HYDROTHERMAL IRON OXIDE COPPER-GOLD & RELATED DEPOSITS



A Global Perspective

VOLUME 2

PGC PUBLISHING

THE AMERICAS | AFRICA | EURASIA | AUSTRALIA

HYDROTHERMAL IRON OXIDE COPPER-GOLD & RELATED DEPOSITS A GLOBAL PERSPECTIVE

Volume 2

Edited
by
T M Porter

PGC
PUBLISHING

a division of
PORTER GEOCONSULTANCY PTY LTD
6 BeattyStreet, Linden Park, SA 5065 Australia
www.portergeo.com.au/publishing

Other titles in the Global Perspective series:

Porphyry and Hydrothermal Copper & Gold Deposits:
A Global Perspective ISBN 978-0-908039-71-5

Hydrothermal Iron Oxide Copper-Gold & Related Deposits:
A Global Perspective - Volume 1 ISBN 978-0-9580574-0-0

Hydrothermal Iron Oxide Copper-Gold & Related Deposits:
A Global Perspective - Volume 3 ISBN 978-0-9871196-0-5

Hydrothermal Iron Oxide Copper-Gold & Related Deposits:
A Global Perspective - Volume 4 ISBN 978-0-9871196-2-9

Super Porphyry Copper and Gold Deposits:
A Global Perspective -Volume 1 ISBN 978-0-9580574-2-4

Super Porphyry Copper and Gold Deposits:
A Global Perspective - Volume 2 ISBN 978-0-9580574-3-1

Contents and abstracts may be browsed, and copies ordered on-line from:
www.portergeo.com.au/bookshop

HYDROTHERMAL IRON OXIDE COPPER-GOLD & RELATED DEPOSITS
A GLOBAL PERSPECTIVE
Volume 2

ISBN 978-0-9580574-1-7

First edition, March 2002

PGC
PUBLISHING

PORTER GEOCONSULTANCY PTY LTD
ABN 15 075 541 632
Trading as: PGC PUBLISHING
6 Beatty Street
Linden Park SA 5065 Australia
Phone: +61 8 8379 7397 Facsimile: +61 8 8379 7397
email: publishing@portergeo.com.au
Web page: http://www.portergeo.com.au/publishing

Citation:
in: Porter, T.M., (ed.), 2000 - Hydrothermal Iron Oxide Copper-Gold and Related Deposits: A Global Perspective, Volume 2, *PGC Publishing, Adelaide.*

Inclusion of a paper in this volume does not necessarily reflect endorsement of its contents by PGC Publishing, Porter GeoConsultancy Pty Ltd., their respective employees, officers or agents, or the editor. Readers should use their own judgement before using or applying any information herein. PGC Publishing, Porter GeoConsultancy Pty Ltd., their respective employees, officers and agents, and the editor, accept no responsibility for any damages or losses in any form that might result from the publication of, or as a result of reading or applying the information included in any part of this volume in any way what-so-ever.

***Cover photograph:** "Perhaps the greatest of them all" - Olympic Dam in South Australia, aerial view 1999, Photograph by T M Porter.*

PGC PUBLISHING

IRON OXIDE COPPER-GOLD AND RELATED DEPOSITS
A GLOBAL PERSPECTIVE

Volume 2

Contents

Page

PREFACE 1

Iron Oxide Alteration/Mineralising Systems and Copper-Gold & Related Mineralisation
T. Michael Porter 3

AUSTRALASIA 91

The Geological Framework, Distribution and Controls of Fe-Oxide Cu-Au Mineralisation in the Gawler Craton, South Australia: Part I - Geological and Tectonic Framework
Gary M. Ferris, Michael P. Schwarz and Paul Heithersay 9

The Geological Framework, Distribution and Controls of Fe-Oxide Cu-Au Mineralisation in the Gawler Craton, South Australia: Part II - Alteration and Mineralisation
Roger G. Skirrow, Evgeniy Bastrakov, Garry Davidson, Oliver L. Raymond and Paul Heithersay 33

Structural and Geochemical Constraints on the Emplacement of the Monakoff Oxide Cu-Au (-Co-U-REE-Ag-Zn-Pb) Deposit, Mt Isa Inlier, Australia.
Garry J. Davidson, Brett K. Davis and Andrew Garner 49

The Selwyn Line Tabular Iron-Copper-Gold System, Mount Isa Inlier, NW Queensland, Australia
David W.W. Sleigh 77

THE AMERICAS 95

Fe Oxide-Cu-Au Deposits in Peru: An Integrated View
Jorge Injoque Espinoza 97

Marcona and Pampa de Pongo: Giant Mesozoic Fe-(Cu, Au) Deposits in the Peruvian Coastal Belt
Nicholas Hawkes, Alan Clark and Timothy Moody 115

The Productora Prospect in North-Central Chile: An Example of an Intrusion-Related, Candelaria Type Fe-Cu-Au Hydrothermal System
Gerry E. Ray and Lawrence A. Dick 131

Geology of the Arizaro and Lindero Prospects, Salta Province, Northwest Argentina: Mid-Miocene Hydrothermal Fe-Ox Copper-Gold Mineralisation
Russell J. Dow and Murray W. Hitzman 153

The Geology of the El Soldado Manto Type Cu (Ag) Deposit, Central Chile
Ricardo Boric, Carmen Holmgren, Nicholas S. F. Wilson and Marcos Zentilli 163

Chilean Strata-bound Cu- (Ag) Deposits: An Overview
Victor Maksaev and Marcos Zentilli 185

Magmatic Iron Ores and Associated Mineralisation: Examples from the Chilean High Andes and Coastal Cordillera
H. Richard Naslund, Fernando Henríquez, Jan Olov Nyström, Waldo Vivallo and F. Michael Dobbs 207

The Epigenetic Sediment-hosted Serra Pelada Au-PGE Deposit and its Potential Genetic Association with Fe-Oxide Cu-Au Mineralisation within the Carajás Mineral Province, Amazon Craton, Brazil
Christian J. Grainger, David I. Groves and Carlos H.C. Costa 227

THE AMERICAS continued

Comparison of the Geology of Proterozoic Iron Oxide Deposits in the Adirondack and Mid-Atlantic Belt of Pennsylvania, New Jersey and New York
Kurt C. Friehauf, Robert C. Smith II and Richard A. Volkert 247

Wernecke Mountains (Yukon) Breccias and Scattered Ore Occurrences: What Contribution to FeOx-Cu-Au-U Metallogeny?
Peter Laznicka 253

EURASIA & AFRICA 273

The Guelb Moghrein Fe-Oxide Copper-Gold-Cobalt Deposit and Associated Mineral Occurrences, Mauritania: A Geological Introduction
Colin D. Strickland and John E. Martyn 275

The Sin Quyen Iron Oxide-Copper-Gold-Rare Earth Oxide Mineralisation of North Vietnam
Robert N. McLean 293

Kiruna-Type Iron Oxide-Apatite Ores and "Apatitites" of the Bafq District, Iran, with an Emphasis on the REE Geochemistry of their Apatites
Farahnaz Daliran 303

The Khetri Copper Belt, Rajasthan: Iron Oxide Copper-Gold Terrane in the Proterozoic of NW India
Joe Knight, Sojen Joy, Jon Lowe, John Cameron, James Merrillees, Sudipta Nag, Nalin Shah, Gaurav Dua and Khamalendra Jhala 321

A Short Review of Palaeozoic Hydrothermal Magnetite Iron-Oxide Deposits of the South and Central Urals, and their Geological Setting
Richard Herrington, Martin Smith, Valeriy Maslennikov, Elena Belogub and Robin Armstrong 343

GENERAL 355

Geophysics of Iron Oxide Copper-Gold Deposits
Robert J. Smith 357

BIOGRAPHY 341

Biographies of Principal Authors 343

Preface

PGC
PUBLISHING

Porter, T.M., 2002 - Preface: Iron Oxide Alteration/Mineralising Systems and Copper-Gold & Related Mineralisation; *in Porter, T.M. (Ed.), Hydrothermal Iron Oxide Copper-Gold & Related Deposits: A Global Perspective*, Volume 2; PGC Publishing, Adelaide, pp 3-6.

PREFACE

IRON OXIDE ALTERATION/MINERALISING SYSTEMS AND COPPER-GOLD & RELATED MINERALISATION

T. Michael Porter

Editor - PGC Publishing
Porter GeoConsultancy Pty Ltd, Adelaide, SA, Australia
mike.porter@portergeo.com.au

This preface presents the background to this book, the second volume of the "Hydrothermal Iron Oxide Copper-Gold & Related Deposits - A Global Perspective" series, and briefly discusses the rationale for inviting the papers it contains, their format and what it is hoped the volume will achieve. It also offers some observations on the unifying characteristics of the iron oxide copper-gold family of deposits and what they may represent in a broader context.

Background to this Volume

The "hydrothermal iron-oxide copper-gold" (IOCG) family and related deposits continue to attract keen interest, both as the subject of academic research and as arguably the most sought after mineral exploration target in the world today.

This interest has been reflected by the strong demand for the first volume of "Porter, T.M. (Ed.), 2000 - Hydrothermal Iron Oxide Copper-Gold & Related Deposits - A Global Perspective". That volume was published as a companion to the conference of the same name convened by the Australian Mineral Foundation in Perth, Western Australia, on 4-5 December 2000, the technical program of which was organised by Mike Porter of Porter GeoConsultancy. The first edition sold out within 6 months and a second printing was commissioned in June 2001. The second edition was published by PGC Publishing in March, 2002.

To further satisfy the obvious need within the industry, it was decided that a second volume should be compiled comprising twenty all new papers to complement the first. This book, also published by PGC Publishing, is the result.

Rationale & Content

This second volume is intended to complement and build upon the first (Porter, 2000). The regions, deposits and subjects in both have been carefully selected to provide a comprehensive global coverage, with appropriate expert authors from both industry and from academia having been invited to contribute papers to achieve that coverage.

While this volume contains a few less papers than did its predecessor, they are on average larger and more exhaustive, resulting in a thicker book. The bulk of the contributions relate to individual deposits, prospects or provinces, and have been geographically sub-divided, as in volume 1, into those from Australasia, The Americas, and Africa & Eurasia, with just one general paper discussing the geophysical expression of the IOCG deposits and their settings.

The editorial intent for both volumes has been to present descriptive detail and observations from a wide variety of IOCG examples from around the world, accompanied by the interpretations and conclusions that may be drawn from those observations.

At the outset, a broad outline of the content and scope of each paper was agreed with the respective author(s), depending on the character of the subject deposit or province and what it might contribute to an understanding of the IOCG family. In addition, each author was asked to include details of the tectonic, geologic and metallogenic setting of the province under discussion or that which embraced the subject deposit, followed by a more detailed description of the geology, structure, alteration, mineralisation, mineralogy, geochemistry and other key characteristics of the subject deposit or deposits of the province. In addition authors were asked to address the occurrence of associated iron oxides, how they were formed/emplaced, the controls of mineralisation, and the spatial, temporal and chemical relationships between the iron oxides and the associated economic mineralisation, both on a property scale, and regionally.

It is not intended that the two volumes be composed of papers that merely reveal the "absolute truths" on the origin of these deposits from positions of authority, but rather that readers are presented with a range of factual descriptions, observations and differing opinions that provide the opportunity for them to draw their own informed

conclusions. Indeed there has been a definite intention to include the conflicting opinions that are argued in the literature, although the authors involved have been asked to support their interpretations by hard observations and careful reasoning (eg. Barton and Johnston, 2000; Pollard, 2000; Naslund, *et al.*, this volume).

In addition, as will become apparent from studying the papers in these two volumes, this family of deposit does not comprise a single ore type, but represents a family of loosely related deposits with a common elemental association and overlapping characteristics. As such the conflicting views presented are found to be applicable to different branches of the family, while none are necessarily all embracing.

Since the recognition of this family of deposits a wide range of examples have been cited within the literature as being members. As we learn more about them it has become apparent that not all should be readily accepted into the family. Never-the-less, papers have been invited to describe some of these less obvious relatives that are found in association with accepted members, and to discuss whether or not they should be incorporated into the family as well as their links, if any to it (eg. Maksaev and Zentilli, this volume and Boric, *et al.*, this volume).

In a similar vein, it is apparent that deposits may belong to the family, while also being classified as another distinct ore style (eg., some are also classified as skarns, *see* Injoque, this volume and Herington, *et al.*, this volume; some have carbonatite associations, *see* Vielreicher, *et al.*, 2000 and Harmer, 2000; while others exhibit the influence of many of the processes normally associated with sediment hosted copper ores, *see* Boric, *et al.*, this volume). This emphasises the earlier observations that the family does not represent a single ore style but a group of deposits with common elemental associations and overlapping characteristics, but no over-arching genetic model.

An Elemental Association

It seems unlikely that a particular model will explain all of the deposits commonly included within the IOCG family, but rather there are several overlapping to separate and/or distinct classes of ores.

The main unifying characteristic of the IOCG family might be that the association of iron oxide alteration and copper ±gold ±silver ±uranium ±LREE ±apatite ±fluorine may represent an association of elements related to their complementary chemical properties, solubilities and ability to be transported and/or to be precipitated together under similar conditions.

A direct analogue of this approach may be the universal association of lead-zinc-silver ±copper ±gold ±barite, usually with accompanying iron-sulphide alteration, in what might be loosely regarded as the 'Pb-Zn-Ag family' of deposits. As we know, this same elemental association occurs together in a wide range of geological settings, from volcanic hosted massive sulphides (Kuroko, Palaeozoic VHMS, Archaean Cu-Zn), to shale/sediment hosted (Mt Isa, Century, McArthur River, Red Dog), sandstone hosted (Laisvall, l'Argentere) and carbonate hosted (often inaccurately grouped together as 'Mississippi Valley Type'), to transgressive pipe like bodies within sedimentary piles (Tsumeb, Kabwe, Kipushi), through to those in high grade metamorphic sequences (Broken Hill, Cannington, Aggeneys, Gamsberg, Rampura-Agucha) and to magmatic/skarn associations (Antamina). These settings range from continental margin arc, to back-arc to intra-continental collapse/extensional settings, and are related to straight magmatic-hydrothermal, to metamorphic-hydrothermal, to mixed magmatic and basinal processes to straight basinal fluids. All produce significant, economic ore deposits, many of which (but not all) have a stratabound character. As such the Zn-Pb-Ag elemental association, or family of deposits, span a variety of ore classes, are found in a range of tectonic settings, host sequences and modes of occurrence, some transitional representing a continuum, while others are markedly different.

It is likely therefore that the IOCG family similarly reflects an association of compatible elements emplaced as the result of a range of different processes in a variety of settings and conditions. The common factor is the elemental association. Never-the-less a study of the deposits included within the family can teach us more about the way in which Cu ±Au ±other metals behave within, or react to, a dominantly oxidised, iron rich environment or mineralising system.

Oxide Mineralising Systems

Until the discovery of Olympic Dam and the subsequent realisation of the existence, and then the significance, of the broad IOCG family, base and precious metal exploration and studies had concentrated almost exclusively on systems where 'iron-sulphides - silicate/carbonate' associations (ie. iron sulphides such as pyrite or pyrrhotite with silicates like k-feldspar, biotite, sericite, chlorite, and/or carbonates including calcite, ankerite, etc.,) dominated, both in the immediate ore and as the surrounding alteration halo on all scales. The exceptions of course were the iron ore systems and supergene environments.

The IOCG family however, is characterised by a much lower total sulphide content within a dominantly 'iron-oxides - silicate/carbonate' mineralogy (ie. iron oxides such as magnetite or hematite with silicates like k-feldspar, biotite, albite, chlorite, and/or carbonates including calcite, ankerite, etc), both in the ore zone and as the surrounding alteration halo. As is demonstrated in Ferris, *et al.*, (this volume), Skirrow, *et al.*, (this volume), Williams & Skirrow (2000), Smith (this volume) these iron-oxide - silicate/carbonate alteration systems may be very extensive, comparable to, or larger than the iron-sulphide - silicate/carbonate halos surrounding the great porphyry systems of the Andes for example.

In addition there is a tendency for significant IOCG deposits and districts to be located in terranes in which other, usually

pre-existing significant iron oxide accumulations are common, ie. in more oxidised sections of the crust or where a strong oxidised component is observed. Examples are the eastern Gawler Craton in South Australia with its widespread banded iron formations, some of which are exploited as ores in the Middleback Ranges (Ferris, *et al.*, this volume; Skirrow *et al.*, this volume), but which also embraces the Olympic Dam deposit (Reynolds, 2000); the Carajas province of Brazil which encompasses enormous high grade, exploited iron formation reserves as well as the IOCG deposits at Salobo (Souza & Vieira, 2000), Igarape Bahia (Tazava & de Olivera, 2000), Alemão (Ronze, *et al.*, 2000;), Sossego, Cristalino and Serra Pelada (Grainger & Groves, this volume); or the Chilean Iron Belt that contains a string of magnetite-apatite deposits (eg. El Romeral) and IOCG ores such as La Candelaria (Marschik, *et al.*, 2000) and prospects like Productora (Ray & Dick, this volume). The pre-existing or early phase iron oxide occurrence may either form a reactive base on which IOCG sulphide mineralisation is nucleated, as at Tennant Creek in Australia (Skirrow, 2000), or is itself altered, overprinted and upgraded by subsequent iron oxide alteration as at Olympic Dam, or in the Middleback Ranges (Skirrow, *et al.*, this volume) and in sections of the Carajas of Brazil.

The discovery of Olympic Dam, has raised the awareness of the potential for economic copper ±gold ±silver ±uranium ±LREE ±apatite ±fluorine, etc., accumulations being found in association with iron-oxide alteration/ mineralising systems in what we now recognise as the IOCG family. Perhaps this may not represent the only elemental association that can occur together to form economic deposits within such 'oxide mineralising systems'. Ores of other metals may yet be found within iron-oxide rich systems in similar or different hosts.

These iron-oxide rich 'oxide mineralising systems' may represent the converse of the iron-sulphide rich reduced systems on which attention has been focused for so long, or the end member of a spectrum that includes both, as described by Haynes (2000). We now know the former may embrace vast IOCG deposits. If we were to concentrate on these 'oxide alteration/mineralising systems', other large, as yet un-recognised ore deposits of different commodities and ore classes may be recognised, or existing deposits may be 're-classified' and better appreciated.

Acknowledgments

The editor and PGC Publishing wish to thank all of the authors who have so willingly contributed so much of their time, experience and expertise to prepare the outstanding collection of papers we have been able to assemble in this volume. We are also very grateful that all agreed to permit PGC Publishing to use their work and for their trust that we will be able to adequately market and distribute the book worldwide. We also very much appreciate the assistance of those throughout the industry, both in Australia and internationally who were consulted and offered advice on the content and the authors to be approached.

Thanks are also due, firstly to Lyn Porter of PGC Publishing who has with diligence and persistence prepared the master electronic file from the many and varied data files received from authors, and to Mark Porter for his invaluable contribution to producing the e-commerce web-site at http://www.portergeo.com.au/publishing required to market, take orders for, and distribute both volumes globally.

References

Barton, M.D. and Johnson, D.A., 2000 - Alternative Brine Sources for Fe-Oxide (-Cu-Au) Systems: Implications for Hydrothermal Alteration and Metals ; *in Porter, T.M. (Ed.), Hydrothermal Iron Oxide Copper-Gold & Related Deposits: A Global Perspective*, Volume 1; PGC Publishing, Adelaide, pp 43-60.

Boric, R., Holmgren, C. & Wilson, N.S.F. & Zentilli, M., 2002 - The Geology of the El Soldado Manto Type Cu (Ag) Deposit, Central Chile; *in this volume.*

Ferris, G.M., Schwarz, M.P. and Heithersay, P., 2002 - The Geological Framework, Distribution and Controls of Fe-Oxide Cu-Au Mineralisation in the Gawler Craton, South Australia: Part 1: Geological and Tectonic Framework; *in this volume.*

Grainger, C.J., Groves, D.I. & Costa, C.H.C., 2001 - The Epigenetic Sediment Hosted Serra Pelada Au-PGE Deposit and its Potential Genetic Association with Fe-Oxide Cu-Au Mineralisation, Amazon Craton, Brazil; *in this volume.*

Harmer, R.E., 2000 - Mineralisation of the Phalaborwa Complex and the Carbonatite Connection in Iron Oxide-Cu-Au-U-REE Deposits; *in Porter, T.M. (Ed.), Hydrothermal Iron Oxide Copper-Gold & Related Deposits: A Global Perspective*, Volume 1; PGC Publishing, Adelaide, pp 331-340.

Haynes, D.W. 2000 - Iron Oxide Copper (-Gold) Deposits: Their Position in the Ore Deposit Spectrum and Modes of Origin; *in Porter, T.M. (Ed.), Hydrothermal Iron Oxide Copper-Gold & Related Deposits: A Global Perspective*, Volume 1; PGC Publishing, Adelaide, pp 71-90.

Herrington, R., Smith, M., Maslennikov, V., Belogub, E. & Armstrong, R., 2002 - A Short Review of Palaeozoic Hydrothermal Magnetite Iron-oxide Deposits of the South and Central Urals and their Geological Setting; *in this volume.*

Injoque, J., 2002 - Fe Oxide-Cu-Au Deposits in Peru: An Integrated View; *in this volume.*

Maksaev, V. & Zentilli, M., 2002 - Chilean Strata-bound Cu-(Ag) Deposits: An Overview; *in this volume.*

Marschik, R., Leveille, R.A., & Martin, W., 2000 - La Candelaria and the Punta del Cobre District, Chile: Early Cretaceous Iron-Oxide Cu-Au(-Zn-Ag) Mineralisation; *in Porter, T.M. (Ed.), Hydrothermal Iron Oxide Copper-Gold & Related Deposits: A Global Perspective,* Volume 1; PGC Publishing, Adelaide, pp 163-175.

Naslund, H.R., Henriquez, F., Nyström, J.O., Vivallo, W. & Dobbs, F.M., 2002 - Magmatic Iron Ores and Associated Mineralisation: Examples from the Chilean High Andes and Coastal Cordillera; *in this volume.*

Pollard, P.J., 2000 - Evidence of a Magmatic Fluid and Metal Source for Fe-Oxide Cu-Au Mineralisation; *in Porter, T.M. (Ed.), Hydrothermal Iron Oxide Copper-Gold & Related Deposits: A Global Perspective,* Volume 1; PGC Publishing, Adelaide, pp 27-41.

Porter, T.M. (Ed.), 2000 - Hydrothermal Iron Oxide Copper-Gold & Related Deposits - A Global Perspective, Volume 1, PGC Publishing, Adelaide, 350p.

Ray, G.E. & Dick, L.A., 2002 - The Productora Prospect in North-Central Chile: An Example of an Intrusion-related, Candelaria Type Fe-Cu-Au Hydrothermal System; *in this volume.*

Reynolds, L. J., 2000 - Geology of the Olympic Dam Cu-U-Au-Ag-REE deposit. *in Porter, T.M. (Ed.), Hydrothermal Iron Oxide Copper-Gold & Related Deposits: A Global Perspective,* Volume 1; PGC Publishing, Adelaide, pp 93-104.

Ronzê, P.C., Soares, A.D.V., Santos, M.G., Barreira, C.F., 2000 - Alemão Copper-Gold (U-REE) Deposit, Carajas, Brazil; *in Porter, T.M. (Ed.), Hydrothermal Iron Oxide Copper-Gold & Related Deposits: A Global Perspective,* Volume 1; PGC Publishing, Adelaide, pp 191-202.

Skirrow, R.G., Bastrakov, E., Davidson, G., Raymond, O.L. & Heithersay, P., 2002 - The Geological Framework, Distribution and Controls of Fe-Oxide Cu-Au Mineralisation in the Gawler Craton, South Australia: Part II: Alteration and Mineralisation; *in this volume.*

Skirrow, R.G., 2000 - Gold-Copper-Bismuth Deposits of the Tennant Creek District, Australia: A Reappraisal of Diverse High Grade Systems; *in Porter, T.M. (Ed.), Hydrothermal Iron Oxide Copper-Gold & Related Deposits: A Global Perspective,* Volume 1; PGC Publishing, Adelaide, pp 149-160.

Smith, R.J., 2002 - Geophysics of Iron Oxide Copper-Gold Deposits; *in this volume.*

Souza, L.H. & Vieira, E.A.P., 2000 - Salobo 3 Alpha Deposit: Geology and Mineralisation; *in Porter, T.M. (Ed.), Hydrothermal Iron Oxide Copper-Gold & Related Deposits: A Global Perspective,* Volume 1, PGC Publishing, Adelaide, pp 213-224.

Tazava, E. & de Oliveira, C.G., 2000 - The Igarapé Bahia Au-Cu-(REE-U) Deposit, Carajás Mineral Province, Northern Brazil; *in Porter, T.M. (Ed.), Hydrothermal Iron Oxide Copper-Gold & Related Deposits: A Global Perspective,* Volume 1; PGC Publishing, Adelaide, pp 203-212.

Vielreicher, N.M. Groves, D & Vielreicher, R.M., 2000 - The Phalaborwa (Palabora) Deposit and its Potential Connection to Iron-Oxide Copper-Gold Deposits of Olympic Dam Type; *in Porter, T.M. (Ed.), Hydrothermal Iron Oxide Copper-Gold & Related Deposits: A Global Perspective,* Volume 1; PGC Publishing, Adelaide, pp 321-329.

Williams, P.J. & Skirrow, R.G., 2000 - Overview of Iron Oxide-Copper-Gold Deposits in the Curnomona Province and Cloncurry District (Eastern Mount Isa Block), Australia; *in Porter, T.M. (Ed.), Hydrothermal Iron Oxide Copper-Gold & Related Deposits: A Global Perspective,* Volume 1; PGC Publishing, Adelaide, pp 105-122.

Australasia

PGC
PUBLISHING

Ferris, G.M., Schwarz, M.P. and Heithersay, P., 2002 - The Geological Framework, Distribution and Controls of Fe-Oxide Cu-Au Mineralisation in the Gawler Craton, South Australia: Part 1: Geological and Tectonic Framework; *In* Porter, T.M. (Ed.), Hydrothermal Iron Oxide Copper-Gold and Related Deposits: A Global Perspective, Volume 2; *PGC Publishing, Adelaide*, pp 9-31.

THE GEOLOGICAL FRAMEWORK, DISTRIBUTION AND CONTROLS OF FE-OXIDE CU-AU MINERALISATION IN THE GAWLER CRATON, SOUTH AUSTRALIA.

PART I - GEOLOGICAL AND TECTONIC FRAMEWORK

Gary M. Ferris, Michael P. Schwarz and Paul Heithersay

Office of Minerals and Energy Resources, PIRSA, Adelaide, South Australia

Abstract - The Archaean to Mesoproterozoic Gawler Craton hosts a range of economic mineral commodities, including Au (central Craton), Ag-Pb-Zn (eastern Eyre Peninsula) and iron ore of the Middleback Ranges. A major iron-oxide copper-gold province containing the world class Olympic Dam Cu-U-Au-Ag-REE deposits extends ~ 500 km along the eastern margin of the Craton, from the Mount Woods Inlier in the north to the Moonta-Wallaroo district in the south. This paper presents new advances in our understanding of the structure, deformation history and tectonic evolution of the Gawler Craton, which may lead to a better understanding of the distribution of these mineral systems. The Craton is subdivided into tectonic domains, each encompassing an area of crust containing similar lithological and structural associations. New tectonic events have been defined within the three major orogenic cycles of the Gawler Craton (the Sleaford, Kimban and Kararan Orogenies). The recent discovery that much of the craton comprises relatively juvenile Proterozoic crust has improved our understanding of cratonic evolution. We propose growth through accretion in magmatic arc settings along the eastern margin of an arcuate Archaean core at ~ 1850 Ma (Donington Suite), and along the southwestern margin at ~ 1680 Ma (Tunkillia Suite) and 1620 Ma (St Peters Suite). We suggest an alternative model to a largely anorogenic setting for emplacement of the Hiltaba Suite, an intracontinental, extensional back-arc, located behind a northeast dipping subduction zone, south of the Nuyts Domain, which produced the arc-related magmatism of the St Peters Suite.

The Hiltaba Suite magmatic event was widespread across the Gawler Craton, and is broadly associated, both temporally and in places spatially, with a major mineralising event. At the Olympic Dam deposit, a close spatial and temporal association is recognised between its host rock, the Roxby Downs Granite, and iron-oxide copper-gold mineralisation. Other mineral prospects related to Hiltaba Suite magmatism include Tarcoola, Tunkillia, Myall, Sheoak, Barns, and possibly Weednana and Menninnie Dam. The presence of Hiltaba Suite granites is an important factor for exploration companies in tenement selection.

Introduction

The Gawler Craton (Fig. 1) is an ancient crystalline shield comprising Archaean to Mesoproterozoic metasediments, volcanics and granites, which has been tectonically stable, with the exception of minor epeirogenic movements, since ~1450 Ma (Thomson, 1975; Parker, 1990, 1993). Due to very sparse basement outcrop, the geology of the Gawler Craton is poorly constrained, compared to other cratonic areas within Australia. The Craton records crust formation and tectono-thermal events in the late Archaean to early Palaeoproterozoic (Sleaford Orogeny), Palaeoproterozoic (Kimban Orogeny), and Palaeoproterozoic to Mesoproterozoic (Kararan Orogeny).

The boundaries of the Gawler Craton have been interpreted from a combination of both total magnetic intensity and gravity data. Limited regional geological outcrop information and irregularly distributed drill hole data have also been used to determine the outer most limit of rock types assigned to the Gawler Craton. The eastern limit of the craton is relatively well defined by the Torrens Hinge Zone, a zone of Neoproterozoic rifting initiated during the development of the Adelaide Geosyncline. Later deformation, during the Delamerian Orogeny, led to reworking of the eastern margin. Fig. 2 illustrates the extent of this domain.

The northern and western extent of the craton is less well defined. The boundaries are obscured by Neoproterozoic and Phanerozoic sediments which increase rapidly in thickness across faulted margins to the Officer Basin. The northwestern boundary is defined to coincide with a linear, magnetic and gravity anomaly which is interpreted to represent the extent of the Kararan Orogeny. The southern margin of the Gawler Craton is presently placed close to the edge of the Continental Shelf, in the southern ocean, along prominent gravity and magnetic features. These may

indicate mafic intrusives associated with rifting during the Jurassic, which eventually led to separation of Australia and Antarctica during Tertiary times.

Continued acquisition of detailed aeromagnetic data, flown as part of the South Australian Exploration Initiative (SAEI) and Targeted Exploration Initiative (TEISA), have greatly enhanced the geological understanding of the Gawler Craton. Greater detail in structural trends and magnetic patterns, which together with regional mapping, further U-Pb geochronology, isotopic analysis and geochemistry have provided the basis for the subdivision of the Gawler Craton into domains (Fig. 2). These domains are considered to represent the major components which were assembled through polyphase tectonic events during the Proterozoic (~1850 to 1540 Ma).

The domain boundaries are based on; major crustal shear/ fault zones (ie: Karari Fault Zone, Yerda Shear Zone); marked difference in metamorphic grade and zones of complex structural/metamorphic transitions where faults and late plutonic rocks have masked the boundary (e.g., Nuyts and Cleve Domain boundary). The geological characteristics of each Domain are summarised below.

The eastern Gawler Craton is a major iron-oxide copper-gold province within South Australia and hosts the world class Olympic Dam Cu-U-Au-Ag-REE deposit, located approximately 520 km north-northwest of Adelaide (Fig. 1). The mineralisation and alteration in this metallogenic belt, termed the Olympic copper-gold province, is described in part II (Skirrow *et al.*, this volume). The Olympic Dam deposit contains ore reserves of >600 Mt averaging 1.8% Cu, 0.5 kg/t U_3O_8, 0.5 g/t Au and 3.6 g/t Ag (Reynolds, 2000). The total resource for the deposit is >2300 Mt containing 30 Mt of Cu, 930 000 t of U_3O_8, 1200 t of Au and 6700 t of Ag (Reynolds, 2000). Olympic Dam is hosted by the Olympic Dam Breccia Complex, which occurs within the Roxby Downs Granite, a member of the Hiltaba Suite. The Olympic Domain also hosts sub-economic mineralisation at Acropolis, Emmie Bluff, Wirrda Well, Oak Dam and within the overlying Pandurra Formation sediments at Mount Gunson (Fig. 1). Within the southern Olympic Domain, the Moonta-Wallaroo region, contains a number of significant historic mines as well as the Wheal Hughes and Poona copper mines (Fig. 1), which were discovered in 1985/86 and mined until 1994. Mineralisation is hosted by the Palaeoproterozoic Moonta Porphyry at Moonta and the Doora Schist at Wheal Hughes. A total of 355 000 t of copper and 2 t of gold have been extracted from the Wallaroo-Moonta region, largely in the late 19th century (Conor, 1995).

The recent discovery of the Prominent Hill prospect within the Mount Woods Inlier by Minotaur Resources Ltd (Minotaur Resources Ltd, 2001) has greatly increased the prospectivity of the Gawler Craton, with significant interest in areas containing oxidised Hiltaba Suite granite. Drill hole DDH URN1 intersected basement at 108 metres, below a cover of barren Mesozoic and Permian shale and sands. Copper mineralisation commences at 200 m with significant intersections of 107 m (200 to 307 m) at 1.94% Cu, 0.65 g/t Au (including 35 m at 3.86%, 272 to 307m) and 152 m (429 to 581 m) at 1.1% Cu, 0.61 g/t Au and 267 ppm U, in a hematite breccia host (Minotaur Resources Ltd, 2001, 2002). Significant intersections of copper have been reported from other prospects in the Mount Woods area, including Manxman, Joes Dam and Cairn Hill. Large resources of iron ore are also present within the Mount Woods Inlier (Polito and Davies, 1997). Drilling at Peculiar Knob outlined a resource of 14 Mt grading 63.2 % Fe to 100 m depth (Morris and Hough, 1997), with enrichment produced by hydrothermal replacement of the host BIF (Davies, 2000).

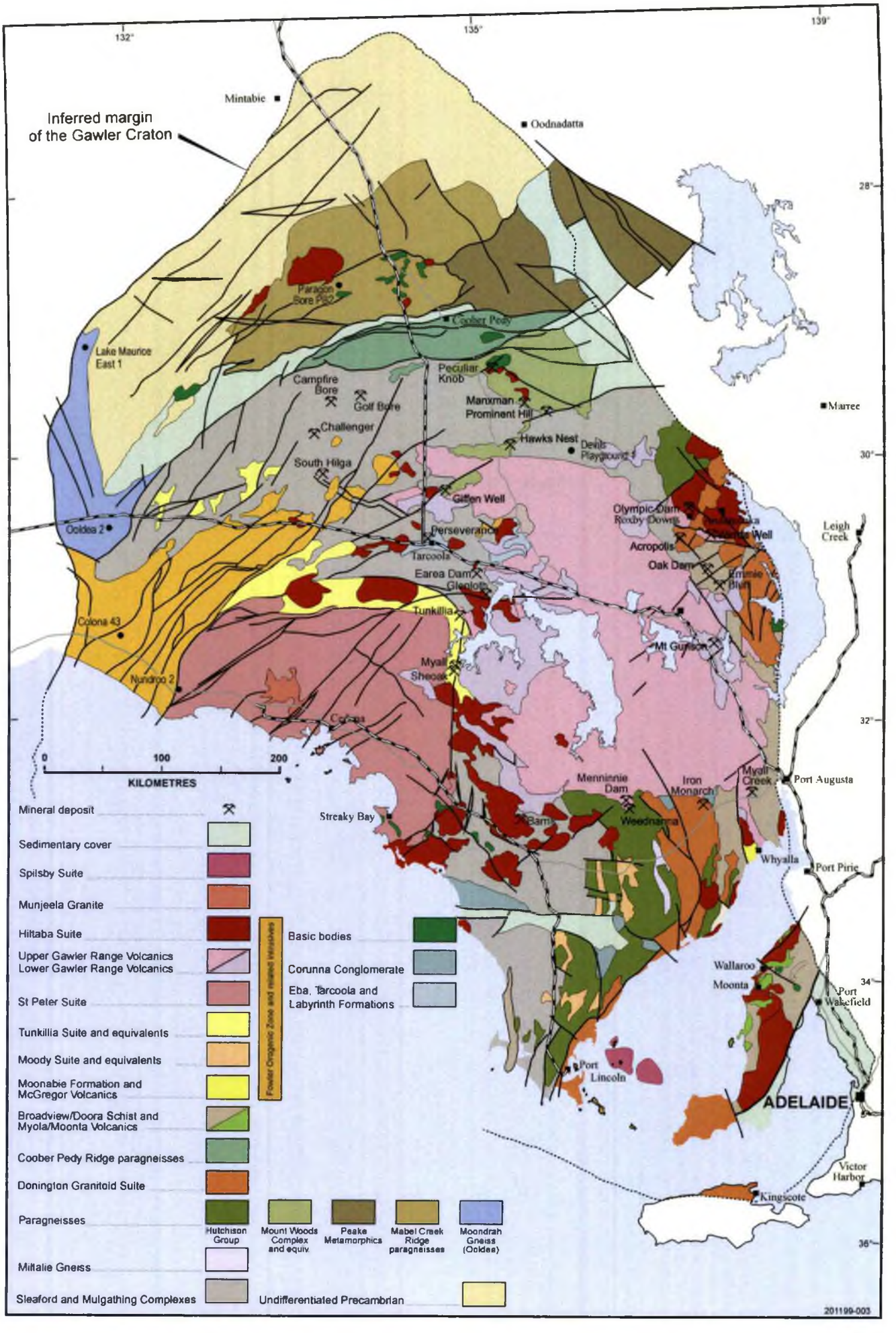
The extent of iron oxide related alteration on the eastern Gawler Craton including the Olympic, Mount Woods and northern Spencer Domains suggest that large volumes of hydrothermal fluids were involved and similar processes were occurring at the same time. The predominantly linear to arcuate nature of the eastern iron oxide alteration system and associated Hiltaba Suite plutons (Fig. 1) suggests control by a major tectonic feature. This may have been a major factor in extensive alteration and mineralisation on the eastern Gawler Craton. Distinct from the iron oxide associated mineralising system on the eastern Gawler Craton, Daly, *et al.* (1998) report gold and base metal mineralisation, with associated sericite-chlorite alteration, at Tarcoola, Tunkillia, Myall-Sheoak, Glenloth and Earea Dam related to central Gawler Craton, Hiltaba Suite magmatism. Hence, there appears to be two distinct arcuate belts of Hiltaba Suite magmatism and a difference between eastern and central, associated mineralisation styles.

Part one of this paper will describe the regional geology and tectonic setting of the Gawler Craton as a framework for the eastern Gawler Craton iron oxide copper-gold province. Part two will discuss the different alteration assemblages associated with regional alteration, and the controls on mineralisation across the eastern Gawler Craton.

Domains of the Gawler Craton

Thomson (1970) and Parker (1990) divided the Gawler Craton into tectonic sub-domains based on structural, metamorphic and stratigraphic characteristics. Teasdale (1997) defined three new sub-domains, the Fowler, Coober Pedy and Lincoln Sub-domains. Based on recent geochronology and geochemical work on the Gawler Craton (Teasdale, 1997; Steward and Foden, 2001; Ferris, 2001), a new domain map of the Gawler Craton has been produced (Fig. 2). This process has been undertaken as a first step into a holistic tectonic interpretation of the Gawler Craton. It is intended to reveal those areas that require further research in order to produce robust tectonic interpretations (and the genetic connotations contained therein) of each domain. It also allows the spatial relationship of mineralising systems to be investigated. Within this map, the term domain is preferred because it is non-genetic and the next subdivision of a province. Each domain of the Gawler

Figure 1 (facing page): Interpreted sub-surface geology of the Gawler Craton, South Australia, modified from Daly *et al.* (1998). Geology of the Stuart Shelf basement courtesy of Geoscience Australia (see also Part II, Skirrow *et al.*, this volume).


Inferred margin of the Gawler Craton
132°
135°
139°
28°
30°
32°
34°
36°
Mintabie
Oodnadatta
Marree
Leigh Creek
Port Augusta
Whyalla
Port Pirie
Port Wakefield
Port Lincoln
ADELAIDE
Victor Harbor
Kingscote
Streaky Bay
Ceduna
Wallaroo
Moonta
Paragon Bore PB2
Coober Pedy
Lake Maurice East 1
Peculiar Knob
Campfire Bore
Golf Bore
Challenger
Manxman
Prominent Hill
Hawks Nest
Devils Playground 1
South Hilga
Gilles Well
Olympic Dam
Roxby Downs
Perseverance
Tarcoola
Acropolis
Oak Dam
Emmie Bluff
Earea Dam
Glenloth
Tunkillia
Mt Gunson
Myall Sheoak
Colona 43
Nundroo 2
Ooldea 2
Menninnie Dam
Weednanna
Iron Monarch
Myall Creek
Barns
0
100
200
KILOMETRES
Mineral deposit
Sedimentary cover
Spilsby Suite
Munjeela Granite
Hiltaba Suite
Upper Gawler Range Volcanics
Lower Gawler Range Volcanics
St Peter Suite
Tunkillia Suite and equivalents
Moody Suite and equivalents
Moonabie Formation and McGregor Volcanics
Broadview/Doora Schist and Myola/Moonta Volcanics
Coober Pedy Ridge paragneisses
Donington Granitoid Suite
Paragneisses
Hutchison Group
Mount Woods Complex and equiv.
Peake Metamorphics
Mabel Creek Ridge paragneisses
Moondrah Gneiss (Ooldea)
Miltalie Gneiss
Sleaford and Mulgathing Complexes
Undifferentiated Precambrian
Fowler Orogenic Zone and related intrusives
Basic bodies
Corunna Conglomerate
Eba, Tarcoola and Labyrinth Formations
201199-003

Reverse of colour plate, intentionally blank

Craton encompasses an area of crust, which has similar lithological and structural associations, which differ broadly, from the surrounding domains. Boundaries are commonly placed along major crustal shear zones or zones of contrasting litho-stratigraphy. Fig. 3 shows a tectono-stratigraphic diagram for the Gawler Craton based on the Domains presented below.

Peake and Denison Domain

The Peake and Denison Domain (Peake and Denison Inlier) is located on the northern margin of the Gawler Craton (Fig. 2) and comprises quartzite (Baltucoodna Quartzite), amygdaloidal basalts and acid volcanics (Tidnamurkuna Volcanics), and quartz-chlorite-muscovite schists collectively termed the Peake Metamorphics. A rhyolite, within the Tidnamurkuna Volcanics, has a SHRIMP U-Pb zircon age of 1780±12 Ma (Fanning, 1997). The syn-tectonic Wirriecurrie Granite has tectonised contacts with the surrounding Peake Metamorphics and gives a 1793±8 Ma age (Fanning, 1997). Younger unnamed granites give a SHRIMP U-Pb zircon age of 1536±6 Ma and intrude the Peake Metamorphics on the eastern side of the inlier (Fanning, 1997). The boundaries of the Peake and Denison Domain are defined by faulted and unconformable contacts with overlying Adelaidean sediments. Delamerian folding of Adelaidean sediments has mildly overprinted the basement units (Rogers and Freeman, 1996).

Nawa Domain

The Nawa Domain contains magnetite-rich metasediments of the Moondrah Gneiss (Daly *et al.*, 1998), thought to represent aluminous, magnesium-rich meta-pelites. Interpretation of regional aeromagnetics suggest the presence of polygonal, relatively non-magnetic, sheet-like intrusives of Hiltaba Suite (Fairclough and Daly, 1995). The domain comprises an intensely faulted, rigid crustal block, which appears relatively unaffected by the ductile, arcuate, roughly northeast-southwest to east-west shear zones which separate domains to the south. It is bounded by the Cambrian to Neoproterozoic Murnaroo Platform to the northwest, the Karari Fault Zone to the south, and the Torrens Hinge Zone to the northeast. Rb-Sr isotope data indicates that samples from drill hole Ooldea 2 (Fig. 2) have a minimum metamorphic age of ~1700 Ma (Parker, 1993). Pb-Pb analysis using the Kober zircon evaporation technique yielded two ages, 1690±9 Ma and 2426±6 Ma (Teasdale, 1997). U-Pb SHRIMP analysis yielded a concordant age of 1653±8 Ma with inherited components at ~1700 Ma (Fanning, 1997; Daly *et al.*, 1998). Teasdale (1997) interpreted the data to indicate two events, one zircon forming event at 1690 Ma, followed by a high temperature event at 1653 Ma. Fanning, (1997) considered initial zircon growth occurred at 1653 Ma, with 1690 Ma inheritance. The difference of opinion remains problematic, however the onset of the Kararan Orogeny buried these sediments. A quartz-plagioclase-garnet-biotite-sillimanite paragneiss, from drill hole Paragon Bore PB2 within the Mabel Creek Ridge, has a U-Pb SHRIMP age of ~1540 Ma, which is interpreted as recording the timing of later high-grade metamorphism (Fanning, 1997). The Mabel Creek Ridge is separated from the Coober Pedy Ridge, and Mount Woods Domain by the Karari Fault Zone. On the north western margin of the Nawa Domain, a U-Pb emplacement age of 1740 Ma was recorded for a foliated granite from the Yoolperlunna Inlier (Fanning, pers comm).

Coober Pedy Domain

The Coober Pedy Domain (formerly known as the Coober Pedy Ridge) comprises sinuous, high magnetic intensity, iron-rich meta-sedimentary granulites. The northern and southern boundaries are defined by the Karari Fault Zone (Fig. 2). The northern boundary is delineated on aeromagnetics and the southern boundary by gravity. U-Pb zircon geochronology of meta-granodiorite or tonalite and cordierite-garnet-biotite-sillimanite paragneiss containing zircons with relic cores which were dated at 1750 Ma, with metamorphic rims recording an age of 1565±8 Ma (Daly *et al.*, 1998; Fanning, 1997). It is inferred that the paragneisses forming the Coober Pedy Ridge were derived from the Mount Woods Domain and deformed under granulite facies conditions at 1568 Ma, an event apparently not recorded in the Mount Woods Domain (Daly *et al.*, 1998).

Mt Woods Domain

The Mt Woods Domain contains fine-grained, finely layered, banded iron formation and calc-silicates (Daly *et al.*, 1998). Aeromagnetic images show ductile metamorphic layering inferring reworking of the underlying Archaean. Within the Mount Woods Domain, metasediments underwent granulite facies metamorphism at 1736±14 Ma (Fanning, 1997), hence these sediments are older than ~1740 Ma. Also within this domain is the Engenina Adamellite which has a SHRIMP U-Pb zircon age of 1691±25 Ma (Fanning, 1997). The Engenina Adamellite has a similar age to the Moody Suite granites of the southern Gawler Craton (Parker, 1993), although the high error may allow for a syn-Kararan intrusive age. The Mt Woods Domain contains undeformed Hiltaba Suite, such as the Balta Granite which has a SHRIMP U-Pb age of 1584±18 Ma (Fanning, 1997). The northern boundary of the Mount Woods Domain is the Karari Fault Zone. The southern boundary in fault controlled and the eastern boundary is defined by a dramatically increasing thickness of overlying sediments.

Economic Geology

The Mount Woods Domain hosts the recently discovered Prominent Hill (copper-uranium-gold) prospect as well as the Joes Dam, Cairn Hill and Manxman prospects (Fig. 2). It appears that the Hiltaba Suite has a strong temporal and spatial association with iron-oxide copper-gold mineralisation within these prospects, as is the case with the Olympic Domain. The Mount Woods Domain also contains significant strike lengths of Palaeoproterozoic BIF within a sequence of metasediments. Depth of cover varies from a few tens of metres deepening to >100 m to the south.

Christie Domain

The original Christie Sub-domain of Parker, 1990, has been subdivided to exclude the Fowler Domain (Fowler Orogenic Zone), the Coober Pedy Domain and the Mount Woods Domain. The Christie Domain comprises Archaean to earliest Palaeoproterozoic rocks, which comprise the original protolith, on which younger units were deposited/ incorporated (Daly and Fanning, 1993; Teasdale, 1997). Major rock units include low magnetic intensity Mulgathing Complex paragneiss (e.g., host of the Challenger gold deposit), interlayered with, linear highly magnetic zones of banded iron formation and ultramafic rocks, including peridotite, and intruded by highly magnetic ~1690 to 1670 Ma intrusives. The western boundary is the Karari Fault Zone and the eastern boundary is the Coorabie and Tallacootra Shear Zones (Fig. 2).

Economic Geology

The Challenger gold deposit was discovered by Dominion Mining Ltd and Resolute Ltd (Gawler Joint Venture) in 1995. Drilling has outlined a combined indicated and inferred resource of 1.71 Mt at 8.5 g/t Au containing 14.5 tonnes (0.465 Moz) of gold (Dominion Mining, 2002). Development of the project to mine status is currently underway with the first gold production expected during the second half of 2002. The mineralised system occurs within a meta-sedimentary plagioclase, perthitic K-feldspar, quartz, cordierite, garnet and biotite variant of the Archaean Christie Gneiss (Mulgathing Complex). Syntectonic, ~2440 Ma, high grade gold mineralisation occurs within and adjacent to a complex array of quartz veins (Dominion, 2002). These veins occur within structurally controlled shoots with a north-northeasterly strike and northerly plunge (Dominion, 2002). The internal vein geometry is oblique to the plunge azimuth of the shoots, probably reflecting Proterozoic overprinting. Numerous other prospects have been identified with a similar mineralisation style including the Birthday, Golf Bore, Campfire Bore, South Hilga and Birdie prospects (Daly *et al.*, 1998). Potential also exists for Archaean, granite-greenstone style gold mineralisation in the Harris Greenstone Domain in the western Gawler Craton.

Harris Greenstone Domain

The Harris Greenstone Domain (formerly part of the Wilgena Domain), comprises supercrustal Archaean ultramafic (komatiite) and mafic volcanics and Archaean aluminous metasediments (Christie Gneiss), felsic extrusives and/or intrusives (Kenella Gneiss) and syn-tectonic acid intrusives (Glenloth Granite) (Daly and Fanning, 1993). Mafic/ultramafic packages in the Christie Domain are generally intrusive whereas in the Harris Greenstone Domain they are dominantly extrusive. This may be due to significantly different crustal levels exposed within the different domains. Alternatively, the intrusive and extrusive ultramafics may be different geological units. The Yerda Shear Zone represents the southern boundary and the northern boundary is a lithological zone boundary with the Wilgena Domain.

Fowler Domain

The Fowler Domain comprises a northeast trending sinuous high magnetic intensity belt of Palaeoproterozoic igneous and metamorphic rocks. Boundaries are the Karari Fault Zone to the west and the Coorabie Shear Zone to the east (Fig. 2). The Fowler Domain was previously termed the Fowler Suture Zone (Daly *et al.*, 1995), but is more recently described as the Fowler Orogenic Belt (Daly *et al.*, 1998). Teasdale subdivided the Fowler Domain into four blocks; the Nundroo, Central, Colona and Barton Blocks which show different metamorphic grade. SHRIMP U-Pb zircon geochronology of mildly deformed, coarse-grained, cumulus gabbro, in drill hole Colona 43, gives an emplacement age of 1730±10 Ma (Fanning, 1997). Small zircons grown during high-grade metamorphism of a gabbro or basalt in drill hole Nundroo 2 define a U-Pb age of 1543±9 Ma (Fanning, 1997). Possible host paragneisses include sillimanite bearing aluminous metasediments and banded iron formation of unknown age (Afmeco, 1982). Deformed Hiltaba Suite granite also occurs within the Fowler Domain. The eastern margin of the Fowler Orogenic Zone is markedly discordant to the gross litho-tectonic trends in the Nuyts Domain to the east and represents a major crustal discontinuity. Aeromagnetic data suggests a significant strike-slip component to this boundary, but outcrop data shows a dominant vertical displacement. This suggests significant transpressive strike-slip displacement.

Nuyts Domain

The Nuyts Domain comprises possible Palaeoproterozoic, ductile deformed metasediments and meta-igneous rocks into which variably magnetic, Palaeoproterozoic to Mesoproterozoic granitoids were emplaced. The Nuyts Domain was previously interpreted to represent Archaean basement, but recent geochronology and isotopic analyses show juvenile crust produced during Palaeoproterozoic orogenic activity. The domain is broadly delineated by a distinctive gravity low, reflecting the predominantly felsic igneous composition. It is bound to the north by the Yerda Shear Zone, and the west by the Coorabie Shear Zone. The overlying Gawler Range Volcanics obscure the eastern boundary but it appears to be strongly controlled by the Yarlbrinda Shear Zone (Fig. 2). The south east boundary remains problematic. A noticeable feature of the Nuyts Domain is the concentration of large Hiltaba Suite plutons around its structurally controlled northern and eastern margins (Fig. 2). Both deformed and undeformed plutons occur within shear zones bounding the Nuyts Domain, suggesting at least a partly syn-orogenic emplacement. Spatially, the plutons form an arcuate belt distinct from a similar belt to the north-east, within the Olympic and Mt Woods Domains. Based on empirical evidence, the Hiltaba Suite within, and adjacent to, this belt appears to be associated with a quartz-sericite-chlorite-gold dominant style of mineralisation as opposed to iron oxide copper-gold in the Olympic and Mount Woods Domains.

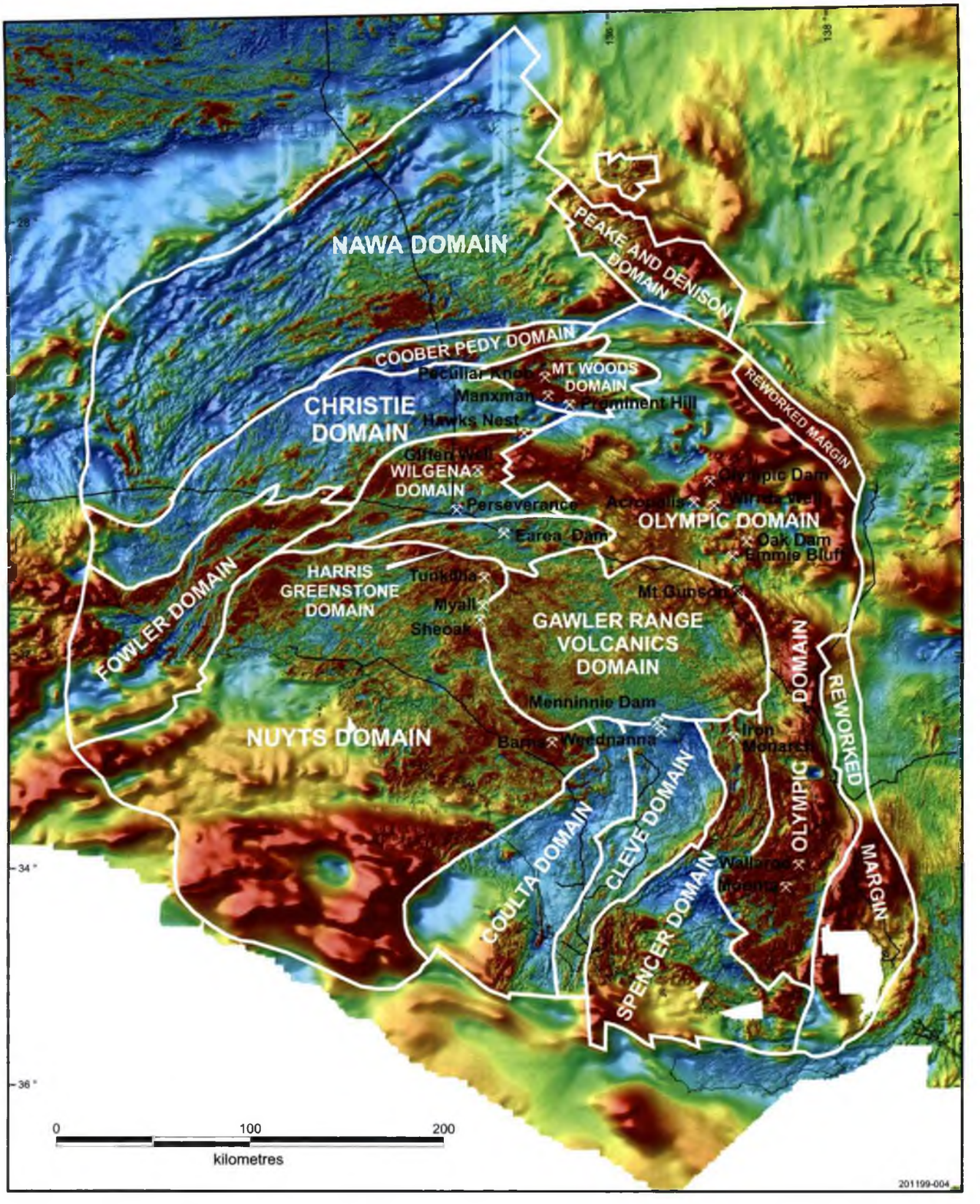


Figure 2: Domains of the Gawler Craton on Total Magnetic Intensity

Reverse of colour plate, intentionally blank

Wilgena Domain

The Wilgena Domain was originally defined by Parker (1990), as a large northeast trending zone. Teasdale (1997) subdivided the Wilgena and part of the Christie Sub-domains into the Christie, Fowler and Coober Pedy Sub-domains, based on different metamorphic histories. The Wilgena Domain comprises high magnetic intensity metasediments, including banded iron formation, intruded by large elliptical Hiltaba Suite plutons. Boundaries are the Coorabie Shear Zone to the north and west, Yerda Shear Zone and the Harris Greenstone Domain to the south and the Olympic Domain to the east (Fig. 2).

Economic Geology

Alluvial gold mineralisation was discovered at Tarcoola in 1893 and gold-bearing quartz reefs were located in 1900. Between 1900 and 1955, gold bullion totalling 2400 kg was recovered from 64 000 t of ore at an average grade of 37.5 g/t. Gold is found in quartz veins within carbonaceous siltstone and interbedded quartzite of the Palaeoproterozoic Tarcoola Formation. Gold also occurs in altered quartz-feldspar granite, inferred to be Hiltaba Suite from a nearby 1575±7 Ma U-Pb zircon age, from unaltered granite. Alluvial gold was also discovered at Glenloth and gold-bearing reefs discovered in 1901. Between 1901 and 1955, ~315 kg of gold was produced from 14 620 t of ore, at an average grade of 21.6 g/t. Mineralised veins are hosted by sheared and fractured Archaean to Palaeoproterozoic Glenloth Granite. North of the Glenloth Goldfield, gold was discovered at Earea Dam in 1899 and during 1899-1903 and 1933-1941 produced 59 kg of gold from ~1870 t of ore at an average grade of 35.5 g/t.

Recent exploration for iron ore, at the Hawks Nest prospect, has identified a series of disconnected ridges of BIF, where magnetite occurs as the dominant iron oxide beneath relatively shallow cover of younger sediments and weathered BIF (Davies, 2000). Close-spaced drilling on one of the strike ridges has identified an inferred resource of 220 Mt to 135 m depth, grading 36% Fe (AuIron Energy, 2000). The potential for further resources is significant. A similar deposit occurs at Giffen Well, 60 km to the southwest, with resources estimated at 240 Mt to 150 m depth, grading 36% Fe.

Gawler Range Volcanics Domain

The Gawler Ranges Volcanics Domain is a large area of dominantly felsic volcanics, which are flat lying and relatively undeformed (Fig. 2). Lower parts of the sequence contain interlayered basalts. U-Pb zircon dating for the Wanganny and Yardea Dacites give ages of 1591±3 and 1592±3 Ma (Fanning *et al.*, 1988) respectively. The boundaries are coincident with the distinct elliptical magnetic signature of the domain. Recent work (Morrow and McPhie, 2000) indicates that the greater part of the Gawler Range Volcanics, originally interpreted as predominantly ignimbrites (Blissett, 1980), may be lavas. This concept has significant implications for exploration.

Olympic Domain

The Olympic Domain (incorporating the Moonta Domain of Parker, 1993) is an arcuate zone of Palaeoproterozoic sediments and felsic igneous rocks and Mesoproterozoic granite, volcanics, quartz-rich sediments and conglomerates.

The oldest rocks known from the Olympic Domain comprise a schistose unit which occurs as enclaves within deformed granites of Suite #1 (Creaser, 1989). These rocks are strongly deformed, containing at least one foliation, and are thought to represent Hutchinson Group metasediments based on relationships with the Suite #1 granites of Creaser (1989). The Hutchinson Group is an extensive sequence of shallow clastic and chemical marine sediments, with minor acid and mafic volcanics (Parker, 1993). Parker and Lemon (1982) subdivided the Hutchinson Group into three main sequences:

- a basal quartzite sequence (Warrow Quartzite)
- a mixed chemical and clastic sequence (Middleback Subgroup)
- an upper pelitic unit (Yadnarie Schist)

Within the Olympic Domain, numerous drill holes intersect coarse grained, deformed granite. U-Pb SHRIMP analysis of zircons from hole PD-2, give a crystallisation age of 1845 Ma; hence this is considered to be part of the Donington Granitoid Suite (Creaser, 1995). The unit is of batholithic extent, which supports a Donington Suite classification (Creaser, 1995). In addition to the coarse-grained, deformed granite, Creaser (1989) recognised two other distinct lithological groups:

- Felsic, medium grained, equigranular granite and pegmatite, and
- Intermediate to mafic lithologies including tonalite, gabbroic anorthosite, granodiorite and quartz monzonite.

The Donington Granitoid Suite is defined from the southern Gawler Craton, where it outcrops on the eastern coast of the Eyre Peninsula through to the west coast of the Yorke Peninsula. In this region the suite forms a batholithic series of intrusions ranging from quartz gabbro-norite to ultra-fractionated granite (Parker *et al.*, 1988). The batholith contains small volumes of mafic to intermediate magmas, voluminous felsic, megacrystic granite and gneiss, and smaller volumes of late, ultra-fractionated, fine, even-grained granite. Distinct lithological units within the Donington Granitoid Suite exhibit abundant co-magmatic relationships, suggesting evolution from a common magma source (Schwarz, 2003). Original anhydrous orthopyroxene ± clinopyroxene bearing compositions have been variably retrogressed to biotite and hornblende. Numerous U-Pb zircon dates on different lithological units have all returned crystallisation ages within error of 1850 Ma (Fanning, 1997).

The Kalinjala Mylonite Zone separates the Donington Granitoid Suite in the south from similar lithologies in the Cowell-Cleve region, northern Eyre Peninsula. In this

region the Minbrie Gneiss is interpreted as an equivalent to the Donington Granitoid Suite (Parker, 1993). Lithological units comprise granite gneiss, granodiorite gneiss and augen gneiss, are multiply deformed and contain enclaves of Hutchison Group metasediments. Rb-Sr analysis on the granite gneiss suggests a crystallisation age >1800 Ma (Webb *et. al.*, 1986).

Within the Olympic Dam region, a sequence of intercalated, deformed felsic volcanics and schists overlie the Donington Granitoid Suite (Creaser, 1989). This unit has not been dated, but is thought to be correlated with either the Myola (~1791 Ma) or Moonta Volcanics (~1760 Ma) or possibly the Tidnamurkuna Volcanics (~1780 Ma).

Unconformably overlying the older granites within the Olympic Domain is a widespread sequence of finely laminated meta-siltstone, feldspathic sandstones, calc-silicates and amphibolites. This sequence is unconformably overlain by Gawler Range Volcanics, hence Creaser (1989) correlated this unit with the Wanderah Meta-siltstone found within the Moonta Domain. Conor (1995) defined the Wallaroo Group to include all meta-sedimentary and meta-igneous units older than the Mesoproterozoic Tickera-Arthurton Granites and the Oorlana Metasomatite within the Moonta Domain. The Wallaroo Group includes the Wardang Volcanics, Willamulka Volcanics, Wanderah Metasediments and Doora Metasediments (Fig. 3). The age of the sequence has been determined from the interbedded Moonta Volcanics, dated by U-Pb zircon analyses at 1760±7 Ma (C.M. Fanning, PRISE, *pers. comm.*, 2002).

The last major magmatic event observed in the area is the Hiltaba Suite/Gawler Range Volcanic magmatic event (1595 to 1575 Ma). The Gawler Range Volcanics cover an area of approximately 25 000 km² and are the dominant Proterozoic outcropping unit on the Gawler Craton. They consist of a series of dominantly felsic lavas and ignimbrites, with minor mafic lavas. The Hiltaba Suite intrudes the Gawler Range Volcanics and is a suite of mostly oxidised, K-feldspar dominant granite. The discovery of the Olympic Dam Cu-U-Au ore body, hosted within the Roxby Downs Granite, a member of the Hiltaba Suite, has greatly increased the prospectivity of the Gawler Craton.

Unconformably overlying these older units is the Pandurra Formation, a thick sequence of undeformed arenaceous red bed sediments that extend over a greater part of the Olympic Domain (Cowley, 1991). Fanning *et al.* (1983) reports that the Pandurra Formation has a minimum depositional age of 1424±51 Ma based on Rb-Sr geochronology. Unconformably overlying the Pandurra Formation in the Cultana area (Moonta Domain) are subaerial basalts of the Beda Volcanics and intercalated coarse fluvial clastics of the Backy Point Formation.

Economic Geology

The eastern Gawler Craton contains one of the largest iron oxide-copper-gold provinces in the world extending for some 700 km from the Peake and Denison Range, in the north, through the Mount Woods Inlier, Olympic Dam, Mount Gunson, to the Moonta-Wallaroo and Iron Monarch areas, in the south.

The Olympic Dam deposit contains ore reserves of >600 Mt averaging 1.8% Cu, 0.5 kg/t U_3O_8, 0.5 g/t Au and 3.6 g/t Ag (Reynolds, 2000). The total resource for the deposit is >2300 Mt containing 30 Mt of Cu, 930 000 t of U_3O_8, 1200 t of Au and 6700 t of Ag (Reynolds, 2000). The Hiltaba Suite/Gawler Ranges Volcanic magmatic event was widespread across the Gawler Craton (Fig. 3) and was a major mineralising event. The timing of mineralisation at Olympic Dam overlaps the emplacement age of the Roxby Downs Granite, suggesting the granite was a source of heat and possibly fluids for the deposit.

Overlying the Olympic Domain, copper mineralisation also occurs in Adelaidean sediments. Copper mineralisation was discovered at Mount Gunson in 1875 with approximately 149 000 t of copper metal and 65 t of silver from 8.4 Mt of ore (grading 1.7% Cu) produced since 1898. Mineralisation is located within the (~1400 Ma) Pandurra Formation and Adelaidean cover sediments.

A joint venture between Australian Selection (Pty) Ltd and Sims Metals Pty Ltd discovered the Myall Creek prospect located south of Port Augusta in March 1975, during exploration for Copperbelt type orebodies on the Stuart Shelf. Drill holes intersected copper sulphides, with lesser zinc and lead, and accessory silver and cobalt, over an area extending 15 km north-south by 3 km east-west, at a depth of approximately 160 metres. Mineralisation occurs at the base of the Tapley Hill Formation within a thin white sandstone and an overlying silt-dolo-laminite facies. Minor copper sulphide mineralisation is also found in underlying Beda Volcanics. The deposit shows metal and mineral zoning both vertically and laterally. Apart from pyrite, the sulphide minerals are of epigenetic origin. The deposit exhibits many features in common with the Kupferschiefer of Europe.

Copper was discovered in the Moonta-Wallaroo are in 1860 and approximately 350 000 t of copper at 3.7% Cu was recovered between 1860 and 1923 mainly from underground workings. The Wheal Hughes and Poona deposits produced 17 500 t of copper (grade 3.7%) between 1988 and 1993. The Wallaroo and Moonta copper deposits also produced approximately 3.6 t of gold with an average grade of 0.4 g/t between 1860 and 1923. Recent mining at Wheal Hughes and Poona produced 423 kg of gold (0.9 g/t) from 476 000 t of ore. The host rocks include feldspar porphyry (Moonta Porphyry) and schists (Doora Schist) with mineralisation associated with the Hiltaba Suite magmatic event (~1590 Ma).

Spatially, the Hiltaba Suite forms an arcuate belt from the Mt Woods Domain in the north through to the Olympic Domain (Moonta Wallaroo region) in the south. Within this belt, apparent concentrations of plutons occur in the Moonta-Wallaroo region, Olympic Dam region and the eastern portion of the Mt Woods-Nawa Ridge region (Fig. 2). Mineralisation associated with the Hiltaba Suite within this belt is dominated by iron oxide copper-gold.

Coulta Domain

The Coulta Domain is dominated by Archaean metasediments and volcanics of the Sleaford Complex, and high level, granitoid intrusives of the Dutton Suite. These rocks comprise the original protolith on which younger units of the southern Gawler Craton were deposited. The Coulta Granodiorite of the Dutton Suite gives a U-Pb zircon age of 2517±14 (Fanning, 1997). The northern boundary is inferred to be an east-west trending shear zone stitched by Hiltaba Suite plutons (Fig. 2). The western boundary represents a faulted margin with the Nuyts Domain, which marks a transition into significantly younger intrusives.

Cleve Domain

The Cleve Domain is dominated by basinal sediments of the Palaeoproterozoic Hutchison Group unconformably overlying Palaeoproterozoic Miltalie Gneiss and Archaean paragneiss and orthogneiss with a metamorphic age of ~2440 Ma. Syn-tectonic intermediate to felsic Moody Suite (~1700 Ma) intrude the Hutchison Group metasediments. The Cleve Domain is separated from the Coulta Domain by a major northeast trending shear zone, which brings high level granites of the Dutton Suite, within the Coulta Domain, into juxtaposition with granulite facies para- and orthogneiss of the Sleaford Complex. The Kalinjala Mylonite Zone separates the Cleve Domain from the Spencer Domain (Fig. 2).

Economic Geology

Within the Cleve Domain, Pb-Zn mineralisation is known from the Palaeoproterozoic Hutchinson Group metasediments. Many small deposits are located on eastern Eyre Peninsula with the largest being the Miltalie Mine (lead-silver). Ore grades up to 61.5% Pb and 118.5 g/t Ag are reported, the mine operating intermittently between 1860 and 1914. Other small mines include Atkinson's Find, Cleve, Elson, Lady Franklin, Mangalo, Mount Miller, Poonana and Yalpoundie.

Drilling of aeromagnetic targets adjacent to the southern margin of the Gawler Ranges in 1981 resulted in discovery of significant lead-zinc-silver mineralisation at the Menninnie Dam and Telephone Dam prospects. Mineralisation is hosted by Hutchison Group serpentine marble, laminated graphitic, ankeritic, dolomitic marble and carbonate-facies BIF, and comprises massive pyrite-sphalerite-galena with minor chalcopyrite and pyrrhotite. The mineralising event is related to intrusion of Mesoproterozoic rhyolitic dykes (Roache and Fanning, 1994). An inferred resource of 1.7 Mt at 5% Pb, 8% Zn and 100 g/t Ag is reported for Menninnie Dam.

Spencer Domain

The Spencer Domain comprises irregularly shaped intrusives of the Donington Granitoid Suite ranging in composition from gabbro-norite to highly evolved leucogranite. Results of U-Pb zircon dating, from the southern part of the domain, give a consistent intrusive age of 1850 Ma (Fanning, 1997). Interfolded inliers of Palaeoproterozoic Hutchison Group metasediments occur within the Donington Granitoid Suite in the northern part of the domain. The Spencer Domain is separated from the Cleve Domain by the Kalinjala Mylonite Zone. The Olympic Domain is distinguished from the Spencer Domain by the development of characteristic iron oxide alteration within the former (Fig. 2).

Economic Geology

Deposits of iron-rich chemical sedimentary rocks occur within the Spencer Domain and are easily recognised by their prominent linear aeromagnetic signature. The Middleback Ranges comprise a series of prominent, discontinuous ridges of Palaeoproterozoic BIF extending north-south for 60 km. Oxidised BIF, with haematite as the dominant iron oxide, occurs from surface to an average depth of 90 m, and is underlain by unoxidised BIF with magnetite as the dominant iron oxide. Currently it is considered to be uneconomic to beneficiate the near surface haematite-rich ore. The first major iron ore mining in Australia began at Iron Knob in the Middleback Range in 1915. From 1915 to the present, over 200 Mt of high-grade ore has been mined from haematite deposits within the Middleback Range (Iron Monarch, ~130 Mt until closed in 1998; Iron Baron - Iron Prince area, ~56 Mt until closed in 1995; Iron Duke - Iron Duchess - Iron Knight area, ~15 Mt). For some 50 years from 1915 to 1965 these deposits were the main supply of ore for Australia's iron and steel industry, and the favourable logistics of the region led to the establishment of an integrated steelworks at Whyalla in 1964. The remaining measured reserves of high-grade ore in the Middleback Range are reported at 26 Mt (Davies, 2000).

Deformation History of the Gawler Craton

Three major tectonic events have fundamentally affected the formation of the Gawler Craton

1. ?2700 to 2300 Ma - Late Archaean sedimentation and volcanism followed by early Palaeoproterozoic plutonism and metamorphism (*Sleaford Orogeny*);
2. 2000 to 1700 Ma - initial basin/platform sedimentation followed by widespread plutonism, metamorphism and deformation (*Kimban Orogeny*) with local volcanism and continental sedimentation; and
3. 1690 to 1450 Ma - development of spatially separated granulite and amphibolite facies rocks during the *Kararan Orogeny* (1690 to 1540 Ma) in the northern and western portion of the craton. This was accompanied by syn-tectonic intrusion of acid, ultramafic and mafic plutons with associated development of major ductile shear zones encroaching on the central Gawler Craton. Emplacement of extensive Hiltaba Suite plutonism and felsic volcanism (Gawler Range Volcanics), accompanying the formation of the iron oxide copper-gold systems on the eastern Gawler Craton. Intra continental clastic sedimentation occurred late in this event.

The following section is a summary of the current understanding of the deformation history of the Gawler

Craton, based of recent work of the Geological Survey and numerous workers referenced within. New tectonic events have been defined within the three major tectonic cycles outlined above. On the southern Gawler Craton the historical Kimban Orogeny (1850 to 1700 Ma) has been separated into two discrete events, the Neill Event (1850 Ma) and the new Kimban Orogeny (1730 to 1700 Ma).

Sleafordian Orogeny ~2700 to 2300 Ma

Effects of the Sleafordian Orogeny are recorded in Archaean crust within the Coulta Domain, Harris Greenstone Domain, Wilgena Domain, and Christie Domain. Very little is known of Sleafordian kinematics as many original structures have been reworked by later tectonic events. The onset of high grade metamorphism is thought to have occurred around 2600 Ma (Fanning *et al.*, 1988) with the most pervasive, peak granulite facies metamorphism occurring between 2440 and 2420 Ma. Waning stages of the orogeny are recorded by Rb-Sr whole rock geochronology at ~2300 Ma (Webb *et al.*, 1986). Following the cessation of the Sleafordian Orogeny at ~2300 Ma there was a period of relative tectonic quiescence until 2000 Ma, the onset of the Miltalie Event.

Miltalie Event, Southern Gawler Craton, ~2000 Ma

The Miltalie Event separates the Sleafordian Orogeny from the Neill Event described below (Fanning, 1997). The Miltalie Gneiss at Plug Range (WHYALLA map sheet, Parker, 1983, Parker and Fanning, 1997), granite west of Tumby Bay and hypersthene gneiss within the Carnot Gneisses at Redbanks, all record zircon crystallisation at about 2000 Ma (Fanning, 1997). Fanning *et al.*, (1995), Fanning (1997) and Daly *et al.*, (1998) have proposed that during this event, the lower crustal, high grade Carnot Gneisses were brought into juxtaposition with higher crustal level, lower grade intrusions of the Dutton Suite. Aeromagnetic data of the southern Gawler Craton reveal a roughly northeast-southwest boundary between magnetically busy Carnot Gneisses to the east and relatively quiet Dutton Suite to the west (Fig. 2). This is interpreted as a major fault or terrane boundary formed during this event. Further evidence that this is a major crustal feature comes from a crustal scale electromagnetic conductor coincident with this boundary (White & Milligan, 1984).

Redefining the Kimban Orogeny

The Kimban Orogeny, as defined by Thomson (1969), Glenn *et al.* (1977), and Parker and Lemon (1982) occurs over a relatively long time period of ~150 Ma. Parker (1993), defines three major events having occurred between ~1845 and ~1710 Ma. Based on relationships to various igneous units, KD_1 was inferred between ~1845 and 1795 Ma, KD_2 between ~1795 and 1745 Ma and KD_3 between ~1745 and 1710 Ma. Subsequent geochronology (principally reported in Fanning, 1997) has led to a refinement of the tectono-thermal history. The first major event is now constrained to the waning stages of intrusion of the Donington Granitoid Suite at 1850 Ma. The second and third major events occurred between ~1730 and ~1700 Ma, constrained by Sm-Nd data on granulite facies assemblages within the Kalinjala Mylonite Zone (Hand *et al.*, 1995), intrusion of the syntectonic Middle Camp Granite at ~1730 Ma and syn- to post-tectonic Moody Suite at ~1700 Ma. Hoek and Schaefer (1998) suggest that the first tectono-thermal event of the Kimban Orogeny be separated from the latter, due to the ~150 Ma separation between the two. Significant crustal extension at ~1770 Ma (Oliver and Fanning, 1997), involving deposition of the Price Metasediments, supports a division. Wilson (1999) has termed the first event, at 1850 Ma, the Lincoln Orogeny and redefined the Kimban Orogeny as the second event correlating with KD_2 and KD_3 of Parker and Lemon (1982). Considering the term "Lincoln" is well established with the term "Lincoln Complex" (Parker, 1993), the authors feel that it would cause much confusion to adopt the nomenclature of Wilson (1999). We suggest that the term Neill Event be applied to the earlier, and Kimban Orogeny be restricted to the later, episodes of deformation.

Neill Event, Southern Gawler Craton, ~1850 Ma

The Neill Event is well constrained by intrusion of the Donington Granitoid Suite. Mortimer *et al.* (1988) identified foliated enclaves of megacrystic granite gneiss within relatively undeformed Colbert Granite. Both rocks have subsequently been dated at ~ 1850 Ma. Parker's early layer parallel foliation in the Hutchison Group metasediments is thought to have formed during this event, as did metamorphic zircons in Corny Point Paragneiss, (Zang and Fanning, 2001)

Kimban Orogeny, Southern Gawler Craton, ~1730 to 1700 Ma

The redefined Kimban Orogeny contains KD_2 and KD_3 of Parker and Lemon (1982). The orogeny is currently constrained by intrusion of the Middle Camp Granite at ~1730 Ma (Fanning, 1997), granulite facies metamorphism within the Kalinjala Mylonite Zone, at ~1730 Ma (Hand *et al.*, 1995), and intrusion of the late to post tectonic Moody Suite at ~1700 Ma (Fanning, 1997).

Transitional Kimban - Kararan Deformation

Metasediments from the Mount Woods Domain underwent high-grade metamorphism at ~1740 Ma, possibly coeval with the Kimban Orogeny outlined above. However, tectonic activity continued within the Mount Woods Domain beyond activity recorded in the southern Gawler Craton (Betts, 1992; Finlay, 1993). Within the Fowler Domain, the host sediments were intruded by voluminous sheets, sills and plutons of strongly magnetised, mafic-intermediate, I-type, cumulus layered intrusives at ~1730 Ma (Teasdale, 1997). Hence, deformation pre-1650 Ma, was occurring on the western and northern Gawler Craton and the relationship between these events and the Kimban Orogeny, on the southern Gawler Craton, is uncertain.

The Kararan Orogeny

The Kararan Orogeny was defined by Daly *et al.* (1995, 1998) to describe high-grade metamorphism and associated deformation between ~1650 and 1540 Ma on the northern and western Gawler Craton. Daly *et al.* (1998) report that deformation associated with the Kararan Orogeny is related to continental collision between the eastern proto-Yilgarn Craton, to the northwest, and the central Gawler Craton-East Antarctic Craton (Mawson Continent) in the south. The name Kararan Orogeny is derived from the Karari Fault Zone, a major crustal feature on the northwestern Gawler Craton. The temporal relationships associated with the Kararan Orogeny are poorly constrained, due to lack of exposures along the northern margin of the Craton.

Daly *et al.* (1998) reported the effective minimum age for the onset of the Kararan Orogeny was ~1650 Ma, defined by metamorphic zircons from the Ooldea Region. Magnetite-rich aluminous metasediments from DDH Ooldea 2 have a mineral assemblage comprising hypersthene-sillimanite and sapphirine-quartz which indicate high grade metamorphic conditions (>950°C and >9.5kb; Teasdale, 1997). Teasdale (1997), using the Kober Pb-Pb technique, reports that the main zircon forming event occurred at ~1690 Ma and these zircons were recrystallised at ~1653 Ma during the ultra-high temperature event. Fanning (1997) records zircon growth at ~1653 with inheritance at ~1700 Ma. This problem has not yet been resolved; however, burial of these sediments is regarded as occurring during the onset of the Kararan Orogeny, so that the metamorphic ages must be regarded as a minimum age for this event. Additional SHRIMP dating, by Fanning, for Teasdale (1997) record abundant syntectonic intrusives from 1690 to 1670 Ma, in the Fowler Domain. This suggests that the Kararan Orogeny should be extended to 1690 Ma.

If this change in concept is accepted, then those deformed granites assigned by Daly *et al.* (1998) to the Kimban Orogeny, now become Kararan Orogeny syntectonic granites. For example, the Symons Granite (1690±10 Ma) immediately west of Mulgathing Homestead and the Engenina Adamellite (1691±10 Ma) in the Mt Woods Domain. Syntectonic granites described by Teasdale (1997), at Wynbring Rocks (1669±10 Ma), Barton South (~1675 Ma) and at Lake Ifould (1672±17 Ma) would also become syn-Kararan Orogeny granites. Included in this group is Little Pinbong from the Coulta Domain (1670±17 Ma; Fanning, 1997).

Teasdale (1997) used the term Ifould Complex for variably deformed I-type granitoids and mafics at Lake Ifould in the western Gawler Craton. Daly *et al.* (1998) used Ifould Complex for all syntectonic Kararan Orogeny intrusives so that further subdivision would be individually named suites within this very large region. To avoid confusion, Teasdale's (1997) usage has precedence and should be used strictly for those granites in the Lake Ifould area. The stratigraphic term proposed here is the Ifould Suite.

Ferris (2001) has now defined a suite of comagmatic felsic and mafic granitoids, within the Yarlbrinda Shear Zone with a U-Pb zircon age of ~1680 Ma, as the Tunkillia Suite. These rocks show an arc-affinity on a Pearce *et al.* (1984) diagram (Fig. 4).

Between ~1630 and 1610 Ma, the St Peter Suite was intruded into the Nuyts Domain, producing a suite of tonalitic to granodioritic rocks, similar in chemistry to Archaean tonalite-trondhjemite-granodiorites. Fig. 4 shows the St Peter Suite plot predominantly within the volcanic arc granite field on a Pearce *et al.* (1984) tectonic diagram. This event is not witnessed within the eastern Gawler Craton.

The Hiltaba Suite/Gawler Range Volcanics magmatic event (~1595 to 1575 Ma) represents a major tectonic/tectono-thermal event which affected much of the Gawler Craton (Fig. 3). Geochemistry and Sm-Nd isotope analysis of the Hiltaba Suite shows that it is highly variable across the Gawler Craton. The suite is dominantly felsic, although intermediate lithologies are known from the northern Gawler Craton (Andamooka and Olympic Dam areas). ε_{Nd} values for Hiltaba Suite granites within the Nuyts Domain record positive values including 0.11 (Nunnyah Rockhole) and 1.19 (Wallala Rock) (Stewart and Foden, 2001), which suggest a depleted mantle source (Rollinson, 1993). Hiltaba Suite samples to the east of the Nuyts Domain record a range of negative ε_{Nd} values indicating a continental crustal source (Stewart and Foden, 2001). Johnson and Cross (1991) record a mixed ε_{Nd} signature, indicating a partial mantle source mixed with older Archaean crust.

The episodic Kararan Orogeny in the western and north western Gawler Craton, (1690 to 1670, 1650 and 1565 to 1540 Ma) has produced ductile gneisses of amphibolite facies to granulite facies metamorphism. In the central and eastern parts of the craton, major ductile shear zones were imposed on older rocks. It is highly likely the Kararan Orogeny has produced major structures into which the St Peters Suite, Gawler Range Volcanics and Hiltaba Suite were emplaced. If, within these areas, deformation is consistent across each domain, magnetic alteration and associated mineralisation sourced from Hiltaba Suite granite or the Gawler Range Volcanics will appear as ductile layering (Daly, *et al.*, 1998).

Major compressional deformation on the western Gawler Craton occurred again between ~1565 and 1540 Ma related to oblique transpression along major shear zones. Metasediments within the Coober Pedy Domain and Nawa Domain underwent ductile deformation at ~ 1565 and ~1550 Ma respectively (Daly *et al.*, 1998). High-grade metamorphism within the Fowler Domain is recorded by zircons from MESA DDH Nundroo 2, which have a U-Pb age of 1543±9 Ma (Fanning, 1997).

Regional Tectonics

Previous tectonic interpretations of the Gawler Craton show a predominant Archaean basement with two major periods of Proterozoic deformation (Kimban Orogeny and Kararan Orogeny). One of the most recent advances in the understanding of the Gawler Craton has been the recognition that large parts of the south western Gawler

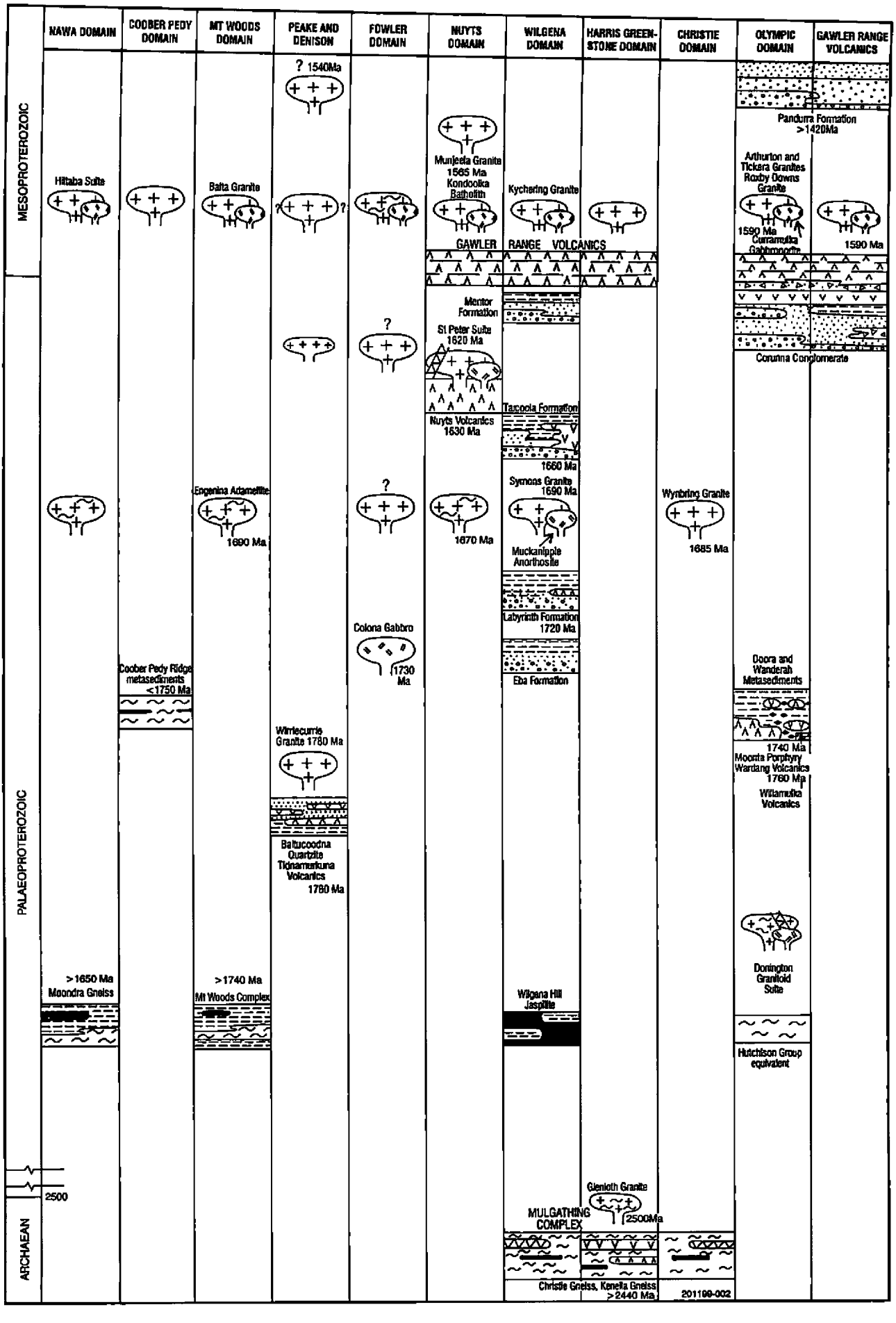


Figure 3: Strato-tectonic elements of the Gawler Craton (adapted from Daly *et al.*, 1998)

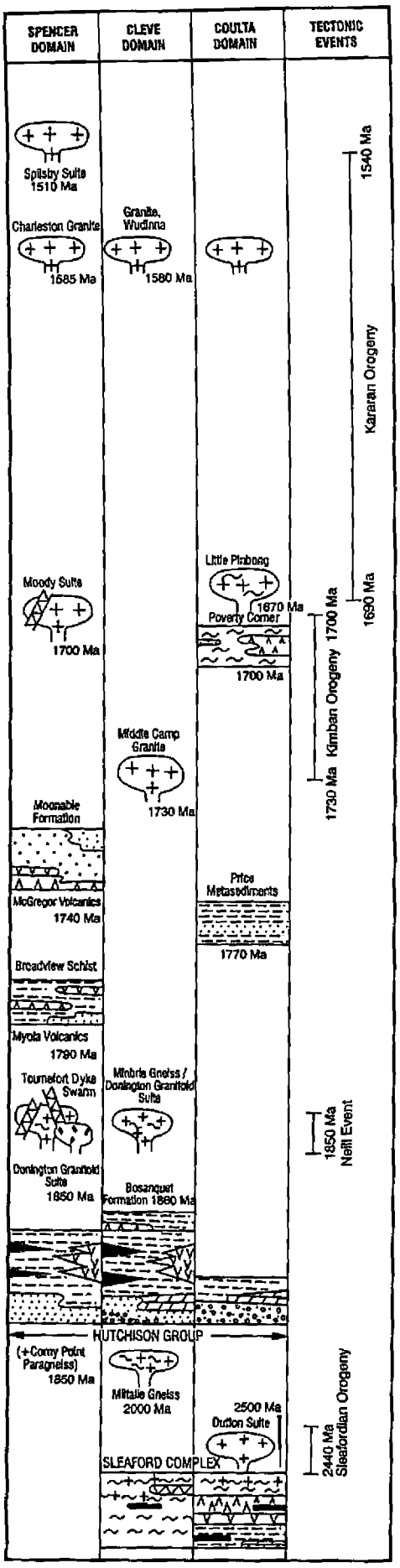
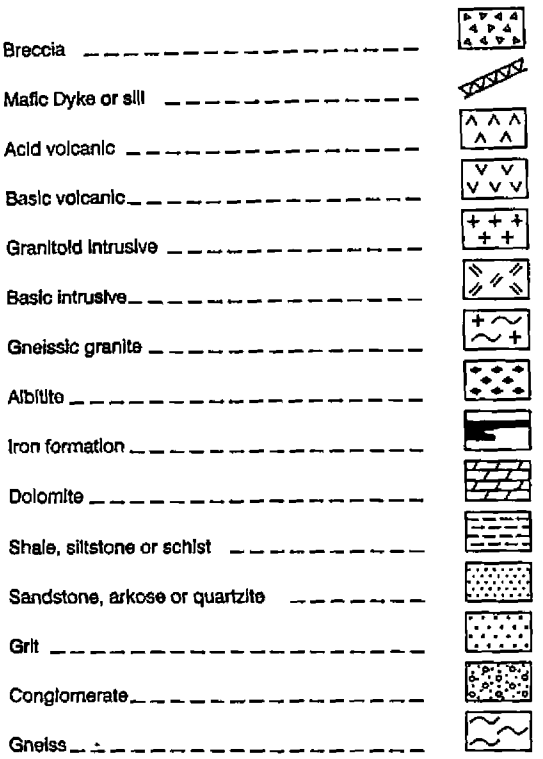


Figure 3: *continued.*



Craton comprise relatively juvenile crust (Ferris, 2001) added to the craton during the early stages (1630 to 1610 Ma) of the Kararan Orogeny. Fig. 1 shows an arcuate zone of known Archaean basement into which major pulses of Palaeo- to Mesoproterozoic igneous suites have been emplaced. Traditional models for crustal growth within the Gawler Craton have suggested growth dominantly through vertical accretion processes (e.g., Donington Granitoid Suite - Schaefer, 1998; Hiltaba Suite - Stewart *et al.*, 1999). In the light of recent information it appears that the tectonic evolution of the Gawler Craton may also be explained through accretion in a series of magmatic arc settings. This model is still at the speculative stage but the authors feel that it is useful to present these ideas to promote discussion and should only be considered as an alternative at this stage. The ideas are currently being investigated further and will be expanded upon in the near future (Ferris *et al.*, 2003; Schwarz *et al.*, 2002).

Recent updates to the interpreted sub-surface geology (Fig. 1) have led to the recognition of an arcuate Archaean core to the Gawler Craton. Various intrusive suites (e.g., Donington Granitoid Suite, Hiltaba Suite) and sedimentary basins (e.g., Hutchison Group Metasediments) form arcuate belts along the margins of the Archaean core suggesting lateral accretion.

The Archaean core contains an arcuate belt of Hutchison Group metasediments on it's eastern margin. This sequence comprises a basal quartzite overlain by a series of clastic and chemical sediments, with interlayered basaltic material. The sequence is interpreted to have been deposited onto a composite Archaean-Proterozoic continent (Sleaford Complex and Miltalie Gneiss), within a passive margin, continental shelf environment, deepening to the east (Daly *et al.*, 1998). We speculate the Hutchison Group was

deformed during the Neill Event at 1850 Ma during the initiation of east dipping subduction and collision between the Gawler and an unknown craton fragment to the east (perhaps basement to the Curnamona Craton; Schwarz *et al.*, 2002).

The Donington Granitoid Suite forms a regionally extensive linear to arcuate belt on the eastern margin of the Gawler Craton, extending from southern Eyre Peninsula, Yorke Peninsula, north to the Olympic Dam region. Previous interpretations for emplacement of the Donington Granitoid Suite have proposed generation within a rift environment via mafic under-plating of the crust (Schaefer, 1998). Several characteristics have been used to support this interpretation; the system has overall chemical and isotopic homogeneity, the suite was emplaced during a relatively restricted time frame, in the order of ~10 Ma and the range of initial ε_{Nd} values are relatively restricted between -2.1 to -4.2 (Schaefer, 1998). However, geochemical and isotopic data from the Donington Granitoid Suite and associated mafic rocks is somewhat equivocal, and do not preclude having formed in an active continental margin or alternatively from partial melting of arc-type under-plates or intrusions. The coincidence of deformation during the Neill Event and emplacement of the Donington Granitoid Suite suggests a convergent tectonic setting at the time of emplacement. Potentially, the Donington Granitoid Suite either, directly marks the existence of a magmatic arc that developed along the margin of the Archaean-Palaeoproterozoic continent, or may have been produced in a back arc environment and then accreted onto the eastern margin of the Gawler Craton during the Kimban Orogeny. Following accretion of the Donington Granitoid Suite, a transition to transpressional convergence resulted in the development of the Kalinjala Mylonite Zone during the Kimban Orogeny between ~1730 and 1700 Ma.

The previously interpreted Ifould Complex, now Ifould Suite (see Kararan Orogeny) was thought to have formed during continental collision within the Fowler Orogenic Zone, producing major crustal thickening, which resulted in the formation of a crustal suite of granites between 1690 and 1670 Ma (Teasdale, 1997). However within the Yarlbrinda Shear Zone, these granites are termed

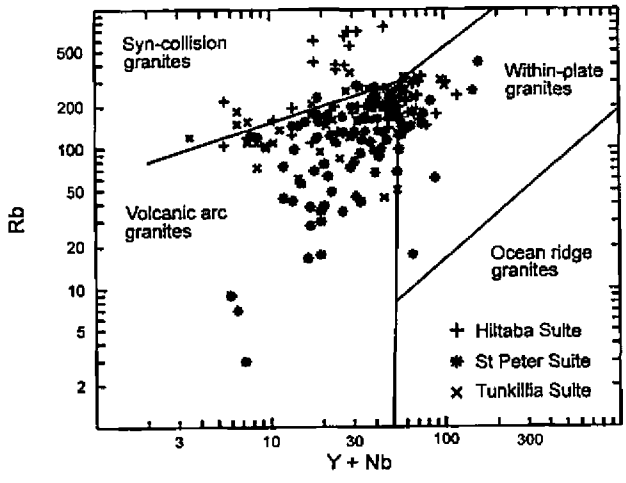


Figure 4: Rb vs (Y + Nb) Pearce *et al.* (1984) plot of Palaeoproterozoic to Mesoproterozoic intrusive suites from the western Gawler Craton.

the Tunkillia Suite and have a geochemical signature consistent with a volcanic arc environment (Fig. 4). The Tunkillia Suite and equivalents are predominantly felsic with minor mafic dykes, but the full extent of this magmatic event is still unknown. At approximately 1630 Ma, the St Peter Suite, a suite of tonalitic to granodioritic rocks, similar in chemistry to Archaean tonalite-trondhjemite-granodiorites, was emplaced within the Nuyts Domain. As with the Tunkillia Suite, the St Peters Suite has a geochemical signature consistent with emplacement in a volcanic arc setting. Alternatively continental extension between ~1640 and 1630 Ma could have resulted in mantle under-plating, producing arc-like chemical signatures in the Tunkillia and St Peters Suites.

Both the Tunkillia Suite and St Peters Suite may have been emplaced in a magmatic arc setting on the south western margin of the arcuate Archaean core during north east dipping subduction. This represents a switch from subduction related convergence on the eastern margin of the Craton to the south western margin coincident with the end of the Kimban Orogeny in the east and onset of the Kararan Orogeny in the west.

Traditionally the formation of Hiltaba Suite/Gawler Range Volcanic magmatic event (~1595 to 1575) Ma has been attributed to development of a mantle plume within an anorogenic, intracontinental environment (Creaser, 1989, Flint, 1993, Stewart and Foden, 2001). An anorogenic interpretation applied because the Hiltaba Suite was thought to be undeformed and contain relatively homogeneous geochemistry across the Craton. However, evidence from the western Gawler Craton shows the Hiltaba Suite ranges from syn-tectonic, within the Yerda Shear Zone to post-tectonic massive, coarse-grained granite. Therefore at least some of the Hiltaba Suite was contemporaneous with activation of crustal scale shear zones. Sm-Nd isotope analysis shows the Hiltaba Suite changes its isotopic characteristics from the western Gawler Craton, where it records juvenile basement rocks, to the eastern Gawler Craton, where it records Archaean to Palaeoproterozoic crust within the Moonta-Wallaroo and Stuart Shelf regions of the eastern Gawler Craton (Stewart and Foden, 2001).

The eastern Gawler Craton has similarities with the Phanerozoic Coastal belt in Chile. Hitzman (2000) describes iron-oxide copper-gold deposits within the Mesozoic of northern Chile and southern Peru, which were formed within a volcanic arc extensional environment.

A possible tectonic setting at the time of the Hiltaba Suite magmatic event may be related to the previously proposed northeast dipping subduction zone located south west of the Nuyts Domain, which produced a major suite of arc-related magmatism at ~1620 Ma (St Peter Suite). Potentially, a period of subduction related transpression followed resulting in the Hiltaba Suite being emplaced within a back-arc, intra-continental environment. The Hiltaba Suite granites, which form a convex plutonic belt located close the margin of the Nuyts Domain (and St Peters Suite), record positive ε_{Nd} values. This indicates a

juvenile source for the western belt of Hiltaba Suite plutons (Fig. 1), possibly related to basaltic under-plating of the subducting slab, at the base of the crust, during subduction. The eastern belt of Hiltaba Suite plutons, in the Olympic Domain, have ε_{Nd} values suggesting derivation from pre-existing older crust. Back-arc environments are characterised by crustal thinning, which results in increased geothermal gradients. The eastern belt may therefore have formed in an extensional back arc environment. Large linear strike-slip structures (Reynolds, 2000) were active at this time along the eastern part of the Gawler Craton providing fluid pathways for deep seated hydrothermal fluids, as well as allowing surface waters to penetrate below the surface providing a suitable environment for fluid mixing. This is consistent with models for the formation of the Olympic Dam deposit which are discussed in Part II (Skirrow *et al.*, This Volume).

Relationship of the Hiltaba Suite to Copper-Gold Mineralisation and Regional Alteration

The Hiltaba Suite is a variable suite of granitoids, which range in composition from granite (*s.s*) to granodiorite. Texturally the Hiltaba Suite ranges from high-level, sub-volcanic, porphyritic granite, to microgranite, to medium to coarse-grained equigranular granite. The Hiltaba Suite shows considerable geochemical variation both within individual plutons and between plutons. This variability is also reflected in the Sm-Nd isotopes which show a range of values from ε_{Nd} of -12.67 to 2.78 (Stewart and Foden, 2001). Table 1 outlines the characteristics of selected Hiltaba Suite granites on the Gawler Craton.

The Hiltaba Suite is typically K-feldspar dominant and is pink to red in colour due to disseminated hematite in feldspar. The suite is dominantly felsic and SiO_2 ranges from 54 to 81 wt %. Drill holes in the Olympic Dam and Andamooka areas intersect mafic lithologies, including hornblende bearing monzodiorite, quartz monzonite and quartz syenite (Creaser, 1989). The Hiltaba Suite is dominantly oxidised (Fig. 5). Major elements show calc alkaline trends with decreasing Al_2O_3, Fe_2O_3, TiO_2, MgO, CaO and P_2O_5 with increasing SiO_2. K_2O and Na_2O show a general increase with increasing SiO_2. The Hiltaba Suite is enriched in Rb, Y, Zr, Th and U and depleted in Ba and Sr. Stewart and Foden (2001) report increasing Rb/Ba ratios with increasing SiO_2, indicating fractionation of K-feldspar. Chondrite normalised REE plots for the Hiltaba Suite show similar REE patterns; steep LREE patterns, significant negative Eu anomalies and relatively flat HREE patterns (Ferris, 2001; Stewart and Foden, 2001). The Hiltaba Suite plots predominantly within the A-type field on Ga/Al plots (Whalen *et al.*, 1987).

The age of the Hiltaba Suite ranges from ~1600 to 1575 Ma, based on U-Pb zircon analysis. Rb-Sr analysis show ages which are approximately 100 m.y. too young, probably reflecting resetting of the isotopic system during later thermal perturbation (Table 1). Fig. 1 shows the interpreted sub-surface extent of the Hiltaba Suite on the Gawler Craton, which appears to form clusters of discrete igneous centres and ongoing collaborative research between PIRSA and Geoscience Australia (formerly AGSO) is aimed at determining the geochemical characteristics and mineral potential of these discrete centres. Emplacement of the Roxby Downs Granite and the formation of the Olympic Dam Breccia Complex overlap at ~1590 Ma. U-Pb zircon geochronology constrains the date of the Roxby Downs Granite and surrounding granites between 1592±8 and 1588±4 Ma (Cooper *et al.*, 1988; Creaser, 1989; Creaser and Cooper 1993). The breccia complex was formed at ~1590 Ma, hence its formation and emplacement of the Hiltaba Suite appear intimately linked. The source of metals at Olympic Dam remains a point of contention. Johnson and Cross (1991) report Sm-Nd isotope data which show a primitive Nd component, suggesting that the mantle was the source of ore fluids. Alternatively, Knutson *et al.* (1992) report that Mesoproterozoic basalts are a possible source of copper for the Olympic Domain deposits.

Budd *et al.* (1998) divided the Hiltaba Suite into two distinct suites, the "Olympic Dam and Kokatha suites" and reported a broad spatial correlation of these types of granites with different mineralising systems. The Olympic Dam Suite are strongly fractionated and oxidised, and are related to copper-gold systems on the eastern Gawler Craton. The Kokatha suite are less fractionated and are generally related to gold, silver and base metal systems (Budd *et al.*, 1998). Fig. 5 shows that the Hiltaba Suite within the Moonta-Wallaroo and Olympic Dam areas, together with granites from the Williams and Naraku Batholiths (of the Mount Isa Inlier, which are linked to copper-gold mineralisation at Ernest Henry and Osborne), are oxidised to strongly oxidised. Only a small number of Hiltaba Suite samples plot within the reduced fields. Wyborn (1992, 1998) reports the Hiltaba Suite is geochemically similar to the Williams and Naraku Batholiths. Wyborn (2001) termed these granites the "Hiltaba Association" and suggests a spatial relationship between these granites and copper-gold mineralisation.

The role of magmatic fluids in the genesis of iron-oxide copper-gold deposits remains ambiguous, with many researchers favouring an orthomagmatic origin, while

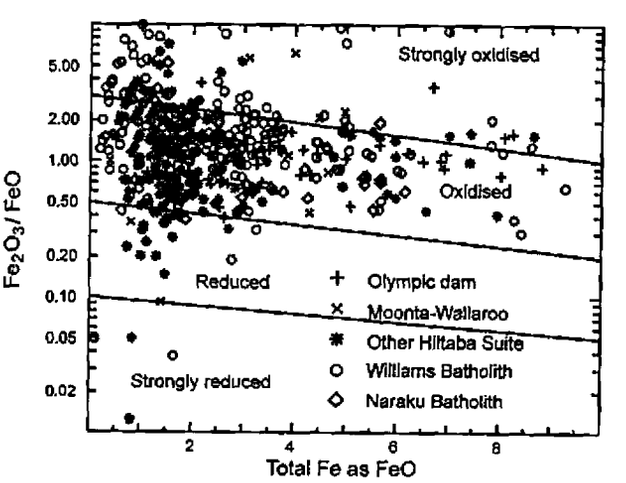


Figure 5: Redox plot of Champion and Heinemann (1994) showing Hiltaba Suite and granites from the Williams and Naraku Batholiths from the Mount Isa Inlier.

Table 1: Summary characteristics of the Hiltaba Suite granite from the Gawler Craton (Flint, 1993).

Unit	Lithology	Petrography	Relationships and extent	Geochronology
Charleston Granite	Homogeneous, coarse-grained, megacrystic granite.	Large K-feldspar phenocrysts (30-40%), greenish plagioclase (10-15%), quartz and biotite. Zoned feldspar phenocrysts.	Intrudes McGregor Volcanics and Corunna Conglomerate as indicated By local hornfelsing, epidotisation and quartz-epidote veins within 10 m of the granite contact (Miles, 1954; Smale, 1966; Giles *et al.*, 1980). Forms discrete pluton 20x15 km.	**~1576 Ma** (U-Pb zircon: Fanning *et al.*,1988); **1585±5 Ma** (U-Pb zircon: Creaser and Fanning, in press); **1556±30 Ma** (Rb-Sr:Crompston *et al.*, 1986); **1445±39 Ma** (Rb-Sr; Webb *et al.*,1986); **1568, 1567, 1532 Ma** (K-Ar Biotite: Webb *et al.*, 1986).
Granite, 'Hiltaba'	Homogenous, coarse-grained, red granite.	Dominantly graphic quartz and perthitic orthoclase, lesser plagioclase and chloritised biotite. Fluorite is a common accessory. Feldspars are intensely reddened.	Intrudes Yardea Dacite (Blissett and Thomson, 1978). Forms several Plutons in a zone 70x20 km.	**1514^{+32}_{-24} Ma** (U-Pb zircon: Cooper *et al.* 1985); **1581±16 Ma** (Reinterpretation: Creaser and Cooper, 1993); **1478±38 Ma** (Rb-Sr: Webb *et al.*, 1986); **1508,1361 Ma** (K-Ar biotite: Webb *et al.*, 1982).
Granite, 'Kokatha'	Leucocratic pink, medium to coarse-grained granite to adamellite, including some porphyritic varieties.	Dominantly graphic quartz and K-feldspar; also plagioclase, interstitial hornblende and biotite. Accessory minerals include apatite and fluorite	Intrudes Chitanilga Volcanic Complex, forming several plutons in A zona 30x10 km. Also includes granitic exposures in an area 70x30 km west of Lake Everard.	**1478±38 Ma** (Rb-Sr isochron pooled with granite at 'Hiltaba': Webb *et al.*, 1986).
Wirrda Subsuite, OlympicDam (Creaser, 1989)	Bimodal suite of medium-grained and porphyritic rock types including quartz monzo-diorite, quartz monzonite, syenite and aplite (eg. drill-holes PD 3, RD 80, 87, 161, WRD 3, BLD 2).	Mafic varieties consist mainly of plagioclase with lesser quartz and K-feldspar; mafic minerals include augite, hornblende and biotite. Apatite and zircon are common accessories. Granites are leucocratic, though containing hornblende, biotite and magnetite. Fluorite is common.	Dykes of porphyritic granite intrude acid volcanics at acropolis prospect.	**1613^{+20}_{-19}, 1606±7, 1590^{+6}_{-4} Ma**, (U-Pb zircon: Mortimer, Cooper *et al.*, 1988); **1598±2, 1590^{+6}_{-4}, 1593±4, 1593±2 Ma** (U-Pb zircon: Creaser & Cooper, 1993).
Roxby Downs Granite	Coarse-grained (<20 mm) equigranular to porphyritic Syenogranite.	Modal composition of 50% alkali feldspar, 20-25% quartz, 20-25% plagioclase, 5-8% amphibole and biotite (halogen-rich <2wt% F, 2wt% Cl). Accessory magnetite, fluorite, sphene, uranothorite.	Hosts the mineralised breccias of the Olympic Dam Cu-U-Au deposit.	**1588±4 Ma**(U-Pb zircon: Creaser and Cooper, 1993).
White Dam Subsuite, Andamooka (Creaser, 1989)	Variety of rock types including quartz monzodiorite, quartz monzonite and aplite (eg. drillholes OFD 1-3).		Restricted to the subsurface.	**1590±10 Ma** (U-Pb zircon: Creaser and Cooper, 1993).
Granitoids Kingoonya	Bimodal suite of fine to coarse-grained and porphyritic Granite (high SiO_2) and syenite to granodiorite (low SiO_2).	Granites consist of perthitic orthoclase and microcline phenocrysts in a matrix of graphic quartz and K-feldspar,plagioclase, and minor biotite and muscovite. Syenite contains orthoclase and hornblende.	Microgranite intrudes Tarcoola Formation, forming abundant quartz-muscovite ± fluorite ± topaz greisen. Restricted to the Lake Labyrinth area (Cowley and Martin, 1990).	
Balta Granite	Even-grained and porphyritic granite and adamellite, brick-red granite, hybrid granite and (?) diorite.	Brick-red granite characterised by high (~60%) microcline content. Hybrid granite contains hornblende and scapolite, feldspar megacrysts and quartz-feldspar xenoliths. Diorite mineralogy includes olivine, hypersthene, clinopyroxene and calcic plagioclase.	Intrudes Palaeoproterozoic Granulites and gneisses, forming several small, discrete plutons; Mt Woods Inlier.	**~1550-1450 Ma** (Rb-Sr: Ambrose and Flint, 1981b).
Granite, Tarcoola	Coarse-grained (~5 mm) red granite and adamellite in Tarcoola DDH 1-3.	Microcline is fresh, plagioclase is heavily sericitised, quartz exhibits strong undulose extinction and sutured grain boundaries. High chlorite content (10-15%). Accessories include apatite, fluorite and sulphides.	Pluton 20x5 km intrudes Tarcoola Formation just west of Tarcoola. Relationships to numerous other Hiltaba Suite granites in the region are not known (Daly, 1985).	**1474±45 Ma** (Rb-Sr: Webb *et al.*, 1986).
Granite, Kychering Rockhole	Medium-grained pinkish granite, adamellite and granodiorite.	Granodiorite is plagioclase-rich (<50%) with high muscovite (<5%) and absence of biotite. Adamellite & granite contain perthitic microcline, quartz, plagioclase and minor biotite.	Discrete plutons at least 10x5 km intrude Tarcoola Formation near Kychering Rockhole (Daly, 1985).	**1475±45 Ma** (Rb-Sr: Webb *et al.*, 1986).
Calca Granite	Distinctive, red, coarse-grained granite.	Very high content of perthitic orthoclase and microcline (50-75%) and low plagioclase (<5%). Characterised by abundant, very fine-grained haematite.	Relationship to Blue Range Beds not exposed. Occurs on Flinders and Waldegrave Islands in the Investigator Group, and in the Calca-Colley Hill area (50x20 km).	**1456±26 Ma** (Rb-Sr: Webb *et al.*, 1986).
Granites, Minnipa, Wudinna, Buckleboo	Pinkish, coarse-grained granite-adamellite, minor porphyritic varieties and minor aplite dykes.	Perthitic K-feldspar crystals range up to 20 mm, with interstitial plagioclase, quartz and biotite. Pyrite is a common accessory.	Occurs as inselbergs and discrete plutons on central Eyre Peninsula and intrude GRV.	**1519±87 Ma**, Wudinna 1 (Rb-Sr: Webb *et al.*, 1986); **1477±34 Ma**, Minnipa and Buckleboo (Rb-Sr: Webb *et al.*, 1986).
Granite, 'Cultana'	Red, coarse grained granite.	Dominantly feldspar (~60-70%) and quartz (~30%), but with tourmaline common (<5%).	Considered intrusive into porphyritic rhyolite along western side of Cultana Inlier.	Disturbed U-Pb systematics.
Tickera Granite	Coarse-grained granite-adamellite.	Equal proportions of microcline, Plagioclase and quartz, with minor Biotite and opaques.	Intrudes Doora Schist. Exposed along coast north of Point Riley.	**1215±554 Ma**, IR=0.7357 (Rb-Sr: Webb *et al.*, 1986).
Adamellite, Moonta	Coarse-grained granite, adamellite and granodiorite.	Varying proportions of quartz, K-feldspar and plagioclase. High chloritised biotite content (7-10%) opaques (2-3%), and accessory apatite and fluorite.	Occurs at least in drillholes WMC DDH 33, 57, 103, 147, 221; full lateral extent unknown. Equivalents include Arthurton Granite.	**1583±7 Ma** (U-Pb zircon from WMC DDH 33: Creaser and Cooper, 1993); **1282±179 Ma** (Rb-Sr: Webb *et al.*, 1986); **1251, 1505 Ma** (K-Ar biotite: Webb *et al.*, 1986).

others report the dominant factor is basinal brines, particularly saline evaporitic basins, or a combination of the two. The orthomagmatic origin for hydrothermal fluids and derivation of some or all of the metals from granites is favoured by Hitzman *et al.* (1992), Pollard *et al.* (1997, 1998), Williams (1998), Menard (1995) and Lindblom *et al.* (1996), or from mafic magmas with alkaline affinity (Johnson and Cross, 1991). Hildebrande (1986) reports that iron oxide copper-gold districts in Scandinavia, and the Great Bear Magmatic Zone in northwest Canada, are closely related to mafic to intermediate intrusions. Menard (1995) reports that iron-oxide copper-gold deposits within the Chilean Iron Belt are closely associated with intermediate intrusives emplaced within an extensional (island arc) setting. Hitzman *et al.* (1992) described iron-oxide copper-gold deposits as expressions of deeper seated, volatile rich igneous hydrothermal systems, with numerous stable isotope studies suggesting a dominantly magmatic source for the hydrothermal fluidsand sulphur.

Barton and Johnson (2000) report the variability of iron-oxide copper-gold deposits cannot be produced by a single model. Table 1 in Barton and Johnson (2000) describes the geological characteristics of a range of deposits from interpreted fluid sources including magmatic, coeval brines, older brines/evaporites and hybrid systems. All groups are believed to source fluids and metals from igneous rocks.

Iron-oxide copper-gold deposits tend to occur within districts (ie: eastern Gawler Craton, Cloncurry, Chilean Iron Belt), and these districts also contain suites of 'late' oxidised granites (eg: Hiltaba Suite on the Gawler Craton and the Williams and Naraku Batholiths at Cloncurry). Davidson and Large (1994) report that major copper-gold mineralisation within Australian copper-gold provinces are correlated with emplacement of regional granites (Fig. 6). The Olympic Dam copper-uranium-gold-silver deposit is hosted within the Roxby Downs Granite, a member of the Hiltaba Suite, but other deposits within the Olympic Domain are hosted in older granitoids and volcanic units. Reynolds (2000) reports that the formation of the Olympic Dam deposit is related to the Hiltaba Suite magmatic event, with the granites and ultramafic and mafic magma, supplying both the hydrothermal fluids and metals. Sulphur isotopes and fluid inclusion data supports a magmatic source (Reynolds, 2000). However, similar granites are located within areas of no iron-oxide copper-gold mineralisation/ alteration. These oxidised suites of granite do not appear to represent the dominant, controlling factor on the location of iron-oxide copper-gold provinces. On the Gawler Craton, the Hiltaba Suite is widespread (Figs. 2 and 3), but iron-oxide copper-gold deposits are dominantly located along the eastern part of the Craton. This may reflect deeper crustal fractures, focussing mafic and ultramafic mantle fluids. The more mafic Hiltaba Suite at Olympic Dam indicates a greater mantle component.

Pollard (2000) reports that meta-igneous rocks, which are the source of many granitoids linked to iron-oxide copper-gold deposits, require high temperatures to initiate partial melting. The higher temperatures increase the solubilities of refractory minerals including iron-titanium phases and zircon, hence leading to enrichment of titanium,

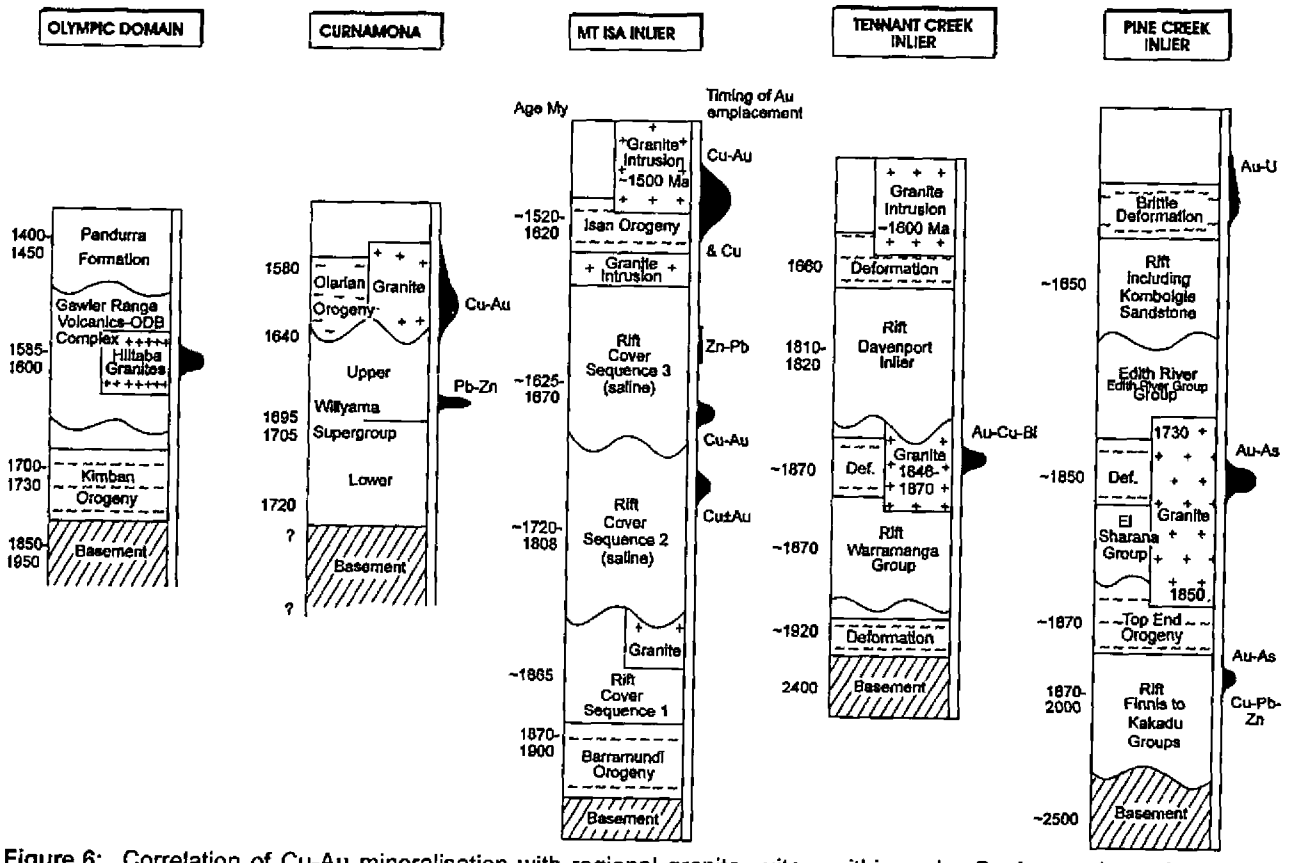


Figure 6: Correlation of Cu-Au mineralisation with regional granite suites, within major Cu-Au provinces in Australia (after Davidson and Large, 1994; Skirrow *et al.*, 2000; Teale and Fanning, 2000).

zirconium, uranium and REE (Pollard, 2000). The different mineralising systems reported on the eastern Gawler Craton may reflect a difference in source rocks, or even more importantly, variations in depth of formation and degree of fractionation.

References

Afmeco Pty Ltd., 1982 - Lake Tallacootra South. Progress reports from 20/5/80 to 25/1/82; *Department of Primary Industries and Resources, South Australia*, Open file Envelope, 03871

Ambrose, G.J. and Flint, R.B., 1981 - BILLA KALINA, South Australia, Sheet SH53-7; *Geological Survey of South Australia*, 1:250 000 Series – Explanatory Notes.

Aulron Energy, 2000 - Announcement on Website 27 July 2000 - Aulron confirms 30 years inferred resources for SASE project, Hawk's Nest, South Australia; www.auironenergy.com.au/asxreleases/asxreleases.asp

Barton, M.D. and Johnson, D.A., 2000 - Alternative brine sources for Fe-Oxide (-Cu-Au) systems: Implications for hydrothermal alteration and metals; *in* Porter, T.M. (ed.) Hydrothermal Iron Oxide Copper-Gold and Related Deposits: A Global Perspective, *PGC Publishing, Adelaide*, v. 1, pp. 43-60.

Betts, P., 1992 - Structure and tectonic history of the Mount Woods Inlier utilising aeromagnetic data and rock property analysis; Unpublished B.Sc (Honours) thesis, *Monash University, Melbourne.*

Blissett, A.H., 1980 - CHILDARA, South Australia, sheet SH53-14; *Geological Survey of South Australia*, 1:250 000 Series - Explanatory Notes.

Blissett, A. H. and Thomson, B.P., 1978 - SADME Gawler Ranges Excursion; *South Australia, Department of Mines and Energy*, Report Book, 78/130.

Budd, A.R., Wyborn, L.A.I. and Bastrakova, I.V., 1998 - Exploration significance of the Hiltaba Suite, South Australia; *Australian Geological Survey Organisation*, Research Newsletter, 29, pp. 1-4.

Champion, D.C. and Heinemann, M.A., 1994 - Igneous rocks of North Queensland: 1:50 000 map and explanatory notes; *Australian Geological Survey Organisation*, Record, 1994/11, 82p.

Conor, C.H.H., 1995 - Moonta-Wallaroo region: an interpretation of the geology of the Maitland and Wallaroo 1:100 000 sheet areas; *Mines and Energy, South Australia*. Open file Envelope 8886.

Cooper, J.A., Mortimer, G.E., Rosier, C.M. and Upphill, R.K., 1985 - Gawler Range magmatism - further isotopic age data; *Australian Journal of Earth Science*, v. 32; pp. 115-123.

Cowley, W.M., 1991 - The Pandurra Formation; *South Australia, Department of Mines and Energy*, Report Book , 91/7.

Creaser, R.A., 1989 - The geology and petrology of middle Proterozoic felsic magmatism of the Stuart Shelf, South Australia; Unpublished Ph.D. thesis, *Latrobe University, Melbourne.*

Creaser, R.A., 1995 - Neodymium isotopic constraints for the origin of Mesoproterozoic felsic magmatism, Gawler Craton, South Australia; *Canadian Journal of Earth Science*, v. 32, pp. 460-471.

Creaser, R.A. and Cooper, J.A., 1993 - U-Pb geochronology of middle Proterozoic felsic magmatism surrounding the Olympic Dam Cu-U-Au-Ag and Moonta Cu-Au-Ag deposits, South Australia; *Economic Geology*, v. 88, pp. 186-197.

Daly, S.J., 1993 - Mineralisation associated with the Gawler Range Volcanics and Hiltaba Suite granitoids: Earea Dam Goldfield Glenloth Goldfield and Tarcoola Goldfield; *in* Drexel, J.E, Preiss, W.Y. and Parker, A.J., (eds.), The Geology of South Australia - The Precambrian, *Geological Survey of South Australia*, Bulletin 54, v. 1.

Daly, S.J., Fairclough, M.C., Fanning, C.M. and Rankin, L.R., 1995 - Tectonic evolution of the western Gawler Craton: A Palaeoproterozoic collision zone and likely plate margin; *Geological Society of Australia*, Abstracts, v. 40, pp. 35-36.

Daly, S.J., Fanning, C.M. and Fairclough, M.C. (1998) - Tectonic evolution and implications for exploration potential of the western Gawler Craton; *AGSO Journal of Australian Geology and Geophysics*, v. 17, pp. 145-168.

Davidson, G.J. and Large, R.R., 1994 - Gold metallogeny and the copper-gold association of the Australian Proterozoic; *Mineralium Deposita*, v. 29, pp. 208-223.

Davies, M. B., 2000 - Iron ore in South Australia; *Primary Industries and Resources, South Australia*, Commodity Review 8.

Dominion Mining Ltd., 2002 - Challenger Gold Project, Geology and Resource; *Dominion Website*, www.dml.com.au

Drexel, J.F., Preiss, W.V. and Parker, A.J., (eds.), 1993 - The geology of South Australia - The Precambrian; *Geological Survey of South Australia*, Bulletin 54, v. 1.

Fairclough, M.C. and Daly, S.J., 1995 - Interpreted basement geology for the northern Gawler Craton; *South Australia, Department of Mines and Energy*, Digital Data Set (unpublished).

Fanning, C.M., 1997 - Geochronological Synthesis of South Australia, Part II: The Gawler Craton; Unpublished PRISE report. *Research School of Earth Sciences, Australian National University.*

Fanning, C.M., Daly, S.J., Bennett, V.B., Menot, R.P., Peucat, J.J., Oliver, R.L. and Monnier, O., 1995 - The "Mawson Continent": Once contiguous Archaean to Proterozoic crust in the east Antarctic Shield and Gawler Craton, Australia; *in* Ricci, C.A. (ed.), The Antarctic Region: Geological Evolution and Processes, Proceedings of the VII SCAR/IUGS International Symposium on Antarctic Earth Sciences, Siena, Italy, *Terra Antartica Publication*, Abstracts, p. 124.

Fanning, C.M., Flint, R.B., Parker, A.J., Ludwig, K.R. and Blissett, A.H., 1988 - Refined Proterozoic evolution of the Gawler Craton, South Australia, through U-Pb zircon geochronology; *Precambrian Research*, v. 40/41, pp. 363-386.

Fanning, C.M., Flint, R.B. and Preiss, W.V., 1983 - Geochronolgy of the Pandurra Formation; *Geological Survey of South Australia*, Quarterly Geological Notes, v. 88, pp. 11-16.

Ferris, G.M., 2001 - The geology and geochemistry of granitoids in the CHILDARA region, western Gawler Craton, South Australia: implications for the Proterozoic tectonic history of the western Gawler Craton and the development of lode-style gold mineralisation at Tunkillia; Unpublished M.Sc. Thesis, *University of Tasmania, Hobart.*

Ferris, G.M., Hand, M. and Barovich, K., 2003 - Putting the Hiltaba Suite into a tectonic context; *in* Preiss, W.V., (ed.), Geoscience 2002: Expanding Horizons, 16th Australian Geological Convention, Adelaide, *Geological Society of Australia*, Abstracts, v. 67, p. 63.

Finlay, J., 1993 - Structural interpretation in the Mount Woods Inlier; Unpublished B.Sc (Honours) thesis, *Monash University, Melbourne.*

Flint, R.B., 1993 - Mesoproterozoic; *in* Drexel, J.E, Preiss, W.Y. and Parker, A.J., (eds.), The Geology of South Australia - The Precambrian, *Geological Survey of South Australia*, Bulletin 54, v. 1.

Glenn, R.A., Laing, W.P., Parker, A.J. and Rutland, W.R., 1977 - Tectonic relationships between the Proterozoic Gawler and Willyama orogenic domains; *Journal of the Geological Society of Australia*, v. 24, pp. 125-150.

Hand, M., Bendall, B.R. and Sandiford, M., 1995 - Metamorphic evidence for Palaeoproterozoic oblique convergence in the eastern Gawler Craton; *Geological Society of Australia*, Abstracts v. 40, p. 59.

Haynes, D.W., 2000 - Iron oxide copper(-gold) deposits: Their position in the ore deposit spectrum and modes of origin; *in* Porter, T.M., (ed.), Hydrothermal Iron Oxide Copper-Gold and Related Deposits: A Global Perspective, *PGC Publishing, Adelaide*, v. 1, pp 71-90.

Haynes, D.W., Cross, K.C., Bills, R.T. and Reed, M.H., 1995 - Olympic Dam ore genesis: A fluid-mixing model; *Economic Geology*, v. 90, pp. 281-307.

Hildebrand, R.S., 1986 - Kiruna-type deposits: Their origin and relationship to intermediate subvolcanic plutons in the Great Bear magmatic zone, NW Canada; *Economic Geology*, v. 81, pp. 640-659.

Hitzman, M.W., 2000 - Iron-Oxide-Cu-Au Deposits: What, where, when and why ?; *in* Porter, T.M., (ed.), Hydrothermal Iron Oxide Copper-Gold and Related Deposits: A Global Perspective, *PGC Publishing, Adelaide*, v. 1, pp. 9-25.

Hitzman, M.W., Oreskes, N. and Einaudi, M.T., 1992 - Geological characteristics and tectonic setting of Proterozoic iron oxide (Cu-U-Au-REE) deposits; *Precambrian Research*, v. 58, pp. 241-287.

Hoek, J.D. and Schaefer, B.R., 1998 - The Palaeoproterozoic Kimban Mobile Belt, Eyre Peninsula: Timing and significance of felsic and mafic magmatism and deformation; *Australian Journal of Earth Sciences*, v. 45, pp. 305-313.

Huston, D.L., Bolger, C. and Cozens, G., 1993 - A comparison of mineral deposits at Gecko and White Devil deposits: implications for ore genesis in the Tenant Creek district, Northern Territory, Australia; *Economic Geology*, v. 88, pp. 1198-1225.

Johnson, M.C. and Cross, K.C., 1991 - Geochronological and Sm-Nd isotopic constraints on the genesis of the Olympic Dam Cu-U-Au-Ag deposit, South Australia; *in* Pagel, M. and Leroy, J.L., (eds.), Source, Transport and Deposition of Metals, *Balkema, Rotterdam*, pp.395-400.

Knutson, J., Donnelly, T.H., Eadington, P.J. and Tonkin, D.G., 1992 - Hydrothermal alteration of Middle Proterozoic basalts, Stuart Shelf, South Australia - a possible source for Cu mineralisation; *Economic Geology*, v. 87, pp. 1054-1077.

Loiselle, M.C. and Wones, D.R., 1979 - Characteristics and origin of anorogenic granites; *Geological Society of America*, Abstracts with Programs, v. 11, p. 468.

Menard, J.J., 1995 - Relationship between altered pyroxene diorite and the magnetite mineralization in the Chilean Iron Belt, with emphasis on the El Algarrobo iron deposits (Atacama region, Chile); *Mineralium Deposita*, v. 30, pp. 268-274.

Minotaur Resources Ltd., 2001 - Announcement, 27 December 2001, Prominent Hill - Drilling Update.

Minotaur Resources Ltd., 2002 - Announcement 29 January 2002 Prominent Hill - Drilling Update.

Morris, B.J. and Hough, J.K., 1997 - South Australia Steel and Energy Project, Peculiar Knob Prospect; *South Australia, Department of Mines and Energy Resources*, Report Book, 97/9.

Morrow, N. and McPhie J., 2000 - Mingled silicic lavas in the Mesoproterozoic Gawler Range Volcanics, South Australia; *Journal of Volcanology and Geothermal Research*, v. 96, pp. 1-13.

Mortimer, G.E., Cooper, J.A. and Oliver, R.L., 1988 - The geochemical evolution of Proterozoic granitoids near Port Lincoln in the Gawler Orogenic Domain of South Australia; *Precambrian Research*, v. 40/41, pp. 387-406.

Oliver, R.L. and Fanning, C.M., 1997 - Australia and Antarctica: precise correlation of Palaeoproterozoic terrains; *in* Ricci, C.A. (ed.), The Antarctic Region: Geological Evolution and Processes, VII SCAR/ IUGS International Symposium on Antarctic Earth Sciences, Siena, Italy, *Terra Antartica Publication*, Proceedings, v. 4, pp. 163-172.

Parker, A.J., 1983 - WHYALLA map sheet; *South Australia, Geological Survey*, Geological Atlas 1:250 000 Series, sheet SI53-8.

Parker, A.J., 1990 - Gawler Craton and Stuart Shelf - regional geology and mineralisation; *in* Hughes, F.E., (ed.), Geology of the Mineral Deposits of Australia and Papua New Guinea; *Australasian Institute of Mining and Metallurgy, Melbourne*, Monograph 14, v. 2, pp. 999-1008.

Parker, A.J., 1993 - Palaeoproterozoic; *in* Drexel, J.E, Preiss, W.Y. and Parker, A.J., (eds.), The Geology of South Australia - The Precambrian, *Geological Survey of South Australia*, Bulletin 54, v. 1. pp. 51-105.

Parker, A.J., Fanning, C.M., Flint, R.B., Martin, A.R. and Rankin, L.R., 1988 - Archaean-Early Proterozoic granitoids, metasediments and mylonites of southern Eyre Peninsula, South Australia; *Geological Society of Australia. Specialist Group in Tectonics and Structural Geology*, Field Guide Series, v. 2.

Parker, A.J. and Lemon, N.M., 1982 - Reconstruction of the Palaeoproterozoic stratigraphy of the Gawler Craton, South Australia; *Journal of the Geological Society of Australia*, v. 29, pp. 221-238.

Parker, A.J. and Fanning, C.M., 1997 - WHYALLA, South Australia, sheet SI 53-8; *South Australia, Geological Survey*, 1:250 000 Series-Explanatory Notes.

Pearce, J.A., Harris, N.B.H. and Tindle, A.G., 1984 - Trace element discrimination diagrams for the tectonic interpretation of granitic rocks; *Journal of Petrology*, v. 25, pp. 956-983.

Polito, P. and Davies, M., 1997 - South Australia Steel and Energy Project, Coober Pedy Iron Ore Investigation, Review of Previous Exploration; *South Australia, Department of Mines and Energy Resources*, Report Book, 97/12.

Pollard, P.J., Blake, K.L. and Dong, G., 1997 - Proterozoic Cu-Au-Co and Pb-Zn-Ag mineralization in the Cloncurry district, eastern Mt Isa Inlier, Australia: Constraints on fluid sources from mineralogical fluid inclusion and stable isotope dataQueensland; *in* Pollard (Compiler), *AMIRA P438 Cloncurry Base Metals and Gold*, Annual Report, section 7, pp. 1-50.

Pollard, P.J., Mark, G. and Mitchell, L.C., 1998 - Geochemistry of post-1540 Ma granites in the Cloncurry district, northwest Queensland; *Economic Geology*, v. 93, pp. 1330-1344.

Pollard, P.J., 2000 - Evidence for a magmatic fluid and metal source for Fe-Oxide Cu-Au mineralisation; *in* Porter, T.M., (ed.), Hydrothermal Iron Oxide Copper-Gold and Related Deposits: A Global Perspective, *PGC Publishing, Adelaide*, v. 1, pp. 27-41.

Reynolds, L.J., 2000 - Geology of the Olympic Dam Cu-U-Au-Ag-REE deposit; *in* Porter, T.M., (ed.), Hydrothermal Iron Oxide Copper-Gold and Related Deposits: A Global Perspective, *PGC Publishing, Adelaide*, v. 1, pp.93-104.

Roach, M.W. and Fanning, C.M., 1994 - Timing of mineralisation at the Menninnie Dam Pb-Zn-Ag deposit, Eyre Peninsula, South Australia; *in* Freeman M.J., (ed.), Geoscience Australia: 1994 and Beyond, *Geological Society of Australia*, Abstracts, v. 37, pp. 376-377.

Rogers, P.A. and Freeman, P.J., 1996 - WARRINA, South Australia, sheet SH53-3; *South Australia, Geological Survey*, 1:250 000 Series-Explanatory Notes.

Rollinson, H., 1993 - Using geochemical data: evaluation, presentation, interpretation; *Longman, Singapore*, 352p.

Schaefer, B.R., 1998 - Insights into Proterozoic tectonics from the southern Eyre Peninsula, South Australia; Unpublished PhD thesis, *The University of Adelaide*.

Schwarz, M.P., 2003 - LINCOLN, South Australia, 1:250 000 map sheet SH 53-11, Second edition; *South Australia, Geological Survey*, Geological Atlas 1:250 000 Series - Explanatory Notes, 1v, Map.

Schwarz, M.P., Hand, M. and Barovich, K, 2002 - A plate margin setting for evolution of the southern Gawler Craton, from detrital zircon and Sm-Nd isotopic data of the Hutchison Group; *in* Preiss, W.V., (ed.), Geoscience 2002: Expanding Horizons, 16th Australian Geological Convention, Adelaide, *Geological Society of Australia*, Abstracts v. 67.

Skirrow, R.G., Ashley, P.M., McNaughton, N.J. and Suzuki, K., 2000 - Time-space framework of Cu-Au (-Mo) and regional alteration systems in the Curnamona Province; *AGSO Record* 2000/10, pp. 83-86.

Skirrow, R.G., Bastrakov, E., Davidson, G., Raymond, O.L. and Heithersay, P. 2002 - The geological framework, distribution and controls of Fe-oxide and related alteration, and Cu-Au mineralisation in the Gawler Craton, South Australia: Part II: alteration and mineralisation; *in* Porter, T.M., (ed.), Hydrothermal Iron Oxide Copper-Gold and Related Deposits: A Global Perspective, *PGC Publishing, Adelaide*, v. 2, pp. 33-47.

Stewart, K.P. and Foden, J., 2001 - Mesoproterozoic granitoids of South Australia: Part 1 - the Gawler Craton; *Department of Geology and Geophysics, University of Adelaide* (unpublished).

Stewart, K., Schaefer, B. and Foden, J., 1999 - Proterozoic magmatism and crustal growth on the Gawler Craton, South Australia; *in* Barbarin, B., (ed.), The Origin of Granites and Related Rocks, Fourth Hutton Symposium, September 20-25, Clermont-Ferrand France, *Documents du BRGM*, Abstracts, p. 191.

Teale, G.S. and Fanning, C.M., 2000 - The timing of Cu-Au mineralisation in the Curnamona Province; *Australian Geological Survey Organistion*, Record 2000/10, pp. 98-99.

Teasdale, J., 1997 - The interpretive geology and tectonothermal evolution of the western Gawler Craton; Unpublished Ph.D thesis, *University of Adelaide*.

Thomson, B.P., 1969 - Precambrian crystalline basement; *in* Parkin, L.W., (ed.), Handbook of South Australian Geology, *South Australia, Geological Survey*, pp. 21-48.

Thomson, B.P., 1970 - A review of the Precambrian and Lower Palaeozoic tectonics of South Australia; *Royal Society of South Australia*, Transactions, v. 94, pp. 193-221.

Thomson, B.P., 1975 - Gawler Craton, S.A.; *in* Knight, C.L. (ed.), Economic Geology of Australia and Papau New Guineau - Metals, *Australasian Institute of Mining and Metallurgy, Melbourne*. Monograph 5, v. 1, pp. 461-466.

Webb, A.W., Thomson, B.P., Blissett, A.H., Daly, S.J., Flint, R.B. and Parker, A.J., 1986 - Geochronology of the Gawler Craton, South Australia; *Australian Journal of Earth Sciences*, v. 33, pp. 119-143.

Whalen, J.B., Currie, K.L. and Chappell, B.W., 1987 - A-type granites: geochemical characteristics, discrimination and petrogenesis; *Contributions to Mineralogy and Petrology*, v. 95, pp. 407-419.

White, A. and Milligan, P.R., 1986 - Geomagnetic variation anomaly on Eyre Peninsula, South Australia; *Exploration Geophysics*, v. 17, pp. 32-34.

Williams, P.J., 1998 - An introduction to the metallogeny of the McArthur River-Mount Isa-Cloncurry minerals province; *Economic Geology*, v. 93, pp. 250-260.

Wilson, C.J.L., (ed.), 1999 - The Great Southern Transect II: a geological section incorporating the Lachlan Fold Belt, Adelaide Fold Belt and Gawler Craton, Halls Gap (Victoria) to Port Lincoln (S.A.); Specialist Group in Tectonics and Structural Geology, *Geological Society of Australia*, Field Guide No. 6,

Wyborn, L.A.I., 1992 - The Williams and Naraku Batholiths, Mt Isa Inlier: An analogue of the Olympic Dam Granites?; *Australian Bureau of Mineral Resources, (BMR)*, Research Newsletter v. 16, pp. 13-16.

Wyborn, L.A.I., 1998 - Younger ca 1500 Ma granites of the Williams and Naraku Batholiths, Cloncurry district, eastern Mt Isa Inlier: geochemistry, origin, metallogenic significance and exploration indicators; *Australian Journal of Earth Sciences*, v. 45, pp. 397-411.

Wyborn, L.A.I., 2001 - Granites and copper gold metallogenesis in the Australia Proterozoic; *in* Budd, A.R., Wyborn, L.A.I. and Bastrakova, I.V. (eds.) The Metallogenic Potential of Australian Proterozoic Granites, *Australian Geological Survey Organisation*, Record 2001/12.

PGC PUBLISHING

Skirrow, R.G., Bastrakov, E., Davidson, G., Raymond, O.L. and Heithersay, P., 2002 - The Geological Framework, Distribution and Controls of Fe-Oxide Cu-Au Mineralisation in the Gawler Craton, South Australia: Part II: Alteration and Mineralisation; *in* Porter, T.M. (Ed.), *Hydrothermal Iron Oxide Copper-Gold & Related Deposits: A Global Perspective*, Volume 2; PGC Publishing, Adelaide, pp 33-47.

THE GEOLOGICAL FRAMEWORK, DISTRIBUTION AND CONTROLS OF Fe-OXIDE Cu-Au MINERALISATION IN THE GAWLER CRATON, SOUTH AUSTRALIA.

PART II - ALTERATION AND MINERALISATION

[1]Roger G. Skirrow, [1]Evgeniy Bastrakov, [2]Garry Davidson, [1]Oliver L. Raymond, and [3]Paul Heithersay

[1]*Geoscience Australia, Minerals Division, Canberra, ACT, Australia*
[2]*University of Tasmania, CODES, Hobart, Tasmania, Australia*
[3]*PIRSA, Office of Minerals and Energy Resources, Adelaide. South Australia, Australia*
Corresponding author: roger.skirrow@ga.gov.au

Abstract - The Olympic Cu-Au province on the eastern margin of the Gawler Craton includes three major regions of hydrothermal alteration and mineralisation: Stuart Shelf basement (including the Olympic Dam Cu-U-Au deposit), Mount Woods Inlier and the Moonta-Wallaroo-Roopena region. Each of these regions contains high-, moderate- and low-temperature Fe-oxide rich alteration, Cu-Au±U mineralisation, and felsic to mafic Mesoproterozoic (~1590 Ma) intrusions of the Hiltaba Suite with or without coeval Gawler Range Volcanics. The three regions are interpreted to represent the 'footprints' of separate crustal-scale thermal anomalies. Three key hydrothermal alteration and ore mineral assemblages are recognised in the metallogenic province: (1) CAM: calcsilicate - alkali feldspar ± magnetite ± Fe-Cu sulphides (generally minor); (2) MB: magnetite-biotite ± Fe-Cu sulphides; and (3) HSCC: hematite-sericite-chlorite-carbonate ± Fe-Cu sulphides ± U, REE minerals. Ore grade Cu-U-Au mineralisation is generally associated with the HSCC assemblage, which is paragenetically later than the CAM and MB assemblages in most deposits and prospects. The crustal level of exposure of the hydrothermal systems may vary significantly between and within the three mineralised regions. The CAM, MB and HSCC assemblages and associated Cu-Au mineralisation represent a possible spectrum of settings from deeper, higher temperature, shear-hosted environments to near-surface, low-temperature breccia and fault settings.

Introduction

The Olympic Cu-Au province is a metallogenic belt in the eastern Gawler Craton (Fig. 1) containing a wide range of Fe, Cu, Au, U, REE, and Ag mineralisation. It includes the giant Olympic Dam Cu-Au-U deposit and the recently discovered Prominent Hill Cu-Au prospect. The province is of early Mesoproterozoic age, and extends over 500 km along the eastern margin of the Gawler Craton from the Mount Woods Inlier in the north, through the basement of the Stuart Shelf, to the Moonta-Wallaroo district in the south. Although its boundaries are not yet well defined, this metallogenic province may transgress several tectonic domains including the Mount Woods Inlier and Olympic Domain (Fig. 1; Ferris *et al.*, this volume). Possible extensions of the Olympic Cu-Au province may include hydrothermal systems of the Peake and Denison Domain, Mabel Creek Ridge (southern Nawa Domain; Fig. 1), and the south-central Gawler Craton. The systems may also transgress the Torrens Hinge Zone (THZ), which has been generally regarded as the eastern boundary of the Gawler Craton (Fig. 1). Adelaidean sedimentary rocks rapidly thicken to the east of the THZ, but most probably overlie Gawler Craton basement.

Much of the Olympic Cu-Au province is covered by flat-lying Neoproterozoic to Recent sedimentary rocks and regolith ranging in thickness from a few tens of metres to a kilometre or more. Outcrop is only present in the Mount Woods Inlier and Moonta-Wallaroo district, albeit sparsely. Consequently, almost all of the geological information available for the Olympic Cu-Au province is derived from drilling and geophysical data.

This review paper presents a first synthesis of hydrothermal alteration and mineralisation types and distribution for the Olympic Cu-Au province. This is followed by summary descriptions of the major hydrothermal systems and mineralisation of the Stuart Shelf basement (Fig. 1), Moonta-Wallaroo district, and Mount Woods Inlier. Finally, ore formation models are reviewed, and a new interpretation of crustal settings of the mineralised hydrothermal systems is presented. The geological framework and stratigraphy of the eastern Gawler Craton are described in the companion paper by Ferris *et al.* (this volume).

In addition to the mineralised systems described here, Fe-oxide related Cu-Au mineralisation is known from a number of other areas of the eastern Gawler Craton. For example,

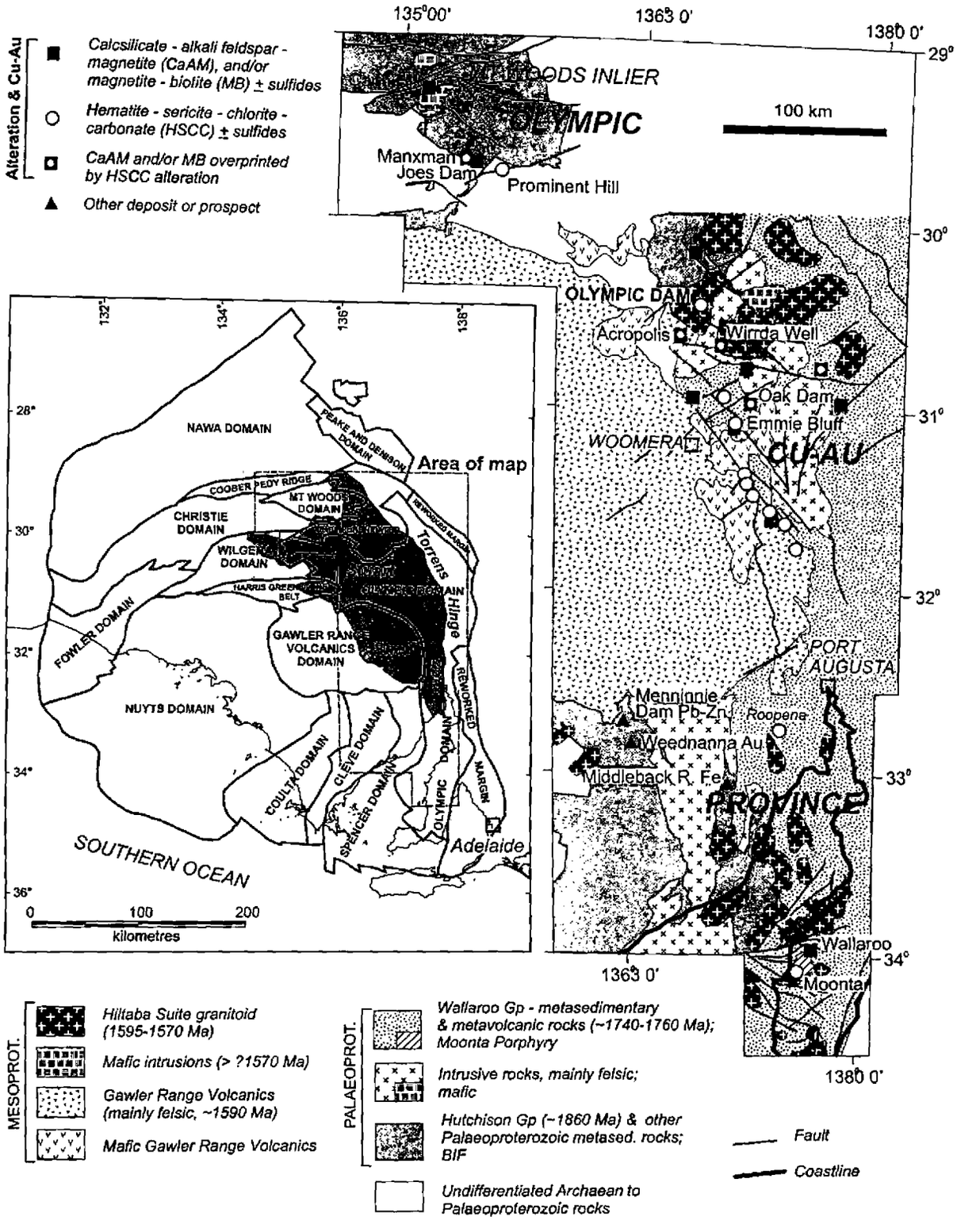


Figure 1: Basement geology interpretation (pre-Pandurra Formation) and alteration in the Olympic Cu-Au province (right), shown in relation to tectonic/magnetic domains of the Gawler Craton (left; from Ferris *et al.*, this volume). Principal Cu-Au±U deposits and prospects are named within the Mount Woods Inlier, basement to the Stuart Shelf, and Moonta-Wallaroo-Roopena regions. The extent of the Mesoproterozoic Pandurra Formation and Neoproterozoic and younger sedimentary rocks of the Stuart Shelf, is shaded in the map at left. Geology map at right compiled from new interpretations of basement to the Stuart Shelf (N. Direen, P. Lyons, L. Jagodzinski, written communication, 2002) and Moonta-Wallaroo district (O. Raymond, written communication, 2002); remaining areas are based on Daly *et al.* (1998).

recent exploration by Helix Resources NL near the Iron Monarch and Iron Prince iron ore deposits in the Palaeoproterozoic Hutchison Group (Fig. 1) has revealed anomalous geochemical values of Cu, Au, Ag, U, Co, Bi (Helix Resources Ltd, 2000). In the Roopena area, to the east of the Middleback Range iron ore deposits, widespread hematitic alteration is accompanied in places by anomalous copper (Drexel *et al.*, 1993). As noted by Budd *et al.* (1998) and Ferris *et al.* (this volume), mineralisation in the central and southern Gawler Craton that is believed to be associated with Hiltaba Suite - Gawler Range Volcanics (GRV) magmatism is dominated by gold (eg., Tarcoola, Tunkillia) and base metals (eg., Menninnie Dam; Fig. 1), and apparently lacks Fe-oxide rich or high-temperature alteration.

Overview of Hydrothermal Alteration in the Olympic Cu-Au Province

The Olympic Cu-Au province contains enormous volumes of hydrothermally altered rock, represented by highly diverse oxide-sulphide-silicate-carbonate mineral assemblages formed under a range of conditions of temperature, pressure, oxidation-reduction and pH. Re-logging of diamond drill core, being undertaken in current studies at Geoscience Australia and PIRSA, has resolved three broad groupings of alteration assemblages, which are now recognised in hydrothermal systems occurring from the Mt Woods Inlier through Stuart Shelf basement to the Moonta-Wallaroo district:

- CAM: calcsilicate (clinopyroxene, amphibole, garnet) - alkali feldspar (K-feldspar, albite) ± magnetite ± Fe-Cu sulphides
- MB: magnetite - biotite ± Fe-Cu sulphides
- HSCC: hematite - sericite - chlorite - carbonate ± Fe-Cu sulphides ± U, REE minerals.

Gow (1996) documented high temperature 'skarn' and lower temperature hematitic assemblages, roughly corresponding to the first and third groups above, in several prospects hosted by basement to the Stuart Shelf. The CAM and MB assemblages were described in the Moonta-Wallaroo district by Conor (1996), whereas Hampton (1997) recorded aspects of all three broad assemblages in the Manxman and Joes Dam prospects in the Mount Woods Inlier. The Olympic Dam deposit is dominated by the HSCC assemblage, although magnetite ± siderite are also present (Reeve *et al.*, 1990) and may be related to the CAM or MB alteration types observed elsewhere in the Olympic Cu-Au province. Not all minerals in each broad assemblage are necessarily present at any particular occurrence, and numerous variations on these themes are present. The assemblages CAM and HSCC may represent end-members of high-temperature and low-temperature hydrothermal conditions, with MB as a transitional style.

Few absolute age constraints exist for hydrothermal activity in the Olympic Cu-Au province. Constraints from U-Pb zircon dating at Olympic Dam indicate that brecciation, ore metal deposition, and Hiltaba Suite-GRV igneous activity occurred at about 1590 Ma (Reeve *et al.*, 1990; Johnson & Cross, 1995). For the Acropolis prospect, southwest of Olympic Dam, Mortimer *et al.* (1988) report U-Pb and Pb-Pb ages of 1601±8 Ma and 1602±7 Ma for apatite in veins containing magnetite.

Multi-stage paragenetic sequences have been identified in individual deposits and prospects, yet, in almost all occurrences one or more of the CAM, MB and HSCC assemblages is recognised. In all cases documented in the present study, the CAM and MB assemblages are paragenetically earlier than the HSCC assemblages. Each of the three assemblages developed in a wide variety of host rocks including metasedimentary, mafic and felsic volcanic, and granitoid rocks, indicating that metasomatism commonly involved major mass transfer between fluid and rock. The products of the most intense metasomatism were only locally or partially controlled by host rock composition, eg., in calcareous sedimentary rocks.

Textural styles of the three alteration assemblages vary widely according to the nature of structural controls, crustal depth, host rock permeability, etc. Open-space fill, brecciation, and vein networks are characteristic of alteration styles in upper crustal environments (eg., Olympic Dam, Reeve *et al.*, 1990; Prominent Hill, Minotaur Resources, 2002), whereas pervasive replacement zones controlled by ductile or brittle-ductile deformation elements are typical of alteration at deeper crustal levels (eg., Moonta-Wallaroo district).

Other minerals that may be present in the CAM assemblages include pyrite, quartz, titanite, scapolite, epidote, and minor pyrrhotite, chalcopyrite, and allanite. Based on drill hole data, CAM assemblages have been documented in the Mt Woods Inlier (Hampton, 1997), the northern Stuart Shelf basement, with the notable exception of the Olympic Dam deposit, and in the Moonta-Wallaroo district. Although calcsilicate-rich metasedimentary rocks are present in the Mt Gunson area, they contain little or no hydrothermal magnetite. These assemblages may reflect isochemical thermal metamorphism of calcareous precursor sedimentary rocks (Gow, 1996). Thus, as at Olympic Dam, hydrothermal alteration found in the Mt Gunson area appears to be dominated by HSCC assemblages.

Magnetite-biotite assemblages are known mainly from the Mt Woods Inlier and Moonta-Wallaroo districts. In the Manxman and Joes Dam prospects, the MB assemblages are interpreted to have overprinted clinopyroxene-scapolite-albite CAM assemblages (Hampton, 1997). One, or more, of pyrite, pyrrhotite, chalcopyrite, molybdenite (Moonta-Wallaroo only), apatite, amphibole, titanite, albite, tourmaline, stilpnomelane, fluorite, and monazite, may be present in MB assemblages. Most Fe-Cu sulphides in Wallaroo-style mineralisation were deposited with the MB assemblage, whereas Hampton (1997) proposed a separate, post-MB chalcopyrite-pyrite ± hematite event at Manxman and Joes Dam.

The HSCC assemblages are the most significant associates of Cu-Au-U mineralisation at the Olympic Dam deposit and Emmie Bluff prospect (Reeve *et al.*, 1990; Gow, 1996).

Based on limited open-file data, this association may also be present at the Wirrda Well and Prominent Hill prospects (Cross, 1993; Minotaur Resources, 2002). The major Fe-Cu sulphides are chalcopyrite, pyrite, and hypogene bornite and chalcocite, although these did not necessarily form synchronously and occur in zoned assemblages at Olympic Dam (chalcopyrite-pyrite and bornite-chalcocite zones; Reeve *et al.*, 1990). Various minerals containing U, LREE, Th, Co, Ni, Pb, and As are found in HSCC assemblages (Reeve *et al.*, 1990; Gow, 1996; Hampton, 1997). Fluorite and barite are locally present in HSCC assemblages, and also form post-sulphide veins (eg., Olympic Dam, Reeve *et al.*, 1990).

Previous studies and recent results from Geoscience Australia and PIRSA studies suggest that occurrences of albite, K-feldspar, sericite, and biotite in hydrothermal alteration assemblages are regionally zoned within the Olympic Cu-Au province. Albitisation is widespread and locally intense in the Moonta-Wallaroo district, and is also present in the Mt Woods Inlier, generally in association with CAM assemblages that may contain scapolite. K-feldspar alteration is known from much of the Olympic Cu-Au province, although it is notably absent from Olympic Dam where sericite is the sole hydrothermal K-silicate. Sericitisation is widely distributed in alteration systems in basement to the Stuart Shelf, but it is uncommon in the Moonta-Wallaroo district where biotite is the dominant layer-silicate alteration mineral. In the Mt Woods Inlier, sericite is not a major constituent at Manxman and Joes Dam, though it is present in the Prominent Hill prospect. The regional distributions of feldspar and K-silicates, along with other minerals in alteration assemblages, provide important constraints on variations in fluid properties and conditions of metasomatism and mineralisation in different parts of the Olympic Cu-Au province. Further documentation and interpretation will be presented elsewhere.

Olympic Dam Cu-Au-U-Ag-REE Deposit

As comprehensive descriptions of the Olympic Dam deposit have been given by Reeve *et al.* (1990), Cross *et al.* (1993), Haynes *et al.* (1995), and Reynolds (2000), only a summary of the broader scale features and paragenesis is given here.

The Olympic Dam deposit (Table 1) was discovered, in 1975, by WMC beneath ~300m of flat lying Stuart Shelf sedimentary rocks, and came into production in 1988. Although the orebody extends more than 3 km in a roughly northwest-southeast direction, it occupies only a small proportion of the Olympic Dam Breccia Complex (ODBC). The ODBC is entirely hosted by the Roxby Downs Granite, a member of the Burgoyne Batholith which, in turn, forms part of the Hiltaba Suite. Brecciated granite forms a zone measuring about 7 km x 5 km in plan, centred on a core of barren hematite-quartz breccias. The core is flanked to the northwest, north and east by diverse and multi-stage hematitic breccias, which are the main host to Cu-U-Au mineralisation. Minor rock types in the ODBC include high-level, ultramafic to felsic intrusives, laminated tuffs, and other volcaniclastics. U-Pb ages of zircons from some of the felsic rocks in the ODBC are indistinguishable from the age of the Roxby Downs Granite and GRV and indicate

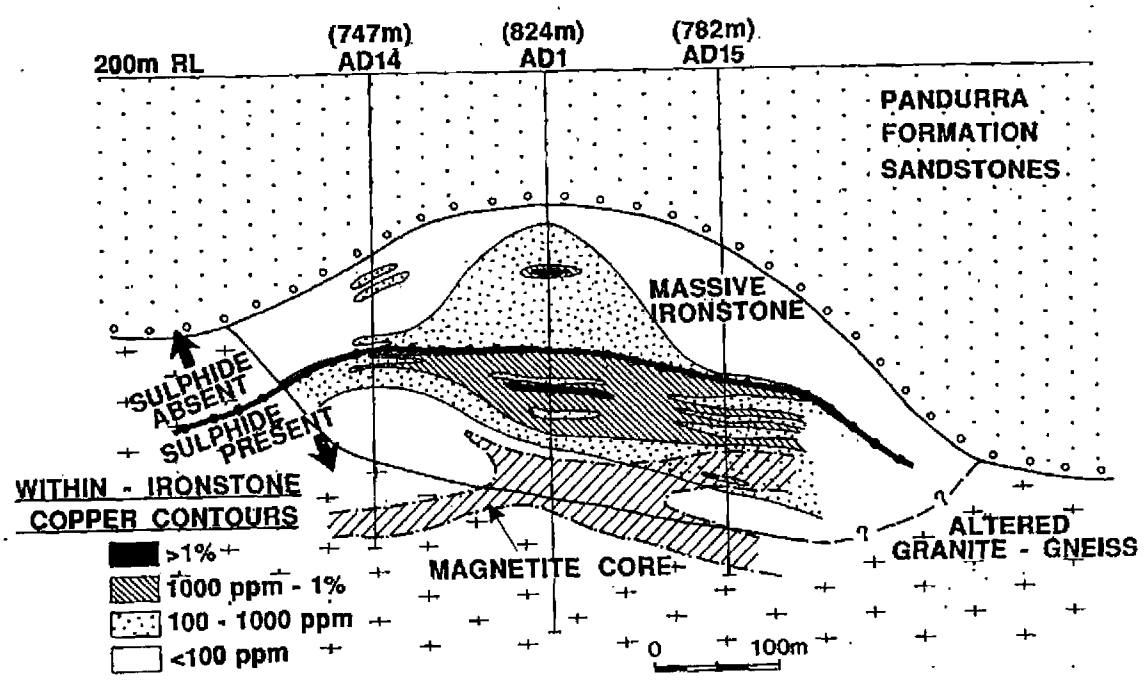


Figure 2: East-west geological cross-section of the Oak Dam East mineralised ironstone, showing the relationship to the Adelaidean unconformity, the location of high susceptibility magnetic zones, and geochemical contours for Cu. Note that the section commences 200 m below surface.

that development of the ODBC was coeval with Hiltaba Suite-GRV igneous activity (Cross *et al.*, 1993; Johnson & Cross, 1995). The volcaniclastic rocks are interpreted to have formed in maar craters by phreatic and phreatomagmatic processes, concurrent with emplacement of ultramafic to felsic dykes (Reeve *et al.*, 1990; Cross *et al.*, 1993; Haynes *et al.*, 1995).

Most of the breccia zones within the ODBC are elongate and have steep dips; north-northwest trends are common along a west-northwest axis. This structure has been interpreted to have developed within a dilational jog related to dextral strike-slip movement on a regional west-northwest trending fault zone (Cross *et al.*, 1993). The hematitic and granitic breccias are the product of a complex interplay between faulting, phreatomagmatic activity, and hydrothermal processes within an eruptive environment.

Three mineral associations are documented (Haynes *et al.*, 1995). The paragenetically earliest (*association 1*) in each of multiple mineralisation episodes comprises magnetite ± hematite, chlorite, sericite, siderite, pyrite, chalcopyrite, and pitchblende. Magnetite is only locally abundant, as this assemblage is in general overprinted by *association 2* containing hematite, sericite, chalcocite, bornite, pitchblende, barite, fluorite, and chlorite. The later stages of mineralisation are characterised by hematite, quartz, and vein barite (*association 3*).

Although overlapping in time and space, there is a gross vertical zonation from *association 3* at higher levels to *association 1* at depth. A key feature mapped across the deposit is the interface between bornite- (± chalcocite) and chalcopyrite-bearing assemblages. This interface undulates at a depth of ~100-300 m below the top of the deposit but locally traces subvertical pinnacle-like extensions, and dips towards the hematite-quartz core. The protruberances in this surface are interpreted to represent upflow zones of fluids responsible for *association 2* (Haynes *et al.*, 1995).

A summary of fluid inclusion and stable isotope data are given in Table 1. Ore deposition mostly occurred at temperatures of 150-250°C (Oreskes & Einaudi, 1992; Cross *et al.*, 1993), and involved a wide range of fluid salinities. Two fluids were present, either during temporally separate stages (Oreskes & Einaudi, 1992) or synchronously (Haynes *et al.*, 1995), as discussed further below.

Wirrda Well and Acropolis Cu-Au Prospects

Brief descriptions of the Wirrda Well Cu-U-Au and Acropolis Cu prospects are given in Paterson (1986), Parker (1990), Cross (1993), and Daly *et al.* (1998). The Acropolis prospect comprises two main zones of iron oxide-rich alteration about 7 km apart. Most of the Cu (-U-Au) mineralisation occurs in the northwestern zone where magnetite, hematite, K-feldspar, quartz, and apatite occur in vein networks and massive replacements within sericitised GRV dacite. The volcanics overlie meta-sedimentary rocks correlated with the Palaeoproterozoic Wandearah Formation, foliated granite, and diorite. A breccia of granite clasts in a magnetite-hematite-rich matrix is developed in the southeastern alteration zone. Breccias and hematisation are more extensively developed at Wirrda Well and are hosted by granite of the Hiltaba Suite, foliated granite, and by Palaeoproterozoic metasedimentary rocks. Other minerals reported at Acropolis and Wirrda Well include pyrite, chalcopyrite, siderite, chlorite, barite, fluorite, phlogopite, and uraninite (Cross, 1993). Bornite is present at Wirrda Well. Oxygen isotope data for magnetite - K-feldspar pairs in veins at Acropolis were reported by Oreskes and Einaudi (1992; Table 1).

Oak Dam Cu-U Prospect

WMC Ltd discovered the Oak Dam prospect in 1976 by targeting coincident intense magnetic and 3-4 mgal gravity anomalies, 39 km west of Lake Torrens (Paterson, 1986). The prospect was described by Davidson (1991) and Davidson and Paterson (1993). Thirteen drill holes revealed two very large iron-oxide bodies (ironstones) whose tops were intersected below an unconformity at the base of 400-500 m of flat-lying Adelaidean cover (Fig. 2). Ironstone cobbles shed into the basal Pandurra Formation during weathering of the basement provides evidence of a minimum age of 1424±51 Ma (Fanning *et al.*, 1983) for the ironstone development. The eastern ironstone, Oak Dam East, was the source of the targeted coincident magnetic and gravity anomalies. Infill drilling delimited ore-grade U (Table 1) to a 200 m x 200 m x 60 m-thick zone within the overall 1200 m x 400 m x 300 m-thick ironstone zone. A second non-magnetic ironstone, termed Oak Dam West, forms a gravity anomaly about 4 km west of Oak Dam East. Limited drilling penetrated a thick sequence of barren hematite sandstones and conglomerates resembling the interpreted maar-fill volcaniclastic facies at Olympic Dam. The underlying rocks have not been drilled.

The Oak Dam East ironstone occurs on the northernmost tip of the regional north-south Pernatty Culmination; basement isopachs and the ironstone itself parallel the north-south trend. Intense brecciation, similar to that in the ODBC, is the dominant feature of Oak Dam East. Fragments of gneissic granite (possible equivalents of the Donington Suite; Creaser, 1989) and minor schist (Hutchison Group?) are common, variably replaced by the dominant hematite ± quartz assemblage. The lower limit of intense iron metasomatism and veining coincides with a distinct decrease in the intensity of brecciation, forming a flat 'base' to the host ironstone body. The lateral margins have not been intersected in drilling.

The basement and small areas of the ironstone are transected by 0.5-5 m-wide dykes of undeformed, weakly sericitised, coarse-grained to pegmatitic alkali granite (Hiltaba Suite?), medium-grained diorite (very altered), and altered thin mafic dykes with peperitic margins. This evidence indicates that felsic and mafic magmatism was contemporaneous with ironstone formation and brecciation, but did not form the main hostrock to ironstone.

Table 1. Characteristics of selected Cu-Au deposits and prospects of the Olympic Cu-Au province.

Deposit/ prospect	Tonnage-grade or intersections	Hostrock geology	Ore/alteration Paragenesis	Mineralisation textures, style	Mineral and metal zoning	Controlling Structure	Fluid properties	References
Olympic Dam	2320 Mt @ 1.3% Cu, 0.5 g/t Au, 0.4 kg/t U_3O_8, 2.9 g/t Ag (resource, 1999)	[1] ODBC hosted by Roxby Downs Granite; ODBC contains multi-stage hematitic breccias & minor volcaniclastics; minor felsic & mafic/ultramafic dykes	1. Mt ± Hm, Chl, Ser, Sid, Py, Cpy, Pit 2. Hm, Ser, Cc, Bn, Pit, Bar, Flu, Chl 3. Hm, Qtz, Bar	Disseminated sulphides in hematitic breccia matrix & clasts; also sulphides in veins	Gross zonation from assoc 1 at depth to 3 at higher levels; sulphide zonation upwards from Py to Cpy to Bn to Cc; higher Au at margin of barren Hm-Qtz core in ODBC	Long dimension of ODBC trends NW	Assoc. 1 fluid: T = 250-400°C, $\delta^{18}O_{fluid}$ ≈10‰; Assoc. 2 fluid: T = 150-400°C, $\delta^{18}O_{fluid}$ <9‰; 7-42 eq.wt% NaCl; $\delta^{34}S_{sulphides}$ = –6 to -10‰ (av.); $\delta^{34}S_{barite}$ =10‰ (av.)	Reeve et al. (1990), Oreskes & Einaudi (1992), Haynes et al. (1995), Eldridge & Danti (1994), Reynolds (2000), Conan-Davies (1987).
Acropolis	66m @ 0.7% Cu	Felsic GRV, granitoid, gniessic alkali granite	Mt and/or Hm, Sid, Qtz, Kfs, Ser, Chl, Bar, Flu, Ap, Phl, Py, Cpy, Uran	Vein networks & granite breccia; massive Fe-oxides		Fault-controlled breccia(?)	T = 440-550°C $\delta^{18}O_{fluid}$ = 10‰	Parker (1990) Cross (1993) Oreskes & Einaudi (1992)
Wirrda Well		Burgoyne granite, breccia clasts of Palaeoproterozoic deformed granite, Hutchison Gp	Hm, Mt, Sid, Qtz, Kfs, Ser, Chl, Bar, Flu, Ap, Phl, Py, Cpy, Uran,	Breccia & vein networks		Fault-controlled breccia(?)		Parker (1990) Cross (1993)
Oak Dam	7 m @ 0.27% Cu & 63 m @ 0.32% Cu & 690 ppm U; ~ 560 Mt massive Fe; 216 m @1480 ppm La, 1615 ppm Ce.	Deformed Palaeoproterozoic granitoids and metasediments; cut by Hiltaba Suite granite dykes, minor diorites, and mafic dykes.	1. Mag-Qtz-Ap-Py 2. Colloform Hm 3. Hm after Mt; chalcedony, Qtz-illite, Chl, Ser, Mon, Cpy, Py, Car, Sp, Ap, Carb, Uran; 4. Vughy Qtz ± Bar.	Disseminated sulphides in hematitic breccia matrix & clasts; sulphides in veins; replacement of colloform bands	Upper ~100 m weathered to hem-limonite; below this, mineralisation forms 25-180 m thick blanket (Cpy after dissem Py only). Main REE-P-Mt zone underlies this.	Ironstone was exposed on Pandurra Fm unconformity at 1424 Ma; this process left an erosional remnant with a strong north orientation, parallel to "Pernatty Culmination"	Early fluids: CO_2-L-V T = 360-495°C, 46.4 wt % NaCl; Syn-Cu-U fluid (L-V; boiled): T = 160-205°C, 1.3-4.7 eq.wt% NaCl; $\delta^{34}S_{sulphides}$ = –14 to 0‰ (av.)	Davidson (1991), Davidson & Paterson (1993)
Emmie Bluff	Up to 2.8% Cu, 0.6 g/t Au	Wandearah Fm, granite (in north); GRV dacite (in south)	1. Mt (+Cpx, Amph, Gt, Qtz, Cal, Kfs, Py, Allan in south) 2. Cpy, Bn, Hm, Chl, Qtz, Cc (in north)	Disseminated sulphides in tectonic breccias	Upper Hm-Chl-Qtz, lower Mt-Chl-Py	?Shallow-dipping splays of major NW-striking fault	Early fluid: T = 490-550°C, $\delta^{18}O_{fluid}$ 6.5-7.5‰; later fluid: T <430°C, $\delta^{18}O_{fluid}$ <4.6-8.2‰	Gow (1996)

Deposit/ prospect	Tonnage-grade or intersections	Hostrock geology	Ore/alteration Paragenesis	Mineralisation textures, style	Mineral and metal zoning	Controlling Structure	Fluid properties	References
Moonta (including Wheal Hughes, Poona)	approx. 6.75 Mt @ 5% Cu, 1-4 g/t Au (Moonta-Wallaroo combined)	Metarhyolite (Moonta Porphyry)	Qtz, Kfs, Bt, Tm, Hm, Cpx, Chl, Cpy, Py, Bn	Fissure veins up to 8 m wide	Bn towards the surface; Cpy at deeper levels	Arcuate sets of steeply dipping veins. Mineralisation along veins and at intersections of veins and fractures		Dickinson (1953) McBriar (1962) Hafer (1991)
Wallaroo		Phyllite, biotite schist (Doora Metasediments)	Qtz, Carb, Tm, Ap, Flu, Amph, Cpx, Mt, Kfs, Bt, Py, Po, Cpy	Replacement and disseminations along foliation and shears		En echelon ductile shears		Dickinson (1953) McBriar (1962)
Manxman, Joes Dam	Up to 1.7% Cu, 2.5 g/t Au; anomalous LREE, Co; 287m @ 0.23% Cu, (Manxman A1)	Mt- & cal-rich breccias of pelitic metaseds; I-type granitoid, felsic to intermediate gneisses, granulite	1. Alb, Scap, Cpx, Qtz, Act, Ap 2. Mt, Bt, Ap, Til, REE mins, Hm 3. Po then Cpy, Py, REE & U & Th mins, Hm, Co-Ni-As-Pb mins, Amph, Chl, Cal, Alb, Flu, Kfs, Sti, Bar, Ser, Ep	Sulphides as vein fill, dissem. & in breccia matrix; massive Mt & Hm zones	Inner & early Po to outer/later Py-Cpy to outermost Py; inner Mt, outer Hm	Fault(?) control on sulphide & oxide zonation	1. <500°C (?) 2. 400-500°C (?) 3. 200-400°C (?)	Hampton (1997)
Prominent Hill	107m @ 1.94% Cu, 0.65g/t Au, 1.6g/t Ag; incl 20m @ 3.0 g/t Au; & 17 m @ 2.35% Cu, 1.07g/t Au, 3.3 g/t Ag, 1398 ppm U	Hematitic breccias hosted by metasediments & 'felsic volcs'	1. Cpy, Bn, Cc, Hm, Ser, silica 2. Flu, Uran	Dissem sulphides in breccia	Upper Cc; Lower Cpy-Bn-Uran	East-West trending gravity anomaly		Minotaur Resources Ltd. (2002)

[1] ODBC: Olympic Dam Breccia Complex (Reeve et al., 1990)

Mineral abbreviations: Alb – albite, Allan – allanite, Amph – amphibole, Ap – apatite, Bar – barite; Bn - bornite, Bt – biotite, Car – carrolite, Carb – carbonate, Chl – chlorite, Cpx – clinopyroxene, Cpy – chalcopyrite, Dol – dolomite, Flu -fluorite, Gal – galena, Hm – hematite, Kfs – K-feldspar, Mar – marcasite, Mon – monazite; Ms – muscovite, Mt – magnetite, Phl – phlogopite, Pit – pitchblende; Po – pyrrhotite, Py – pyrite, Qtz – quartz, Scap – scapolite, Ser – sericite, Sid – siderite, Sp – sphalerite, Sti – stilpnomelane, Tm – tourmaline; Uran – uraninite.

Ironstone textures provide evidence for an early high temperature magnetite - apatite - calc-silicate ± pyrite assemblage, which is still partly preserved near the base of the ironstone. Brecciation was followed by development of large-scale open space infill by colloform hematite and quartz in the upper part of the body, as well as isolated development of hematite oolite-filled fractures interpreted to have been deposited from boiling of fluids. Approximately synchronous with the onset of sulphide mineralisation, a second, very widespread, steely hematite phase then partially replaced earlier fabrics.

Chalcopyrite and pitchblende are concentrated in a blanket-like 20-180 m-thick subhorizontal layer about 100 m below the unconformity. Above the blanket, there is a rapid transition to a hematite-limonite oxide zone, with evidence of replacement of pre-existing pyrite and chalcopyrite. This is interpreted as pre-Pandurra Formation Proterozoic weathering (Davidson and Paterson, 1983). Within the 'blanket', hydrothermal chalcopyrite, sphalerite, pitchblende, and carollite (associated with illite replacement), sericite, quartz, and monazite, have commonly replaced disseminated pyrite adjacent to fractures and veins.

Emmie Bluff Cu-Au Prospect

The Emmie Bluff Cu-Au Fe-oxide deposit was discovered by drilling coincident gravity and magnetic anomalies in basement, under 800-900 m of Pandurra Formation and younger cover. The following summary is based on Gow (1996). Two major zones of Fe-oxide rich alteration have been located about 3 km apart, as follows.

1 The northern, stratabound alteration zone is up to ~150 m thick, ~3 km in diameter, and is hosted by chert, shale, and carbonate-bearing metasedimentary rocks of the Wandearah Formation. The alteration is characterised by magnetite, hematite, chlorite, and quartz, and hosts the principal zone of Cu-Au mineralisation.
2 The southern, discordant alteration zone contains veins and replacements within rhyodacite of the Gawler Range Volcanics, intersected at more than1 km depth. Veins contain skarn-like, high-temperature mineral assemblages with combinations of clinopyroxene, amphibole, magnetite (<10% vol.), garnet, quartz, calcite, K-feldspar, pyrite, and allanite. Magnetite occurs disseminated in alteration selvages adjacent to veins. Albite veins are found within the rhyodacite. Sulphides, other than pyrite, are rare.

The chemical meta-sedimentary host sequence and underlying medium- to coarse grained meta-arkosic rocks and Palaeoproterozoic metagranite are interpreted to have been faulted against the Gawler Range Volcanics along the Southern Arcoona Fault Zone (Gow, 1996). Initial movement on the northeast-trending, southwest-dipping, fault zone was normal. This was followed by inferred reverse reactivation along shallow-dipping splays that resulted in tectonic emplacement of meta-granite wedges within the Wandearah Formation.

Copper-gold mineralisation in the northern alteration zone is hosted by brecciated, laminated meta-sedimentary and meta-granitic rocks. Grades of up to 2.8% Cu and 0.6 g/t Au are reported. The Fe-Cu-Au deposit is crudely zoned downwards from breccia and cataclasite zones with intense hematite-chlorite-quartz alteration and containing chalcopyrite-pyrite-bornite-covellite, to less brecciated magnetite-chlorite-pyrite altered laminated metasedimentary zones with lower abundances of Fe and Cu sulphides. Gow (1996) interpreted the breccias in the northern alteration zone to be of tectonic origin, related to reverse reactivation of the Southern Arcoona Fault Zone. Hematisation of pre-existing magnetite, and accompanying Cu-Au mineralisation, were also envisaged to have occurred during the fault reactivation.

Moonta-Wallaroo Cu-Au District

The Moonta-Wallaroo district is situated in the southern part of the Olympic Cu-Au province (Figure 1). During the latter part of the 19th century the Moonta and Wallaroo Mines were largely responsible for South Australia being one of the world's largest copper producing provinces at that time. The historic yield from the Moonta-Wallaroo district, mostly during that period, totalled approximately 355 000 tonnes of contained copper and 2 tonnes of gold (Conor, 1995).

Basement outcrop in the Moonta-Wallaroo district is very poor, and is typically covered by up to 100 metres of Neoproterozoic to Quaternary sediments. The basement comprises meta-sedimentary and meta-volcanic rocks of the Palaeoproterozoic Wallaroo Group, which were intruded by Mesoproterozoic granitoids of the Hiltaba Suite. Fine grained albitic meta-sedimentary rocks, in places scapolite-bearing, are common in the Wallaroo Group. Calcsilicate skarns were commonly developed within calcareous meta-sedimentary rocks. SHRIMP zircon U-Pb ages of felsic volcanic rocks in the Wallaroo Group range from 1737±5 Ma to 1763±14 Ma (Fanning *et al.*, 1988, Conor 1995). Regional upper greenschist to amphibolite facies metamorphism and deformation of the Wallaroo Group occurred during the Kimban Orogeny (ca. 1720 Ma; Ferris *et al.*, this volume).

Well-constrained ages of Hiltaba Suite magmatism within the Moonta-Wallaroo district range from 1575±7 Ma to 1598±7 Ma (compiled in Zang, 2002). Intrusion of these granitoids was accompanied by contact metamorphism, shearing, and high temperature Fe-Na-Ca±K metasomatism of the adjacent Wallaroo Group and, in places, of the granitoids themselves. Conor (1996) referred to these altered rocks as the Oorlano Metasomatites, although metasomatic mineral assemblages vary widely. At a regional scale, there is a strong spatial association of Fe-Na-Ca metasomatism with the contact aureoles of Hiltaba Suite granites. At a drillhole scale, metasomatic alteration zones emanate away from granite bodies and dykes, with fluids commonly focussed along foliation and shear zones within the host rocks.

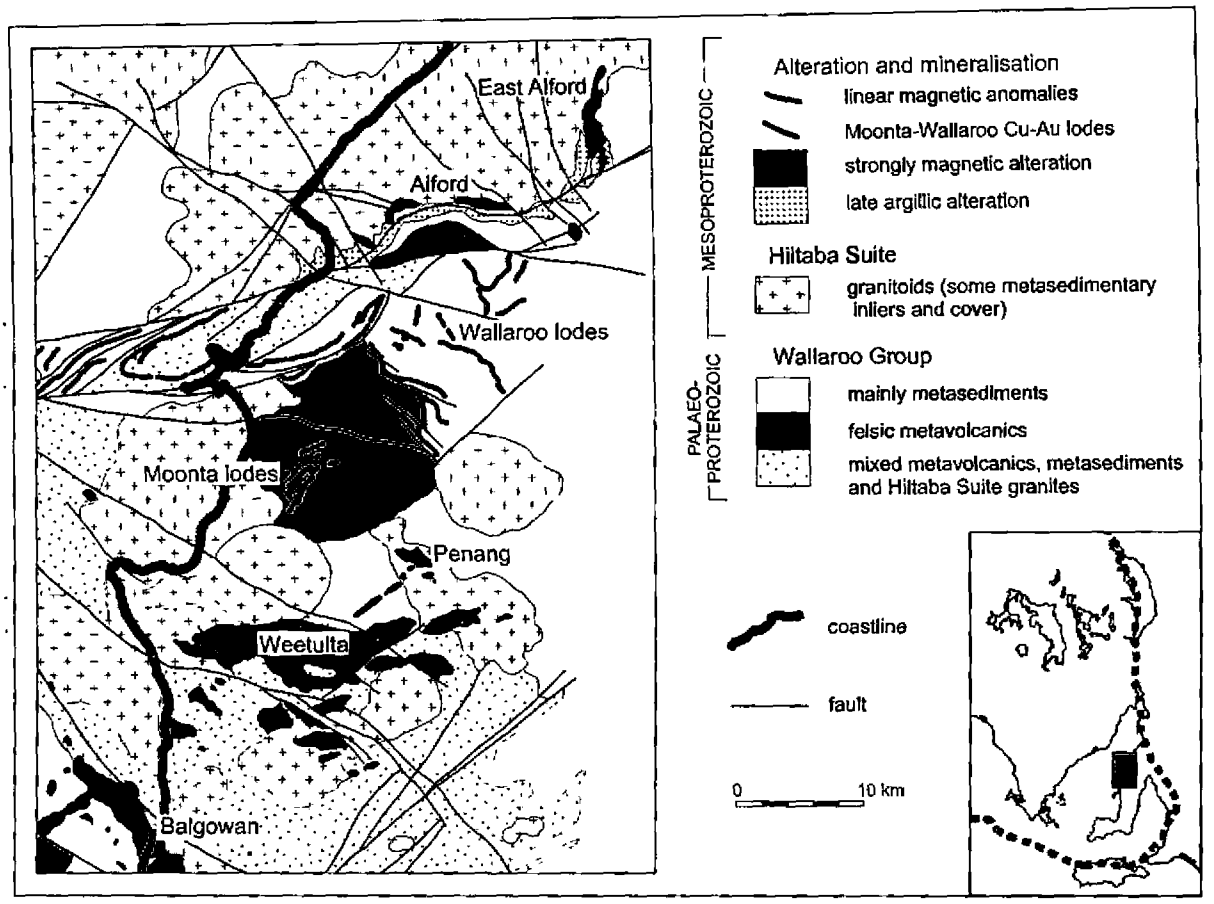


Figure 3: Basement geology sketch map of part of the northern Yorke Peninsula, showing the distribution of Hiltaba Suite granitoids and magnetic alteration. Inset shows location of map and the boundary of the Gawler Craton.

Albite-actinolite-magnetite ± carbonate ± pyrite replacement of metasedimentary rocks (i.e., the 'type' Oorlano Metasomatite) occurs primarily adjacent to Hiltaba Suite granites, notably the Tickera Granite in the Alford and Port Broughton areas (Fig. 3). More distal and widespread albitisation of metasedimentary and volcanic rocks is common. This alteration is not generally associated with significant sulphides.

Biotite-magnetite ± pyrite metasomatism in the Wallaroo mines district is focussed in brittle-ductile shear zones within metasedimentary rocks, forming strong magnetic anomalies and hosting the Wallaroo Cu-Au mineralisation (Fig. 4). A large area (~30 km x 40 km) of strongly magnetic rock, beneath the waters of Spencer Gulf west of Moonta, is interpreted to be a further zone of extensive biotite-magnetite metasomatism of Wallaroo Group metasedimentary rocks. South of Moonta, in the region between Penang and Balgowan, biotite-magnetite-albite ± K-feldspar ± amphibole ± pyrite veining and pervasive metasomatism forms irregular magnetic anomalies, including a major 5 km x 15 km alteration zone at Weetulta (Fig. 3). Apatite, monazite, allanite, and fluorite are locally important alteration components, indicating significant P, REE, and F in the hydrothermal fluids. Chlorite is locally significant - typically as a late alteration phase replacing biotite and/or actinolite and may occur with quartz ± K-

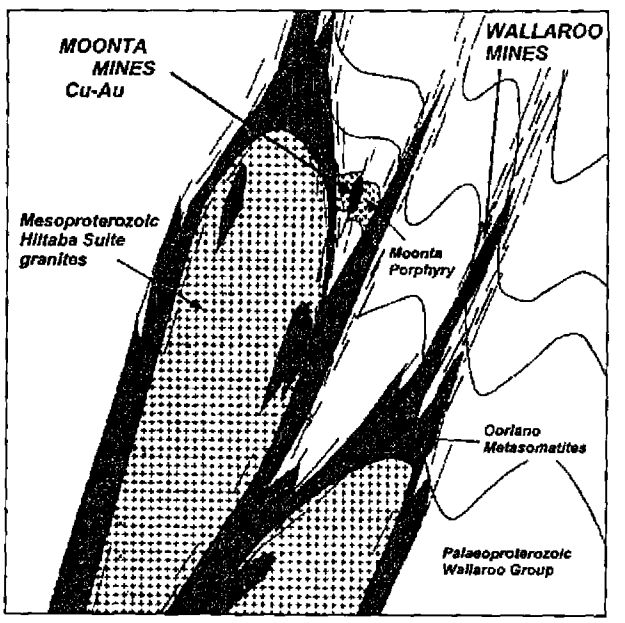


Figure 4: Diagrammatic cross section showing the geological setting of the Moonta and Wallaroo mineralisation associated with intrusion of Hiltaba Suite granites and syn-intrusive shearing (from Conor, 1995).

feldspar ± pyrite ± chalcopyrite. While magnetite is typically associated with broad alteration domains, it may show antithetic relationships with the more restricted chloritic alteration and/or Cu mineralisation.

Other metasomatic styles in the Moonta-Wallaroo district include minor carbonate breccias which may bear minor Cu mineralisation. Widespread hematite-quartz-chlorite-calcite alteration is generally a minor and late stage overprint, and is not associated with sulphides. Local kaolinite alteration and epithermal quartz-carbonate ± hematite veins overprint early albitic metasomatism, particularly within a major structural corridor along the southern margin of the Tickera Granite. The age and possible genetic relationship of this high-level alteration to the earlier higher temperature metasomatism is unclear, although some Moonta-style Cu mineralisation has kaolinitic wallrock-alteration.

Although the Moonta-Wallaroo district contains regional Fe-Na-Ca metasomatism typical of iron oxide-Cu-Au mineral systems, as well as deposits of this style (eg., Wallaroo), iron oxides do not constitute a major part of the mineralisation in the Moonta mines area. The Cu-Au mineralisation in the Moonta deposits occurs as steeply dipping quartz - K-feldspar - biotite - tourmaline ± hematite ± magnetite ± chlorite ± sericite, coarse-grained veins up to 8 m wide, developed within a competent metarhyolite host, the Moonta Porphyry. Chalcopyrite-pyrite-bornite mineralisation occurs in the veins, commonly at the intersection of cross structures.

Mount Woods Inlier

Archaean to Mesoproterozoic basement of the Mount Woods Inlier is mostly covered by 30-160 m of Permian to Cretaceous sediments, and by the Mesoproterozoic Pandurra Formation in the southeast. Basement comprises Archaean gneisses in the south and west and Palaeoproterozoic metamorphic rocks to the north and east, including paragneiss, orthogneiss, and extensive banded iron formation. Metamorphic zircons in the upper amphibolite to granulite facies rocks record a SHRIMP age of 1736±14 Ma (Fanning, 1997). The weakly deformed Engenina Granite (1691±2 Ma, Fanning, 1997) and undeformed Balta Granite (1584±18 Ma, Daly *et al.*, 1998) and related Hiltaba Suite equivalents, intruded the metamorphic rocks. Several large mafic intrusive complexes are believed to be Palaeoproterozoic in age (Daly *et al.*, 1998), but Hiltaba-aged mafic intrusions may also be present.

The Mount Woods Inlier is separated from high grade gneisses of the Coober Pedy Ridge to the north by shears associated with the Karari Fault Zone, which was active during the Kararan Orogeny. Tectonism in the Gawler Craton around 1650 Ma and in the period ~1565-1540 Ma has been ascribed to the Kararan Orogeny (Daly *et al.*, 1998). The Mount Woods Inlier appears to have escaped the high grade metamorphic event that affected basement rocks of the Coober Pedy Ridge at 1565±8 Ma (Daly *et al.*, 1998). Juxtaposition of the Mt Woods Inlier and Coober Pedy Ridge tectonic domains therefore probably occurred after about 1565 Ma, during the Kararan Orogeny. Although still poorly understood, this tectonic scenario may have important implications for the distribution of hydrothermal alteration and mineralisation in the Mount Woods region.

Iron-oxide-rich metasomatic rocks are widely distributed in the Mount Woods Inlier (PIRSA, 2000). For example, the Peculiar Knob iron ore prospect, which contains high grade hematite, has been interpreted to represent Palaeoproterozoic banded iron formation that was recrystallised and remobilised by the adjacent Balta Granite (PIRSA, 2000). The Skylark iron ore prospect, and Hawksnest prospect in the Wilgena Domain, to the south of the Mount Woods Inlier, both contain metamorphosed banded iron formation.

Magnetite- and hematite-rich alteration, breccias and 'skarns' have been widely reported in exploration drill holes. Only some of these Fe-oxide-rich alteration zones contain significant Cu or Au mineralisation. The most important are the recently discovered Prominent Hill prospect, the Manxman and Joes Dam prospects, described below, and the Cairn Hill prospect (Fig. 1).

Manxman and Joes Dam Cu-Au Prospects

Exploration by CRAE, Normandy Group and Burmine NL in the late 1980s to mid 1990s led to the discovery of major magnetite-rich alteration systems with anomalous Cu-Au-REE mineralisation in the southern part of the Mount Woods Inlier. The best intercepts occur in the vicinity of the White Hill mafic complex, and include 287 m @ 0.23% Cu and up to 1.7% Cu, 2.5 g/t Au at the Manxman A1 prospect, and 186 m @ 0.13% Cu at the Joes Dam South prospect (Table 1). Both prospects, described most recently by Hampton (1997), are highly anomalous in Co, Ce and La, whereas only Manxman is anomalous in U. The principal host lithologies at Joes Dam South are fine-grained, laminated, quartz - plagioclase - biotite meta-sedimentary rocks. Magnetite-rich breccias and lesser hematite-rich zones at the Manxman A1 prospect are hosted predominantly by various granitoid rocks and by subordinate fine-grained laminated quartz - albite - diopside ± biotite metasedimentary rocks (Hampton, 1997). Granitoids at Manxman A1 range from granitic gneiss and pegmatite gneiss to granite, microgranite and pegmatite. The granitoids are all I-type and range in composition from monzonite (similar to the Engenina Adamellite) to granite (similar to the Balta Granite; Hampton, 1997).

Granitoid and metasedimentary rocks have been overprinted by hydrothermal alteration during three main paragenetic stages which are observed at both Manxman and Joes Dam. Alteration styles include vein networks, infill of breccia matrix, and pervasive replacements. The stages proposed by Hampton (1997) are as follows:

1 Na-Ca metasomatism: albite - scapolite - clinopyroxene (diopside-hedenbergite) - quartz.
2 K-Fe metasomatism: magnetite - biotite - apatite - titanite - LREE minerals ± hematite.

3 'Regression' and Cu-Au mineralisation: Na-amphibole - chlorite - LREE minerals - calcite - albite - fluorite - hematite - K-feldspar; mineralisation comprises early pyrrhotite and later chalcopyrite - pyrite - LREE minerals with a range of minor ore minerals such as uraninite, pyrosmalite, siengite, arsenopyrite, glaucodot, galena, tellurobismuthite and thorite. Other minor minerals reported for stage 3 include sericite, barite, zoisite, and stilpnomelane.

It is likely that stage 3 of Hampton (1997) includes several separate assemblages: for example, hematite and pyrrhotite would not have formed in equilibrium, nor is it likely that albite, K-feldspar and sericite grew in the same assemblage.

Fine hematite dusting of alkali feldspars has locally imparted a pinkish colouration ('red-rock') to some alteration assemblages and to most of the granitoid rocks at Manxman A1. Only very minor hydrothermal hematite is associated with sulphides at Manxman and Joes Dam. A hypogene, massive hematite zone at Manxman A1, apparently at the margin of the Fe-oxide rich alteration system, is low in Cu and Au.

In general, there is a strong spatial association between Cu, Fe, Co and Au contents, and most Cu (as chalcopyrite) occurs within magnetite-rich zones in veins, and as replacements of magnetite. Pyrite is widespread, whereas pyrrhotite at both Manxman A1 and Joes Dam South forms zones within which higher Cu±Au grades are commonly, but not exclusively, developed. Hampton (1997) suggested that these zones at Manxman A1 formed around faults, interpreted from geophysical data, near the centre of the hydrothermal system.

Prominent Hill Cu-Au-U Prospect

Significant copper and gold mineralisation was recently discovered at the Prominent Hill prospect in the southern Mt Woods Inlier (Fig. 5, Table 1) by Minotaur Resources Ltd in joint venture with BHP Billiton, Normandy Exploration Pty Ltd, Sons of Gwalia Ltd and Sabatica Pty Ltd. DDH URN1 (see Figure 5 for intersection widths and grades) was targeted on part of an E-W trending gravity 'high' about 2 km long, which has mostly low magnetic response; coincident gravity and magnetic 'highs' lie immediately to the north of the drilled gravity anomaly. Basement (from 108 m depth) comprises variably altered and brecciated metasedimentary rocks, underlain by a sequence described as amygdaloidal, felsic, volcanic rocks, agglomerate and silica-hematite breccia (Minotaur Resources Ltd, 2002). Mineralised hematitic breccia is developed within the metasedimentary rocks, which are cut by an unmineralised dolerite dyke. Clasts in the matrix-supported, 'milled' breccia are hematite-sericite-silica

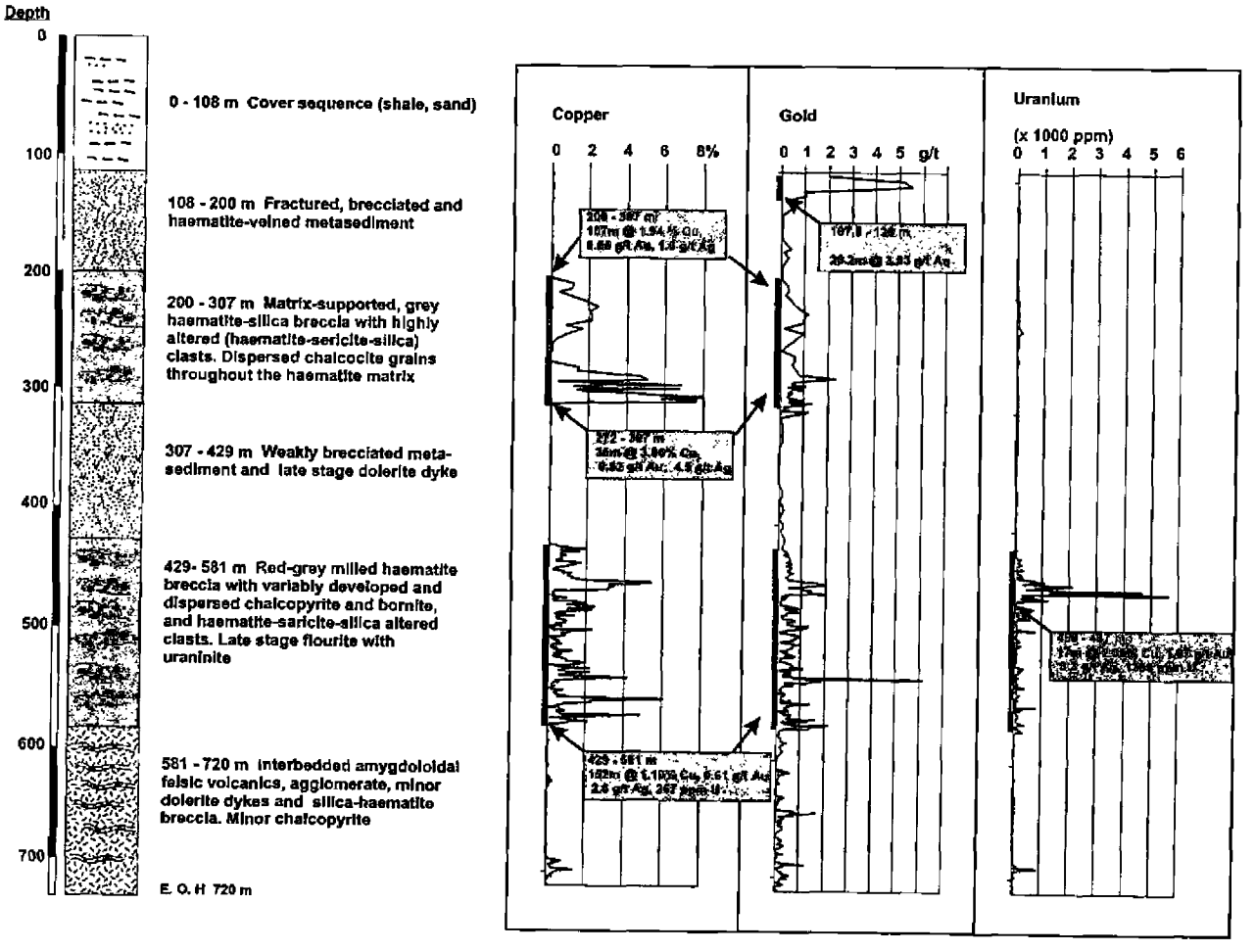


Figure 5: Prominent Hill prospect. Summary geological log and assay results, DDH URN1 (courtesy Minotaur Resources Ltd)

altered and are enclosed in a hematite-silica rich matrix containing disseminated copper sulphides.

Based on limited open file data (Minotaur Resources Ltd, 2002), mineralisation is zoned from an upper Au-rich zone, downwards through a Cu-Au zone containing chalcocite, to a lower zone of Cu-Au ±U containing chalcopyrite and bornite. Uraninite is reported with late-stage fluorite. Lanthanum and cerium are highly enriched, with REE grades of 0.2-0.6% throughout the Cu and Au mineralised zones. The copper sulphide zoning, Cu-Au-U-LREE association, brecciation and hematite-sericite alteration, bear strong similarity to the Olympic Dam deposit (Minotaur Resources Ltd, 2002).

Fe-oxide Cu-Au Ore Formation

Key geological criteria widely applied in exploration for Olympic Dam style Cu-Au deposits in the Gawler Craton include:

1. Broad temporal association of Cu-Au mineralisation with magmatism of the Hiltaba Suite and Gawler Range Volcanics, at ~1590 Ma; note that absolute age constraints on hydrothermal events are sparse.
2. Fe-oxide-rich alteration and Cu-Au mineralisation have a broad spatial associated with this magmatism, but evidently only in the eastern Gawler Craton. The Fe-oxide rich zones produce gravity anomalies, with or without major magnetic anomalies.
3. The presence of breccias (tectonic, hydrothermal, or magmatic-related) in localising mineralisation.
4. High crustal level of Cu-Au ore formation.
5. Strong (brittle) structural control on the location of breccias and ore.
6. Hematite-sericite-chlorite alteration accompanying higher grade Cu-Au mineralisation.
7. Association of Cu-U-Au with LREE, Ag, F, Ba, P, Co.

Several models of ore formation have been published for the Olympic Dam Cu-U-Au deposit in the past decade. The key differences between models relate to the role of granites versus other sources of metals and fluids, the timing of fluid-rock interaction, and which of two fluids carried the ore metals. The implications of the differences in the models for exploration are profound. Some of the components in the Olympic Dam style ore-forming system are shown schematically in Figure 6.

1 Reeve *et al.* (1990) proposed a model of near-surface formation of Fe-oxides and Cu-U-Au-Ag-REE mineralisation, within breccias of diverse phreatomagmatic, tectonic, and hydrothermal origin. Primary Cu-U-Au ore deposition resulted from

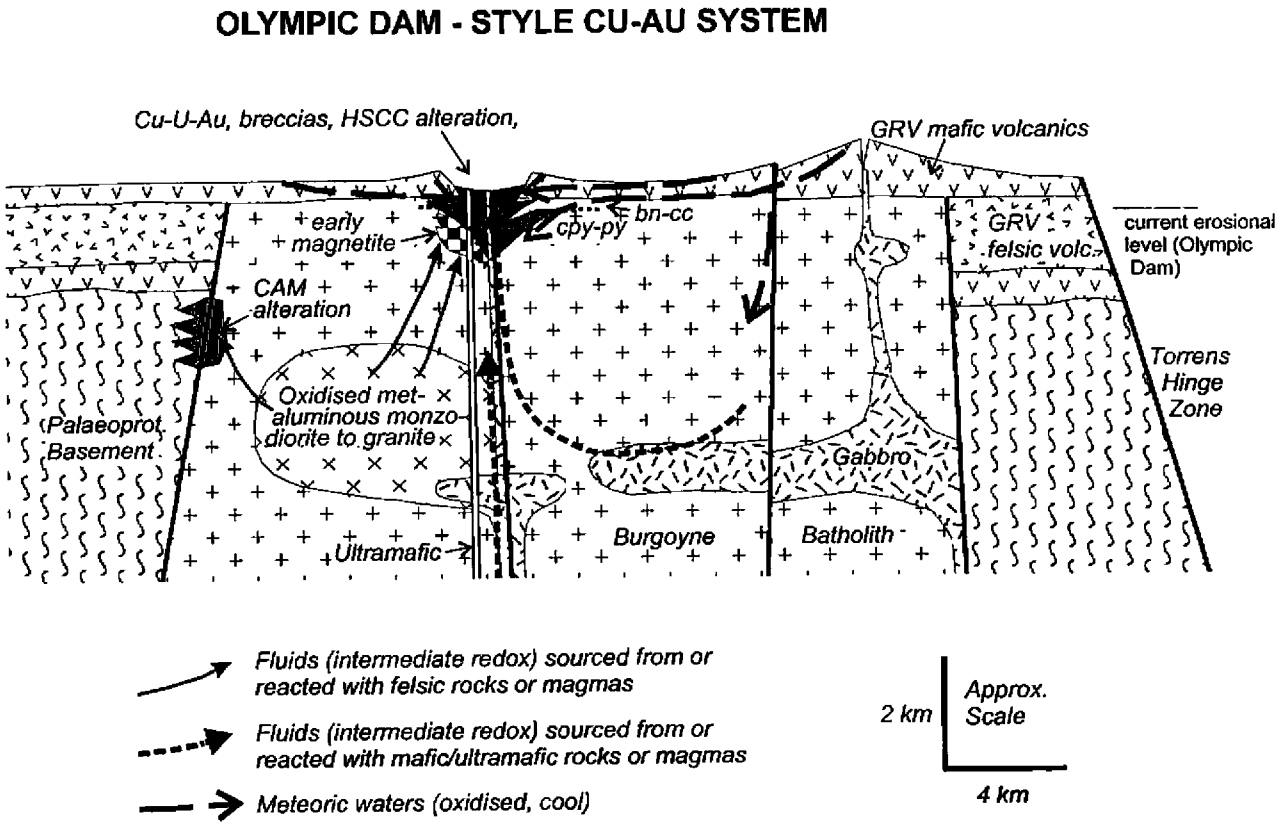


Figure 6: Schematic cross section of an Olympic Dam style hydrothermal system, showing Cu-U-Au mineralisation asssociated with hematite-sericite-chlorite-carbonate (HSCC) alteration. Deeper level and/or distal calcsilicate-alkali feldspar-magnetite alteration (CAM), and alternative fluid types that may have been active in the system, are also shown (see text). The interface between chalcopyrite-pyrite (cpy-py) and bornite-chalcocite (bn-cc) assemblages is indicated. Geology based on Reeve *et al.* (1990) and Haynes *et al.* (1995).

interaction of ascending hot, relatively reduced, metal-rich brines and descending cooler, oxidised, meteoric waters, producing a broad zonation from lower chalcopyrite ± pyrite to upper bornite ± chalcocite.

2 Based on the geological model in (1) and on thermodynamic modelling, Haynes *et al.* (1995) also advocated fluid mixing as a depositional mechanism for Fe-oxides and ores, but favoured Cu-U-Au transport in the cooler, descending, oxygenated meteoric waters (modelled at 150°C). The authors acknowledged the alternative possibility that ore metals were introduced in the hotter fluid (250°C in model). Basalts of the Gawler Range Volcanics were preferred as a source of the copper, leached by saline waters derived from a playa lake.

3 Oreskes and Einaudi (1990, 1992) postulated that the ODBC and associated Cu-Au-Au-Ag-REE mineralisation formed ~190 Ma later than the host Roxby Downs Granite, at and immediately below the palaeosurface following uplift and erosion of the granite. Brecciation was viewed as hydrothermal in origin, with major amounts of Cu-Fe sulphides introduced during the waning stages of brecciation. Like Reeve *et al.* (1990) and Haynes *et al.* (1995), two fluids were suggested by Oreskes and Einaudi (1990, 1992), but with hotter (~400°C) deep-sourced fluids of possible felsic magmatic origin preceding rather than mixing with cooler oxidising surficial waters (seawater, groundwater, or closed-basin water). According to Oreskes and Einaudi (1990, 1992), the hotter fluid may have carried Fe, Cu and other metals but the oxidising fluids responsible for the formation of hematitic breccias were considered the key to the higher grade Cu mineralisation. Oreskes and Einaudi (1990, 1992) further proposed that Proterozoic surface weathering led to local development of supergene chalcocite ores.

4 Johnson and McCulloch (1995) suggested that the Cu-REE-enriched fluid may have been an ascending volatile phase exsolved from mafic/ultramafic magma chamber(s), and which post-dated the magnetite-forming fluid. They presented Sm-Nd isotopic evidence supporting involvement of two fluids in ore genesis, one of which was in isotopic equilibrium with Hiltaba Suite granites and which precipitated the early magnetite. The other fluid, responsible for introduction of at least some Cu, had a more primitive ε_{Nd} signature, which demanded a significant contribution of Nd (and by implication, Cu) from mafic/ultramafic rocks or magmas.

5 Reynolds (2000) alluded to magmatic sources for both ore fluids and metals at Olympic Dam. However, only limited supporting data have been published (eg., Eldridge and Danti, 1994)

At the Emmie Bluff deposit, Gow *et al.* (1994) and Gow (1996), proposed a two stage model resembling that of Oreskes and Einaudi (1990, 1992) for Olympic Dam. The calcsilicate - K-feldspar - magnetite vein networks in the southern alteration zone at Emmie Bluff were interpreted to be the product of contact metamorphism, and attributed the rock fracturing to high fluid pressures and volatile release associated with emplacement of Hiltaba Suite intrusion(s). Oxygen isotope compositions of quartz and magnetite in the veins are consistent with a magmatic source of fluids (Table 1). A shift towards lower temperatures and lower ($\delta^{18}O$) values of fluids associated with hematitic alteration and Cu-Au deposition (quartz-hematite pairs; Table 1) was interpreted to be from the influx of evolved meteoric-hydrothermal waters (Gow *et al.*, 1994; Gow, 1996). The proposed two-stage model involves early high-temperature magnetite-rich assemblages, that were overprinted by hematitic alteration possibly during the later stages of Hiltaba Suite magmatism (Gow *et al.*, 1994; Gow, 1996). In this model fluid flow was strongly controlled by northwest-trending faults.

At Oak Dam East, Davidson (1991) and Davidson and Paterson (1993) attributed brecciation to overpressuring during large-scale volatile release from underlying Hiltaba Suite magma. Some magnetite-calcsilicate skarn formed prior to brecciation and unroofing of the hydrothermal complex. Hot, saline waters of magmatic/meteoric origin (Table 1) formed magnetite, pyrite, and quartz near the base of the system. Colloform hematite-quartz formed towards the top of the system where cooler oxidised meteoric water dominated within 100-200 m of the Mesoproterozoic palaeo-surface. Minor brecciation occurred along narrow fracture zones during rapid 'gas-streaming' events, the results of phase separation at depth. Boiling of fluid almost to the top of the existing body produced widespread chalcedony and K-phyllosilicates. Late in the development of the iron-oxide body, an upwelling, boiling, Fe-Cu-U-bearing fluid mixed along a sub-horizontal boundary with oxidised, low-temperature meteoric water (Table 1), depositing oxidised metal assemblages and phyllosilicates. The processes of phase separation and fluid mixing in a high-level crustal setting are analogous to those forming some epithermal precious metal deposits. Prior to 1424±51 Ma, a weathering interface probably migrated downwards into the metal-rich blanket, potentially leaching a significant portion of the hydrothermal mineralisation.

Crustal Settings of Cu-Au Mineralisation

There are three major regions of hydrothermal activity broadly associated with Hiltaba Suite ± GRV magmatism (Fig. 1): Stuart Shelf basement, the Mount Woods Inlier and the Moonta-Wallaroo-Roopena region. Each of these regions contains high- to moderate-temperature Fe-oxide rich alteration as well as low temperature alteration, Cu-Au mineralisation and felsic Mesoproterozoic intrusions. At least two of the regions contain Mesoproterozoic intermediate or mafic intrusions. The three regions have a broad spatial correlation with regional-scale, positive gravity anomalies, and may represent the 'footprints' of separate crustal-scale thermal anomalies. To date, a world-class Cu-Au deposit has been identified only in the central region.

The crustal level of exposure of the hydrothermal systems may vary significantly between and even within the three

regions of hydrothermal activity. This is suggested by (1) the temperature range of hydrothermal alteration from high (~450-500°C, CAM assemblages, above) to low (HSCC assemblages), and (2) the variation in styles of structures controlling fluid flow, which range from brittle-ductile shear zones to breccias and brittle faults. Shear-hosted CAM and MB assemblages in the Moonta-Wallaroo district probably formed at deeper crustal levels than breccia and vein network styles of some CAM assemblages in the basement of the Stuart Shelf. The products of near-surface hydrothermal processes are also preserved (beneath sedimentary and regolith cover) in all three regions, particularly in the basement to the Stuart Shelf (eg., at Olympic Dam), and possibly at Prominent Hill. We suggest that uplift or unroofing of some of the hydrothermal systems occurred during and/or after their development, resulting in telescoping of deeper and shallower alteration patterns. The CAM, MB and HSCC assemblages and associated Cu-Au mineralisation, therefore, may represent a continuum from deeper, higher-temperature, shear-hosted settings to near-surface, low-temperature breccia and fault environments. The larger systems discovered, to date, in the Olympic Cu-Au province are of the higher-level style, but this does not rule out the presence of deeper-level styles of economic Cu-Au mineralisation similar to those in the Mt Isa Eastern Succession.

Ongoing investigations of the crustal structure, magmatism, fluid pathways, and timing of hydrothermal and tectonic events are aimed at elucidating the district- to crustal-scale controls on the location of major Cu-Au deposits in the Gawler Craton.

Acknowledgements

The authors wish to thank our colleagues at Geoscience Australia, CODES and at PIRSA for sharing the results of research, discussions, and reviews which have assisted us in the preparation of this paper. We also would like to acknowledge the cooperation of MIM Exploration, Minotaur Resources Ltd, Gunson Resources, WMC, and Adelaide Resources. Brian Logan at the PIRSA drill core facility is thanked for efficiently arranging core layouts.

Roger Skirrow, Evgeniy Bastrakov and Oliver Raymond publish with the permission of the CEO, Geoscience Australia.

Reference List

Budd, A., Wyborn, L. A. I., and Bastrakova, I., 1998 - Exploration significance of the Hiltaba Suite, South Australia. *AGSO Research Newsletter* No. 29 (November), 1-4.

Conan-Davies, M., 1987 - A sheet silicate and fluid inclusion study of the mine area DNW, Olympic Dam, South Australia. Australian National University, unpublished B.Sc. Hons thesis.

Conor, C. H. H., 1995 - Moonta-Wallaroo region: An interpretation of the geology of the Maitland and Wallaroo 1:100 000 sheet areas. Mines and Energy South Australia, Open File Envelope 8886, DME 588/93 (Appendices including drill hole logs).

Creaser, R. A., 1989 - The geology and petrology of Middle Proterozoic felsic magmatism of the Stuart Shelf, South Australia. La Trobe University, unpubl. Ph.D.

Cross, K. C., 1993a - Acropolis and Wirrda Well. *In* Drexel, J. F. Preiss W. V. and Parker A. J., (Eds), The geology of South Australia. Geological Survey of South Australia, Bulletin 54, Vol. 1, p. 138.

Cross, K. C. Daly S. J. and Flint R. B., 1993b - Olympic Dam deposit. *In* Drexel, J. F. Preiss W. V. and Parker A. J., (Eds), The geology of South Australia. Geological Survey of South Australia, Bulletin 54, Vol. 1, p. 132-138.

Daly, S. J., Fanning, C. M., and Fairclough, M. C., 1998 - Tectonic evolution and exploration potential of the Gawler Craton. *AGSO Journal of Australian Geology and Geophysics* 17, no. 3, 145-168.

Davidson, G. J., 1991 - Chemical and physical controls on the development of Oak Dam East: a prodigious uranium-bearing, massive oxide body. Unpublished report to Western Mining Corporation, University of Tasmania Centre for Ore Deposit Studies, 37 p.

Davidson, G. J. and Paterson H. L., 1993 - Oak Dam East: a prodigious, uranium-bearing, massive iron-oxide body on the Stuart Shelf. *Geological Society of Australia Abstracts* 34, 18-19.

Dickinson, S. B., 1953 - The Moonta and Wallaroo Copper Mines. In: Edwards, A. B. (Ed.), Geology of Australian ore deposits. Vol.1:487-504.

Drexel, J. F., Preiss, W. V., and Parker, A. J., 1993 - The geology of South Australia. Mines and Energy South Australia, Geological Survey of South Australia, Bulletin 54.

Eldridge, C. S., and Danti, K., 1994 - Low sulfur isotope ratios; high gold values - a closer look at the Olympic Dam deposit via SHRIMP. The Geological Society of America, Annual Meeting, Abstracts with Programs, Seattle, p.A-498 -A-499

Fanning, C. M., 1997 - Geochronological synthesis of Southern Australia. Part II. The Gawler Craton. South Australia Department of Mines and Energy.

Fanning, C. M. Flint R. B. and Preiss W. V., 1983 - Geochronology of the Pandurra Formation. *South Australia Geological Survey Quarterly Geological Notes* 88, 11-16.

Fanning, C. M. Flint R. B. Parker A. J Ludwig K. R and Blissett A. H., 1988 - Refined Proterozoic evolution of the Gawler Craton, South Australia, through U-Pb zircon geochronology. *Precambrian Research* 40-41, 363-386.

Gow, P. A., 1996 - Geological evolution of the Stuart Shelf and Proterozoic iron oxide - associated mineralization: Insights from regional geophysical data. Unpubl. Ph.D., Monash University.

Gow, P. A. Wall V. J. Oliver N. H. S. and Valenta R. K., 1994 - Proterozoic iron oxide (Cu-U-Au-REE) deposits: further evidence of hydrothermal origin. *Geology* 22, 633-636.

Hafer, M. R., 1991 - Origin and controls of deposition of the Wheal Hughes and Poona copper deposits, Moonta, South Australia. BSc Honours thesis, University of Adelaide, 115 pp.

Hampton, S., 1997 - A study of the paragenesis and controls on Proterozoic (Cu-Fe-Au-REE) mineralisation at the Manxman A1 and Joes Dam South prospects, Mount Woods Inlier, South Australia. Unpubl. Hons thesis, Department of Economic Geology, James Cook University of North Queensland.

Haynes, D. W., Cross, K. C., Bills, R. T., and Reed, M. H., 1995 - Olympic Dam ore genesis: a fluid mixing model. *Economic Geology* 90, 281-307.

Helix Resources Ltd, 2000 - Eyre Peninsula projects including Middleback Range Project, South Australia (web page), *Available at* http:// helix.net.au/pdf/proj/SA-EPMidAuCu.pdf.

Johnson, J. P., and Cross, K. C., 1995 - U-Pb geochronological constraints on the genesis of the Olympic Dam Cu-U-Au-Ag deposit, South Australia. *Economic Geology* 90, 1046-1063.

Johnson, J. P., and McCulloch, M. T., 1995 - Sources of mineralizing fluids for the Olympic Dam deposit (South Australia): Sm-Nd isotopic constraints. *Chemical Geology* 121, 177-199.

McBriar, E. M., 1962 - Primary copper mineralisation at Moonta and Wallaroo, South Australia. MSc thesis, University of Adelaide, 104 pp.

Minotaur Resources Ltd, 2002 - Announcements at http://www.minotaurresources.com.au.

Mortimer, G. E. Cooper J. A. Paterson H. L. Cross K. Hudson G. R. T. and Uppill R. K., 1988 - Zircon U-Pb dating in the vicinity of the Olympic Dam Cu-U-Au deposit, Roxby Downs, South Australia. *Economic Geology* 83, 694-709.

Oreskes, N., and Einaudi, M. T., 1990 - Origin of rare earth element-enriched hematite breccias at the Olympic Dam Cu-U-Au-Ag deposit, Roxby Downs, South Australia. *Economic Geology* 85, 1-28.

—, 1992 - Origin of hydrothermal fluids at Olympic Dam: preliminary results from fluid inclusions and stable isotopes. *Economic Geology* 87, 64-90.

Parker, A. J., 1990 - Gawler Craton and Stuart Shelf. *In* Hughes, F. C., (Ed.), Geology of the mineral deposits of Australia and Papua New Guinea, Australasian Institute of Mining and Metallurgy, p. 999-1008.

Paterson, H. L., 1986 - The Acropolis Prospect. *In* Paterson, H. L., (Compiler), Basement geology of the Stuart Shelf region, 8th Australian Geological Convention, p. 17-23.

PIRSA, 2000 - Iron ore in South Australia. Department of Primary Industry and Resources South Australia.

Reeve, J. S., Cross, K. C., Smith, R. N., and Oreskes, N., 1990 - Olympic Dam copper-uranium-gold-silver deposit. *In* Hughes, F. E., (Ed.), Geology of the mineral deposits of Australia and Papua New Guinea. Melbourne, The Australasian Institute of Mining and Metallurgy, Monograph 14, p. 1009-1035.

Reynolds, L. J., 2000 - Geology of the Olympic Dam Cu-U-Au-Ag-REE deposit. *In* Porter, T. M., (Ed.), Hydrothermal iron oxide copper-gold & related deposits: A global perspective. Adelaide, South Australia, Australian Mineral Foundation, p. 93-104.

Zang, W.-L., 2002 - Late Palaeoproterozoic Wallaroo Group and early Mesoproterozoic mineralisation in the Moonta Subdomain, eastern Gawler Craton, SA South Australia. Geological Survey Branch, Department of Primary Industry and Resources South Australia., Report Book 2002/001

PGC PUBLISHING

Davidson, G.J., Davis, B.K. & Garner, A., 2002 - Structural and Geochemical Constraints on the Emplacement of the Monakoff Oxide Cu-Au (-Co-U-REE-Ag-Zn-Pb) Deposit, Mt Isa Inlier, Australia; *in Porter, T.M. (Ed.), Hydrothermal Iron Oxide Copper-Gold & Related Deposits: A Global Perspective*, Volume 2; PGC Publishing, Adelaide, pp 49-76.

STRUCTURAL AND GEOCHEMICAL CONSTRAINTS ON THE EMPLACEMENT OF THE MONAKOFF OXIDE Cu-Au (-Co-U-REE-Ag-Zn-Pb) DEPOSIT, MT ISA INLIER, AUSTRALIA.

[1]Garry J. Davidson, [2]Brett K. Davis and [1]Andrew Garner

[1]*Centre for Ore Deposit Research (CODES SRC), University of Tasmania, Hobart, Tasmania, Australia.*
[2]*Geology Department, James Cook University, Townsville, Queensland, Australia.*

Abstract - Within the Eastern Succession of the Australian Mount Isa Inlier, Monakoff is a 1 million tonne (mt) Mesoproterozoic, oxide Cu-Au deposit only 13 km from the large (167 mt) Ernest Henry mine. The two deposits share similar geochemical signatures (Ba-Cu-Au-U-Pb-Zn-As-Sb-Co-W-Mo-Mn-F-REE), suggesting commonality of origin. This signature is far more complex than those of most other Eastern Succession Cu-Au oxide systems, but it is extremely similar to the signatures of some recently discovered large Brazilian examples, such as Alemão. Monakoff ore has a barite-carbonate-fluorite-magnetite-chalcopyrite-dominated mineralogy, and contains economic quantities of Cu, Au, Co, U and Ag; the 1–2% levels of both Pb and Zn are unusually high for oxide Cu-Au deposits. However, it lacks the distinctive K-feldspar alteration halo of Ernest Henry. It occurs on the northern south-dipping limb of the Pumpkin Gully Syncline, considered to be a regional, EW-oriented, D2 fold, bounded to the north and west by D1 thrust contacts. A splay of the northern thrust hosts the main Monakoff mineralisation. Naraku Batholith elements outcrop ~2 km north of Monakoff; and ore alteration records post-ore hornfels recrystallisation.

Two lenses of mineralisation occur: the main Monakoff Western Zone, which is a sub-vertical sheet within the shear, and the Monakoff Eastern Zone, which replaced meta-dolerite in the core of a tight D2 fold adjacent to a D1 shear, forming a narrow west-plunging pipe of unknown depth extent. A 10–20 m wide symmetric alteration halo grades inward from carbonate spotting and garnet overgrowths in regional muscovite-quartz-plagioclase schist, through biotite-spessartine-magnetite-plagioclase, to chlorite-spessartine-magnetite. This zoned sequence overprints an earlier biotite-magnetite alteration system that was focussed upon the D1 shear. A large F anomaly extends into adjacent amphibolites and porphyroblastic garnet-biotite schists, at least 130 m across strike, expanding the geochemical halo by more than 10x the dimensions of the observed alteration. The Monakoff Shear experienced movement during the regional D1 and D2 to D2.5 events. Dextral shear during D1 was the major fabric-forming event. Ore formation was synchronous with D2.5 on the basis of: (1) pseudomorphing of earlier fabrics by the ore and alteration assemblage; (2) crenulation of the biotite alteration by D3; (3) preferential development of some ore phases (carbonate, sulphide) in D2.5 crenulations; (4) a lack of pressure-shadowing on alteration garnets; and (5) use of D2 fold structures as fluid conduits. Although evidence mainly favours an epigenetic timing for mineralisation, the footwall shows evidence of minor pre-deformational Mn-Al-K-Fe metasomatism, associated with BIF formation.

Our Monakoff ore formation model involves flexural slip and production of dilatancy in broad, near-horizontal, D2.5 folds, a mechanism which accounts for the sheet-like ore geometry in vertical beds. Flexural slip was concentrated on the lubricated D1 shear system, with packages of ore fluid being drawn in by extensional failure at various scales. The geometry of extension during D2.5 favoured the inflow and mixing of fluids from above and below. As at Ernest Henry, mixing deposited barite, U-phases, carbonate, Mn-minerals, and fluorite; the components of these phases are not effectively transported and deposited from one fluid. The metals and oxidised S were carried in a corrosive, F-rich, >500° C magmatic vapour and fluid, which condensed in, and reacted with, reduced K-Ca-Ba-Mn-Cl-rich waters, as well as Fe^{2+}-rich assemblages in the wallrocks, such as pre-existing magnetite.

Editor's note: This paper has been included to report the details of an important integrated, structural and geochemical study by two major research centres. It provides new insights into the formation of iron oxide copper-gold mineralisation within the Mount Isa Inlier, and by inference with other major deposits and districts around the world with similar geochemical signatures. Monakoff's significance is not in its size or economic value, but in what it can contribute to the understanding of this style of mineralisation. It has been mined and studied since well before the discovery of the nearby much larger Ernest Henry orebody, which has both similar and contrasting but complementary characteristics.

Introduction

Monakoff, which outcropped in the Proterozoic Soldiers Cap Group 20 km ENE of Cloncurry (in NW Queensland, Australia) has long been regarded as a significant ore deposit in the Mt Isa Eastern Succession, with an indicated reserve of 1 mt (million tonnes or 'metric tons') @ 1.5% Cu and 0.5 g/t Au (Milner, 1993). It is distinguished by its association with iron formation, its unusual Ba-Cu-Au-U-Pb-Zn-As-Sb-Co-W-Mo-Mn-F-REE geochemistry, and its barite-carbonate-dominated mineralogy. The metal association is extremely similar to that of the large Ernest Henry deposit (167 mt @ 1.1% Cu and 0.54 g/t Au; Mark et al., 2000), which lies only 13 km to the north. In the Mount Isa Inlier, other geochemically similar but sub-economic occurrences are known at Milo, Dairy Bore and Blockbuster-Mobs Lease (Davidson, 1998). Globally the metal association closely resembles that of the recently discovered Alemão copper-gold deposit (Carajás, Brazil), as well as having many geochemical features in common with Olympic Dam (Australia), Igarapé Bahia (Brazil) and Salobo (Carajás, Brazil) (Ronzê et al., 2000; Reeve et al., 1990; Tazava and Oliveira, 2000; Souza and Vieira, 2000). Most other Cu-Au occurrences in the Mt Isa Inlier, such as Starra, Mt Elliott, Eloise, Osborne and Mt Freda, (Fig. 1; Rotherham, 1997; Garrett, 1992; Baker, 1998; Adshead, 1995; Davidson, 1998), lack Ba-Mn-As-Sb-F-U-REE-Pb-Zn enrichment. This paper aims to provide a detailed geological, mineralogical and geochemical context for the Monakoff deposit, and to gain a greater insight into the mechanism of formation of these geochemical groupings amongst oxide Cu-Au deposits. Our findings are based upon logging of 3 deep diamond drill holes (Ashley, 1983), detailed field mapping of a 1.5 x 0.5 km area, magnetic susceptibility measurements, major and trace element profiles, examination of spatially oriented thin sections, and a compilation of previous mineral exploration and research (Ashley, 1983; Laing, 1991; Milner, 1993).

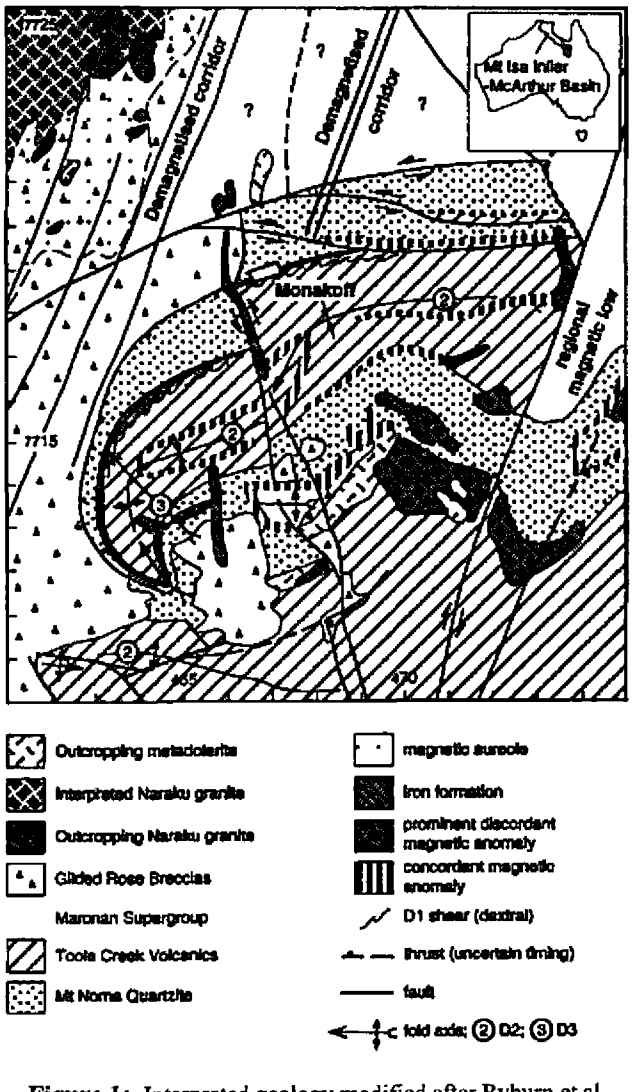


Figure 1: Interpreted geology modified after Ryburn et al. (1988), constructed using aeromagnetic data.

Stratigraphy and Regional Geology

The Eastern Succession consists of poly-deformed Palaeo- and Mesoproterozoic volcano-sedimentary sequences that were intruded by voluminous granite batholiths at 1540–1500 Ma (Williams and Naraku Batholiths; Pollard et al., 1998, Wyborn, 1998). All sequences were deposited in intracontinental rift settings, though the relationship between some sequences is obscured by the deformation history, and is the subject of continuing detailed research. Thin skinned deformation (~1600 Ma to 1520 Ma) of the Isan Orogeny resulted in gross eastward tectonic transport (Macready et al., 1998), interleaving of major lithostratigraphic units, and a dominant north-south tectonic grain. Deformation is conventionally divided into: (D_1) large-scale thrusts and isoclinal folds; (D_2) major north-south upright to inclined isoclinal fold trains; and (D_3) brittle-ductile spaced NW and NE-trending corridors of faulting, kinking, and folding. Major epigenetic hydrothermal activity was largely coincident with granite intrusion, and with brittle-ductile deformation phases of the orogeny. It produced regional sodic-calcic metasomatism and globally significant oxide Cu-Au deposits (De Jong and Williams, 1995; Mark, 1998; Williams, 1998). Large sediment hosted Zn (Dugald River) and Broken Hill-Type Pb-Zn-Ag deposits (Cannington, Pegmont) also occur within the Eastern Succession.

Two sequences predominate in the Monakoff area: the Soldiers Cap Group (1660–1680 Ma; Page and Sun, 1998) of the informally defined Maronan Supergroup (Beardsmore et al., 1988), and the Corella Formation of the Mary Kathleen Group (~1740 Ma; Page, 1988). Surface geology and seismic interpretation indicates the two to always be in tectonic contact (Beardsmore et al., 1988, O'Dea et al., 1997). The two major contacts are the Cloncurry Overthrust and the Pumpkin Gully Fault. In fact the Cloncurry Overthrust changes from a single NW-trending strand south of Cloncurry, to several NE-trending *en echelon* segments and splays (including the Pumpkin Gully Fault) north of Cloncurry. Regionally, the outcropping Soldiers Cap Group north of the Weatherley Creek Syncline differs from equivalent stratigraphy further south in its low metamorphic grade (greenschist transitional to amphibolite; Ashley, 1983, Rubenach and Barker, 1996), and less intense structural fabrics; consequently many primary igneous and sedimentary structures are preserved.

The Soldiers Cap Group is a conformable carbonate-poor stratigraphic succession younging from the Llewyllen Creek Formation (pelite, arenite), through the Mount Norna Quartzite (quartzo-feldspathic arenite, carbonaceous pelite, metagreywacke, metabasalt, iron formation) to the Toole Creek Volcanics (metabasalt, minor carbonaceous metasediment, iron formation) (Derrick et al., 1976). Dolerite sills and dykes were widely intruded, largely prior to the main metamorphism, in some cases prior to consolidation. These were followed by the Corella Formation which consists of well bedded scapolitic carbonate and quartzo-feldspathic layers, inferred to have been deposited within a shallow marine to evaporitic shelf environment (Reinhardt,1986); it is widely suggested to have been a major source of saline fluids during metamorphism (eg., Oliver, 1995). Where it is strongly intra-formationally brecciated it is referred to as Corella breccias (Ryburn et al., 1988), and where it is brecciated and contains exotic clasts it is referred to as Gilded Rose breccia, considered to be hydrothermal in origin (Marshall and Oliver, 2001).

Cu-Au mineralisation is hosted mainly within the Soldiers Cap Group, with only minor occurrences adjacent to or within the Corella Formation breccias within 1 km of more significant accumulations. The dominant Cu-Au mineralisation styles in the Cloncurry area are:

1). replacement Cu-Au-U barite-siderite lenses associated with iron formations, of which Monakoff is the largest known example;

2). brittle Mt Freda-style carbonate vein and replacement deposits;

3). albitite-associated vein and replacement deposits;

4). brittle-ductile quartz vein and vein networks, subdivided into a). Gilded Rose-type, and b). Eloise-type (Davidson, 1998).

Monakoff occurs within an unusual east-west trending, south-younging belt of Soldiers Cap, which is separated from Corella breccia to the north and west by D1 thrust contacts. The deposit occurs on the northern south-dipping limb of the D2 Pumpkin Gully Syncline, on a tectonic contact between the Mount Norna Quartzite and the Toole Creek Volcanics (Ashley, 1983). This position corresponds to a regionally extensive linear magnetic anomaly, with sporadic iron formations and ironstones as its outcrop expression. Approximately 1 km west of Monakoff, the ore stratigraphy is off-set by ~500 m across a sinistral, sub-vertical, north-striking fault which can be traced magnetically southwards through the Pumpkin Gully Syncline down to a major fault intersection close to the Matilda Highway (Fig. 1). This fault is of interest because it hosts intrusive calc-silicate breccia bodies, and contains carbonate-quartz breccia veins similar to those that host Mount Freda-style mineralisation (Davidson, 1998). Around 3 km of the fault has a positive magnetic expression near Monakoff. A second set of east-west faults and fault-splays, again with sinistral offset, are visible in aeromagnetic images some 1 to 2 km north of Monakoff. These are interpreted to repeat the ore horizon several times to the north-east under cover. A fault with an orientation and offset that is consistent with this fault generation separates the Monakoff West Zone from the Monakoff East Zone of mineralisation (Fig. 2). No granitic intrusives have been identified at Monakoff. The nearest granites, 2 km north of Monakoff, are outcropping sentinels of the Naraku Batholith, with the main metamorphic aureole to the batholith occurring a further 2 km NW (Fig. 1).

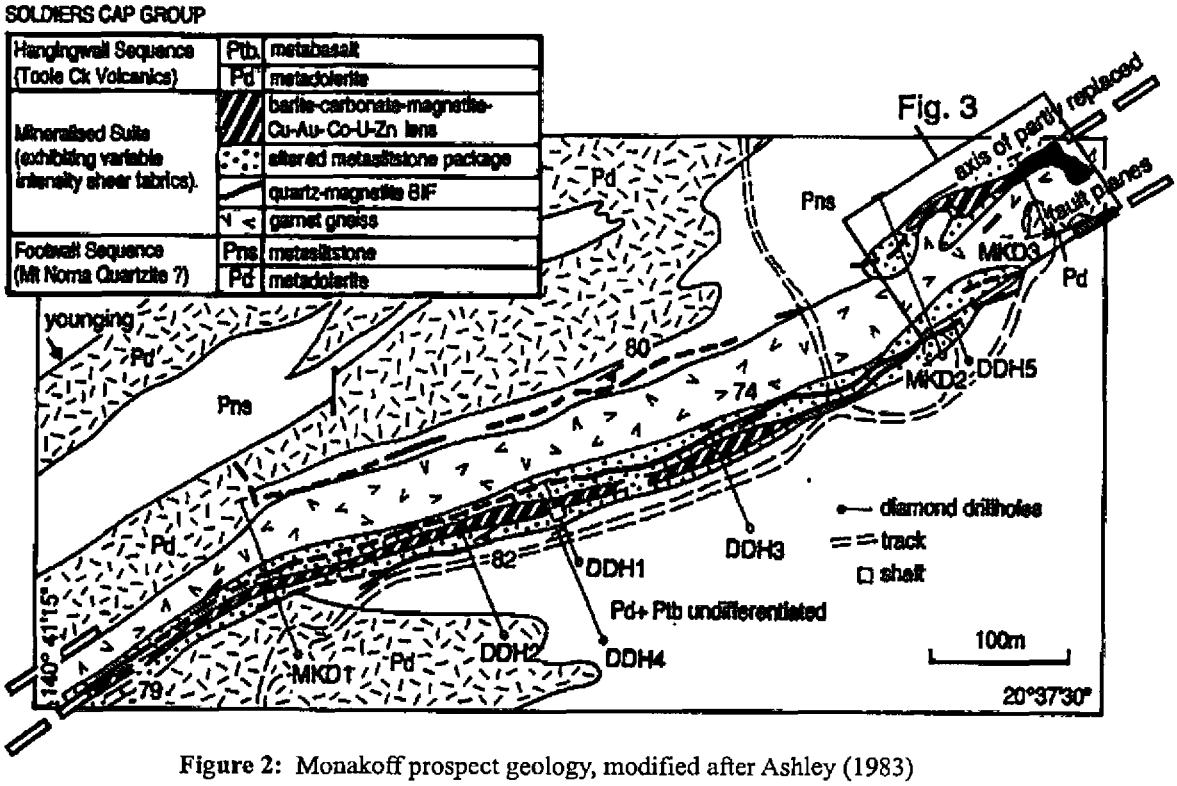


Figure 2: Monakoff prospect geology, modified after Ashley (1983)

Deposit Geology

Discovered by prospectors prior to 1908, Monakoff was drilled in several phases by companies between 1954 and 1997, including Gold Mines of Australia (3 holes, one shaft), Mount Isa Mines (2 holes), Esso Minerals (3 holes) and Cloncurry Mining (30 shorter holes during mining delineation). Most exploration programs adopted a syngenetic ore genesis model because of the sheet-like nature of the ore. Laing (1991) briefly interpreted Monakoff as an epigenetic ironstone-hosted deposit at the conjunction of a D1 mylonite and a later structure. Cloncurry Mining removed approximately 300 000 tonnes by open pit mining, ceasing operations in 1997. The deposit stratigraphy was originally preserved in a low 1 km long ridge, now partly removed by mining, rising 30-40 m above the plains to the north. Outcrop is moderate in the footwall, good to excellent in the ore stratigraphy, and moderate in the hangingwall.

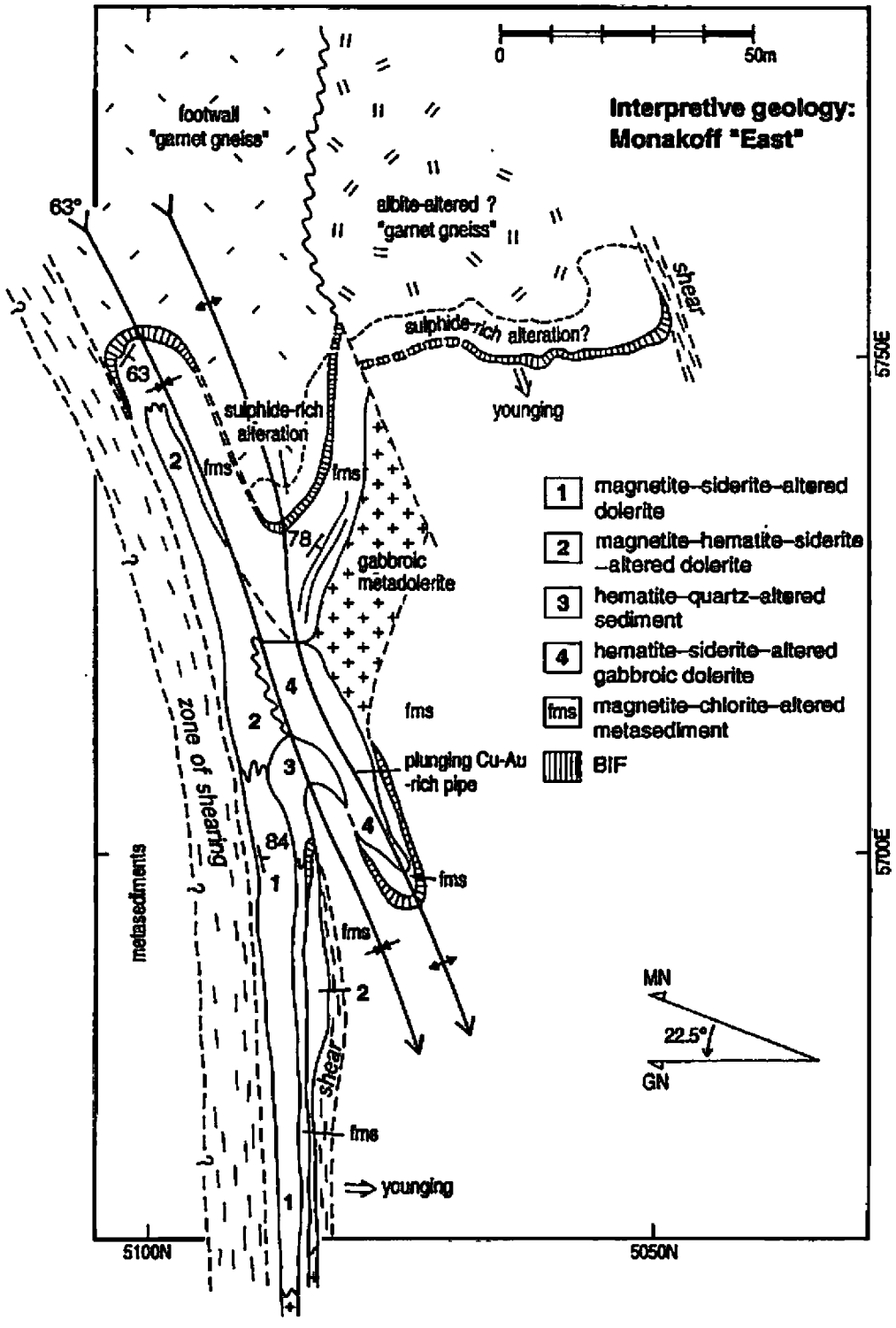


Figure 3: Interpretive map of the Monakoff East Zone mineralisation, emphasising the fold hinge control on the replacement of a meta-dolerite. The factual surface map is presented in Davidson (1995).

Footwall

The upper 100 m of footwall lithologies comprise intercalated magnetite-bearing muscovite pelites, psammo-pelites, and meta-dolerites of the uppermost Mount Norna Quartzite, overlain by massive porphyroblastic garnet-biotite schist, then a persistent iron formation, and lastly by strongly sheared metasediments immediately hosting the Monakoff West ore. The metadolerites form continuous sills with locally angular contacts and variable epidote alteration, particularly adjacent to sediment contacts. Most also either preserve peperitic margins or contain peperitised silicified sediment for 0.2–1.0 m away from their margins (Plate 1b), indicating that they intruded un-lithified host sediment (Davidson and Davis, 1997; Hatton et al., 2000). The pelites, which dominate the upper 100 m of Mount Norna Quartzite stratigraphy at this location, contain only fine 1–3 mm laminations, which may be either sedimentological or tectonic in origin. Conversely, psammo-pelites are present below 100 m as 0.5 m thick graded beds containing cross-bedding, plane lamination, convoluted bedding, flame structures and rip-up clasts, all consistent with a turbiditic emplacement origin and indicating upward-facing stratigraphy. The predominant metamorphic assemblage in the sediments is muscovite-plagioclase-quartz-magnetite±tourmaline.

The porphyroblastic garnet-biotite schist (Plate 2a) is mainly massive, with randomly oriented lathes of plagioclase, and a lower peperitic contact indicating an intrusive origin during lithification. However, the upper 3-5 m contains quartz-magnetite-filled vesicles consistent with an extrusive coherent lava origin. Thus a partly intrusive, partly extrusive igneous origin is indicated. Ashley (1983) favoured an andesitic parentage for this unit, with significant pre-metamorphic Si-K-Fe-Mn alteration to account for the mineralogy. Detailed geochemistry (see "geochemistry" section) confirms that the unit is far more felsic than the majority of igneous products in the Toole Creek Volcanics, possessing high field strength element abundances that are consistent with an andesitic to dacitic precursor.

The continuous, thin (1-2 m), prominently banded, quartz-magnetite±hematite BIF can be traced through the whole prospect ~5–10 m above the top of the porphyroblastic garnet-biotite schist, hosted by pelitic metasediment. Bands vary from 1-2 mm wrinkly lamination (possibly crenulations; Plate 2b), to 0.5 cm interbands of quartz-barite, and spessartine-magnetite. The unit regularly and preferentially contains F1, F2 and F3 micro- to meso-scale folds (Plate 2e), which is evidence that it formed prior to any regional deformation. Approximately 3 km west along strike from Monakoff, iron formations at this stratigraphic position are interbedded with sedimentary or hydrothermal carbonate beds 30 cm thick, all folded by D1-folds (Plate 2e). Ryburn et al. (1988) describe stromatolitic structures in carbonates of this horizon. This association has not however been recognised at Monakoff. BIF defines the major D2 fold structure hosting the Monakoff East Zone, where it is also enclosed in places by carbonate-barite alteration (Fig. 7). The Monakoff West Zone mineralisation consistently occurs 20–30 m above the BIF (Fig. 2, and detailed geological maps in Davidson and Davis 1996), although the BIF is strongly anomalous in most ore elements. The immediate footwall and hangingwall to ore are bedded and strongly sheared fine to medium-grained, dark-grey magnetite-bearing siltstones.

Several minor transgressive lithologies occur in the footwall. These include: 1). areas of variable muscovite-alteration, particularly associated with orthogonal fractures, which become more abundant westwards; 2). north-south oriented 'pebble' dykes, with clasts of sericitised wallrock, and matrices of albite-actinolite-carbonate-sulphide (weathered), together with parallel calcite-siderite-muscovite-scapolite-quartz-chalcopyrite veins up to 0.5 m thick (Plates 1f & 2c); and 3). one isolated, 30 m diameter outcrop of "Gilded Rose" breccia approximately 200 m north of the main shaft at Monakoff, which field relations indicate to be vertical and intrusive. The carbonate-bearing veins are magnetite destructive and have halos in core that extend away from the vein for ~10x the vein-width (Plate 1f). This vein generation also occurs on lithological contacts west of Monakoff, where its orientations indicate an emplacement during strike-slip movement. Their lack of deformation indicates a D3- to post-D3 timing.

Hangingwall

A 20-30 m thick interval of short strike-length metabasalts, minor iron formation, volcanic conglomerate, breccia-bearing limestone, and meta-dolerites occur immediately above the thin strip of sheared metasediment that hosts ore. A local spectacular pillow breccia outcrops close to the ore package near the centre of the deposit, although this was not encountered in core. Ryburn et al. (1988) also report black carbonaceous limestone and stromatolitic chert from this stratigraphic position, but these lithologies were not observed by the authors. More common elements of the Toole Creek Volcanics occur above this complex facies assemblage, consisting of massive medium to coarse-grained meta-dolerite to gabbro in the west, and mixed meta-dolerite, meta-basalt, siliceous siltstone and minor iron formations in the east. Unlike the upper Mount Norna Quartzite, no regional spessartine-biotite alteration is present in the hangingwall. Epidote alteration is present inhomogeneously along thin vein zones and particularly along mafic unit contacts, where it may form 1-5 m wide epidote-quartz pods. Along-strike from the Monakoff mineralisation, a zone of this material is deformed by D1 structures, suggesting that it is a pre-deformational alteration type. In core, small post-metamorphic biotite-carbonate-magnetite veins occur that appear to be mineralogically similar to some parts of the ore package alteration.

"Ore Package"

Ashley (1983) considered the "ore package" to include the altered rocks adjacent to the ore, the ores themselves, and the overlying sediments and basaltic tuff, all younging and

dipping southward (Fig. 2). It consequently includes some units already described above. Ryburn et al. (1988) defines the base of the Toole Creek Volcanics at Monakoff as the top of the ore "package", or the base of the first meta-basalt/meta-dolerite above the ore. The ore package contains two structurally separate mineralisation zones: 1). Monakoff East, which has a steep pipe-like geometry, and was not included in the quoted ore reserve; and 2). Monakoff West, which was mined and has the form of a steeply dipping sheet. Monakoff East is slightly deeper in the stratigraphy than the Monakoff West Zone.

Near-ore alteration commences in the footwall with distinctive porphyroblastic spessartine-biotite-quartz-plagioclase-chloritoid-tourmaline-biotite development in the meta-andesite (Plate 2a), in which the idioblastic garnet is disseminated or forms irregular bands localised on peperite zones. In places pink spessartine is overgrown by coarse-grained almandine + quartz, indicating that Monakoff peak metamorphism exceeded the almandine isograd. It is not certain if almandine stability was attained during regional D2, or whether it occurred during a local contact metamorphic effect that developed during intrusion of an unexposed granite. However, almandine does provide an important time constraint on spessartine growth, which itself required a Mn-rich stratigraphy or fluid for growth. Chloritoid has a randomly oriented distribution, and contains a magnetite-defined foliation, S1 or S2.

Post-peak metamorphic alteration is abundant above the garnet-biotite schist, exhibiting zoning around the ores, low-angle shears, and tension gashes. The general alteration sequence spanning scales of from 0.5 to 10 m distant from mineralised zones is an outer chlorite-spessartine (Plate 3e), inward to biotite-magnetite ±pyrite, to siderite-magnetite ±pyrite alteration as ore or sulphide-bearing veins/fractures are approached. In meta-siltstones this alteration forms pseudo-breccias (Plate 1a, 3g), in which 'clasts' have distinct dark biotite-rich centres. Carbonate alteration also preferentially affects thin basaltic dykes or extrusives. The general complexity of the fabrics are heightened by probable peperitic relationships, pillow basalt fabrics, and autoclastic brecciation that formed during volcanism.

A constraint on timing of ore and alteration is provided by a 1.5 m wide post-ore dyke in MKD2 (Fig. 2), which is not exposed in outcrop. This dyke contains only minor chlorite alteration of olivine, but is chilled against barite-chalcopyrite ore on one hand, and severely altered dyke host rock on the other. Furthermore, barite-carbonate ore is metamorphosed at the dyke contact, producing 1 cm long siderite porphyroblasts. Insufficient K was present in the dyke to obtain an Ar-Ar age estimate. However, a lack of ore-related alteration indicates that the dyke post-dates D2.5 (see structural section) and could be part of the Lakeview Dolerite swarm (~1100 Ma) which intrudes parts of the Mount Isa Inlier. It plots in the sub-alkaline basalt field (Nb/Y ~ 0.30–0.34) of Winchester and Floyd (1977), ie. more alkaline than the small surrounding amphibolite host rock population (Nb/Y~0.1–0.2), assuming that the relative abundances of the high field strength element have not been altered.

Structural History of Monakoff

A multistage deformation history is well developed at Monakoff, particularly in the main ore-related shear zone and rocks bounding it. The deformation history comprises four events, herein termed D1, D2, D2.5 and D3. These correlate well with events of the same generation recognised for the Isan Orogeny regionally, although some orientations are unusual. D1 was responsible for formation of the main central shear zone, hereafter referred to as the Monakoff Shear Zone, which is apparent as a zone of S1 foliation intensification several metres to tens of metres wide that trends sub-parallel to lithological layering (bedding) within the ore package. Production of the shear zone would appear to represent deformation partitioning involving accommodation of D1 shear strain by the phyllosilicate-rich horizons between the hangingwall mafic Toole Creek Volcanics and the massive porphyroblastic garnet-biotite schist (Fig. 2), with strain enhanced dissolution causing a relative increase in the amount of phyllosilicate. Interestingly, D1 potentially comprises two phases of deformation, producing a deformation history similar to that noted by Davis et al. (2001a) in the Quamby area to the north.

S1 in the Monakoff Shear Zone is a subvertical mylonitic fabric that anastomoses around elongate, ellipsoidal pods of relatively more quartz-rich material that have

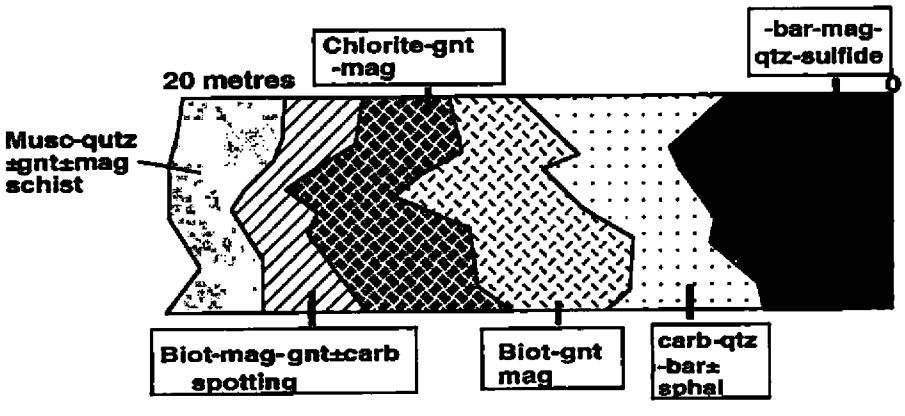


Figure 4: A schematic view of alteration types spreading away from ore on the right hand side of the figure, Monakoff Western Zone.

accommodated D1 shortening strain (Plate 1c). These pods vary in scale from centimetres to tens of centimetres, and generally have aspect ratios in plan of 2:1 to 4:1. Their extent in the third dimension is unknown. In the shear zone, the mylonitic fabric is folded about steeply plunging folds that are tight to isoclinal, and centimetres to tens of centimetres in wavelength. Microscale crenulations exhibit locally consistent asymmetries that change across cm-scale F1 fold hinges, indicating that folds and crenulations are of the same generation. These F1 folds are in turn deformed by a subvertical fabric that is continuous with, but distinguishable from, that interpreted to represent the regional S2 fabric. As such, there appears to have been two stages of deformation comprising D1, namely formation of the main shear fabric representing the initial stage, and ongoing reactivation of this fabric during formation of the folds and micro-crenulations of the latter stage. Alternatively, fabric formation and overprinting folds represent complex patterns of repartitioning of shearing and shortening strain during progressive D1 deformation.

Maximum inter-limb angles of the folds produced during the second stage of D1 are of the order of 30°. These folds are generally isolated, intrafolial and rootless, although some fold couplets and triplets have been noted. Fold asymmetries are common and the dominant population indicates that sense of shear during D1 was dextral. This is in good agreement with the shear sense movement resolved from other kinematic indicators such as foliation geometries and clast asymmetries. However, west of Monakoff in the Pumpkin Gully Syncline, the axes of decimetre- to metre-scale F1 are near-horizontal, probably as a combined result of strong rotational strain in the main shear during D1 and the effect of overprinting deformation.

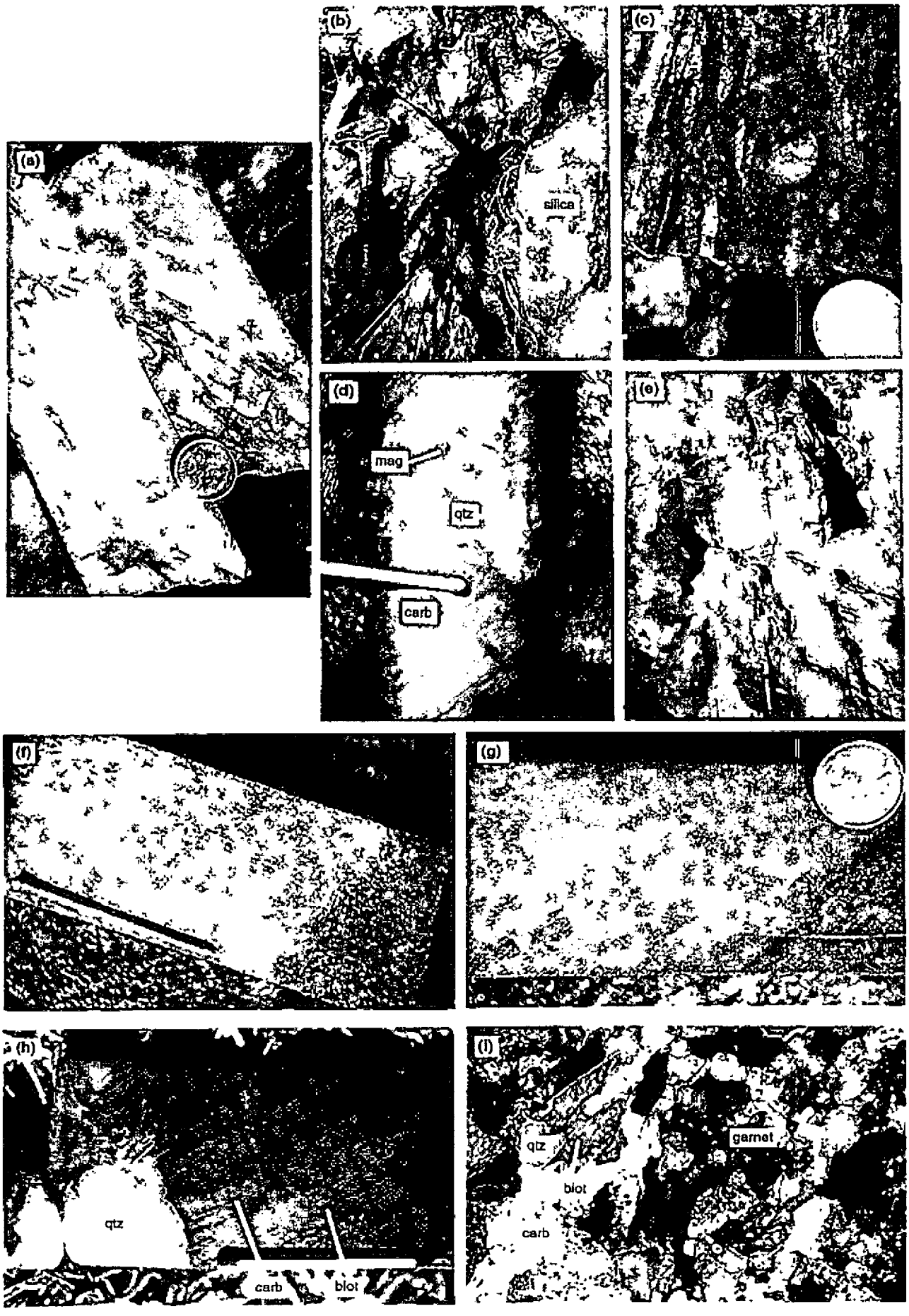
D1 kinematic indicators are best represented by foliation geometries around and within clasts (Fig. 5), and indicate an overall dextral sense of movement on the shear zone (Plate 2f). Local shear reversals, which have produced geometries indicative of sinistral shear, have also been observed but are uncommon. Dramatic volume loss was experienced by shear zone rocks and we interpret this to be due to shear enhanced dissolution of minerals such as quartz. This is evident where zones of high D1 shearing strain have impinged on individual lithological layers and caused marked reductions in thickness. Such zones of high shearing strain are most evident against large quartzose clasts where strain accumulation has occurred.

At the outcrop scale, D2 produced meso-scale folds, generally of centimetres to tens of centimetres in wavelength and amplitude. Folds vary from open to tight (Fig. 5), and commonly deform D1 folds within the central shear zone. S2 is a pervasive, approximately northwest trending cleavage that varies from a fracture cleavage to a schistosity. The similar orientations of S1 and S2 have produced a composite S1-S2 fabric, particularly on F1 fold limbs. Alignment of magnetite within this composite fabric suggests D2 growth. L_1^2 lineations are steeply plunging sub-parallel to F_1^2 fold axes. The L_2^2 stretching lineation is steeply pitching in S2. The structure of the Monakoff East Zone is dominated by a large, steeply plunging, tight F2 fold with a wavelength of ~20 m, the hinge of which is defined by a cylindrical mineralised breccia pipe (Fig. 3). A syn- to post-D2 age of brecciation is implied by the control of the F2 hinge on the location and orientation of brecciation (although this does not necessarily imply the same age for the mineralization contained within it). Kinematics for D2 are indicated by a dominance of crenulation asymmetries exhibiting north-side-up sense of shear, which are also preserved within the core of garnet porphyroblasts. These garnet cores are interpreted to have grown syn-D2.

D2.5 structures (Plates 2h, 3e) are best developed at the northern end of the deposit, particularly within zones of chlorite schist in the central shear zone. F2.5 folds are rare and restricted to open flexures. Accumulation of D2.5 shearing strain against the margins of the syn-D2 garnet porphyroblasts has rotated the D2 differentiated crenulation with a top-to-the-southwest sense of shear, producing sigmoidal and spiral foliation geometries. The rotated fabric is continuous with S2 in the early garnet cores and subsequent D2.5 growth of garnet has preserved this geometry as sigmoidal and spiral inclusion trails. Elsewhere the S2.5 fabric is pervasively developed but the earlier S2 crenulation has been destroyed, restricting fabric geometries to sigmoidal D2.5 crenulations. S2.5 is best developed within chlorite-rich zones that are associated with biotite-garnet-chlorite alteration. This alteration forms a halo to the deposit and is potentially associated with the mineralising event.

Given that the garnets are an integral part of the alteration assemblage and that the majority of them show micro-structural relationships consistent with growth during D2.5 (Plate 3e), a post-D2 to syn-D2.5 age is interpreted for the emplacement of mineralisation. Furthermore, this suggests that the D2 and D2.5 events may have been very closely spaced in time. Emplacement of mineralisation during progressive deformation is indicated by the occurrence of ore phases in oblique-chocolate block boudinage veins, observed both in core and in outcrop, with extension occurring in competent units in both near horizontal and near-vertical directions. Boudinaged neck zones in the intense metasomatic halo, or in the weakly altered host rock, generally consist of quartz vein-fill with minor garnet, monazite ± galena-pyrite-sphalerite (Plates 1d, 1h). They are surrounded by radiating fracture networks of magnetite, that cross-cut pervasive siderite replacement zones, surrounded in turn by strong biotite alteration. In outcrop, a string of such failure zones sub-parallel to bedding, and associated layer-parallel alteration, resemble original Fe-Mn-rich beds, but in fact such zones result from the preferential flow of fluids parallel to S0/S1/S2. In mineralised zones, the main boudin neck mineralogy is barite-carbonate-fluorite.

Deformation during D3 was coarsely partitioned on the meso-scale, resulting in corridors of well developed decimetre-scale folds with local intense S3 developments that are separated by zones of relatively less intense cleavage development and an almost total absence of folding (eg., 5200E, see Davidson & Davis 1996 for maps).


(a)
(b)
silica
(c)
(d)
mag
qtz
carb
(e)
(f)
(g)
(h)
qtz
carb
biot
(i)
qtz
biot
carb
garnet

In the zones of intense deformation, S3 is present as a steeply dipping, approximately north-northeast striking, crenulation or differentiated crenulation cleavage (Plate 2g). The best overprinting evidence for S3 occurs where it has cross-cut the shallow S2.5. In zones of high D3 shearing strain, the accumulation of D3 strain against garnet porphyroblasts has destroyed pre-D3 geometries except in very rare strain shadows adjacent to the garnets. Locally, S3 is present as a planar fabric displaying consistent asymmetry. This consistent asymmetry is observed on both sides of some folds, indicating that the folds are products of pre-D3 deformation. On the limb of the earlier folds, where the asymmetry was the same as that for the late sub-vertical event, an intense composite foliation has been produced. Foliation asymmetries (crenulations, S-C fabrics) for pre-D3 fabrics have been noted on the limbs of folds where the asymmetry of the earlier fabric was opposite to that of the late one. S3 is also defined by crenulations in biotite alteration, and this biotite is considered part of the alteration halo to the mineralisation (see "alteration" section).

In the zones of relatively less intense D3, zones of unfolded material between F3 fold corridors commonly contain pre-D3 surfaces (bedding and foliations) that have been in orientations favourable for accommodating D3 shearing strain. In general, S2 in zones of foliation reactivation has been deformed but not destroyed, indicating that deformation associated with this process was quite minor in many places within the deposit. This supports the view that the dextral asymmetries noted throughout the shear zone are preserved D1 geometries, and that the shear sense during D3 was the same as that in D1. Depending on how the deformation was partitioned and redistributed during progressive D3, these pre-existing surfaces accommodated both synthetic and antithetic shear relative to the overall D3 shear sense in adjacent folded layers. The reactivation of pre-D3 surfaces also produced apparently ambiguous structural overprinting relationships. S1 planes that were reactivated by D3 now lie axial planar to crenulations of S2.

Of interest are micro-structural relationships indicating that a final stage of garnet growth occurred late-syn- to post-the formation of S3. The late planar S3 is continuous with planar inclusion trails in the garnet rims, and deflection of the fabric at the margin of porphyroblasts is minimal to absent. The late stage of garnet growth is only detectable via inclusion style and content. The final rim-phase of garnet growth locally occurs as elongate crystals that have grown syntaxially from zones of quartz-rich folia out into, and at right angles to, the adjacent chlorite-rich foliation zones. Magnetite crystals are generally larger in the matrix than in the garnet porphyroblasts (Plate 3e), indicating ongoing magnetite growth into the late stage of deformation and porphyroblast growth (D3?). Furthermore, these micro-textural relationships suggest that some magnetite at least is not temporally related to mineralisation as it post-dates it.

Mineralisation

The main western ore zone forms an east-dipping sheet 700 m long x 2-10 m thick, with unknown depth extent, whereas the smaller eastern mineralisation, ~100 m northeast of the end of the western zone, forms a pipe-like body that plunges very steeply west, with a 40 m strike length at surface. Between the two zones, porphyroblastic garnet-biotite schist is replaced by unmineralised albite around a sinistral D3- to post-D3 fault (Fig. 3); this alteration style is not seen elsewhere in the prospect, but is regionally common around post-orogenic granites (Mark, 1998). The textures, settings and associations of the two mineralised zones are very different.

The western zone is enclosed by, and replaces, magnetite-bearing meta-siltstones. At surface it is manifested as a friable, resistant, massive unit with variable black pyrolusite and malachite staining, sometimes given the field term "garnet sandstone", on the basis of its arenaceous texture and pink colour (Plate 1e). At depth it is a remarkably massive unit compared to surrounding alteration (Plate 1g, 3a, 3b, 3c), and consists of barite, ponite (Fe-rhodochrosite; see ore mineralogy section), magnetite, chalcopyrite, pyrite, spessartine, fluorite ±K-feldspar, sphalerite, galena, arsenopyrite, mackinawite, molybdenite, brannerite/davidite, pentlandite and linnaeite (Ashley, 1983). This mineralogy gives rise to the cosmopolitan element assemblage Cu-Au-Ag-U-Zn-Pb-Co-Mo-W-Sn-F-Mn-Ba-Sr-LREE-As-Sb-Bi.

The eastern zone is distinctive because it appears to be mainly a replaced medium-coarse-grained amphibolite, within a tight D2 fold adjacent to an unexposed east-west fault (Fig. 3). In outcrop it is represented by a 50 m long

Plate 1: (see page opposite)

(a) MKD2/40m In situ tectonic breccias broadly related to boudinage, with pyrite-magnetite veining carbonate (rims) and biotite (centres) clasts;
(b) peperitic amphibolite margin, displaying characteristic silicified sediments, and sediment clasts;
(c) magnetite-infiltrated silicified mylonite, immediate ore hangingwall;
(d) MKD1/64.7m Small boudinage neck vein in muscovite-quartz schist, with quartz fill, a fine garnet and pyrite selvage, brown carbonate alteration, and crack-filling magnetite;
(e) Typical weathered Monakoff Western Zone ore, with a planar foliation, and pink barite-fluorite with black Mn staining;
(f) MKD1/51.5m. Epidote alteration around thin quartz veins in amphibolite, hangingwall;
(g) MKD1/78.0 m. Typical chalcopyrite-rich mineralisation, Monakoff Western Zone
(h) MKD1/64.3m. Quartz vein-fill in a boudin-neck zone, with corresponding dark Mn-Fe-carbonate and magnetite metasomatism (dark laminae), fringed by biotite-garnet alteration;
(i) MKD1/74.5m. (f.o.v. 2mm, crossed polars) sample at the biotite-garnet and carbonate-barite boundary, showing garnet-biotite breakdown.

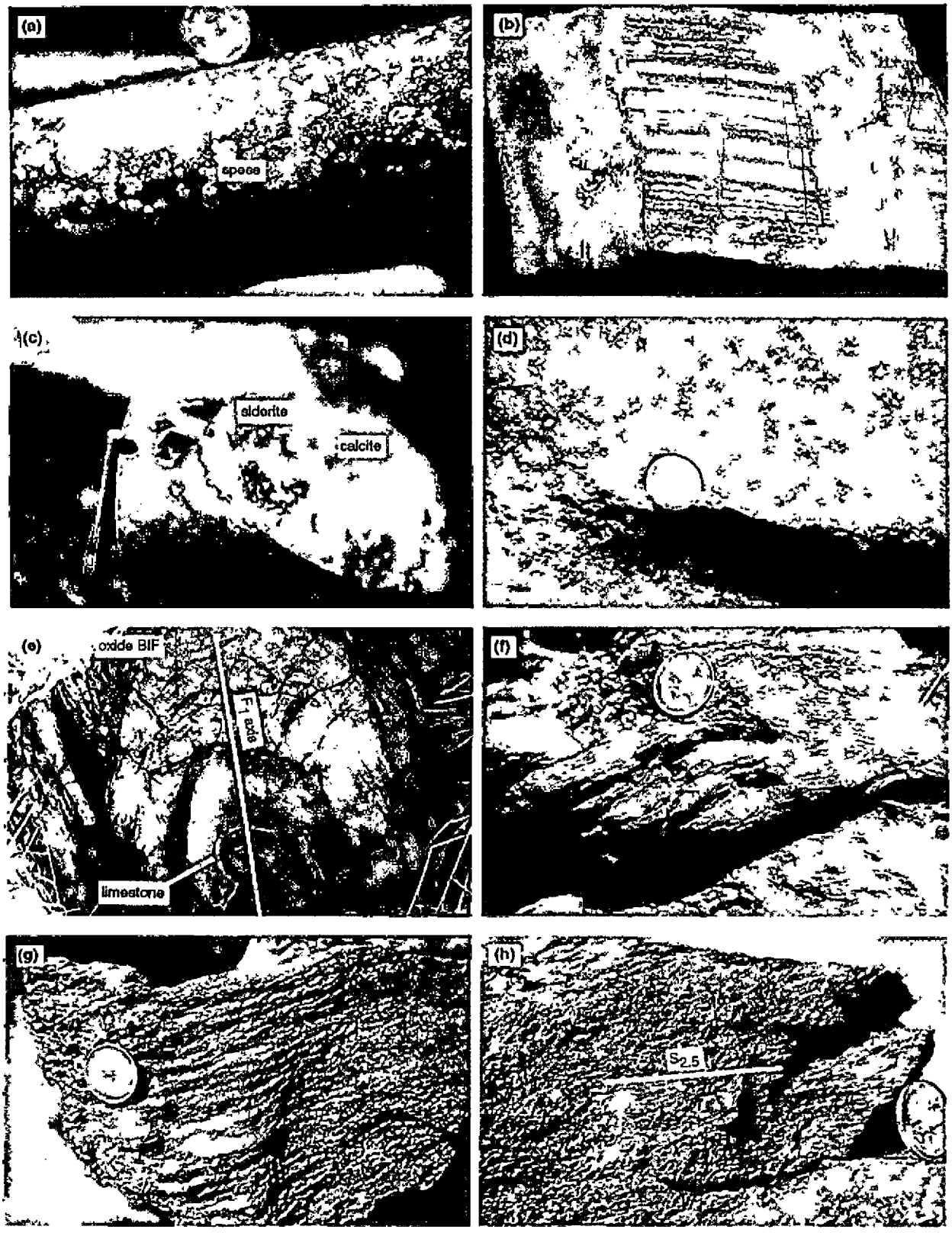


Plate 2:

(a) MKD1/93.3m Typical porphyroblastic garnet-biotite schist, identified as a meta-dacite/andesite;
(b) Banded iron formation from the "ore package", transected by numerous coarse and fine weathered sulphide veins;
(c) MKD1/115.7 m. Siderite (brown)-calcite vein (post-ore) with a magnetite-destructive halo in footwall porphyroblastic garnet-biotite schist;
(d) Coarse magnetite-barite assemblage from the Monakoff Eastern Zone, representing altered coarse amphibolite;
(e) F1 shallowly west-plunging isoclinal fold in carbonate and oxide iron formation, 4 km west of Monakoff;
(f) Dextral shear indicator (looking straight down at vertical S1) in the Monakoff Shear, ~ 5175E; prospect grid;
(g) D3 crenulations in massive biotite ore selvage (~5175E; not in situ);
(h) F2.5 fine crenulations in chlorite-spessartine schist adjacent to ore (~5175E), viewed in situ looking north at a vertically dipping S1 surface.

hill edged by small cliffs. This hill consists of buff silica, studded with randomly oriented crystals of coarse magnetite, magnetite-hematite, and hematite, that are unlike any fabric in the western zone, and are consistent with faithful pseudomorphing of meta-gabbro (Plate 2d). The silica may be a surficial replacement product of carbonate, since silica is not abundant in the ore at depth here. The hill occurs within a steeply west-plunging fold structure defined by bedding trends in banded iron formation and metasediment. 100 m west along strike, drill hole MKD2 indicates that the less altered equivalents of the folded package are comparatively thin massive meta-dolerites and intercalated peperitised sediments. The meta-dolerite/sediment contacts are preferentially silicified in MKD2, with an alteration zonation into the sediment of siderite-magnetite-pyrrhotite-chalcopyrite, magnetite-siderite-quartz, to biotite-quartz-magnetite over 1 m or less. The adjacent dolerite contains incipient siderite alteration. It is interpreted that in the core of the fold, severe alteration affected the interior of the folded metadolerite as well as the sediment margins, with fluids tightly focussed by the fold structure, resulting in wholesale replacement of dolerite. This produced a narrow west-plunging pipe with Cu grades of 1.4-3.0%, consisting of siderite-barite-magnetite-chalcopyrite, which is likely to have considerable depth extent. The fold-hinge control, the transgressive character, and dolerite host-rock all indicate that the Monakoff East Zone developed during deformation, rather than before it.

In addition to the two main ore zones, minor mineralisation occurs on many steeply dipping contacts within both the footwall and hangingwall sequence, although mainly in the footwall. In particular, amphibolite-sediment contacts display mineralisation, with local alteration haloes in each lithology. This is evidence that steeply dipping contacts were dilational during ore formation not only on the main shear zone, but also generally in the host-sequence, at least 200 m into the footwall. The early silicification (pre-ore) which preferentially characterises amphibolite contacts, is fractured, and commonly contains disseminated siderite-magnetite-pyrrhotite-chalcopyrite, grading out to disseminated magnetite-siderite, and then to biotite-magnetite over 0.5–2.0 m (eg., from 114.0 to 119.2 m, in MKD2), probably resulting from local gradients in the activity of S and CO_2.

Alteration and Ore Mineralogy

The following alteration zones are recognised around the Monakoff Western Zone, and are summarised in Fig. 4:

Weakly Altered Host Rock

Meta-siltstone constitutes the immediate ore hangingwall and footwall. It consists of 1-3 mm wide segregated bands of alternating phyllosilicate and quartz-dominated assemblages. In detail each assemblage consists of: 1). muscovite-biotite-garnet-magnetite-quartz±chlorite, and 2). quartz-albite±magnetite (some albite grains are much coarser than the deformed quartz matrix, up to 200 μm, which is consistent with a local immature feldspar sediment source). 1-3 cm scale folds (F_3) defined by banding, in detail contain an earlier muscovite-defined differentiation schistosity, crenulated by a second muscovite-defined cleavage (S_2/S_1). Thin (250 μm) veins of recrystallised quartz-magnetite-pyrite-chalcopyrite are sub-parallel to S_1/S_2, but are folded by S_3. Chalcopyrite was invariably formed by replacement of some coarser magnetite. Garnet (white, euhedral; 100–200 μm diameter), does not contain any inclusion-defined cleavage, leading to the conclusion that at least some garnet grew prior to S_2. As a possible distal ore halo within 10 m of mineralisation, and as small halos to isolated zones of epigenetic mineralisation, a second garnet generation overgrew the widely distributed garnet porphyroblasts: the overgrowths are a white, birefringent, uvarovitic variety. The overgrowths do not show substantial pressure shadowing even where quartz in the same rock displays large grain-preferred aspect ratios parallel to the muscovite-defined cleavage. Biotite defines a separate cleavage at ~15° to the main muscovite cleavage (S_2), and preferentially forms fine lenses that in hand-specimen impart a dark flecked appearance. It is not possible to say whether this is $S_{2.5}$ or S_3. A second foliated biotite generation occurs with spessartine in a proximal alteration shell, and a third occurs as isolated, ragged, disoriented brown biotite throughout the prospect. On the basis of very strong pressure-shadowing around magnetite-carbonate intergrowths, some small magnetite and carbonate porphyroblasts grew prior to S_1/S_2, whereas the location and orientation of most other carbonate porphyroblasts is controlled by the crests of $S_{2.5}$ crenulations, and quartz within the porphyroblasts is crenulated by $S_{2.5}$ (eg., in MKD1 at 66.4 m). This indicates that most carbonate was introduced during or post $S_{2.5}$ development.

Alteration Associated with Local Boudinage

Oblique boudinage zones occur both in the weakly altered and main alteration zones, and are surrounded by distinct small metasomatic haloes that provide information on the timing of general mineralisation. These boudinage zones vary in scale from a few centimetres to >5 m in scale, and are also gradational to fracture networks. The metasomatic haloes around boudinage neck veins are similar to those that characterise small mylonitic breccias in the hanging wall, and appear to be sites where more proximal alteration types are favoured, particularly massive magnetite metasomatism (Plate 1h). Veins are zoned from an internal fill of quartz-sphalerite-galena-pyrite-carbonate (quartz is strongly undulose, with serrated grain boundaries), with pink garnet edges, to an immediate wallrock alteration zone of fine pink euhedral garnet+magnetite, both embayed by carbonate. Garnet is cracked and altered by chalcopyrite (Plate 3b) and fibrous stilpnomelane in radiating aggregates immediately adjacent to veins, where it also shows maximum replacement by carbonate. Pyrite within veins is replaced by dolomite rhombs along fractures. Magnetite occurs both as intense replacement along and around fractures adjacent to veins, and as disseminated crystals

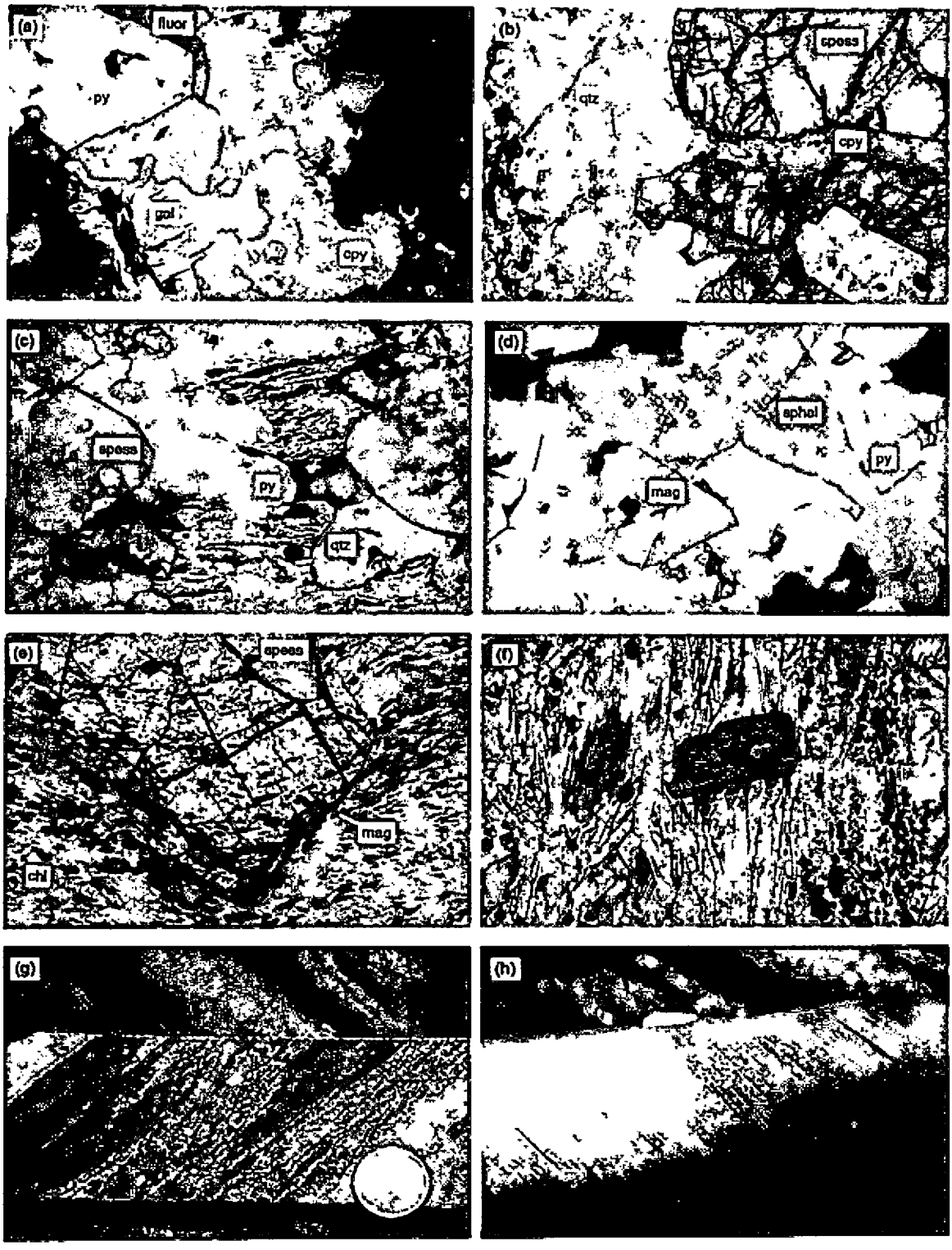


Plate 3:

(a) MKD1/78.2m Reflected light of typical ore relationships, galena distributed around the margins of a fluorite grain, which is in contact with euhedral pyrite;

(b) MKD1/93.3m (f.o.v. 2mm; transmitted and reflected light) Spessartine with a quartz halo in the garnet-bearing footwall, cut by a chalcopyrite-chlorite vein, filling fractures;

(c) MKD1/87.0m chalcopyrite-garnet replacing an antecedent cleavage;

(d) MKD1/79.0m (f.o.v. 1mm; reflected light) Euhedral to subhedral magnetite overgrowing chalcopyrite riddled sphalerite, and pyrite;

(e) MKD1/71.8m (f.o.v. 1mm) Chlorite and garnet overgrowth of a D2.5 crenulation that is defined by elongate magnetite foliation, with post-crenulation magnetite concentrating around the garnet; (f) MKD1/74.5m (f.o.v. 0.5mm) biotite-garnet alteration used for garnet-biotite geothermometry, illustrating the dominant early biotite fabric (syn-D2.5), overgrown by younger disoriented biotite, a typical feature of the whole area;

(g) MKD2/58.5m Near-foliation parallel fractures infilled by carbonate-barite ore, with the clasts consisting of fine-grained precursor magnetite-quartz;

(h) MKD2/ 170m. Fine tectonic/sedimentary compositional lamination with small dark biotite concentrations in the foliation, shear zone adjacent to the Monakoff eastern Zone, Mt Norna Quartzite.

throughout the host rock. Chalcopyrite is not an obvious vein fill, but instead replaces magnetite, garnet and carbonate along fractures (Plate 3b).

Chlorite-Garnet Alteration

The main minerals in this zone are chlorite, plagioclase, garnet (3 growth phases described earlier), 2 biotite generations, carbonate and sphalerite. Compared to the weakly altered host rock, fine euhedral isotropic garnet is mainly absent, but minor granular relics on the edges of carbonate lenses are evidence of its former presence. Chlorite is foliated and also crenulated (Plate 3e), and replaces foliated biotite, which is commonly only present as slight brown streaks in the chlorite (eg., in drill hole MKD1 at 71.8 m). Garnet (pink spessartine) and chlorite appear to have been in metamorphic equilibrium. Garnet however, where in contact with carbonate, is embayed and granulated (Plate 1I). In terms of timing, it is not clear whether chlorite overgrew or was foliated by S2. As noted earlier, garnet preserves a crenulated quartz inclusion-defined foliation, consequently, most garnet grew syn- to post-S2.5. Elongate relict subhedral plagioclase defines a cleavage (S1), which is crenulated by the chloritised biotite cleavage (S2), forming a weak segregation cleavage relationship.

Biotite-Garnet Alteration

The transition inward to biotite -garnet ± plagioclase-magnetite assemblages is gradational over 10 cm, forming a massive foliated rock dominated by biotite (Plate 2g). Inward, some biotite-garnet to carbonate-quartz metasomatic contacts preferentially contain sphalerite disseminated immediately within the carbonate-quartz zone, and fine pink garnet concentrated close to the contact within the biotite zone. Biotite defines two moderate cleavages (an early cleavage, and a second crenulating cleavage at a small angle to the first), but is more randomly crystallised than adjacent relict host-rock muscovite. There is minor evidence of a second randomly oriented third biotite generation (Plate 3f). Garnet contains randomly-oriented inclusions of plagioclase rather than a foliation, has pronounced pressure shadows of carbonate-quartz±magnetite, and also distorted biotite around its margins, suggesting that some garnet cores grew prior to S1/S2, growing in the prograde metamorphic episode prior to S1 (O'Dea et al., 1997). This conclusion is based upon the principle that garnet will always preserve a pre-existing foliation. Consequently, there is evidence of early garnet, syn-metasomatic garnet (Syn-D2.5), and post-D3 garnet overgrowths in this part of the Monakoff shear zone, and the textural difference between them is not as clear as in outer alteration zones. Magnetite is concentrated around the margins of garnet (Plate 3e) and follows distortions in the biotite schistosity, indicating that it grew syn- to post-biotite. Magnetite is notably absent in the carbonate-quartz zone. Propagation of the metasomatic zonation occurred preferentially along small ductile faults (plate 3g). Here micro-zonation occurs inward from biotite ±sphalerite, to carbonate-quartz-garnet-biotite (in which garnet displays severe breakdown to carbonate), inwards to quartz-only, with minor relic biotite grains remaining on the triple point margins of recrystallised quartz.

Carbonate-Quartz/Barite-Carbonate Ore Zones

In the contact transition between metasomatic zones, several of the macroscopically identified assemblages may occur in close proximity in foliation-sub-parallel breccias. These include multiple planar low-angle metasomatised faults and fractures in which breaks contain barite-carbonate alteration around clasts of biotite-plagioclase ±disseminated magnetite, with carbonated rims, or alternatively biotite-altered rims and carbonated cores. Beyond the contact zones in massive ore, there is a general antipathetic relationship between sulphides and magnetite. A compressed broader alteration zonation can occur over 5-10 cm in this contact region, with for instance, a transition from biotite-plagioclase, to coarse garnet (with evidence of carbonate replacement), to massive carbonate, to carbonate-quartz-barite-chalcopyrite-pyrite. Minor phases in the carbonate-barite zone include: 1). monazite on contacts between biotite and quartz; 2). epidote in places displaying replacement by carbonate; 3). fluorite occurring as ovoid inclusions within quartz and carbonate; and 4). hematite occurring as <1-5 μm inclusions along barite grain boundaries with carbonate. Fluorite and coarse magnetite are enriched in the centres of ore intersections (Fig. 4).

The barite-carbonate zone does not contain definitive timing criteria to assist correlation with external deformation events. It possesses a granofelsic texture, with only a moderate cleavage in the adjacent biotite 2 zones. Crude petrographic timing evidence for ore includes: 1). overgrowth of foliation by unfoliated chalcopyrite; and 2). replacement of spessartine in porphyroblastic garnet-biotite schist by chalcopyrite along veins and fractures. There is evidence of magnetite breakdown to form sulphides, indicating that magnetite is paragenetically earlier than most sulphide. The evidence consists of an antipathetic relationship between the two, the occurrence of magnetite inclusions in euhedral coarse pyrite crystals, and a general highly amoeboid grain habit for magnetite, compared to its euhedral habit in adjacent zones. This occurs in both Monakoff East and West zones. Barite commonly does not contain any magnetite inclusions and only rare sulphide inclusions, but chalcopyrite and pyrite inclusions are commonly present in magnetite. However, in the central high-grade sections of ore intervals, coarse magnetite is stable in contact with pyrite, sphalerite and galena. This inherent paragenetic contradiction for magnetite over short intervals could be explained if the coarse magnetite described here, and mapped in the Monakoff Eastern Zone at surface, is metamorphic, and like some biotite in the surrounding alteration, was produced by a thermal event following the main ore event.

Summary

The following metasomatic paragenesis is observed:

Pre-ore - Epidote alteration of mafic sill margins, and silicification of mafic sill sediment contacts. K-Fe-Mn alteration of meta-andesite, which recrystallised to spessartine-biotite-chloritoid during pre-D1 metamorphism;

Stage 1 - Biotite-magnetite alteration, focussed upon a D1 shear zone;

Stage 2 - Chlorite-garnet/biotite-garnet/carbonate-fluorite-barite zonation (ore formation);

Stage 3 - "Mt Freda"-style ferro-carbonate veining and minor breccia, with haloes of sericitisation in amphibolites; and

Stage 4 - Pervasive albitisation focussed along NW oriented faults.

Stage 1 was an early post-D2 event in which fine-grained biotite pseudomorphed 2 muscovite-defined cleavages. Stage 2 was timed closely to D2.5, which overprinted the more extensive but disseminated Stage 1 assemblage. Given that brecciation and well-developed mineralisation coincide with higher magnetite concentrations, it is possible that the earlier phase, which produced variable abundances of fine-grained magnetite, partly controlled the location of ore development in the later phase. However, primary magnetite concentrations, such as the persistent BIF horizon

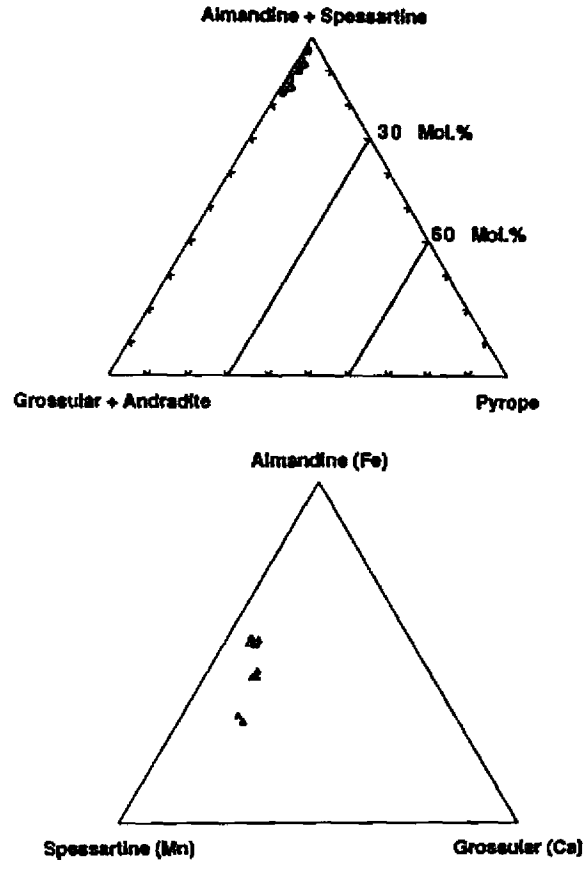


Figure 6: Monakoff garnet compositions

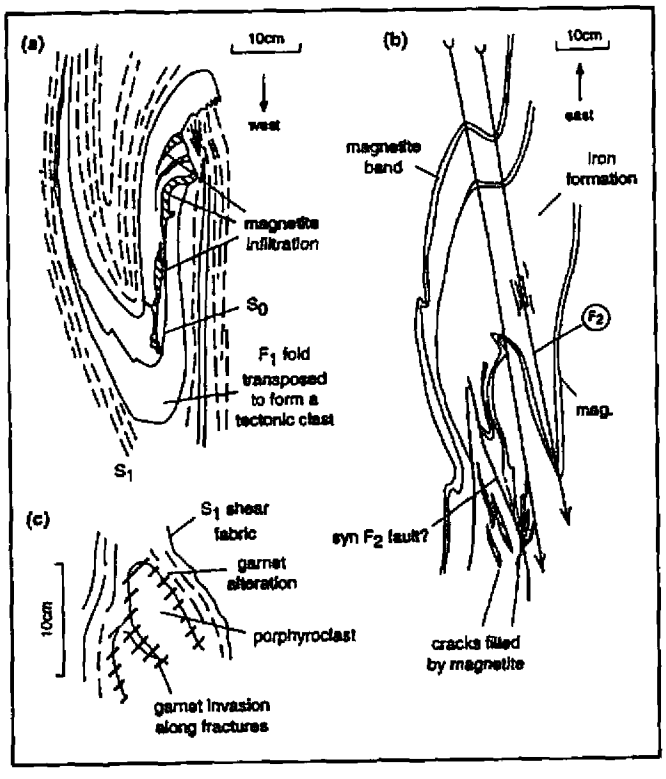


Figure 5: Plan views at varying scales of:
(a) an F1 dismembered fold-hinge with preserved magnetite infiltration around the clast margins;
(b) a typical small-scale F2 fold plunging steeply west, emphasising the variable effect of F2 on adjacent lithologies;
(c) garnet metasomatism around a tectonic clast within the Monakoff Shear.

in the footwall package, experienced metasomatism and moderate infiltration by barite-forming fluids, but were not severely replaced. Consequently magnetite was an important but not vital prerequisite for ore formation. The solution to this contradiction may lie in the location of the main shear zone relative to magnetite concentrations, with zones of shear-hosted magnetite being subject to greater extension, permitting greater fluid access during the ore event.

Mineral Chemistry

8 thin-sections were analysed across the Monakoff Western Zone from drill hole MKD1 from 66.3 to 93.3 m, targeting biotite, garnet, chlorite, carbonate and sundry phases, with the aim of: 1). characterising the compositions of the important alteration phases; 2). determining whether mineral chemistry is a more effective tool than whole rock geochemistry for exploration for Monakoff-style targets; and 3). to determine if there is a significant compositional difference between pre-metamorphic and metamorphic alteration. Analyses were obtained with an SX50 Cameca microprobe running at 15kV and 10 nA.

Garnet

Garnets divided into low Ca-Mg spessartines and Mn-almandine varieties, with X_{spess} = 0.23–0.58 (Fig. 6). A typical metasomatic garnet has a composition of $Py_{0.00}Alm_{0.47}Gro_{0.06}Spess_{0.47}$. The porphyroblastic garnets of the altered meta-dacitic footwall contain lower Mn

contents (X_{spess} = 0.23–0.35) than garnets in the ore halo. Rim contents of some garnets vary significantly (are more Fe-rich) from core compositions in some samples, particularly where distinct garnet overgrowths occur (Mn content in garnet increases through the metasomatic halo towards the ore zone, and is highest in the biotite-garnet zone. However, even weakly altered schist garnets contain 15–20 wt.% MnO (Fig. 7). The lower garnet Mn values in footwall schist are consistent with the observed whole-rock Mn decrease away from ore.

Biotite

Biotite compositions are very variable, with (Mg+Mn)/(Mg + Mn + Fe) ratios of 0.1–0.65, and octahedral aluminium values of 0.03–1.16. Consequently they cover most of the solid solution between annite and siderophyllite varieties. They possess high F and low Cl contents, typically F ~2 wt.% [maximum 3.12 wt.%] and Cl ~ 0.02–0.2 wt% in ore, with cation F/Cl ratios of 20–200 adjacent to the ore zone, grading to 0.5–20 in the peripheral weakly altered areas, where F descends to 0.5–0.8 wt.%. The physical variation of F in biotite across the Monakoff Western Zone closely mimics Mn variation in garnet - F is elevated in weakly altered muscovite-garnet schist, is highest in the biotite-garnet zone adjacent to ore, and lowest in foliated biotites of the porphyroblastic garnet-biotite footwall. A clear control on F is the Mg content of biotite, itself a function of metamorphic conditions. F is strongly positively correlated with Mg, which is an expression of the well-documented 'Fe-avoidance' rule for F in mica and amphiboles (Munoz, 1984).

Carbonate

Carbonates have not been extensively analysed, but carbonate spotting in the biotite-garnet alteration consists of manganoan calcite, which is typically $(Ca_{0.87}Mg_{0.02}Mn_{0.07}Fe_{0.03})CO_3$, with Mn varying from 6 to 7 wt. % in a slide, whereas the adjacent carbonate-barite mineralisation contains iron-rich rhodochrosite, known as the variety "ponite" (Deer et al., 1992), defined as rhodochrosite with up to 20 wt. % Fe. The ore carbonate has a typical composition of $(Ca_{0.07}Mg_{0.04}Mn_{0.6}Fe_{0.29})CO_3$. This follows the behaviour of ore elements in other phases as the ore conduit is approached, with very large increases occurring over a short distance.

Whole Rock Geochemistry

Methods and Results

Samples were selected regularly across the mineralised zones in three separate diamond drill holes, with representative samples of adjacent lithologies also taken for comparison. The aim of this work was to: 1). characterise the composition of alteration and ore; 2). identify any important trends in the alteration geochemistry away from ore; and 3). identify elemental relationships that constrain genetic models for Monakoff. Samples were processed at James Cook University, and analysed both by XRF and neutron activation. A comparison of results of the exploration data for Cu, taken at 1 m intervals, compared to samples taken by this study (30 cm sticks of quarter- to half-core at 1–5 m intervals)

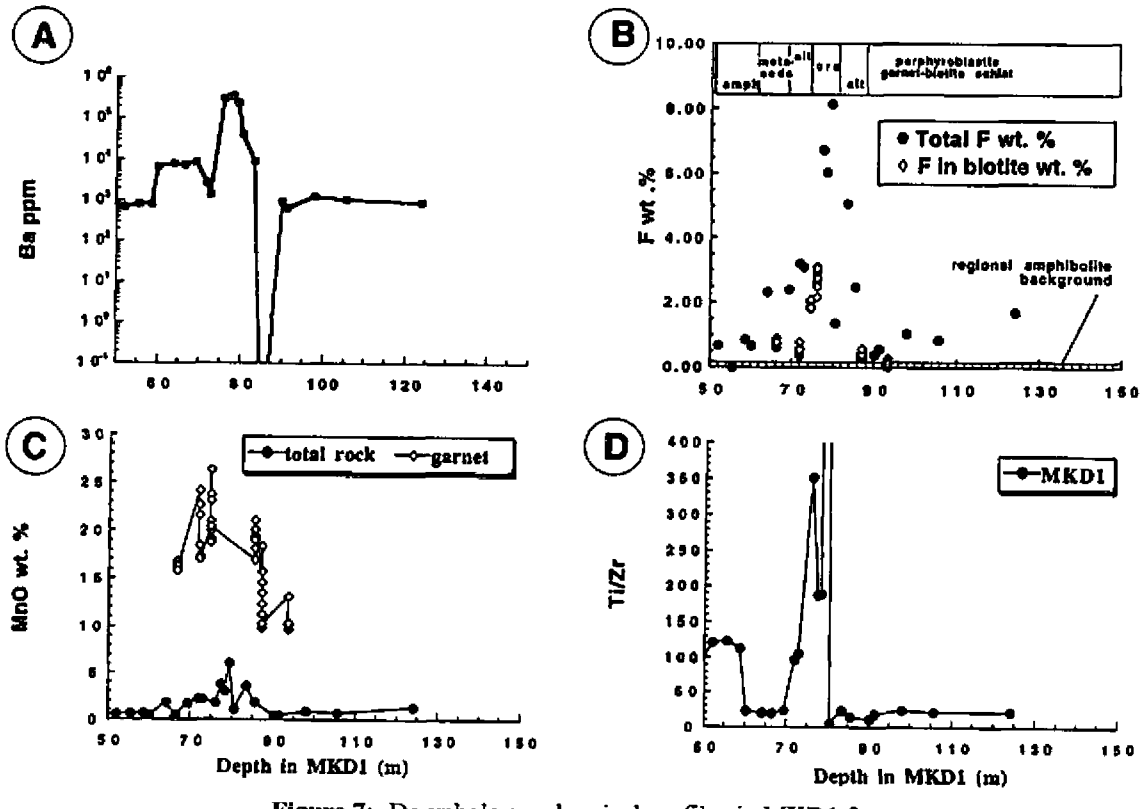


Figure 7: Downhole geochemical profiles in MKD1 for:
(A) Ba; (B) F, including trends in mineral chemistry biotite;
(C) MnO including garnet composition trends; (D) Ti/Zr.

	MKD1/7 6.0m	MKD 1/77.4m	MKD1/ 78.2m	MKD1/7 9.3m	MKD1/49. 8m	MKD1/6 4m	MKD1/66. 3m	MKD1/72. 8m	MKD1/12 4m
	Ore	Ore	Ore	Ore	Weakly altered amphib	Host musc schist	Stage 1 biotite alteration	Stage 2 chlorite-garnet	footwall garnet-biotite
SiO_2	9.29	0.59	0.45	1.33	47.93	56.32	59.74	42.48	61.17
TiO_2	0.15	0.11	0.11	0.08	0.99	0.61	0.67	1.07	1.02
Al_2O_3	2.28	0.79	0.79	0.71	14.43	15.44	16.92	13.30	12.64
Fe_2O_3T	12.84	15.01	15.38	23.27	13.37	14.10	11.67	13.01	13.62
MnO	1.82	3.76	3.05	6.13	0.51	1.79	0.54	2.22	1.33
MgO	0.43	0.39	0.35	0.49	8.29	1.32	1.10	5.05	0.55
CaO	11.97	11.99	12.48	9.55	9.61	2.09	0.73	9.26	3.01
Na_2O	0.00	0.00	0.00	0.00	2.69	0.28	0.38	2.42	3.12
K_2O	0.62	0.00	0.03	0.04	0.54	4.56	5.31	0.40	2.04
P_2O_5	0.35	0.25	0.26	0.17	0.07	0.59	0.18	0.09	0.29
S	22.05	22.85	23.20	21.46	0.09	0.14	0.19	0.55	0.02
F	2.62	6.74	6.06	8.16	0.59	2.33	0.62	3.10	1.72
BaO	30.75	34.36	34.79	26.40					
CuO	4.08	2.70	2.81	1.91					
L.O.I	0.00	0.63	0.00	1.63	1.40	2.11	1.93	7.90	1.60
minusO=F	1.10	2.83	2.54	3.43	0.25	0.98	0.26	1.30	0.72
SUM	**97.23**	**96.46**	**96.08**	**96.85**	100.35	101.58	100.54	99.67	101.47
Ag	72.50	63.70	71.30	-20.00					
As	2010	2350	2280	1360	8.59	53.9	7.1	6.12	2.02
Au ppb	699	795	665	481					
Ba	303000	336000	352000	239000	726	7800	7170	1410	873.00
Cs					4.93	13.1	9.46	5.57	6.30
Co	1260	1670	1700	1490	56.2	44.2	10.4	52.7	11.20
Cu					189.4	8872.6	31.2	937.5	58.10
Ga *	2.40	0.00	6.30	7.10	19	21.1	28.6	15	19.90
Hf	5.34	3.58	5.09	2.64	1.3	90.1	4.98	1.64	8.07
Ir ppb	-20.00	-20.00	-20.00	-20.00					
Mo	-500	-400	-500	-200					
Nb *	0.00	0.00	0.00	0.00	3.6	0	1.1	2.5	17.80
Ni *	41.10	51.90	50.10	37.10	124.1	36.9	34.8	113.3	8.20
Pb *	2694	3210	5076	5998	21.1	12.2	11.2	79.4	7.00
Rb *	10.70	0.00	0.00	0.00	45.2	333	353	35.5	97.70
Sb	402	226	120	24.70	2.4	1.52	0.93	1.87	-0.20
Sc	2.01	0.44	0.48	0.56	39.7	13.7	14.7	38.7	20.70
Sr *	66701	10675	8406	5089	221.3	112.1	65	163.6	45.70
Ta	-2.00	-2.00	-2.00	-1.00	1.04	1.24	2.01	-1	2.09
Th	3.41	3.85	-1.00	1.75	0.74	17.2	18.7	1.08	10.90
U	334	284	307	164	-2	10	-2	-2	-2.00
V					275.2	106.2	69	292.5	16.30
W	80.90	150.00	151.00	169.00	44.3	16.1	7.76	-4	-4.00
Y					18.3	21	23	14.6	54.20
Zn	7060	10300	10900	9540	465	262	176	3300	139.00
Zr *	1.00	1.00	1.00	1.00	55.2	170.7	194.7	66.8	319.20
Ce	1150	880	920	436	9.34	105	104	30	57.50
Eu	6.72	4.64	5.83	4.44	0.79	1.57	1.51	0.56	2.12
La	1680	1420	1470	753	3.96	67.5	56.5	25	27.80
Sm	6.95	6.22	6.15	4.13	2.31	7.88	8.14	3.2	8.60
Tb	1.09	0.85	0.90	0.63	0.53	1.02	1.13	0.52	1.77
Yb	0.53	0.50	0.50	-0.50	1.59	2.71	3.03	1.65	6.45

Table 1: Typical composition of ore zones and host rocks in diamond drill hole MKD1.

* indicates XRF data, with all other data derived by neutron activation;
\# Detection Limit numbers only apply to neutron activation data;
Negative indicates "less than" in neutron activation data.
Sn was measured at 0.0 in all ore samples.

were surprisingly different, and indicate that the research sampling, although detailed, does not provide as accurate a guide to elemental distribution as the exploration sampling (Fig. 8). Typical analyses are presented in Table 1.

Ores

Monakoff ores are geochemically very complex, although their major components (>10 wt.% oxide) are, in order: S, Ba, F, Fe and Ca, with the significant minor element enrichments including (* denotes elements at economic concentration) Sb, As, Co*, Cu*, Au*, Pb, Ag*, W, U, La, Ce and Zn, as well as an astonishing Sr abundance (Sr = 0.5-1%; highest recorded value of 1.07 wt.%). Mo and Sn are high in surface samples (Davidson, 1994), but detection limits by neutron activation were a problem for these elements. Other elements with high neutron activation detection limits that have not been adequately characterised are Ir, Br, Ce, and Se. Considering the previous comparisons between Monakoff and BHT-style Pb-Zn systems (Ashley, 1983; Derrick, 1996), P_2O_5 abundances are surprisingly low, with most ores containing only 0.2–0.4 wt.% P_2O_5. The highest values were systematically found in the iron formation, although several high Fe samples in the immediate ore halo in Monakoff Eastern Zone possess values of up to 1.88 wt.%. However, no strong Fe-P correlation exists when all the data is considered. La and Ce abundances are also very high, with typical values of >1000 ppm. Rather than apatite, the host phase for REE, U, and possibly P_2O_5, is monazite, which is common in ore intersections (see petrography), and concentrates the LREE. Zr is unusually low, 1–5 ppm.

Host Rocks

The broad physical patterns of geochemical behaviour of the host rocks are reviewed herein. The three major lithologies (amphibolite, footwall porphyroblastic garnet-biotite schist, and meta-pelite) all have distinctive Ti/Zr ratios (Fig. 7) unless they are visibly altered, at which point Ti/Zr is disturbed. The alteration and ore Ti/Zr signature is very high (>100), but the uncertainty caused by Sr interference with XRF Zr remains a problem (see above). Of the elements found to be enriched in ore, Mn and F have the most consistent regional distribution in the associated alteration, and F is particularly interesting in terms of exploration potential because of the low F background in normal crustal rocks. Mn in the alteration is consistently >2 wt% MnO, but the whole sequence has a high Mn background >0.5 wt.%, compared to the regional amphibolite MnO background of 0.15-0.30 wt.% (Unpublished AGSO geochemical database). As previously discussed, on the basis of textures, this Mn enrichment is considered to at least partly relate to a pre-metamorphic hydrothermal alteration event (Ashley, 1983).

Less ambiguously, F is >0.5 wt.% over the entire 132 m length of MKD1, a drill hole that terminates in footwall garnet-biotite schist. The enrichment occurs in footwall garnet schist, the alteration and ore, and the hangingwall

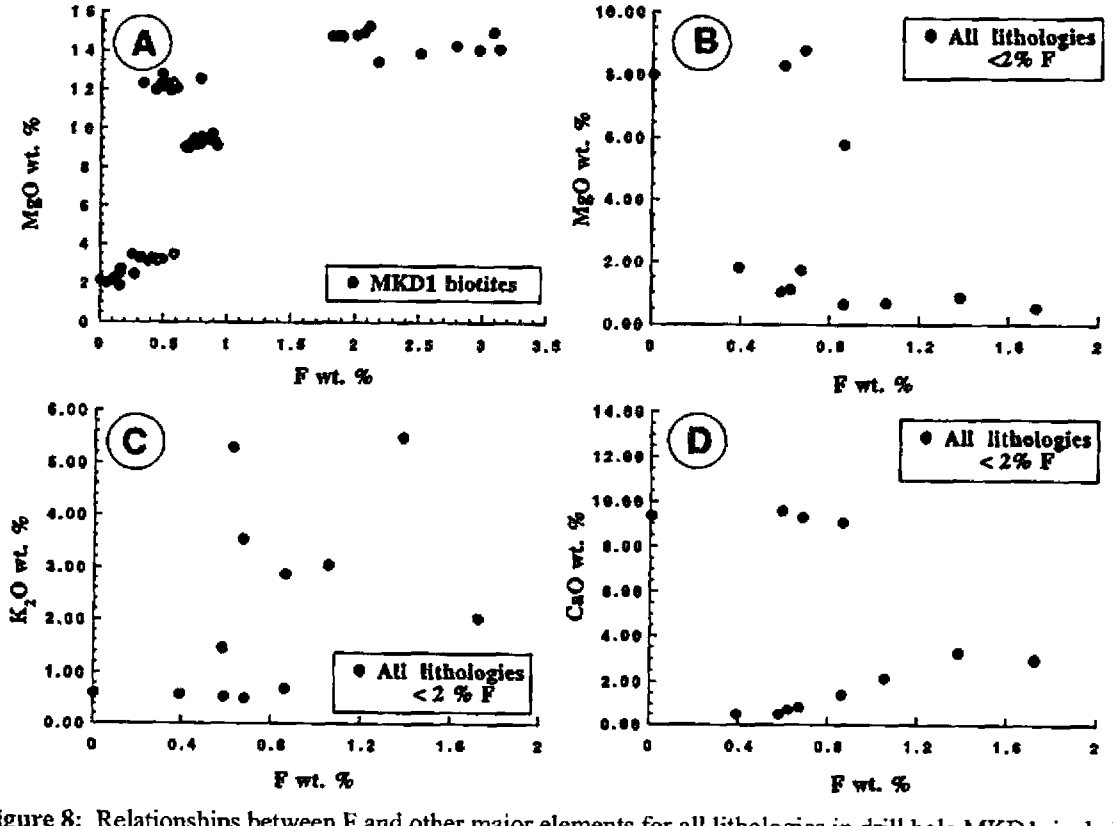


Figure 8: Relationships between F and other major elements for all lithologies in drill hole MKD1, including
(A) the mineral chemistry of biotite; (B) MgO;
(C) K_2O; (D) CaO.
These elements were plotted to evaluate the behaviour of F compared to fluorite and biotite variation.

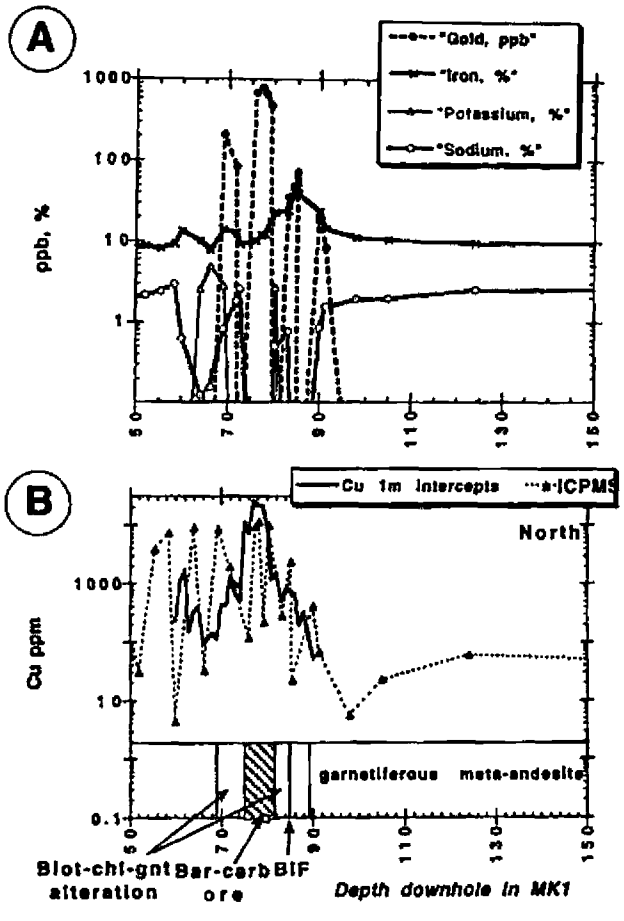


Figure 9:

(A) Downhole behaviour of Au, Fe, K, Na, and Cu in MKD1

(B) Cu behaviour, at >1 m sampling intervals, by ICPMS, in this study, compared to 1 m intercepts data obtained by Esso Minerals (Ashley, 1983) by atomic absorption.

amphibolites. Regional Toole Creek Volcanic amphibolites contain F <200-500 ppm. In MKD2, the Monakoff F halo terminates sharply at the base of the garnet schist, dropping to background (200 ppm F; unpublished AGSO geochemical database) within the metasediment (Fig. 10), a behaviour that is closely mirrored by Mn. The F enrichment has great potential as an exploration indicator, because it enlarges the ore halo by >10X the width of the visible alteration zone. The control on fluorine enrichment has already been examined mineralogically, where the Fe-avoidance rule was shown to be operating for Monakoff alteration biotite, and presumably also for other hydrous phases. However, plots of potential element correlations, such as K as a measure of biotite enrichment, or Ca as a measure of available Ca for fluorite precipitation, do not show any coherent co-variation with F (Fig. 8). High background F concentrations may therefore be caused by substitution into several different phases with different major element compositions, rather than into a single phase. There is nevertheless a clear enrichment in igneous over sedimentary lithologies which is not yet understood.

Ore elements U, Zn and Ba all also have large haloes (Fig. 11), although not as extensive as F. There is no definite zoning in the ore elements through the alteration, with U, Zn, Ba and Cu all displaying similar peaks through the MKD1 ore zone, dropping off into the alteration in a symmetric fashion, with the exception of Ba, which is enriched in hangingwall alteration relative to footwall (Fig. 11). These elements display positive linear co-variance with F, which is consistent with F-metal complexing. However, simple co-precipitation of phases can also produce similar geochemical behaviour on binary plots, as demonstrated for Ba (Fig. 11), so that fluorine complexing is likely but not proven.

Fluid Inclusions

Workable fluid inclusions are not abundant in the Monakoff replacement ores, but are present in minor quantities in some boudin neck veins, such as found in drill hole MKD1 at 60.8 m (Quartz-garnet-pyrite-sphalerite-galena in boudinage fill). No heating and freezing data are reported here, but the veins have the following inclusion populations:

Type 1. Primary inclusions: 5-15 μm vapour-only and L-V inclusions, with strong negative crystal forms, occur in patches in quartz and garnet. Those in garnet are round-edged circular- to pear-shaped 5-40 μm inclusions arranged centripetally around growth zones, with variable liquid-vapour ratios, from ~20% liquid, up to nearly 100%, and no daughter salts. The liquid-rich examples have complex decoration within the inclusions, whereas the vapour-rich examples have negative crystal shapes. These inclusions are additionally most pronounced where they are completely surrounded by a sulphide phase. Similar examples in open areas of quartz are collapsed and emptied, consistent with destruction during subsequent deformation.

Type 2. Secondary or pseudo-secondary inclusions: 5-25 μm square liquid-dominated inclusions with 5-10% vapour by volume, and two isotropic square daughter salts (probably halite and sylvite). Inclusions occur in patches in quartz, in close proximity to sulphide inclusions, and also in continuous planes.

Type 3. Secondary or pseudo-secondary inclusions: 2-15 μm square liquid-dominated inclusions with 5% vapour by volume, and no daughter salts. Inclusions occur in planes in quartz, but are not related to quartz grain boundaries.

The primary inclusion types correspond most closely with liquid-dominated type 2 inclusions of Dong (1996), which she regionally correlates through a wide variety of Cu-Au deposits. Dong (1996) type 2 inclusions occur with mineralisation. The variable L-V ratio of inclusions in Monakoff boudin necks can be accounted for by: 1). fluid mixing; 2). boiling; or 3). condensation.

Discussion

The most detailed previous ore genesis model (Ashley, 1983) envisaged 'stratiform polymetallic ore' to have formed in 'a marine environment at a time when conditions were changing from possible turbidite sedimentation to a

major pulse of mafic magmatism'. Exhalation at this time 'precipitated chemical sediments of iron formation which were commonly rich in base metals, Ba, S, F and Mn, as well as containing highly anomalous values of U, REE and chalcophile pathfinder elements'. These views were supported by Derrick (1996), who described the ore as 'layered granoblastic exhalite containing barite-Mn carbonate-garnet-quartz-magnetite-fluorite-pyrite-chalcopyrite'. Conversely, Laing (1991, 1998) interpreted the deposit as a replaced D1 mylonite, localised at the intersection of a later structure, although he concluded that the iron formation also had a structural-replacement origin. Davidson and Large (1998) included the deposit in an 'Iron formation associated' sub-class within the iron-oxide Cu-Au deposits of Australia, ascribing an epigenetic origin to the ore.

The following deposit features require an epigenetic origin for the ore and most associated alteration:

1) Symmetric shells of high temperature alteration around the mineralisation;
2) Textural evidence of pervasive replacement of a D1 mylonite fabric by ore, and the exploitation of structural fabrics by alteration:
3) Specific growth of ore alteration carbonates and garnets during D2.5 deformation;
4) Common boudinage neck zones containing the ore assemblages; and
5) The pipe-like geometry of the Monakoff Eastern Zone within a replaced D2 antiform, in detail texturally replacing coarse-grained amphibolite.

However, no evidence could be found to support the view of Laing (1991) that the underlying iron formation was also epigenetic in origin, although its high metal contents in places indicate that it participated in the ore event. It is extremely continuous at regional scales, is folded by D1 folds adjacent to the prospect area, exhibits anomalous box-fold geometries indicative of a distinctive rheological response to deformation, shows no association with the boudinage that is common in the ore package, and is well banded, with banding defined by alternating magnetite and quartz dominated layers. Detailed mapping shows that it is never the locus of the main mineralisation at either lens within the deposit, so that description of the deposit as 'iron formation associated' is misleading in the connotation that iron formation hosts ore; it does not. Fe-K-Mn alteration of the interpreted footwall meta-andesite is an asymmetric feature of the ore site. Here, spessartine, almandine garnet,

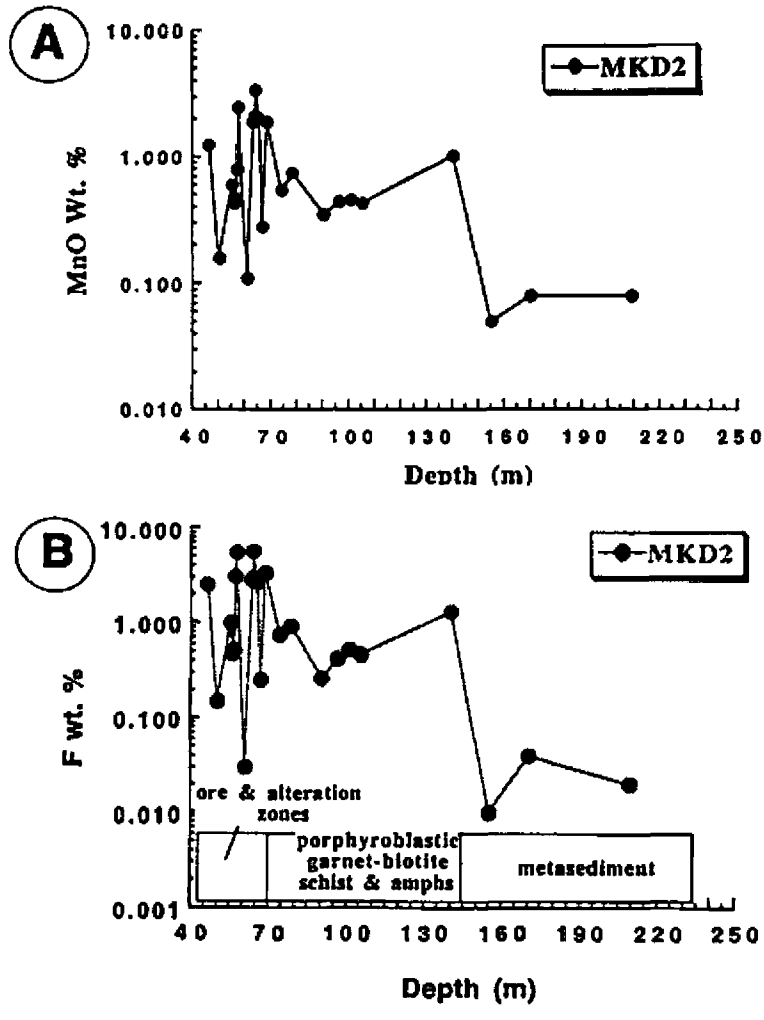


Figure 10: Downhole behaviour of (A) Mn; and (B) F in MKD2.
The northern edge of the F anomaly occurs at the meta-andesite/sediment boundary; this is the only hole in which the fluorine anomaly is fully defined in the footwall.

biotite and chloritoid occur pervasively within a thick massive rock mass. The random orientation of chloritoid could be accounted for by post-deformational growth. However, this observation, combined with the lack of foliation overgrowth by spessartine in this unit (in contrast to spessartine within the shear), and the overgrowth of spessartine by peak metamorphic almandine, forms a mass of evidence favouring development of the main mineral assemblage prior to foliation formation. Biotite orientation is controlled by several separate cleavages, and while it likely crystallised during pre-deformational metamorphism, there is little evidence of this now. It is concluded that an early hydrothermal history influenced the bulk geochemical character of the sequence below the iron formation. This low temperature hydrothermal event enriched the footwall sequence in Fe, K and Mn at ~1650 Ma, and its spatial association with metre-scale BIFs provides circumstantial evidence that this occurred during sedimentation. The F enrichment of the unit conjecturally developed later during the Cu-Au ore event, with preferential F uptake by pre-existing biotite. A more detailed structural model for ore formation is outlined below.

Structural Factors

The ore event is closely associated with D2.5, which regionally produced recumbent folds and a shallow-dipping foliation, indicating that the main stress field had a near-vertical σ_1, a factor that must be considered for ore genesis models at this time. Evidence presented indicates that D2.5 generated moderately strong crenulations through the ore sequence, as well as broad dip changes of beds, and particularly, numerous zones of oblique and chocolate-block boudinage in and around the ore zone. These features are not present everywhere in the Eastern Succession (Bell, 1991; Pollard et al., 1997), so it is argued that Monakoff lies close to the hinge of a large D2.5 fold with a near-horizontal axial trace. Development of S2.5 is associated with the formation of open parasitic folds. Monakoff Western Zone ore formed during the flexural slip, extension, and production of dilatancy in a broad D2.5 fold, a structural mechanism which accounts for the sheet-like ore geometry (parallel to bedding), and which has its best structural analogue in the saddle reefs and bedding parallel veins of slate-belt-hosted gold deposits, forming prior to fold lock-up (Cox et al., 1991). Fold lock-up also has the effect of causing strain accumulation due to the inability of the deforming sequence to accommodate the deformation and any changes in volume (eg., Davis et al., 2001b). Saddle reef mechanisms, and processes associated with the lock-up of both folds and thrusts, have been proposed for other Proterozoic gold-only deposits, such as parts of the Cosmopolitan Howley (Northern Territory, Australia), Telfer (Western Australia) and Sabie-Pilgrim's Rest (South Africa) deposits (Partington and McNaughton, 1997; Rowins et al., 1997; Harely and Charlesworth, 1992), and Archaean gold-only deposits such as Mulgarrie (Davis et al., 2001b). In these instances the axial planes are sub-vertical rather than sub-horizontal.

At Monakoff, strain was not distributed evenly across the package, but was focussed at unit contacts and older shear zones, with dilatancy occurring in those areas with near-vertical orientations. This is supported by the occurrence of mineralisation not only in the Monakoff Shear, but on numerous amphibolite-sediment contacts well into the footwall in DDH MKD2. However, a degree of pervasive fluid flow was also required, to account for the high geochemical background of fluorine and other ore elements in both the footwall and hangingwall.

The features of the boudin necks provide several constraints on the ore system. Firstly, the formation of boudin necks was synchronous with the arrival of ore fluid at the site,

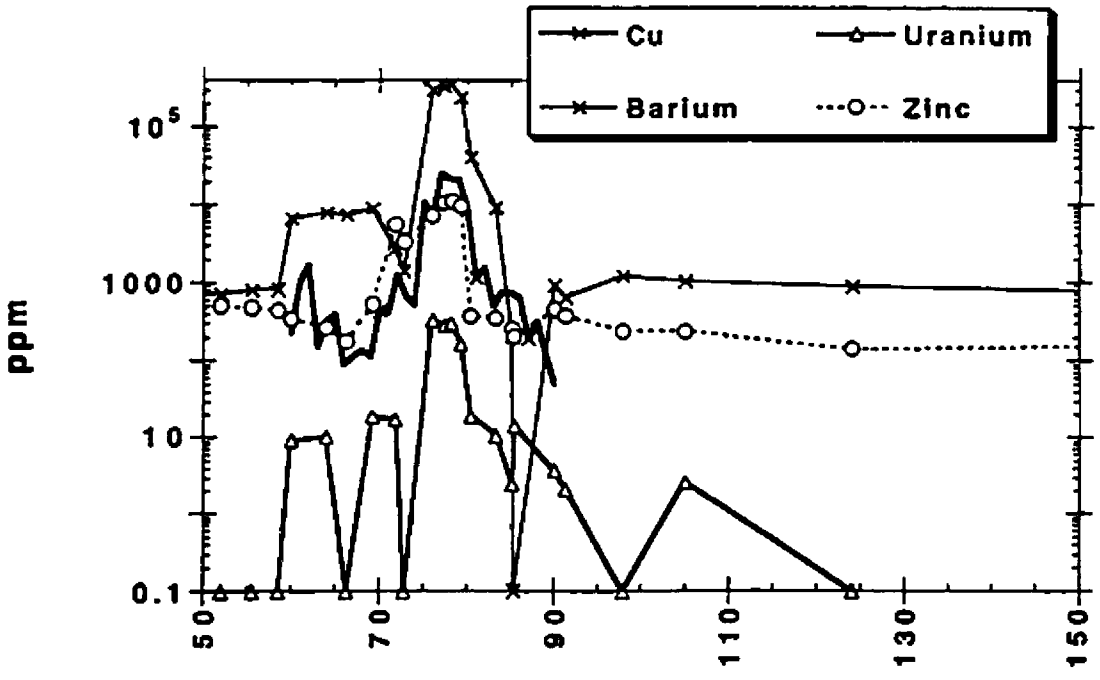


Figure 11: Downhole behaviour of Cu, Ba, Zn and U in MKD1.

because boudin necks contain many of the ore assemblages. Although this may be coincidence, it is more likely to be directly related to an increase in fluid pressures, increasing the probability of rupture on the failure envelope, resulting in movement of ore fluids into low mean stress sites offered by boudin necks. This is supported by the general lack of boudinage in the surrounding sequence, and by the curvilinear nature of associated fracture arrays within the metasomatic halo, which is symptomatic of brittle failure under high fluid pressures (McClay, 1987). Secondly, the enrichment of metals in many boudin-neck zones, each interpreted to have formed in a single failure episode, provides evidence that the ore forming fluid or fluids were extremely metal-rich, and consequently that ore deposition likely occurred in only a few failure episodes. Unfortunately the corrosive and reactive quality of the mineralising fluids obliterated much of the evidence of how the fluid infiltrated into the sequence to form the massive replacement orebodies.

Mineralogical and Geochemical Constraints

The fluid oxidation state during ore formation was high, to account for the dominance of sulphate in ores (S ~25–30%). Hematite is generally not observed except in the upper near-surface of the Monakoff Eastern Zone, where it forms large primary bladed crystals replacing amphibolite. Magnetite is the dominant iron oxide in the Western Zone, although there is doubt that it was precipitated at the same time as the ore, because of post-ore metamorphic recrystallisation. Magnetite grains at the margins of the ore zone were replaced by sulphide minerals. Oxidation-sensitive minerals mainly comprise pyrite, with minor pyrrhotite and arsenopyrite disseminated asystematically.

There is evidence in the whole rock geochemistry for more than one fluid at the time of ore formation. This arises from the abundant barite, fluorite and high background Mn; Ba does not have a high solubility in the presence of abundant dissolved sulphate, and the transport of both Mn and Ba is enhanced under reduced conditions (Cook et al., 2000). On the other hand, U transport is enhanced under oxidised conditions (Wilde et al., 1988) although the effect of F-complexing on U transport is not clear. The abundant barite could be accounted for: 1). from the mixing of a sulphate-rich oxidised fluid with a reduced Ba-bearing fluid; or 2). from the oxidation of a very reduced fluid to a sulphate-stable condition, thus precipitating barite. Option (2) is discounted because it should have produced large massive sulphide bodies, that are not evident. Option (1) could very effectively account for fluorite deposition by mixing of Ca-rich with F-rich fluids (Williams-Jones et al., 2000), although Bethke (1996) demonstrates that cooling is also an efficient depositional mechanism.

The small number of primary fluid inclusions that are available from mineralised open-growth sites do not contain daughter salts (consequently the fluids are <26.5 wt.% NaCl), but do possess variable L-V ratios, supporting mixing, boiling or syn-ore condensation. Given the brittle-ductile conditions of ore formation, boiling can be discounted as a viable ore formation mechanism. Secondary inclusions do contain saline fluid inclusions with two daughter phases, but their timing with respect to mineralisation is not known.

The thermal conditions of ore formation are constrained by the stabilities of the alteration envelope phases of coexisting biotite and the almandine component of garnet. A broad estimate of 460–950° C is calculated for this assemblage in pelitic rocks (Ferry and Spear, 1978; Gessman et al., 1997). However, Mahar et al. (1997), Gessman et al. (1997) and others have found that high Mn stabilises garnet below its normal range at higher and lower pressures in pelites, and additionally permits the growth of garnet at ~100° C below normal conditions, so that these thermal constraints will be adjusted with future precise work on garnet and biotite mineral chemistry (preliminary results are reported in Davidson and Davis, 1997 and 2001). The brittle-ductile behaviour during ore formation favours pressures of ~3 kB, which is consistent with regional estimates of pressures (Jaques et al., 1982) for the northern Eastern Succession between D2 and D3, a likely period of episodic uplift (O'Dea et al., 1997).

An Integrated Genetic Model

The early syn-sedimentary hydrothermal history influenced the bulk geochemical character of the sequence that was leached during the subsequent metamorphic history. This low temperature hydrothermal event enriched the footwall sequence in Fe, K and Mn at ~1650-1640 Ma, and produced metre-scale BIFs over a large area; it may have had a broad relationship with Broken Hill-type deposit formation, which some workers interpret to have accompanied Soldiers Cap Group sedimentation (Bodon, 1998; Walters and Bailey, 1998). All lithologies in the ore sequence were emplaced during sedimentation, with the exception of a narrow sub-alkaline dolerite dyke.

The structural history involved the development of a narrow shear system by strain partitioning around rigid blocks of mafic igneous rocks during D1, with folding and mild reactivation in a regionally unusual orientation during D2, producing the broad east-west oriented Pumpkin Gully Syncline (Fig. 12). Steeply plunging F2 folds are a product of both the steep dips imposed upon the sequence during D1, and the variation in D2 strain along the hinge line of the folds. These local events were part of a regional duplexing of the Mary Kathleen Group meta-carbonates and evaporites, with the dominantly clastic carbonate-poor Soldiers Cap Group rocks; a tectonic contact between these packages is hypothesised to deeply underlie the Pumpkin Gully Syncline (O'Dea et al., 1997 and references therein). Mild vertical compression reactivated the Monakoff Shear system during D2.5, ie. at ore-time.

Flexural slip during D2.5 was concentrated on the east-west, near vertical, D1 shear system, with fluid packages being drawn in by extensional failure resulting in transient low pressure sites. High fluid pressures enhanced the local development of extensional failure by boudinage. During

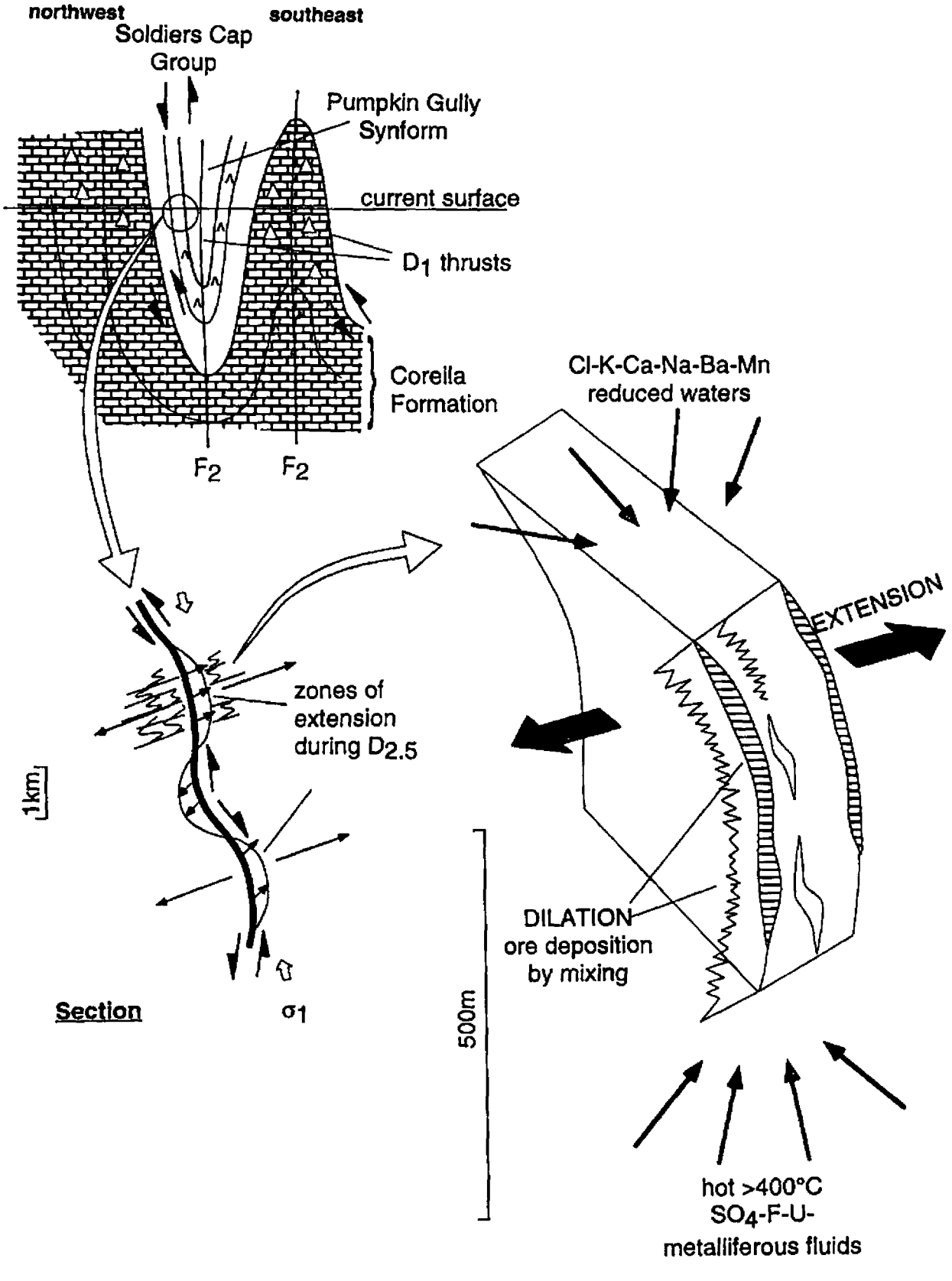


Figure 12: Genetic model for Monakoff, involving dilation in a broad D2.5 hinge zone, which induced mixing of a metal-bearing, >400° C, F-S-metal-rich fluid (granite derived?), with a reduced Ca-K-Ba rich fluid (meta-evaporite-derived), stimulating sulphide, barite and fluorite deposition.

D2.5, steeply plunging F2 folds (and hinge breccias) adjacent to dilating shear surfaces also channelled some fluids into the D2 hinge zones, producing pipe-like mineralisation zones. These pipes likely pinch and swell at depth, due to different dilational behaviour of changing D2 fold-plunge during D2.5. The geometry of extension during D2.5 favoured the inflow and mixing of fluids from above and below, producing a pronounced thermal anomaly compared to the temperatures of surrounding metamorphic rocks.
The paragenesis indicates that an early stage (Stage 1) of high temperature alkali metasomatism formed knots of massive magnetite surrounded by a shell of biotite 1 within the D1 shear system. Conditions of formation for stage 1 are not well constrained, but the assemblage characterises the early hydrothermal history of many shears in the vicinity of the Naraku Batholith, most notably at Ernest Henry, where they provide much of the magnetic response that initially attracted the attention of explorers (Craske, 1995). The breakdown of Stage 1 magnetite to form sulphide minerals is evidence that Stage 1 products may have played a role in ore precipitation. Stage 1 magnetite replaces D1 foliations and D2 folds, but its relationship to D2.5 could not be ascertained. In the Eastern Succession, control of later hydrothermal deposition by reaction with earlier hydrothermal products was first noted at the Eloise Cu-Au deposit by Baker (1994, 1998).

Stage 2 of the hydrothermal system was responsible for most ore and alteration assemblages. Mixing in dilatant zones was critical to the formation of abundant ore-stage barite, since Ba and oxidised S transport is not effective within the same fluid (Cooke et al., 2000). The proposed fluid chemistry was:

Fluid 1 - reduced, Ca-K-Fe-Mn-Ba rich, CO_2-rich, and saline, buffered mainly to the Mary Kathleen Group carbonates at regional metamorphic temperatures.

Fluid 2 - sulphate-rich, metal-bearing, 400–600° C, and F-rich. To account for the high F, fluid 2 may have been granite derived.

Mixing of these fluids deposited abundant barite, and possibly anhydrite (subsequently replaced by carbonate). The reaction of fluid 2 with earlier disseminated magnetite and Fe^{2+}-rich assemblages, acted to increase the concentration of H_2S available for sulphide deposition. However, an important feature of the mixing was the destabilisation of metal- and REE-F complexes when abundant fluorite deposition was stimulated by mixing with the calcic fluids. Such destabilisation may also have occurred where the wallrocks themselves were very calcic, which may account for the preferential replacement of amphibolite in the Monakoff Eastern Zone.

Very high metal concentrations in fluid 1 are suggested by: 1). the occurrence of high metal abundances in one-pass fluid circulation systems such as boudin neck zones; and 2). metal deposition at extreme temperatures, where most metals are still under-saturated. To account for the presence of hematite in some areas, and pyrrhotite in others, steep oxidation gradients must have been present on local scales, with hematite-stable zones representing the most oxidised parts of the system. CO_2-gradients, likely also displaced carbonate for hematite, because the stability field of Fe-Mn carbonate is enhanced by high pCO_2 relative to hematite under oxidised conditions at low to moderate temperatures (Cooke et al., 2000). This may also account for the general lack of hematite in an otherwise very oxidised environment at Monakoff.

Paragenetic Contrasts to the Ernest Henry Cu-Au Deposit

Ernest Henry exhibits the following alteration events, summarised from Mark et al. (2000) (and given new titles for ease of reference here), in order of occurrence:
Stage 1 - Regional Na-Ca alteration;
Stage 2 - Pre-ore disseminated biotite-magnetite alteration up to kilometres from the deposit, and spessartine-K feldspar (Ba)-manganiferous biotite veining transitional to the ore event;
Stage 3 - K-feldspar-hematite alteration transected by quartz-calcite-magnetite-fluorite-titanite/rutile veins) within 2 km of ore, transitional to two ore vein and breccia matrix stages consisting of magnetite, calcite, pyrite, biotite, chalcopyrite, K feldspar, titanite and quartz, with accessory garnet, barite, molybdenite, fluorite, amphibole, apatite, monazite, arsenopyrite, LREE fluoro-carbonate, galena, cobaltite, sphalerite, scheelite, uraninite and tourmaline;
Stage 4 - Post-ore carbonate 'flooding', forming veins and breccias of carbonate-quartz-biotite-actinolite-pyrite-magnetite-minor garnet-chalcopyrite.

In comparison, Monakoff is missing the early regional Na-Ca alteration, but conspicuous albite alteration post-dates all other types (Monakoff Stage 4), and is focussed on NW-trending faults. Most obviously, the massive K-feldspar-hematite alteration which is the hallmark of Ernest Henry ore and alteration is absent from Monakoff. However, the abundant biotite in Monakoff Stages 1 and 2 attests to similar K-metasomatism during and prior to the ore events. Conditions of alteration are likely to have been more reduced at Monakoff compared to Ernest Henry, thus stabilising biotite-magnetite over K-feldspar-hematite. Additionally, fluid flow at Monakoff was highly partitioned and subjected to lower fluid pressures, on the basis of the confinement of ore formation and alteration to the major zones of structural weakness, and the far lower abundance of fluid-related brecciation.

Exploration implications

Our improved structural understanding of the Monakoff deposit provides potential new target areas in the district. Ore forms a 1.5 km long sheet which is basically continuous to the north-south fault (to the west), and to the east extends to a large D2 fold, which is now offset in a left-lateral sense by a D3 fault (Fig.1 and Fig. 3). This compartment may have experienced dilation across its whole length during D2.5, with the greatest dilation occurring near the centre of the sheet. The western fault may either have accommodated

shearing strain if it was present during D2.5, or more likely it offset the mineralisation obliquely as well as in a strike-slip sense, such that mineralisation does not now continue to the west. To the east, D2.5 dilation may have been interrupted by the medium-scale D2 fold zone, but repetitions could be expected at the intersection between D2.5 fold hinges and steeply-dipping D1 shear positions to the east, and within amphibolite in reactivated D2 fold hinges.

Previous exploration attention has mainly focussed on the magnetic and outcropping BIFs, but this study indicates the importance of early steep shears, steep lithological contacts, and large-scale inhomogeneities in competency, as alternate targets. Notably the structural-aeromagnetic interpretation suggests the occurrence of fault repetitions of the ore package several kilometres to the north east under cover (Fig. 1). Broadly the model would favour ore positions close to Mary Kathleen Group/Soldiers Cap Group contacts, to facilitate fluid mixing. Given the probable granitic fluid source for F, sub-surface granites close to D2.5 dilational sites should be targeted, but other than a post-D2.5 thermal peak (evidenced by randomly oriented disseminated biotite 3 throughout the area), there is no surface evidence of granites within 2 km of Monakoff. The obvious conduit to these granites is a north-south vertical fault system 1 km west of Monakoff, but the timing of this fault is not known, other than it contains probable D3-age carbonate-vein systems.

Comparison with the Ernest Henry paragenesis indicates that widespread or intense K feldspar alteration is not a prerequisite to form the polymetallic element assemblage that characterises both Ernest Henry and Monakoff. We do not yet know whether the more oxidised style of K-metasomatism at Ernest Henry, and the higher fluid pressures that resulted in extensive brecciation, were critical features in the formation of large tonnages there, compared to Monakoff.

Acknowledgements

This work was supported by collaborative ARC-AMIRA Project P438, an Australian Post-doctoral Research Fellowship for BKD, and an Australian Research fellowship for GJD. Cloncurry Mining, and in particular Steve Milner, Jim and Annette, and Julie Hugenholtz, kindly allowed access and provided logistical support. Simon Stephens, Wieslaw Jablonski, Debbie Harding and Sharon Ness (JCU) all assisted in production of the many numbers and figures in this paper. Discussions with Peter Pollard, Pat Williams, Kevin Blake, James Lally and many JCU post-graduate students improved our understanding of the Monakoff system, in its context as a small part of Mt Isa Inlier hydrothermal activity. Lastly, a firm thankyou! to all of the companies and their geologists who financially supported this project, and encouraged us during our fieldwork and reporting.

References

Adshead, N.D., 1995 - Geology, alteration and geochemistry of the Osborne Cu-Au deposit, Cloncurry district, NW Queensland, Australia. Unpublished Ph.D thesis (James Cook University), 382 p.

Ashley, P.M., 1983 - Recent exploration results at the Monakoff prospect, near Cloncurry, northwest Queensland. Esso Minerals internal report, Dec. 1983 (held by Terra Search, Townsville).

Baker, T., 1994 - Localization of sulphides by a hornblende-biotite alteration system at the Eloise Cu-Au deposit, Cloncurry district, NW Queensland. Geological Society of America 1994 abstracts with programs, A-379.

Baker, T., 1998 - Alteration, mineralization and fluid evolution at the Eloise Cu-Au deposit, Cloncurry district, northwest Queensland, Australia. Economic Geology 93, 1213–1236.

Beardsmore, T.J., Newbery, S.P. and Laing, W.P., 1988 - The Maronan Supergroup— an inferred early volcanosedimentary rift sequence in the Mount Isa Inlier, and its implications for ensialic rifting in the Middle Proterozoic of northwest Queensland. Precambrian Research 40/41, 487–507.

Bell, T.H., 1991 – The role of thrusting in the structural development of the Mt Isa Mine and its relevance to exploration in the surrounding region. Economic Geology 86, 1602–1625.

Bethke, C.M., 1996 - Geochemical reaction modelling. Oxford University Press, New York, 397 p.

Bodon, S. B., 1998 - Paragenetic relationships and their implications for ore genesis at the Cannington Ag-Pb-Zn deposit, Mt Isa Inlier, Queensland, Australia. Economic Geology 93, 1463–1488.

Cooke, D.R., Bull, S.W., Large, R.R. and McGoldrick, P.J., 2000 - The importance of oxidized brines for the formation of Australian Proterozoic stratiform sediment-hosted Pb-Zn (Sedex) deposits. Economic Geology, 95, 1–18.

Cox, S.F., Wall, V.J., Etheridge, M.A. and Potter, T.F., 1991 - Deformational and metamorphic processes in the formation of mesothermal vein-hosted gold deposits— examples from the Lachlan Fold Belt in central Victoria, Australia. Ore Geology Reviews 6, 391–423.

Craske, T., 1995 - Geological aspects of the discovery of the Ernest Henry Cu-Au deposit, northwest Queensland. Australian Institute of Geologists Bulletin16, 95–109.

Davidson G.J., 1994 - A geochemical and geological reconnaissance study of alteration, copper-gold ores, and iron-rich lithologies in the Cloncurry area, Mt Isa Inlier. Unpublished CODES report, March 1994, University of Tasmania, 185p.

Davidson, G.J., 1995 - Progress Report 1: Monakoff— macroscopic geology in Pollard, P. (compiler) Cloncurry base metals and gold annual report, October 1995, AMIRA P438, 3A-1/3A-10.

Davidson G.J., 1998 - Variation in copper-gold styles through time in the Proterozoic Cloncurry goldfield, Mt Isa Inlier: a reconnaissance view. Australian Journal of Earth Sciences, 45, 445-462.

Davidson, G.J. and Davis, B.K., 1996 - Progress report 2: Monakoff— S isotope geochemistry and descriptive structural geology. Cloncurry base metals and gold annual report, October 1996, AMIRA P438, 8-1–8-13.

Davidson, G.J. and Davis, B.K., 1997 - Characteristics of the Monakoff Cu-Au-F-Ba-Mn deposit, Mt Isa Eastern Succession. Final report Cloncurry base metals and gold project, September 1997, AMIRA P438, 13-1–13-53.

Davidson, G.J. and Davis, B.K., 2001 - Structural and geochemical constraints on the emplacement of the oxide Cu-Au Monakoff deposit. In: Williams, P.J., ed., A Hydrothermal Odyssey, Townsville, 17–19th May 2001, EGRU Contribution 59, 44–45.

Davidson, G.J. and Large, R.R., 1998 - Proterozoic Au-Cu deposits. AGSO Journal Jubilee Papers, 17, 105–114.

Davis, B.K., Pollard, P.J., Lally, J.H., McNaughton, N.J., Blake, K. and Williams, P.J., 2001a - Deformation history of the Naraku Batholith, Mt Isa Inlier, Australia: implications for pluton ages and geometries from structural study of the Dipvale Granodiorite and Levian granite. Australian Journal of Earth Sciences 48, 113–129.

Davis, B.K., Hickey, K.A. and Rose, S., 2001b - Superposition of gold mineralisation on pre-existing carbonate alteration: structural evidence from the Mulgarrie gold deposit, Yilgarn Craton. Australian Journal of Earth Sciences 48, 131-149.

Deer, W.A., Howie, R.A. and Zussman, J., 1992 - An introduction to the rock-forming minerals. Longman, Hong Kong.

De Jong, G., and Williams, P.J., 1995 - Evolution of metasomatic features during exhumation of mid-crustal Proterozoic rocks in the vicinity of the Cloncurry Fault, NW Queensland. Australian Journal of Earth Sciences 42, 281–290.

Derrick, G.M., 1996 - The 'geophysical approach to metallogeny of the Mt isa Inlier. Proceedings of the Australasian Institute of Mining & Metallurgy Annual Conference, Perth, 24–28 March, 1996, 349–366.

Derrick, G.M., Wilson, I.H. and Hill, R.M., 1976 - Revision of stratigraphic nomenclature in the Precambrian of northwestern Queensland. V. Soldiers Cap Group. Queensland Government Mining Journal 77: 600-604.

Dong, G., 1996 - Fluid inclusions from Cloncurry ore systems. Cloncurry base metals and gold annual report, September 1996, AMIRA P438, 5-1/5-17.

Ferry, J.M. and Spear, F.S., 1978 - Experimental calibration of the partitioning of Fe and Mg between biotite and garnet. Contributions to Mineralogy and Petrology, 66, 113–117.

Garrett, S., 1992 - Geology and geochemistry of the Mount Elliott copper-gold deposit, N.W. Queensland. Unpublished M.Sc thesis, University of Tasmania, 139 p.

Gessman, C.K., Spiering, B. and Raith, M., 1997 - Experimental study of the Fe-Mg exchange between garnet and biotite: constraints on the mixing behaviour and analysis of the cation-exchange mechanisms. American Mineralogist 82, 1225–1240.

Harely, M. and Charlesworth, E.G., 1992 - Thrust-controlled gold mineralization at the Elandshoogte mine, Sabie-Pilgrim's Rest goldfield, South Africa. Mineralium Deposita 27, 122–128.

Hatton, O.J., Bull, S.W. and Davidson, G.J., 2000 - A review of the geological setting and sedimentology of the Proterozoic upper Soldiers Cap Group, Eastern Succession, rift fill in a Pb-Zn-rich basin (Mt Isa Inlier, NW Queensland). Proceedings of New Ideas for a New Millenium, Cranbrook Workshop, May 6–7 2000. http://www.cyberlink.bc.ca/-ekcm/Abstracts.htm

Jaques, A., Blake, D. and Donchak, P., 1987 - Regional metamorphism in the Selwyn Range area, northwest Queensland. Australian Bureau of Mineral Resources Journal of Geology & Geophysics 7, 181-196.

Laing, W., 1991 - Base metal + gold mineralisation styles in the Cloncurry terrane. Economic Geology Research Unit Contribution 38: 77–88.

Macready, T., Goleby B.R., Goncharov, A., Drummond, B.J. & Lister, G.S., 1998 - A framework of overprinting orogens based on the interpretation of the Mount Isa deep seismic transect. Economic Geology 93, 1422–1434.

Mahar, E.M., Baker, J.M., Powell, R., Holland, T.J.B. and Howell, N., 1997 - The effect of Mn on mineral stability in metapelites. Journal of Metamorphic Geology 15, 223–238.

Mark, G., 1998 - Albitite formation by selective pervasive sodic-alteration of tonalite plutons in the Cloncurry district, NW Queensland. Australian Journal of Earth Sciences 45, 765–774.

Mark, G., Oliver, N.H.S., Williams, P.J., Valenta, R.K., Crookes, R.A., 2000 - The evolution of the Ernest Henry Fe-oxide-(Cu-Au) hydrothermal system; In Porter T.M., Ed., Hydrothermal iron oxide copper-gold & related deposits, Australian Mineral Foundation, Adelaide, 123–136.

Marshall, L.J. and Oliver, N.H.S., 2001 - Regionally extensive tectonic and hydrothermal breccias in the Cloncurry Fe-oxide-Cu-Au district, NW Queensland. In: Williams, P.J., ed., A Hydrothermal Odyssey, Townsville, 17–19th May 2001, EGRU Contribution 59, 126–127.

McClay, K., 1987 - The mapping of geological structures. Geological Society of London handbook series, Wiley & Sons, Chichester, 161 p.

Milner, S., 1993 - The Monakoff Cu-Pb-Zn-Au-Ag-Co-Ba-F deposit— geological summary. In: Derrick, G., ed., Core Shack Explanatory Notes, AMF Course 832/93, Australian Mineral Foundation, Glenside, South Australia, 31–39.

Munöz, J.L., 1984 - F-OH and Cl-OH exchange in mica with applications to hydrothermal ore deposits. In: Bailey, S.W., ed., Micas. Reviews in Mineralogy13, 469–491.

O'Dea, M.G., Lister, G.S., MacCready, T., Betts, P.G., Oliver, N.H.S., Pound, K.S., Huang, W. and Valenta, R.K., 1997 - Geodynamic evolution of the Proterozoic Mount Isa terrain; In: Burg, J.-P. and Ford, M., eds., Orogeny through time, Geological Society Special Publication 121, 99-122.

Oliver, N.H.S., 1995 - Hydrothermal history of the Mary Kathleen Fold Belt, Mt Isa Block, Queensland. Australian Journal of Earth Sciences 42, 267–280.

Page, R.W., 1988 - Geochronology of early to middle Proterozoic fold belts in northern Australia: a review. Precambrian Research 40/41, 1–19.

Page, R.W. and Sun, S-s, 1998 - Aspects of geochronology and crustal evolution in the Eastern in the Eastern Fold Belt, Mount Isa Inlier. Australian Journal of Earth Sciences 45, 343–362.

Partington, G.A. and McNaughton, N.J., 1997 - Controls on mineralization in the Howley district, Northern Territory: a link between grantie intrusion and gold mineralization. Chron. Rech. Min., 529, 25–44.

Pollard, P.J., Davis, B.K. and Williams, P.J., 1997 - Structural and physicochemical controls on ore formation in Cloncurry Cu-Au deposits, eastern Mount Isa Inlier, Queensland. Final report Cloncurry base metals and gold project, September 1997, AMIRA P438, 2-1–2-41.

Pollard, P.J., Mark, G. and Mitchell, L.C., 1998 - Geochemistry of post-1540 Ma granites in the Cloncurry district, northwest Queensland. Economic Geology 93, 1330–1344.

Reeve, J.S., Cross, K.C., Smith, R.N. and Oreskes, N., 1990 - Olympic Dam copper-uranium-gold-silver deposit; In: Hughes F.E., ed., Geology of the mineral deposits of Australia and Papua New Guinea: Australasian Institute of Mining & Metallurgy Mon. 14, p. 1009–1035, Melbourne, Australia.

Reinhardt, J., 1987 - Cordierite-anthophyllite rocks from north-west Queensland, Australia: metamorphosed magnesian pelites. Journal of Metamorphic Geology 5: 451-472.

Ronzê, P.C., Soares, A.D.V., dos Santos, G. S. and Barreira, C.F., 2000 - Alemão copper-gold (U-REE) deposit, Carajás, Brazil; In Porter T.M., Ed., Hydrothermal iron oxide copper-gold & related deposits, Australian Mineral Foundation, Adelaide, 191–202.

Rotherham, J. F., 1997 - A metasomatic origin for the iron-oxide Au-Cu Starra orebodies, Eastern Fold Belt, Mt Isa Inlier. Mineralium Deposita 32, 205–218.

Rowins, S.M., Groves, D.I., McNaughton, N.J., Palmer, M.R. and Steward, C.S., 1997 - A reinterpretation of the role of granitoids in the genesis of Neoproterozoic gold mineralization in the Telfer Dome, Western Australia. Economic Geology 92, 133–160.

Rubenach, M.J. and Barker, A.J. 1996 - Episodic metamorphism and metasomatism in pelitic rocks of the Snake Creek Anticline; In: Baker, T., Rotherham, J., Richmond, J., Mark, G. and Williams, P., eds., MIC '96 New developments in metallogenic research: the McArthur, Mt Isa, Cloncurry minerals province; EGRU Contribution 55, 127–130.

Ryburn, R.J., Wilson, I.H., Grimes, K.G. and Hill, R.M., 1988 - Cloncurry 1:100 000 geological map commentary. Australian Bureau of Mineral Resources.

Souza, L.H. and Vieira, E.A.P., 2000 - Salobo 3 Alpha deposit: geology and mineralisation ; In Porter T.M., Ed., Hydrothermal iron oxide copper-gold & related deposits, Australian Mineral Foundation, Adelaide, 213–224.

Tazava, E.and de Oliveira, C.G., 2000 - The Igarapé Bahia Au-Cu-(REE-U) deposit, Carajãs Mineral Province, Northern Brazil ; In Porter T.M., Ed., Hydrothermal iron oxide copper-gold & related

deposits, Australian Mineral Foundation, Adelaide, 203–212.

Walters, S. and Bailey, A., 1998 - Geology and mineralization of the Cannington Ag-Pb-Zn deposit: an example of Broken Hill-type mineralization in the eastern Succession, Mount Isa Inlier, Australia. Economic Geology 93, 1307–1329.

Wilde, A.R., Bloom, M.S., Wall, V.J., 1989 - Transport and deposition of gold, uranium and platinum-group elements in unconformity-related uranium deposits. Economic Geology Monograph 6, 637–650.

Williams, P.J., 1998 - An introduction to the metallogeny of the McArthur River-Mount Isa-Cloncurry minerals province. Economic Geology 93, 1120–1131.

Williams-Jones, A.E., Samson, I.M. and Olivo, G.R., 2000 - The genesis of hydrothermal fluorite-REE deposits in the Gallinas Mountains, New Mexico. Economic Geology 95, 327–342.

Winchester, J.A. and Floyd, P. A., 1977 - Geochemical discrimination of different magma series and their differentiation products using immobile elements. Chemical Geology 20, 325-343.

Wyborn, L.A.I., 1998 - The younger ca 1500 Ma granites of the Williams and Naraku Batholiths, Cloncurry district, eastern Mt Isa Inlier: geochemistry, origin, metallogenic significance and exploration indicators. Australian Journal of Earth Sciences 45, 397–412.

PGC PUBLISHING

Sleigh, D.W. 2002 - The Selwyn Line Tabular Iron-Copper-Gold System, Mount Isa Inlier, NW Queensland, Australia; *in Porter, T.M. (Ed.), Hydrothermal Iron Oxide Copper-Gold & Related Deposits: A Global Perspective*, Volume 2; PGC Publishing, Adelaide, pp 77-93.

THE SELWYN LINE TABULAR IRON-COPPER-GOLD SYSTEM, MOUNT ISA INLIER, NW QUEENSLAND, AUSTRALIA

D.W.W. Sleigh

Group Geologist, Selwyn Operations Pty Ltd

Abstract - The Selwyn Line is the name adopted for an open arcuate zone of iron-copper-gold mineralisation, located ~150 km southeast of Mount Isa, in the Mount Isa Proterozoic inlier, northwest Queensland, Australia. Since the discovery of gold mineralisation in the Selwyn Hills in the 1970's, five small mines have been operated. These exploited high grade ironstone hosted gold-copper mineralisation, located within a zone of poly-aged shearing and complex alteration. The mines are located within the Starra Shear which has a history of ductile-brittle, brittle-ductile and brittle deformation. The structure is altered over widths of between 100 and 500 m, and for more than 10 km along strike. The alteration involved early albite +quartz +calcite +scapolite +actinolite replacement of the host sheared meta-sediments of the Staveley Formation. This was followed by a magnetite/hematite+biotite+quartz(+pyrite) overprint, and finally post tectonic oxidation of the magnetite, and chlorite-calcite alteration with associated chalcopyrite and gold mineralisation, and limited pyrite formation (Rotherham 1997). The high grade zones exhibit indications of strong structural controls. They typically plunge steeply to the north along magnetite bearing extensional duplex structures and shear planes which include portions of the hanging wall bounding shears and link structures to the footwall bounding shears. The dimensions of the mined and mineable resource (<8 Mt) have always been regarded as small for typical Fe-Cu-Au systems. However resource work done on lower cut-off grades indicates that the system is more typical of the large systems of this sort found elsewhere in the district, with a pre-mining global resource of at least 29 Mt @ 2.5 g/t Au and 1.4% Cu (at a 1.5% $Cu_{equiv.}$ cutoff using a factor of ~ 0.8 depending on where the ore is from), 49 Mt @ 1.76 g/t Au and 1.05% Cu using a 1.0% cut off, or 95 Mt @ 1.1 g/t Au and 0.74% Cu at a 0.5% cutoff. These are embraced within a larger mineralised system with a global resource of 253 Mt @ 0.48 g/t Au and 0.34% Cu at measured, indicated and inferred categories, to a depth of ~300 m below surface (using a 0.2% $Cu_{equiv.}$ cutoff cut off).

The main observations made in this paper are: (1) The Selwyn Line is fairly typical of iron-copper-gold systems in NW Queensland in that it is part of a very large alteration system containing large tonnages of mineralised magnetite ironstones with associated low tenor Cu and Au grades; (2) In the Selwyn Line (excluding the 222 Mine) the ore grade zones discovered to date have been confined to duplexes within crudely tabular "tramway" shear systems, in which multiple localised sites for ore mineral deposition were generated. The cumulative tonnage of these sites is substantial but still remains constrained by the overall tightness of the late (brittle-ductile) strain zones which were dominated by flattening (D_4). The dimension of ore grade zones in these systems is mostly a function of the volume of the zones in which late extensional deformation was developed (D_4 to D_6, Adshead-Bell, 2000); (3) At 222 Mine to the south, the structural location is more complex with multiple "north" trending S_2/S_4 shears intersecting the S_1 'hinge zone' shear and its associated intra-folial ironstones at higher angles. This has provided a site for greater volumes of late stage alteration and mineralisation. The resultant lower grade tonnages drilled to date have already intersected larger orebodies here (>5 Mt), and suggest there is further potential for the delineation of a major deposit in this system.

Introduction

The Selwyn Line is the name adopted for an arcuate zone of iron-copper-gold mineralisation, located in north west Queensland, Australia (Fig. 1), some 150 km southeast of Mt Isa. This linear zone contains five dormant iron-copper-gold mines which where exploited from May 1988 until March 1999. This mining principally exploited high grade gold (and copper) mineralisation hosted by sheared iron oxide-feldspar-chlorite-silica-carbonate (± biotite and sericite) altered metasediments. On the basis of the mineral and metal associations observed within these deposits, the Selwyn deposits were grouped by Hitzman *et al.* (1992) into the iron-copper-gold metallogenic family of deposits, including Olympic Dam as one end member and the Kiruna iron deposits as another.

In total only 6.84 million tonnes of ore at 4.6 g/t Au and 2.1% Cu, were removed from the five Selwyn deposits in

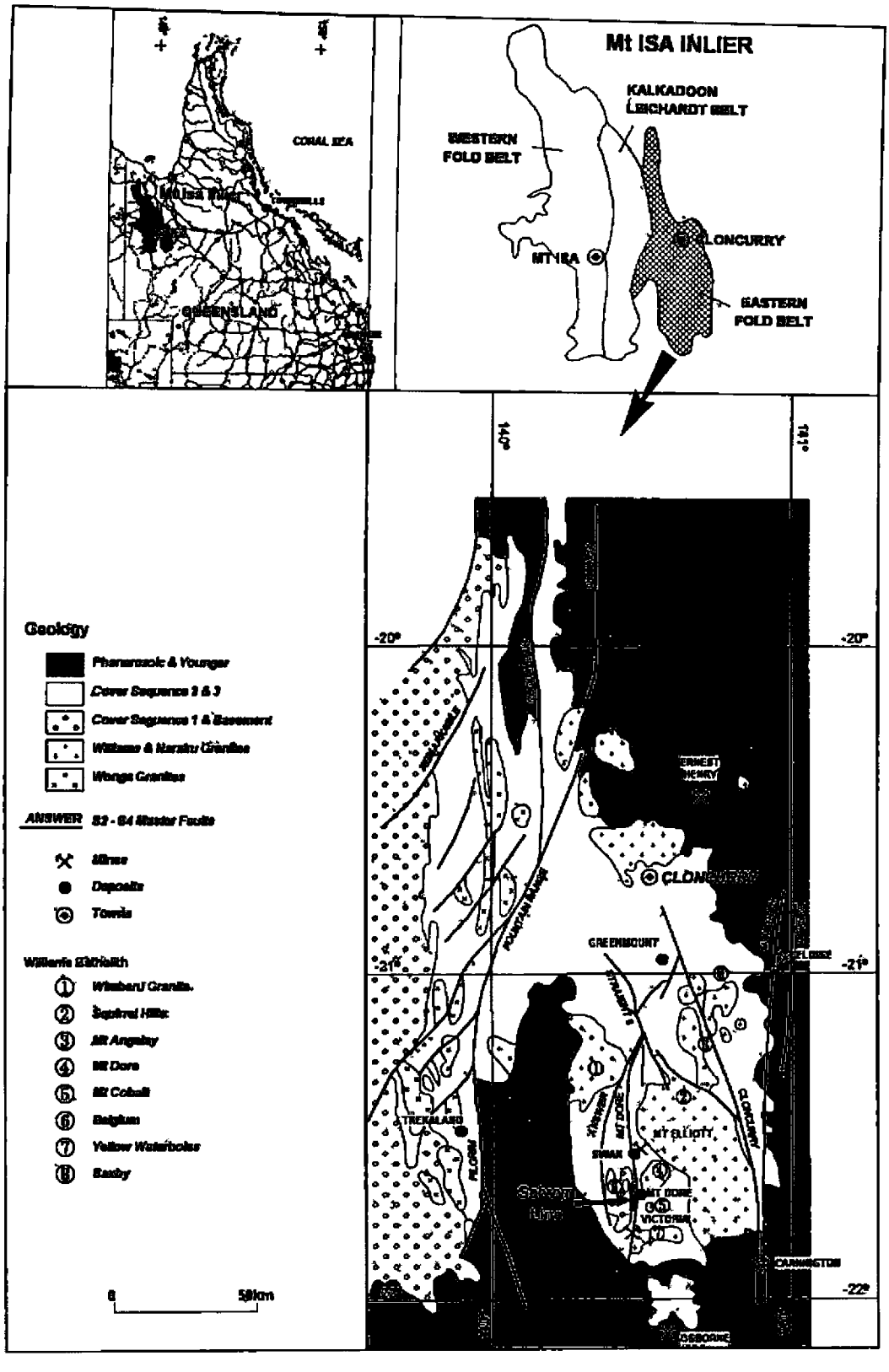


Figure 1: Selwyn Line location map and regional geological setting

both open pit and underground mining operations to their closure during March 1999 (Selwyn Mines Prospectus, 2000). The residual reserve at this stage was listed at 0.1 mt @ 4.51 g/t gold and 2.26% copper. This relatively modest historical mined tonnage and high gold grade is unusual in relation to other typical iron-copper-gold deposits, where huge tonnages at lower grades are more characteristic (eg. Ernest Henry Mine located 170 km north of Selwyn had a reported resource of 166 mt @ 1.6% Cu and 0.54 g/t Au (Ryan 1998)). Laing (1998) suggested that mineralised systems such as those at Selwyn and Osborne had potential to represent major deposits if lower grade cut offs were applied. The possibility that the Selwyn Line deposits formed part of a major mineralised system

was also arrived at independently by the current operating company during 2000. A full review of the existing data was undertaken resulting in scoping and feasibility studies during 2000 and 2001, with the decision to proceed with the exploitation of the resultant enlarged resource being made in the final quarter of 2001. This paper endeavours to present an update on the setting of the Selwyn Line and convey the outcome of the resource review.

It is noted at this point that in the literature, the mines of the Selwyn Line have historically been called both the Starra Mines and the Selwyn Mines. To avoid further changes and confusion the author and current mining company have retained the name adopted by the previous mining company, namely the "Selwyn Mines".

Regional Setting

The Selwyn Line is hosted by highly altered, sheared metasediments of the Staveley Formation of the Mary Kathleen Group and Maronan Supergroup. These units are located in the eastern tectono-stratigraphic domain of the Proterozoic aged Mount Isa Inlier. This eastern domain has been variously referred to as the Eastern Succession, the Eastern Fold Belt and more recently as the Eastern Mount Isa Block (Laing, 1998) and is indicated in Figure 1. Regionally the area of interest is underlain by a package of metamorphosed shales, siltstones, pelites, calcic metasediments, evaporites, and metavolcanics intruded by several generations of felsic and mafic magmatism. The bulk of the stratigraphy of the Mount Isa Inlier is thought to be composed of 4 main units (Beardsmore et al. 1988; Blake and Stewart 1992; Page and Sun, 1996), as follows:

1) A pre-1875 Ma ***gneissic and schistose basement.*** In the Selwyn area the Double Crossing Metamorphics and the gneissic components of the Gin Creek "Granite" (Figure 2) were interpreted as being part of this basement (Blake, 1987). Eastward of this, the highly deformed Answer Slate unit was thought to form part of this early "basement" although this interpretation has been questioned by newer work. Dating in recent years has suggested these units are younger, falling within the same time bracket as the last phases of Cover Sequence 1 and the early phases of Cover Sequence 2 listed below (Page and Sun , 1998). Never the less, the Answer Slate still forms part of a higher grade (amphibolite facies) "basement" to the upper greenschist facies Cover Sequence 2 and 3 rocks in the Selwyn Line Area across a tectonised contact.

2) The ***Isan Cover Sequence 1,*** which is dominated by felsic meta-volcanic rocks of between 1875 and 1850 Ma age (Blake, 1987) . These are not developed in the Selwyn district.

3) The ***Isan Cover Sequence 2,*** composed of calc-silicates, metasediments, and both mafic and felsic metavolcanic suites. Importantly these also include the carbonaceous shales, evaporites, and carbonate formations of the Mary Kathleen Group.

4) The ***Isan Cover Sequence 3,*** composed of mafic metavolcanics, turbidites, psammites, and assorted amphibolites, schists and gneisses of the Soldiers Cap Group. A date of 1677±9 Ma was established by Page, 1994 for the Fullarton River Group which conformably underlies the basal Soldiers Cap strata.

Age dating by Nisbet et al. (1983), Wyborn et al. (1988), Pearson et al. (1992), Page (1994), Page and Sun (1996), and Pollard and McNaughton (1997) combined with petrographic, geochemical, and structural data have grouped the principal intrusive bodies in the region into three main affiliations.

1) The ***Wonga Batholith*** involved extensive A and I type bimodal magmatism in the western parts of the Eastern Fold Belt, during the pre-Isan extensional deformation (1760-1720 Ma, Pearson et al. 1992).

2) The ***Naraku Batholith*** which includes a pre-peak metamorphic microgranite phase of plutons dated at 1754±25 Ma (Wyborn et al. 1988), foliated granodiorite of 1752±8 Ma (Pollard and McNaughton, 1997), and coarse grained unfoliated hornblende-biotite sodic/ calcic granite plutons with an age range of 1508±70 Ma (Wyborn et al. 1988). These are typically strongly fractionated A-type intrusives, located in the northern and eastern parts of the Eastern Fold Belt.

3) The ***Williams Batholith*** dominates the southern parts of the Eastern Fold Belt. It is also composed of at least two main phases. The older is a foliated leucogranite while the younger post dates the main regional deformational events. The main older phase observed in the Selwyn District is the Gin Creek Granite which was dated by Page and Sun (1996) at ~1740 Ma. The younger Williams intrusives typically comprise coarse grained unfoliated granites. The Selwyn district was intruded by numerous granitoids of this generation including the Mount Dore, Yellow Waterhole, Mount Cobalt, Squirrel Hills, Belgium, Saxby and Wimberu granite bodies. The Mount Dore granite was dated at 1509±22 Ma by Nisbet et al. (1983) and 1510±10 Ma by Pollard and McNaughton (1997). Further south the Yellow Waterhole granite was dated at 1480±28 Ma (Page, 1994), and 1510±8 Ma (Pollard and McNaughton, 1997). Eastward the Squirrel Hills have an age of 1514±5 Ma (Pollard and McNaughton, 1997). Pollard et al. (1998) recognised that these granitoids were distinctly potassic, meta-aluminous, and sub-alkaline in character, and belonged to a Super-suite of A-type granitoids within the Williams Batholith. Modelling of gravity and magnetic data indicates the Williams batholith has flat upper and lower bounding surfaces, implying sheet-like emplacement or thrusting. The seismic profiles support this (Wyborn et al. 1996). Modelling of CSAMT data and drilling information (Selwyn Operations Pty Ltd unpublished data, 2001) across the western margin of the Mount Dore granite body supports the view that at least towards their margins, these granites are not emplaced as deep plutonic or diapiric bodies, but rather form sheet-like features, due to thrusting and/or crudely tabular igneous emplacement.

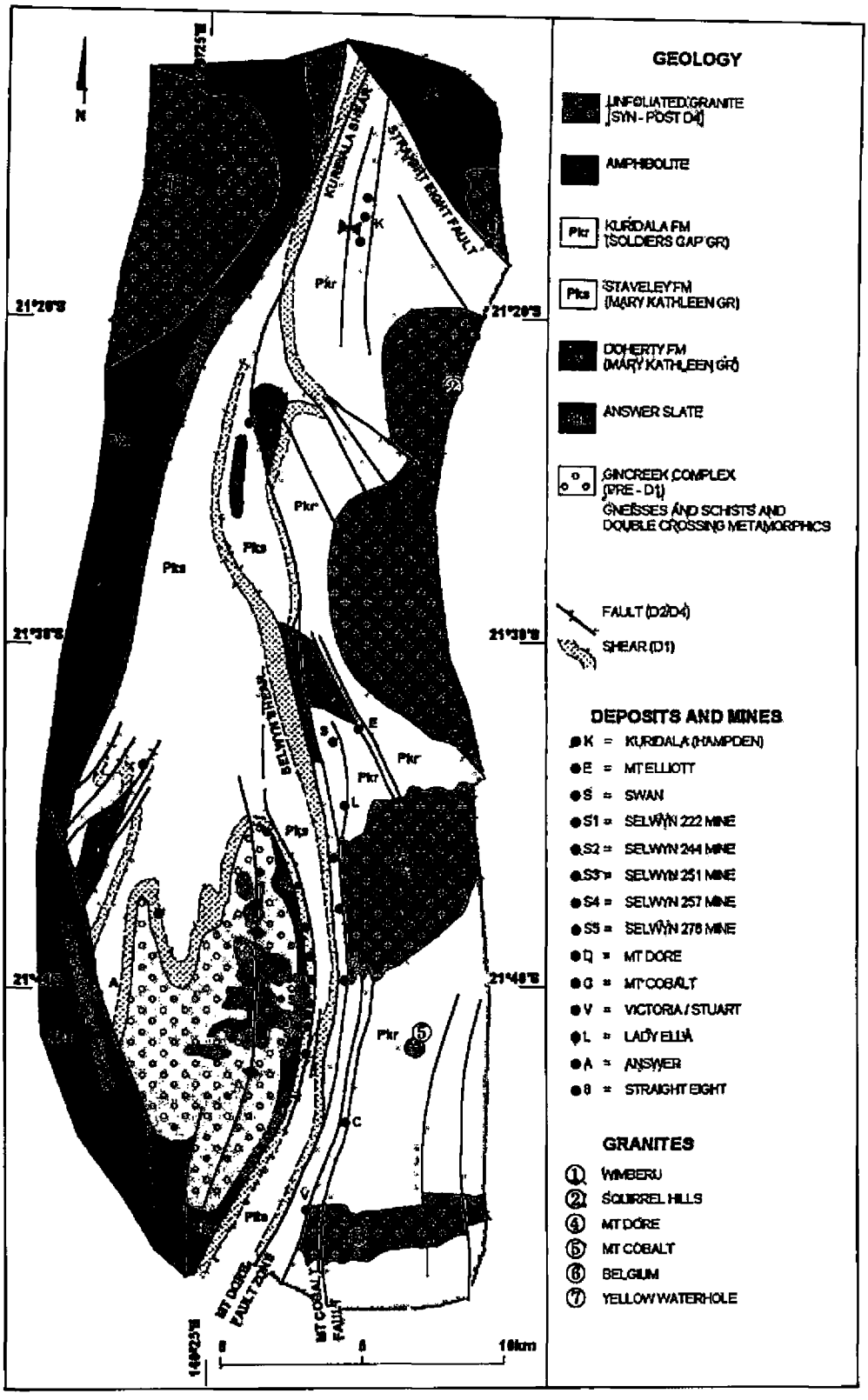


Figure 2: District geology (modified from Switzer et al.1988, and Beardsmore 1992)

Throughout the region there are also numerous intrusive mafic bodies for which no collective name has been given. They are emplaced as dykes, sills and pods, and belong to several age groupings. These include earlier pre- and syn-tectonic metadolerite and amphibolite, and later gabbroic and dioritic dykes considered to be coeval with the ~1500 Ma unfoliated granite phases of the Williams and Naraku batholiths (Pollard et al., 1996).

Tectono-stratigraphic Framework of the Eastern Fold Belt

The Double Crossing Metamorphics, dated at 1840±20 Ma (Page and Sun, 1998), and possibly the Gin Creek granite gneisses and the Answer Slate are the oldest units exposed in the Selwyn region of the Eastern Fold Belt. Their age,

combined with their comparatively high metamorphic grade and un-correlated early structural history, suggests they were probably emplaced and deposited late during the first major tectonic event to influence the region, namely the Barramundi Orogeny, which was bracketed at between 1880-1850 Ma by Etheridge et al. (1987).

The main stratigraphic units in the Eastern Fold Belt belong to the second and third supracrustal cover sequences. These are interpreted as having been emplaced during a prolonged period of ensialic extensional and strike slip tectonics (Loosveld, 1989) between 1725 Ma (Page, 1994) and 1650 Ma (Page, 1993; Page and Sun, 1996). These supracrustal sequences were then subjected to 3 major regional compressional events (Page and Bell, 1986) which comprise the second main orogeny to effect the region, namely the Isan Orogeny. This occurred between 1590 Ma and 1500 Ma (Blake et al., 1990) with peak metamorphism at ~1545 Ma (Page and Bell, 1986).

The first compressional event, (D_1) is most evident in the development of regionally extensive, flat lying mylonite zones deformed by subsequent D_2 and D_3 aged folds (Laing, 1998), and east-west trending fold-thrust complexes (Bell, 1983). One of these mylonite zones (the Starra Shear) is interpreted to separate the sheared greenschist facies Staveley metasediments, from the amphibolite facies Gin Creek-metamorphic "basement" to the west (Figure 2).

The second deformation (D_2) produced the prominent north-south trending, regional fabric and fold axis orientation, evident in most regional geological maps. D_2 deformation involved strong east-west shortening which generated north trending, steeply west verging to upright folds with a well developed axial planar foliation and sub-parallel ductile-brittle shears.

D_3 was also compressional in an east-west orientation and also resulted in north-south trending upright folding. This event caused east over west rotation of the D_2 aged folds (Adshead-Bell, 1998) and activation of the north-south trending faults in a more brittle environment.

This is a simplistic framework, with many areas in both the western and eastern Isan domains exhibiting several additional phases of local deformation (Bell and Hickey, 1998; Adshead-Bell, 2000). Laing 1998, using seismic profiles as support, suggests the entire Eastern Fold Belt is an allochthonous block, composed of interleaved carbonate and siliclastic units separated by listric faults. Structural and seismic data suggests these are eastward dipping but become flat dipping along a major detachment plane at depth. Bett and Lister (2001) and MacCready et al. (1998) suggest that towards the end of the Isan Orogeny, there was a transition from thin to thick skinned tectonics, and wrenching. This was marked by the development of increasingly brittle deformation (Drummond et al., 1998). In the western parts of the Mount Isa Inlier, economically important "master faults" were identified as zones where earlier basin forming structures were overprinted by deep penetrating, brittle, strike slip, reverse slip and wrench faults (Lister et al., 1999). In the Eastern Fold Belt similar reactivated "master faults" were also identified although they are in a different structural domain (Blake, 1987; De Jong and Williams, 1995; Oliver, 1995). Prominent structures of this sort in the Selwyn region include the Mt Dore and Cloncurry fault systems (Beardsmore et al., 1988), which are spatially closely associated with many of the principal deposits in the region. The Starra Shear which hosts the Selwyn mines, is interpreted to be a similar feature. It involves a zone containing several steeply dipping S_2 aged reverse shears. On the western side these overprint an earlier S_1 decollement structure. The S_2 structures are themselves over printed by "D_3" (local D_4 aged) aged zones of high flattening strain (Adshead-Bell, 2000). These stresses induced both normal and oblique slip movement along the earlier structures. This interpretation of the Starra Shear is supported by modelled CSAMT and magnetic data, which indicate the shear zones are more steeply dipping than the ironstone altered shears, which themselves form duplex features linking 'hangingwall and footwall' displacement planes.

Metallogenic Setting

There is an abundance of copper and copper-gold deposits associated with late epigenetic fluid systems utilising structures along the length of the Eastern Fold Belt, with at least 25 significant deposits and mines discovered to date. Numerous mapping and research programs through the last 80 years have established that the region has been influenced by extensive and in many areas very powerful fluid systems of several generations, with distinct characteristics. Where these fluids have been introduced under the right physical and chemical conditions they have shown the capacity to generate substantial metal accumulations. Many of these copper-gold deposits exhibit characteristics common to the iron-copper-gold systems found elsewhere in the world.

The deposits of this style found to date within the Eastern Fold Belt range in size from several hundred thousand, to more than 150 million tonnes (Table 2 and Figures 1 and 2). They are characteristically reduced iron-copper-gold systems, but invariably most contain portions which are dominated by hypogene oxidised ore and gangue assemblages. These typically include hematite, low-iron copper sulphides, copper "oxides" and even native copper as the predominant ore species. These deposits are commonly associated with district scale master faults.

Textural data from black shale hosted copper deposits in the Selwyn area suggest many of them formed due to the passage of late to post deformational mineralising fluid into brecciated zones within the "master faults". The Mt Dore deposit is an example. This timing is apparently similar to that characteristic of the iron-copper-gold deposits (late to post regional D_3). In the latter, iron oxides already in the host unit provided the reductive environment to capture economic metals. Fluids entering black shales in the absence of earlier iron oxide alteration, produced iron sulphides (pyrrhotite and pyrite) as the preferred iron alteration species (over oxides) and copper was confined

Regional Structural Record			Selwyn Structural Record (Adshead-Bell 2000)		
	Orientation	Evidence / Event		Orientation	Evidence
D1	N-S compression – northward transport direction (Laing et al. 1989)	Early during the Isan Orogeny (1584 ±17 Ma, Page and Sun, 1998)	D1	N-S compression	S1 - foliation parallel to S0 S1 - Decollement Zone resulting in the Starra Shear precursor (and the Selwyn shear)
D2	E-W compression, N-S dominated fabric & fold axis orientation in the Selwyn Region (Beardsmore, 1992)	Principle regional fabric and fold forming event. Upright to eastward dipping fold axes and penetrative fabric	D2	E-W compression. This generated the dominant regional fabric (approx. N-S trending fold axes and foliations)	S2 – steeply dipping penetrative cleavage and foliation, axial planar to tight or isoclinal folding
D2.5	E-W compression in both the Western (Bell and Hickey,1998) and Eastern Fold Belts	Correlates to : - D3 in the Snake Creek Anticline (Rubenach and Barker, 1998) - D4 in the Soldiers Cap Group (Mares, 1998)	D3	E-W compression	Resulted in top-to-the-west overturning of D2 aged folds and fabrics Local flat dipping crenulation and folding
D3	E-W compression	- Late Isan Orogeny 1493-1508 Ma (Page & Sun, 1998) and (1510 ± 13 Ma, Page & Bell, 1986)	D4	E-W compression (late Isan Orogeny)	Localized N-S trending upright folds with a foliation sub-parallel to the S2 fabric.
			D5	E-W compression	Overturns some S2-S4 fabric and structures, (top-to-the-east). Best developed within the Selwyn Line
			D6	E-W compression	Re-activation of S2-S4 structures. Best developed in the Selwyn Line

Table 1. The Selwyn Line structural record relative to the generalized regional deformation history

to oxide, carbonate and relatively oxidised sulphide species. In these instances copper-gold ratios are higher (See Table 2) and abundant late stage copper oxides are prominent due to high porosity in the breccias.

Similarly where primary or metasomatic calcium was abundant in host rocks, such as in the metabasalts and calc-silicates at the Mount Elliott Mine and the Swan deposit, skarns are developed where major structures were intruded by magmas which released abundant fluids on freezing. These deposits typically contain abundant magnetite and pyrrhotite with lesser peripheral pyrite, and are also post regional D3 in their timing.

Several key features are common to most of these deposits within the terrain, and include many typical features found in similar hypabyssal epigenetic iron-copper-gold terrains:

- proximity to major, deep seated, steeply dipping district and regional scale reactivated fault systems;
- reductive host units containing earlier ferruginised units and structures, black shales, and evaporite bearing beds within the stratigraphic pile;
- major zones of early sodic-calcic metasomatism, subsequent potassic-ferric metasomatic overprinting and late stage copper-gold (+ iron?) alteration in and adjacent to brittle structures;
- abundant late to post tectonic, anorogenic, granitoids intruding the district in sheet-like, diapiric and batholithic forms. These range from granitic through to dioritic in composition.

All these features are all present in the Selwyn Line district.

Geology of the Selwyn Deposits

The most comprehensive mapping of the surface geology of the Selwyn deposits was conducted by Leishman between the late 1970's though to the early 1990's. He identified the prominent feldspar-magnetite alteration and chloritisation associated with the mineralised systems of the Selwyn Line, and noted the general absence of this style of alteration from the apparently barren Eastern Hematites. Numerous other workers have studied the local geology, but due mainly to its complex structural and alteration history, no definitive understanding has been proposed to date.

The Selwyn Line deposits, with the exception of the 222

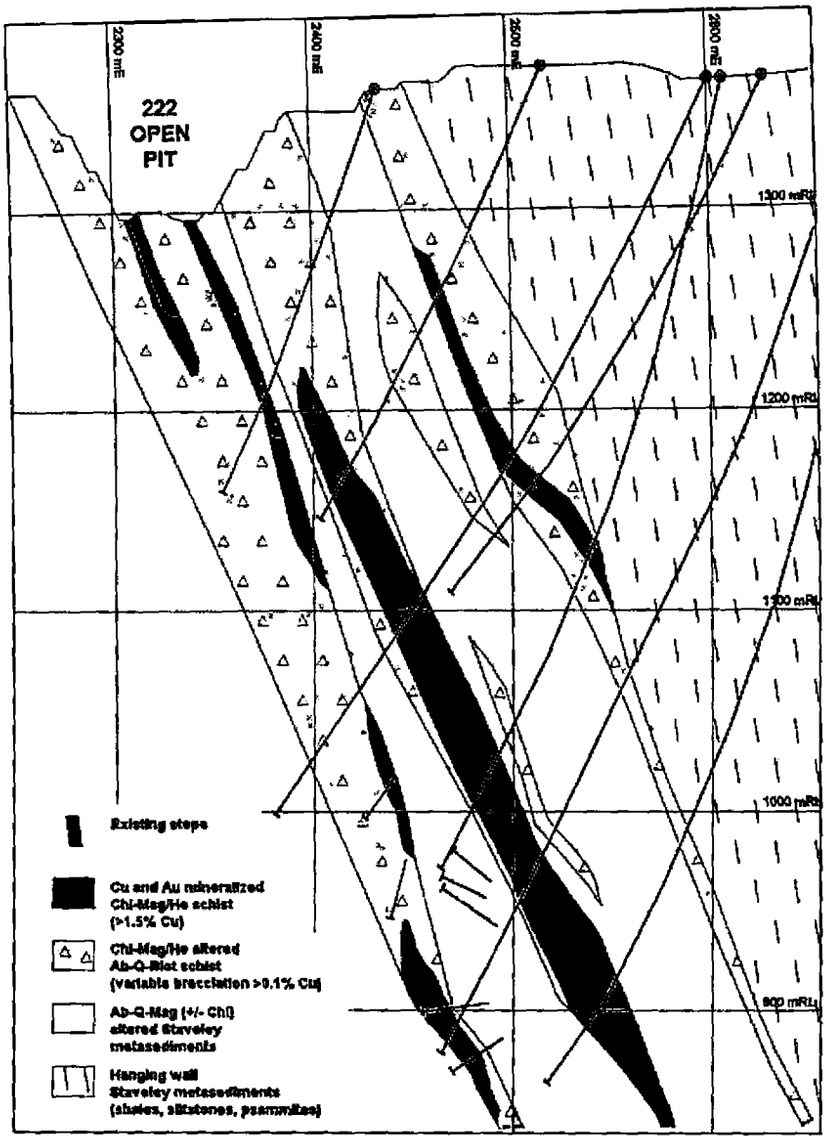


Figure 3: Section 7850N in 222 Mine – simplified E-W cross section illustrating the distribution of grade within altered breccia zones. The higher grade zones plunge steeply northward into the section.

Mine, all exhibit the same basic alteration and lithological cross section. There are however, local variations in the dominance of different alteration minerals, and structural complexities, within the Selwyn Line system. These variations are observed both vertically and laterally.

Lithologies

The stylised section through the line from the east (hanging wall) to the west (footwall) involves :

Metasediments

This is the mine term used collectively, for the package of interlayered carbonate bearing meta-psammites and meta-pelites belonging to the Staveley Formation and located in the hanging wall of the main mineralised zones. They exhibit variable quartz-albite-calcite-magnetite/hematite ±scapolite, pyrite and biotite alteration, overprinting an earlier greenschist facies metamorphic assemblage. The metasediments are increasingly strained to the west, as demonstrated by local intensification of shear fabric and breccia development. Westward, clasts in the breccias are increasingly flattened and imbricated or parallel to the host shear fabric. The clasts are dominantly composed of quartz and albite (Rotherham 1997a, Adshead-Bell 2000), and westward the matrix is increasingly replaced by biotite/chlorite, and magnetite/hematite. In many parts of the Selwyn Line the brecciated hangingwall and footwall metasediments are overprinted by calcite matrix crackle breccias, with dominant orthogonal tensional fractures indicating a strong post-foliation flattening strain at high angles to the dominant north-south foliation. These are similar in orientation and character to breccias and fracture sets observed in the altered black shales adjacent to the western faulted contact of the Yellow Water Hole granite and the Mount Dore granite, at the Victoria and Mount Dore copper deposits. The increased deformation to the west is attributed to the development of the hangingwall bounding shears of the main Starra Shear zone. The metasediments commonly overlie extensive lenses of near massive ironstones. These contacts are typically sheared, with the development of chlorite and clays defining the change in unit.

DEPOSIT		PRE-MINING RESOURCE TONNES & GRADE (MEASURED & INDICATED) * denotes reserve					
Name	Type	Cut off	Mt	Au g/t	Cu %	Cu/Au ratio	Source
Selwyn	Fe-Au-Cu	high (>3g/t Au Eq)	6.9*	4.6	2.1	0.5	Selwyn Prospectus and Annual Reports, 2000 & 2001
		mod (>1.5% CuEq)	14.6*	2.1	1.1	0.5	Selwyn Annual Report, 2001
Ernest Henry	Fe-Cu-Au - Global	Low	166.0	0.5	1.6	3.0	Ryan 1998
	Fe-Cu-Au	Low (>0.4% Cu)	127.0*	0.55	1.1	2.0	Ernest Henry Mines Annual Report, 2001
Eloise	Fe-Cu-Au	High	3.2*	1.5	5.8	3.9	Baker and Laing 1998
Osborne	Fe-Cu-Au (skarn? & ironstone?)	mod (>1.5% CuEq)	36.0	1.0	2.0	2.0	Adshead 1995
		high (>3% Cu) *	15.2*	1.1	3.0	2.9	Gauthier et al., 2001
Mt Elliott	Fe-Cu-Au skarn & black shales	high (>2.5%Cu)	6.3*	1.8	4.6	2.6	Selwyn Prospectus and Annual Reports, 2000 & 2001
		mod (>1.5% CuEq)	11.0	1.2	2.9	2.5	Selwyn Annual Report, 2001
Swan	Fe-Cu-Au calcsilicate & black shales	v.low (0.3% Cu)	13.5	0.5	0.9	1.8	Selwyn Annual Report, 2001
Greenmount	Cu-Au calcsilicate & black shales	low (0.5% Cu)	3.6	0.8	1.5	1.9	Homestake Quarterlyl Report, March 1995.
		?	20-30	?	0.5	?	Hodgson 1998
Trekelano	Cu-Au calcsilicate (skarn?)	?	3.6	0.7	2.7	3.9	Shepherd, 1953
Mt Dore	Cu - black shales	v. low (0.2%Cu)	27.3	0.1	0.7	6.6	Selwyn Annual Report, 2001
Victoria	Cu - black shales	low (0.5% Cu)	2.4	0.2	1.3	6.5	Selwyn Annual Report, 2001

Table 2. Tonnages and grades of several Fe-Cu-Au and related deposits in the Eastern Fold Belt, Mt Isa Inlier.

Massive Ironstones

These are developed as crudely tabular or lensoid bodies composed of variable proportions of magnetite and hematite, with quartz, albite, calcite, sulphides and chlorite in their matrix. The majority of the massive ironstones are typically medium to coarse grained, and dominated by granular hematite. The hematite is however variably replaced by concordant and discordant, coarse grained magnetite/martite. The latter are commonly associated with chalcopyrite or bornite. In portions of the Selwyn Line, the hematite ironstones delineate hangingwall and footwall bounding shears in the S2 Starra Shear zone. These tend to be relatively straight zones. Internal to these "tramway" structures and in areas where the Starra Shear is dislocated, or develops splays or flexures, the magnetite replacement becomes dominant (excluding the effects of weathering). The magnetite ironstones are typically developed along obliquely discordant, sigmoidal structures linking hangingwall to footwall structures, both along strike and down dip. These typically strike at 10^0 to 15^0east of the principal hematitic S2 shears (Figure 4).

The hematitic ironstones occur in both massive and brecciated forms. Both the massive form, and the clasts in the breccias, are usually granular with a moderately developed internal fabric. The magnetite dominated ironstones typically exhibit both concordant and discordant replacement along the main S1 and S2 foliations, folding of these foliations, S4 foliation and crosscutting shear structures (Adshead-Bell, 2000). In several areas the earlier fabric is folded about S2/S4 axes, but the textural evidence supports the iron replacement postdating the formation of the folds, with iron oxides and sulphides penetrating the associated axial planar cleavage. This replacement can be observed on scales from millimetres to tens of metres in width, and over hundreds of metres down dip and along strike. The influence of the magnetite replacement is particularly evident in the 276, 257, 251 and 244 deposits. It is of note that in many zones the magnetite has undergone partial to complete hypogene oxidation to martite (Rotherham, 1997a).

The Starra Shear Schists

This is new terminology for the mine, and is used to describe the chlorite/biotite-magnetite/hematite-albite-quartz-carbonate schists that comprise the central portions of the Starra Shear zone. They represent the altered and sheared Staveley Formation metasediments that are developed in the main zones of dislocation within the Starra Shear. The proportions of chlorite, feldspar, magnetite and hematite in this unit vary significantly along the Selwyn Line. In many parts the texture and alteration mineral composition is closely linked to the type of mineralisation present. The distribution of the alteration minerals is also strongly linked to the development of structures. In the south at the 222 deposit high proportions of chlorite ±biotite ±sericite define broad breccia zones and shear fabrics (Figure 3) which demarcate north through to north east trending shears. These are accompanied by coarse magnetite/martite disseminations which are commonly accompanied by chalcopyrite with minor gold. Gold grades increase in the presence of bornite, high concentrations of chalcopyrite and in reworked, non-sulphidic, massive hematite breccias which are both sub-parallel with, or subtly discordant to, the principal foliations.

Further north at 244 Starra Shear Schists are chlorite dominated and developed in elongate duplexes and lenses within the main shear, but are typically still located in the footwall of the massive magnetite ironstones that mark portions of the principal hangingwall bounding shears. These chlorite dominated Starra Shear Schists are mineralised to ore grades in parts, and overlie the dominantly hematitic massive ironstones and the albite-quartz-magnetite ±pyrite ±scapolite schists which form the western or footwall stratigraphy of the Selwyn Line. In many areas these schists become increasingly deformed westward until they form a mylonitic straightening zone which together with the hematitic footwall ironstones forms the western bounding shears.

Further north at the 276 deposit, chloritic schists are less well developed compared to the magnetite bearing metasediments and footwall feldspar-quartz-magnetite schists.

Feldspar-Quartz-Magnetite Schists

This unit is separated from the Starra Shear Schists by its distinctive mineralogy (only minor biotite/chlorite). They are typically developed in the footwall of the main shear zone but are also present as extensive lenses and zones within the body of the shear. The unit is variably brecciated, and the degree of strain is crudely related to the amount of chalcopyrite present. These schists typically contain zones of abundant coarse deformed pyrite ±scapolite in the vicinity of the footwall bounding shears. The contact with the Answer Slates in its footwall is not well exposed, but is interpreted as an alteration front across shear boundaries. These schists are typically between 50 and 100 m in thickness, and this combined with their abundance of disseminated magnetite, results in their close correspondence with the regional magnetic anomaly. It is noted at this point that the relatively non-magnetic Eastern Ironstones do not exhibit the abundant albite-magnetite alteration evident in the Western Ironstones.

Amphibolites

Amphibolite masses are developed as concordant and discordant bodies within the metasediments on both the eastern and western sides of the Selwyn Line. They are not observed to crosscut the mineralised units, preferring instead to remain within the fabric of the sediments. The amphibolites are medium to fine grained actinolite (after pyroxene) - plagioclase - magnetite bearing rocks. They exhibit a weak fabric associated with chlorite development along their margins but tend to be ophitic within the body of the intrusives.

Ore Mineralogy

Through out the Selwyn Line the ore mineralogy is broadly similar with the main variations derived from local differences in oxidation state. These changes in oxidation

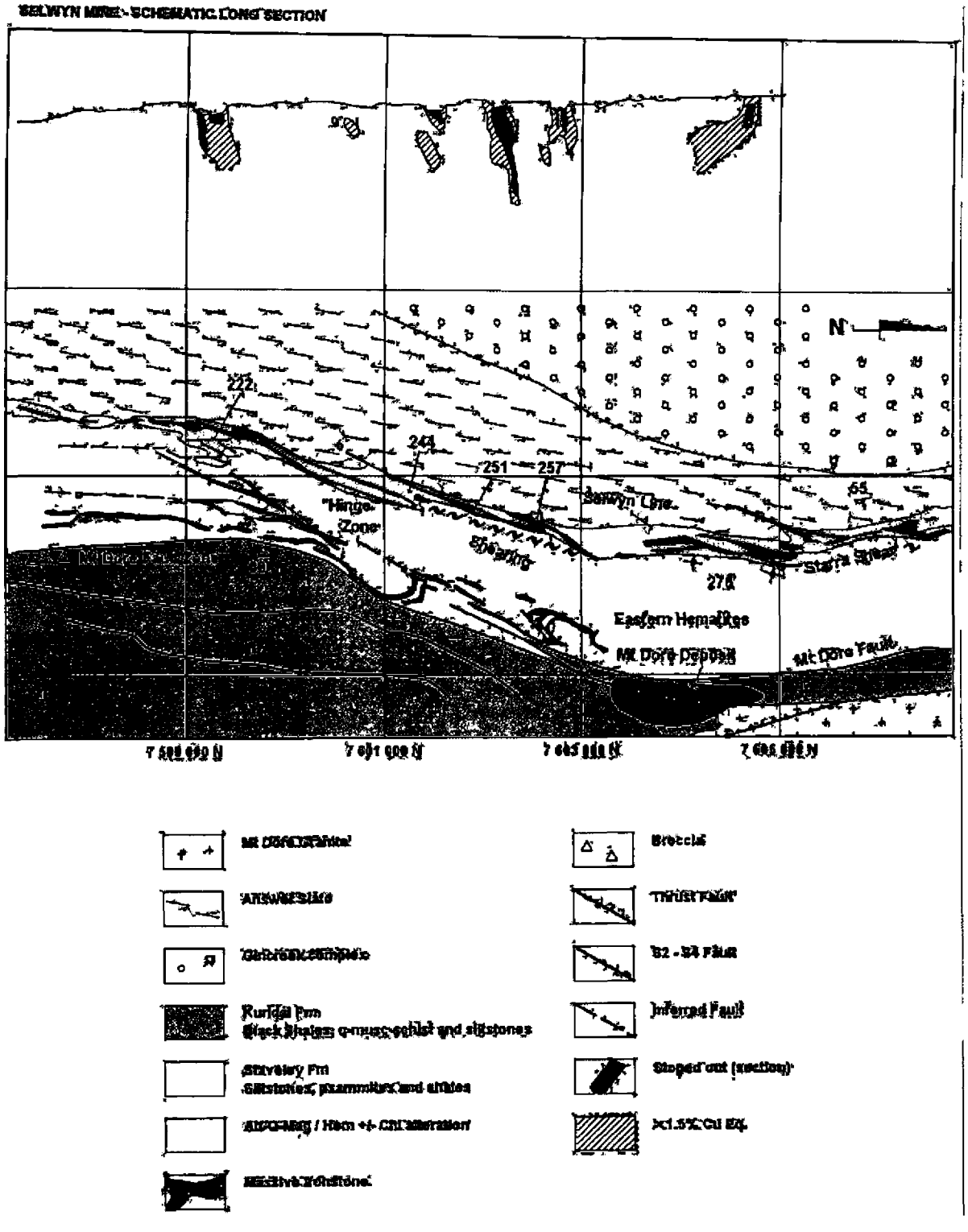


Figure 4: Selwyn Line – local geology and schematic distribution of grade in long section

state are observed over both sub-horizontal and sub-vertical boundaries. The main primary copper ore minerals are chalcopyrite and bornite with trace chalcocite. Principal weathered zone "oxide minerals" include malachite, chrysocolla, chrysoprase, cuprite, a variety of cupriferous sulphur-salts, while in many areas native copper is a prominent ore mineral. Petrographic studies on the gold distribution indicate it is mostly <50μm (Kary and Harley 1990). Gold is commonly present as intergranular particles, and is also included within chalcopyrite, bornite, magnetite, martite, hematite, hematised rims to magnetite, pyrite, calcite and quartz (Adshead-Bell, 2000; Rotherham 1997a).

Primary gangue minerals include magnetite, martite, hematite, quartz, calcite/anchorite, barite, sodic feldspar, potassic feldspar, scapolite, actinolite, biotite, chlorite, sericite, pyrite, tourmaline, apatite, and trace scheelite.

The alteration paragenesis and its relationship to structure and the mineralisation are indicated in Table 3.

Structure

The structural record within the Selwyn Line is complex, with evidence of both major regional orogenic deformations as outlined in Section 2, and local or district specific deformation. Numerous workers have studied the structure within the Selwyn District. The most recent and most comprehensive detail was provided by Adshead-Bell (2000) who's work is summarised in the Table 1. The principal difference between Adshead-Bell's work that of earlier workers lies in the detailed interpretation of specific micro- and meso- scale structures. Adshead-Bell interprets the Starra Shear as being of both D2 and D4 age while others such as Blake (1987) and Laing et al. (1989) perceive it as being the product of a D2 remobilisation of a D1 aged decollement zone. This latter view is supported by a difference in metamorphic grade from greenschist facies assemblages east of the Selwyn Shear (and Mount Dore fault) to amphibolite facies assemblages west of the Starra Shear.

Originally Laing et al. (1989) indicated the Selwyn Line of deposits as being located on the eastern side of a 2 km wide zone of ductile shearing known as the Starra Shear (Figures 2 and 4). Beardsmore (1992) and Adshead-Bell (2000) identified 2 main shears in proximity to the Selwyn Line, namely the Starra Shear in the west and the Selwyn Shear 2 km to the east, abutting but still west of the more brittle Mount Dore fault zone. High flattening strains and zones of intense straightening are evident in the Starra Shear, but there is less evidence for the same intensity of straightening in the Selwyn Shear. It is notable that the bulk of the Selwyn Shear, which to date is apparently poorly mineralised, does not host the intense albite-magnetite alteration prevalent in the Starra Shear.
The distribution of many of the principal S2 aged shears in the Selwyn Line is typically highlighted by massive hematite dominated iron oxide replacement of the original sheared metasediments. It is postulated that the S4 aged shears tend to be traced by magnetite dominated replacement ironstones, but several are less obvious and are traced by local intensification in S4 foliation, and shear fabric.

Geometry

Of the 5 mined deposits of the Selwyn Line, three are located in the southern half arc, namely the 244, 251 and the 257 orebodies. The high grade portions of each are typically developed in broad ribbon-like shoots within near massive ironstone lenses, extending for more than 600 m down plunge, between 50 and 300 m along strike and are 2 to 30 m in width. They plunge consistently at between 60^0 and 80^0 to the north-northeast, and clearly reflect a relatively constant structural regime along this portion of the line. The geometry of these high grade shoots is spatially associated with the junction zone of the principal north-northeast trending hanging wall shears, and prominent southwest trending link structures developed beneath this shear within the body of the Starra Shear zone. Lower grade mineralisation is commonly developed in the footwall and along strike from the high grade zones, in intervals of less massive iron replacement, and more abundant chlorite and biotite development. In several areas the mineralised zones hosted in the "footwall" Starra Shear Schist are developed as sizeable higher grade zones such as the "B-zone" in the 244 Mine open pit.

The southernmost deposit in the Selwyn Line (the 222 Mine) is located in the junction zone of the main north to north-northeast trending (S2/S4) Starra Shear structures, and a northeast-southwest trending (S1?) cross shear (the "hinge zone"). The latter was originally interpreted by previous workers (Switzer et al., 1988; Kary and Harley, 1990; Davidson et al., 1989; Beardsmore et al., 1988) as an S2 aged fold closure, deforming the early ironstones. Later work by Switzer et al. (1988), Beardsmore (1992) and Adshead-Bell (2000), has this zone incorporated in the Selwyn Shear as it tracks southward to link onto the Starra Shear. It is interpreted in this paper, as being part of the S1 aged Starra Shear system which is largely defined by iron replacement parallel to the S0/S1 fabric. Crudely north-south trending S2 upright shears intersect the S1 structure in several locations, and are themselves overprinted by S4 aged E-W compressional strain associated with the shearing in the main Selwyn Line. The north-south structures are also characterised locally by iron oxide replacement, and intense feldspar, silica, chlorite and carbonate alteration. At 222 the orebodies are located within multiple zones of alteration, which form broad envelopes. The high grade zones mined to date involve tabular ironstones which extend down dip for >500 m, along strike for 250 m and which are 2 to 20 m wide. These plunge at 60^0 to 80^0 to the northeast. Recent drilling combined with existing data however, indicates the mined zones at 222 are only a part of the economically mineralised system, and that far greater widths (up to 100 m) are developed, particularly to the northeast along the strike from the "hinge zone". At lower cut offs (eg. 1.5 g/t Au or 1.5% Cu) multiple large shoots are evident, plunging at 75^0 to the northeast. These define the junction lineation between the north to north-northeast trending S2 and S4 shearing and the northeast trending S1 aged "hinge zone" structures. This supports the continued use by mineralising fluids, of zones where early sodic-silica-calcic alteration in S1/S2 structures, have been overprinted by more brittle S4 structures. Drilling to-date has not closed off these systems and the potential for significantly larger deposits still exist.

In the northern arc of the Selwyn Line, only the 276 deposit has been mined to date (Figure 4). Here the exploited high grade ore zone is located in the junction zone of an eastward dipping (70^0) hanging wall shear (magnetite/martite dominated) where it converges on the main S1-S2 Starra Shear (pre-D4 hematite dominated replacement). The geometry of this deposit is not fully defined as yet due to a lack of definitive drilling. Indications are that the northern end of the high grade zone is controlled by the steep southward plunging junction lineation of the two shears. This converges at depth (>400 m) with a second controlling intersection lineation formed where the eastward dipping hangingwall ore zone is incorporated into a near vertical

Stage	Alteration Type	Alteration Paragenesis	Mineralisation	Structure	Magmatism	Comment
1	Na – Ca metasomatism	Albite, quartz, scapolite, actinolite, apatite		Used mainly D2 Faults and foliation (replacement of ductile-brittle structures)	Fluids associated with early Williams granites?	Changed laminated host rocks prone to deformation by simple shear, into more massive textured brittle rocks
2a				D4 brecciation of brittle sodic altered rocks		Tectonic brecciation
2b	K - Fe metasomatism	Biotite, magnetite, hematite, quartz, pyrite, tourmaline, apatite	Pyrite – no associated Au or Cu minerals	Mostly replacement of D1 foliation and shearing, and D2-D4 structures, fabric and breccias.	Associated with emplacement of Mt Dore aged granites ? (~1510Ma?)	o Replacement and hydraulic breccia textures, over-printing earlier breccia o Main development of the bulk of the ironstone units
3a -early	Au – Cu mineralization & Si-Ca alteration	Quartz, calcite, chlorite, magnetite, hematite, anhydrite, sericite/k-spar	Au (2 sub-stages?), pyrite, barite, bornite, & chalcopyrite	D2/D4 structures – mineralization of available low pressure areas. Fluid overpressure.	Late phases of Mt Dore aged intrusives ? (~1500Ma?)	Magnetite/martite over-printing earlier iron-oxides, and associated with chalcopyrite. Au with martite, calcite, quartz ± pyrite
3b - late	Au-Cu mineralization associated Ca-K ?	Calcite, chlorite, epidote, sericite	Au , chalcopyrite & pyrite	D5/D6 – overprinting earlier mineralization/alteration	Waning system (cooler)	Au & chalcopyrite in late calcite-silica-Mg chlorite veins
4	Supergene oxidation	Hematite, siderite, goethite, limonite, kaolin, smectite, illite	Native Cu, cuprite, malachite, chalcocite chrysocolla,	Existing faults, joints and fratures - commonly sub-horizontal, but dipping sub-vertically into faults	Weathering	

Table 3. Alteration, mineralization and structure : sequence of events (modified after Rotherham (1997a), and Adshead-Bell (2000))

(S4 aged ?) shear. The mineralised magnetic hangingwall ironstone is poorly developed within this shear due to attenuation and/or weaker iron replacement. Movement indicators suggest the main magnetite ore body developed in a regime of east over west reverse faulting (typical of S2?). This was overprinted by a subsequent (S4?) west side up normal displacement which resulted in decreasing dip and structural thickening of the hangingwall magnetite shear as the subvertical S4 shear is approached. Once in the shear, the dip then steepens and the ironstones become dismembered and/or attenuated. This junction zone has a shallow southward plunge (15^0 to 35^0). The 276 mineralised system clearly exhibits a different geometry to the deposits to the south, and this is apparently linked to a different set of structural conditions and orientations. As per the other deposits in the Selwyn line, the economic mineralisation in the 276 system is larger than the high grade zones mined to date, with abundant slightly lower grade copper dominated ore developed in the hangingwall magnetites, down dip and along strike, and down plunge towards the south of the current workings.

Timing

Comprehensive studies on the timing of the copper and gold mineralisation by Rotherham (1997a) and Adshead-Bell (2000) have laid to rest many of the uncertainties suffered by previous workers. Metallogenic models originally proposed followed the typical "syngenetic versus epigenetic" lines of debate, and ranged from variably remobilised exhalative styles (Davidson 1989) through various shear hosted epigenetic models (Ransom, 1986; Laing et al., 1989). Rotherham (1997b) and Adshead-Bell (2000) integrated petrographic, geochemical, textural and structural data, and provided a solid control on the timing of alteration and mineralisation in the Selwyn Line. This is summarised in the Table 3, which indicates that the economic metals were introduced late and post D4 by hot dominantly magmatic derived fluids, emplaced into a brecciated structural environment. The brittle character was derived from a combination of the post peak metamorphic (cooler) conditions during S4/S5/S6, and by the intensive to pervasive early alteration of rocks within the large S2 aged shears (Starra and Mt Dore) by albite and silica, which decreased the capability of the host rocks to deform by simple shear. Various degrees of hydraulic brecciation are also associated with the emplacement of the mineralising fluids, but the principal pathways were tectonic in origin.

The timing of mineralisation is also seemingly linked to the emplacement of the non-foliated granites in the region. In the Selwyn area these include the Mount Dore granite to the east, the Yellow Water Hole granite further south, and the Belgium granite which intrudes the older foliated Gin Creek granite west and north of the Selwyn Line. Drill holes through the western margins of the Mount Dore granite and mapping by Beardsmore (1992) and Leishman (1990) has indicated that the basal contact of the granite is tectonically brecciated. Kinematic indicators combined with modelled CSAMT, magnetic and gravity data suggests the Mount Dore granite was thrust westward post-S2, along a number of listric thrust planes, in a series of sheets, rather than emplaced as a simple diapiric body. This relationship is complicated by the fact that most of the western contact of the granite is planed straight by the Mount Dore fault (Beardsmore, 1992) which is interpreted as a syn to post S4 remobilisation of the S2 aged, steeply dipping, regional Mount Dore fault system. This may have been in response to the ongoing intrusion of the granites further to the east (ie. the granite emplacement, thrusting and remobilisation of the Mount Dore shear may have all taken place as a single evolving event during S4). Similar planing of the western margin of the Yellow Waterhole Granite further south is also observed. Here there is evidence from aeromagnetic and spectral data, that the Yellow Waterhole Granite is also a composite intrusive with indications of westward thrusting.

The westward thrusting of the Mount Dore granite is interpreted to have been a fundamental factor in the strong development of the S4 aged high strain shears in the Selwyn Line (Adshead-Bell, 2000). The east-west stress field set up by the westward displacement of the Mount Dore granites resulted in increased crushing of the Staveley Formation metasediments and the interbedded amphibolites against the Gin Creek Granite buttress in the west. Similar buttressing effects are reported by Betts and Lister (2001), for the deformation of the Mt Isa and Twenty Nine Mile faults around the Sybella granite buttress. In this later case the faults and sediments are arched around the curvature of the buttress granite in a similar fashion to the S2 Starra Shear and the Staveley metasediments north of Selwyn. Betts and Lister (2001) invoke high strain zones associated with the buttressing. At Selwyn similar higher strain zones are observed and mapping by Leishman (1983) and by Beardsmore (1992) indicates these coincide spatially with the distribution of a discrete zone of increased calc-silicate and "granofels" alteration developed in the Staveley Formation metasediments.

The timing of the economic mineralisation is proposed by Adshead-Bell (2000) and Rotherham (1997a) as being late to post D4. This is also late to post Mount Dore granite (1516±10 Ma, Pollard and McNaughton, 1997) emplacement and it is proposed that the special conditions under-which the main zone of mineralisation in the Selwyn Line developed, where largely due to the more intense S4 strain features developed in the compressed zone west of the Mount Dore granite body, and east of the Gin Creek buttress. Brittle deformation of the already intensely albitised-silicified Starra Shear, created structural pathways for deeply tapped fluids associated with the last phases of the "Mount Dore aged" regional magmatic event (~1500 Ma).

The Selwyn Line Resource

Perceptions

Throughout the life of these deposits the indications were that the best economics have been associated with the mining of small tonnes at high grades. This enabled the

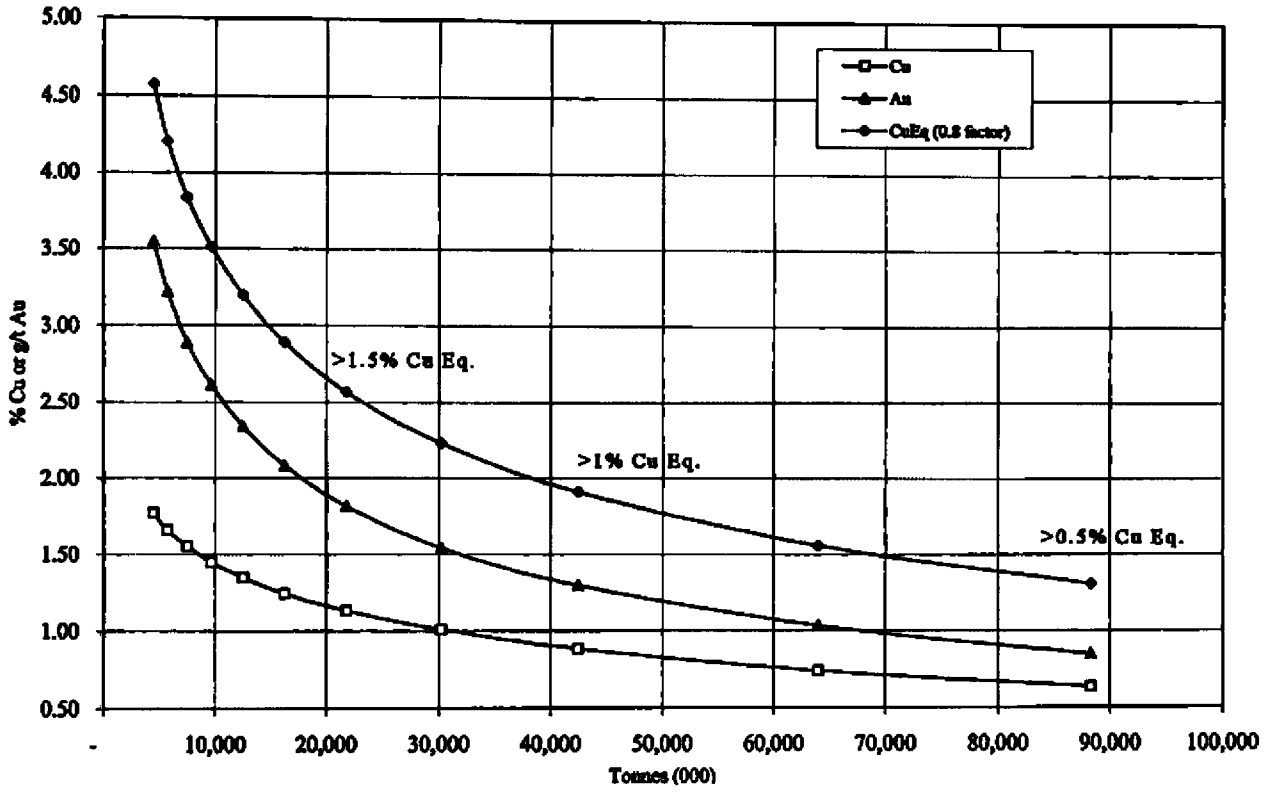


Figure 5: Grade tonnage curve for the post mining Selwyn Line Resource

	Cut off Cu Eq %	Tonnes (000s')	Cu Eq %	Cu %	Au g/t	Cu (t)	Au (oz)	Cu:Au Ratio
Mined	3.5	6 840	5.78	2.1	4.6	143 640	1 011 704	0.46
Post-mined	1.50	21 786	2.56	1.13	1.81	246 182	1 267 931	0.62
	1.00	42 463	1.91	0.88	1.3	373 674	1 774 981	0.68
	0.50	88 270	1.30	0.63	0.84	556 101	2 384 141	0.75
Global	0.2	253 000	0.72	0.34	0.48	860 200	3 917 419	0.71
Pre-mined	1.50	28 626	3.3	1.36	2.48	389 822	2 279 635	0.55
	1.00	49 303	2.4	1.05	1.76	517 314	2 786 685	0.60
	0.50	95 110	1.6	0.74	1.11	699 741	3 395 846	0.66
Global	0.2	259 840	0.9	0.39	0.59	1 003 840	4 929 124	0.66

Assumes : Cu Equivalence = (Cu% + (0.8*Au g/t)) & Global includes measured, indicated and inferred

Table 4: Selwyn Line June 2001 resources (Selwyn Mines June 2001 Resource Statement).

declines to be sunk and the construction to proceed. The resultant perception has thus been that this is what these systems are comprised of. Examination of the entire data set however suggests this is not the case, and these high grade shoots only form parts of far larger systems which are mineralised to economic grades, by processes not dissimilar to those understood for the large Ernest Henry deposit 160 km to the north of the Selwyn Mine.

Resources

Initial resource studies for the 276 Mine in mid 2000 produced a relatively open grade tonnage curve. This prompted a global resource study for the Selwyn Line from the 222 Mine in the south to the 280 area, 5.8 km to the north using the ~168 km of drilling data available, during late 2000. Using a 0.2% Cu Equivalent cut off to define

the mineralised zones, a resource of 253 mt @ 0.48g/t Au and 0.34% Cu in measured, indicated and inferred categories, was identified above ~300m depth below surface (~local RL of >1000 m). The shape of this grade tonnage curve provoked a more detailed revision of the resources, which was completed by June 2001. The resultant grade tonnage curve for measured, indicated and inferred post mining resources, is indicated in Figure 5 and the simplified numbers behind them in Table 4. Studies indicated that the steeply dipping and largely tabular geometry of the Selwyn Line system, precluded the large open pit option for the mining of bulk tonnes, and forced the economics toward higher grade bulk mining underground. Subsequent resource studies focusing on each deposit have identified the current optimal economic cut off at ~1.5% Cu Equivalent. Using this the calculated resources for the Selwyn Line as at July 2001 are ~22 mt @ 1.81 g/t Au and 1.13% Cu (Selwyn Mines Annual Report, 2001). Combining this with the already mined resources for the 5 known deposits in the Selwyn Line, results in a pre-mining global resource of ~29 mt @ 2.48g/t Au and 1.36% Cu (containing 71.5 t, or 2.3 million oz. Au, and 390 000 t Cu metal) . There is also a high probability that this resource will be substantially increased once the open ended portions of the 222, 244, and 276 systems are drilled out. In addition, there are indications that at the lower cutoffs, new deposits in the mineralised gaps between the main zones mined to date, will become evident. The transformation in the image of the Selwyn systems is due to the simple application of reduced grade cutoffs within a large mineralised system. A graphic example of this is the 222 mine reserve which changed from a post mining reserve of zero in 1999 to 5 mt @ 1.61g/t Au and 0.77% Cu in 2001, with open ended mineralised shoots to the northeast and at depth. It is also of note that the Cu:Au ratios (Table 4) from the high grade zones are enriched in gold relative to copper, compared to the ratios for the global tonnes.

Conclusion

The Selwyn orebodies are unusual for iron-copper-gold systems in that they have high grade gold rich zones and relatively low cobalt, rare earth and uranium concentrations. Their petrological and metallogenic indicators suggest however that the mineralised system is not far removed from that at Ernest Henry. The late to post regional D_3 timing, the character of the alteration, and the style of mineralisation at Ernest Henry are also very similar to those features in the Selwyn Line deposits.

The main controlling factors on the dimensions of the economic deposits in the Selwyn Line have been structural. The high flattening strains at Selwyn during the local D_4 event, may have generated numerous planar less voluminous low pressure zones compared to the wider breccia zone common in large deposits such as Ernest Henry. Indications of larger mineralised breccia zones within the Selwyn Line are evident where the Starra Shear type alteration is developed away from zones exhibiting the most intense D_4 flattening, but which still retain significant late fragmentation. These areas hold potential for the development of broader breccia complexes, and the resultant larger deposits.

The Selwyn Line iron-copper-gold system prior to mining was host to nearly 5 million oz. of gold and a million tonnes of copper. Conversion of these resources to reserves is largely only viable by under ground mining. It is anticipated that approximately half of this will have been removed by the end of the current phase of mining.

References

Adshead N.D., 1995. Geology, alteration and geochemistry of the Osborne Cu-Au deposit, Cloncurry district, NW Queensland, Australia. PhD thesis (unpubl.), James Cook University, Townsville .

Adshead-Bell, N.S,. 1998. Evolution of the Starra and Selwyn high strain zones, Eastern Fold Belt, Mount Isa Inlier: Implications for Au-Cu mineralization: Economic Geology, 93, p. 1450-1462.

Adshead-Bell, N.S, 2000. Structural Constraints of the Ironstone Hosted Au-Cu Starra Deposit and Selwyn Range Region, Eastern Fold Belt, Mt Isa Inlier. Unpublished PhD thesis, James Cook University, Queensland, Australia.

Baker T., and Laing W.P., 1998. The Eloise Cu-Au deposit, Mt Isa Block: structural controls on ore. Australian Journal of Earth Sciences, 45, p. 429-444.

Beardsmore, T.J., 1992. Petrogenesis of Mount Dore-style breccia-hosted copper +/- gold mineralisation in the Kuridala-Selwyn region of northwestern Queensland. Unpublished PhD Thesis, James Cook University, Queensland, Australia.

Beardsmore, T.J., Newbery, S.P., and Laing, W.P., 1988. The Maronan Supergroup: An inferred early volcano-sedimentary rift sequence in the Mount Isa inlier and its implications for ensialic rifting in the Middle Proterozoic of northwest Queensland. Precambrian Research, 40/41, p. 487-507.

Bell, T.H., 1983. Thrusting and duplex formation at Mt Isa, Queensland, Australia. Nature, 304, p. 493-497.

Bell, T.H., and Hickey, K.A., 1998. Multiple deformations with successive subvertical and sub-horizontal axial planes: their impact on geometric development and significance for mineralisation and exploration in the Mount Isa region. Economic Geology, 93, p. 1369-1389.

Betts, P.G., and Lister, G.S., 2001. Comparison of the 'strike-slip' versus the 'episodic rift-sag' models for the origin of the Isa Super-Basin. Australian Journal of Earth Science, 48, p. 265-280.

Blake, D.H., 1987. Geology of the Mount Isa inlier and environs, Queensland and Northern Territory : Australian Bureau of Mineral Resources Bull., 225, p. 83.

Blake, D.H., Etheridge, M.A., Page, R.W., Stewart, A.J., Williams, P.R. and Wyborn, L.A.I., 1990. Mt Isa Inlier Regional geology and mineralisation, in Geology of Mineral Deposits of Australia and Papua New Guinea. Australasian Institute of Mining and Metallurgy, 14, p. 915-925.

Blake , D.H. and Stewart, A.J., 1992. Stratigraphic and tectonic framework, Mount Isa Inlier, in Stewart, A.J. and Blake, D.H., (eds). Detailed Studies of the Mount Isa Inlier, AGSO Bulletin, 243, p. 1-11.

Davidson, G.J., Large, R.R., Kary, G., and Osborne, R., 1989. The deformed iron formation hosted Starra and Trough Tank Au-Cu mineralization: a new association from the Proterozoic Eastern Succession of Mount Isa, Australia. Economic Geology Monograph, 6, p. 135-150

De Jong, G., and Williams, P.J., 1995. Evolution of metasomatic features during the exhumation of mid crustal Proterozoic rocks in the vicinity of Cloncurry Fault, NW Queensland. Australian Journal of Earth Sciences, 42, p 281-290.

Drummond, B.J., Golesby B.R., Goncharov, A.G., Wyborn, L.A.I. Collins, C.D.N., and MacCready T., 1998. Crustal-scale structures in the Proterozoic Mount Isa Inlier of North Australia: their seismic response and influence on mineralization. Tectonophysics, 288, p. 43-56.

Etheridge, M.A., Rutland, R.W.R. and Wyborn, L.A.I., 1987. Orogenesis and tectonic process in the Early to Middle Proterozoic of northern Australia, in; Kroner, A. (ed.), Proterozoic Lithosphere Evolution. Geodynamics Series, 17. American Geophysical Union, Geological Society of America, p. 131-147.

Gauthier, L., Hall, G., Stein, H, Schltegger, U., 2001 The Osborne Deposit, Cloncurry District: A 1595 Ma Cu-Au Skarn Deposit. In: Williams P.J. (ed.), Economic Geology Research Unit, Contribution 59. Extended Conference Abstracts, p. 58 – 59.

Hitzman, M.W., Oreskes, N., and Einaudi, M.T., 1992. Geological characteristics and tectonic setting of Proterozoic iron oxide (Cu-U-Au-REE) deposits. Precambrian Research,.58, p. 241-287

Hodgson, G.D., 1998. Greenmount copper-cobalt deposit: Australasian Institute of Mining and Metallurgy Monograph, 22, p. 769-774.

Kary, G.L., and Harley, R.A., 1992. Selwyn Gold-Copper Deposits. Geology of the Mineral Deposits of Australia and Papua New Guinea (ed. F.E. Hughes) Institute of Australasian Mining and Metallurgy, p. 955-960.

Laing, W.P., 1998. Structural-metasomatic environment of the East Mt Isa Block base metal-gold province: Australian Journal of Earth Sciences, 45, p. 413-428.

Laing, W.P., Rubenach, M.J., and Switzer, C.K., 1989. The Starra gold-copper deposit: syndeformational metamorphic mineralisation in a folded early regional zone of decollement. Geological Society of Australia Abstracts, 21, p. 229.

Leishman, J., 1983. Report on 1:25 000, 1: 5 000 and 1:10 000 geological mapping, Starra/Selwyn area, northwest Queensland. Unpublished report (Selwyn Library).

Lister, G.S., O'Dea, M.G., and Somaia, I., 1999. A tail of two synclines: rifting, inversion and transpressional pop-outs at Lake Julius, northwestern Mt Isa terrane, Queensland. Australian Journal of Earth Sciences, 46, p. 233-250.

Loosveld, R.J.H., 1992. Structural Geology of the central Soldiers Cap Belt, Mt Isa Inlier, Australia, in: Stewart, A.J., and Blake, D.H., (eds), Detailed Studies of the Mount Isa Inlier, AGSO Bulletin, 243, p. 349-359.

Mares, V.M., 1998. The structural development of the Soldiers Cap Group within a portion of the Eastern Fold Belt of the Mount Isa Inlier: A succession of horizontal and vertical deformation events and large-scale shearing. Australian Journal of Earth Sciences, 45, p. 373-387.

MacCready T., Golesby, B.R., Goncharov, A., Drummond, B.J., and Lister, G.S., 1998. A framework of the Mount Isa deep seismic transect. Economic Geology and the Bulletin of the Society of Economic Geologists, 93, p. 1422-1434.

Nisbett, B.W., Devlin, S.P., and Joyce, P.J., 1983. Geology and suggested genesis of cobalt tungsten mineralisation at Mount Cobalt, northwestern Queensland. Proceedings of the Australian Institute of Mining and Metallurgy, 287, p. 9-17.

Oliver, N.H.S. 1995. Hydrothermal history of the Mary Kathleen Fold Belt, Mt Isa Block, Queensland. Australian Journal of Earth Sciences, 38, p. 425-455.

Page, R.W., and Bell, T.H., 1986. Isotopic and structural response of granite to successive deformation and metamorphism. Journal of Geology,94, p. 365-379.

Page, R.W., 1993. Geochronological results from the eastern fold belt, Mount Isa Inlier: AGSO Research Newsletter, 19, p. 4-5.

Page, R.W., 1994. Mount Isa geochronology. Australian Geological Survey Organisation 1993 year book, p. 60.

Page, R. and Sun, S., 1996. Age and provenance of the granites and host sequences in the Eastern Fold Belt, Mount Isa Inlier. James Cook University EGRU Contribution no. 55, p. 95-98.

Page, R.W., and Sun, S., 1998. Aspects of geochronology and crustal evolution in the Eastern Fold Belt, Mt Isa Inlier. Australian Journal of Earth Sciences, 45, p. 343-361.

Pearson, P.J., Holocombe, R.J. and Page, R., 1992. Synkinematic emplacement of the middle Proterozoic Wonga Batholith into the a mid-crustal extensional shear zone, Mount Isa Inlier, Queensland, Australia. Australian Geological Survey Organisation Bull., 243, p. 289-328.

Pollard, P.J., Mark, G., and Mitchell, L., 1996. Granitoids of the Mt Angelay and Wiley Igneous Complexes: links to alteration and Cu-Au-Co mineralisation in the Cloncurry district. James Cook University EGRU Contribution No. 55, p. 104-107.

Pollard, P.J., and McNaughton, N.J., 1997. U/Pb geochronology and Sm/Nd isotope characterisation of Proterozoic intrusive rocks in the Cloncurry district, Mount Isa Inlier, Australia: constraints on fluid sources from mineralogical, fluid inclusion and stable isotope data: AMIRA P438 Cloncurry Base Metals and Gold Final Report, Section 4, p. 19.

Pollard, P.J., Mark, G., and Mitchell, L., 1998. Geochemistry of post-1540 Ma granites in the Cloncurry district. Economic Geology, 93, p. 1330-1344.

Ransom, D.M., 1986. Structural environment of the Starra auriferous ironstone deposits, Selwyn Region, Northwest Queensland. Cyprus Minerals Australia. Unpublished Report (Selwyn Library).

Rotherham, J.F., 1997a. Origin and Fluid Chemistry of the Starra Ironstones and High Grade Au-Cu Mineralisation, Cloncurry District, Mount Isa Inlier, Australia. Unpublished PhD Thesis, James Cook University, Queensland, Australia.

Rotherham, J.F., 1997b. A metasomatic origin for the iron-oxide Au-Cu Starra orebodies, Eastern Fold Belt, Mount Isa Inlier. Mineralium Deposita, 32, p. 205-218.

Ruebenach, M.J., and Barker, A.M., 1998. Episodic metamorphism and metasomatism in pelitic rocks of the snake creek Anticline. Australian Journal of Earth Sciences, 45, p. 363-372.

Ryan, A.J. 1998. Ernest Henry copper-gold deposit. In Berkman, D.A. and Mackenzie, D.H. (eds.) Geology of Australasian and Papua New Guinean Mineral Deposits, The Australian Institute of Mining and Metallurgy, Melbourne, p. 759-767.

Shepherd, S.R.L., 1953. Trekelano copper mine: In Edwards, A.B., (ed.) Geology of Australian Ore Deposits, Melbourne, Australasian Institute of Mining and Metallurgy, p. 404-410.

Switzer, C.K., Laing, W.P., and Rubenach, M.J., 1988. The Proterozoic Starra Au + Cu ironstone deposit-syntectonic mineralisation in a folded early regional zone of decollement. Bicentennial Gold '88, Geological Society of Australia Abstracts, 23, p. 212-214.

Wyborn, L.A.I., Page, R., McCulloch, M., 1988. Petrology, geochronology, and stable isotope geochemistry of the post-1820 Ma granites of the Mt. Isa Inlier: mechanisms for the generation of Proterozoic anorogenic granites. Precambrian Research, 40/41, p. 509-543.

Wyborn, L.A.I., Goleby, B., Drummond, B., and Gallagher, R., 1996. A 2.5 dimensional metallogenic GIS analysis. AGSO Research Newsletter, 24, p. 10-12.

The Americas

PGC
PUBLISHING

Injoque, J., 2002 - Fe Oxide-Cu-Au Deposits in Peru: An Integrated View, *in* Porter, T.M. (Ed.), Hydrothermal Iron Oxide Copper-Gold and Related Deposits: A Global Perspective, Volume 2; *PGC Publishing, Adelaide*, pp 97-113.

Fe OXIDE-Cu-Au DEPOSITS IN PERÚ AN INTEGRATED VIEW

Jorge Injoque Espinoza

Noranda Perú S.A.C, Lima, Perú

Abstract - Within Perú, Fe oxide-Cu-Au deposits are found mainly in the Western Andes range and on the coast, associated with the Jurassic-Cretaceous alkaline to calc-alkaline volcanism of the aborted ensialic Cañete-Huarmey marginal basin. They also exist in the calc-alkaline plutons of the Coastal Batholith and the tholeiitic Patap Super-unit, associated with continental margin processes. The exception is Cobriza (100 Mt[1] @ 1.5% Cu, Fe oxide-Cu-Au type; Cu calcic distal skarn) which is located in the eastern range, associated with Permian late-Hercynian extensional tectonics and alkaline granites.

Marcona (apatite-magnetite type; Callovian-Oxfordian), an orebody of >1500 Mt with 60% Fe, and Raúl-Condestable (Fe oxide-Cu-Au type; Hauterivian-Barremian), with ~50 Mt of 1.5% Cu, are Fe calcic skarns, characterised by a pattern of stratabound calc-silicate alteration, coinciding with a fissure intrusive-volcanic centre. This is the reason why they are classified as geothermal skarns. The Cañete Basin is characterised by the presence of ocoites[2], a thick crust, with 20 to 30°C/km geothermal gradients, burial greenschist to zeolite facies metamorphism, and a moderate intrusion of mantle into the crust. Further to the north, deeper oceanic conditions resulted in the formation of VMS deposits. Marcona also has a direct relationship with the dextral northwest-trending Treinta Libras Fault, similar to the Atacama Fault in Chile.

Fe-Acarí and Yaurilla (magnetite-apatite type) contain 40 Mt of 66% Fe, while Eliana, Monterrosas and Cata Cañete (Fe oxide-Cu-Au) comprise to 2.5 Mt with 1.5 to 2.6% Cu. All of these skarns are Fe-calcic type and late-tectonic. The first-mentioned examples are related to the Albian Patap Super-unit while the latter is associated with the Late Cretaceous Cochahuasi Pluton. Cobrepampa is a Cu calcic skarn (Fe oxide-Cu-Au) containing 5 Mt with 2 to 5% Cu, associated with the alkaline Linga Super-unit, and with local dextral faulting. All these deposits are auto-reaction skarns.

The district wide alteration associated with most of these deposits comprises an outer zone of propylitisation with abundant albite, surrounding an internal halo of clinopyroxene, amphibole, sodic-scapolite, epidote, chlorite and garnet. The exception is Cobrepampa where the alteration is K feldspar with biotite, amphibole, garnet and tourmaline representing the most important accessory minerals. The mineralogy of these deposits is characterised by actinolite, chlorite, biotite, phlogopite, sericite, apatite, sphene and minor amounts of rutile, albite, tourmaline, K feldspar, quartz and calcite. The dominant metallic minerals are magnetite, pyrite, chalcopyrite, and variable contents of pyrrhotite, with less abundant bornite, chalcocite, covellite, ilmenite, molybdenite, galena and sphalerite. Cobriza however, has silver and bismuth by-products and significant amounts of arsenopyrite that are generally very scarce in Andean deposits. In addition, tungsten and tin appear at Cobrepampa and Cobriza, suggesting a relationship with felsic and alkaline magmas. However, in the coastal belt, gold (native, electrum and solid solution), silver (in galena), and traces of cobalt and nickel are frequently present.

Editor's note: This paper integrates the observations and characteristics of the important Peruvian magnetite-apatite deposits, many with associated iron and copper sulphides, and the primarily copper (-gold) occurrences with significant accompanying iron oxides within the same districts. Some of the former are among the largest hydrothermal iron-oxide systems in the world, although many, particularly of the latter have been, and still are, classified as skarns. The information provided allows the reader to draw their own conclusions on the inter-relationship and classification of these ores, and their association with the other deposits described within this volume.

Introduction

The Fe oxide-Cu-Au deposits of Perú (Fig. 1) have been known since ancient times, although they were not exploited by modern mining in most cases until the end of the 1950s and the early 1960s, with the exception of Eliana and Monterrosas, where production commenced a decade later (Samamé, 1992).

Marcona was the only producer of iron ore in Perú from the very beginning, except for a small contribution from the Fe-Acarí Mine in the 1960s, which was quickly depleted.

[1] Mt = million tonnes. Tonnage includes past production and remaining reserves.

[2] Ocoite (Ocoita) is the name given in Chile to andesites or basalts with phenocrysts of large plagioclase (>1 cm.) which seem to be regional tectonic guides of abortive ensialic marginal basins in thick crustal areas with environments favourable to Manto-type Cu deposits (Injoque, 1999, 2000).

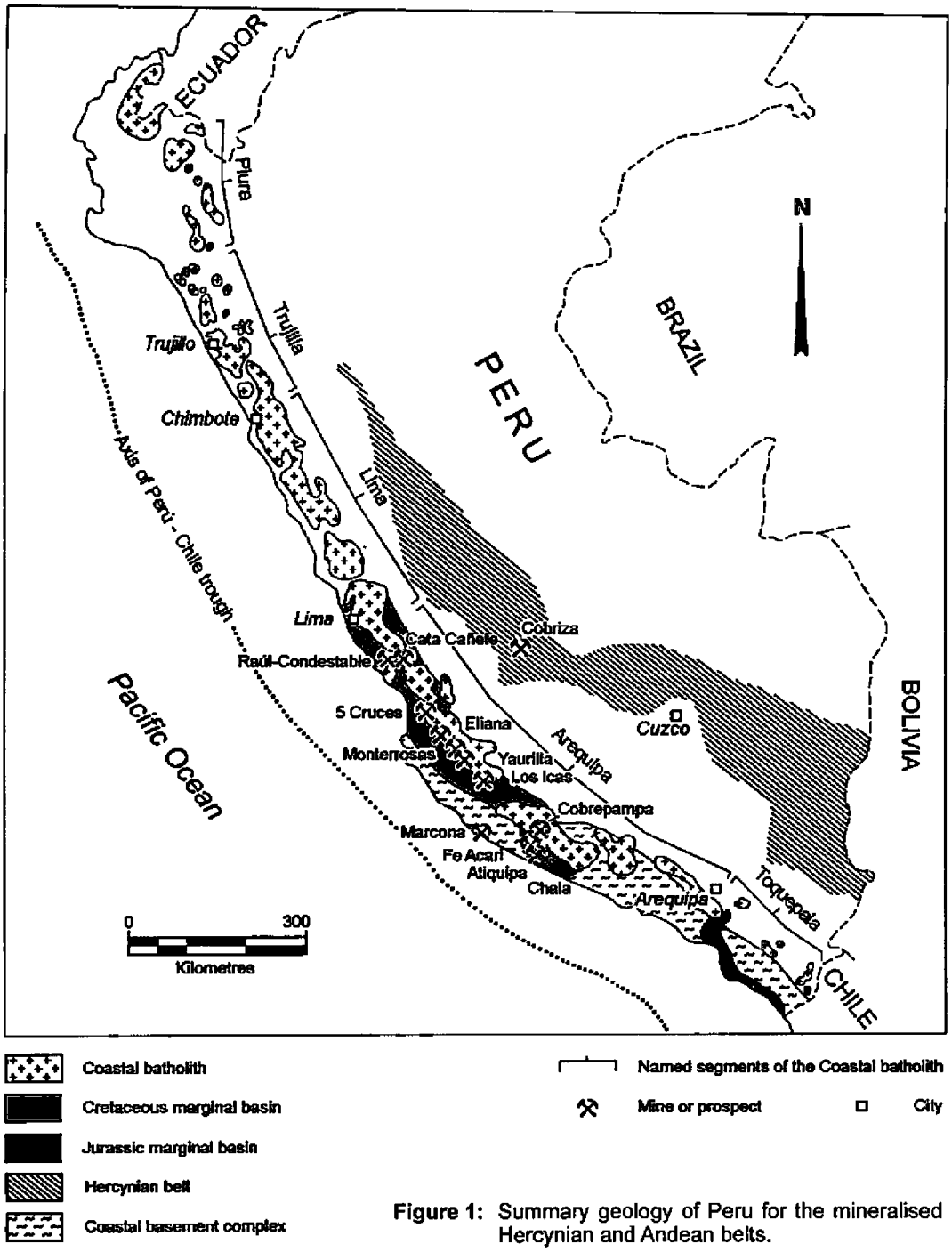


Figure 1: Summary geology of Peru for the mineralised Hercynian and Andean belts.

The main sources of Perúvian copper are the Cu-Mo porphyries. The Fe-Cu-Au deposits only accounted for 5 to 6% of total production in the 1990s (www.snmpe.org.pe).

The study of these deposits commenced in the 1950s with a PhD on Marcona (Atchley, 1956) and another in the 1960s on Cobriza (Petersen, 1965). Subsequently, in the 1970s and 1980s, there was an important research pulse fostered by mining operations, but also by regional works performed in Perú by INGEMMET, ORSTOM from France, BGS and Liverpool University from the United Kingdom, and the University of Heidelberg from Germany, as well as a number of other institutions. This research produced an important body of descriptions of these deposits as well as genetic interpretations by both syngenetists and epigenetists which significantly expanded the available knowledge. The main papers from this period are referenced later in this contribution, while a search of the reference lists from each will provide a supplementary bibliography.

This paper does not discuss genetic issues, which are well supported in the works cited. It is assumed that individual deposits were generated by late magmatic-hydrothermal activity within the respective district. Within this context, these deposits were classified in the past as Fe and/or Cu skarns or as hydrothermal deposits, but with no clear understanding of the regional geology and metallogenic context. This synthesis aims at filling in this blank, summarising the particular, district and regional characteristics of each deposit to place them in a modern geotectonic-metallogenic framework.

Regional Geology

The deposits of this family in Perú (Fig. 1) are related with the Andean Orogeny and Mesozoic rocks in the western range and in most of the Perúvian coast, except for Cobriza which is related to the Hercynian Orogeny and Paleozoic rocks in the eastern range.

A metamorphic Precambrian basement forms the eastern range and Lower Paleozoic continental clastic rocks cover it. These rocks, metamorphosed into slates during the Eohercian deformation and were covered by molasses and some marine deposits during Carboniferous times. During the Late Hercynian, deformation was reactivated in a soft and coaxial manner and in Permian-Triassic times, there was extensional and block-faulting tectonics followed by a deposition of red beds, as a transition to the Andean Cycle (Laubacher and Megard, 1985). This extensional stage coincided with the activation of an ensialic rift, the deposition of alkaline and per-alkaline lavas and intrusion of sub-alkaline crustal-derived granodiorites and monzogranites (Kontak *et al.*, 1985; Soler, 1991).

Mesozoic and Cenozoic Andes are built over the rocks of this mountain range, but towards the coast; the deposition and Mesozoic volcanism started in the Jurassic and followed through the Cretaceous in the Cañete-Huarmey Marginal Basin (Cobbing, 1999), extending to the north into the Lancones Basin (Injoque, 1999, 2000). This basin is the result of the breaking of the continental crust along a continental rift, that has a structure similar to an oceanic rift, in which the axial zone contributed filling the basin with volcanic material through a process of extension and subsidence. In the central part, this basin shows a quasi-ophiolitic character, while towards the south, in the surroundings of the Precambrian Coastal Basal Complex, this is an abortive ensialic marginal basin with alkaline to shoshonitic affinities. Transition from volcanism to the Coastal Batholith intrusion occurred at the end of the Cretaceous volcanic activity, during the intrusion of early tholeiite gabbros and diorites called Patap Super-unit, precursors of Batholith; this event coincided with the Mochica Deformation Phase in the Albian. The Coastal Batholith intruded along the coast, from 100 to 60 Ma, coinciding partially with the Perúvian late Cretaceous Deformation Phase, existing also late eastern units of about 40 Ma. The Coastal Batholith intrusion and the volcanic activity in the area seem to have been the result of a "mantle plume" formed in the continental margin, even though their relationship with subduction processes (Cobbing, 1999) may not have been necessary to its formation (Atherton, 1990).

Hercynian Deposits

Cobriza

(Petersen, 1965; Cerro de Pasco Corporation, 1969; Valdez, 1983b; Rivera *et al.*, 1989)

The Cobriza deposit (Fig. 2), currently developed by Doe Run Perú, is located 300 km to the ESE of the city of Lima, near to the town of Coris. The mine produces about 10 000 tpd of copper ore with silver and bismuth by-products.

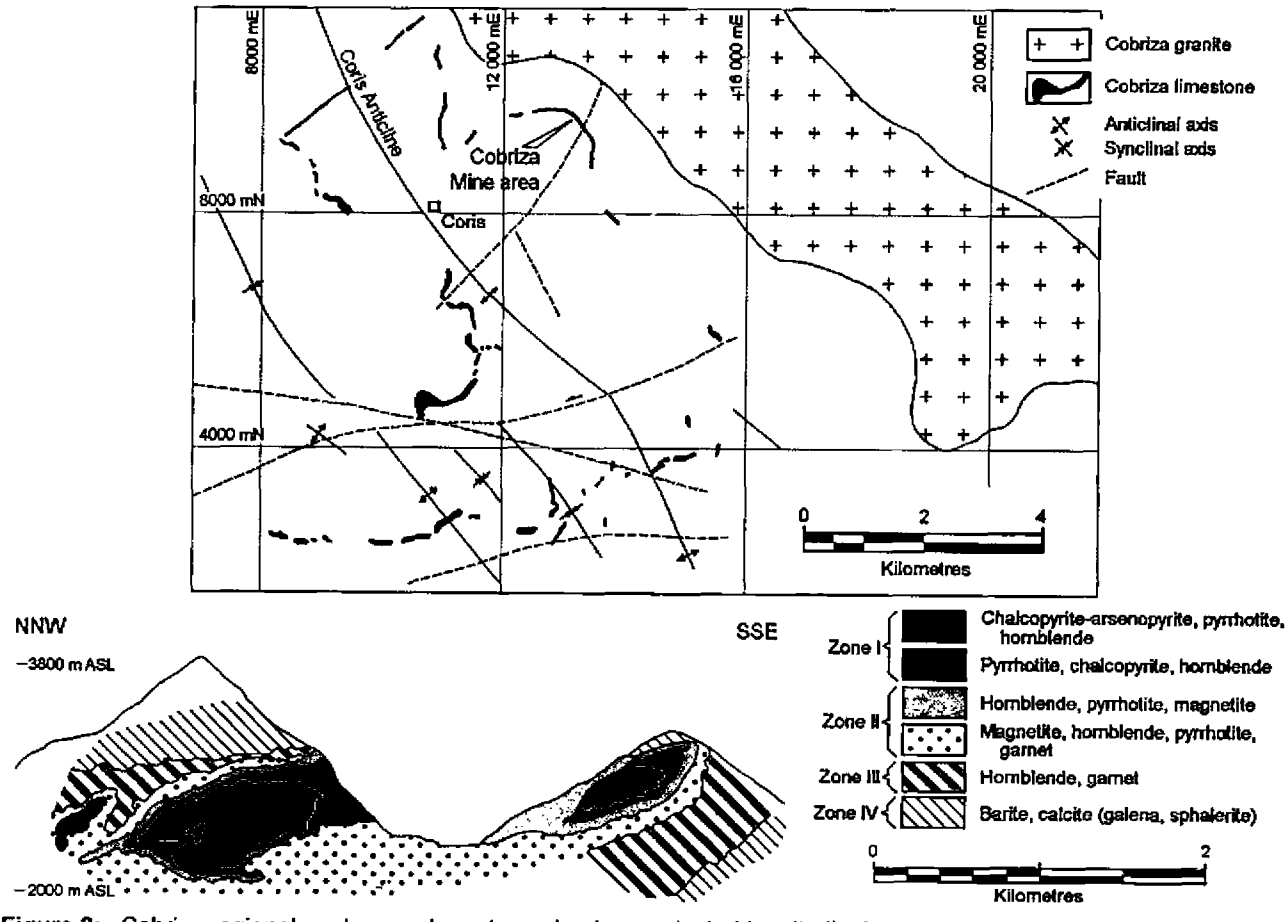


Figure 2: Cobriza regional geology and manto zoning in a projected longitudinal section through the Cobriza Mine area (approximately NNW orientation, after Rivera *et al.*, 1989)



Figure 3: Geology of the Marcona iron deposits

Mineralisation is hosted within a 2000 m thick calcareous package, mainly composed of shales, sandy- and calcareous-shales and limestones, that belongs to the Carboniferous (Pennsylvanian) Tarma Group. Up to six concordant mineralised horizons have been recognised within this sequence. The most important of these is the Cobriza limestone, which is some 800 m above the base of the sequence. The other. less well developed mineralised bands are also conformable to the stratification and are associated with calcareous and calc-silicate bands intercalated with quartzite, slates and slaty-mudstones (Megard, 1978).

The host sedimentary package is folded, forming the northwest-oriented Coris Anticline, which is part of a regional anticlinorium. The sequence is intruded to the northeast by the Cobriza two-mica granite, which is part of the 253±11 Ma Villa Azul Batholith (Noble *et al.*, 1995), and by minor apparently Miocene-Pliocene dykes of basalt and diorite (Valdez, 1983b). Late Hercynian, northwest-trending reverse faults cut the whole district.

The deposit is a Cu-calcic skarn consisting of a large mineral lens (manto) with a strike length of 5500 m, 15 to 25 m thickness and over 2000 m depth extent, replacing a favourable calcareous horizon sandwiched by impermeable shales. The orientation of the manto is 315° with a 30 to 50°NE dip. It comprises magnetite, pyrrhotite, arsenopyrite and chalcopyrite in a matrix of diopside, garnet, hornblende, actinolite, phlogopite and quartz. The principal ore mineral is chalcopyrite, which carries silver in solid solution (Valdez, 1993a). The zoning described for this manto is complex, with an apparent high temperature core towards the northwest (Cerro de Pasco Corp., 1969), although subsequent work suggest the existence of 4 to 5 superimposed foci located at intersections of high angle reverse northwest faults (Valdez, 1983b).

The zoning comprises a core rich in diopside and garnet, successively and subsequently replaced towards the margins by hornblende, actinolite-tremolite and talc, passing finally in a periphery to dolomitic marble. Among the minor minerals in these assemblages, there are varieties of epidote, sodic-scapolite with calcite, predominatly towards the core, and phlogopite towards the border. From the core outwards, there are successive zones of (1) magnetite-actinolite with accessory hematite, (2) pyrrhotite, with rare pyrite, (3) arsenopyrite-pyrite-quartz-phlogopite and minor bismuthinite, native bismuth and lollingite, and, finally, (4) the external zone of chalcopyrite with exsolutions of marmatite and stannite. However, it is outstanding to find at the base of the deposit a more or less continuous, centimetres in thick manto of galena-sphalerite-baryte-calcite, with an unclear relationship to the Cu ores, although it seems to be late (Huamán, pers. comm.).

Reserves plus past production are estimated to be 100 Mt (Samamé, 1992) with 1.4 to 1.6 % Cu and 14 to 19 g/t Ag (Centromin Perú, 1995) and the age of the mineralisation as determined by K-Ar on non-deformed gangue amphibole is 263.4±8 Ma (Noble *et al.*, 1995). The presence of gold, although it is not reported at Cobriza, is evidenced by the name of the associated town, Coris, which in quechua means 'gold', and was also reported in mineragraphic studies at the laboratories of La Oroya (Gagliufi, pers. comm.). Finally, there are reports of the presence of 0.5 to 1 g/t Au in the prospects surrounding the mine site (Centromin Perú, 1995).

Pb isotope studies of these minerals indicate that the Pb and, perhaps other metals, originated in the ancient Precambrian crust present in the neighbourhood (Noble *et al.*, 1995).

It is not clear if there is relationship between the Cobriza mineralisation and the Cobriza Granite. However, the age of both is close and the latter intrusive belongs to the group of granites within the region, which have alkaline affinities and anorogenic characteristics, products of an extensional regime (Soler, 1991) in a intracontinental rift, with no relationship to subduction (Kontak *et al.*, 1985).

Andean Deposits

The Andean deposits of this family known in Perú correspond to two types. Those related to Jurassic and Cretaceous volcanism of the Cañete-Huarmey Marginal Basin in the Perúvian coast and those related to the Coastal Batholith and associated early gabbros and diorites.

Jurassic-Cretaceous Volcanic-related Deposits

Marcona and Minor Jurassic Prospects

(Atchley, 1956; Adrian, 1958; Atkins *et al.*, 1985; Injoque, 1985; Injoque *et al.*, 1988)

The Marcona Mining District (Fig. 3), located 500 km to the south of Lima, consists of major Fe and medium sized Cu deposits, located in pelitic rocks of the Upper Precambrian to Lower Paleozoic Marcona Formation, and volcanic-sedimentary rocks of the Callovian-Oxfordian (Jurassic) Río Grande Formation. This district has been commercially exploited for iron since 1956, while the upper portions, which are rich in copper have been worked in by artisanal miners since the 1960's. The deposit has reserves plus past production of more than 1500 Mt of @ 60% Fe (Samamé, 1992), comprising magnetite ore with associated Cu, Ag and Au byproducts, and traces of Co and Ni. Its K-Ar age is 160 to 154 Ma, corresponding to the late-Río Grande Formation (Injoque *et al.*, 1988). The Marcona mine is currently operated by the Chinese state-owned Shougang Hierro Perú company.

The geological environment consists of dolomites and pelites of the Marcona Formation, which are overlain above an angular unconformity by the lavas and volcano-sedimentary rocks of the Río Grande Formation. Together these two formations make up the elevated coastal block, subdivided into the Coastal Andean Range to the west, and the Pre-Andean Depression to the east where

the conformable Río Grande, Jahuay (Kimmeridgian-Tithonian) and later formations are represented. The transition between these two blocks is marked by the Treinta Libras Fault, which dates from ancient times and has at least two known pulses: an early dextral transcurrent movement followed by later normal displacement. This fault controlled volcanism and intrusive activity in the area during Lower Jurassic-Cretaceous times. Effusive activity is evidenced as a rift, a large swarm of dykes and regional subvolcanic plugs.

The Río Grande and Jahuay volcanics and the subvolcanic instrusives of the area exhibit alkaline to shoshonitic affinities, clinopyroxene, hornblende and plagioclase fractionation and a "within plate" character.

The iron ores are stratabound and conformable, comprising 9 major deposits and 35 to 40 minor occurrences, with east-west to northeast strikes and 35 to 65°NW dip orientations. However, in detail, they are irregular and discontinuous, partially due to the irregularity of surrounding layers, but also to faults and intrusives that cut them.

All of the Marcona ore is hosted by the Marcona Formation as magnetite mantos. The magnetite is massive, with dodecahedral grains of up to 1 mm across and a saccharoid texture. The mantos are located in two favourable levels reaching 1 to 2 km in length. The upper level, known as "E-grid", is structurally persistent with a thickness of up to 150 m, and is enclosed by dolomitic marble on both sides. The lower level or "Mina 7", occurs towards the base of the formation with manto thicknesses somewhat less than those at the "E-grid" level. The depth extent of the mantos has not as yet been determined, although it is known to exceed 500 m.

In the Río Grande Formation, magnetite mantos are predominantly localised within 3 favourable horizons: "N-13", "Flor del Desierto" and "Cerritos de la A", where their thicknesses are characteristically 160, 40 and 60 m, respectively. These mantos are composed of massive magnetite intergrown with copper minerals. None have been developed as iron ores as the accompanying copper constitutes a deleterious metallurgical contaminant. Haloes of disseminated magnetite commonly surround these mantos with grades of up to 15% Fe. In addition there are also veins and minor stockwork bodies within the Río Grande Formation. All of the styles of mineralisation within this younger unit are in general characterised by the abundance of copper.

Residual sedimentary and volcanic structures are observable within the ore and surrounding metamorphic rocks that have been formed as a result of the hydrothermal replacement mineralising process. Mineralisation commenced with the formation at lower stratigraphic levels of diopsidic-clinopyroxene, garnet, cordierite, and hornblende. These assemblages were subsequently replaced by actinolite-tremolite, and minor amounts of Na-scapolite, phlogopite, chlorite-sericite, and apatite-epidote, which also developed towards the upper levels. Finally massive magnetite formed mineralised mantos with interstitial fillings of late pyrite (~0.1%), pyrrhotite, chalcopyrite (~0.01%), bornite, pentlandite, sphalerite, galena, molybdenite, gold, rutile, tourmaline, sphene, prehnite, albite and quartz.

Sulphur isotopes ($\delta^{34}S$) from two samples of pyrite, yielded values of -1.76 and +4.72‰ (Baruj Spiro, BGS; pers. comm.), suggesting a partially magmatic source and maybe some contribution from sea water for sulphur.

Mineralisation within the immediate Marcona district has also been reported cutting the younger Jahuay Formation ocoites. Similarly, 15 km to the northwest of Marcona, the Huaricangana copper Prospect comprises swarms of small secondary copper deposits hosted by Jahuay ocoites with strong associated thermal metamorphism represented by the development of actinolite, scapolite, magnetite, pyrite and oxidised chalcopyrite. The copper grade averages 0.25%, with accompanying traces of Au.

Pampa Pongo is another major prospect with a similar style of mineralisation and tonnage potential to that at Marcona. It is some 20 km southeast of Marcona and is completely concealed, but reflected by a large magnetic anomaly. Mineralisation at Pampa Pongo cuts both Marcona Formation dolomites and Jahuay ocoites similar to those seen at Marcona. These two deposits, together with the late mineralisation at Marcona, indicate that along a 50 km northwest-trending corridor, there are at least 4 mineralising foci corresponding to at least two separate mineralising pulses: One late-Río Grande phase generating Fe-Cu mineral in Marcona and a late-Jahuay phase, responsible for the mineralisation of Huaricangana, Pampa Pongo and part of the Jahuay level Cu-mineralisation at Marcona. Detailed information on Marcona. Pampa Pongo and related prospects are covered by Moody *et al.*, in this volume.

The Río Grande-Jahuay geological environment represents an alkaline to shoshonitic fissural volcanic backarc regime, characterised by northwest-trending dyke swarms that run parallel to the main Treinta-Libras Fault. This fault has a dextral transcurrent sense of movement and controls the eastern border of the Coastal range where Marcona is located. This structural-magmatic system was active from Jurassic times when volcanism started in the area, and continued to at least the Aptian (117 Ma) when the later felsic dykes appear in that system. This ensialic rift marks the break-up of continental crust and the beginning of volcanic activity in the region.

Considering the stratigraphic distribution of metamorphic and alteration minerals observed in the sequence and their association with the late Río Grande events, Marcona has been interpreted to have formed as a geothermal system, in the sense described by Bird *et al.* (1984) and Schiffman *et al.* (1984). This coincides with dextral movement along the Treinta Libras Fault, during the final stages of the Río Grande volcanism.

In the same region, there are two minor prospects: Chala and Los Icas. Chala, which only has a meagre tonnage potential, is located 620 km to the south of Lima. It comprises around 10 separate mantos of magnetite each of up to 10 m in thickness and several tens of metres in length (Olchauski, 1980), located in the middle of a complex of ocoite lavas, dykes and volcanic-sedimentary rocks associated with the Liassic age fissural-effusive Chocolate Formation arc. Los Icas has only produced copper from artisanal workings and consists of a series of discrete copper dissemination zones and mantos, in a sub-volcanic environment associated with a generally north-south-trending Río Grande age fissure-rift (Osterman, 2001).

Raúl-Condestable and Minor Cretaceous Prospects

(Atkin *et al.*, 1985; Injoque, 1985; Vidal *et al.*, 1990)

The Raúl-Condestable deposit is hosted by the Upper Valanginian-Barremian (early Cretaceous) age Chilca Formation, part of the Copara Volcanics that extend for 500 km to the south of Lima, and is the centre of a district that has been an active mining centre since the late 1950s. The deposit has a total endowment comprising reserves and past production, of approximately 50 Mt @ 1.5% Cu with Ag and Au by-products.

The volcanic-sedimentary Chilca Formation is distributed around a northeast-trending effusive fissure controlled centre located in Quebrada Calicantro, immediately to the South of the Raúl Mine. This fissure is flanked by a 1000 to 2000 m thick package of basalt-andesite lavas, tuffs and pyroclastics, which grade towards the north and south into marine limestones, shales, sandstone and volcaniclastics. The stratigraphic sequence contains exhalative pyrite as nodules, smokers and replaced fossils. This volcanic-sedimentary pyrite, which produces a reddish colouration in the surrounding volcanics, disappears to the north and south, and it is not associated with copper mineralisation.

The volcanic centre, also hosts a set of dykes, sills and small stocks of andesite, dacite and granodiorite of 124 Ma in age (Vidal *et al.*, 1990).

Lavas and intrusives from the Raúl-Condestable Volcanic Centre have calc-alkaline to tholeiite affinities, with clinopyroxene, hornblende and plagioclase fractionation and a transitional arc basalt character. This deposit has chalcopyrite associated with pyrite, magnetite, actinolite and lesser apatite, forming disseminated orebodies, mantos and veins within the volcanic-sedimentary sequence of the host formation. Mantos (Fig. 4) are up to 250 x 200 m and have thicknesses of 1 to 5 m. They replace limestones, permeable tuffs and lava blocks. Veins extend for hundreds of metres and appear both in the volcanic-sedimentary sequence and in the dacitic intrusives. Finally, disseminated orebodies may be hundreds of metres across and appear as replacements in tuffs and andesitic lavas.

Mineralisation within the district is surrounded by a recognisable pattern of alteration. It commences as a thermal metamorphic suite, characterised by the presence of calcareous marbles, calc-silicate hornfels and sericite-biotite-talc hornfelses, surrounding cores of amphibolite and rocks rich in pyroxene and garnet. The amphibolites are composed of tremolite, actinolite, hornblendic-actinolite, tschermakite and hastingsite. These rocks are in their turn, extensively and irregularly replaced by tremolite, actinolite, chlorite and to a lesser extent by prehnite, albite, apatite and silica. Metallic mineralisation occurred at a late stage as disseminations, fracture fillings and replacements, following the typical skarn sequence. Alteration, is in general extensive and pervasive, but does not destroy the original rock textures, suggesting non-explosive and long lasting processes. The original fossils, nodules, sedimentary structures and geopetal textures are preserved in sedimentary protoliths, while volcano-clastic, pyroclastic and porphyritic textures are readily recognisable in rock of volcanic origin.

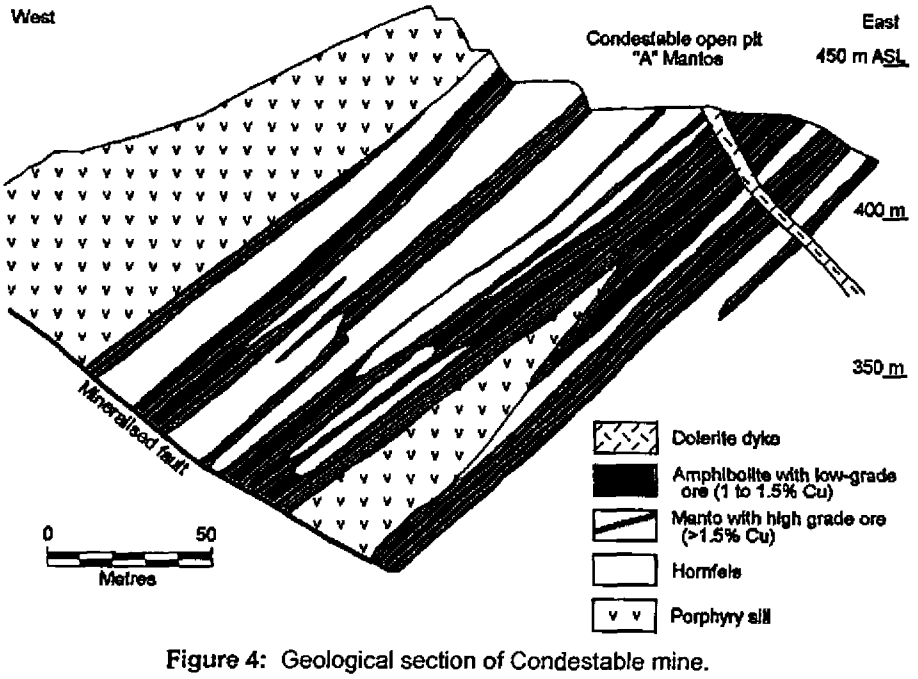


Figure 4: Geological section of Condestable mine.

The most important characteristic of this alteration is that the first stages of thermal metamorphism were zoned parallel to stratigraphy, with pyroxene, hornblende and garnet present towards the bottom of the stratigraphic sequence, while tremolite, actinolite, sericite, biotite and talc formed towards the top. This mineral distribution is similar to the one observed in active geothermal systems (Bird *et al.*, 1984; Schiffman *et al.*, 1984). Therefore, the pattern of alteration is considered to be the product of an ancient volcanic geothermal system.

Metallic mineralisation occurs in two associations. The first of these, iron-copper comprises chalcopyrite ore, together with pyrite, magnetite and minor amounts of pyrrhotite, galena, sphalerite, ilmenite, molybdenite, bornite, mackinawite, valleriite, marcasite, electrum and cobaltite. silver and gold are common by-products. Lead-zinc is the later association and it occurs as subsequent and minor veins and veinlets of galena and sphalerite with minor amounts of pyrite, chalcopyrite, tetrahedrite, melnikovite, gold and calcite. There are no exhalative iron-copper nor lead-zinc occurrences. The maximum formation temperature was around 320 to 414°C and isotope geochemistry (S, O, H) and fluid inclusion studies indicate that sulphur and the mineralising fluids had a sea-water source and that there was no boiling (Ripley and Ohmoto, 1977, 1979).

Within the district, metamorphic and hydrothermal alteration, mineralisation, volcanic activity and the emplacement of dacitic subvolcanic and hypabyssal intrusions are virtually all centred on the northeast-trending Calycantro Fault, which apparently controlled fissure volcanism, alteration and mineralisation.

Other minor copper-prospects of this kind are 5 Cruces, hosted in the Albian-Cenomanian Quilmana volcanics and Cerro La Loza, hosted in the volcanic-intrusive Bella Union Complex of Upper Cretaceous age.

Plutonic-related Cretaceous Deposits

The Coastal Batholith is composed of a large number of smaller granite plutons which have been grouped into super-units, while the batholith has been sub-divided into five lateral segments along its length as shown in Fig. 1. The early gabbros and diorites of this batholith, commonly known as the Patap Super-unit, occupy the same locus as the granite units of the batholith, but because of their tholeiitic nature are not considered to be part of the batholith from a geochemical and petrographical viewpoint (Pitcher *et al.*, 1985).

Fe oxide-Cu-Au deposits are associated with the early Albian (mid Cretaceous) gabbros and diorites of the Coastal Batholith and also with Cenomanian-Santonian (mid to upper Cretaceous) felsic super-units. They all occur in the Arequipa Segment of the Coastal Batholith, except for minor prospects in the Piura Segment, which are not described in this work.

Deposits Associated with Early Gabbros and Diorites of the Coastal Batholith (Patap Super-unit)

(Injoque, 2001; Injoque, 1985; Atkin *et al.*, 1985; Vidal *et al.*, 1990)

These deposits fall into two groups, iron and copper deposits. Yaurilla and Fe-Acarí (Fig. 5) belong to the first group (Dunin-Borkowski 1970; Zevallos, 1966) and are located 300 and 550 km respectively to the south of Lima. Both deposits were worked on a small scale in the 1960s and their production and reserves are of the order of 19 Mt @ 60% Fe and 20 Mt @ 66% Fe respectively.

Both Yaurilla and Fe-Acarí are associated with pyroxene-bearing diorite plutons having the geochemical characteristics of continental margin tholeiites and containing mineral veins of between 1 and 10 m in width

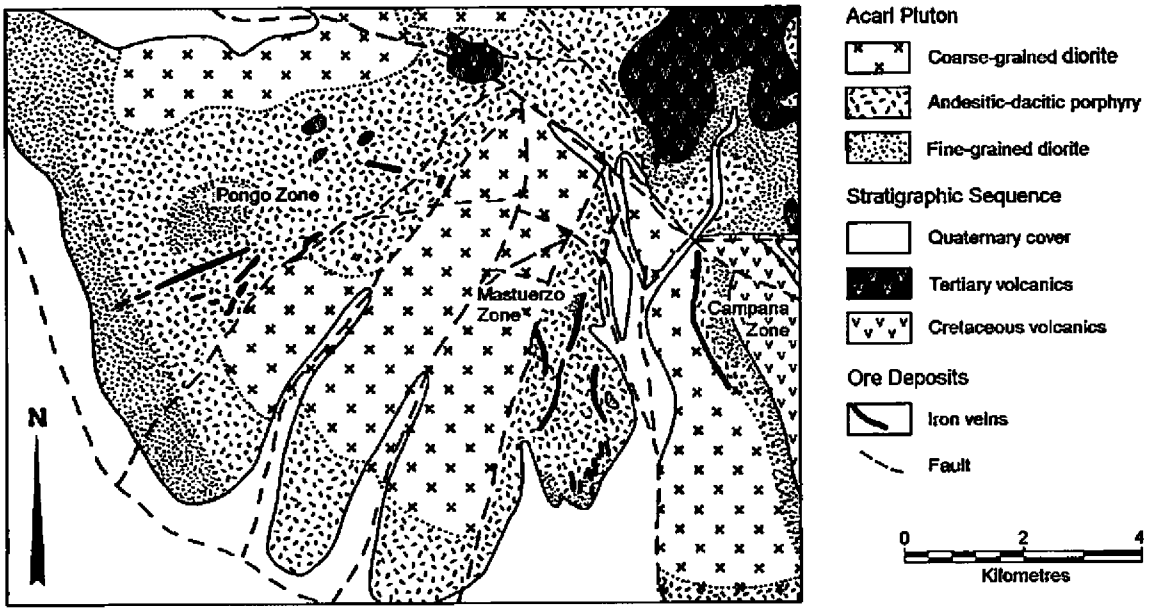


Figure 5: Geology of the Fe-Acari Deposit (modified after Dunin, 1970).

and up to 1 km in length. These veins show a vertical zoning pattern, with pyroxene dominant towards the lower levels and magnetite toward the upper sections.

The associated alteration is propylitic with magnetite disseminations farthest from the mineralised structures, while magnetite and associated epidote, clinopyroxene and amphiboles becoming more abundant towards the veins. The magnetite veins frequently have a banded appearance. This banding is made conspicuous by the less frequent occurrence of apatite, quartz and calcite accumulations between the magnetite bands. In the pyroxene rich magnetite veins of the lower levels, pyroxene has clearly crystallised first, from the walls of the host rock, while the magnetite has filled the space between pyroxene crystals. Many of these veins exhibit symmetric crustiform textures and marked poly-ascendant stages, with pyroxene or amphibole growing normally to the host rock, a clear indication that the veins were open-space during deposition. The delicate growth of magnetite and pyroxene, together with fault controls in the main veins and the transition from fresh diorite to altered diorite towards the contact with mineralisation, are a clear indication that the mineralising process was not magmatic as suggested by other authors, but that it was in fact metasomatic to hydrothermal (Injoque, 1985).

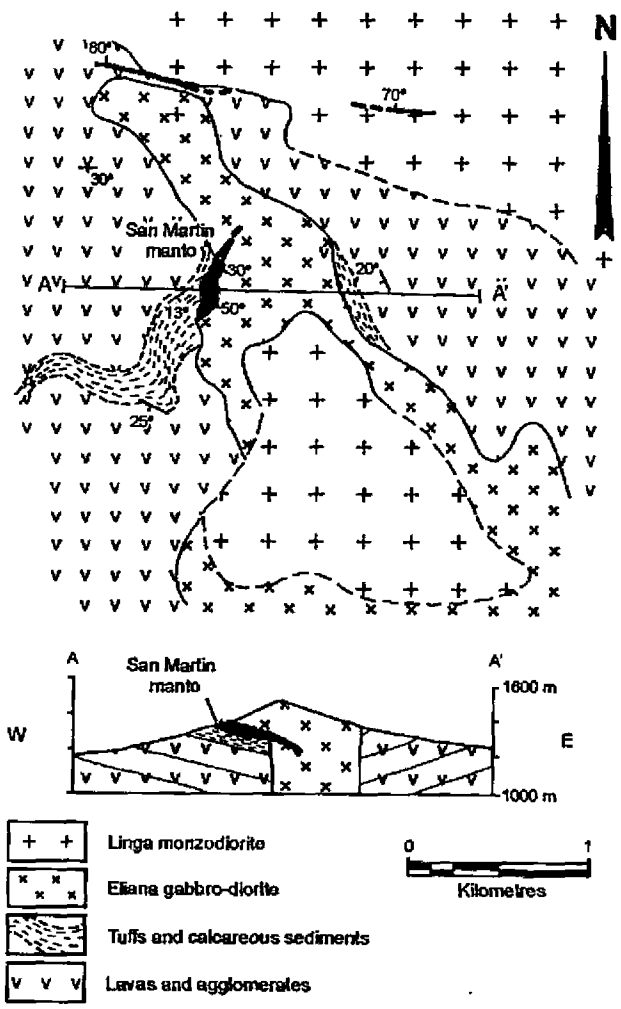


Figure 6: Geology of the Eliana Mining District (after Vidal, 1980)

The K-Ar age of the porphyry immediately preceding the iron mineralisation at Fe-Acari is 109 Ma (Vidal *et al.*, 1990).

The Cu deposits are represented by the San Martin Manto at the Eliana mine (Fig. 6) and by Monterrosas (Fig. 7; Vidal *et al.*, 1990), located 230 and 300 km to the south of Lima respectively. Both are now exhausted. Eliana produced 0.4 Mt @ 2.7% Cu from an up to 12 m thick manto located at the contact between a folded gabbro-dioritic sill and the andesite volcanics of the Albian Casma Volcanics. Monterrosas, on the other hand, is a 1.1 to 2% Cu vein linked to the sinistral Canzas fault. The vein is 430 m long, 150 m deep and up to 20 m thick and it is hosted by diorites. In both deposits, intrusives are continental margin tholeiites, but in contrast to those related to the iron deposits, they are hornblende- and biotite-bearing.

The alteration at Eliana includes of an outer zone of amphibole, chlorite, calcite and titanite. At the contact with the mineralised structure there is abundant amphibole and scapolite (Mei 25 to 33), together with disseminations of apatite, magnetite, pyrite and chalcopyrite, while the three latter and actinolite dominate within the mineralised structure. K-Ar dating of alteration amphiboles (hastingsite) associated with the Cu mineralisation, yielded ages of between 112 and 114 Ma (Vidal *et al.*, 1990), indicating a relationship between the gabbro and mineralisation. Furthermore, sulphur isotopes ($\delta^{34}S$) from 2 samples of pyrite gave values of -3.245 and -7.801‰ (Baruj, Spiro, BGS, personal comment) suggesting a source in part magmatic and perhaps partly sedimentary(?) for the sulphur, probably related to the surrounding Casma rocks.

At Monterrosas, late magmatic-hydrothermal alteration of the diorite generally resulted in the replacement of magmatic clinopyroxene and plagioclase by actinolite, with chalcopyrite and variable amounts of chlorite, epidote, scapolite (Me 25 to 29), tourmaline, sphene, apatite, magnetite and traces of K feldspar, calcite and muscovite.

Petrographic textures in both the diorite and ores indicate that metasomatic replacement was important, as well as fracture filling. The dominant mineral assemblage consists of chalcopyrite, magnetite, pyrite and actinolite in variable proportions, together with smaller quantities of clinopyroxene, Na-scapolite, tourmaline, quartz, pyrrhotite and cubanite. Underground mapping reveals a transitional zoning from the diorite walls towards the centre of the vein. The contact is irregular and gradational and is occupied by vein swarms composed of an outer zone of Na-scapolite and then by actinolite inwards. Immediately following is an interval of crystalline acicular actinolite, changing further toward the centre to massive magnetite in which small sulphide veins and disseminations appear and increase to form a central ore zone of massive chalcopyrite. Silicates, magnetite and sulphides are sigmoidal, while supergene processes replaced chalcopyrite with covellite and martitisation of magnetite.

A geochemical comparison of the total rock (balance) between fresh and altered diorites (Sidder, 1981, 1984), shows that the total iron content increases towards the central ore zone, while silica is reduced. Metals such as copper and cobalt are found at a background levels in diorites while abnormal concentrations of these elements and of Au, Ag and Mo characterise the actinolite and sulphides.

Fluid inclusion studies of quartz and sulphur isotope studies of pyrite and chalcopyrite indicate hydrothermal alteration and ore deposition temperatures of between 300 and 500°C, salinities of 30 to >50 wt.% $NaCl_{equiv.}$ and values of 1.6 to 3.3‰ for $\delta^{34}S$. High temperature, saline and magmatic fluids produced by the Patap Super-unit gabbro-diorite crystallisation are considered to have originated, transported and deposited the Monterrosas amphibole-copper-iron ores as a consequence of a drop in temperature and acidity of the mineralising fluid (Sidder, 1984).

Deposits Associated with the Coastal Batholith

The known iron oxide copper-gold family deposits of the main Coastal Batholith (other than the Patap Super-unit) occur within the Linga Super-unit (Cobrepampa) and the Cochahuasi Pluton (Cata Cañete).

Linga Super-unit: Cobrepampa District: (Hudson, 1974; Lavado, 1973; Valera, 1982) The Cobrepampa copper deposit is located 550 km to the south of Lima and consists of a cluster of veins hosted in the Cobrepampa Alkaline Monzonite, a 15 x 10 km northwest oriented pluton, belonging to the Linga Super-unit of the Coastal Batholith. The district has produced copper on small scale from the late 1950s to early 1960s, but at present is abandoned. The pluton varies from monzonite to grey-pink quartz-monzonite with dioritic facies.

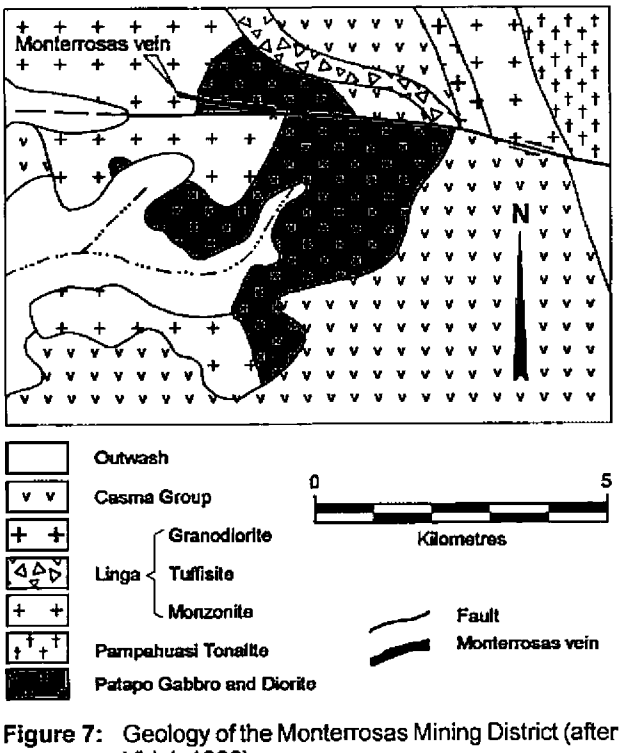


Figure 7: Geology of the Monterrosas Mining District (after Vidal, 1980)

The most primitive facies show 30 to 35% orthoclase and 40 to 45% andesine plagioclase, with hornblende, clinopyroxene and quartz as accessory minerals, while in the more evolved facies orthoclase becomes dominant with abundant biotite, usually forming aplitic dykes.

The principal structures of the district are northwest-trending faults that crosscut the entire area, with important dextral and normal components of displacement. The movement on these faults was in general late relative to the consolidation of the pluton and in part synchronous with the mineralisation.

Towards the mineralised zone, secondary biotite occurs at the transition from the magmatic to the late magmatic stages, and towards the core of the pluton. Subsequent abundant K feldspar alteration is widespread throughout the pluton but especially close to the mineralised bodies and takes the form of small veins and dissemination, increasing in density to finally alter the whole rock. This alteration has associated amber and brown garnet, actinolite and tourmaline as accessories. Towards the periphery of the feldspathised zone, transitional and sequential zones of quartz-sericite and, finally, propylitisation are developed.

The mineralisation occurs as a cluster of northwest-trending veins dipping at from 60 to 70°NE to subvertical, crosscutting practically the whole central zone of the intrusion. These veins form orebodies that are 100 to 300 m long, 5 to 10 m thick and 100 to 200 m deep, distributed in a sigmoidal pattern. On average, ore occupies 33 to 50% of the length of the veins. In total the vein swarm, spread throughout the pluton, covers an area of at least 10 x 5 km. It is suggested that the historic production (Samame, 1992; Valera, 1982; Lavado, 1973) plus reserves within the district may be of the order of 3 to 5 Mt with of 2 to 5% Cu, ~15 g/t Ag and Au as by-products.

The ore worked in these veins is mainly chalcopyrite and bornite, which associated pyrite and minor specularite, sphalerite and magnetite. However, during the early phase of mining activity in the district, the main ores were chalcocite, covellite and copper-oxides. The vertical zonation within the veins, commences with copper- and iron-oxides over the first 50 m below the surface. This is followed downwards by a secondary enriched copper-zone with chalcocite, covellite, digenite and Cu-oxides overprinting the primary ores in the lower sections to form bornite-chalcocite to a depth of 100 m. The next lower zone is a 50 to 100 m pyrite-chalcopyrite interval, which is followed downward by a magnetite-rich zone. Subordinate amounts of tungsten and tin are also found at depth (Samame, 1992).

The non-metallic gangue is K feldspar-rich towards the more potassic sections of the pluton with clinopyroxene and actinolite as the dominant gangue and some quartz towards the periphery. There are also smaller quantities of tourmaline, apatite, garnet, biotite, chlorite, quartz and calcite. The principal orebodies are associated with propylitic alteration. The gangue minerals grow mainly towards the host rocks, with a comb-like texture while the sulphides and magnetite grow towards the centre of

the structure. Nevertheless, towards the central and wider parts of the orebodies, the sulphides and gangue grade into a crackled zone, followed by a breccias with a high concentration of sulphides, indicating a relation between mineralisation and the dextral movement that formed the veins.

At Atiquipa, which is some 600 km to the south of Lima, there is a prospect comprising 10 to 15 smaller veins. Mineralisation occurs as Cu-oxides, magnetite, clinopyroxene, actinolite, Na-scapolite, epidote, quartz and chlorite. The veins are hosted within the alkaline Chala gabbro, which also belongs to the Linga Super-unit. These veins have been worked by artisanal miners to extract the Cu oxides which contain traces of Au and have a potential of a few thousand to tens of thousands of tonnes.

Cochahuasi Pluton, Cata Cañete District: (Injoque *et al.*, 1995) The Cata Cañete District is located 100 km to the southeast of Lima and consists of veins and small clusters of Cu minerals within the Cochahuasi Pluton of the Coastal Batholith.

The Cochahuasi Pluton is an northwest-trending, elongate, 20 x 10 km body composed of two principal units. The Mafic Unit is melanocratic, mainly monzo-dioritic, intruding and metamorphosing the surrounding Mesozoic volcanic-sedimentary formations to the south and west. It is intruded by the later leucocratic quartz-dioritic Felsic Unit. Both units have subsequently been intruded by swarms of lamprophyric dykes and are strongly affected, especially the Mafic Unit, by a northwest-trending, Cretaceous, amphibolite facies, dynamo-metamorphic event. The whole pluton was then intruded to the east by the late post-tectonic felsic Tiabaya Pluton.

The Cu mineralisation is distributed virtually throughout the pluton and into the neighbouring Mesozoic formations, as veins containing defined orebodies and as minor vein-swarms. The veins display sigmoidal patterns. The orebodies within the pluton attain lengths of several hundred metres and have widths of 2 to 10 m, although in the surrounding Mesozoic formations they only reach some tens of metres in length.

The mineralisation towards the base of the veins and within the host rock develop clinopyroxene, garnet, epidote and hornblende assemblages, which are generally obliterated by later mineralisation comprising chalcopyrite, pyrite, magnetite, quartz, chlorite, biotite and calcite, with minor bornite, sphalerite, galena, pyrrhotite, cobaltite, molybdenite, ilmenite, arsenopyrite, marcasite, melnikovite and gold.

This district has been mainly worked by informal and small miners and reserves plus historic production is believed to only be of the order of some hundreds of thousands of tonnes @ 1.5% Cu with Ag and Au by-products, although the upper oxidised levels are generally richer.

[1] REE: rare earth elements

Discussion

Geotectonic Environmental and Sources of Magma and Metals *(Refer to Tables 1 and 2)*

Iron oxide rich deposits with variable amounts of accompanying copper and/or gold are found in two very different environments within Perú.

The first of these is represented by the Cobriza deposit which is found in the Hercynian eastern range, hosted by the Tarma Group that occurs within an ensialic rift subsequent to Hercynian deformation, together with anorogenic intrusions (Soler, 1991; Kontak *et al.*, 1985).

In the western range, volcanic related deposits occur in the southern sector of the Cañete-Huarmey Marginal basin (the Cañete Basin proper), where its ensialic character produced volcanism of alkaline and shoshonitic affinities with markedly inter-plate (Jurassic) to arc basalt (Cretaceous) character. The plutonic related deposits associated with the Patap Super-unit and the Coastal Batholith, have also formed in this section of the Andes, are localised in the Arequipa Segment, and are also ensialic in nature. The plutons of the Coastal Batholith are generally arc-related magmas, indicating a possible relationship with subduction processes, as are the Cretaceous volcanics.

The REE signatures of the Coastal Batholith hosts indicate plagioclase, clinopyroxene and hornblende fractionation in different proportions, but no garnet fractionation, implying that the magmas originated at depths of less than 40 to 60 km in the mantle (Injoque, 1985; Pitcher *et al.*, 1985). The exception is the Cochahuasi Pluton (Cata Cañete) where garnet fractionation was important. Nevertheless, the magmas of this segment of the batholith are enriched in radiogenic Pb and LIL-elements (Atherton and Plant, 1987), because of their emplacement within the Precambrian crust. This enrichment is not recorded in the Lima Segment, where Precambrian crust is absent.

The Pb isotopes in the deposits also indicate that they originated in the mantle but with enrichment from the upper sedimentary layers of the crust, except for Marcona and Cobriza where Precambrian crustal Pb is important (Mukasa *et al.*, 1990; Noble *et al.*, 1995). This suggests that basement crustal sources may have contributed by providing copper and iron at Cobriza, while deposits formed away from this ancient crust, have derived metal from more mantle-related sources.

The source of sulphur and water for Raúl-Condestable was predominantly seawater (Rypley and Ohmoto, 1977, 1979). In contrast, the source of sulphur at Monterrosas (Sidder, 1981, 1984), Eliana and Marcona is magmatic, although minor sedimentary (Eliana) or marine (Marcona) sources cannot be discounted.

The relationship between deformation and mineralisation is another interesting aspect of these deposits. Cobriza, in the eastern range of the Andes, appears to be a post-tectonic deposit and coincides in time with the late Hercynian

Table 1: Plutonic related deposits

	Hercynian Cycle: Cobriza	Andean Cycle: Cata Cañete	Eliana	Yaurilla	Monterrosas	Fe-Acari	Cobrepampa
Regional Aspects							
Regional Igneous Body	Villa Azul Batholith	Coastal Batholith	Coastal Batholith	Coastal Batholith	Coastal Batholith	Coastal Batholith	Coastal Batholith
Associated Type Pluton	Two mica granite	Cochahuasi diorite	Patap Gabbro, Diorite	Patap Diorite	Patap Diorite	Patap Diorite	Linga Monzonite
Geotectonic Character	Anorogenic	Extensional, continental margin	Extensional, continental margin	Extensional, continental margin	Extensional, continental margin	Extensional, continental margin	Extensional, continental margin
Petrochemistry	Alkaline	Calcalkaline-alkaline	Tholeiite	Tholeiite	Tholeiite	Tholeiite	Alkaline
Magma Fractionation	Plagioclase*	Garnet	Plagioclase, (clinopyroxene)		Plagioclase, (clinopyroxene)	Plagioclase, (clinopyroxene)	Plagioclasa, (hornblende)
Regional Tectonics	Intracontinental rift	Late Cretaceous	Late Albian	Late Albian	Late Albian	Late Albian	Late to deformation
Important Structures	NW Reverse faults	Dextral NW faults	NW Synclinal		E-W sinistral Canzas Fault	NW & NE normal faults	Dextral NW normal faults
Exposed basement	+	-	+	+	+	+	+
Local Aspects							
Type of structures	Manto	Multiple	Manto	4 Veins	1 Vein	15 Veins	Multiple veins
Alteration							
External			Propylitic, albite	Propylitic, clinopyroxene	Propylitic, albite	Propylitic, clinopyroxene	K-feldspar, biotite, tourmaline
Internal	Diopside, garnet, hornblende, skarn type	Chlorite, sericite, silica, pyrite	Diopside, hornblende, Na-scapolite (skarn), pyrite	Clinopyroxene, actinolite	Diopside, hornblende, Na-scapolite skarn type, pyrite	Clinopyroxene, actinolite	K-feldspar, actinolite, tourmaline
Ores, by products	Chalcopyrite, Ag, Bi	Chalcopyrite, Ag, Au	Chalcopyrite, Ag, Au	Magnetite	Chalcopyrite, Ag, Au	Magnetite	Chalcopyrite, bornite, chalcocite, Ag, Au
Metallic Gangue	Magnetite, pyrrhotite, arsenopyrite	Magnetite, pyrite, pyrrhotite	Magnetite, pyrite, pyrrhotite		Magnetite, pyrite, pyrrhotite		Magnetite, pyrite
Non-metallic Gangue	Actinolite, phlogopite, quartz	Quartz, chlorite, calcite	Actinolite, chlorite, apatite, quartz, calcite	Clinopyroxene, apatite	Actinolite, chlorite, apatite, quartz, calcite	Clinopyroxene, apatite, quartz, calcite	Actinolite, chlorite, albite, K-feldspar, apatite, quartz, calcite
Trace Elements	W, Sn	Co, Ni	Co, Ni		Co, Ni		Co, Ni, W, Sn
Main Metasomatism					Fe, Mg, Al, K	Fe, Mg, Ca, (-Mn)	
Minor Metasomatism					Si, Na, Ca	Si, Al, Na, P	
Pressure, Kbars			0.5		0.5	0.5	
Ore Source			Patap Diorite		Patap Diorite	Patap Diorite	
Sulphur Source			Magmatic, (-sedimentary?)		Magmatic		
Lead Source	Precambrian crust	Enriched Mantle & upper sedimentary crust	Enriched Mantle & upper sedimentary crust		Enriched Mantle & upper sedimentary crust		Enriched Mantle & upper sedimentary crust
Fluid Source							
Salinity, NaCl eq. %					30-50		10-60**
Size and grade	100 Mt @ 1.5% Cu (Ag, Bi)	~1 Mt @ 1.5% Cu (Ag, Au)	0.4 Mt @ 2.6% Cu	19 Mt @ 60% Fe	1.9 Mt @ 1.6% Cu (Ag, Au)	20 Mt @ 66% Fe	5 Mt @ 2-5%Cu
Metallic Cu content (Mt)	15	~0.3	0.12		0.34		~1.5
Age (Ma)	263	>66***	114-112			<109	>96***
Deposit Type							
Skarn (Einaudi et al., 1981)	Cu calcic skarn	Fe calcic skarn	Fe calcic skarn	Fe calcic skarn	Fe calcic skarn	Fe calcic skarn	Cu calcic skarn
Other	Distal skarn	Autoreaction/hydrothermal	Autoreaction skarn	Autoreaction skarn	Autoreaction skarn	Autoreaction skarn	Autoreaction skarn
Hitzman et al. (1992)	Fe oxide-Cu-Au	Fe oxide-Cu-Au	Fe oxide-Cu-Au	Magnetite-apatite	Fe oxide-Cu-Au	Magnetite-apatite	Fe oxide-Cu-Au

* Soler, 1991; ** For the Linga Superunint Linga, Pisco Pluton, Agar, 1981; *** Estimated after Beckinsale *et al.*, 1985

extensional event, although the deposit is apparently focused on a northwest-trending reverse fault set (Valdez, 1983b). Marcona is associated with the transcurrent Treinta Libras Dextral Fault and a localised Jurassic rift which was the source of local volcanism (Injoque *et al.*, 1988). In this same period, volcanic activity in northern Chile coincided with the initial activation on the Atacama Fault (Brown *et al.*, 1991; Scheuber and Adrienssen, 1990), and with important mineralisation such as at Mantos Blancos and Michilla (Munizaga *et al.*, 1991; Venegas *et al.*, 1991). Raúl-Condestable (Injoque, 1985) and los Icas (Osterman, 2001) display a similar association with local rifts, but so far have no apparent relation to transcurrent faults. The plutonic related deposits however, are later associated with the Albian Mochica Deformation (Patap Super-unit; Injoque, 2001) or the Late Cretaceous Perúvian Deformation (Cata Cañete; Injoque *et al.*, 1995). For Monterrosas (Injoque, 1985) and Cobrepampa (Valera, 1982) however, there is a clear relationship with district scale transcurrent faults. Thus there appears to be a correlation between transcurrent faulting and mineralisation, the main mineralisation coinciding with the most notable fault (eg., Marcona).

Table 2: Volcanic Related Deposits

	Andean Cycle:	Raúl-Condestable	Marcona
Regional Aspects	*Type of basin*	Ensialic aborted marginal basin	Ensialic aborted marginal basin
	Petrochemistry	Calc-alkaline	Alkaline-shoshonitic
	Magma fractionation	Clinopyroxene, hornblende, (plagioclase)	Clinopyroxene, hornblende, (plagioclase)
	Thickness of the basin (m)	1000 to 2000	>4000
	Geothermal gradient (°C/km)	<100°	
	Type of metamorphism	Burial Type	Burial Type
	Metamorphic facies	Prehnite-pumpellyite to zeolite	
	Geotectonic character	Extensional, continental margin	Extensional, continental margin
	Regional tectonics	Extensional, local rift	Dextral transcurrent, local rift
	Important structures	Calycantro NE Extensional Fault	Treinta Libras NW Dextral Fault
	Ocoite presence	No	Yes
	Mantle intrusion into the crust	Yes	No
	Basement in the vicinity	No	Yes
Local Aspects	*Type of structures*	Mantos, veins, disseminated ore bodies	Mantos, veins, disseminated ore bodies
	Alteration		
	External	Propylitic, albite, K feldspar, hematite	Propylitic, albite, K feldspar, hematite
	Internal	Diopside, garnet, hornblende, Na-scapolite (skarn type), biotite, sericite, talc, pyrite	Diopside, garnet, hornblende, Na-scapolite (skarn type), Phlogopite (skarn type), pyrite
	Ores, by-products	Chalcopyrite, Ag, Au	Magnetite, chalcopyrite, Ag, Au
	Metallic gangue	Magnetite, pyrite, pyrrhotite	Pyrite, pyrrhotite
	Non-metallic gangue	Actinolite, chlorite, albite, K-spar, apatite, quartz, calcite	Chlorite, albite, K-spar, apatite, quartz, calcite
	Trace elements	Co, Ni	Co, Ni
	Metasomatism - addition	Fe, Mg, Cu, Co, Ni	Fe, Cu, Co
	Metasomatism - depletion	Na, P	
	Prograde stratigraphic zoning		
	Upper Part	Biotite, chlorite-sericite, talc	Phlogopite, chlorite-sericite
	Lower Part	Diopside, garnet, hornblende, Na-scapolite	Diopside, hornblende, Na-scapolite
	Maximum formation temp. (°C)	414	500
	Pressure, Kbars	0.5	1
	Local gradient (°C/km)	~100°	~100°(?)
	Ore metal source	Surrounding Volcanics	
	Sulphur source	Sea water, magmatic	Magmatic, sea water?
	Lead source	Enriched mantle and upper sedimentary crust	Precambrian crust
	Mineralising fluid source	Sea water	
	Salinity, equivalent % NaCl	20 to 30	
	Size (millons of tonnes & grade)	~50 Mt @ 1.5 % Cu (Ag, Au)	>1500 Mt of Fe; 0.01% Cu, Ag, Au
	Metallic Cu content in Mt	~7.5	1.5?
	Age (Ma)	124 to 127	154 to 160
Deposit type	*Skarn type (Einaudi et al., 1981)*	Fe Calcic skarn	Fe Calcic skarn
	Other classifications	Geothermal skarn, CuTM Peruvian type*	Geothermal skarn, CuTM Peruvian type*
	after Hitzman et al. 1992	Fe oxide-Cu-Au	Magnetite-apatite

*Copper Manto-Type deposits, Peruvian type (Injoque 1999, 2000)

Mineralogy and Formation Conditions *(Refer to Tables 1, 2 and 3)*

The principal alteration associated with these deposits of the coastal volcanic environment and the Patap Super-unit intrusives is propylitisation, with albite present to a greater or lesser extent and minor proportions of K feldspar. Immediately adjacent to the mineralisation clinopyroxene, amphiboles (hornblende and tremolite-actinolite), Na-scapolite, epidote, chlorite and garnet alteration patterns become important.

At Cobrepampa, however, K feldspar alteration and weak secondary biotite are observable on a district scale. At Marcona and Raúl-Condestable, furthermore, pyrite disseminations can be found surrounding the mineralisation giving way to an outer halo of weak pinkish hematite.

The mineralogy of these deposits generally consists of actinolite, hornblende, Na-scapolite and chlorite, with variable amounts of biotite, phlogopite, sericite, garnet (grandite), diopsidic clinopyroxene, apatite, sphene and minor presence of rutile, albite, tourmaline, K feldspar, quartz and calcite, the latter being developed mainly towards the hydrothermal stage. The dominant metallic minerals are magnetite, pyrite, chalcopyrite and variable quantities of pyrrhotite, with bornite, chalcocite, covellite, ilmenite, molybdenite galena and sphalerite being generally less abundant. Cobriza, however, contains Ag and Bi as by-products as well as noteworthy contents of arsenic minerals that are otherwise absent or very rare in Andean deposits. Trace amounts of W and Sn are also present, elements that are only found on the coast at Cobrepampa, which appears to indicate a relation to felsic alkaline magmas in both cases. On the coast, however, almost all of the deposits contain by-

Table 3: Comparative mineralogy table for the main Fe Oxide-Cu-Au Deposits of Perú.

	Hercynian Cycle	Andean Cycle						
	Cobriza	Raúl-Condestable	Eliana	Monterrosas	Marcona	Fe-Acari	Cata Cañete	Cobrepampa
Garnet	●	O			O		O	O
Clinopyroxene	●	O		Tr	O	●	O	O
Scapolite	O	O	O	O	Tr	Tr		O
Amphibole	●	●	●	●	●	O	O	●
Apatite		O	O	O	O	O	O	O
Sphene	O	O	O	O	O	O	O	O
Biotite/phlogopite/sericite	O	O	O	O	O	Tr	O	O
Albite		O	O	O	Tr	Tr	O	
Prehnite		O			Tr			
Tourmaline/axinite	O	Tr	Tr	O	O			O
Chlorite	O	●	O	O	O	Tr	●	O
Epidote	O	O	O	O	Tr	Tr	O	Tr
K-Feldspar		O	Tr	Tr	Tr			O
Quartz	O	O	O	O	Tr	Tr	●	O
Calcite	O	O	O	O	O	O	●	O
Talc	O	Tr			Tr	Tr		
Barite	O							
Magnetite	●	●	●	●	●	●	O	●
Hematite	O	Tr			O	O	Tr	O
Ilmenite		Tr	Tr	Tr	Tr		Tr	
Molybdenite		Tr	Tr	Tr	Tr		Tr	Tr
Pyrite	●	●	●	●	●	O	●	●
Cobaltite/Gersdorfite		Tr	Tr				Tr	
Pentlandite					Tr			
Pyrrhotite	●	O	Tr	Tr	Tr			
Arsenopyrite	●	Tr	O				Tr	
Lollingite	Tr							
Rutile	●	Tr	Tr	Tr	Tr	Tr		
Chalcopyrite		●	●	●	●	Tr	●	●
Bornite	Tr	Tr	Tr	Tr	Tr		O	O
Cubanite		Tr	Tr	Tr				
Sphalerite/Marmatite	Tr	O	O	O	Tr		O	Tr
Galena	Tr	O	Tr	Tr	Tr		O	Tr
Mackinawite/valerite		Tr	Tr		Tr		Tr	
Au/electrum	Tr	Tr	Tr	Tr	Tr		Tr	Tr
Marcasite	O	Tr	Tr	Tr	O		O	
Tetrahedrite		Tr						
Bismuthinite/Native Bi	Tr							
Melnicovite		Tr	Tr		Tr			
W, Sn	Tr							Tr

Principal = ● Minor = O Trace = Tr

products gold (native, electrum and solid solution), silver (in galena) and traces of cobalt and nickel, indicating an association with basic magmas (Injoque *et al.*, 1985).

The formation temperature for these deposits is generally estimated between 400 and 500°C considering their mineral assemblages. Only at Raúl-Condestable there are temperature estimations based on isotope geochemistry (320 to 414°C). The formation pressure for the coastal deposits has been estimated from the stratigraphy at around 0.5 Kbars although it appears that Marcona was somewhat deeper (1 Kbar).

Classification *(Refer to Tables 1 and 2)*

The iron oxide rich deposits with variable amounts of accompanying copper and/or gold found in Perú are considered to be classical Fe and/or Cu skarns. According to the classification used by Einaudi *et al.*, (1981) they are "Fe calcic skarns", except for Cobrepampa which, because of its relationship with the Cobrepampa monzonite is a "Cu calcic skarn". Cobriza, because of its mineralogy and proximity to granitic rocks also belongs to the second group. Cata Cañete, however, although it has skarn roots, is volumetrically an hydrothermal deposit.

On the other hand Raúl-Condestable and Marcona are deposits formed at sub-volcanic levels in the final stages of the Chilca and Rio Grande volcanisms, respectively. Their initial stages of thermal metamorphism produced a zoning pattern that parallels the stratigraphy, with pyroxene, hornblende and garnet development towards the base of the sequence, while tremolite, actinolite, sericite, biotite and talc occur towards the top. This mineral distribution is similar to that observed in active geothermal systems (Bird *et al.*, 1984; Schiffman *et al.*, 1984). For this reason the pattern of alteration is considered to have originated in an ancient volcanic geothermal system and deposits are classified as geothermal skarns or Perúvian Manto type Cu deposits (Injoque, 1985, 1999, 2000). These deposits coincide on a regional scale with the presence of ocoites, a thick crust, geothermal gradients of 20 to 30°C/km, green schist to zeolite facies metamorphism and a moderate intrusion of the mantle into the crust in the Cañete Basin. To the north however (Huarmey Basin), ocoites are absent, although there is an association with episodic burial metamorphism, geothermal gradients of >300°C/km, an oceanic environment within the basin, together with a deep intrusion of the mantle into the crust (Aguirre *et al.*, 1989). Under these conditions VMS type deposits occur instead (Injoque, 1999, 2000), with Raúl-Condestable being found at the transition between the two basins.

The deposits related to the Coastal Batholith, however, are classified as auto-reaction skarns in the sense of Zharikov (1970).

Hitzman *et al.* (1992) separate this family into two groups. The magnetite-apatite or Kiruna-type deposits, which include Marcona, Chala, Fe-Acari and Yaurilla, given the massive presence of magnetite in these deposits. The second group corresponds to the Fe oxide-Cu-Au deposits because of their greater copper content, although of these only Cobrepampa and Cobriza are related to felsic rocks. Cata Cañete, however, has developed further towards the hydrothermal stage and is richer in quartz and calcite, corresponding to higher systems as described by Ray and Lefebure (2000). The development of these deposits towards systems rich in magnetite or rich in copper appears to be related to the evolution of pyroxene-rich magmas or hornblende-rich magmas respectively (Osborn, 1959; Helz, 1976; Oyarzun, and Frutos, 1984), within the typical metallogenic evolution processes of island arcs (Stanton, 1978).

Acknowledgements

The author is thankful to Miguel Huamám and Elsiario Antunez de Mayolo for their comments on Cobriza and also to Noranda Perú S.A.C. for the facilities to publish this paper.

References

Adrian, E., 1958 - The geology and iron ore bodies of the Marcona District, Perú; *Marcona Mining Co., Perú*, Internal Report.

Aguirre, L., Levi, B. and Nystrom J.O., 1989 - The link between metamorphism, volcanism and geotectonic setting during the evolution of the Andes; *in* Daly, J.S., Cliff, R.R. and Yardley, B.W.D., (eds.), Evolution of Metamorphic Belts, *Geological Society of London*, Special Publication, v. 43, pp. 223-232.

Agar, R., 1981 - Copper mineralization and magmatic hydrothermal brines in the Rio Pisco section of the Perúvian Coastal Batholith; *Economic Geology*, v. 76, pp. 677-693.

Atchley, F., 1956 - Geology of the Marcona Iron Deposits, Perú; Unpublished Ph.D, thesis, *Stanford University, California*, 150p.

Atherton, M., 1990 - The Coastal Batholith of Perú: the product of rapid recycling of "new" crust formed within rifted continental margin; *Geological Journal*, v. 25, pp. 337-349.

Atherton, M., and Plant, J., 1987 - High heat production granites and the evolution of the Andean and Caledonian continental margins; *in* Halls, C. (ed.), High Heat Production Granites, Hydrothermal Circulation and Ore Genesis, *Institute of Mining and Metallurgy, London*, pp. 459-478.

Atkin, B., Injoque, J. and Harvey, P., 1985 - Cu-Fe-amphibole mineralization in the Arequipa segment; *in* Pitcher, W.S., Atherton, M.P., Cobbing, E. J. and Beckinsale, R.D., (eds.), Magmatism at a Plate Edge - the Perúvian Andes, *Blackie and Son Ltd, Glasgow*, pp. 261-270.

Beckinsale, R., Sanchez-Fernández, A., Brook, M., Cobbing, E., Taylor, W. and Moore, N., 1985 - Rb-Sr whole-rock isochron and K-Ar age determinations for the Coastal Batholith of Perú; *in* Pitcher, W.S., Atherton, M.P., Cobbing, E. J. and Beckinsale, R.D., (eds.), Magmatism at a Plate Edge - the Perúvian Andes, *Blackie and Son Ltd, Glasgow*, pp. 177-202.

Bird, D., Schiffman, Pe., Elders, W.A., Williams, A.E. and McDowell, S.S., 1984 - Calc-silicate mineralisation in active geothermal systems; *Economic Geology*, v. 79, pp. 671-695.

Brown, M., Díaz, F., and Grocott, J., 1991 - The Atacama Fault System: History of displacement and tectónic significance for the Mesozoic-recent evolution of Northern Chile; Proceedings, *6th Congreso Geológico Chileno, Viña del Mar*, pp. 129-132.

Centromin Perú, 1995 - Gerencia de Operaciones Mineras, Planeamiento a Mediano y Largo Plazo U.P. Cobriza 1995-2000.

Cerro de Pasco Corporation, 1970 - Geología de la Mina Cobriza; *en* Geología de los Yacimientos Minerales Operados por la Cerro de Pasco Corporation, *1er. Congreso Latinoamericano de Geología, Lima-Perú*, Nov. 1970, pp. 36-61.

Dunin-Borkowski, E., 1970 - Der Acari-pluton (Perú) als Berspiel der Differentiation del Tonalitishchen Magmas; *International Journal of Earth Sciences: Geologische Rundschau*, v. 59, pp. 1141-1180.

Einaudi, M., Meinert, L and Newberry, R., 1981 - Skarn deposits; *Economic Geology*, 75th Anniversary Volume, pp. 317-391.

Helz, R., 1976 - Phase relation of basalts in their melting ranges at P_{H_2O} 5 Kbars. Part III, Melt compositions; *Journal of Petrology*, v. 17, pp. 139-193.

Hitzman, M., Oreskes, N. and Einaudi, M, 1992 - Geological characteristics and tectonic setting of Proterozoic iron oxide (Cu-U-Au-REE) deposits; *Precambrian Research*, v. 58, pp. 241-287.

Huamán, M., Rivera, G., Antúnez de Mayolo, E. and Kobe, H., 1987 - Manto Cobriza: mineralización estratoligada y estratiforme en los sedimentos del Grupo Tarma; *6th Congreso Perúano de Geología, Lima*, Resúmenes, pp. 117.

Hudson, C., 1974 - Metallogenesis as related to crustal evolution in S.W. Central Perú; Unpublished Ph.D. thesis, *University of Liverpool*, 150p.

Injoque, J. 1985 - Geochemistry of Cu-Fe-amphibole skarn deposits of the Perúvian Central Coast; Unpublished Ph.D. thesis, *University of Nottingham, U.K.*, 597p.

Injoque, J., 1999 - The location and extent of volcanic massive sulphide and manto-type copper deposits in the Cretaceous Volcanic Arcs in the Perúvian Andes; PACRIM'99 Proceedings, Bali, Indonesia, *Australasian Institute of Mining and Metallurgy, Melbourne*, pp. 327-334.

Injoque, J., 2000 - Distribución de yacimientos de sulfuros masivos (VMS) y de cobre tipo manto (CuTM) en el arco volcánico Cretáceo de los Andes Perúanos y Sudamericanos; *Boletín de la Sociedad Geológica del Perú*, v. 90, pp. 19-34.

Injoque, J., 2001 - Segmentación de los Gabros y Dioritas Tempranos del Batolito de la Costa (SuPerúnidad Patap), la Fase Deformativa Mochica y Mineralización Asociadas, como parte de la Segmentación Cretácea de la Costa Perúana; *Boletín de la Sociedad Geológica del Perú*, v. 92, pp 7-22.

Injoque, J., Mendoza, J., Aranda, A., Ramírez, L. and Andrade, R., 1985 - Sobre la presencia de Co, Ni, Ag y Au en los yacimientos de Cobre y Hierro de la Costa Centro-Sur Perúana; *Minería* N°191, Nov. Issue, pp 41-50.

Injoque, J., Atkin, B., Harvey, P. and Snelling, N., 1988 - Mineralogía y geocronología del skarn geotermal de hierro de Marcona; *Boletín de la Sociedad Geológica del Perú*, v. 78, pp. 65-80.

Injoque, J., Valera, J., and Miranda, C., 1995 - Geología del Distrito Minero de Cata Cañete, Aspectos Petrológicos y Estructurales con Mención en la mineralización de Cobre; *Boletín de la Sociedad Geológica del Perú*, v. 84, pp. 43-78.

Kontak, D., Clark, A., Farrar, E. and Strong, D., 1985 - The rift-associated Permo-Triassic magmatism of the Eastern Cordillera: a precursor to the Andean orogeny; *in* Pitcher, W.S., Atherton, M.P., Cobbing, E. J. and Beckinsale, R.D., (eds.), Magmatism at a Plate Edge - the Perúvian Andes, *Blackie and Son Ltd, Glasgow*, pp. 36-44.

Laubacher, G. and Megard, F., 1985 - The Hercynian basement: a review; *in* Pitcher, W.S., Atherton, M.P., Cobbing, E. J. and Beckinsale, R.D., (eds.), Magmatism at a Plate Edge - the Perúvian Andes, *Blackie and Son Ltd, Glasgow*, pp. 29- 41

Lavado, M., 1973 - Geologia de la Mina La Argentina, Cobrepampa, Acari; Unpublished Bachiller en Geologia thesis, *Universidad Nacional Mayor de San Marcos, Lima.*

Megard, F., 1978 - Etude geologique des Andes du Perou Central; *Mémoires ORSTOM, Paris*, v. 86, 310p.

Mukasa, S., Vidal, C. and Injoque, J., 1990 - Pb isotope bearing on the metallogenesis of sulfide ore deposits in Central and Southern Perú; *Economic Geology*, v. 85, pp. 1438-1446.

Munizaga, F., Ramirez, R., Drake, R., Tassanari, C. and Zentilli, M., 1991 - Nuevos antecedentes geocronológicos del yacimiento Mantos Blancos, Región de Antofagasta. Chile; Proceedings, *6th Congreso Geológico Chileno, Viña del Mar*, pp. 221-224.

Noble, D., McKee, E., Petersen, U., Alvarez, A. and Yupanqui, M., 1995 - The Cobriza copper skarn deposit, Central Perú: Permian age, radiogenic lead isotope composition and association with two mica granite; Volumen Jubilar Alberto Benavides, *Sociedad Geológica del Perú*, pp. 239-242.

Olchauski, E., 1980 - Geologia de los cuadrangulos de Jaqui, Coracora, Chala y Chaparra; *Instituto Geologico Minero y Metalurgico, Lima*, Boletín. N°34A, 71p.

Osborn, E., 1959 - Role of Oxygen pressure in the crystallisation and differentiation of a basaltic magma; *American Journal of Science*, v. 257, pp. 609-647.

Osterman, G., 2001 - Geología del Distrito Los Icas; *Boletín de la Sociedad Geológica del Perú*, v. 92, pp 91-96.

Oyarzun, J. and Frutos, J., 1984; Tectonic and Petrological Frame of the Cretaceous Iron Deposits of North Chile; *Mining Geology*, v. 34, pp. 21-31.

Petersen, U., 1965 - Regional geology and major ore deposits of central Perú; *Economic Geology*, v. 30, pp. 407-476.

Pitcher, W.S., Atherton, M.P., Cobbing, E. J. and Beckinsale, R.D., (eds.), Magmatism at a Plate Edge - the Perúvian Andes, *Blackie and Son Ltd, Glasgow*.

Ray, G. and Lefebure, D., 2000 - A synopsis of iron oxide±Cu±Au±P±REE deposits of the Candelaria-Kiruna-Olympic Dam Family; *in* Geological Fieldwork 1999, *British Columbia Ministry of Energy and Mines*, Paper 2000-1, pp. 267-271.

Ripley, E.M. and Ohmoto, H., 1977 - Mineralogic, sulphur isotope and fluid inclusion studies of the stratabound copper deposits at the Raúl mine, Perú; *Economic Geology*, v. 72, pp. 1017-1041.

Ripley, E.M. and Ohmoto, H., 1979 - Oxygen and hydrogen isotopic studies of the ore deposition and metamorphism at the Raúl mine, Perú; *Geochimica et Cosmochimica Acta*, v. 43: pp. 1633-1643.

Rivera, A., Huamán, M., Antunez de Mayolo, E. and Kobe, H., 1989 - Manto Cobriza: mineralización estratoligada y estratiforme en los sedimentos de Grupo Tarma; *Boletín de la Sociedad Geológica del Perú*, v. 79, pp 23-32.

Samamé, M., 1992 - El Perú Minero, Tomo IX Empresas; *Instituto Geologico Minero y Metalurgico, Lima*,

Scheuber, E. and Andrienssen, P., 1990; The kinematic and geodynamic significance of the Atacama fault zone, Northern Chile; *Journal of Structural Geology*, v. 12, pp. 243-257.

Schiffman, P., Elders, W.A., Williams, A.E., McDowell, S.S. and Bird, D., 1984 - Active metasomatism in the Cerro Prieto geothermal system, Baja California, México: A telescoped low pressure, low temperature metamorphic facies series; *Geology*, v. 12, pp. 12-15.

Sidder, G., 1981 - Metallization and alteration at the Monterrosas mine, Ica, Perú; Unpublished M.Sc. thesis, *University of Oregon*, 110 p.

Sidder, G., 1984 - Ore genesis at the Monterrosas deposit in the Coastal Batholith of Ica, Perú; Unpublished. Ph.D. thesis, *Oregon State University*, 221 p.

Soler, P., 1991 - Contribution a l'etude du magmatisme associe aux marges actives - petrographie, geochimie et geochimie isotopique du magmatisme cretace a pliocene le long d'une transversale des Andes du Perou central - implications geodynamiques et metallogeniques; Unpublished Docteour es-Sciences thesis, *Academie de Paris, Universite Pierre et Marie Curie, France*. 845p.

Stanton, R.L., 1978 - Mineralisation in Island Arcs with particular reference to the South-west Pacific Region; *Proceedings of the Australasian Institute of Mining and Metallurgy*, v. 268, pp. 9-19.

Valdez, M. 1983a - Estimación cuantitativa de Plata en el Manto Cobriza - Mina Cobriza; *Boletín de la Sociedad Geológica del Perú*, v. 71, pp. 63-68.

Valdez, M. 1983b - Alteración y mineralización hidrotermal del Manto Cobriza - Mina Cobriza; *Boletín de la Sociedad Geológica del Perú*, v. 72, pp. 111-126.

Valera, J, 1982 - Estudio geológico de la Veta Cobrepampa en el Distrito Minero de Acarí-Arequipa. Unpublished Ingeniero Geólogo thesis, *Universidad Nacional de Ingeniería, Lima*.

Venegas, R., Munizaga, F. and Tassanari., C., 1991 - Los yacimientos de Cu-Ag del Distrito Carolina de Michilla, Región de Antofagasta, Chile: Nuevos antecedentes geocronológicos; Proceedings, *6th Congreso Geológico Chileno, Viña del Mar*, pp.452-455.

Vidal, C., Injoque, J., and Sidder, G., 1990 - Amphibolitic Cu-Fe skarn deposits in the Central Coast of Perú; *Economic Geology*, v. 85, pp. 1447-1461.

Zevallos, R., 1966 - Geology of the Acari Iron Mining District, Arequipa, Perú; Unpublished M.Sc. Thesis, *Univ. of Missoury, Rolla*, 170p.

Zharikov, V., 1970 - Skarns I, II, III; *International Geology Review*, v. 12, pp. 541-559, 619-647, 760-775.

PGC
PUBLISHING

Hawkes, N., Clark, A.H. & Moody, T.C., 2002 - Marcona and Pampa de Pongo: Giant Mesozoic Fe-(Cu, Au) Deposits in the Peruvian Coastal Belt; *in Porter, T.M. (Ed.), Hydrothermal Iron Oxide Copper-Gold & Related Deposits: A Global Perspective*, Volume 2; PGC Publishing, Adelaide, pp 115-130.

MARCONA AND PAMPA DE PONGO: GIANT MESOZOIC Fe-(Cu, Au) DEPOSITS IN THE PERUVIAN COASTAL BELT

[1]Nicholas Hawkes, [2]Alan H Clark and [1]Timothy C Moody

[1]Rio Tinto Mining & Exploration, Lima, Peru
[2]Department of Geological Sciences & Geological Engineering, Queen's University, Kingston, Ontario, Canada

Abstract – Located approximately 400 km south of Lima, Peru, the Marcona and Pampa de Pongo deposits are the largest iron accumulations with associated copper and gold along the western coast of South America. Approximate resources include more than 1400 Mt of iron ore at Marcona and 1000 Mt of magnetite mineralisation at Pampa de Pongo. Both deposits contain some copper and gold and exhibit numerous features that allow their inclusion in the "Iron Oxide-Copper-Gold" clan of deposits, alongside such examples as Candelaria and Mantos Blancos in Chile. The two deposits form part of a cluster of similar occurrences that together define the "Marcona Fe-Cu District".

The Marcona iron deposits were first identified in 1915 and mining commenced in 1953, while artesenal copper mining had been carried out in the district from the late 19th century. The larger iron bodies are hosted by the Lower Paleozoic Marcona and Middle to Upper Jurassic Río Grande Formations. The Marcona Formation is dominated by arenites and both calcitic and dolomitic carbonates, whereas the Río Grande Formation comprises a thick sequence of basaltic andesites and andesites (sills and flows), volcaniclastics and minor limestones. Although including major carbonate replacement facies, the iron deposits widely exhibit previously undocumented, intra-mineralisation hydrothermal breccia textures and multistage iron oxide ± sulphide/copper mineralisation. Copper mineralisation is mainly associated with magnetite and lesser specularite. The iron oxide bodies strike northeast and north-northwest and show both fault and lithological controls on ore geometry. Intra- and post-iron mineralisation igneous activity in the Marcona Mine area included dacitic/granodioritic dykes and andesitic "ocöite" dykes.

The hitherto undocumented Pampa de Pongo Fe (-Cu-Au) deposit, covered by at least 20 m of sand, was discovered in 1994 by drilling a large magnetic anomaly 30 km southeast of Marcona. Host rocks to the mineralisation are dolostones and andesitic volcanics of the Oxfordian-Tithonian Jahuay Formation, which are higher in the sequence than the Marcona iron deposits. The iron mineralisation exhibits both replacement and breccia-fill facies within a steeply northwest-dipping fault corridor. Magnetite mineralisation in the andesites is associated with Fe-chlorite, talc and clinochrysotile, whereas replacement of the underlying dolostone includes magnetite-amphibole-serpentine associations.

The age of the Pampa de Pongo deposit is uncertain, although the preferred genetic model for the district involves a large metal flux coeval with deep-seated Jurassic, and probably Cretaceous igneous intrusive activity. This was triggered by the introduction of mantle-derived melt along the root zone of the extensional faults within an active continental arc. At a local scale, iron oxide-associated mineralisation at Marcona, Pampa de Pongo and the surrounding district probably formed in an environment characterised by repeated crustal extension over a +20-60 my period. The anomalous concentration of thick andesitic volcanics or sills and dykes at Marcona, and evidence for district-scale thermal anomalies preceding and during the main introduction of iron oxide mineralisation, indicate that the area was also an important volcanic centre and the site of a long-lived thermal anomaly.

Introduction

The Marcona Fe (-Cu, Au, Zn, Co) deposit and Pampa de Pongo Fe (-Cu-Au) prospect represent two large Fe-oxide -rich Mesozoic hydrothermal centres situated approximately 400 km south of Lima, Peru. (Figure 1). Together with the granitoid-hosted magnetite-apatite system at Hierro Acarí (Injoque, 1985, and Vidal, *et al.*, 1990) and Cu-Fe-Au vein system at Cobrepampa, the two deposits make up a strongly mineralised segment of the littoral zone, herein termed the Marcona Fe-Cu District, which constitutes the apparent apogee of this mineralisation style in the Central Andes.

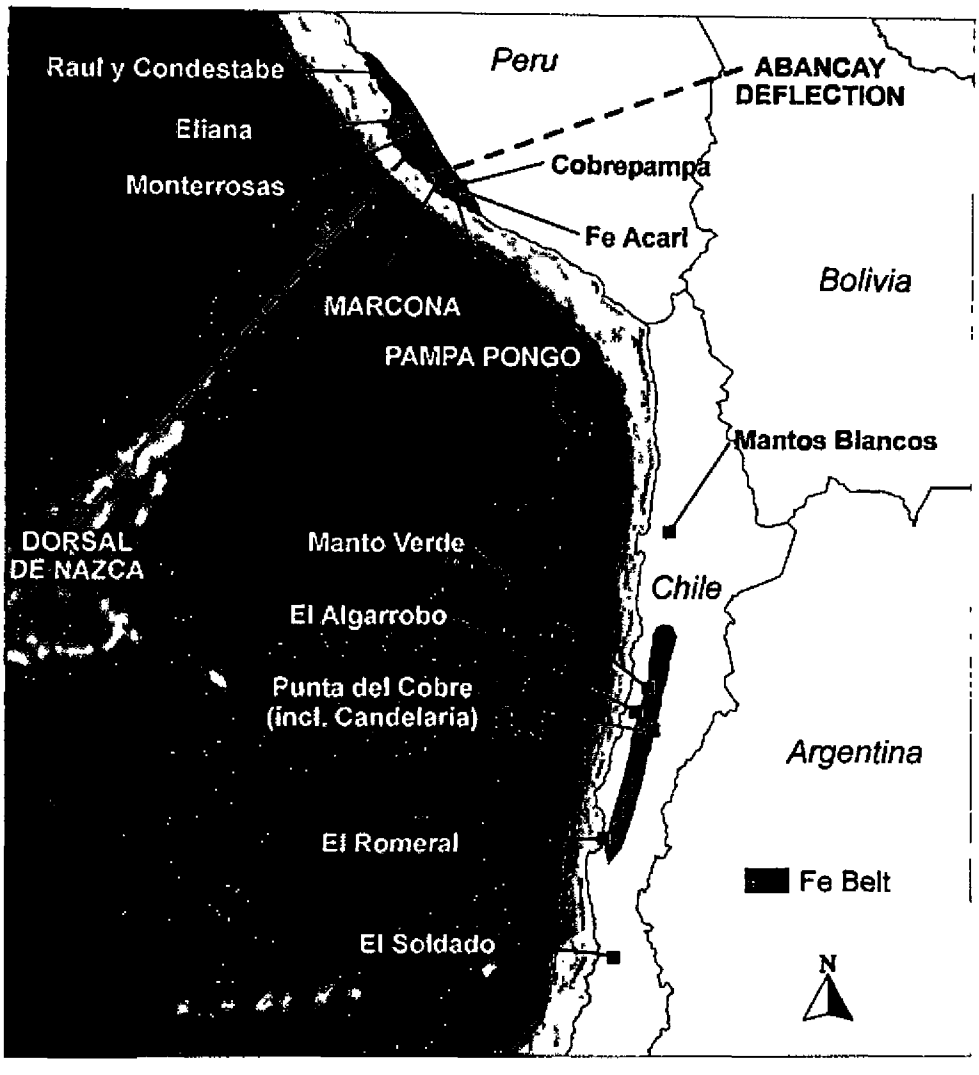


Figure 1: Map of South America showing the location of major FeOx-Cu-Au deposits.

Total resources at the Marcona mine include approximately 1440 Mt @ 54.1% Fe and 0.11% Cu, dispersed in eight major and at least 47 minor orebodies. Preliminary drilling at Pampa de Pongo infers a resource of more than 1000 Mt @ 75% magnetite. Each of these centres incorporates more ore-grade magnetite than the entire Chilean Cretaceous iron belt, and together they represent the most important metallogenic episode of Mesozoic age in the Central Andes. Although Cu has been only modestly produced at Marcona and economic grade Cu and Au has not yet been identified at Pampa de Pongo, these deposits clearly correspond in all salient aspects to the iron oxide-rich copper-gold-polymetallic clan. Megascopic and microscopic petrographic relationships at Marcona and Pampa de Pongo indicate many points of comparison with the Chilean deposits, particularly Candelaria (Ryan, *et al.*, 1995; Ullrich & Clark, 1997; 1999; Ullrich, *et al.*, 2001).

The Marcona deposit has been widely described since its original development, having been the subject of a dedicated PhD thesis (Atchley, 1956) and included in comprehensive overviews of the "Cu-Fe-amphibole [skarn] deposits" of the coastal area of central Peru (Injoque, 1985; Atkin, *et al.*, 1985; Vidal, *et al.*, 1990). However, there is little detailed information on *mesoscopic* textural relationships. Hence, key aspects of ore genesis remain obscure. Information on the early history of mining and exploration at Marcona is summarised from Adrian (1858) and Bourret and Hayes (1957). Pampa de Pongo has not been previously described.

Geological Setting

A belt approximately 70 km wide and stretching 400 km along the Peruvian coast from Lima to south of Chala (*ca.* 16° S) hosts numerous mineral occurrences grouped together under the general heading of iron oxide-copper-gold deposits (*eg*, Clark, *et al.*, 1990; Figure 1). The belt consists locally of a series of Precambrian gneisses and schists overlain by subordinate Palaeozoic sediments and volcanics and by more extensive volcano-sedimentary rocks of Triassic-Jurassic age. Numerous dykes and stocks ranging from acidic to basic composition intrude the belt. Tertiary ignimbrites and Quaternary aeolian deposits cover a large part of the area. The geological relationships at Marcona (Figure 2) have been well documented by, *inter alios*, Atchley (1956), Caldas (1978) and Injoque (1985), and the regional setting is clearly described by Shackleton, *et al.* (1979) and Pitcher, *et al.* (1985).

The Marcona Fe-Cu District lies athwart the intersection of the aseismic, NE-trending Nazca Ridge (*Dorsal de*

Nazca) and the continental margin, delimiting the southern limit of the major Peruvian flat-slab domain and the northern limit of the Central Volcanic Zone. It also lies in the region of the Abancay Deflection. The latter forms a continental-scale NE-SW sinistral shear zone centred in the *Cordillera Oriental.*

Stratigraphy in the Marcona Fe-Cu District includes a Mesoproterozoic (Wasteneys, *et al.*, 1995) basement gneiss complex, overlain by Paleozoic dolomites, limestones and sediments and a thick sequence of Jurassic volcanics and sediments. Caldas (1978) subdivides the Palaeozoic sequence into the San Juan Formation and Marcona Formation, with the upper distinguished from the lower unit by the presence of a quartzite layer and thin chert laminations within the carbonates. The Jurassic sequence has also been subdivided by Caldas (1978) into the Río Grande, Jahuay and Yauca Formations. The Río Grande Formation and overlying Jahuay Formation include mostly andesitic volcanics, sediments and limestones. The Yauca Formation includes mostly fine-grained sediments and lesser sandstone. The iron bodies at Marcona are sufficiently extensive to be distinguished as a distinct unit (*"fierro"*) on the 1:100 000 scale geological map of the San Juan quadrangle (Caldas, 1978). Figure 3 is a summarised stratigraphic column illustrating both the older classification of Atchley (1956) which is still used by the mine geologists at Marcona, and the more comprehensive work of Caldas (1978) together with published dates for mineralisation and host formations from Vidal, *et al.* (1990) and Wasteneys *et al.* (1995).

A wide-range of intrusive rocks are recognised in the Marcona area. The San Nicolás Batholith intrudes the basement metamorphic complex and the Palaeozoic sediments, but predates the Jurassic sequence. Compositional variations within the batholith include monzogranite in the centre passing outwards to granodiorite and gabbro-diorite. U-Pb zircon ages for the batholith include 390±23-46 Ma and, more reliably, 425±4 Ma (Mukasa and Henry, 1990). It is inferred that upper greenschist-amphibolite facies metamorphism in the basement rocks predates intrusion of the San Nicolás Batholith (*eg.* Atchley, 1956). Units of the more extensive Coastal Batholith occur east of Pampa de Pongo but are not found in the Marcona mine area. Several intra- and post-mineral hypabyssal intrusives and dykes occur in close proximity to the iron mineralisation. Andesitic "ocöite" dykes cut the iron mineralisation in the Marcona mine area while rocks of similar composition are also present at Pampa de Pongo.

Marcona

Location and General Geology

The Marcona iron deposits are centred at Latitude 15°12'30"S, Longitude 75°7'30"W. Small-scale copper mining probably commenced in the district during the late 19th century and continued episodically up to the mid-1980s. Discovery of the Marcona iron deposits was announced in 1915 and mining has been in progress since 1953. In the mine area, the iron deposits are mainly hosted by the Marcona Formation, but also occur in the Río Grande Formation and locally cut the basement. The San Nicolás Batholith crops out to the east of the mines and shows only restricted alteration, suggesting it played no significant role in the genesis of the Marcona iron deposits.

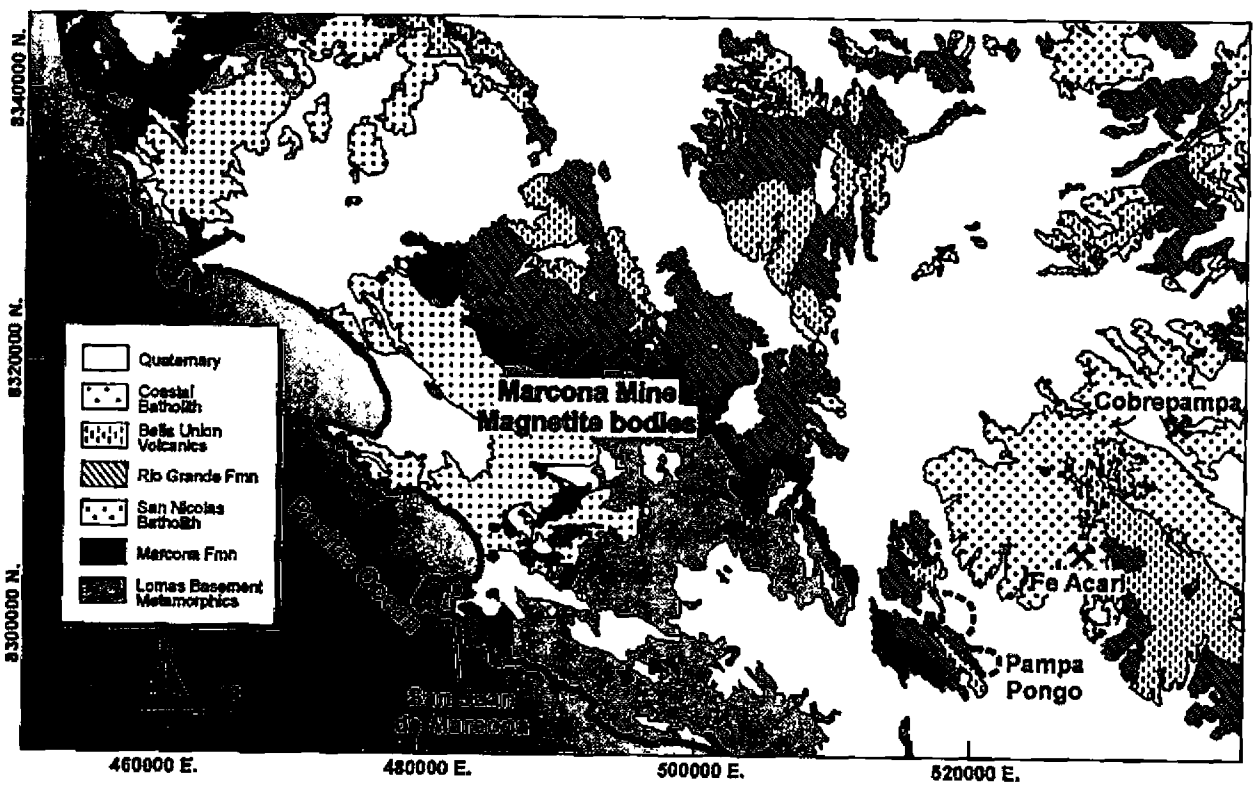
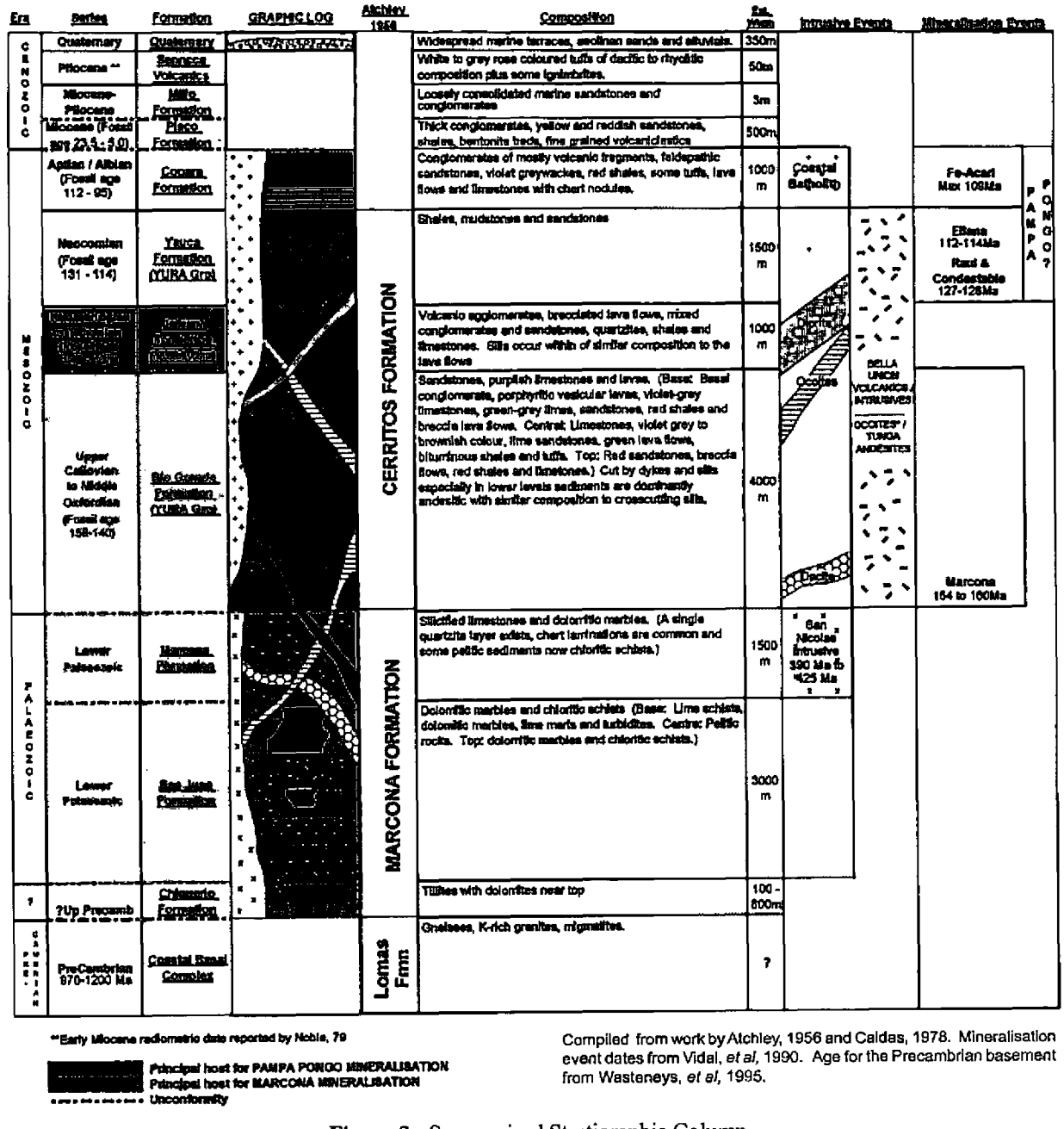


Figure 2: Marcona District Geology

In the mine area, the Marcona Formation is dominated by calcareous rocks, pelites and minor quartzites.

The overlying Río Grande Formation is dominated by porphyritic basaltic-andesitic and andesitic volcanics/sills, volcaniclastics and restricted intercalated shallow-marine limestones containing Toarcian to Oxfordian fauna (*ie.*, *ca.* 143-156 Ma, Caldas, 1978). Dacite and "granodiorite" dykes are observed to exhibit a close relationship to mineralisation. The significance of these dykes has not been studied.

Injoque (1985) and others describe the majority of the volcanic rocks in the Marcona area as shoshonites or latitic andesites, on the basis of K_2O contents of 2.79-3.76 wt.% at SiO_2 contents of *ca.* 52-53 wt.% SiO_2 (*cf.* Peccerillo and Taylor, 1976). However, there is no petrographic evidence for primary magmatic K-enrichment and even the least altered flows and dykes exhibit strong sericitisation of plagioclase phenocrysts. In a study of burial metamorphism in the Río Grande volcanic succession, Aguirre and Ottley (1985) document such sericite as a component of prehnite-pumpellyite assemblages, but its abundance strongly implies a hydrothermal origin (A.H.C., unpubl.). Hence, on the basis of petrographic observations and alteration characteristics, the volcanics are more-correctly termed high-K calc-alkaline augite andesites. The numerous volcanic and hypabyssal units in the Río Grande Formation near Marcona are frequently characterised by closely spaced, large (# 1.5 cm diameter), glomerophyric aggregates of plagioclase phenocrysts recording multiple magmatic dissolution/overgrowth events, but do not appear to be otherwise unusual. The Chilean term "ocöite" is used locally to describe the dykes due to their characteristic porphyritic appearance in hand specimen. A low-grade metamorphic overprint assemblage is also recognised in the volcanics comprising albite-actinolite-chlorite-titanite ± epidote/clinozoisite (Reynolds, 2002).



Compiled from work by Atchley, 1956 and Caldas, 1978. Mineralisation event dates from Vidal, *et al*, 1990. Age for the Precambrian basement from Wasteneys, *et al*, 1995.

Figure 3: Summarised Stratigraphic Column

The Marcona deposits have received only scant attention from the standpoint of modern geochemical techniques. Thus, only two sulphur isotopic analyses are reported by Injoque (1985): values of -1.76 ‰ and +4.72 ‰ for pyrite are in permissive agreement with a magmatic-hydrothermal origin, but no explanation is given for the compositional difference. Vidal, *et al.* (1990) provide a single Pb isotopic analysis for pyrite. The data, *viz.* $^{206}Pb/^{204}Pb$ = 18.208, $^{207}Pb/^{204}Pb$ = 15.567 and $^{208}Pb/^{204}Pb$ = 38.381 fall in the range for the wider Arequipa segment of the Mesozoic Coastal Batholith. The very low $^{206}Pb/^{204}Pb$ ratio reveals extensive "contamination" by the U-depleted Mesoproterozoic granulitic basement, presumably through assimilation-fractional crystallisation processes. The other comparable deposits analysed by Vidal, *et al.*, Raúl, Eliana, Monterrosas and Leonila, are not demonstrably underlain by the Arequipa Massif, and exhibit more radiogenic $^{206}Pb/^{204}Pb$ and $^{207}Pb/^{204}Pb$ ratios.

Structure

Three principal structural systems are recognised in the mine area (Atchley, 1956). The Pista Faults, probably the oldest, strike 295° and dip at 60° to the north. These normal faults were active before and after mineralisation. The Repiticion fault system comprises a series of reverse faults paralleling stratigraphy and with a strike direction of 045° and a 65° northerly dip. Finally the major Huaca fault system which parallels the Cordillera also comprises normal faults with a strike of 335° and dip of 60° to the east. The late stage ocöite dykes are generally aligned parallel to this trend. The Huaca faults have probably been sites of repeated reactivation since at least the early Mesozoic and have a strong influence on present-day topography which would have formed during Miocene to Pliocene uplift and erosion.

Ore Deposit Geology

The gross form and setting of the numerous magnetite orebodies have been well described by Atchley (1956) and subsequent workers. Although iron and copper mineralisation occurs in both the Marcona Formation and in the stratigraphically overlying Río Grande Formation, the iron bodies in the former tend to be larger and higher grade. The main iron bodies are massive, lensoid to tabular

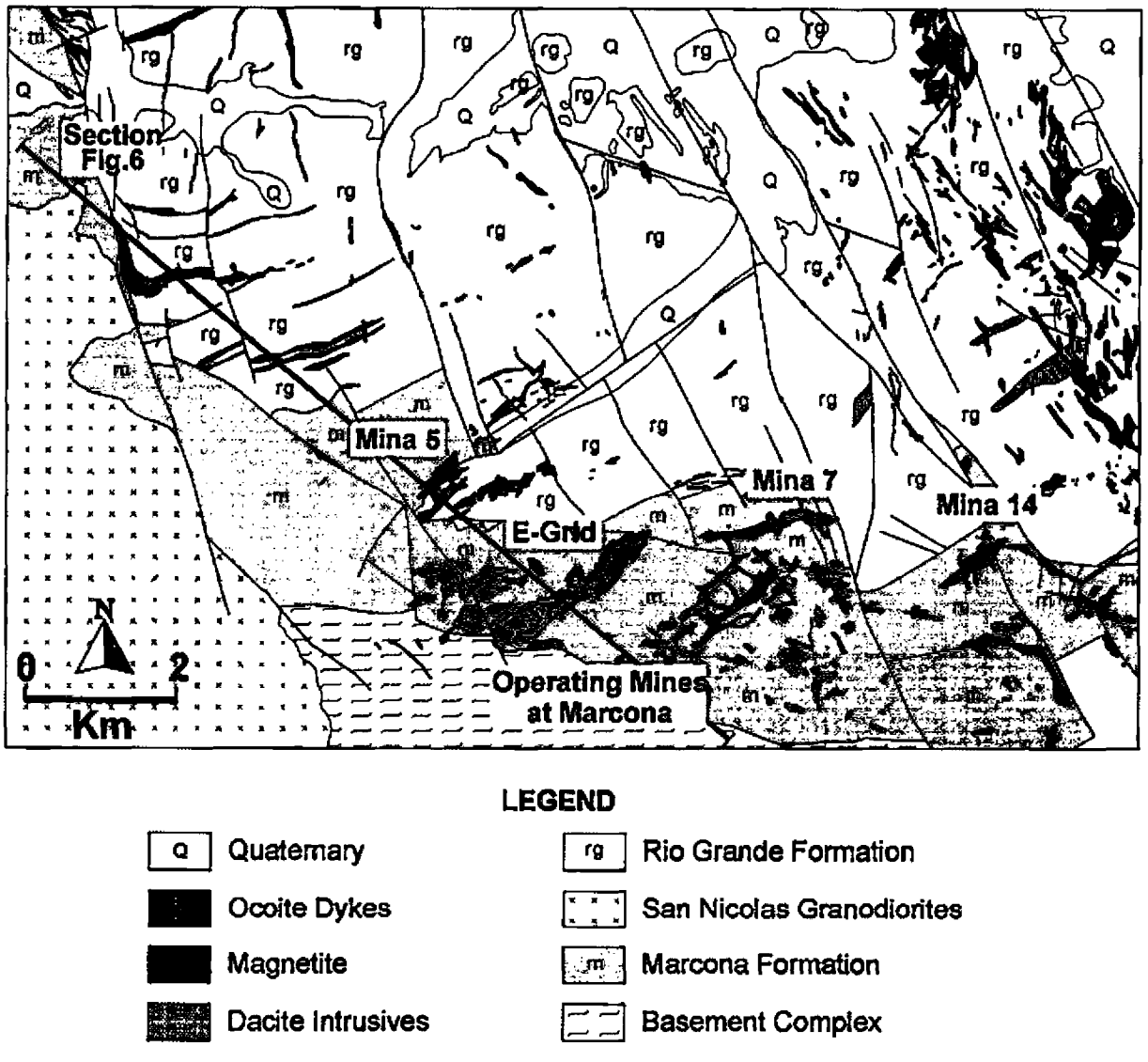


Figure 4: Marcona Mine area geology, adapted from Shougang Heirro Peru.

and broadly concordant with the stratification. These occur as crudely *en echelon* arrays of thick, NE-elongated bodies which dip at *ca.* 35°-65°NW, sub-parallel to lithological contacts, and are concentrated in two horizons, termed "E-grid" and 600 m lower stratigraphically, "Mina 7" (Figures 5 & 6). Stockwork-style and disseminated iron mineralisation is also present. Magnetite and specular hematite iron mineralisation occurs in the Río Grande Formation and shows a similar geometry to that in the Marcona Formation. Both the more massive and stockwork iron mineralisation carry some copper.

Ore-waste contacts are irregular in detail and dyke-like bodies of magnetite widely crosscut all host-rock fabrics. Igneous intrusions, broadly coeval with magnetite emplacement, and including strictly intra-mineralisation bodies, comprise dyke swarms of dacitic "granodioritic" and andesitic composition.

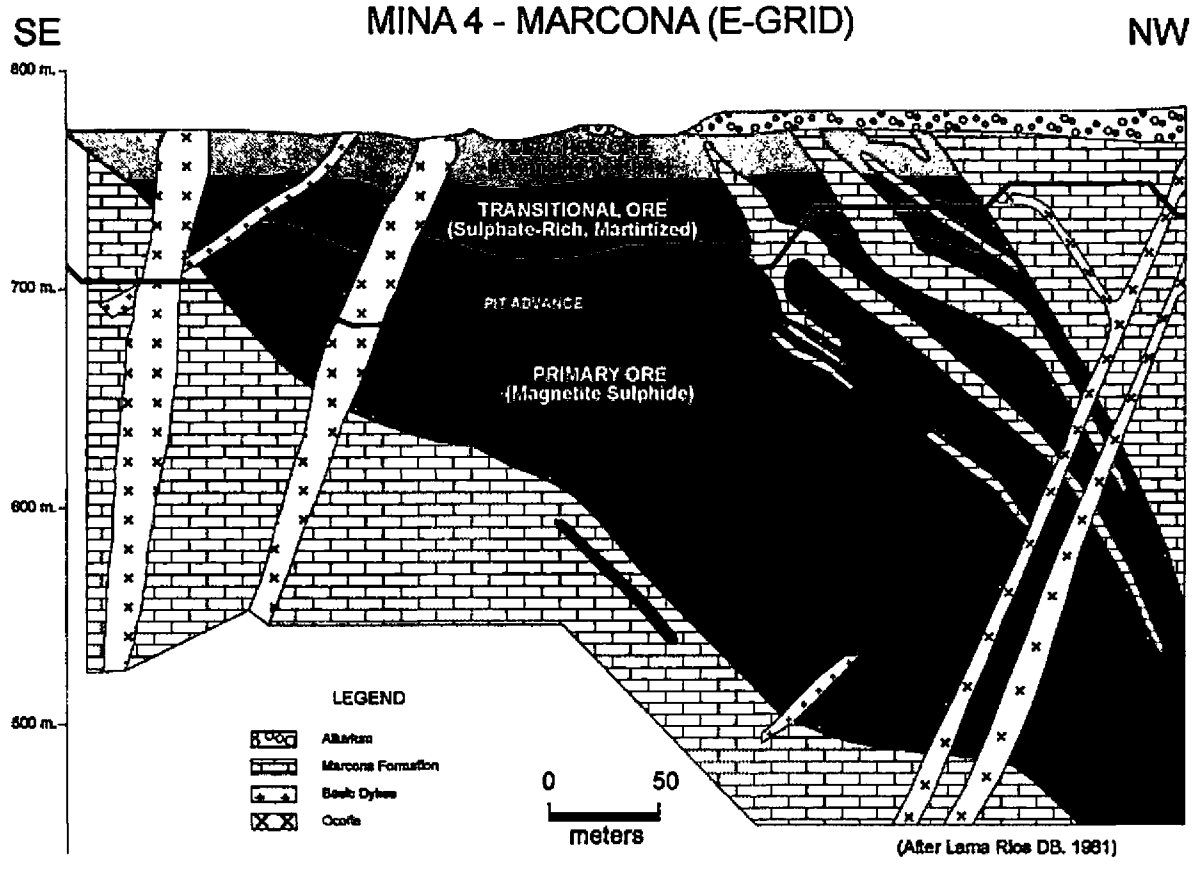


Figure 5: Marcona Section E-Grid (Mine 4) area.

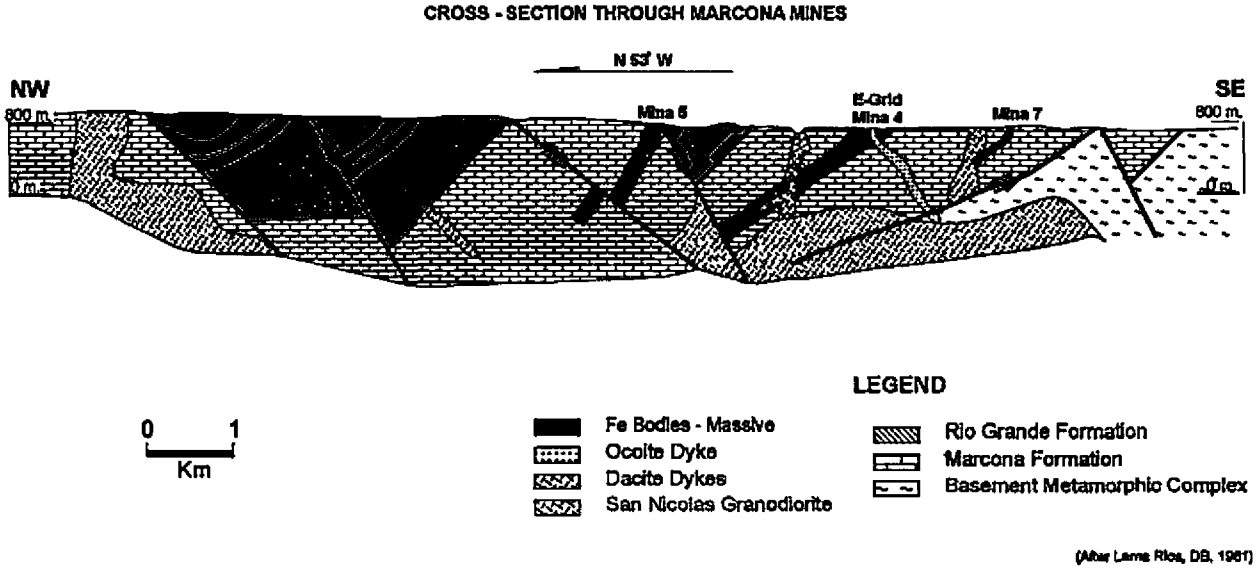


Figure 6: Marcona Section Regional Interpretation

Conventional K-Ar dates of 160±4 and 154 Ma from hydrothermal phlogopite and sericite (Injoque, *et al.*, 1988) would assign the mineralisation to the late stages of arc development. This is supported by the pre-, intra- and post-mineralisation context of swarms of andesitic dykes that probably constitute feeders for the younger Río Grande Formation flows. Vidal, *et al.* (1990) reported whole rock K-Ar dates of 118±3.0 to 137±3.0 Ma for three intermediate post-ore dykes: these ages are unremarkable, but whole-rock dates for such lithologies are notoriously unreliable.

Inferred orebody protoliths include both calcareous and quartzo-feldspathic clastic and pyroclastic horizons intercalated in the andesitic succession (Injoque, *et al.*, 1988). These authors also suggest that extensional fracture zones controlled both fluid circulation, and the emplacement of sill and dyke complexes. In such zones, it is implicit that permeable andesitic rocks have suffered intense Fe-metasomatism, a process more clearly shown by the Pampa de Pongo mineralisation. Moreover, it seems likely that the Fe orebodies hosted by the Palaeozoic and Jurassic strata represent a single, large-scale hydrothermal system.

Finely laminated fabrics are widely exhibited by magnetite- and/or sulphide-rich ores at Marcona and are interpreted as relict bedding (*eg.* Atchley, 1956; Injoque, 1986). Certainly, such textures are commonly observed on the margins of the Marcona orebodies and at Pampa de Pongo, and in such cases selective replacement of carbonate-rich laminae may reasonably be inferred. However, some cases of non-sedimentary fabrics are apparent, such as crudely cylindrical alternating layers of magnetite and/or sulphide and amphibole or chlorite. We interpret such textures as "wrigglitic" (*cf.* Kwak and Askin, 1981), reflecting the progress of a metasomatic front through a relatively homogeneous protolith. Such textures are widespread in true skarn deposits, but are not restricted to carbonate hosts.

A further important textural question concerns the role of *breccias*, which, to our knowledge, have not been recorded by previous workers. Preliminary field studies of the largest mineralised zone, comprising Minas 2, 3 and 4 in the Marcona Formation, as well as examination of drill-core from Mina 11 and Mancha 13, indicate that hydrothermal breccias dominate large proportions of the high-grade (>50% Fe) mineralisation. The breccias exhibit matrices with varying proportions of magnetite, amphibole, phlogopite-biotite-chlorite and sulphides. Two or more superimposed brecciation events are evident in some of the pits and segments of drill core. The breccias range from "jigsaw" fabrics, in which little relative displacement of clasts has occurred, through angular, matrix-supported to "amoeboid" or "ductile" fabrics. A similar spectrum of breccia-types occurs at the Candelaria Cu-Au deposit, Chile (Ullrich and Clark, 1996, 1997). In some outcrops, the clasts exhibit strong variations in lithology or, more typically, alteration type and intensity, and in such cases significant transport of clasts may be inferred.

Our observations, although not comprehensive, suggest that intense hydrothermal fragmentation played a major role in ore formation. Injoque (1985) favoured a more passive replacement process. It should be emphasised that the breccias, well exposed in for example, Minas 2 and 3, are strictly *intra-mineralisation*, and thus reveal the conditions of emplacement of magnetite and sulphides (mostly pyrite and/or chalcopyrite), rather than recording merely post-ore disturbance. The irregular hanging-wall contact of orebody 3 clearly shows apophyses of magnetite+sulphide-cemented breccia that are re-brecciated and cemented by magnetite-amphibole assemblages.

Weathering and supergene leaching has resulted in a vertical zonation through the iron ore bodies. The upper parts are characterised by massive hematite with actinolite together with minor malachite, atacamite, brochantite and chrysocolla grading down through a transitional zone containing hematite, jarosite and gypsum that overlies the primary zone dominated by magnetite-actinolite-pyrite±chalcopyrite. The main period of weathering related oxidation occurred prior to deposition of the uppermost Pliocene to Pleistocene shallow marine sediments (*eg.* Atchley, *op cit.*; Ortlieb and Macharé, 1990).

Alteration-Mineralisation Relationships

There are few detailed descriptions of the paragenetic relationships of the Marcona orebodies and systematic studies have not been carried out. Previous studies have tended to oversimplify the sequence of events, conforming to traditional skarn models in which "prograde" (anhydrous) silicate minerals precede "retrograde" (hydrous) and magnetite precedes sulphides (*eg.* Injoque, 1985). Preliminary logging of core from Mina 11, Mancha 13 and bench faces in Minas 2, 3 and 4, all in sulphide-rich ore facies, indicate that no such simple transitions occurred. Observations on alteration relationships described here are mostly anecdotal, but the increasing development of several minerals in the vicinity of mineralisation is a guide to the major processes. The main iron minerals are magnetite and haematite. Sulphides include pyrite, pyrrhotite, chalcopyrite, lesser bornite, chalcocite, sphalerite, galena and minor carrollite. Molybdenite, pentlandite, mackinawite and gold have also been reported (*eg.* Injoque, 1988). The paragenesis of the principal iron oxide and sulphide minerals is summarised in Table 1 based on the authors' observations and preliminary studies of areas immediately adjacent to the Marcona Mines.

District-scale Alteration

A salient characteristic of the clan of ore deposits under discussion is the development of quasi-pervasive district to regional-scale alteration, far more extensive than for example propylitisation surrounding porphyry Cu centres. Because the alteration minerals, such as albitic plagioclase and calcic amphiboles, are commonly developed in low-grade regional metamorphism, distinction between metamorphism and hydrothermal alteration may be difficult. The nature, extent and age of strictly metamorphic effects in the Marcona Formation remain uncertain, although the lack of convincingly metamorphic foliation favours thermal rather than regional processes. Injoque

Table 1: Marcona Deposit - Summary paragenesis of Fe oxide minerals and principal sulphides.

	HYPOGENE							SUPERGENE
	Magnetite, Ca-amphibole, albite	Magnetite-sulphide-Ca-amphibole	Brecciation + sulphide, magnetite, Ca-amphibole	Magnetite-sulphide-Ca-amphibole+ Kspar/albite	Sulphide veins	Sulphide + anhydrite veins	Anhydrite	
MAGNETITE	■	■	■	■				
PYRRHOTITE		■	■	■				
SPECULAR HEMATITE		■	■	----				
"MARTITE"		■	■	----	----	----	----	----
PYRITE		----	■	■	■	----		
CHALCOPYRITE		----	----	■	■	----		
BORNITE				■	■	----	----	
CHALCOCITE				----	■	■	----	----
"MUSHKETOVITE"				■	----	----	----	----
JAROSITE								■
GOETHITE								■
ANHYDRITE						■	■	
Cu OXIDES								■

Other major mineral species: Ca-amphibole, clinopyroxene, sericite, chlorite, titanite, k-feldspar, quartz, calcite, apatite, albite, garnet, biotite.
Other minor mineral species: Galena, sphalerite, ilmenite, carrollite; plus additional minerals reported by Injoque, 2001: molybdenite, pentlandite, cubanite, mackinawite, valleriite, tourmaline, marcasite, sepentinite, zeolite, talc, scapolite, electrum(Au).

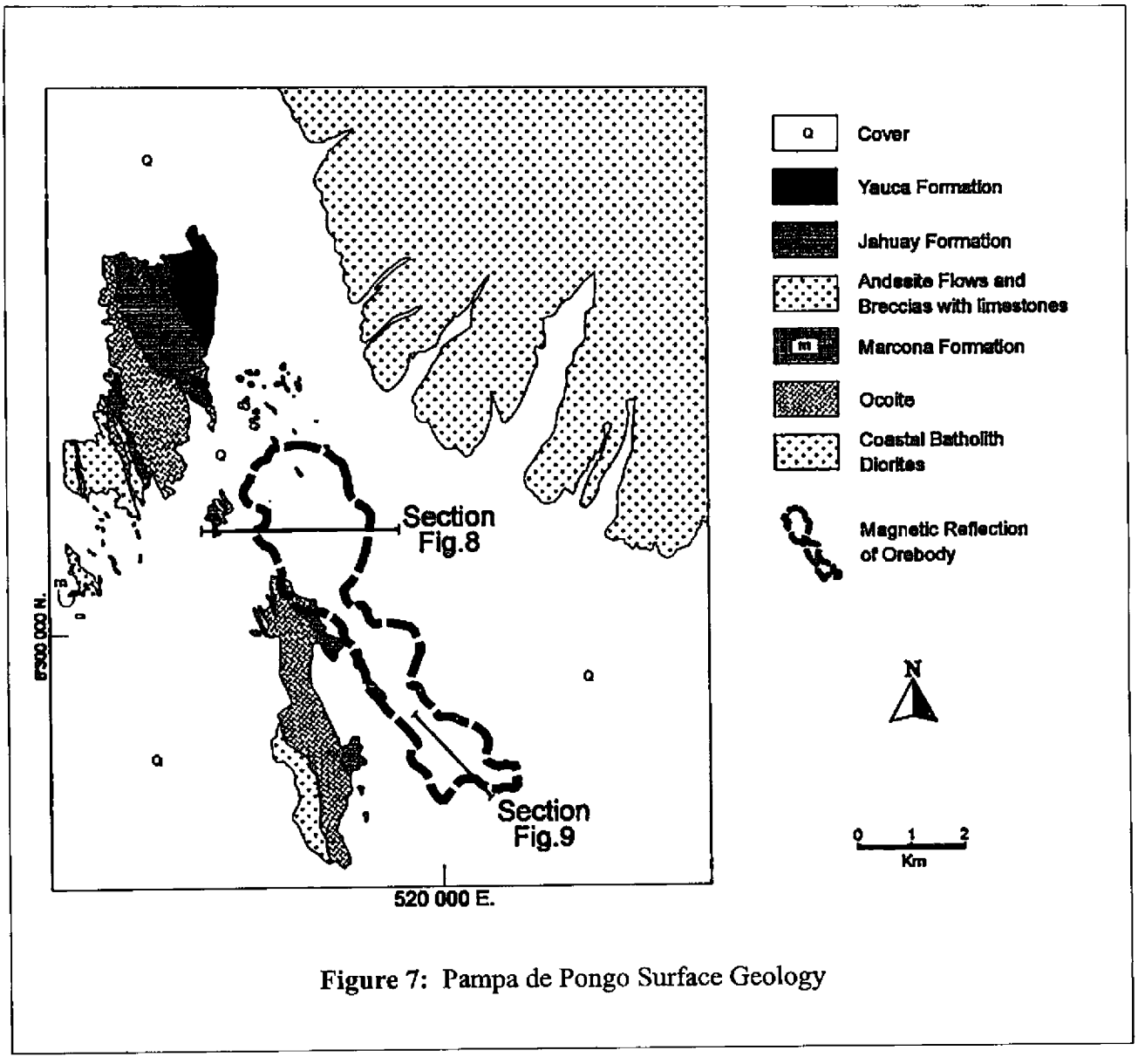


Figure 7: Pampa de Pongo Surface Geology

(1985) records the occurrence of cordierite, and we tentatively ascribe this to the intrusion of the San Nicolás Batholith.

The areal extent of the district-scale alteration assemblages is poorly documented. Chlorite and sericite are widespread in andesites of the Río Grande Formation north of the iron mines. Late epidote and calcite commonly occur as patches or veinlets in many outcrops. Different timings for the district-scale alteration assemblage is suggestive of multiple events.

Pervasive Albitisation

Pervasive albitisation ($An_{<2}$) widely replaces plagioclase phenocrysts in the Río Grande Formation, yielding a pink to cream cast in outcrop, and, closer to magnetite bodies, develops in the rock matrix. Complete albitisation of the andesitic host-rocks, as occurred in the Candelaria deposit, Chile (Ullrich and Clark, 1997) was not attained in the Marcona district despite the greater overall scale of hydrothermal activity. Albite is also developed in ocöitic andesite dykes cutting the magnetite bodies (*eg.*, the south contact of the Mina 1 orebody). Here, pink albitic selvages form on the margin of actinolite-chalcopyrite-pyrite veinlets and provide evidence for a resumption of Na metasomatism late in the hydrothermal history.

Potassic Alteration

Post-albite, low temperature red-pink potassic alteration is recognised within the volcanics of the Río Grande Formation associated with fracturing and brecciation together with late stage hematite and sulphides.

Main Iron Oxide Stages

Up to four episodes of magnetite+Ca-amphibole mineralisation are recognised, each forming the matrix of hydrothermal breccias. Of these sub-stages, only the first was apparently sulphide-free. The earliest sulphide assemblage is pyrrhotite-dominant with minor chalcopyrite, pyrite and cubanite. Thereafter, chalcopyrite and pyrite and eventually chalcopyrite are increasingly abundant. Successive overgrowth and replacement of chalcopyrite by bornite and chalcocite has also been recognised in the area. Concentrations of chalcopyrite are associated with pink albite and buff orthoclase as well as with amphibole (locally hornblende rather than tremolite-actinolite). As in many FeOx-Cu-Au deposits, *eg.*, Candelaria, magnetite and specular hematite exhibit mutual, probably multistage pseudomorphous replacement ("martite" and "mushketovite"), demonstrating that the hydrothermal fluids remained close to the magnetite/hematite phase boundary in aO_2 *vs.* aS_2 space. Specularite has at least locally been an important phase in the early to intermediate stages of iron oxide mineralisation. Specularite occurs most commonly as an open-space filling, associated with episodic fracturing during ore formation.

Late Stage Sulphide + Anhydrite

The polyphase hydrothermal brecciation that dominates the Marcona paragenesis was followed successively by magnetite-actinolite±chalcopyrite veins with pink K-feldspar selvages, minor, local, chalcopyrite-pyrite, chalcopyrite-anhydrite and mauve anhydrite vein types. The latest phases of hydrothermal activity at Marcona overlapped the emplacement of ocöitic dykes which, although locally sericitised, chloritised and epidotised contain negligible magnetite or sulphides.

These associations are very similar to those at Candelaria (*eg.*, Ullrich and Clark, 1999), with the exception of biotite, which is pre-magnetite when present at Marcona. In contrast, K-feldspar antedates the highest-grade Cu sulphide associations at least locally in the area.

Pampa de Pongo

Location and General Geology

The Pampa de Pongo Fe (±Cu-Au) deposit is centred at Latitude 15°22'30"S, Longitude 74°49'30"W and was discovered by Rio Tinto Mining and Exploration in 1995 while testing a large NNW-SSE trending magnetic anomaly for Fe-Cu-Au mineralisation. Wide-spaced drilling suggests a potential resource of 1000 Mt comprising approximately 75% magnetite (approx. 40% Fe). Hole 1 cut 168.7 m of magnetite grading 52.9% Fe with anomalous Cu and Au.

The Oxfordian-to-Tithonian (Jurassic) Jahuay Formation (Caldas, 1978) hosts the Pampa de Pongo deposit. Lithologies observed in drill-core include thick sequences of coarse volcaniclastics, and conglomerates, banded siltstones, shales, sandstones and carbonate-rich sediments. Clastic and carbonate sediments with plagioclase-phyric andesites are exposed to the northwest and southeast of the mineralised zone, the latter considered to represent both sills and dykes. Drill holes suggest the upper 400-450 m are mostly andesitic dyke/sills, bedded flows and tuffaceous units. These are underlain by more than 600 m of white, predominantly dolomitic marbles, which, outside of the mineralised zone exhibit sparse tremolite porphyroblasts and networks of talc veinlets. To the authors' knowledge, no direct evidence exists for the age of these units. Several holes also cut basement gneiss, implying that a steep angular unconformity cuts out the entire Marcona Formation and possibly the Río Grande Formation.

The dioritic Acari pluton is exposed 800 m to the east of the prospect. This intrusion is considered part of the Arequipa segment (Caldas, 1978) of the Coastal Batholith and, therefore is assigned ages of 96 and 80 Ma by Cobbing (1977, 1998). To our knowledge, the Acari and the more easterly Cobre Pampa plutons have not been dated. However, these dioritic to granodioritic bodies intrude (Caldas, 1978) strata assigned to the Neocomian-Aptian Copara Formation and the Bella Union hypabyssal complex. These intrusive relationships and the 109±4 Ma whole-rock date for a pre-ore dacitic dyke at Hierro Acari (Vidal, *et al,* 1990) strongly suggest the Acari pluton post-dates hydrothermal activity at Marcona. Despite the faulted contact with the Acari porphyry, proximity of this intrusion to the Pampa de Pongo deposit may also imply a Cretaceous age for the mineralisation.

Structure

Bedding across the property dips consistently at 15 to 20° and tectonic breccias are recognised in several sections of drill-core. The magnetite has been emplaced along a steep NW-trending fault corridor. This structural zone parallels the Huaca fault system at Marcona and the main ocöite dyke orientation. There are sharp cutoffs to the iron body to the east and west. Copper shows higher grades in the hanging wall and SW footwall (up to 0.42% Cu) and 0.68 g/t Au). Copper and gold content is significantly lower in the majority of the iron mineralisation.

Alteration-Mineralisation Relationships

Preliminary documentation by Carbonell (1996) and Taylor (1996) established the salient features of the mineralisation. These authors emphasised the importance of widespread albitisation, serpentinisation and replacement of all rock-types, in particular dolomitic units, by magnetite. In cross-section a massive magnetite zone up to 1 km in width is haloed by stockwork iron mineralisation. The importance of both fractures and hydrothermal breccias as hosts for magnetite (-pyrrhotite) mineralisation is consistent with the present authors' observations. Taylor (1996) interpreted

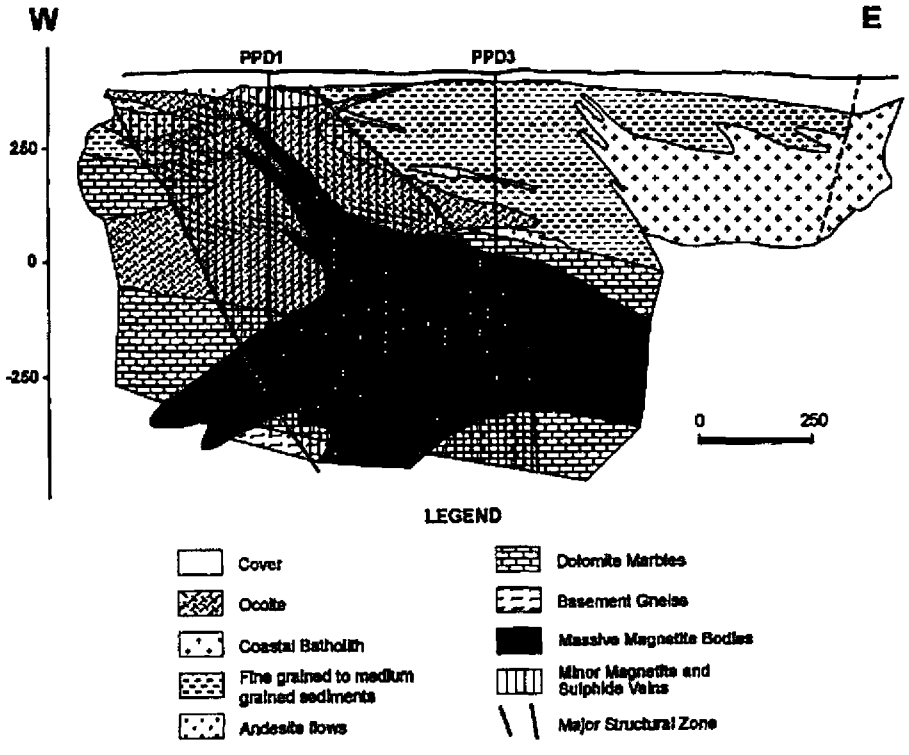


Figure 8: Pampa de Pongo E-W Cross Section (Adapted from drawings by J. Carbonell).

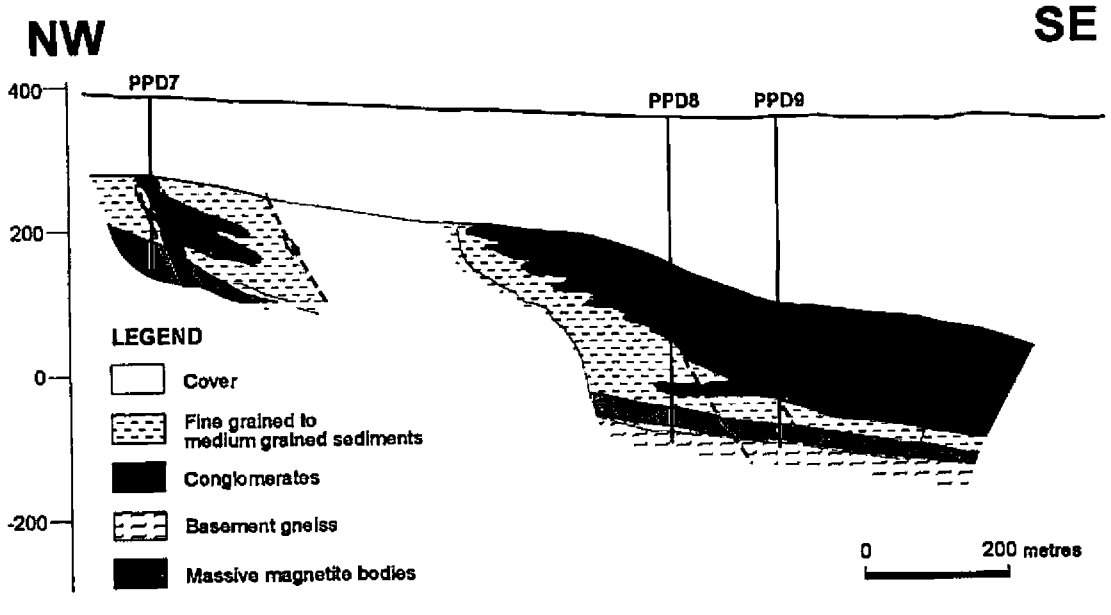


Figure 9: Pampa de Pongo SE-NW Cross Section (Adapted from drawings by J. Carbonell).

the range of fabrics as the product of a spectrum of brecciation conditions, ranging from "crackle" through "mosaic" to "hydraulic" with increasing intensity related to increasing micro-fracture-controlled Fe metasomatism of host-rocks.

Present observations focus on the ore-types and alteration facies developed in the largely ocöitic/andesitic rocks intersected in the upper 400 m of diamond drill-holes PPD-001 (centre-west) and PPD-002 (northeast), *ie.*, in the hanging-wall of the major concentration of magnetite. These drill-holes exhibit striking textural relationships that reveal the processes involved in the emplacement of this exceptionally large magnetite body. Over this interval ore is hosted entirely by andesitic rocks, the majority of which are crowded plagioclase porphyries with complex phenocrysts of ocöite type, and with augite as the dominant magmatic ferromagnesian mineral. The andesites have been extensively altered, although replacement of igneous minerals is rarely complete, even within 10 cm of magnetite bodies. Almost all the observed iron mineralisation occurs as veins, commonly sinuous, and as cements to hydrothermal breccias.

The alteration-mineralisation relationships at Pampa de Pongo are described briefly in sequence from host-rock to magnetite bodies, based on hand-specimen study, and limited petrographic, X-ray powder diffraction, cathode luminescence and electron microprobe investigation.

Peripheral Alteration

Although sericitisation of plagioclase appears to represent an outer alteration facies, the initial process unambiguously related to mineralisation is the development of white rims of albite ($An_{<1}$) on plagioclase phenocrysts. With increasing alteration the rims expand into the phenocrysts and fine-grained, buff, decussate grains of albite form in the matrix, together with local 0.5-1.5 cm rounded patches of epidote + actinolite. These associations are similar to "sodic-calcic" alteration resulting from prograding incursion of non-magmatic fluids in, for example the Yerington district, Nevada porphyry Cu deposits (Dilles and Einaudi, 1992) but here record *Na Metasomatism*. Albite development increases in relatively restricted zones accompanying progressive destruction of igneous plagioclase. The phenocrysts lose definition and the rock is converted to a blotchy association of white and buff albite and ultimately to an extremely fine-grained, porcelaneous "albitite". Although some albite development occurs as envelopes to individual magnetite bodies, Na metasomatism appears to have been a more widespread "precursor" event controlled by sheeted- structures in the andesites with the appearance of a spaced cleavage, as at Marcona.

"Skarn" Development

Several intersections in drill-hole 001 exhibit coarse-to-fine grained assemblages of andraditic garnet ($Grossular_{4-7}$ $Andradite_{93-96}$) intergrown with diopsidic clinopyroxene ($Hed_{<9}$). Such associations would normally be interpreted as evidence for high-temperature "skarnification" of carbonate units. However, some intervals (*eg.* 115-118 m) show relict albitised plagioclase phenocrysts. The calc-silicate alteration assemblages indicate *Ca metasomatism* of igneous protoliths and could be considered as endoskarn or, more appropriately, "anti-skarn". Similar relationships are widespread in the hanging wall of the main orebody at Candelaria (Ullrich and Clark, 1997, 1999), where "skarn" development is routinely, and erroneously, interpreted as evidence for the former presence of carbonate sediments (*eg.*, Marschik and Fontboté, 2002). The calc-silicate zones at Pampa de Pongo appear to represent a restricted Ca-metasomatism that post-dated the albitisation, as at Candelaria. However, the andradite-diopside rocks also incorporate large (# 3 cm), crudely-spheroidal white patches dominated by K-feldspar with orthoclase Si-Al ordering, providing strong evidence for *K-metasomatism*, presumably occurring at approximately the same time as the Ca-metasomatism.

Main Magnetite (-Pyrrhotite) Stage

In the upper part of the deposit, magnetite occurs both as exceptionally coarse (to 3 cm) euhedral (octahedral) and subhedral crystals and, probably less commonly, as extremely fine-grained massive grain-aggregates. The former constituted the first stage in the development of veins cutting altered andesite or in the cementation of hydrothermal breccias. The veins range from sinuous ("A-type" in appearance, but continuous for 10's of cms.) to planar. These may be regarded as the initial stage or peripheral facies of the breccias. Fine magnetite invades the andesite as networks of thin veins, coalescing as irregular patches that in part may be metasomatic. Coarse magnetite is almost everywhere intergrown with Fe sulphides. X-ray studies confirm the presence of both hexagonal and monoclinic pyrrhotite, pyrite and, locally, marcasite. Although pyrite occurs sparsely as coarse (1 cm) cubes and pyritohedra, as well as a fine-grained cement, the characteristic mode of occurrence of the Fe sulphides is as blades up to 15 cm, but averaging 5-7 cm in length and 1-3 mm in width. The coarse pyrrhotite plates, with long axes paralleling the {0001} planes, are extensively pseudomorphed by pyrite (Plate 2) and marcasite (*ie.* Fe loss). The porous pseudomorphs are commonly in-filled by white calcite and some laths are entirely of calcite. In numerous core-sections, pyrrhotite has been pseudomorphed by magnetite. Petrographic relations also reveal the replacement sequence pyrrhotite-pyrite-magnetite. It is implicit that, although these relationships record an overall transition from magnetite-pyrrhotite equilibrium to that of pyrite-calcite, fluctuations in $f\,S_2$ clearly took place. Only rarely do coarse intergrowths of chalcopyrite and calcite infill the lath-forms. Textures of this type occur in a wide range of ore deposits, but appear to be most characteristic of carbonate-replacement mineralisation of Leadville-type (*eg.*, the "eutectic texture" of Emmons, *et al.*, 1927; the "rod texture" of Thompson and Arehart, 1990), although growth in pre-existing open-space or an abruptly dilating environment is probably a prerequisite.

Minor minerals associated with the magnetite-pyrrhotite assemblage include mackinawite with 0.5-0.7 wt.% Ni and

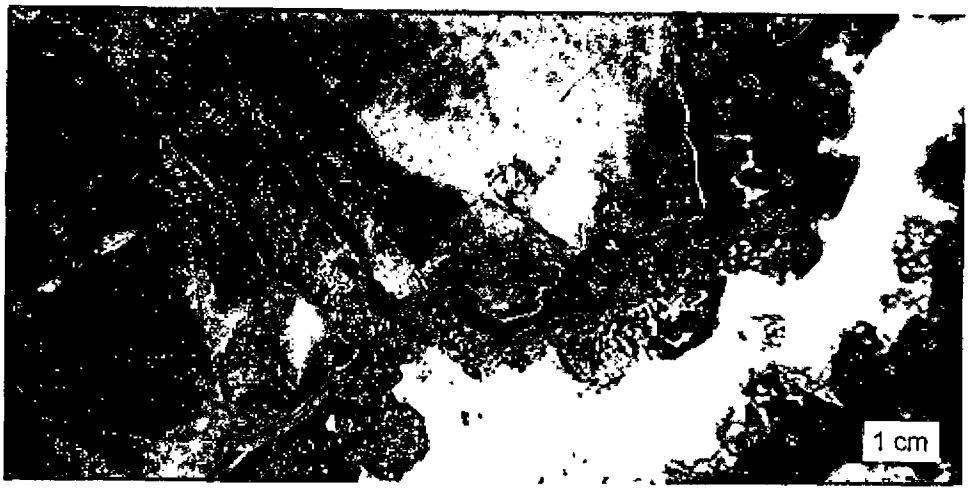


Plate 1: Strongly albitised and chloritised andestite (phenocryst outlines obliterated) with thin, black chlorite – talc selvages, cut by sinuous veins in which early magnetite has been almost entirely engulfed and overgrown by coarse white calcite. DDH 001 - 145.3 m.



Plate 2: Characteristic texture of main magnetite –Fe sulphide ore in the upper section of the Pampa de Pongo deposit. Coarse-grained massive magnetite is intergrown with plates, originally single crystals of pyrrhotite, now pseudomorphed by fine grained pyrite. DDH 001-81.9 m.

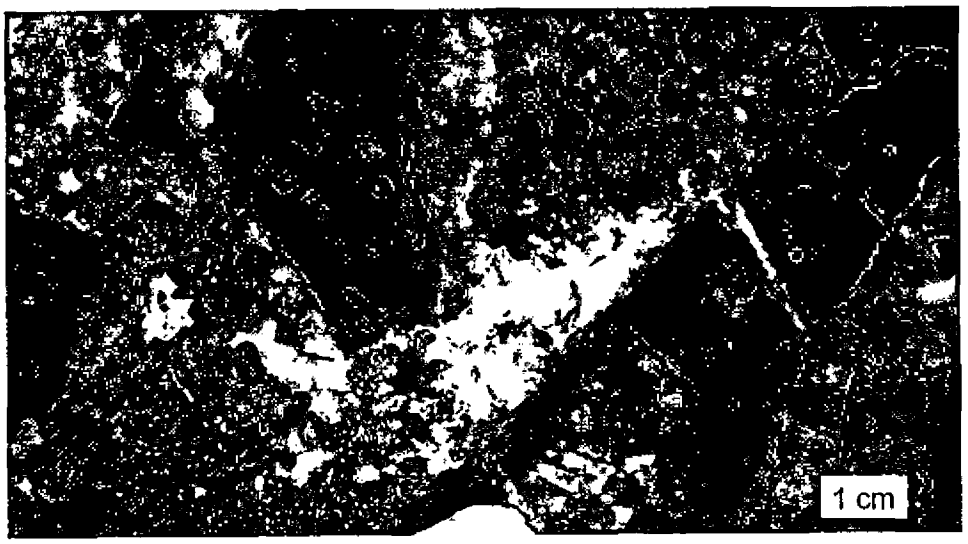


Plate 3: Hydrothermal breccia, with matrix of magnetite, coarse grained pyrite and calcite. Clasts are of moderately altered "ocoite". Plagioclase phenocryst outlines are well preserved in the pale-green cores of the clasts, but are extensively replaced by buff albite, and the andesitic groundmass is strongly chloritised. Black alteration selvages are dominated by biotite (inner) and chlorite (outer). DDH 001-86.9m.

0.1-0.2 wt.% Co in solid solution, Co-rich pentlandite and lollingite. Microprobe analysis reveals up to 0.15 wt.% Ni in the hexagonal pyrrhotite. The magnetite contains very minor Ti (< 0.1 wt. %) and V was not detected (*ie.*, < 0.05 wt.%).

Emplacement of these texturally-unusual magnetite-pyrrhotite veins and breccias was almost everywhere associated with the development of black to dark-green and locally dark-brown alteration selvages (Plates 1 and 3) comprising an extremely fine-grained association of various phyllosilicate minerals and minor magnetite. These average 8-10 mm in width and locally reach several cms. X-ray diffraction analysis shows these selvages include various proportions of biotite ($Annite_{82-90}$), Fe-rich chlorite (clinochlore), talc and clinochrysotile. Biotite is most widely associated with chlorite, talc with chlorite, and occasional biotite-clinochrysotile. The alteration envelopes exhibit abrupt interfaces with the variably albitised host-rocks and some display a fine layering paralleling the contact with the overgrowing magnetite. Textural relationships, and hence crystallisation sequence, are difficult to determine, but in two samples the biotite content increased outwards relative to chlorite, *ie.*, towards the andesite. On this basis, biotitisation, and hence K-, and possibly Fe metasomatism probably occurred prior to the development of chlorite and other K-free minerals. Moreover, because brown to buff clinochrysotile is locally concentrated at the contact between the alteration selvages and the later magnetite, and serpentine was locally precipitated as pale apple-green sheaves in cavities in the magnetite, the suggested overall order of phyllosilicate formation was biotite → chlorite → talc → serpentine. In the upper-part of the deposit the main deposition of magnetite took place during serpentine development. The inferred sequence of alteration events that coincided and overlapped with magnetite mineralisation in this part of the Pampa de Pongo deposit, although in broad conformity with retrograde processes in magnesian skarns, is entirely unlike that at Marcona. Thus, Ca-amphiboles have not been observed in association with the magnetite and/or sulphide minerals in the upper part of the deposit. Carbonell (1996 and pers. comm. 2002) observed minor tremolitic amphibole in association with Cu-rich sulphide mineralisation. These are reported as late stage and occurring on the margins of the deposit.

Sulphide-Calcite Stage

The commonly euhedral surfaces of the magnetite crystals are widely overgrown by coarse and vughy white carbonate (Plate 1). Taylor (1996) interpreted this as dolomite, but X-ray and acid testing suggests that calcite is much more abundant. Locally, the magnetite-calcite contact is "hazy", owing to the development of extremely fine-grained chlorite in both minerals. The calcite, representing the final stages of dilation of the ore-zones, is widely intergrown with subhedral to granular pyrite, showing no evidence of an origin through replacement of pyrrhotite, and minor chalcopyrite. However, as noted above, Taylor (1996) describes an Au-rich chalcopyrite-pyrrhotite zone, implying sulphidation conditions varied markedly at this stage. Single grains of sphalerite, galena, tennantite and arsenopyrite have also been observed or reported previously. Petrographic work shows pale-mauve anhydrite overgrows calcite in one sample. Valleriite has been confirmed as a coating on several late-stage fractures, intergrown with finely platy magnesite.

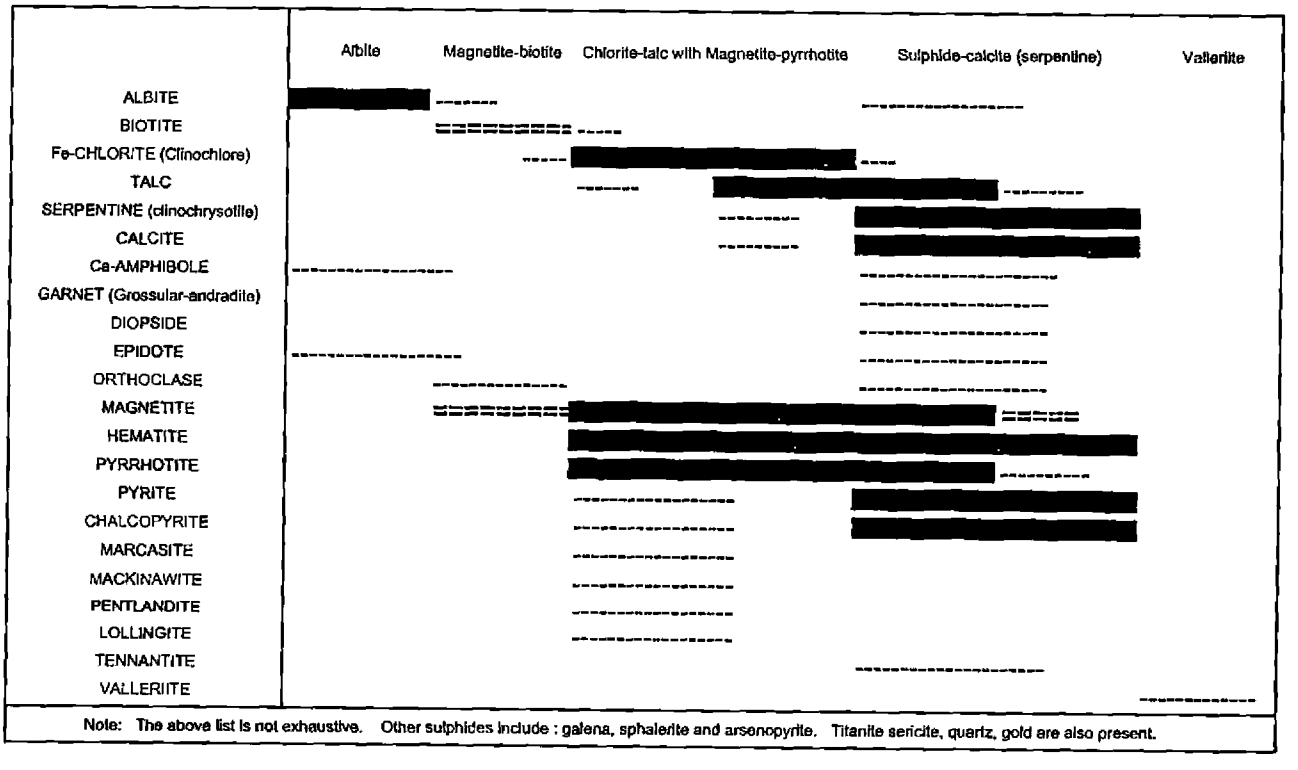


Table 2: Pampa de Pongo deposit - Summary mineral paragenesis of Fe oxide and principal sulphides

Discussion

Both the Marcona and Pampa de Pongo deposits share many characteristics of Iron Oxide-Copper-Gold deposits. These include abundance of iron oxide with anomalous and locally ore grade copper and gold, a generally low-sulphidation state, widespread precursor albitisation / Na metasomatism, and more erratic K-metasomatism and Ca-metasomatism. Despite the subordinate development of brittle stockwork, hydrothermal breccias are a major ore-host. Control by large scale, and probably multiply reactivated, fault systems is also a characteristic feature. Both Marcona and Pampa de Pongo incorporate carbonate replacement domains but we argue that andesitic country rocks were at least as widely metasomatised and mineralised. Pampa de Pongo apparently differs from all other Fe-oxide deposits of the Peruvian Coastal Belt in the sparse development of Ca-amphibole alteration. In this context, it is of interest that its overall Cu content appears lower than those with greater amphibole. Considered overall, the paragenetic evolution of the Pampa de Pongo deposit appears simpler than that at Marcona. Although brecciation and replacement was important in both centres, no evidence has been found for more than a single major fragmentation event in the former.

Lead isotope data suggest the Marcona ore has a composition differing markedly from that of broadly coeval Mesozoic granitoids from southern Peru which, although also intruded into the Arequipa Massif, show only minimal evidence of AFC processes (Barreiro and Clark, 1984). The ore-Pb compositions of the largest lower Eocene porphyry Cu deposits of southern Peru, Toquepala and Cuajone, similarly record only minimal crustal contamination, implying a marked metallogenetic difference between these centres and Marcona (Clark, 1997). All of these deposits, however, have Pb isotopic compositions indicative of mixing of lead derived from deep crustal and/or upper mantle and upper crustal reservoirs.

Hydrothermal activity occurred during construction of a major Jurassic volcanic arc, represented locally by thick successions of largely andesitic strata assigned to the Río Grande Formation. Dates for mineralisation at Marcona and the age of host formations at Pampa de Pongo suggest iron oxide mineralisation commenced around 160 Ma, >20 my. before the formation of the Pampa de Pongo iron deposit. Although Pampa de Pongo is within the contact aureole of the Coastal Batholith, a genetic affiliation with iron mineralisation has not been established. It is postulated likely that the later stages of the hydrothermal system at Marcona may have overlapped in time with the development of the Pampa de Pongo deposit. Extensive high-level iron oxide-Cu-Au veins in the Coastal Batholith, such as at Cobrepampa, suggest that this style of mineralisation may have continued well after Pampa de Pongo was formed and possibly after considerable uplift. The numerous small iron and copper deposits in the coastal batholith show alteration characteristics and vein orientations similar to Marcona and Pampa de Pongo, suggesting a common origin and genesis that is independent of host rock except on a very local scale.

There is a very close relationship between the timing of the mineralisation at Marcona and the intrusion of porphyritic andesite sills and dykes (including the ocöites). Some have intruded just prior to the main mineralisation event, and some shortly afterwards but are affected by waning stages of the alteration and mineralisation. These high-level intrusives and Fe-oxide associated copper gold in the Marcona District potentially share a common deep magmatic source. The combined effect of both deep and high level intrusives are postulated as the causative bodies for the widespread alteration assemblages characteristic of low grade thermal metamorphism.

The role of the Abancay Deflection on Mesozoic mineralisation remains obscure, as does the significance of the intersection with the other major crustal linear, the Dorsal de Nazca. The close proximity of the mineralisation of the Marcona district to these structures is consistent with the observations of Hitzman (2000) who recognises that Fe-oxide-Cu deposits are generally located on splays off deep structural features. The Dorsal de Nazca has certainly played an important role in the erosional and supergene history of the deposit but it is believed very unlikely that this structure was present in its current form during the Jurassic. Nevertheless it may be an indication of a far longer lived deep crustal suture in the region.

Acknowledgements

Field work by technical staff of Rio Tinto Exploration, Peru since 1994 are acknowledged as having played a vital role in the production of this manuscript even when not directly involved. Jorge Carbonell requires a special mention as much of the work at Pampa de Pongo is based on his summary observations from drilling and the geological sections relating to the deposit were originally constructed by him. His constructive comments on the draft version of the paper were greatly appreciated. Petrographic reports by Ivan Reynolds have been extensively utilised in attempts to construct the paragenesis for these deposits and his valuable contributions are gratefully acknowledged.

Shougang Hierro Peru is thanked for permission to publish the paper and for the valuable comments from their geological team at the Marcona Mine. Extensive reference has been made to the work of Jorge Injoque whose early investigations on the Marcona Deposit deserve a high commendation.

Petrographic and analytical studies at Queens University were supported by grants from the Natural Sciences and Engineering Council of Canada to A.H.C. The latter further thanks Farhad Bouzari for assistance with the X-ray work and Joan Charboneau for uncomplainingly typing numerous versions of the manuscript.

Finally the authors wish to reserve Mike Porter and his wife Lyn a special place in these acknowledgements for patiently waiting an inordinately long time for the paper to be prepared and then in addition editing a substantially revised version of the paper before final printing.

References

Adrian, E., 1958 - The geology and iron ore bodies of the Marcona District, Peru. *Internal Report Marcona Mining Co., Peru.*

Atchley, F.W., 1956 - Geology of the Marcona Iron Deposits, Peru. *Ph.D thesis, University of Stanford, USA.*

Aguirre, L. and Offler, R., 1985 - Burial metamorphism in the western Peruvian trough: its relation to Andean magmatism and tectonics; *in* Pitcher, W.S., Atherton, M.P., Cobbing, E.J., and Beckinsale, R.D., eds., Magmatism at a Plate Edge: the Peruvian Andes, *Blackie and Sons Ltd.*, Glasgow, p. 59-71.

Atkin, B.P., Injoque-Espinoza, J., Harvey, P.K., 1985 - Cu-Fe-amphibole mineralisation in the Arequipa segment, *in* Pitcher, W.S., Atherton, M.P., Cobbing, E.J., and Beckinsale, R.D., eds., Magmatism at a plate edge: The Peruvian Andes, *Blackie and Son Ltd.*, p. 261 –270.

Barreiro, B.A., and Clark, A.H., 1984 - Lead isotopic evidence for evolutionary changes in magma-crust interaction, central Andes, southern Peru: *Earth and Planetary Science Letters*, v. 69, p. 30-42.

Bookstrom, A.A., 1995 - Magmatic features of iron ores of the Kiruna type in Chile and Sweden: ore textures and magnetite geochemistry – a discussion: *Economic Geology*, v.90, p. 469-473.

Bourrett, W. & Hayes, J.J., 1957 - The role of geology in developing the Marcona Iron District. Paper presented to the *American Institute of Mining, Metallurgical and Petroleum Engineers.* New Orleans, Louisiana. Feb 28.

Caldas, J., 1978 - Geologia de los cuadrangulos de San Juan, Acari y Yauca. *Boletin N.30 Institution GeologicaMin Peru.*

Carbonell, 1996, *Internal Rio Tinto Report*, Unpublished.

Clark, A.H., 1998-1999 - Magmatic-Hydrothermal Ore-Genesis and Metallogenesis in the Central Andes: *Short course notes for Rio Tinto Mining & Exploration Ltd. Antafogasta, Lima and Mendoza*, 753pp.

Clark, A.H., Farrar, E., Kontak, D.J., Langridge, R.J., Arenas, M.J., France, L.J., McBride, S.L., Wasteneys, H.A., Sandeman, H.A., and Archibald, D.A., 1990 - Geologic and geochronologic constraints on the metallogenic evolution of the Andes of southwestern Peru: *Economic Geology*, V 85, p 1520-1583.

Cobbing, J., 1998 - The Coastal Batholith of Peru and other aspects of Andean Magmatism, *Boletin Sociedad Geologica del Peru*, Vol. 88, p 5-20.

Dilles, J.H. and Einaudi, M.T., 1992 - Wall-rock alteration and hydrothermal flow paths about the Ann-Mason porphyry copper deposit, Nevada - a 6km vertical reconstruction: *Economic Geology*, v. 87, p 1963-2001.

Dunin-Borkowski, 1978 - Los yacimientos de oxidos de Hierro en los departamentos de Cuzco y Apurimac. *XIV Convencion de Ingeneiros de Mina*, Lima Peru.

Eaton L., 1941 - The iron ore deposits at Marcona and Yaurilla. The limestone deposits at Zaña, Saltur and San Juan in Peru. *H.A. Brassert*, New York.

Emmons, S.F., Irving, J.D., and Loughlin, G.F., 1927 - Geology and Ore Deposits of the Leadville Mining District, Colorado: *U.S. Geological Survey, Professional Paper* 148, 368p.

Holmberg, C.J. 1941 - The iron ore deposits at Marcona in Peru: H.A. Brassert & Company, NY. Reprinted in Spanish: *Informaciones y memorias de la Sociedad de Ingenieros del Peru*, tome XLVI, no.2, p.107-186, 1945.

Hitzman, M.W., 2001 - Iron Oxide-Cu-Au Deposits: What, Where, When and Why. *in* Porter, T.M. (Ed), Hydrothermal Iron Oxide Copper-Gold & Related Deposits: A Global Perspective, *Australian Mineral Foundation*, Adelaide, p 9-25.

Injoque, J.E., 1985 - Geochemistry of the Cu-Fe-amphibole skarn deposits of the Peruvian central coast. *PhD thesis University of Nottingham, U.K.*

Injoque, J., Atkin, B., Harvey, P., and Snelling, N., 1988 - Mineralogia y geocronologia del skarn geothermal de Hierro de Marcona. *Boletin de la Sociedad Geologica del Peru* 78, 65-80.

Injoque, J., 2001 - Segmentacion de los gabbros y diorites tempranos del Batolito de la costa (Superunidad Patap), la fase deforativa Mochica y mineralisacion asociadas, como parte de la segmentacion Cretacea de la Costa Peruana. Unpublished.

Kwak, T.A.P., and Askin, P.W, 1981 - The nomenclature of carbonate replacement deposits, with emphasis on Sn-F (-Be-Zn) "wrigglite" skarns: *Journal of the Geological Society of Australia*, v. 28, p. 123-136.

Lama Rios, D. 1981 - Geología Planamiento y control de calidad: Hierro Peru, Minas Marcona. Provincia Nazca, Ica. *Programa de Ingenieria Geologica. Universidad Nacional Mayor de San Marcos*, Peru.

Marschik, R, and Fontboté, L., 2002 - The Candelaria-Punta del Cobre iron oxide Cu-Au (-Zn, Ag) deposits, Chile: *Economic Geology*, v. 96, p.1799-1826.

Mukasa, S.B., and Henry, D.J., 1990 - The San Nicolás Batholith of coastal Peru: early Paleozoic continental arc or continental rift magmatism?: *Journal of the Geological Society of London*, v.147, p. 27-39.

Nyström, J.O, and Henriquez F., 1995 - Magmatic features of iron ore of the Kiruna type in Chile and Sweden: ore textures and magnetite geochemistry. *Economic Geology*, v. 90, p 473 -475.

Peccerillo, A., and Taylor, S.R., 1976 - Geochemistry of Eocene calc-alkaline volcanic rocks from the Kastamonu area, Northern Turkey. *Contributions to Mineralogy and Petrology*, v. 58, p 63-81.

Pitcher, W.S., Atherton, M.P., Cobbing, E.J., and Berkinsale, R.D., 1985 - Magmatism at a plate edge: The Peruvian Andes: *Blackie and Sons*, Glasgow.

Ryan, P.J., Lawrence, A.L., Jenkins, R.A., Matthews, J.P., Zamora, J.C., Marino, E., and Urqueta, I, 1995 - The Candelaria copper-gold deposit, Chile: *Arizona Geological Society Digest*, v.20, p. 625-645.

Reynolds, I., 2002, *Internal Rio Tinto Report*, Unpublished.

Shackleton, R.M., Ries, A.C., Coward, M.P. & Cobbold, P.R., 1979 - Structure, metamorphism and geochronology of the Arequipa massif of Coastal Peru. *Journal Geological Society*, London 136, 195-214

Taylor, R.G., 1996, *Internal Rio Tinto Report*, Unpublished.

Thompson, T.B., and Arehart, G.B., 1990 - Geology and the origin of ore deposits in the Leadville district, Colorado: *in* Beaty, D.W., Landes, G.P., and Thompson, T.B., (Eds.), Carbonate-Hosted Sulphide Deposits of the Colorado Mineral belt, *Economic Geology Monograph*, 7, p. 130-154.

Ullrich, T.D & Clark, A.H. 1997 - Paragenetic Sequence of Mineralisation in the Main Orebody, Candelaria Copper Gold Deposit, Chile, *Progress Report #3 for Phelps Dodge Exploration Corp.* Unpublished internal report.

Ullrich, T.D & Clark, A.H. 1998 - Evolution of the Candelaria Cu-Au deposit, III Region, Chile. *Geol. Soc. America, Abstracts with Programs*, v. 30, 7, A-75

Ullrich, T.D & Clark, A.H. 1999 - The Candelaria Cu-Au deposit, III Region, Chile: Paragenesis, geochronology and fluid composition, *in* Stanley, C.J., *et al.*, (Eds.), Mineral deposits. Processes to processing: *Balkema*, Rotterdam, p. 201-204.

Ullrich, Thomas. D & Clark, Alan. H., Kyser, T. Kurtis, 2001 - The Candelaria Cu-Au deposit, III Region, Chile; product of long-term mixing of magmatic-hydrothermal and evaporite-sourced fluids, Abstracts with programs - *Geological Society of America*, 33 (6), p.3.

Vidal, C.E., Injoque, J., Sidder, G.B. & Mukasa, S.B., 1990 - Amphibolitic Cu-Fe skarn deposits in the Central Coast of Peru: *Economic Geology*, 85, 1447-1461

Wasteneys, H.A., Clark, A.H., Farrar, E. and Langridge, R.J., 1995 - Grenvillian granulite facies metamorphism in the Arequipa massif, Peru: a Laurentia-Gondwana link: *Earth and Planetary Science letters*, v.132, p 63-73.

PGC PUBLISHING

Ray, G.E. & Dick, L.A., 2002 - The Productora Prospect in North-Central Chile: An Example of an Intrusion-related, Candelaria Type Fe-Cu-Au Hydrothermal System; *in Porter, T.M. (Ed.), Hydrothermal Iron Oxide Copper-Gold & Related Deposits: A Global Perspective*, Volume 2; PGC Publishing, Adelaide, pp 131-151.

THE PRODUCTORA PROSPECT IN NORTH-CENTRAL CHILE: AN EXAMPLE OF AN INTRUSION-RELATED, CANDELARIA TYPE Fe-Cu-Au HYDROTHERMAL SYSTEM

[1]Gerry E. Ray, [2]Lawrence A. Dick

[1]British Columbia Geological Survey, Victoria, BC, Canada.
[2]Former Exploration Vice President, General Minerals Corporation, Vancouver, BC, Canada.

Abstract - The Productora prospect is situated 15 km SSW of the town of Vallenar in the Third Region, north-central Chile. It lies within the "Chilean Iron Belt" close to the north-trending Atacama Fault system. The belt contains a variety of Fe oxide ±Cu ±Au-bearing deposits including Candelaria (366 million tonnes averaging 1.08 % Cu, 0.26 g/t Au) which is situated in the Punta del Cobre region approximately 150 km north of Productora. The age, structural setting, alteration assemblages and styles of mineralisation in the Productora area resemble those present at Candelaria, but Productora differs in its spatial association with intrusive rocks and its lack of skarn assemblages.

Productora includes a north-trending zone of hydrothermal alteration (Fe oxide-albite-K spar-tourmaline-sericite-silica) that exceeds 8 km in strike length and 3 km in width. This zone contains 13 small former mines, 8 of which were worked for magnetite and the remaining 5 for Cu-Au. In addition, there are over 80 shallow pits and surface occurrences containing some Fe oxide ±Cu ±Au ±U ±REE ± apatite mineralisation.

The mineralisation and alteration are structurally and stratigraphically controlled. They are preferentially developed in more permeable tuffaceous units of a presumed Cretaceous package but also follow NW-striking and, to a lesser extent, N-trending structures related to the Atacama Fault system.

Hydrothermal alteration is mainly centred around two Early Cretaceous (c. 130 Ma) felsic intrusions, the Cachiyuyito and El Molle stocks. Six proximal to distal alteration zones are recognised. Zone I alteration assemblages in the stocks comprise pervasive albite with veins of actinolite, magnetite and epidote. The immediately adjacent country rocks are overprinted by Zone II alteration dominated by albite, chlorite, actinolite, magnetite, apatite and coarse calcite veins. More distal still is Zone III with widespread K-spar and tourmaline, as well as magnetite, hematite, secondary biotite and silica. This passes out to Zone IV in which the volcaniclastics are strongly replaced by albite and silica ± epidote and hematite. Zones V and VI represent the uppermost and lowest temperature alteration. The former is largely preserved in an elongate, 1.5 km-wide down-faulted block and is characterised by massive silica, specular hematite, sericite and dumortierite, whilst the outermost Zone VI has pervasive propylitic and albitic alteration with rare jasper veins.

Three styles of Fe-oxide dominant mineralisation are identified, each of which tends to occur within a specific alteration zone. The most proximal and common of these is magnetite ± apatite veins and replacements hosted by Zone II alteration assemblages. This style seldom contains significant Cu or Au and is represented by the Mariposa, La Bandera, La Chulula, La Negrita and the El Molle magnetite mines.

The second and most economically important style of mineralisation is typified by the Cu-Au ± REE ± U ± Mo ± Co mineralisation at the Productora and Santa Innes mines. It is more commonly associated with Zone III alteration (K-spar-silica and tourmaline) but in the case of the Monseratt Mine and Remolina pit it is hosted by Zone II mineral assemblages. Hypogene mineralisation includes magnetite, chalcopyrite, pyrite and native gold. Surface leaching has resulted in the development of irregular leached caps containing Cu-oxide and phosphate mineralisation at surface and secondary Cu enrichment locally at depth. Both the hypogene and secondary Cu mineralisation is Au-rich (100 to 9700 ppb) and they contain anomalous REE's (50 to 560 ppm La). Trace quantities of the U oxide mineral, torbernite, are also present. Sulphur isotope ratios for chalcopyrite, pyrite and chalcocite collected from Style 2-type mineralisation show $\delta^{34}S$ values ranging from -8.2 to +1.2 which are lower than those recorded in the Punta del Cobre region further north.

The third style of mineralisation is developed in the outermost parts of the Productora hydrothermal system (Zone VI). Here, small veins and mantos of magnetite and/or hematite are associated with epidote, albite and silica alteration. This distal mineralisation may be geochemically anomalous in Cu, Au, Zn, As, Co, Pb and Mn.

Introduction

The Productora property is located approximately 625 km north of Santiago and 15 km SSW of Vallenar in Region III, north-central Chile (Figure 1). It lies less than 4 km west of the Pan American Highway (Ruta 5) and is geographically centred around the Productora Valley (Figure 2) which comprises several talus-filled basins. The basins are surrounded by, and lie on strike with, a north-trending zone of hydrothermal alteration (Fe oxide-albite-K-spar-biotite-tourmaline-sericite-silica) that is discontinuously traceable over an 8 km length. This zone reaches 3 km in outcrop width and contains five small, shallow former mines (Productora, Santa Innes, Monseratt, Remolina and Fortuna; Figure 3) that were worked for Cu oxides and Au, as well as eight magnetite mines and more than 80 pits and occurrences with Fe oxides ±Cu ±Au ±U ±REE ±apatite mineralisation.

The Productora area lies within the "Chilean Iron Belt" which is associated with the long-lived, north-trending Atacama Fault Zone (Figure 1). This brittle-ductile structure has been active since the Early Cretaceous and has involved recurrent sinistral strike-slip displacements (Brown et al., 1993). The belt contains a large number of

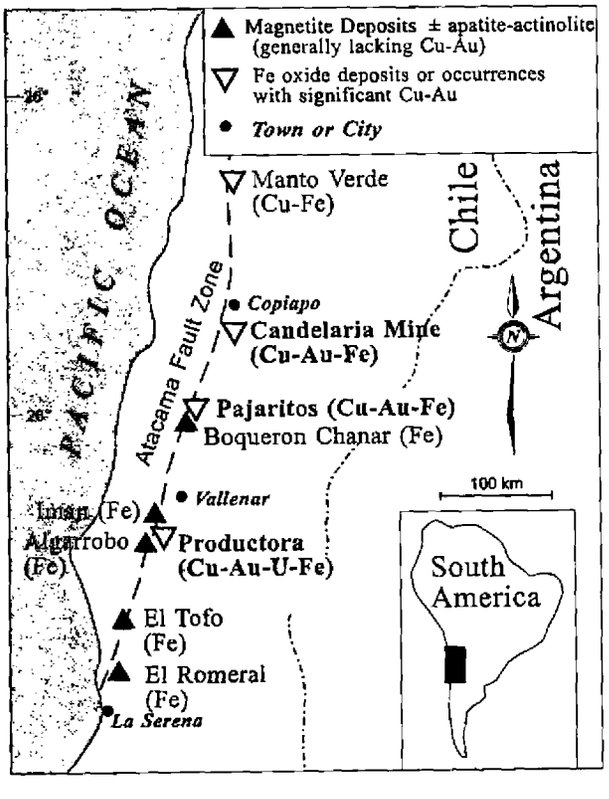


Figure 1: The Atacama Fault Zone, north-central Chile, showing locations of various Fe oxide deposits including the Productora Prospect and the Candelaria Deposit.

Fe oxide-rich occurrences as well as several large deposits. The occurrences and deposits can be separated into two types (Figure 1), namely magnetite-dominant ± actinolite ± apatite systems that generally lack Cu sulphides (eg. El Romeral, El Tofo, Algarrobo and Iman) and those where the magnetite or hematite is associated with significant amounts of Cu and Au (eg. Candelaria, Manto Verde; Bookstrom, 1977; Ryan et al., 1995; Vila et al., 1996; Marschik et al., 1996). The Productora prospect and the lesser known Pajaritos occurrences north of Vallenar (Ray, 1997b; Figure 1) represent examples of the latter type. In particular, the structural setting, Na, K and Si alteration zoning and Cu-Au-Co-REE geochemical signature of the mineralisation at Productora show strong similarities to the Cretaceous-age Candelaria deposit (c. 366 Mt grading 1.08 % Cu, 0.26 g/t Au and 4.5 g/t Ag; Marschik et al., 1996; Jenkins et al., 1998), situated approximately 150 km further north (Figure 1). Unlike Candelaria, however, the Productora alteration is spatially related to a suite of elongate, albitised felsic intrusions that have yielded a U-Pb zircon date of 129.8 Ma (Fox, 2000).

Previous Work

Despite the long history of sporadic mining and exploration in the Productora area, the only published report is a brief description by Dick and Ray (2000). Maus (1997a and b) completed reconnaissance mapping and also noted the earlier exploration by Noranda and Newcrest Mining. At least 10 short (35 m to 101 m long) holes were drilled during the 1980's by the Commission Chilena Energia Nuclear (CCEN). This drilling was targeting uranium mineralisation, but later assaying revealed significant intersections with Cu-Au mineralisation (Maus, 1997a). Later, General Minerals Corporation (GMC) completed an initial phase of eight percussion drill holes close to the Productora and Santa Innes mines. This totalled 1607 m of drilling along an 800 m strike length. The intersected mineralisation was typically 30 to 70 m thick and averaged 0.3 to 0.6 % Cu with elevated quantities of Au, Mo, Co, U, and REE's.

Descriptions of reflected light and scanning electron microprobe studies of rock chips collected from the GMC percussion drilling at Productora were presented by Osterman (1997, 1998), who also noted the presence of the uranium oxide mineral torbernite as well as some tourmaline breccias and stockworks. Later, 1:10 000 and 1:5000 geological mapping and sampling was completed over a 40 km^2 area (Ray, 1997a, 1998 a and b, 2001; Arcos, 1998). In addition, more detailed work was undertaken in the field and at the Colorado School of Mines (Fox, 2000). The latter work included U-Pb and K-Ar radiometric dating of the intrusions and the potassic alteration, as well as some sulphur isotope studies.

Regional Setting

The geology of the region includes a generally poorly exposed Paleozoic basement overlain by Mesozoic and Cenozoic volcanic and sedimentary sequences. Jurassic and younger deposition comprised mainly calc-alkaline andesitic lavas and flow breccias with some continental clastic sediments (Aguirre et al., 1974; Clarke et al., 1976), laid down in a continental margin, back-arc environment (Coira et al., 1982). The Andean Orogeny commenced during the early Jurassic (Clark et al., 1976), and the subsequent volcanism and plutonism moved progressively eastwards with time. Jurassic plutons occur along the coast, whereas Cretaceous and younger plutons outcrop further east. Compressional deformation in the region resulted in large amplitude folds, but it was generally subordinate to extensional movements that resulted in abundant normal faulting, accompanied by doming and the emplacement of some plutons (Jordan et al., 1983). The four main geological elements of Cretaceous age in the Productora-Candelaria region include the Chanarcillo back-arc basin marine carbonates in the east, the Bandurrias volcanic arc in the central part of the region, and the Coastal batholith and Atacama Fault Zone to the west (Marschik, 1996; Fox, 2000).

Geology of the Productora Area

Introduction

Most of the mapped area illustrated in Figure 3 is underlain by a gentle to moderately inclined stratigraphic package of andesitic to dacitic tuffs that are interpreted to have been deposited in a sub-aerial to shallow aqueous environment. In addition, there are some mafic volcanic flows, bedded tuffaceous siltstone, volcanic sandstone, and very rare examples of thin (<15 m thick) impure limestones. The precise age of the Productora rocks is unknown due to a lack of fossil and radiometric data. Fox (2000) suggests they may belong to the Jurassic-Lower Cretaceous age Bandurrias Formation; an alternative possibility is that the package at Productora represents part of the pre-late Valanginian Punta del Cobre Formation which hosts the Candelaria deposit further north (Marschik et al., 2000; Figure 1).

A north to south facies change is recognised along the Productora belt. In the northern part of the area and north of the Productora Fault (Figure 3), volcanic flows are rare and the sequence mainly comprises ash and lapilli tuffs with minor volcanic breccias. South of the fault, however, the tuff package includes an extensive flow unit of massive andesite-basalt. The unit is economically important because it forms a comparatively impermeable cap whose base, together with the immediately underlying tuffaceous rocks, have been the locus of intense hydrothermal alteration with the local development of Fe oxide-Cu-Au mineralisation.

The following bottom-to-top stratigraphic succession is recognised south of the Productora Fault (Figure 3):

1. a lower unit of ash flows and lapilli tuffs of andesitic to dacitic composition (Dick and Ray, 2000; Fox, 2000) which is estimated to be >500 m thick.
2. a middle unit of widespread basaltic to andesitic flows that reaches 220 m in thickness (Ray, 2001).
3. a thin upper tuffaceous unit that generally occurs as minor erosional remnants along the Eastern Ridge (Figures 2 and 3).

Lower Tuffs

The lowest part of the sequence comprises dacitic and andesitic ash and lapilli tuffs, some volcaniclastic debris flows and a 100 m thick unit of devitrified welded tuff (Fox, 2000). These lower permeable rocks host most of the magnetite and Cu-Au mineralisation in the belt, including that present at the Productora, Monseratt and Santa Innes mines and the Remolina pit (Figure 3). Most tuffs are massive, poorly to moderately sorted and lack grading. Rounded, water-worn lapilli are present but layering and sedimentary bedding are uncommon except in the finer grained ash tuffs or in the tuffaceous siltstones. In some lapilli tuffs the elongated clasts possess an alignment that records a crude layering. Many tuffaceous outcrops also display a well marked sub horizontal to gently dipping parting that may mimic original depositional layering in the tuffs. This parting is widespread and is well developed, for example, at the Productora Mine. Most tuffs display some degree of hydrothermal or thermal alteration. The fine grained ground mass contains crystals of K-feldspar and albite-oligoclase plagioclase with lesser amounts of glassy quartz, highly altered amphibole and minor pyroxene. In the dacitic tuffs, rounded to broken crystals of glassy quartz are a variable but widespread feature. The quartz crystals reach 5 mm in diameter and contain prominent bands of fluid inclusions and delicately embayed margins. The quartz crystals in many of the more silicified tuffs are characterised by ragged and thin overgrowths of secondary silica.

The heterolithic lapilli tuffs contain angular to well rounded clasts of volcanic and tuffaceous rocks. The lapilli include dark coloured feldspar porphyritic basalts and andesites, pale flow banded rhyodacites, and fragments of either mafic or quartz-bearing felsic tuffs. Also present are rare fragments of massive silica, bedded sediments and felsic intrusive rocks. Some mafic tuffs contain up to 10% amphibole and lesser augite that are extensively replaced by epidote and pale to dark green chlorite. Accessory minerals include zircon, zoisite, sericite and traces of apatite.

Middle Unit of Mafic Flows

The lower tuffs are overlain by the widespread unit of dark, mafic andesite-basalt that predominates in the southern part of the area (Figure 3). To the west, underlying the Silica Ridges (Figures 2 and 3) there is an extensive, thin unit of hydrothermally altered, Fe-rich basalts that may be part of the same flow unit. This generally massive volcanic unit includes equigranular and porphyritic types. The latter contain plagioclase phenocrysts up to 0.5 cm in length with smaller crystals of hornblende, pyroxene and olivine (Fox, 2000) in a highly chloritised and epidotised groundmass. Close to some presumed original volcanic feeder fissures, there are flow breccias containing clasts of

intrusive felsic quartz diorite and monzonite up to 0.3 m in diameter (Ray, 1998b). Analyses indicate the volcanic flow rocks are sub-alkaline and calc-alkaline, being of basalt-andesite composition (Dick and Ray, 2000).

Upper Tuffs

These represent the uppermost sequence seen in the area. Along the Eastern Ridge (Figures 2 and 3) they occur as small remnants on the hilltops where they comprises fine grained ash tuffs and tuffaceous sediments. South and west of the Quebrada Escondido Fault, however, they pass laterally into heterolithic lapilli tuffs and very coarse grained volcanic breccias.

Intrusive Rocks

Two major intrusive phases are recognised. The youngest and least altered of these is the Ruta 5 Batholith, a small portion of which outcrops in the south-east part of the area

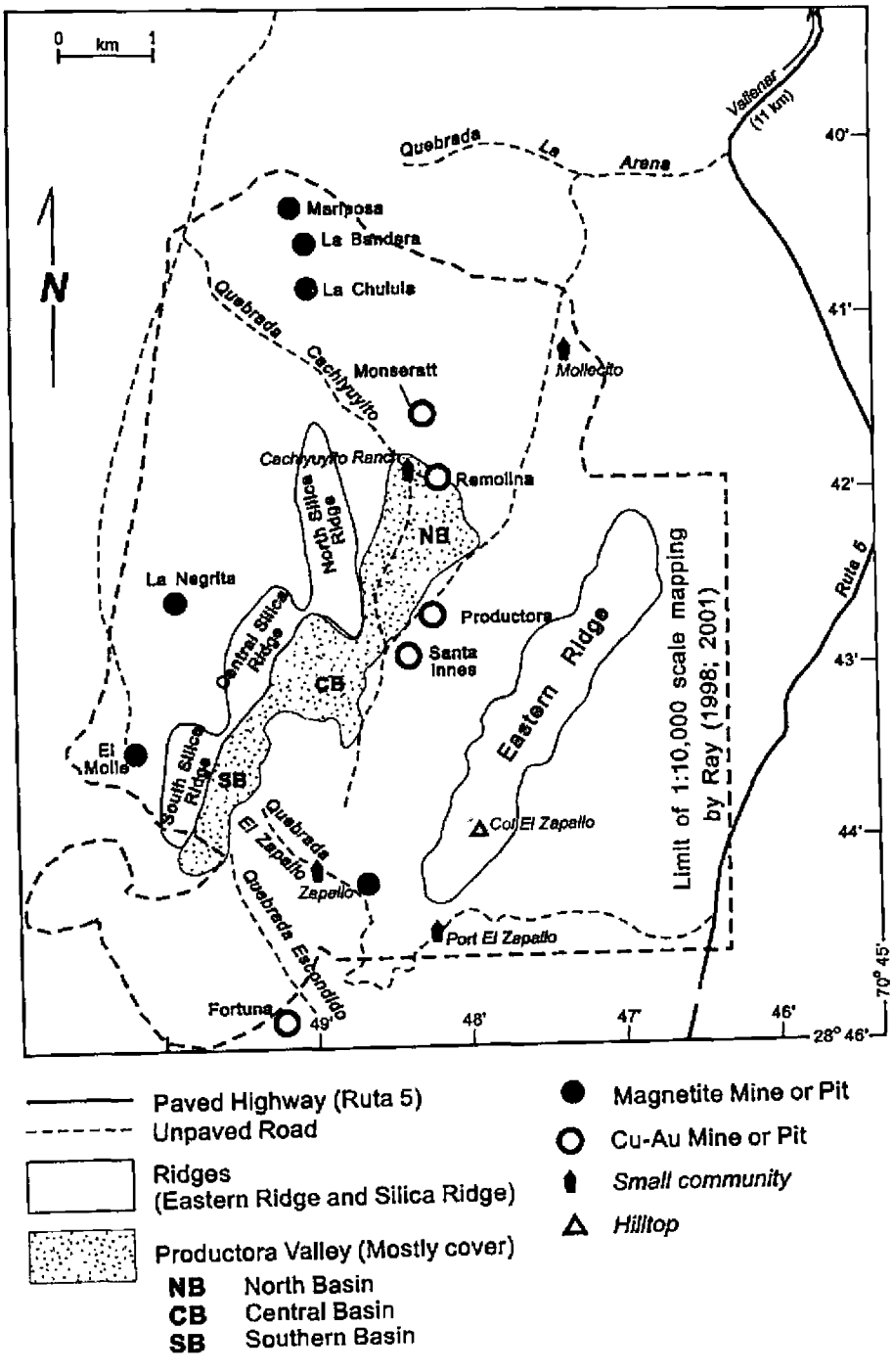


Figure 2: Location of mines, roads and main topographic features in the Productora area, Chile.

(Figure 3). It is medium to coarse grained, equigranular and leucocratic body with a biotite-dominant granodiorite-quartz monzonite core and a mafic, hornblende-rich border phase. The batholith has been dated by U-Pb zircon methods at 96.1 Ma (Fox, 2000). It is cut by swarms of Au-bearing quartz ± barite veins. These veins trend NNW to NW and some are still being mined on a small scale for their Au. Locally, the batholith is strongly supergene kaolin-altered but it post-dates the Productora Fe oxide-Cu-Au-REE-U mineralisation and the associated Na-K-Si alteration. The contact aureole includes a biotite ± garnet ± cordierite hornfels, a wide zone of epidote alteration (Figure 4), and several small Cu-bearing skarn occurrences (Ray, 1998b).

The older intrusive phase was responsible for the El Molle, Zapallo and Cachiyuyito stocks (Figure 3). It pre-dates the Fe oxide-Cu-Au-U-REE mineralisation and Na-K-Si alteration but is believed to be genetically related to the Productora hydrothermal system. Fox (2000) reports a U-Pb zircon age of 129.8 Ma for the Cachiyuyito Stock which is somewhat older than the 114-116 Ma ages determined for the Candelaria Fe-oxide mineralisation further north (Marschik et al., 2000).

Chemical analyses and various plots for the Cachiyuyito Stock are shown in Table 1 and Figure 5. The stock is sub-alkaline, meta-aluminous and calc-alkaline and its Rb, Y and Nb contents indicate it represents a "volcanic arc" granitoid as defined by Pearce et al (1984). Plots also suggest a tonalite-quartz diorite composition although this conclusion must be treated with caution due to the intense secondary albitisation and local silicification. The stocks are leucocratic, equigranular to weakly porphyritic and medium to coarse grained. Primary and secondary plagioclase totals between 60 and 90% of the rock, with hornblende, pyroxene and quartz generally comprising < 10%. Accessory minerals include zircon, apatite, carbonate, zoisite, ilmenite and late K-spar.

Intense hydrothermal alteration in these older stocks is ubiquitous, both as pervasive albitisation and veins of actinolite, epidote, chlorite and magnetite (Figure 6C and I). Rarely, veins of tourmaline or quartz are seen. The adjacent country rocks are overprinted by pervasive actinolite-chlorite-albite alteration with numerous magnetite ± apatite veins but no contact metamorphic hornfels aureole is recognised.

Geological and structural history

The geological history for the Productora area is believed to be:

1. Deposition of Early Cretaceous flows and tuffs in a shallow aqueous to subaerial, volcanic back-arc environment. Locally, the volcanism and sedimentation was controlled by intersecting sets of N and NW-trending structures related to the Atacama Fault system.
2. Early Cretaceous (c. 130 Ma) emplacement of the Cachiyuyito, El Molle and Zapallo stocks, closely followed by
3. Formation of the Productora Fe oxide-Cu-Au-U-REE-apatite hydrothermal system which was controlled on an outcrop scale by NW and N-trending structures (Figure 6A, B and J), as well as stratigraphic host-rock permeability.
4. Ductile movements resulting in the formation of several narrow N-striking quartz-sericite schist zones followed by normal down-faulting (Figure 3).
5. Late Cretaceous (c. 96 Ma) intrusion of the Ruta 5 Batholith and subsequent development of NW trending Au-bearing quartz ± barite veins.
6. Multiphase brittle minor movement along the sets of N and NW trending structures. This late movement along the cross-faults resulted in right lateral offset of the original lithologies and mineralisation.

No major folds have been identified in the area apart from drag structures adjacent to some major faults. However, the stratigraphy is complicated by abrupt volcanic facies changes and later brittle faulting. Two sets of fractures are recognised, a generally N to NNE-striking set and a more dominant NW trending cross-set (Figure 7). On a local scale, both sets have controlled the veins of Fe oxide-Cu-Au, feldspar, silica, actinolite and tourmaline, although the NW-trending fractures are more abundant (Figure 7).

The north-trending, steeply dipping structures, including the Quebrada Verde and Quebrada Mollecito faults (Figure 3), are probably related to the main Atacama Fault Zone which is believed to lie 10 km further west. These older faults have undergone both vertical and sinistral sub-horizontal recurrent movements, and have controlled the intrusion of the elongate Cachiyuyito and El Molle stocks and some of the Fe oxide-Cu-Au-REE mineralisation.

The area is also cut by swarms of NW-trending, steep-dipping cross structures, including the Rancho and Productora faults (Figures 3 and 6A and B). Offset of the stratigraphy, the stocks and the hydrothermal alteration, together with sub-horizontal slickensides show that the latest movements along these cross structures were right lateral. However, these faults have had a long history and locally have had important controls on the Fe oxide-Cu-Au mineralisation and its associated alteration (Figure 7). Mapping (Ray, 1998a and b) also suggests that the Productora Fault was a precursor fissure for some of the extrusive volcanism in the area. Thus, some of the older cross structures are probably Cretaceous in age.

The El Molle Stock is thought to be a SSW strike extension of the Cachiyuyito body (Dick and Ray, 2000). However, the stocks have been separated from each other by an elongate, 1.5 km wide down-faulted block of intensely silicified ± kaolin ± specular hematite ± dumortierite-bearing rocks (Figures 3 and 4; Dick and Ray, 2000). Two narrow (< 70 m), north-trending zones of quartz-sericite schist mark the eastern and western margins of the block. Most movement along the schist zones postdates the hydrothermal silicification in the adjacent rocks, and the eastern schist obliquely truncates the Cachiyuyito Stock and the Quebrada Verde Fault (Figures 3 and 4).

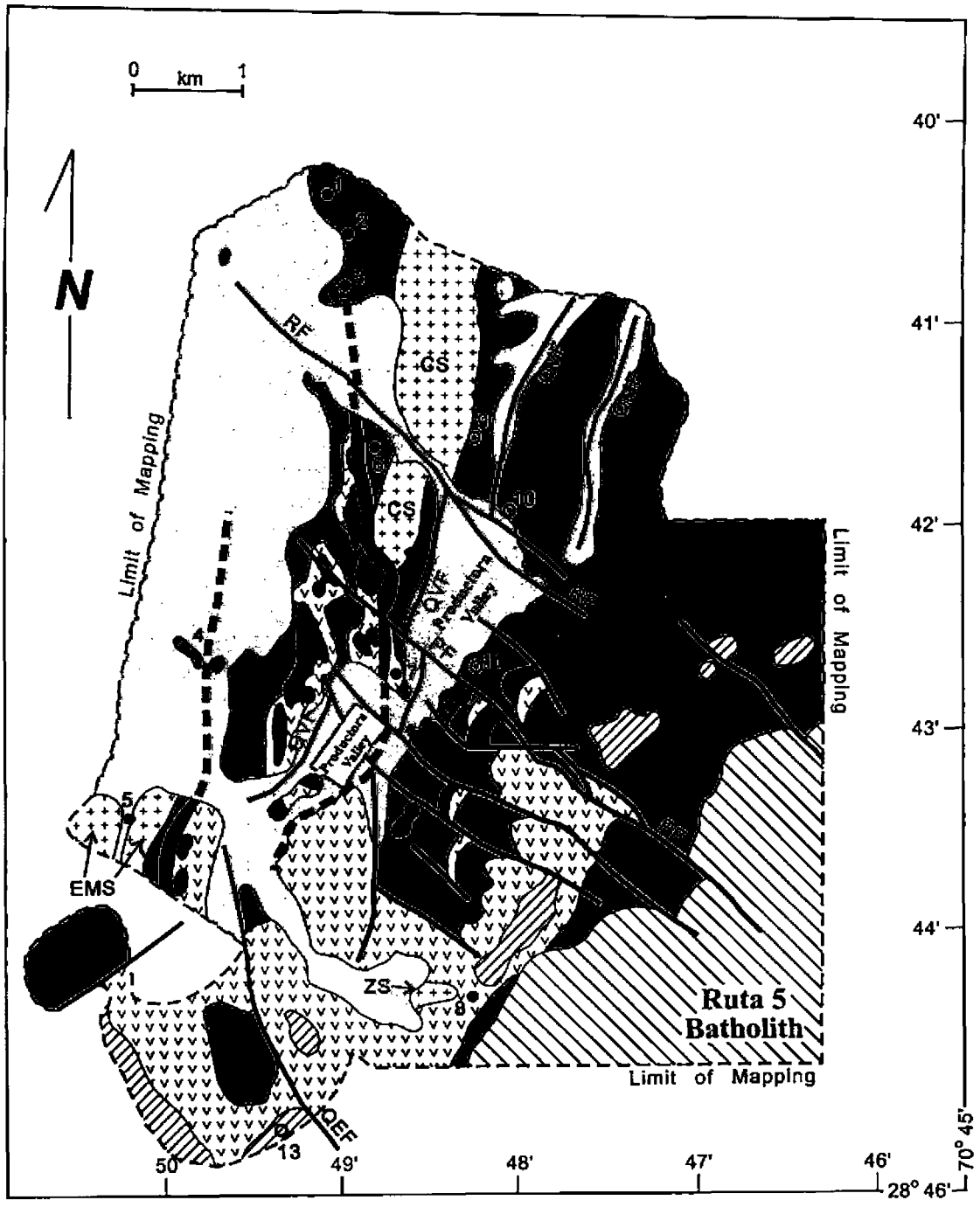


Figure 3: Geology of the Productora Prospect and location of the principal Fe oxide and Cu-Au workings.

Economic Geology

Introduction

Past small-scale metal mining in the Productora area has mainly been carried out on:

1. Gold in late quartz ± barite veins that cut the 96 Ma Ruta 5 Batholith and its adjoining hornfelsed country rocks.
2. Placer Au derived from the above quartz veins.
3. Magnetite in lenses, pods or veins, commonly associated with actinolite ± apatite, as seen at the Mariposa, La Bandera, La Chulula, La Negrita and El Molle Fe mines (Figure 3).
4. Copper-gold mining from Fe oxide-Cu ±Au ±U ±REE mineralisation. Most of this was extracted from secondary Cu oxide ore (Figure 6J) with lesser amounts of hypogene Cu-sulfide material. This mineralisation occurs along vertical structures or, less commonly, as small stratiform replacements and is seen at the Monseratt, Productora, Fortuna and Santa Innes mines and the Remolina pit (Figure 3).

Numbers 1 and 2 above are probably directly or indirectly related to the Ruta 5 Batholith whereas numbers 3 and 4 belong to the older Productora hydrothermal system.

Alteration

The Productora area is marked by an elongate zone of hydrothermal alteration that is > 3 km wide and > 8 km in semi-continuous strike length (Figure 4). Virtually all the tuffs and many of the volcanic flows along the belt show varying degrees of alteration that involved the introduction of large volumes of Fe, Si, Na and K. Alteration occurs either in veins, disseminations or as pervasive, selective replacements, and is locally so intense that the nature of the original lithology is uncertain. Where alteration is less strong, lapilli in the tuffs may be rimmed by halos of either albite, silica or K-feldspar (Figure 6O), and the lapilli fragments partially or totally replaced by various silicates (including tourmaline) or Fe-oxides (Figure 6E and G). The alteration mineral assemblages include albite, K-feldspar, specular and non-specular hematite, tourmaline, chlorite, actinolite, magnetite and apatite, together with extensive developments of massive silica and numerous Cu-Au ± REE ± U occurrences. Dumortierite (Figure 6H) and secondary biotite are sporadically developed, as well as some minor jasper veining. In addition, REE-enriched allanite has been identified with some of the Cu-Au mineralisation (Osterman, 1997). Adjacent to some massive silica zones, the alteration is characterised by veins, up to 5 cm wide, of massive bright green sericite-muscovite. Areas with strong supergene alteration include abundant disseminated kaolin (some of which has been mined) and rare veins of alunite.

Various paragenetic sequences of mineral alteration occur in different parts of the area which reflect the diachronous development of the Productora hydrothermal system. However, the overall mineral paragenesis suggests the system involved the early introduction of Na, followed in turn by K, Si, Fe and B. It ended with widespread Fe and Si metasomatism. The general mineral paragenesis is:

(1) albite, (2) K-spar (3) pervasive silica (4) tourmaline (5) magnetite and/or actinolite (6) specular hematite (7) chlorite and/or epidote (8) jasper veins, and (9) late hematite veins.

The Cu-Au-REE mineralisation was either syn or immediately post the chlorite event (No. 7 above). It postdates the magnetite which accounts for the poor spatial relationship between magnetite and Cu-Au throughout the area.

Alteration Zoning

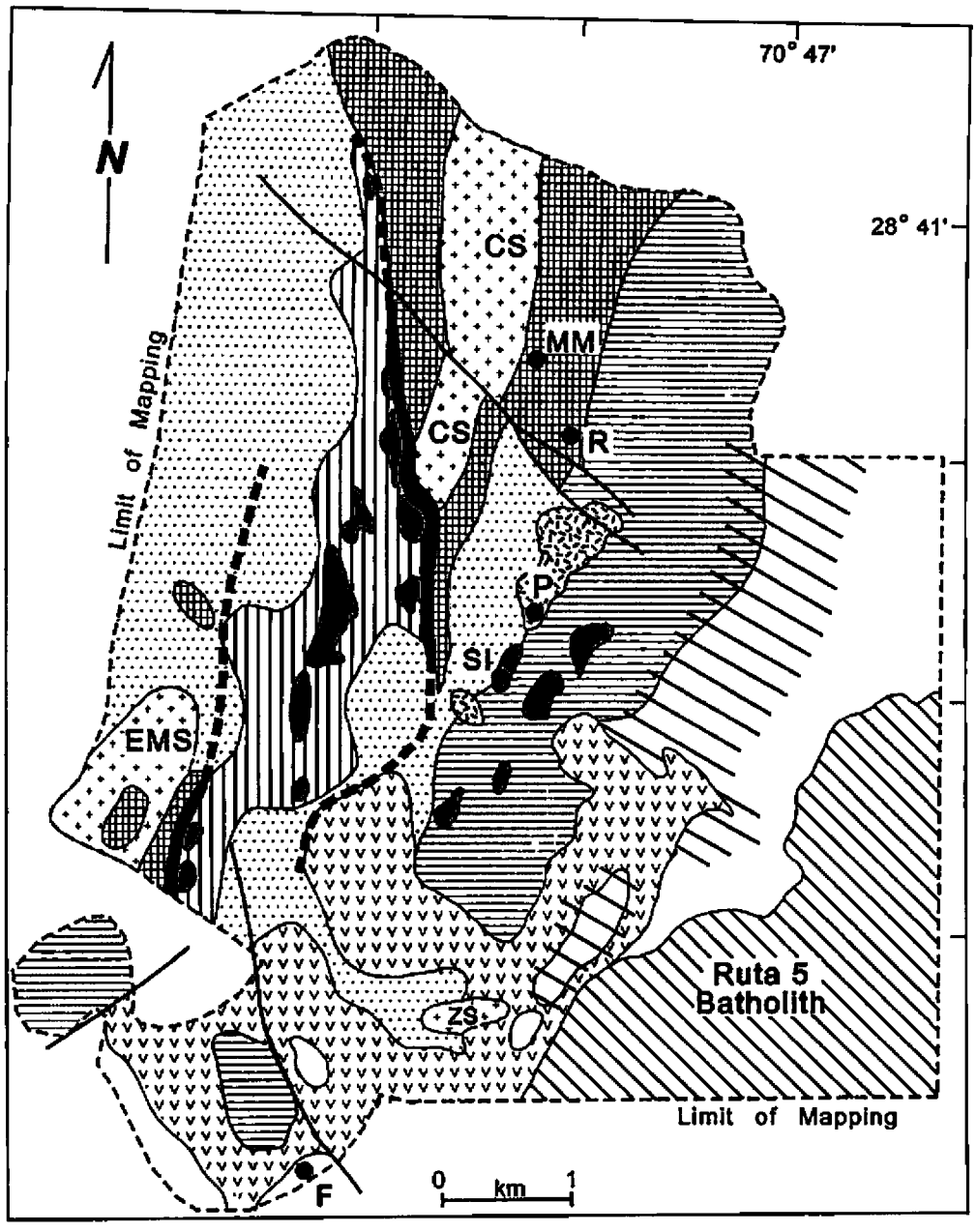
The hydrothermal alteration along the belt can be broadly separated into extensive zones of higher temperature, prograde assemblages (albite, K-spar, tourmaline and some early magnetite), and more restricted areas with lower temperature retrograde assemblages marked by actinolite, chlorite, epidote, hydrothermal biotite, sericite and some late magnetite-hematite. Development of massive silica was protracted and took place as prograde and retrograde events. The pyrite-chalcopyrite mineralisation is temporally and often spatially associated with the retrograde Fe-Mg assemblages.

The prograde alteration appears to be centred and zoned around the Cachiyuyito-age stocks (Figure 4), which suggests that these intrusions and the Productora hydrothermal system are related. However, while some of the retrograde alteration (eg. actinolite, chlorite and late magnetite) is centred around the stocks, most of the better Cu sulphides mineralisation found to date is not. Copper mineralisation appears to be best associated with K-spar ± tourmaline prograde alteration and mainly lies along a N-trending zone that can be discontinuously traced along the east side of the Productora valley (Figure 4).

The intensity and nature of the prograde and retrograde alteration assemblages throughout the belt were strongly influenced by a number of factors including:

1. the presence of controlling NW and, to a lesser extent, N to NNE-trending faults,
2. distance from either the structural conduits or the stocks, and
3. the composition and permeability of the original host-rocks. Mafic volcanics and tuffs, tend to produce epidote-chlorite-actinolite-rich assemblages while the Fe-poor dacitic tuffs tend to be more readily overprinted by albite, K-spar and silica alteration.

Most of the prograde and retrograde alteration along the belt appears to follow the original, gently dipping stratigraphy, which suggests that rock permeability was an overall important controlling factor. This is seen, for example, along the Silica Ridges (Figure 2) where fluids have passed selectively along certain permeable tuffaceous horizons to produce thick, gently dipping zones of massive silica. Elsewhere, however, alteration crosscuts the stratigraphy at a high angle, probably due to the influence of steeply dipping structural conduits.



Cover

Ruta 5 Batholith

Epidote-silica ± garnet (possibly related to the Ruta 5 Batholith)

Mafic flows. Propyllitic alteration ± albite ± local silica

ZONE I ALTERATION

Albitized stocks ± actinolite, magnetite and epidote veins

ZONE II ALTERATION

Magnetite-chlorite-actinolite-apatite with remnant albite

ZONE III ALTERATION

Pink K-spar ± tourmaline ± silica

ZONE IV ALTERATION

Bleached, albitized & silicified rocks ± epidote ± hematite

ZONE V ALTERATION

Quartz-sericite schist: outcrop/assumed

Massive silica

Disseminated sericite and specular hematite ± kaolin ± dumortierite

STOCKS

CS Cachiyuyito
ZS Zapallo
EMS El Molle

Cu-Au MINES

● **P** Productora Mine
● **SI** Santa Innes Mine
● **MM** Monseratt Mine
● **R** Remolina Pit
● **F** Fortuna Mine

Figure 4: Distribution of hydrothermal alteration on the Productora Prospect

Table 1: Major and trace element data of altered plutonic & tuffaceous rocks, Productora

	CACHIYUYITO STOCK (Zone I-type alteration)						Zone III-type alteration				Zone IV-type alteration					
Sample No.	GR 15	GR102	GR103	GR105	GR106	GR123	71416	71417	71421	71422	GR159	GR 232	GR244	71411	71414	71415
SiO_2	59.04	71.04	73.83	66.98	60.74	64.47	69.29	66.84	69.02	65.34	74.43	68.89	74.54	70.15	75.64	74.75
$Al2O_3$	17.32	15.27	13.99	18.19	15.61	17.23	12.87	12.85	12.03	12.38	13.69	17.46	13.80	13.81	13.29	13.37
$Fe2O_3$	3.34	1.51	1.70	2.03	4.35	3.45	2.12	4.11	2.91	5.25	1.72	1.13	1.19	1.07	0.55	0.95
MgO	3.50	0.79	0.57	0.27	2.90	2.22	0.73	0.67	0.57	3.08	0.53	0.30	0.25	0.19	0.19	0.18
CaO	7.06	2.85	1.48	3.52	7.41	2.23	0.54	0.28	1.9	2.24	0.34	0.65	0.50	2.34	0.37	0.43
Na_2O	5.61	5.81	6.66	5.49	4.09	7.39	0.41	0.34	2.25	2.41	7.06	9.13	6.88	8.02	7.52	7.7
K_2O	1.34	0.82	0.26	1.04	2.56	0.97	11.51	12.9	7.9	5.64	0.37	0.60	0.45	0.54	0.89	0.37
TiO_2	1.14	0.67	0.35	1.23	1.03	0.53	0.32	0.34	0.37	0.54	0.29	0.41	0.29	0.51	0.29	0.51
P_2O_5	0.04	0.05	0.06	0.01	0.17	0.02	0.21	< .01	0.07	0.14	0.12	0.12	0.12	0.13	0.05	0.05
MnO	0.14	0.04	0.02	0.07	0.11	0.10	0.02	0.02	0.03	0.06	0.02	0.01	0.01	0.1	0.01	0.02
LOI	1.80	1.20	1.00	1.40	1.20	1.60	1.40	1.10	2.30	2.30	1.30	1.30	1.60	2.60	1.10	1.60
S	0.15	0.08	0.01	0.04	0.02	0.03	0.04	0.02	0.86	0.08	0.01	0.01	0.01	< .01	< .01	0.04
Sum	100.48	100.13	99.93	100.27	100.19	100.24	99.46	99.47	100.21	99.46	99.88	100.01	99.64	99.46	99.90	99.97
Total alk	6.95	6.63	6.92	6.53	6.65	8.36	11.92	13.24	10.15	8.05	7.43	9.73	7.33	8.56	8.41	8.07
Na/K	4.19	7.09	25.62	5.28	1.60	7.62	0.04	0.03	0.28	0.43	19.08	15.22	15.29	14.85	8.45	20.81
Ba	117	59	15	144	527	71	1260	1279	1537	805	47	45	157	45	112	86
Ni	20	25	28	24	25	22	NA	NA	NA	NA	24	20	34	NA	NA	NA
Zr	126	275	139	261	173	123	125	106	103	121	117	178	127	168	131	115
Y	20	12	13	10	27	10	11	6	16	28	10	12	17	39	11	16
Sc	22	12	10	10	16	10	10	4	5	9	10	10	10	8	6	7
Nb	2	4	3	6	5	2	3	5	6	6	3	4	5	10	5	4
Rb	30	10	1	12	46	14	NA	NA	NA	NA	8	10	10	NA	NA	NA
La	4	6	12	2	3	3	NA	NA	NA	NA	23	1	11	NA	NA	NA
Cr	31	71	51	34	65	24	NA	NA	NA	NA	116	61	127	NA	NA	NA
V	18	29	32	15	77	23	NA	NA	NA	NA	17	10	11	NA	NA	NA
Th	2	26	20	2	10	6	NA	NA	NA	NA	5	7	6	NA	NA	NA
Sr	33	21	16	24	36	10	64	65	70	79	5	6	13	29	23	27

CACHIYUYITO STOCK (Zone I-type alteration)

GR 15 Porphyritic tonalite with actinolite veins
GR102 Feldspathic & silicified diorite-tonalite
GR103 Feldspathic & silicified hornblende tonalite
GR105 Feldspathic hornblende-quartz bearing tonalite
GR106 Hornblende-quartz bearing diorite with minor late K-spar
GR123 Feldpathic, hornblende bearing tonalite

Zone III-type alteration (K spar-silica-tourmaline)

71416 K spar-silica-tourmaline altered tuff, NNE of Productora Mine, UTM 323975; 6823035
71417 K spar-silica-tourmaline altered tuff, NNE of Productora Mine, UTM 323958; 6823071
71421 K spar altered tuffs, hole PR 24 @ 210-212m, UTM 323887; 6823105
71422 K spar altered tuffs, hole PR 24 @ 138-140m, UTM 323887; 6823105

Zone IV-type alteration (albite-silica)

GR159 White, albitized & silicified tuffs, north Productora Basin
GR 232 Albitized dacitic tuff west of Cachiyuyito Ranch
GR 244 Silicified & albitized dacitic tuff, Productora Mine trench
71411 Silicified & albitized tuff, NNW of Zapallo, UTM 334055; 6900566
71414 Albite-silica altered dacitic lapilli tuff, NNE of Productora Mine, UTM 324144; 6822956
71415 Albite-silica altered dacitic lapilli tuff, NNE of Productora Mine, UTM 323983; 6822844

Analyses at ACME Analytical Laboratories, Santiago, Chile.
Major elements by XRF, minor elements by ICP.
Major elements in percent; trace elements in ppm.
NA = elements not determined.

Six proximal to distal zones of mineral alteration are recognised together with at least three different styles of mineralisation (Figure 8). The mineralogy and width of individual alteration zones reflect depth and proximity to the Cachiyuyito-type stocks as well as the composition and pervasive character of the original host-rocks. The mineral zoning is as follows (Figures 4 and 8):

Zone I is represented by the pervasively albitised Cachiyuyito-type stocks with veins of actinolite, quartz, epidote and magnetite (Figure 6C and I).

Zone II includes pervasive early albitisation, overprinted by actinolite-rich alteration with magnetite ± apatite ± actinolite veins and breccias (Figure 6K and L), together with abundant retrograde epidote, chlorite and coarse crystalline calcite veining. This is best seen adjacent to the Cachiyuyito and El Molle stocks. It hosts a number of magnetite occurrences, including the La Negrita, La Mariposa, La Bandera and La Chulula magnetite mines (Figure 3).

Zone III is characterised by pervasive pink K-feldspar and tourmaline ± pervasive silica ± veins of magnetite-hematite. This alteration occurs with local retrograde epidote-chlorite, secondary biotite and Fe and Cu sulphides. It outcrops as a belt along the east side of the Productora valley (Figure 4), and is characterised by low Na/K ratios (<0.43; Table 1), numerous Cu ± Au ± U ± REE occurrences, and hosts the Productora and Santa Innes mines mineralisation. Although

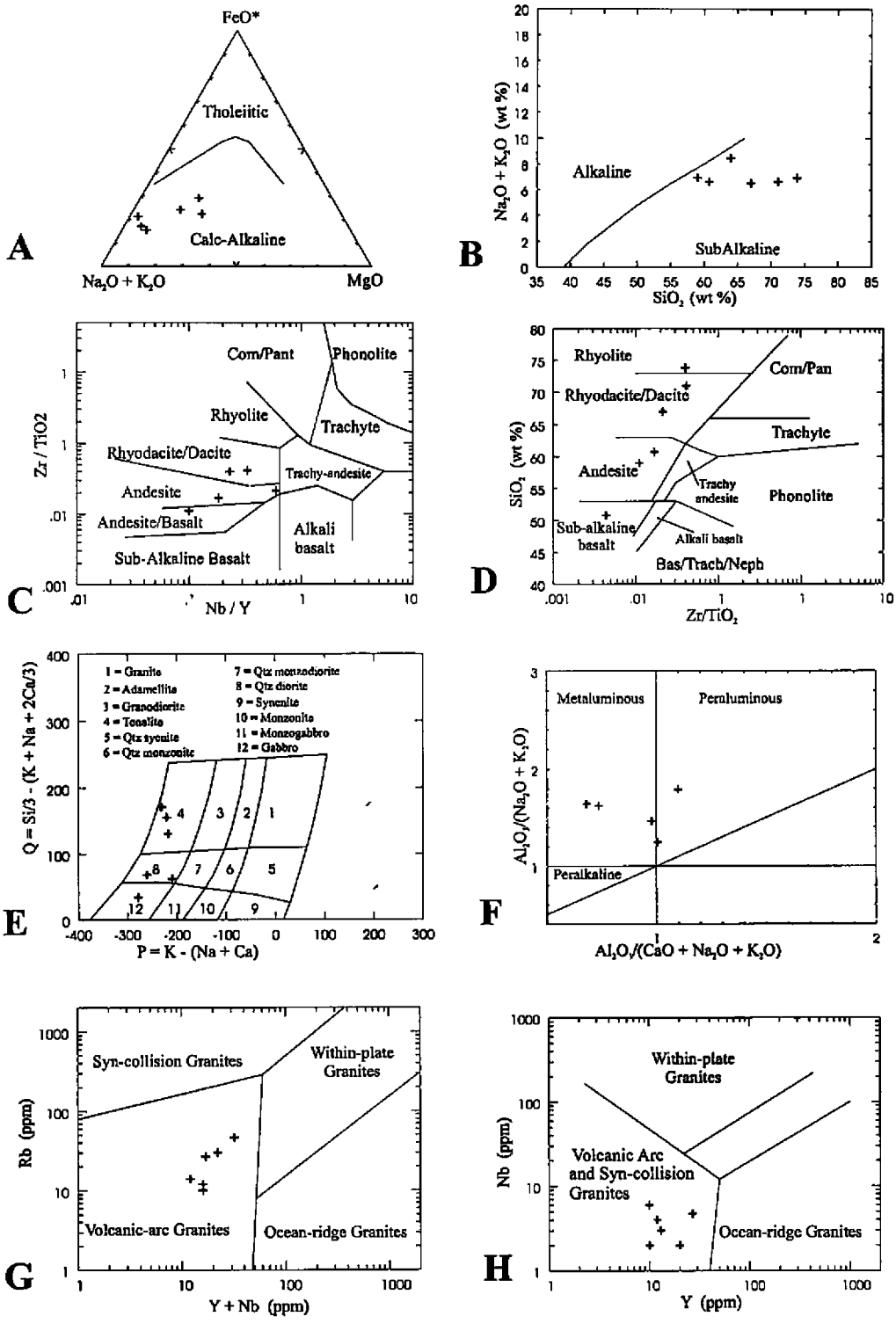


Figure 5: Major and trace element plots of the Cachiyuyito Stock (data from Table 1)

A & B: AFM & alkali-silica plot (after Irvine and Baragar 1971).
C: Zr/TiO_2 versus Nb/Y discrimination plot (after Winchester & Floyd, 1977).
D: SiO_2 versus Zr/TiO_2 discrimination plot (after Winchester & Floyd, 1977).
E: Q - P plot (after Debon and Le Fort, 1983).
F: Aluminium saturation plot (after Maniar and Piccolli, 1989).
G: Log Rb versus Log Y+Nb tectonic discrimination plot (after Pearce et al., 1984).
H: Log Nb versus Log Y tectonic discrimination plot (after Pearce et al., 1984).

isolated and widespread veins of black tourmaline occur in Zones I and II, in Zone III assemblages the mineral may locally form > 50 % of the rock. Tourmaline occurs mostly in veins (Figure 6D and F), many of which are controlled by fractures related to the north and NW-trending fault sets. However, in Zone III tourmaline also occurs as disseminations, as selective replacements of lapilli and in breccias where fragments of silicified pink K-spar are enclosed in a matrix of massive black tourmaline (Figure 6E and F). Intense tourmaline alteration is always spatially associated with abundant pink K-spar, although the latter mineral is invariably older. There is also a tendency for Cu oxide showings to be more common in areas with intense tourmaline and K-spar alteration.

Zone IV is marked by intense bleaching because virtually all the primary mafic minerals have been removed and replaced by albite and silica ± epidote ± specular hematite (Figure 6G). The amount of epidote present depends on the original host-rocks; epidote is abundant (up to 10%) in the bleached middle unit basalts but is generally absent in the altered dacitic tuffs. This extensive alteration is seen on the slopes east of the Productora and Santa Innes mine, as well as in the south part of the belt (Figure 4). It is marked by high Na/K ratios (8-20; Table 1).

Zone V is characterised by replacement zones of massive pale coloured silica ± disseminated white sericite ± specular hematite ± pyrite ± green sericite-muscovite veins. Generally, the silicification is so strong that no original tuffaceous or sedimentary textures are recognisable, although in rare cases remnant bedding or layering are seen (Figure 6M). Where the narrow, N-trending quartz-sericite schist zones cut the silica alteration, sporadic veins of dumortierite and alunite are developed (Figure 6H). This higher-level alteration, which includes that present along the Silica Ridges, is best displayed in the 1.5 km-wide, down-faulted block that separates the El Molle and Cachiyuyito stocks (Figures 3 and 4). In surface outcrops, most of the original disseminated pyrite (Figure 6N) has been leached and replaced by hematite-jarosite.

Zone VI. Rocks in the very highest or most distal parts of the system are weakly to moderately bleached and propylitically altered with epidote, chlorite and sporadic silica, minor albite and rare veins of jasper. Lapilli in the tuffs may be haloed by pale rims of silica or albite alteration (Figure 6O). This outer propylitic zone hosts veins and small irregular mantos of massive magnetite and/or hematite (Figure 8) some of which contain anomalous amounts of Cu, Au, Zn, Pb, Ag, Co and Mn (Table 2).

Mineralisation

The following three styles of Fe-oxide dominant mineralisation are identified in the Productora area, each of which tends to occur in a specific alteration zone (Figure 8):

Style 1, which is the most proximal and common, is represented by magnetite veins and replacements associated with Zone II-type actinolite-chlorite-epidote ± apatite assemblages, as well as thin veins of coarse calcite. This style of mineralisation seldom contains significant Cu or Au values and examples include the Mariposa, La Bandera, La Chulula, La Negrita and the El Molle mines (Figure 3). Apatite may occur in fine disseminations, in pegmatite-like veins where it is intergrown with coarse grained actinolite, or in irregular breccia bodies where it forms brecciated fragments enclosed in a magnetite-actinolite matrix (Figure 6K and L).

Style 2 mineralisation is typified by the Cu-Au ± REE ± U occurrences seen at the Productora and Santa Innes mines (Figure 3). It appears to be more commonly associated with Zone III alteration (K-spar, silica and tourmaline) but in the case of the Monseratt Mine and Remolina pit it is hosted by Zone II mineral assemblages. It is dominated by secondary Cu minerals; malachite, chalcocite, chrysocolla, brochantite, tenorite and turquoise have been tentatively identified, and rare native Cu is reported. Hypogene mineralisation in the deeper pits and mines comprises disseminations and veinlets of chalcopyrite, some of which cut and post-date the pyrite (Fox, 2000). Microprobe studies (Osterman, 1997) recognised an association between chalcopyrite and allanite; the latter mineral contains up to several percent combined REE's (Ce, La, Nd, Pr, Sm, Yb and Gd). This study also noted that the chalcopyrite and chalcocite occur with variable amounts of pyrite, covellite, apatite and minute grains of molybdenite.

Chalcocite is common at the Monseratt and Productora mines; at the latter property it appears to form a blanket beneath a leached, argillised horizon that contains Cu and U oxides. Some chalcocite grains contain up to 5% Co but no cobalt minerals have been identified (Osterman, 1997). There are several generations of Au, including a very late supergene phase which overgrows coatings of black Cu-Mn oxides at the Productora Mine. Most of the near surface supergene and hypogene Cu mineralisation is fracture controlled, although in the deeper parts of the Productora and Monseratt mines some mineralisation is disseminated and stratiform.

The assay results of Style 2 mineralised grab samples from some of the Cu mines and pits in the area and examples of the Cu mineralisation intercepted by drilling are shown in Tables 2 and 3 respectively. Most of the Cu mineralisation contains between 200 and 600 ppb Au, although Au values up to 9.7 g/t Au are present locally. In the hypogene mineralisation a good correlation exists between Cu:Au, Cu:Co and Co:V. However, no positive relationship between Au and Cu is seen in the oxide ore. The Cu ±Au mineralisation is sporadically anomalous in Mo, Co, Zn, U, La and P (Table 2). The highest REE values occur in hypogene and supergene mineralisation at the Productora and Monseratt mines where samples containing up to 563

ppm La are recorded. There is also a good positive correlation between La:P, indicating that some of the REE's are held in the apatite. The U oxide, torbernite, occurs in veinlets but the low Th content of the mineralised rocks sampled (maximum 12 ppm) suggests that no primary U minerals are present.

Sulphur isotope ratios were determined for chalcopyrite, pyrite and chalcocite collected from Style 2-type mineralisation along the eastern margin of the Productora valley (Fox, 2000). The isotopic ratios for these minerals show a range of $\delta^{34}S$ values from -8.2 to +1.2 which is lower than values recorded for the Punta del Cobre region where they range from -0.7 to +1.1 (Marschik, 1996). At Productora, pyrite and chalcopyrite average -3.5 and -1.8 respectively, and Fox (2000) notes that the absence of isotopically heavy values suggests that the sulphur was not derived from an evaporitic source, as modelled for some other worldwide Fe oxide deposits (Barton and Johnson, 1996).

Style 3 mineralisation is developed in the propylitically altered, upper and outermost parts of the Productora hydrothermal system (Figure 8). It consists of generally small veins, irregular replacements and mantos dominated by massive magnetite and/or hematite that is commonly associated with epidote, albite and silica

Figure 6: Photographs showing various aspects of the Productora Prospect:

A: View looking south down the northern basin of the Productora valley. Note the locations of the Productora Mine and the north-trending Quebrada Verde Fault. This structure separates the basin from the Silica Ridge further west. The northwest-trending cross-structure, the Rancho Fault, is in foreground.

B: View looking north from the Productora Mine. The northern basin is bounded to the north and west respectively by the Rancho and Quebrada Verde faults. Note the ridge underlain by the Cachiyuyito Stock (CS) and the location of the Monseratt Mine (MM).

C: Zone I alteration. Magnetite veinlets cutting the altered Cachiyuyito Stock, 1.75 km north-northwest of the Productora Mine.

D: Zone III alteration. Narrow veins of black tourmaline cutting pink K-spar and silica altered tuffs. Located on the eastern edge of the northern Productora basin, approximately 800 m southeast of the Cachiyuyito Ranch (Figure 2).

E: Zone III alteration. Black tourmaline selectively replacing lapilli fragments in a K-spar and silicified lapilli tuff. Length of photo represents 45 cm. Located 330 m south-southwest of the Santa Innes Mine.

F: Zone III alteration. Intensely K-spar-altered and silicified pink tuffs, brecciated and cut by a black tourmaline vein. Located 330 m southwest of the Santa Innes Mine.

G: Zone IV alteration. Bleached, silicified and strongly albitized dacitic tuff with some lapilli selectively replaced by specular hematite. Located 950 m east of the Santa Innes Mine at UTM 324540E; 6822150N.

H: Zone V alteration. Massive silica cut by veins of blue dumortierite. Located on the south segment of Silica Ridge at UTM 321030E; 6821190N.

I: Zone I alteration. Albitized Cachiyuyito Stock cut by intersecting sets of dark actinolite veins, 1.75 km north-northwest of the Productora Mine.

J: Small-scale surface mining of Cu-oxides and phosphates along northwest-trending fractures that cut albitized and silicified tuffs. Note the seated figure in trench for scale. Workings lie south of the El Molle magnetite Mine at UTM 320785E-6820026N.

K: Zone II alteration. Apatite-magnetite breccia with rounded to angular clasts of pale apatite in a dark matrix of magnetite and minor hematite. Float from a small pit located north of the Rancho Fault at UTM 323994E-6824599N.

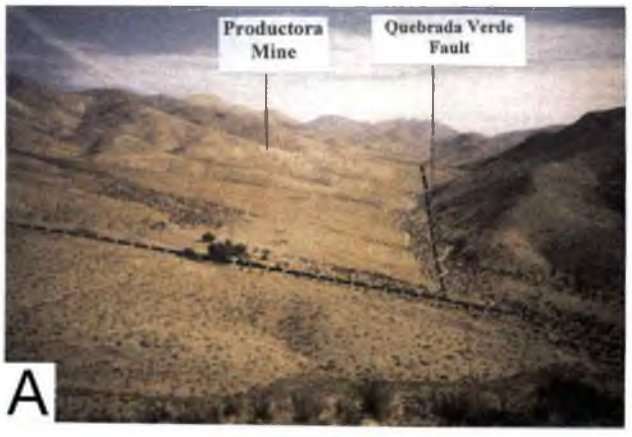
L: Zone II alteration. East-striking pegmatitic vein containing elongate crystals of dark actinolite and pale apatite that have grown normal to the vein margins. The 2 m-wide vein is located 950 m northeast of the Cachiyuyito Ranch (*see* Figure 2).

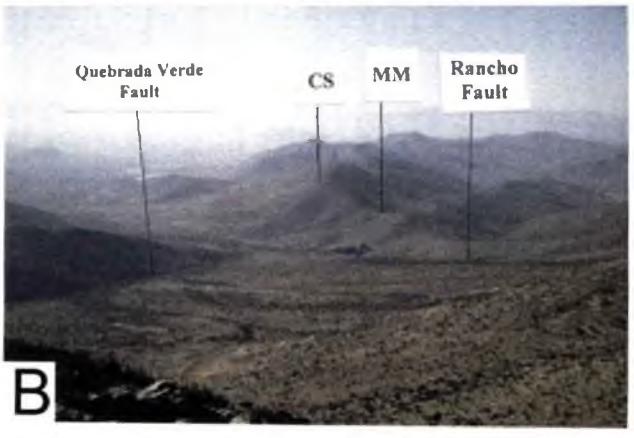
M: Zone V alteration. Massive pale silica showing remnant tuffaceous layering. Boulder float near the central segment of the Silica Ridge, UTM 322211E-6823137N.

N: Zone V alteration. Euhedral, coarse-grained crystals of pyrite in massive silica. Located on the north segment of Silica Ridge, 1.6 km NW of the Santa Innes Mine.

O: Zone VI alteration. Hydrothermally altered andesitic lapilli tuff and tuff breccia. Dark, angular to sub-angular clasts of andesite with pale alteration halos of silica and albite. Located on ridge southwest of Quebrada Escondido at UTM 321031E- 6818271N (*see* Figure 2).

P: Hematitic breccia containing pale silica-albite-altered clasts cemented by a dark, earthy hematite with sulphide boxwork. Located west of the Quebrada Escondido at UTM 320016E-6819354N (*see* Figure 2).

















Continued on page 145

Reverse of colour plate, intentionally blank

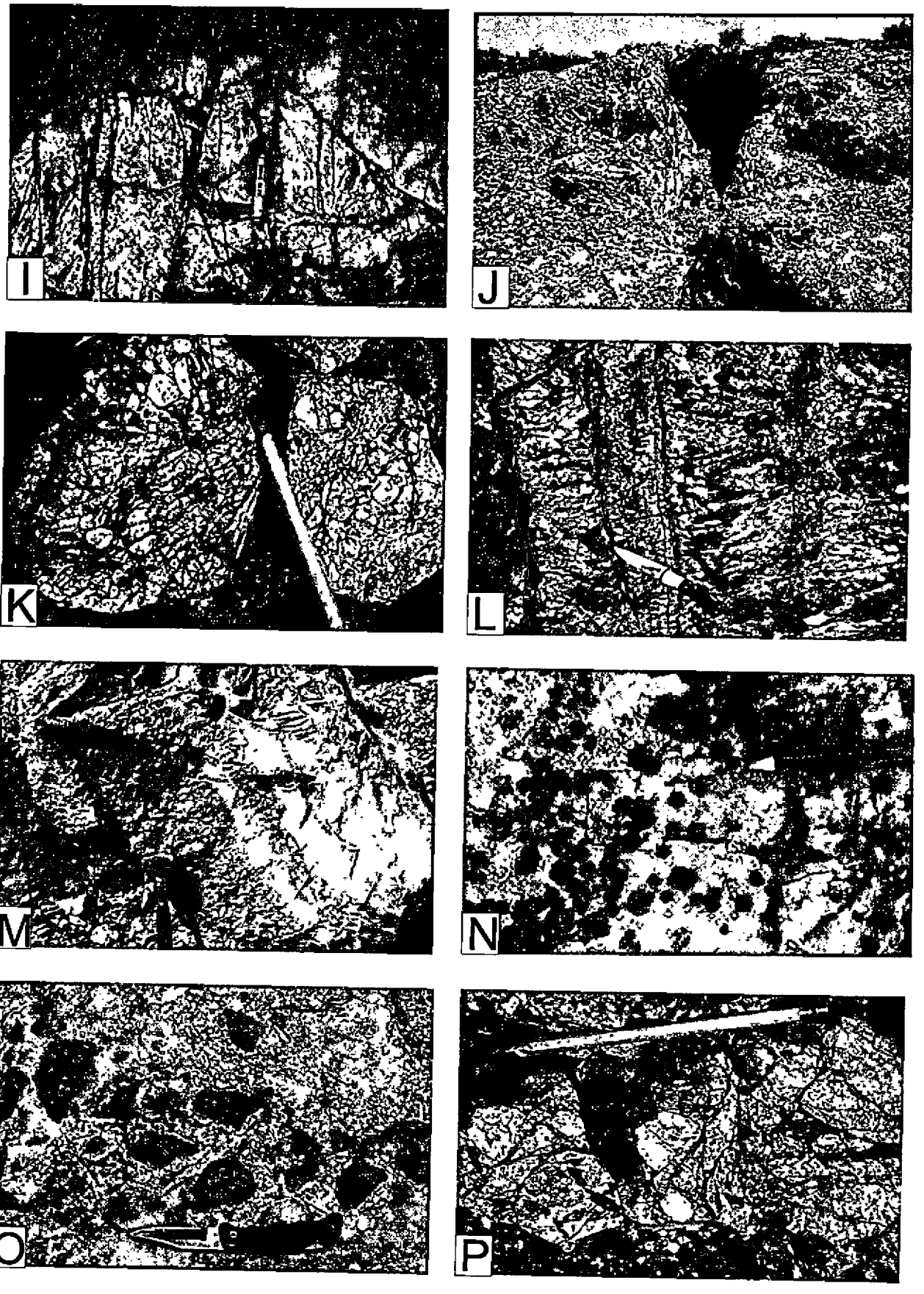
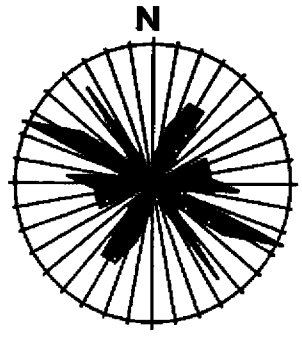
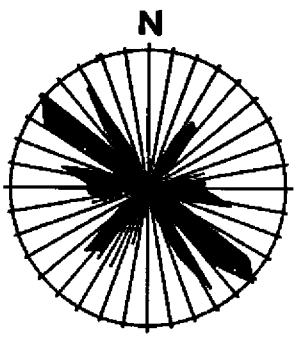


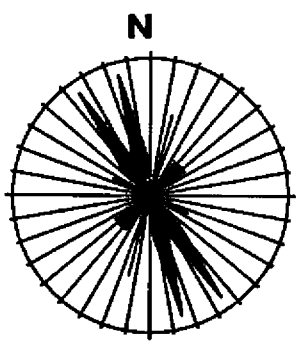
Figure 6: Continued from page 143. See caption on p. 142.



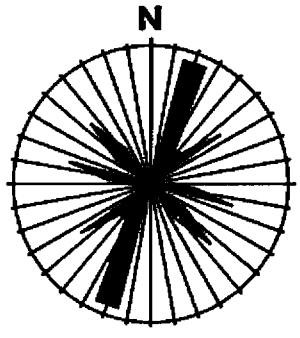
Area 1
N = 34
Mean = 63 degrees N



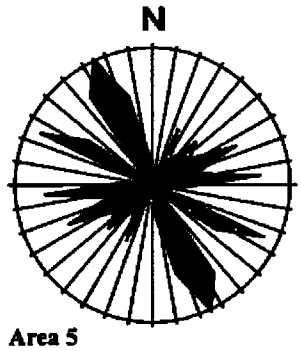
Area 2
N = 45
Mean = 135 degrees N



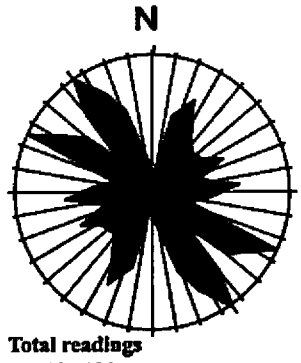
Area 3
N = 15
Mean = 173 degrees N



Area 4
N = 18
Mean = 69 degrees N



Area 5
N = 74
Mean = 146 degrees N



Total readings
N = 186
Mean = 129 degrees N

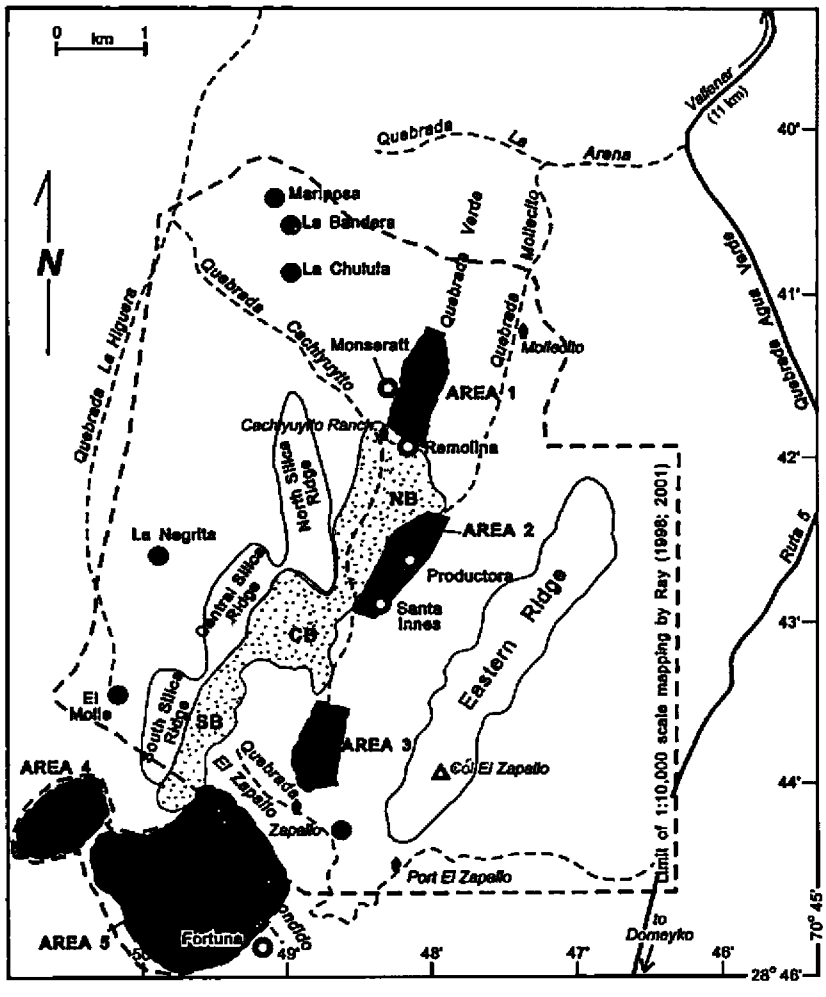


Figure 7: Rose diagrams showing the main strike of fractures controlling the Fe and/or Cu oxides, K spar, silica, actinolite or tourmaline veins in five parts of the Productora Prospect. Note the variations in vein orientation throughout the prospect and the abundance of the NW-trending vein set. See Figure 2 for map legend.

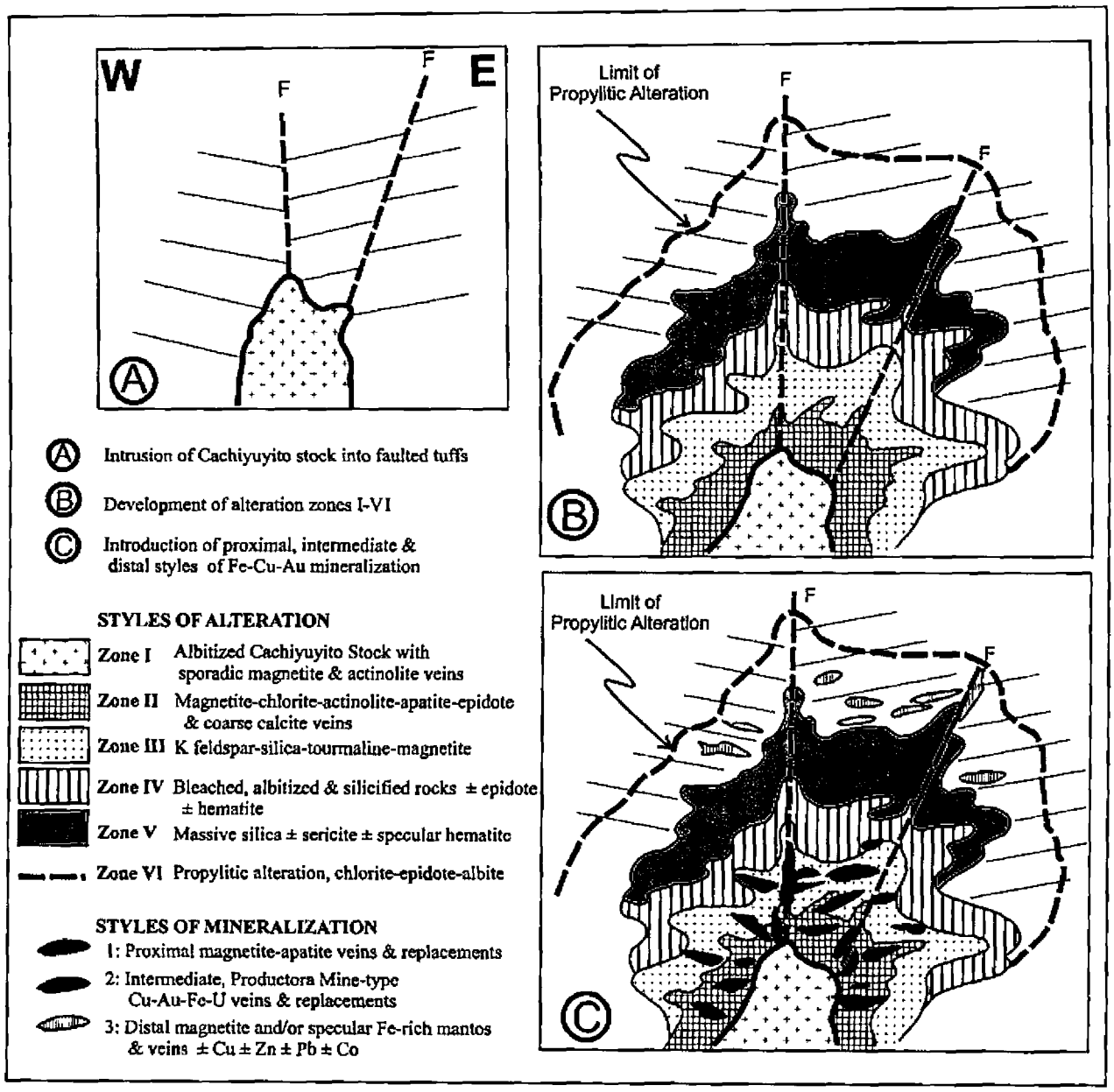


Figure 8: Model showing the distribution of the alteration zones at Productora and location of various styles of Fe oxide ± Cu ± Au mineralization.

alteration together with minor jasper veining. Locally, these Style 3 occurrences contain minor pyrite and trace chalcopyrite together with Cu oxides and phosphates. Assays indicate that this distal type of mineralisation may contain anomalous quantities of Cu, Au, Zn, As, Co, Pb and Mn (Table 2).

Discussion and Conclusions

The age, structural setting, alteration assemblages and varied styles of mineralisation in the Productora area are similar to those present at the Pajaritos property (Ray, 1997b), the Candelaria Cu-Au deposit and other Fe oxide-Cu-Au occurrences in the Punta del Cobre belt further north (Figure 1; Ryan et al., 1995; Marschik and Fontboté, 1996, Marschik et al., 1996, 2000). However, the alteration and Fe oxide mineralisation at Productora differ from Candelaria in their clear spatial association with intrusive rocks and their lack of garnet-pyroxene-scapolite skarn assemblages; these differences may reflect deeper erosion at Productora and the absence of calcareous host-rocks.

Certain aspects of the alteration at Productora (eg. K-spar, secondary biotite, tourmaline, dumortierite and green sericite-muscovite veins) resemble those present in certain Au and magnetite-rich Cu porphyry systems, such as the Highland Valley and Island Copper deposits in British Columbia, and the Los Pelambres porphyry in Chile (Perello et al., 1995; Casselman et al., 1995: Atkinson et al., 1996). However, other features such as the presence of abundant Fe oxides, together with apatite, allanite, anomalous Au, REE's and U, are similar to those described in deposits of the Fe oxide-Cu-Au family (Williams, 1998).

Studies by workers such as Oreskes and Einaudi (1990), Einaudi and Oreskes (1990), Vidal et al. (1990), Hitzman et al. (1992), Oreskes and Hitzman (1993) and Williams

Table 2: Analytical data of mineralized samples, Productora.

Sample	GR-36	GR-84	GR-124	GR-155	GR-209	GR-257	GR-258	GR-260	46510	46519	46520
Au	609	16	203	3061	9730	23	303	218	161	402	137
Mo	10	2	128	9	9	4	180	571	128	52	27
Cu	16279	2734	42592	22904	26659	15274	14772	37753	11981	4447	2316
Ag	0.9	0.3	0.3	1.1	2.0	0.3	1.1	1.5	0.3	0.5	0.3
Ni	148	437	327	19	114	16	60	340	7	18	12
Co	88	497	832	17	97	23	149	660	33	118	30
As	63	18	77	13	27	7	56	93	7	10	8
U	10	8	8	30	8	8	8	8	8	8	8
Th	3	5	2	2	12	6	3	2	8	5	5
Sr	15	19	166	22	11	11	11	15	17	21	16
V	1297	329	304	194	1033	154	176	271	6	58	44
P	0.98	0.18	0.39	0.07	0.54	0.16	0.12	0.13	0.02	0.07	0.06
La	2	28	498	26	37	219	25	52	5	347	563
Cr	25	56	51	48	13	112	66	27	47	11	18
Ba	12	21	8	33	12	8	7	9	130	140	145
Ti	0.08	0.16	0.02	0.12	0.01	0.01	0.01	0.01	0.01	0.02	0.02
B	3	45	3	11	3	12	9	6	71	6	8
Pb	9	3	7	11	33	3	3	12	NA	NA	NA
Zn	27	76	13	57	126	27	67	19	NA	NA	NA

Sample	71326	71350	71314	71348	71404	71408	71410	71412	71413	71418	71420
Au	1105	350	594	20	989	195	173	10	43	134	3440
Mo	21	42	< 1	3	69	2	11	3	52	130	6
Cu	32246	56771	26070	14731	22072	21864	19537	9644	27029	6527	26318
Ag	2	0.5	5.1	1.6	2.7	3.5	0.8	1.2	< .3	0.4	2
Ni	81	95	24	9	29	227	1173	19	83	16	4
Co	265	125	72	44	391	246	1240	160	904	46	7
As	489	575	< 2	25	95	73	23	8	7	13	13
U	< 8	< 8	< 8	< 8	< 8	40	< 8	< 8	< 8	< 8	< 8
Th	< 2	3	< 2	< 2	5	9	6	< 2	< 2	8	2
Sr	11	31	6	63	24	29	18	5	8	13	23
V	416	93	75	110	284	679	520	70	169	54	59
P	0.02	0.06	< .001	0.02	0.04	0.94	0.25	0.13	0.02	0.09	0.07
La	3	< 1	3	3	26	23	30	4	3	76	3
Cr	29	15	17	81	40	43	38	17	18	39	45
Ba	3	2	23	1	10	6	29	3	7	77	17
Ti	0.04	< .01	0.01	0.12	0.1	0.05	0.07	0.07	0.06	0.05	0.05
B	3	7	35	3	14	11	8	< 3	4	3	< 3
Pb	87	48	1237	73	13	56	4	8	4	4	< 3
Zn	47	21	7803	1193	48	88	197	81	83	17	12

Au in ppb; Ti & P in %; All other elements in ppm: Analytical methods: Au by MIBK; other elements by ICP
Analyses by ACME Analytical Laboratories, Santaigo, Chile
Sample descriptions:

GR-36 Altered tuff with magnetite & apatite veins & Cu oxides; 300m north of Productora Mine.
GR-84 Highly altered tuff with minor tourmaline & Cu oxides; adjacent to the Zapallo Stock.
GR-124 Hematite-magnetite-Cu oxide ore, Monseratt Mine.
GR-155 Altered tuff with Cu oxides; 400m NE of Productora Mine.
GR-209 Chalcopyrite-cuprite-magnetite ore: pit 900m NE of Monseratt Mine.
GR-257 Albite-actinolite-altered tuff with Cu oxides; Remolina Pit.
GR-258 Albite-actinolite-altered tuff with magnetite & Cu oxides; small pit 700m south of Monseratt Mine.
GR-260 Chalcopyrite-chalcocite-magnetite ore; Monseratt Mine.
46510 Altered, tourmaline-bearing tuff with Cu oxides, trench at Productora Mine.
46519 Altered tuff with Cu oxides; trench at Productora Mine.
46520 Altered tuff with Cu oxides; trench at Productora Mine.
71326 Cu oxides with epidote & chlorite. South of El Molle Mine, UTM 320557; 6819626
71350 Cu oxides from pit. South of El Molle Mine, UTM 320459; 6819783
71314 Massive magnetite float with Cu oxides, west of Quebrada Escondido, UTM 321506; 6819229
71348 Cu oxides with epidote, calcite & magnetite, SW of Zapallo, UTM 322156; 6819863
71404 Massive specular hematite-magnetite with Cu oxides. West of Quebrada Escondido, UTM 321094; 6818208
71408 Hematite-magnetite with Cu oxides. NE of Zapallo, UTM 322893; 6820344
71410 Albite with hematite-magnetite & Cu oxides. NE of Zapallo, UTM 323002; 6820251
71412 Magnetite-hematite with actinolite, Cu oxides & pyrite. North of the Rancho Fault, UTM 323905; 6824821
71413 Actinolite-chlorite with magnetite & Cu oxides. North of the Rancho Fault, UTM 323867; 6824772
71418 K spar-silica alteration with pyrite & Cu oxides. North of Productora Mine, UTM 323952; 6823111
71420 Cu-oxides with specular hematite. Fortuna Mine, UTM 322241; 6817884

(1998), and summarised by Ray and Lefebure (2000), suggest that this Fe oxide family is worldwide and includes the Olympic Dam and Ernest Henry deposits in Australia, Kiruna in Sweden, and those in the Chilean and Peruvian Iron belts such as Candelaria, El Romeral, Manto Verde, Productora, Condestable, Raul and Eliana. The idea that these varied deposits share any family link is controversial, which is hardly surprising given the wide variation in their ages, tectonic settings and non-ferrous metal contents. However, there is now increasing evidence that the ideas presented by early workers such as Hitzman et al. (1992) are valid and that the Fe oxide-Cu-Au family represents a spectrum of hydrothermal deposits that varies from magnetite ± apatite systems which are barren of economic Cu and Au (eg. Kirunavaara; El Romeral) to more sulfide-rich Fe oxide-Cu ± U ± Au ± REE ± apatite-bearing examples as seen at Olympic Dam and Candelaria. Candelaria, Productora and Pajaritos (Figure 1) probably represent a subtype of this family; they differ notably from the better known Proterozoic examples by their younger ages, the presence of B-rich alteration, and their development in a volcanic back-arc rather than a continental crustal environment.

Acknowledgements

We thank General Minerals Corporation President, Mr. R. Fitch, for permission to publish this data. Discussions with the following people are appreciated: R. Arcos, A.C. Correa, W.C. Cuadra, K.A. Fox, M.W. Hitzman, D. Jones, A.R. King, F. Malbran, D. Maus, C. Osterman, W. Palma, A. Pope, J. Skokan, J.F.H. Thompson, J. Toohey and I.C.L. Webster. We thank M.A. Fournier for drafting some of the figures and Rene Aguillar and Celso Carvajal for assistance in the field.

Table 3: Examples of mineralised drill intersections at the Productora property.

Hole	From (metres)	To (metres)	Length (metres)	Average Cu (%)
S1-7	27.5	48	20.5	1.01
S1-11	31.5	44.5	13	1.13
PR-2	68	140	72	0.60
including	68	92	24	0.93
PR-5	52	96	44	0.72
including	84	96	12	1.23
PR-7	96	140	44	0.41
S8-4	0	25	25	0.75
S8-5	7	40	33	0.97
including	21	36.5	15.5	1.44
PR-9	102	214	112	0.65
including	102	130	28	1.00
PR-13	200	316	116	0.41

References

Atkinson, W.W., Souviron, A., Vehrs, T.I., and Faunes, G., 1996 - Geology and mineral zoning of the Los Pelambres porphyry copper deposit, Chile. *In* Andean copper deposits: new discoveries, mineralization, style and metallogeny, *Society of Economic Geologists Special Publication No. 5*, Camus, F., Sillitoe, R.H., and Peterson, R., eds. 1996, pages 131-155.

Aguirre, L., Charrier, R., Daidson, J., Mpodozis, A., Rivano, S., Thiele, R., Tidy, E., Vergara., and Vincente, J.C., 1974 - Andean Magmatism: its palegeography and structural setting in the central part (30-35°S) of the Southern Andes. *Pacific Geology*, Volume 8, pages 1-38.

Arcos, R., 1998 - Productora. monthly field report. Unpublished report, *General Minerals Corporation*, May 1998, 3 pages.

Barton, M.D., and Johnson, D.A., 1996 - Evaporite-source model for igneous-related Fe oxide-(REE-Cu-Au-U) mineralization, *Geology*, Volume 24, Number 3, pages 259-262.

Bookstrom, A.A., 1977 - The magnetite deposits of El Romeral, Chile, *Economic Geology*, Volume 72, pages 1101-1130.

Brown, M., Diaz, F., and Grocott, J., 1993 - Displacement history of the Atacama Fault System 25°00'S-27°00'S, northern Chile. *Geological Society of America* Bulletin, Volume 105, pages 1165-1174.

Casselman, M.J., McMillan, W.J., and Newman, K.M., 1995 - Highland Valley porphyry copper deposits near Kamloops, British Columbia: A review and update with emphasis on the Valley deposit. *In* Porphyry Deposits of the Northwest Cordillera on North America, *Canadian Institute of Mining and Metallurgy and Petroleum*, T.G. Schroeter, ed. Special Volume 5, pages 161-191.

Clark, A.H., Caelles, J.C., Farrar, E., Haynes, S.J., Lortie, R.B., McBride, S.L., Quirt, S.G., Robertson, R.C.R., and Zentilli, M., 1976 - Longitudinal variations in the metallogenic evolution of the central Andes: A progress report, *Geological Association of Canada*, Special Paper No. 14, pages 25-58.

Coira, B., Davidson, J., Mpodozis, C., and Ramos, V., 1982 - Tectonic and magmatic evolution of the Andes of northern Argentina and Chile, *Earth Science Reviews*, Volume 18, pp 303-332.

Debon, F., and Le Fort, P., 1983 - A Chemical-mineralogical classification of common plutonic rocks and associations, *Royal Society of Edinburgh Transactions*, Earth Sciences 73 (for 1982), pp135-149.

Dick, L.A., and Ray, G.E., 2000 - Iron oxide-Cu-Au-U-REE-apatite mineralization at the Productora property, north-central Chile, *In* Iron oxide copper-gold deposits: Separating fact from fantasy, *Vancouver Mining Exploration and British Columbia and Yukon Chamber of Mines*, Shortcourse notes, November 16th 2000, Vancouver, British Columbia, pages E19-E33.

Einaudi, M.T., and Oreskes, N., 1990 - Progress towards an occurrence model for Proterozoic iron oxide deposits - a comparison between the ore provinces of South Australia and southeast Missouri. *In* The Midcontinent of the United States - Permissive Terranes for an Olympic Dam Deposit?, *U.S. Geological Survey,* Bulletin 1392.

Fox, K.A., 2000 - Fe oxide (Cu-Au) mineralization and alteration at the Productora prospect, Chile, Unpublished Master of Science thesis, *Colorado School of Mine*, CO, 141 pages.

Hitzman, M.W., Oreskes, N., and Einaudi, M.T., 1992 - Geological characteristics and tectonic setting of Proterozoic iron oxide (Cu-U-Au-REE) deposits; *Precambrian Research*, Volume 58, pp 241-287.

Irvine, T.N., and Baragar, W.R.A., 1971 - A guide to the chemical classification of the common volcanic rocks; *Canadian Journal of Earth Sciences*, Volume 8, pp 523-547.

Jenkins, R.A., Leveille, R.A., and Marin, W., 1998 - Discovery and geology of the Candelaria deposit, Chile. Pathways '98, extended abstract volume, *B.C. & Yukon Chamber of Mines and Society of Economic Geologists*. pp 78-79.

Jordan, T.E., Isacks, B.L., Allmendinger, R.W., Brewer, J.A., Ramos, V.A., and Ando, C.J, 1983 - Andean tectonics related to geometry of subducted Nazca Plate, *Geological Society of America Bulletin*, Volume 94, pp 341-361.

Maniar, P.D., and Piccoli, P.M., 1989 - Tectonic discrimination of granitoids, *Geological Society of America,* Bulletin, Volume 101, pp 635-643.

Marschik, R., 1996 - Cretaceous Cu (-Fe) mineralization in the Punta del Cobre belt, northern Chile, Unpublished Ph.D. Thesis, *University of Geneva*, Thesis No. 2827, 197 pages.

Marschik, R., and Fontboté, L., 1996 - Copper (-Iron) mineralization and superposition of alteration events in the Punta Del Cobre Belt, Northern Chile. *In* Andean copper deposits: new discoveries, mineralization, style and metallogeny, *Society of Economic Geologists Special Publication No. 5*, Camus, F., Sillitoe, R.H., and Peterson, R., eds. 1996, pages 171-190.

Marschik, R., Singer, R., Munizaga, F., Tassarini, C., and Fontbote, L., 1996 - Age of the Cu (-Fe) mineralization and Cretaceous to Paleocene thermal evolution of the Punta del Cobre district, northern Chile. *In* Proceedings of the XXXIX Brazilian Geological Congress, Bahia. Anais 7, pages 306-309.

Marschik, R., Leveille, R.A., and Martin, W., 2000 - La Candelaria and the Punta del Cobre district, Chile: Early Cretaceous Iron-Oxide Cu-Au (-Zn-Ag) mineralization, *in* Hydrothermal Iron Oxide Copper-Gold and Related Deposits, *Australian Mineral Foundation Inc.*, T.M. Porter, ed., pages 163-175.

Maus, D., 1997a - Geological Map - Productora Project (1:10 000 scale), unpublished report, *General Minerals Corporation*, November, 1997.

Maus, D., 1997b - Productora area reconnaissance mapping, unpublished report, *General Minerals Corporation*, June 1997, 4 pages.

Oreskes, N. and Einaudi, M.T., 1990 - Origin of rare earth-enriched hematite breccias at the Olympic Dam deposit, Roxby Downs, South Australia; *Economic Geology*, Volume 85, Number 1, pages 1-28.

Oreskes, N., and Hitzman, M.W., 1993 - A model for the origin of Olympic Dam-type deposits. *In*, Mineral Deposit Modeling, *Geological Association of Canada*, Special Paper No. 40, pages 615-633.

Osterman, C., 1997 - Mineralogical notes on the Productora project, Region III, Chile. Unpublished report, *General Minerals Corporation*, May 1997, 8 pages.

Osterman, C., 1998 - Field notes on the Productora Project, Region III, Chile. Unpublished report, *General Minerals Corporation*, March 1998, 8 pages.

Pearce, J.A., Harris, N.B.W., and Tindle, A.G., 1984 - Trace element discrimination diagrams for the tectonic interpretation of granitic rocks, *Journal of Petrology*, Volume 25, pages 956-983.

Perello, J.A., Fleming, J.A., O'Kane, K.P., Burt, P.D., Clarke, G.A., Himes, M.D., 1995 - Porphyry copper-gold-molybdenum deposits in the Island Copper cluster, northern British Columbia. *In* Porphyry Deposits of the Northwest Cordillera on North America, *Canadian Institute of Mining and Metallurgy and Petroleum*, T.G. Schroeter, ed. Special Volume 5, pages 214-238.

Ray, G.E., 1997a - Summary report on the Productora Cu-Au Claim, Vallenar Area, North-central Chile. Unpublished report, *General Minerals Corporation*, May 17th 1997, 7 pages.

Ray, G.E., 1997b - A new drill target for the Pajaritos (West) property, Vallenar district, Chile, Unpublished report, *General Minerals Corporation*, June 15th 1997, 4 pages.

Ray, G.E., 1998a - Productora project - summary of work completed between the 21st Feb. and 8th April

1998. Unpublished report, *General Minerals Corporation*, April 1998, 4 pages.

Ray, G.E., 1998b - Geology and geochemistry of the Productora-Cachiyuyito Cu-Au-Fe-U-REE Belt, Vallenar, Region III, Chile. Unpublished report and geological maps, *General Minerals Corporation*, September 1998, 59 pages.

Ray, G.E., 2001 - Alteration and mineralization in parts of the Productora Cu-Au-Fe Belt, Vallenar, Chile, Unpublished report and geological maps, *General Minerals Corporation*, May 2001, 57 pages.

Ray, G.E., and Lefebure, D.V., 2000 - A synopsis of iron oxide ± Cu ± Au ± P ± REE deposits of the Candelaria-Kiruna-Olympic Dam family, *In* Geological Fieldwork 1999, *British Columbia Ministry of Energy and Mines*, Paper 2000-1, pages 267-272.

Ryan, P.J., Lawrence, A.L., Jenkins, R.A., Matthews, J.P., Zamora, J.C., Marino, E.W. & Diaz, I.U., 1995 - The Candelaria copper-gold deposit, Chile; *In* Porphyry Copper Deposits of the American Cordillera, editors Pierce, F.W. and Bolm, J.G, *Arizona Geological Society Digest*, 20, 625-645.

Vidal, C.E., Injoque-Espinoza, J., Sidder, G.B., and Mukasa, S.B., 1990 - Amphibolitic Cu-Fe skarn deposits in the central coast of Peru; *Economic Geology*, Volume 85, pages 1447 -1461.

Vila, T., N. Lindsay, and R. Zamora (1996)- Geology of the Manto Verde copper deposit, Northern Chile, A Specularite-Rich, Hydrothermal-Tectonic Breccia Related to the Atacama Fault Zone, *In* "Andean copper deposits: new discoveries, mineralization, style and metallogeny", *Society of Economic Geologists Special Publication No. 5*, Camus, F., Sillitoe, R.H., and Peterson, R., eds. 1996, pages 157-170

Williams, P.J., 1998 - Metalliferous economic geology of the Mount Isa Eastern Succession, northwest Queensland. *Australian Journal of Earth Sciences*, Volume 45, pages 329-341.

Winchester, J.A., and Floyd, P.A., 1977 - Geological discrimination of different magma series and their differentiation products using immobile elements. *Chemical Geology*, Volume 20, pages 325-343.

PGC
PUBLISHING

Dow, R.J. & Hitzman, M.W., 2002 - Geology of the Arizaro and Lindero Prospects, Salta Province, Northwest Argentina: Mid-Miocene Hydrothermal Fe-Ox Copper-Gold Mineralisation; *in Porter, T.M. (Ed.), Hydrothermal Iron Oxide Copper-Gold & Related Deposits: A Global Perspective*, Volume 2; PGC Publishing, Adelaide, pp 153-161.

GEOLOGY OF THE ARIZARO AND LINDERO PROSPECTS, SALTA PROVINCE, NORTHWEST ARGENTINA: MID-MIOCENE HYDROTHERMAL Fe-Ox COPPER-GOLD MINERALISATION

Russell. J. Dow and Murray. W. Hitzman

Department of Geology and Geological Engineering
Colorado School of Mines, Golden, CO, USA

Abstract – The Arizaro and Lindero prospects are possibly the youngest recognised examples of the hydrothermal iron oxide-copper-gold class of deposits in the world. These two prospects, and numerous other iron-oxide manifestations, form a newly discovered district within northwest Argentina. The Arizaro and Lindero prospects are hosted within mid-Miocene, calc-alkaline, dominantly andesitic, volcanic complexes that formed within a convergent plate margin tectonic setting. This descriptive paper presents observations from surface geology and petrographic studies.

Alteration at the Arizaro prospect is zoned from distal calcite-epidote-chlorite alteration (propylitic) inwards to actinolite-potassium feldspar-magnetite-biotite ± diopside-albite alteration (calcic-potassic) and finally to a central core of intense potassium feldspar-magnetite-biotite alteration (potassic). Weak hydrolytic alteration (quartz-sericite-clay) occurs on the periphery of the system and overprints other alteration types. Alteration at Lindero forms near-complete, concentric rings that are zoned from a central chlorite-calcite core, outwards into potassic alteration (potassium feldspar-magnetite-biotite), into hydrolytic alteration (quartz-sericite-clay-limonite), and finally to an outer propylitic alteration zone (epidote-calcite). Both prospects contain magnetite-rich, pyrite-absent assemblages with Cu-Au and elevated Pd and REE concentrations (La-Ce-Nd). Sulphides are largely restricted to zones of strong to intense potassic alteration and consists of disseminated chalcopyrite and minor bornite.

The interplay between extensional tectonics, magmatism, and thermal convection of saline basinal brines is probably critical for the development of the Arizaro - Lindero alteration systems.

Introduction

The Arizaro-Lindero prospects were discovered by Mansfield Minerals S.A. in 1999 and 2000 respectively and form part of a newly discovered, extremely young (ca 15 Ma), hydrothermal iron oxide copper-gold district within the Puna Plateau of northwest Argentina (Figure 1). Prospects within the district are hosted within both the cores of mid-Miocene, calc-alkaline, dominantly andesitic, volcanic complexes (eg. Arizaro, Lindero, Rio Grande) and within Miocene-age(?), high-angle splays off major structural lineaments (eg. El Camino, La Sarita) (Figure 2). These prospects formed within a convergent plate margin tectonic setting. The Arizaro-Lindero prospects represent a unique opportunity to further our understanding of the iron oxide-copper-gold class of deposits, primarily due to their youth (14 to 15.5 Ma), absence of post-mineralisation alteration or deformation, and location within a tectonic and regional geological setting that is well-constrained relative to other global districts. This paper focuses on description of the surface geology and includes petrographic information on alteration assemblages. Additional laboratory studies to constrain the genesis of mineralisation of these prospects is currently underway.

Regional Geological Setting

The Arizaro-Lindero prospects are located at the southern limit of the Salar de Arizaro, one of the largest salars in South America (Figure 2). The salar occupies the western third of a large 100x100 km intra-arc basin, which is referred to as the Arizaro Basin within this paper. The Arizaro Basin is bounded by major normal, strike-slip and reverse/thrust fault systems and is interpreted to contain approximately 4000 m of sedimentary fill (Jordan and Alonso, 1987). The basin is bounded to the north by the northwest-trending Calama-El Toro Transverse Zone, in the south by the northwest-trending Archibarca Transverse Zone and in the west by the NNE-trending 'East Fissure' Longitudinal Zone (Figure 2). These three structural zones controlled the emplacement of large volumes of mid-Miocene to recent intrusive and extrusive igneous rocks. The eastern extent of the basin is bounded by a NNE-trending reverse/thrust fault structural zone that is currently un-named. The major NNE-trending structures probably represent terrane boundaries, whereas northwest-trending structures were possibly initially established during Triassic extension of the Pangea super-continent. These large basin-bounding structural zones are surface expressions of deep-

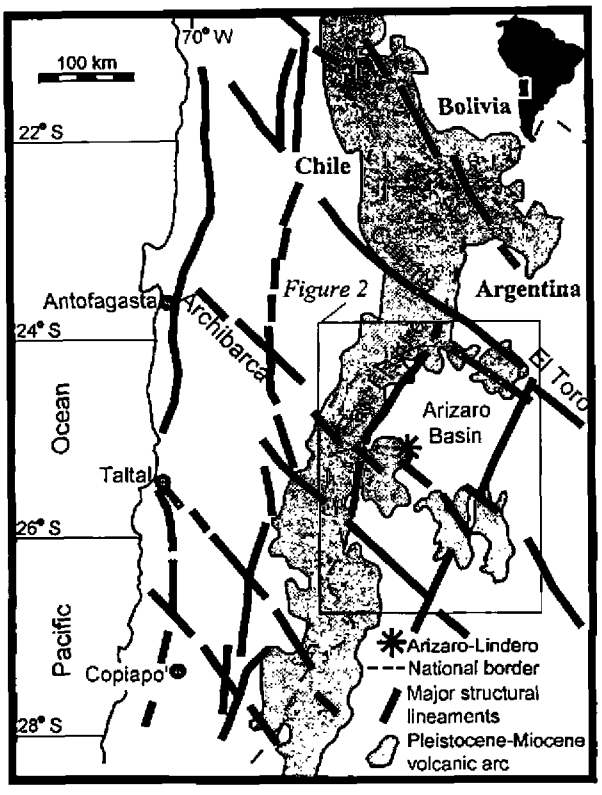


Figure 1: Location map of the Arizaro and Lindero prospects in the Puna area of northwest Argentina. The map indicates the location of the Pleistocene-Miocene Andean volcanic arc, major structural lineaments and the Arizaro Basin (modified after Richards, 2000).

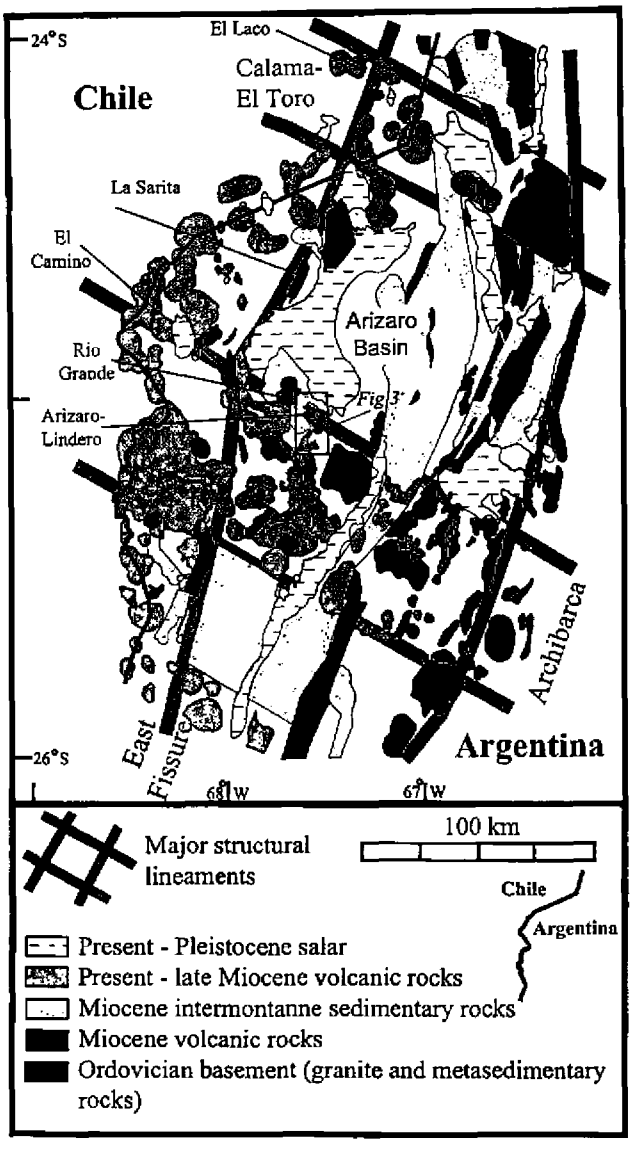


Figure 2: Regional geology of northwest Argentina showing the location of major crustal lineaments, the Arizaro Basin and key geological units. Note that Cretaceous to Late Oligocene arkosic sedimentary rocks are not defined on this map, due to poor regional mapping. Arkosic sedimentary rocks of Cretaceous through Late Oligocene age are believed to underlie most of the Miocene intermontane strata (modified after Richards, 2001).

crustal structures and have been periodically reactivated since at least the early Tertiary (Richards, 2000). Episodic movement along these structures, related to subduction of the Pacific oceanic plate below the South American continent, created high-permeability tensional and transtensional tectonic regimes.

The basement of the Arizaro Basin comprises Early to Middle Ordovician granitic plutons and Precambrian through Paleozoic volcanic and sedimentary sequences (Amengual, et al., 1979, Vandervoort, 1993). This basement is unconformably overlain by Cretaceous - latest Oligocene continental arkosic sedimentary rocks. Oligocene strata accumulated in a foreland depositional basin of low relief in which clastic playa, aeolian, and fluvial depositional environments predominated (Jordan and Alonso, 1987). The regional extent of the Oligocene strata clearly distinguish them from the much less extensive Neogene and younger sedimentary rocks (Vandervoort, 1993).

Initiation of Puna Plateau development, at approximately 16-17 Ma (Jordan et al., 1997, Vandervoort et al, 1995), imposed significant changes on the depositional environment and tectonic-structural framework of this region as well as coinciding with the establishment of an extremely arid environment. This plateau is 1800 km long and 300-400 km wide and has an average elevation of greater than 3000 m. The plateau is characterised by numerous structurally-controlled, internally-draining basins (eg. Arizaro) that probably started forming around the time of initial plateau development.

Plateau uplift occurred due to subduction-related crustal thickening produced by horizontal shortening of a thermally softened crust (Allmendinger et al, 1997). Rapid uplift promoted high erosion rates and resulted in accumulation of thick sequences of immature clastic and evaporitic sediments within internally-draining basins. Measured sections in the Arizaro Basin indicate greater than 1500m of evaporitic sediments (Vandervoort, 1993) with an interpreted thickness of up to 4000m (Jordan and Alonso, 1987, Vandervoort, 1993). The Arizaro Basin stratigraphic package consists of first generation red beds and evaporitic halite deposits.

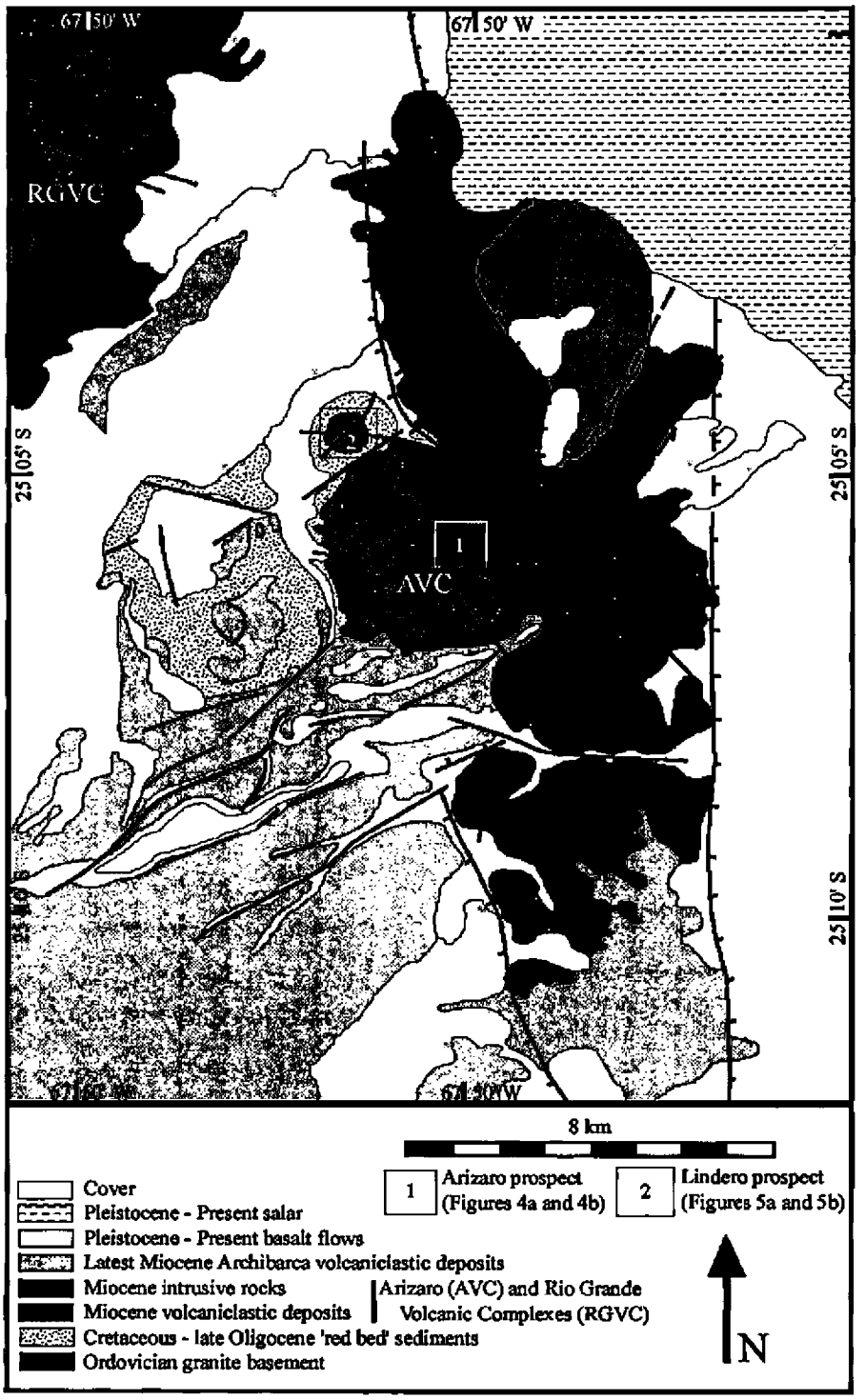


Figure 3: Geology map of the broader Arizara Volcanic Complex.

Mid-Miocene to recent igneous rocks occur along the modern Andes magmatic arc, and within northwest-trending 'magmatic fingers' (Figure 2) which coincide with northwest-trending structural lineament zones. At least four distinct ages of igneous rocks have been identified within the broader Arizaro-Lindero area including: porphyry copper intrusions at Cerro Samenta and Taca Taca (28-30 Ma, Rojas et al, 1999), the Arizaro and Rio Grande volcanic complexes (16-17 Ma, Dow, 2001), Archibarca Volcano (<5 Ma ?) and very young basalt dykes and lava flows (2 Ma-present).

Local Geology

The Cretaceous to late Oligocene red arkosic sandstones are unconformably overlain by mid-Miocene volcanic flows and volcaniclastic sediments and are cross-cut by intrusive rocks. These mid-Miocene igneous rocks comprise the Arizaro volcanic complex which covers an area of approximately 6x4 km. Lithologically similar rocks to the northwest make up the area around the Rio Grande prospect (Figure 3). Mid-Miocene volcaniclastic rocks also outcrop north, northeast and east of the Arizaro volcanic complex,

although, it is unclear where these deposits originated. The Arizaro volcanic complex consists of three zones containing abundant calc-alkaline intrusive rocks which are each surrounded by lava flows and volcaniclastic rocks. These extrusive rocks are cut by calc-alkaline dykes which extend radially away from each of the intrusive centres.

The intrusive rocks are generally porphyritic although minor equigranular phases are also present. Porphyritic minerals are dominated by medium-grained plagioclase and hornblende with minor augite. The groundmass of the intrusive rocks consists dominantly of plagioclase and potassium feldspar. Extrusive rocks immediately adjacent to the intrusive units are generally weakly hornfelsed. Relatively unaltered intrusive rocks from the Arizaro prospect have yielded an $^{40}Ar/^{39}Ar$ age of 16.35±0.35 Ma while relatively unaltered intrusive rocks from the Lindero prospect yield an $^{40}Ar/^{39}Ar$ age of 16.75±0.35 Ma.

The lava flows and volcaniclastic rocks surrounding the intrusive centres are typically slightly more felsic than adjacent intrusive rocks. Lava flows are subordinate to volcaniclastic rocks. The volcaniclastic rocks are dominated by mass-flow units consisting of blocks of andesite and/or dacite in a fine- to medium-grained, crystal-rich, andesitic matrix. The volcaniclastic rocks also contain minor thin-bedded ashfall deposits.

The Arizaro complex appears to be a series of partially dissected volcanic edifices. The Arizaro prospect is located in a relatively large zone of intrusions while the Lindero prospect occurs in a small intrusion that forms a prominent hill. The largest volcanic edifice is located to the south of the Arizaro prospect and appears to be unmineralised.

Igneous rocks of the Arizaro complex are unconformably overlain by late-Miocene (?) volcanic rocks which are believed to be derived from the Archibarca volcanic complex 15 km to the southwest of Arizaro. In the Arizaro area, these Archibarca volcanic rocks comprise white, poorly lithified, pumice flows and heterogeneously coloured volcaniclastic massflow deposits. The youngest volcanic rocks in the area are Quaternary basalt flows and dolerite dykes.

The Arizaro prospect area is cut by northeast-, north-northeast-, and northwest-trending, high angle faults. Most faults occupy covered valleys. Maximum displacement on the faults is probably several hundred metres. The Arizaro area is bound to the northeast by a northeast-trending, left-lateral strike-slip fault zone.

Geology of the Arizaro Prospect

The Arizaro prospect is located within an intrusive centre of the Arizaro volcanic complex. The intrusive core is surrounded by volcaniclastic breccias which are cut by radial dykes (Figure 4a). The prospect area is cut by a number of northeast-trending valleys that are interpreted to mark the location of high angle faults. The southern limit of the prospect is a major northeast-trending valley which separates the prospect from the main intrusive centre of the Arizaro volcanic complex.

Sulphides were discovered at Arizaro in 1999 through prospecting. Mineralisation occurs in both intrusive and extrusive igneous rocks of the Arizaro volcanic complex. Early grab samples for the prospect returned an average grade of 0.36% Cu and 0.73g/t Au. Distinctive alteration zones similar to the previously discovered Rio Grande system quickly highlighted the similarities between these two prospects. This initial work was followed-up with the excavation of two small trenches over the best exposed mineralisation, which returned assay values of 22m @ 0.63% Cu, 1.12 g/t Au and 8m @ 0.8% Cu, 1.44 g/t Au. During late 2000, a 1400x1200 m soil survey, at 100x50 m spacings, was completed and identified a moderate sized anomaly of 600x400 m @ >800 ppm Cu and >300 ppb Au (Figure 4b). A second trenching program was completed in early 2001 to confirm the continuity of the identified soil anomaly. This trenching program confirmed the continuity of the alteration and mineralisation system, although it also highlighted the low grade nature of the exposed system. The two longest trenches returned assays of 636m @ 0.13% Cu, 0.22 g/t Au and 516m @ 0.13% Cu, 0.24 g/t Au. These and most other trenches intersected small and discontinuous higher grade zones (ie. >15m @ 0.4% Cu, 0.8 g/t Au). Copper-gold ratios typically range from 1:2 to 1:1.5 (ie. 0.5%Cu:1g/t Au to 0.5% Cu : 0.75 g/t Au).

Hydrothermal Alteration

Hydrothermal alteration at Arizaro (Figure 4b) is zoned from distal calcite-epidote-chlorite alteration (propylitic) inwards to actinolite-potassium feldspar-magnetite-biotite ± diopside-albite alteration (calcic-potassic) and to a central core of intense potassium feldspar-magnetite-biotite alteration (potassic). Weak hydrolytic alteration (quartz-sericite-clay) occurs on the periphery of the system and overprints other alteration types. The central potassic and calcic-potassic alteration zones have a strike length of almost 2 km. Propylitic alteration extends from the edge of the central alteration zone to the limit of exposures of the Arizaro volcanic complex.

Potassic Alteration

Three distinctive styles of potassic alteration are observed: potassium feldspar flooding with magnetite veins, biotite vein breccia, and biotite spots. Alteration is generally pervasive and results in the destruction of primary igneous texture. Altered rocks are primarily cream to dark brown coloured.

Potassium feldspar flooding with magnetite vein zones is the dominant potassic alteration style observed at Arizaro. This alteration style is characterised by massive potassium feldspar with variable amounts of disseminated magnetite and biotite. These zones are cut by chaotic magnetite veins which locally give the rock a brecciated appearance. Magnetite veins within these zones have irregular shapes, are angular and discontinuous. Zones with well-developed breccia texture are typically round in shape with diameters

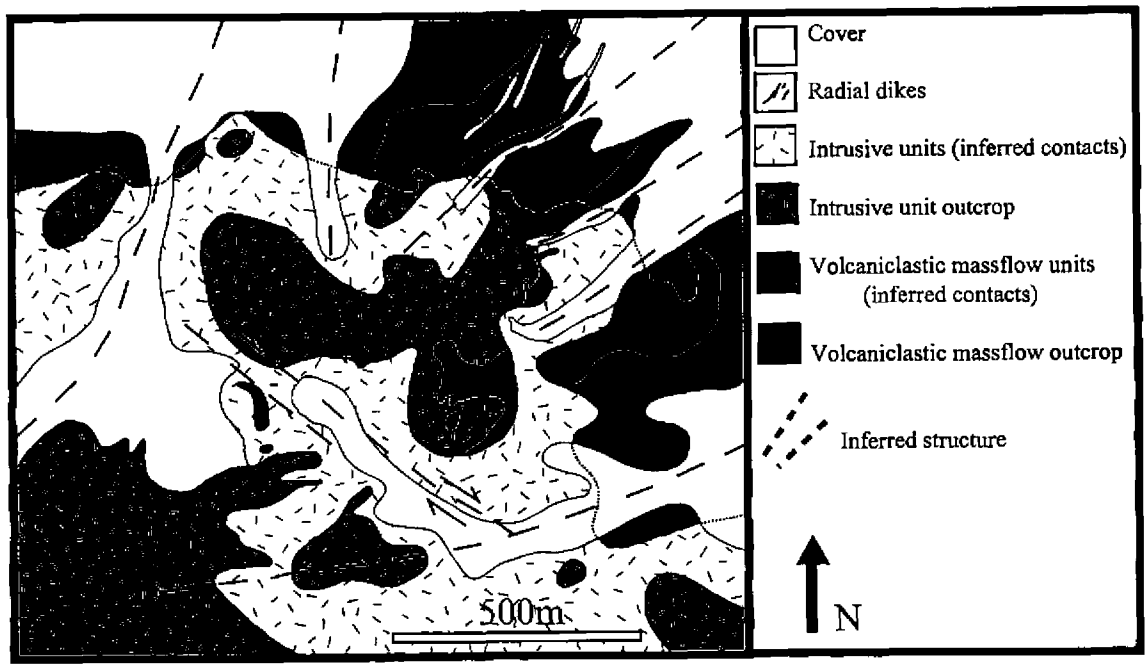


Figure 4a: Outcrop geology map of the Arizaro prospect

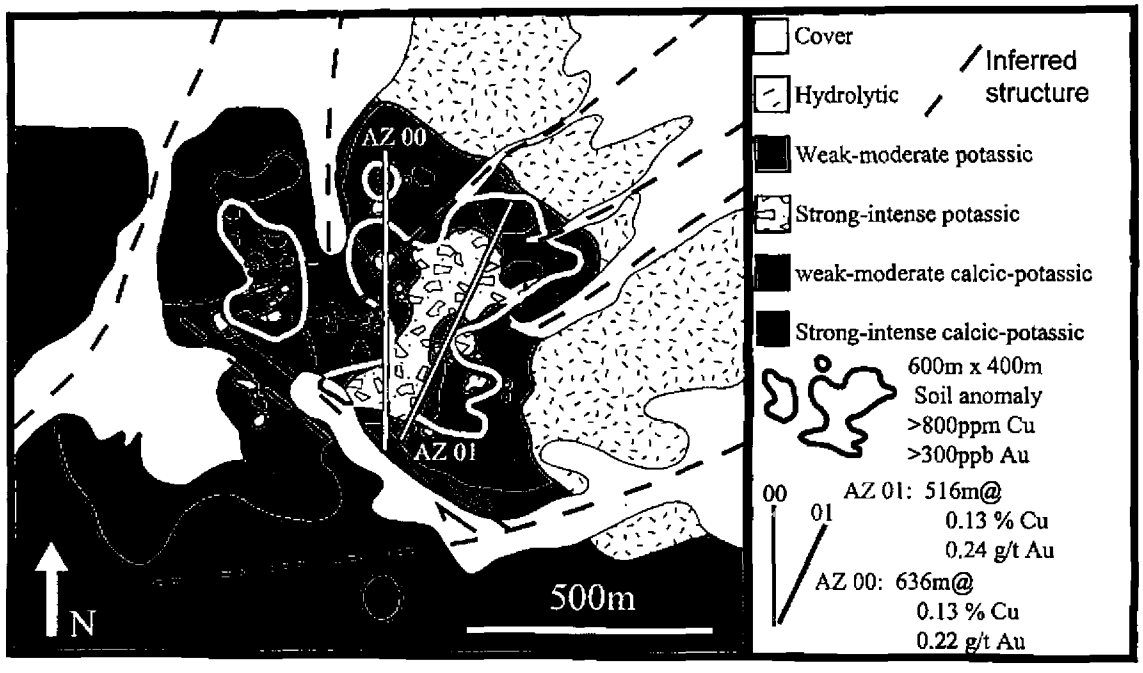


Figure 4b: Alteration and mineralisation map of the Arizaro prospect

that range in size from 3 to 40 m. Wallrock alteration decreases in intensity with increasing distance from breccia zones. Magnetite veins outside of the breccia zone generally display a rectilinear geometry.

Biotitic alteration is characterised by thin (<1 mm) biotite ± potassium feldspar-magnetite veins that locally coalesce to form a breccia texture. Biotite veins typically have a straight to curvilinear morphology. Individual biotite veins commonly have potassium feldspar-biotite-magnetite alteration halos. In zones with abundant biotite veins the wallrock may be pervasively replaced by a biotite-potassium feldspar-magnetite assemblage. Biotite from a thoroughly biotitically altered area yielded an $^{40}Ar/Ar^{39}$ age of 15.46 ± 0.11 Ma.

Biotite spots represent the least common form of potassic alteration. This textural style of alteration is present in rocks which have been pervasively altered to potassium feldspar. The biotite spots are 2-5 mm in diameter, and are amoeboidal to tube-like (up to 50 mm long) in shape. The spots generally consist of a central biotite-potassium feldspar ± chalcopyrite core surrounded by a biotite-magnetite rim. This alteration style is observed in both intrusive and extrusive protoliths indicating that the texture is not lithologically controlled.

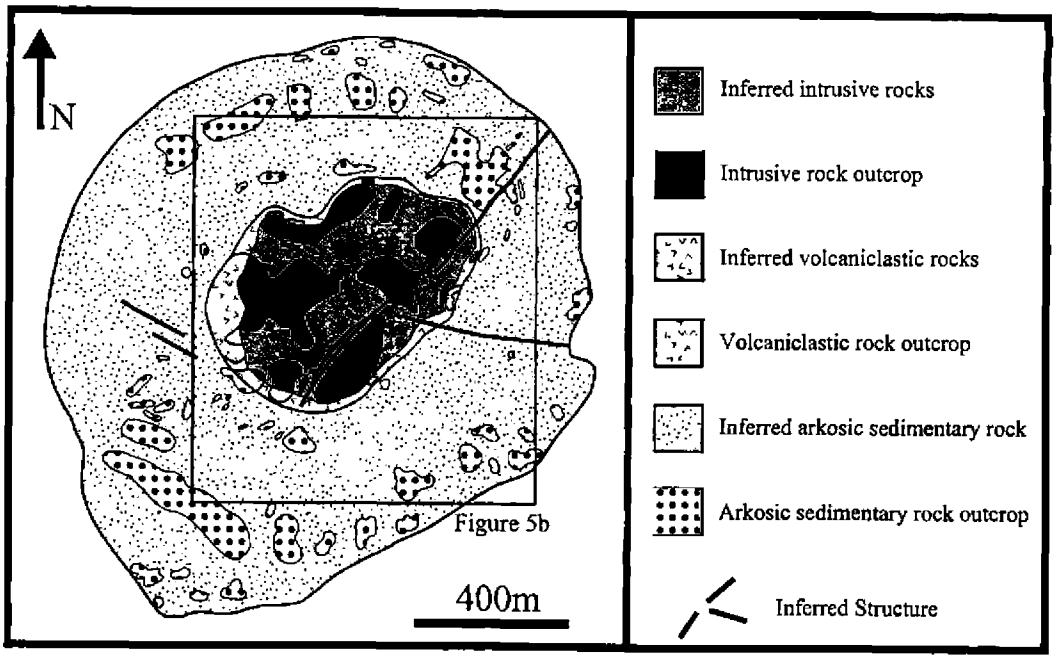


Figure 5a: Outcrop geology map of the Lindero prospect.

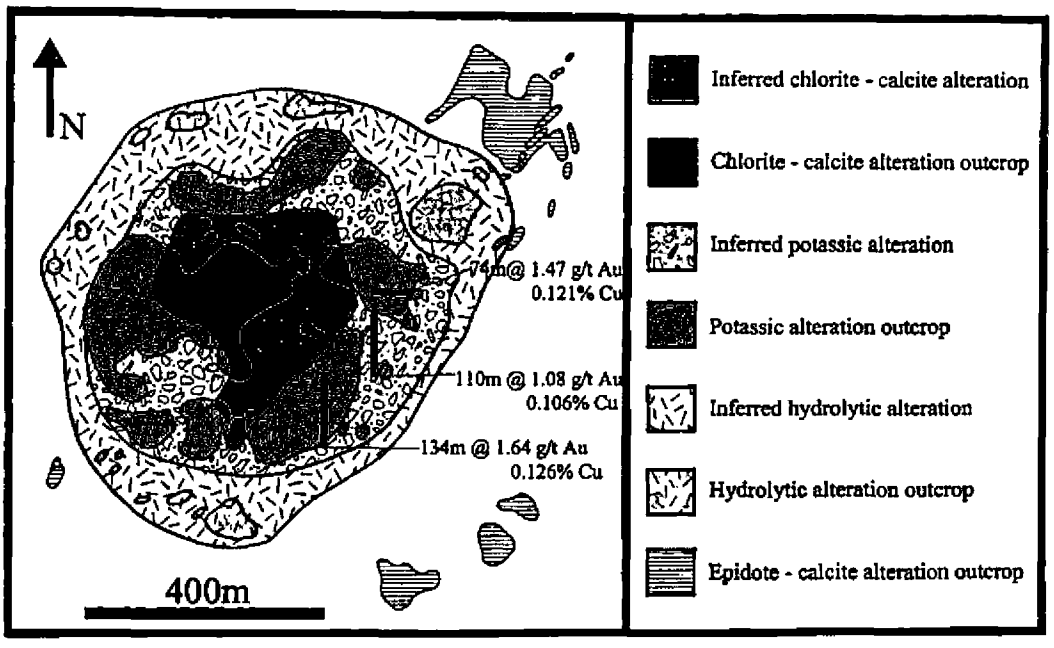


Figure 5b: Alteration and mineralisation map of the Lindero prospect.

Calcic-potassic Alteration

Calcic-potassic alteration is poorly developed relative to potassic alteration. Altered outcrops typically have a green colour, display well preserved primary igneous textures, and megascopically appear unaltered. Alteration mineralogy and intensity, outcrop colour and texturally non-destructive nature of alteration allow for easy mapping distinction between this alteration type and potassic alteration zones. Calcic-potassic alteration occurs primarily as an envelope around the central potassic alteration zone (Figure 4b).

Calcic-potassic alteration is characterised by vein and vein stockworks which have selvages and halos containing similar alteration minerals. Vein mineralogy is dominated by actinolite-magnetite ± quartz-potassium feldspar-biotite-chalcopyrite. Outside of the veins, actinolite generally replaces igneous hornblende and augite, while potassium feldspar, magnetite, and biotite replace the finer-grained groundmass.

Age relationships between the calcic-potassic and potassic styles of alteration are unclear. However, in the northeast and central portion of the prospect, actinolite is locally replaced by biotite, suggesting that calcic-potassic alteration may predate potassic alteration.

Two zones of strong to intense, calcic-potassic alteration are shown in Figure 4b. The northern outcrop comprises a

zone of diopside-albite-biotite-magnetite vein breccia. The southern outcrop consists of an intensely developed, massive potassium feldspar-actinolite-magnetite ± biotite vein with strong actinolite-magnetite replacement of adjacent wallrock. Massive potassium feldspar from this vein returned an $^{40}Ar/Ar^{39}$ age of 13.98 ± 0.38 Ma, significantly younger than the alteration age from biotite in the potassic zone. This age relationship contrasts with the petrographic evidence that actinolite is replaced by biotite.

Propylitic Alteration

Propylitic alteration is characterised by weak to strong calcite and weak epidote alteration of plagioclase phenocrysts and groundmass and weak chlorite alteration of mafic phenocrysts. Alteration is typically controlled by calcite micro-veinlets. Propylitic alteration intensity gradually decreases away from the central potassic core and affects most of the Arizaro volcanic complex.

Hydrolytic Alteration

Hydrolytic alteration is present around the north, northeast and eastern parts of the prospect in the volcaniclastic rocks which surround the intrusive core. Hydrolytically altered rocks are generally light cream to white in colour, and contain a quartz-sericite-clay mineral assemblage.

Mineralisation

Exposed mineralisation at Arizaro is dominated by supergene, copper oxide minerals which replace chalcopyrite and minor bornite. Chalcopyrite is generally fine-grained (<0.5 mm), is commonly associated with bornite and intergrown with magnetite. Micron-sized gold (±Pd) grains occur with chalcopyrite-copper oxide accumulations, although chalcopyrite-gold intergrowths have not yet been identified. The highest copper and gold grades are contained almost exclusively within the strong to intense potassic alteration zone. Sulphides are primarily disseminated but also occur within magnetite veins. Copper-gold anomalies are strongly coincident, suggesting that the two metals share a similar fluid transport and precipitation mechanism. Mineralised samples show minor enrichments in silver (<6.5 g/t), zinc (<0.2%) and lanthanum (<50 ppm) relative to unaltered samples.

Geology of the Lindero Prospect

The Lindero prospect was discovered by the senior author during completion of 1:20 000 scale mapping of the Arizaro Volcanic Complex during late 2000. Since discovery, the prospect has been soil sampled and trenched. The soil sampling program led to the discovery of a large, partially covered gold soil anomaly at the southern end of the prospect (500x300 m, >1g/t Au). An 1100 m trenching program, started in early 2001, confirmed the bedrock source for the large soil anomaly. Unfortunately, significant areas of cover limited testing of the anomaly. Nevertheless, 1100 m of trenching returned an average of 0.66 g/t Au and 0.13% Cu. These assay results define a semi-circular mineralised zone approximately 900 m long and >70 m wide.

Outcrop Geology

The Lindero prospect forms a semi-circular mineralised halo around a steep hill containing an intrusive core (Figure 5a and 5b). The hill is isolated from the main Arizaro Volcanic Complex by a northeast-trending valley. The Lindero hill comprises a central intrusive core consisting of at least four individual andesite intrusive bodies. One of these intrusions has yielded an $^{40}Ar/Ar^{39}$ age of 16.75 ± 0.12 Ma. These intrusive rocks cross-cut both Oligocene(?) arkosic sedimentary rocks and volcaniclastic rocks of the Arizaro volcanic complex. The volcaniclastic rocks display both monolithic and polylithic breccia textures and have been classified as both mass-flow deposits and intrusion-related breccias. These deposits form a thin ring that separates the central intrusive complex from the host rock arkosic sediments. The hill is cross-cut by two andesite radial dykes that are aligned parallel to the main observed structural trends (northwest and NNE).

Hydrothermal Alteration

Alteration types at Lindero are similar to those observed at Arizaro. However, calcic-potassic alteration has not been identified at Lindero and the core of the Lindero system contains calcic (chlorite-calcite) alteration. Alteration at Lindero forms near-complete, concentric rings that are zoned from a central chlorite-calcite core, outwards into potassic alteration (potassium feldspar-magnetite-biotite), then hydrolytic alteration (quartz-sericite-clay-limonite), and finally to an outer propylitic alteration zone (epidote-calcite). The contact between potassic and propylitic alteration is obscured by a >100 m wide ring of colluvial cover. Biotite from the potassic alteration zone has recently been dated by $^{40}Ar/Ar^{39}$ methods at 15.21 ± 0.11 Ma.

Chlorite-calcite Alteration

The central intrusive core of the Lindero hill is weakly to moderately altered to a chlorite-calcite alteration assemblage. Chlorite replaces igneous hornblende and augite. Calcite is present as minor veins and disseminated throughout the porphyry groundmass.

Potassic Alteration

Potassic alteration forms a ring around the intrusive centre and has a length of 1500 m with an average width of 150 m. The strongest potassic alteration is located along a linear northeast-trending ridge in the southwest portion of the prospect. Potassic alteration appears to extend under cover to the south and east of this ridge. The potassic alteration within this ridge has an abrupt western contact with the central chlorite-calcite alteration zone, a feature most easily explained by a fault offset. Potassic alteration at Lindero is typically more intense than that observed at Arizaro. The potassic zone contains four distinct assemblages: early magnetite-biotite ± quartz rectilinear veins, potassium feldspar-magnetite-biotite breccias, magnetite vein breccias, and late quartz-magnetite vein stockworks.

Early magnetite-biotite ± quartz veins are rectilinear and have thin potassium feldspar-magnetite-biotite alteration selvages. These veins are also accompanied by weak to

moderate potassium feldspar-magnetite-biotite alteration of adjacent wallrock. This early alteration event is crosscut by massive potassium feldspar-magnetite-biotite breccia zones which contain weakly to moderately altered wallrock clasts in a potassium feldspar-magnetite-biotite matrix. These breccias make up the majority of the potassic alteration zone.

These breccias are cross-cut by magnetite veins which locally form stockwork breccias. The magnetite veins have moderately developed potassium feldspar-magnetite alteration selvages. The veins commonly have unfilled (open) centres. Magnetite veins are locally cross-cut by late quartz ± magnetite veins.

Hydrolytic and Propylitic Alteration

Hydrolytic alteration is developed around the entire intrusive body. This alteration type is typically cream to tan coloured. The rock is weak to moderate clay altered with minor quartz-sericite development. Yellow limonite is commonly observed. Epidote-calcite alteration (propylitic) forms the most distal alteration type. Epidote veins cross-cut the host 'red bed' sediments and weak epidote-calcite forms a pervasive alteration of the matrix.

Mineralisation

Rock chips, soils and trenching confirm the presence of a mineralised zone that is 900 m long, >70 m wide and has an average grade of 0.66 g/t Au and 0.13 % Cu. This mineralised zone contains significant widths with higher grades: 134 m @ 1.65 g/t Au, 0.126% Cu; 110 m @ 1.08 g/t Au, 0.106% Cu; and 74 m @ 1.47 g/t Au, 0.121% Cu (Figure 5b). High copper and gold values at Lindero are restricted to the potassic alteration zone. Mineralisation is strongest along a northeast-trending zone in the southeast part of the prospect. Mineralisation at Lindero is dominated by copper oxides; chalcopyrite is rarely observed. The highest copper concentrations occur within potassium feldspar-magnetite-biotite breccia zones.

Summary

The Arizaro and Lindero prospects are believed to be extremely young examples of the iron oxide-copper-gold class of deposits (Hitzman 2000). Both prospects contain magnetite-rich, pyrite-absent assemblages with significant Cu-Au and elevated REE concentrations (La, Ce, Nd). Both prospects are characterised by intense potassic alteration (potassium feldspar-biotite). The rocks display veinlet-controlled, disseminated and pervasive styles of alteration. Iron oxide-copper-gold systems typically display zoning from a deep sodic zone upward to potassic and hydrolytic alteration zones (Hitzman et al, 1992). Although sodic alteration has not been recognised at Arizaro and Lindero, the nearby Rio Grande prospect (Figure 2) does contain a sodically altered core. It is probable that sodic alteration is present at depth below the potassic zone at Arizaro and Lindero.

The Arizaro and Lindero prospects are hosted within the cores of mid-Miocene (≈ 16-17 Ma), calc-alkaline andesitic volcanic complexes. Geochronology suggests that these two prospects may be the youngest currently recognised examples of the hydrothermal iron oxide copper-gold deposit class in the world. Geochronology also indicates a significant time gap (≈ 1 Ma) between the age of host rock intrusions and hydrothermal alteration. These data strongly suggest that the observed host rocks are not the direct source of hydrothermal fluids. In addition, the preliminary geochronology suggests hydrothermal alteration may have occurred during a 1.5 million year period. Work is ongoing to better constrain the duration of the hydrothermal event.

The development of the Arizaro Basin and the emplacement of the Arizaro volcanic complex coincided with uplift of the Puna Plateau. It is probable that the Arizaro Basin was an active depocentre during hydrothermal alteration processes at Arizaro-Lindero, however, what is unclear is the size, depth and nature of contained sediments and basinal fluids. The dominance of magnetite and the sulfur-deficient nature of the two systems is not typical of a magmatic-fluid dominated hydrothermal system (Barton and Johnson, 1996, 2000). It is probable that an oxidised, saline fluid was required to form the observed alteration at Arizaro and Lindero. The interplay between tensional tectonics, magmatism, and induced thermal convection of saline basinal brines is probably critical for the development of the Arizaro - Lindero alteration systems and the multitude of other iron-oxide manifestations observed surrounding the Arizaro Basin.

References

Allmendinger, R.W., Jordan, T.E., Kay, S.M., and Isacks, B.L., 1997. The evolution of the Altiplano-Puna plateau of the central Andes. *Annual Review of Earth and Planetary Science* 25, pp 139-174.

Amengual, R., Mendez, V., Navarini, A., Viera, O., and Zanettini, J.C., 1979. Geologia de la region norosete, Republica Argentina, Provincias de Salta y Jujuy: Buenos Aires, *General de Direccion Fabricaciones Militares,* scale 1:400,000.

Barton, M.D. and Johnson, D.A., 1996. Evaporitic-source model for igneous related Fe oxide-(R.E.E.-Cu-Au-U) mineralization. *Geology* 24 (3), pp 259-262.

Barton, M.D. and Johnson, D.A., 2000. Alternative brine sources for Fe-oxide (-Cu-Au) systems: Implications for hydrothermal alteration and metals; *in* Porter, T.M. (ed.), Hydrothermal Iron Oxide Copper-gold and Related Deposits: A Global Perspective. Vol 1, *Australian Mineral Foundation Inc,* Adelaide, pp 43-60.

Dow, R.J., 2001. $^{40}Ar/Ar^{39}$ age dating of the Arizaro and Lindero prospects. *Unpublished Mansfield Minerals report.*

Hitzman, M.W., Oreskes, N., and Einaudi, M.T., 1992. Geological characteristics and tectonic setting of Proterozoic iron oxide (Cu-Au-REE) deposits. *Precambrian Research*, V 58, pp 214-287.

Hitzman, M.W., 2000. Iron oxide Cu-Au deposits: What, where, when and why; *in* Porter, T.M. (ed.), Hydrothermal Iron Oxide Copper-gold and Related Deposits: A Global Perspective. Vol 1, *Australian Mineral Foundation Inc*, Adelaide, pp 9-25.

Jordan, T.E., and Alonso, R.N., 1987. Cenozoic stratigraphy and basin tectonics of the Andes Mountains, 20° - 28° south latitude. *American Association of Petroleum Geologists Bulletin* V 71, pp 49-64.

Jordan, T.E., Reynolds 3rd, J.H., and Erikson, J.P., 1997. Variability in age of initial shortening and uplift in the central Andes, 16° - 33°30'S; *in* Ruddiman, W.F., (ed.) Tectonic Uplift and Climate Change. *Plenum Press*, New York, pp 41-61.

Richards, J.P., 2000. Lineaments revisited. *Society of Economic Geologists*, SEG Newsletter, July 2000, Number 42, p1 and pp 14-20.

Richards, T.A., 2001. Summary of the geology of northwest Argentina. *Unpublished Mansfield Minerals Inc company report.*

Rojas, N., Drobe, J., Lane, R., and Bonafede, D., 1999. El porfiro cuprifero de Taca Taca Bajo, Salta. in Zappettini, E, O, Recursos Minerales de la Republica Argentina. *Institudo de Geologia y Recursos Minerales, SEGEMAR, Anales 35*, Buenos Aires pp 1321 – 1331.

Vandervoort, D.S., 1993. Non-marine evaporite basin studies, southern Puna Plateau, central Andes. Ph.D Thesis, *Cornell University, New York*, pp 1-40.

Vandervoort, D.S., Jordan, T.E., Zeitler, P.K., and Alonso, R.N., 1995. Chronology of internal drainage development and uplift, southern Puna Plateau, Argentine central Andes. *Geology* 23 (2), pp 145-148.

PGC PUBLISHING

Boric, R., Holmgren, C. & Wilson, N.S.F. & Zentilli, M., 2002 - The Geology of the El Soldado Manto Type Cu (Ag) Deposit, Central Chile; *in Porter, T.M. (Ed.), Hydrothermal Iron Oxide Copper-Gold & Related Deposits: A Global Perspective*, Volume 2; PGC Publishing, Adelaide, pp 163-184.

THE GEOLOGY OF THE EL SOLDADO MANTO TYPE Cu (Ag) DEPOSIT, CENTRAL CHILE

[1]Ricardo Boric, [2]Carmen Holmgren, [3]Nicholas S. F. Wilson and [1]Marcos Zentilli

[1]Department of Earth Sciences, Dalhousie University, Halifax, Nova Scotia, Canada.
[2]Consultant, Santiago, Chile.
[3]Energy and Environment, Geological Survey of Canada, Calgary, Alberta, Canada.

Abstract - El Soldado is the largest (>200 Mt @ 1.4% Cu) of the known Cu manto-type deposits in central Chile. It is strata-bound within a submarine, bimodal calc-alkaline basalt - rhyodacite unit of the Lower Cretaceous Lo Prado Formation., which also contains marine carbonaceous shales and volcaniclastic sandstones. Although stratigraphically restricted, the clustered orebodies are mostly vein-like and discordant, controlled by a system of N-S to NNW faults formed within a transtensional zone (cymoid loop) of a sinistral, strike-slip brittle shear system. Individual orebodies are zoned, with an external and deeper zone of barren pyrite, followed inward by concentric zones with chalcopyrite-pyrite, chalcopyrite bornite, bornite-chalcocite, and a central zone of chalcocite (± digenite ± covellite) and abundant hematite. The deposit was formed in two main phases: 1) a low-temperature, diagenetic phase during which framboidal pyrite developed in association with migrated petroleum, at ca. 130 to 120 Ma; 2) a high-temperature (>300°C from fluid inclusions) hydrothermal phase at ca. 103 Ma, (coinciding with batholith emplacement), that deposited early hematite (± magnetite), followed by chalcopyrite, bornite and chalcocite, mostly replacing pre-existing pyrite, with the excess Fe forming hematite. Gangue minerals are calcite, albite, k-feldspar and chlorite. The hydrothermal Cu mineralization is associated with an increase in Na and depletion in K in host rocks, although there are localised zones of K increase in bornite-chalcocite assemblages near structures. Isotopic studies indicate that: a) the sulphur in diagenetic pyrite provided the bulk of the sulphur for Cu sulphides; b) petroleum was the source of carbon in bitumen and part of the carbonate; c) osmium in diagenetic pyrite was derived from the black shales; d) strontium in calcites was inherited from the Cretaceous arc lavas; e) oxygen isotopes in carbonates, and K-feldspar and atmospheric argon in K-feldspar plus the high salinity of fluid inclusions (21-26% NaCl equivalent) suggest a basinal connate-metamorphic brine was responsible for Cu transport, yet a (distal) magmatic component to the fluids cannot be ruled out.

Introduction

The El Soldado copper deposit (32° 38' Lat S; 71° 04' Long W; 500-1000 m above sea level.) is located in the Coastal Cordillera of Central Chile, 120 Km northwest of the capital city Santiago, and 30 km from the Pacific coast (Figure 1). The total identified resources at El Soldado, comprising production plus reserves, is well over 200 million tonnes (metric tons) @ 1.35% Cu, including 70 million tonnes @ 1.8 % Cu mined out from rich zones (Contador and Glavic, 2000), thus making it equivalent, in terms of total metal content, to a medium size porphyry copper deposit, yet smaller than Mantos Blancos and Candelaria (eg. Maksaev and Zentilli, this volume).

This paper offers an updated description of the geology, petrography, structure, ore and gangue mineralogy, hydrothermal alteration, and paragenesis of the El Soldado deposit, incorporating previous information (eg. Holmgren, 1987; Klohn et al., 1990), and adding new data accumulated in the last decade during development and mining of new orebody clusters at the mine. We also incorporate summaries of detailed studies developed during the last decade in a collaborative effort between the CMDLC staff, various consultants, and faculty and students at Dalhousie University, Halifax, Canada.

Editors note: The El Soldado deposit has been included within the Iron Oxide Copper-Gold (IOCG) family by a number authors in the existing literature, although others would disagree. It does have significant hematite and specularite associated with the copper mineralising phase. However, it differs from many of the recognised members of the family (such as Olympic Dam and La Candelaria) in that there appears to be much less evidence for a magmatic contribution to the mineralisation, but instead a more definite link to basinal processes, perhaps driven by a magmatic heat engine. In fact it exhibits the influence of many of the processes normally associated with sediment hosted copper deposits such as White Pine (USA) and the Kupferschiefer (Europe). This excellent, well reasoned paper which presents a series of carefully researched observations and cogent arguments for the formation of this deposit was invited for the reader to assimilate and ponder whether El Soldado is a member of, or is related to, the IOCG family of deposits.

Manto Type Copper Deposits

Chile contains one of the largest copper concentrations on Earth and annually produces around 37% of the world's copper (Camus and Dilles, 2001). Most of that production comes from the giant porphyry copper deposits of Cenozoic age, although a significant proportion is from Mesozoic

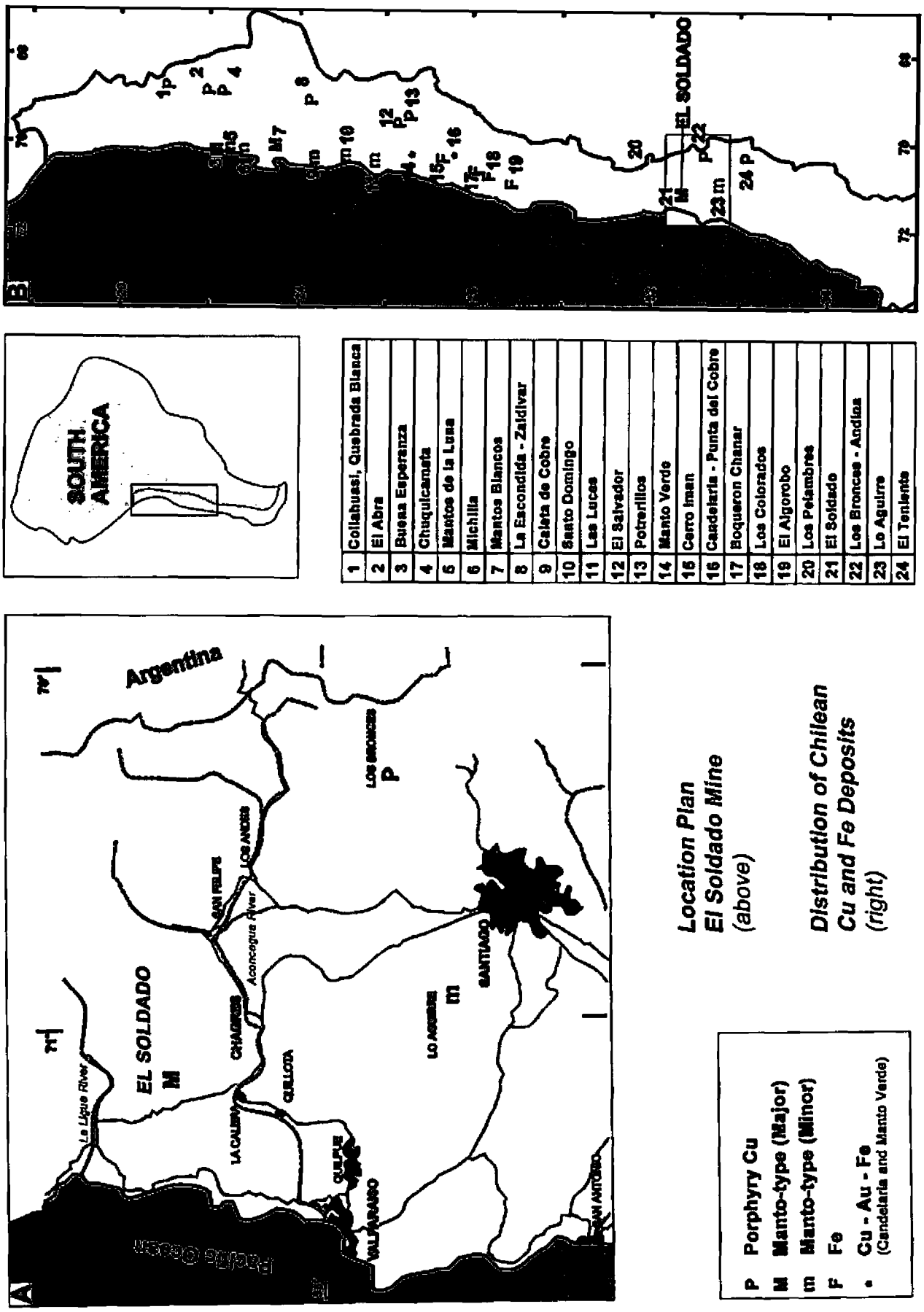


Figure 1: Location of El Soldado in central Chile, and in relation to other Chilean Cu and Fe deposits.

strata-bound copper (silver) and copper (gold-iron) deposits (Figure 1). These stratabound deposits are distributed in the western part of the Andean orogen between 21° to 34 ° latitude S and the most significant are hosted by volcanic and volcano-sedimentary sequences of Jurassic to Lower Cretaceous age, which were accumulated in intra-arc basins.

Among the strata-bound deposits, the copper (silver) family, also known as "mantos" or "manto-type" copper deposits in the literature, are the better understood. This family of deposits usually has a high copper grade (1.5-2% Cu), relatively low contents of silver (5-20 g/t) and are practically devoid of gold. They are hosted by Jurassic volcanic rocks in northern Chile (21°- 26° latitude S; eg. Mantos Blancos, Michilla) and by Early Cretaceous volcano sedimentary sequences (27° to 34° latitude S; eg. Punta del Cobre, El Soldado). The most important mines of this subtype are Mantos Blancos in northernmost Chile, and El Soldado, in central Chile (Figure 1). The ore in these deposits is only strata-bound in a regional sense, meaning that they are epigenetic, and although the ores are restricted to certain stratigraphic units, in detail they are discordant; their orebodies are structurally controlled or follow relatively permeable horizons in the strata. Hypogene mineralogy is relatively simple, and consists of bornite, chalcocite (± digenite), chalcopyrite, pyrite and hematite. The sulphide ores tend to occur in reduced (probably sub-marine) strata rather than in oxidised (sub-aerial) strata, suggesting to most authors that oxi-reduction reactions were important in their genesis. Supergene metal enrichment related to surficial weathering, which has been significant in making some porphyry copper deposits economic, is not a main factor in the mantos, although oxidised ores are exploited in many. Gangue minerals are relatively scarce and the effects of hydrothermal alteration are difficult to distinguish from low-grade regional metamorphic assemblages (eg. Sato, 1984; Sillitoe, 1992).

The genesis of these manto type deposits has been the subject of much controversy (eg. Fontboté, 1990), with the proposed genetic models ranging from volcanogenic syngenetic (eg. Ruiz, et al., 1965; Camus, 1980; Ruiz and Peebles, 1988), through hypotheses that call for fluids liberated during low-grade metamorphism of the volcanic piles (eg. Sato, 1984: Westra, 1988; Sillitoe, 1992); fluids directly derived from granitoid plutons (eg. Carter, 1961; Palacios, 1986; Klohn et al., 1990), to a combination of these last two mechanisms (eg. Fontboté, 1990). The scarcity of effectively datable minerals has made absolute dating difficult, and the pronounced alkali metasomatism of the host rocks (Boric, 2002) complicates their interpretation. Nevertheless, available geochronological data suggest that, in this family of deposits, ores were emplaced at least 10 Ma after the deposition of the host strata, mainly during two metallogenic pulses, in the Late Jurassic and in the Early Cretaceous (Munizaga et al., 1988; Boric et al., 1990; Tassinari et al., 1993; Vivallo and Henriquez, 1998; Wilson et al., submitted; Maksaev and Zentilli, this volume).

Geography and History

The El Soldado mine (Figure 1) is located within 8 km of the Pan American Highway, railway links and major power grids. The mine is currently owned and operated by Cia. Minera Disputada de las Condes Ltda. (CMD), an affiliate of ExxonMobil Coal and Minerals Co. (EMCMC). El Soldado's primary operations (Figure 2) comprise an open

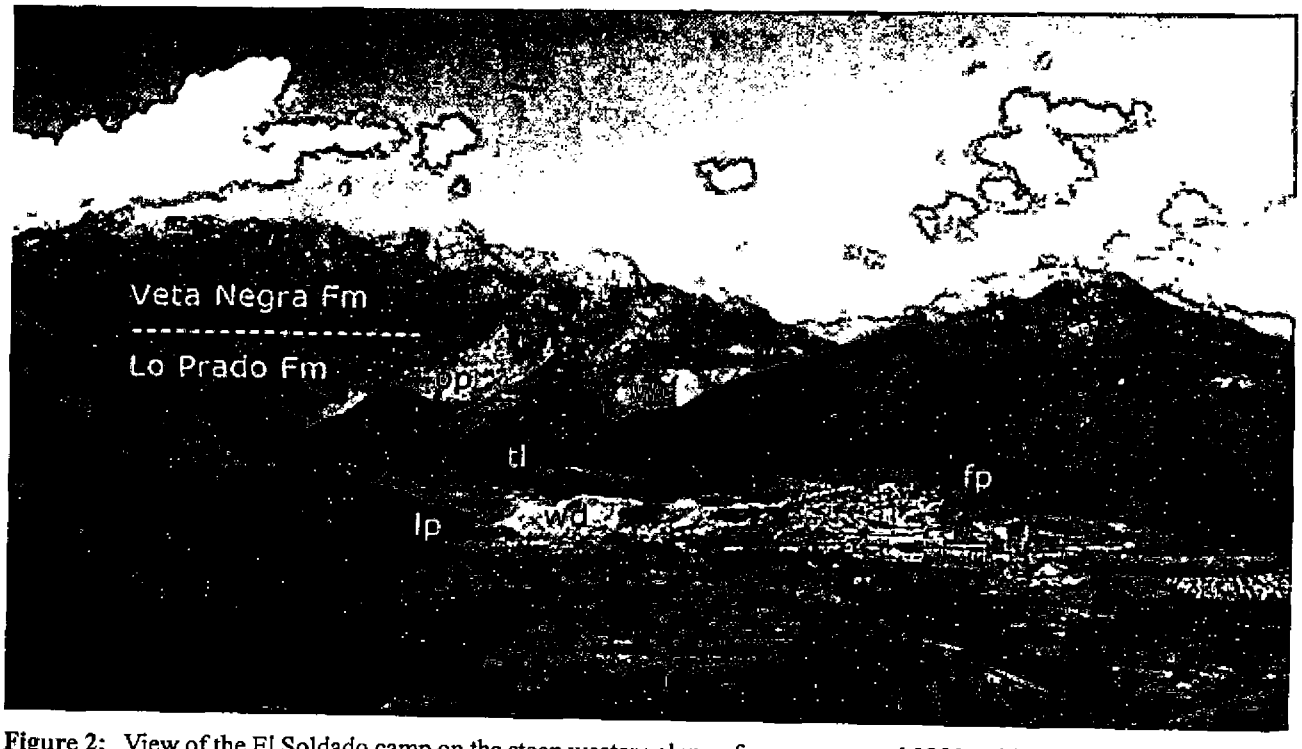


Figure 2: View of the El Soldado camp on the steep western slope of a snow-capped 2300 m high range. The dotted line marks the approximate boundary between the marine Lo Prado Formation and the sub-aerial andesitic lavas and red beds of the Veta Negra Formation. Also shown are the Morro open pit (op), waste dumps (wd) the transport level for the underground operation (tl), the flotation plant (fp) and the leaching plant (lp).

pit mine (the Morro pit), an underground mine, the El Cobre sulphide flotation concentrator plant, and a leaching plant with Solvent Extraction Electro Winning (SXEW). Concentrates are sent to the CMD Chagres smelter located north of the Aconcagua River, southeast of El Soldado (Figure 1), or to the Ventanas port on the Pacific coast.

The mine lies on the steep west flank of a 2300 m high, moderately vegetated range (brush and small deciduous trees), in a zone of warm-temperate climate, with abundant winter fog, irregular precipitation in the form of rain (~ 400 mm/year), and occasional snow during May to August (Figure 2). Temperatures range from –2°C in winter to ~30°C in summer, with a yearly median of ~15°C (Fuenzalida, 1965).

At El Soldado, mining of exposed high-grade pods began in the eighteenth century, although the first modern exploitation did not commence until 1919, when ore grading between 7 and 15 % Cu was extracted from an underground mine. Since then, under a number of subsequent owners, production has been almost continuous, but was limited to less than 600 t/day until the late 1960s, when it was increased to 3300 t/day. Exxon Minerals, today EMCMC,

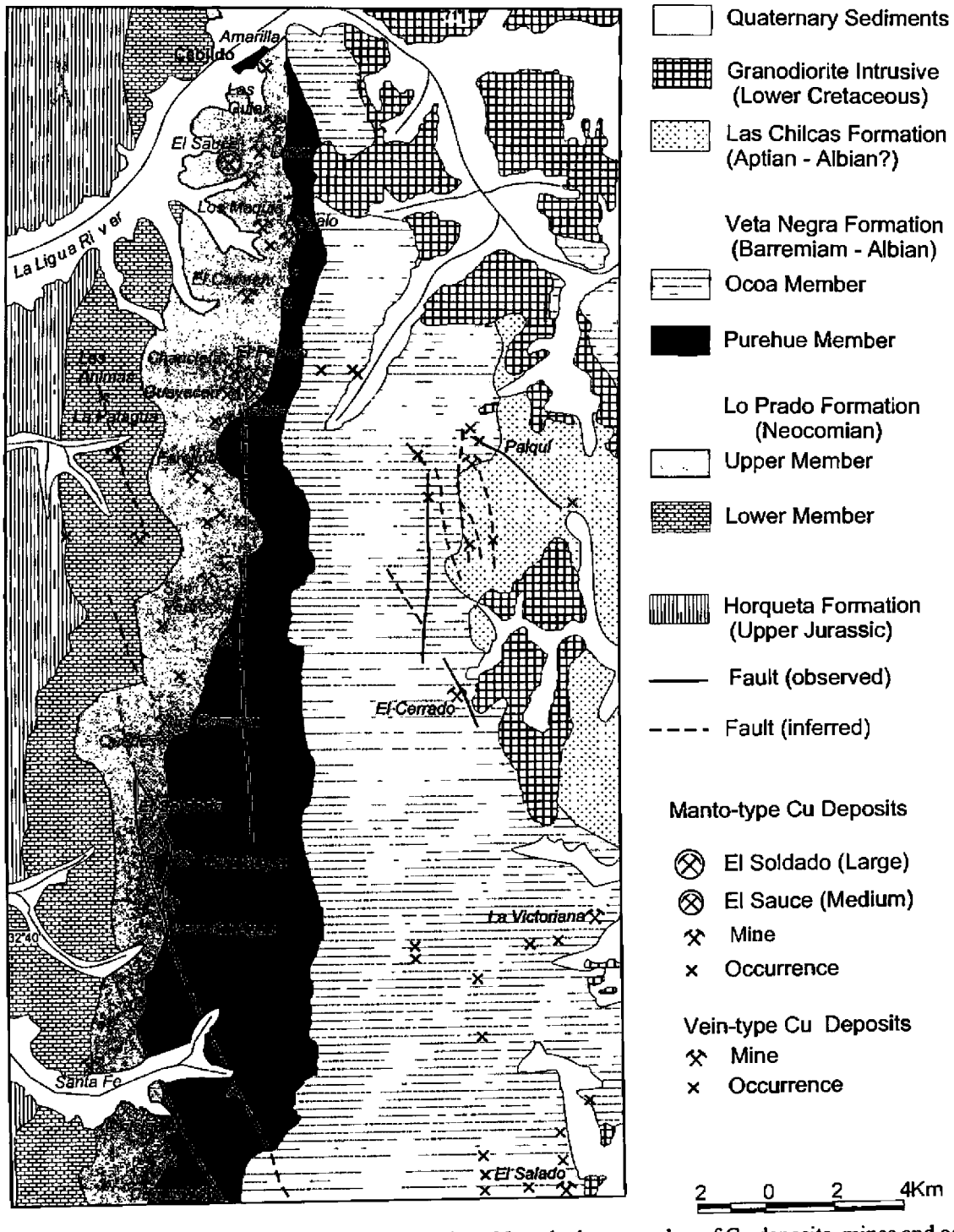


Figure 3: El Soldado in its regional stratigraphic setting. Note the large number of Cu deposits, mines and occurrences hosted by the Lower Cretaceous Lo Prado Formation and the distal location of El Soldado with respect to outcrops of the Cretaceous batholith.

also owner of the Los Bronces porphyry copper deposit in the high Cordillera (Figure 1), assumed control of El Soldado in 1978 and developed an intensive drilling campaign, which led to the discovery of many unexposed sulphide orebodies, significantly increasing ore reserves. These discoveries and the change in underground mining method to sub-level open-stoping, allowed stepwise expansions in sulphide ore treatment to 5500 and 11 500 t/day. In 1989 the Morro open pit (Figure 2) began operating, to support an increase in the production rate up to the current 17 500 t/day, with the SXEW leaching plant (Figure 2) being added in 1990 to treat the oxide ore from the Morro pit. In 2001 the open pit mine provided 70% of total production, with a copper grade at 1.2% Cu. Total identified resources at El Soldado, comprising production plus reserves, is well over 200 million metric tons @ 1.35% Cu, including 70 million metric tons @ 1.8% Cu mined out from rich zones (Contador and Glavic, 2000).

Regional Geologic Setting

The El Soldado deposit is hosted by the upper member of the Lower Cretaceous Lo Prado Formation (Piraces and Maksaev, 1977), a volcaniclastic arc suite, which represents an important regional metallotect, hosting more than 20 copper deposits mined at one time or another, between the Aconcagua and the La Ligua rivers (Figures 1 and 3). At El Soldado, this unit is 500 m thick and composed of bimodal rhyodacitic (felsic) and basaltic (mafic) flows and pyroclastics with sedimentary volcaniclastic and marine limestone lenses (Figure 4). These strata are underlain by the lower member of Lo Prado Formation, a marine, organic-rich calcareous shale-siltstone-sandstone unit, which is at least 1500 m thick. The Lo Prado Formation conformably overlies the volcanic Upper Jurassic Horqueta Formation (Figure 3), and is conformably overlain by 5-7 km of basaltic andesites, tuffs, volcanic epiclastic breccias, redbeds and lacustrine sediments of the continental Lower Cretaceous (Barremian-Albian) Veta Negra Formation, which in turn is overlain by the Cretaceous (Lower - Upper Cretaceous) Las Chilcas Formation (eg. Rivano et al., 1993; Rivano, 1996).

Deposition of the sedimentary-volcanic sequence took place in a transitional marine-terrestrial environment during the Early Cretaceous. The Lo Prado Formation contains both marine (ammonites and pelecypods of Berriasian to Hauterivian age; Vergara et al., 1995; Wall et al., 1999) and plant remains, indicating proximity to a coast. Pillow basalts are locally developed in the upper member of Lo Prado Formation (Vergara et al 1995), but at the mine area, basalt flows and rhyodacite flows, domes and feeder dykes predominate. The overlying Veta Negra Formation marks a transition to a terrestrial environment, and is characterised by oxidised lavas and intercalated volcaniclastic breccias and redbeds. The presence of Lower Cretaceous marine fossils in the overlying Las Chilcas Formation (Rivano et al., 1993; Wall et al., 1999) indicates that brief marine transgressions occurred after deposition of the Veta Negra Formation in a subsiding basin.

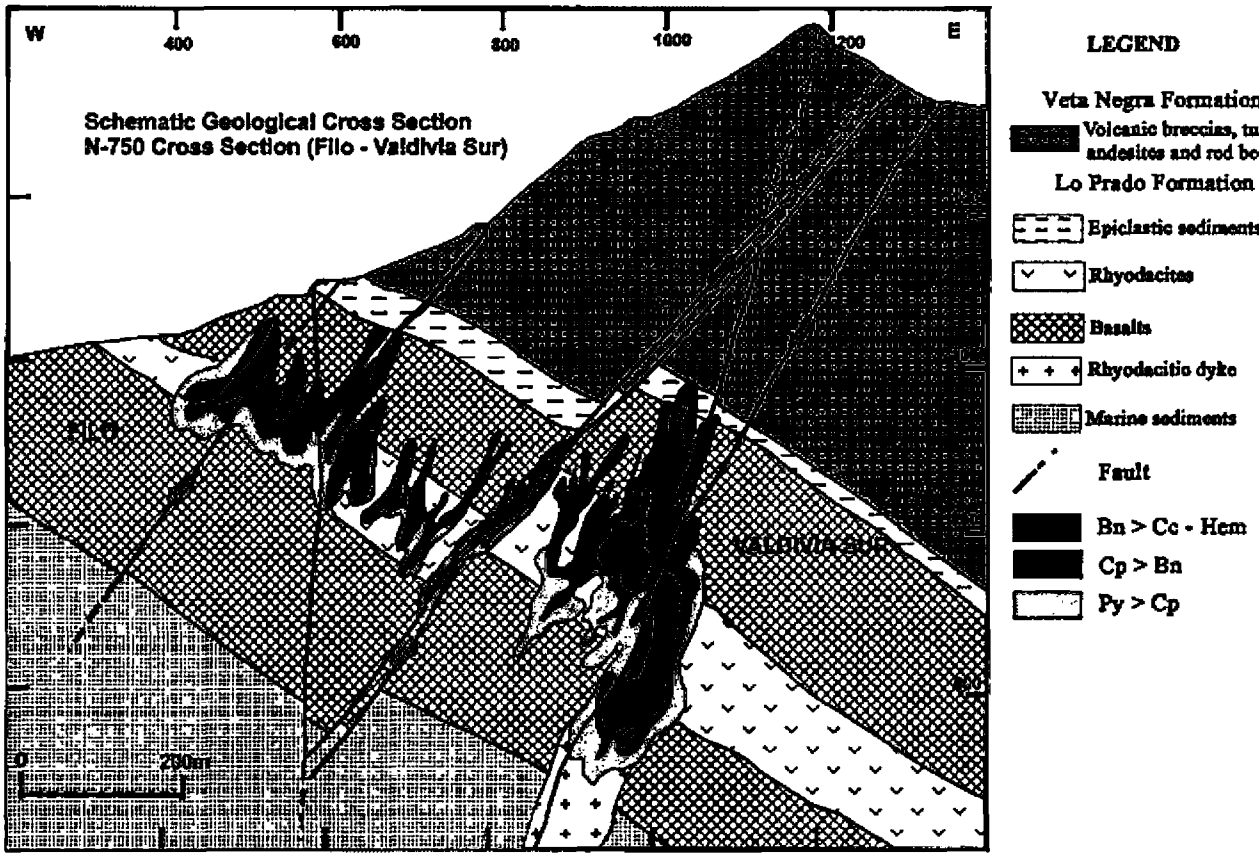


Figure 4: Cross-section at the N-750 coordinate. Note the structurally controlled and yet stratabound nature of the orebodies within the upper member of the Lo Prado Formation.

Lower Cretaceous, calc-alkaline granitoids intrude the Veta Negra Formation in the mountains 13 km to the east of El Soldado (Figure 3) and the Lo Prado Formation both 20 km along the range to the north (Figure 3), and 28 km directly south of El Soldado at La Campana-Caleu, and may well subcrop much closer at the level of the mine. In these localities the batholith has generated skarnoid and vein copper deposits (eg. Ruiz and Peebles, 1988). The age of this batholith is bracketed by K/Ar dates on biotite (118-94 Ma; Rivano et al., 1993; Wall et al 1999), and on more precise $^{40}Ar/^{39}Ar$ dates on hornblende (117-103 Ma), and on biotite (101-94 Ma; Parada and Larrondo, 1999).

Major structures recognised at the district scale are N-S to NNW left lateral strike-slip faults and reactivated normal faults; the latter dipping at 60° to the west (Figures 4 & 5). The strata have been tilted into a ca. 30° east-dipping homocline, but the dip of the strata decreases progressively to the east.

In terms of tectonics, these Lower Cretaceous volcano-sedimentary sequences and granitoids, are inferred to represent a volcano-plutonic arc, developed at a continental margin (eg. Charrier and Muñoz, 1994; Vergara et al, 1995). The great thickness of shallow water formations and the recurrence of marine facies are suggestive of subsidence and deposition under extensional conditions, which had prevailed at the arc and back arc domains (Åberg et al., 1984; Vergara et al., 1995). This environment is consistent with conditions associated with a steep subduction regime

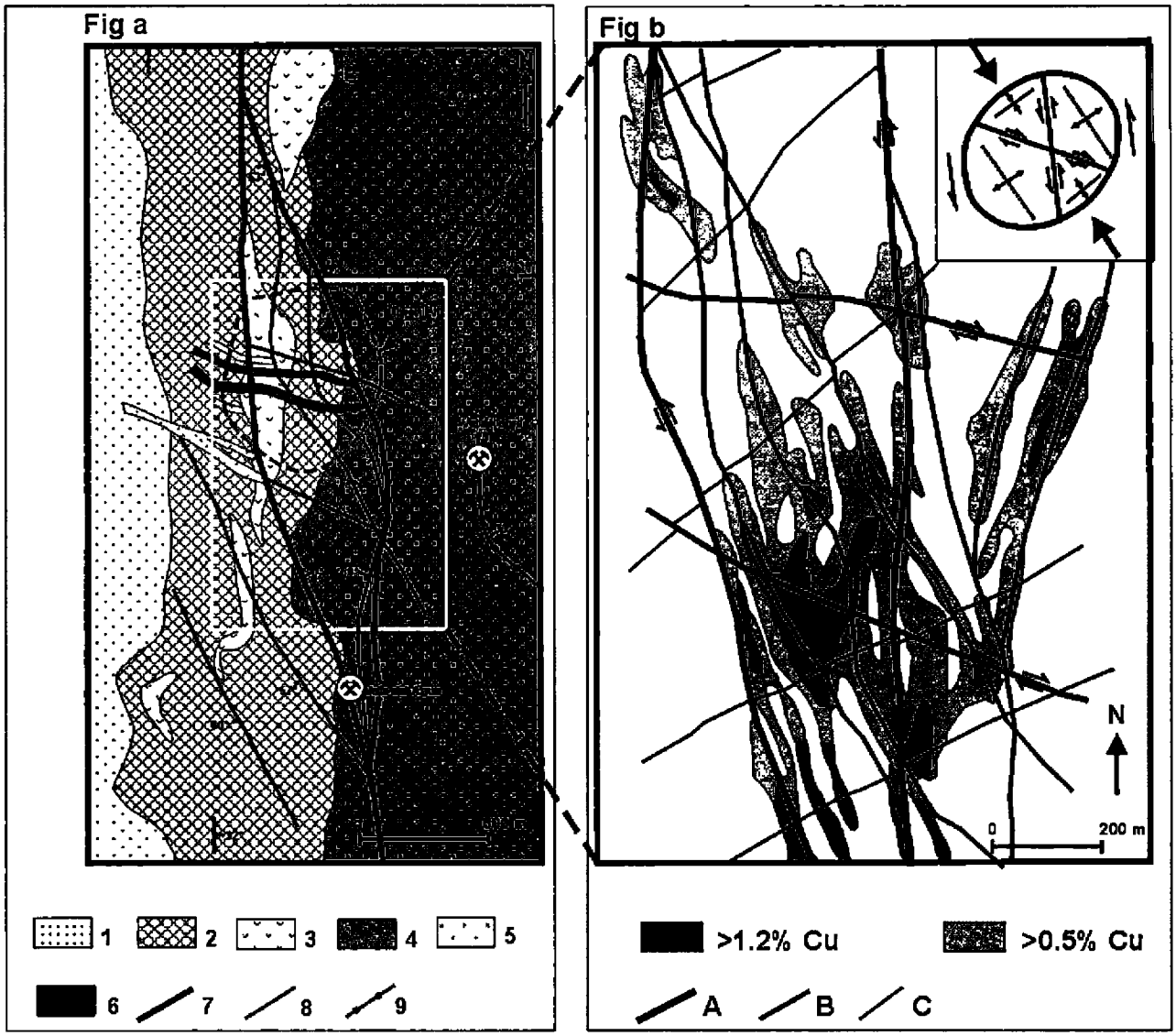


Figure 5: Simplified structural map of El Soldado orebodies in relation to a regional wrench fault. Note outline of open pit.

a) Location of the deposit within a cymoid loop. 1: Lower sedimentary member of the Lo Prado Formation; 2: Upper member of Lo Prado Formation; 3: rhyodacite flows and domes; 4: Veta Negra Formation; 5: Rhyodacite feeder dykes; 6: Andesite feeder dykes for Veta Negra Formation; 7: Major regional wrench faults (generalized); 8: Lesser faults and veins; 9: Mineralized (Cu) lacustrine shale at Veta Negra mine, showing dip of strata; due to generalization, dyke displacements are not shown.

b) Generalized structural plan of orebodies, detail from 5A: A: Main shear faults; B: Secondary Faults; C: Fractures. Inset shows hypothetical model of conjugate faults in response to a sinistral wrench system with a regional NNW (horizontal) main stress axis (modified from Boric, 1997).

(*Marianas Type*) inferred to have been active in this segment of the Andes during most of the Early Cretaceous (eg. Mpodozis and Ramos, 1990; Sillitoe, 1992; Maksaev and Zentilli, this volume).

Lithological Control

Figure 4 is a cross-section showing the main stratigraphic units recognised at the mine through the Filo and Valdivia Sur orebody clusters, namely: 1) the lower member of the Lo Prado Formation, composed of marine sediments, mostly volcaniclastic sandstones, organic-rich siltstones, and calcareous shales; 2) the upper member of the Lo Prado Formation, a 500-m-thick sequence of interlayered basaltic and rhyodacite flows and domes, with intercalations of tuffs, epiclastic sandstones and breccias, some with calcareous cement, also of marine origin, and 3) the lower (Purehue) member of the Veta Negra Formation, composed of red, oxidised, subaerial basaltic andesite flows (many of them breccia flows), intercalated tuffs, red sandstones, and a few lenses of lacustrine siltstones with abundant carbonised plant remains and minor copper sulphides (eg. at the Veta Negra deposit, Figures 3 and 5; Villalobos 1995).
In addition there are 3 different types of subvertical dykes (Figure 5): 1) rhyodacite dykes with a 290-300° trend, some of which are the feeders of the host rhyodacite flows and domes of the Lo Prado Formation; 2) basaltic and andesite dykes with a 280-290° trend; some of these are feeders to the Veta Negra Formation lavas; and 3) microdiorite dykes that cut all the above units and have a NW and NE trends. The only faneritic intrusive recognised in the camp is a gabbro-diorite stock, which has been intercepted by deep drill holes in the northern part of the mine; it does not outcrop, and it is interpreted to be coeval with the Veta Negra volcanic sequence.

Basaltic flows can be correlated within the camp, although they have notable textural and thickness variations. Most significant as a host rock, the rhyodacite flows are thicker above the feeder dykes, forming domes, with spectacular columnar jointing (Figure 6), and locally a brecciated top, interpreted to be a syn-volcanic structure. Away from their feeder dykes, the rhyodacites grade into coarse to fine volcaniclastic rocks. Large angular boulders of rhyodacite in overlying epiclastic strata that cap the ore deposit indicate that the rhyodacite domes were elsewhere undergoing erosion soon after emplacement (Wilson, 1998).

In most previous publications, such as the company reviews by Klohn et al. (1986, 1990) the host rocks to ore at El Soldado have been referred to as "anomalous", "alkaline" "trachytes" and "andesites", and the title of the papers (if not their conclusions) imply that the ores are related to alkaline magmatism. Other workers suggested that the felsic rocks are either albitised (Na metasomatised) andesites (Olcay and Alarcon, 1975), or represent rhyolitic

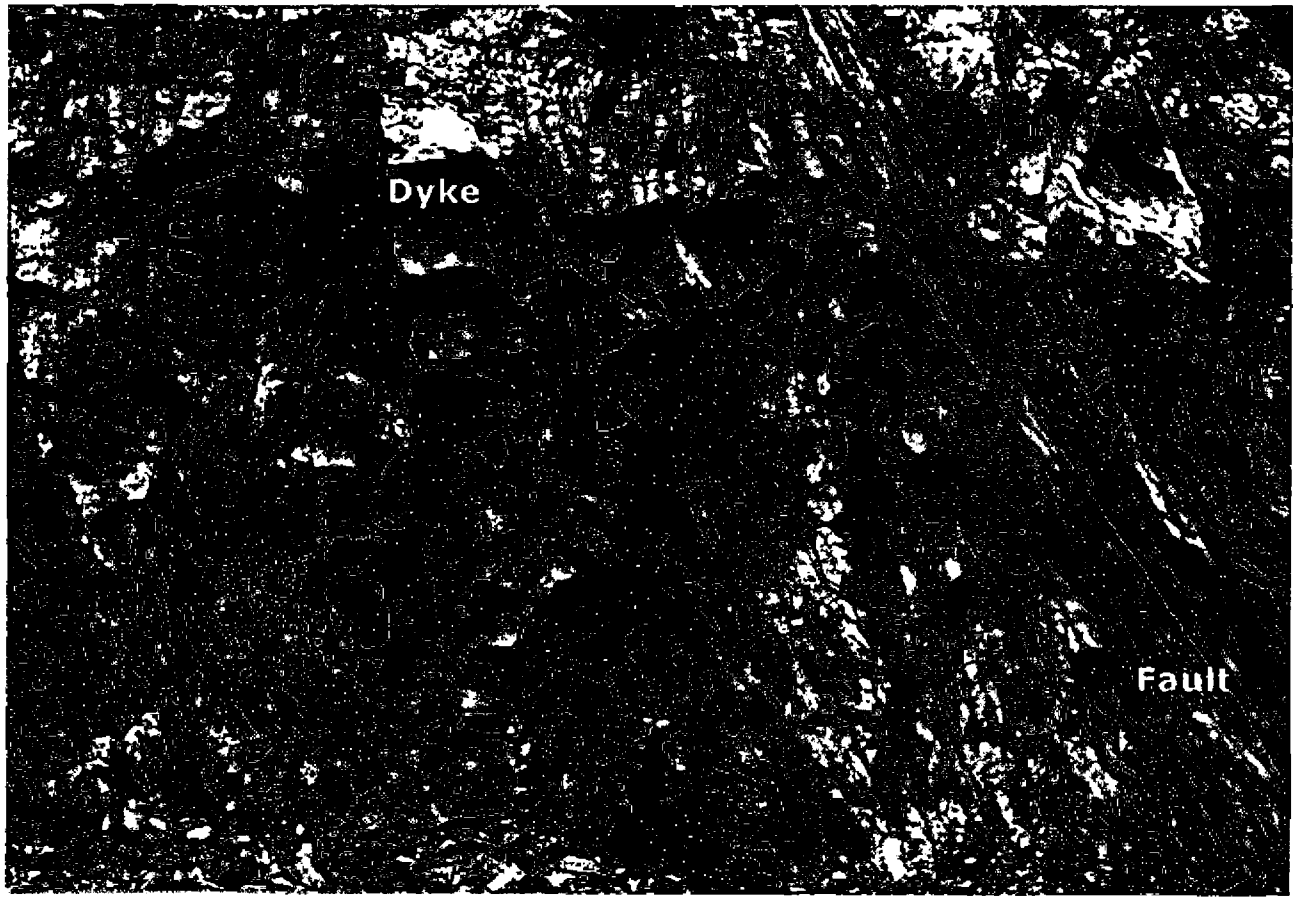


Figure 6: Strongly developed columnar jointing in mineralized rhyodacite unit exposed in Morro open pit. Primary porosity and the competent nature of the rhyodacite makes it the most favourable host rock. Note the different style of fracturing in andesite dyke, and steep fault plane.

Table 1. Geochemistry, Average Values by Ore Zone

| 1. Averages Values by Ore Zone | | |

primary and secondary) and zircon are scarce, and U/Pb dating indicates that part of the (visibly resorbed) zircon is xenocrystic (Zentilli et al., 2001). Even though there is no textural evidence for Na alteration, the albite phenocrysts are interpreted to be the result of an event of regional metasomatism/metamorphism rather than a primary factor or a product of hydrothermal alteration *per se*. It is the trachytic texture and the abundant feldspar laths that led to this rock being named a trachyte. Rhyodacites also have minor ferromagnesian phenocrysts altered to calcite, chlorite, epidote, titanium oxides (leucoxene, titanite, rutile), and minor hematite and pyrite. Although less abundant than in the basalts, pyrite is a very common secondary mineral in the least-altered, "background" rhyodacites. Pyrite occurs as small crystals (1 to 100 μm), disseminated in the groundmass, included in albite phenocrysts, and very commonly replacing or rimming ferromagnesian minerals or titanomagnetite (see Figure 9A). These rhyodacites have the characteristics of altered and Na-metasomatised felsic rocks referred to in the past as *keratophyres* (Boric 2002).

It is interesting to note that 60-65% of copper production has come from rhyodacitic host rocks, 30-25% from basaltic hosts and 5-10% from the volcaniclastic sediments, reflecting their respective behaviour during deformation. As shown in Figure 4, economic copper mineralization is restricted to the upper member of the Lo Prado Formation, although narrow veins continue upwards into the lowermost strata of the Veta Negra Formation. This clearly indicates that copper mineralization postdates the deposition of the base of that unit. The roots of orebodies are usually located well above (100-150 m) the lower sedimentary member of the Lo Prado Formation. The lowermost unit of the upper member of the Lo Prado Formation, which is composed of basalt breccia flows with minor volcaniclastics is mostly barren, containing only minor pyrite (Boric, 2002).

Structural Control

El Soldado comprises numerons vein-like orebodies with intervening barren zones, distributed in about a dozen orebody clusters (Figures 5 and 8). The known clusters are spatially distributed within a volume that is about 2 km long by 0.8 km wide and 600 m in vertical extent (Figures 4 and 8). Within the blocks, individual sub vertical orebodies are extremely variable in size, from very small to 450 m long, 150 m wide, and 450 m in vertical extent (Boric, 1997). Clusters of orebodies occur mainly where structural permeability has been generated by brittle fracturing, such as in fault intersections, where subvertical (pipelike) bodies are developed. The best example is the Valdivia Sur chimney (Figure 4), which contains 14 Mt @ >2% Cu, including core zones grading 5% Cu and 20-30 g/t Ag. At an individual orebody scale, the copper sulphides occupy mainly structural porosity, in the form of veins, faults and joints, including columnar joints. Fracturing is most intense in the rhyodacite (Figure 4), which was not only the hardest and most brittle, but was pre-fractured by columnar jointing (Figure 6) and syn-volcanic breccias. Primary porosity was also important locally, in the form of vesicles and irregular gas structures in basalts, and inter-clast pores in breccias and tuffs. However, the tuffs in the uppermost Lo Prado Formation were relatively incompetent (ductile) during faulting, and in general formed an impermeable seal to all fluids, both petroleum and hydrothermal solutions.

The master faults are shears that form a cymoid loop (eg. Anhaeusser, 1965) - a dilational jog or trans-tensional zone (eg. Cox et al., 2001) - within the confines of which the best orebodies were developed. This loop is closed both to the south and north of the mine (Figure 5). Intersections of N-S and NNW faults with 290°-300° conjugate faults form particularly rich orebodies within this transtensional domain. North and south of the loop orebodies are narrow and can

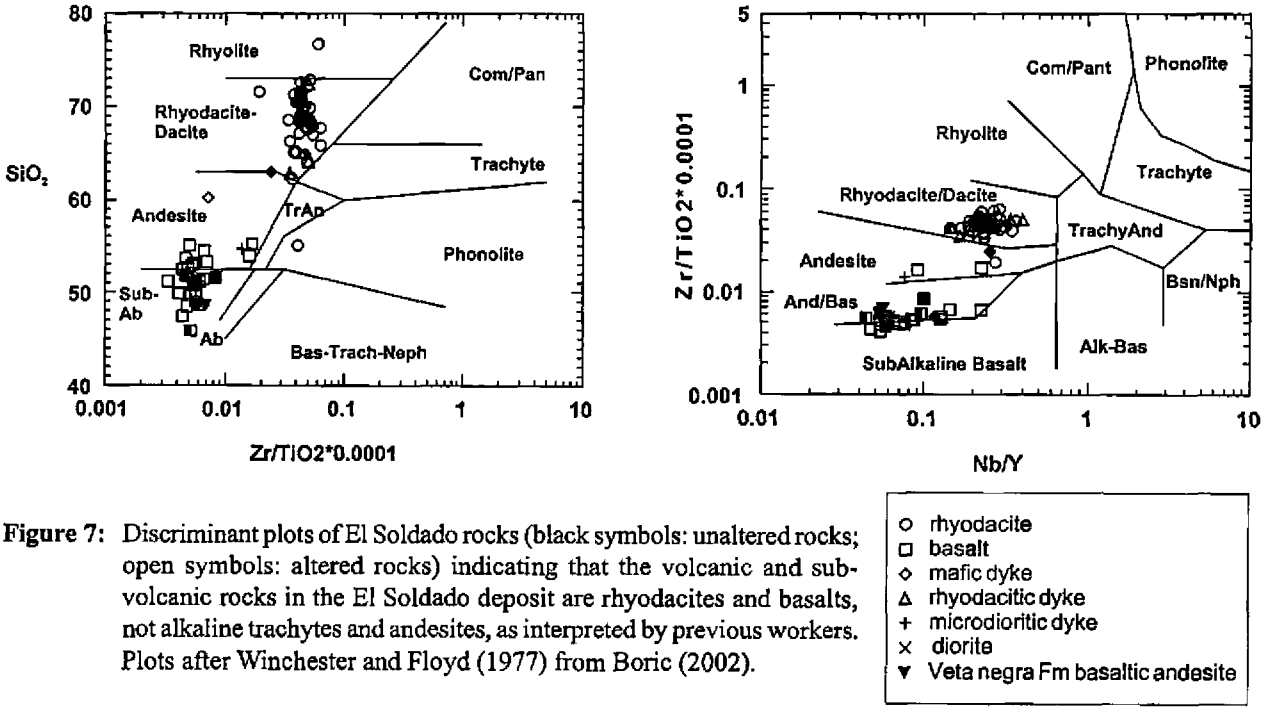
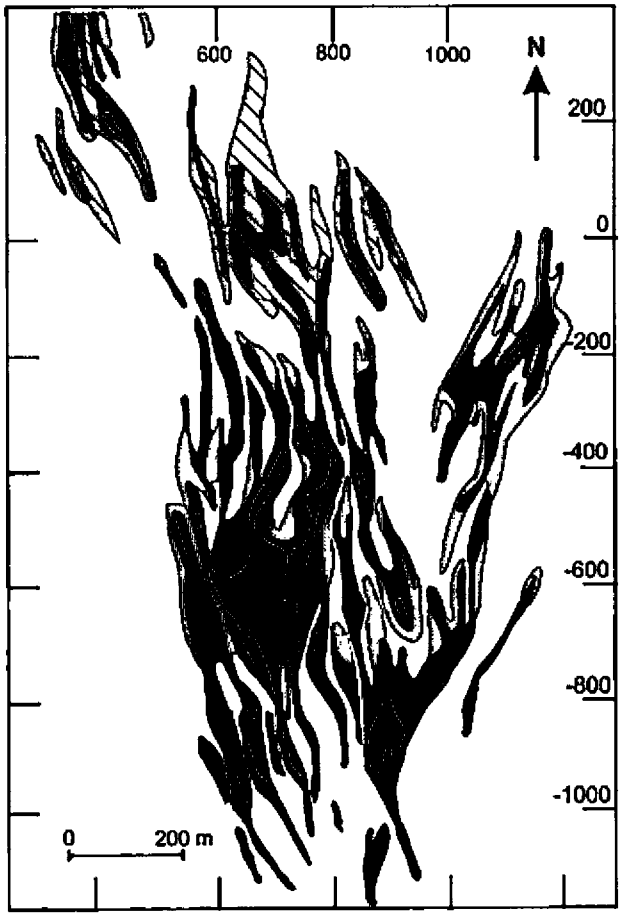


Figure 7: Discriminant plots of El Soldado rocks (black symbols: unaltered rocks; open symbols: altered rocks) indicating that the volcanic and sub-volcanic rocks in the El Soldado deposit are rhyodacites and basalts, not alkaline trachytes and andesites, as interpreted by previous workers. Plots after Winchester and Floyd (1977) from Boric (2002).

be best described as veins (eg. Veta del Agua, Figures 3 and 5). Intermediate and mafic dykes which were emplaced in a general WNW trend, are cut and displaced by most faults and predate the hydrothermal event, although they are generally unmineralised (Boric, 1997). This structural pattern can be explained by a fracturing-reactivation event under brittle strain conditions. Judging by the orientation of conjugate shears and of dilatant fractures, the main stress ($\sigma 1$) is inferred to have been sub-horizontal and oriented NNW - SSE; the minimum stress ($\sigma 3$) perpendicular to it, and the intermediate stress ($\sigma 2$) subvertical (eg. Boric, 1997; 2002; S. Caddey, CMD internal report, 2001). This inferred local tectonic stress is consistent with the regional stress field active during the Early Cretaceous and responsible of the left lateral motion along the Atacama fault system in the Early Cretaceous of northern Chile (eg. Maksaev and Zentilli, this volume). Chavez (1988), in a detailed rock-mechanics analysis of meso- and micro-structures in the underground workings, computed probable maximum ($\sigma 1$) and minimum ($\sigma 3$) confining stresses of 1050 and 850 bar respectively, and pore fluid pressures for the main fracturing-mineralising event of between 1250 and 850 bar.



Mineral Zoning and Paragenesis

Hypogene ore minerals (Figures 9 & 10) are chalcopyrite, bornite, chalcocite (and digenite) and minor covellite that occur as disseminations and veinlets. Common waste or gangue minerals are pyrite, hematite, calcite, chlorite, albite, K-feldspar (adularia, microcline), solid bitumen, quartz, opaline silica, rutile, titanite, and minor amounts of magnetite, sphalerite, galena, and arsenopyrite. Hydrothermal alteration mimics the gangue associations (Table 1; Figure 11), and consists of abundant calcite, chlorite, albite, microcline, epidote, titanite-leucoxene and rutile, and some quartz, sericite and clay minerals, but primary rock textures are largely preserved (Holmgren, 1987, Boric, 1997).

Individual orebodies in a cluster (Figure 8) show a remarkable mineralogical zoning (eg. Martin, 1981, Ruge, 1985; R. Sillitoe, CMD internal report, 1995; Boric 1997, Ponce 2001), from a core of chalcocite - (covellite) - hematite or chalcocite- (covellite) -bornite-hematite; followed outward by approximately concentric zones of bornite-chalcopyrite, chalcopyrite, chalcopyrite-pyrite and pyrite in the most peripheral zone. Furthermore, the deeper roots of the orebodies contain relatively more pyrite than their upward terminations, which are richer in bornite, chalcocite and fine hematite (Figure 8B; Boric, 1997; 2002; Ponce, 2001). As shown in Figure 8A, a more global zoning

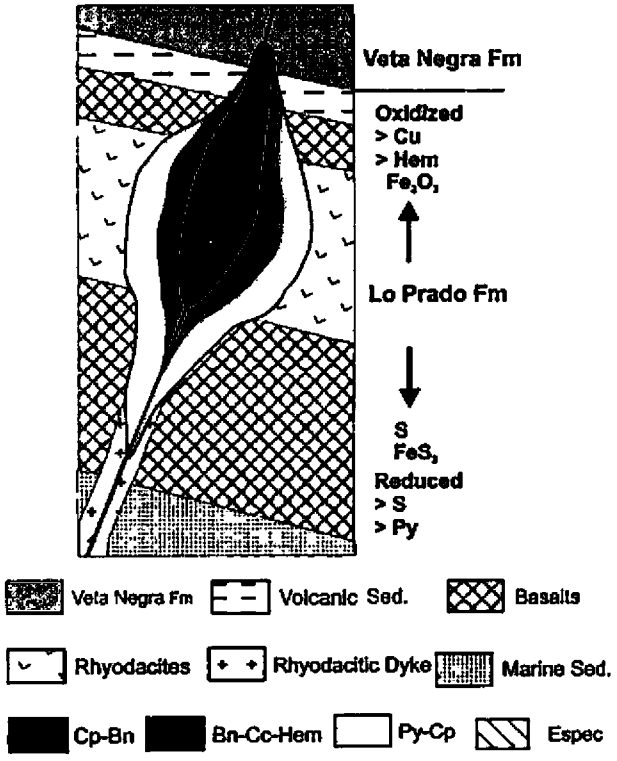


Figure 8:

Left Plan view of El Soldado orebodies (Level Zero), showing mineral zoning of orebody clusters. Note a general increase of specular hematite (Spec Hem) towards the north, and an increase of chalcocite and bornite toward the south.

Right Generalized model (adapted from Sillitoe, CMD internal report, 1996 and Boric, 1997), for the vertical mineralogical zoning of individual orebodies: outward pyrite-chalcopyrite zone, followed inwards by a chalcopyrite-bornite zone, and an internal and uppermost bornite-chalcocite-hematite zone

at the camp scale has also been noted. The southern orebodies have relatively more chalcocite and bornite, whereas chalcopyrite and pyrite predominate towards the north (Martin, 1981; Holmgren and Gonzalez, 1988; Boric, 1997; Boric, 2002). In addition, new exploration drill holes have shown that specular hematite becomes gradually more abundant towards the north (Boric, 2002).

Matching their mineralogical zoning, the orebodies display a strong variability in copper grades, especially laterally (Figures 4, 5 & 8). Their lateral margins are similarly characterised by abrupt changes in the copper content (Ruge, 1985). The transition from internal high-grade (~1.2 - 2.0% Cu), to lateral medium-grade (0.5 - 1.2% Cu), to external low-grade (0.2 - 0.5% Cu) zones, takes place within few metres or less. Country (or "background") rocks between the orebodies are "barren" (usually below 0.1% Cu; Table 1; Figure 11). Variations in copper grade are less marked along strike and down plunge of the orebodies. The cut-off grade is generally 0.8% Cu for the underground mine, and 0.5% Cu for the open pit. The silver content averages about 6 g/t Ag, although in the bornite-chalcocite core it is 20-30 g/t Ag. Microprobe analyses indicate that silver is mainly in the bornite and chalcocite, as inclusions and in solid solution (M.C.Graves, Cuesta Research Ltd. report for CMD, 1995; Boric, 1997; Ponce, 2001). It is important to emphasise that globally, Cu grades increase southwards (Boric, 2002).

In previous studies (eg Klohn et al, 1990), the external pyrite zone (Figures 4 & 8) had been considered a distal unit within the hydrothermal assemblage. However, it is now recognised that at least part of this pyrite (background values where pyrite is less than 2% by volume) grew at low temperatures in association with liquid petroleum in the realm of sulphur-reducing bacterial activity. Geopetal structures of gas bubbles at the top of oil-filled cavities indicate that petroleum migrated and solidified before the tilting of the strata (Wilson and Zentilli, 1999). Therefore it is necessary to contrast the pyrite of diagenetic origin (Stage I of Wilson and Zentilli, 1999) and that of possible hydrothermal origin (Figure 12); zones with more than 2% pyrite could be a combination of both processes (Boric, 2002).

Part of the pyrite grew by sulphidation of titanomagnetite (Figure 9A) and ferromagnesian minerals, and is present as fine disseminations in all rocks as a background, usually comprising about 1% by volume. However, most of the pyrite in El Soldado occurs as framboidal spherules associated with bitumen (Figures 9B, 9C). Framboids are spheroidal aggregates with a diameter ranging from a few micrometers to 70 μm (mean 16 μm; Wilson, 1998) made

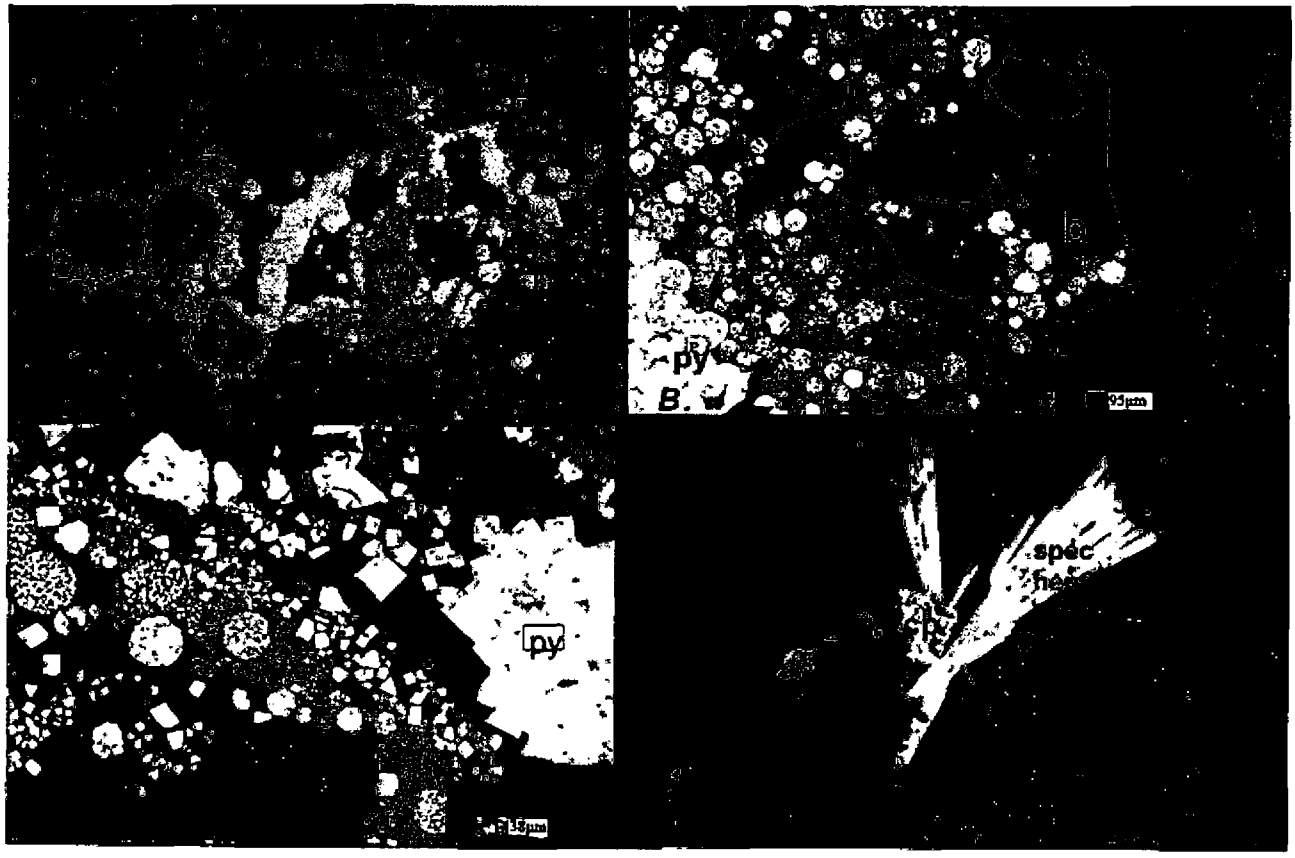


Figure 9: Photomicrographs of Diagenetic (A,B,C) and early hydrothermal assemblages (D).

- A: Altered titanomagnetite rimmed by diagenetic pyrite (white), in calcite (dark) (field of view 4 mm);
- B: Diagenetic, framboidal pyrite (py) within and around solid bitumen (b) and calcite (ca) (scale bar 95 micrometers);
- C: Framboidal and euhedral pyrite in calcite (ca) (scale bar 38 micrometers);
- D: Specular hematite (spec hem) and chalcopyrite-pyrite from the earliest hydrothermal stage, in altered rock (field of view 2 mm).

of euhedral pyrite crystals of 1 μm and larger. These framboids developed mostly, but not exclusively, within globules of liquid petroleum, now bitumen. Around a nucleus of framboidal pyrite, later growth of pyrite, probably as a result of increasing temperatures, developed large euhedral pyrite crystals (Figure 9C). Minor amounts of sphalerite, sphalerite with inclusions of chalcopyrite (Wilson, 1998), and very rare arsenopyrite (Zentilli et al., 1997) exist within this early sulphide assemblage. It remains open to question how much, if any of the pyrite at El Soldado developed during the hydrothermal phase. Low values of arsenic are associated with (and perhaps restricted to) the diagenetic pyrite (Wilson, 1998; Collins et al., 2002).

Organic matter occurs as bitumen and graphite. In hand specimen bitumen looks glassy black and is brittle like anthracite. It is particularly significant in the south of the camp (eg. Filo). Under transmitted light it is opaque, and under reflected light it is light brown (Figures 9B, 10B, 10D) with low reflectance (less than 5%), and thus easily overlooked; it is relatively soft and brittle and is easily plucked out during manufacture of polished sections. Although identified and analysed by microprobe (C.Holmgren & F.Barbagelata, CMD internal company report, 1985), its genetic significance was not recognised until recently (Zentilli et al., 1994; 1997). Bitumen started as liquid petroleum, and is found forming globules, commonly showing degassing bubbles that have risen to the top of cavities (Wilson and Zentilli, 1999). Solidification led to shrinkage and fragmentation into angular granules (Figures 9B, 10D). Bitumen occupies primary and fracture porosity in rhyodacites and basalts, and it is commonly associated with calcite, which fills brittle (post-solidification) fractures, indicating that calcite is paragenetically later. It occurs with framboidal pyrite, and in all sulphide zones, but is more abundant in the Filo orebody cluster in the southern part of the camp (Wilson, 1998). Graphite (graphitised bitumen) occurs in the north of the camp in chalcopyrite and bornite veins (Wilson, 1998). Bitumen in the richest bornite ores is highly enriched in chlorine, as detected in microprobe analyses. This chlorine is interpreted to have been inherited from chloride copper complexes during mineralization, suggesting an active-carbon role for the bitumen (Wilson and Zentilli, 1999).

During the hydrothermal stage (Stage II) chalcopyrite was the first copper mineral to crystallise; chalcopyrite clearly

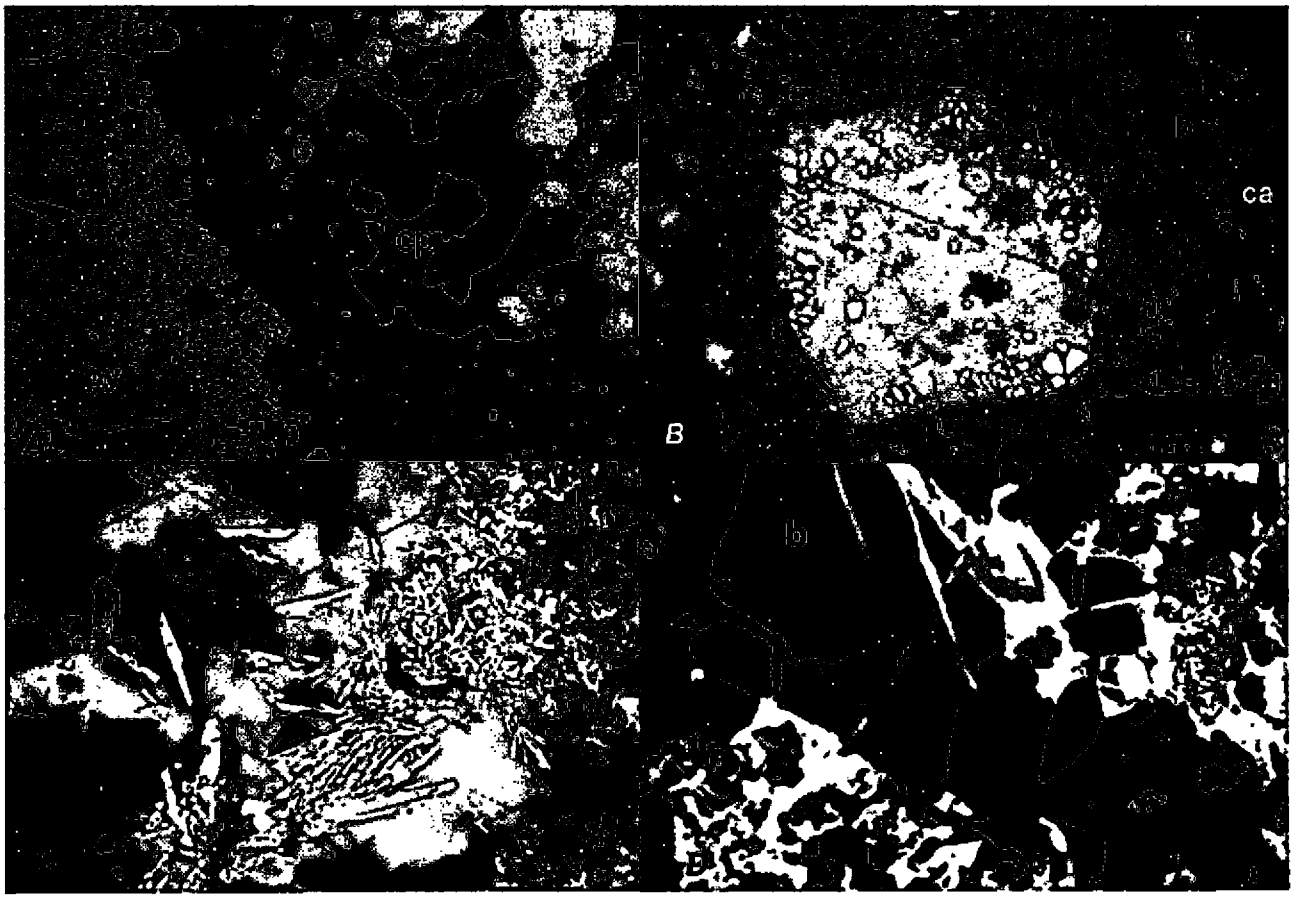


Figure 10: Mineral assemblages of the hydrothermal stage (II).

- A: Pyrite-chalcopyrite zone; pyrite (py) replaced by chalcopyrite (cp) [field of view 1 mm];
- B: Bornite-chalcocite zone; bornite (light grey) and chalcocite (darker grey) replace pyrite (white), part of which was framboidal; solid bitumen (b) has up to 1.7% S, and is veined by calcite (ca) [scale bar 90 microns];
- C: Bornite-chalcopyrite zone; assemblage of bornite (grey), chalcopyrite (light grey) and hematite (white); [field of view 1 mm];
- D: Chalcocite (white)-covellite (grey) assemblage with solid bitumen (b) and calcite; [field of view 1.5 mm].

replaces pyrite (Figure 10A). The pyrite-chalcopyrite zone contains mainly pre-existing pyrite of Stage I, although some proportion of the pyrite may have grown in Stage II.

Chalcopyrite, bornite and chalcocite pseudomorphically replace the framboidal pyrite and thus the texture of the framboidal precursor can be observed even in massive parts of sulphide veins (Figure 10B).

Bornite is associated with chalcocite, although many microprobe analyses indicate that locally the sulphide has the composition of digenite (M.C.Graves, Cuesta Research Ltd., internal report CMD, 1995). Where replacement of pyrite by bornite and chalcocite-digenite is complete, expelled excess iron formed hematite (Holmgren, 1987; Figure 10C), with textural relationships suggesting co-precipitation of the 3 phases. Bornite and chalcocite contain Ag measurable by microprobe (M.C.Graves, Cuesta Research Ltd., internal report CMD, 1995; Ponce, 2001; Boric, 2002).

Covellite is common in the southern part of the camp, together with chalcocite and bitumen (Figure 10D; Ponce, 2001).

The first mineral to crystallise (Figure 11) during the hydrothermal phase (Stage II) was probably specular hematite (Figure 9D) locally accompanied by minor magnetite (Martin, 1981; Wilson, 1998). However, this aspect has not been addressed systematically and needs more work.

Although relatively insoluble oxidised copper minerals (eg. malachite, chrysocolla, copper pitch) exist near the surface (10-30 m, to 60 m in faults), and mixed sulphide-oxide ores are exploited, supergene enrichment is not significant. The lower margin of the oxidised zone is gradual, and displays secondary minerals (eg. chalcocite) passing gradually into hypogene sulphides, but does not represent a supergene enriched zone; in fact mixed ores have lower copper grades than the primary sulphide mineralisation. The absence of supergene copper enrichment has been ascribed to high erosion rates, the relative scarcity of pyrite in the upper levels of orebodies, and the abundance of calcite, which would neutralise the oxidising solutions necessary to produce enrichment (Gonzalez and Holmgren, 1993; Ponce, 2001).

Alteration

Previous studies (Klohn et al., 1990) recognised 4 main alteration effects: 1) *carbonatisation*, expressed as abundant calcite halos and veinlets in proximity to ore; 2) *chloritisation*, which is particularly pronounced in the host basalts and tuffs, where it is associated with epidote and calcite; 3) *silicification*, mainly associated with the bornite zones of the orebodies; and, 4) *albitisation*, which they considered to be late and patchy, and only locally developed. The present study points out the importance of previously unrecognised alkali metasomatism and particularly sodic, and locally potassic alteration in the deposit (Boric 2002). Furthermore, it is necessary to distinguish between the effects of the diagenetic phase, of regional metamorphism, and hydrothermal alteration proper. To this effect, the geochemistry of representative samples of rocks from the different mineralogical zones have been analysed for major and trace elements and compared with the "freshest", "least altered", or "background" rocks distal from ore (Table 1, Figure 11). Specific gravity (S.G.) was measured with a beam balance, and magnetic susceptibility (M.S.) systematically with a hand-held EDA K-2 Magnetic Susceptibility Meter.

The alteration effects on rhyodacites (Figure 11A) are divided into 4 zones: 1) pyrite; 2) chalcopyrite; 3) bornite-chalcocite-sodic; and 4) bornite-chalcocite-potassic, the latter to emphasise alkali metasomatic effects. For the basalts (Figure 11B) the bornite-chalcocite association is not sub-divided. The plots represent the ratios between the different groups and the background or "least altered" rock, taken away from ore but still in mappable continuity to ensure internal consistency.

In the rhyodacites, all zones are enriched in Cu when compared with background rocks (Table 1). There is no significant change in specific gravity, while magnetic susceptibility, SiO_2, TiO_2, Al_2O_3, CaO, C, REE, Y, Zr, Th, U and V all show no change. Most significant in the rhyodacites is the moderate increase in Na_2O (due to albitisation), FeO(total), S, MgO (chloritisation), P_2O_5 (secondary apatite), Ag, As, and Zn, with the anomaly that Na_2O is depleted in the K-feldspar rich bornite-chalcocite zone. K_2O is depleted in the sulphide zones, except where it occurs as adularia. This K-rich zone is also depleted in Zn and Sr, but contains some of the highest Cu grades. Other important depletions are Co, Ni (not reliable because both values are close to the detection limits; Table 1). Rb and Ba are depleted, except in the bornite-chalcocite-potassic zone, where they increase sympathetically. Sr behaves like CaO, as expected. In retrospect it appears that the rocks selected as background rhyodacite were somewhat enriched in carbonate, and this fact distorts the apparent behaviour of LOI, MnO and C (Boric, 2002).

For the basalts (Figures 11B), again there is no change in S.G, SiO_2 (no hint of silicification, even in the bn-cc zone), TiO_2, Al_2O_3, FeO(total) and the immobile trace elements. In contrast to the rhyodacites, the basalts exhibit a drastic loss of magnetic susceptibility, reflecting the wholesale sulphidation of magnetite, associated with a large gain in S; this extreme effect should be useful in exploration. Other uneven losses are MgO, K_2O, Ba, Rb and Sr. Arsenic is lost from the chalcopyrite zone, but increases in the other two zones. Zentilli et al. (1997) showed how early-formed arsenopyrite has been almost totally replaced by bornite-chalcocite; it appears some of the As is redistributed in Cu sulphides. Significant increases are Na_2O, Na_2O/K_2O, LOI, and C (as total C including bitumen and CO_2).

Fluid Inclusion Data

Fluid inclusion data from previous studies are summarised in Table 2. This work was carried out by Holmgren (1985; 1987) and M. Skewes (CMD internal report, 1988), and

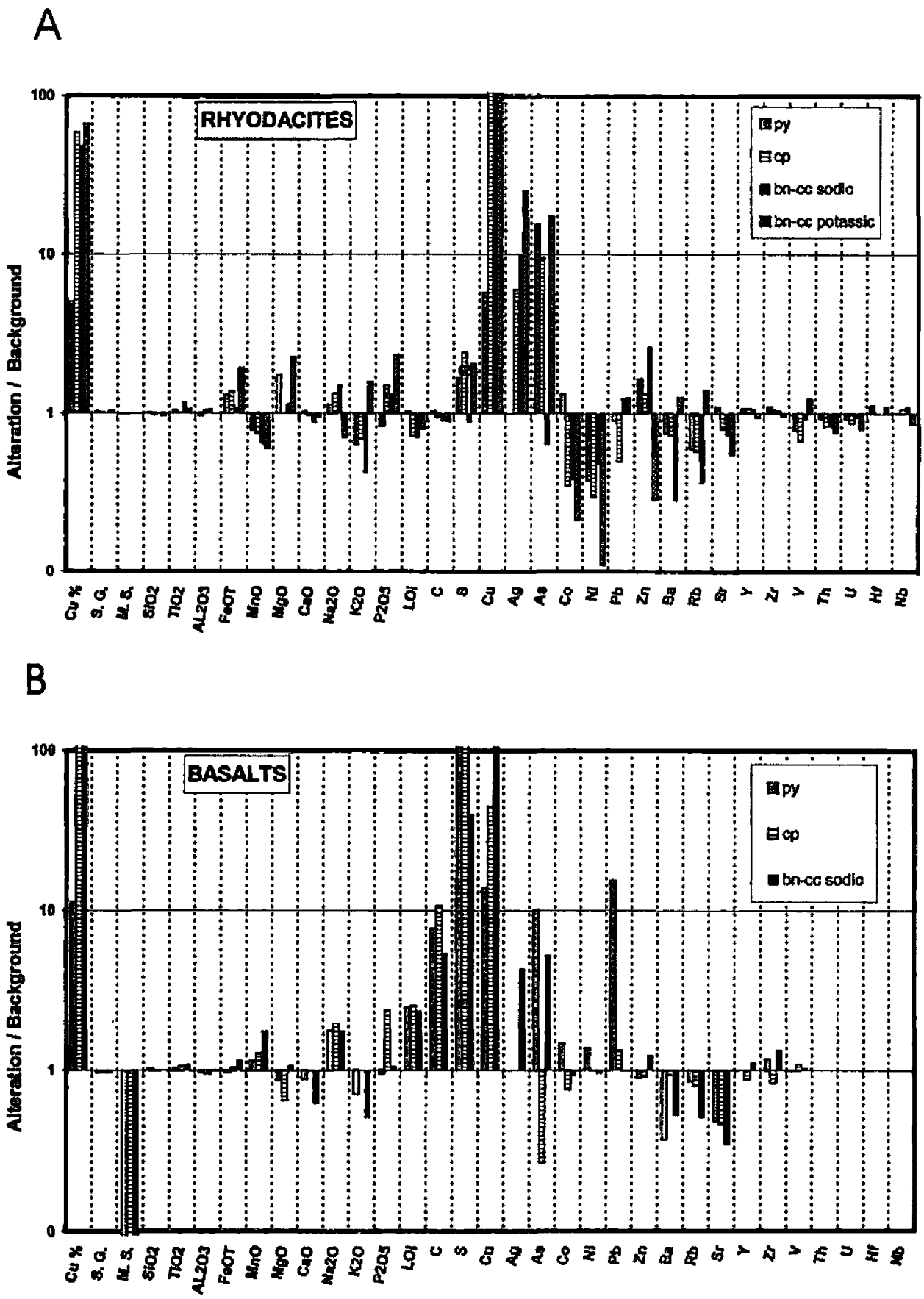


Figure 11: Plots of gains and losses, normalized to least altered (background) rocks (see Table 1); in each case the columns represent different mineral zones in the orebodies (see Figure 8).

A: Major and trace elements in rhyodacites;

B: Major and trace elements in basalts. Note that there is no change in specific gravity, but a complete removal of magnetic susceptibility (M.S) in the basalts.

Table 2. Range of Homogenization Temperatures (1) and Salinities of Fluid Inclusions in El Soldado											
Ore Zone	Hom. Temp. Min. °C			Hom. Temp. Max. °C			n	Salinity %			n
Stage II	Low	High	Average	Low	High	Average	Samples	Min	Max	Average	Samples
py-cp	118	240	172	155	296	249	5	10	31	26	3
cp-bn	102	239	153	119	303	178	12	3	31	22	8
bn-cc	93	244	138	137	204	181	9	3	31	21	5
late barren veins	82	122	102	104	170	137	6	22	29	25	2

Compiled from data in Holmgren (1985;1987); M.Skewes (CMD internal report, 1988) in Boric (2002);
(1) Uncorrected homogenization temperatures

Table 2: Range of Homogenization Temperatures (uncorrected for pressure) from reports by Holmgren (1985;1987) and M. Skewes (CMD internal report, 1988) in Boric (2002).

partially reported in Klohn et al. (1990). For this summary paper, Table 2 groups results of over 400 T_H measurements, ice melting and NaCl dissolution measurements made in veinlets of calcite and quartz, grouped by mineralogical zones. The homogenisation temperatures for the 4 groups overlap somewhat as follows: 1) pyrite-chalcopyrite (172-249°C); 2) chalcopyrite-bornite (153-178°C); 3) bornite-chalcocite (138-181°C); 4) late barren veins (102-137°C), suggesting a cooling trend from a maximum of ca. 200°C; all these temperatures are uncorrected for pressure. No evidence of boiling of the fluids was observed in the fluid inclusions.

Klohn et al. (1990) assumed the depth of formation to be 7 km and applied pressure corrections to the data, suggesting temperatures of Cu-rich hydrothermal fluids to have been ca. 300°C (hydrostatic, 680 bar) or ca. 400°C (lithostatic, 1800 bar), and for the late barren veins 175°C (hydrostatic) and 250°C (lithostatic). The maximum burial of the deposit by Lower Cretaceous strata is poorly constrained, but the absence of high-temperature alteration minerals such as biotite or actinolite, which in the Salton Sea basin appear at temperatures higher than 300°C (eg. Elders et al. 1979) it is unlikely that temperature was much higher than 300-350°C.

Salinities are consistently high (21-26% NaCl equivalent) with some analyses as high as 34%, suggesting $CaCl_2$ in addition to NaCl in the fluids. A few samples indicated salinities as low as 3% NaCl equivalent. Although no evaporites are known in the Lo Prado and Veta Negra Formations, the consistently high salinities suggest their presence in what may represent basinal fluids. Klohn et al. (1990) interpreted these high salinities as evidence for magmatic fluids. We prefer to interpret this salinity as representing deeply circulating basinal brines analogous to those in the Salton Sea geothermal system of southern California (23-30 wt % NaCl equivalent), with maximum temperatures of ca. 350°C (eg. Elders et al. 1979).

Isotopic data

Sulphur isotope data on the pyrite have a wide range in $\delta^{34}S$ ratios (-11.1 ‰ and 28.0 ‰), consistent with strong fractionation in compartmentalised pore domains where variable proportions of sulphate are incompletely reduced; the fractionation is probably biogenic, such as with the intervention of sulphur-reducing bacteria (eg. Love, 1967), most likely at temperatures below 100°C (Wilson et al., in press a). Sulphur isotope data on copper sulphides, which pseudomorphically replace framboidal pyrite (Figure 9B), also has a wide range in $\delta^{34}S$ ratios (-12.7 ‰ and 19 ‰), indicating that sulphur was inherited from the pyrite during replacement of pyrite by Cu sulphides (Wilson et al, in press a). A few sulphide samples have $\delta^{34}S$ ratios near zero, and were originally interpreted by Klohn et al. (1990) to be evidence for a magmatic source, although the wide range observed in many new analyses suggests that a "magmatic" signature is volumetrically insignificant.

The $\delta^{13}C$ ratios of gangue calcite at El Soldado vary between -4 ‰ and -20 ‰ and represent a mixing line with consistent $\delta^{18}O$ values (12.0 - 14.7 ‰) between pyrobitumen-derived organic and inorganic C reservoirs (Wilson 1998; Wilson et al., in press a). The observed range is compatible with incorporation of bitumen-derived organic carbon into the gangue calcite, and is greatest (lowest $\delta^{13}C$) where solid bitumen was replaced during mineralization. Bitumen associated with gangue calcite has $\delta^{13}C$ values of -30 ‰ to -26 ‰, indicative of representing solidified petroleum (Wilson, 1998).

The $\delta^{18}O$ ratios of K-feldspar (adularia) range between 12.0 and 12.7 ‰, and are compatible with the fluids being of

Table 3. Summary Table of Geochronological Data				
Unit	Material	Age Ma	Method	Source
Rhyodacitic dyke	zircon	138-126	U/Pb	Heaman in Boric (2002)
Rhyodacitic dyke	k-spar	132 ± 3	$^{40}Ar/^{39}Ar$	Boric & Munizaga (1994)
Basalt dyke	k-spar	119 ± 2	$^{40}Ar/^{39}Ar$	Boric & Munizaga (1994)
Alkali metasomatism in rhyodacite	k-spar	109-112	$^{40}Ar/^{39}Ar$	Wilson (1998)
Veins and vugs in ore	k-spar	101-106	$^{40}Ar/^{39}Ar$	Wilson (1998)
Amygdules (distal)	k-spar	101-105	$^{40}Ar/^{39}Ar$	Boric & Munizaga (1994)
Rhyodacite flow	apatite	88 ± 18	AFT	Wilson et al. (submitted b)

metamorphic/basinal origin (Wilson et al., in press a). Oxygen isotope ratios of calcite vary between 12.0 and 14.7 ‰, a range of less than 3 ‰. The relatively small range in $\delta^{18}O$ ratios in calcite and K-feldspar suggest that the external fluid was relatively homogeneous and there was no great variation in temperature during crystallisation. The $\delta^{18}O$ ratios of water in equilibrium with calcite at the estimated temperatures of 300 °C to 400 °C can be calculated using the equations of O'Neil and Clayton (1969), and gives a range of 6.4 - 9.12 and 8.8 - 11.5 respectively, hence overlapping with the range of primary magmatic waters, if slightly on the heavy (metamorphic) side, hence a magmatic contribution to the mineralising brines cannot be ruled out. If the temperature of equilibration of calcite had been lower, say between 100 and 200 °C, then the participation of meteoric waters could be invoked.

The $^{87}Sr/^{86}Sr$ ratios in calcite (which contain less than 60 ppm Rb) of 0.7041 to 0.7051 are similar to those of the host basaltic rocks at the time of mineralization (eg. Munizaga et al., 1995), and different from values obtained from marine carbonates in the Lo Prado Formation (0.7051-0.7071; F. Munizaga, CMD internal report, 1992). These results are consistent with a basinal or metamorphic fluid having inherited the low $^{87}Sr/^{86}Sr$ ratios during water-rock reaction for several million years. Furthermore, during the geochronological study (Wilson, 1998; Wilson et al., submitted b), it was noted that all $^{40}Ar/^{39}Ar$ dated samples of K-feldspar (adularia) contain high proportions of atmospheric argon; this is interpreted to indicate a high proportion of meteoric water in the basinal mineralising fluids, lessening the probable importance of any magmatic component.

Re-Os-isotope data for El Soldado (Ruiz et al., 1997) are significantly more radiogenic than those of the porphyry copper type deposits of Chile. Whereas the initial $^{187}Os/^{188}Os$ ratios in pyrite from El Soldado is 3.95, in the Los Bronces (Disputada) porphyry copper southeast of El Soldado (Figure 1) the pyrite has $(^{187}Os/^{188}Os)_i$ of 0.18 (mantle ~0.12). Ruiz et al. (1997) suggest that black shales are the one crustal reservoir (continental crust ~ 1.0) that could possibly account for the anomalously high $(^{187}Os/^{188}Os)_i$ of El Soldado sulphides. These results are consistent with the present interpretation that the diagenetic pyrite in El Soldado is related to petroleum (Wilson and Zentilli, 1998); they say little about the source of the Cu deposited during the hydrothermal stage.

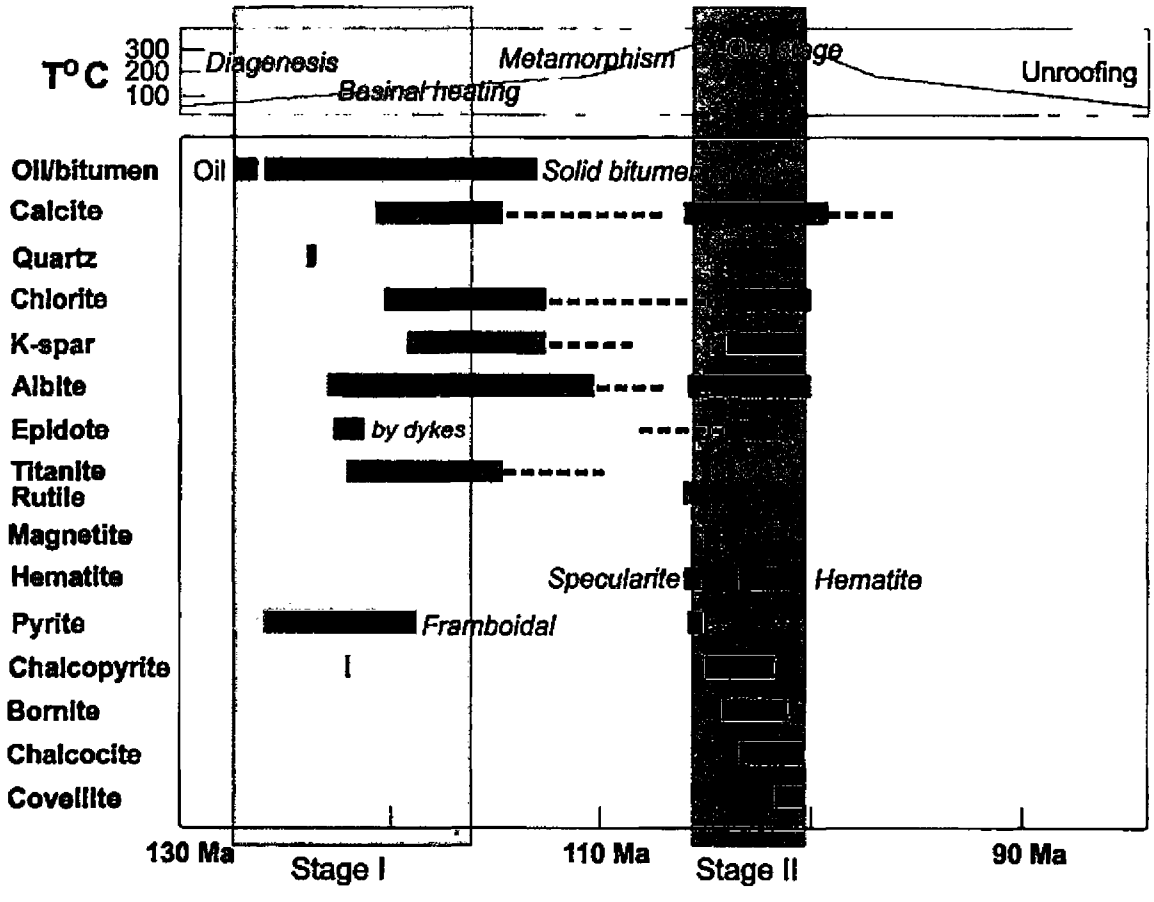


Figure 12: Generalized paragenesis for the El Soldado ore deposits. Temperature and time scales approximate only. Dashed lines indicate high uncertainty. The most signifiucant minerals are indicated in black. See text for discussion.

Geochronology

Table 3 summarises the state of knowledge of the age of rocks and alteration/gangue minerals. The age of the host basalts and rhyodacites is based on marine fossils in the Lo Prado Formation, Berriasian to Hauterivian (Lower Cretaceous). According to the time scale of Okulitch (1999), the marine rocks were emplaced between 145 and 127 Ma. This is consistent with 126-138 Ma U/Pb dates on zircon from a host rhyodacite dyke (L.Heaman in Boric, 2002) and a 132±3 Ma $^{40}Ar/^{39}Ar$ in K-feldspar (Boric and Munizaga, 1994). A basalt dyke that may be a feeder to the Veta Negra Formation yielded a $^{40}Ar/^{39}Ar$ in K-feldspar of 119±2Ma (Boric and Munizaga, 1994). Wilson (1998) dated K-feldspar developed by alkali metasomatism in rhyodacite with ages of 109-112 Ma, and K-feldspar (adularia) veinlets in ore with ages between 101 and 106 Ma, with an average of 103±2 Ma, which we consider to be the age of Cu (Ag) mineralization. A similar age was obtained by Boric and Munizaga (1994) on K-feldspar in amygdules in basalt distal from ore at El Soldado. One fission track age in apatite of 88±18 Ma was reported from a rhyodacite flow within the mine, interpreted to represent final cooling of the hydrothermal system to ca. 100°C (Wilson et al., submitted b).

In summary, the copper-silver mineralization was emplaced at least 20 Ma after the deposition of the host rocks, broadly coinciding with the emplacement of the Cretaceous batholith and the peak of regional low-grade metamorphism as determined elsewhere in the basin (eg. Fuentes et al., 2001; Morata et al., 2001; Maksaev and Zentilli, this volume).

Evolution of the Deposit

Figure 12 is a generalised summary of the evolution of El Soldado, taking into account the mineral paragenesis, fluid inclusion constraints, and the geochronology. The evolutionary model is significantly different from the interpretation of Klohn et al. (1990). The deposit can be best understood by distinguishing 2 phases: a first *(Stage I) diagenetic stage* of rock preparation and deposition of low-temperature pyrite, probably related to petroleum migration, and a second *(Stage II) hydrothermal phase* (eg. Wilson, 1998; Wilson and Zentilli, 1999). An intervening metamorphic stage can be assumed, involving the burial of the sequence until the time of batholith emplacement.

During Stage I, burial must have been relatively rapid, since liquid petroleum was generated and migrated into the upper Lo Prado Formation, before tilting, implying oil-window temperatures of >60°C in the underlying source rocks (Wilson and Zentilli, 1999; Wilson, 2000). The presence of petroleum as a liquid, and the formation of framboidal pyrite with the assistance of bacteria (Wilson et al., submitted a), suggest that the temperature was less than 100°C. The source of oil was the dark shales of the lower member of the Lo Prado Formation; it migrated upwards through extensional normal faults that must have been active during sedimentation and volcanism that filled the basin, and probably represent growth faults, which were later reactivated during Stage II. Permeability was provided by primary porosity such as columnar jointing, syn-volcanic breccias, inter-particle spaces in coarse volcaniclastic rocks, vesicular zones in basalts, and secondary fracture porosity related to faults. The uppermost tuffaceous unit of the Lo Prado Formation acted as a relatively impervious cap for the petroleum reservoir.

After petroleum solidified and fractured as it shrank, calcite crystallised in the open spaces. This calcite (as the carbon isotope data show) was in part generated by the oxidation of organic matter. The diagenetic stage must have developed between deposition of the volcanic host rocks at ca. 130 Ma, and peak metamorphism, although calcite precipitated after solidification of the bitumen, probably at temperatures above 100°C, consistent with the minima for homogenisation temperatures of fluid inclusions (Table 2).

During the diagenetic and metamorphic stages, redistribution of alkalis in the rhyodacites formed interstitial K-feldspar with argon dates of variable age, but averaging ca. 110 Ma (Table 3).

During Stage II, temperatures peaked to 300-350°C, probably soon after intrusion of the Cretaceous Batholith, and the age of mineralization is probably close to 103±2 Ma, on the basis of the ages obtained in previous and current work for adularia associated with copper sulphides (Wilson and Zentilli, 1999). This age is similar to $^{40}Ar/^{39}Ar$ dates obtained by Fuentes et al. (2000) for adularia and sericite in Veta Negra Formation lavas in the Chacana area, only 10 km south of El Soldado. Also, this is the age obtained for alteration K-feldspar and sericite associated with a dacitic porphyry at the La Isla Cu mine, also in the Chacana area (Boric and Munizaga, 1994). Apatite fission track dating suggests rapid cooling and exhumation, such that by 90 Ma the rocks had cooled to ca. 100°C (Wilson et al., submitted b) and were never substantially reheated.

In addition to the age and duration of the ore-forming process no genetic model is complete without consideration of the possible source(s) of fluids, metals, sulphur, gangue constituents, of energy, the fluid transport mechanism and the fluid focusing through the deposit, the conditions and controls of precipitation in the ore deposit, and post-ore modifications (eg. Zentilli et al., 1997; Boric, 2002).

The diagenetic pyrite precursor turns out to be a fundamental prerequisite for mineralization at El Soldado. Cu was preferentially precipitated where it could replace pyrite, and chalcopyrite and the subsequently replacing sulphides (Figure 12) recycling the sulphur and incorporating it into their structure (Wilson et al., in press a). Little sulphur appears to have been added during Cu mineralization. From isotopic studies we know the sulphur was derived from low-temperature (probably bacterial) reduction of sulphate in the pore waters. Since Fe is not easily transported in oxidised waters (eg. Love, 1967), Fe for the pyrite was most likely derived from the reduced pore waters accompanying the petroleum in their

rise through the basinal normal faults. This concept is totally consistent with the Re-Os data on (diagenetic) pyrite (Ruiz et al., 1997).

The growth of specularite in the northern part of El Soldado, locally associated with pyrite, seems to have preceded the introduction of Cu. Either this specularite represents abundance of Fe in solution after bacterial reduction of sulphate became ineffective by rising temperature, and precipitation near an oxidising front, or otherwise the first pulses of hydrothermal brines did not carry significant Cu, nor sulphur, to create sulphides. This part of the paragenesis remains doubtful. It is reminiscent, however, of an early phase of specular hematite present in Punta del Cobre-Candelaria (eg. Ortiz et al., 1966; Marschik and Fontbote, 1996) and Mantos Blancos districts (Chavez 1985).

Sulphur was inherited wholesale from diagenetic pyrite during the hydrothermal stage, as indicated by the matching extremely wide range in sulphur isotopic ratios in pyrite and Cu sulphides. The source of the Cu is speculative, but as forcefully put forward by Westra (1988) for El Soldado, by analogy with other low-grade metamorphic sequences such as the Karmutsen volcanics in British Columbia (Lincoln, 1981), and the Keweenawan tholeiitic lavas of northern Michigan (Jolly and Smith, 1972), it is most likely that the Cu was extracted during prograde low-grade metamorphism from the oxidised Veta Negra Formation mafic and intermediate volcanics, volcaniclastics and redbeds.

The salinity of fluid inclusions (21-26% NaCl equivalent) indicates that the solutions that transported the Cu were high-salinity brines. The presence of chlorine has been detected within the bitumen associated with high grade Cu ores (Wilson, 1998; Wilson and Zentilli, 1999). Eh-pH relationships allowing for the precipitation of chalcocite-covellite-hematite assemblages must have been highly oxidising, and mildly acidic at ca. 300°C (eg. Lincoln, 1981). The oxygen and carbon isotope data, the strontium isotopes and the presence of atmospheric argon in the alteration and gangue K-feldspar (adularia) are compatible with the fluids having been connate, in part meteoric waters within the subaerial volcanic Veta Negra Formation, in partial equilibrium with the rocks during prograde metamorphism, which culminated with peak temperatures during intrusion of the batholith.

The energy source for fluid migration may have been the tectonic tilting of the strata and the intrusion of the huge Cretaceous batholith. Focusing was provided by the development of a brittle shear system parallel to the Andean margin in response to oblique subduction (eg. Maksaev and Zentilli, this volume) generating transtensional regimes such as the cymoid loop at El Soldado. The reactivation of pre-existing normal faults and the resulting fracturing generated structural permeability in vertical zones thus attracting and channelling large volumes of hot, Cu-rich brines into the more brittle lithologies of the Lo Prado Formation, such as the rhyodacites, from the overlying Veta Negra Formation.

The access of Cu-rich, oxidised chloride brines to zones with pyrite accompanied by still-reactive bitumen, which acted as active carbon to destabilise the chloride complexes (Wilson and Zentilli, 1999), led to the progressive replacement of the pyrite by Cu sulphides. The replacement of pyrite by chalcopyrite only requires the addition of Cu, but any further replacement by Cu leads to an excess of Fe, which results in the co-precipitation of hematite (Figure 10C).

As indicated above, after ore formation and batholith intrusion, the region underwent rapid cooling and exhumation during inversion of the Cretaceous Basin. This interpretation is compatible with apatite fission track dates of ca. 90 Ma at El Soldado, and 82-95 Ma at the Caleu Pluton revealing rapid denudation during the Late Cretaceous (eg. Parada and Larrondo, 1999; Gana and Zentilli, 2000).

Supergene oxidation is not insignificant, in particular in the upper levels of the mine near the surface, and in the proximity of open faults, such that mixed sulphide-oxide ores are exploited by leaching. However, oxidation has led to a decrease in Cu grades rather than to supergene enrichment. The lack of sufficient pyrite to generate sulphuric acid during oxidative weathering, the presence of reducing bitumen, and of abundant calcite to neutralise any acid formed, have worked against supergene enrichment (eg. Gonzalez and Holmgren, 1993).

Conclusions and Implications for Exploration

The main controls of orebody development at El Soldado are:

1. ***Pyrite and bitumen.*** Copper minerals replaced pre-existing pyrite, which developed within a degraded petroleum reservoir, probably through the interaction of sulphur reducing bacteria, at temperatures below 100°C (Wilson and Zentilli, 1999; Wilson et al., in press a). Petroleum migration and pyrite growth preceded tilting of the strata (Wilson and Zentilli, 1999; Wilson et al., in press a). Therefore the locus for pyrite within the potential petroleum reservoir could extend long distances down dip and to the east. Solid bitumen acted as a reductant for hydrothermal solutions and probably destabilised chloride complexes carrying Cu (Wilson, 1998). Other palaeo-petroleum reservoirs within the Cretaceous basin could be the locus of mineralization even if no pyrite was developed. As pointed out by Zentilli et al. (1997) interaction of hydrothermal solutions with petroleum source rocks (organic-rich Lo Prado Formation or any other), migrating hydrocarbons, or hydrocarbon reservoirs could be good loci for sulphide precipitation. Petroleum has had both physical roles, such as preserving pore spaces by preventing cementation, providing new porosity during shrinking to a solid, and because of its negligible tensile and shear strength, enhancing reactivation of bitumen-sealed faults (Zentilli et al., 1997), as well as chemical roles, such as promoting pyrite growth, and acting as a reductant to oxidising solutions.

2. ***Structural Permeability.*** Early formed extensional faults controlled the migration of petroleum and localised the formation of the essential pyrite before and during petroleum migration. Later remobilisation of these faults and development of a sinistral strike-slip regime with a transtensional zone (cymoid loop) responding to a horizontal maximum principal stress σ1 oriented NNW-SSE. The best extensional structures should have an orientation somewhat parallel to the above, and the permeability zones formed should have a sub-vertical extension, parallel to the intermediate stress direction (eg. Sibson, 2001). Within this brittle regime, the most favourable rock types for ore are the brittle rhyodacites, and basaltic lavas of the upper member of the Lo Prado Formation, whereas the more ductile tuffaceous units and fine-grained clastic sediments are relatively less favourable (eg. Klohn et al., 1990).

Other important conclusions are:

3. The *trachyte* of previous reports (eg. Klohn et al., 1990) is in fact a metasomatised rhyodacite; the *andesite* is in fact basalt. There is no evidence of alkaline magmatism in the El Soldado camp, and the rocks are calc-alkaline (Boric, 2002). The alteration of these rocks has given them characteristics of *keratophyres* and *spilites*. The same effects are recognised in the Punta del Cobre - Candelaria district (Marschik and Fontboté, 1996).
4. Hydrothermal Cu mineralisation is associated with an increase in Na related to albitisation and a depletion in K in host rocks. Nevertheless, there are localised zones of K increase in bornite-chalcocite assemblages near structures, where K-feldspar has precipitated as adularia.
5. The complete disappearance of magnetic susceptibility in basalts as they approach mineralised bodies resulted from sulphidation of the magnetic minerals, and should be a useful empirical tool in logging and geophysical exploration.
6. The El Soldado deposit is epigenetic, but the fluids that formed it were not magmatic. The data available suggest that the fluids were highly saline connate basinal brines, modified by prograde very low grade metamorphism, but with a significant component of meteoric water. Evaporites may have been involved, although they have not been recognised in the basin.

Generalisations about very large manto type deposits:

7. This study suggests that very large manto type Cu (Ag) deposits hosted by volcanic rocks, such as El Soldado, Mantos Blancos and Punta del Cobre have some common features, perhaps suggesting that these deposits form part of a continuum between the Cu (Ag) and Cu-Au-Fe stratabound deposits (Maksaev and Zentilli this volume):
   - They are hosted by bi-modal calc-alkaline volcanic sequences including rhyodacite intrusive-extrusive units that have been strongly albitised.
   - They are associated with transtensional domains in brittle strike-slip shear systems.
   - They have a similar paragenesis that starts with specular hematite, followed by increasingly copper-rich sulphides.
   - They are associated with strong Na and locally K alteration, clearly distinguishable from regional metamorphic assemblages.
   - Their mineralization event is roughly coeval with emplacement of granitoid intrusives that are proximal (Punta del Cobre) or distal (El Soldado, Mantos Blancos).
   - The importance of petroleum involvement, or the generation of diagenetic pyrite as rock preparation is important in El Soldado, but has not been associated with Mantos Blancos and Punta del Cobre; possibly El Soldado is an anomaly.

Acknowledgements

We thank the El Soldado CMD Management for encouraging this publication and allowing the comprehensive study, for which they provided logistic support and many analyses. Funding came from Cuesta Research Ltd., NSERC grants to MZ, and a Killam Fellowship to NSFW.

References

Aberg, G., Aguirre, L., Levi, B., and Nystrom, J.O., 1984. Spreading subsidence and generation of ensialic marginal basins, an example from the Early Cretaceous of central Chile. *In:* Kokelaar, B.P. Howells, M.F. (eds.), Marginal Basin Geology. *Geol. Soc. Spec. Publ.*, pp. 185-193.

Anhaeusser, C.R., 1965. Wrench faulting and its relationship to gold mineralization in the Barberton mountain land. Information Circular - Economic Geology Research Unit, University of the Witwatersrand, v. 24, 20p.

Boric, R., 1997. Nuevos antecedentes sobre el modelo genético del yacimiento de cobre El Soldado, Chile central. *VIII Congr. Geol. Chileno, Antofagasta*, pp. 862-866.

Boric, R., 2002. The Geology of the El Soldado Manto Type Copper Deposit, Chile. *Unpublished M.Sc. Thesis*, Dalhousie University, Halifax, Canada, 150p.

Boric, R., Díaz, F. and Maksaev, V.,1990. Geología y yacimientos metalíferos de la Región de Antofagasta. Servicio Nacional de Geología y Minería, *Boletín* N° 40, Santiago, 246 p.

Boric, R. and Munizaga, F., 1994. Geocronología Ar-Ar y Rb-Sr del depósito estratoligado de cobre El Soldado (Chile Central). *Comunicaciones, Universidad de Chile*, v. 25-26, pp. 57-75.

Camus, F., 1980. Distrito Punta del Cobre. Modelo de Interpretación. *Revista Geológica de Chile*, N° 11, pp. 51-76.

Camus, F. and Dilles, J.H., 2001. A special issue devoted to porphyry copper deposits of northern Chile. Econnomic Geology, 96, p. 233-237.

Carter, W.D., 1961. Yacimientos de Cobre Tipo Manto, su distribución en franjas mineralizadas. Provincia de Aconcagua. *Boletín* N° 10, Instituto de Investigaciones Geológicas, Chile, 30 p.

Charrier, R., and Muñoz, N., 1994. Jurassic Cretaceous paleogeographic evolution of the Chilean Andes at 23°-24°S and 34°-35°S latitude: a comparative analysis. *In* Reuter, K.,J., Sheuber, E., and Wigger P.J., (Eds.), Tectonics of the Southern Central Andes, Springer Verlag, pp. 233-242.

Chavez, A., 1988. Relaciones entre fracturas, campos de esfuerzos y mineralizacion en el yacimiento El Soldado, V Region. *Unpublished B.Sc.Thesis*, Departamento de Geología y Geofisica, Universidad de Chile, Santiago, 141 p.

Chavez, W., 1985. Geological setting and the nature and distribution of disseminated copper mineralization of the Mantos district, Antofagasta Province, Chile. *Unpublished Ph.D. Thesis*, California University, Berkeley, USA, 142 p.

Collins, P., Boric, R. Zentilli, M., and Wilson, N.S.F., 2002. Fixation of sulphur during framboidal pyrite development in a petroleum reservoir in Cretaceous volcanics in the Andesimplications for Cu metallogenesis. Abstract, Atlantic Geoscience Society Colloquium, Antigonish, Nova Scotia, February 9-10, 2002.

Contador N., and Glavic, M., 2001. Sublevel Open Stoping at El Soldado Mine: A Geomechanic Challenge. *Underground Mining Methods, Engineering Fundamentals and International Case Studies, Society for Mining, Metallurgy, and Exploration, Inc. (SME)*, Chapter 29, pp. 263-269.

Cox, S.F., Knackstedt, M.A., and Braun, J., 2001. Principles of structural control on permeability and fluid flow in hydrothermal systems. Chapter 1 *in* J.P.Richards and R.M.Tosdal (Eds.) Structural Controls on Ore Genesis, Reviews in Economic Geology, v. 14, p. 1-24.

Elders, W.A., Hoagland, J.R., McDowell, S.D., and Cobo, J.M., 1979. Hydrothermal mineral zones in the geothermal reservoir of Cerro Prieto.. In W.A.Elders (editor) Geology and geothermics of the Salton Trough, Field Trip Guidebook No. 7, Geological Society of America 92nd Annual Meeting, San Diego, November 1979, p. 36-43.

Fontboté, L., 1990. Stratabound Ore Deposits in the Andes: A Review and a Classification According to their Geotectonic Setting. *in* Fonbote, L., Amstutz, G.C., Cardozo, M.,Cedillo, E. and Frutos,J., (eds.), *Stratabound ore deposits in the Andes*, pp. 79-110.

Fuentes, F., Féraud, G., Aguirre, L. and Morata, D., 2001. Convergent strategy to date metamorphic minerals in sub-greenschist facies metabasites by the $^{40}Ar/^{39}Ar$ method. *III South American Symposium on Isotope Geology, Extended Abstract Volume* (CD), Sociedad Geológica de Chile, Santiago, pp. 34-36.

Fuenzalida, H. 1965. Clima, *In Geografía Económica de Chile*, Corporación de Fomento de la Producción, Santiago, Chile, pp. 98-152.

Gana, P., Wall, R., Gutierrez, A., 1996. Mapa Geologico del area de Valparaiso-Curacavi, Region de Valparaiso y Region Metropolitana. Servicio Nacional de Geologia y Mineria, Chile, *Mapas Geologicos*, N° 1, Escala 1:100,000, 1 mapa, 1 anexo.

Gana, P. and Zentilli, M., 2000. Historia termal y exhumación de intrusivos de la Cordillera de la Costa de Chile Central. *Congreso Geológico Chileno IX*, Puerto Varas, Chile, V. 2, pp.664-668.

Gonzalez, F. and Holmgren, C. 1993. Caracteristicas mineralogicas de la zona de oxidacion y su implicancia en la recuperacion de sulfuros en el yacimiento El Soldado, *Congreso Internacional de Ingenieria de Minas*, III Region, Copiapo, Chile, Actas, pp. 270-279.

Holmgren, C., 1985. Antecedentes para un modelo genético del yacimiento El Soldado, V Región. *IV Congr. Geol. Chileno, Antofagasta, IV*, pp. 626-650.

Holmgren, C., 1987. Antecedentes para un modelo genético del yacimiento El Soldado, V región de Valparaíso, Chile. *Rev. Geol. Chilena*, 30, pp. 3-18.

Klohn, E., Holmgren, C., and Ruge, H., 1986. El Soldado, a peculiar copper deposit associated with anomalous alkaline volcanism in the Central Chilean Coastal Range. *Proc., 115th Annual Meeting, Soc. Mining Eng.*, New Orleans, AIME, 8p.

Klohn, E., Holmgren, C., and Ruge, H., 1990. El Soldado, a Stratabound Copper Deposit Associated with Alkaline Volcanism in the Central Chilean Coastal Range. *in* Fonbote, L., Amstutz, G.C., Cardozo, M., Cedillo, E. and Frutos, J., (eds.), *Stratabound ore deposits in the Andes* pp. 435-448.

Love, L.G., 1967. Sulphides of metals in recent sediments. Proceedings of the 15th Inter-University Geological Congress, University of Leicester, England. p. 30-60.

Maksaev, V., and Zentilli, M., 2002. Chilean Strata-bound Cu-(Ag) Deposits: An Overview, *in* Porter TM. (Ed.) *Hydrothermal Iron-oxide copper-gold & related deposits: A global perspective, Volume 2.*

Marschik, R., and Fontboté, L., 1996. Copper (Iron) mineralization and superposition of alteration events in the Punta del Cobre Belt, Northern Chile. *SEG, Special Publication* N°5, pp. 171- 189.

Martin, W., 1981. Distribucion de la Mineralizacion en el Yacimiento Cuprifero El Soldado, V Region. *Unpublished B. Sc. Thesis*, Departamento de Geologia y Geofisica, Universidad de Chile, Santiago, 92 p.

Morata, D., Aguirre, L., Féraud, G., Fuentes, F., Parada, M.A. and Vergara, M., 2001. The Lower Cretaceous Volcanism in the Coastal Range of Central Chile: Geochronology and Isotopic Geochemistry. *III South American Symposium on Isotope Geology, Extended Abstract Volume* (CD), Sociedad Geológica de Chile, Santiago, pp. 321-324.

Mpodozis, C., and Ramos, V., 1989. The Andes of Chile and Argentina. *In*: Ericksen, G.E., Cañas, M.T., and Reinemund, J.A. (editors), *Geology of the Andes and its relation to hydrocarbon and mineral resources*, Circum-Pacific Council for Energy and Mineral Resources, *Earth Science Series*, V. 11, pp. 59-90.

Munizaga, F., Holmgren, C., Huete, C., and Kawashita, K., 1988. Geocronología de los yacimientos de cobre El Soldado y Lo Aguirre, Chile central. *V Congr. Geol. Chileno, Santiago*, III, G177-193.

Olcay, L., and Alarcón B., 1975. Alteración Hidrotermal Sódica de Mina El Soldado, Provincia de Valparaíso, Chile, *II Congr. Geol. Iberoam. Geol. Econ., Buenos Aires*, II, pp.1-9.

Ortiz, F.J., Araya, R., Franquesa, F., Moraga, A. and Zentilli, M., 1966. Informe Geologico del Distrito Minero de Punta del Cobre. Instituto de Investigaciones Geologicas, Chile. *Special Publication* N°1, 4 volumes, 86 maps.

Palacios, C., 1986. Subvolcanic Copper deposits in the Coastal Range of Northern Chile. *Zentralblatt für Geologie und Paläontologie*, Teil I, 1985, H.9/10, Stuttgart, pp. 1605-1615.

Parada, M.A. and Larrondo, P., 1999. Thermochronology of the Lower Cretaceous Caleu Pluton in the Coast range of Central Chile: Tectono-stratigraphic implications. *Fourth ISAG, Goettingen (Germany)*, pp. 563-566.

Piraces, R. and Maksaev, V. 1977. Geologia de la Hoja Quillota. Instituto de Investigaciones Geologicas Chile, unpublished report, 64 p., 1 map escale 1:250,000.

Ponce, R. , 2001. Geologia, mineralizacion y distribucion de elementos trazas en el sector Filo , mina El Soldado, V Region. Unpublished B.Sc. thesis, Depto. de Geologia, Universidad de Chile, Santiago, 104 p.

Rivano, S., Sepúlveda, P., Boric, R., and Espiñeira, D., 1993. Hojas Quillota y Portillo. Servicio Nacional de Geología y Minería, *Carta Geológica de Chile* N° 73, only geological map published.

Rivano, S. 1996. Geologia de las Hojas Quillota y Portillo. Servicio Nacional de Geologia y Mineria, *limited circulation, preliminary report 7644C1*, 202 p, plus 30 p tables, to accompany Rivano, S., Sepúlveda, P., Boric, R., and Espiñeira, D., 1993. Hojas Quillota y Portillo. Servicio Nacional de Geología y Minería, *Carta Geológica de Chile* N° 73.

Ruge, H., 1985. Geología y Mineralización del Yacimiento de Cobre El Soldado, V Región, Chile, *IV Congr. Geol. Chileno, Antofagasta*, IV, pp. 855-872.

Ruiz, C., Aguirre, L., Corvalan, J., Klohn, C., Klohn, E., and Levi, B., 1965. Geología y yacimientos metalíferos de Chile. *Instituto de Investigaciones Geológicas, Santiago, Chile,* 302 p.

Ruiz, C. and Peebles, F., 1988. Geología, distribución y génesis de los yacimientos metalíferos chilenos. *Editorial Universitaria*, Santiago, Chile, 305 p.

Ruiz, J., Freydier, C., McCandless, T., Chesley, J. and Munizaga, F., 1997. Re-Os-Isotope systematics of sulfides from base-metal porphyry and manto type mineralization in Chile. International Geology Review, v. 39, p. 317-324.

Sato, T., 1984. Manto type copper deposits in Chile: a review. *Bulletin of the Geological Survey of Japan*. V. 35, pp. 565-582.

Sillitoe, R. H., 1992. Gold and copper Metallogeny of the central Andes: Past, present and future exploration objectives. Econ. Geol. Vol. 87, pp. 2205-2216.

Tassinari, C., Munizaga, F. y Ramírez, R., 1993. Edad y geoquímica isotópica Rb-Sr del yacimiento de cobre Mantos Blancos: relación temporal con el magmatismo Jurásico. *Revista Geológica de Chile*, V. 20, N° 2, pp. 193-206.

Terrazas, R., 1977. Petrografia, alteracion hidrotermal y mineralizacion del yacimiento cuprifero El Soldado, Provincia Valparaiso, Chile. *Unpublished Ph.D. thesis*, Universidad de Chile, 105 p.

Vergara, M., Levi, B., Nyström, J.O. and Cancino, A., 1995. Jurassic and Early Cretaceous island arc volcanism, extension, and subsidence in the Coast Range of Central Chile. *Geological Society of America Bulletin*, V. 107, N°12, pp. 1427-1440.

Villalobos, H., 1995, Antecedentes para un modelo genetico del yacimiento Veta Negra y su relacion con el yacimiento de cobre El Soldado, V Region, *Unpublished B.Sc, Thesis*, Universidad de Concepcion, 91p.

Vivallo, W. and Henriquez, F., 1998. Génesis común de los depósitos estratoligados y vetiformes de cobre del Jurásico Medio a Superior en la Cordillera de la Costa, Región de Antofagasta, Chile. *Revista Geológica de Chile*, V. 25, N° 2, pp. 199-228.

Wall, R., Gana, P., and Gutierrez, A., 1996. Mapa Geologico del area de San Antonio-Melipilla, Regiones de Valparaiso, Metropolitana y del Libertador General Bernardo O'Higgins. Servicio Nacional de Geologia y Mineria, Chile, *Mapas Geologicos*, N° 2, Escala 1:100,000, 1 mapa, 1 anexo.

Wall, R., Selles, D., and Gana, P., 1999. Area Tiltil-Santiago, Region Metropolitana. Servicio Nacional de Geologia y Mineria, Chile, *Mapas Geologicos*, N°11, Escala 1:100,000, 1 mapa, 1 anexo.

Westra, G., 1988. La importancia del metamorfismo de carga en la formación de yacimientos de cobre de tipo manto: preprint, Keynote Address, *V Cong. Geol. Chileno, Santiago*, 18 p.

Wilson, N.S.F., 2000. Organic petrology, chemical composition, and reflectance of pyrobitumen from the El Soldado Cu deposit, Chile. *International Journal of Coal Geology*, 43, pp. 53-82.

Wilson, N.S.F., 1998. The role of petroleum in the formation of the El Soldado copper deposit, Chile: Hydrothermal replacement of a biodegraded petroleum reservoir. *Unpublished Ph.D. Thesis*, Dalhousie University, Canada, 418 p.

Wilson, N.S.F and Zentilli, M., 1999. The role of organic matter in the genesis of the El Soldado volcanic-hosted manto-type Cu deposit, Chile, Economic Geology, v.94, pp. 1115-1136.

Wilson, N.S.F., Zentilli, M., and Spiro, B. , in press a, The Essential Role of Bacteria and Petroleum in the Formation of the Volcanic-hosted El Soldado Manto-type Cu Deposit, Chile: a Sulfur, Carbon, Oxygen, and Strontium Isotope Study. Submitted to *Economic Geology*.

Wilson, N.S.F., Zentilli, M., Reynolds, P.H. and Boric, R. (submitted b). $^{40}Ar/^{39}Ar$ Geochronology of K-feldspar (Adularia) from the El Soldado Manto-Type Copper Deposit, Chile. Submitted to *Chemical Geology*.

Winchester J.A. and Floyd, P.A., 1977. Geochemical discrimination of different magma series and their differentiation products using immobile elements. *Chemical Geology*, v. 20, pp. 325-343.

Zentilli, M., Boric, R., Munizaga, F., and Graves, M.C., 1994. Petroleum involvement in the genesis of some strata-bound copper deposits of Chile. *VII Congr. Geol. Chileno, Concepción*, II, pp.1542-1546.

Zentilli, M., Munizaga, F., Graves, M. C., Boric. R., Wilson. N.S.F., Mukhopadhyay, P. K., and Snowdon, L.R., 1997. Hydrocarbon Involvement in the genesis of Ore Deposits: an example in Cretaceous Strata-bound (Manto Type) Copper Deposits of Central Chile, International Geology Review, Vol.39, p.1-21.

Zentilli, M, Heaman, L., Pop, N., and Boric, R. (2001) Evidence of Precambrian crust under the Coastal Cordillera of Chile: xenocrystic zircons in Cretaceous volcanic rocks. (Abstract). *III South American Symposium on Isotope Geology* Comunicaciones, Universidad de Chile.

PGC PUBLISHING

Maksaev, V. & Zentilli, M. 2002 - Chilean Strata-bound Cu-(Ag) Deposits: An Overview; *in Porter, T.M. (Ed.), Hydrothermal Iron Oxide Copper-Gold & Related Deposits: A Global Perspective*, Volume 2; PGC Publishing, Adelaide, pp 185-205.

CHILEAN STRATA-BOUND Cu- (Ag) DEPOSITS: AN OVERVIEW

[1]Victor Maksaev and [2]Marcos Zentilli

[1]*Departamento de Geología, Universidad de Chile, Santiago, Chile*
[2]*Department of Earth Sciences, Dalhousie University, Halifax, Nova Scotia, Canada*

Abstract - Strata-bound Cu- (Ag) deposits, long known as 'Chilean manto-type', occur along the Coastal Cordillera of northern Chile (22°-30°S) hosted by Jurassic and Lower Cretaceous volcanic and volcano-sedimentary rocks. These deposits are typical of the first stage of Andean evolution characterised by an extensional setting of the arc magmatism along the active margin of South America. Strata-bound Cu- (Ag) deposits were formed during two metallogenic epochs in the Late Jurassic and uppermost Early Cretaceous. The mineralisation took place at the time of structurally controlled emplacement of batholiths within the Mesozoic volcanic and sedimentary strata. The volcanic-hosted strata-bound Cu- (Ag) deposits invariably occur distal, but peripheral to coeval batholiths emplaced within tilted Mesozoic strata. The prevalent view that these deposits have an inherent genetic relationship with hydrothermal fluid derivation from subvolcanic stocks and dykes is contended here, because these minor intrusions are largely barren and this hypothesis does not fit well with Sr, Os and Pb isotopic data that call for crustal contribution of these elements. The strata-bound Cu- (Ag) mineralisation appears to be produced by fluids of mixed origin that were mobilised within permeable levels and structural weakness zones of the Mesozoic arc-related volcano-sedimentary sequence during the emplacement of shallow granodioritic batholiths under transtensional regimes. These hydrothermal fluids deposited copper and subordinate silver when reacted with organic matter, pyrite and/or cooled away from their heat sources. Although strata-bound Cu- (Ag) mineralisation took place during the same Cretaceous metallogenic event that formed the magnetite-apatite bodies, and Fe-oxide-Cu-Au deposits along the present Coastal Cordillera, the conceivable relationships with these other types of deposits are hampered by the inconclusive debate about the origin of the Chilean Fe-oxide deposits. However, the available data strongly suggest that the Fe oxide-rich deposits are metasomatic in origin and genetically related to contact zones of Lower Cretaceous dioritic batholiths, whereas the iron-poor volcanic-hosted Cu-(Ag) stratabound deposits constitute distal mineralisation peripheral to Upper Jurassic of Lower Cretaceous granodioritic batholiths.

Introduction

Strata-bound copper deposits with subordinate silver, long known as 'Chilean Manto-type', occur along the Coastal Cordillera of northern Chile hosted by Jurassic and Lower Cretaceous volcanic and volcano-sedimentary rocks. These Mesozoic strata-bound deposits historically were the second source of Chilean copper production after Cenozoic porphyry copper deposits, but have recently been displaced to third place by the exploitation of large Lower Cretaceous Fe-oxide-Cu-Au deposits (eg. Candelaria and Manto Verde mines; Marschik et al., 2000, Vila et al., 1996, Zamora and Castillo, 2001).

Two groups of significant strata-bound Cu- (Ag) occur in Chile: (a) from 22° to 26° lat. S hosted by a Jurassic volcanic sequence (La Negra Formation) and (b) from 30° to 34° lat. S hosted by Lower Cretaceous volcanic and volcano-sedimentary rocks. Although a group of Lower Cretaceous Fe-oxide-Cu-Au strata-bound deposits in the Punta del Cobre district (~27°30' S) have traditionally been included in the manto-type in Chile (eg. Camus, 1980, 1985), the present review excludes them, being exclusively focused on the Fe-poor volcanic-hosted strata-bound copper deposits with subordinate silver that are hosted by Mesozoic andesitic-basaltic volcanic sequences along the Coastal Cordillera of northern Chile. For lack of space, this paper does not discuss Cu- (Ag)±(Hg) mantos hosted by Cenozoic rhyolitic ignimbrites such as: Jardin, Amolanas, Venado, Elisa de Bordo (Camus, 1985, Lortie and Clark, 1987, Mayer and Fontboté, 1990, Jurgeit and Fontboté, 1990). These relatively small deposits represent a different metallogenic problem altogether.

Editors note: The Chilean strata-bound Cu-(Ag), or "Manto" deposits, particularly Mantos Blancos and El Soldado, have been included within the Iron Oxide Copper-Gold (IOCG) family by many authors in the existing literature. Others however, have argued a contrary view. Consequently, these two renowned authorities on this group of deposits were invited to contribute a paper describing the characteristics of the "Chilean Mantos", and then on the basis of their observations to discuss whether they are members of the IOCG family and their relationship to the ores of the family within the same belt.

Volumes and Grades

The largest strata-bound Cu- (Ag) deposit of the Jurassic group is Mantos Blancos in the Coastal Cordillera of Antofagasta in northern Chile, where 120 mt (million metric tons or tonnes) of ore were extracted during the period 1960-1995 producing 1 643 715 tonnes of copper. In 1995 the

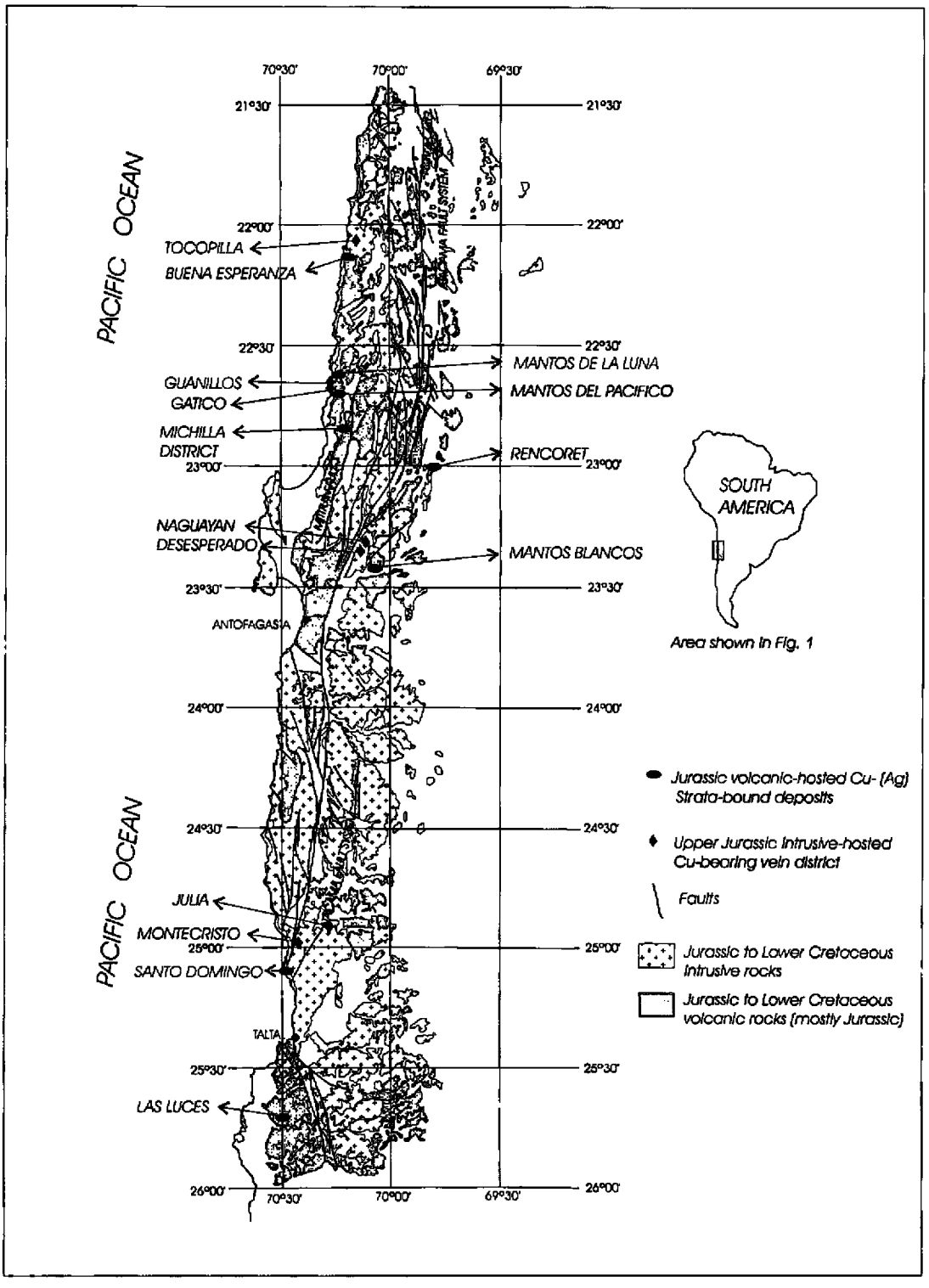


Figure 1: Upper Jurassic volcanic-hosted Cu-(Ag) strata-bound deposits and Cu-bearing vein districts hosted by Upper Jurassic intrusives in the Coastal Cordillera of northern Chile from 22° to 26°S. Simplified geology after Boric et al., 1990.

remaining reserves amounted to 43 mt of oxide ore at 0.86% Cu and 62 mt of sulphide ore at 1.18% Cu and 12 g/t Ag (Pizarro, 1997). The second in volume is the Mantos de la Luna deposit that has measured resources of 40.5 mt at 1.39% Cu plus inferred resources of 6 mt at 1.4% Cu (Minería Chilena, 2001). The other Jurassic deposits are smaller, although the reserves and production of some commonly total some millions of tonnes of ore at 1 to 3.8% Cu and 8 to 25 g/t Ag. The most significant deposits are Susana and Juarez in the Michilla district, and Santo Domingo, with other examples such as Buena Esperanza and Mantos del Pacifico (Fig. 1). The largest strata-bound Cu- (Ag) deposit hosted by Lower Cretaceous volcanic rocks is El Soldado in the Coastal Cordillera of central Chile, whose production plus ore reserves amounts to over 200 mt at 1.35% Cu. The second in volume of the Lower Cretaceous group is Lo Aguirre (now exhausted), located immediately west of Santiago city, where 11.1 mt at 2.14% Cu were exploited. Lower Cretaceous volcano-clastic rocks in central Chile host another group of relatively small strata-

bound Cu- (Ag) deposits. Typical examples are: Talcuna (Boric, 1985) and Cerro Negro (Elgueta et al., 1990). At Cerro Negro 6 mt of ores at 1-3% Cu and 31 g/t Ag were exploited, whereas the average tonnage of other deposits is about 2 mt at 1.7% Cu and 25 g/t Ag (Camus, 1990).

Geological Setting of the Strata-bound Cu-(Ag) Mineralisation

The Andean Cordillera in northern Chile (18°-34° Lat. S) is a section of the Central Andes that has long been regarded a classic example of a "simple" orogen developed along a convergent plate margin (eg. Dewey and Bird, 1970, James, 1971). This is a non-collisional orogen formed over a long-lived, currently active, subduction system, whose distinctive feature is the occurrence of a great volume of igneous rocks generated throughout its geologic history. Therefore the Andes have been referred to as a "magmatic mountain range" (Zeil, 1979) or a "volcano-plutonic orogen" (Sillitoe, 1976). Most of the rich metallic ore deposits of the Andes are of hydrothermal origin. They have an inherent and temporal relationship to the magmatic arc activity, and they are believed to derive most of their metallic content from underlying subduction-related processes (eg. Sillitoe, 1972, 1974, 1976, Clark and Zentilli, 1972, Clark et al., 1976, Maksaev, 1990, Maksaev and Zentilli, 1999). Successive supra-subduction volcano-plutonic arcs were developed since the Early Jurassic on the western continental margin of South America in response to plate convergence with an east-dipping Benioff zone. The magmatic front systematically shifted position inland as geological time progressed, the eastward change of position of the arc system followed periods of crustal thickening by compressive deformation, so that tectonism also migrated inland with time (Boric et al., 1990).

Two major stages are recognised in the geological evolution of the Andes in the northern half of Chile: 1). from the Jurassic to the end of the Early Cretaceous, when a magmatic arc-system flanked to the east by a sedimentary marine back-arc basin developed within an extensional tectonic setting, and, 2). since the Late Cretaceous to the present, when arc-systems developed on a continental environment within an overall compressive tectonic setting. Fold and thrust belts were locally developed eastward from the arc systems during the second stage.

Strata-bound Cu-(Ag) mineralisation was conspicuous during the first extensional stage of Andean evolution in Chile, whereas porphyry copper deposits strongly dominated during the second. These two major stages in the geological evolution of the north Chilean Andes reveal a major change of geodynamic conditions on the active continental margin during orogen formation that was also reflected in Andean metallogeny.

Most of the Andean Cordillera of the northern half of Chile was built above a basement that corresponds to an accretionary prism and arc system related to a pre-existing subduction regime on the border of the Gondwana super-continent during the Late Paleozoic to Early Triassic (Mpodozis and Ramos, 1990). The main N-S orientation of the Andean structures in northern Chile are oblique relative to the largely NNW to NW-trending fabric of the Upper Paleozoic basement rocks (eg. Tosdal and Richards, 2001). A 2500 km long belt that extends from northern Chile to southern Argentina and consists of rhyolitic ignimbrites and andesites several thousand metres thick, known as the Choiyoi Formation, represents the Upper Carboniferous to Lower Triassic arc system. The striking abundance of felsic rocks of this pre-Andean belt has been taken to represent either crustal anatexis-related processes during an extensional stage or as calc-alkaline subduction-related differentiated felsic rocks (Mpodozis and Ramos, 1990).

The Late Paleozoic–Early Triassic accretionary prism and magmatic arc system were replaced during Middle to Late Triassic time by a palaeogeography dominated by a number of NW-trending fault-bounded isolated basins or grabens (Charrier, 1979, Suarez and Bell, 1993, Ramos and Aleman, 2000). The formation of these grabens is believed to be related to extensional tectonics that preceded the fragmentation of the Gondwana super-continent (Mpodozis and Ramos, 1990). The Middle-Upper Triassic basins were filled by continental red-beds and lacustrine sediments, but also by marine sedimentary deposits along the present Coastal and Domeyko Cordilleras of northern Chile, and by local basaltic and rhyolitic bimodal volcanic rocks (Mpodozis and Cornejo, 1997; Ramos and Aleman, 2000). Subduction-related igneous activity resumed in the Early Jurassic some 100 to 150 km west from the former position of the Late Paleozoic–Early Triassic magmatic arc, while the area formerly occupied by the Late Paleozoic arc subsided to originate the Jurassic back-arc marine basin that persisted during the Early Cretaceous.

During the Jurassic and Early Cretaceous a subduction-related magmatic arc system was established along the whole length of the present Coastal Cordillera of northern Chile. It is now represented in northernmost Chile (21°-26°S) by a thick basaltic to andesitic volcanic pile (>7000 m thick) of calc-alkaline to K-rich calc-alkaline nature, with initial stages of tholeiitic affinity (Rogers and Hawkesworth, 1989, Pichowiak, et al., 1990). The volcanic strata were episodically intruded by a number of Jurassic and Lower Cretaceous calc-alkaline dioritic to granodioritic batholiths, many smaller intrusions and conspicuous dyke swarms (eg. Marinovic et al., 1995, Dallmeyer et al., 1996). Numerous Cu-bearing vein districts occur within Upper Jurassic batholiths (Boric et al., 1990). Most of the Jurassic - Lower Cretaceous volcanic rocks of the Coastal Cordillera of northernmost Chile were erupted in subaerial conditions, although minor marine fossiliferous calcareous sedimentary intercalations and local pillow lavas attest a persistent depositional environment more or less at sea level (Ferraris and Di Biase, 1978, Naranjo and Puig, 1984, Marinovic et al., 1995, Gröschke et al., 1988; Bogdanic et al., 1994). The extrusion of this volcanic sequence had to be accompanied by considerable crustal subsidence probably related to the extensional tectonic setting of the whole arc system (Dallmeyer et al., 1996). The fact that a thick Jurassic-Lower Cretaceous volcanic pile was deposited without significant relief building indicates that magmatic

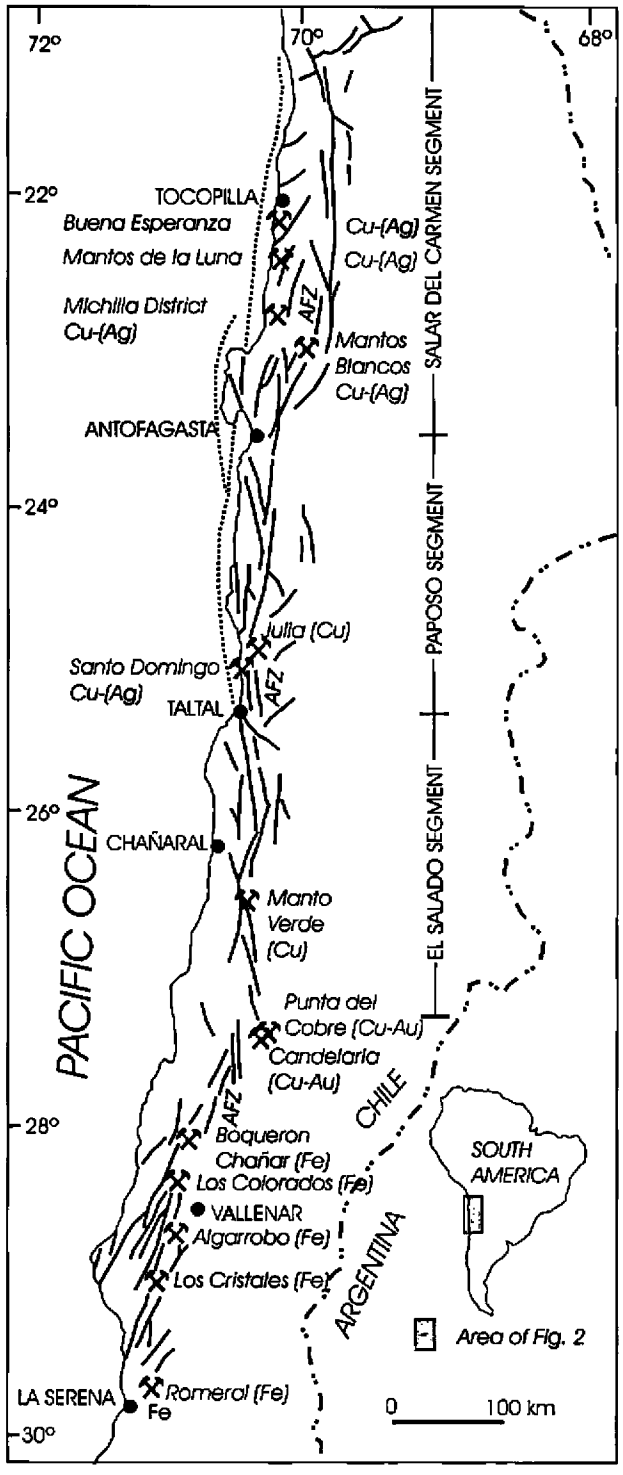


Figure 2: Major faults of the sinistral Atacama Fault Zone (AFZ) along the Coastal Cordillera of northern Chile, modified after Brown et al. (1993) and Vila et al. (1996). Main Fe, Cu-Au, and Cu-(Ag) deposits within the domain of the fault zone are shown.

arc evolution was accompanied by crustal thinning that accommodated steady subsidence. Foliated intrusions and mylonites along the Coastal Cordillera of the Antofagasta area (23°-26° Lat. S) indicate changes of stress regime with local transpressive conditions during the Jurassic and transtension during the Early Cretaceous (Gonzalez, 1999). These foliated intrusions and mylonites are related to the Atacama Fault Zone that is a major trench-linked sinistral strike-slip fault system that extends more than 1000 km along the Coastal Cordillera of northern Chile from latitude 20° to 30° S (Fig. 2). This fault system developed through the Jurassic-Early Cretaceous as an intra-arc regional structure related to oblique subduction of the Aluk (Phoenix) plate relative to the South American continent (Boric et al., 1990, Scheuber and Andriessen, 1990; Scheuber and Gonzalez, 1999).

The development of the Jurassic to Early Cretaceous magmatic arc along the present Coastal Cordillera was accompanied by subsidence and formation of a back-arc basin system farther east in the area now occupied by the Intermediate Depression and Domeyko Cordillera (Tarapaca Basin, Mpodozis and Ramos, 1990). In northern Chile (21°-27°S) the back-arc basin sequences are preserved as a belt of marine and continental sedimentary rocks exposed 70 to 110 km east of the coeval magmatic arc (Reutter and Scheuber, 1988, Ardill et al., 1998). In addition, local continental and marine sedimentation took place during the Early Cretaceous within the domain of the magmatic related sinistral to pull-apart basins (eg. El Way basin; Maksaev, 1990).

In the Coastal Cordillera of north-central Chile (~30°-34°S) the subsiding Jurassic to Lower Cretaceous magmatic arc is represented by a >10 000 m thick sequence of mafic lavas intercalated with marine clastic and carbonate rocks. This volcano-sedimentary sequence is thought to be deposited over thinned crust (Vergara et al., 1995; Aguirre et al., 1999). Episodic emplacement of plutonic complexes also took place during arc development in central Chile. The intrusion of large Aptian-Albian (upper-Early Cretaceous) granodioritic to dioritic batholiths (K-Ar 118-96 Ma; Rivano et al., 1993, Rivano and Sepulveda, 1991, Dallmeyer et al., 1996) appear to be particularly relevant to copper mineralisation. Iron, copper and gold occur within and on the periphery of these batholiths that were emplaced along extensional or sinistral transtensional faults within the Lower Cretaceous section of the volcanic-sedimentary sequence: eg. the Illapel Super-unit along the Manquegua and associated faults (Rivano y Sepulveda, 1991) and the La Borracha Plutonic Complex within the domain of the Atacama Fault Zone (Dallmeyer et al., 1996). In detail the Aptian-Albian batholiths are composed of a number of individual plutons that conform to relatively narrow N-S-trending belts indicating that batholiths largely expanded by episodic injection of magma batches that were emplaced along transtensional faults within the Lower Cretaceous volcanic-sedimentary pile and older intrusions. This is consistent with emplacement models postulated for Mesozoic plutonic complexes along the Coastal Cordillera of the Copiapo region (26°-29°S) of Chile (eg. Dallmeyer et al., 1996, Wilson and Grocott, 1999). Tilting of the Jurassic-Lower Cretaceous sequence also appears to be related to Aptian-Albian sinistral transtensional tectonics along the Coastal Cordillera of central Chile (~30°-34°S).

On the other hand, Tithonian-Neocomian (Late Jurassic to Early Cretaceous) marine limestones that outcrop in the High Andes between 32°-34°S attest that a marine platform developed to the east of the extensional magmatic arc in central Chile (Aconcagua Platform of Mpodozis and Ramos, 1990).

Tectonic inversion took place during the Cenomanian to Santonian (lower Late Cretaceous) as result of compressive deformation pulses that affected the whole Central Andes. This included contraction and emergence of the of the arc and back-arc basin system (Megard, 1987, Coira et al., 1982, Mpodozis and Ramos, 1990, Ladino et al., 1999, Tomlinson et al., 2001). The igneous activity along the former Jurassic - Lower Cretaceous magmatic arc ceased at the onset of compression and subsequently a new magmatic arc was developed some 50 km eastward from the previous location. Subsequent Late Cretaceous and Cenozoic volcanic activity in the Andes of northern Chile took place exclusively in a subaerial environment, with further episodes of crustal shortening/thickening by compressive deformation events.

The tectonic inversion of the former Jurassic to Lower Cretaceous marine back-arc basin domain, waning of the igneous activity along the westernmost section of the South American continental border and the establishment of a new magmatic arc farther inland are major Late Cretaceous palaeogeographic changes that have been interpreted as an adjustment of the active continental margin of South American from a Mariana type (extensional) to a Chilean (compressive) type of subduction (Davidson and Mpodozis, 1991). These significant geological and tectonic changes correlate with a rapid separation between Africa and South America, with the latter overriding the oceanic plate to the west (Ramos and Aleman, 2000).

The stratigraphic position and geochronological data indicate that the Chilean volcanic-hosted strata-bound Cu-(Ag) deposits were generated during the Late Jurassic and uppermost Early Cretaceous. The overall extensional tectonic setting, crustal thinning, active subsidence, extensional tilting of the volcano-sedimentary strata and episodic batholith emplacement within these strata during the development of the Jurassic - Lower Cretaceous magmatic arc are singular to this early stage of Andean evolution in Chile. However, it appears that distinct periods of transtensional tectonics facilitated shallow emplacement of batholitic masses, provided structural weakness zones for hydrothermal fluid circulation, and modified the hydraulic regime within the permeable strata of tilted volcano-sedimentary strata. The concurrence of these specific factors and probably other still unknown ingredients may account for the occurrence of two discrete periods of strata-bound Cu-(Ag) mineralisation.

Jurassic Volcanic-hosted Strata-bound Cu-(Ag) Deposits

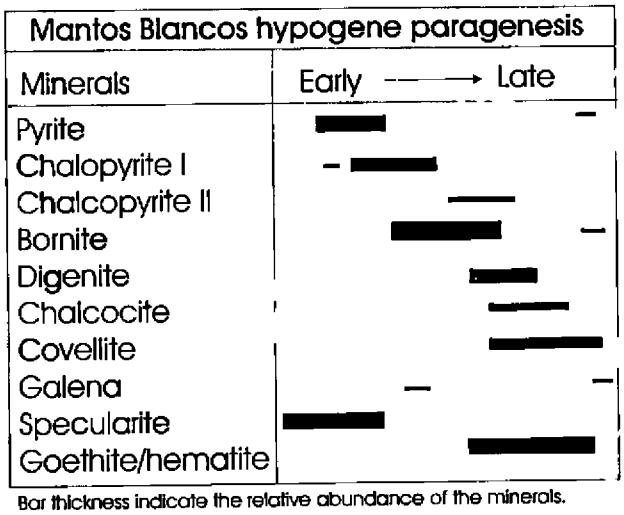
The strata-bound Cu-(Ag) deposits of the Jurassic belt are distributed along the Coastal Cordillera of northern Chile between 22°-26°S (Fig. 1). They are primarily hosted by mafic Jurassic basaltic to andesitic porphyritic lavas or breccia bodies, although the largest deposit of this group Mantos Blancos is hosted by a bimodal suite of rhyolitic and andesitic rocks, with some ore-grade mineralisation also occurring within dacitic and andesitic sills and dykes (Chavez, 1985). Strata-bound Cu-(Ag) deposits often occur near gabbroic, dioritic or andesitic subvolcanic intrusive bodies, such as dykes, sills, stocks, or volcanic necks, but these intrusives are largely un-mineralised and some post-date copper mineralisation (eg. at Buena Esperanza, Susana, and Santo Domingo; Palacios, et al., 1986, Espinoza et al., 1996). These subvolcanic intrusives have been interpreted as feeder conduits of the Jurassic volcanism (Palacios and Definis, 1981, 1981b, Espinoza, 1981, Espinoza et al., 1996).

The strata-bound Cu-(Ag) deposits have long been known as "Chilean Manto-type", because initial mining exploited the stratiform sections of the deposits (referred to as "mantos" by miners). However, the complete orebodies are commonly composite, including stratiform, lenticular, pipe, and irregular forms, that are either concordant or discordant to the bedding of the host Jurassic volcanic strata. Mantos Blancos for example includes at least four main lenticular disseminated and fracture-filling sulphide orebodies (Sorpresa, Aida, Nora, and Marina) forming an overall, slightly unconformable, sub-horizontal tabular ore deposit (Chavez, 1985). The thicknesses of mineralised zones at Mantos Blancos range from 150 to 350 m and the deposit extends irregularly over an area of 2.6x1.2 km. At Buena Esperanza and Susana copper sulphides cement the matrix of a central breccia pipe and are also disseminated in a number of conformable stratiform orebodies ("mantos") around the breccia pipes (Palacios, 1990; Espinoza et al., 1996). The stratiform orebodies (2 to 25 m thick) are commonly restricted to the amygdaloidal and brecciated sections of the Jurassic lava flows while minor veins occur along local faults and fractures (Palacios and Definis, 1981, 1981b, Dreyer and Soto, 1985). The main hypogene sulphides are chalcocite and bornite, minor chalcopyrite, and at times covellite and digenite. Hypogene gangue minerals are quartz, hematite, pyrite, chlorite, albite, and calcite. Minor magnetite occurs as dissemination within mineralised rocks, but is mostly replaced by hematite or maghemite. At Mantos Blancos, where specularite occurs, it is early in the paragenesis and mostly concentrated within a barren andesite flow that overlies the orebody, whereas a fine reddish hematite dissemination occurs within mineralised rocks. A lateral hypogene zonation has been described at Mantos Blancos and Santo Domingo that includes copper-rich cores dominated by chalcocite-bornite-digenite surrounded by a peripheral halo of bornite-chalcopyrite or chalcopyrite alone, and an external halo (mostly uneconomic) of chalcopyrite-pyrite (Chavez, 1985, Definis, 1985). The hydrothermal alteration assemblage of albite - chlorite - hematite - quartz - calcite - epidote - sphene - scapolite - anatase - minor sericite is associated with ore minerals in these strata-bound Cu- (Ag) deposits, with the primary textures of the volcanic rocks being preserved (Losert, 1973, Chavez, 1984, 1985, Palacios, 1986, 1990). This local alteration appears to be superimposed upon a regional low grade alteration/ metamorphism of the volcanic sequence characterised by a chlorite-calcite-epidote-zeolite-prehnite-pumpellyite assemblage, with little or no alteration contrast macroscopically visible between mineralised and barren volcanic country rocks. The hydrothermal alteration is

particularly pervasive in Mantos Blancos, where litho-geochemistry shows significant metasomatism of the host rocks with addition of Na, Fe and Mg (Chavez, 1985).

Paragenetic studies of these strata-bound Cu-(Ag) deposits have shown that pyrite-chalcopyrite-bornite and minor magnetite were deposited first, followed by subordinate amounts of hypogene chalcocite-covellite-digenite accompanied by hematite (Fig. 3). This sequence indicates a gradual increase in the proportion of copper in the sulphides, and probably a decrease of sulphur activity in the mineralising fluids with time (Chavez, 1985, Losert, 1974, Wolf et al., 1990; Trista, 2001). The paragenetic sequence is characterised by the successive hypogene replacement of iron rich sulphides (pyrite, chalcopyrite) by copper-rich sulphides (bornite, chalcocite, covellite, digenite) which may account for iron release and formation of hypogene hematite associated with the copper sulphides (Chavez, 1984).

Two phase, liquid-rich fluid inclusions in quartz and calcite with sulphides from Mantos Blancos have yielded homogenisation temperatures in the 225°-400°C range (mostly concentrated within 284°-355°C) and salinities from 8 to 17 wt.% NaCl equivalent (Collao, 1993). Fluid inclusions in gypsum from the same deposit have lower homogenisation temperatures in the 112°-225°C range and lower saline content (3-10 wt.% NaCl equivalent). Pressure estimations from the fluid inclusion data range from 145 to 222 bars in hydrostatic conditions (Collao, 1993). At the Buena Esperanza deposit saline fluid inclusions (up to 35 wt.% NaCl equivalent) in calcite that contains copper sulphides have produced homogenisation temperatures ranging from 65° to 195°C, whereas fluid inclusion in quartz-filled amygdules yielded homogenisation temperatures between 130°C and 235°C; minimum formation pressures were estimated at about 285-315 bars (Nisterenko et al., 1973). However, Palacios (1990) reported higher fluid inclusion homogenisation temperatures (440°-500°C) of hyper-saline (52-59 wt.% NaCl eq.) fluid inclusions in hydrothermal quartz from the vicinity of the central gabbroic stock of Buena Esperanza, which was regarded as the mineralising fluid source by this author. Two phase, liquid-rich fluid inclusions in quartz from the Buena Vista deposit (Michilla District) have yielded homogenisation temperatures ranging from 214° to 360°C (mostly concentrated within 220°-300°C) and salinities from 16 to 21 wt.% NaCl equivalent; a trapping pressure of 90 bars was estimated for an average homogenisation temperature of 270°C and hydrostatic pressure conditions (Trista, 2001). Although the last author estimated that the fluid at Buena Vista was trapped close to the boiling point, no evidences of boiling of hydrothermal fluids were observed by any of the above mentioned authors. The limited data available for the formation conditions of the Jurassic strata-bound Cu- (Ag) deposits suggests that saline fluids, at moderate temperatures, within a depth range of about 1000 to 3000 m deposited metals within the Jurassic volcanic pile assuming hydrostatic pressure conditions. This estimate of depth of emplacement for the Jurassic strata-bound Cu-(Ag) deposits is consistent with independent estimations of unroofing based on apatite fission track data (<2 km assuming a palaeo-geothermal gradient of 30°C/km) from Jurassic and Cretaceous intrusions along the Coastal Cordillera of the northern section of the Antofagasta Region (Maksaev, 1990, 2000, Andriessen, 2000).



Bar thickness indicate the relative abundance of the minerals. (After Chavez, 1985)

Figure 3: Paragenetic sequence of hypogene minerals in Mantos Blancos volcanic-hosted Cu-(Ag) strata-bound deposit. After Chavez (1985).

Sparse and imprecise K-Ar and Rb-Sr minimum radiometric dates indicate that the main strata-bound deposits hosted by Jurassic volcanic rocks of northern Chile were formed at about 150-140 Ma (Boric et al., 1990, Venegas et al., 1991, Tassinari et al., 1993, Vivallo and Henriquez, 1998). This radiometric age range is younger than the volcanic host rocks that have been dated by Rb-Sr and K-Ar methods in the 186-165 Ma range, but overlapping with ^{40}Ar-^{39}Ar, Rb-Sr and K-Ar ages of granodioritic batholiths that intrude the volcanic sequence along the coastal area (age compilation in Vivallo and Henriquez, 1998). Minor stocks and dykes spatially related to the strata-bound Cu-(Ag) deposits have minimum K-Ar ages ranging between 154 and 133 Ma, except for the gabbroic stock at Buena Esperanza that have yielded a K-Ar age of 168 ± 5 Ma in plagioclase (Boric et al., 1990).

On the other hand, numerous iron oxide and copper bearing veins are hosted by the Upper Jurassic dioritic to granodioritic batholiths that are emplaced within the same Jurassic volcanic sequence that hosts strata-bound Cu-(Ag) deposits along the Coastal Cordillera. The most significant occur at the Tocopilla, Gatico, Desesperado, Julia and Montecristo districts (Fig. 1). These vein districts were of primary economic importance in the second half of the 19th Century and early 20th Century when most of the Chilean copper production came from veins, but most are long abandoned. The largest vein deposits are Minita-Despreciada (Tocopilla District), Toldo-Velarde (Gatico District), and Julia-Reventon (Julia District). These are mostly NE-trending, steeply-dipping veins (though some veins strike WNW, E-W and N-S), from 750 to 2000 m long, 1 to 12 m wide and about 370 to 670 m of known vertical extent. Copper ores concentrate in rich pockets along these structures, separated by low grade or barren

sections. The hypogene paragenetic sequence of the largest veins is tourmaline-actinolite-quartz-magnetite-hematite-pyrite-chalcopyrite-bornite-calcite (Ferraris et al., 1973, Boric et al., 1990). Strong silicification, argillic alteration and chloritisation occur within these copper bearing veins, and extends some metres into their intrusive wall rocks. The hypogene minerals fill fractures and openings, either as irregular and discontinuous veinlets or massive pockets with banded textures, or as fine dissemination. The structure of the Cu-bearing veins is regular and continuous within the intrusive bodies, but quite irregular and discontinuous when the veins extend into the intruded volcanic rocks, as at the Naguayán - Desesperado district (Boric et al., 1990), although a transition from these magnetite and copper bearing veins to strata-bound Cu-(Ag) mineralisation has not been observed. Cu-bearing veins from the Tocopilla and Guanillos Districts contain hyper-saline fluid inclusions (48-68 wt.% NaCl eq.) with homogenisation temperatures from 320° to 540°C, but mostly between 380°-420°C (Trista, 2001). The characteristics of this type of magnetite and copper-bearing veins indicate that they are high to moderate temperature mesothermal deposits (Ruiz et al., 1965, Ferraris et al., 1973, Boric et al., 1990, Vivallo and Henriquez, 1998, Trista, 2001). They are genetically related to the emplacement and cooling of Upper Jurassic Batholiths (K-Ar and ^{40}Ar-^{39}Ar ages ranging from 167 to 140 Ma, Maksaev, 1990).

The apparent time and space relationships between the Jurassic volcanic-hosted Cu-(Ag) strata-bound deposits and the mesothermal Cu-bearing veins hosted by plutonic rocks, plus geochemical and isotopic comparisons led Vivallo and Henriquez (1998) to postulate that the batholith-hosted, iron-rich, Cu-bearing veins were the deep feeder structures of the hydrothermal fluids that originated the strata-bound deposits within the Jurassic volcanic strata. Although this hypothesis cannot be discarded, these two types of deposits were formed in rather different pressure and temperature conditions, their timing of formation is poorly constrained, and there are no direct field relationships between them (Trista, 2001).

Most of the strata-bound Cu-(Ag) deposits of the Jurassic belt have an upper oxidised zone that extends to a maximum depth of 250 m. The degree of supergene oxidation is variable; some deposits comprise almost exclusively oxidised copper ores (eg. Mantos de la Luna, Juarez), whereas others are completely composed of hypogene sulphides (eg. Buena Esperanza). When present, the boundary between the supergene and hypogene ores is gradual, so that some deposits include a zone with a mixture of copper sulphides and oxidised minerals (eg. Susana, Santo Domingo). The oxidised ores include mainly atacamite, minor chrysocolla, malachite, and rare cuprite and native copper; the oxidised rocks show profuse goethite and hematite stains on fracture surfaces. Copper grades are similar in the oxidised upper section and the underlying hypogene sulphide zone of the deposits, so that no significant Cu transport occurred during the supergene oxidation (largely *in situ* oxidation). Only the largest deposits such as Mantos Blancos and Susana have local enriched pockets with supergene chalcocite group minerals and covellite (Astudillo, 1984, Chavez, 1985, Wolf et al., 1990).

The poor development of secondary enrichment within the Jurassic strata-bound Cu-(Ag) deposits could be explained by the insufficiency of hypogene pyrite to release supergene acid solutions under oxidation, and the profuse occurrence of calcite gangue that may have readily neutralised any supergene acid solutions precluding the leaching of metallic cations from the oxidised zone.

Lower Cretaceous Strata-bound Cu-(Ag) Deposits

Lower Cretaceous volcanic rocks with marine sedimentary intercalations form a N-S-trending belt in north central Chile that is located about 30 to 60 km east from the Pacific coast. Significant volcanic-hosted strata-bound Cu-(Ag) deposits occur within this belt, particularly in central Chile (eg. El Soldado, Lo Aguirre) (Fig. 4). In addition, there is a distinct group of strata-bound Cu-(Ag) deposits within

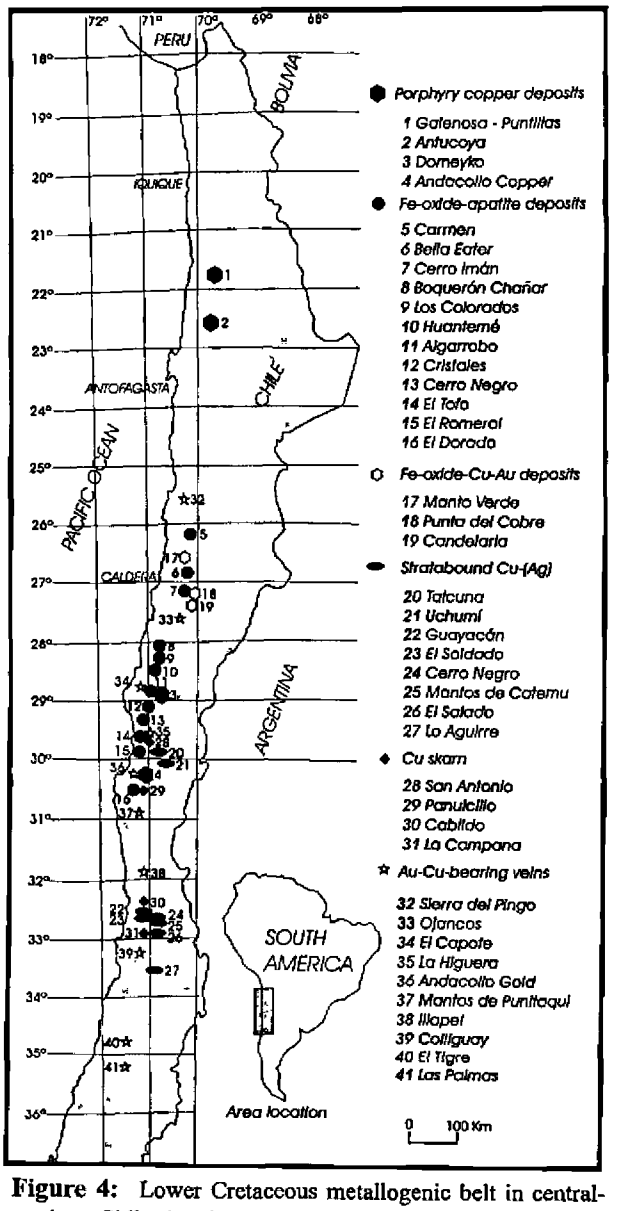


Figure 4: Lower Cretaceous metallogenic belt in central-northern Chile showing the variety of deposit types that occur along this belt besides the Cu- (Ag) strata-bound deposit.

volcano-sedimentary strata formed in intermontane basins with red-beds and carbonaceous mudstones (eg. Cerro Negro, Talcuna, Uchumi) (Figs. 4-5). Furthermore, the belt of Lower Cretaceous volcano-sedimentary rocks and plutonic complexes hosts a diverse suite of copper, iron and gold deposits including: Fe-oxide Cu-Au deposits (Candelaria, Manto Verde, Manto Ruso, Farola, Generosa), porphyry copper deposits and prospects (Andacollo, Antucoya, Puntilla, Domeyko), Cu skarns (Panulcillo, Cabildo and La Campana districts), magnetite-apatite deposits of the "Chilean Iron Belt" (eg. Los Colorados, El Algarrobo, and Romeral, Espinoza, 1990) (Fig. 3), and mesothermal Au-Cu-bearing veins (Andacollo Gold, Capote, Mantos de Punitaqui, and Colliguay districts) (Fig. 4). The most significant deposits of the Lower Cretaceous belt are: strata-bound Cu-(Ag), Fe-oxide Cu-Au, magnetite-apatite, porphyry copper, and Cu skarn deposits. According to available geochronological data all these deposits were formed in the uppermost Early Cretaceous.

The largest deposit of this group of strata-bound Cu- (Ag) deposits is El Soldado, that is located about 120 km north

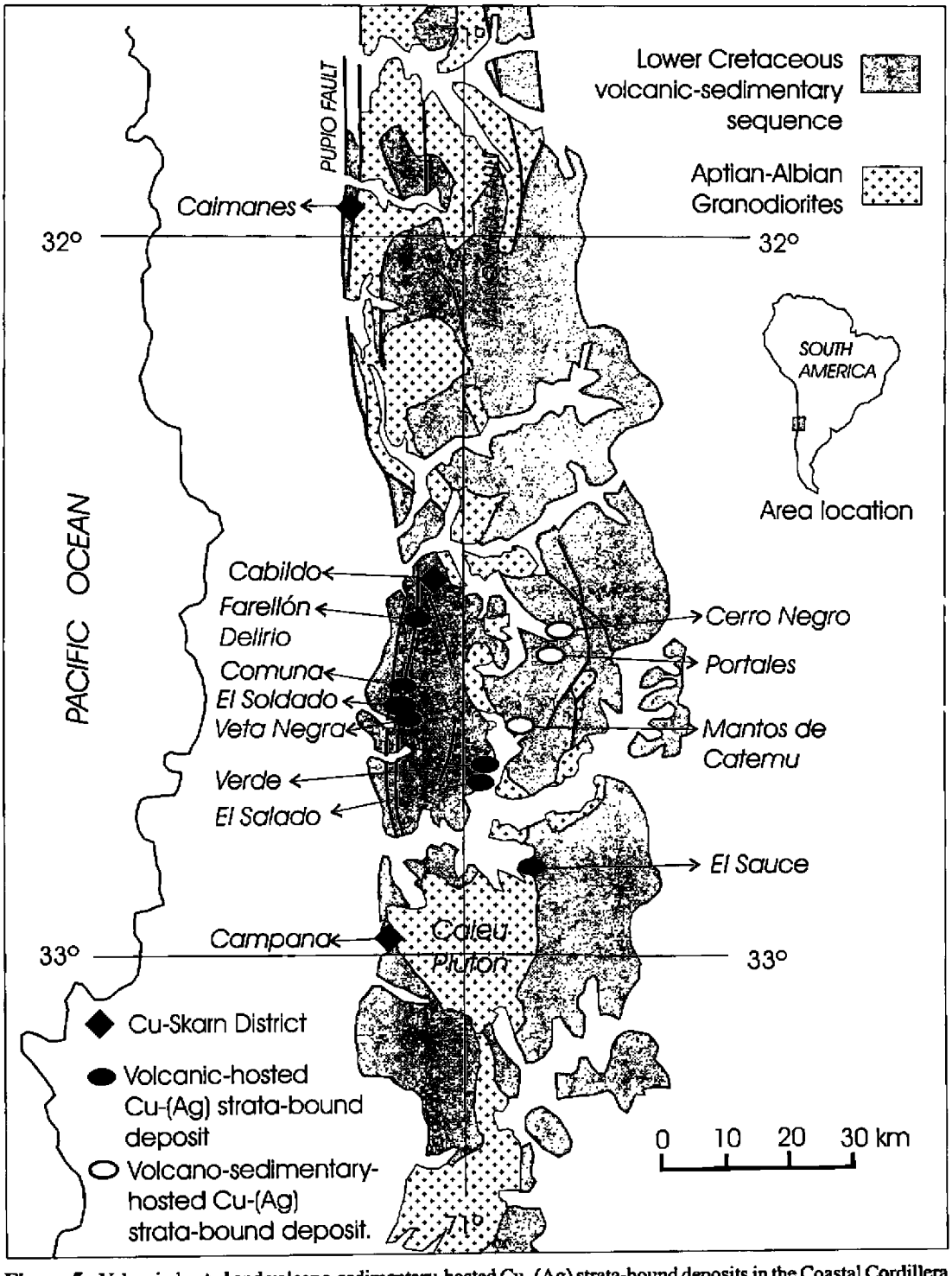


Figure 5: Volcanic-hosted and volcano-sedimentary-hosted Cu- (Ag) strata-bound deposits in the Coastal Cordillera of central Chile between 32° and 33°S. The belt of Lower Cretaceous volcanic sequence with sedimentary intercalations and Aptian - Albian granodioritic plutons emplaced within this unit are shown. Geology simplified after Rivano et al., 1993 and Rivano and Sepulveda, 1991.

of Santiago, in the Coastal Cordillera of central Chile (Fig. 5). The deposit is hosted by a sequence of felsic and basaltic units (Boric, et al., this volume) dipping ~30° to the east, that constitutes the Upper Member of the Lower Cretaceous Lo Prado Formation (Rivano et al., 1993). El Soldado consists of numerous isolated orebodies with intervening barren zones, distributed in about a dozen individual orebody clusters or blocks. These blocks are spatially distributed within a volume of about 2 km in length by 1 km wide and 600 m in vertical extent (Wilson and Zentilli, 1999). Within the blocks, individual subvertical orebodies are extremely variable in size, from very small to 450 m long, 150 m wide, and 450 m in vertical extent (Boric, 1997). Although described as strata-bound at a regional scale, in detail the El Soldado orebodies are distinctly discordant, displaying a strong structural control (Ruge, 1985). The orebodies are preferentially developed within a generally N-S to NNW regional fracture system, especially where N-S, E-W, and NW faults intersect. The overall fault pattern at El Soldado is consistent with transtensional zones along a longitudinal sinistral fault system. Away from these zones of structural permeability, orebodies can be best described as veins (Boric, 1997). Lithologic control is exerted by the relatively more brittle felsic flows (trachyte-rhyolite) and their feeders, which are more richly mineralised in comparison of more mafic (andesite-basalt) flows and tuffs (Martin, 1981, Ruge, 1985). Late andesitic-basaltic dykes are generally barren (Boric, 1997). Hypogene ore minerals are chalcopyrite, bornite, and chalcocite that occur as dissemination and veinlets, largely filling primary and secondary porosity of the volcanic host rocks. According to Boric (1997) many individual orebodies in a block show a mineralogical zoning: a core of chalcocite-hematite or chalcocite-bornite-hematite is followed outward by approximately concentric zones of bornite-chalcopyrite, chalcopyrite, and pyrite in the most external zone. The deeper roots of the orebodies contain relatively more pyrite than their upward terminations. Although oxidised copper zones exist near the surface and mixed ores were exploited, supergene enrichment is not significant. Common waste or gangue minerals are pyrite, hematite, magnetite, calcite, chlorite, albite, microcline, bitumen, and minor amounts of sphalerite, galena, and arsenopyrite. The copper grade is extremely variable (Klohn et al., 1990). Lateral limits of the orebodies are characterised by abrupt changes of Cu grade from a nucleus at about 2% Cu to marginal zones at 1.2-0.5% Cu within a few metres (Ruge, 1985, Klohn et al., 1990). The wall rock between the orebodies is generally barren (<0.15% Cu, Klohn et al., 1990). Hydrothermal alteration consists of abundant calcite, chlorite, albite, microcline, epidote, opaline silica, titanite, and rutile-anatase, and some sericite and clay minerals, with primary rock textures largely being preserved (Holgrem, 1987, Boric, 1997).

Highly saline (ca. 30-40 wt.% NaCl equivalent) three-phase fluid inclusions in quartz related to sulphide mineralisation at El Soldado yielded minimum homogenisation temperatures ranging between 200°-257°C (without pressure correction), with no evidences of boiling being observed (Holgrem, 1987). The same study found that fluid inclusions within late barren calcite at El Soldado are also highly saline but with lower homogenisation temperatures from 82° to 104°C. On the other hand, three-phase fluid inclusions in quartz from quartz-bornite amygdules at El Salado yielded homogenisation temperatures from 250° to 430°C, whereas the occurrence of some vapour-rich inclusions suggests boiling (Nisterenko et al., 1973). El Salado is a minor volcanic-hosted stratiform Cu-(Ag) deposit located 18 km SE from El Soldado (Fig. 5), and close to the western border of a granodioritic intrusion with a biotite K-Ar ages of 118 ± 3 Ma (Rivano et al., 1993).

Many radiometric dates (K-Ar, $^{40}Ar/^{39}Ar$, Rb/Sr) reported from El Soldado range from 131 to 99 Ma supporting the Early Cretaceous age for this copper deposit (Munizaga et al., 1988, Boric and Munizaga, 1994, Boric, 1997). The oldest radiometric ages at El Soldado are from 131 to 118 Ma and are in agreement with the stratigraphic Neocomian (lower Early Cretaceous) age of the host volcanics. A group of younger ages from 113 to 96 Ma are considered to represent the alteration/mineralisation event; this group of radiometric ages includes dates of veinlets of K-feldspar and albite associated with copper sulphides that are mostly concentrated between 105 and 101 Ma (Boric, 1997). According to this radiometric data mineralisation at El Soldado temporally coincides with the K-Ar age range of Cretaceous batholiths that are emplaced within the Lower Cretaceous volcano-sedimentary sequence and outcrop some 12.5 km NE and 18 km SE of El Soldado (118-96 Ma; Rivano et al., 1993). This is also true for the 117-94 Ma ^{40}Ar-^{39}Ar age range of the Caleu Pluton that crosscuts the Lower Cretaceous sequence some 25 km south of El Soldado (Parada and Larrondo, 1999, Parada et al., 2001) (Fig. 5). Cu-bearing skarn deposits occur in metamorphosed limestone intercalations of the Lower Cretaceous sequence within the contact aureole of Aptian-Albian (upper Early Cretaceous) intrusions, whereas volcanic-hosted Cu-(Ag) strata-bound deposits are present farther from the same plutons (eg. the Cabildo and La Campana districts; Carter, 1961, Tidy, 1970, Moya, 1980). Therefore, Cu-(Ag) mineralisation at El Soldado coincides temporally with an Aptian-Albian regional plutonic event characterised by the emplacement of large batholithic masses within the previously deposited Lower Cretaceous volcanic-sedimentary sequence, but was also coeval with Cu skarn mineralisation associated with the contact zones of the Aptian - Albian plutons.

Recently, Wilson et al. (submitted) have dated 10 samples of K-feldspar (adularia) from El Soldado by the stepwise-heating ^{40}Ar-^{39}Ar method. For hydrothermally precipitated K-feldspar in close association with copper sulphides, the ages range from 100.5±1.5 Ma to 106±1.1 Ma, with a mean of 103±1.3 Ma, which these authors interpret to be the main age of copper mineralisation at El Soldado. K-feldspar unrelated (or with dubious relationship) to ore, yields ages between 109.4±1.1 Ma and 112±2 Ma (mean = 110±1.4 Ma). They interpret these older ages to represent redistribution of alkalis in response to low-grade metamorphism of the host sequence. The ca. 110 Ma well-

defined argon release spectra are variably reset by the ca. 100 Ma hydrothermal mineralisation episode. High levels of atmospheric Ar were detected in all K-feldspar samples. They are tentatively attributed to connate basinal and metamorphic fluids that were heavily contaminated by meteoric waters. Fission track dating of apatite in the host rocks yields an age of ca. 90 Ma, indicating fast cooling of the system post-mineralisation; time-temperature modelling of fission track-length data are compatible with initial fast exhumation, followed by slow exhumation and cooling to surface temperatures (Wilson et al, submitted).

The timing of the copper mineralisation of El Soldado coincides with the 100-96 Ma ^{40}Ar-^{39}Ar age range of secondary K-feldspar and sericite from volcanic rocks of the Lower Cretaceous sequence some 10 km south of El Soldado (Fuentes et al., 2001, Morata et al., 2001). The occurrence of secondary albite, K-feldspar, prehnite-pumpellyite, laumontite, epidote, calcite and minor sericite is widespread within the Lower Cretaceous sequence in central Chile, with the primary textures of the rocks being preserved (eg. Levi et al., 1989). These secondary minerals are traditionally interpreted as products of a low-grade regional metamorphism of the Mesozoic sequence (Levi et al. *op. cit.*, Fuentes et al., 2001, Morata et al., 2001). The geochronological data now available show that this regional metamorphic event may in part coincide temporally with the emplacement of large batholithic masses within the Lower Cretaceous volcano-sedimentary pile and also with the Cu-(Ag) mineralisation at El Soldado and Cu-bearing skarns, although adularia may have also crystallised earlier during the burial history of the basin according to the data of Wilson et al. (submitted).

At the Lo Aguirre deposit, on the western outskirts of Santiago city, Cu-bearing ores occur within andesitic-basaltic lavas and breccias of the Barremian-Aptian Veta Negra Formation forming a main irregular orebody 600 m long, 200 m wide, and 150 m in vertical extent. Lo Aguirre and two minor satellite orebodies (San Antonio and Carreton) are peripheral to a barren dioritic stock. Hypogene mineralisation comprises disseminated chalcocite and bornite with successive outer zones of bornite-chalcopyrite, chalcopyrite-pyrite and pyrite. The copper sulphides concentrate within the more porous levels of the host volcanic rocks and were partly oxidised by supergene activity. Hydrothermal alteration minerals are calcite, quartz, hematite, chlorite, epidote, and clay minerals. At Lo Aguirre a whole rock K-Ar age of 110±4 Ma was obtained for an andesite sample and a Rb-Sr isochron of 113±3 Ma, which were interpreted to represent the probable age of hydrothermal alteration related to mineralisation in this deposit (Munizaga et al., 1988). However, a later ^{40}Ar-^{39}Ar dating of albite from mineralised rocks yielded a date of 102±5 Ma that places the mineralisation at Lo Aguirre as temporally concurrent with that at El Soldado (Munizaga, verbal communication).

Another group of relatively small strata-bound Cu-(Ag) deposits in central Chile is hosted by Lower Cretaceous sedimentary or volcano-clastic rocks (Cerro Negro, Uchumi, Talcuna, Camus, 1990). These are roughly tabular conformable orebodies ("mantos") restricted to a specific stratum, being interconnected by poorly mineralised sections. Copper mineralisation is concentrated in the upper few metres of a specific sedimentary or pyroclastic level that normally underlies either a massive volcanic or mudstone impervious stratum. Typical examples occur at Talcuna (Boric, 1985), and Cerro Negro (Elgueta et al., 1990). At Talcuna, stratiform Cu-(Ag) mineralisation mostly occurs along a 10 to 15 m thick bituminous lapilli tuff band, with economic-grade ore-shoots extending for only some tenths of metres from the intersection between the lapilli tuff level and subvertical NNW-trending veins. These veins have open-space filling textures, evidence of hydraulic fracturing and have been interpreted as feeders of hydrothermal fluids that mineralised the bituminous lapilli tuff band beneath an impervious manganese-rich level of tuffaceous sandstones and mudstones (Boric, 1985, Moreno, 2001). Present exploitation within the Talcuna district concentrates on NW-elongate ore shoots that developed along the intersection of the above mentioned lapilli tuff level with veins; rich pockets coincide with the occurrence of abundant bitumen (Moreno, 2001). Coexisting liquid-rich and vapour-rich fluid inclusions in calcite (suggesting trapping of a boiling hydrothermal fluid) associated with copper sulphides at the Talcuna orebodies yielded homogenisation temperatures from 70° to 170°C and salinities from 5 to 27 wt.% NaCl equivalent (Oyarzun et al., 1998). These authors interpreted the wide range of salinity variation as the result of complex interaction between boiling of the hydrothermal fluid and mixing with non saline waters during mineralisation at Talcuna. In addition, fluid inclusions in calcite from cavity filling in andesites in the area of the deposits yielded homogenisation temperatures in the range of 120° - 205°C and salinities from 11 to 19 wt.% NaCl equivalent. These were taken to represent an earlier stage of mineralisation at Talcuna (Oyarzun et al., 1998).

The strata-bound deposits of this group have been formed within the Lower Cretaceous sequences deposited in shallow marine to intermontane lacustrine sedimentary basins with coeval volcanic deposits (Camus, 1990). Hypogene minerals are bornite, chalcopyrite, chalcocite, pyrite and minor sphalerite and galena. Gangue minerals are calcite, chlorite, hematite, epidote, zeolites, and local magnetite. In addition, Zentilli et al. (1997) and Wilson and Zentilli (1999) documented that bitumen commonly occurs within these strata-bound Cu- (Ag) deposits hosted by Lower Cretaceous volcano-sedimentary strata (Uchumi, Talcuna, Cerro Negro) suggesting that copper mineralisation in these deposits was deposited within degraded petroleum reservoirs.

Isotopic Constraints

The volcanic-hosted strata-bound copper deposits (Upper Jurassic and Lower Cretaceous) are characterised by $\delta^{34}S$ values ranging from -10 to +10‰ suggesting magmatic derivation of sulphur, whereas the Lower Cretaceous strata-bound deposits within sedimentary-volcanic strata contain isotopically lighter sulphur($\delta^{34}S$ -10 to -40‰) suggestive

of reduction by organic matter or biogenic fractionation (Munizaga et al., 1994, 1995). However, barite present in the upper levels of the mineralised bodies at Cerro Negro with $\delta^{34}S$ +10 suggests an ultimate magmatic source for the sulphur of these sulphates (Munizaga, et al., 1994). Isotopic data for gangue calcite ($\delta^{13}C$ = -10 to 13‰; $\delta^{18}O$ = +12 to +18‰; initial $^{87}Sr/^{86}Sr$ = 0.7040 to 0.7056) preclude a major involvement of seawater in most Cu-(Ag) strata-bound deposits as suggested by Chavez (1985). At Mantos Blancos the initial $^{87}Sr/^{86}Sr$ ratio of 0.7056 from ore-bearing calcite and from altered rocks contrasts with the lower initial $^{87}Sr/^{86}Sr$ ratios (0.7031-0.7041) of the Jurassic volcanics and plutonic rocks. According to Tassinari et al. (1993) these data imply that the hydrothermal fluids that formed Mantos Blancos were not entirely magmatic in nature, nor seawater, but probably they were a mixture of fluids from different origin or fluids that partially equilibrated isotopically with the host rocks. At the El Soldado and Lo Aguirre deposits initial $^{87}Sr/^{86}Sr$ ratios of 0.7047 and 0.7048 have been obtained respectively, which are higher than the average value of 0.7040 obtained for Lower Cretaceous un-mineralised volcanic rocks (Munizaga et al., 1988). These ratio values are compatible with a predominant magmatic derivation of the hydrothermal fluids at this deposits with minor crustal contribution of Sr, which are not compatible with marine or metamorphic waters that would have had higher initial $^{87}Sr/^{86}Sr$ ratios (Munizaga et al., 1988).

Initial $^{187}Os/^{188}Os$ ratios from sulphides of Mantos Blancos, El Soldado, Cerro Negro and Talcuna range from 0.5 to 4. These values are more radiogenic relative to the range of 0.2 to 0.5 obtained for major porphyry copper deposits (Chuquicamata, El Teniente) suggesting the involvement of crustal Os in the strata-bound deposits (Munizaga et al., 2000). Pb isotopic data for the Lower Cretaceous volcanic and sedimentary-hosted strata-bound Cu-(Ag) deposits of central Chile ($^{206}Pb/^{204}Pb$ = 18.316-18.574, $^{207}Pb/^{204}Pb$ = 15.557-15.605, $^{208}Pb/^{204}Pb$ = 38.115-38.456; Tosdal and Munizaga, 1996, and in press) form a field that extends along the average crustal growth curve of Stacey and Kramers (1975) on the $^{208}Pb/^{204}Pb$ versus $^{206}Pb/^{204}Pb$ diagram, although data for sedimentary-hosted deposits plot slightly beneath the curve on the less radiogenic side (Fig. 6a). On the $^{207}Pb/^{204}Pb$ versus $^{206}Pb/^{204}Pb$ diagram the strata-bound, Pb isotopic compositions for strata-bound Cu-(Ag) deposits lie below the average crustal growth curve (Fig. 6b). The Pb isotopic compositions for strata-bound deposits overlap the limited Pb isotopic data available for Cretaceous sedimentary and igneous rocks (Fig. 6) consistent with Pb derivation from the Lower Cretaceous volcanic and sedimentary rocks that host the strata-bound Cu-(Ag) mineralisation. This suggests that the lead at these deposits was derived from the host crustal rocks.

Discussion

The origin of the strata-bound Cu-(Ag) deposits hosted by the Jurassic volcanics of Northern Chile has long been a matter of controversy. Stratiform orebodies were first regarded as syngenetic volcanic exhalative (Ruiz et al., 1965, 1971, Stoll, 1965). However, their epigenetic origin is now widely demonstrated, by the subsequent discovery of unconformable orebodies, the spatial relationship of copper mineralisation around Upper Jurassic intrusive stocks and sills, and significant hydrothermal alteration (albite, chlorite, quartz, sericite, calcite, sphene, scapolite, anatase) associated with copper-rich sulphide disseminations (chalcocite, bornite) within the volcanic host rocks (Palacios and Definis, 1981, 1981b, Dreyer and Soto, 1985, Orquera, 1987, Espinoza et al., 1996). The hydrothermal derivation of these volcanic-hosted copper deposits, related to subvolcanic intrusive bodies is the most accepted hypothesis (Espinoza, 1981, 1982, Chavez, 1985, Palacios, 1990, Espinoza et al., 1996), although hydrothermal derivation from batholiths has also been proposed by Vivallo and Henriquez (1998), while some authors have alternatively suggested a diagenetic-metamorphic origin (Sato, 1984, Sillitoe, 1990).

Although the overall geochronological data for the Jurassic strata-bound Cu-(Ag) deposits is rather poor, it indicates that hydrothermal copper and subordinate silver mineralisation was introduced within the volcanic sequence after its accumulation and at a time coincident with a regional plutonic event characterised by the emplacement of large batholithic masses within the previously deposited Jurassic volcanic pile. The spatial and possibly temporal relationship of the strata-bound deposits with stocks and dykes appears to be suggestive of a direct genetic connection of the Cu-(Ag) mineralisation with subvolcanic intrusive bodies and this view has been widely postulated by different authors (Espinoza, 1981, 1982, Chavez, 1985, Palacios, 1990, Wolf et al., 1990, Espinoza et al., 1996). However, most of the subvolcanic intrusions are barren or poorly mineralised, a fact that could be taken to indicate that the mentioned relationship is accidental rather than genetic. In fact, both the subvolcanic intrusive bodies and hydrothermal fluid flow that deposited copper sulphides may have followed similar paths along zones of structural weakness within the volcanic pile. Structural control is apparent for some strata-bound deposits, but also for adjacent minor intrusions (eg. the Buena Vista and Nucleo X deposits of the Michilla district, Trista, 2001).

The origin of the Lower Cretaceous strata-bound Cu-(Ag) deposits has also long been a matter of controversy. Models range from volcanogenic syngenetic (Ruiz and Peebles, 1988, Camus, 1980), through hypotheses that call for fluids liberated during crustal thinning and low-grade metamorphism of the volcanic and volcano-sedimentary piles (Sato, 1984, Westra, 1988, Sillitoe, 1990), or fluids derived from granitoid plutons (Holgrem, 1987). An epigenetic hydrothermal origin is substantiated by new data of the largest deposit of this type (Holgrem, 1987, Boric, 1997, Wilson and Zentilli, 1999). In addition, Wilson and Zentilli (1999) suggested that organic matter was an essential component in the formation of El Soldado and other Lower Cretaceous strata-bound deposit. They recognise two main stages in the evolution of the El Soldado copper deposit. The first occurred at low temperatures (<100°C) when petroleum was introduced into the Lower

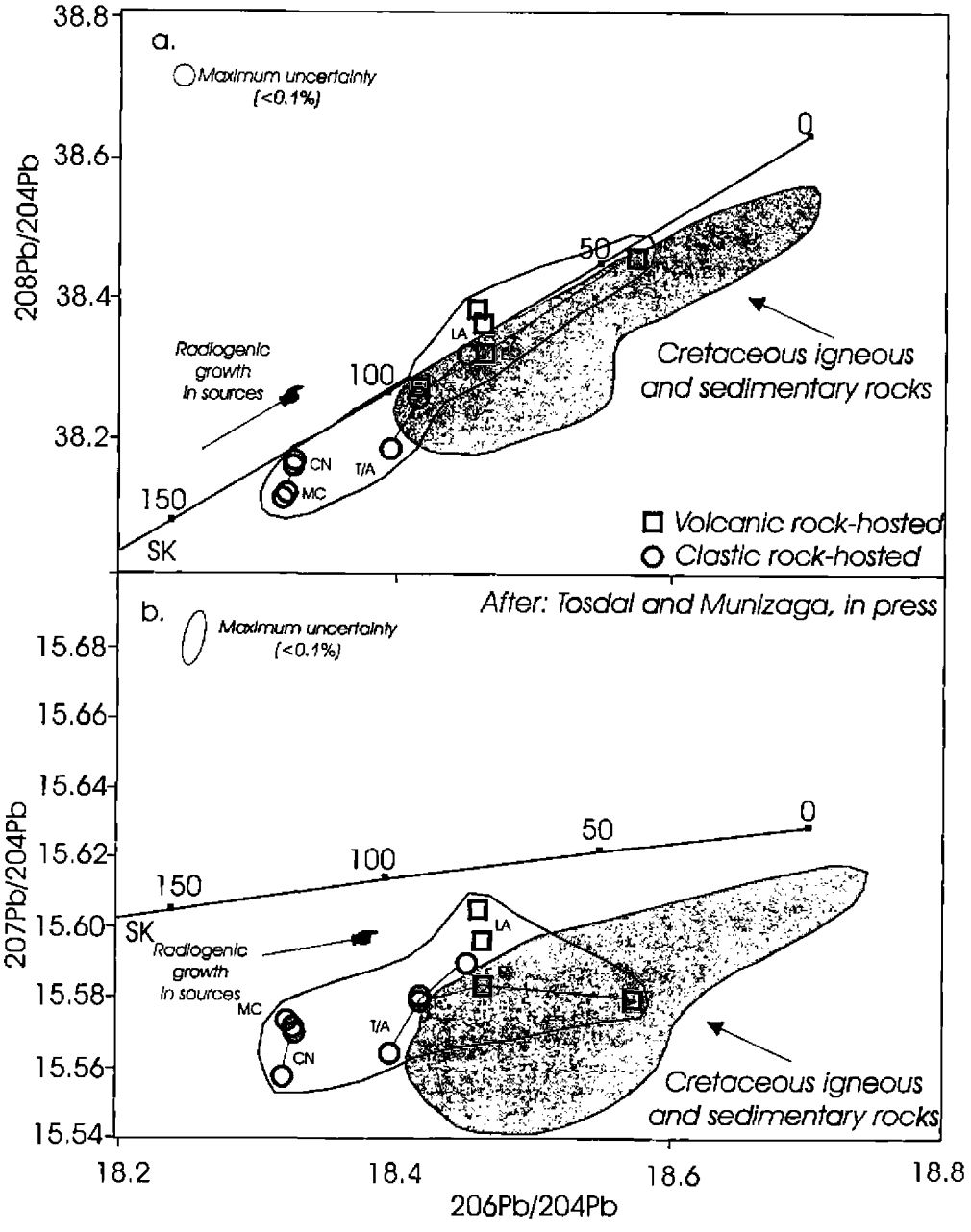


Figure 6: Lead isotopic evolution diagrams (extracted from Tosdal & Munizaga, 1996, in press)

(a) $^{208}Pb/^{204}Pb$ versus $^{206}Pb/^{204}Pb$ and (b) $^{207}Pb/^{204}Pb$ versus $^{206}Pb/^{204}Pb$ comparing sulphide Pb isotopic compositions of strata-bound Cu- (Ag) deposits with the field of major Cretaceous volcanic and plutonic rocks units and sandstone from the Talcuna-Corral Quemado basin. Tie lines link Pb isotopic composition for sulphide minerals from the same deposit. Time-integrated growth of Pb isotopic compositions of potential sources are, at the scale of the diagrams, subparallel to the average crustal growth curve, as indicated by the arrow. SK, average crustal growth curve of Stacey and Kramers (1975). Volcano-hosted Cu-(Ag) strata-bound deposit: ES, El Soldado; LA, Lo Aguirre. Volcano-sedimentary-hosted Cu- (Ag) strata-bound deposit: CN, Cerro Negro; MC, Mantos de Catemu; T/A, Talcuna and Arqueros.

Cretaceous rocks of the upper Lo Prado Formation and diagenetic (framboidal) pyrite formed during degradation of the petroleum, which later solidified as bitumen. The second stage was hydrothermal, with temperatures of 200° to >300°C when copper sulphides precipitated due to reduction of mineralising fluids by the organic matter in the host rocks and replacement of the pre-existing pyrite by copper sulphides; bitumen also acted as activated carbon, destabilising chloride complexes responsible for copper transport (Wilson and Zentilli, 1999). According to these authors the presence of bitumen within other strata-bound Cu-(Ag) deposits hosted by Lower Cretaceous strata (eg. Uchumi, Talcuna, Cerro Negro) suggests that degraded petroleum reservoirs were suitable sites for mineralisation by Cu-bearing solutions of different origins in north-central Chile. In fact the location of mineralised intervals within permeable clastic units that underlie impervious strata suggests that the sediment-hosted strata-bound deposits were formed by the invasion of hydrothermal fluids into older oil traps within particular stratigraphic levels

(eg. Zentilli et al., 1994; 1997). These levels probably represented zones of fluid over-pressure (above hydrostatic) within the Lower Cretaceous sequence. Furthermore, the regional occurrence of bitumen within Chilean Lower Cretaceous volcanic rocks associated with minor copper deposits has also been described in the Copiapó Region of northern Chile (Cisternas et al., 1999; Hermosilla et al., 2001).

The radiometric data and metallogenic setting of El Soldado strongly suggest that this deposit is a distal copper mineralisation genetically related to hydrothermal fluid flow triggered by batholith emplacement and is concurrent in age with Cu skarn formation within contact aureoles of the same intrusions. Mineralising fluids could have been a mixture of magmatic, connate, and meteoric waters thermally mobilised by the large Aptian - Albian igneous masses that were emplaced within the Lower Cretaceous sequence along sinistral transtensional faults.

The early occurrence of bitumen at El Soldado and other Lower Cretaceous strata-bound deposits, combined with the radiometric data available, imply that diagenetic processes released hydrocarbons from the intercalated Jurassic-Lower Cretaceous marine sediments. Petroleum was accumulated within lithologic-structural reservoirs within the stratigraphic sequence and transformed into bitumen due to the relatively high geothermal gradient within the extensional and subsiding arc developed over attenuated crust. Later hydrothermal fluids, probably mobilised by Aptian - Albian plutons emplaced within the Lower Cretaceous volcanic-sedimentary sequence, appear to have utilised similar flow paths to those followed by the early hydrocarbons, so that Cu-(Ag) were deposited by reduction reactions with the organic matter and/or replacement of pre-existing diagenetic pyrite. Although the occurrence of organic matter has not been described within the Jurassic volcanic-hosted strata-bound Cu-(Ag) deposits of northern Chile, they also appear to be distal copper precipitation genetically related to igneous masses that were emplaced within the thick volcanic pile during the Late Jurassic. Their origin was probably similar, but cooling or dilution of the hydrothermal solutions could have controlled metal precipitation.

If subduction was essentially continuous since the beginning of the Jurassic, why were the major strata-bound Cu-(Ag) deposits restricted to relatively brief periods of geologic history? Many of the largest deposits show structural control, and in most cases the structural permeability seems to have facilitated access to primary permeability within the host formations. One common denominator to several of these Cu-(Ag) deposits is the presence within the metallogenic provinces of large scale, orogen-parallel strike-slip faults (eg. Fig. 2). These faults accommodated a sinistral shear component produced by oblique subduction between the Aluk (Phoenix) and South American plates during the Early Cretaceous (Naranjo et al., 1984; Herve, 1987; Brown et al., 1993; Reijs and McClay, 1998), although $^{40}Ar/^{39}Ar$ and Rb-Sr data from ductile shear zones indicate that the strike-slip fault system had been active since the Jurassic (Scheuber at al., 1995). Transtensional and tensional regimes within these fault systems have controlled both basin development, and access to magmas for volcanism and plutons as postulated by Dallmeyer et al. (1996). In addition, they led to large-scale tilting and inversion of basins, and probably modified basinal hydraulic systems.

In a structural analysis of the El Soldado deposit, Chavez (1988) concluded that the mineralised system developed simultaneously with, and represents the effects of, a short-lived sinistral brittle shear system; a similar structural control is apparent in the richest ore shoots of the Cu-skarn deposits in the Cabildo district some 20 km farther north (personal observation). Considering that the K-feldspar present in veins at El Soldado is ca. 103 Ma (Wilson et al., submitted), it can be suggested that a sudden influx of hydrothermal fluids coincided with regional sinistral shear congruent with the Atacama Fault Zone further north (eg. Maksaev 1990). Mesozoic plate configuration reconstructions are hampered by to the lack of any oceanic crust older than around 50 Ma off-shore from South America (Müller et al, 1997). Therefore the only reconstructions of Mesozoic plate configurations in the Pacific realm are based on investigations of remnants of Jurassic and Cretaceous oceanic crust in the western Pacific (Larson and Pitman, 1972, Zonenshayn et al., 1984). These reconstructions indicate that a spreading centre existed off South America and during this time the Aluk (Phoenix) plate converged with the South American Plate at a very oblique angle. In contrast, during the Late Cretaceous, the convergence approached orthogonal. This change correlated with the rapid separation of Africa and South America, with the latter overriding the oceanic plate to the west (Ramos and Aleman, 2000). We contend that it is at this time that inversion of the Cretaceous Basin occurred. This interpretation is compatible with apatite fission track dates of ca. 90 Ma at El Soldado, and 82-95 Ma at the Caleu Pluton revealing rapid denudation during the Late Cretaceous (Parada and Larrondo, 1999, Gana and Zentilli, 2000).

Pop et al. (2000) concluded that in the Punta del Cobre-Candelaria district in the Copiapo region, Fe-oxide-Cu mineralisation occurred during a brief interval between 111 and 103 Ma. Structurally, this region represents a brittle sinistral shear system where the large Fe-oxide-Cu-Au Candelaria and other lesser deposits of this type occur. At Candelaria mineralisation and shearing deformation took place at ca. 111 Ma according to ^{40}Ar-^{39}Ar data (Ullrich and Clark, 1999; Arevalo et al., 2000). In addition, a sinistral transtensional fault subsidiary of the Atacama Fault Zone hosts the breccias with Fe-oxide-Cu-Au matrix at the Manto Verde deposit. Its mineralisation is thought to be genetically related to intrusives that have been dated by K-Ar at 117±3 and 121±3 Ma (Vila et al., 1996).

The Jurassic Cu-(Ag) stratabound deposits likewise appear to be formed within an overall sinistral transtensional regime, although Scheuber and Gonzalez (1999) established a distinct stage of strong arc-normal extension between 160-

150 Ma revealed by brittle low-angle normal faults, tilting of the Jurassic volcanics, some ductile normal faults and the intrusion of N-S elongated batholiths in the Coastal Cordillera of northern Chile. According to these authors NE-SW trending dykes intruded within the period between ~155-147 Ma indicate subsequent oblique dilation and a reversal in shear sense. At Mantos Blancos a 150 Ma Rb-Sr errorchron in altered rocks has been taken to represent the mineralisation age (Tassinari et al., 1993), whereas andesitic dykes of NE-SW orientation crosscut mineralised bodies and were dated by K-Ar at 147-149±13 Ma (Chavez, 1985). Albeit imprecise, these age data for the largest Jurassic Cu-(Ag) strata-bound deposit suggest that mineralisation took place during late stages of pluton emplacement preceding a possible short-lived shear sense reversal.

Other authors have alternatively proposed that the emplacement of Fe-P magmas (Kiruna-type) originated Lower Cretaceous magnetite-apatite bodies along the Coastal Cordillera of northern Chile, whereas Fe-oxide-Cu-Au and volcanic-hosted strata-bound Cu-(Ag) deposits were generated by different levels of emplacement and release of hydrothermal fluids from these primogenitor Fe-P magma intrusions (Vivallo and Henriquez, 1997, Gelcich, 1999). However, there is an inconclusive and classic debate over the origin of the Chilean magnetite-apatite deposits. Some authors (eg. Nyström and Henriquez, 1994, 1995) contend that many such deposits are derived by melt crystallisation, whereas others suggest that they are hydrothermal replacements (eg. Hitzman et al., 1992; Bookstrom, 1995) and possibly formed from fluids that had little or no interaction with magmas (Barton and Johnson, 1996, Rhodes and Oreskes, 1999). In fact, the balance of evidence seems to favour a metasomatic origin for most magnetite-apatite deposits, related to the contact zones of Lower Cretaceous diorite bodies (Menard, 1995, Bookstroom, 1977, 1995). On the other hand, while the association with intrusions is controversial, a metasomatic origin is also obvious for the Fe-oxide-Cu-Au deposits of the Coastal Cordillera of northern Chile, although these iron-rich deposits have undergone paragenetically late additions of copper sulphide and Au (eg. Sillitoe, 1996). The Lower Cretaceous volcanic-hosted strata-bound Cu-(Ag) deposits have an uncertain association with intrusions, but their distribution peripheral to granodioritic batholiths has been long known (eg. Carter, 1961).

The available geochronological data indicate that strata-bound Cu-(Ag) deposits, Cu-bearing skarns, magnetite-apatite bodies, and Fe-oxide-Cu-Au deposits were formed along the present Coastal Cordillera of northern Chile during the same metallogenic episode in the uppermost Early Cretaceous. This metallogenic epoch was concurrent with fault-controlled emplacement of large batholithic masses within the Lower Cretaceous volcano-sedimentary sequence. Therefore the volcanic-hosted strata-bound deposits are regarded here as distal Cu-(Ag) mineralisation formed by hydrothermal fluids mobilised during batholith emplacement at shallow crustal levels and cooling. The actual fluids could have been derived from magmatic, connate, and meteoric sources that may have contributed in different proportions, whereas copper precipitation may have taken place either by interaction with organic matter or early pyrite as documented for the Lower Cretaceous deposits or mainly by fluid cooling or mixing/dilution in the case of Upper Jurassic deposits. Despite the controversial origin of the Lower Cretaceous magnetite-apatite bodies, and Fe-oxide-Cu-Au deposits of the Chilean Coastal Cordillera these deposits are certainly proximal to coeval batholitic masses, whereas the volcanic or sedimentary-hosted, iron-poor Cu-(Ag) strata-bound deposits occur distal from coeval batholiths. The actual metal association in the different Lower Cretaceous deposits could not only be conditioned by the distance from plutons, but also may reflect the composition of the magmas involved and different degrees of hydrothermal fluid mixing.

Conclusions

Volcanic-hosted strata-bound deposits, known as "Chilean manto-type", are characteristic of a first period of Andean evolution during which subduction-related arc magmatism took place under an overall extensional tectonic setting. However, there were two distinct periods of strata-bound Cu-(Ag) mineralisation, in the Upper Jurassic and uppermost Early Cretaceous respectively, both of which were coincident with batholith emplacement within the Mesozoic volcanic pile, probably controlled by transtensional sinistral regional faults. The strata-bound Cu-(Ag) deposits are always peripheral to, but distal from, coeval batholiths.

The prevalent view that these Cu-(Ag) deposits have an inherent genetic relationship with hydrothermal fluid derivation from subvolcanic stocks and dykes is contended here as these minor intrusions are largely barren and this hypothesis does not fit well with Sr, Os, and Pb isotopic data that call for contribution of these elements from the country rocks. Instead the strata-bound Cu-(Ag) mineralisation is regarded here as the product of hydrothermal fluids of mixed origin that were mobilised during the emplacement and cooling of batholiths within the Mesozoic sequence and deposited copper either where they reacted with organic matter, pyrite, or cooled/mixed with meteoric fluids away from their heat sources. The spatial relationship with minor intrusions, dykes and sills could be accidental and related to the structural control of both subvolcanic intrusions and hydrothermal fluid circulation.

Although strata-bound Cu-(Ag) mineralisation took place during the same metallogenic event that formed the magnetite-apatite bodies, and Fe-oxide-Cu-Au deposits along the present Coastal Cordillera, the possible relationships with these other types of deposits are hampered by the inconclusive debate of the magma injection versus hydrothermal replacement models. However, the balance of evidence seems to favour a metasomatic origin of the iron-rich deposits and they are certainly more proximal to batholiths than the iron-poor Cu-(Ag) strata-bound deposits.

References

Aguirre, L., Féraud, G., Morata, D., Vergara, M. and Robinson, D., 1999. Time interval between volcanism and burial metamorphism and rate of basin subsidence in a Cretaceous Andean extensional setting. *Tectonophysics*, V. 313, No4, pp. 433-447.

Andriessen, P.A.M., 2000. Late Jurassic to Mid Cretaceous Unroofing and Neogene Topographic Evolution of the Coastal Cordillera, Northern Chile, Response to the Eastward Migration of the Andean Subduction Regime Assessed by FT Analyses. In: Noble, W.P., O'Sullivan, P.B. and Brown, R.W. 9th International Conference on Fission Track Dating and Thermochronology, Lorne, Australia, Geological Society of Australia Abstracts Series #58, p. 3-4.

Ardill, J., Flint, S., Chong, G., Wilke, H., 1998. Sequence Stratigraphy of the Mesozoic Domeyko Basin, northern Chile. *Journal of the Geological Society* 155, pp. 71-88.

Arévalo, C., Grocott, J., Pringle, M. and Martin, W., 2000. Edad 40Ar/39Ar de la mineralización en el yacimiento Candelaria, Región de Atacama. *Congreso Geológico Chileno, IX*, Puerto Varas, Chile, V. 2, pp. 92-98.

Astudillo, O., 1984. Geología y Metalogénesis del distrito minero Carolina de Michilla, Antofagasta, II Región, Chile. *Unpublished B.Sc. Thesis*, Departamento. de Geociencias, Universidad del Norte, Antofagasta, Chile, 131 p.

Barton, M.D. and Johnson, D.A., 1996. Evaporitic source model for igneous related Fe oxide-(REE-Cu-Au-U) mineralization. *Geology*, V. 24, p. 259-262.

Bogdanic, T., Standen, R. and Wilke, H., 1994. Nuevos antecedentes de sedimentitas calcáreas intercaladas en la Formación La Negra, a la latitud del Distrito Michilla, II Región de Antofagasta. *Congreso Geológico Chileno VII*, Concepción, V.1, p. 414-417.

Bookstrom, A.A., 1977. The magnetite deposits of El Romeral, Chile. *Economic Geology*, V. 64, pp. 1101-1130.

Bookstrom, A.A., 1995. Magmatic features of iron ores of the Kiruna-type in Chile and Sweden: Ore textures and magnetite geochemistry: a discussion. *Economic Geology*, V. 90, pp. 469-473.

Boric, R., 1997. Nuevos antecedentes sobre el modelo geológico del yacimiento de cobre El Soldado, Chile Central. *Congreso Geológico Chileno, VIII, Antofagasta, Chile*, V. II, p. 862-866.

Boric, R., 1985. Geología y yacimientos metálicos del Distrito Talcuna, Región de Coquimbo. *Revista Geológica de Chile*, N° 25-26, pp. 57-75.

Boric, R., Díaz, F. and Maksaev, V., 1990. Geología y yacimientos metalíferos de la Región de Antofagasta. Servicio Nacional de Geología y Minería, *Boletín* N° 40, Santiago, 246 p.

Boric, R. and Munizaga, F., 1994. Geocronología Ar-Ar y Rb-Sr del depósito estratoligado de cobre El Soldado (Chile Central). Universidad de Chile, *Comunicaciones*, V. 45, p. 135-148.

Brown, M., Díaz, F., and Grocott, J., 1993. Displacement history of the Atacama fault system 25°00'-27°00'S, northern Chile. *Geological Society of America Bulletin*, V. 105, pp. 1165-1174.

Camus, F., 1990. Geological characteristics of Strata-bound Deposits Associated with Lacustrine Sediments, Central Chile. In: Fontboté, et al. (editors) *Stratabound Ore Deposits in the Andes*. Berlin, Springer-Verlag, p. 449-462.

Camus, F., 1985. Los yacimientos estratoligados de Cu, Pb-Zn y Ag de Chile. In: Frutos, J., Oyarzún, R. and Pincheira, M. (editors) Geología y Recursos Minerales de Chile. Editorial de la Universidad de Concepción, Concepción, Chile, Tomo II, p. 547-635.

Camus, F., 1980. Distrito Punta del Cobre. Modelo de Interpretación. *Revista Geológica de Chile*, N°11, pp. 51-76.

Carter, W.D., 1961. Yacimientos de Cobre Tipo Manto, su distribución en franjas mineralizadas. Provincia de Aconcagua. *Boletín* N° 10, Instituto de Investigaciones Geológicas, Chile, 30 p.

Cisternas, M.E., Frutos, J., Spiro, B., and Galindo, E., 1999. Lavas con bitumen en el Cretácico Inferior de Copiapó, petroquímica e importancia metalogénica. *Revista Geológica de Chile*, V. 26, N° 2, pp. 205-226.

Charrier, R., 1979. El Triásico de Chile y regiones adyacentes de Argentina: una reconstrucción paleogeográfica y paleoclimática. *Comunicaciones*, Santiago, Chile, V. 26, pp.1-37.

Chavez, A., 1988. Relaciones entre fracturas, campos de esfuerzos y mineralización en el Yacimiento El Soldado, V Región. Unpublished B.Sc, Thesis, Departamento de Geología, Universidad de Chile, Santiago, 141 p.

Chavez, W., 1984. Alteration mineralogy and chemistry of rhyolitic and andesitic volcanic rocks of the Mantos Blancos copper-silver district, Chile:

Society of Mining Engineers of AIME. Pre-print, N° 84-153, 5 p.

Chavez, W., 1985. Geological setting and the nature and distribution of disseminated copper mineralization of the Mantos district, Antofagasta Province, Chile. *Unpublished Ph.D. Thesis*, California University, Berkeley, USA, 142 p.

Clark, A.H.. and Zentilli, M., 1972. The evolution of metallogenic province at a consuming plate margin: The Andes between latitudes 26° and 29° South (extended abstract): *Canadian Institute of Mining Metallurgy Bulletin*, V. 65, p. 37.

Clark, A.H., Caelles, J.C., Farrar, E., Haynes, S.J., Lortie, R.B., Mc.Bride, S.L., Quirt, G.S., Robertson, R.C.R. and Zentilli, M., 1976. Longitudinal variations in the metallogenic evolution of the Central Andes: a progress report. In: Strong, D.F. (editor) *Metallogeny and Plate Tectonics*. Geological Association of Canada, Special Paper N°14, pp. 23-58.

Coira, B., Davidson, J., Mpodozis, C. and Ramos, V., 1982. Tectonic and magmatic evolution of the Andes of northern Argentina and Chile. *Earth Science Reviews*, V. 18, pp. 303-332.

Collao, S., 1993. Inclusiones Fluidas en el Yacimiento Mantos Blancos. *Unpublished Report*, Departamento de Ciencias de la Tierra, Universidad de Concepción, Concepción, Chile, 27 p.

Dallmeyer, R.D., Brown, M., Grocott, J., Taylor, G.K. and Treolar, P.J., 1996. Mesozoic Magmatic and Tectonic Events within the Andean Plate Boundary Zone, 26°-27°30'S, North Chile: Constraints from 40Ar/39Ar Mineral Ages. *The Journal of Geology*, University of Chicago, V. 104, pp. 19-40.

Davidson, J. and Mpodozis, C., 1991. Regional Geologic Setting of Epithermal Gold Deposits, Chile. *Economic Geology*, V. 86, pp. 1174-1186.

Definis, A. 1985. Antecedentes geológicos del yacimiento de cobre Santo Domingo, Taltal y discusión acerca de su relación con un sistema de filones gabrodioríticos. *Congreso Geológico Chileno, IV, Antofagasta, Chile*, Vol. 2, p. 3-204 - 3-215.

Dewey, J.F. and Bird, F.M., 1970. Mountain belts and the new global tectonic. *Journal of Geophysical Research*, V. 75, pp. 2625-2647.

Dreyer, H. and Soto, H., 1985. Geología de Mina Susana, un yacimiento novedoso en Carolina de Michilla. *Congreso Geológico Chileno, IV, Antofagasta, Chile*, Vol. 2, p. 3-354 - 3-382.

Elgueta, S., Hodgkin, A., Rodriguez, E. and Schneider, A., 1990. The Cerro Negro Mine, Chile, Mineralization in a Volcanoclastic Environment. In: Fontboté. L., et al. (editors) *Stratabound Ore Deposits in the Andes*. Berlin, Springer-Verlag, pp. 463-472.

Espinoza, S., 1990. The Atacama-Coquimbo Ferriferous Belt, Northern Chile. . In: Fontboté, L., et al. (editors) *Strata-bound ore deposits in the Andes*: Berlin, Springer-Verlag, p. 353-364.

Espinoza, S., 1981. Esbozo metalogénico del distrito de Michilla, II Región, Chile. *Primer Coloquio sobre volcanismo y metalogénesis*, Departamento de. Geociencias, Universidad del Norte, Antofagasta, Chile, p. 71-81.

Espinoza, S., 1982. Definición del tipo diseminado infravolcánico de súlfuros de cobre. *Congreso Geológico Chileno, III, Concepción*, Chile, Vol. 3, p. E201-E219.

Espinoza, S., Véliz, H., Esquivel, J., Arias, J., y Moraga, A., 1996. The Cupriferous Province of the Coastal Range, Northern Chile. In: Camus, F., Sillitoe, R.H., and Petersen, R. (editors) *Andean Copper Deposits: New Discoveries, Mineralization, Styles and Metallogeny*. Society of Economic Geologists, Special Publication Number 5, pp. 19-32.

Ferraris, F. and Di Biase, F., 1978. Hoja Antofagasta, Región de Antofagasta, Carta Geológica de Chile, N°30, Instituto de Investigaciones Geológicas, Santiago, Chile, 48 p.

Ferraris, F., Rojas, N., Ortiz, F., et al., 1973. Geología y yacimientos metalíferos de la región de la mina Julia, distrito minero de Paposo, Provincia de Antofagasta, (*Unpublished Report*), Instituto de Investigaciones Geológicas, SERNAGEOMIN Archive, Santiago, Chile, 106 p.

Fuentes, F., Féraud, G., Aguirre, L. and Morata, D., 2001. Convergent strategy to date metamorphic minerals in sub-greenschist facies metabasites by the 40Ar/39Ar method. *III South American Symposium on Isotope Geology, Extended Abstract Volume* (CD), Sociedad Geológica de Chile, Santiago, pp. 34-36.

Gana, P. and Zentilli, M., 2000. Historia termal y exhumación de intrusivos de la Cordillera de la Costa de Chile Central. *Congreso Geológico Chileno IX*, Puerto Varas, Chile, V. 2, p. 664-668.

Gelcich, 1999. Fe and Cu±Fe Mineralization in the Coastal Cordillera of Chañaral, Northern Chile. (extended abstract) *Proceedings of the Fourth ISAG*, October 4-6, 1999, Goettingen, Germany, p. 261-265.

González, G., 1999. Mecanismo y profundidad de emplazamiento del Plutón de Cerro Cristales, Cordillera de la Costa, Antofagasta, Chile. *Revista Geológica de Chile*, Vol. 26, N° 1, pp. 43-66.

Gröschke, M., Von Hillebrandt, A., Prinz, P., Quinzio, L.A., and Wilke, H.-G., 1988. Marine Mesozoic Paleogeography in Northern Chile between 21° and 26°S. In: Bahlburg, H., Breitkreutz, C., and Giese, P., (editors) *The Southern Central Andes. Lecture Notes in Earth Sciences*, 17, p. 105-117.

Hermosilla, J.M., Cisternas, M.E., and Spiro, B., 2001. C and S Isotope characteristics of bitumen, calcite, Fe and Cu sulfides in the metallogenic analysis of the Ocoita Metallotect. *III South American Symposium on Isotope Geology, Extended Abstract Volume (CD)*, Sociedad Geológica de Chile, Santiago, pp. 476-479.

Herve, M., 1987. Movimiento sinistral en el Cretácico Inferior de la Zona de Falla Atacama al norte de Paposo (24°S), Chile. *Revista Geológica de Chile*, N° 31, pp. 37-42.

Hirtzman, M.W., Oreskes, N., and Einaudi, M.T., 1992. Geological characteristics and tectonic setting of Proterozoic iron oxide (Cu-U-Au-REE) deposits. *Precambrian Research*, V. 58, p. 241-287.

Holgrem, C., 1987. Antecedentes para un modelo genético del yacimiento El Soldado, V Región de Valparaíso, Chile. *Revista Geológica de Chile*, N° 30, pp. 3-18.

James, D.E., 1971. Plate tectonic model for the evolution of the central Andes: *Geological Society of America Bulletin*, V. 82, pp. 3325-3346.

Jurgeit, M. and Fontboté, L., 1990. The Stratabound Tuff-Hosted Elisa de Bordos Silver-Mercury Deposit, Northern Chile. In: Fontboté. L., et al. (editors), *Stratabound Ore Deposits in the Andes*. Berlin, Springer-Verlag, p. 647-658.

Klohn, E., Holgrem, C., and Ruge, H., 1990. El Soldado, a strata-bound copper deposit associated with alkaline volcanism in the central Chilean Coastal Range. In: Fontboté, L., et al. (editors) *Strata-bound ore deposits in the Andes*: Berlin, Springer-Verlag, p. 435-448.

Ladino, M., Tomlinson, A., and Blanco, N., 1999. New constrains for the age of Cretaceous compressional deformation in the Andes of northern Chile (Sierra de Moreno, 21°-22°10'S). (Extended Abstract), *Proceedings of the Fourth ISAG*, Goettingen, Germany, p.407-410.

Larson, R.L. and Pitman, W.C., 1972. World-wide correlation of Mesozoic magnetic anomalies and its implications. *Geological Society of America Bulletin*, V. 83, pp. 3645-3662.

Levi, B., Aguirre, L., Nyström, J.O., Padilla, H. And Vergara, M., 1989. Low-grade regional metamorphism in the Mesozoic-Cenozoic volcanic sequences of the Central Andes. *Journal of Metamorphic Geology*, V. 7, p. 487-495.

Lortie, R.B. and Clark, A.H., 1987. Strata-bound cupriferous sulfide mineralization associated with continental rhyolitic volcanic rocks, Northern Chile: I. The Jardin copper-silver deposit. *Economic Geology*, V. 82, pp. 546-570.

Losert, J., 1973. Genesis of copper mineralization and associated alterations in the Jurassic volcanics rocks of Buena Esperanza mining area. *Publicación* N°40, Departamento de Geología, Universidad de Chile, Santiago, 104 p.

Losert, J., 1974. Alteration and associated copper mineralization in the Jurassic volcanic rocks of Buena Esperanza mining area (Antofagasta Province, Northern Chile). In Klohn E. (editor), *Coloquio sobre fenómenos de alteración y metamorfismo en rocas volcánicas e intrusivas*, p. 51-85.

Maksaev, V., 1990. Metallogeny, geological evolution, and thermochronology of the Chilean Andes between latitudes 21° and 26° South, and the origin of major porphyry copper deposits. *Unpublished Ph.D. Thesis*, Dalhousie University, Halifax, Nova Scotia, Canada, 554 p.

Maksaev, V., 2000. Significado tectónico y metalogénico de datos de trazas de fisón en apatitas de plutones de la Cordillera de la Costa de la Región de Antofasta. Congreso Geológico Chileno IX, Puerto Varas, Chile, p. 129-134.

Maksaev, V. and Zentilli, M., 1999. Fission Track Thermochronology of the Domeyko Cordillera, Chile: Metallogenetic Implications for Andean Porphyry Copper Metallogenesis. *Exploration and Mining Geology*, Special Issue on Latin American Mineral Deposits, Vol. 8, Nos. 1 & 2, pp. 65-89.

Marinovic, N., Smoje, I., Maksaev, V., Hervé, M., Mpodozis, C., 1995. Hoja Aguas Blancas, Región de Antofagasta. Servicio Nacional de Geología y Minería, *Carta Geológica de Chile* N° 70, 150 p.

Marschik, R., Leveille, R.A. and Martin, W., 2000. La Candelaria and the Punta del Cobre District: Early Cretaceous Iron-Oxide Cu-Au (-Zn-Ag) Mineralization. In: Porter, T.M. (editor), Hydrothermal Iron Oxide Copper-Gold & Related Deposits: A Global Perspective, Volume 1, Australian Mineral Fundation, Adelaide, 350 p.

Martin, W.R., 1981. Distribución de la mineralización en el yacimiento cuprífero El Soldado, V Región. *Unpublished B.Sc. Thesis*, Departamento de Geología, Universidad de Chile. 92 p.

Mayer, C.K. and Fontboté, L., 1990. The Stratiform Ag-Cu Deposit El Jardin, Northern Chile. In: Fontboté. L., et al. (editors), *Stratabound Ore Deposits in the Andes*. Berlin, Springer-Verlag, p. 637-646.

Megard, F., 1987. Cordilleran Andes and Marginal Andes: a review of Andean geology north of the Arica elbow (18°S). In: Monger, J.W.H. and Francheteau, J. (editors), *Circum-Pacific orogenic belts and evolution of the Pacific Ocean basin.* American Geophysical Union - Geological Society of America, *Geodynamic Series*, V. 18, pp. 71-95.

Menard, J.J., 1995. Relationship between altered pyroxene diorite and the magnetite mineralization in the Chilean Iron Belt, with emphasis on the El Algarrobo iron deposits (Atacama Region, Chile). *Mineralium Deposita*, V. 30, p. 268-274.

Minería Chilena, 2001. Mantos de la Luna. *Minería Chilena* N° 245, November 2001, Santiago, Chile, p. 37.

Morata, D., Aguirre, L., Féraud, G., Fuentes, F., Parada, M.A. and Vergara, M., 2001. The Lower Cretaceous volcanism in the Coastal Range of Central Chile: Geochronology and Isotopic Geochemistry. *III South American Symposium on Isotope Geology, Extended Abstract Volume* (CD), Sociedad Geológica de Chile, Santiago, pp. 321-324.

Moreno, A., 2001. Geología del yacimiento 21 de Mayo, Talcuna, Cuarta Región. *Unpublished B.Sc. Thesis*, Departamento de Geología, Universidad de Chile, Satiago, 81 p.

Moya, V., 1980. Zonación mineralógica y química yacimiento de cobre tipo skarn mina Sauce, Cabildo, V Región. *Unpublished B.Sc. Thesis*, Departamento de Geología, Universidad de Chile, Santiago, 123 p.

Mpodozis, C. and Cornejo, P., 1997. El rift Triásico-Sinemuriano de Sierra Exploradora, Cordillera de Domeyko /25°-26°S): Asociaciones de facies y reconstrucción tectónica. *Congreso Geológico Chileno, VIII, Antofagasta*, Chile, V.1, pp. 550-554.

Mpodozis, C., and Ramos, V., 1990. The Andes of Chile and Argentina. In: Ericksen, G.E., Cañas, M.T., and Reinemund, J.A. (editors), *Geology of the Andes and its relation to hydrocarbon and mineral resources*, Circum-Pacific Council for Energy and Mineral Resources, *Earth Science Series*, V. 11, pp. 59-90.

Müller, R.D., Roest, W.R., Royer, J.-Y., Gahagan, L.M. and Sclater, J.G., 1997. Digital isochrons of the world's ocean floor. *Journal of Geophysical Research*, V. 102, pp. 3211-3214.

Munizaga, F., Mathur, R. and Ruiz, J., 2000. Geoquímica isotópica Re-Os en yacimientos de Cu en Chile, una respuesta diferente de pórfidos y mantos. *Congreso Geológico Chileno* IX, Puerto Varas, Chile, V. 1, p. 303-305.

Munizaga, F., Zentilli, M., Tassinari, C., Boric, R., Ramirez, R. and Reynolds, P.H., 1995. Geochronological and isotopic signatures of Mesozoic Stratabound "manto-type" copper deposits of Chile. (abstract) 1995 GSA Annual Meeting, New Orleans, *Geological Society of America, Abstract with Programs*, 27: 6: A-410..

Munizaga, F., Reyes, J.C. and Nyström, J.O., 1994. Razones isotópicas de S de los sulfuros del distrito minero de Cerro Negro: un posible indicador de los depósitos estratoligados de Cu hospedados en rocas sedimentarias lacustres. *Revista Geológica Chilena*, V. 21, N° 2, p. 189-195.

Munizaga, F., Holgrem, C., Huete, C. and Kawashita, K., 1988. Geocronología de los yacimientos de cobre El Soldado y Lo Aguirre, Chile Central. *Congreso Geológico Chileno V, Santiago*, Chile, V. 3, pp. G177-G193.

Naranjo, J.A. and Puig, A., 1984. Hojas Taltal y Chañaral, Regiones de Antofagasta y Atacama. Carta Geológica de Chile, Escala 1:250.000, SERNAGEOMIN, Santiago, Chile, N° 62-63, 140 p.

Naranjo, J.A., Herve, F., Prieto, X. And Munizaga, F., 1984. Actividad Cretácica de la Falla Atacama al este de Chañaral: Milonitización y Plutonismo. Departamento de Geología, Universidad de Chile, *Comunicaciones*, N° 34, p. 57-66.

Nisterenko, G.V., Losert, J., Chavez, L. and Naumov, V.B., 1973. Temperaturas y presiones de formación de algunos yacimientos cupríferos de Chile. *Revista Geológica de Chile*, N°1, pp. 74-84.

Nyström, J.O., and Henríquez, F., 1994. Magmatic features of iron ores of the Kiruna type in Chile and Sweden: Ore textures and magnetite geochemistry. *Economic Geology*, V. 89, p. 820-839.

Nyström, J.O., and Henríquez, F., 1995. Magmatic features of iron ores of the Kiruna type in Chile and Sweden: Ore textures and magnetite geochemistry – A Reply. *Economic Geology*, V. 90, p. 473-457.

Orquera, W., 1987. Geología y geoquímica de alteración en el "Area de Superficie" de la mina de cobre Buena Esperanza, Chile. *Unpublished B.Sc. thesis*, Depto. Geociencias, Universidad del Norte, Antofagasta, 221p.

Oyarzun, R., Ortega, L., Sierra, J., Lunar, R. and Oyarzun, J., 1998. Cu, Mn, and Ag mineralization in the Quebrada Marquesa Quadrangle, Chile: the Talcuna and Arqueros districts. *Mineralium Deposita*, V. 33, p. 547-559.

Palacios, C., 1990. Geology of the Buena Esperanza Copper-Silver Deposit, Northern Chile. In: Fontboté. L., et al. (editors), *Stratabound Ore Deposits in the Andes*. Berlin, Springer-Verlag, p. 313-318.

Palacios, C., 1986. Subvolcanic Copper deposits in the Coastal Range of Northern Chile. *Zentralblatt für Geologie und Paläontologie*, Teil I, 1985, H.9/10, Stuttgart, Juni 1986, pp. 1605-1615.

Palacios, C., Hein, U.F. and Dulski, P., 1986. Behaviour of rare earth elements during hydrothermal alteration at the Buena Esperanza copper-silver deposit, northern Chile. Earth and Planetary Science Letters, V. 80, p. 208-216.

Palacios, C. and Definis, A., 1981. Petrología del yacimiento Buena Esperanza, II Región, Norte de Chile. *Primer Coloquio sobre volcanismo y metalogénesis, Departamento de Geociencias*, Universidad del Norte, Antofagasta, Chile, p. 48-67.

Palacios, C. and Definis A., 1981b. Geología del yacimiento estratiforme Susana, distrito Michilla, Antofagasta. *Primer Coloquio sobre volcanismo y metalogénesis, Departamento de Geociencias*, Universidad del Norte, Antofagasta, Chile, p. 82-91.

Parada, M.A., Féraud, G., Aguirre, L., Fuentes, F., Morata, D., Vergara, M., Larrondo, P. and Palacios, C., 2001. U-Pb, 40Ar-39Ar and fission-track geochronology of the Early Cretaceous Caleu pluton and its volcanic envelope, Coastal Range of central Chile: tectonic and metamorphic implications. *III South American Symposium on Isotope Geology, Extended Abstract Volume (CD)*, Sociedad Geológica de Chile, Santiago, pp. 612-615.

Parada, M.A. and Larrondo, P., 1999. Thermochronology of the Lower Cretaceous Caleu Pluton in the Coast range of Central Chile: Tectono-stratigraphic implications. *Fourth ISAG, Goettingen (Germany)*, pp. 563- 566.

Pichowiak, S., Buchelt, M., and Damm, K.W., 1990. Magmatic activity and tectonic setting of early stages of Andean cycle in northern Chile. *Geological Society of America Special Paper* 241, pp. 127-144.

Pizarro, J., 1997. Estudio geológico de la unidad dacita cuarcifera del yacimiento Mantos Blancos, Antofagasta-Chile. *Unpublished B.Sc. Thesis*, Departamento de Geología, Universidad de Chile, Santiago, 87 p.

Pop, N., Heaman, L., Edelsein, O., Isache, C., Zentilli, M., Pecskay, Z., Valdman, S., Rusu, C., 2000. Geocronología de las rocas ígneas y los productos de alteración hidrotermal relacionadas a la mineralización de Cu-Fe (Au) del sector Adriana - Carola - Cobriza (parte este del Distrito Punta del Cobre - Candelaria) en base a dataciones U-Pb (en circón), $^{40}Ar/^{39}Ar$ y K-Ar. Congreso Geológico Chileno IX, Puerto Varas, Chile, V. 2, p. 155-160.

Ramos, V. and Aleman, A., 2000. Tectonic evolution of the Andes. In: Cordani, U.G. et al. (editors), *Tectonic Evolution of South America*, Rio de Janeiro, Brazil, pp. 635-685.

Reijs, J., and McClay, K., 1998. Salar Grande pull-apart basin, Atacama Fault System, northern Chile. In: Holdsworth, R.E.; Strachan, R.A. and Dewey, J.F. (editors). *Continental Transpressional and Transtensional Tectonics. Geological Society of London, Special Publications*, 135, pp. 127-141.

Reutter, K-J., and Scheuber, E., 1988. Relation between tectonics and magmatism in the Andes of Northern Chile and adjacent areas between 21° and 25°S. *Congreso Geológico Chileno, V*, Santiago, Chile, Vol. III, p. 1345-1363.

Rhodes, A.L. and Oreskes, N., 1999. Oxygen Isotope Composition of Magnetite Deposits of El Laco, Chile: Evidence of Formation from Isotopically Heavy Fluids. In: Skinner, B.J. (editor), *Geology and Ore Deposits of the Central Andes, SEG Special Publication Number 7*, p. 333-351.

Rivano, S. And Sepulveda, P., 1991. Hoja Illapel, Región de Coquimbo. *Carta Geológica de Chile*, Servicio nacional de Geología y Minería, N° 69, 132 p.

Rivano, S., Sepúlveda, P., Boric, R., and Espiñeira, D., 1993. Hojas Quillota y Portillo. Servicio Nacional de Geología y Minería, *Carta Geológica de Chile* N° 73, only geological map published.

Rogers, G. and Hawkesworth, C.J., 1989. A geochemical traverse across the North Chilean Andes: evidence for crust generation from the mantle wedge. Earth and Planetary Science Letters, V. 91, pp. 271-285.

Ruge, H., 1985. Geología y mineralización del yacimiento de cobre El Soldado, V Región, Chile. *Congreso Geológico Chileno, IV, Antofagasta, Chile*, Vol. IV, p. 3-854-3-872.

Ruiz, C., Aguirre, L., Corvalan, J., Klohn, C., Klohn, E., and Levi, B., 1965. Geología y yacimientos metalíferos de Chile. *Instituto de Investigaciones Geológicas, Santiago, Chile*, 302 p.

Ruiz, C., Aguilar, A., Egert, E., Espinosa, W., Peebles, F., Quezada, R. and Serrano, M., 1971. Strata-bound copper sulphide deposits of Chile. In: *Proceedings IMA-IAGOD, 7th General Meeting*, Tokyo-Kyoto, Japan, 1970. Soc. Min. Geol. Japan, *Special Issue* 3, pp. 252-260.

Ruiz, C. and Peebles, F., 1988. Geología, distribución y génesis de los yacimientos metalíferos chilenos. Editorial Universitaria, Santiago, Chile, 305 p.

Sato, T., 1984. Manto type copper deposits in Chile: a review. *Bulletin of the Geological Survey of Japan*. V. 35, pp. 565-582.

Scheuber, E. and Gonzalez, G., 1999. Tectonics of the Jurassic - Early Cretaceous magmatic arc of the north Chilean Coastal Cordillera (22°-26°S): A story of crustal deformation along a convergent plate boundary. *Tectonics*, V. 18, N° 5, pp. 895-910.

Scheuber, E. and Andriessen, P.A.M., 1990. The kinematic and geodynamic significance of the Atacama fault zone, northern Chile. *Journal of Structural Geology*, V. 12, No 2, pp. 243-257.

Scheuber, E.; Hammerschmidt, K.; and Friedrichsen, H., 1995. $^{40}Ar/^{39}Ar$ and Rb-Sr analyses from ductile shear zones form the Atacama fault Zone, northern Chile: The age of deformation. *Tectonophysics*, V. 250, pp. 61-87.

Sillitoe, R.H., 1972. Relation of metal provinces in Western America to subduction of oceanic lithosphere. *Geological Society of America Bulletin*, V. 83, pp. 813-818.

Sillitoe, R., 1974. Tectonic segmentation of the Andes: Implications for magmatism and metallogeny: *Nature*, V. 250, pp. 542-545.

Sillitoe, R.H., 1976. Andean mineralization a model for the metallogeny of convergent plate margins. In: Strong, D.F. (editor), *Metallogeny and plate tectonics, Geological Association of Canada, Special Paper*, N°14, pp. 59-100.

Sillitoe, R.H., 1990. Copper Deposits and Andean Evolution. In: Ericksen, G.E., Cañas, M.T., and Reinemund, J.A. (editors), *Geology of the Andes and its relation to hydrocarbon and mineral resources*, Circum-Pacific Council for Energy and Mineral Resources, *Earth Science Series*, V. 11, pp. 285-311.

Sillitoe, R.H., 1996. Granites and metal deposits. *Episodes*, V. 19, pp. 126-133.

Stacey, J.S. and Kramers, J.D., 1975. Approximation of terrestrial lead isotopes evolution by a two-stage model. Earth and Planetary Science Letters, V. 26, p. 207-221.

Stoll, W.C., 1965. Metallogenic provinces of South America. *Mining Magazine*, V. 112, pp. 22-33, and 90-99.

Suarez, M. and Bell, C.M., 1993. Triassic rift-related sedimentary basins in northern Chile (24°-29°S). *Journal of South American Earth Sciences*, V. 6, N°3, pp.109-121.

Tassinari, C., Munizaga, F. y Ramírez, R., 1993. Edad y geoquímica isotópica Rb-Sr del yacimiento de cobre Mantos Blancos: relación temporal con el magmatismo Jurásico. *Revista Geológica de Chile*, V. 20, N° 2, pp. 193-206.

Tidy, E., 1970. Geología del distrito minero La Campana, provincia de Valparaiso. *Unpublished B.Sc. Thesis*, Departamento de Geología, Universidad de Chile, Santiago, 286 p.

Tosdal, R.M. and Munizaga, F., 1996. Age and geographical variations in sulfide Pb isotopic compositions of Mesozoic and Cenozoic Andean Ore Deposits between La Serena and Santiago, Chile (30°-34°S). *XXXIX Congresso Brasileiro de Geologia*, Geologia e Sociedade, Anais, Vol. 7, Bahia, Brazil, P. 332-336.

Tosdal. R.M. and Munizaga, F., in press. Changing Pb sources in Mesozoic and Cenozoic Andean ore deposits, North-Central Chile (30°-34°S). *Mineralium Deposita* (in press).

Tosdal, R.M. and Richards, J.P., 2001. Magmatic and Structural Controls on the Development of Porphyry Cu ± Mo ± Au Deposits. Society of Economic Geologists, *Reviews in Economic Geology*, V. 14, p. 157-181.

Tomlinson, A.J., Martin, M.W., Blanco, N., and Pérez de Arce, C., 2001. U-Pb and K-Ar Geochronology from the Cerro Empexa Formation, 1st and 2nd Regions, Precordillera, Northern Chile. *III South American Symposium on Isotope Geology, Extended Abstract Volume (CD)*, Sociedad Geológica de Chile, Santiago, pp. 632-635.

Trista, D., 2001. Mineralización y microtermometría de inclusiones fluidas de yacimientos cupríferos de la Cordillera de la Costa, entre los 22°04' - 22°44' latitud Sur. II Región de Antofagasta, Chile. *Unpublished B.Sc. Thesis*, Departamento de Ciencias Geológicas, Universidad Católica del Norte, Antofagasta, Chile, 127 p.

Ullrich, T.D. and Clark, A.H., 1999. The Candelaria copper-gold deposit, Region III, Chile: Paragenesis, geochronology and fluid composition. In: Stanley, C.J. et al. (editors), *Mineral Deposits: Processes to Processing*, Balkema, Rotterdam, pp. 201-114.

Venegas, R., Munizaga, F., Tassinari, C., 1991. Los yacimientos de Cu-Ag del Distrito de Carolina de Michilla, Región de Antofagasta, Chile: nuevos antecedentes geocronológicos. *Congreso Geológico Chileno, VI, Viña del Mar, Chile*, Vol. 1, p. 452-455.

Vergara, M., Levi, B., Nyström, J.O. and Cancino, A., 1995. Jurassic and Early Cretaceous island arc volcanism, extension, and subsidence in the Coast Range of central Chile. *Geological Society of America Bulletin*, V. 107, no. 12, p. 1427-1440.

Vila, T., Lindsay, N. and Zamora, R., 1996. Geology of the Manto Verde Copper Deposit, Northern Chile: A Specularite-Rich, Hydrothermal-Tectonic Breccia Related to the Atacama Fault Zone. In: Camus, F. et al. (editors), *Andean copper deposits:*

new discoveries, mineralization styles and metallogeny, Society of Economic Geologists Special Publication N° 5, pp. 157-170.

Vivallo, W. and Henriquez, F., 1997. Relación genética entre los yacimientos estratoligados de Cu ("tipo manto"), de Cu-Fe±Au y de hierro del tipo Kiruna. *Congreso Geológico Chileno, VIII, Antofagasta, Chile*, p. 1189-1193.

Vivallo, W. and Henriquez, F., 1998. Génesis común de los depósitos estratoligados y vetiformes de cobre del Jurásico Medio a Superior en la Cordillera de la Costa, Región de Antofagasta, Chile. *Revista Geológica de Chile*, V. 25, N° 2, pp. 199-228.

Westra, G., 1988. La importancia del metamorfismo de carga en la formación de yacimientos de cobre tipo manto: Keynote Address, *Congreso Geológico Chileno, V*, Santiago, Chile, August 8-12, 1988, Preprint 18 p.

Wilson, J. and Grocott, J., 1999. The emplacement of the granitic Las Tazas complex, northern Chile: the relationship between local and regional strain. *Journal of Structural Geology*, V. 21, pp. 1513-1523.

Wilson, N.S.F., Zentilli, M., Reynolds, P.H. and Boric, R. (submitted). $^{40}Ar/^{39}Ar$ Geochronology of K-feldspar (Adularia) from the El Soldado Manto-Type Copper Deposit, Chile. Submitted to *Chemical Geology*.

Wilson, N.S.F. and Zentilli, M., 1999. The Role of Organic Matter in the Genesis of the El Soldado Volcanic-Hosted Manto-Type Cu Deposit, Chile. *Economic Geology*, V. 94, pp. 1115-1136.

Wolf, F.B., Fontboté, L. and Amstutz, G.C., 1990. The Susana Copper (-Silver) deposit in Northern Chile, Hydrothermal mineralization Associated with a Jurassic Volcanic Arc. In: Fontboté. L., et al., editors, *Stratabound Ore Deposits in the Andes*. Berlin, Springer-Verlag, pp. 319-318.

Zamora, R. and Castillo, B., 2001. Mineralización de Fe-Cu-Au en el Distrito Mantoverde, Cordillera de la Costa, III Región de Atacama, Chile. In: *II Congreso Internacional de Prospectores y Exploradores*, ProEXPLO 2001 Compact Disk, 24-27 Abril, 2001, Lima, Peru, , 13 p.

Zeil, W., 1979. The Andes, A geological Review. Gebrüder Borntraeger, Berlin, Stuttgart, Germany, 260 p.

Zentilli, M., Boric, R., Munizaga, F. and Graves, M.C., 1994. Petroleum involvement in the genesis of some strata-bound copper deposits of Chile. *Congreso Geológico Chileno VII*, Concepción, Chile, V. II, p. 1542-1546.

Zentilli, M., Munizaga, F., Graves, M.C., Boric, R., Wilson, N.S.F., Mukhopadhyay, P.K., and Snowdon, L.R., 1997. Hydrocarbon Involvement in the genesis of Ore Deposits: An Example in Cretaceous Stratabound (Manto-Type) Copper Deposits of Central Chile, *International Geology Review*, V. 39, p.1-21.

Zonenshayn, L.P., Savostin, L.A. and Sedov, A.P., 1984. Global Paleogeodynamic reconstructions for the last 160 million years. *Geotectonics*, V. 18, N° 3, pp. 181-195.

PGC PUBLISHING

Naslund, H.R., Henríquez, F., Nyström, J.O., Vivallo, W. & Dobbs, F.M., 2002 - Magmatic Iron Ores and Associated Mineralisation: Examples from the Chilean High Andes and Coastal Cordillera; *in Porter, T.M. (Ed.), Hydrothermal Iron Oxide Copper-Gold & Related Deposits: A Global Perspective*, Volume 2; PGC Publishing, Adelaide, pp 207-226.

MAGMATIC IRON ORES AND ASSOCIATED MINERALISATION: EXAMPLES FROM THE CHILEAN HIGH ANDES AND COASTAL CORDILLERA

[1]H. Richard Naslund, [2]Fernando Henríquez, [3]Jan Olov Nyström, [4]Waldo Vivallo, and [2]F. Michael Dobbs

[1]*Department of Geological Sciences, SUNY, Binghamton, NY, USA*
[2]*Departamento de Ingeniería en Minas, Universidad de Santiago, Santiago, Chile*
[3]*Swedish Museum of Natural History, Stockholm, Sweden*
[4]*Servicio Nacional de Geología y Minería, Santiago, Chile*

Abstract - The El Laco magnetite-apatite ore deposits in the Andean Cordillera of northern Chile occur as massive, tabular bodies, as stratified, pyroclastic ores, and as crosscutting dykes and vein complexes. The ore deposits and surrounding volcanic rocks, mainly andesites, are Plio-Pleistocene in age and preserve many of their original volcanic textures and structures. All the field and laboratory data are consistent with an origin by eruption and shallow intrusion of a high-temperature, volatile-rich, iron-oxide magma. A number of other iron-oxide-apatite deposits of Cenozoic age in the Andean Cordillera, and a belt of Cretaceous iron deposits in the Coastal Cordillera of Chile also have features that suggest a magmatic origin. Associated with these magmatic ore deposits are economic and sub-economic concentrations of Cu, Au, U, and REE.

Introduction

The discovery of the enormous Cu-Au-U-REE hematite breccias at Olympic Dam in Australia (Roberts and Hudson, 1983; Oreskes and Einaudi, 1990, 1992; Haynes et al., 1995) has made iron-oxide-apatite deposits of considerable economic interest for commodities other than iron. Indeed, many deposits are associated with nearby Cu, Au, U, or REE mineralisation (Bai and Yuan, 1983; Crocker, 1985; Einaudi and Oreskes, 1990; Hauck, 1990; Kisvarsanyi, 1990; Marikos et al., 1990; Vivallo et al., 1993a, 1994a, 1995a, 1995b; Espinoza et al., 1994; Förster and Jafarzadeh, 1994; Rojas and Henríquez, 1994; Foose and McLelland, 1995; Porter, 2000). Although iron-oxide-apatite deposits share many common features, it is clear that they did not all form by the same process or processes. Many deposits show evidence of formation in evolving magmatic systems: some deposits present clear magmatic features whereas others are predominantly hydrothermal in character; others still have such complicated histories or such poor exposures, that their origins are unclear.

Low-Ti, magnetite-apatite ore deposits occur associated with volcanic rocks in two belts in northern Chile (Figure 1); one of Cenozoic age in the High Andean Cordillera, and one of Cretaceous age in the Coastal Cordillera. The best preserved orebodies are the Plio-Pleistocene, El Laco deposits in the High Andes, which were first described by Park (1961), who reported iron-oxide orebodies that resembled lava flows. He suggested that the deposits formed from a volatile-rich, iron-rich magma which intruded the local volcanic sequence at shallow depth and in places erupted to the surface. This interpretation has been assumed by many subsequent investigators (Rogers, 1969; Haggerty, 1970; Frutos and Oyarzún, 1974; Henríquez and Martin, 1978; Frutos et al., 1990; Nyström and Henríquez, 1994, 1995; Naslund et al., 1997, 1998; Henríquez and Nyström, 1998; Broman et al., 1999; Nyström et al., 2002). Although not as well preserved, similar magmatic iron ore deposits occur in the High Andes of Chile at Incahuasi and Magetita Pedernales, and at numerous localities in the Cretaceous iron belt (Figure 1) (Grez et al., 1991; Henríquez et al., 1994; Travisany et al., 1995). A number of recent reports, however, have suggested that the El Laco iron-oxide deposits are hydrothermal in origin (Hildebrand, 1986; Hitzman et al., 1992; Larson and Oreskes, 1993; Larson, 1994; Rhodes and Oreskes, 1995a, 1995b, 1996, 1999; Oreskes et al., 1994, 1995; Rhodes, 1996; Sheets et al., 1997; Rhodes et al., 1997, 1999; Hitzman, 2000).

Editor's note: One of the aims of this two volume set has been to present the differing views on what constitutes a member of the "iron-oxide copper-gold" family of deposits, and how they were formed so that the reader can study the reasoning behind the varying opinions and make their own informed decision. There is a well reasoned argument that some of the important magnetite-apatite deposits are in fact magnetite lavas, including those found in districts that also host hydrothermal iron-oxide copper-gold ores. As a consequence, this group of authors, who through years of careful observation and research have supported this interpretation, were invited to contribute a paper outlining and arguing the case for their viewpoint. Their work is largely based on the El Laco deposits in Chile which are probably the best example available for such a study. The El Laco magnetite deposits fall within the Puna Belt, which also includes the Arizaro and Lindero Cu-Au Prospects described by Dow and Hitzman in this volume.

El Laco is, therefore, a critical locality. If the best-preserved, seemingly magmatic iron ore deposits in this district are hydrothermal in origin, then all similar deposits are likely to be hydrothermal as well. If, however, it can be demonstrated that iron-oxide magmas erupted at even one place on Earth, then a magmatic origin must be considered for other similar, less-well-preserved, deposits.

Although there are some features at El Laco that are clearly hydrothermal in origin, as one would expect at any volcanic centre, all of the available evidence indicates that the magnetite ore deposits were formed from iron-oxide magmas and magmatic fluids released by the magmas as they cooled and solidified. This paper will outline the field relationships at El Laco and the available analytical data, and discuss how they fit with both the magmatic and hydrothermal hypotheses. The paper will then describe the general geology of the Cretaceous iron belt, and the mineralisation associated with magmatic iron-oxide deposits in Chile.



Figure 1: Magnetite-apatite ores and some associated Fe-Cu-(Au, Ag) mineralisation in northern Chile (the Toldo-Velarde deposit is situated 125 km north of Antofagasta.

Field Relationships at El Laco

Tectonic Setting

The El Laco iron deposits are exposed at altitudes between 4,700 to 5,300 m on the flanks of El Laco, a calc-alkaline volcanic complex in the Central Andes of northern Chile at 23°48' S latitude and 67°30' W longitude (Figures 1-2). Within an area of 30 km^2 there are seven deposits with total resources on the order of 500 million tons of high-grade, iron ore (Nyström and Henríquez, 1994). With the exception of the orebodies, El Laco is similar to other volcanic complexes in the area in terms of silicate lava compositions, phenocryst assemblages, general eruptive history, and degree and distribution of alteration. The ore deposits have been dated at 2.1 Ma by apatite fission track analysis (Maksaev et al., 1988). Andesitic to dacitic lavas predate and postdate the ore deposition. Fumarolic activity has continued at El Laco to the present day.

El Laco is located slightly behind the active volcanic arc, as defined by the volcanoes Láscar, Licancabur, and Putaria to the north, and Socompa, Lastarria, and Antofalla to the south. Crustal thickness beneath El Laco is ca. 60 km (Tassara, 1997), and the depth to the well-defined, Benioff zone beneath the volcano is approximately 125 km (Frutos, 1990). Calc-alkaline lavas within the Central Andes (21° to 26° S) have systematically higher $^{18}O/^{16}O$ and $^{87}Sr/^{86}Sr$ ratios than do lavas in the rest of the volcanic chain, which may be related to the thicker crust in this segment (Harmon and Hoefs, 1984). Tectonic reconstructions suggest that the crustal section below El Laco contains a Lower Paleozoic basement of marine sedimentary rocks, unconformably overlain by Mesozoic and Lower Tertiary continental sediments and Upper Tertiary volcanic rocks (Frutos, 1990). Small evaporitic basins are common in the high Altiplano around El Laco. Glacial deposits are present to the west of El Laco, and glacial erosion has removed the upper part of the San Vicente Bajo orebody.

General Features of the Deposits

The El Laco ore deposits, which are composed mostly of primary magnetite or martite pseudomorphs after magnetite, occur as pyroclastic material, lava flows and related dykes (Laco Norte, Laco Sur, and San Vicente Alto), subvolcanic bodies (San Vicente Bajo, Rodados Negros, and Laquito), and an intrusive dyke-vein network (Cristales Grandes). Due to its friable nature, the pyroclastic material is exposed only in mined areas (Laco Sur), road cuts and exploration pits. Apatite is locally abundant in the intrusions, but is only a minor accessory phase in the lavas. The ore contains variable amounts of partly to completely altered pyroxene. Hematite is a ubiquitous oxidation product after magnetite in intrusive and pyroclastic ore, and is in places primary. Dykes and veins of magnetite, ± pyroxene, and ± apatite are abundant in the massive units and in the surrounding host rocks, but comprise less than 1% of the ore volume. Many of the host rocks surrounding the deposits have been pervasively altered, and massive mounds of fumarolic sulphate and sulphur occur in the volcanic complex. Late-stage, low-temperature, quartz veins are common.

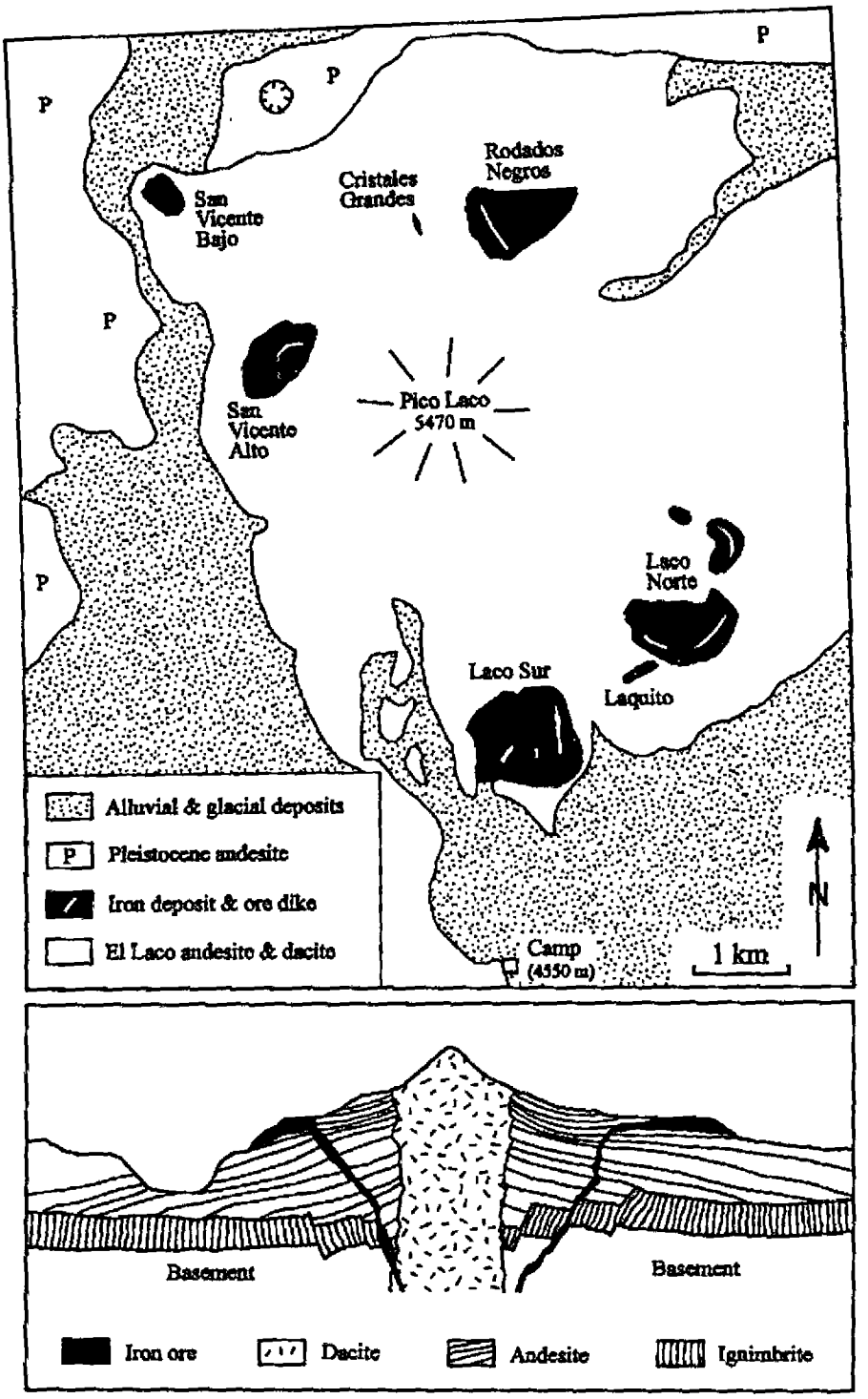


Figure 2: Geological sketch map and profile of the El volcanic complex and iron deposits (modified after Nyström and Henríquez, 1994 and Frutos and Oyarzún, 1974).

Massive Iron Ores

The term massive is used here for ore without bedding and includes ore lava, pyroclastic material and intrusive ore. Massive orebodies in excess of 100 m thick, composed of >98% iron-oxide, are present at Laco Norte, Laco Sur, San Vicente Alto, and San Vicente Bajo. Evidence for a direct magmatic origin for these massive units includes: 1) pahoehoe and aa flow surfaces; 2) contorted flow layering; 3) razor-sharp, chilled contacts; 4) vesicular textures with open vesicles; 5) friable, porous aggregates of euhedral magnetite crystals which locally pass into stratified ore ± apatite; 6) abundant gas escape tubes; and 7) coarse, spherulitic and dendritic magnetite crystals (Henríquez and Martin, 1978; Nyström and Henríquez, 1994; Naslund et al., 1997, 1998). It has been argued that these textures are relicts of an original silicate rock replaced by hydrothermal iron-oxide. Such a process would require the gradual replacement of a silicate lava or tuff while retaining their fine-scale textures. No samples showing a progression from altered andesite to massive iron-oxide (rocks with 20%, 40%, or 60% iron-oxide, for example) have been reported by any investigators. The only partial "replacement" by iron-oxide reported, is where thin (1 mm

to 1 cm) crosscutting veins cement fractured and brecciated host andesites. Such vein "replacement", however, does not preserve original textures, nor is it likely to result in rock bodies 100 m thick with >98% iron-oxide. The proposed hydrothermal replacement process for El Laco (Rhodes et al., 1999), involves the replacement of initial silicate lavas by smectite, scapolite, and feldspar, followed by a second stage in which the altered lavas are replaced with coarse, massive pyroxene, followed by a final stage in which the pyroxene rock is replaced by magnetite. Such a multistage process would certainly obliterate any original textures. In fact, although in some places rocks adjacent to the massive orebodies have been completely replaced by smectite, scapolite, and feldspar, and in other places rocks have been replaced by coarse, massive pyroxene, none of the replaced rock preserves any of the volcanic textures observed in the massive iron ores.

It has been suggested that the contacts of the massive magnetite units at El Laco are gradational (Larson, 1994; Rhodes and Oreskes, 1995a; Oreskes et al., 1995) based on the fact that altered andesite talus gradually changes to iron-ore talus below the iron-ore outcrops. Where exposed, however, the contacts of the massive magnetite units are razor-sharp, and in many cases a fine-grained chilled margin is present in the magnetite adjacent to the contact (Figure 3). Within the Laco Sur deposit there are a number of large (>1m diameter) xenoliths of altered andesite. There is no iron mineralisation within the xenoliths, the surrounding massive iron-oxide ore is chilled against the xenoliths, and the contact between rock with <5% iron-oxide and rock with >99% iron-oxide is razor-sharp. Similar razor-sharp, chilled contacts are present in vesicular dykes below the Laco Sur orebody. At the base of San Vicente Bajo thin veins of magnetite crosscut the host andesite for tens of metres below the contact of the orebody, and the adjacent andesite is badly altered, and in places brecciated. The contact, however, is marked by a change from altered andesite to massive iron ore over a distance of <1mm (see Figures 13B-C in Rhodes et al., 1999). Semi-horizontal fracture patterns in the andesite below the contact and in the ore above the contact are similar, and give the rocks a crude layered appearance. It has been suggested that this "layered morphology" in the ore was inherited from an original andesite protolith (Rhodes, 1996; Rhodes et al., 1999). Regardless of how the ore deposit formed, however, these fractures are clearly a post-mineralisation feature. Had they been present at the time of mineralisation, whether by iron-oxide magmas or by hydrothermal fluids, they would have acted as channel ways for the mineralising liquids. The fractures are unmineralised.

The vesicular textures common in many of the massive magnetite units (Figure 4) are hard to reconcile with an origin by hydrothermal alteration or replacement which usually fills pores and vesicles during the initial stages of alteration. Vesicular textures are ubiquitous in the massive ores, and almost all of the vesicles are unfilled, open pore spaces. Some vesicular dykes that crosscut the massive iron-oxide bodies are so rich in open spherical vesicles that they have densities of 1.9 g/cm^3 and yet are almost pure iron-oxide. It has been suggested that the porosity in the magnetite ores is a relict of angular pore spaces in brecciated andesite protolith or of pore spaces between coarse pyroxene crystals formed during replacement of andesite by pyroxene (Rhodes et al., 1999). The iron-oxide orebodies contain both angular and rounded vesicles, but neither resemble the angular pore spaces in breccias or in the pyroxene rocks adjacent to the deposits.



Figure 3: Contact between iron ore (below) and altered andesite (above) with a fine-grained chilled margin in the ore, Laco Sur. Knife handle is 6.0 cm long.

Open, vertical pipes metres to tens of metres long, and centimetres to tens of centimetres in diameter, with circular to oval cross sections are common in the massive orebodies (Figure 5). Such features are common in cooling silicate lava flows and ignimbrites and represent internal degassing conduits. At El Laco, these degassing pipes are typically lined with coarse magnetite octahedra. In some tubes the magnetite is intergrown with coarse pyroxene and apatite, and other tubes contain fine-grained ore with vesicles and locally even bedding. The tubes appear to represent conduits along which high-temperature gases escaped from the crystallising, volatile-rich, iron-oxide magma (Henríquez and Martin, 1978). Externally derived, hydrothermal fluids would be more likely to have been transported along planar fractures than along open, vertical tubes.

Stratified and Scoriaceous Ores

Mining of the Laco Sur deposit has uncovered bedded ash layers beneath the main orebody (Figure 6). The ash which is almost pure iron-oxide in composition, is crystalline, friable, size-sorted, and contains numerous magnetite spindle bombs up to 0.5 m in length. In some layers, rounded masses of diadochite ($Fe_2PO_4SO_4OH{\cdot}6H_2O$), 2 to 10 cm in diameter are present in the bedded ash, and appear to be a primary feature. These deposits are fresh, and have not been altered by any later folding, metamorphism, or fluid interaction. Bedded ore can also be found at several places within the massive orebody. The bedding within the more massive ore bodies, is best seen where it is marked by thin layers of apatite needles (see Figures 4A-B in Nyström and Henríquez, 1994). The textural features and friable nature of the bedded ash along with the solid magnetite spindle bombs, conclusively demonstrate that it is a near-vent, volcanic, pyroclastic deposit. An origin by hydrothermal replacement of a "normal" silicate ash is precluded by the friable, porous nature of the deposit, and the lack of veining or alteration along the upper or lower contacts of the unit. While the surface venting of a hydrothermal system could produce bedded hematite fragments, the magnetite spindle bombs require the eruption of an iron-oxide magma (Henríquez and Nyström, 1998). It is extremely difficult to imagine how a hydrothermal replacement process could convert an originally silicate, near-vent facies deposit to iron-oxide and leave the bedded ash and lapilli as unconsolidated magnetite and hematite fragments, while replacing the enclosed spindle bombs with solid (but vesicular) magnetite.

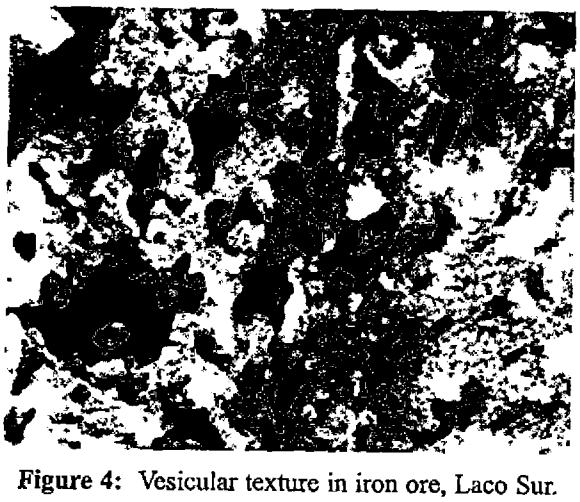


Figure 4: Vesicular texture in iron ore, Laco Sur. Width of view is ~3.3 cm.

At Laco Norte, pyroclastic iron ore is present in drill core from beneath and within the main orebody and is exposed in exploration pits north of the orebody. In the exploration pits, loose, vesicular iron-ore fragments centimetres to tens of centimetres in diameter with the appearance of basaltic scoria overlie an unaltered andesite lava flow and are overlain by a second unaltered lava flow. This scoriaceous ore appears to be formed by a strombolian-like eruption of iron-oxide magma. An origin by hydrothermal replacement would require the complete replacement of individual fragments while leaving their vesicles unfilled, the fragments un-cemented, and the lavas above and below the fragmental ore unit unaltered.

Dykes and Veins

Some of the smaller orebodies at El Laco are dykes (Rodados Negros and Laquito) or dyke-vein systems with prominent ore breccia and aggregates of magnetite, pyroxene and apatite in open spaces (Cristales Grandes). Crosscutting veins or dykes of magnetite, with pyroxene and apatite are common within and around many of the massive iron orebodies. Some veins 1 to 10 cm wide have open centres lined with magnetite crystal terminations showing clear evidence that magnetite crystals grew from the walls of the vein inward. In a few of these open veins, the central part has been filled with later, lower-temperature quartz or quartz plus apatite.

It has been suggested that the pyroxene crystallisation preceded magnetite crystallisation (Rhodes et al., 1999). Although in some places, pyroxene rock near the margins of the massive orebodies is cut by later magnetite veins, in most places pyroxene grew simultaneously with magnetite. Veins of intergrown magnetite and pyroxene cut the massive magnetite orebody at Laco Sur demonstrating that at least some of the pyroxene crystallisation postdates the main ore forming process (Broman et al., 1999). In some veins parallel layers of elongate pyroxene crystals are completely surrounded by coarse magnetite, demonstrating that in these veins magnetite crystallisation proceeded, occurred simultaneously with, and followed pyroxene crystallisation. In some other veins, magnetite ± pyroxene crystallisation alternated with magnetite ± apatite crystallisation, and in a few veins magnetite, apatite, and pyroxene clearly crystallised simultaneously. Some open veins contain perfectly formed crystal terminations of octahedral magnetite, prismatic pyroxene, and hexagonal apatite indicating that all three were in equilibrium with the liquid that filled the open space during the final stage of crystallisation. The idea that such veins represent the initial crystallisation of a layer of elongate pyroxene crystals, that the space between the pyroxene crystals was later "filled in" with magnetite, and that the parallel, elongate apatite crystals represent original pyroxene laths that were



Figure 5: Gas escape tube in iron ore, Laco Sur.

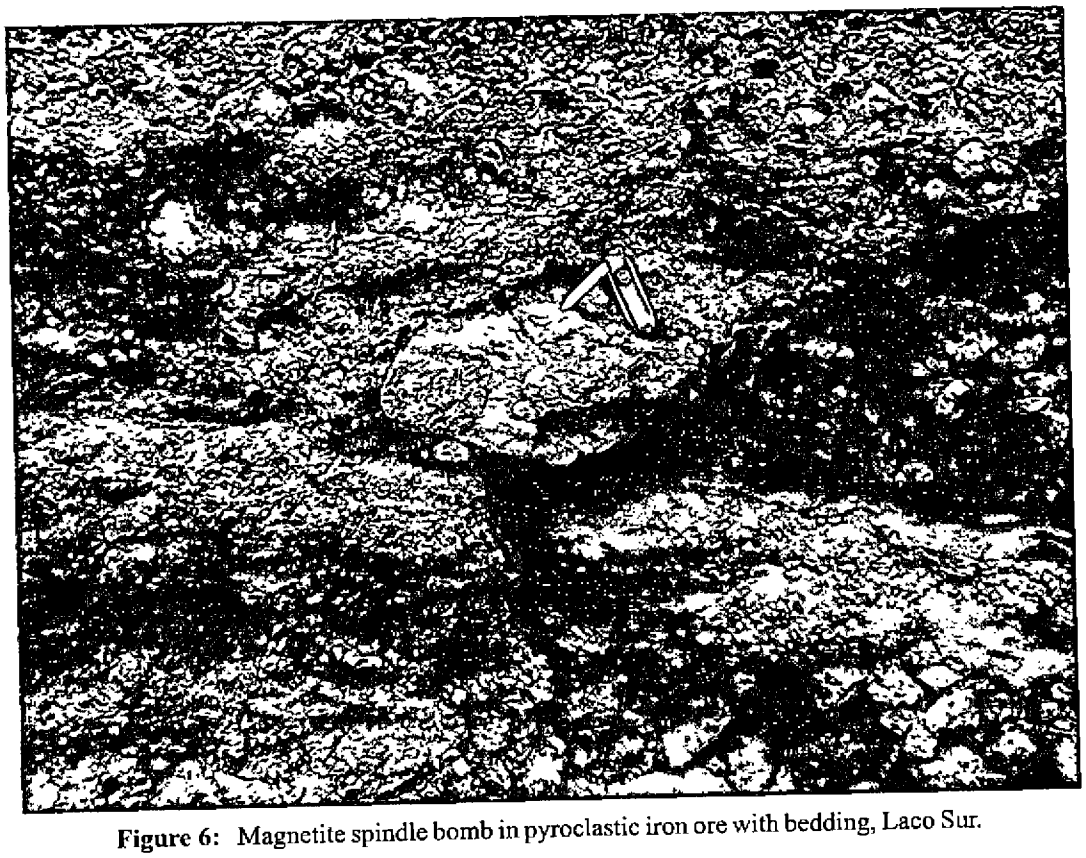


Figure 6: Magnetite spindle bomb in pyroclastic iron ore with bedding, Laco Sur.

completely replaced by apatite (Rhodes et al., 1999) is clearly incorrect.

It is suggested that "hydrothermal magnetite-quartz veins" are common in the host rocks (Larson and Oreskes, 1993; Larson, 1994; Rhodes and Oreskes, 1995a, 1995b, 1996; Oreskes et al., 1995; Rhodes et al., 1997, 1999). There are numerous veins cutting the host rock that contain an early magnetite selvage and an open or quartz-filled interior. These are, however, not "magnetite-quartz" veins. The magnetite is clearly of high-temperature origin, and the quartz is a later, lower-temperature, fracture-filling mineral. No data has been reported to suggest that magnetite and quartz were deposited in equilibrium; in fact, all the reported data indicates that they were not (see discussion of oxygen isotopes below). The texture of the quartz in hand specimen and thin section, indicates that it is a late, low-temperature mineral, unrelated to the crystallisation of the coarse magnetite crystals in the veins or to the massive magnetite orebodies. Calcite, which is present in some samples, is also a late, low-temperature mineral unrelated to the iron mineralisation.

At San Vicente Bajo, abundant magnetite dykes one to several metres wide cut sub-horizontal flow layering in the massive magnetite orebody (see Figure 13A in Rhodes et al., 1999). Previous workers attributed the close proximity of subvertical and sub-horizontal "layers" in the ore to replacement of an andesite protolith that had undergone "normal faulting" (Rhodes et al., 1999). There is no indication of any faulting at El Laco that could have rotated originally horizontal layers into a vertical position on such a large scale and over such short horizontal distances.

Alteration

Two types of alteration patterns are recognised at El Laco. The first type is restricted to the margins of the intrusive iron orebodies, and occurs as halos around them and as minerals deposited in open spaces within the extrusive ores. This first type is overprinted by hydrothermal alteration affecting large areas in the district.

Alteration assemblages seemingly related to the emplacement of the ore (Vivallo et al., 1993b, 1994b; Nyström and Henríquez ,1994; Broman et al., 1999) form metasomatic aureoles (halos) around the ore dykes and the San Vicente Bajo intrusion. The width of the aureoles (up to 20 m) varies with the size of the orebody and the permeability of the host rock. The aureoles consist of pyroxene, magnetite, quartz, and scapolite (marialite) in altered andesite lava and tuff. The contacts between the orebodies and the altered host rock are sharp at the few places where they are exposed, and in drill cores. Quartz is common in partly filled cavities and as veins within or outside the magnetite bodies, but textural relations show that the quartz invariably is younger than the iron-oxide.

Metasomatic aureoles like those around the intrusive orebodies and dyke-vein systems have not been observed at the margins of the extrusive deposits. In general, the andesitic lavas and tuffs immediately below the magnetite flows at Laco Sur and Laco Norte are hydrothermally altered. Illite, mixed-layer clays (smectite-illite) and pyrophyllite are present in the drill core, in addition to quartz, feldspar, and a few irregular magnetite veins without pyroxene fringes. In one trench on the northwest edge of the Laco Norte deposit coarse pyroxene rock is present adjacent to magnetite ore, but these samples appear to be associated with a feeder dyke for the Laco Norte flows.

Open spaces in the extrusive ore contain tridymite, quartz, amorphous silica, hematite, and small amounts or traces of Na-alunite, Fe-bearing phosphates, plagioclase (labradorite), sanidine, and rutile. These minerals (not listed according to temperature of formation) were deposited during degassing and subsequent stages of hydrothermal activity.

The El Laco deposits and associated metasomatic alteration are overprinted by hydrothermal alteration formed at low temperature that has affected large areas of the volcanic complex without a clear zonation pattern (Vivallo et al., 1993b, 1994b). It is expressed as a pervasive, strong silicification and advanced argillic alteration with destruction of the original textures, grading outwards to rocks with moderate or weak alteration. The degree and extent of the hydrothermal alteration show a good correlation with lithology and permeability, the most strongly affected being pyroclastic rocks. The silicified rocks consist of quartz, tridymite, cristobalite, alunite and jarosite, and minor amounts of K-feldspar, anatase and some unidentified iron sulphates and phosphates. Rocks affected by argillic alteration are characterised by quartz, alunite, kaolinite, gypsum, cristobalite, smectite, bassanite, pyrite and pyrophyllite.

In the less altered volcanic rocks there is only a partial replacement of pyroxene by chlorite and plagioclase by sericite and clay minerals; a hematite-epidote association is common. Locally, there are fumarolic deposits dominated by gypsum with subordinate alunite, jarosite, sulphur, cristobalite, tridymite and calcite. These exhalative deposits are restricted in extent and thickness and were deposited around several discrete centres in the district. The orebodies are crosscut by numerous veins of gypsum, which clearly postdate the ore forming process.

Analytical Data from El Laco

General Features

In terms of the reported analytical data, there do not appear to be any serious disagreements between those advocating a magmatic origin and those advocating a hydrothermal origin for El Laco. Where data have been reported by both groups, for example oxygen isotope analyses and fluid inclusion homogenisation temperatures, the results are similar. The interpretations of the results, however, are very different.

The main orebodies at El Laco are composed of almost pure magnetite or magnetite partly replaced with hematite pseudomorphs. Most ore samples are >98% iron-oxide.

The bulk ores are rich in REE with some samples containing in excess of 1% total REE-oxides. An average of 13 samples of randomly selected bulk ore from Laco Sur contained 0.33% REE-oxides (Heriberto Fortín, Compañía Minera del Pacifico internal report, 2001). The REE in the bulk ores are concentrated in apatite and Fe-phosphates. Apatite is abundant in veins, gas escape tubes, and locally in the ore, but on average makes up a very small percentage of the deposit (<1%). Pyroxene is only abundant in veins, gas escape tubes, and some contact rocks, and in most samples where it would be expected, it is only present as badly altered relict crystals. In some cases the former presence of pyroxene is indicated by empty, elongate, prismatic holes in coarse magnetite crystals lining gas escape tubes. Near the margin of some of the massive magnetite bodies, the host rock has been completely converted to a coarse pyroxene rock completely destroying any original features so that the protolith is unknown. The volume of such pyroxene rock is very small relative to the orebodies (<0.01%).

Oxygen Isotopes

It has been suggested that since the oxygen isotopes in magnetite from veins and massive units are very similar, both must be hydrothermal (Larson, 1994; Rhodes and Oreskes, 1995a, 1995b, 1996, 1999). If the veins and massive units both had hydrothermal isotope signatures, a logical conclusion might be that both were hydrothermal. However, both the veins and the massive units have igneous oxygen isotope signatures (Vivallo et al., 1994b; Rhodes and Oreskes, 1999; Nyström et al., 2002). An alternative explanation is that the veins have similar isotopic signatures as the massive units, because the veins were deposited at near-magmatic temperatures from fluids exsolved from iron-oxide magmas as they solidified. In fact, all of the available oxygen isotopic data suggest that the iron-oxide deposits are unrelated to the hydrothermal alteration at El Laco (Figure 7). Unaltered andesites and dacites at El Laco have a narrow range of oxygen isotope values ($\delta^{18}O$ = 7.9, Vivallo et al., 1994b; $\delta^{18}O$ = 7.2 to 7.9, Rhodes and Oreskes, 1999), while all of the hydrothermally altered samples analysed have much higher values ($\delta^{18}O$ = 11.8 to 35.3, Vivallo et al., 1994b; $\delta^{18}O$ = 8.5 to 24.2, Rhodes and Oreskes, 1999). Altered magnetite, on the other hand, has lower oxygen isotope values ($\delta^{18}O$ = 2.3 to 3.5 in samples with 7 to 75% hematite, Nyström et al., 2002; $\delta^{18}O$ = -8.9 to 3.5 in samples with 6 to 96% hematite, Rhodes and Oreskes, 1999) than does unaltered magnetite ($\delta^{18}O$ = 3.1 to 4.2, Nyström et al., 2002; $\delta^{18}O$ = 3.5 to 5.2, Rhodes and Oreskes, 1999). This indicates that the processes responsible for the hydrothermal alteration of the silicate lavas are unrelated to those responsible for the formation of the ore deposits or for the alteration of the ore deposits.

As described above, numerous veins cutting the host rock contain an early magnetite selvage and an open or quartz-filled interior. In contrast to the narrow range of values for magnetite ($\delta^{18}O$ = 3.1 to 5.2; Rhodes and Oreskes, 1999; Nyström et al., 2002), quartz displays a wide range of oxygen isotope values ($\delta^{18}O$ = 11.9 to 25.0, Vivallo et al., 1994b; $\delta^{18}O$ = 6.0 to 27.9, Rhodes and Oreskes, 1999). Moreover, quartz shows wide $\delta^{18}O$ variations within individual veins (Larson, 1994; Vivallo et al., 1994b; Rhodes and Oreskes, 1995b, 1999), confirming that the magnetite and quartz are not in equilibrium, and did not precipitate from the same liquids.

The proposed hydrothermal model (Rhodes and Oreskes, 1999; Rhodes et al., 1999) would require a series of fluids with a very complicated history of oxygen isotope changes. The unaltered andesites with a narrow range of $\delta^{18}O$ (7.2 to 7.9) would be first converted to altered andesites with a range of higher $\delta^{18}O$ during propylitic alteration and Na-K metasomatism ($\delta^{18}O$ values = 8.5 to 10.1), followed by high-temperature replacement and Ca metasomatism to produce pyroxene with a narrow range of low $\delta^{18}O$ (7.1 to 8.9), followed by low-temperature replacement to produce magnetite ores with a narrow range of still lower $\delta^{18}O$ (3.5 to 5.2), followed by quartz precipitation and argillic alteration at low temperature with a wide range of higher $\delta^{18}O$ (6.0 to 27.9) and apatite replacement at low temperature with a narrow range of $\delta^{18}O$ (7.8 to 8.0), followed finally by hematite alteration at low temperature to produce very low $\delta^{18}O$ altered ores (-8.9 to 3.5) (all data from Rhodes and Oreskes, 1999). A simpler model would be to produce the andesites, magnetites, apatites, and pyroxenes at high temperature with all four related to magmas or magmatic fluids with narrow ranges of $\delta^{18}O$, to then produce the altered andesites and quartz veins during a single, post Fe-mineralisation, hydrothermal, alteration event from fluids with a range of high $\delta^{18}O$ values, and to finally produce the hematite by alteration of the magnetite by low $\delta^{18}O$ meteoric water.

The difference in oxygen isotopes between unaltered iron ores and unaltered silicate lavas is similar to what would be predicted for immiscible liquids of these compositions. Experimental studies of immiscible silicate liquids have shown that iron-rich liquids have lower oxygen isotope ratios than do iron-poor liquids (Kyser et al., 1998). A difference of 0.6 per mil was observed for immiscible liquids which differed in iron content by only 22% (42% vs. 20% Fe-oxides). For liquids that differ in iron content by 90% (98% vs. 8% Fe-oxides, for example), a difference of ~2.5 per mil might be predicted, similar to that observed for the El Laco iron ores and silicate lavas. The difference in oxygen isotopes between magnetite and pyroxene is consistent with the crystallisation of these minerals at high temperatures (Nyström et al., 2002). The observed $\Delta\ \delta^{18}O$ for pyroxene-magnetite is 1.9 to 5.4 per mil (Rhodes et al., 1999) which corresponds to crystallisation temperatures of 1090 to 540 °C (Chiba et al., 1989).

Fluid Inclusions

Magmatic to near-magmatic fluid inclusion homogenisation temperatures have been reported for pyroxenes associated with magnetite in dykes and veins at El Laco (710 to 840 °C, Sheets et al., 1997; Rhodes et al., 1997; Rhodes and Oreskes, 1999; >800 °C, Broman et al., 1999). Lower fluid inclusion homogenisation temperatures have been

reported for El Laco apatites (219 to 360 °C, Oreskes et al., 1994; 250 to 350 °C, Sheets et al., 1997, Rhodes et al., 1997; 150 to >600 °C, Broman et al., 1999). The low apatite temperatures may represent: 1) a low-temperature origin for at least some of the apatite; 2) the post-crystallisation trapping of later, low-temperature fluids; or 3) annealing and/or re-equilibration of apatite as it cooled. Fission tracks in apatite anneal at 100 °C, so it is possible that fluid inclusions in apatite also anneal at low temperatures during slow cooling. The fluid inclusions in apatite that yield the low homogenisation temperatures contain a wide range of salinities (0.2 to 59 wt% NaCl equivalent, Sheets et al., 1997, Rhodes et al., 1997) suggesting that these inclusions probably do not accurately preserve the fluids from which they formed. In some El Laco ore samples, apatite fluid inclusions (hydrous saline Na-K chloride melt inclusions) failed to homogenise at 600 °C, and in other samples the apatite host decrepitated before fluid inclusion homogenisation was achieved (Broman et al., 1999), demonstrating that some of the fluid inclusions in apatite formed at higher temperatures. Some of the apatite in veins is intergrown with quartz and is clearly a low-temperature phase. In most other samples from El Laco, however, apatite has grown simultaneously with magnetite and pyroxene and must be of higher temperature origin. The high fluid inclusion temperatures reported for pyroxene are in agreement with the temperatures obtained from pyroxene geothermometry (see below). The temperatures reported for the pyroxene are too high for hydrothermal systems *sensu stricto*, and imply crystallisation from a magma or from magmatic fluids. The minor amounts of magnetite deposited as magnetite veins with pyroxene and/or apatite near the contacts of massive iron-oxide bodies, are therefore, best explained as the product of the degassing of a volatile-rich magma during crystallisation. The most likely source for these magmatic fluids, are the magmas that formed the adjacent iron-oxide lavas and intrusive bodies.

Mineral Compositions

Analyses of pyroxene phenocrysts in unaltered El Laco silicate lavas and pyroxenes in magnetite-pyroxene dykes and veins demonstrate that they are almost identical in composition (Figure 8) and have similar crystallisation temperatures based on the Lindsley (1983) pyroxene geothermometer (silicate phenocrysts = 770 to 950 °C; "vein" pyroxene = 500 to 850 °C). The silicate lavas contain both Ca-rich and Ca-poor pyroxenes, and as a result, the pyroxene geothermometer is directly applicable. In the ore, however, unaltered low-Ca pyroxene is rare, and therefore, the pyroxene geothermometer will yield only minimum crystallisation temperatures. The similarity in major and minor elements between the pyroxenes in rock and ore suggests that both have "magmatic" compositions. In addition, the El Laco pyroxenes are very dry (<0.001 % OH, Broman et al., 1999), confirming that they are most likely of magmatic and not hydrothermal origin. If the centimetre- to metre-wide dykes and veins cutting andesite host rock tens of metres away from the massive orebodies record temperatures in excess of 800 °C, it is likely that the 100 m thick massive orebodies were formed at even higher temperatures. Pyroxene associated with the El Laco orebodies is REE-rich with La values 280 to 1240 times chondritic abundances and Lu values >100 times chondrites (Rhodes et al., 1999).

Apatite is locally abundant (>20%) in some of the dykes and veins, but is much less abundant in the massive bodies and stratified ores. Apatite is also a common inclusion in phenocrysts in unaltered El Laco silicate lavas, suggesting that the silicate magmas were saturated or nearly saturated in apatite. Analysed apatites from El Laco andesites, ores and ore veins are almost identical in terms of F, Cl, SO_3, and OH (Figure 9) suggesting that all have magmatic compositions. Hydrothermal transport of iron by NaCl-rich brines, as has been proposed for other iron-oxide-apatite orebodies (Barton and Johnson, 1996), would be

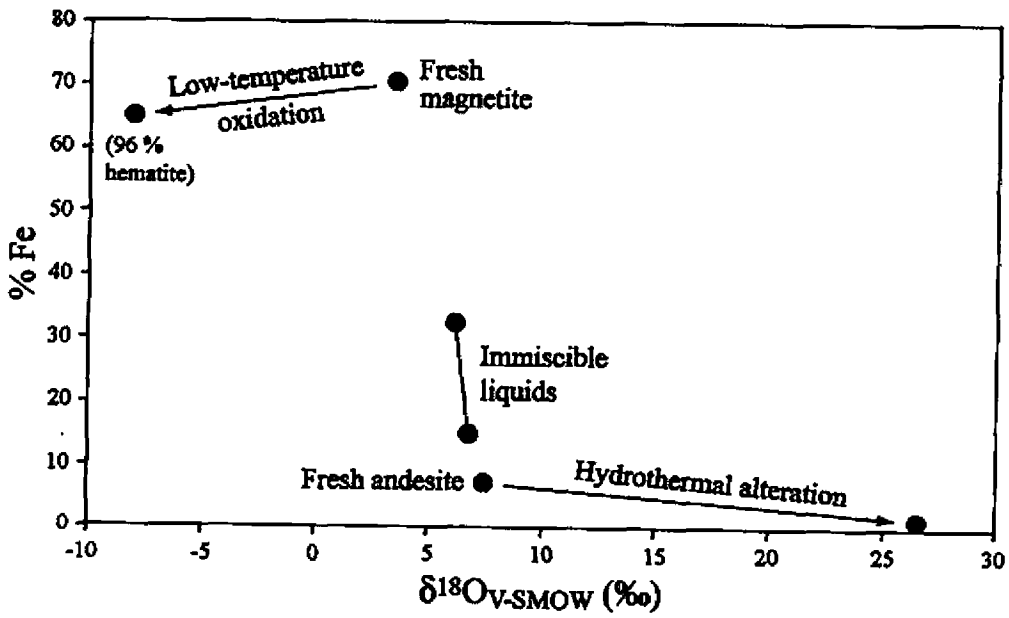


Figure 7: Oxygen isotope composition of iron-oxide-apatite ores and host rocks at El Laco, and immiscible liquids (Kyser et al., 1998).

expected to produce Cl-rich apatites. In fact, Cl-rich apatite is generally cited as evidence for hydrothermal deposition, while F-rich apatite is cited as an indication of magmatic crystallisation (Boudrou, 1995). Apatite associated with the El Laco orebodies is REE-rich with La values >10,000 times chondrites and average Lu values >200 times chondrites (Rhodes et al., 1999).

El Laco magnetite samples are rich in V (900 to 2500 ppm), Ni (90 to 360 ppm), and Mg (3000 to 8000 ppm) and poor in Cr (generally <10ppm), Ti (<5000 ppm), Co (<150 ppm), Zn (<150 ppm), Cu (<50 ppm), and Mn (<750 ppm), and they are similar in composition to magnetite in ores from the Cretaceous iron belt in Chile and the Kiruna iron ores in Sweden (Nyström and Henríquez, 1994). Average REE contents in El Laco magnetite samples range from 150 times chondrites for La to 15 times chondrites for Lu (Rhodes et al., 1999). Some magnetite samples in the El Laco deposits are rich in SiO_2 with contents up to 0.7 % (Nyström and Henríquez, 1994). XRD analysis shows distortion of the unit cell, suggesting that the SiO_2 is structurally incorporated in the magnetite.

Discussion of Magmatic and Hydrothermal Hypotheses for El Laco

Proposed Models for the Development of Massive Magnetite Ores

The origin of massive magnetite-apatite deposits is not well understood, and in fact, although they share a number of similarities, it is not likely that all of these deposits are produced by the same mechanisms. Proposed origins include: 1) separation of an immiscible iron-rich melt from a silica-rich melt during cooling; 2) partial or complete melting of iron-rich crustal rocks; 3) contact metamorphism and/or replacement of wall rocks by high-temperature, iron-rich magmatic fluids; 4) hydrothermal deposition or replacement; and (5) sedimentary-exhalative deposition. Processes 1 and 2, described below under "a magmatic model", both involve the transport of iron as an extremely iron-rich magma; they differ primarily in how that magma was formed. Processes 3, 4, and 5, described below under "a hydrothermal model", all involve the transport of iron as a dissolved component in a fluid, and differ mainly in where the fluid originates and in how and where the fluid interacts with the surrounding rocks to release the dissolved iron.

Agreement Between Magmatic and Hydrothermal Models

In addition to the analytical data described above there are a number of other features at El Laco that are agreed upon by both those advocating a hydrothermal origin and those advocating a magmatic origin for the deposits. The general geology of the El Laco deposits, including the composition and distribution of the main orebodies, vein complexes, and alteration zones is not in dispute. The textures within the deposits, including the size, shape, and distribution of magnetite, pyroxene, apatite, and quartz are features that have been observed and similarly reported by both groups. The preservation of volcanic features within the orebodies and in the surrounding friable, pyroclastic, iron-oxide deposits are also not in question. Although the two groups disagree about many of the interpretations, they agree that most of the hematite is secondary and formed by reaction between original magnetite and meteoric water and that this process is unrelated to the main alteration events. Both groups agree that the large, fumarolic sulphate mounds, generally located inside of the "ring" of magnetite orebodies, were deposited after the main ore forming event. Both groups also agree that in places, in particular at Cristales Grandes, magnetite-pyroxene and magnetite-apatite veins cut altered andesite host rock, and that these veins appear to have been precipitated from high-temperature fluids.

A Magmatic Model for El Laco

Experimental studies (Philpotts, 1967; Naslund, 1983) suggest that iron will dissolve readily in silica-rich melts at high temperatures, but upon cooling, immiscible silica-rich and iron-rich liquids will separate. In an experimental study of the effect of fO_2 on the development of immiscible iron-rich melts, the most iron-rich compositions (>78% Fe-oxides), occurred in melts at 1465 °C formed in equilibrium with magnetite and hematite at the highest oxygen partial

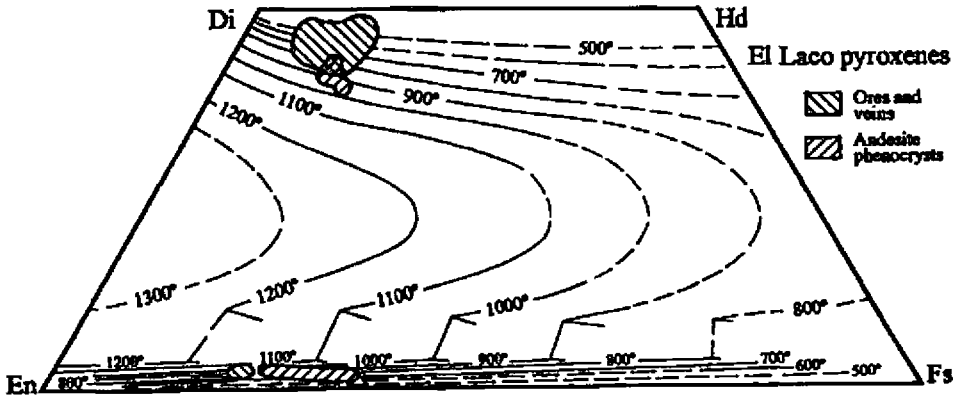


Figure 8: Pyroxene composition at El Laco and inferred crystallisation temperatures based on the Lindsley (1983) geothermometer.

pressures (Naslund, 1983). The addition of volatiles such as CO_2, H_2O, P, F, or SO_3 can lower the temperature of these iron-rich melts to more geologically reasonable values (< 1200°C), and expand the immiscibility field to more iron-rich compositions (Lester, 2002). Weidner (1982) produced iron-oxide melts in CO_2 saturated experimental runs at 880 °C, and Gibbon and Tuttle (1967) produced immiscible iron-oxide-rich melt in H_2O saturated experiments at 1060 °C. The immiscible relationship between silicate liquids and FeS liquids has been long recognised (Naldrett, 1989). Recent field and laboratory research has suggested that there is a continuum between FeS liquids and Fe-S-O liquids that extends from pure FeS liquids to liquids with O/S > 1.3 (Larocque et al., 2000; Rose and Brenan, 2001). Such liquids are immiscible with silicate melts, and are characterised by high Fe and low Ti contents. The abundance of vesicles and gas escape tubes in the El Laco flows suggest that they contained considerable amounts of dissolved gas, and this is probably an important feature of iron-oxide deposits of magmatic origin. The presence of F-apatite indicates that F was present in the volatile phase. The abundance of sulphate around the El Laco volcanic centre, and the presence of anhydrite in pyroxene fluid inclusions (Sheets et al., 1997; Broman et al., 1999), suggests that SO_3 may also have been important in the system.

The relatively low Ti and P contents of the El Laco deposits relative to nelsonites, has been cited as evidence that they do not represent immiscible melts (Larson, 1994; Rhodes and Oreskes, 1996). The Ti and P contents of immiscible melts, however, will be determined by an equilibrium distribution between the melts. Experimental data for Ti and P distribution between immiscible melts (Visser and Koster van Groos, 1979; Naslund, 1983) suggest that an iron-rich liquid in equilibrium with a dacite or rhyolite containing 0.5% TiO_2 and 0.15% P_2O_5 would contain 0.75 to 2.0% TiO_2 and 0.3 to 1.8% P_2O_5. Eutectic proportions of ilmenite and apatite, as observed in nelsonites, would only be expected from magmas produced by partial melting or magmas derived from extreme crystal fractionation. In addition, the titanium content of magnetite, is controlled not by the amount of titanium in the melt from which it crystallised, but by the temperature and oxygen fugacity at which it forms, and at the high oxygen concentrations necessary to crystallise coexisting magnetite and hematite (observed locally in the stratified ore below Laco Sur), both minerals should have very low titanium contents (Buddington and Lindsley, 1964). The dissolved volatiles present in the El Laco magma will also influence the distribution of elements between immiscible liquids. If SO_3 was an important component of the volatile phase, the ores would be expected to be low in TiO_2.

An alternate to the immiscibility theory is that iron-rich magmas are formed by partial melting of iron-rich crustal rocks. Magmas formed from partial melting of sedimentary iron ores would be expected to have a distinct chemical signature (low La/Lu; anomalous Ce; low V; high Pb), and distinct isotopic signatures which are not observed. In addition, many sedimentary rocks are quite refractory, and a melt derived from partially melting a sedimentary sequence would be likely to contain xenoliths of unmelted sedimentary layers. Although rumoured to exist (Thomas, 1970; Frutos and Oyarzún, 1974), no such xenoliths have been described by any investigators.

It has been argued that iron-rich liquids, such as those advocated for El Laco, would have such low viscosity that they would form very thin, laterally extensive flows, not the thick, almost dome-like orebodies observed (Hitzman et al., 1992; Larson, 1994). While some pahoehoe features are preserved at El Laco, most of the flow features suggest a much more viscous magma. It is likely that the El Laco magmas were very fluid at depth, but upon reaching the surface they began to degas and crystallise, and as a result became very viscous. The ubiquitous presence of gas vesicles and gas escape tubes demonstrates that the magmas were very gas-rich and underwent extensive degassing upon eruption. It has also been suggested that the pyroclastic

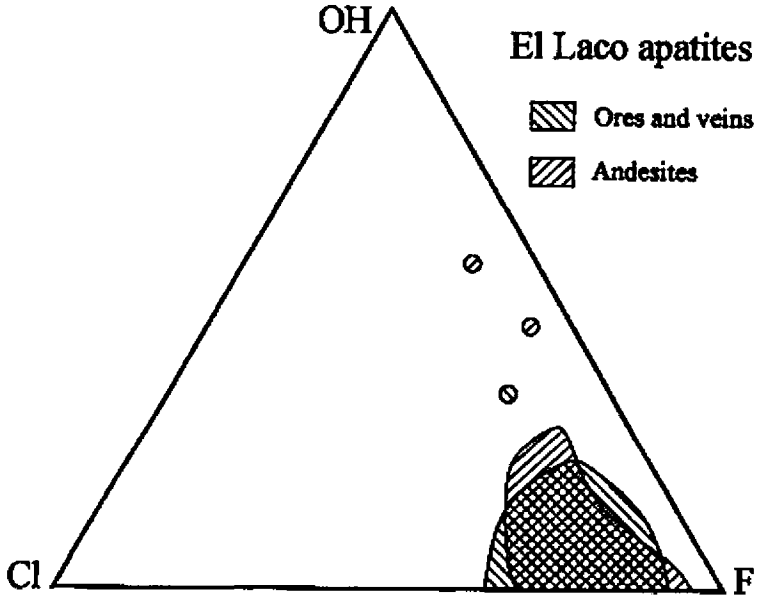


Figure 9: F-OH-Cl composition of apatites at El Laco.

deposits around and within the main orebodies do not represent the eruption of an iron-rich magma because they contain well-developed magnetite octahedra, and not the poorly formed crystals or iron-oxide glass that would be expected by rapid cooling of an iron-oxide magma according to Rhodes and Oreskes (1995a). Unlike silicate magmas, however, iron-oxide magmas should not form glasses upon quenching. As a result of the extremely low nucleation energy for magnetite, even under laboratory conditions with extremely rapid quench rates, high-temperature, iron-oxide liquids quench to a crystal mosaic of magnetite or magnetite ± hematite and not to glass.
The high density of iron-oxide magmas might be expected to decrease the likelihood that they would reach the surface (McBirney and Naslund, 1990). This may, in part, explain why localities like El Laco are so rare. Many magmas, however, are denser than the crustal rocks through which they erupt. Even a magma with a density of 5.0 could easily erupt if it was 50% vesiculated. Many of the ore samples at El Laco have densities <3.0, and a few of the most vesicular have densities <2.0. The existence of iron-oxide lavas at El Laco indicates that the processes responsible for the formation of the ore magma occurred high enough in the crust that the magma was able to vesiculate and erupt.

A Hydrothermal Model for El Laco

Traditionally, the word "hydrothermal" has been used to describe hot fluids derived from meteoric or intraformational water with or without contributions from magmatic fluids, and restricted to temperatures below ~500°C (Lindgren, 1933). Higher-temperature "magmatic" or "skarn" fluids are derived directly from degassing magmas, and can reach temperatures in excess of 1000 °C. The evidence at El Laco indicates that the main, massive, orebodies were crystallised from volatile-rich, iron-oxide magmas, and that the nearby magnetite-pyroxene and magnetite-apatite veins were formed from magmatic fluids released from these crystallising magmas. There is no evidence that replacement of pre-existing rocks by iron transported in either hydrothermal or magmatic fluids is responsible for any of the massive orebodies at El Laco.

The main El Laco orebodies formed at or near the surface. The area to the west of Pico Laco (Figure 2) was glaciated, and the San Vicente Bajo deposit appears to have been formed at shallow depth, and then uncovered by glaciation. There is no evidence, however, that the San Vicente Alto, Laco Norte, or Laco Sur deposits were ever glaciated, or that any significant amount of erosion has occurred since they formed. There is no evidence that these three orebodies were ever covered. The San Vicente Alto, Laco Norte, and Laco Sur deposits appear to have formed at the surface, and to have remained there ever since. The total replacement of near-surface silicate lavas or tuffs with coarse magnetite crystals by hydrothermal fluids is difficult to imagine. In general, in near-surface hydrothermal deposits "replacement is lacking and impregnation occurs only to quite a small extent" (Ramdohr, 1980). In fact, hydrothermal magnetite "is generally an indication of high temperature and considerable depth" (Ramdohr, 1980).

The formation of iron-oxide-apatite ores by fluid transport requires a system that can efficiently transport iron while limiting most other cations (except P) to low abundances. Experimental studies suggest that Fe can be transported in Cl-rich or Cl-poor hydrothermal solutions as Fe, Fe-Cl, or Fe-OH complexes (Chou and Eugster, 1977; Eugster and Chou, 1979; Whitney et al., 1985; Crerar et al., 1985). Although there is little available data for higher temperatures, existing data suggest that this process is more efficient at lower temperatures. Replacement of pre-existing silicate rocks would require the complete removal of Si, Al, Ca, Mg, Na, and K. Although there is a great deal of hydrothermal alteration at El Laco, there is no evidence for such massive movement of these other components. In addition, hydrothermal fluids would be expected to leave a distinctive trace element signature, rich in easily transported elements, and poor in less-easily transported elements. The El Laco ores, however, are rich in V, Ni, and REE, which are not easily transported in hydrothermal fluids and poor in Mn, Zn, Cu, and Co, which are more easily transported. The ores appear to be the source of fluids rather than the product of fluids.

One of the most persistent arguments that has been presented as evidence of a hydrothermal origin for the El Laco deposits, is that the magnetite in the massive ores and the magnetite in small veins cutting the host andesite near the massive orebodies have similar isotopic and trace element compositions, and since the veins are hydrothermal, both must be hydrothermal (Larson, 1994; Rhodes and Oreskes, 1995a, 1995b, 1996, 1999; Rhodes, 1996; Rhodes et al., 1997, 1999). This postulated hydrothermal system at El Laco, however, covered a range of temperatures (150 to >800 °C), a range of fluid compositions (Na-K metasomatism, Ca metasomatism, argillic alteration, siliceous alteration), and a wide range of isotopically heavy fluids ($\delta^{18}O$ in altered rocks = 7.1 to 35.8). As such, if the El Laco deposits were produced by hydrothermal processes, one would expect magnetites with a wide range of isotopic and trace element compositions that varied from one texture to the next. If, however, the deposits were formed from volatile-rich, iron-oxide magmas, and from the high-temperature, magmatic gases released from and in equilibrium with those magmas, one would expect that the magnetites would have similar, magmatic, isotopic and trace element signatures with little variation between textural types.

El Laco magnetites, like those at other iron-oxide-apatite deposits (Gleason et al., 2000), have igneous REE patterns consistent with the interpretation that they formed from iron-oxide magmas and high-temperature magmatic fluids in equilibrium with those magmas. The similarity in bulk REE content between El Laco magnetites and andesites has been cited as evidence that the magnetites inherited their REE contents from andesite protolith during replacement (Rhodes et al., 1999). The magnetites, however, are more strongly enriched in LREE and have flatter HREE patterns than either unaltered or altered El Laco andesites. Average magnetites have chondrite-normalised La/Sm = 8.5 and Sm/Lu = 1.7, while average

andesites have La/Sm = 4.6 and Sm/Lu = 2.3 (Rhodes et al., 1999). These differences cannot be attributed to alteration (altered andesite samples have lower La/Sm and higher Sm/Lu than the analysed magnetites), nor can it be attributed to contamination of the magnetite samples with pyroxene or apatite (average El Laco pyroxene has La/Sm = 2.7 and Sm/Lu = 2.5; average El Laco apatite has La/Sm = 7.4 and Sm/Lu = 6.8; Rhodes et al., 1999). The fact that the El Laco magnetites and unaltered andesites have similar total REE, was also cited as evidence that the iron ores did not form by liquid immiscibility which would be expected to concentrate REE in the iron-rich magma (Rhodes et al., 1999). Average Laco Sur bulk iron ores, however, have REE contents 20 times higher than average unaltered El Laco andesites (Heriberto Fortín, Compañía Minera del Pacífico internal report, 2001). REE in the bulk samples are concentrated in late-crystallising minor phases. In addition, the bulk iron ore has undergone degassing and some of the original REE content, which would presumably be concentrated in residual liquids during early magnetite crystallisation, may have been carried off in the volatile phase.

The strongest evidence against a hydrothermal or fluid-replacement origin and in favour of a magmatic origin, are the field relationships and well-preserved volcanic textures and intrusive structures. The pahoehoe and aa flow structures, the razor-sharp contacts with chilled margins, the open vesicular textures, the abundant open gas escape tubes, and the unconsolidated, massive, as well as size-sorted and bedded ash deposits are inconsistent with a replacement origin for these deposits. Although it has been suggested that these features are "palimpsest textures" inherited from an original andesite protolith (Rhodes et al., 1999) many of these features are not common in the surrounding unaltered lavas, and no partially replaced rocks that preserve original textures have been reported by any investigator. In fact, all of the proposed replacement processes for El Laco destroy textures. In addition, all of the analytical data is consistent with a magmatic model, and much of it is difficult to reconcile with a hydrothermal origin. The high-temperature fluid inclusions and pyroxene geothermometry results, the unusual oxygen isotope patterns, and the magmatic mineral compositions are unlike those reported from any hydrothermal or replacement deposit.

General Geology of the Cretaceous Iron Belt

The Cretaceous iron belt is approximately 600 km long and 25 km wide. It consists of seven large (>100 million tonnes of high-grade ore) and about 40 medium-sized and small deposits of magnetite-apatite ore (Figure 1). Three of the large deposits (Boquerón Chañar, Cerro Negro Norte, and Cristales) are unexploited or only partially mined and a fourth (Los Colorados) has been mined only since 1999.

The iron deposits consist of primary magnetite with varying amounts of secondary hematite. The apatite content is variable within and between different orebodies, and genetically related apatite veins are abundant in the ore districts. Unlike El Laco, magnetite orebodies in the iron belt contain large bladed amphibole crystals and pyroxene has not been reported; however, in some deposits pseudomorphs morphologically resembling pyroxene at El Laco have been observed. Based on field relationships, structures and textures, the different deposits in the iron belt have been interpreted as dykes, domes, sills, and stratiform subaerial orebodies, the latter including lava flows and pyroclastic deposits (Henríquez et al., 1994; Nyström and Henríquez, 1994, 1995; Travisany et al., 1995). Iron ore breccias and stockworks are present in many deposits close to massive ore, and occur in other parts of ore districts without obvious relationships to massive orebodies.

The deposits are considered to have formed in a magmatic arc along an Early Cretaceous shallow–marine basin (Vivallo et al., 1994c, 1995b). Some of them are hosted by volcanic rocks and others by granitoids, but most of them, including the largest deposits, occur associated with altered volcanic rocks in tectonic contact with granitoids within the north-trending Atacama mega-fault zone. The iron belt coincides spatially with this zone, and individual orebodies are elongated parallel to it. Most of the granitoids are dioritic members of large plutons, and appear to postdate the lavas. The volcanic host rock is dominated by basaltic to andesitic lava flows. The lavas away from ore deposits and granitoids are affected by non-deformational regional metamorphism, usually at prehnite-pumpellyite facies. Available radiometric ages of the rocks associated with the ores fall in the range of 100 to 128 Ma (Vivallo et al., 1995b).

Pyrite and less abundant chalcopyrite occur as dissemination and veinlets in the magnetite orebodies. The grade of the alteration, as reflected by extensive development of actinolite, is higher near large orebodies. The imprint of a subsequent episode of extensive silicic-argillic alteration is evident in the outer zone, and albite, K-feldspar (or biotite), and tourmaline are also present. The hydrothermally altered host rocks display a mineralogical and geochemical zonation around the iron orebodies, with an internal halo of actinolitised rocks passing outward into quartz-feldspar (albite, K-feldspar or biotite) alteration and silicified ± tourmalinised rocks (Vivallo et al., 1995a; Vivallo and Henríquez, 1997, 1998). As a result of the hydrothermal activity, the original textures of the volcanic rocks have been obliterated and hydrothermal breccias have been formed. Breccias located close to the orebodies are typically composed of magnetite, actinolite, and sulphides (mostly pyrite). Other ore breccias, composed of specularite hematite and sulphides (mostly pyrite and chalcopyrite), occur further away from massive ore. Quartz-feldspar alteration is commonly found in these breccias. The mineralogical and geochemical zoning around the iron orebodies reflect thermal and compositional gradients in the hydrothermal fluids during and after the emplacement of the massive iron orebodies (Vivallo et al., 1995a).

Mineralisation Associated with Magmatic Iron-oxide Deposits in Chile

No Cu-Au mineralisation has been reported from El Laco, but there are anomalous values of Au and U in areas affected by hydrothermal alteration, and pyrite has been found in a drill core at Pasos Blancos south of Pico Laco. A gold prospect, El Perro, is spatially related to the magmatic iron ore at Magnetita Pedernales (Grez et al., 1991). In the Coastal Cordillera, iron-oxide-Cu mineralisation can be divided into a northern group (18° to 26° S) and southern group (26° to 32° S) according to the concentrations of Au and Ag, the age of the host rocks, and the genetic relationship with tectonic and magmatic events (Henríquez and Vivallo, 2000).

Deposits Located Between 18° and 26° S

The Cu-mineralisation associated with iron deposits in this segment are related to Jurassic and Cretaceous magmatic arcs and the Atacama fault system (Espinoza, et al., 1996). The Jurassic deposits are veins in gabbroic to granitic intrusive rocks, and stratiform bodies ("mantos") and breccia pipes in basalts and andesites of the La Negra Formation. Vein deposits hosted by intrusive rocks consist of Fe-Cu-Au mineralisation with magnetite, pyrite, chalcopyrite, actinolite and scarce apatite as primary minerals. Examples of these deposits are Toldo-Velarde, Montecristo and Mina Julia (Figure 1). The veins range from tens of metres to 2 km in length, from 1 to 12 m in width, and they are up to 700 m deep. They are fault-controlled and the mineralisation shows a vertical supergene zonation with an upper Cu-oxide zone, followed by a secondary enrichment level, and hypogene mineralisation at depth. The primary mineralisation is also vertically zoned: magnetite and actinolite increase with depth, whereas quartz and specularite are more abundant in the upper levels. Alteration halos with albite, quartz, chlorite, actinolite and sericite surround the veins.

The stratiform bodies consist of Cu ± Ag mineralisation with a lower Fe content than the veins. The host rocks are mainly andesitic to basaltic lava flows; dacites-rhyolites and andesites host the mineralisation at one deposit, Mantos Blancos. The mineralisation shows a vertical zonation similar to that of the vein deposits: copper-oxide minerals in the upper part are followed by a mixed zone with copper-oxides and sulphides, and a primary sulphide zone at depth. Hypogene mineralisation consists of bornite, chalcocite and chalcopyrite with specularite, pyrite, quartz and calcite as gangue minerals. The host rocks are altered and contain albite, chlorite, epidote and quartz.

Mineral-chemical and isotopic (Pb, S, C) studies, radiometric dating, and spatial relationships between the two types of deposits suggest a common hydrothermal origin related to Jurassic granitoids (Vivallo and Henríquez, 1998). The vein mineralisation was deposited in a high-temperature, plutonic environment, from neutral to slightly alkaline, magmatic solutions in equilibrium with magnetite, as shown by the association of magnetite, sulphides, and albite or potassic feldspar. These hydrothermal fluids moved up to a near-surface volcanic environment characterised by lower temperature and higher oxygen fugacity, with hematite as the stable phase, to form stratiform deposits (Vivallo and Henríquez, 1998).

Deposits Located Between 26° to 32° S

As in the previous segment, the distribution of the Fe-Cu-Au deposits is related to the evolution of Jurassic-Cretaceous magmatic arcs and especially to the Atacama fault system. In addition, there is a relationship with the iron orebodies of the Cretaceous iron belt. Manganese deposits are also spatially related to the iron and sulphide ores (Henríquez and Vivallo, 2000).

The Fe-Cu-Au deposits consist of veins, hydrothermal and tectonic breccias, and stratabound bodies hosted by Jurassic and Lower Cretaceous volcanic rocks; examples are Candelaria (Ryan et al., 1995), Manto Verde (Vila et al., 1997; Gelcich and Ugalde, 1997), Punta del Cobre (Marschick et al., 2000), and Panulcillo (Hopper and Correa, 2000) (Figure 1). Magnetite and/or hematite, variable amounts of pyrite and chalcopyrite, and traces of molybdenite and arsenopyrite characterise the primary ore. Common gangue minerals are actinolite, quartz, albite, K-feldspar and calcite. Most of the deposits show a vertical, primary zonation defined by an increasing Fe/Cu ratio with depth. Mineralogically, this zonation is represented by magnetite at depth, passing successively to magnetite-pyrite, pyrite-magnetite-chalcopyrite, and specularite-pyrite-chalcopyrite at higher levels. Supergene oxidation processes were important in some deposits (eg., Manto Verde), resulting in oxidation minerals of higher copper grade. Ore breccias with abundant specularite in the matrix are found in most of these deposits. The host rocks of the Fe-Cu-Au mineralisation and the Cretaceous iron deposits show the same alteration characterised by a zonal arrangement around the iron orebodies (Figure 10): an inner zone of actinolitised rocks passes outward into albitised (or K-feldspar-rich) rocks; outside these zones the rocks are silicified and locally contain tourmaline; this silicification generally overprints the actinolitised and albitised rocks. Some districts have an additional zone of quartz-sericitic alteration. Garnet and pyrrhotite are present in some districts (Panulcillo).

Based on field, textural and geochemical relationships, two main hydrothermal events are suggested (Vivallo et al., 1995a, b). The first event is characterised by neutral to slightly alkaline, high-temperature solutions, rich in Mg, Fe, Ca, CO_2, F, P, Cl, which produced the actinolitisation and albitisation in the rocks hosting the iron ores. This hydrothermal activity is related to the emplacement of the iron orebodies, which released volatiles rich in Cl, capable of remobilising Cu and Au originally contained in magnetite. A second hydrothermal stage, overprinting the first, consists of neutral to slightly acid hydrothermal solutions of lower temperature, rich in silica, F and B, resulting in an outer zone of silicified ± tourmalinised rocks.

Manganese deposits (eg., Venus, Coquimbana) composed of Mn-oxides, subordinate magnetite, and chert occur in many iron districts situated in limestones immediately overlying the volcanic rocks containing Fe ores and Fe-Cu-Au mineralisation (Henríquez et al., 2000). They appear to represent a last, volcanic-exhalative stage in the evolution of the mineralisation system with magmatic iron ore and hydrothermal Fe-Cu-Au schematically depicted in Figure 10.

Conclusions and Implications

The field relationships and the well-preserved volcanic structures and textures at El Laco indicate that the main, massive orebodies were crystallised from volatile-rich, iron-oxide magmas, and that the nearby magnetite-pyroxene and magnetite-apatite veins were formed at high temperature from magmatic fluids released from the crystallising magmas. All of the available analytical data are consistent with a magmatic origin for these deposits. There is no evidence to suggest that any of the iron orebodies at El Laco were produced by hydrothermal fluids. The clear evidence for iron-oxide magmas at El Laco suggests that a magmatic origin should be considered for other similar, less-well-preserved, deposits. The nature of such volatile-rich magmas is that they alter their host rock during emplacement and crystallisation. As such, even orebodies with alteration halos and gradational contacts may have formed from iron-oxide magmas. In other localities, hydrothermal breccias and vein deposits may be related to the degassing of an iron-oxide magma at depth.

Economic and subeconomic concentrations of Cu, Au, U, and REE are often associated with iron-oxide-apatite ores, either within the iron-oxide orebodies, or occurring nearby as breccias, veins, or stockworks, or in areas without known magnetite-apatite deposits. From an exploration standpoint it is important to determine if a Cu-(Au-U-REE) deposit is associated with the intrusion or eruption of iron-oxide magma, or unrelated to such magma and formed from hydrothermal processes alone. Iron-oxide magmas that have vented to the surface as ignimbrites, airfall ash, or lavas are less likely to have associated Cu or Au mineralisation because these elements are likely to be partially lost during degassing. Exploration targets for these "vented" systems will be at depth below the iron ores. U and REE are less likely to escape in the vented gases and may be present within the iron orebodies. Iron-oxide magmas that have intruded as sills or dykes are more likely to have associated Cu, U, Au, or REE mineralisation within, adjacent to, or stratigraphically above the iron ores, although additional mineralisation at depth can not be ruled out. Systems, formed by hydrothermal solutions, may have Cu, U, Au, or REE mineralisation as well. In these deposits, Cu, U, Au, and REE distribution will be most likely controlled by fluid circulation pathways, temperature gradients, host-rock compositions and permeabilities, and fluid mixing within the hydrothermal system, but may be derived from an iron-oxide magma at depth.

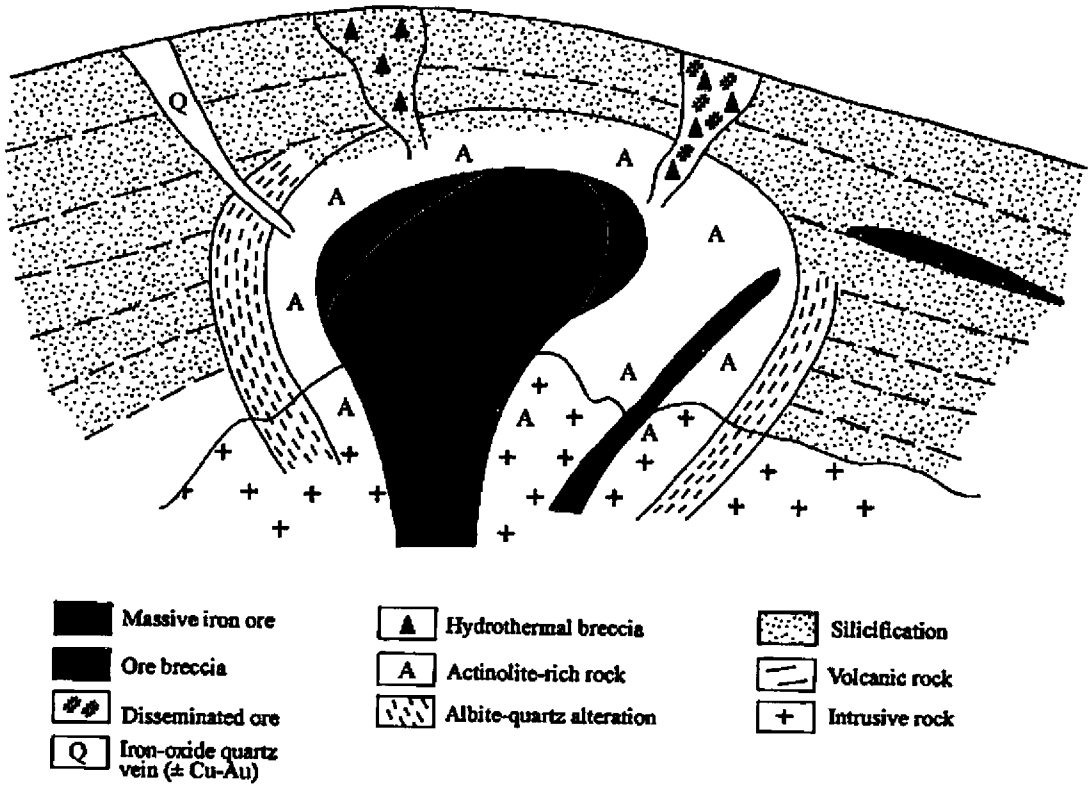


Figure 10: Model of the alteration zone distribution and Fe-Cu-Au mineralisation around magnetite-apatite orebodies based on the Cretaceous iron belt in Chile.

Acknowledgements

This paper summarises the results of many years of research during which the authors have had discussions with numerous colleagues that have helped to shape our thinking about these deposits. Recent discussions with Hugo Aguirre, Ramón Aguirre, Heriberto Fortín, Greg Lester, Beatriz Levi, Donald Lindsley, Haroldo Lledó, José Antonio Naranjo, Vinicio Travisany, Leonardo Vergara, and Gonzalo Yañez have been particularly helpful. The help of the Compañía Minera del Pacifico, Chile is gratefully acknowledged. This research has been partly supported by the U.S. Fulbright Commission, by National Science Foundation grant EAR-9814761 to HRN, by FONDICYT grants 1950571 and 1970671 to FH and WV, by DICYT grant 05-97-15HB to FH, by Servicio Nacional de Geología y Minería de Chile, and by the Swedish Natural Science Research Council grant GU 04535-301 to JON.

References

Bai, G. & Yuan, Z.X., 1983 - On the genesis of the Bai Yun Obo ore deposit, *Chinese Academy of Geological Science, Institute of Mineral Deposits, Bulletin* 4, 1-17.

Barton, M.D. & Johnson, D.A., 1996 - Evaporitic-source model for igneous-related Fe-oxide-(REE-Cu-Au-U) mineralization, *Geology* 24, 259-262.

Boudreau, A.E., 1995 - Fluid evolution in layered intrusions: evidence from the chemistry of the halogen-bearing minerals; *in* Thompson, J.F.H. (ed.), Magmas, fluids, and ore deposits, *Mineralogical Association of Canada, Short Course Series* 23, 25-45.

Broman, C., Nyström, J.O., Henríquez, F. & Elfman, M., 1999 - Fluid inclusions in magnetite-apatite ore from a cooling magmatic system at El Laco, Chile, *GFF* 121, 253-267.

Buddington, A.F. & Lindsley, D.H., 1964 - Iron-titanium oxide minerals and synthetic equivalents, *Journal of Petrology* 5, 310-357.

Chiba, H., Chacko, T., Clayton, R.N., & Goldsmith, J.R., 1989 - Oxygen isotope fractionations involving diopside, forsterite, magnetite, and calcite: Application to geothermometry, *Geochimica et Cosmochimica Acta* 53, 2985-2995.

Chou, I.M. & Eugster, H.P., 1977 - Solubility of magnetite in supercritical chloride solutions, *American Journal of Science* 277, 1296-1314.

Crerar, D., Scott, W. & Brantley, S., 1985 - Chemical controls on solubility of ore-forming minerals in hydrothermal solutions, *Canadian Mineralogist* 23, 333-352.

Crocker, I.T., 1985 - Volcanogenic fluorite-hematite deposits and associated pyroclastic rock suite at Vergenoeg, Bushveld complex, *Economic Geology* 80, 1181-1200.

Einaudi, M.T. & Oreskes, N., 1990 - Progress towards an occurrence model for Proterozoic iron oxide deposits - a comparison between the ore provinces of South Australia and southeast Missouri; *in* Pratt, W.P. & Sims, P.K., (eds.), The midcontinent of the United States - permissive terrane for an Olympic Dam-type deposit?, *U.S. Geological Survey Bulletin* 1932, 58-69.

Espinoza, S., Vivallo, W. & Henríquez, F., 1994 - Geología y genésis de mineralización metálica en el distrito ferrífero de Cerro Imán, Copiapó, Chile. *VII Congreso Geológico Chileno, Actas* 2, 799-802.

Espinoza, S., Véliz, G.H., Esquivel, L.J., Arias, F.J. & Moraga, B.A., 1996 - The cupriferous province of the Coastal Range, Northern Chile; *in* Camus, F., Sillitoe, R.H. & Petersen, R, (eds.), Andean copper deposits: new discoveries, mineralization, styles and metallogeny, *Society of Economic Geologists Special Publication* 5, 19-32.

Eugster, H.P. & Chou, I.M., 1979 - A model for the deposition of Cornwall type magnetite deposits, *Economic Geology* 74, 763-774.

Foose, M.P. & McLelland, J.M., 1995 - Proterozoic low-Ti iron-oxide deposits in New York and New Jersey: Relation to Fe-oxide (Cu-U-Au-rare earth element) deposits and tectonic implications, *Geology* 23, 665-668.

Förster, H. & Jafarzadeh, A., 1994 - The Bafq mining district in central Iran - a highly mineralized Infracambrian volcanic field, *Economic Geology* 89, 1697-1721.

Frutos, J., 1990 - The Andes Cordillera: A synthesis of the geologic evolution; *in* Fontboté, L., Amstrutz, G.C., Cardozo, M., Cedillo, E. & Frutos, J., (eds.), Stratabound ore deposits in the Andes, *Springer-Verlag, Berlin*, 3-35.

Frutos, J. & Oyarzún, J., 1974 - Tectonic and geochemical evidence concerning the genesis of El Laco magnetite lava flow deposits, Chile, *Economic Geology* 70, 988-990.

Frutos, J., Oyarzún, J., Shiga, Y. & Alfaro, G., 1990 - The El Laco magnetite lava flow deposits, Northern Chile: An up-to-date review and new data; *in* Fontboté, L., Amstrutz, G.C., Cardozo, M., Cedillo, E. & Frutos, J., (eds.), Stratabound ore deposits in the Andes, *Springer-Verlag, Berlin*, 681-690.

Gelcich, S. & Ugalde, H., 1997- Anomalía magnética dipolar en el distrito Los Pozos (Mina Manto

Verde), Provincia de Chañaral: su relación a los yacimientos de Fe y Cu-Fe-Au, *VIII Congreso Geológico Chileno, Actas* 2, 983-987.

Gibbon, D.L. & Tuttle, O.F., 1967 - A note on the system FeO-Fe_2O_3-SiO_2-H_2O, *American Mineralogist* 52, 886-889.

Gleason, J.D., Marikos, M.A., Barton, M.D. & Johnson, D.A., 2000 - Neodymium isotopic study of rare earth element sources and mobility in hydrothermal Fe oxide (Fe-P-REE) systems, *Geochimica et Cosmochimica Acta* 64, 1059-1068.

Grez, E., Aguilar, A., Henríquez, F. & Nyström, J.O., 1991 - Magnetita Pedernales: a new magmatic iron deposit in northern Chile, *Economic Geology* 86, 1346-1349.

Haggerty, S.E., 1970 - The Laco magnetite lava flow, Chile, *Carnegie Institution of Washington Yearbook* 68, 329-330.

Harmon, R.S. & Hoefs, J., 1984 - Oxygen isotope ratios in Late Cenozoic Andean volcanics; *in* Harmon, R.S. & Barreirro, B.A. (eds.), Andean magmatism, chemical and isotopic constraints, *Shiva Publishing Ltd.*, 9-21.

Hauck, S.A., 1990 - Petrogenesis and tectonic setting of middle Proterozoic iron oxide-rich ore deposits - an ore deposit model for Olympic Dam-type mineralization; *in* Pratt, W.P. & Sims, P.K., (eds.), The midcontinent of the United States - permissive terrane for an Olympic Dam-type deposit, *U.S. Geological Survey Bulletin* 1932, 4-39.

Haynes, D.W., Cross, K.C., Bills, R.T. & Reed, M.H., 1995 - Olympic Dam ore genesis: a fluid-mixing model, *Economic Geology* 90, 281-307.

Henríquez, F. & Martin, R.F., 1978 - Crystal growth textures in magnetite flows and feeder dykes, El Laco, Chile, *Canadian Mineralogist* 16, 581-589.

Henríquez, F. & Nyström, J.O., 1998 - Magnetite bombs at El Laco volcano, Chile, *GFF* 120, 269-271.

Henríquez, F., Dobbs, F., Espinoza, S., Nyström, J., Travisany, V. & Vivallo, W., 1994 - Origin of Chilean magnetite-apatite ore deposits, *VII Congreso Geológico Chileno, Actas* 1, 822-824.

Henríquez, F. & Vivallo, W., 2000 – Unidades metalogénicas y estilos de mineralización en la Cordillera de la Costa Chilena: una revision, *IX Congreso Geológico Chileno, Actas* 2, 127-128.

Henríquez, F., Dobbs, F.M., Naslund, H.R., Nyström, J.O. & Travisany, V., 2000 - Yacimientos de Fe estratiformes de Sierra Bandera, Distrito Huantemé-Los Colorados, III Región, *IX Congreso Geológico Chileno, Actas* 2, 123-126.

Hildebrand, R.S. 1986 - Kiruna-type deposits. Their origin and relationship to intermediate subvolcanic plutons in the Great Bear magmatic zone, Northwest Canada, *Economic Geology* 81, 640-659.

Hitzman, M.W., 2000 - Iron oxide-Cu-Au deposits: What, where, when, and why; *in* Porter, T.M., (ed.), Hydrothermal iron oxide copper-gold and related deposits: A global perspective, *Australian Mineral Foundation, Adelaide*, 9-25.

Hitzman, M.W., Oreskes, N. & Einaudi, M.T., 1992 - Geological characteristics and tectonic setting of Proterozoic iron oxide (Cu-U-Au-REE) deposits, *Precambrian Research* 58, 241-287.

Hopper, D. & Correa, A., 2000 - The Panulcillo and Teresa de Colmo copper deposits: Two contrasting examples of Fe-Ox Cu-Au mineralization from the Coastal Cordillera of Chile, *in* Porter, T.M. (ed.), Hydrothermal iron oxide copper-gold & related deposits: A global perspective, *Australian Mineral Foundation, Adelaide*, 177-189.

Kisvarsanyi, E.B., 1990 - General features of the St. Francis and Spavinaw granite-rhyolite terranes and the Precambrian metallogenic region of Southeast Missouri; *in* Pratt, W.P. & Sims, P.K., (eds.), The mid-continent of the United States - permissive terrane for an Olympic Dam-type deposit, *U.S. Geological Survey Bulletin* 1932, 48-57.

Kyser, T.K., Lesher, C.E. & Walker, D., 1998 - The effects of liquid immiscibility and thermal diffusion on oxygen isotopes in silicate liquids, *Contributions to Mineralogy and Petrology* 133, 373-381.

Larocque, A.C.L., Stimac, J.A., Keith, J.D. & Huminicki, M.A.E., 2000 - Evidence for open-system behavior in immiscible Fe-S-O liquids in silicate magmas: Implications for contributions of metals and sulfur to ore-forming fluids, *Canadian Mineralogist* 38, 1233-1249.

Larson, A.C. & Oreskes, N., 1993 - Evidence of vapor-phase transport in the genesis of magnetite deposits at El Laco, Chile, *EOS Transactions of the American Geophysical Union* 74, 651.

Larson, A.C., 1994 - Evidence of pneumatolytic processes in the genesis of magnetite deposits at El Laco, Chile. M.Sc. thesis, *Dartmouth College, Hanover, New Hampshire*, 51p.

Lester, G.W., 2002 - The effects of excess H_2O and H_2O in combination with F, Cl, S or P on liquid immiscibility in the system Si-Fe-Al-K-O at 2 KBar: Implications for the generation of Fe-oxide magmas. M.Sc. thesis, *State University of New York, Binghamton, New York*, 66p.

Lindgren, W., 1933 - Mineral deposits, *McGraw-Hill, New York*, 930 p.

Lindsley, D. H., 1983 - Pyroxene thermometry, *American Mineralogist* 68, 477-493.

Maksaev, V., Gardeweg, M., Ramírez, C.F. & Zentilli, M., 1988 - Aplicación de método trazas de fisión a la datación de cuerpos de magnetita de El Laco e Incahuasi en el Altiplano de la Región de Antofagasta, *V Congreso Geológico Chileno, Actas* 1, B1-B23.

Marikos, M.A., Nuelle, L.M. & Seeger, C.M., 1990 - Geologic mapping and evaluation of the Pea Ridge iron ore mine (Washington County, Missouri) for rare-earth element and precious metal potential - a progress report; *in* Pratt, W.P. & Sims, P.K., (eds.), The mid-continent of the United States - permissive terrane for an Olympic Dam-type deposit?, *U.S. Geological Survey Bulletin* 1932, 4-39.

Marschick, R., Leveille, R.A. & Martin, W., 2000 - La Candelaria and the Punta del Cobre District, Chile: Early Cretaceous iron-oxide Cu-Au (Zn-Ag) mineralization; *in* Porter, T.M. (ed.), Hydrothermal iron oxide copper-gold & related deposits: A global perspective, *Australian Mineral Foundation, Adelaide*, 163-175.

McBirney, A.R. & Naslund, H.R., 1990 - The differentiation of the Skaergaard intrusion, a discussion of Hunter and Sparks (Contributions to Mineralogy and Petrology 95:451-461), *Contributions to Mineralogy and Petrology* 104, 235-240.

Naldrett, A., 1989 - Magmatic sulfide deposits. *Oxford University Press, Oxford*, 186 p.

Naslund, H.R., 1983 - The effect of oxygen fugacity on liquid immiscibility in iron-bearing silicate melts, *American Journal of Science* 283, 1034-1059.

Naslund, H.R., Dobbs, F.M., Henríquez, F.J. & Nyström, J.O., 1997 - Irrefutable evidence for the eruption of iron-oxide magmas at El Laco volcano, Chile, *EOS Transactions of the American Geophysical Union* 78, S333.

Naslund, H.R., Dobbs, F.M., Henríquez, F.J. & Nyström, J.O., 1998 - Evidence for iron-oxide magmas at El Laco, Chile, *Geological Society of America, Abstracts with Program* 30, (7), A-91.

Nyström, J.O. & Henríquez, F., 1994 - Magmatic features of iron ores of the Kiruna type in Chile and Sweden: Ore textures and magnetite geochemistry, *Economic Geology* 89, 820-839.

Nyström, J.O. & Henríquez, F., 1995 - Magnetite features of iron ores of the Kiruna type in Chile and Sweden: ore textures and magnetite geochemistry - a reply, *Economic Geology* 90, 473-475.

Nyström, J.O., Billström, K., Henríquez, F. & Fallick, A.E., 2002 - Oxygen isotope composition of magnetite in iron ores of the Kiruna type, (*submitted*).

Oreskes, N. & Einaudi, M.T, 1990 - Origin of rare earth element enriched hematite breccias at the Olympic Dam Cu-U-Au-Ag deposit, Roxby Downs, South Australia, *Economic Geology* 85, 1-28.

Oreskes, N. & Einaudi, M.T, 1992 - Origin of hydrothermal fluids at Olympic Dam: preliminary result from fluid inclusions and stable isotopes, *Economic Geology* 87, 64-90.

Oreskes, N., Rhodes, A.L., Rainville, K., Sheets, S.A., Espinoza, S. & Zentilli, M., 1994 - Origins of magnetite deposits at El Laco, Chile: new evidence from field studies, fluid inclusions, stable isotopes, and fission track analysis, *Geological Society of America, Abstracts with Program* 26, A379.

Oreskes, N., Rhodes, A.L., Sheets, S.A. & Espinoza, S., 1995 - Evidence for formation of magnetite by hydrothermal processes at El Laco, Chile, Part I: Field relations and alteration assemblages, *Geological Society of America, Abstracts with Program* 27, A467.

Park, C.F. Jr., 1961 - A magnetite "flow" in northern Chile, *Economic Geology* 56, 431-441.

Philpotts, A.R., 1967 - Origin of certain iron-titanium oxide and apatite rocks, *Economic Geology* 62, 303-315.

Porter, T.M., 2000 - Hydrothermal iron oxide copper-gold & related deposits: a global perspective, *Australian Mineral Foundation, Adelaide*, 349 p.

Ramdohr, P., 1980 - The ore minerals and their intergrowths, (2nd edition), *Pergamon Press*, 1205 p.

Rhodes, A.L., 1996 - Geology and geochemistry of the El Laco magnetite deposits, Chile. Ph.D. thesis, *Dartmouth College, Hanover*, 198p.

Rhodes, A.L. & Oreskes, N., 1995a - Magnetite deposition at El Laco, Chile: Implications for Fe-oxide formation in magmatic-hydrothermal systems; *in* Clark, A.H., (ed.), Giant ore deposits II: Controls on the scale of orogenic magmatic-hydrothermal mineralization, *Proceedings of the Second Giant Ore Deposits Workshop, Kingston, Ontario*, 582-622.

Rhodes, A.L. & Oreskes, N., 1995b - Evidence for formation of magnetite by metasomatic alteration of host rock andesite, El Laco, Chile, Part II: Rare earth (REE) trace element, and oxygen isotope data, *Geological Society of America, Abstracts with Program* 27, A467.

Rhodes, A.L. & Oreskes, N., 1996 - Magnetite deposits at El Laco, Chile: a transition between magmatic and epithermal processes or all hydrothermal?, *Geological Society of America, Abstracts with Program* 28, A335.

Rhodes, A.L. & Oreskes, N., 1999 - Oxygen isotope composition of magnetite deposits at El Laco,

Chile: Evidence of formation from isotopically heavy fluids; *in* Skinner, B.J. (ed.), Geology and ore deposits of the Central Andes, *Society of Economic Geologists Special Publication* 7, Littleton, Co., 333-351.

Rhodes, A.L., Oreskes, N. & Sheets, S.A., 1997 - Recognition of a paleo-hydrothermal system responsible for magnetite formation at El Laco, Chile, *EOS Transactions of the American Geophysical Union* 78, F748.

Rhodes, A.L., Oreskes, N. & Sheets, S.A., 1999 - Geology and rare earth element geochemistry of magnetite deposits at El Laco, Chile; *in* Skinner, B.J. (ed.), Geology and ore deposits of the Central Andes, *Society of Economic Geologists Special Publication* 7, Littleton, Co., 299-332.

Roberts, D.E. & Hudson, G.R.T., 1983 - The Olympic Dam copper-uranium-gold deposit, Roxby Downs, South Australia, *Economic Geology* 78, 799-822.

Rogers, D.P., 1969 - The extrusive iron oxide deposits, "El Laco", Chile, *Geological Society of America, Special Paper* 121, 700.

Rojas, M.G. & Henríquez, F., 1994 - Contenido y distribución de tierras raras en apatitas del yacimiento de hierro El Algorrobo, III Región, *VII Congreso Geológico Chileno, Actas* 2, 1177-1178.

Rose, L.A. & Brenan, J.M., 2001 - Wetting properties of Fe-Ni-Co-Cu-O-S melts against olivine: Implications for sulfide melt mobility, *Economic Geology* 96, 145-157.

Ryan, P.J., Lawrence, A.L, Jenkins, R.A., Matthews, J.P., Zamora, J.C., Marino, E. & Urqueta, I., 1995 - The Candelaria copper-gold deposit, Chile; *in* Pierce, F.W. and Bolm, J.G. (eds.), Porphyry copper deposits of the American Cordillera, *Arizona Geological Society Digest* 20, 625-645.

Sheets, S.A., Oreskes, N., Rhodes, A.L., Bodnar, R.J. & Szabo, C., 1997 - Fluid inclusion evidence for hydrothermal origin for magnetite-apatite mineralization at El Laco, Chile, *Geological Society of America, Abstracts with Program* 29, A50.

Tassara, A., 1997 - Segmentación andina desde el análisis flexural de la anomalía de Bouger. M.Sc. thesis, *Universidad de Chile, Santiago*, 140 p.

Thomas, A., 1970 - Beitrag zur Tektonik Nordchiles, *Geologische Rundschau* 59, 1013-1027.

Travisany, V., Henríquez, F. & Nyström, J.O., 1995 - Magnetite lava flows in the Pleito-Melón district of the Chilean iron belt, *Economic Geology* 90, 438-444.

Vila, T., Lindsay, N. & Zamora, R., 1997 - Geology of Manto Verde copper deposit, Northern Chile: a specularite-rich hydrothermal-tectonic breccia related to the Atacama Fault Zone; *in* Camus, F., Sillitoe, R.H. & Peterson, R. (eds.), Andean copper deposits: New discoveries, mineralization, style and metallogeny, *Society of Economic Geologists, Special Publication* 5, 157-169.

Visser, W. & Koster van Groos, A.F., 1979 - Effects of P_2O_5 and TiO_2 on liquid-liquid equilibria in the system K_2O-FeO-Al_2O_3-SiO_2, *American Journal of Science* 279, 970-988.

Vivallo, W. & Henríquez, F., 1997 - Relación genética entre los yacimientos estratoligados de Cu ("Tipo Manto"), de Cu-Fe-Au y de hierro del tipo Kiruna, *VIII Congreso Geológico Chileno, Actas* 2, 1189-1193.

Vivallo, W. & Henríquez, F., 1998 - Génesis común de los yacimientos estratoligados y vetiformes del Jurásico Medio a Superior en la Cordillera de la Costa, Región de Antofagasta, Chile, *Revista Geológica de Chile* 25, 199-228.

Vivallo, W., Espinoza, S. & Henríquez, F., 1993a - Magnetite-apatite type iron ore and gold mineralization in the Cerro Negro Norte district, Chile; *in* Fenoll Hach-Alí, Torres-Ruiz and Gervilla (eds.), Current research in geology applied to ore deposits, *University of Granada, Granada, Spain*, 587-590.

Vivallo, W., Henríquez, F. & Espinoza, S., 1993b - Hydrothermal alteration and related mineralization at El Laco mining district, northern Chile, Low-temperature metamorphism, processes, products and economic significance, *Symposium, IGCP Project 294, Santiago, Chile*, 142-146.

Vivallo, W., Espinoza, S. & Henríquez, F., 1994a - Significado de la distribución del oro en menas y rocas de caja en los depósitos de hierro de los distritos Cerro Negro Norte y Cerro Imán, Chile, *VII Congreso Geológico Chileno, Actas* 2, 926-930.

Vivallo, W., Henríquez, F. & Espinoza, S., 1994b - Oxygen and sulfur isotopes in hydrothermally altered rocks and gypsum deposits at El Laco mining district, northern Chile, *Revista Comunicaciones* 45, 93-100.

Vivallo, W., Espinoza, S. & Henríquez, F., 1994c - Geología y mineralización del distrito ferrífero Cerro Imán, Copiapó, Chile, *Revista Geológica de Chile* 21, 197-212.

Vivallo, W., Espinoza, S. & Henríquez, F., 1995a - Metasomatismo y alteración hidrotermal en el Distrito Ferrífero Cerro Negro Norte, Copiapó, Chile, *Revista Geológica de Chile* 22, 75-88.

Vivallo, W., Espinoza, S. & Henríquez, F., 1995b - Los depósitos de hierro del tipo magnetita-apatita: geoquímica de las rocas volcánicas asociadas y potencialidad de la mena de hierro como fuente de mineralización de oro, *Revista Geológica de Chile* 22, 159-175.

Weidner, J.R., 1982 - Iron-oxide magmas in the system Fe-C-O, *Canadian Mineralogist* 20, 555-566.

Whitney, J.A., Hemley, J.J. & Simon, F.O., 1985 - The concentration of iron in chloride solutions equilibrated with synthetic granite compositions: the sulfur-free system, *Economic Geology* 80, 444-460.

PGC PUBLISHING

Grainger, C.J., Groves, D.I. & Costa, C.H.C., 2002 - The Epigenetic Sediment Hosted Serra Pelada Au-PGE Deposit and Its Potential Genetic Association with Fe-Oxide Cu-Au Mineralisation, Amazon Craton, Brazil; *in* Porter, T.M. (Ed.), Hydrothermal Iron Oxide Copper-Gold and Related Deposits: A Global Perspective, Volume 2; *PGC Publishing, Adelaide*, pp 227-245.

THE EPIGENETIC SEDIMENT-HOSTED SERRA PELADA AU-PGE DEPOSIT AND ITS POTENTIAL GENETIC ASSOCIATION WITH FE-OXIDE CU-AU MINERALISATION WITHIN THE CARAJÁS MINERAL PROVINCE, AMAZON CRATON, BRAZIL

[1]Christian J. Grainger, [1]David I. Groves and [2]Carlos H.C. Costa

[1]*Centre for Global Metallogeny, Department of Geology and Geophysics, University of Western Australia, Crawley, WA, Australia.*
[2]*Companhia Vale do Rio Doce (CVRD), Serra dos Carajás, Parauapebas, PA, Brazil.*

Abstract - The Serra Pelada Au-PGE deposit is located within the Carajás Mineral Province of the southeastern Amazon Craton, Brazil. Gold-PGE ores are epigenetic and display a strong structural control, being hosted in sub-greenschist facies carbonaceous and calcareous meta-siltstone, within the hinge zone of a reclined, tight, regional-scale F2 synform. Although the entire orebody has undergone deep tropical weathering, some evidence of the original hydrothermal alteration is preserved. Gold-PGE mineralisation is associated with the formation of magnetite- and hematite-rich hydrothermal breccias, massive zones of hematite metasomatism, intense sericite (white mica)-kaolin metasomatism, siderite veining and a jasperoid envelope of amorphous silica alteration hosting rare disseminated pyrite. All other Au-PGE ore-related mineral assemblages have undergone intense weathering to hydrated Fe-oxides and secondary clay minerals, preventing further description of primary ore and alteration features. The geochemistry of the primary Au-PGE ores at Serra Pelada displays many similarities to that of Fe-oxide Cu-Au deposits within the Carajás Mineral Province, and indeed world-wide, in terms of metal association (e.g., Co, Ni, Cu, U), LREE enrichment and accompanying Fe-metasomatism. The Au-Pd-Pt association also suggests ore metal transport in acid, oxidising, chloride-rich fluids, similar to those for Fe-oxide Cu-Au deposits. In combination with these similarities, and the location of the Serra Pelada Au-Pd-Pt deposit, it is suggested that the latter represents a distal equivalent to the Fe-oxide Cu-Au deposits and, as such, a target that may have been overlooked during exploration programs around such terrains globally.

Introduction

Serra Pelada, a world-class Au-PGE deposit, is located adjacent to a complex strike-slip system within the Itacaiúnas Belt of the northern Carajás Mineral Province, southeastern Amazon Craton, Brazil (Figs. 1 and 2). The Itacaiúnas Belt comprises an Archaean meta-volcano-sedimentary sequence, the Itacaiúnas Supergroup, intruded by a suite of granitic magmas ranging from Archaean to Proterozoic in age (Fig. 3). Originally identified in the 1960's as a major iron-ore province hosting the giant Carajás iron mines, the metallogenic province has more recently been recognised as a premier Cu-Au province, hosting a number of large (>300 Mt) Fe-oxide Cu-Au (±Mo±Ag±U±REE) deposits (e.g., Cristalino, Igarapé Bahia-Alemão, Salobo, Sossego).

Since the discovery of the Serra Pelada Au-PGE deposit in the early 1980's by garimperos, a local commune of miners and prospectors, it has been subjected to one of the largest gold rushes in South American history, being worked by more than 100 000 garimperos at the peak of production activity (Fig. 4). Although the deposit has been exploited sporadically for almost 20 years, exclusively by garimperos, very little scientific research has been carried out. The original metal content of the deposit has been difficult to calculate given the extensive working by garimperos. However, a current estimated resource, in the unmined portion of the deposit, is 56 t Au, 15 t Pd and 7 t Pt, grading 15.20 g/t Au, 4.09 g/t Pd and 1.89 g/t Pt (CVRD, 1998). Original pre-mining resources have been estimated at ~110 t Au, ~35t Pd and ~18 t Pt, although the uncertainty of these figures is high.

Previous scientific studies carried out on the Serra Pelada orebody and in the surrounding area include brief structural descriptions of the Au-PGE ore-hosting regional-scale synform exposed in the Serra Pelada open-pit and of the mine sequence geology (Jorge João *et al.*, 1982; Meireles and Teixeira, 1982; Lab and Costa, 1992; Pinheiro, 1997). Petrographic studies, mapping and drill-core analysis, by Tallarico *et al.* (2000a), led to their interpretation that the Serra Pelada deposit was genetically linked to an Archaean diorite and associated skarn mineralisation. They suggested that Serra Pelada constituted a unique mineral occurrence, distinct from the Fe-oxide Cu-Au deposits in the Carajás

Mineral Province. The object of this paper is to briefly describe the Serra Pelada deposit, and to examine its possible relationship to the Fe-oxide Cu-Au deposits in the Carajás Mineral Province. Field-based observations are stressed, together with geochemical data, although the extreme weathering of the entire deposit hinders application of many conventional analytical techniques.

Regional Setting

The Carajás Mineral Province comprises two Archaean tectonic blocks, the older southern Rio Maria granitoid-greenstone terrain (Fig. 3), represented by rocks of the Andorinhas Supergroup (Huhn *et al.*, 1988), and the northern Itacaiúnas Belt (Fig. 4; Araújo *et al.*, 1988). In contrast to typical granitoid-greenstone terrains, which are widely considered to have developed in arc and back-arc environments, rocks of the Itacaiúnas Supergroup of the Itacaiúnas Belt, display similarities to volcanic and sedimentary rock sequences developed on continental crust adjacent to rift zones (Olszewski *et al.*, 1989) or intracratonic basins (Machado *et al.*, 1991). Rocks of the Itacaiúnas Supergroup, which host the Serra Pelada Au-PGE deposit and the Carajás Fe-oxide Cu-Au deposits, form a structural province represented by the major E-W- to NNW-trending Carajás and Cinzento strike-slip systems (Figs 2 and 3). Transpressional to transtensional deformational phases throughout the Late Archaean, and transpressional reactivation of the Carajás and Cinzento strike-slip systems in Proterozoic times, dominate the tectonic evolution of the region (Pinheiro, 1997). Deposited during the Late Archaean (ca 2.75 Ga), the Itacaiúnas Supergroup consists of a sequence of volcano-sedimentary rocks, dominated by mafic volcanic rocks, metamorphosed to greenschist and amphibolite facies (Machado *et al.*, 1991). Unconformably overlying the volcano-sedimentary sequence are rocks of

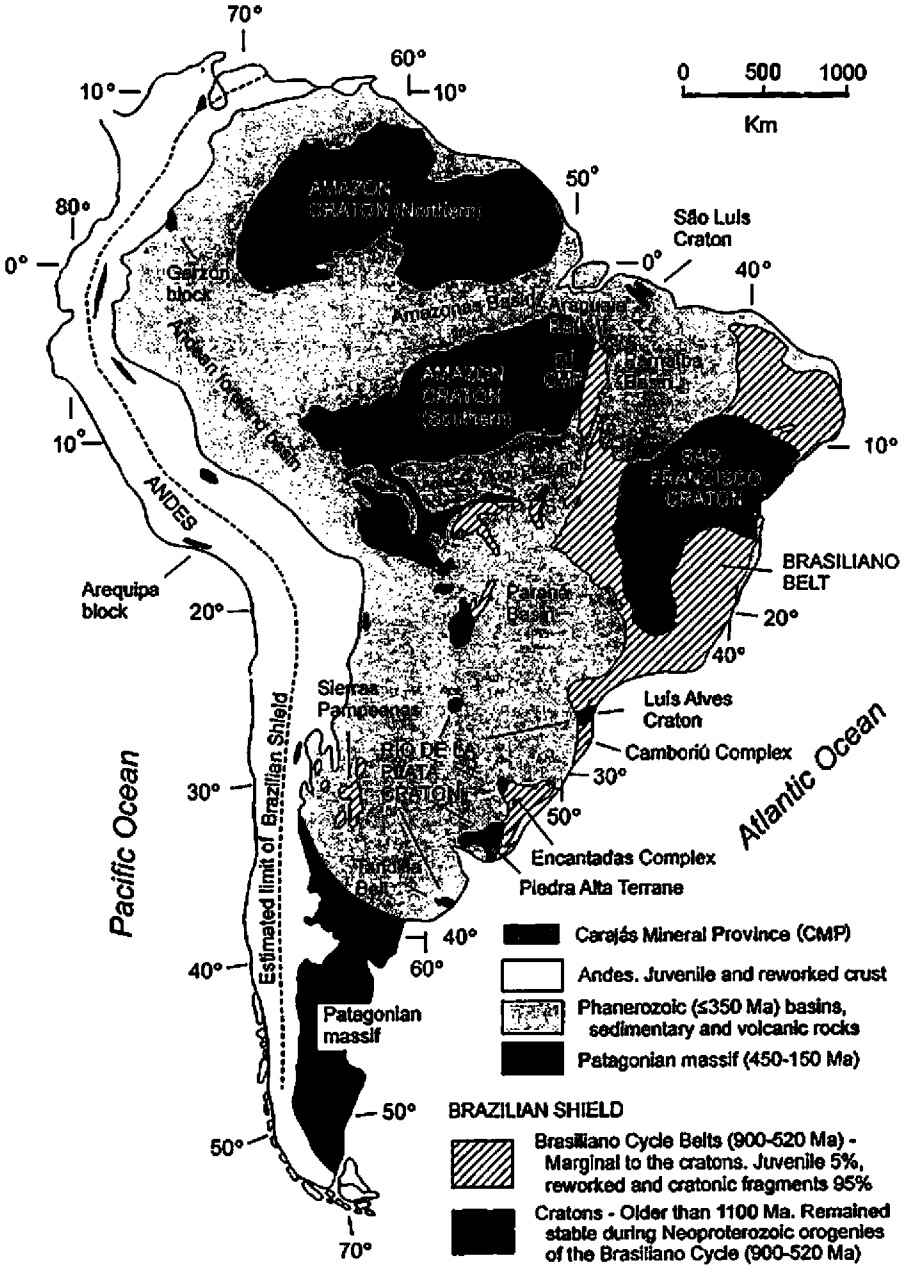


Figure 1: Geological map of the South American Platform showing the location of the Amazon Craton and the Carajás Mineral Province, designated CMP (after Hasui and Almeida, 1985).

the Aguas Claras and Rio Fresco Formations, extensive platform sequences of Archaean (ca 2.68 Ga) sandstones, conglomerates and siltstones, metamorphosed to lower greenschist and sub-greenschist facies (Trendall *et al.*, 1998). The supracrustal rocks of the Itacaiúnas Supergroup have been intruded by several Archaean to Proterozoic granitoids. These include calc-alkaline granitoids and diorites of the ca 2.74 Ga Plaquê Suite (Huhn *et al.*, 1999), the ca 2.57 Ga A-type Old Salobo granite/Estrela alkaline granitoid complex (Machado *et al.*, 1991; Barros *et al.*, 1997), and Paleoproterozoic alkaline to sub-alkaline A- and I-type granitoids of the ca 1.88 Ga Carajás Suite (Machado *et al.*, 1991). There are also ultramafic to mafic intrusions, including the ca 2.75 Ga Luanga mafic-ultramafic complex (Machado *et al.*, 1991).

The Rio Maria granitoid-greenstone terrain and the Itacaiúnas Belt can be differentiated in terms of both their geological setting and associated mineral deposits. The Itacaiúnas Belt is unusual for an Archaean greenstone belt in that it contains a number of Fe-oxide Cu-Au (±Mo±Ag±U±REE) deposits, including Aguas Claras, Cristalino, Igarapé Bahia-Alemão, Salobo and Sossego (Fig. 3). These deposits display a number of characteristic features: (i) strong structural control, commonly in vertical breccia pipes; (ii) epigenetic formation; (iii) strong iron-metasomatism in the form of magnetite and/or hematite; and (iv) copper-gold ores with LREE, Co, Ni, Pb, Zn, As, Bi, W and U enrichment (Soares *et al.*, 2000; Requia and Fontboté, 2000; Souza and Viera, 2000; Tazava and de Oliveira, 2000; Tallarico *et al.*, 2000b; Ronzê *et al.*, 2000). In contrast to the Itacaiúnas Belt, the Rio Maria granitoid-greenstone terrain is more typical in that it is characterised by orogenic lode-gold deposit types (cf. Groves *et al.*, 1998). These are characteristically gold deposits that are poor in base metals, in contrast to the Fe-oxide Cu-Au deposits from the Itacaiúnas Belt, and they generally occur as structurally-controlled quartz veins within the rocks of the greenstone belt (Villas and Santos, 2001).

Geology and Structural Setting of the Serra Pelada Area

The Serra Pelada Au-PGE deposit is located in the northeastern part of the Carajás Mineral Province, at the eastern termination of the Cinzento strike-slip system of the Itacaiúnas Belt (Fig. 3). Stratigraphic contacts between rocks of the Rio Novo Group and the Rio Fresco Formation, adjacent to the Serra Pelada deposit, display an E-W trend parallel to the regional trend of most units. The Rio Novo Group is an Archaean greenstone sequence composed mainly of mafic volcanic rocks, BIF and ultramafic schists that were metamorphosed to greenschist facies, and it represents the basal sequence within the Serra Pelada area. Unconformably overlying the Rio Novo Group are the Archaean Rio Fresco Formation metasedimentary rocks, represented by a platform sequence of quartzites, impure marble, meta-conglomerate, carbonaceous and calcareous beds and red meta-siltstone units metamorphosed to sub-greenschist facies (Fig. 5). The Rio Fresco Formation metasedimentary rocks are intruded by diorite plugs, possibly related to the 2.74 Ga Plaquê Granitoid Suite, 1.88 Ga A-type granite of the Carajás Suite, represented by the Cigano granite (Machado *et al.*, 1991), and much younger 198 Ma NW-trending gabbro dykes (Rb/Sr; Meireles and Teixeira, 1982). A mafic-ultramafic intrusion, possibly genetically related to the 2.75 Ga Luanga mafic-ultramafic complex that lies to the east of the Serra Pelada area (Fig. 3), intrudes only the greenstones of the Rio Novo Group (Fig. 5). Additionally, a number of circular, sub-surface, pipe-like breccia bodies, identifiable only by gravity/magnetic data and deep drilling (unpublished CVRD company reports), associated with intense chlorite ±sericite ±magnetite ±biotite ±siderite ±pyrite alteration, occur in the eastern part of the Serra Pelada area. These pipe-like breccia bodies (Fig. 9a) are currently of unknown origin and age.

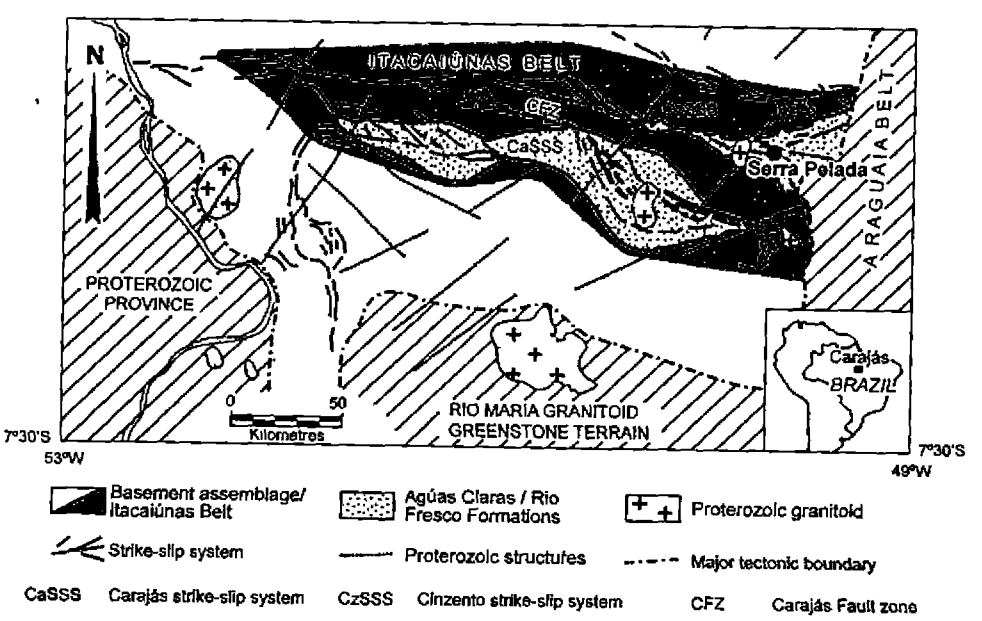


Figure 2: Simplified structural lineament map of the Itacaiúnas Belt displaying the two major strike-slip systems and the location of the Serra Pelada Au-PGE deposit (after Holdsworth and Pinheiro, 2000).

The structural evolution of the Serra Pelada area is complex, incorporating five identifiable deformation events (D_1-D_5) that produced a polyphase-deformed terrain. These deformation events are associated with a series of transpressional and transtensional reactivation phases of major E-W faults, locally represented by movement along the Cotia Fault (Fig. 6). The D_1 event, restricted to the metavolcanic rocks of the Rio Novo Group, incorporated the development of sinistral NNE-SSW-trending shear zones resulting from WNW-ESE transpression. Following deposition of sedimentary cover rocks of the Rio Fresco Formation, D_2 dextral strike-slip transpressional movement occurred along major east-west faults. The syn-tectonic intrusion of diorite (ca 2.74 Ga), and the associated thermal aureole within rocks of the Rio Fresco Formation (with sub-economic skarn-like Cu-Au mineralisation), occurred during the initiation of dextral east-west fault movement. Continued transpressional movement resulted in NNW-SSE compression, which formed regional-scale, reclined, tight, asymmetrical F_2 folds. These folds are the main structural hosts of Au-PGE mineralisation. The north-facing, kilometre-scale folds plunge gently (15°-25°) to

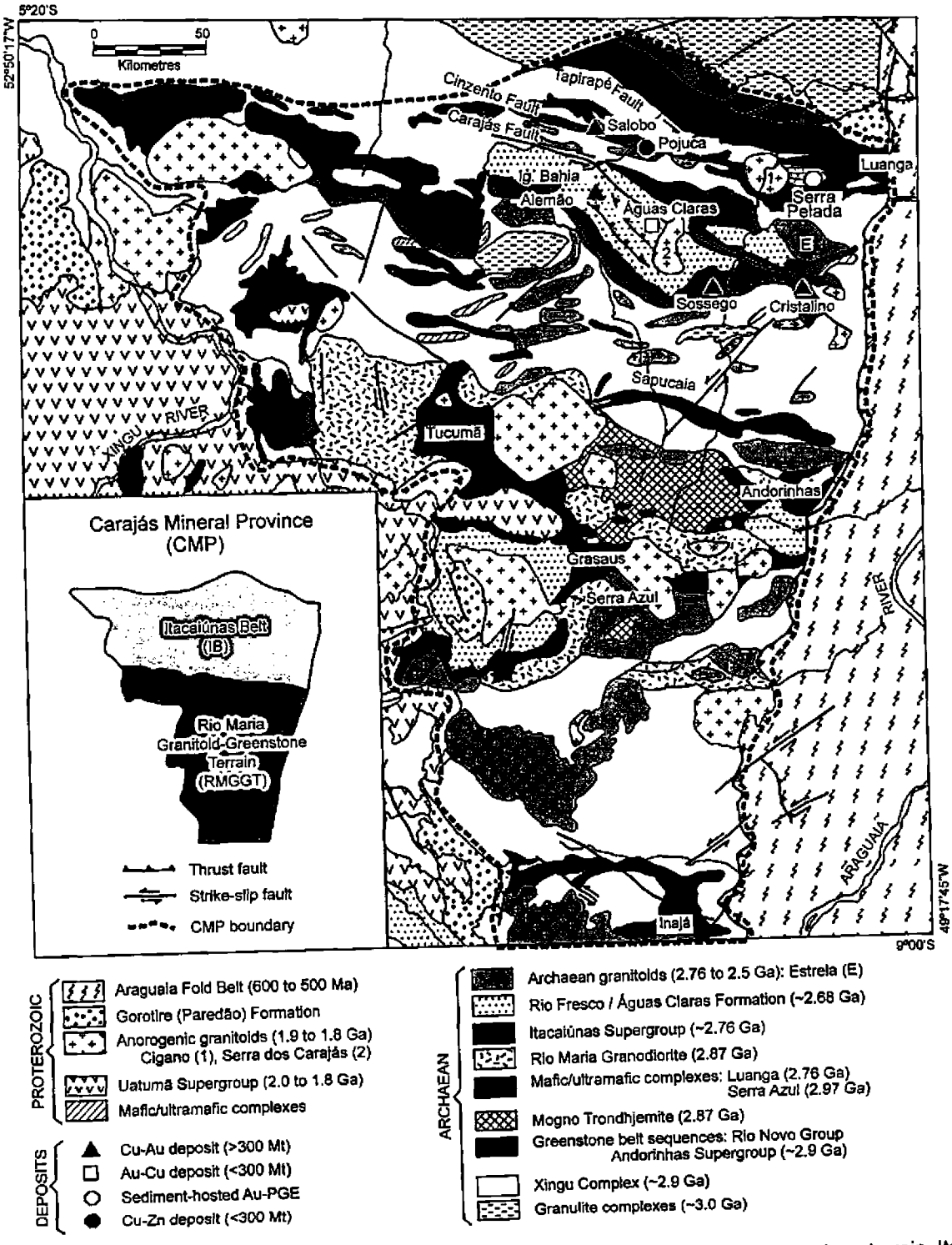


Figure 3: Geological map of the Carajás Mineral Province showing the Rio Maria granite-greenstone terrain, Itacaiúnas Belt and the location of the Serra Pelada Au-PGE and other major deposits of the Itacaiúnas Belt (after Villas and Santos, 2000).

the west-southwest. Their formation was associated with thin-skinned thrusting within the sedimentary rocks of the Rio Fresco Formation. This thrusting caused the structural emplacement of a diorite block, dismembered from the main diorite body at depth, along a hangingwall thrust to the Serra Pelada reclined fold, and caused major truncation of other lithological units. Peak metamorphic conditions within the Rio Fresco Formation metasedimentary rocks occurred late during the D_2 event, based on observed textural relationships between prograde metamorphic minerals and D_2 fabrics.

The third deformation event, D_3, is directly related to the formation of open F_3 folds that plunge to the south-southwest and deform the D_2 thrust planes and F_2 folds. This brittle-ductile deformation event was related to WNW-ESE transpression. Continued WNW-ESE compression, and oblique-slip along compressional surfaces, is also responsible for the development of sinistral NNE-NE faults and shear zones, due to competency contrasts in lithologies.

The fourth deformation event, D_4, is directly related to transtensional tectonism, resulting in the sinistral reactivation of the major E-W faults, locally represented by the Cotia Fault and parallel faults. The sinistral fault movement, with a minor SSW-NNE compressional component, produced open, gently WNW-plunging F_4 folds, which locally deform both F_2 and F_3 folds. Sinistrally deformed NNW- to NW-trending faults are inferred as acting as major fluid conduits to the Serra Pelada F_2 fold hinge. Gabbroic dykes were intruded along NW to NNW structures, which offset F_2 folds and S_2 foliation, and are interpreted as products of the last deformation event, D_5. The D_5 event is possibly related to a SW-NE extensional episode and the reactivation of NW- to NNW-trending faults.

Geology of the Serra Pelada Au-PGE Deposit

The Serra Pelada Au-PGE mineralisation is hosted entirely by metasedimentary rocks of the Rio Fresco Formation (Fig. 5) that include, in sequence from oldest to youngest, impure marble, carbonaceous and calcareous meta-siltstone, and red meta-siltstone. The majority (>75%) of the ore is hosted in the black, carbon-rich, lower part of the carbonaceous and calcareous meta-siltstone.

Impure marble: The impure marble is composed of a sequence of dolomitic marble, dolomitic quartzite, and minor dolomitic meta-conglomerates and quartzite beds that represent a dolomitised arenite sequence. The dolomitic marble and dolomitic quartzite, which form the majority of the unit, consist of rounded quartz grains (5 to 60%) in a matrix of granoblastic dolomite (30 to 95%), with rare (<2%) clasts of quartz, banded iron formation, chert and mafic volcanic rocks.

Carbonaceous and calcareous meta-siltstone: The carbonaceous and calcareous meta-siltstone forms a well-bedded (1- to 4-cm-thick beds), grey to black, carbonaceous horizon of amorphous carbon (2 to 10%), quartz (40 to 60%), dolomite (2 to 20%), fine-grained clays (5 to 20%), and rare disseminated pyrite (<1%). The basal part of the unit is dominantly a black, carbon-rich layer occurring as discontinuous lenses, which are concentrated in the hinge zone and along the lower limb of the Serra Pelada F_2 synform. These carbon-rich lenses become increasingly interbedded and grey in colour upwards.

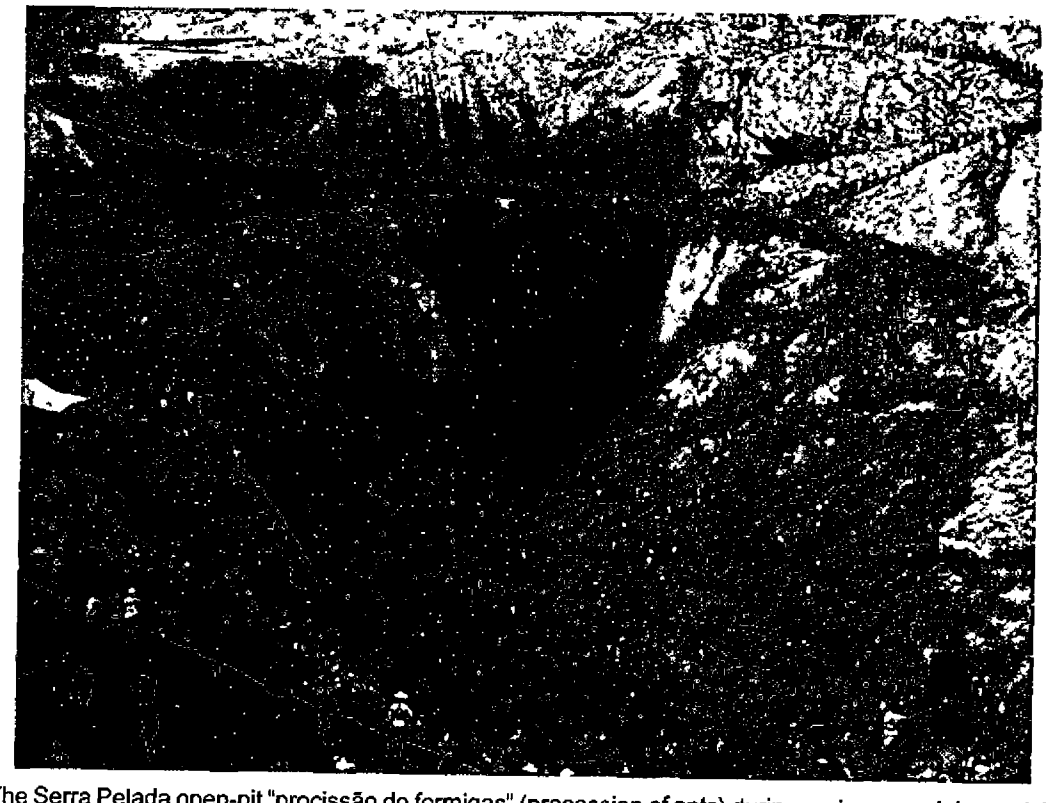


Figure 4: The Serra Pelada open-pit "procissão do formigas" (procession of ants) during garimpero mining activity, October 1982 (photo courtesy of CVRD).

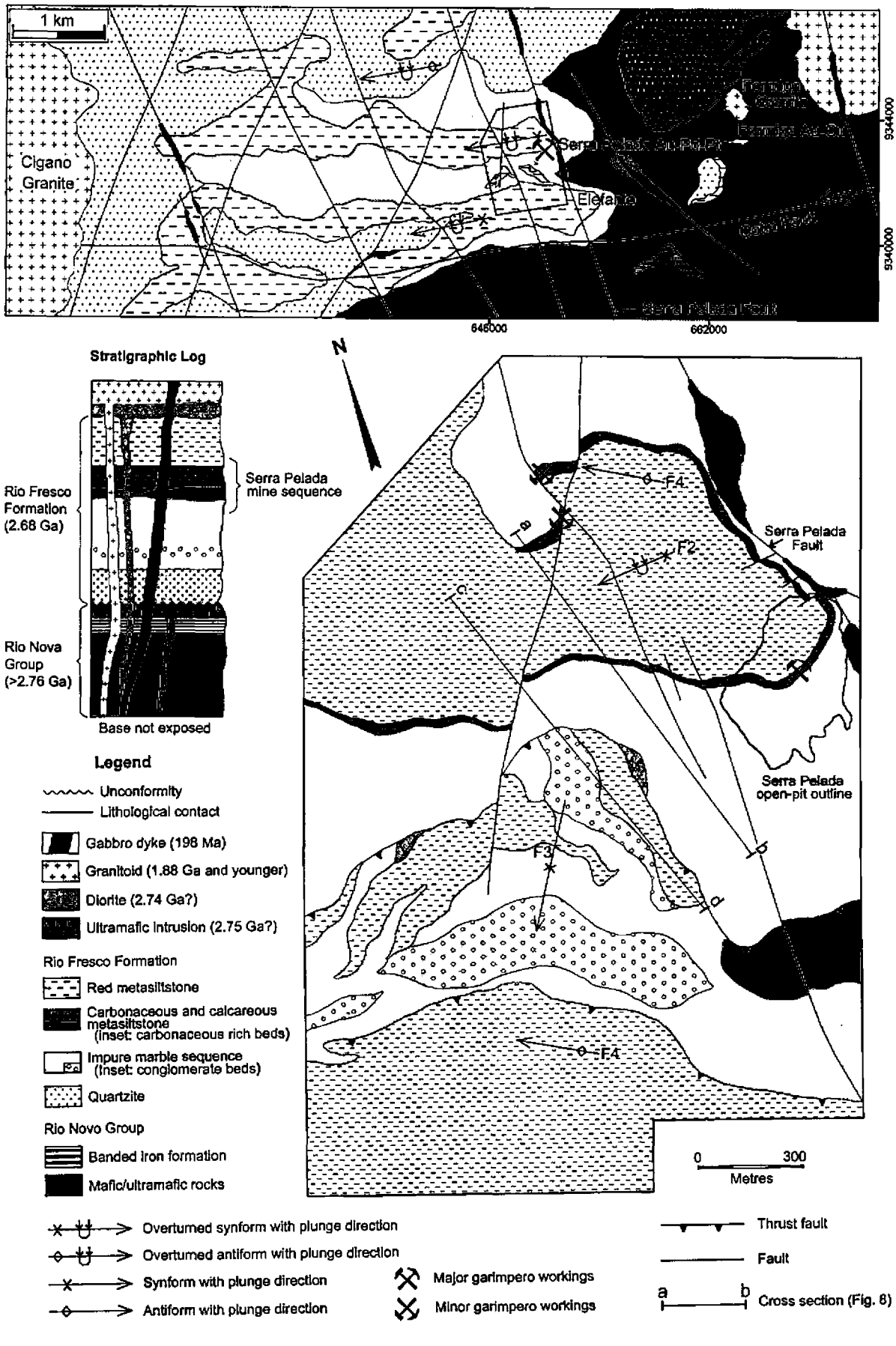


Figure 5: Simplified geological map of the Serra Pelada area (top) and geological map of the area surrounding the Serra Pelada Au-PGE deposit (bottom) showing the stratigraphic log of the area and location of cross sections.

Red meta-siltstone: The red meta-siltstone is a uniform, well-bedded (1- to 7-cm thick beds), red to off-white unit composed of quartz (30 to 60%), fine-grained clays (20 to 50%), and fine-grained hydrated Fe-oxides (1 to 15%). Minor interbeds (1- to 10-cm-thick) of both grey and black carbonaceous meta-siltstone occur irregularly in the lower parts of the red meta-siltstone lithology.

Lode Geometry

The geometry and localisation of high-grade ore shoots within the Serra Pelada deposit are controlled by three structural factors. These are: (1) the plunge of the major F2 fold hinge within the black carbonaceous and calcareous meta-siltstone, which is the main host for Au-PGE mineralisation; (2) the proximity of the F2 fold hinge to NNW-trending faults that were the ore-fluid channel; and (3) the lithological contacts between the carbonaceous and calcareous meta-siltstone and impure marble units. Each of these factors is described below, as are vertical changes in ore styles.

Geometric Features of Lodes

Structural analysis of the Serra Pelada deposit reveals that the plunge of individual ore shoots is controlled by the gentle plunge of the reclined, tight, F2 synformal fold hinge within the carbonaceous and calcareous meta-siltstone. The size of individual ore shoots in the meta-siltstone are closely related to the amplitude of the fold hinge and the amount of dilation associated with the hinge zone. Long-sections of the deposit show that the orebody plunges at approximately 15 to 25° WSW, parallel to the F2 fold hinge (Fig. 7). The main ore shoots reach 40 m in width in the thicker parts of the meta-siltstone (ie. F2 fold hinge; Fig. 8a). These major ore zones are located immediately down plunge from the Serra Pelada open-pit. The reduction in dimension, and ultimate termination of the Serra Pelada orebody down plunge, is associated with the tightening of the F2 fold hinge. F3 deformation is supported by an orthogonally-orientated F3 synformal hinge (Fig. 5). This caused the F2 fold hinge to tighten and pinch-out (Fig. 8a), preventing fluid flow down-plunge of this intersecting structure during the D4 mineralising event.

Location of Fluid Conduits

There are a number of faults that are inferred to have acted as fluid conduits to the Serra Pelada deposit. Intense hydrothermal alteration is located along the strike of the east-west-trending Cotia Fault and parts of the NNW-trending Serra Pelada Fault (Fig. 5). This alteration is interpreted to be related to the Au-PGE mineralisation event, as supergene mineralogy and trace-element geochemistry are similar for both. High-grade Au-PGE intersections in the carbonaceous and calcareous meta-siltstone at Elefanto (Fig. 5), southeast of the Serra Pelada open-pit, occur in high-angle faults of unknown orientation with normal vertical offset (Fig. 9b). This mineralisation is inferred as having been along strike of the NNW-trending Serra Pelada Fault, or within a parallel fault. The Serra Pelada Fault truncates the F2 synform and the Cotia Fault. Cross-sections show that the majority of the Serra Pelada orebody is located within the fold hinge adjacent to the Serra Pelada Fault, where the meta-siltstone is intersected by the fault (Fig. 8a). In addition, the volume of ore within the hinge zone decreases with increasing distance from the Serra Pelada Fault (Fig. 8b). This evidence suggests that the latter acted as a major fluid conduit for ore fluids entering the dilated, F2 fold-hinge during the D4 event.

Lithological Contacts

The lithological contact zones between the meta-siltstone and marble, particularly at fold hinge zones, are interpreted to have acted as major loci for fluid flow. Slip along these contact zones, due to contrasting rock rheologies during folding, and the influence of fold hinge dilation, are interpreted to have produced planar zones for fluid flow. Ore shoots were formed along these lithological contacts at the hinge of the Serra Pelada F2 synform, predominantly within the carbonaceous meta-siltstone (Fig. 8a).

Vertical Change of Structural Control and Mineralisation Style

Sections through the deposit show that the sub-surface orebody is complex down-dip, and is controlled by a combination of tight to open folding of F2 fold hinges, which cause structural thickening of the carbonaceous and calcareous meta-siltstone. Tight F2 fold hinges result in structural thickening of the meta-siltstone, which occurs as lenses, and not a continuous stratigraphic layer, within and adjacent to the Serra Pelada deposit. These structurally thickened areas at the dilational zone of the F2 fold hinge define the most prospective areas for Au-PGE mineralisation, which continue with depth along the plunge of the F2 fold hinge, and comprise the major ore shoots of the deposit (Fig. 8a).

Primary Mineralisation and Hydrothermal Alteration

Primary mineralisation within the Serra Pelada deposit is epigenetic and represented by two distinct ore types: (1) the predominant Au-Pd-Pt ore that is mainly hosted within the carbonaceous and calcareous meta-siltstone, but also associated with magnetite- and hematite-bearing hydrothermal breccias, intense sericite (white mica)-kaolin alteration zones, and an extensive jasperoid alteration halo with rare disseminated pyrite; and (2) Au (±Pd±Pt) ore associated with massive hematite metasomatism and siderite veins in marble. All other minor zones of Au-PGE mineralisation, located in both the red meta-siltstone and impure marble, are inferred to be related to supergene processes that redistributed the original epigenetic Au-PGE mineralisation. The different mineralisation styles are described below.

Carbonaceous and Calcareous Meta-siltstone-hosted Au-Pd-Pt Ore

High-grade Au-PGE mineralisation (grades of as much as 110 000 g/t Au and 16 000 g/t Pd and Pt) is associated with zones of high carbon content (≤10% C), predominantly within the hinge zone of the Serra Pelada F2 fold. Associated hydrothermal alteration in this ore type is subtle, with kaolin-sericite (white mica) ±hematite ±quartz ±muscovite ±hydrated Fe-oxide ±monazite ±rutile ±manganese oxide being the only indicators of hydrothermal activity (Fig. 9c). Rare zones of micro-brecciated meta-siltstone host rock, associated with a kaolin-quartz-monazite-muscovite alteration assemblage, also occur within this ore type.

Intense zones of sericite-kaolin alteration possibly indicate areas of high fluid flow and the destruction of carbonaceous matter.

Magnetite and Hematite Breccia-Hosted Au-Pd-Pt Ore

Magnetite-rich breccias, mainly weathered to hydrated Fe-oxides (Fig. 9d), commonly contain high-grade Au-PGE mineralisation (as much as 100's g/t of each Au, Pd and Pt). These breccias are typically sited within the hinge zone of the Serra Pelada F2 fold, but are also located along the lower limb. The breccias are matrix supported and contain angular clasts of quartzite and meta-siltstone. Grades of gold and PGE are highly erratic within these breccias, with a strong correlation of these to the amount of matrix material and to the proximity to the carbonaceous and calcareous meta-siltstone. Commonly, barren magnetite breccias are sited within the quartzite and impure dolomite sequence, distal to the F2 fold hinge. Characteristically, hematite-rich breccias display more consistent ore grades

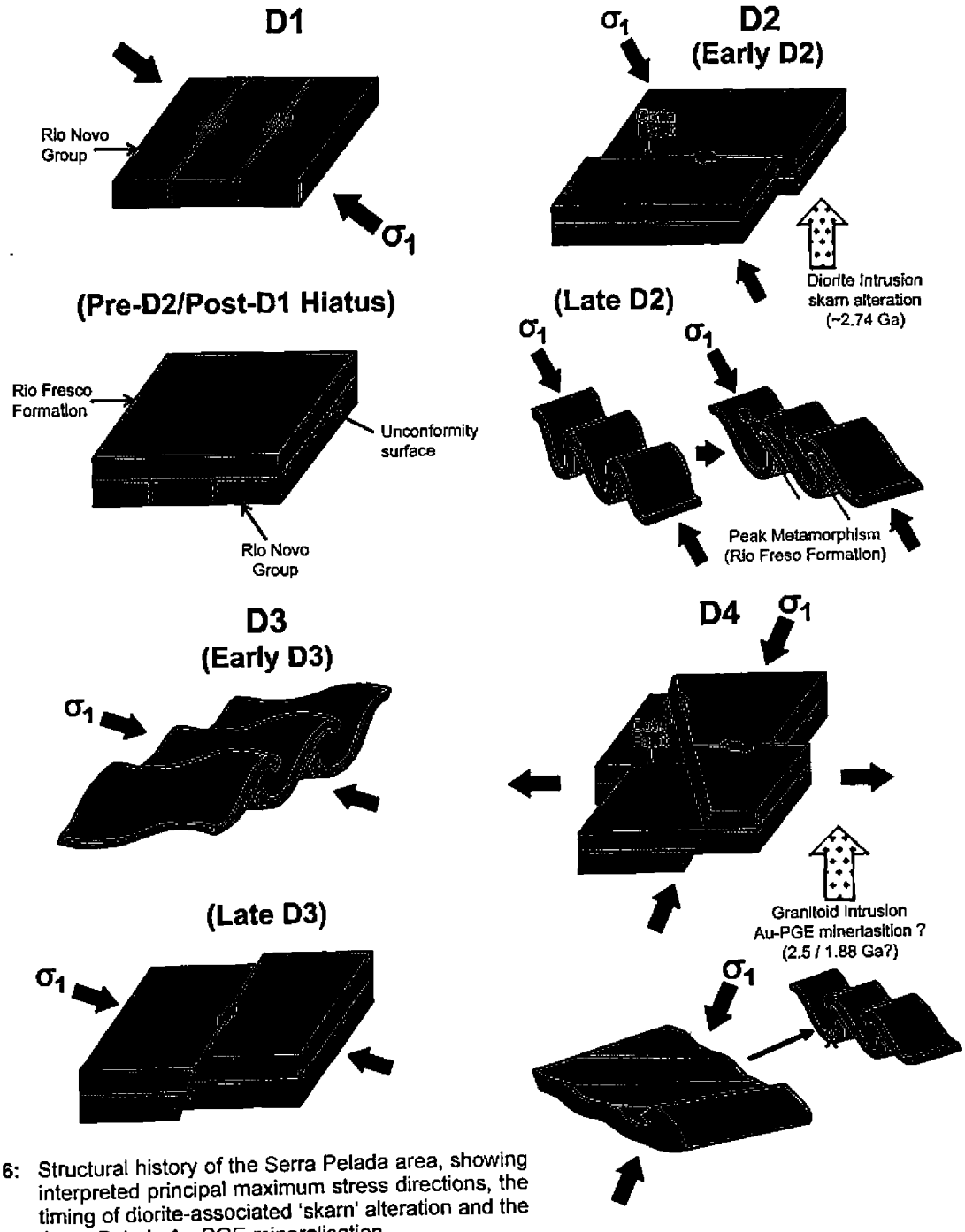


Figure 6: Structural history of the Serra Pelada area, showing interpreted principal maximum stress directions, the timing of diorite-associated 'skarn' alteration and the Serra Pelada Au-PGE mineralisation.

and are located primarily within the F2 fold hinge at the contact between the carbonaceous and calcareous meta-siltstone and marble, and within the carbonaceous and calcareous meta-siltstone. This hydrothermal breccia contains clasts of marble and meta-siltstone in a matrix of hematite, and is associated with intense alteration to kaolin-sericite-hydrated Fe-oxide (Fig. 9e and f).

Jasperoid-hosted Gold-PGE Ore

An extensive jasperoid alteration zone envelops the main ore zone within the hinge of the Serra Pelada F2 fold (Figs. 8a and b). The jasperoid envelope, which occurs as an amorphous, fine-grained silica alteration zone, also extends along the limbs of the fold. The Au-PGE mineralisation occurs where the jasperoid replaces the carbonaceous parts of the meta-siltstone, and is associated with a kaolin-hydrated Fe-oxide ±muscovite ±monazite ±hematite assemblage and rare fine-grained disseminated pyrite (Fig. 9g). Jasperoid replacements of the impure marble sequence generally contain little or no mineralisation.

Massive Hematite Gold Ore

Massive hematite, located on the lower limb of the Serra Pelada F2 fold hinge, displays Au (±Pd±Pt) enrichment. This ore type is characterised by massive hematite-chlorite metasomatism ±monazite ±apatite ±rutile alteration of the impure marble sequence (Fig. 9h), and is associated with minor siderite veins (Fig. 9i).

Fracture-fill Gold-PGE Ore

To the southeast of the Serra Pelada open-pit, and along a NNW-trending fault corridor, high-grade Au-PGE mineralisation occurs within the Elefanto area (Fig. 5). High-angle fractures displaying a normal vertical offset are host to high-grade Au-PGE mineralisation (as much as hundreds of g/t of Au, Pd and Pt) within the carbonaceous and calcareous meta-siltstone (Fig. 9b). Free gold, palladium and platinum occur within micro-fractures that display minor selvages of kaolin associated with minor Fe-oxide ±monazite alteration.

Deep Weathering of the Serra Pelada Au-PGE Deposit

The Serra Pelada Au-PGE deposit is located within a heavily-weathered tropical terrain of sub-greenschist facies Archaean metasedimentary rocks. Since its discovery, the deposit has been mined extensively, but intermittently, leaving no surface expression of the original Au-PGE mineralisation. Access to the mined open-pit is impossible due to flooding, and the remaining sub-surface orebody has also undergone extensive tropical weathering. The calcareous rocks have been decalcified generally to ~350 m below surface (Figs. 8a and b). Whereas this may be due to decalcification during hypogene alteration, by analogy with similar decalcification in the Carlin-type gold deposits (Hofstra and Cline, 2000), deep weathering is more likely because the decalcification everywhere terminates at essentially the same depth below surface, irrespective of position with respect to the reclined synformal fold and the orebody.

Decalcification has resulted in the transformation of the carbonaceous and calcareous meta-siltstone to an amorphous carbonaceous unit, and the impure marble to a loose, friable sandstone, within the vicinity of the Serra Pelada deposit. Weathering has also transformed pre-existing magnetite and/or hematite and/or Fe-sulphides to hydrated Fe-oxides, such as goethite, and has probably transformed hydrothermal sericite, minor amounts of which are preserved, into kaolinite. Secondary manganese oxides are common, and extensive collapse breccias rich in manganese oxides occur on the limbs and hinge of the Serra Pelada F2 fold.

These collapse breccias are inferred to be related to volume reduction due to decalcification of the impure marble, under secondary weathering conditions, and are not associated with the Au-PGE mineralisation. Most of the ore components have been redistributed during weathering, with REE now mainly concentrated in secondary minerals, base metals concentrated in manganese oxides, and Au-Pd-Pt being primarily associated with amorphous carbon and Fe- and Mn-oxides. Gold and PGE's also occurred as nuggets, to 60 kg in mass, in the open-pit workings.

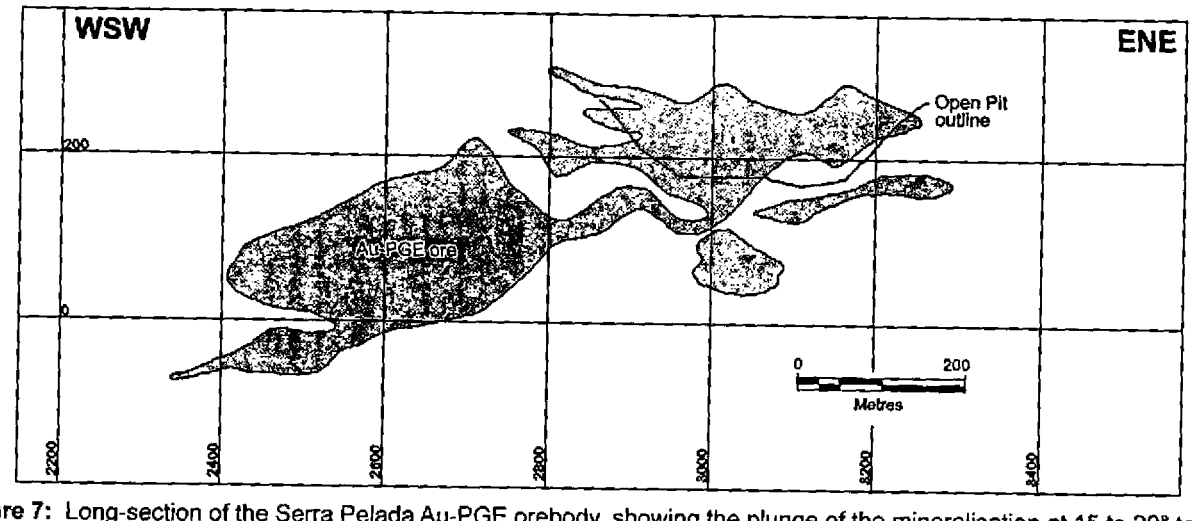


Figure 7: Long-section of the Serra Pelada Au-PGE orebody, showing the plunge of the mineralisation at 15 to 20° to the WSW. Outline of mineralisation at 1 g/t Au+PGE cut-off

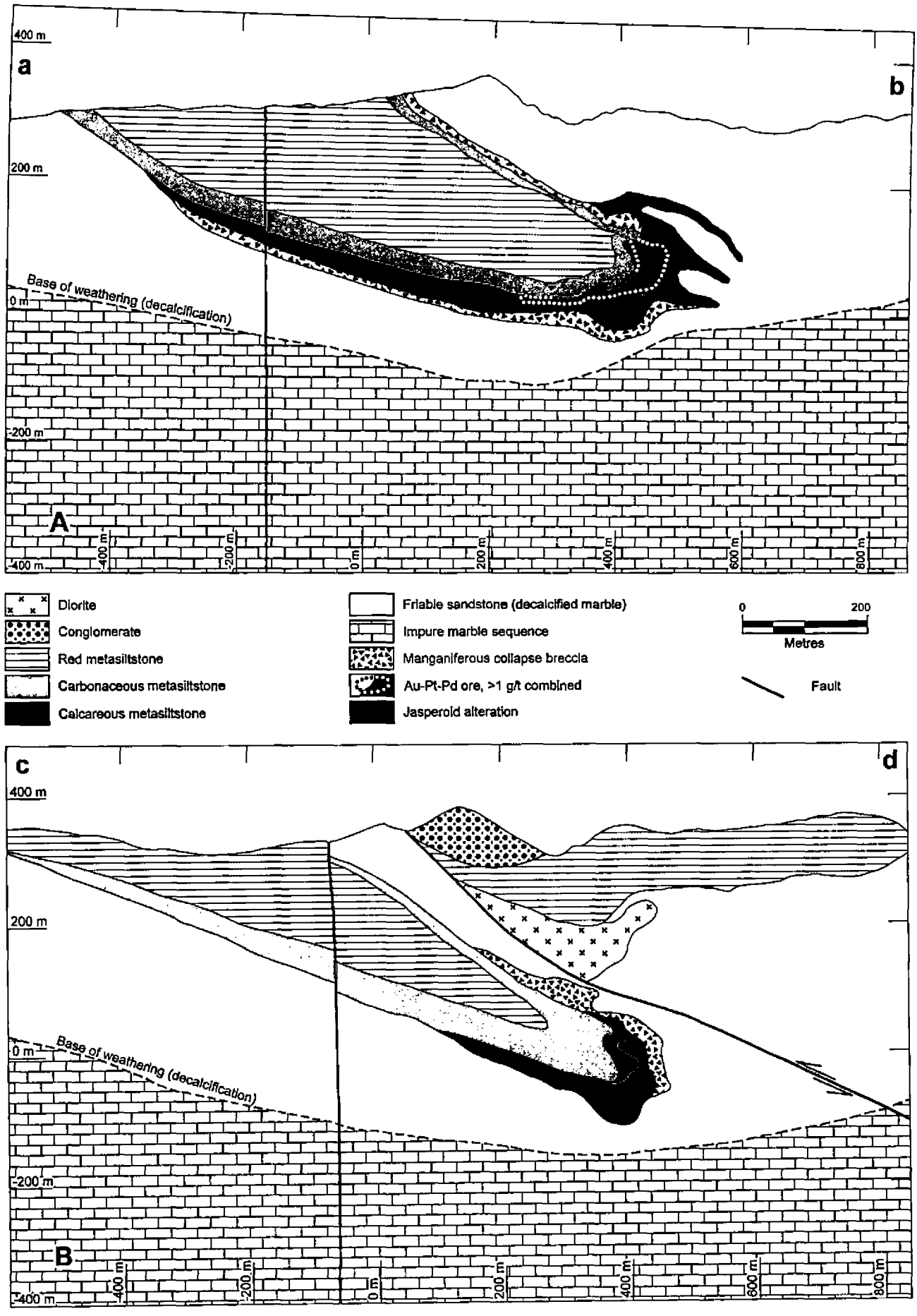


Figure 8: Cross-sections through the Serra Pelada Au-PGE deposit (section lines shown on Fig. 5). **A** - down plunge extension of the ore deposit showing the location of the Au-PGE mineralisation within the F_2 fold hinge; **B** - showing the termination of ore due to the tightening of the F_2 fold hinge. Note the thrust fault on the upper limb of the synform and the dislocated diorite intrusion from depth.

Ore Geochemistry

Whole-rock analyses of major, trace and REE for gold and PGE enriched samples display anomalous values for LREE, Co, Cu, Ni, Pb, Zn, As, Bi, W and U (Table 1). The Au-PGE enrichments, related to the carbonaceous meta-siltstone ore, magnetite and hematite breccias, and intense zones of kaolin alteration, display a constant enrichment signature of these trace elements. The magnetite breccias commonly display additional enrichment in Ni and Zn. The Au-PGE mineralisation within the jasperoids generally is also anomalous in Ag, Bi and W. The Au (±PGE) enrichment associated with massive hematite metasomatism displays similar enrichment in many of the above trace elements.

Stable Isotopes

Carbon and oxygen isotope ratios were measured on hydrothermal siderites associated with massive hematite Au (±Pd±Pt) ore from Serra Pelada, and from petrographically and texturally similar siderite veins from the barren pipe-like breccia bodies adjacent to the Serra Pelada deposit. Only four samples from the Serra Pelada deposit were analysed, due to a lack of suitable fresh carbonate material. Carbon isotope data for the samples exhibit a narrow range of $\delta^{13}C$ (-0.6 to -2.2‰) and $\delta^{18}O$ (13.8 to 14.7‰). The pipe-like breccia bodies also display a narrow, although different range of $\delta^{13}C$ (-7.1 to -7.6‰) and $\delta^{18}O$ (8.8 to 14.2‰). These results are plotted in Fig. 10, and compared with other known reservoirs and the Igarapé Bahia Fe-oxide Cu-Au deposit.

Although the data are not definitive, the narrow range of negative $\delta^{13}C$ values indicates the presence of magmatic fluids in the Au-PGE ore forming process of Serra Pelada. A magmatic origin may also be suggested for the pipe-like breccia bodies adjacent to Serra Pelada. Their isotopic association with the carbonatite reservoir may designate an alkaline magmatic genetic association, as does the isotopic similarity of the Serra Pelada Au-PGE ores with the Olympic Dam reservoir (Oreskes and Einaudi, 1992).

Preliminary Genetic Model for Au-PGE Mineralisation

The Serra Pelada Au-PGE deposit is clearly epigenetic, based upon its strong structural control by F_2 folds and the associated wallrock alteration within stratigraphic horizons and along D_4 faults. It appears most likely that fluids were initially channelled during D_4 along E-W faults, such as the Cotia Fault, into NW- to NNW-trending faults, such as the Serra Pelada Fault, and finally into the dilated, reclined F_2 fold-hinge within the carbonaceous and calcareous meta-siltstone. Such a model is consistent with the occurrence of additional Au-PGE mineralisation adjacent to a reclined synformal fold-hinge at Elefanto, which is close to the southeastern extension of the Serra Pelada Fault (Fig. 5). The structural timing of mineralisation is inconsistent with the models of Villas and Santos (2001) and Tallarico *et al.* (2000a), which postulate that the Au-PGE mineralisation is related to diorite-associated skarn development. This skarn is also geochemically very distinct from the Serra Pelada ores, in particular, it does not display the LREE enrichment shown by Fe-oxide-dominated mineralisation styles in the Serra Pelada orebody (Table 1).

The extreme weathering of the deposit, with destruction of primary ore and alteration minerals, means that deduction of fluid conditions from mineralogical assemblages and compositions is not possible. Similarly, the main mineralised zones contain no minerals suitable for fluid inclusion studies. Hence, the nature of the ore fluids and transport and depositional mechanisms must be surmised from the metal association of the ores. Gold and PGE's, particularly palladium, can be efficiently transported in highly saline, oxidising, and acidic fluids, as chloride complexes in equilibrium with hematite (e.g., Mountain and Wood, 1988; Wood *et al.*, 1992). Deposition of the gold and Pd-Pt can be induced by a decline in temperature, with a rapid decrease in solubility of all three elements below 300° C, by reduction of the fluid, and/or by an increase in pH. The most obvious mechanism for deposition of high-grade Au-Pd-Pt ores is reduction caused by the extremely carbonaceous meta-siltstone host rocks, with an increase in pH due to carbonate dissolution being an additional factor. Fluid reduction would also explain the deposition of other redox-sensitive elements such as U, As, Cu, Co and Ni. Temperature decline could similarly be a factor, because the source of the fluids was presumably below the present exposure level, and the deposit is sited in the low metamorphic-grade, stratigraphically and structurally highest parts of the Carajás Basin lithostratigraphic section, where temperatures would have been relatively low during the mineralisation event.

Although the present distribution of decalcified carbonate rocks appears to mainly relate to tropical weathering, the occurrence of extensive jasperoid, some with preserved pyrite, that forms an envelope around the ore zone, suggests that acidic hydrothermal fluids also dissolved carbonate with resultant silica replacement. The co-existence of hypogene sericite and kaolin is also consistent with acidic fluids during alteration and mineralisation.

The deposit is clearly unusual in the association between gold and PGE, particularly palladium. There appear to be two potential sources for the PGE's. The most obvious is leaching, by hydrothermal fluids, of the PGE's from the adjacent Luanga mafic-ultramafic complex (Fig. 3) or other ultramafic intrusions in the Serra Pelada area. Such leaching and remobilisation of PGE's, particularly palladium and platinum, have been documented in several studies, for example at Rathbun Lake, Ontario (Rowell and Edgar, 1986) and New Rambler, Wyoming (McCallum *et al.*, 1976). However, hydrothermal fluids in these deposits are suggested to contain bisulphide or hydroxide complexes for Au-PGE transport. These are clearly not responsible for the transport of metals in Serra Pelada, given the extensive acidic alteration in the form of sericite and/or kaolin and oxidised mineral assemblages (e.g., hematite; Wood *et al.*, 1992). Potentially more interesting is the association between gold and some PGE's, particularly palladium and platinum,

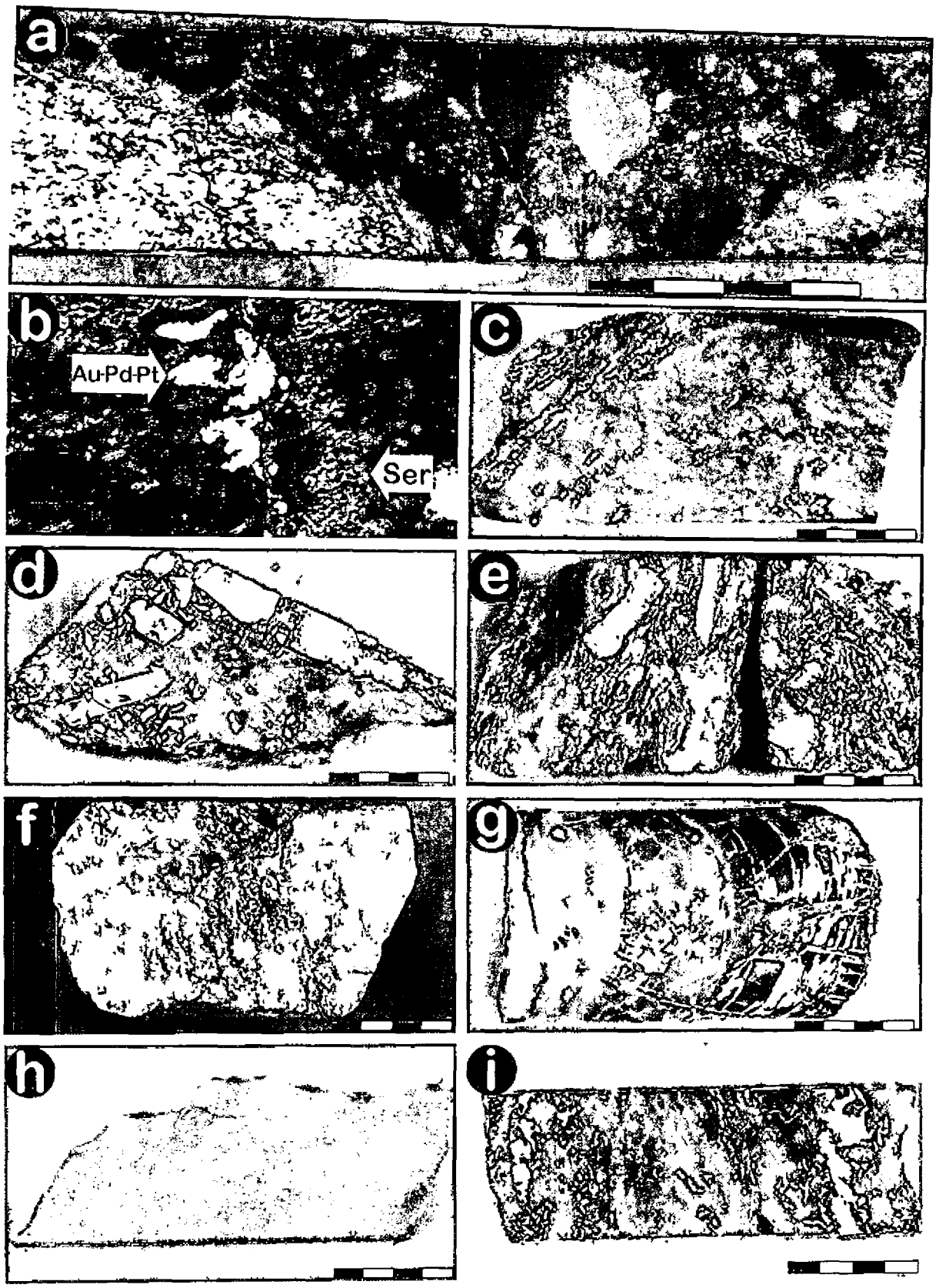


Figure 9: **a** Chlorite-rich breccia pipe, hosting granite, mafic metavolcanic and BIF clasts;
b Thin-section (x10 magnification; reflected light) of high-grade Au-PGE mineralisation associated with high angle fractures and sericite alteration within the carbonaceous and calcareous metasiltstone from the Elefanto area;
c Carbonaceous and calcareous metasiltstone Au-PGE ore with minor kaolin alteration;
d Limonite-goethite (after magnetite) breccia Au-PGE ore;
e Hematite-rich hydrothermal breccia Au-PGE ore within the carbonaceous and calcareous metasiltstone;
f Kaolin alteration in Au-PGE ore zone within the carbonaceous and calcareous metasiltstone;
g Jasperoid Au-PGE ore within the carbonaceous and calcareous metasiltstone;
h Massive hematite Au (±PGE) ore.
i Siderite veins adjacent to massive hematite Au (±PGE) ore.

in alkaline porphyry-style deposits that include the Allard Stock, Colorado (Werle *et al.*, 1984), the Similkameen deposit, British Colombia (Fahrni *et al.*, 1976), and the Skouries copper deposit, northern Greece (Eliopoulos and Economou-Eliopoulos, 1991; Frei, 1995). Such deposits were formed from acidic, oxidising fluids, with metals transported as chloride complexes, as is inferred for Serra Pelada.

Importantly, there are two generations of sub-alkaline to alkaline intrusive rocks in the Carajás Mineral Province, the 2.57 Ga Old Salobo granite/Estrela A-type alkaline granitoid complex and the 1.88 Ga A-type granitoid suite, which includes the Cigano granite of the Serra Pelada area. The latter are associated with hematitic breccias not unlike those at Serra Pelada. Furthermore, a genetic association with alkaline (or shoshonitic) magmatism is proposed for a number of Fe-oxide Cu-Au deposits, notably Olympic Dam (Hauck, 1990; Reeve *et al.*, 1990; Mutschler and Mooney, 1993; Pollard *et al.*, 1998; Jensen and Barton, 2000), which are located withincratonic areas with Archaean basement, such as at Carajás.

Geological Similarities and Genetic Relationship to Fe-Oxide Cu-Au Mineralisation

Deposits of the Fe-oxide Cu-Au class (e.g., Hitzman *et al.*, 1992) display a strong structural control, are epigenetic, and display a direct association with extensional tectonism of Paleoproterozoic to Mesoproterozoic age (Kerrich *et al.*, 2000). Classic economic examples of this deposit type include Olympic Dam, South Australia (Reeve *et al.*, 1990; Campbell *et al.*, 1998) and Ernest Henry, Queensland (Twyerould, 1997; Mark *et al.*, 2000). From the viewpoint of Serra Pelada, it is important that it is sited in the same Carajás Mineral Province, which arguably is a region with the most extensive group of world-class deposits of this type, including Igarapé Bahia-Alemão, Cristalino, Salobo and Sossego (e.g., Huhn and Nascimento, 1998; Tallarico *et al.*, 2000b; Kerrich *et al.*, 2000). The province is also at the margin of one of the world's largest A-type granite provinces (Santos *et al.*, 2000).

The Serra Pelada deposit displays many similar characteristics to the Fe-oxide-Cu-Au class of mineral deposits in that: (1) the Au-PGE mineralisation is genetically related to strong Fe-metasomatism in the form of magnetite and hematite breccias; (2) the Au-PGE ore is associated with LREE, Co, Cu, Ni, Pb, Zn, As, Bi, W and U enrichment; (3) the REE distribution in the ores shows similar patterns and enrichment factors (Fig. 11); (4) the ore is epigenetic and displays a strong structural control; (5) there is a potential alkaline magmatic source; and (6) mineralisation is interpreted to be associated with an extensional tectonic event (D_4).

The recent suggestions that the Palabora carbonatite magnetite-copper deposit may be an end member of the Fe-oxide Cu-Au deposit group (Groves and Vielreicher, 2001) provides a potential connection between gold and PGE's, particularly palladium and platinum, as Palabora produces about 0.28 tonnes per annum of both metals as a by-product of copper mining (Verwoerd, 1986). It also indicates that the Au-Pd-Pt association may reflect an alkaline magmatic source, in agreement with the same associations in alkaline porphyry systems, as discussed above.

If the Serra Pelada deposit is, in fact, related to the Carajás Fe-oxide Cu-Au deposits, it is important to establish the nature of the connection. Clearly, the fluids implicated for

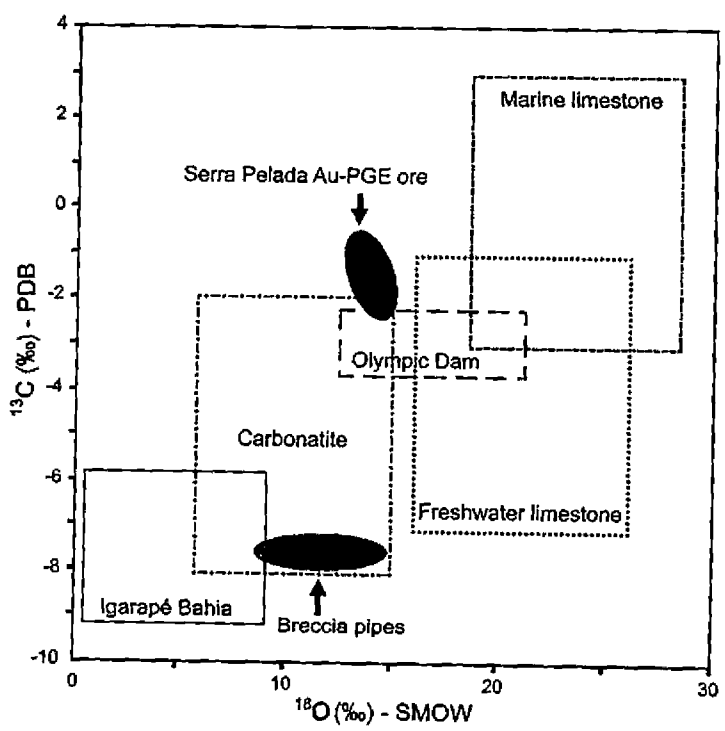


Figure 10: Plot of $\delta^{13}C$ vs. $\delta^{18}O$ showing the isotopic composition of siderite from the Serra Pelada Au-PGE deposit and adjacent Aeroporto breccia pipes, relative to carbonatites, siderite and calcite from the Igarapé Bahia Fe-oxide Cu-Au mineralisation (Tallarico *et al.*, 2000b), Olympic Dam mineralisation, freshwater limestone and marine limestones (Oreskes and Einaudi, 1992).

Au-PGE mineralisation at Serra Pelada are similar acid, oxidising fluids to those depositing Fe-oxide Cu-Au deposits (e.g., Large *et al.*, 1989, Murphy *et al.*, 1999). Hitzman *et al.* (1992) suggested that there was vertical zonation in Fe-oxide Cu-Au systems in terms of their Fe-oxide mineralogy, magnetite versus hematite, and wallrock alteration, as well as structural style. Both Kerrich *et al.* (2000) and Groves and Veilreicher (2001) emphasise this theme, and suggest that there could be vertical temperature gradients within the systems that produce the vertical zonation. Gold solubility as chloride complexes is strongly dependant on temperature, with declining solubility at lower temperatures (e.g., Seward and Barnes, 1997). There is some evidence that this is reflected in Cu:Au ratios of the ores, with those inferred to be higher-temperature, deeper-level deposits on the basis of their mineralogy (e.g., Salobo, Ernest Henry) having lower gold contents and higher Cu:Au ratios than those inferred to have been deposited at higher crustal levels (e.g., Olympic Dam, Igarapé Bahia-Alemão, Aguas Claras). It is significant that the Palabora deposit, inferred to be the most proximal to source, has a very high Cu:Au ratio (Groves and Veilreicher, 2001), and that there is evidence of copper to gold zonation in the potentially most distal, hematite-dominated Olympic Dam deposit (Reeve *et al.*, 1990).

Table 1: Chemical composition of Serra Pelada Au-PGE ores types, regional alteration of the Serra Pelada area, and the Igarapé Bahia and Salobo Fe-oxide Cu-Au deposits. Major elements (wt.%) and trace elements (ppm). Sample identification by drill core and depth (m): CMS = Carbonaceous and calcareous metasiltstone Au-PGE ore (Serra Pelada); HB = Hematite breccia Au-PGE ore (Serra Pelada); MB = Magnetite breccia Au-PGE ore (Serra Pelada); MH = Massive hematite metasomatism Au-PGE ore (Serra Pelada); KZ = Kaolin-sericite alteration Au-PGE ore (Serra Pelada); SK = Skarn alteration magnetite (adjacent Serra Pelada); Abx = Breccia pipe (adjacent Serra Pelada); IgBah = Magnetite breccia Cu-Au ore (Igarapé Bahia; Tazava and Oliveira, 2000); Sal = Magnetite Cu-Au ore (Salobo; Requia and Fontboté, 2000).

Locality	Serra Pelada (S.P.) Ore Types					Adjacent S.P.		Fe-Oxide Cu-Au	
	FD-156	FD-126	FD-172	FD-201	FD-126	FD-196		353AC	KRI-65
Sample	236.6	179.2	141	145	181	192.35		184.7	IR I
Type	CMS	HB	MB	MH	KZ	SK	Abx	IgBah	Sal
SiO_2	66.1	64.6	48.4	14.3	67.6	48.4	67.4	21.1	10.9
Al_2O_3	17.1	12.6	7.0	6.2	10.8	12.4	9.6	3.3	1.6
Fe_2O_3	1.3	13.2	33.3	62.1	12.8	17.5	12.6	55.5	83.4
MnO	1.1	<0.01	1.9	0.1	0.4	0.1	0.1	0.5	0.4
MgO	0.3	0.2	<0.01	10.9	0.1	4.9	3.8	1.8	0.2
CaO	0.1	0.1	<0.01	<0.01	0.1	10.6	0.1	4.6	3.7
Na_2O	0.2	0.1	<0.01	<0.01	<0.01	<0.01	0.1	0.5	<0.01
K_2O	1.5	0.2	0.06	<0.01	<0.01	<0.01	2.6	0.5	0.1
TiO_2	0.9	0.6	0.3	0.4	0.4	2.2	0.5	0.2	0.1
P_2O_5	1.0	0.7	0.9	<0.01	0.7	0.3	0.1	1.1	0.2
LOI	7.5	6.8	7.6	5.0	6.4	2.8	2.6	0.4	0.3
Total	97.0	99.1	99.4	99.2	99.2	99.3	99.4	89.6	101.0
Au	71.5	6.0	26.0	47.6	6.0	2.5	<0.01	7.7	2.6
Ag	88.7	0.6	<0.5	<0.5	<0.5	<0.5	<0.5	29.3	4.2
Pd	29.5	3.5	691.0	0.2	1.5	<0.01	<0.01	na	na
Pt	18.6	4.0	180.0	0.2	1.0	<0.01	<0.01	na	na
Co	1552.0	158.0	558.0	153.0	1650.0	34.0	45.0	94.0	87.0
Ni	123.0	117.0	608.0	155.0	655.0	87.0	59.0	141.0	46.0
Cu	1102.0	469.0	337.0	1825.0	1234.0	353.0	41.0	55127.0	31521.0
Zn	192.0	187.0	400.0	372.0	443.0	66.0	71.0	58.0	6.0
Pb	1636.0	921.0	335.0	180.0	763.0	8.0	6.0	119.0	na
Mo	<2.0	<2.0	<2.0	20.0	4.0	<2.0	<2.0	110.0	269.0
Bi	345.0	54.0	17.3	277.0	21.0	0.5	0.4	<5.0	na
As	134.0	50.0	106.0	17.0	16.0	<0.5	<0.5	59.0	14.4
W	133.0	179.0	86.0	23.0	48.0	72.0	120.0	<0.3	126.0
U	23.0	115.0	158.0	31.0	251.0	1.0	2.2	160.0	57.4
La	1039.0	1314.0	569.0	145.0	53.0	17.0	25.0	777.0	712.0
Ce	1178.0	1617.0	712.0	355.0	109.0	32.0	48.0	940.0	681.0
Nd	282.0	286.0	158.0	106.0	60.0	24.0	22.0	280.0	166.0
Sm	12.0	32.0	7.5	15.0	17.0	6.4	4.2	31.0	35.2
Eu	1.5	8.0	1.6	1.7.0	4.9	1.9	1.0	9.6	13.2
Tb	1.0	4.0	1.5	1.6	2.9	1.2	0.5	4.0	na
Yb	3.4	9.0	4.8	6.4	7.9	5.0	1.6	4.7	4.4

Although it is not possible to make palaeo-reconstructions of the Carajás Mineral Province at the time of Fe-oxide Cu-Au mineralisation, as the timing of mineralisation is currently poorly constrained, it is significant that the inferred higher-temperature deposits (e.g., Salobo) occur in, or adjacent to, the basement complex, whereas the inferred lower-temperature deposits (e.g., Igarapé Bahia-Alemão, Aguas Claras) are sited in, or adjacent to, the low metamorphic-grade sedimentary rocks of the uppermost Aguas Claras Formation (Fig. 12). Serra Pelada also occurs in rocks of the stratigraphically high Rio Fresco Formation in a position that is distal to the major concentration of Fe-oxide Cu-Au deposits, which occur in a corridor adjacent to the Cinzento and Carajás strike-slip fault systems (Figs 2 and 3). It is, therefore, possible that the Serra Pelada deposit represents a distal equivalent of the Fe-oxide Cu-Au deposits in a broadly zoned mineral district.

Conclusions

1. Serra Pelada is a Au-PGE (Pd-Pt) deposit sited within the Carajás Mineral Province of the southeastern Amazon Craton, Brazil. This province is best known for its giant iron-ore deposits and its world-class Fe-oxide Cu-Au deposits.

2. The deposit has been strongly affected by tropical weathering, such that its original mineralogy and wallrock alteration is largely destroyed. Despite this, there is strong evidence for the former existence of magnetite and hematite, plus sericite-kaolin, siderite and quartz alteration minerals, in a deposit with an element association of Au-PGE with LREE, Co, Cu, Ni, Pb, Zn, As, Bi, W and U.

3. The deposit is clearly epigenetic with a strong structural control. It is hosted in a sub-greenschist facies, carbonaceous and calcareous meta-siltstone unit within the hinge zone of a reclined, tight, regional-scale F_2 synform. The deposit is sited close to the E-W trending D_2 Cotia Fault, near its intersection with numerous northwest- to NNW-trending D_4 faults, the most easterly one being the Serra Pelada Fault. These are interpreted as the major ore-fluid conduits.

4. Despite weathering, the high-grade Au-PGE deposit within the exceptionally carbon-rich meta-siltstone is considered to have been associated with magnetite- and hematite-rich hydrothermal breccias, massive zones of hematite metasomatism, siderite veins, intense zones of sericite (white mica)-kaolin alteration, and a jasperoid envelope related to hydrothermal decalcification of the calcareous rocks.

5. The deposit is interpreted to have formed from acid oxidising fluids that migrated along east-west and northwest- to NNW-trending fault systems during D_4 into the dilated fold hinge in the highly carbonaceous and calcareous meta-siltstone host unit. Gold and Pd-Pt are interpreted to have been transported as chloride complexes and deposited due to declining temperature, reduction by the carbonaceous host rock, and possibly increase in pH due to carbonate dissolution.

6. Although the PGE is could have been leached from adjacent ultramafic complexes by the mineralising fluid, it is more likely that they are from fluids exsolved from an alkaline magmatic source, as Au-Pd-Pt-bearing copper-rich porphyry systems are consistently associated with alkaline intrusive rocks.

7. The Serra Pelada deposit shows a number of similarities to the Fe-oxide Cu-Au deposits (e.g., Aguas Claras, Cristalino, Igarapé Bahia-Alemão, Salobo, Sossego) in the Carajás Mineral Province. These include similar element associations (particularly LREE, Co, Ni, U), very similar REE patterns, association with magnetite- and/or hematite-rich breccias, epigenetic character and strong structural control.

8. Based on its distal position to the strike-slip fault corridor containing the Carajás Fe-oxide Cu-Au deposits, and its siting in the upper part of the exposed lithostratigraphic sequence, Serra Pelada is tentatively interpreted to have a distal relationship to the Fe-oxide Cu-Au deposits. It is interpreted to have been deposited at lower temperatures from similar, acid, oxidising ore fluids.

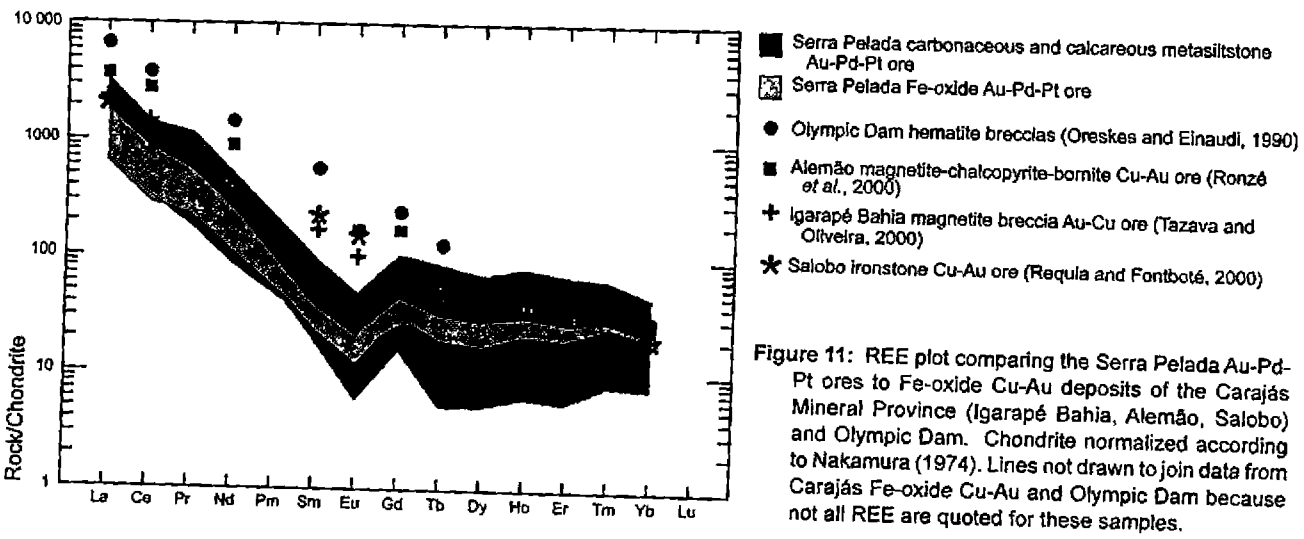


Figure 11: REE plot comparing the Serra Pelada Au-Pd-Pt ores to Fe-oxide Cu-Au deposits of the Carajás Mineral Province (Igarapé Bahia, Alemão, Salobo) and Olympic Dam. Chondrite normalized according to Nakamura (1974). Lines not drawn to join data from Carajás Fe-oxide Cu-Au and Olympic Dam because not all REE are quoted for these samples.

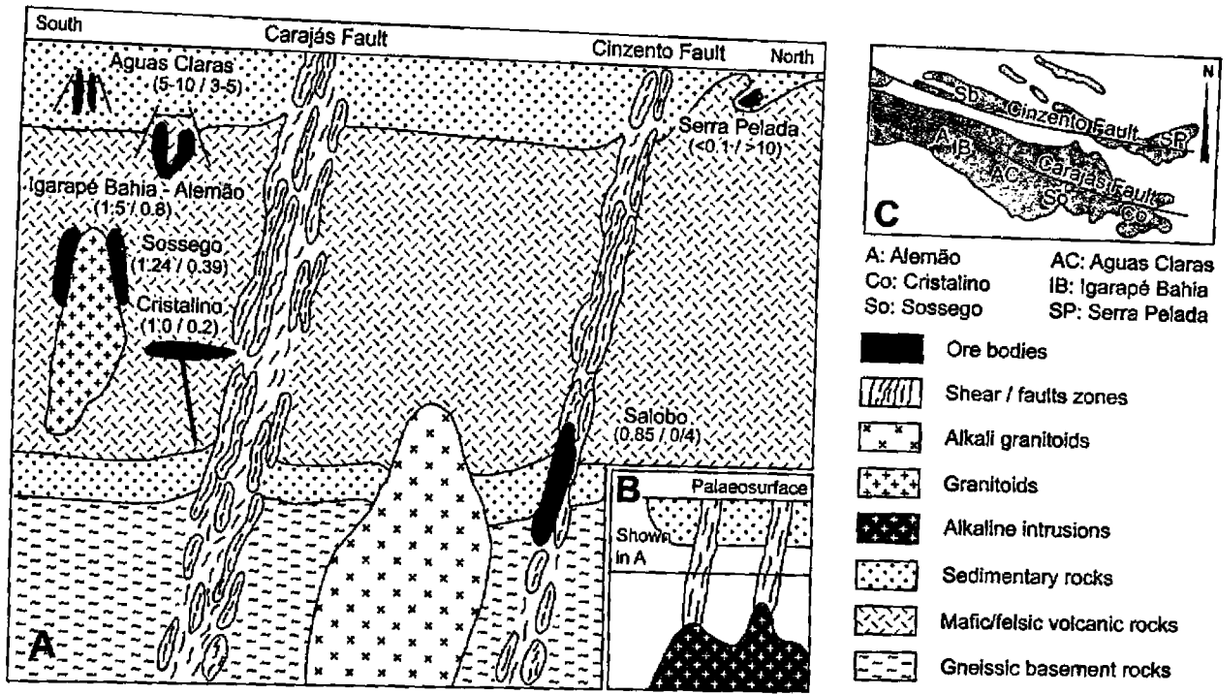


Figure 12: Schematic diagram of Fe-oxide-Cu-Au deposits in the Carajás Mineral Province, showing the interpreted spatial and depth position of the Serra Pelada Au-PGE deposit. A is a schematic cross section; B shows the conceptual relationship between the cross section, crustal-scale faults and alkaline intrusions below the depth of exposure of the ore bodies, and C is a schematic plan showing the spatial position of the deposits relative to the Cinzento and Carajás Faults. Average Cu (%) and Au (g/t) grades are shown (1.0 / 0.2 = 1.0% Cu, 0.2 g/t Au). Aadapted from a figure in Kerrich *et al.* (2000).

9. In terms of its structural timing (Fig. 6), the Serra Pelada Au-PGE deposit was most likely genetically related to either the ca 1.88 Ga sub-alkaline to alkaline granites that form small plutons within a few kilometres of the deposit, or possibly the alkaline A-type ca 2.57 Ga Old Salobo granite/Estrela granitoid complex. However, there is no published dating of the deposit, and the ages of the Fe-oxide Cu-Au deposits, with which Serra Pelada is compared, are also poorly constrained.

10. If Serra Pelada is a distal equivalent of the Fe-oxide Cu-Au deposit group, it may represent a deposit style that has been overlooked in provinces of this deposit group. In view of the current high price of PGEs, it is an attractive target type, although the geometry of the Serra Pelada ore would make it a particularly difficult target in a geologically poorly-defined terrain.

Acknowledgements

The authors wish to express gratitude to the Companhia Vale do Rio Doce (CVRD) and Rio Doce Geologia Mineração S.A. (DOCEGEO), particularly Diogenes Vial, for permitting the funding and research of the Serra Pelada deposit and surrounding Serra Leste Prospect. All geologists and staff of the Serra Leste Project are gratefully thanked for their expertise, geological input, professionalism and support during extended fieldwork. Fernando Tallarico is thanked for enlightening discussions. The paper was improved by the comments of the reviewers Chuck Thorman, Pat Williams, Warren Day and Mark Barton, and by the editorial comments from Rich Goldfarb.

References

Araújo, O.J.B., Maia, R.G.N., Jorge-João, X.S. and Costa, J.B.S., 1988 - A megaestruturação arqueanada folha Serra dos Carajás; in Congresso Latino-Americano Geologia, 7, Belém, *Sociedade Brasileira de Geologia/DNPM*, Anais, pp. 324-333.

Barros, C.E. de M., Dall'Agnoll, R., Barbey, P. and Boullier, A.M., 1997 - Geochemistry of the Estrela Granite Complex, Carajás region, Brazil: an example of an Archean A-type granitoid; *Journal of South American Earth Sciences*, v. 10, pp. 321-330.

Campbell, I.H., Compston, D.M., Richards, J.P., Johnson, J.P. and Kent, A.R.J., 1998 - Review of the application of isotopic studies to the genesis of Cu-Au mineralization at Olympic Dam and Au mineralization at Porgera, Tennant Creek district and Yilgarn Craton; *Australian Journal of Earth Science*, v. 45, pp. 201-218.

CVRD, 1998 - The Serra Leste gold project; Internal company report, *Companhia Vale do Rio Doce*, pp. 1-25.

Eliopoulos, D.G. and Economou-Eliopoulos, M., 1991 - Platinum-group element and gold contents in the Skouries Porphyry Copper Deposit, Chalkidiki Peninsula, Northern Greece; *Economic Geology*, v. 86, pp. 740-749.

Fahrni, K.C., Macauley, T.N. and Preto, V.A.G., 1976 - Copper Mountain and Ingerbelle; *Canadian Institute of Mining and Metallurgy*, Special Volume 15, pp. 368-375.

Frei, R., 1995 - Evolution of mineralising fluid in the porphyry copper system of the Skouries Deposit, Northeast Chalkidiki (Greece): Evidence from combined Pb-Sr and stable isotope data; *Economic Geology*, v. 90, pp. 746-762.

Groves, D.I., Goldfarb, R.J., Gebre-Mariam, M., Hagemann, S.G. and Robert, F., 1998 - Orogenic gold deposits: A proposed classification in the context of their crustal distribution and relationship to other gold deposit types; *Ore Geology Reviews*, v. 13, pp. 7-27.

Groves, D.I. and Vielreicher, N.M., 2001 - The Phalabowra (Palabora) carbonatite-hosted magnetite-copper sulfide deposit, South Africa: an end-member of the iron-oxide copper-gold-rare earth element deposit group?; *Mineralium Deposita*, v. 36; pp. 189-194.

Hasui, Y. and Almeida, F.F.M., 1985 - The Central Brazilian Shield revisited; *Episodes*, v. 8, pp. 29-37.

Hauck K.I., 1990 - Petrogenesis and tectonic setting of middle Proterozoic iron oxide-rich ore deposits: An ore deposit model for Olympic Dam-type mineralization; *U.S. Geological Survey*, Bulletin 1932, pp. 4-39.

Hitzman, M.W., Oreskes, N. and Einaudi, M.T., 1992 - Geological characteristics and tectonic setting of Proterozoic iron-oxide (Cu-U-Au-REE) deposits; *Precambrian Research*, v. 58, pp. 241-287.

Hofstra, A.H. and Cline, J.S., 2000 - Characteristics and models for Carlin-type gold deposits; *in* Hagemann, S.G. and Brown, P.E., (eds.) Gold in 2000, *Reviews in Economic Geology*, v. 13, pp. 163-214.

Holdsworth, R.E. and Pinheiro, R.V.L., 2000 - The anatomy of shallow-crustal transpressional structures: insights from the Archean Carajás fault zone, Amazon, Brazil; *Journal of Structural Geology*, v. 22, pp. 1105-1123.

Huhn, S.R.B. and Nascimento, J.A.S., 1997 - São os depósitos cupríferos de Carajás do tipo Cu-Au-U-ETR?; *in* Costa, M.L., Angélica, R.S. (eds.), Contribuições a Geologia da Amazônia, Belém, *FINEP/SociedadeBrasileira de Geologia-Núcleo Norte*, pp. 143-160.

Hunh, S.R.B., Santos, A.B.S., Amaral, A.F., Ledsham, E.J., Gouveia, J.L., Martins, L.P.B; Montavão, R.M.G. and Costa, V.C., 1988 - O terreno granito greenstoneda região de Rio Maria - Sul do Pará; *in* Congresso Brasileiro de Geologia, 35, Belém, *Sociedade Brasileira de Geologia*, Anais, v.3, pp.1438-1452.

Huhn, S.R.B., Souza, C.I.de J., Albuquerque, M.C. de, Leal, E.D. and Brustolin, V., 1999 - Descoberta do depósito Cu(Au) Cristalino: gelogia e mineralização associada - Região da Serra do Rabo - Carajás - PA; *in* Simpósio de Geologia da Amazônia, 6, Manaus, *Sociedade Brasileira de Geologia-Núcleo Norte*, Boletim, pp. 140-143.

Jensen, E.P. and Barton, M.D., 2000 - Gold deposits related to alkaline magmatism; *in* Hagemann, S.G. and Brown, P.E., (eds.) Gold in 2000, *Reviews in Economic Geology*, v. 13, pp. 279-310.

Jorge João, X., da S., Neves, A.P. and Leal, J.W.L., 1982 - Ouro da Serra Pelada, aspecto da geologia e garimpagem; *in* Simpósio de Geologia da Amazônia 1, Belém, *Sociedade Brasileira de Geologia*, Anais, v. 3; pp. 52-61.

Kerrich, R., Goldfarb, R., Groves, D.I. and Garwin, S., 2000 - The geodynamics of world-class gold deposits: characteristics, space-time distribution, and origins; *in* Hagemann, S.G. and Brown, P.E., (eds.) Gold in 2000, *Reviews in Economic Geology*, v. 13, pp. 501-551.

Lab, K.O. and Costa, J.B.S., 1992 - Evolução lito-estrutural do Duplex Serra Pelada; *in* Semana de Seminários do Curso de Pós-Graduação em Geologia e Geoquímica, Centro de Geociências, *Universidade Federal do Pará, Belém.*

Large, R.R., Huston, D.L., McGoldrick, P.J., Ruxton, P.A. and McArthur, G., 1989 - Gold distribution and genesis in Australian volcanogenic massive sulfide deposits and their significance for gold transport models; *Economic Geology Monograph*, v. 6, pp.520-536.

Machado, N., Lindenmayer, Z., Krogh, T.E. and Lindenmayer, D., 1991 - U-P geochronology of Archean magmatism and basement reactivation in the Carajás area, Amazon Shield, Brazil; *Precambrian Research*, v. 49, pp. 329-354.

Mark, G., Oliver, N.H.S., Williams, P.J., Valenta, R.K. and Crookes, R.A., 2000 - The evolution of the Ernest Henry hydrothermal system; *in* Porter, T.M. (ed.), Hydrothermal Iron Oxide Copper-Gold and Related Deposits: A Global Perspective, *PGC Publishing, Adelaide*, v. 1, pp. 123-136.

McCallum, M.E., Loucks, R.R., Carlson, R.R., Cooley, E.F. and Doerge, T.A., 1976 - Platinum metals associated with hydrothermal copper ores of the New Rambler Mine, Medicine Bow Mountains, Wyoming; *Economic Geology*, v. 71, pp. 1429-1450.

Meireles, E. de M. and Teixeira, J.T., 1982 - Depósito de ouro de Serra Pelada; *in* Sympósio de Geologia da Amazônia, 1, Belém, *Sociedade Brasileira de Geologia*, v. 3, pp. 75-85.

Mountain, B.W. and Wood, S.A., 1988 - Chemical controls on the solubility, transport and deposition of platinum and palladium in hydrothermal solutions: a thermodynamic approach; *Economic Geology*, v. 83, pp. 492-510.

Murphy, P.J., Stevens, G. and La Grange, M.S., 1999 - Gold-chloride speciation in hydrothermal fluids: a Raman spectroscopic study at geologically relevant pressures and temperatures; *Economic Geology Research Unit, University of Witwatersrand, Johannesburg*, Information Circular 334.

Mutschler, F.E. and Mooney, T.C., 1993 - Precious-metal deposits related to alkalic igneous rocks: Provisional classification, grade-tonnage data and exploration frontiers; *in* Kirkham, R.V., Sinclair, W.D., Thorpe, R.I. and Duke, J.M. (eds.), Mineral Deposit Modeling, *Geological Association of Canada*, Special Paper 40, pp.479-520.

Nakamura, N., 1974 - Determination of REE, Ba, Fe, Mg, Na and K in carbonaceous and ordinary chondrites; *Geochimica et Cosmochimica Acta*, v. 38, pp. 757-775.

Olszewski, W.J., Wirth, K.R., Gibbs, A.K. and Gaudette, H.E., 1989 - The age, origin, and tectonics of the Grão Pará Group and associated rocks, Serra dos Carajás, Brazil: Archean continental volcanism and rifting; *Precambrian Research*, v. 42, pp. 229-254.

Oreskes, N. and Einaudi, M.T., 1990 - Origin of rare earth element-enriched hematite breccias at the Olympic Dam Cu-U-Au-Ag deposit, Roxby Downs, South Australia; *Economic Geology*, v. 85, pp. 1-28.

Oreskes, N. and Einaudi, M.T., 1992 - Origin of hydrothermal fluids at Olympic Dam: preliminary results from fluid inclusions and stable isotopes; *Economic Geology*, v. 87, pp. 64-90.

Pinheiro, R.V.L., 1997 - Reactivation history of the Carajás and Cinzento strike-slip systems, Amazon, Brazil; Unpublished PhD Thesis, *University of Durham, England*, 408p.

Pollard, P.J., Mark, G. and Mitchell, L.C., 1998 - Geochemistry of post-1540 Ma granites in the Cloncurry District, northwest Queensland; *Economic Geology*, v. 93, pp. 1330-1344.

Reeve, J.S., Cross, K.C., Smith, R.N. and Oreskes, N., 1990 - Olympic Dam copper-uranium-gold-silver deposit; *in* Hughes, F.E., (ed.) Geology of the Mineral Deposits of Australia and Papua New Guinea, *The Australasian Institute of Mining and Metallurgy, Melbourne*, Monograph No. 14, v. 2, pp. 1009-1035.

Requia, K. and Fontboté, L., 2000 - The Salobo iron oxide copper-gold deposit, Carajás, Northern Brazil; *in* Porter, T.M., (ed.), Hydrothermal Iron Oxide Copper-Gold and Related Deposits: A Global Perspective, *PGC Publishing, Adelaide*, v. 1, pp. 225-236.

Ronzê, P.C., Soares, A.D.V., Giovanni, S. and Barreira, C.F., 2000 - Alemão copper-gold (U-REE) deposit, Carajás, Brazil; *in* Porter, T.M., (ed.), Hydrothermal Iron Oxide Copper-Gold and Related Deposits: A Global Perspective, *PGC Publishing, Adelaide*, v. 1, pp. 191-202.

Rowell, W.F. and Edgar, A.D., 1986 - Platinum-group element mineralization in a hydrothermal Cu-Ni sulfide occurrence, Rathbun Lake, northeastern Ontario; *Economic Geology*, v. 81, pp. 1272-1277.

Santos, J.O.S., Hartmann, L.A., Gaudette, H.E., Groves, D.I., McNaughton, N.J. and Fletcher, I.R., 2000 - New understanding of the Amazon Craton Provinces, based on field work and radiogenic isotope data; *Gondwana Research*, v.3, pp. 453-488.

Seward, T.M. and Barnes, H.L., 1997. Metal transport by hydrothermal ore fluids; *in* Barnes H.L. (ed.), Geochemistry of Hydrothermal Ore Deposits, 3rd edition, *Wiley, New York*, pp. 435-486.

Soares, A.D.V., Ronzê, P.C., Santos, M.G.S., Leal, E.D. and Barreira, C.F., 2000 - Geologia e mineralizações do depósito de Cu-Au Alemão - Provincia Mineral de Carajás (PA); in Simpósio de Geologia da Amazônia, 6, Manaus, *Sociedade Brasileira de Geologia-Núcleo Norte*, Resumos Boletim, pp. 144-147.

Souza, L.H. and Vieira, E.A.P, 2000 - Salobo 3 Alpha Deposit: geology and mineralization; *in* Porter, T.M., (ed.), Hydrothermal Iron Oxide Copper-Gold and Related Deposits: A Global Perspective, *PGC Publishing, Adelaide*, v. 1, pp. 213-224.

Tallarico, F.H.B, Coimbra, C.R. and Costa, C.H.C., 2000a - The Serra Leste sediment-hosted Au-(Pd-Pt) mineralization, Carajás Province; *Revista Brasileira de Geociências*, v. 30, pp. 226-229.

Tallarico, F.H., Oliveirs, C.G. and Figueiredo, B.R., 2000b - The Igarapé Bahia Cu-Au mineralization, Carajás Province; *Revista Brasileira de Geociências*, v. 30, pp. 230-233.

Tazava, E. and de Oliveira, C.G., 2000 - The Igarapé Bahia Au-Cu-(REE-U) deposit, Carajás Mineral Province, Northern Brazil; *in* Porter, T.M., (ed.), Hydrothermal Iron Oxide Copper-Gold and Related Deposits: A Global Perspective, *PGC Publishing, Adelaide*, v. 1, pp. 203-212.

Trendall, A.F., Basei, M.A.S., de Laeter, and Nelson, D.R., 1998 - SHRIMP zircon U-Pb constraints on the age of the Carajás Formation, Grão Pará Group, Amazon Craton; *Journal of South American Earth Sciences*, v. 11, pp. 265-277.

Twyerould, S.C., 1997 - The geology and genesis of the Ernest Henry Fe-Cu-Au deposit, NW Queensland, Australia; Unpublished PhD thesis, *University of Oregon*, 494p.

Verwoerd, W.J., 1986 - Mineral deposits associated with carbonatites and alkaline rocks; *in* Anhaeusser C.R., Maske S., (eds.), Mineral Deposits of Southern Africa, *Geological Society of South Africa, Johannesburg*, v. 2, pp. 2173-2191.

Villas, R.N. and Santos, M.D., 2001 - Gold deposits of the Carajás mineral province: deposit types and metallogenesis; *Mineralium Deposita*, v. 36, pp. 300-331.

Werle, J.L., Ikramuddin, M. and Mutschler, F.E., 1984 - Allard Stock, La Plata Mountains, Colorado – an alkaline rock-hosted porphyry copper – precious metal deposit; *Canadian Journal of Earth Science*, v. 21, pp. 630-641.

Wood, S.A., Mountain, B.W. and Pan, P., 1992 - The aqueous geochemistry of platinum, palladium and gold: recent experimental constraints and a re-evaluation of theoretical predictions; *Canadian Mineralogist*, v. 30, pp. 955-983.

PGC
PUBLISHING

Friehauf, K.C., Smith, R.C., Volkert, R.A., 2002 - Comparison of the Geology of Proterozoic Iron Oxide Deposits in the Adirondack and Mid-Atlantic Belt of Pennsylvania, New Jersey and New York; *in Porter, T.M. (Ed.), Hydrothermal Iron Oxide Copper-Gold & Related Deposits: A Global Perspective*, Volume 2; PGC Publishing, Adelaide, pp 247-252.

COMPARISON OF THE GEOLOGY OF PROTEROZOIC IRON OXIDE DEPOSITS IN THE ADIRONDACK AND MID-ATLANTIC BELT OF PENNSYLVANIA, NEW JERSEY AND NEW YORK

[1]Kurt C. Friehauf, [2]Robert C. Smith II, [3]Richard A. Volkert

[1]*Dept. of Physical Sciences, Kutztown Univ., Kutztown, PA, USA*
[2]*Pennsylvania Geol. Survey, Harrisburg, PA, USA*
[3]*New Jersey Geol. Survey, Trenton, NJ, USA*

Abstract - Proterozoic hydrothermal iron oxide deposits occur within two metallogenic belts in the northeastern U.S.: the Adirondack region, and the Mid-Atlantic (Reading Prong) belt. A 175 km wide belt of Palaeozoic cover separates these two regions, although some iron deposits occur in Proterozoic rocks near the unconformity, suggesting a possible continuation beneath the cover. Although potentially part of the same continuous metallogenic province sharing similar mineralogy, host rock composition and hydrothermal alteration, deposits in the two regions differ in degree of deformation. Differences in the degree of metamorphic deformation fuel the debate of the relative timing of mineralisation, igneous activity, and metamorphism. Generally less deformed textures in the Adirondack deposits led workers in the New York deposits to conclude iron ores in the Adirondacks are associated with anorogenic granites that post-date peak metamorphism. Folded iron ores in granitic gneiss of the Mid-Atlantic belt suggest some deposits in eastern Pennsylvania, northern New Jersey, and southern New York predate peak metamorphism. REE-enriched deposits in both belts are characterised by abundant apatite, tourmaline, and manganese concentrations, as well as the presence of hematite-chlorite alteration in addition to magnetite. Unlike deposits hosted exclusively within granite gneisses, deposits within supracrustal rocks commonly contain significant sulphides and so are potential hosts for copper mineralisation.

Introduction

Iron ores played a prominent role in American history dating back to British colonial times. The earliest workings in the New Jersey Highlands produced magnetite ore for smelting in charcoal furnaces in the late 1600's. Continued exploration and development ultimately revealed the region to host many of these small deposits, in addition to several larger districts such as Benson Mines (NY), Dover (NJ), and Cornwall (PA). Iron mining in the eastern U.S., however, declined as production from large banded iron formations began to dominate the market.

The recognition of a link between some iron oxide deposits and REE, U, Cu, and/or Au mineralisation in the last two decades and publication of Foose and McLelland's paper (1995) sparked renewed interest in the region. Several iron oxide deposits in each region contain elevated REE, U, and Th concentrations, although few copper and no significant gold deposits are known. The purpose of this paper is to compare the geology of the major Proterozoic iron oxide deposits in the Adirondack and Reading Prong regions of the northeastern U.S. and highlight regional trends with implications for mineral exploration in the region.

Regional Setting and Tectonic Overview

The rock record contains evidence for at least five major compressional orogenies in the northeastern United States since Proterozoic times. The high grade metamorphic event associated with the Grenville orogeny occurred in two stages. Arc-derived sedimentary and volcanic rocks were metamorphosed to upper amphibolite and granulite facies first during the 1300-1200 Ma Elzevirian Orogeny, and then again during the 1100-1050 Ma Ottawan Orogeny (Grauch and Aleinikoff, 1985). A rift sequence of supracrustal gneisses of sedimentary and volcanic origin and marble were deposited in the intervening interval (Volkert and Drake, 1999). Anorogenic granites and granitic pegmatites intruded the region both between these Mesoproterozoic orogenies, and afterward (Drake et al., 1991, Drake and Volkert, 1991). Neoproterozoic rift-related clastic sedimentary and bimodal volcanic rocks unconformably overly the Mesoproterozoic rocks (Drake, 1999, Volkert et al., 1999). Rifting resumed circa 575 Ma, primarily south of the Adirondack region, producing a sequence of bimodal volcanic and clastic sedimentary rocks. Iron oxide mineralisation is thought to have occurred both during the Mesoproterozoic and Neoproterozoic events.

Palaeozoic sedimentary rocks unconformably overlie the Proterozoic section, covering a 175 km wide belt between the Adirondack region and the Reading Prong to the south. Compression during the Ordovician Taconic Orogeny, Devonian Acadian Orogeny, and Permian Alleghany Orogeny resulted in lower greenschist facies metamorphism of sedimentary rocks, development of a fold and thrust belt range of mountains (Appalachian range), and ultimately the formation of the Pangea Super-continent. Little igneous activity and no iron oxide mineralisation is known to be associated with the Palaeozoic compressional orogenies.

Rifting during the late Triassic and early Jurassic led to the opening of the Atlantic Ocean, intrusion of voluminous dolerite sills, and formation of restricted red bed rift basins. Metasomatism of carbonate rocks near the dolerite intrusions formed several large magnetite skarns (eg., Cornwall, Pennsylvania). The eastern margin of the North American continent has remained passive since the Jurassic with minor isostatic uplift associated with erosion of the highlands.

Types of Iron Oxide Deposits in the Northeastern U.S.

Several types of iron oxide-rich mineral deposits occur in the northeastern U.S. Large, titanium-rich orthomagmatic magnetite-ilmenite deposits associated with anorthosite intrusions such as the Sanford Lake district (Stephenson, 1945) are restricted to the Adirondack region. Although Proterozoic in age, these are not the focus of this paper.

Sedimentary oolitic ironstones of the Silurian Clinton Formation (Newland and Hartnagel, 1908) occur in northwestern New York. Although they were a historic source of iron, they will not be discussed in this paper due to their sedimentary nature.

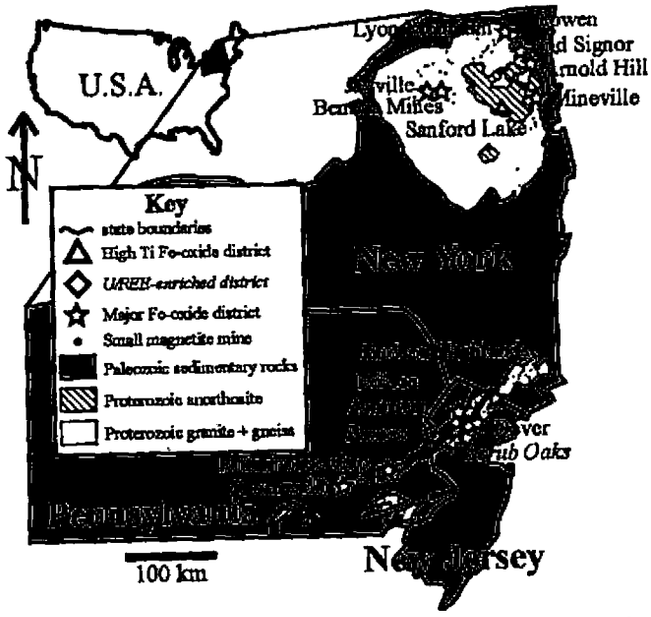


Figure 1: Generalised geological map of the Mid-Atlantic States region showing locations of major deposits described in text.

Several large magnetite skarns occur in Palaeozoic carbonate rocks along the margins of Triassic rift basins. These deposits are closely associated spatially with early Jurassic dolerite intrusions related to the Atlantic rifting event. Magnetite veins cut the dolerite sills. Rose, et al., (1985) demonstrated that, although the dolerite may have provided the heat that drove the circulation of hydrothermal fluids, the dolerite was an unlikely *source* for the hydrothermal fluids responsible for the formation of the Cornwall deposit. The Mesozoic magnetite skarns are generally richer in sulphide than the granite/gneiss-hosted Proterozoic deposits, and so host more copper and cobalt. Unlike the Proterozoic iron oxide deposits in the region, though, none of the Mesozoic deposits have known elevated uranium and rare earth concentrations, nor are the magnetite skarns related to granitoid intrusions. Although the absence of associated granites might preclude the inclusion of these Mesozoic magnetite skarns from the iron oxide class of deposits in the view of proponents of magmatic fluid models, advocates of non-magmatic sources for iron-oxide deposit mineralising brines may see the adjacent rift basin sediments as a potential source of evaporitic brines (eg., Rose, et al., 1985; Barton and Johnson, 1995).

The low-titanium, Proterozoic iron oxide deposits associated with anorogenic granites and large-scale hydrothermal alkali exchange alteration zones occur in both the Adirondack and Reading Prong regions (Figure 1). Foose and McLelland (1985) brought attention to these deposits as members of the large-scale hydrothermal iron oxide family of which Kiruna and Olympic Dam are members. Several of the deposits in the northeastern U.S. are enriched in uranium and REE, although most lack significant copper and gold resources.

Major Deposits of the Adirondack Region

The Lyon Mountain Granite Gneiss (LMG) hosts most of the major magnetite deposits in Adirondack region. There are several phases of the Lyon Mountain Granite Gneiss which differ primarily in their feldspar mineralogy. McLelland, et al, (2001) report the relative abundances of these phases in the Adirondacks to be quartz-microperthite leucogranite (45%), quartz-albite leucogranite (20%), quartz-microcline leucogranite (10%), and micro-antiperthite granite (25%). Minor sphene, aegerine-augite, and disseminated magnetite occur in addition to the quartz and feldspar. Uranium-lead dates by Chiarenzelli and McLelland (1991) and McLelland, et al. (2001) on zircons in the LMG constrain granitic intrusion ages to 1055-1035 Ma. McLelland (1984) notes that the LMG lacks strong deformation, indicating intrusion postdates peak metamorphism.

Magnetite deposits throughout the region occur as lenses and veins within the LMG, associated with apatite and minor amounts of ilmenite and locally trace pyrite. All magnetite deposits in the region are associated with alkali exchange hydrothermal alteration and some of the apatite is enriched in REE (McKeown and Klemic, 1956; Lindberg

and Ingram, 1964), leading Foose and McLelland (1995, 2001) to draw the comparison with Kiruna-type / Olympic Dam-type deposits.

Lyon Mountain / Clinton County District, New York

Total production from the Clinton County district was less than 20 mt (million 'metric tons' or tonnes) (Postel, 1952). Most orebodies occur in pyroxene-rich microperthite phases of the LMG and/or pyroxene skarns, although sodic phases of the LMG host almost 25% of the ores in the district (Postel, 1952). There is not a clear spatial regional trend segregating deposits in potassic rocks from those in sodic rocks, but deposits in sodic rocks generally occur in the centre, surrounded by ores in potassic rocks where several deposits cluster.

The Chateaugay or Lyon Mountain Mine was the biggest single producer in Clinton County, yielding 15 mt of magnetite ore. Ore in the Lyon Mountain Mine occurs in pyroxene-bearing, pink, microperthite-rich phases of the LMG (Postel, 1952). Gallagher (1937) describes "miarolitic cavities" up to a metre in diameter, lined with pegmatitic orthoclase, microperthite, hastingsite, and quartz overgrown by magnetite and albite, in the LMG of the Lyon Mountain Mine area. Gneissic foliation and pegmatites in the district are clearly folded, leading Newland (1908) to interpret the concordance of massive magnetite mineralisation with gneissic foliation to indicate mineralisation predated metamorphism. Trace amounts of ilmenite occur with magnetite in ore lenses, along with highly variable apatite contents and extremely scarce pyrite (Gallagher, 1937). Quartz, feldspars, aegerine-augite, and hastingsite also occur as minor gangue in magnetite bodies. McLelland, et al. (2001) report data on quartz-magnetite oxygen isotope pairs that indicate equilibrium at temperatures between 600° and 700°C and $\delta^{18}O$ values consistent with an evolved basinal brine source for the ore-forming fluids.

Martite ores in the Ausable group of mines south of the Lyon Mountain Mine occur in sodic plagioclase-rich phases of the LMG (albite-oligoclase composition). Nearby magnetite ores occur primarily in pink microperthite-rich, ferromagnesian mineral-poor phases of the LMG associated with variable amounts of purple fluorite (Postel, 1952).

Mineville District, New York

The largest producer in the Adirondacks, the Mineville district, hosts ore in relatively sodic phases of the LMG ("syenite" of Kemp, 1908). Host rock LMG consists of sodic plagioclase, microperthite, microcline, and quartz with minor augite, sphene, and magnetite, commonly assaying up 6% Na_2O (McKeown and Klemic, 1956). Magnetite lenses, pinching and swelling, but conformable to the metamorphic foliation, are accompanied by variable amounts of REE-bearing fluorapatite. McKeown and Klemic (1956) reported monazite and bastnaesite associated with hematite fill fractures in and rim apatite, giving fourteen apatite separates from magnetite ores an average of 0.032% U, 0.15% Th, and 11.14% REE oxides. Kemp's (1908) description suggests REE-bearing apatite is particularly abundant in "Red Ore" (p. 80). Traces of pyrite and tourmaline occur as gangue.

Benson Mines Deposit, New York

Although the most recent production statistics indicate a total production of 18.6 mt as of 1965 (Crump and Beutner, 1968), the 3.5 km long pit suggests significant additional production occurred before mine closure in 1976. Unlike most other magnetite deposits in the Adirondack region, the Benson Mines deposit is closely associated with metasedimentary rocks in addition to granitic gneisses. Garnet-quartz-K-feldspar gneiss, sillimanite-quartz-microcline gneiss, and pyroxene-hornblende-quartz-orthoclase gneiss all host ore (Crump and Beutner, 1968). A significant amount of specular hematite occurs with magnetite, in addition to traces of molybdenite, fluorite, apatite, sphene, rutile, and ilmenite. Minor copper as bornite, chalcopyrite, chalcocite, covellite, azurite, malachite, and native copper occurs at Benson Mines (Crump and Beutner, 1968). Overgrowths of poikiloblastic garnet and sillimanite led Hagni, et al. (1969) to conclude that at least some iron mineralisation predated metamorphism.

Jayville Mine, New York

Magnetite in the Jayville deposit occurs with biotite "sköls" that are strongly altered to earthy chlorite cut by calcite-hematite-pyrite-jasper veinlets (Leonard and Buddington, 1964). Abundant limonite throughout the deposit suggests the gneiss contained large amounts of sulphide prior to supergene oxidation. Abundant vonsenite ($(Fe^{+2})_2Fe^{+3}BO_5$), and elevated Mn, Ba, and F also characterise the Jayville deposit. Whether the calcite veins were derived from leaching of now-eroded overlying metasediments or much younger rocks remains undetermined.

Major Deposits of the Mid-Atlantic Iron Belt (Reading Prong)

Rittenhouse Gap, Pennsylvania

The Rittenhouse Gap mines are the largest and best studied of the Proterozoic deposits in Pennsylvania. En echelon magnetite veins cut granitic gneiss. The foliated granitic gneiss host rock is composed largely of sodic plagioclase and quartz with only trace amounts of biotite and K-feldspar. Sharp-walled magnetite veins contain quartz, biotite, and riebeckite, whereas disseminated ores consist of magnetite-quartz-plagioclase±biotite. Magnetite-quartz-feldspar intergrowths show granoblastic texture with magnetite forming interstitial to quartz-feldspar grains, suggesting equilibrium during high-grade metamorphism of the ores. Riebeckite is partially altered to brown sericite along cleavage planes. Coarse-grained quartz-feldspar-magnetite-allanite "pegmatites" also occur in the district, but do not constitute ore. Flow-banded, aphanitic felsite dykes with sparse feldspar phenocrysts and metabasalt

dykes crosscut magnetite veins. These dykes contain high Nb, Ta, Zr, Hf, Be, Ga, Sn, and W concentrations characteristic of volcanic rocks related to the Neoproterozoic event, supporting a Mesoproterozoic age of mineralisation. Pyrite, molybdenite, and fluorite-bearing veinlets with trace sphalerite cut felsite dykes, and do not appear to be related to the magnetite mineralisation.

Dover District, New Jersey

The Dover district is the largest iron oxide district in the Mid-Atlantic (Reading Prong) belt, having produced over 26 mt of magnetite ore. Ore occurs as high-grade magnetite veins that pinch and swell cutting highly sodic Losee Gneiss. Magnetite is locally associated with minor amounts of ilmenite and highly variable amounts of apatite. Pyrite, chalcopyrite, and pyrrhotite occur with magnetite in quantities less than 2%. Leucocratic alaskite consisting essentially of pure K-feldspar and quartz is spatially associated with ore (Sims and Buddington, 1958). These potassic alteration zones lie within a larger area dominated by strongly sodic leucocratic rocks such as albite-oligoclase gneiss. Granitic pegmatites are also spatially associated with some deposits within the district, although cross-cutting relationships suggest they pre-date iron mineralisation (Sims and Buddington, 1958).

The Scrub Oaks deposit contained significant REE mineralisation in magnetite veins that cut sodic-altered metavolcanic gneisses. The coarse-grained magnetite at Scrub Oaks was associated with lesser amounts of apatite, rutile, tourmaline, and biotite (Sims, 1953, Williams, 1965). "Pegmatites" are spatially associated with some magnetite deposits in the Scrub Oaks deposit. REE concentrations are locally up to 3% oxides in coarse-grained magnetite partially altered to hematite (Klemic et al., 1959).

Andover / Sulfur Hill District, New Jersey

The Andover/Sulfur Hill district produced less than half a million tonnes of iron ore (Sims and Leonard, 1952), but exemplifies hematite-rich deposits in the Mid-Atlantic Iron Belt. Ore in the Andover deposit occurs primarily as massive black hematite (martite) in highly potassic metasedimentary rocks. Ores are rich in manganese (up to 0.45 % MnO), lack sulphides, and consist primarily of hematite, magnetite, and quartz with minor chlorite and sericite alteration of the wall rocks (Volkert and Puffer, 2001). Host rocks experienced only greenschist facies metamorphic grades, leading Volkert to conclude that, unlike the magnetite deposits at Dover and Rittenhouse Gap, they are Neoproterozoic and postdate high-grade metamorphism. The Sulfur Hill deposit hosts ore in skarns consisting of andradite garnet, salite pyroxene, scapolite, stilpnomelane/biotite, apatite, and fluorite (Neumann, 1952, Sims and Leonard, 1952) associated with pyrite, pyrrhotite, sphalerite, galena, chalcopyrite, and minor molybdenite (Neumann, 1952).

Discussion

Relative Timing of Mineralisation and Metamorphism

The principal debate in the northeastern iron oxide metallogenic belt focuses on the timing of mineralisation relative to metamorphism and granitic magmatism. Foose and McLelland, who have studied the Adirondack deposits extensively, interpret the relatively undeformed textures of those rocks to indicate mineralisation significantly post-dates peak metamorphism (Foose and McLelland, 1995). They note that the close spatial relationship between magnetite ores and the 1055-1035 Ma Lyon Mountain

	Reading Prong Region	Adirondack Region
Granite-hosted deposits	Rittenhouse Gap, PA Edison, NJ Dover, NJ	Lyon Mountain, NY Mineville, NY
Supracrustal metasedimentary/metavolcanic gneiss-hosted deposits	Andover, NJ Dover, NJ	Benson Mines, NY
Carbonate-hosted deposits	Hudson Highlands, NY	Jayville, NY
REE-enriched deposits	Scrub Oaks, NJ	Mineville, NY
Mesozoic deposits	Cornwall, PA French Creek, PA	None known

Table 1: Comparison of Major Proterozoic Fe-oxide Deposits in the Northeastern U.S.

Granite Gneiss suggests a genetic relationship. Based on their oxygen isotopic analyses, McLelland, et al. (2001) concluded that the Adirondack ores may have formed by circulation of evolved brines following intrusion of the Lyon Mountain Granite in a model similar to that proposed by Battles and Barton (1995) and Barton and Johnson (1996).

Geologists working in the Mid-Atlantic (Reading Prong) belt, on the other hand, interpret the folded veins, conformity of magnetite mineralisation with metamorphic foliation, and anhydrous character of mafic minerals in rocks hosting the ores to indicate mineralisation predated the intense metamorphism of the Grenville Orogeny (eg., Buddington, 1966; Baker and Buddington, 1970; Volkert and Puffer, 2001). Although earlier workers proposed metamorphic origins for hydrothermal fluids in the Mid-Atlantic belt, we are currently exploring hypotheses involving evolved brines or magmatic fluids. Whatever the source of the ore fluids in the Mid-Atlantic Belt, the occurrence of hematitic ores in greenschist facies rocks suggests that some iron mineralisation postdates metamorphism.

Analogous Deposits and General Geological Trends

In spite of differences in the interpretation of metamorphic fabrics and timing issues, similarities between deposits in the Adirondack region and the Mid-Atlantic Iron Oxide belt are striking (Table I).

The Jayville deposit of New York (Leonard and Buddington, 1964) and some of the hematitic deposits in the Mid-Atlantic Belt such as the Scrub Oaks deposit in the Dover district, NJ (Klemic, et al., 1959; Sims and Buddington, 1958) are characterised by hematite-stable high oxidation states, chloritic alteration, anomalous boron and manganese mineralisation. These deposits host the most significant concentrations of REE minerals, primarily as fluorapatite, monazite, and bastnaesite. Highly oxidised hematite-dominant deposits such as Andover, NJ, however, have only traces of apatite and lack REE mineralisation.

In general, sulphides are more common in the Mid-Atlantic Belt than in the Adirondack region. Within the Mid-Atlantic Belt, sulphides are most common in deposits spatially associated with supracrustal metasedimentary and metavolcanic (amphibolite) rocks. Sulphides are significant only in the Benson Mines and Jayville deposits of New York, both of which are characterised by the presence of supracrustal rocks. Adirondack deposits hosted exclusively within the Lyon Mountain Granite Gneiss lack sulphides. These relations suggest a possible sedimentary source for the sulphur. The fact that Mesozoic magnetite skarn deposits such as Cornwall, PA occur primarily in sedimentary rocks, contain abundant sulphides, and constitute the largest copper (and cobalt) resources in the region further supports this hypothesis. The relationship between sulphide content and supracrustal rocks (metasedimentary gneisses and amphibolites) is important because copper mineralisation occurs only in deposits with appreciable amounts of sulphide and so has implications for mineral exploration.

Acknowledgements

We would like to thank Mark Barton, Mike Foose, Eric Force, Craig Johnson, David Johnson, Jim McLelland, and John Puffer for enlightening discussions and feedback. We would also like to thank Mike Porter for his patience and hard work in editing this volume.

References

Crump, R. M., and Beutner, E. L., 1968 – The Benson Mines iron ore deposit, Saint Lawrence County, New York: *in*, Ridge, J. D., *ed.*, Ore Deposits of the United States – The Graton-Sales Volume, *American Institute of Mining, Metallurgical, and Petroleum Engineers*, 49-71.

Drake, A. A., Jr., 1999 – Precambrian and Lower Paleozoic metamorphic and igneous rocks – South Mountain and Reading Prong. *in* Shultz, Charles H., *ed., The Geology of Pennsylvania – Pennsylvania Geological Survey Special Publication* 1, pp.36-49.

Drake, A.A., Jr., and Volkert, R. A., 1991 – The Lake Hopatcong Intrusive Suite (Middle Proterozoic) of the New Jersey Highlands. *in* Drake, A.A., Jr., *ed.*, Contributions to New Jersey Geology - *U. S. Geological Survey Bulletin* 1952, p. A1-A9.

Drake, A.A., Jr., Aleinikoff, J.N., and Volkert, R.A., 1991 – The Byram Intrusive Suite of the Reading Prong – Age and tectonic environment. *in* Drake, A.A., Jr., *ed.*, Contributions to New Jersey Geology - U.S. Geological Survey Bulletin 1952, p. D1-D14.

Gallagher, D., 1937 – Origin of the Magnetite Deposits at Lyon Mountain, N.Y.: *New York State Museum Bulletin* no 311, 85p.

Grauch, R. I., and Aleinikoff, J. N., 1985 – Multiple thermal events in the Grenvillian orogenic cycle: Geochronologic evidence from the northern Reading Prong, New York-New Jersey [abs.]. *Geological Society of America Abstracts with Programs*, v. 17, p. 596.

Hagni, R. D., Masiello, R.A., and Tumialan, P.H., 1969, Metamorphic aspects of the magnetite-hematite deposit at Benson Mines, New York: *Economic Geology*, v. 64, 183-190.

Hunter, R. E., 1970 – The Valley and Ridge and Appalachian Plateau – Stratigraphy and sedimentation, facies of iron sedimentation in the Clinton Group: *in* Fisher, G. W.; Pettijohn, F. J.; Reed, J. C., Jr.; Weaver, K. N., *eds., Studies of Appalachian geology, central and southern*, 101-121.

Kemp, J. F., 1908 – The Mineville-Port Henry mine group: *in* Newland, David H., Geology of the Adirondack magnetite iron ores, *New York State Museum Bulletin* 119, 57-123.

Klemic, H., Heyl, A.V., Jr., Taylor, A.R., and Stone, Jerome, 1959 – Radioactive rare-earth deposit at Scrub Oaks mine, Morris County, New Jersey. *U. S. Geological Survey Bulletin* 1082-B, 59p.

Leonard, B. F., and . Buddington, A. F., 1964 – Ore deposit of the St. Lawrence County Magnetite district, Northwest Adirondacks, New York: *U. S. Geological Survey Professional Paper* 377, 259p.

Lindberg, M. L, and Ingram, B., 1964 – Rare-earth silicatian apatite from the Adirondack Mountains, New York: *U. S. Geological Survey Professional Paper* 501-B, B64-B65.

McKeown, F. A., and Klemic, H., 1956 – Rare-earth-bearing apatite at Mineville, Essex County, New York: *U. S. Geological Survey Bulletin* 1046-B, 9-23.

McLelland, J., Foose, M. P., and Morrison, J., 2001 – Kiruna-type low Ti, Fe oxide ores and related rocks, Adirondack Mountains, New York – High-temperature hydrothermal processes: *in* Slack, J. F., Johnson, C.A., Foose, M. P., and McLelland, J. M., *eds.*, Zinc and Iron Deposits of the Adirondack Mountains and New Jersey Highlands, *Society of Economic Geologists Guidebook*, November 2001, v. 35, 7-17.

McLelland, J., Kelly, W. M., and Petersen, E. U., 1993 – Magnetite-ilmenite ores at Sanford Lake: *in* Slack, J. F., and Offield, T. W., *eds.*, Selected mineral deposits of Vermont and the Adirondack Mountains, New York; I, Mineral deposits of the Adirondack Mountains; II, Besshi-type massive sulfide deposits of the Vermont copper belt *Society of Economic Geologists Guidebook*, October 1993, v. 17, 10-16.

Neumann, G. L., 1952 – Diamond drilling for zinc ore at Andover-Sulphur Hill iron mines, Sussex County, NJ. *U. S. Bureau of mines Report of Investigations* 4911, 13p.

Newland, D. H., 1908 – Geology of the Adirondack magnetic iron ores: *New York State Museum Bulletin* no. 119, 177p.

Newland, D.H., and Hartnagel, C.A., 1908 – Iron ores of the Clinton Formation in New York State: *New York State Museum Bulletin* no. 123, 76p.

Postel, A. W., 1952 – Geology of Clinton County Magnetite District, New York: *U. S. Geological Survey Professional Paper* 237, 87p.

Sims, P. K., and Buddington, A. F., 1958 – Geology and magnetite deposits of Dover District, Morris County, New Jersey: *U. S. Geological Survey Professional Paper* 287, 162p.

Sims, P. K., and Leonard, B. F., 1952 – Geology of the Andover mining district Sussex County, New Jersey. *New Jersey Department of Conservation and Economic Development, Geologic Series Bulletin* 62, 46p.

Stephenson, R. C., 1945 – Titaniferous magnetite deposits of the Lake Sanford Area, New York: *New York State Museum Bulletin* 340, 95p.

Volkert, R. A., and Puffer, J. H., 2001 – Field Trip Day Five: Road Log for the Sulfur Hill and Andover Iron Mines, New Jersey, *in in* Slack, J. F., Johnson, C.A., Foose, M. P., and McLelland, J. M., *eds.*, Zinc and Iron Deposits of the Adirondack Mountains and New Jersey Highlands, *Society of Economic Geologists Guidebook*, November 2001, v. 35.

Volkert, R. A., Monteverde, D.H., Gates, A. E., and Dalton, R. F., 1999 – Late Proterozoic Rapitan-type iron-formation in the Chestnut Hill Fm., New Jersey Highlands [abs.]: *Geological Society of America Abstracts with Programs*, v. 31, p. A-76.

Volkert, R.A., and Drake, A.A., Jr., 1999 – Geochemistry and stratigraphic relations of the Middle Proterozoic rocks of the New Jersey Highlands. *U. S. Geological Survey Professional Paper* 1565-C, 77p.

PGC PUBLISHING

Laznicka, P. 2002 - Wernecke Mountains (Yukon) Breccias and Scattered Ore Occurrences: What Contribution to FeOx-Cu-Au-U Metallogeny? *in* Porter, T.M. (Ed.), *Hydrothermal Iron Oxide Copper-Gold & Related Deposits: A Global Perspective*, Volume 2; PGC Publishing, Adelaide, pp 253-271.

WERNECKE MOUNTAINS (YUKON) BRECCIAS AND SCATTERED ORE OCCURRENCES: WHAT CONTRIBUTION TO FeOx-Cu-Au-U METALLOGENY ?

Peter Laznicka

Data Metallogenica Centre, Adelaide, Australia.

Abstract - The Wernecke and Southern Ogilvie Mountains in Yukon are part of an almost east-west trending range in the northern Canadian Cordillera in which several areas of the Palaeo-Mesoproterozoic basement are exposed, enveloped by a Phanerozoic miogeoclinal sequence. The oldest division, the ~1.8-1.4 Ga Wernecke Supergroup, is interpreted as a "clastic rift". It is an up to 15 km thick pile, the bulk of which is a monotonous, well-bedded siltite-quartz rich litharenite-argillite, topped by carbonate-pelite units. Less than 1% of the area consists of small gabbro to diorite intrusions of several, mostly Palaeoproterozoic and Mesoproterozoic, generations. The predominantly brittle deformation regime produced extensive tracts of disrupted and dismembered units grading to tectonic (not subduction !) melange. These have been overprinted by large scale Na, Ca, Mg, Fe, CO_2 and lesser Si, K metasomatism to produce widespread albitisation, chloritisation, carbonatisation, hematitisation and less extensive sericitisation (with local biotite) of the fractured sedimentary >> magmatic rocks as well as tectonic fragmentites. The "Wernecke Breccia" is a metasomatised disaggregated breccia series and it is associated with hundreds of small scattered showings of specular hematite, magnetite and chalcopyrite, several occurrences of U and Co minerals, and anomalous gold. Not even a marginally economic orebody has so far been discovered despite intermittent exploration going back to the 1960s. It appears that we are dealing with a moderately deep (closely above the ductile-brittle interface) level of regional release and displacement of metals from source rocks (Fe, Cu and Co from gabbros; U perhaps from carbonaceous argillites) by metasomatic destruction of the carrier minerals. However, the system lacked sufficient plumbing and the channelling required to produce better metal accumulations at higher levels.

Introduction

Ever since the Fe-oxide, Cu, U, Au, REE association were recognised as a "family" by Hitzman et al. (1992), the Wernecke Mountains and their Fe, Cu and U "deposits" have been widely quoted as key examples in the international literature. There are some 20 citations accumulated to date in which the Werneckes figure in an international context (eg. Bell, 1989; Hitzman et al., 1992; Hitzman, 2000). Many of these publications are directed more towards proposing concepts than reporting factual observations, while many salient facts are probably concealed in proprietary reports inaccessible to the international reader, including this writer. This contribution is based on considerable personal field experience, although not exhaustive or recent, and hence the conclusions and interpretations are certainly biased and may suffer from a lack of awareness of recent work or sites not visted by this writer.

The Werneckes are over 100 km from the nearest road and only accessible to those with a corporate budget, or to the most hardy. The area has only recently been de-glaciated and there are several small receding remnants of cirque glaciers. The rugged alpine physiography offers up to 100% absolutely fresh outcrop on ridges and upper mountain slopes, although the lower slopes are masked by talus and valleys are filled by drift and a few lakes. This exposure makes it possible to directly observe and graphically record the geology of some 60% of the area, over a relief of some 900 m, representing at least 12-15 km of stratigraphic column. The superb visibility is the main asset of the Werneckes, which compares favourably with areas like the Stuart Shelf where the "facts" have to be laboriously pulled up from 300-500 m depths by drilling. As a consequence, the geological continuity is a luxury directly observed only in a tiny fraction of the Stuart Shelf, namely in the Olympic Dam mine.

The problem with the Werneckes is that, although there have been numerous intermittent exploration campaigns since the 1960s, not even a marginally economic orebody has been found. It is thus one of the few provinces embracing members interpreted to belong to the "Fe-Ox" family that has not yet yielded an economic deposit. Do the Werneckes have "potential" ? Who knows, but if there is a large deposit, it should be much easier to actually see than is the case in the predominantly covered and deep

regolith surfaces in Australia, Zambia, Brazil, or even the Ozarks. These areas where more than 90% of the bedrock is concealed, appear to have a greater discovery potential than the Werneckes where some 60% of the bedrock is exposed. An undiscovered major deposit in the Werneckes would most likely be below the slope and valley debris if at all, although the recent discovery of the Voisey's Bay Cu-Ni orebodies demonstrate that some ore outcrops in the Canadian outback that could be directly seen have not been recognised, until very recently.

The Werneckes have the greatest value for basic research. The brittle tectonics is outstanding. This is one of the best regions in the world to study coarse fragmentites (especially breccias) in their natural setting (Laznicka, 1988), as some of the field relationships of these rocks, laboriously interpreted elsewhere, can often be directly exposed on the mountain slope, ready to be recorded. There is a striking interplay of breccias with areal hydrothermal alteration and metasomatism, especially albitisation. This is not to say that the origin of many of these breccias is known or interpreted without controversy, as we do not know what is and what has happened at depth, a crucial key to understanding. The Werneckes are also a field laboratory to study and appreciate the initial "small steps" in the formation of metallic deposits, that is the release of some trace metals at source, their transport and redeposition, in the form of a myriad "failed ore formation attempts": A veinlet of specularite here, a few specks of chalcopyrite there, over a large area, but nothing major. Again, the breccias, metasomatism and metal accumulation go together and many secrets remain to be revealed.

The lithology and stratigraphy of the Wernecke's is monotonous over much of the exposed sequence, with no volcanics, and only a few small mafic intrusions at the present level of exposure. However it is likely that the latter contribute more than the rest to the feeble mineralisation. This paper will also compare the Werneckes with other sequences around the world where some of the similar conditions and processes were at work, but with better results in terms of metal accumulation.

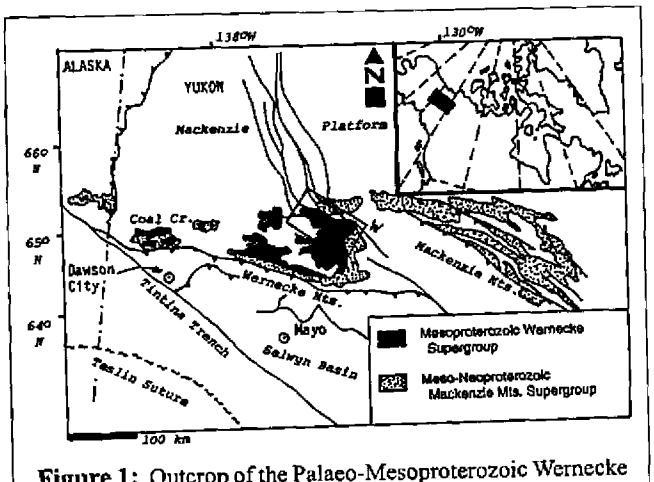


Figure 1: Outcrop of the Palaeo-Mesoproterozoic Wernecke Supergroup in the northern Canadian Cordillera in the Yukon. Modified after Laznicka 1992.

Regional Geology

The WNW to almost E-W trending Wernecke Mountains, together with the Southern Ogilvie Mountains farther west, conspicuously depart from the prevalent Cordilleran NW-SE structural grain (Fig. 1). They are located between the longitudes of 132° and 141° west, and latitudes of 64° and 66° north. The nearest settlements are Elsa in the Keno Hill Ag-Pb-Zn district (about 80 km by air to the southern limit of the Wernecke Palaeo-Mesoproterozoic), and Dawson City (and the same distance to the Ogilvie Palaeo-Mesoproterozoic). There is no road access to the region.

The Mountains are situated in the Foreland Belt of the Ancestral North America (Gabrielse and Yorath, eds., 1991), west of the North American Platform and east of the Tintina Fault Zone. They are a discontinuous erosion-exhumed Proterozoic core within a broader east-west trending spur of the thrust- and fold- belt of the Paleozoic platform and passive margin ("miogeoclinal") sequence (predominantly carbonates). This belt is terminated in the east by the N-S to NW-SE trending Richardson Trough (a fault-bounded Paleozoic sedimentary basin) and the East Richardson fault array. The latter coincide with a cluster of increased seismicity probably related to a continuing right-lateral movement (Sweeney et al., 1991). The Foreland Belt is an area of low Bouger anomalies but the topographically higher Richardson Mountains coincide with a gravity high. Cratonic basement, the continuation of the Canadian Shield, is believed to underlie the thrust belt.

The Wernecke-Ogilvie Palaeo-Mesoproterozoic core is a "clastic rift", sub-greenschist to greenschist metamorphosed member of the 1.8-1.2 Ga old Purcell-Wernecke "Sequence A" of Aitken and McMechan (1991), believed to have been deposited at a stable continental margin or in an intracratonic basin. The 14 km thick Wernecke Supergroup is considered a distal analogue of the proximal Hornby Bay and Dismal Lake groups in the Coppermine Homocline 600 km to the east, in the Bear Province of the Canadian Shield. The latter has a thick unit of subaerial flood basalts, the former is entirely sedimentary. The Wernecke Palaeo-Mesoproterozoic core is intermittently flanked by the Meso-Neoproterozoic "Sequence B" (the Mackenzie Mountains mostly detrital, platformal to shelf assemblage with provenance in the Canadian Shield), and the Neoproterozoic (0.78-0.57 Ga) "Sequence C" that includes red beds, the Rapitan Group diamictites (a glaciogene suite ?) and mafic volcanics. The Neoproterozoic rifting events are also responsible for the 780 Ma Mount Harper volcanic complex in the Ogilvies (Parrish, 1991; Roots and Thompson, 1992) and for the rare 778-780 Ma old diorite bodies in the Mackenzie Mountains.

The Cordilleran Foreland arc in NW Canada is pierced by clusters of Proterozoic mafic dykes and "diatremes" shown on the map in Gabrielse and Yorath, eds. (1991). The Wernecke Mountains and the Coal Dome in the Ogilvies host two of the "diatreme" clusters. The term diatreme is unfortunate as it suggests a presence of near-surface volcanic vents, a concept difficult to demonstrate. The Cordilleran (Mid-Cretaceous) granitic plutonism east of the

Tintina Fault, affects the more internal Omineca terrain and the nearest granitoid outcrops (Deadman and Tombstone) are more than 50 km from the margin of the Palaeo-Mesoproterozoic outcrop.

Wernecke and Ogilvie Mountains Geology

The Palaeo to Mesoproterozoic (probably pre-1.72 Ga, but see the high degree of uncertainty reviewed in Aitken and McMechan, 1991) Wernecke Supergroup, which is 13 to 14 km thick, is usually compared and correlated with the Belt-Purcell Supergroup 2000 km farther south in British Columbia, Alberta and Montana. Its anomalous east-west disposition makes it a regional misfit, and it is not known whether it is autochthonous or allochthonous which, in turn, makes speculations about the type and position of the sedimentary basin and detritus provenance tenuous. Aitken and McMechan (1991) seem to favour the allochthonous nature of the Wernecke Supergroup and if so, it was probably transported from the south, from a closer proximity than today to the autochthon preserved in the Coppermine Homocline, of which it could have been the distal part of a miogeoclinal wedge.

Basement of the Wernecke Supergroup is not exposed. The bulk of the Supergroup is represented by a monotonous pile of thin- to medium-bedded siltstone (siltite) interbedded and interlaminated with fine quartz-rich sandstone (sublitharenite) and "argillite" (slate), divided by Delaney (1981) into the lower Fairchild Group and the upper Quartet Group (Fig. 2). This lower greenschist-metamorphosed sequence contains minor "carbonate beds", some of which are almost certainly zones of carbonatisation, and occasional slump features grading to intraformational conglomerates. A major lithologic change comes only in the top 4 km of the Supergroup where the Gillespie Lake Group comprises fine-grained siliciclastics cemented by dolomite, grading to a well-bedded orange-weathering silty dolomite. Stromatolites, molar-tooth structures and minor edgewise conglomerate intervals indicate shallow shelf to carbonate platform setting. The enigmatic Pinguicula Group (Eisbacher, 1981) is exposed in a small area in the eastern Werneckes, sandwiched between the erosion-bevelled folded Wernecke Supergroup below, and the Neoproterozoic Rapitan diamictites above. Considered a member of the "B Sequence" of Aitken and McMechan (1991), it is a "varicoloured beds" association with red litharenite and siltstone with reduced (green) intervals, topped by thinly bedded dolomites. Thorkelson et al. (2000) constrained its age to be <1.6 Ga, the presumed age of the Racklan Orogeny.

Neoproterozoic (about 780 to 730 Ma) units flank the Wernecke's in the east and include the Mackenzie Mountains Supergroup (Sequence B of Aitken and McMechan, 1991) and Sequence C (equivalent to the Windermere Supergroup in southern British Columbia (Gabrielse and Campbell, 1991). The former is a "miogeoclinal" suite of shallow water clastics with minor platform carbonates and evaporites (anhydrite and gypsum).

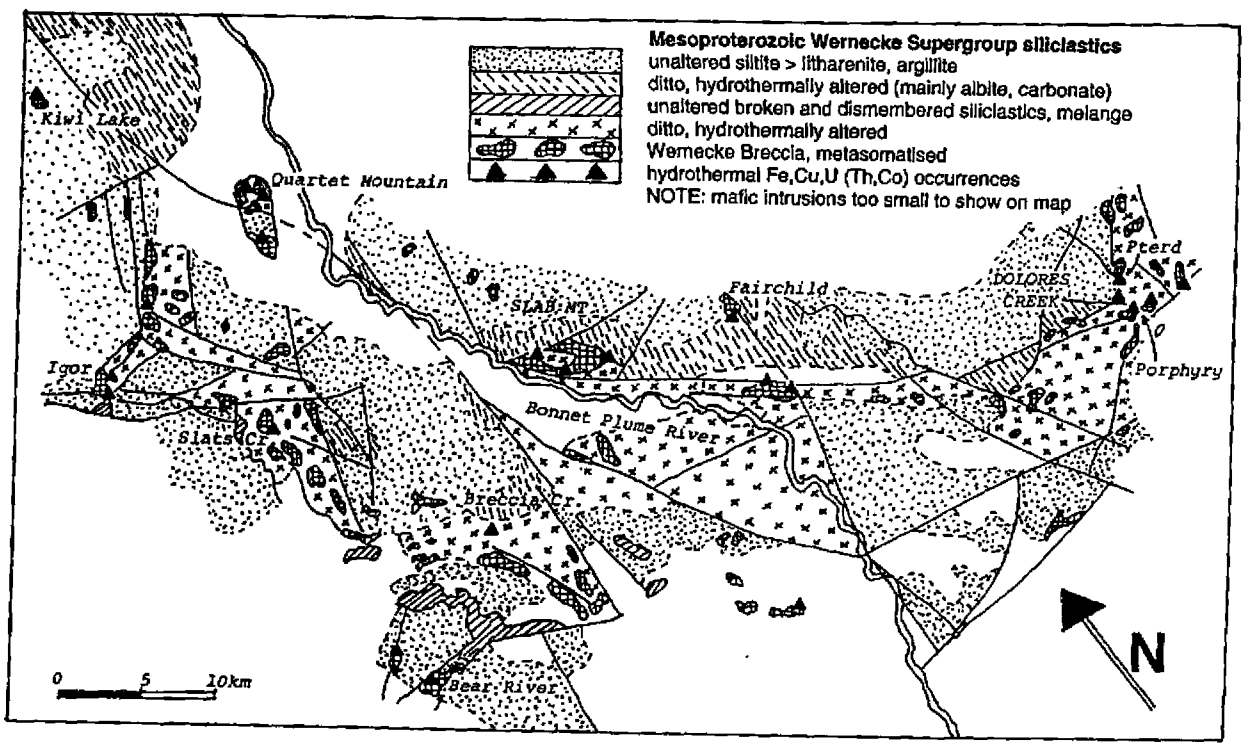


Figure 2: Wernecke Mountains, northern part in the Bonnet Plume River valley and environs, showing distribution of disrupted, brecciated and hydrothermally altered areas and of the better known Fe, Cu, U occurrences. Modified after Laznicka (1992); a simplified and reinterpreted map based on Bell (1986).

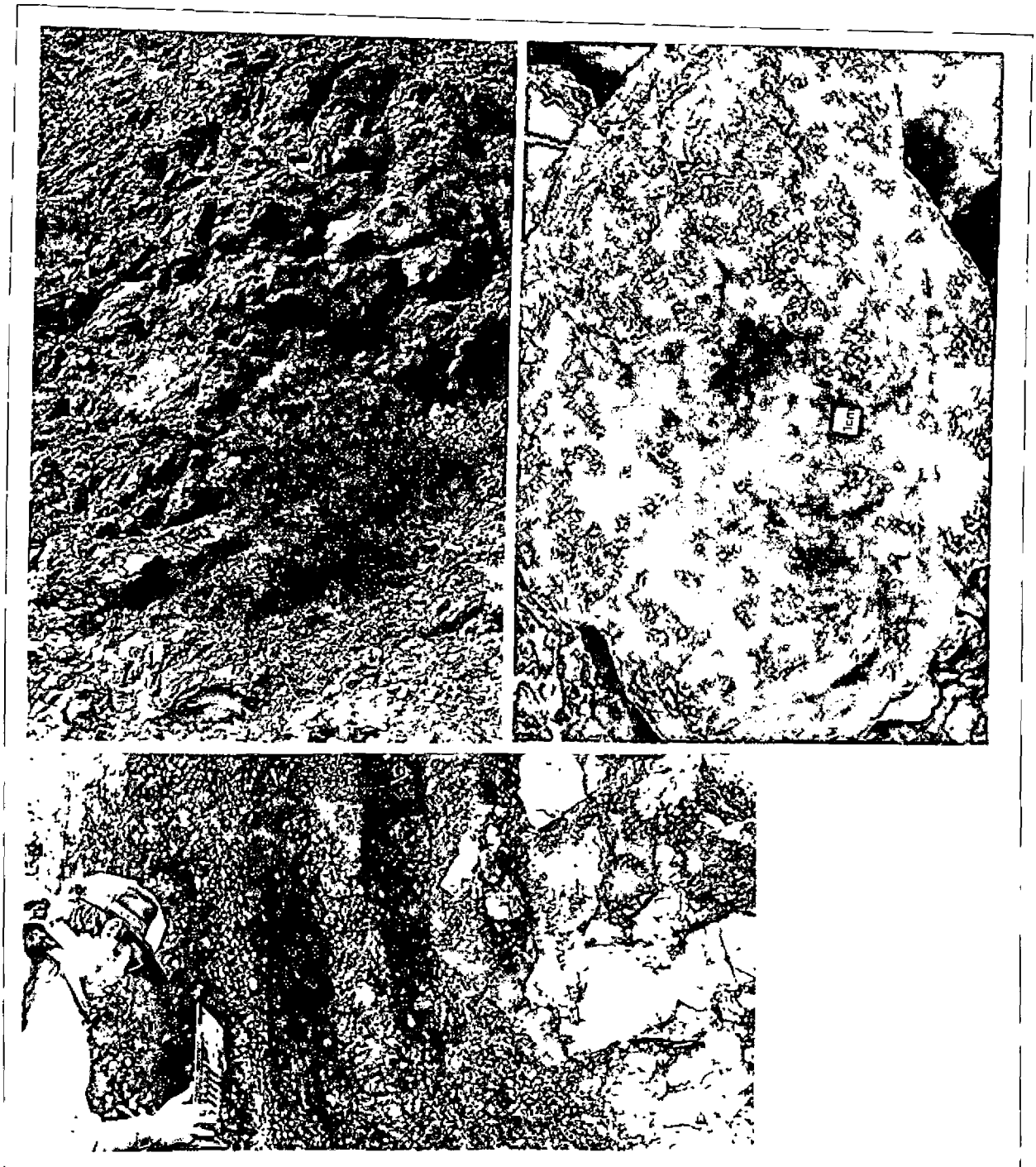


Figure 3: Tectonic fragmentites unmodified by superimposed metasomatism.

TOP LEFT: a "broken formation", internally disrupted but with preserved continuity;
TOP RIGHT: tectonic melange of brittle but attrition rounded fragments in mylonitic rock flour matrix;
BOTTOM: composite brittle fault zone.

The latter is a polygenetic rift assemblage of mafic volcanics, grey and varicoloured clastics, diamictites and carbonates. The Neoproterozoic units are on the fringe of the Wernecke's core that contains the bulk of the breccias ("diatremes") and related Fe, Cu and U occurrences. They contain the "right" lithologies on which to base various metallogenic theories (eg. basalts and probably comagmatic gabbro-diorite; red beds, Kupferschiefer-style redox interfaces, carbonates and evaporites), and two significant metallic deposits: the large, diamictite hosted Crest (Snake River) siliceous banded hematite (11,620 Mt. Fe @46%; Young, 1976), and the Redstone stratabound Cu horizon (1.77 Mt of Cu @3.92% and 418 t of Ag @ 11.3 ppm; Ruelle, 1982). Although there is no physical contact between the supracrustal members of the Neoproterozoic "rift facies" and the Wernecke Breccias, the latter could well be, at least partly, a component of the intermediate depth infrastructure of the former. Even if not, this possible connection provides a welcome ground for genetic speculations.

There are no proven volcanic members, at least in the two lower thirds of the Wernecke Supergroup, although Thorkelson et al. (2000) introduced a new stratigraphic unit, the Slab Volcanics, based on a 250 m thick mega-fragment found within the Wernecke Breccia. However, as the "rhyolites" of 1970s vintage reports were subsequently found to be quartz-sericite altered fragmented sediments and the "basalts" from the same period were sheared, chloritised gabbroids, this writer is cautious to endorse the Slab Volcanics at this stage. There is a minor (less than 1% of the area) but genetically significant presence of mafic plutonic rocks variously designated as gabbro, diorite or diabase (dolerite). Their exact age is uncertain as they most likely represent several generations from the ages contributed by Thorkelson et al. (2000), namely 1.72 Ga, 1.38 Ga and 1.27 Ga. The older, tectonised and almost always Ca-Na altered (epidote, albite, chlorite) suite are mostly hornblende gabbros. They form small irregular bodies, dykes and sills and overlap with the main phase of Proterozoic deformation and hydrothermal activity. The younger (Phanerozoic ?), undeformed and unaltered intrusions, are rare thin lamprophyre dykes filling dilational fractures.

Wernecke Breccias

All the Fe, Cu, U occurrences in the core of the Wernecke Mountains are associated with hydrothermalites (ie. products of hydrothermal void filling, metasomatism and alteration) which, in turn, are controlled by predominantly brittle structures. The natural progression of events is brittle deformation - areal to localised hydrothermal alteration and metasomatism - Fe, Cu, U emplacement, although there is a substantial overlap caused by (a) the broadly contemporaneous interference of fluids emitted from numerous centres; and b) sequential interference of numerous overprinting phases, the bulk of which had taken place in the late Proterozoic.

The Wernecke's are crisscrossed by numerous, predominantly NW-SE and N-S oriented brittle structures. Although their trends coincide with the late Mesozoic Cordilleran direction (due to NE directed thrusting) and the N-S to NNW-SSE trends of the Richardson fault array, most of the tectonics in the Wernecke's core is Proterozoic, overprinted by Cordilleran tectonics. The alteration-mineralisation and their immediate structural control are clearly pre-Cordilleran. Penetrative deformation is rare and confined to several narrow zones of fracture cleavage and hydrothermally altered shears. The rest of the meta-sedimentary pile is gently open folded and undisturbed over much of the region, where well bedded sequences can be visually traced for large distances. This continuity is interrupted by both single, sharply outlined brittle faults, as well as by broad intervals of disrupted strata, coarse fragmentite (breccia) bodies, and faults. In contrast with, for example, the San Andreas fault zone of California or the gold-bearing "breaks" of the Canadian Shield (eg. Destor-Porcupine, Cadillac), the Wernecke deformation lacks continuity. There have been a variety of structural interpretations advanced based on alternate models, including megabreccias of diapiric origin; diatremes; and submarine slope debris, although none are entirely consistent with a careful analysis of the field evidence.

What can be seen in the field include some low-angle, bedding parallel reverse faults as well as steep, crosscutting transtensional ? faults. Rather than being represented by a single discrete slip surface, the structures expand into broken units, or a sequence of: a broken (disrupted, disturbed) unit to a dismembered unit to a melange (eg. Raymond, ed., 1984; read also the discussion in Laznicka, 1988, p. 141). In a broad zone say, 100 m or even several km wide, the internally fragmented rocks, sometimes interspersed with sub-parallel planar slip surfaces, assumed the role of single faults and facilitated the lateral movement between two adjacent blocks over a myriad of internal slip surfaces without significantly losing stratigraphic continuity (Fig. 3). Whole mountain slopes are composed of a close fitting, packed, "rubble" of siltstone or sandstone where the individual fragments consist of an unmodified rock interior smeared with a gouge or mylonitic paste over an attrition rounded surface. The fragments are irregular, equant, elongated to lozenge-shaped and exhibit some similarity to lodgement till, although the fragments to matrix ratio is much higher than in the till. The fragment size varies from millimetres to metres, while some mega-blocks measure more than 100 m (hence a mega-breccia of Bell, 1986). There is no established term for this sort of fragmentite (breccia): some would call that a melange but, by definition, melange requires fragment mixing which could be the next evolutionary step.

A typical field traverse, initiated in undisturbed rock, can record the following phases of the disaggregated fragmentite series (Laznicka, 1989):

- Solid, undisturbed rock, for example a thinly banded siltite-litharenite (quartzite)-slate set 50 cm thick;
- Crackle breccia where the rock set is interrupted by a network of thin fractures with less than 10% of inter-fragmental space;
- Mosaic breccia, where fragments have expanded, but can still be mentally fitted together;
- Rubble breccia of rotated fragments; variable degrees of physical interference of the adjacent fragments; the gouge/mylonite coated fragments mentioned above are an extreme case;
- Melange breccia where fragments mix; given the initial heterogenous rock set the melange will be a mix of fragments of quartzite, siltite and slate where the slate will show the highest degree of milling and attrition and greatest contribution to the matrix.

The above fragmentite (breccia) series will be of local derivation with mono-lithologic (homo-lithologic) fragment population if produced from a uniform progenitor (eg. siltstone). When more than one lithology alternates as in the above example, the fragmentite will be hetero-lithologic. This is another source of confusion in the Werneckes, as hetero-lithology is interpreted as an evidence for breccia assembly from several widely spaced parent lithologies.

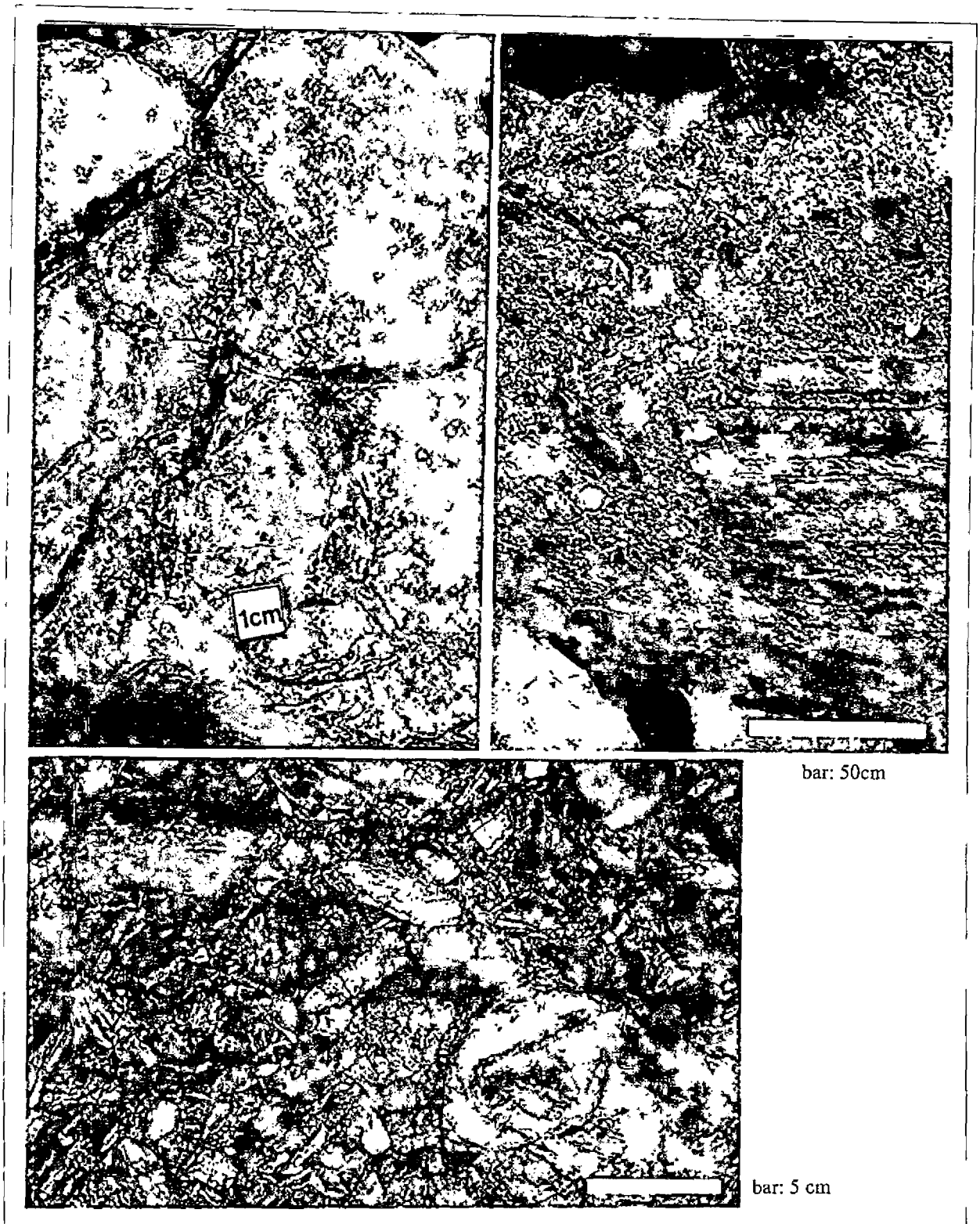


Figure 4: "Wernecke Breccia", a series of disaggregated metasomatised fragmentites.
TOP LEFT: Mosaic breccia in albitised meta-quartzite;
TOP RIGHT: Intrusive breccia, forcibly injected into dilations in fractured albitized (meta)sediments;
BOTTOM: (tectonic) melange breccia of albitized > carbonatized, hematite-pigmented fragments in chlorite, specularite rich matrix.

Once formed, every phase of the disaggregated fragmentite progression can be wasted (by erosion) and the fragments dispersed, or transported somewhere else and retextured in the process. When fluids under pressure intervene, the fragment mixture can be made to forcibly fill dilations (the intrusive breccia of Bryant, 1968; Fig. 4b). Alternatively, upward-streaming pressurised volatiles can carry the fragments with a rock flour matrix to fill planar dilations between two joints, fractures or fault planes to form breccia or pebble dykes, or diatremes in the shallow sub-crustal region. Typical diatremes have roughly circular cross-section and are common in volcanic areas or at least above shallow chambers of volatile-rich fractionating magma, hardly the case in the Wernecke. We have, however, observed an extended fracture filled by a hetero-lithologic breccia of attrition-subrounded, but still locally derived

fragments, directly above a terminating gabbro dyke. This was most likely a product of a small local phreatomagmatic explosion where the hot magma created the pressurised propellant by volatilisation of the rock moisture. The rock fragments probably fell from the roof and underwent a period of milling. We found no exotic fragments except one of gabbro. To conclude, much of the Wernecke fragmentites were, at least initially, related to tectonism, sometimes accompanied or followed by a complementary process. This took place at a relatively deep level, close to, but above, the brittle-ductile transition of Sibson (1977), under lower greenschist conditions. It is unlikely that near-surface equivalents were preserved. A portion of these fragmentites remain as described above, unmodified by hydrothermal alteration, and these are free of mineralisation.

Hydrothermal Alteration and Albite-chlorite-hematite Altered Breccias

Conspicuous, spotted pink, maroon, green and beige breccias were noted by the early prospectors in float and glacial drift in, and downstream from, the Wernecke and Ogilvie Mountains (Fig. 4). Later they were informally referred to in the literature as "Wernecke Breccia". They are typical but not the only breccia variety found and are the product of hydrothermal alteration (metasomatism) superimposed upon (or simultaneous with) the tectonic fragmentation described above. A typical "Wernecke Breccia" will have angular to subrounded pink or maroon fragments of fine-crystalline ("sugary") albitite surrounded by a chlorite-rich matrix (Fig. 4c). There is a range from fragment-supported to matrix-supported textures. The albitite is a metasomatically replaced quartzite (usually pink) or brittle siltstone (usually maroon) and the chlorite replaces the rock flour matrix originally enriched in the pelitic component. Relict sedimentary lamination is often preserved in the fragments. Although the breccias appear heterolithologic, the overwhelming majority are of local derivation, corresponding to the unaltered "melange breccia" that could have been derived from a single 30 to 50 cm thick mixed sedimentary unit. Exotic fragments are virtually nonexistent, except for an occasional gabbro block. Scattered crystals of specularite are ubiquitous, both in fragments and matrix, and isolated specks of chalcopyrite also occur. Sericite, sericite-carbonate, and Ca-Mg-Fe carbonate (ankerite and ferro-dolomite, less commonly siderite) alteration is also widespread. The former is most common in sheared material, both in previously albitised breccias and non-brecciated rocks as well as in the non-altered rock; the latter is either a distal zone contemporaneous with albitisation, or it overprints the albitised materials. Sericitised fragments are rarely found in breccias, whereas carbonatisation both predates and is superimposed on the "Wernecke Breccia". The carbonatised material has a beige colour when fresh, and is satin brown when (surficially) oxidised.

In outcrop, the "Wernecke Breccia" is gradational into crackle (Fig. 4a) or mosaic brecciated wallrocks or, alternatively, the contacts are sharp indicating emplacement of a transported breccia (intrusive breccia?). According to Thorkelson et al. (2000) this happened during the Racklan Orogeny (ca 1.6 Ga). The albitisation and subordinate chloritisation, however, continue past the breccia into the solid or crackle-brecciated metasediment, with the same colour effects caused by the background lithology, to produce areas of thorough to partial albitisation hundreds to thousands of metres across changing to carbonatisation. There is a permeability control to alteration and consequently the "broken formations" are preferentially altered.

Hydrothermal alteration also affects the gabbro bodies that are densely fractured and in places sheared, although breccias granulometrically comparable with the Wernecke Breccia are relatively rare. Most gabbros contain earlier quartz-epidote (albite, calcite) fracture veinlets and inhomogeneities, while some have been caught in the Na-Ca metasomatic front together with the surrounding metasediments or breccias. Albitised gabbros retain their coarse crystalline texture and are altered to pseudo-syenites of hypidiomorphic pink albite with scattered specks of chlorite and specularite.

Fe, Cu, and/or U, Th Occurrences

The pink, maroon, bluish grey albitised breccias and non-brecciated rocks contain ubiquitous hematite in the form of dispersed pigment and scattered flakes of specularite (Fig. 6c, 6a). Specularite accumulates along fractures and short discontinuous faults to form several small orebodies with almost massive sections of steely hematite. The largest recorded, explored body for which resources were estimated, is Pagisteel (Bear River) with approximately 1 Mt @ 29% Fe material. Magnetite is rare in the area and mostly occurs in carbonate replacements and veins in association with pyrite. Chalcopyrite is also widely scattered in the albite-chlorite metasomatites and is particularly common when alteration overprints gabbro bodies as at Dolores Creek (Fig. 6b). Most explored copper prospects contained chalcopyrite stringers and small masses (Fig. 6d) in discontinuous quartz and carbonate fault and fracture veins and in patches of ferro-dolomitic or ankeritic carbonatisation. U and Th occurrences have several forms and Gabelman (1988) recognised at least three generations. The oldest (1249 to 1153 Ma) has brannerite occurring as scattered crystals in albite veinlets and albite, chlorite, hematite spots in the "Wernecke Breccia" as at Quartet Mountain, and is an accessory to most Fe and Cu occurrences elsewhere where it accounts for slight radioactivity. The younger generation has pitchblende, usually in quartz-carbonate gangue, sometimes with barite, associated with fractures near the margin of large Wernecke Breccia bodies (Bond, Igor prospects) or outside the breccia but in association with sericite and carbonate alteration. Gabelman (1988) quotes discordant pitchblende ages from 107 to 929 Ma that suggest several episodes of remobilisation. At the Igor prospect, most of the pitchblende and minor yellow U oxides occur in a zone of intense red hematite alteration and impregnations suggestive of a palaeo-regolith relict beneath an unconformity (presumably under the Pinguicula "red beds"; Fig. 6d). Unconformity control to the Wernecke uranium is also suggested by the observation of Bell (1989)

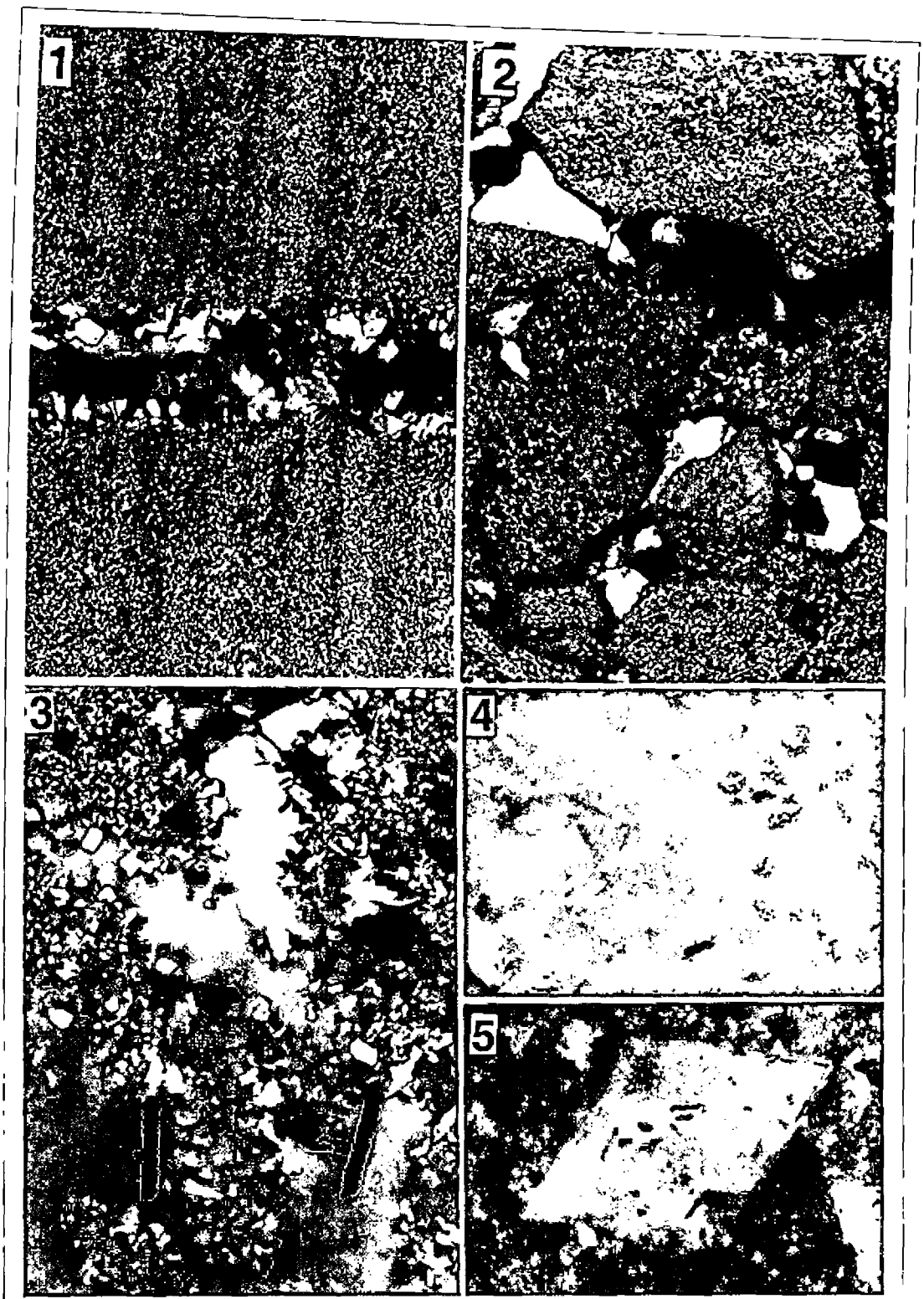


Figure 5: Hydrothermal metasomatites showing multiple alteration phases.

1, 2 Early stage, fine-grained albitised sedimentary rock is intersected by later stage dilation-filling albite veinlet (left) or interfragmental cement (right).
3 Later stage albite (discernible crystals) advanced into a "cherty" groundmas of an earlier albinte; dark bars are cross sections of specularite flakes.
4 Ghosts of albitized former breccia fragments, with impurites, overprinted by stage 2 albite that also provides cement.
5 Dolomite metacryst growing over the equivalent of (4) #1-3 field of vision: 14x8 mm, #4,5: 8x5 mm

that the majority of occurrences is in the eastern Wernecke's, that is closest to the preserved Pinguicula remnants.

Gold is rumoured to have been detected in some assays of predominantly chalcopyrite-rich ores, but hard data are scarce. Thorkelson and Wallace (1993) quote 1.5 g/t Au at the Sihota occurrence in the Werneckes and Burke (1997) mentions gold values from 0.2 g/t Au to 1 g/t Au assayed at the Monster prospect in the South Ogilvies. Also enigmatic is the presence of the "alkaline association" of metals (REE, Nb, Ti, Zr, Th, U) reported from a Dempster Highway occurrence in the Ogilvie Mountains (Gabelman, 1988) and from the NOR "breccia pipe", well outside the Werneckes in the Richardson Mountains (Tempelman-Kluit, 1981).

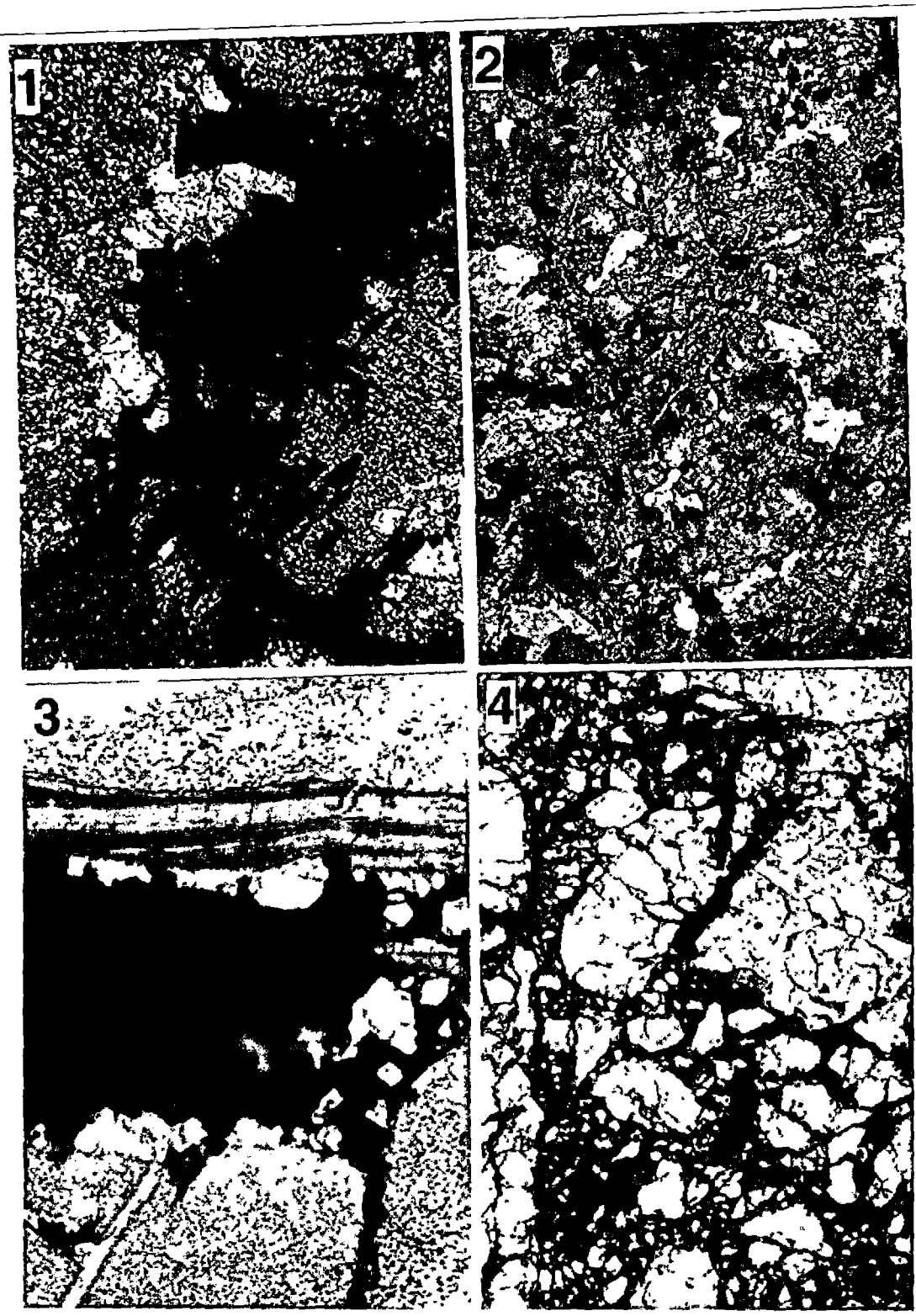


Figure 6 Ore minerals in Wernecke metasomatites.

1. Specularite replacing albite and carbonate along grain boundaries, 0.25 x 0.35 mm;
2. Scattered specularite intergrown with chalcopyrite (black) in a quartz-rich portion of albite "syenite" (metasomatite over gabbro), 12x18 mm.
3. Small chalcopyrite mass filling dilations and replacing earlier albite.
4. Infiltrations of supergene hematite in multiphase breccia, under paleosurface; #3, 4: 14x8 mm.

Mineral Exploration and Example Deposits

Serious prospecting started late in the Wernecke's because of the difficult access, and few claims were staked before the 1960s (Findlay, 1969). The first major wave of prospecting, claim staking and limited drilling took place in the late 1960s and early 1970s, thanks mainly to the efforts of Archer & Cathro consultants, and also to the mapping projects of the Geological Survey of Canada that provided the first reliable geological background (eg. Green, 1972; Blusson, 1974). In addition to discovering and staking a number of prospects of their own, Archer & Cathro Ltd. assembled a comprehensive Northern

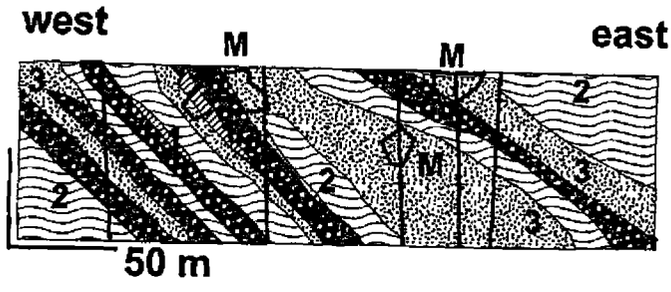


Figure 7: "Porphyry" prospect, Dolores Creek. Disseminated chalcopyrite with specularite in irregular bodies of "Wenecke Breccia" superimposed on the meta-sediments and gabbro.
M = orebodies, +0.2% Cu
1. Gabbro bodies
2. Finely albitized Wernecke Supergroup meta-sediments
3. Coarse albite pseudosyenite after gabbro > Wernecke Breccia
4. Wernecke Breccia, predominantly albite-chlorite altered tectonic melange breccia of local derivation.

Cordillera Mineral Inventory database, available for purchase, since 1973. This provided an excellent overview of the Yukon mineral occurrences that included 54 copper showings in the Wernecke's. About a dozen uranium occurrences were discovered during the "uranium rush" throughout the 1970s (Bell, 1978), after which few new showings have been found during the intermittent "mopping operations" stage. The "gold rush" of the 1980s had little impact, while periodic staking and early stage exploration have been taking place in part of the Coal Creek Dome in the Southern Ogilvie Mountains, accessible by the recently constructed Dempster Highway (eg. Burke, 1997). By the end of the century there have been some 80 occurrences of Cu, U or Fe, recorded in the Yukon MINFILE database maintained by the Yukon Government (www.geology.gov.yk.ca/minfile/index.html). Dolores Creek and Igor are two of the few prospects studied in some detail and are described in the literature. Most recent descriptions of Fe, Cu, U occurrences in the Slats Creek, Fairchild Lake and Dolores Creek area are available from Thorkelson et al. (2000).

Dolores Creek, "Porphyry" Disseminated Cu Prospect.

The Dolores Creek group of Cu >U, Co prospects (Laznicka and Edwards, 1979; Fig. 7) is in the eastern Werneckes, 155 km NE of Elsa, the nearest permanent settlement, at about 64° 55'N and 133° 20' W. It was discovered by L. Brown, who noticed the malachite-stained outcrop at the "Porphyry" prospect, in the early 1960s. Seven shallow diamond drill holes were drilled into "Porphyry" between 1967 and 1969 and the area has been dormant since, with only periodic short campaigns of outcrop examination, sampling and light portable geophysics. The prospect area is close to the core of a NE-trending, NE plunging complex antiform in which the moderately to steeply dipping open folds are severely faulted and displaced along predominantly NE and NNW trends. Spectacular fracture cleavage is developed locally and the deformation is multiphase. The predominantly meta-sedimentary, pre-alteration lithology of the Palaeo-Mesoproterozoic Fairchild Lake and Quartet Groups of Delaney (1981) is monotonous. The bulk of the area is occupied by thick- to thin-bedded sub-mature detrital sedimentary rocks dominated by meta-siltstone ("silite") grading into quartzite and "argillite". A unit of dolomite-marble grading to carbonatised meta-pelite contains scattered scapolite and magnetite and it is not clear how much of this rock is sedimentary and how much metasomatic. Equally problematic is the occurrence of a stratabound jasper and quartz-laced silicite ("chert"). A small body of altered gabbro at the Porphyry prospect and several gabbro dykes in the area probably correspond to the 1.72 Ga Bonnet Plume River intrusions Thorkelson et al. (2000).

The evidence of brecciation and albite-chlorite-hematite metasomatism producing the spectacular Wernecke Breccia is most prominent in what appears to have been the centre of the alteration system. There, the Porphyry prospect contains several irregular bodies of pervasively disseminated fine grained chalcopyrite with abundant specularite in chlorite specks and matrix of medium to coarse crystalline pink massive "pseudo-syenite" (largely albitised gabbro) and the Wernecke Breccia. The host breccia and pseudo-syenite appear as a series of east-dipping sheets intercalated with unbrecciated but albitised meta-sediments. About five "orebodies" of erratic mineralisation estimated at several tens of thousand tonnes of material with better than 0.25% Cu have been identified. The best intersection returned 12.5 m with a grade better than 0.5% Cu.

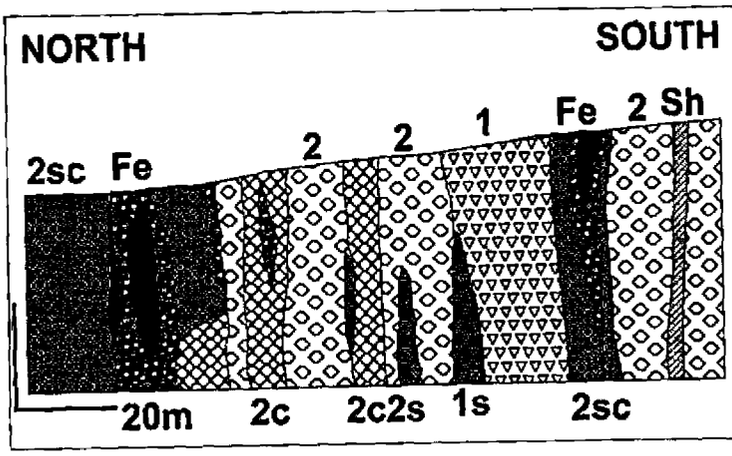


Figure 8: Igor Fe,Cu,U prospect, Quartet Lakes area. Cross-section of the ore zone, an interval of intersecting multiphase deformation, alteration and mineralisation zones overprinted by supergene modification under paleosurface.
Fe: 80% plus (black) and 10-80% (dense lace pattern) hematite impregnations, discontinuous barite veinlets, local U oxide impregnations.
Sh: phyllonite-filled shear.
1. Albite-chlorite-hematite altered Wernecke Breccia.
2. Strained and sheared "augen breccia". Letter symbols indicate alteration assemblages that overprint 1 & 2:
s=sericite and paragonite;
c=Ca,Mg,Fe carbonate.

Albitisation at the Porphyry prospect area has reduced the original K_2O content in the unaltered siltite from about 4% to between 0.22 and 1.68%. The displaced K_2O most likely accumulated in abundant sericite and occasional biotite along the albitised margin where two samples gave 8.41% and 7.28% K_2O, respectively while minor hydrothermal biotite occurs along late fractures in the Porphyry showing itself. This occurrence may provide a link with the "diorite model" of porphyry style Cu-(Au) deposits. Several showings of impersistent chalcopyrite, cobaltite, tetrahedrite, Pb-Zn sulphides or pitchblende as fracture and fault veins occur in the sericite-carbonate altered fringe.

Igor Fe-Cu-U prospect, Quartet Lakes area.

This prospect, discovered and drilled by Archer, Cathro and Associates during the "uranium" phase between 1976 and 1982, is located 14 km WSW of Quartet Lakes at about 134° 38' W and 65° 02' N (Laznicka and Gaboury, 1988). The local geology is comparable to that at Dolores Creek with well bedded siltite > quartzite > argillite sets of the lower Wernecke Supergroup, small gabbro bodies, Wernecke Breccias and albite-chlorite-hematite and carbonate metasomatites extending beyond the fragmentites into the meta-sediments. What is different here is the strong ductile fabric superimposed on the earlier brittle assemblage along a N-S high strain zone and an E-W set of faults, accompanied by a strong sericite (paragonite) and Ca-Mg-Fe carbonate alteration (Fig. 7). The ductility could be the result of deformation at a lower crustal level, perhaps accomplished during the Mesoproterozoic Racklan Orogeny, or later. Alternatively, the depth level of the site need not have changed but the alteration phyllosilicates and carbonates facilitated plastic slip. Magnetite is more common here than at Dolores Creek and it forms scattered metacrysts and lenticular masses accompanied by red (powdery) hematite, part of which is martite and the rest primary and supergene hematite. Chalcopyrite with pyrite and pyrrhotite form stringers in the sericite-carbonate phyllonite and small replacement masses in carbonate metasomatites. Barite accompanies the Fe oxides as thin lenticular masses and there is scattered and fracture coating pitchblende. This prospect preserves the remains of a palaeo-regolith of which the "secondary" hematite, minor malachite, azurite and chrysocolla, and yellow U oxides, are a part. The wide spread of radiometric ages obtained for the Werneckes U occurrences (Archer et al., 1986) suggest several episodes of rejuvenation at variable crustal levels ranging from the greenschist-stable to near-surface conditions. The estimated ore resource at Igor, quoted by Hitzman et al. (1992), is 0.5 million tonnes of ore with 1% Cu.

Wernecke Breccias: What Contribution to FeOx, Cu, U Metallogeny?

In the Werneckes, we believe (supported by calculations) that the meagre Fe-Cu(-Co) accumulations were derived from the rock-forming minerals and trace Fe, Cu and Co in gabbros that were released, transported and redeposited by hydrothermal fluids as evidenced by the regionally altered rocks. The uranium was probably sourced from the meta-sediments. The mineral occurrences most likely formed close to or within the source rocks from which the metal was derived. They are small and widely dispersed because of the limited metal source base and lack of metal collecting and channelling mechanism (Fig. 8). Even if the gabbros were the passive source of metals, did they also provide the thermal energy to drive the scavenging and ore depositing fluids - or was there another engine ? Were the earlier (~1.7 Ga) gabbros the passive metal source and the later gabbros (~1.38, 1.28 Ga and younger; ages from Thorkelson et al., 2000) the fluids driving force ? Granites and especially alkaline or carbonatite magma systems at depth have been invoked in the literature (eg. Hitzman et al., 1992) or was it a geothermal heat ? What was the source of fluids ? There is no credible answer yet available for most of the genetic questions raised. However there is a set of empirical facts available that can be applied elsewhere in the world to finding and examining mineral occurrences that have some similarities to those of the Werneckes.

International Comparisons

The facts considered most typical and relevant to the Werneckes, if viewed from the premise of field lithologic association (compare Laznicka, 2001), are: 1). the presence of gabbro, diorite or diabase (dolerite); 2). low-grade metamorphosed sedimentary hosts; 3). intracratonic or passive margin palaeo-setting; 4). brecciation or dense fracturing combined with Na>>K feldspathisation, albite-chlorite, sericite, carbonate alteration; 5). hydrothermal Fe oxides and Cu sulphides and minor U oxides. By contrast, the similarity of the Wernecke breccias and mineralisation to the ores at Olympic Dam, as often suggested (eg. Bell, 1986; Thorkelson et al., 2000) does not seem convincing when the empirical attributes are compared (Laznicka, 1993, p.1067), nor is there good evidence that the Wernecke breccias are former diapirs (Bell, 1989). To stay close to the facts, the remainder of this paper briefly reviews hydrothermal Fe and/or Cu and/or U ore types that are directly or indirectly associated with predominantly tholeiitic (meta-)basalt, diabase (dolerite) and gabbro in intracratonic or passive margin settings, of which the Wernecke occurrences are a member (Fig. 9, Table 1).

Subvolcanic Magnetite (and/or Cu,U) in Diatremes Related to Flood- and Plateau-basalt Provinces

The Angara-Ilim Fe province in central Siberia (about 450 km north of Irkutsk on the BAM railway) is economically significant (total endowment about 3 billion tonnes of 40-50% Fe ore) but enigmatic and little publicised in the West. It comprises over one hundred scattered pipes drilled through the almost flat lying sedimentary cover of the Siberian Platform (mostly Cambrian limestone, dolomite and shale with anhydrite and halite units), mineralised by magnetite with minor hematite, pyrite and chalcopyrite. The pipes were emplaced in the lower Triassic and are coeval with the tholeiitic plateau basalt volcanism ("traps") to which the giant Noril'sk-Talnakh Cu-Ni-PGE deposits, located over 1000 km farther NW, are also related. In a rich magnetite deposit such as Korshun (Korshunovskoye;

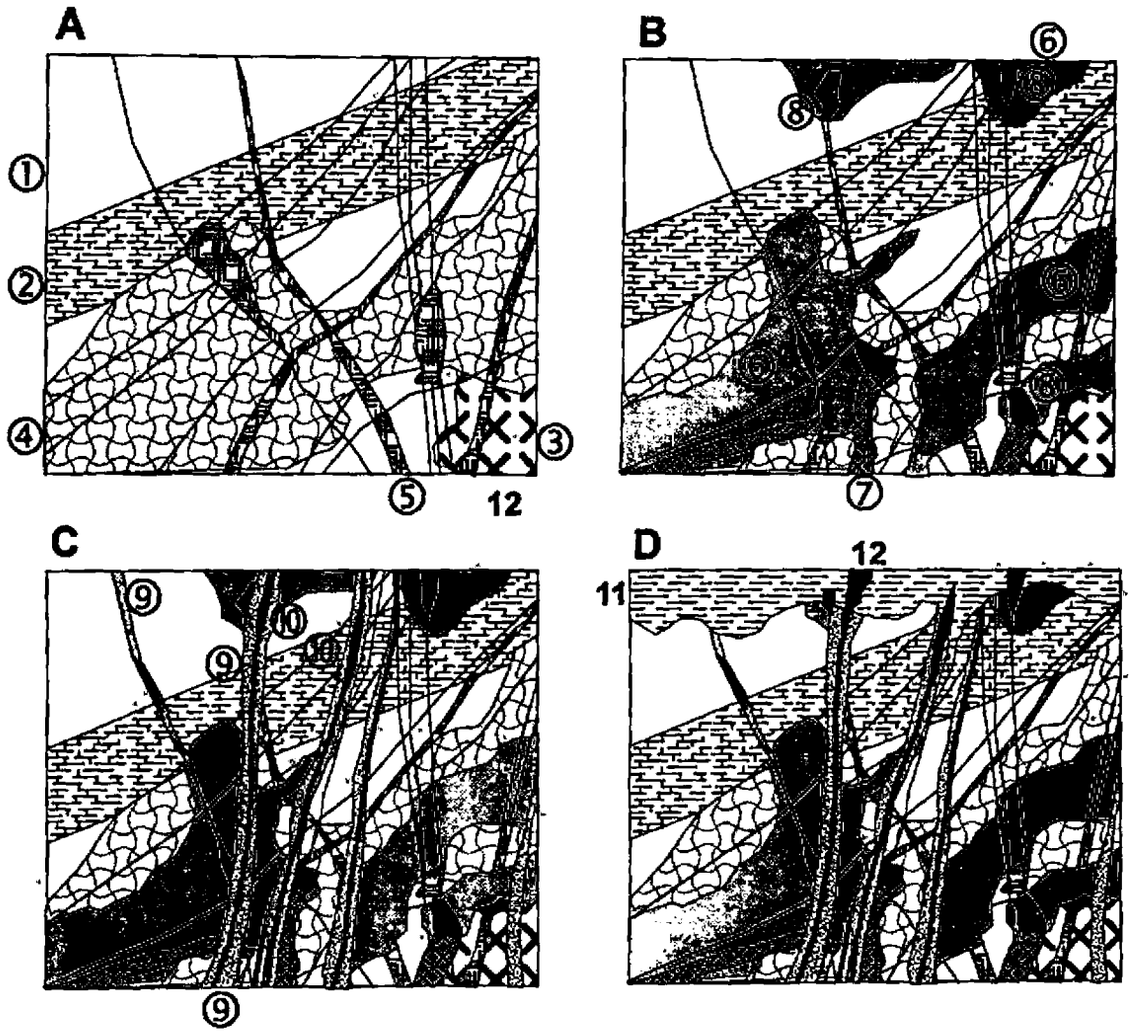


Figure 9: Evolution of the Wernecke Fe,Cu and U occurrences.

A: Brecciation and dilation development.

B: Formation of the altered Wernecke Breccia under essentially brittle conditions; albitization, chloritization and carbonatization with local Fe,Cu (U) accumulation.

C: Sericite, paragonite, silica, pyrite alteration overprinting earlier albitization, partly along ductile shears.

D: Supergene oxidation, hydration and redeposition of earlier minerals under paleosurface.

EXPLANATIONS:

1. Lower Wernecke Supergroup, siltite > sublitharenite.
2. Ditto, carbonaceous argillite.
3. Early gabbro and diorite.
4. Disrupted strata.
5. Dilated fragmentites (fault breccias).
6. Albite-chlorite-hematite metasomatites.
7. Younger gabbro.
8. Disseminations and masses of specularite > chalcopyrite.
9. Ductile and brittle fault-controlled sericite (paragonite) and carbonate alteration.
10. U oxides occurrences.
11. Later Proterozoic (Pinguicula Group ?) and Paleozoic cover at unconformity.
12. Rare ore (Cu in malachite) occurrences above unconformity (in the Pinguicola Group), and oxidation-hydration under unconformity.

Pukhnarevich et al., 1985), an elliptical vertical column of wallrock-derived disaggregated limestone and halite breccia, pierced by a vertical dolerite dyke, are both replaced by garnet-pyroxene skarn which, in turn, is replaced by semi-massive magnetite with irregular patches of massive magnetite. There are offshoots of skarn and magnetite skarn into the Cambro-Ordovician carbonates, evaporites and clastics. A composite magnetite-hydrothermal (remobilised) halite ore is a local curiosity, as it is at the Neryundinskoye deposit and NaCl brines are present in abundance throughout the system. The structure has an elliptical cross-section, more than 1000 m vertical extent, and is rooted in depth in a dolerite intrusion situated within Lower Cambrian carbonate-evaporite sequence close to the Precambrian basement of the Siberian Shield. Less eroded pipes such as Nerunda (Neryundinskoye; Von der Flaas, 1990) flare into a cone filled by basalt-dolerite auto-breccia, eruptive breccia, tuffisite and tuff partially replaced and

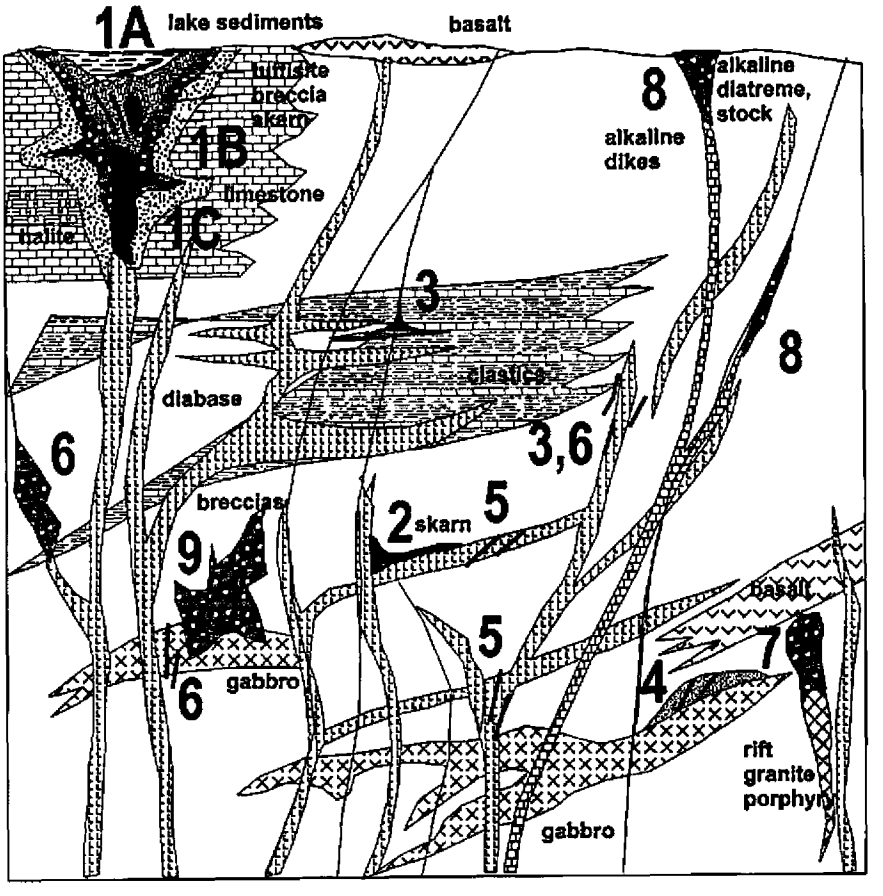


Figure 10: Selected examples of Fe oxide, Cu, U ore accumulations in intracratonic or continental margin extensional terrains associated with mafic intrusions (please see Table 1 for description and examples).

veined by magnetite stockwork, topped by a remnant of bedded tuff and tuffaceous lacustrine sediments. Breccia fragments and mega-fragments derived from above are also present.

At the Krasnoyarskoe magnetite deposit (Pavlov, 1960) tuff and volcanic breccia fill most of the vent and are intersected by sheet-like veins of massive magnetite and densely magnetite-replaced tuff. Nikulin et al. (1991) geophysically traced the magma sources to a depth of 25-30 km under the present surface where the intermediate chambers were established near the upper boundary of the granulitic continental crust. These chambers were filled by alkaline basaltic magma melted in the undepleted sub-continental mantle at a depth of 50-80 km below the present surface. The magma travelled to the surface by way of deep faults. The earlier concept of carbonatite magma involvement seems to be waning, as the abundant hydrothermal carbonate and also halite matrix were clearly locally derived from the wall rocks. It is interesting that scapolite and other silicates usually attributed to evaporite metasomatism are rare to non-existent and instead hydrothermal halite abounds. This is probably the consequence of a very shallow level of emplacement (0 to about 1500 m under the lower Triassic palaeosurface). Of all this writer has seen and read, the Angara-Ilim magnetite pipes are the most relevant for comparison with Olympic Dam, although the Cu content in accessory sulphides is only of the order of 0.1-0.2% Cu, the oxidation of magnetite to hematite is only embryonic, and the presence of U and Au, if any, has not yet been reported in the secretive Soviet/Russian literature. There is, however, no similarity with the Wernecke breccias; the writer is not sufficiently familiar with the "real" NOR diatreme (Tempelman-Kluit, 1981) in the Richardson Mountains to make a comparative judgment.

Sub-Greenschist to Greenschist Levels, Skarns at Diabase or Gabbro Exocontacts and Remobilized Synsedimentary Ores

The Triassic Newark Rift Basin in Pennsylvania contains a belt of iron skarn deposits associated with diabase sills emplaced into early Paleozoic carbonates or along their unconformable contact with Triassic sandstones and conglomerates. The largest of these, the Cornwall Mine, has produced 100 Mt of 40% Fe, 0.29% Cu and 0.04% Co from lenticular bodies of massive to disseminated magnetite with minor pyrite, chalcopyrite and pyrrhotite in a serpentinite matrix (Lapham, 1968). The orebodies are in the hydrous skarn association superimposed on an early clinopyroxene, garnet, tremolite exoskarn. Fissure-controlled K-feldspar, biotite, actinolite, chlorite and

TABLE 1: Styles of hydrothermal Fe oxides, Cu, Au, U deposits associated with diabase and gabbro intrusions in intracratonic or craton margin extensional settings

NO.	SETTING & STYLE	REGION & DEPOSITS EXAMPLES	METAL TONNAGE & GRADE (%); Au g/t	REFERENCES	REPRESENTATION IN THE WERNECKES
1	High-level basalt-diabase subvolcanic diatremes and dikes	Angara-Ilim Triassic magnetite province, Siberian Platform, Russia --**1A**, minor occurrences: Fe oxide impregnations in lake sediments; traces of Cu,U --**1B**, Neryudinskoye, Krasnoyarskoye deposits: mag veins, replacements in mafic tuff, tuffisite, volcanic breccia --**1C**, Korshunovskoye deposit: mag >> cp, po, py massive to densely dissem. replacements in skarn after limestone breccia; also magnetite-halite ore Hopi Buttes & Navajo late Tertiary volcanic province --Small occurrences, U oxide infiltrations in lake sediments	~1.2 Bt @ 40%Fe, some Cu; U ?	Nikulin et al. 1991 Von der Flaas, 1990 Pavlov, 1960 Pukhnarevich et al., 1985	None; too high a level unlikely to be preserved (NOR prospect in the Richardson Mts. possible candidate)
2	Subgreenschist to greenschist setting, early postmagmatic Fe skarn at gabbroid exocontact	Late Triassic Fe province in Pennsylvania (Newark Trough) –Cornwall Mine: mag in paraserpentinite matrix (hydrous skarn) superimposed on garnet-cpx exoskarn; minor Co-pyrite, chalcopyrite --Grace Mine, Morgantown: similar to Cornwall –Severnaya River Fe field, Siberia, Russia: mag exoskarn	100 Mt @ 40% Fe 0.29% Cu, 0.04% Co ~11 Mt @44% Fe	Lapham, 1968 Sims, 1968	None; only rare mineralogical occurrences of skarn association in gabbro
3	Remobilized pre-intrusion FeOX, Cu,U in gabbroid thermal aureole	--Pretoria area, South Africa, Daspoort Horizon in Bushveld contact aureole altered to specularite, magnetite, roscoelite --Lewis Range, Rocky Mts., SW Canada; weak stratabound Cu impregnations in Belt quartzite remobilized near gabbro	~1 Mt @50% Fe; V Cu	Schweigart, 1965 Morton et al., 1973	Not observed
4	Late magmatic-early postmagmatic feldspathic metasomatites at gabbroid contacts	–Kruisrivier, Groblersdal District, South Africa; veins of safflorite, niccolite, cobaltite in feldspathised quartzite at gabbro exocontact --Kuusamo belt, Finland: Cu,Au,U,Co minerals with quartz, carbonate disseminations and veinlets in albitic & Fe,Mg,K metasomatites in and near diabase dike	25 t Co, 10 kg Au Cu,Au,U,Fe	Hammerbeck, 1976 Pankka and Vanhanen, 1992	In most cases gabbros are older, overprinted by metasomatites

5	Early postmagmatic hydrothermal veins, disseminations, replacements mainly in gabbroids	--Yarrow Creek & Spion Kop, Rocky Mts., SW Canada: disseminated chalcopyrite in mafic sills	Cu	Morton et al. 1973	Few cases observed Probably several age groups of gabbroids
		--Laurel Hill, New Jersey: magnetite veins in Triassic diabase pluton along steeply dipping joints, narrow alteration rims	Fe	Puffer & Peters, 1974	
6	As above, mainly in hydrothermally altered gabbroid exocontact	--Cobalt-Gowganda Ag district, Ontario; fissure carbonate veins with silver, Co-Ni arsenides, Pb,Zn,Cu sulfides in & outside Nipissing gabbro sill	15 Tt Ag, 20 Tt Co	Andrews et al., 1986	As above; most exo-contact Fe,Cu,Co,U show no clear metal zoning in respect to a presently exposed mafic body; both meta-sediments and gabbroids are jointly altered and ore-hosting
		--Kitchener-Iron Range Fe zone, SE British Columbia: veins and stockworks of hem, mag>cp in chlorite & albite altered Aldridge sediments subparallel to Moyie gabbro dikes.	Fe >> Cu	MINFILE, 2001	
		--Dripping Springs, Arizona: uraninite in tabular quartz, chlorite, calcite altered fissures, breccias near gabbro sills	21 Tt @0.18% U	Granger & Raup, 1969	
		--Racing R.-Gataga R., NE British Columbia: quartz, calcite, cp veins in lustrous slates // faults in extension of or at contact of diabase sills	115 Tt @ 3-4%Cu	Preto, 1972	
		--Paukkayanvaara, Finland: uraninite replacements in basal conglomerate and veins along contacts of gabbro dikes	U	Krendelev, 1974	
7	Ores related to interaction of small rift-related felsic intrusions with gabbroids, basalts	--Tribag breccia pipes, Batchawana, Ontario: scattered py, cp in quartz and calcite matrix in heterolithologic breccia above quartz-feldspar porphyry stock associated with Neoproterozoic rift controlled diabase dikes & flood basalts	256 Mt @ 0.18% Cu	Norman and Sawkins, 1985u	Not observed
		--Ossura River (Svinholer) prospect, SE Iceland: cp scattered in breccia of basalt and rhyolite fragments, in plateau basalt; (rift) setting	Cu	Laznicka, 1985, p.1441	
8	Ores related to interaction of alkaline magmas and fluids with mafic source rocks	--Phalaborwa, South Africa: cp & Zr,Th,U minerals with mag in hydrothermal vein system associated with late stage carbonatite; Cu probably scavenged from mafics in depth	~1.3 Bt @1% Cu, 18% Fe	Eriksson, 1989	Not observed
9	Hydrothermal veins, disseminations, replacements superimposed on or close to older gabbroids; no genetic connection	--Messina, South Africa; 5 deposits of massive to scattered chalcopyrite, bornite, specularite in albite, chlorite, etc. altered breccia bodies ("pipes") in Archean metamorphics, in fault zone; some diabase dikes; Mesozoic age	45 Mt @ 1,8% Cu	Bahnemann, 1986	The majority of Wernecke gabbroids are passive hosts to alteration and ores
		--Bruce Mines, S-C Ontario: quartz, calcite, cp anastomosing fissure veins and breccias in diabase and quartzite	10 Tt Cu	Pearson, 1979	

magnetite metasomatites are developed at the diabase endocontact. In the Werneckes the garnet-clinopyroxene assemblage is exceptionally developed in calcareous inhomogeneities in some gabbros, with more abundant epidote. Diabase dykes and sills emplaced into sedimentary or volcanic sequences cause thermal recrystallisation and limited hydrothermal remobilisation of synsedimentary ores, when present, as at Martin Lake in Labrador (Swinden and Santaguida, 1993).

Sub-Greenschist to Greenschist Level, Hydrothermal Veins, Disseminations, Breccia-Hosted Ore Minerals in Hydrothermally Altered Gabbroids and Adjacent Rocks (Mostly Meta-sediments)

Large differentiated mafic intrusions often contain granophyric units near the top, generally considered to be magmatic differentiates, contaminates or remelted exocontact sedimentary rocks. Smaller and/or undifferentiated diabase or gabbro dykes or sills are sometimes associated with white, pink or red patches of hydrothermal feldspathic metasomatites (both Na- and K-feldspars may participate), usually designated as "aplite" or "red rock" in the literature. These patches may occur at either side of the contact and many contain scattered blebs and veinlets of chalcopyrite with pyrrhotite, pyrite and rarely Ni sulphides (eg. the Shakespeare prospect, Ontario; Pearson, 1979). There is little doubt about the genetic association of gabbroids and metasomatites, and the latter are popularly considered as products of the "deuteric phase" of the former. The provenance of fluids responsible for the metasomatic change is controversial and either attributed to magmatic water, or to externally supplied waters (meteoric, connate, or released by metamorphic dehydration at depth).

In the Cobalt-Gowganda silver district of Ontario, "aplite" in the Nippissing gabbro sill is particularly common near the carbonate-filled fissure veins with silver and Fe, Co, Ni arsenides (Andrews et al., 1986) and it seems reasonable to associate the origin of such veins with hydrothermal convection driven by the heat from a mafic magmatic body. There are tens of mostly small Fe, Cu, Co, U deposits and occurrences probably formed in a similar way, some of which are included in Table 1 (rows 4 through 6). One problem here is that some of these hydrothermal ores are in a (usually slightly) altered gabbroid itself, hence they are younger than the intrusion. How much younger is difficult to determine, although the magmatic body can still be the source of fluid-driving heat a long time after crystallisation as most of the fluids are low-temperature hydrotherms (200° C and less). It seems logical, however, that in many cases the mafic intrusions were long dead in the time of hydrothermal mineralisation and that the source of heat driving hydrotherms was elsewhere, usually at greater depth. Four such sources are usually quoted in the literature: 1). mafic intrusions of a younger generation; 2). felsic rocks (granites, porphyries, syenites and corresponding volcanics as in SW Iceland) in a rift setting (row 7 in Table 1); 3). alkaline rocks and carbonatites; 4). geothermal heat driving metamorphic dehydration.

The economically important Messina Cu field of South Africa (Bahnemann, 1986) resembles the Werneckes in terms of genetic uncertainty and a steady flow of one-sided genetic interpretations. Five major chalcopyrite and bornite orebodies are all controlled by the Messina Fault zone of fracturing in the high-grade Archaean metamorphics of the Limpopo Orogen. They have the form of schistosity-peneconcordant gneiss replacements, pipe-like breccia bodies, and mineralised brittle fractures associated with albite, zoisite, chlorite and hematite alteration. Mafic (dolerite) dykes probably of several generations, from Mesoproterozoic to Jurassic, are very common, apparently sharing the same controlling structures as the Cu orebodies and both pre- and post-dating the ore emplacement. It is conceivable that the dykes may have provided the "engine" to drive convecting fluids scavenging and precipitating copper at an intermediate crustal level near the ductile to brittle transition. There is no evidence of the copper sources and although early investigators generally embraced the magmatic-hydrothermal concept of metals and fluids coming from (mainly alkaline) magmas at depth, Sawkins and Rye (1979) invoked the Karoo (Mesozoic) lavas, believed once present at the palaeo-surface, as the likely source of copper extracted by convecting low-temperature brines. Alternatively, the mafic source rocks could have been of Waterberg (Mesoproterozoic) age (Bahnemann, 1986). The idea of Cu (and U, Fe) sources above the present ore sites has potential application in the Werneckes, where mafic volcanics and "red beds" with traces of copper occur in the Pinguicula Group and even more in the Neoproterozoic associations.

Cu, Fe (Au, ~U) Accumulations Resulting from Interaction of Felsic and/or Alkaline Intrusions with Mafic Metal Sources in Rift and Extensional Setting

Felsic volcanics (rhyolite), subvolcanic porphyries and related breccias, and granite-quartz monzonite are present in small volumes in most rifting-related plateau basalt provinces (in the Cainozoic Iceland province and the Meso-Neoproterozoic Keweenawan province, for example) and Cu sulphides are very common in a variety of styles where the felsics interacted with the broadly contemporaneous or older mafics (basalts, diabase, gabbroids). A thorough review of examples would fill a book and Table 1 lists just two of them (the Tribag breccia pipes in Ontario and the Ossura River breccia body in Iceland). In extreme cases a genuine porphyry Cu-Mo can develop in the rift association (the sub-grade Jogran prospect, Batchawana, Ontario). A similar interaction is probably responsible for the rare and small Cu occurrences in carbonatites and foidite complexes, although the giant Phalaborwa deposit in South Africa (Eriksson, 1989) is exceptional and it has it all: Fe in magnetite, Cu in bornite and chalcopyrite, U, Th and REE.

The Verdict

When Hitzman et al. (1992) consolidated the hitherto scattered information available for a set of Proterozoic deposits of iron-oxide, sometimes with variable accompanying P, Cu, U, Au, Ag or REE, to create a new "family" of metallic deposits, they opened a Pandora's box.

Their paper arrived during a conceptual vacuum and a short-lived exploration upturn and set in place a progression whereby numerous authors focused on a single premise and kept adding more members to the growing "family"*. Some of these members would appear to have only a tenuous connection to the key examples of the "family", while at the same time, important deposits that have more to contribute to the Fe-oxide discussion have been excluded - an outstanding example being the Angara-Ilim magnetite province in Siberia. The Werneckes are a "poor cousin" in the Fe-Ox "family" and have little in common with such deposits as Olympic Dam, although an appreciation of their occurrence can contribute to the understanding of this important class of ore deposits and which examples should be included in the "family".

***Authors footnote** - the only practical way to make such comparisons is to visit the deposits in question and make a personal judgement. However, if this is impractical, at least peruse representative sample sets while reading the litereature. The Data Metallogenica collection in Adelaide - soon to be available on-line - with >60 000 specimens from 3500 ore deposits and mineral occurrences world wide has been established for just this purpose.

References

Aitken, J.D. and McMechan, M.E., 1991. Middle Proterozoic assemblages. In Gabrielse, H. and Yorath, C.J., 1992. Geology of the Cordilleran Orogen in Canada. Geology of Canada No.4, Geological Survey of Canada, p. 97-124.

Andrews, A.J., Owsiacki, L., Kerrich, R. and Strong, D.F., 1986. The silver deposits at Cobalt and Gowganda, Ontario,I: geology, petrography and whole-rock geochemistry. Canadian Journal of Earth Sciences, v.23, p.1480-1506.

Archer, A., Bell, R.T. and Thorpe, R.I., 1986. Age relationships from U-Th-Pb isotope studies of uranium mineralization in Wernecke Breccias, Yukon Territory. Geological Survey of Canada Paper 86-1A, p. 385-391.

Bahnemann, K.P., 1986. A review of the geology of the Messina copper deposits, northern Transvaal. In C.R. Anhauesser and S. Maske, eds., Mineral Deposits of Southern Africa. Geological Society of South Africa, Johannesburg, p.1671-1688.

Bell, R.T., 1978. Breccias and uranium mineralization in the Wernecke Mountains, Yukon – a progress report. Geological Survey of Canada Paper 78-1A, p. 317-322.

Bell, R.T., 1986. Megabreccias in northeastern Wernecke Mountains, Yukon Territory. Geological Survey of Canada, Paper 86-1A, p. 375-384

Bell, R.T., 1989. A conceptual model for development of megabreccias and associated mineral deposits in Wernecke Mountains, Canada, Copperbelt, Zaire, and Flinders Ranges, Australia. In: Uranium Resources and Geology of North America, Proceedings of the I.A.E.A., Saskatoon 1987, 149-169.

Blusson, S.L., 1974. Nadaleen River map-area of Operation Stewart. Geological Survey of Canada Open File Report No. 2005.

Bryant, D.G., 1968. Intrusive breccias associated with ore, Warren (Bisbee) mining district, Arizona. Economic Geology, v.63, p.1-12.

Burke, M., 1997. Yukon mining and exploration overview 1996. Yukon Exploration and Geology 1996, Indian and Northern Affairs Canada, p.5-32.

Delaney, G.D., 1981. The mid-Proterozoic Wernecke Supergroup, Wernecke Mountains, Yukon Territory. Geological Survey of Canada Paper 81-10, p. 1-23.

Eisbacher, G.H., 1981. Sedimentary tectonics and glacial record in the Windermere Supergroup, Mackenzie Mountains, northwestern Canada. Geological Survey of Canada, Paper 80-27, 40 p.

Eriksson, S.C., 1989. Phalaborwa: a saga of magmatism, metasomatism and miscibility. In K. Bell, ed., Carbonatites: Genesis and Evolution. Hyman & Unwin, London, p.221-254.

Findlay, D.C., 1969. The mineral industry of Yukon and southwestern District of Mackenzie, 1967. Canada Geological Survey Paper 68-68, 131 p.

Gabelman, J.W., 1988. Representative uranium deposits and occurrences exclusive of sandstone impregnations and quartz conglomerate. Ore Geology Reviews, v.3, p.31-159.

Gabrielse, H. and Yorath, C.J., 1992. Geology of the Cordilleran Orogen in Canada. Geology of Canada No.4, Geological Survey of Canada, 844 p.

Granger, H.C. and Raup, R.B., 1969. Geology of uranium deposits in the Dripping Springs Quartzite, Gila County, Arizona. U.S. Geological Survey Professional Paper 595, 108 p.

Green, L.H., 1972. Geology of Nash Creek, Larsen Creek, and Dawson Creek map-areas, Yukon Territory. Geological Survey of Canada, Memoir 364,157 p

Hammerbeck, E.C.I., 1976. Cobalt. In Mineral Resources of the Republic of South Africa, 5th ed. South Africa Department of Mines, Geological Survey, Handbook 7, Pretoria, p.123-124.

Hitzman, M.W., 2000. Iron oxide-Cu-Au deposits: what, where, when and why. In Porter, T.M., ed., Hydrothermal Iron Oxide Copper-Gold and Related Deposits, a Global Perspective. Australian Mineral Foundation, Glenside, p. 9-26.

Hitzman, M.W., Oreskes, N. and Einaudi, M.T., 1992. Geological characteristics and tectonic setting of Proterozoic iron oxide (Cu-U-Au-REE) deposits. Precambrian Research, v. 58, p. 1-47.

Krendelev, F.P., 1974. Ore-bearing conglomerates of the world (in Russian). Nauka, Novosibirsk, 238 p.

Laznicka, P., 1985. Empirical Metallogeny. Elsevier, Amsterdam, 1754 p.

Laznicka, P., 1988. Breccias and Coarse Fragmentites. Elsevier, Amsterdam, 832 p.

Laznicka, P., 1989. The place of breccias in the universal system of rocks and their regimes of formation. International Geological Congress, 28 Session, Washington, Abstracts v.2, p.267-268.

Laznicka, P., 1992. Breccia-related metallogenesis in the Proterozoic core of the Wernecke Mountains, Northwest Canada (Cordilleran Orogen); in S.C. Sarkar, ed., Metallogeny related to tectonics of the Proterozoic Mobile Belts. Oxford and IBH Publishers, New Delhi, p.225-252.

Laznicka, P., 1993. Precambrian Empirical Metallogeny. Elsevier, Amsterdam, 1622 p.

Laznicka, P., 2001. Total Metallogeny-Geosites. Australian Mineral Foundation, Glenside, 720 p. and two posters.

Laznicka, P., and Gaboury, D., 1988. Wernecke Breccias and Fe,Cu,U mineralization: Quartet Mountain-Igor area (NTS 106E). Yukon Geology, v.2, Indian and Northern Affairs Canada, p.42-50.

Laznicka, P. and Edwards, R.J., 1979. Dolores Creek, Yukon- a disseminated copper mineralization in sodic metasomatites. Economic Geology, v.74, p. 1352-1370.

Lapham, DD.M., 1968. Triassic magnetite and diabase at Cornwall, Pennsylvania. In J.D. Ridge, ed., Ore Deposits of the United States 1933-1967. AIME, New York, p.72-94.

Morton, R., Goble, E. and Goble, R.J., 1973. Sulphide deposits associated with Precambrian Belt-Purcell strata in Alberta and British Columbia, Canada. Belt Symposium, Idaho Bureau of Mines and Geology, v.1, p.159-179.

Nikulin, V.I., Von der Flaas, G.S. and Baryshev, A.S., 1991. Explosive-volcanogenic basaltoid ore-forming system (Angara iron ore province); in Russian. Geologiya Rudnykh Myestorozhdenii, No.3, 1991, p.26-40.

Norman, D.,L. and Sawkins, F.J., 1985. The Tribag breccia pipes: Precambrian Cu-Mo deposits, Batchawana Bay, Ontario. Economic Geology, v.80, p.1593-1621.

Pankka, H.S. and Vanhanen, E.J., 1992. Early Proterozoic Au-Co-U mineralization in the Kuusamo district, northeastern Finland. Precambrian Research, v.58, p.387-400.

Parrish, R.R., 1991. Precambrian basement rocks of the Canadian Cordillera. In Gabrielse, H. and Yorath, C.J., 1992. Geology of the Cordilleran Orogen in Canada. Geology of Canada No.4, Geological Survey of Canada, 844 p.

Pavlov, N.V., 1960. Structural geological characteristics of the magnetite deposits in the Tunguska Syneclise (in Russian). In Osnovnye Voprosy i Metody Izucheniya Struktur Rudnykh Polei i Myestorozhdenii. Gosgeoltekhizdat' Moscow, p.456-468.

Pearson, W.N., 1978. Copper metallogeny, Lake Huron area, Ontario. Geological Survey of Canada, Paper 78-1A, p.263-268.

Preto, V.A., 1972. Lode copper deposits of the Racing River-Gataga River area. Geology, Exploration and Mining in British Columbia in 1971, Victoria, p.75-107.

Puffer, J.H. and Peters, J.J., 1974. Magnetite veins in diabase of Laurel Hill, New Jersey. Economic Geology, v.69, p.1294-1299.

Pukharevich, M.M., Naumov, V.B., Bannikova, L.A., Devirc, A.L. and Sharif-Zade, V.B., 1985. The origin of ore-forming fluids at the Korzhuna iron deposit (In Russian). Geologiya Rudnykh Myestorozhdenii, no.6, 1985, p.51-68.

Raymond, L.A., 1984. Classification of melanges. Geological Society of America Special Paper 198, p.7-20.

Roots, C.F. and Thompson, R.I., 1992. Long-lived basement weak zones and their role in extensional magmatism in the Ogilvie Mountains, Yukon Territory. Proceedings of the 8th International Conference on Basement Tectonics, Kluver Academic Publishers, Dordrecht, p.359-372.

Ruelle, J.C.L., 1982. Depositional environments and genesis of stratiform copper deposits of the Redstone copper belt, Mackenzie Mountains, NWT. Geological Association of Canada Special Paper 25, p.709-738.

Sawkins, F.J. and Rye, R.O., 1979. Additional geochemical data on the Messina copper deposits, Transvaal, South Africa. Economic Geology, v.74, p.684-689.

Schweigart, H., 1965. Genesis of the iron ores of the Pretoria Series, South Africa. Economic Geology, v.60, p.269-298.

Sibson, R.H., 1977. Fault rocks and fault mechanisms. Journal of the Geological Society of London, v.133, p.191-213.

Sims, S.J., 1968. The Grace Mine magnetite deposit, Berks County, Pennsylvania. In J.D. Ridge, ed., Ore Deposits of the United States 1933-1967. AIME, New York, p.108-124.

Sweeney, J.F., Stephenson, R.A., Currie, R.G. and De Laurier, J.M., 1991. Crustal geophysics. In Gabrielse, H. and Yorath, C.J., 1992. Geology of the Cordilleran Orogen in Canada. Geology of Canada No.4, Geological Survey of Canada, p. 39-59.

Swinden, H.S. and Santaguida, F., 1993. Argillite-hosted sulphide occurrences in the eastern part of the Labrador Trough. Newfoundland Geological Survey Branch, Report 93-1, p.401-418.

Tempelman-Kluit, D.J., 1981. NOR, summary of assessment work and description of mineral properties. Yukon Exploration and Geology, DIAND, 1979-1980, p.300-301.

Thorkelson, D.J. et al., 2000. Geology and mineral occurrences of the Slats Creek, Fairchild Lake and "Dolores Creek" areas, Wernecke Mountains (106D/16, 106C/13, 106C/14), Yukon Territory. Yukon Geology Program, Bulletin 10, 76 p.

Thorkelson, D.J. and Wallace, C.A., 1993. Development of Wernecke Breccia in Slats Creek (106D/16) map area, Wernecke Mountains, Yukon. Yukon Exploration and Geology, 1992, p.77-87.

Von der Flaas, G.S., 1990. Tuffisites of the subalkaline basaltoids and their role in formation of the iron-bearing diatremes of the south of Siberian platform. Geotectonica et Metallogenia, v.14, p.351-364.

Young, G.M., 1976. Iron formation and glaciogenic rocks of the Rapitan Group, Northwest Territories, Canada. Precambrian Research, v.3, p.137-158.

Eurasia & Africa

PGC PUBLISHING

Strickland, C.D., 2001 - The Guelb Moghrein Fe-Oxide Copper-Gold-Cobalt Deposit and Associated Mineral Occurrences, Mauritania: A Geological Introduction; *in Porter, T.M. (Ed.), Hydrothermal Iron Oxide Copper-Gold & Related Deposits: A Global Perspective*, Volume 2; PGC Publishing, Adelaide, pp 275-291.

THE GUELB MOGHREIN Fe-OXIDE COPPER-GOLD-COBALT DEPOSIT AND ASSOCIATED MINERAL OCCURRENCES, MAURITANIA: A GEOLOGICAL INTRODUCTION.

[1]Colin D. Strickland and [2]John E. Martyn

[1]*General Gold International SA, Perth, Australia.*
[2]*John Martyn Associates Pty Limited, Turramurra, NSW, Australia.*

Abstract – The Guelb Moghrein deposit is located within the Mauritanide Mobile Zone, north east of Nouakchott in the Islamic Republic of Mauritania, West Africa. The copper, gold and iron deposits of the Mauritanides fold/thrust belt of the Akjoujt area have many of the characteristics of the hydrothermal iron oxide copper-gold class of deposits as well as showing distinctive features of their own. Exploration by General Gold International SA since 1994 has concluded that they represent, perhaps, a carbonate-rich sub class and show considerable diversity of form and setting.

The Mauritanides in Mauritania incorporate a great diversity of rocks in multiple, thrust-bounded domains including metamorphosed siliciclastic sediments, meta-felsic volcanics, meta-basic volcanics, serpentinite, and bodies of granitoid rocks.

The Akjoujt area features a supracrustal suite of metamorphosed mafic to felsic volcanic, volcaniclastic and epiclastic rocks, with a number of banded iron formation (BIF) horizons, that have been overthrust northwards and eastwards onto the Archaean Amsaga Basement and the Taoudeni Basin edge. The supracrustal stratigraphy has recently been revised by the authors because previously published schemes were found to be inconsistent with field observations. Carbonate alteration is widespread in the supracrustal suite and the BIFs are commonly carbonate rich.

All of the Fe-oxide copper-gold mineralisation of the Akjoujt area is associated with coarse-grained Fe-Mg-Ca carbonate occurrences. These are widespread throughout the Akjoujt area and they range in size from clusters of carbonate porphyroblasts in BIF, through small pods and lenses, to large lenses, irregular sheets, and from single narrow veins to extensive stockworks and vein systems. Some form of structural control is usually apparent and emplacement has occurred at various stages in the tectonic history from early to syn-thrusting through to upright folding and doming.

The Guelb Moghrein Cu-Au-Co mineralisation within both the Occidental and Oriental bodies is hosted by a massive magnetite-sulphide bearing iron-magnesium carbonate representing a CO_2 metasomatised shear zone or 'tectonite and is characterised by prominent magnetic anomalism. A total measured and indicated resource of 23.6 Mt @ 1.88 % Cu, 1.41 g/t Au and 143 ppm Co has been calculated and currently the mineralised zone is open at depth, presenting a significant geophysical target for the discovery of additional down dip and satellite deposits.

At El Khader the carbonate vein system is interpreted to belong to a different stage in tectonic evolution than at Guelb Moghrein. There the brittle fracture event is considered to have occurred later than the ductile shear setting of Guelb Moghrein.

Given the abundance of carbonate in the country rocks, and the structurally controlled settings of the coarse grained occurrences it is likely that the carbonate bodies in the Akjoujt area evolved by remobilisation from within the system during tectonism. This would probably have involved recycling of basin fluids, however there is no evidence that magmatism played any role in this. The introduction of the metallic components is assumed to be along the same structural channels but the source of metal is unclear. The most likely origin is, like the carbonate, from within the pile, in this case from the abundant, leachable mafic volcanic rocks.

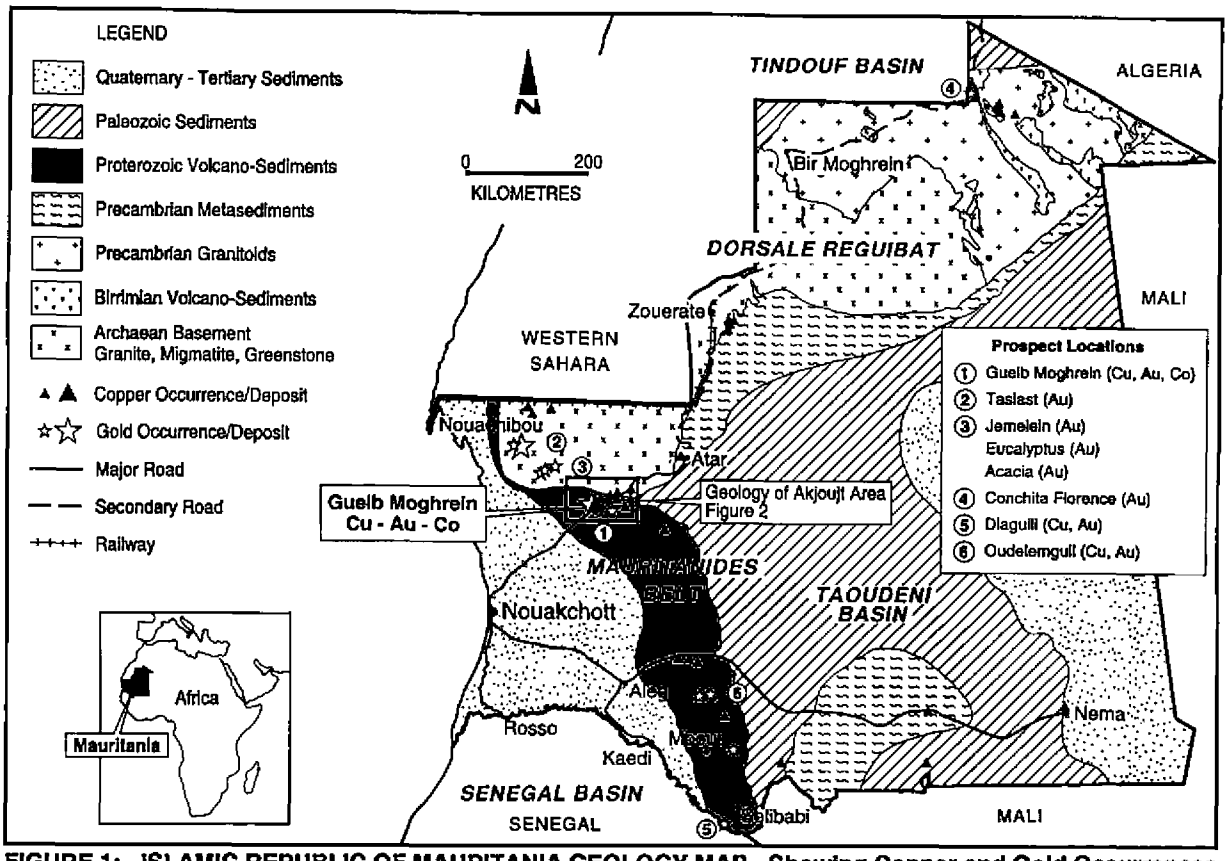


FIGURE 1: ISLAMIC REPUBLIC OF MAURITANIA GEOLOGY MAP - Showing Copper and Gold Occurrences

Introduction

The Islamic Republic of Mauritania is a sub-Saharan country occupying approximately one million square kilometres on the West Coast of North Africa, north of the Senegal River. The Akjoujt area is located 260 kilometres northeast of Nouakchott on the main national highway between the capital and the town of Atar (Figure 1). The copper, gold and iron deposits of the Mauritanides fold/thrust belt of the Akjoujt area have many of the characteristics of the hydrothermal Fe-oxide copper-gold class of deposits as well as showing distinctive features of their own. They represent, perhaps, a carbonate rich sub class and show considerable diversity of form and setting.

This paper is based on the detailed reverse circulation and diamond drilling evaluation of the Guelb Moghrein deposit together with a geological, geophysical, mineragraphic and petrographic study of the ores and host units. It also incorporates the results of a regional mapping programme based on air photographs and enhanced SPOT and TM images. The mapping was supported by an airborne magnetic and radiometric survey over the Guelb Moghrein deposit and the surrounding 300km^2. This survey data was examined in detail in order to identify target sources that had similarities to the magnetic expressions of the known Guelb Moghrein mineralisation (Dockery 2000).

Mining History

The principal deposit, Guelb Moghrein, was exploited for copper in Neolithic times and the ancient workings were noted in 1931 by the French military, however it was not until 1946 that A. Blanchot of the Bureau Minier systematically sampled the malachite impregnated rocks at Guelb Moghrein. (Figure 2). The *Syndicat de l'Inchiri*, an association involving the Bureau Minier, Federation of French West Africa and the Territory of Mauritania, investigated the potential of the Guelb Moghrein mineralisation for large scale mining in the late 1940's. The first modern mining venture on the deposit in the early 1950's, by the *Societe des Mines Cuivre de Mauritanie* (MICUMA) failed to develop a viable metallurgical technology and the company was disbanded in 1958.

In July 1967 *Societe Miniere de Mauritanie* (SOMIMA), commenced development of the oxide copper resource and infrastructure. Oxide reserves at the time were 7.7Mt at 2.7% Cu and 3.1g/t Au overlying open pit sulphide reserves totalling 15Mt of 1.8% Cu and 1.0g/t Au. This led in 1968 to construction of the world's largest oil fired TORCO plant (treatment of refractory copper ore). Design capacity of the TORCO was seldom achieved and in 1974 a combination of increasing fuel prices and a fall in the copper price placed SOMIMA in difficulty. The Mauritanian Government transferred operational responsibility to *Societe Nationale Industrielle et Miniere* (SNIM) which commenced ordering equipment for the future US$50 million dollar sulphide project on which Charter Consolidated had prepared a feasibility study. The continuing deteriorating financial situation however forced SNIM-SOMIMA to close the mine in May 1978.

In 1982 *Societe Arabe des Mines l'Inchiri* (SAMIN) commenced stripping overburden from the sulphide orebody and contracted SOFREMINES to complete an

updated sulphide feasibility study. Although the latter indicated a total sulphide resource of between 34-39Mt at 1.45% Cu and 0.8g/t Au, the copper price was experiencing a 50 year low and SAMIN was forced to abandon their future mining plans. *Minproc Engineers Pty Ltd* then became involved in the resampling of the mine tailings in 1990 and established a resource of 2.4Mt at 3.08 g/t Au. *Mines d'Or d'Akjoujt* (MORAK) was incorporated in 1991 to treat the tailings using the Hunt process, but metallurgical recovery problems plagued the operation and *General Gold International SA* (GGISA) took up Minproc's equity position in 1993. Further research confirmed that the addition of oxygen was a major requirement for the successful cyanide leaching of gold in the presence of copper and ammonia. Gold recoveries of 85% were characteristic of the 50,000t per month treatment till the operation was completed in 1996. The retreated tailings produced a total 158,000 oz Au and during the project's life gold represented the third most valuable export commodity in Mauritania.

GGISA entered into a 50:50 joint venture agreement with SAMIN in 1994 and formed *Guelb Moghrein Mines d'Akjoujt SA* (GEMAK) in 1995 to conduct a feasibility study into the development of the remaining oxide and sulphide resources at Akjoujt, known as the Guelb Moghrein deposit. Following extensive RC and diamond drilling, resource estimation, metallurgical sampling and test work, flowsheet design and costing, marketing studies, provision for dust control measures for asbestiform minerals, and environmental auditing, a bankable feasibility study was commissioned and completed in April 1997 by Kilborn-SNC-Lavalin Europe.

Exploration of the El Khader mineralisation, situated 25km south-east of Akjoujt, (Figures 2 and 7) commenced in 1953. Mapping for the delineation of potential iron ore resources by A. Allon in 1956-57 resulted in the definition of a number of zones of haematite and goethite derived mainly from the weathering of a 60m thick ferruginous carbonate unit. Minor accessory malachite, chrysocolla, cuprite, and native copper locally stain the carbonate. Exploratory pits by MICUMA in 1958 resulted in a resource estimate of 18 Mt of iron ore grading 51% Fe.

The Sainte Barbe prospect, located 27km north-east of Akjoujt, (Figure 2) consists of ancient Neolithic workings that were first explored by MICUMA with trenches and adits in 1955. The mineralisation in the form of malachite, chrysocolla and azurite is associated with quartz-ankerite veining within a massive ferruginous carbonate unit up to 25m thick.

Regional Geological Setting of the Akjoujt Area

The Akjoujt area lies on a bend, or orocline, in the Mauritanides chain, a complex, generally east-verging fold/thrust belt that extends from Senegal in the south to Western Sahara in the north (Figure 1). It is bounded to the east and north by a variety of terrains including the Amsaga Basement, part of the Archaean Reguibat Shield, in the north, the vast, continental sedimentary Taoudeni Basin of Neoproterozoic to Devonian age in the centre, and the Lower Proterozoic Birrimian fold belt emerging from beneath the Taoudeni Basin in the far south. A series of overthrust basement sheets defines the western edge in the Akjoujt area, however thin marine sediments obscure the western boundary of the Mauritanides for much of its length.

The Mauritanides in Mauritania incorporate a great diversity of rocks in multiple, thrust bounded domains. These include metamorphosed siliciclastic sediments, meta-felsic volcanics, meta-basic volcanics, serpentinite, and bodies of granitoid rocks. Low to medium metamorphic grades predominate however amphibolites and eclogites occur locally, especially in the north. Stratigraphic relationships are problematic due to the intensity of deformation and thrust bounded relationships. There is very little information on the age of the various lithological units of the Mauritanides. Given the complexity of the terrain there are undoubtedly domains of diverse age dragged in by the thrusting.

Lecorche et al. (1989) summarised the thermal history of the Mauritanides from the limited data available in the southern part of the belt. These include Rb-Sr and ^{40}Ar / ^{39}Ar dates on the felsic igneous rocks of the Mbout area, 500 km to the south of Akjoujt (Figure 1) of ca. 675 to 685 Ma. This they compared to a more northerly-located U-Pb zircon age on similar rocks of 680±10. A later event of ca.620-650 Ma was also recorded representing a major tectonothermal event, the first phase of the PanAfrican orogeny. A second phase event at around 575 to 550 Ma was also distinguished, followed much later by a late Palaeozoic resetting of muscovite at ca.300 Ma.

It is probable that at least some, and possibly all of the events discriminated from further south are manifest in the Akjoujt area, however the overthrust supracrustals of Akjoujt present a suite of rocks rather unlike those to the south. They are dominated by volcanic and volcaniclastic rocks with prominent banded iron formation units (BIF). Currently we do not have any definitive data on the age of these rocks except that they are certainly pre-Hercynian. The presence of extensive BIF may be age critical. Isley and Dallas (1999) distinguished world-wide iron formation depositional peaks at around 1850, 2450, 2700 and 3000 Ma. Iron Formations also occur in the Neoproterozoic in association with glacigene sediments in Australia, Africa and South America (eg. Lottermoser & Ashley, 2000, Urban et al., 1992) and with volcanics and clastics in the Ordovician of the Tetagouche Group of New Brunswick, Canada (Saif, 1980). Based on the chronology of BIF deposition this presents a wide choice and it is wise to be circumspect until definitive dating information becomes available.

The Mauritanides of Mauritania contain a number of copper gold occurrences, mainly in two areas, the Selibabi-Mbout area in the south and the Akjoujt area (Figure 1). Occurrences in the former, such as Kadiar and Diaguili, are associated with sheared, carbonate-altered serpentinite or with faults and shears in mafic volcanics. Those of the Akjoujt area are the more substantial.

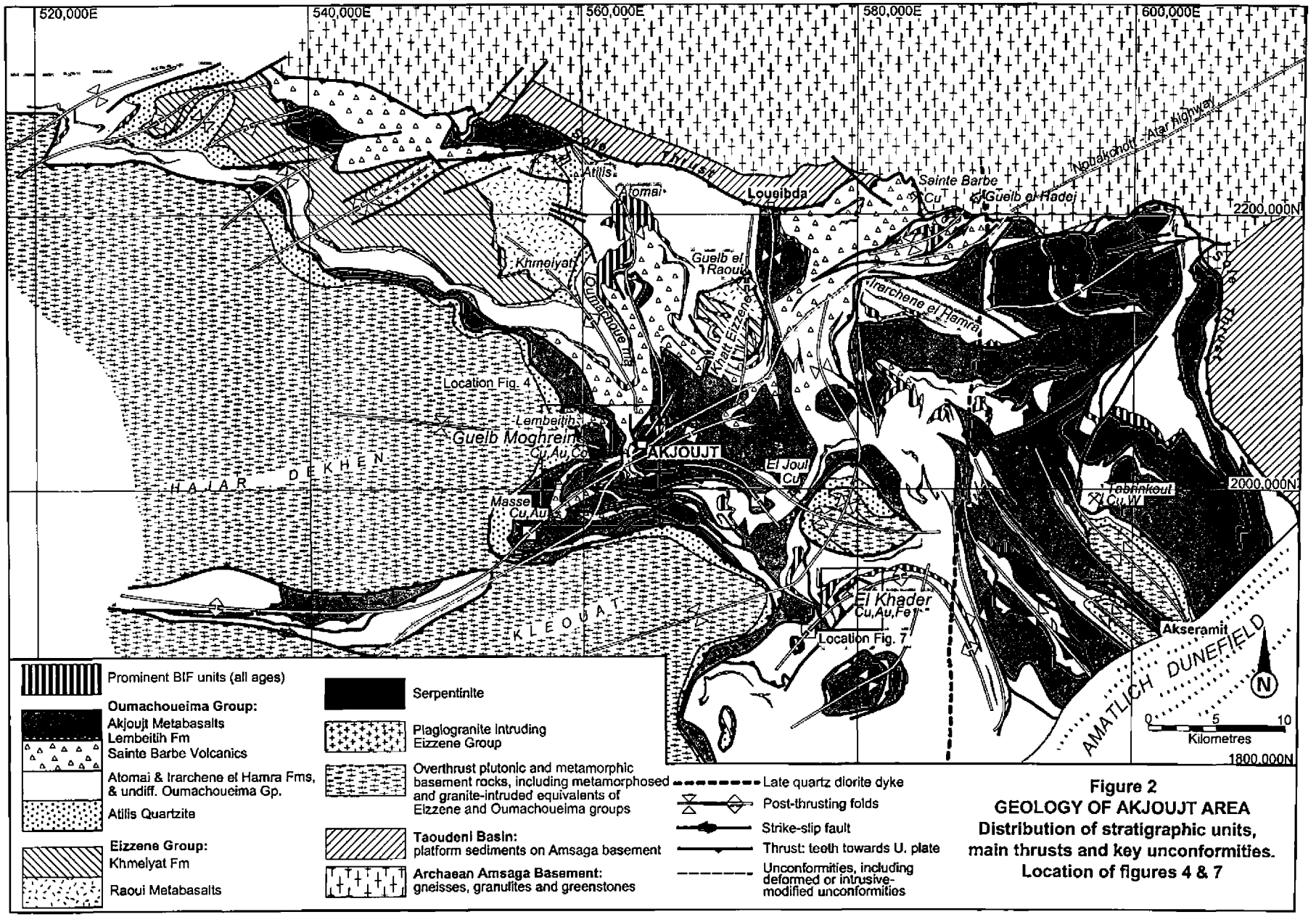


Figure 2
GEOLOGY OF AKJOUJT AREA
Distribution of stratigraphic units, main thrusts and key unconformities. Location of figures 4 & 7

Geology of the Akjoujt Area

Stratigraphy

The Akjoujt area features a supracrustal suite of metamorphosed volcanic, volcaniclastic and epiclastic rocks that has been overthrust northwards and eastwards onto the Archaean Amsaga Basement and the Taoudeni Basin edge (Figure 2). The Amsaga Basement consists of gneisses and granulites with embryonic greenstones, while the Taoudeni Basin sediments are of continental, shallow water character and consist of red and grey conglomerate, sandstone, siltstone and carbonate. To the southwest the supracrustals have been overthrust by their own basement rocks that consist of gneisses, granitoids and older, more metamorphosed supracrustals.

The supracrustal stratigraphy has recently been revised by the authors as previously published schemes (eg Giraudon, 1964, Michaud, 1963) were found to be inconsistent with field observations. The proposed new scheme has yet to be published separately. The sequence is presently believed to consist of two suites separated by an unconformity (Figure 3). The lower assemblage, for which the name Eizzene Group is proposed, consists of altered basalt flows, the Raoui Metabasalts, overlain by fine grained clastics and quartz-magnetite BIF, the Khmeiyat Formation. These are intruded by small plagiogranite plutons.

The Eizzene Group is overlain unconformably by a volcanic and clastic succession for which the name Oumachoueima Group has been proposed. This begins with a basal quartzite, the Atilis Quartzite, followed by fine grained meta-greywacke and siltstone, the Irarchene el Hamra Formation. This is overlain by fine grained intermediate to mafic volcaniclastics with BIF units up to tens of metres thick, the Atomai Formation. A massive BIF at the top of the Atomai Fm is followed by increasingly felsic lavas and volcaniclastics of andesite to rhyodacite composition, the Sainte Barbe Volcanics. These are capped by a widespread BIF/chert marker, the Lembeitih Formation, which is overlain by thick and extensive basalt flows with dolerite intrusives, the Akjoujt Metabasalts.

The BIF units of the Oumachoueima Group are variable but commonly rich in Fe carbonate as well as magnetite. Carbonate is also pervasive throughout the volcanics and volcaniclastics as an alteration phase. Carbonate is locally concentrated in schistose, sheet like zones associated with layer parallel ductile thrusts and these had been previously interpreted as carbonate sediments (eg. Pouclet et al., 1987).

The Oumachoueima Group has not suffered any intrusive activity other than synvolcanic dolerites. The only granitic intrusives to have affected it are where the basal quartzitic units are preserved attached to overthrust basement and multiple leucogranite sheets are intruded.

Structure and tectonic history

The overthrust and allochthonous nature of the supracrustals, with respect to the basement to the north and east, was first recognised by Giraudon & Sougy (1963).

Preliminary work by the authors has suggested that principal thrusting took place on multiple planes during two main periods, the first from a south southwest direction, followed by a second event from the west southwest. These events also brought the basement to the supracrustals over the top. Subsequent open to tight, upright-folding contorted the thrust sheets and this operated above a sole thrust on which the entire supracrustal mass was carried onto the Archaean Amsaga Basement and Taoudeni Basin. The later folding down-folded the overthrust basement which is preserved in synformal remnants and embayments (Figure 2).

Metamorphic grade varies from lower to upper greenschist or low amphibolite and rises upwards towards the overthrust basement which is generally amphibolite grade. This suggests that the sequence was first metamorphosed and then partially inverted during subsequent thrusting. Retrogression and carbonate alteration is widespread.

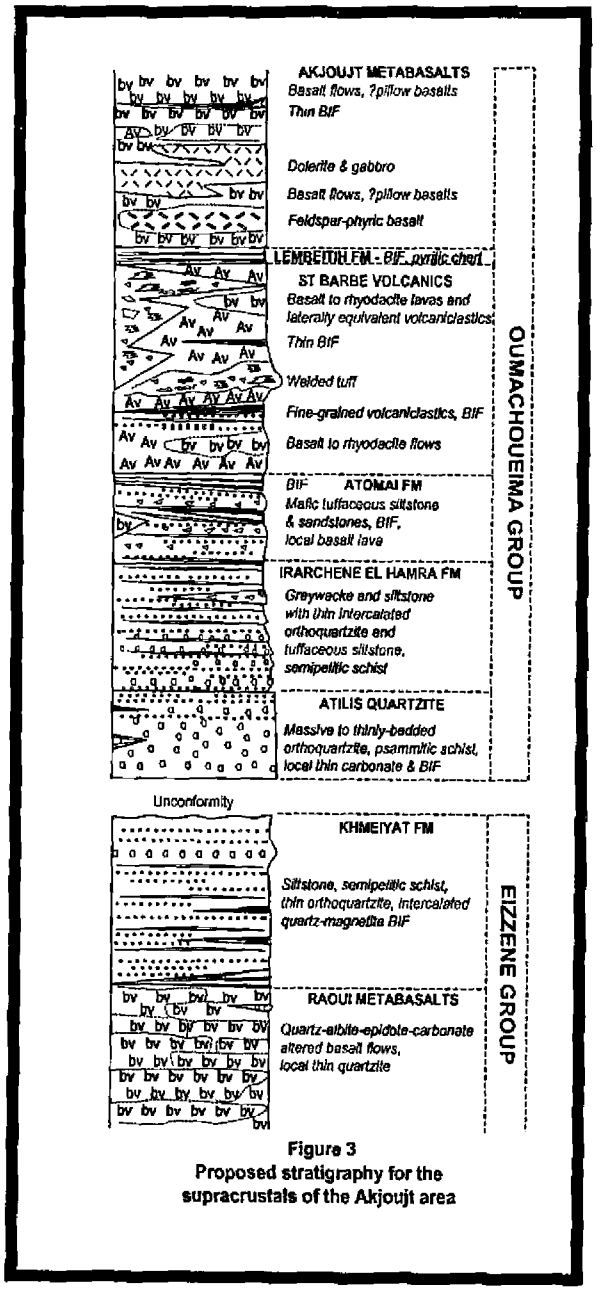
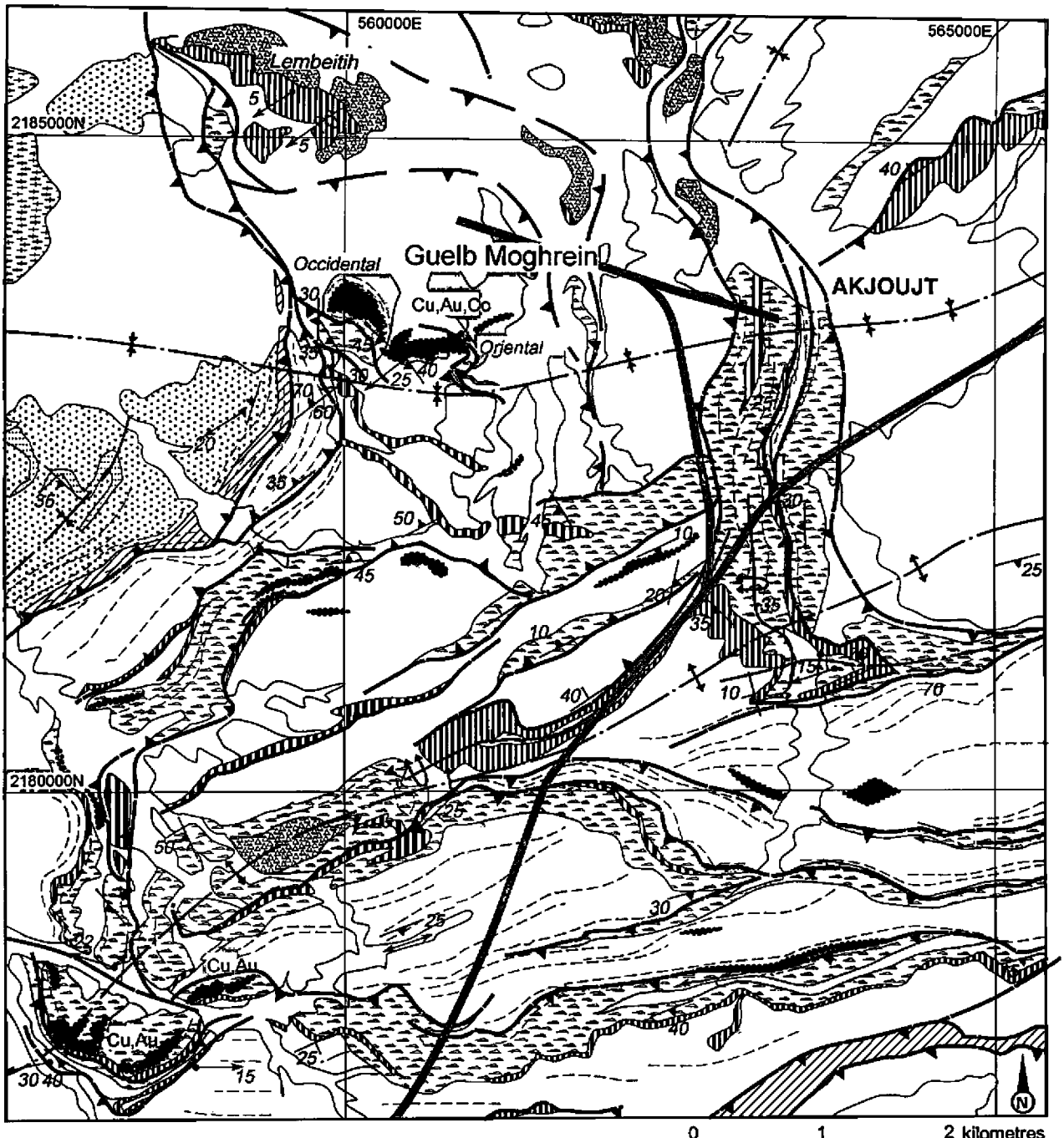


Figure 3
Proposed stratigraphy for the supracrustals of the Akjoujt area



Akjoujt Metabasalts

Metadolerite

Lembeitih Fm Pyritic chert & BIF

Sainte Barbe Volcanics intermediate to felsic volcanics

Undifferentiated schistose to mylonitic volcanics and clastics, BIF, Sainte Barbe Volcanics and Atomai Fm

Irarchene el Hamra Fm, pelitic and semipelitic schist, thin BIF

Atilis Quartzite, psammitic schists granitic and pegmatitic sheets and migmatite, thin marble

Granitic and pegmatitic gneiss and migmatite

Carbonate-magnetite – sulphide bodies

Plunge of minor recumbent fold

Plunge of minor upright fold

Subhorizontal lineation

Plunge of lineation

Dip of foliation or cleavage

Dip of layering

Upright open folds

Overturned to recumbent folds

Thrusts

Figure 4 GEOLOGICAL SETTING OF GUELB MOGHREIN based on field traverses and air photo interpretation showing multiple thrust repititions, refolding of thrusts and carbonate-magnetite bodies.

General Character of the Iron Oxide Copper Gold Occurrences

All of the Fe oxide copper gold mineralisation of the Akjoujt area is associated with coarse-grained Fe-Mg-Ca carbonate occurrences. These are widespread throughout the Akjoujt area and they range in size from clusters of carbonate porphyroblasts in BIF, through small pods and lenses, to large lenses, irregular sheets, and from single narrow veins to extensive stockworks and vein systems. Some form of structural control is usually apparent and emplacement has been at various stages in the tectonic history from early-to syn-thrusting through to upright folding and doming. The carbonate may be accompanied by Mg rich silicates such as cummingtonite, tremolite or anthophyllite or by quartz or magnetite. Porphyroblasts of garnet, cummingtonite and biotite are locally present in schistose rocks enveloping some of the lenses in the Guelb Moghrein vicinity.

Most coarse grained carbonate occurrences do not contain significant Fe oxide or Cu sulphides but there are a number of exceptions, the main ones being the mineral occurrences shown on Figure 2. The two principal deposits, or systems, described below, are Guelb Moghrein and El Khader. They have some features in common with one another but in other respects are contrasting in style, setting and timing in relation to tectonic events.

Guelb Moghrein

Guelb Moghrein outcrops in a zone linking two abrupt hills rising from the low undulating desert terrain on the western outskirts of Akjoujt townsite. (Plate 1). Structurally the deposit is situated just north of the axis of a gentle east-west synform which folds an assemblage of multiple thrust sheets in which elements of the upper part of the Oumachoueima Group, mainly the Akjoujt Metabasalts, Lembeitih Formation and Sainte Barbe Volcanics, are repeated several times. (Figure 2). Immediately west of the deposit lies the eroded eastern edge of a major, downward facing, gently west-dipping overthrust sheet. Within this overthrust structure the basement granitic gneisses and intrusive granites grade downwards into granite sheets interlayered with quartzites, psammitic schists and thin carbonates correlated with the Atilis Quartzite. They rest in turn on pelitic schists of the Irarchene el Hamra Formation in a completely overturned sequence. Throughout the Guelb Moghrein area thrusts are accompanied by zones of strong ductile deformation expressed as intense schistosity and mylonitic fabrics. (Figure 4).

The country rocks in the immediate vicinity of the Guelb Moghrein mine are dominated by amphibolite or meta-dolerite but also include narrow shear bounded sheets or lenses of strongly deformed felsic metavolcanic rocks and BIF. The meta-dolerite is believed to be part of the Akjoujt Metabasalts while the other units belong to the Sainte Barbe Volcanics and Lembeitih Formation.

Mineralisation

The Guelb Moghrein ore system (Figure 5) consists of two lensoid bodies of carbonate known as Occidental and Oriental, linked by an attenuated zone of carbonate in mafic schists. (Plate 2). The Oriental body is a massive, thick pod about 250 m long and at least 150 m thick, largely preserved in the oxide zone and lacking a major down-dip extension. Occidental however is a broader, flatter and more extensive lensoid body about 500 m across and up to 150 m thick, apparently tapering down-dip, but open at depth.

X-ray diffraction analysis of the Guelb Moghrein carbonate shows it to be a magnesian siderite with the main peak at 2.77Å (compared to 2.80Å for siderite and 2.74Å for magnesite) (Henley 1995). This ferromagnesian carbonate falls within the range of pistomesite and is characterised



Plate 1 Guelb Moghrein Deposit
View from the crest of the Oriental mineralisation showing the footwall mafics within the existing Occidental open cut and the TORCO plant.

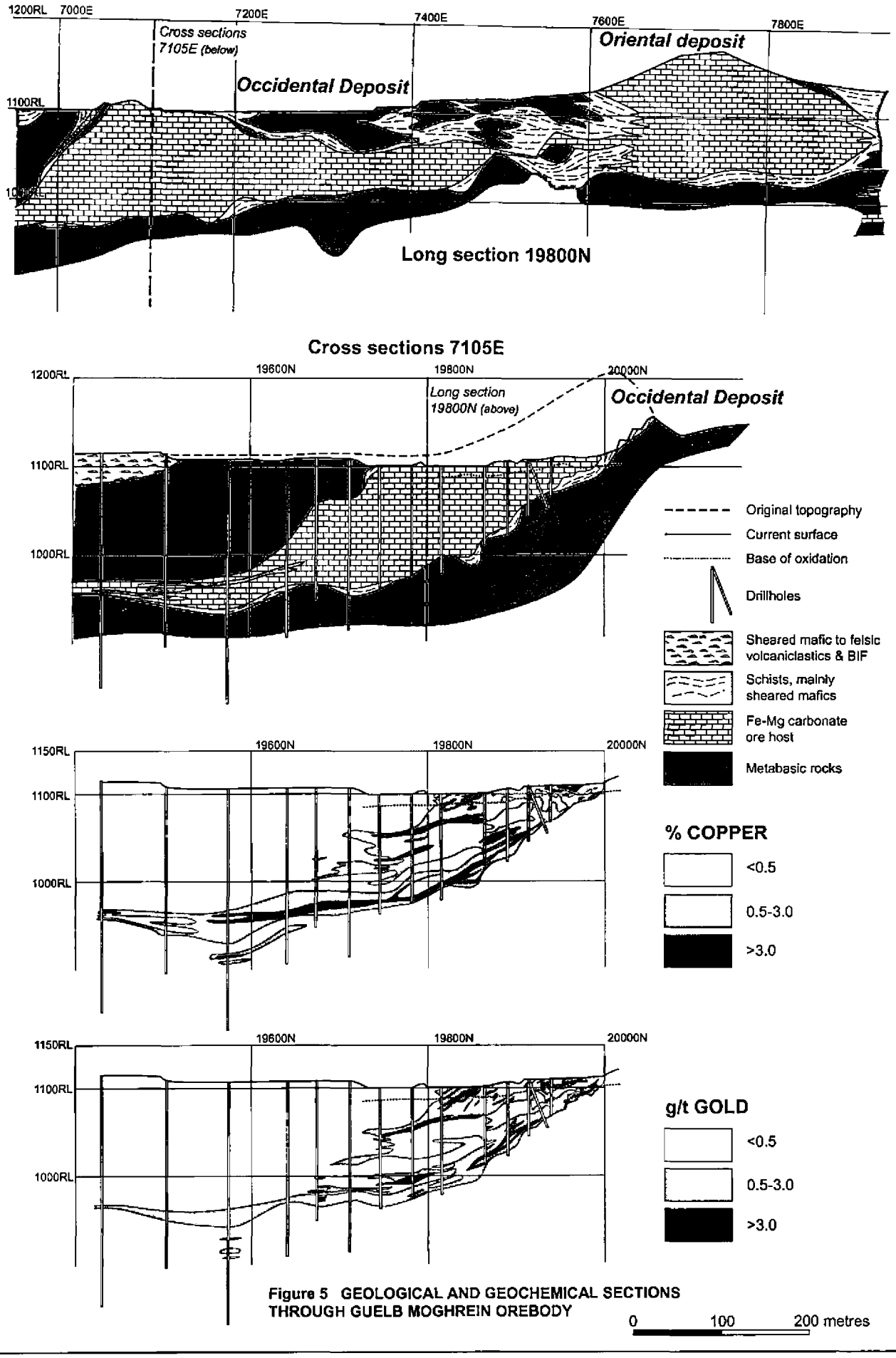


Figure 5 GEOLOGICAL AND GEOCHEMICAL SECTIONS THROUGH GUELB MOGHREIN OREBODY



Plate 2 Guelb Moghrein Deposit
View west from Oriental showing exploratory development of the sulphide mineralisation within the Occidental oxide open cut.

by an intergrowth of massive brown or grey irregular crystals up to several millimetres in size. The carbonate body at Guelb Moghrein has been subdivided into oxide, transition and sulphide zones on the basis of colour, texture and mineralogy.

Copper and gold rich zones are interpreted from drilling to occur as multiple, coalescing lenses that are broadly elongate in the direction of the elongation of the carbonate envelope (Figure 5). There is a concentration of lenses in the upper, thicker part of the body, and at the base.

Within the sulphide zones the carbonate is grey to dark grey in colour, coarsely crystalline with intergrowths of chalcopyrite, pyrrhotite, cubanite, arsenopyrite and cobaltite. Magnetite is dominant, accounting for up to 35% of the mineralisation. The magnetite commonly occurs as irregular to euhedral grains up to several millimetres in size and granular masses intergrown with both the carbonate and the sulphides, it is also observed to occur as narrow cross-cutting veins. Euhedral grains of magnetite in places contain inclusions of chalcopyrite. Both the chalcopyrite and cubanite form anhedral grains, which typically are associated with the magnetite or occur as individual anhedral aggregates up to a few millimetres in diameter. Lamellar intergrowths of chalcopyrite and cubanite are occasionally observed, although they commonly form marginal intergrowths or interstitial intergrowths between the magnetite crystals.

Electron microprobe analyses determined that the cobalt in the sulphide zone occurred as cobaltite, whereas in the oxidised ore samples the cobalt was associated with goethite and malachite. An examination of the native gold particles from the reverse circulation drill cuttings indicated irregular shaped grains with a hackly character and either a very bright surface with no coating or a dull reddish brown appearance due to an iron-oxide coating.

There is approximately 2% by volume of fibrous amphibole minerals. Asbestiform minerals including actinolite, tremolite and anthophyllite occur as discrete fibrous aggregates, along fractures or attached to the carbonate. Rarer mineral species include pentlandite, graphite, valleriite and sylvanite. Simultaneous deposition of magnetite, chalcopyrite, pyrrhotite and arsenopyrite is evident, with exsolution of pentlandite, cubanite, cobaltite and valleriite. The epigenetic sulphides were emplaced in the pre-existing ferromagnesian carbonate body. The sulphide ore zones are characterised by high iron and magnesium with relatively low levels of sulphur. During late folding events the sulphides were probably locally remobilised within the major fold axes and fractures. Physical characteristics of the sulphide mineralisation relevant to future mining are the hard yet unabrasive nature of the ore and it's significant density of 3.7 t/m^3.

The transition zone, containing iron and copper oxides, native copper and trace sulfides occupies a thin irregular blanket between the oxide and sulphide zones. This ore consists of siderite with lesser amounts of magnetite, haematite, goethite and anthophyllite, with trace amounts of graphite, quartz, native copper, malachite and chalcocite. The transition mineralisation is characterised by siderite, with lesser amounts of magnetite, quartz, chalcopyrite, pyrrhotite, anthophyllite, cubanite and arsenopyrite. Trace amounts of pentlanditite, graphite, molybdenite and sylvanite were also observed. Native gold, electrum and melonite ($NiTe_2$) were observed associated with arsenopyrite (Ramdohr et al, 1956).

The oxide zone at Occidental was originally capped by a siliceous iron gossan, depleted in copper and up to 15m thick, few remnants of the mineralised outcrop now remain. This oxide mineralisation at the Oriental deposit currently is present as an undisturbed silicified cap. Haematite, goethite and residual magnetite are the dominant iron minerals present. Goethite coats and partially replaces the carbonate forming a carbonate gossan and haematite commonly coats the magnetite. X-ray diffraction and ore microscopy of thin and polished sections show that the

TABLE 1
GUELB MOGHREIN OCCIDENTAL
ANALYSES OF METALLURGICAL SAMPLES.

Species	Oxide Ore	Sulphide Ore	Species	Oxide Ore	Sulphide Ore
Cu %	1.47	1.76	Al ppm	105	1800
Cu (sol) H_2SO_4 %	1.05	0.016	As ppm	730	101
Cu (sol) Cyanide %	0.89	0.033	Ba ppm	6.4	9.5
Co %	0.02	0.018	Be ppm	<1	<1
Fe %	45.0	38.2	Ca ppm	11700	8520
S %	0.09	2.77	Cd ppm	45	41
S= %	<0.01	2.49	Co ppm	215	186
Au g/t	1.7	2.0	Cr ppm	24	20
Ag g/t	-	-	Cu ppm	14900	19000
CO_3 %	17.8	29.7	Fe ppm	547000	467000
CO_2 %	13.1	21.8	K ppm	689	538
SiO_2 %	5.3	4.7	La ppm	<100	<100
Al_2O_3 %	0.09	0.31	Mg ppm	63100	89000
Fe_2O_3 %	65.5	57.3	Mn ppm	9450	8450
MgO %	8.4	11.8	Mo ppm	<10	<10
CaO %	1.72	1.19	Na ppm	392	870
Na_2O %	<0.05	<0.05	Ni ppm	148	163
K_2O %	0.02	0.03	P ppm	200	303
TiO_2 %	0.03	0.04	Pb ppm	48	36
P_2O_5 %	0.04	0.09	Sb ppm	<10	<10
MnO %	1.28	1.11	Se ppm	<50	<50
Cr_2O_3 %	0.05	0.03	Sn ppm	<20	<20
V_2O_5 %	0.02	<0.01	Te ppm	<50	<50
Loss On Ignition	16.3	21.0	Zn ppm	43	39

TABLE 2.
GUELB MOGHREIN OCCIDENTAL
GEOPHYSICAL PROPERTY MEASUREMENTS

Sample Description	Density g/cm^3	IP Effect mrad	Conductivity S/m	Resistivity ohm.m	Susceptibility cgs x 10^{-6}	Remanence Q factor
Stringer sulphides	4.12	630	1130	0.000780	81700	8.1
Low grade ore	3.70	697	113	0.038000	49100	2.5
High grade ore	3.77	603	472	0.001900	13300	3.2
Massive sulphides	4.29	564	3122	0.000170	28900	0.3
Massive sulphides	4.23	420	5836	0.000032	31700	0.5
Dissem. sulphides	3.88	585	89	2.000000	68300	0.4

oxide ore beneath the siliceous cap is characterised by goethite, siderite, haematite and magnetite with lesser amounts of anthophyllite, graphite, malachite, chalcopyrite and covellite. Carbonate and oxide copper minerals dominate the remainder of this zone including malachite, azurite, cuprite, native copper and chrysocolla. Native gold is commonly attached to goethite and haematite and minute telluride inclusions were observed in the magnetite, chalcopyrite and arsenopyrite.

The spatial distribution of both the carbonate and the economic copper, gold and cobalt mineralisation appears to be a function of total fluid movement throughout the shear structure. Well-defined thin, tabular shoots are typically present, complicated by sulphide enrichment on late fractures, representing a remobilisation overprint. (Figure 5).

A detailed analysis of two composite metallurgical samples, representing oxide and sulphide ore types is presented in Table 1.

Hangingwall and Footwall Lithologies

Petrographic examination of the hangingwall and footwall amphibolites has indicated that the primary textures have been obliterated by upper greenschist to lower amphibolite facies metamorphism. The hangingwall amphibolite is

composed of intergrowths of amphibole and quartz, with minor feldspar, biotite, ilmenite and trace amounts of chlorite, carbonate, sphene and pyrite. Chlorite is intergrown with hornblende and biotite, and porphyroblasts of plagioclase feldspar are common. Discordant streaks and lenses of hornblende-biotite and quartz-carbonate-chlorite intergrowths probably representing shears, disrupt the amphibolites.

The highly sheared footwall examples, although mineralogically similar to the host amphibolites, contain a pronounced fine-grained, lenticular-banded structure and increased fine-grained phyllosilicates and carbonate. The texture is commonly porphyroblastic with quartz and amphibole in a fine grained groundmass of phyllosilicates. Feldspars are sericitised and silicified, and tremolite is developed along the cleavage. The footwall is cut by numerous shear zones, often with a pinched or boudinaged core of carbonate and lenses of fine-grained quartz.

Sulphide mineralisation and tremolite are observed within the highly sheared, carbonated footwall and hangingwall 'schists'. These narrow ore zones occur as irregular selvages to the main body and appear to rapidly decrease in frequency and thickness outwards from the body (Figure 5).

Geophysical Characteristics

The Guelb Moghrein Cu-Au-Co mineralisation within both the Occidental and Oriental deposits is characterised by prominent magnetic anomalism and has the following geophysical properties (Emerson 1998).

- All samples are generally dense with the massive sulphide examples averaging over 4.2 g/cc.
- IP measurements show the samples to be highly polarisable with little difference between strongly or weakly mineralised samples.
- Inductive electromagnetic measurements show all the samples to be conductive, ranging from a low of 89 siemens/m for disseminated sulphides, up to extremely high values of up to 5836 siemens/m for the massive sulphides.
- Galvanic resistivity results show all samples to have low resistivity, with the massive sulphides having extremely low resistivity.
- Magnetic susceptibility values for all samples are very high and equate to between 1% and 27% magnetite equivalent.
- Significant remnant magnetisation was indicated in all samples. Precise measurement of the direction of the remnant magnetism is required prior to any detailed quantitative interpretation of magnetic surveys.

A summary of the measured parameters and results is presented in Table 2.

The Guelb Moghrein mineralisation forms an ideal target for a large variety of geophysical survey methods. For reasons of cost and efficiency a magnetic survey is considered as a first pass method, with the transient electromagnetic (TEM) method the preferred follow up technique, as it allows both deep detection of mineralisation and quantitative interpretation. Figure 6 presents an image of the surface source enhanced total magnetic intensity data and a 3D model of the results viewed from the southeast. The data clearly highlights the Guelb Moghrein mineralisation at Occidental and Oriental and has identified additional magnetic anomalies in the mine environs for future exploration.

Mineral Resources

A 105 hole exploratory drilling programme by GGISA in 1994-95 together with the results from previous drilling campaigns has resulted in a comprehensive database of over 220 diamond drill and reverse circulation holes. Computer studies have involved solid modeling, statistical and geostatistical analysis, and the interpolation of the copper, gold and cobalt grades according to copper cut-off grade and bench elevation.

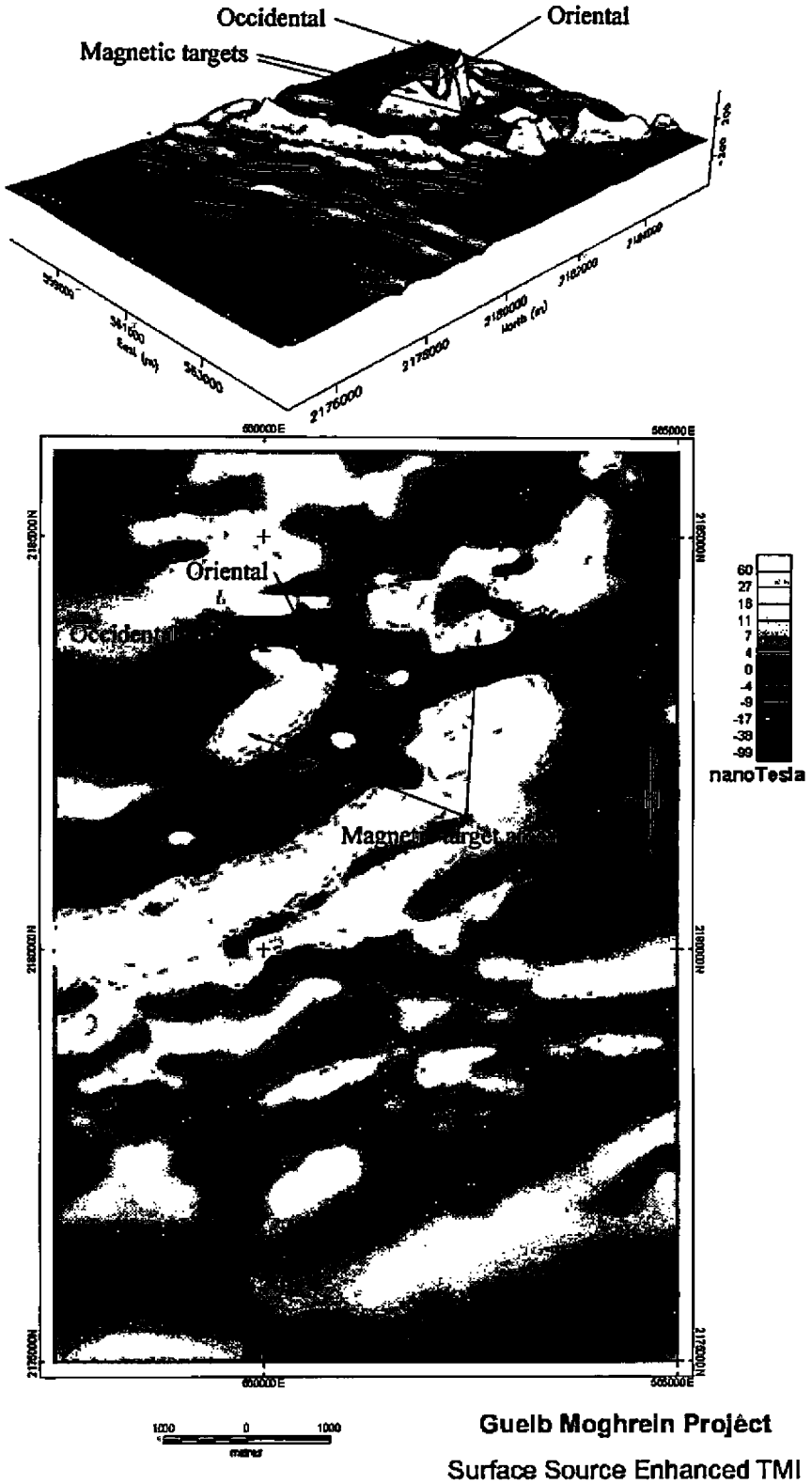
Using a 1% Cu cutoff the Total Resource (including Measured and Indicated) for the Guelb Moghrein Deposit has been independently calculated as 23.6 Mt @ 1.88 % Cu, 1.41 g/t Au and 143 ppm Co. (Kilborn SNC-Lavalin Europe. 1997).

A polygonal resource estimate by GGISA in 1999 using a 0.5 % Cu cutoff and incorporating the existing oxide stockpiles and the Guelb Moghrein Oriental mineralisation, resulted in a Total Resource (including Measured and Indicated) of 32.3 Mt @ 1.61 % Cu, and 1.36 g/t Au.

El Khader

The El Khader prospect (Figure 7) is situated in a hilly dissected area known as Legleitat el Khader. The domal structural setting is formed by the intersection of a moderate, slightly north-verging, arcuate, northeast-southwest asymmetric antiform with a gentle north-northwest trending antiform. The doming is a part of the later folding that warps an extremely complex system of early, stacked thrust sheets.

The southern side of the dome consists of quartz-muscovite-chlorite schists representing meta-siltstone and meta-greywackes of the Irarchene el Hamra Formation. Overlying BIFs and tuffaceous siltstone of the Atomai Formation form a north dipping range on the northern side. The core of the dome is complex and outcrop is partially obscured by supergene ironstone rubble. Meta-dolerite is the most common rock type exposed in the deeper gullies on the south side, but the eastern side of the core is formed from quartz-sericite altered felsic volcaniclastic rocks, interpreted as part of the Sainte Barbe Volcanics. Similar rocks occur as infolds and enclaves within the meta-dolerite. Reverse circulation drilling to shallow depth at various points on the dome encountered interlayered felsic volcaniclastics and 'amphibolites'. A thrust plane is interpreted to separate the core of the dome from the rim in order to explain the disordered stratigraphic succession.



Guelb Moghrein Project

Surface Source Enhanced TMI

Figure 6

The El Khader vein system has not been studied in detail as a coherent system. Mapping has been carried out as part of regional programme and a few selected examples of country rock and hydrothermal alteration have been examined petrographically. Exploration to evaluate the iron ore resource in the supergene cap was carried out by MICUMA in 1958 and resulted in the delineation of a resource of 18 Mt of iron ore grading 51% Fe.

Essentially El Khader consists of an extensive Fe-Mg-Ca carbonate vein system or stockwork, up to 2 km across at the surface, in which the veins of coarsely crystalline brown Fe-rich carbonate thicken and coalesce towards the top. This top is generally represented by a massive supergene goethite cap in which the rock type definition is blurred. Gullies on the southeast side of the vein system cut into its roots where the carbonate veins narrow downwards and become widely spaced in altered meta-dolerite country rock. Reconnaissance petrography has revealed a complex suite of alteration phases in this part of the system. Meta-dolerites are commonly rich in alteration plagioclase ranging from almost pure andesine rock with interstitial

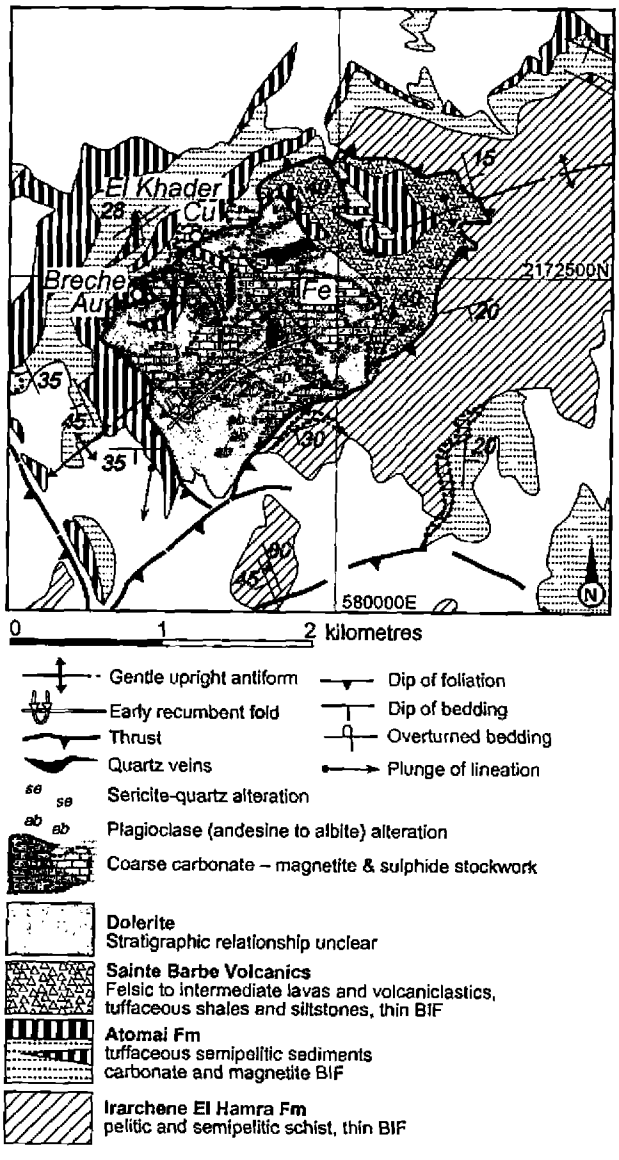


Figure 7 GEOLOGICAL OUTCROP MAP OF EL KHADER
based on field traverses and air photo interpretation

magnetite close to the carbonate vein margins to more disseminated albitic plagioclase further away. Plagioclase also occurs as quartz-albite veinlets. These plagioclase-altered rocks were previously interpreted as 'oligoclasite' or 'albitophyre' intrusives (eg. Marcelin, 1968). Other samples reveal strong sericite and chlorite alteration and there is evidence of a sericite event that post-dated the plagioclase. Meta-felsic volcaniclastic rocks, to the northeast, and in enclaves within the dolerite, are generally quartz-sericite altered and there are localised zones of strong silicification and quartz veining (Figure 7). The top of the carbonate vein system corresponds approximately to the interpreted thrust though it appears to slightly transgress, and therefore post date this structure.

The El Khader supergene copper occurrence is in the oxidised capping to the upper part of the carbonate vein system and consists of malachite staining in the weathered, veined country rocks and goethitic cap. Minor gold has been recorded at the Breche prospect, a quartz-rich breccia developed as a late, cross-cutting phase towards the northwest of El Khader. Drilling of the El Khader prospect has encountered only patchy, low grade supergene copper values in the 0.1-0.3% range, accompanied by anomalous barium and arsenic. More recently the gold and copper potential of the upper, northern rim of the system was investigated by Normandy La Source with a programme of reverse circulation drilling, however no primary mineralisation was encountered. The results of the drilling suggest that, despite the impressive scale of this vein and alteration system, there is little potential for the discovery of a significant Cu, Au resource in close proximity to the surface.

The carbonate vein system at El Khader is interpreted as belonging to a later stage in the tectonic evolution than at Guelb Moghrein. El Khader's brittle fracture event is considered a later event than the ductile shear setting of Guelb Moghrein. Localisation of the veining in a dome structure, and the upward intensification of the veining, suggest that the principal control may be extension across the crest of the dome. No evidence of contemporaneous igneous intrusion has been encountered and the meta-dolerites are believed to belong to an earlier, pre-thrusting event.

Other Deposits

There are a number of smaller occurrences of copper mineralisation in the Akjoujt area with or without iron oxide or gold. The Masse and El Joul groups of deposits close to Akjoujt (Figure 2) are similar to Guelb Moghrein, consisting of numerous pods of coarse-grained ferromagnesian carbonate with magnetite, and copper sulphides. They are crudely concordant to, and hosted by, intensely sheared metavolcanic and metasedimentary rocks showing multiple thrust repetition, and the larger occurrences in the two groups are localised on antiformal refold structures.

The historic Sainte Barbe workings 25 km northeast of Akjoujt (Figure 2) are of oxide copper hosted by quartz-

ankerite stockworks in discordant carbonate bodies hosted by chloritised mafic and felsic flows and volcaniclastics of the Sainte Barbe Volcanics. The mineralisation is located 100-200 metres above the regional sole thrust which rests on Archaean basement and thin cover sediments.

At Tabrinkout, 30 km east of Akjoujt (Figure 2), schistose mafic to felsic volcanics are the hosts to an extensive zone of complex carbonate stockworks, which is broadly controlled by a strong, late-stage north-south fracture. The irregularly distributed lenses of coarse-grained ferromagnesian carbonate are intercalated with narrow quartz veins and contain tungsten mineralisation in the form of wolfram, scheelite and tungstite. Secondary copper in the form of malachite, chalcocite and covellite accompany the tungsten within the quartz veins. Minor bismuthinite and native gold are found at the quartz-carbonate contacts.

Discussion

All of the iron, copper and gold occurrences at Akjoujt and within the broader Inchiri area, feature coarse-grained carbonate as a host. Carbonate is also a pervasive mineral phase in the country rocks as iron carbonate in BIF and as alteration carbonate in a wide variety of rock types. A detailed study of the carbonate has so far been limited to petrographic and mineragraphic work. No oxygen, carbon or indeed sulphur isotope studies have been conducted on the hosts or ores and therefore this discussion lacks the critical analysis such data could provide. Mapping has revealed very little bedded carbonate sediment in the supracrustal sequence, other than iron carbonate in BIF. It is deduced that the carbonate either entered the system at the volcanic-hydrothermal or sea floor alteration stage during the deposition of the BIF, or during tectonism, or perhaps in both periods. Given the abundance of carbonate, and the structurally-controlled settings of the coarse grained occurrences it is likely that the carbonate bodies evolved from within the system during tectonism.

Previously the Guelb Moghrein deposits were thought to be stratiform within a sedimentary carbonate sequence and confined to the nose of southerly plunging syncline (Pouclet et al., 1987). An alternative genetic model as a VHMS style deposit had earlier been proposed by Ba Gatta, (1982). The features of the deposit do not however match any known deposits of these types, and the folded carbonate sediment model of Pouclet et al. is not supported by drilling data (Figure 5). The host rocks are predominantly metabasic igneous rocks, which have been strongly altered along low angle, 10-30 degree thrusts or shears. It is postulated that extensive carbonate alteration has occurred along these zones of structural weakness, and the carbonate has acted as the favourable host for later mineralising fluids. The mineralisation is open at depth and presents a significant target for the discovery of satellite deposits of the Guelb Moghrein type.

There is no evidence of an igneous intrusive event that could have brought about the introduction of the mineralised carbonate bodies. However there is sporadic evidence of a thermal peak that post-dated early thrusting from the garnet, cummingtonite and biotite porphyroblasts that are scattered through the schistose margins of many of the smaller carbonate-magnetite bodies to the southwest of Guelb Moghrein. These porphyroblasts in turn have suffered subsequent partial retrogression to phases such as chlorite, so the thermal history is complex and as yet poorly understood. The domal setting and strong plagioclase and sericite alteration in the deeper exposures at El Khader is suggestive of an intrusive body at depth, but apart from the altered host meta-dolerite, no intrusive rocks have been identified.

The alteration style of the country rocks to the various bodies is quite variable. At Guelb Moghrein the presence of tremolite and biotite in the schistose envelope rocks points to minor magnesium and potassium metasomatism but the effect does not appear to extend very far into the amphibolite country rocks. In contrast, El Khader features strong albite to andesine alteration of the rocks in the roots of the carbonate vein system, and widespread but patchy sericite and chlorite. The sodium, calcium and potassium alteration at El Khader is more typical of the iron-oxide, copper gold class described in (Porter, 2000) but that alteration style is by no means a universal feature of the deposits described therein.

The variation in style of the carbonate bodies of the Akjoujt area is consistent with their development at different times during the tectonic history. The character of the Guelb Moghrein mineralisation is compatible with emplacement during an early thrusting. The asymmetry of the obliquely-bevelled western edge featured in Figure 5 may be interpreted as a response to a second period of thrusting from the west. In contrast the style of El Khader is extensional and related to a late-stage doming event rather than to early compression. It is interpreted that the doming took place as an interference effect in the folding, above the decollement of the sole thrust. El Khader thus would have evolved when the supracrustals were in an allochthonous position above a 'cold', underthrust basement.

The occurrence and origin of the metallic phases and magnetite in the Akjoujt area is more problematic since their distribution is much more localised. Evidence from Guelb Moghrein suggests an introduction of at least the sulphides and gold at a later period than the host carbonate. The very weak copper and gold at El Khader seems to be concentrated at the top of the system, and is therefore related to the evolution of the system, but its very localised distribution suggests that it was also a late stage event.

Although the Akjoujt supracrustal sequence evolved in a rifted continental setting and features strong compression and shortening, it lacks the other two key elements of Hitzman's model (Hitzman, 2000), the evaporites and later magmatism. The formation of the carbonate bodies by remobilisation or concentration of carbonate during tectonic processes seems to be the essential preparation process, and this would have involved recycling of basin fluids, although there is no evidence that magmatism played any

direct role in this. The introduction of the metallic components is assumed to be along the same structural channels that controlled the localisation of the carbonate but the source of the metals is unclear. The most likely origin is, like the carbonate, from within the pile, in this case from the abundant, leachable mafic volcanic rocks.

Literature research has yet to unearth any analogues to the Akjoujt deposits although a number of districts worldwide show some comparative features or processes. Regional metamorphism of sedimentary intervals of BIF, chert and marble has been invoked to explain the so-called 'skarn iron ores' of the Pajala District of northeast Sweden (Carlon, 2000). These consist of lenses rich in magnetite, with carbonate, actinolite, diopside, hornblende, chlorite and biotite. Some of them contain minor pyrite, pyrrhotite and chalcopyrite. Many iron-rich carbonate lenses in the Akjoujt area are within the BIF-rich part of the sequence, and porphyroblasts and segregations of coarse carbonate are common in some of the BIFs.

Carbonate is the principal host of the 1500 Mt Bayan Obo Fe-REE-Nb deposit in northern China (Smith & Chengyu, 2000). Here the setting is a major subduction boundary involving northwest to southeast thrusting of Proterozoic sequences during Caledonian and Hercynian times, a setting and timing comparable to the Mauritanides. The host carbonates show sedimentary features, while the O and C isotopic signatures are comparable to carbonatite, leading those authors to conclude that they were carbonate sediments modified by magmatic fluids. As at Akjoujt, no igneous intrusives were located in the vicinity of the Bayan Obo mineralisation.

Also comparable in overall orogenic setting and timing are the Bou Azzer deposits in the Anti Atlas of Morocco (Leblanc & Billaud, 1982). These consist of bodies of epigenetic cobalt arsenide mineralisation in quartz-carbonate gangue, with accessory nickel, copper and molybdenum. They are located in the tectonised contacts of Neoproterozoic ophiolitic serpentinite and its unconformable cover, in a complex orogenic belt of PanAfrican to Hercynian age like the Mauritanides, and possibly an extension of them. The difference in ore mineralogy to Guelb Moghrein may be more a function of host rocks than style or genesis, the copper and iron of the latter being related to the mafic host in contrast to the cobalt and nickel of the country rocks at Bou Azzer. The carbonate hosted, shear related, copper occurrences of the Selibabi-Mbout region such as at Kadiar, further south in the Mauritanides of Mauritania (Figure 1), may also have comparable paragenesis to those of the Akjoujt area.

A significant feature of the collection of papers in the AMF monograph (Porter, 2000) is the diversity of style and setting of the deposits in the hydrothermal Fe oxide, copper gold class. When an apparently unifying theme is discerned, conspicuous exceptions seem to emerge. For example the Olympic Dam (Reynolds, 2000) and Tennant Creek deposits (Skirrow, 2000) provide a major exception to the characteristic sodium and calcium alteration of the country rocks as seen in most other districts. In the Akjoujt area the El Khader system features moderately strong sodium, calcium and potassium alteration but the Guelb Moghrein system shows only moderate magnesium enrichment of the host envelope.

Descriptions of iron, copper gold mineral provinces like Tennant Creek, or the Curnamona and Cloncurry districts (Williams & Skirrow, 2000) reveal a diversity of style, setting and mineralogy even within one province. Hitzman (2000) discusses a variety of tectonic settings ranging from anorogenic magmatism to orogenic basin collapse. In the latter case, a rifted continental basin is subjected to compression and under plating, leading to a high heat flow and the formation of hydrothermal cells of basin fluids. Examples that were cited include the Cloncurry District of Australia and the Lufilian Orogen of Southern Africa. Key features of the model are the presence of evaporitic continental sediments as a source for brines, and also extensive magmatism driving the cells. Although the Akjoujt supracrustal sequence evolved in a rifted continental setting and features strong compression and shortening, it lacks the other two key elements.

In conclusion, the essential preparation process for the occurrence of the mineralised carbonate bodies in the Akjoujt region has been the remobilisation or concentration of carbonate during tectonism and involving the recycling of basin fluids. However there is no evidence that magmatism played any direct role in this process. The later introduction of the metallic components is assumed to have been along the same structural channels that controlled the localisation of carbonate but the source of the metal is unclear. The most likely origin of the metallic species is, like the carbonate, from within the pile, in this case from the abundant, leachable mafic volcanic rocks.

Further exploration and geological research is necessary at the Guelb Moghrein deposit and associated mineral occurrences to assist in the definition of this style of mineralisation as a carbonate rich sub class of the hydrothermal Fe-oxide copper-gold class of deposit. The ability to effectively target both the magnetic and conductive characteristics of the Guelb Moghrein mineralisation has encouraged the future exploration for extensions to the existing ore resources and satellite deposits. Research during this programme should help address the age, origin and occurrence of both the carbonate, magnetite and the metallic phases of this style of mineralisation.

Acknowledgments

The authors wish to thank GGISA and SAMIN for permission to publish this paper, and especially Mr. Cliff Harding, Managing Director of GGISA and Mr. Talal Al-Saadi, General Director of ARMICO and Vice Chairman of SAMIN for their encouragement and assistance. They also would like to express gratitude to numerous colleagues for their data contribution and constructive criticism during preparation, in particular Mr. Karsten Eden. The support of Dr. John Chappell was, as always crucial.

References

Ba Gatta, A., 1982 –Contribution à l'etude geologique et mineralogique du giesment d'Akjoujt, Mauritanie. *These de Geologie, Univ Orleans.*

Carlon, C.J., 2000 - Iron Oxide systems and base metal mineralisation northern Sweden; in Porter, T.M. (Ed.), Hydrothermal Iron Oxide Copper-Gold & Related Deposits: A Global Perspective, *Australian Mineral Foundation*, Adelaide, 283-296.

Dockery, B.A., 2000 - Report on Interpretation of Airborne Magnetometer Data, Guelb Moghrein Prospect, Mauritania. *B.A. Dockery & Associates Pty Ltd. Perth, Australia.* Unpublished report.

Emerson, D., 1998 - Core Physical Properties Tests, *Systems Exploration (NSW) Pty Limited.* Unpublished report.

Evans, J.H., 1978 - A Brief Guide to the Copper Mineral Property at Akjoujt, Islamic Republic of Mauritania. *Societe Nationale Industrielle Et Miniere – Societe D'Economie Mixte.* Unpublished report.

Giraudon, R., 1964 - La serie d'Akjoujt et le mine de cuivre de Guelb Moghrein. *Rapport Bureau de Recherches Geologiques et Minieres*, Dakar 64-B.

Giraudon, R., Sougy, J., 1963 - Position anormale du socle granitiquedes Hajar Dekhen sur la Serie de Akjoujt et participation de ce socle l'edification des Mauritanides hercyniennes. *C.R. Academie Science*, France, 258, 937-940.

Henley, K.J., 1995 - Mineralogical Analysis of Samples from Akjoujt, Mauritania. *AMDEL Limited*, Thebarton, South Australia. Unpublished report G877500G/95

Hitzman, M.W., 2000 - Iron oxide-Cu-Au deposits: what, where, when and why; in Porter, T.M. (Ed.), Hydrothermal Iron Oxide Copper-Gold & Related Deposits: A Global Perspective, *Australian Mineral Foundation*, Adelaide, 9-25.

Isley, A.E., Dallas, H., 1999 - Plume-related mafic volcanism and the deposition of banded iron formation. *Journal of Geophysical Research*, Vol. 104, No. 87, 15461-15477.

Kilborn SNC-Lavalin Europe,. 1997- Guelb Moghrein Feasibility Study. Volume 2. Project Description, *Mineral Resources and Mining.* Unpublished report

Leblanc, M., Billaud, P., 1982 - Cobalt arsenide orebodies related to an Upper Proterozoic ophiolite: Bou Azzer (Morocco). *Economic Geology* Vol 77 pp162-175

Lecorche, J.P., Dallmeyer, R.D., Villeneuve, M., 1989 - Definition of Tectonostratigraphic Terranes in the Mauritainide, Bassaride, and Rokelide orogens, West Africa. *Geological Society of America Special Paper 230.*

Lottermoser, B.G., Ashley, P.M., 2000 - Geochemistry, petrologyand origin of Neoproterozoic ironstones in the eastern part of the Adelaide Geosyncline, South Australia. *Precambrian Research 101*, 49-67.

Marcelin, J., 1968 - Carte Geologique de la Region d'Akjoujt. *Bureau de Recherches Geologiques et Minieres.* Scale 1:200,000

Martyn, J., 1998 - Preliminary Report to Accompany 1:50,000 Geology Map of Inchiri Area. *General Gold International SA.* Unpublished Report.

Martyn, J., Strickland, C., 2001 - A Reappraisal of the Stratigraphy, Structure and Mineralisation of the Akjoujt Area, Islamic Republic of Mauritania. In Press.

Michaud, J.G., 1963 - Carte Geologique de la Region d'Akjoujt de puis le Guelb Moghrein jusqu'a Legletat el Khader et desmassifs d'Irarchene et d'Araguibe. *Bureau de Recherches Geologiqueset Minieres*, Scale 1:50,000.

Porter, T.M., 2000 - Hydrothermal Iron Oxide Copper-Gold & Related Deposits. A Global Perspective. *Australian Mineral Foundation, Adelaide, Australia.*

Pouclet, A,. Guillot, P,. Ba Gatta, A., 1987 - Nouvelles donnees lithostructurales, petrographiques, mineralogiques et geochimiques sur le gisement de cuivre d'Akjoujt et son environnement geologique (Republique Islamique de Mauritanie). *Journal of African earth Science. Vol.6, No.1, 29-43.*

Ramdohr, H., Blanchot, A., Servant, J., 1956 - Recherches Microscopiques sur les Minerais du Gisement de Guelb Moghrein Akjoujt (Mauritanie). *Extrait du Bulletin de la Direction Federale des Mines et de la Geologie. No 20.*

Reynolds, L.J., 2000 - Geology of the Olympic Dam Cu-U-Au-Ag-REE deposit; in Porter, T.M. (Ed.), Hydrothermal Iron Oxide Copper-Gold & Related Deposits: A Global Perspective, *Australian Mineral Foundation*, Adelaide, 93-104.

Saif, S.I., 1980. - Petrographic and geochemical investigation of iron formation and other iron-rich rocks in Bathurst district, New Brunswick: *Geological Survey of Canada Paper* 80-1A, 309-317.

Skirrow, R.G., 2000 - Gold-copper-bismuth deposits of the Tennant Creek District, Australia: A reappraisal of diverse high grade systems; in Porter, T.M. (Ed.), Hydrothermal Iron Oxide Copper-Gold & Related Deposits: A Global Perspective, *Australian Mineral Foundation*, Adelaide, 149-160.

Snowden and Associates Pty Ltd. 1995. - SAMIN-GGI Joint Venture Guelb Moghrein Copper Project. Resource Estimation Update May 1995. Unpublished report.

Smith, M,. Chengyu, W., 2000 - The geology and genesis of the Bayan Obo Fe-REE-Nb deposit: A review; in Porter, T.M. (Ed.), Hydrothermal Iron Oxide Copper-Gold & Related Deposits: A Global Perspective, *Australian Mineral Foundation*, Adelaide, 271-281.

Strickland, C.D., 1999 - Gold Exploration in Mauritania, *Australian Journal of Mining*, August 1999

Watts, Griffs and McOuat Limited, Canadian Bechel Limited., 1963 - Review and Evaluation of Akjoujt Copper-Gold Deposits for Northfield Mines Inc. Unpublished report.

Williams, P.J., 1999 - Fe-oxide-Cu-Au Deposits of the Olympic Dam/Ernest Henry-Type. In short course Proceedings 'New Developments in the Geological Understanding of some Major ore Types and Environments, with Implications for Exploration'. *Prospectors and Developers Association of Canada.*

Williams, P.J., Skirrow, R.G., 2000 - Overview of iron oxide-copper-gold deposits in the Curnamona Province and Cloncurry District (Eastern Mount Isa Block), Australia; in Porter, T.M. (Ed.), Hydrothermal Iron Oxide Copper-Gold & Related Deposits: A Global Perspective, *Australian Mineral Foundation*, Adelaide, 105-122.

Wright, J.B., 1985 - Geology and Mineral Resources of West Africa. Department of Earth Sciences, *The Open University.*

Urban, H., Stribmy, B., Lippolt, H.J., 1992 - Iron and manganese deposits of the Urucum district, Matto Grosso do Sul, Brazil. *Economic Geology* Vol. 87, 1375-1392.

PGC
PUBLISHING

McLean, R.N., 2001 - The Sin Quyen Iron Oxide-Copper-Gold-Rare Earth Oxide Mineralisation of North Vietnam; *in* Porter, T.M. (Ed.), Hydrothermal Iron Oxide Copper-Gold and Related Deposits: A Global Perspective, Volume 2; *PGC Publishing*, Adelaide, pp 293-301.

THE SIN QUYEN IRON OXIDE-COPPER-GOLD-RARE EARTH OXIDE MINERALISATION OF NORTH VIETNAM

Robert N. McLean

AQ Geological Consultants, Hanoi, Vietnam

Abstract - The Sin Quyen deposit in northern Vietnam is an unusual example of the Fe oxide-Cu-Au-REE group of deposits. Magnetite-orthite-chalcopyrite-gold mineralisation is hosted by extremely altered amphibolite and biotite-gneiss lenses within highly deformed and metamorphosed sediments of the Proterozoic Sin Quyen Formation. The deposit formed in a wide fault zone which acted as a channel for pre-mineralisation amphibolite and granitic dykes, mineralising fluids as well as post mineralisation granite, pegmatite and amphibolite. Metasomatic alteration produced a variety of assemblages predominantly composed of variable amounts of quartz, hastingsite and biotite but also including small zones of hedenbergite-garnet skarn. Alteration is closely associated with magnetite and orthite (allanite) development. Sulphide mineralisation, mainly chalcopyrite and pyrrhotite with lesser pyrite is a later and lower temperature hydrothermal phase, although the majority of the sulphides were deposited within the alteration zones.

Introduction

The Sin Quyen deposit is the largest of a number of zones of chalcopyrite-gold-orthite-magnetite and magnetite only mineralisation in the Bat Xat area of Lao Cai Province in northwestern Vietnam. It is situated approximately 300 km northwest of Hanoi and 1 km from the bank of the Red River which marks the boundary between Vietnam and China in this area. The deposit was discovered in 1961 when a number of radio-metric anomalies including one at Sin Quyen were investigated. Trenching revealed copper mineralisation beneath shallow soil cover.

An extensive exploration program was conducted, including 146 diamond drill holes (41 957 m) and over 7 km of underground development. Fortunately the results of this work, along with petrological, metallurgical, geophysical and ore reserve studies were compiled in great detail in 1975 as an unpublished report by Ta Viet Dung *et al.*; "The Geological Report on Detailed Exploration of the Sin Quyen Copper Deposit". A concurrent regional exploration program (mapping, soil geochemistry, radiometrics and ground magnetics) was conducted on 250 m spaced lines over 50 km of prospective strike. Anomalies were followed up with trenching and drilling. This work was curtailed by the Chinese invasion of Vietnam in 1979 during which 39 scientists and technicians working on site were killed. All drill core and equipment plus much data was lost. In addition, all adits and underground access to the Sin Quyen deposit were destroyed or damaged prior to the Chinese withdrawal three months later.

By early 1993 the tension along the border had subsided and two Australian companies (Northstar Resources NL and Auridiam Consolidated NL) were granted an Exploration Licence over the area. The companies drilled 19 holes designed to twin previous drilling and carried out metallurgical and feasibility studies. The drilling substantiated the previous results with respect to copper. A measured resource of 52.8 million tonnes (Mt) @ 0.91% Cu was determined using both sets of drill data at a 0.5% Cu cutoff. Inferred grades of 0.44 g/t gold, 5.4% magnetite and 0.70% combined Ce, La, Pr and Nd were calculated for this resource. Magnetite and orthite also occur in significant quantities outside the defined copper resource. Due to falling copper prices and pressure from authorities to include copper metal production in the development plans, the Australian companies withdrew from the project. Currently a high-grade near-surface section of the deposit is being mined by a Vietnamese state company. Copper-gold concentrate is shipped to Yunnan Province in China and magnetite is sold into the domestic market.

As the underground workings and previous drill core are no longer accessible and the author has only viewed core from 19 drill holes all textural, mineralogical and petrological observations of the deposit are from Ta Viet Dung *et al.*, 1975 unless otherwise attributed.

Tectonic Setting

Sin Quyen is situated adjacent to the Red River Fault Zone on the northeastern margin of the Da River Mobile Belt which separates the South China and Indochina tectonic plates in northern Vietnam (see Fig. 1). The mobile belt has a complex history of accretion, folding, subduction, rifting, and magmatism. A second inter-plate boundary marked by the Dien Bien Phu Fault truncates the mobile belt to the northwest. This zone is a strike extension of the Pak Lay fold belt in Laos which formed by the late Jurassic collision of the Shan Thai and Indochina blocks (Stokes *et al.*, 1995). It has subsequently acted as dextral strike slip fault and is currently active. All northwest trending structures within northern Vietnam were re-activated as sinistral strike slip faults in the Cenozoic due to Himalayan tectonics which led to the "extrusion" of Indochina along these faults.

Most workers (eg., Tran Van Tri, 1979) regard the Cambrian-Devonian Ma River Terrane on the southern margin of the mobile belt as the boundary between the South China and Indochina plates. This is a belt of greenschist facies oceanic sediments and volcanics (calc-alkaline to mafic) characterised by ophiolites along the Ma River Fault plus large scale folding, thrusting and nappe formation indicating continent-continent collision in the early-middle Carboniferous (Metcalfe, 1995).

The Da River rift zone developed during the Permian-Triassic and comprises a variety of marine volcanics and associated marine sedimentary sequences which formed in an extensional basin on continental crust (Le Dzuy Bach and Ngo Gia Thang, 1995). Volcanics include spilites, tholeiitic to calc-alkaline porphyritic basalt and komatiites (Poliakov *et al.*, 1991). The rift closed during the Jurassic as indicated by folding, thrusting and red-bed formation. Magmatism recommenced with Cretaceous and Miocene volcanics in the Tule Rift.

A ductile shear belt between the Red River and Chay River Faults, which developed in Proterozoic metamorphic basement rocks marks the northeast margin of the mobile belt. The basement comprises a variety of gneiss and schists derived from mafic volcanics and associated volcano-sedimentary rocks that have been metamorphosed to amphibolite facies. There is widespread development of migmatites and evidence of multiple deformation. The major regional metamorphic and deformation event has been dated at between 1960 and 2360 Ma (Tran Ngoc Nam, 2001). Strata to the southwest of the Red River Fault is intruded by a variety of younger magmatic complexes and was uplifted in the Tertiary forming the Hoang Lien Son mountain range.

Stratigraphy

The Sin Quyen deposit is situated within highly deformed amphibolite grade migmatised gneiss and schist of the Proterozoic Sin Quyen Formation. The formation is approximately 800 m thick, strikes between 280 and 320° and is steeply dipping, generally to the northeast. It is divided into upper and lower units; the lower unit predominantly graphitic schist and the upper predominantly gneiss. It is underlain conformably by Proterozoic meta-sediments of the Lung Po Formation (Bui Phu My, 1978). The Upper Sin Quyen Formation is in fault

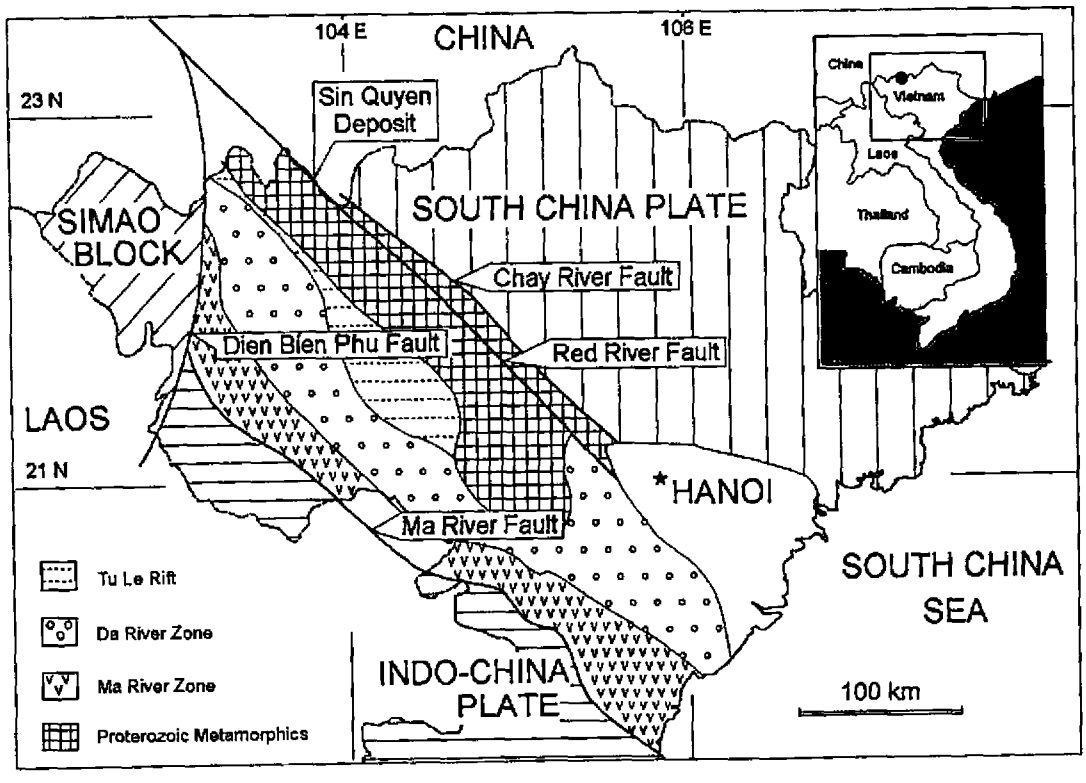


Figure 1: Location and setting of the Sin Quyen deposit.

contact with Cambrian sediments of the Cam Duong Formation at the surface and limestone and marble of the upper Proterozoic / lower Cambrian Sa Pa Suite at depth. The Cam Duong Formation hosts significant sedimentary apatite deposits some 40 km to the southeast of Sin Quyen.

The Lower Sin Quyen Formation is predominantly a quartz (50%), graphite (15%), muscovite (12%), biotite (10%) schist, with minor plagioclase, tourmaline, garnet and sillimanite. It contains bands of plagioclase (42%), quartz (24%), biotite (18%), graphite (15%) gneiss with traces of apatite. Graphite is variably distributed, locally reaching 20%. The sequence is intruded by pegmatites.

Gneiss of the Upper Sin Quyen Formation comprises plagioclase (61%), quartz (21%) and biotite (15%) with accessory apatite, sphene, calcite and garnet. Bands of schist within the gneiss consist of quartz (67%), muscovite (14%) and biotite (15%) with minor garnet, sphene, chlorite and tourmaline. The gneiss is host to extensive intrusions of "granito-gneiss", granite, pegmatite, amphibolite and the great majority of Sin Quyen alteration and mineralisation. Apart from rare isolated patches, graphite is absent from the Upper Sin Quyen Formation.

Intrusives

The Sin Quyen Formation and particularly the mineralised zone is host to a variety of crosscutting but sub-conformable intrusions. These have been sub-divided into Proterozoic and Permian suites based on their petrological similarity to other intrusions in the region and their presence or absence in overlying Palaeozoic strata.

Proterozoic

The older intrusive suite of Proterozoic age comprises both amphibolites and granitic gneisses. The amphibolites represent the earliest intrusive phase, occurring as small (5-50 by 10-100 metre) bodies with variable geometries, although generally lensoidal both in strike and dip directions, with a well defined foliation, and often a banded texture. They are composed of hornblende (66%), plagioclase (19%) and biotite (6%) with minor sphene, epidote, apatite, chlorite and calcite. Plagioclase is commonly sericitised, while hornblende has tremolite, calcite, epidote and biotite alteration on its rims. Amphibolites are intimately associated with mineralisation, particularly where they are locally intensely altered. These altered amphibolite intervals host approximately 70% of the mineralisation and all of the higher grade zones.

The term "granito-gneiss" was applied to highly deformed and migmatised granitic intrusives which occur as dykes and lenses from 2 to 200 by 10 to 300 m in extent, that contain enclaves of amphibolite and biotite gneiss and are invariably found adjacent to mineralised zones. They comprise plagioclase (66%), quartz (26%), and biotite (7%) with lesser microcline, muscovite, sphene, chlorite and calcite, occurring as banded migmatites and augen gneisses, overprinted by cataclastic and mylonitic fabrics.

Permian

The younger intrusions have been grouped together and tentatively assigned a Permian age, based on the interpretation that the most voluminous member of the suite, a plagio-granite, is a co-magmatic equivalent of the Permian Dien Bien Phu Complex. The plagio-granite occurs as small lensoid bodies (1 to 20 m thick by 10 to 300 m long) which cut both the upper Proterozoic to lower Cambrian Sa Pa Suite rocks and Proterozoic intrusions, intrude along faults, and are common within the mineralised zone. They are composed of plagioclase (63%), quartz (26%) and biotite (6%) with minor microcline, muscovite, apatite and chlorite, and have an idiomorphic texture. Ta Viet Dung *et al.*, 1975 observed that these intrusives were mineralised and pre-dated sulphide development. They noted that elsewhere in the region, magnetite mineralisation only contained significant sulphides when these intrusives were present and thus they were interpreted to be genetically linked to the introduction of copper. The author however, logged these same intrusives as being post mineralisation as they intrude and separate zones of mineralisation (including sulphide accumulations) but are themselves barren apart from minor sulphides remobilised into fractures adjacent to their margins.

Un-mineralised plagioclase-quartz pegmatite bodies are associated with the plagio-granite and intrude amphibolite, granito-gneiss and biotite gneiss. Gabbro-dolerite is a minor phase occurring within the Sin Quyen fault, along the contact with the Sa Pa Suite. It comprises amphibole (64%), plagioclase (18%), biotite (7%), chlorite (5%), and calcite (3%) along with pyroxene and rare disseminated pyrrhotite, pyrite and chalcopyrite. Idiomorphic textures are evident and it is only weakly foliated.

Structure

The structural history of the region is complex and poorly understood. The stratigraphy is cut by a number of regional dislocations, including the Sin Quyen, Pin Ngan Chai and Thung Sang faults (see Fig. 2), all of which are parallel to, and interpreted to be splays of the major Red River Fault. Mineralisation in the area is concentrated adjacent to these structures and at Sin Quyen was deposited in extensive fault zones adjacent to the Sin Quyen reverse fault which is parallel to, and northeast of the main ore deposit. Ta Viet Dung *et al.* (1975) described the Sin Quyen fault as being a 50 m wide zone characterised by rocks which are "crushed, folded and sheared".

Mineralisation occurs as a series of anastomosing lenses enclosed within an elongate northwest trending zone which dips steeply and plunges shallowly to the southeast. This zone varies from 100 to 200 m in width, is approximately 2.5 km long and is usually less than 500 m in vertical extent. In cross-section, individual lenses generally dip at a high angle to the northeast, but are stacked in a steeply southwest dipping zone (see Fig. 3). In plan the main mineralised zone defines a weak "S" shaped flexure with the best grades being localised in the middle arm.

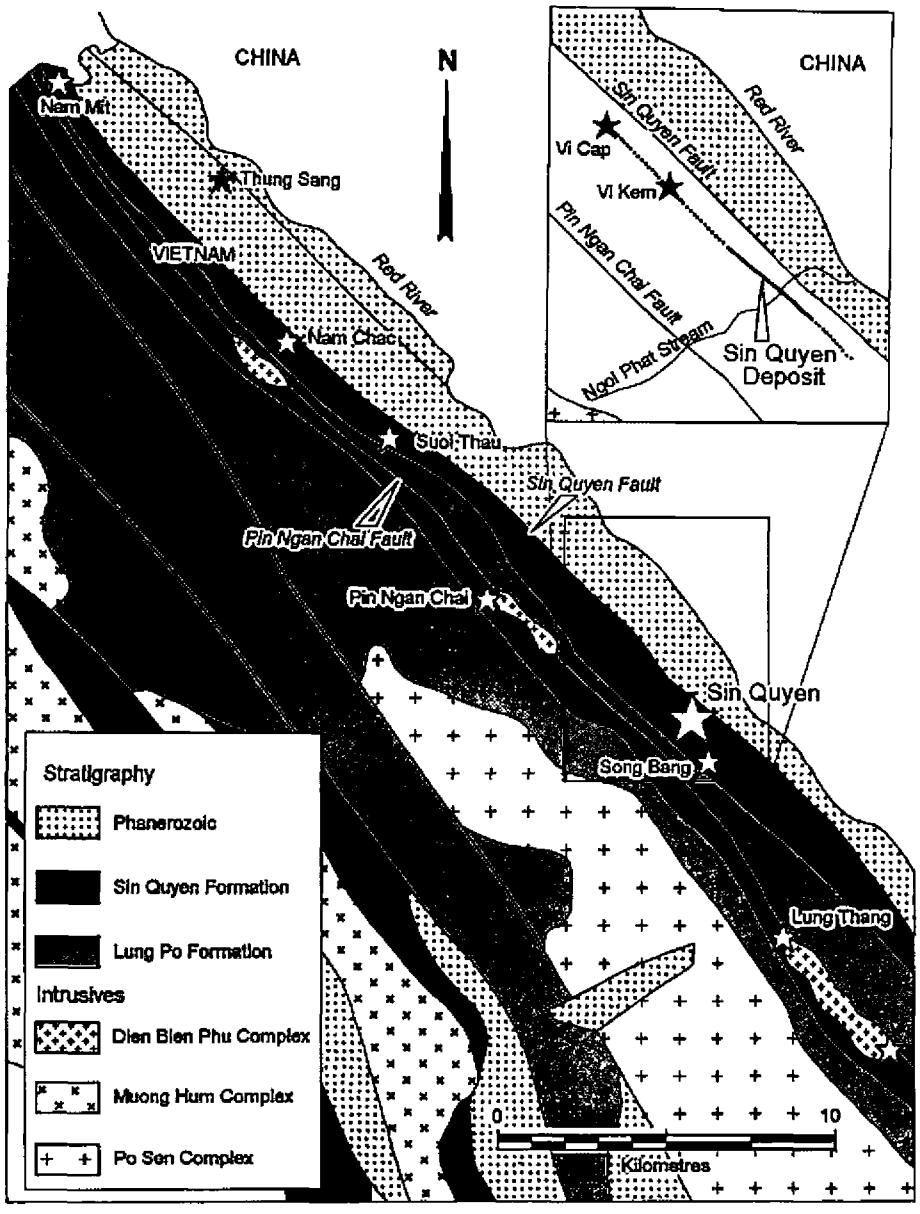


Figure 2: *Geological map of the area surrounding the Sin Quyen deposit.*

This main zone of mineralisation coincides with one of four steeply dipping northwest trending, discontinuous "broken zones" developed within banded quartz-feldspar gneisses. These four zones are thought to represent splays of the Sin Quyen Fault. They are intensely deformed, enclosing rocks that have been strongly fractured and dislocated, characterised by clay matrix breccias, and by minerals with slickensided faces which have been severely crushed and shattered. The largest of these zones hosts the main orebody, while a second contains adjacent low grade mineralisation (see Fig. 3). The other two, including the Sin Quyen fault to the northeast and a fourth zone to the southwest are barren or only weakly and sporadically mineralised. The majority of individual structures within these four zones are sub-parallel.

A second fault or fracture set strikes northeast at between 30 and 40° and is near vertical. This set is well developed regionally and controls the secondary drainage, including a stream, which transects the Sin Quyen deposit. These structures do not however displace stratigraphy and mineralisation to any significant extent.

In outcrop, rocks of the Sin Quyen Formation are strongly deformed with flat-lying mineral stretching lineations, mylonitic fabrics, and asymmetrical tails on feldspars indicating sinistral shearing. The best mineralisation is developed within a weak "S shaped" flexure consistent with a dilational jog related to sinistral movement. Similarly the geometry of individual lenses, which are stacked in an en echelon pattern within the fault zones indicates a strong structural control on the emplacement of amphibolite, granito-gneiss, metasomatic alteration zones and magnetite-orthite mineralisation. Sulphide mineralisation however, appears to be post deformation.

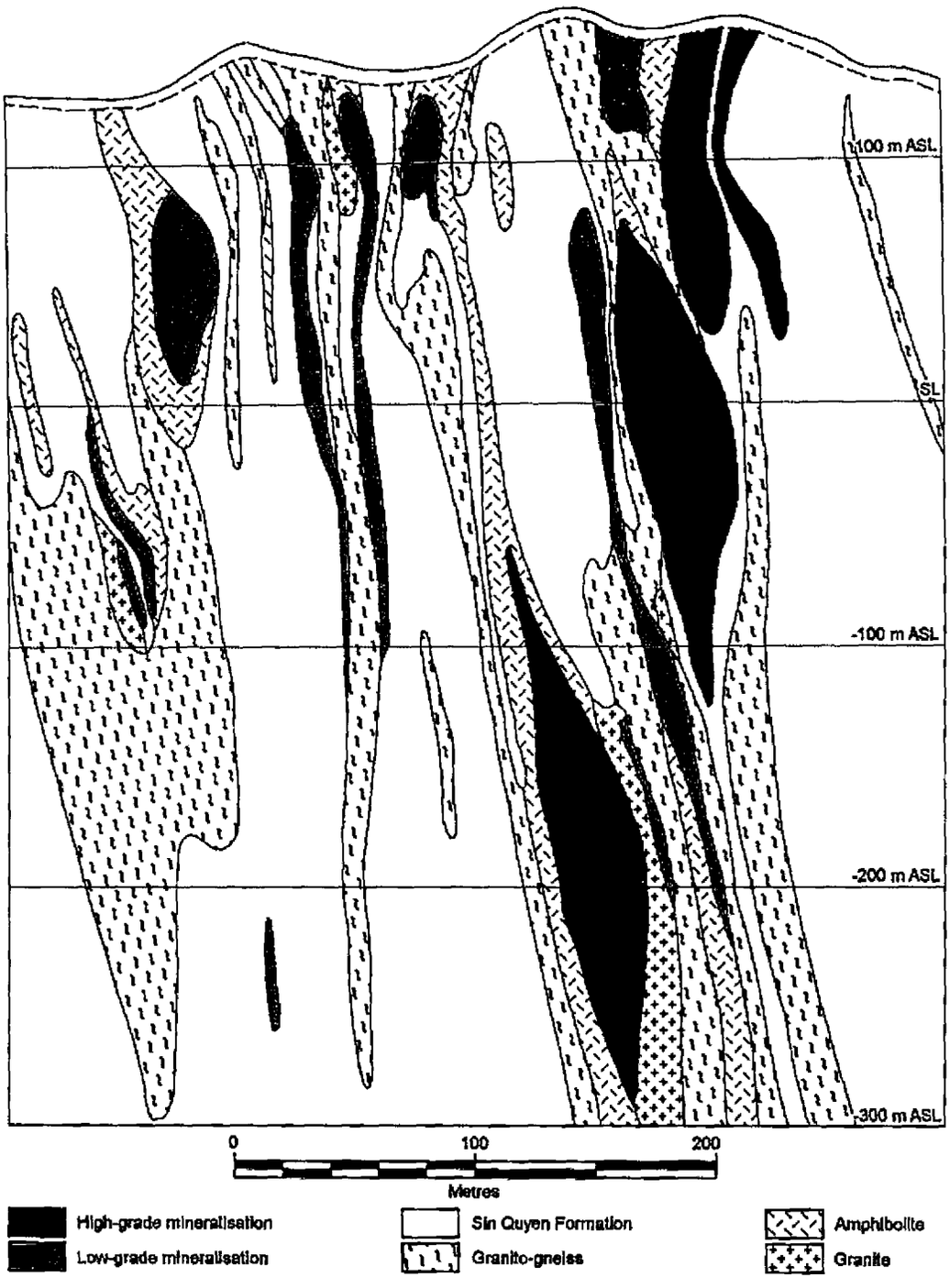


Figure 3: Generalised cross section through the Sin Quyen deposit.

Alteration

The deposit is characterised by early widespread Na alteration (albitisation), followed by the more localised and intense Fe-K phase seen in many other deposits of this type. At Sin Quyen, Fe-K metasomatism completely altered amphibolite and biotite-gneiss such that the resultant rocks were termed "metasomatites". These rocks host almost all of the magnetite and orthite mineralisation and the bulk of the sulphides. They may extend beyond the zones of sulphide mineralisation, both along strike and down dip, and in places are barren or only contain weak developments of magnetite and orthite. The alteration paragenesis is summarised in Table 1.

The metasomatites are predominantly a hastingsite-biotite-quartz rock which replaces amphibolite and adjacent biotite gneiss to form lenses up to 100 m thick and 1000 m in length. Their average composition is 27% hastingsite, 27% biotite, 13% quartz, 10% plagioclase and 7% orthite, with accessory apatite, calcite, chlorite and epidote. Ore (mainly magnetite with lesser sulphides) on average, comprises 14% of this rock type. Mineral contents vary greatly with maximum contents of 60% hastingsite, 70% biotite, 25% quartz and 85% orthite. Magnetite often occurs as massive mono-minerallic bands.

In places the alteration is skarn-like comprising 35% hedenbergite, 27% hessonite-grossularite garnet, 5% idocrase, 10% orthite, 7% calcite, 5% epidote 5% quartz and 3% amphibole with minor apatite and sphene. This rock type is not common and is irregularly distributed. It generally occurs as small zones within large metasomatite bodies and is transitional with other types of metasomatite. Apart from orthite, the skarn alteration tends to be poorly mineralised with only minor magnetite and sulphides (mainly pyrrhotite).

The transition from amphibolite to metasomatite is generally sharp and characterised by green biotite replacing brown biotite, and biotite or biotite-hastingsite rich zones developing in conjunction with an increasing quartz content, leading to variable hastingsite-biotite-quartz rock. The transition is more gradational in gneiss where biotite rich bands of gneiss grade into biotite rich metasomatite. The metasomatite is strongly foliated and commonly has a banded texture.

Mineralisation

Mineralisation occurred in two distinct phases. Orthite, magnetite, uraninite and other minor oxides formed during the metasomatic alteration phase and thus their spatial distribution is closely related to the metasomatite. Sulphides and gold were deposited by a later hydrothermal stage, mainly in metasomatite, but also in schist, biotite gneiss and amphibolite.

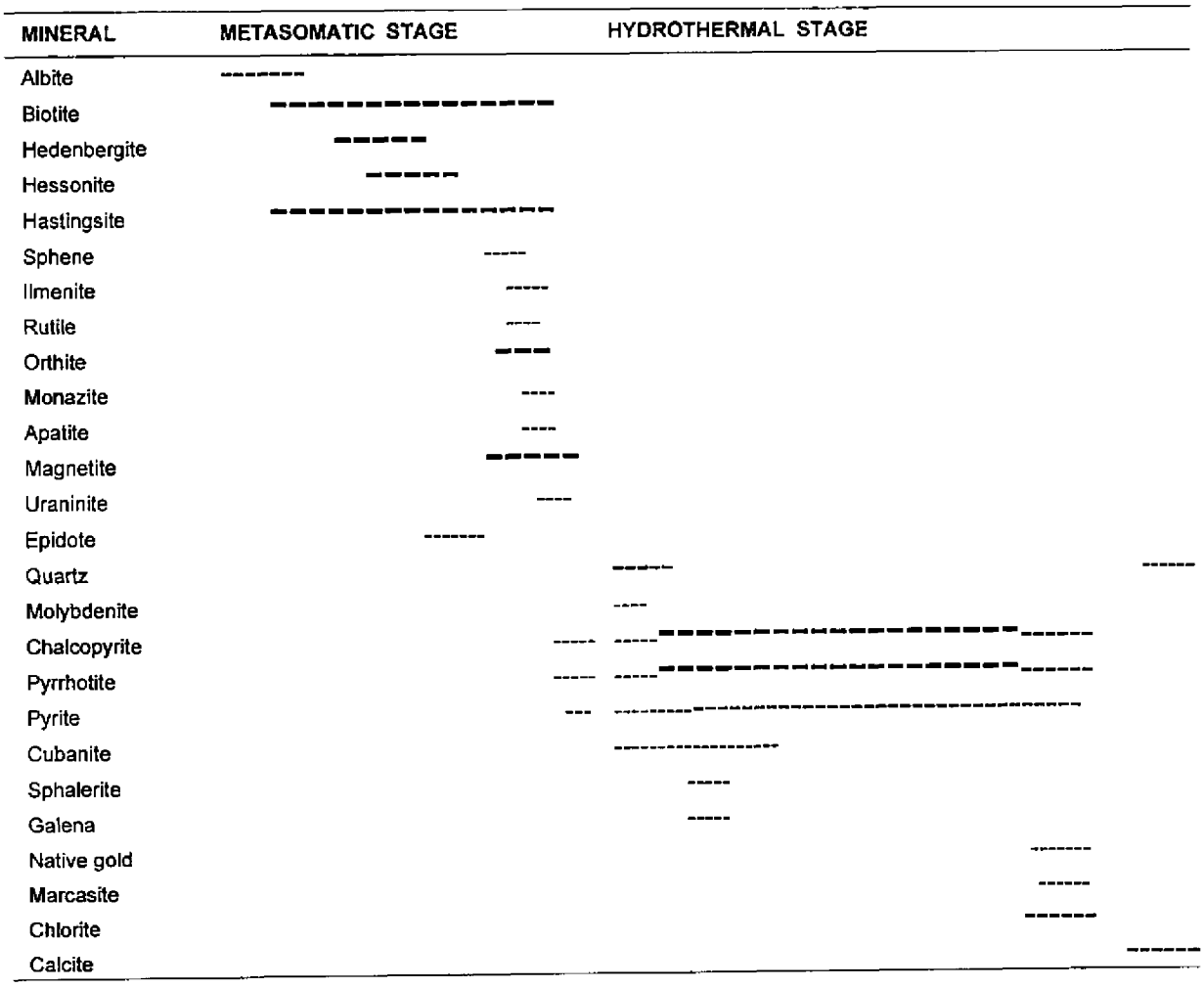
Magnetite

Magnetite formed late in the metasomatic alteration process as disseminations and veins and is strongly developed as bands along foliations and as massive accumulations, generally in metasomatite, but also in biotite gneiss adjacent to the metasomatite. It occurs as grains on the margins of biotite and hastingsite, and in mono-minerallic bands. Commonly these mono-minerallic bands and magnetite rich metasomatite have subsequently been brecciated prior to being cemented with sulphides, mainly chalcopyrite and lesser pyrrhotite. Magnetite is eroded and replaced where adjacent to pyrrhotite.

Orthite

Orthite also formed late in the metasomatic alteration process as disseminations, predominantly within the metasomatite. It is commonly associated with magnetite but also occurs in magnetite and sulphide poor skarn-type alteration. Two types are recognised, namely an early dark brown more iron rich variety and a later greyish coloured phase which in places rims the earlier formed orthite.

Table 1: Mineral Paragenesis (after Ta Viet Dung *et al.*, 1975).



Sulphides

The main sulphide minerals are chalcopyrite and pyrrhotite with lesser pyrite. They occur predominantly as disseminations and bands along foliation planes and fractures within the metasomatite, and to a lesser extent in biotite gneiss, but are also found in veins, breccias and impregnations. A number of generations of sulphides are recognised with initial high temperature phases being followed by progressively lower temperature sulphides.

In general, two main stages of sulphide formation have been recognised. The first of these is a very early but minor phase of chalcopyrite-pyrrhotite-pyrite associated with quartz, which forms veins cross-cutting metasomatite and magnetite bands. Sulphides of this generation have commonly been deformed. The second and main stage consists of chalcopyrite and pyrrhotite with lesser pyrite, and is by far the most common. Different sub-stages of chalcopyrite and pyrrhotite are recognised reflecting deposition at progressively lower temperatures. Sulphides of the second stage are rarely deformed.

Gold

Gold occurs within the sulphides, and as free gold, and is irregularly distributed and difficult to analyse accurately. Metallurgical test work showed that 15% of all gold was free, 68% reported in the copper concentrate and 17% remained in the pyrrhotite-pyrite concentrate.

Other Mineralisation in the Region

Sin Quyen Area

Exploration within the region has located a number of zones of Sin Quyen-type mineralisation, developments of magnetite only, and zones in which copper predominates (see Fig. 2). These have been tested and all found to be smaller, less continuous and of lower grade than Sin Quyen. They are interpreted to fall in four zones, as follows:

Sin Quyen - Nam Mit Zone

This zone is developed adjacent to the Sin Quyen Fault, and includes the main Sin Quyen deposit itself. Along strike to the southeast from Sin Quyen, ore grade mineralisation ends abruptly, becoming low grade and deep seated, although it is possible that further higher grade shoots which have not been intersected by drilling may re-develop down plunge. At the surface, over the same interval, mineralisation is confined to magnetite, with only weakly anomalous accompanying copper values being encountered in trench samples and drill core. To the northwest the prospective zone has been eroded and is characterised by small discontinuous pods of alteration and mineralisation.

Approximately 2 km further along strike to the northwest significant alteration and mineralisation is developed at Vi Kem and is interpreted to represent another south plunging mineralised zone. Ta Viet Dung *et al.*, 1975 reported that this zone was smaller, lower grade and less continuous, with a calculated resource of 35.5 Mt @ 0.54% Cu. The author estimated that the largest lens contains approximately 6 Mt @ 0.75 % Cu. Two magnetite veins were reported a further 2 km along strike at Vi Cap.

Nam Mit lies 25 km along strike to the northwest of Sin Quyen and was considered the best prospect after Sin Quyen on the basis of its similar structural position and because of the surface geology which included copper grades of 0.70%. The results of over 6000 m of diamond drilling however, were disappointing with only weak copper grades being encountered within the well developed metasomatite and magnetite. Results from Nam Chac along strike to the southeast of Nam Mit were similarly disappointing.

Suoi Thau - Song Bang Zone

The Suoi Thau - Song Bang zone is not located on a recognised regional structure but appears to be confined to a particular horizon within the lower Sin Quyen Formation. At Suoi Thau two zones of weak copper-magnetite and a single zone of magnetite only were encountered. At Song Bang there is a single magnetite vein in weak biotite-sericite-chlorite-calcite alteration.

Pin Ngan Chai – Lung Thang Zone

This zone is developed along the Pin Ngan Chai Fault which also hosts a number of intrusive bodies, variously described as quartz-diorite, albite-diorite, biotite-granite and plagio-granite of the Permian Dien Bien Phu Complex (Bui Phu My, 1978). The plagio-granite intrusives within the Sin Quyen ore zone are generally regarded as being associated with this same intrusive suite. At Pin Ngan Chai four zones of low-grade mineralisation were reported to occur in metasomatite, in migmatised gneiss, and along the margins of intrusions. Low grade copper was associated with pyrrhotite, pyrite and orthite, although magnetite was weak or absent. At Lung Thang, chalcopyrite, orthite and pyrrhotite mineralisation was reported occurring as veins within biotite gneiss at the northwestern and southeastern extremities of the intrusion, in hornfels graphite schist along the margins of, and in fractured zones within, the intrusive body. The mineralisation is not typical Sin Quyen-type as metasomatite alteration and magnetite are absent.

Thung Sang Zone

Thung Sang is a distinctly different zone of mineralisation, lying to the northeast of the Sin Quyen Formation within Palaeozoic sediments. Mineralisation occurs as discontinuous thin veins along a northwest trending fault zone within dolerite and gabbro intruded into Permian limestone. The primary ore minerals are chalcopyrite, pyrite, titano-magnetite and specularite. Alteration minerals include chlorite, calcite and epidote. Gold was reported to be rare while orthite and metasomatite alteration are absent. Oxide zone copper (covellite and chalcocite, plus malachite and azurite) is locally high grade and was exploited on a small scale in ancient times.

Elsewhere in the Region

Iron oxide-copper mineralisation is reported further along strike in both China and Vietnam. In Vietnam mineralisation has been located some 100 km along strike to the southeast of Sin Quyen at Ngoi Hut and a further 100 km southeast at Lang My (Ta Viet Dung pers. com.). In both cases magnetite and metasomatic alteration have been reported in Proterozoic gneiss, schists and amphibolites. Copper is reported at Ngoi Hut but not Lang My. Neither area has been drilled.

In China extensive magnetite and chalcopyrite-magnetite mineralisation occurs at Dahongshan approximately 250 km northwest of Sin Quyen within the Red River Fault zone. Seventy nine discrete orebodies are associated with spilitic and keratophyric volcanics, and associated sediments within the lower Proterozoic Dahongshan Formation. One magnetite and two magnetite-copper ore bodies are considered to be large. Mineralisation is characterised by extensive Na alteration which can be directly correlated with the Fe content. Carbonatisation is present but K alteration is subdued. Magnetite is the dominant Fe oxide with minor hematite and titano-magnetite. Copper is associated with Au, Ag, Co, Pt and Pd, with minor pyrite and bornite, although pyrrhotite is rare. Chinese workers have suggested that initial iron mineralisation was related to magmatic and volcanogenic processes. Post magmatic hydrothermal and metamorphic processes led to enrichment of some of the magnetite mineralisation and the introduction of copper mineralisation.

Timing

The timing of the Sin Quyen mineralisation is uncertain and unconstrained by modern geochronological dating methods. The major gneiss forming metamorphic event in the Red River Fault Zone has been variously dated as Oligocene (Tapponnier *et al.*, 1990) and as between 1960 and 2360 Ma (Tran Ngoc Nam, 2001). Ta Viet Dung *et al.*, 1975 proposed a Proterozoic date for the metasomatic alteration and magnetite-orthite mineralisation which they considered to be formed by metamorphic replacement or related to a post magmatic fluid associated with the "granito-gneiss". As the plagio-granite intrusives and the sulphide mineralisation are both relatively undeformed and absent from the magnetite only mineralisation zones in the area, the sulphides were interpreted to be a separate hydrothermal event related to the Permian plagio-granite.

The author prefers a Proterozoic age for all Sin Quyen mineralisation because the plagio-granite can be interpreted to postdate all mineralisation. Early formed sulphides are deformed while the later lower temperature varieties are undeformed suggesting deposition during waning metamorphism and tectonism. A Tertiary age for the mineralisation is unlikely because evidence of the regional metamorphic event is not seen in any post-Proterozoic rocks in the region. The younger Thung Sang mineralisation is clearly different to the typical Sin Quyen mineralisation-alteration assemblage.

Conclusions

The deposit shares a number of important features with some other deposits of this type including the characteristic alteration pattern of early widespread Na alteration, followed by a more intense localised Fe-K phase, formation of magnetite and rare earth minerals prior to deposition of sulphides, the characteristic Cu-Au ratio of approximately 20 000 : 1, a location adjacent to a major intra-cratonic crustal structure and a probable Proterozoic age. The presence of nearby graphitic metasediments, extensive magmatism and intensive replacement of host rocks is also observable in other deposits.

Sin Quyen differs from many deposits of this type in that although located in a sequence or feldspathic rocks the mineralisation is hosted by iron rich metasomatic rocks, which formed by Fe-K alteration of pre-cursor mafics rather than feldspathic rocks. There is no evidence of evaporites in the sequence which in conjunction with the voluminous and varied magmatism, both within the sequence and within the deposit itself, suggests it belongs to the group formed from de-volatilisation of a magmatic fluid without input from sedimentary brines.

Detailed structural interpretation, in conjunction with isotopic and fluid inclusion studies would provide a better understanding of the genesis of this deposit.

References

Bui Phu My, 1978 - Lao Cai and Kim Binh 1:200 000 Geological Map Series of S.R.Vietnam; *Geological Survey of S.R. Vietnam.*

Le Dzuy Bach and Ngo Gia Thang, 1995 - Phanerozoic Ophiolites in Indochina; *in* Proceedings of the International Symposium on the Geology of South East Asia and Adjacent Areas, *Vietnam Journal of Geology,* Special Issue, v. 5-6, pp. 212-221.

Metcalfe, I., 1995 - Gondwana Dispersion and Asian Accretion; *in* Proceedings of the International Symposium on the Geology of South East Asia and Adjacent Areas, *Vietnam Journal of Geology,* Special Issue, v. 5-6, pp. 223-266.

Poliakov, G.V., Balykin, P., Glotov, A.I., Trong Quoc Hung, Ngo Thi Phuong, Hoang Huu Thanh and Bui An Nien, 1991 - High Magnesian Volcanites in the Da River Zone; *in* Tran Van Tri (ed.), Proceedings of the Second Conference on Geology of Indochina, *Geological Survey of Vietnam*, pp. 247-261.

Stokes, R.B., Smith, P.F.L. and Soumphonphakdy, K., 1995 - Timing of the Shan-Thai-Indochina Collision: New Evidence from the Pak Lay Fold Belt of the Lao PDR; *in* Proceedings of the International Symposium on the Geology of South East Asia and Adjacent Areas, *Vietnam Journal of Geology,* Special Issue, v. 5-6, pp. 321-2.

Tapponnier, P., Lacassin, R., Lelaup, H., Scharer, U., Zhong Dalai, Wu Haiwei, Lui Ziaohan, Ji Shaocheng, Zhang Lianshang and Zong Jiayou, 1990 - The Ailo Shan /Red River Metamorphic Belt: Tertiary Left Lateral Shear Between Indochina and South China; *Nature*, v. 342, pp. 431-437.

Ta Viet Dung *et al.*, 1975 - The Geological Report on Detailed Exploration of the Sin Quyen Copper Deposit; *General Department of Geology, Hanoi*, unpublished report.

Tran Ngoc Nam, 2001 - The Age of the Ca Vinh and Xom Giau Complexes Dated by SHRIMP U-Pb Analysis of Zircon; *Vietnam Journal of Geology*, v. 1-2, pp. 1-10. (*in Vietnamese*).

Tran Van Tri, 1979 - Geology of Vietnam (the North Part). *Science and Technology Publishing House, Hanoi*, pp. 78-95

PGC PUBLISHING

Daliran, F., 2002 - Kiruna-Type Iron Oxide-Apatite Ores and "Apatitites" of the Bafq District, Iran, with an Emphasis on the REE Geochemistry of their Apatites; *in Porter, T.M. (Ed.), Hydrothermal Iron Oxide Copper-Gold & Related Deposits: A Global Perspective*, Volume 2; PGC Publishing, Adelaide, pp 303-320.

KIRUNA-TYPE IRON OXIDE-APATITE ORES AND "APATITITES" OF THE BAFQ DISTRICT, IRAN, WITH AN EMPHASIS ON THE REE GEOCHEMISTRY OF THEIR APATITES

Farahnaz Daliran

Institute of Mineralogy and Geochemistry, Technical University of Karlsruhe, Germany
E-mail: farahnaz.daliran@bio-geo.uni-karlsruhe.de

Abstract - The Bafq metallogenic province in Iran contains world class Kiruna-type apatite-iron oxide ores, apatite-rich magmatic rocks called "apatitites", REE, Th-U, Pb-Zn and recently reported Cu(-Au?) mineralisation. The metallogenesis is related to magmatic events that accompanied a major late Precambrian rifting event within Gondwanaland. The magmatic activity is subvolcanic to volcanic, is characterised by the bimodal association of rhyolites and spilitic basalts and is accompanied by a regional alkali metasomatism.

The iron deposits are commonly hosted by hydrothermally altered and metasomatised rhyolitic rocks, which are either interstratified with volcano-sedimentary sequences, or form large subvolcanic and volcanic masses. The iron ore is dominantly a Ti-V-poor massive magnetite with subordinate hematite, and is commonly accompanied by apatite. Apatite also occurs within the magmatic "apatitites" which are spatially and temporally closely associated with the iron ores.

The behaviour of trace elements in the Bafq apatites from both associations is identical. Both apatites are enriched in REE up to 2 weight% REE oxides, and have a REE distribution pattern marked by a strong LREE/HREE fractionation, pronounced negative Eu and slightly positive Ce anomalies. They are also characterised by depletion in Sr (to 300-400 ppm) and Th (to 100 ppm) and are practically devoid of U and Pb.

The REE geochemistry of the apatites from the Bafq region is similar to other global apatite-magnetite ores, including those of Kiruna in Sweden, but also in part to both nelsonites and to the carbonatite association. However, they differ fundamentally from the sedimentary phosphorites, thus excluding a marine source.

The identical chemistry of apatites from both the iron ores and "apatitites" in the Bafq district reflects the composition of a homogeneous source reservoir and confirms the geological, mineralogical, and petrographic evidence that apatites of both associations are cogenetic. These observations strongly imply that fluids have played a crucial role in the formation of the iron ores and the "apatitites", putting the previously proposed iron-phosphorous liquid magma source into question. The fluid model also explains the large spectrum of modes of emplacement, from submarine hydrothermal to hydrothermal and metasomatic. The source of the mineralising fluids is assumed to be an evolved magmatic fluid rich in volatiles and incompatible elements, that was generated during late Precambrian intra-continental rifting within the Bafq district.

Introduction

The town of Bafq is located 115 km south-east of the city of Yazd, in central Iran. It has given its name to the Bafq district, a large metallogenic province containing world class iron ore, magmatic phosphate, Th-U and Pb-Zn deposits and recently discovered Cu (Au?) mineralisation.

Editors note: The Iranian location 'Bafq' may be translated into the Roman alphabet as either 'Bafq' or 'Bafg'. The former has been used in the text of this paper throughout, although the latter may appear on some plans and in citations in the reference list.

The district comprises a narrow rift zone extending from south of the town Bafq to Sagand and Robat-Posht-Badam in the north. The reserves of mostly high grade (65% Fe) iron ores, which are estimated at 1500 million tonnes, are distributed over 34 zones of aeromagnetic anomalies (Fig. 1). Iron ore is currently being mined to supply local steel works. In addition, economic apatite deposits, ignored for many years, have recently become attractive. The first phosphate plant was established at the Esfordy deposit, which has an estimated reserve of 17 million tonnes of apatite with 2-3% REE (Phosphate Mines Development Co., 1999).

In the Bafq district, apatite is associated with both magnetite (-hematite) ore and with apatite-bearing silicate-phosphate-magnetite-carbonate rocks ("apatitites"). The iron ore deposits are classified as Kiruna-type (Williams & Hushmandzadeh, 1966; Borumandi, 1973; Daliran, 1990, 1991; Daliran et. al., 1994; Förster & Jafarzadeh, 1994; Mücke & Younessi, 1994). Kiruna-type iron ores are low-Ti, low-V, magnetite(-hematite)-apatite mineralisation associated with near surface to surface felsic to intermediate magmatic systems (Daliran, 1990). The genesis of the Kiruna-type ores has been controversial for several decades. A wide spectrum of ore genesis models from liquid magmatic (Geijer, 1910; Geijer & Ödeman, 1974; Frietsch, 1984; Wright, 1986; Lyons, 1988; Nyström & Henriquez, 1994) to sedimentary (Parak, 1975) have been proposed for Kiruna-type ores worldwide. Recently volatile and hydrothermal ore forming processes have gained more prominence (Hildebrand, 1986; Oreskes & Einaudi, 1990; Hiztman et al., 1992; Oreskes et al., 1994; Bookstrom, 1995; Treloar & Colley, 1996; Rhodes & Oreskes, 1999; Rhodes et al., 1999) and their generation within a continental rift tectonic environment has been stressed. Broadly, the origin of the Iranian iron ores has been attributed to liquid magmatic processes, in analogy to that proposed for the Kiruna deposits in Sweden (Williams & Hushmandzadeh, 1966; Borumandi, 1973; Förster & Jafarzadeh, 1994; Mücke & Younessi, 1994).

A re-evaluation of the available data and recent fieldwork, demonstrates a close spatial and temporal association between the iron ores and "apatitite" rocks in the Bafq region. Field geological relationships, mineralogy and petrological studies support a common origin for the apatite-iron ores and the "apatitites" with varying modes of emplacement, which can not be explained by a liquid ore magma alone (Daliran, 1990; Daliran & Amstutz, 1991). This association thus offers an appropriate opportunity to approach the problem of the genesis of Kiruna-type ores by means of a comparative study of the geochemistry of apatites of both affiliations in the Bafq district.

Geological Setting

Regional Setting

The Precambrian basement of Iran was consolidated with the neighbouring Arabian Shield, to become part of Gondwanaland during the Upper-Precambrian Assyntic orogenesis (Stöcklin, 1968, Haghipour, 1994). Davoudzadeh et al. (1986) proposed that this event should be termed "Katangan/Pan-African" on the basis of the geodynamic linkage of the structural history of Iran with that of the African-Arabian plate.

During the post-Assyntic, Iran continued to be part of this larger craton within Gondwanaland until the Late Triassic when disruptions, such as that along the Zagros Line, developed an oceanic trough (Stöcklin 1968). Recent studies have indicated however, that there are deep seated faults and rift zones observed in the Bafq district that date from the end of the Precambrian (Haghipour, 1974, Daliran, 1990, Samani, 1993). This rifting took place as a part of the Pan-African tectono-thermal event from 750 Ma to 550 Ma (Illin, 1991, Samani et al., 1994). The geology of the Bafq region was studied in detail by Haghipour (1974) and NISCO (eg., 1980) and was reviewed recently by Hushmandzadeh (1989) and Samani (1993, 1994, 1998).

The orogenesis of the Upper-Precambrian is responsible for the earliest preserved structural patterns observed in Iran with a quasi north-south trend in eastern Central Iran that was reactivated during subsequent rifting. The Bafq district coincides with a narrow north-south striking rift zone from Chogart in the south to Sagand and Robat-Posht-Badam to the north (Fig. 1). Samani (1998) distinguished a southern sector (the Chogart-Esfordy domain) and an 80 Ma younger northern sector (the Sagand-Khoshumi domain). The Chador Malu deposit lies on the dividing line between the two sectors, which corresponds to an east-west trending deep crustal fault. The rift sediments are overlain by platformal Cambrian formations, signifying the termination of the rifting event.

According to Samani (1998), rift-related tectono-magmatic activity in the Bafq district began with mantle doming, alkaline ultrabasic magmatism, and intrusion of late K-syenites in the southern sector. In the northern sector, rifting was associated with carbonatitic metasomatism and by intrusion of granitic masses of metasomatic origin that were accompanied by a regional Na metasomatism. The first rifting stage was accompanied by bimodal volcanic rocks (alkali-feldspar rhyolite and spilitic basalt), whereas the second stage was dominated by K-rich acid volcanism. These two rifting stages have been dated at 750-583 Ma and 583-550 Ma respectively, and are locally separated by a disconformity and a basal conglomerate (Samani et al., 1994). Large volumes of magmatic rocks in the Bafq district are represented by the Zarigan- or Narigan-type subvolcanic granites and by rhyolites, which are the most common host to the apatite-magnetite and "apatitites". Haghipour (1974) and Samani et al. (1994) attributed the formation of these granites to metasomatism of the rhyolites.

Host Sequences

The iron-apatite ores, the "apatitites", REE-, Th-U, Pb-Zn and recently discovered Cu, Co, U (Au?) mineralisation all occur within a series of volcanic and volcano-sedimentary rocks of rhyolitic composition, subordinate spilitic basalts, carbonates and detrital sediments with local evaporites. Syenite sills (albitites) and diabase dykes intrude these rift-related formations, which overly the older Precambrian basement above an angular unconformity. The basement comprises calc-alkaline magmatic and green-schist facies metamorphic rocks. The mineralised rift sequences are dis-conformably overlain by Cambrian platform sediments. The basal conglomerate of the Cambrian units contains reworked fragments of the iron ore and of metasomatic rocks marking the limit of the mineralising epoch.

The rift-related sequences that were previously known as the Rizu, Dezu, Esfordy and Sagand formations and were attributed to the Infracambrian, are now assigned to two

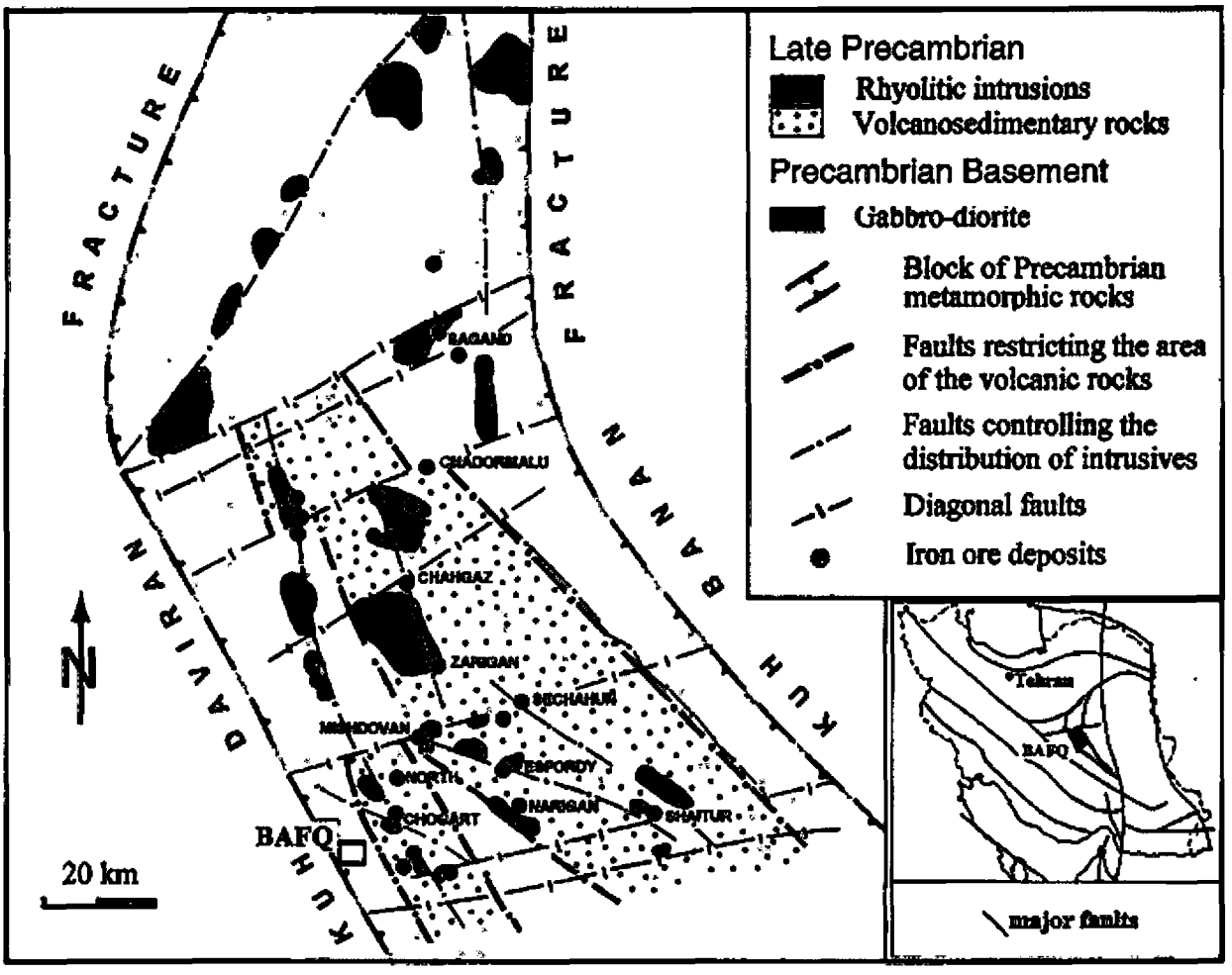


Figure 1: Structural map of the Bafq zone with location of the studied deposits (modified after NISCO, 1980).

new stratigraphic units (Fig. 2). The lower unit, which is now referred to as the Sagand Formation, formed during the major late Precambrian rifting, while the upper unit has been defined as the Rizu-Dezu Series and is related to the later subsidiary stage (Samani, 1998).

The ***Sagand Formation*** is a 1200-1500 m thick sequence that commences with a basal conglomerate, overlain by bimodal volcanics (rhyolite-basalt), volcanic-exhalites, and then by submarine volcanic rocks with intercalated carbonate beds at the top. The upper volcanic member progresses up-section from mainly basic rocks into more acid varieties. This unit that is strongly metasomatised and is the major host to the iron-apatite ore, "apatitites" and U-Th mineralisation of the region. Thick-bedded recrystallised limestones with intercalations of clastic-volcaniclastic rocks and evaporites form the end member of this mineralised volcanic unit.

The ***Rizu-Dezu Series*** comprise a sequence of high-K acid volcanic rocks with carbonates at the top, minor basic volcanics, carbonatic shales and evaporites. The basal conglomerate that overlies the angular unconformity with the Sagand Formation, contains pebbles of metasomatised Sagand Formation, marking the upper limit of metasomatism. The Rizu-Dezu Series is host to sulphide mineralisation (Pb-Zn ore at the Kushk mine) and to the Fe-Mn ores of the region (eg., the Narigan deposit).

Mineralisation

The iron ores of the Bafq district are estimated to total approximately 1500 million tonnes and are distributed over 34 zones of aeromagnetic anomalism, from the Chogart mine in the south, to Sagand and Robat-Posht-Badam in the north. The ore reserves of the individual deposits vary from low tonnage examples (eg., Mishdovan, 20 mt) to larger bodies of several hundred (up to 300-400) million tonnes (eg., the Chogart, Chador Malu, and Seh Chahun deposits). Most are high grade (65% Fe) with some low grade mineralisation (20-30% Fe) that is a function of the ore mineralogy.

Systematic investigation of the iron ore resources of the Bafq district began in 1968 with exploration by the former NISCO, National Iranian Steel Corporation) assisted by Soviet geologists. The results of this work were compiled in a series of internal reports by NISCO between 1969 and 1980. Despite this extensive body of geological and exploration data, the fundamental questions regarding the genesis of the iron ores remains open.

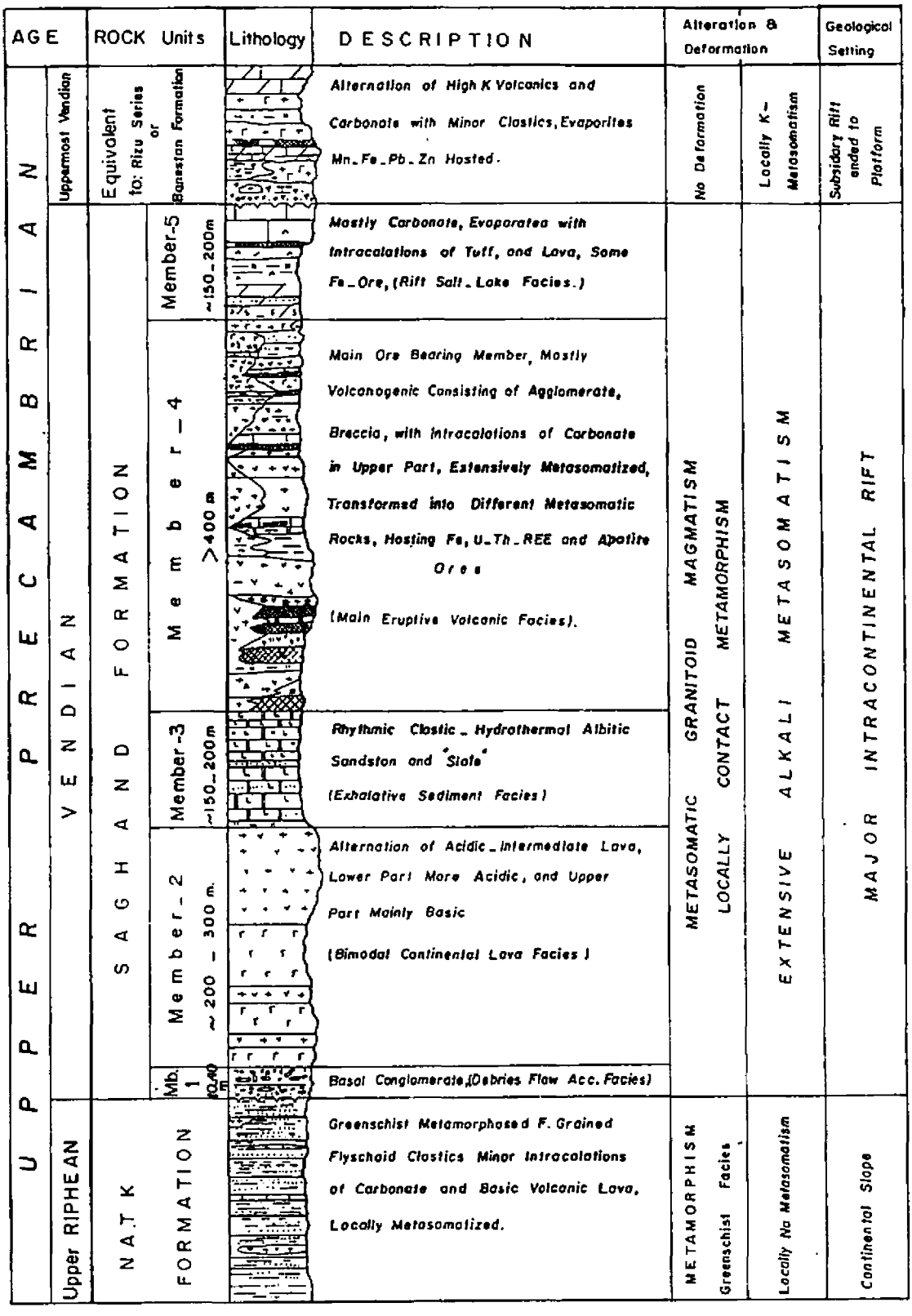


Figure 2: Stratigraphic column of Sagand Formation and Rizu Series (after Samani, 1993)

The iron deposits of the Bafq district exhibit a wide variation in their geology, relationship with host rocks, geometry, and their ore and gangue mineralogy, particularly the REE-bearing species. On the basis of current knowledge, these deposits may be grouped into two main styles:

1. The first is interpreted to have been generated by the discharge of ore fluids onto sedimentary basin floors to precipitate and form ***syngenetic submarine hydrothermal*** deposits. The ore bodies are bedded to lenticular, concordant, and have gradational boundaries with the enclosing host rocks (eg., Mishdovan and Narigan).
2. In the second style, which includes the majority of the ore deposits, the ore fluids penetrated sub-volcanic and volcanic rhyolitic rocks. The passage of the ore fluids resulted in strong metasomatic and hydrothermal alteration of the host rocks, producing ***epigenetic replacement*** deposits (eg. Chogart, Chador-Malu and the North anomaly). This type of iron ore passes gradationally into "apatitites" in some deposits, as is observed at Esfordy and Chogart.

Each of these two mineralisation styles may be further sub-divided on the basis of their ore and gangue assemblages. With few exceptions however, (one being Mishdovan, Daliran, 1990), no systematic studies have been undertaken to allow the assignment of many of the deposits to specific sub-types.

Examples of the variation and sub-types recognised from the ***syngenetic submarine hydrothermal*** style include: apatite-magnetite±hematite (eg., Mishdovan) and Fe-Mn-jaspilite (eg., Narigan) deposits. Barite is a common mineral in the Fe-Mn-jaspilites which are characterised by very low Ti and V (< 0.01%), low P (0.05-0.17%), relatively higher S (0.01 to 1.94%) and up to 10% Mn. Apatite while rare, is reported from Narigan (NISCO, 1980), although it's distribution within other ore deposits of this type is unclear.

The ***epigenetic replacement*** style deposits are commonly massive bodies of apatite-magnetite±hematite. The principal ore mineral is a low Ti-V (2-3%) magnetite that is commonly martitised with subordinate amounts of primary hematite. This basic mineralogy may however be accompanied by a variety of temperature dependant assemblages of silicates, REE minerals, carbonates and quartz, which permits two sub-types to be distinguished. The first of these is a *low-temperature hydrothermal* type which is characterised by the presence of hydro-silicates. An example of this type is the North Anomaly where the iron ore is hosted by rhyolites which form large masses of volcanic (perlites) to subvolcanic rocks. The mineralisation is accompanied by albitisation and actinolitisation of the rhyolites. Magnetite ore is intergrown with quartz, albite and actinolite and is paragenetically associated with chlorite, epidote, allanite, sphene, zircon, calcite, tourmaline and leucoxene. Only minor apatite is present, resulting in low P type deposits. In contrast, the *high-temperature metasomatic* types (eg., Chogart and Esfordy) are commonly accompanied by "apatitites" on a deposit scale containing high temperature minerals such as pyroxenes and garnets, and are enriched in REE-bearing apatite and REE minerals (silicates and phosphates).

In some aspects, this classification supports the observations of the Soviet geologists (NISCO, 1980) who recognised four types of deposits: (a) Red banded, ferruginous quartzite (jasper) with hematite ±siderite and mangano-siderite, (b) Mn-rich ores with siderite and mangano-siderite, (c) Pyrolusite-limonite±hematite ore, and (d) "Contact metasomatic" ore, the grouping into which the Soviet geologists classified the majority of the Bafq district iron ores. This latter group of deposits were defined as having formed at the „crushed and metasomatised" contact zone between granite porphyry intrusions and the Infracambrian (late Precambrian) sequences. The composition of the majority of the metasomatic rocks is given as albite±chlorite±actinolite, grading into a monominerallic albitite with 4-10% magnetite. Other less common metasomatites contain biotite, microcline, carbonate, and actinolite, while those characterised by talc and skarn garnet-diopside carbonate-bearing varieties are rare. In many deposits classified in this group however (eg., Mishdovan), no contact metasomatic zone can be revealed between the volcano-sedimentary sequences and the subvolcanic granites. The "contact metasomatic" ores of the Soviet geologists, correlates in many respects with the *"epigenetic replacement"* style of mineralisation described in the present work.

The spatial and temporal distribution of the different styles of mineralisation in the Bafq region was described by Daliran (1990) who observed that the Pb-Zn ores were deposited in a separate environment to that in which the apatite-iron formed. Samani (1993, 1998) recognised two stages of mineralisation. The first was developed in association with the early rifting accompanied by alkali magmatism, Na-metasomatism, apatite-iron ores and the mineralisation of incompatible elements REE, U and Th. He related the formation of Pb-Zn and Fe-Mn and Cu, Co, U(-Au?) deposits to the later subsidiary rifting stage.

Iron ore deposits

The most systematically studied of the many iron-apatite deposits of the Bafq district is Mishdovan (Daliran, 1990), which is described in more detail below as an example of one of the main styles of ore found in the region.

Mishdovan Deposit

The Mishdovan iron deposit is located some 30 km to the north of the town of Bafq in the southern segment of the rift that defines the Bafq district. It is a high-grade, low tonnage deposit of 20 mt at around 65% Fe, whose morphology is illustrated by the geological map and section of Fig. 3. The orebody is made up of more than 20 individual lenses that are interstratified within, and are clearly concordant with, the host volcano-sedimentary sequence which comprises rhyolitic tuffs with intercalated carbonate lenses in its lower sections. These volcanics and sediments

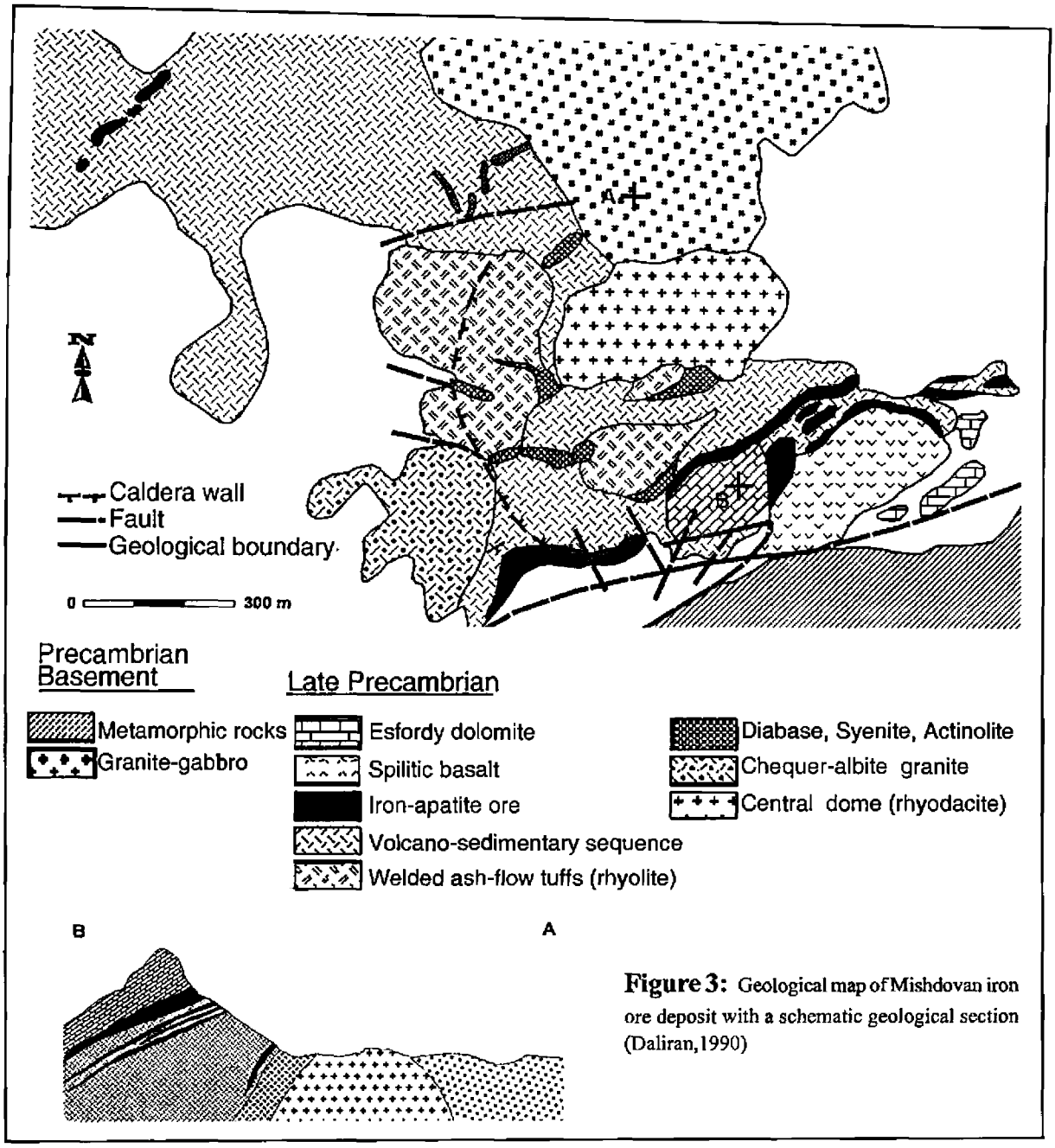


Figure 3: Geological map of Mishdovan iron ore deposit with a schematic geological section (Daliran, 1990)

are unconformably overlain by the massive cherty dolomites of the Esfordy Formation. The dolomites have a sharp contact with the underlying ore body, which is in the uppermost member of the volcano-sedimentary sequence. A small outcrop of spilitic basalt outcrops on the southern flank and may be intercalated within the dolomites. Welded ash flow tuffs are found on the western margin of the deposit, while a central dome of rhyodacitic composition has intruded the host rocks. Syenitic sills (albitites) and diabase (dolerite) dykes cross cut the host rocks and represent the latest magmatic activity at the deposit. The granite-gabbro-diorite massif to the north of the deposit and the metamorphic rocks to the south represent the Precambrian basement and are pre-mineralisation.

Hematite lenses predominate in the lower stratigraphic levels of the ore zone (Fig. 4A). These grade upwards to an interval of intercalated hematite laminae within rhyolitic tuffs, which in turn pass into the overlying main massive magnetite ore body in the uppermost member of the host volcano-sedimentary sequence. Syn-sedimentary deformation features such as interbedding and slumped beds, and the local admixture of the rhyolitic agglomerates with the ore minerals suggest synsedimentary precipitation of the iron ore minerals. The hematite-tuff strata grade laterally into hydrothermally altered chloritic tuffs-magnetite to the east beneath the massive ore body zone (Fig. 4B). The hematite ore is accompanied by a number of minerals that show some local and partly stratigraphic control. These minerals include authigenic quartz and feldspar, micro pockets of barite, tourmaline, chlorite, talc?, carbonates and late rutile, pyrite and goethite. Pockets of actinolite have been locally formed.

"Sandy ore", which is composed of lithified sand and blocks of iron ore, is a conspicuous feature at Mishdovan. It

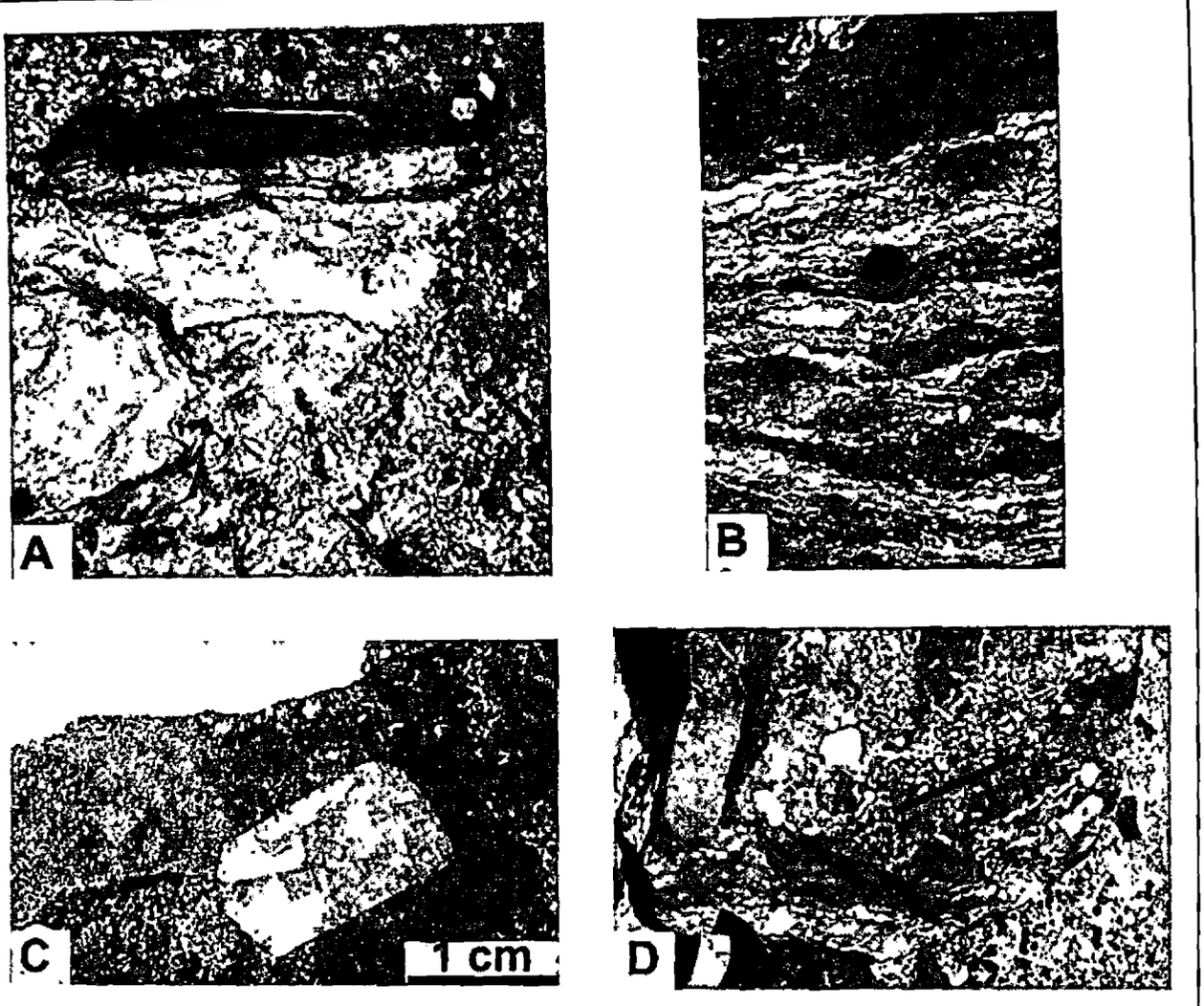


Figure 4: Field features and hand specimen from Mishdovan iron ore deposit.

(A) Lense of hematite ore interbedded within the rhyolitic tuffs.

(B) Interbedding of the magnetite ore with hydrothermally altered (chloritised) tuffs at the base of the massive main ore body.

(C) Hematite-apatite ore.

(D) Magnetite-apatite ore. Note the concentration of apatite crystals (and crystal mush) in a layer.

represents a localised "V"-shaped channel filling that was formed by the erosion and local deposition of the primary ore (Daliran, 1990). This channel which is cut into the volcano sedimentary sequence, indicates a period of erosional at the end of the ore-sedimentary cycle prior to the deposition of the cherty dolomites.

Apatite is virtually the only "gangue" mineral within the high grade ore and accompanies both the magnetite and hematite mineralisation. In the hematite ore it occurs as isolated crystals (Fig. 4C) and as tiny yellow "authigenic" crystals in the carbonate-rich hematite ore lenses. Apatite commonly forms accumulations of large yellow crystals and crystal fragments that are occasionally found in "schlieren" of calcite within the magnetite ore (Fig. 4D). Apatite crystals as well as the magnetite commonly exhibit a fragmented texture and crystal mush. In the so-called "banded ore" (Daliran, 1990), mush of apatite and of magnetite crystals are concentrated in distinct laminae and are cemented by calcite with associated monazite (Fig. 5A, B). Some apatite crystals showed a pronounced oscillatory growth zoning filled with fluid inclusions.

The principal ore mineral within the Mishdovan deposit is magnetite. It is largely martitised (supergene) and contains up to 2-3% TiO_2 and <1% V_2O_3 in solid solution (Daliran, 1990). Discrete exsolutions of black spinel and ilmenite trellis (an oxidation exsolution) can occasionally be observed (Fig. 5C, D). Primary sulphides occur as rare submicroscopic inclusions of chalcopyrite in the magnetite. The hematite ore consists of densely packed xenomorphic grains or as specularite blades and contain occasionally inclusions of pyrite.

Single sheets within the welded ash flow tuffs contain submicroscopic hematite developed along the flow lineation. This hematite, which contains occasionally rutile, is associated with apatite, and tourmaline which is believed to have formed from fumaroles (Daliran, 1990).

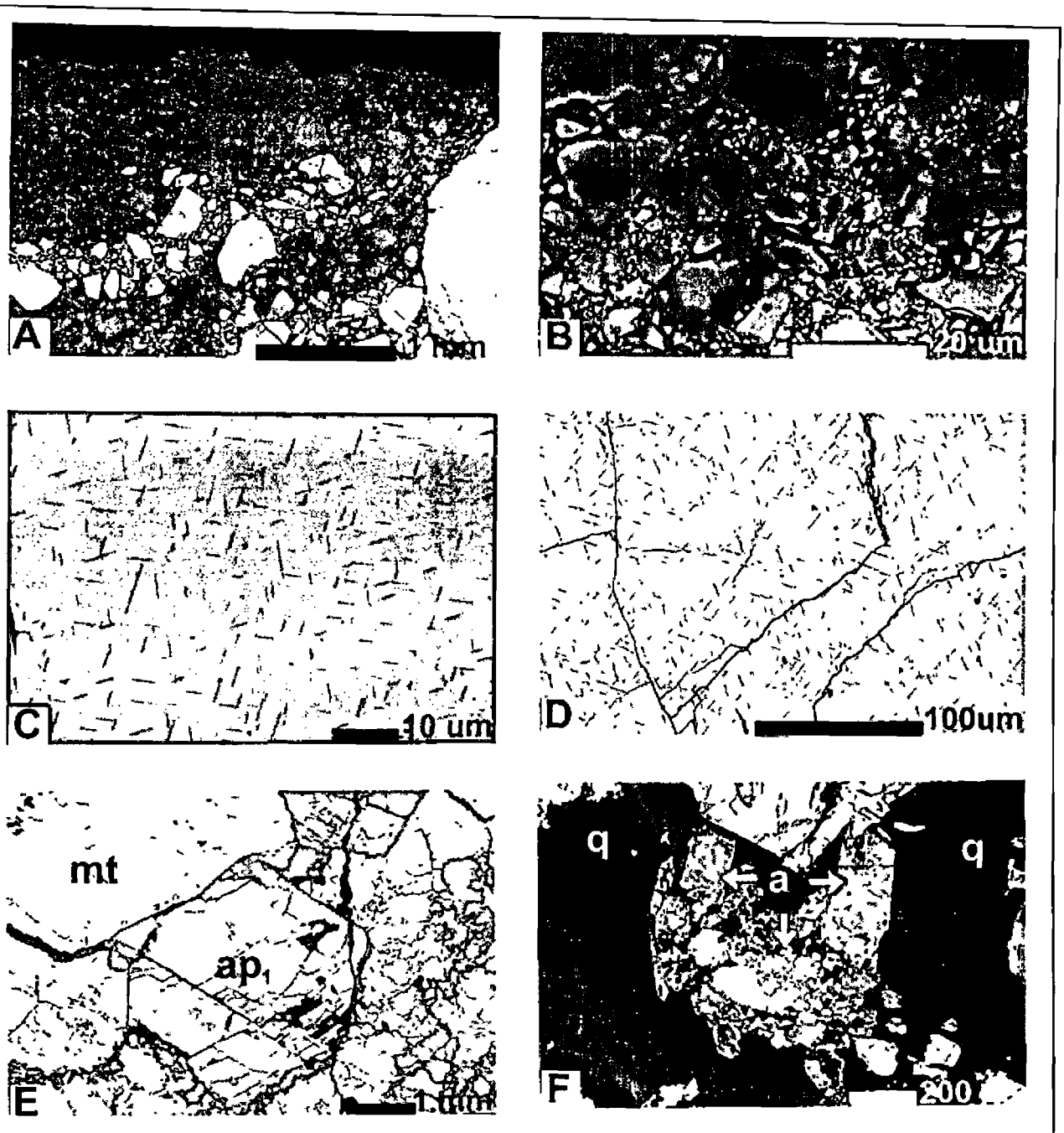


Figure 5: BSE images from the iron ores.

(A-D Mishdovan deposit).

(A) "Fragmented" texture of the banded ore showing a heterogeneous mush of magnetite (white) and of apatite crystals (gray) concentrated along distictinct layers.

(B) Mush of apatite cemented by calcite associated with submicron monazite (white).

(C) Spinel exsolution in magnetite ore.

(D) Ilmenite exsolution trellis in magnetite ore.

(E-F Chahgas deposit).

(E) Apatite (ap)-magnetite (mt) ore.

(F) Idiomorphic allanite crystals (a) associated with late quartz (q) infiltrating the early crystallised magnetite. Lighter allanite grains are richer in REE.

Chahgas Deposit

Magnetite ore from the Chahgas deposit which consists of hypidiomorphic granular magnetite with rare pyrite inclusions, is infiltrated by a network of apatite, which are in turn infiltrated by later fluids that formed talc, chlorite, calcite and quartz with sporadic idiomorphic allanite crystals (Fig. 5E, F). Minor hematite was also deposited in this late stage. This mineral assemblage indicates a metasomatic origin for the deposit.

"Apatitites"

The informal term "apatitite" refers, in a broad sense, to rocks consisting essentially of apatite accompanied by silicates, iron oxides, phosphates and silicates of REE,

titanite, calcite, quartz, talc, scapolite and (phlogopite?). To date, these rocks are only poorly studied, and their relationship to the iron ores is not well documented.

Most of the "apatitite" occurrences are closely associated with iron ore deposits as at Esfordy and Chogart. In these deposits, there is a transition from apatite-magnetite ore to the "apatitite" rocks by the addition of other minerals at the expense of magnetite. At the Chogart iron mine, which is hosted by subvolcanic rhyolites the "apatitites" are mainly confined to the crushed wall-zones between the orebody and the host rhyolite, or as veins, veinlets, and pockets cutting cross the orebody (Fig. 6). The dyke-like body at the Zarigan deposit (Fig. 7A) consists of extraordinarily large apatite crystals (>20 cm) that are crushed or show torsional deformation (Fig. 7B), and are cemented by large laths of calcite (Fig. 8A). Information from an unpublished manuscript of the GSI, appears to indicate that the different rock types at the Esfordy deposit have a concentric configuration.

The "apatitites" have undergone a complex multi-stage history of crystallisation and alteration that has resulted in a heterogeneous pegmatoidal texture with an extensive mineralogical variation and partly in the total destruction of the primary minerals and textures. The heterogeneous pegmatoidal texture has resulted from a two stage crystallisation. In the first stage, the megacrysts of yellow apatite (locally >20 cm across), pyroxene and occasionally garnet grains with magnetite have crystallised. The early crystals are commonly crushed and/or "cataclased", apparently as a result of the filter-pressure exerted by the rest fluid, and sometimes occur as a crystal mush (Fig. 8B, C). Occasional torsion of the early crystals (see Fig. 7B) may indicate a kind of plastic deformation due to a large scale flow movement of the rest fluids that entrained the early crystals at shallower levels. The rest fluids were

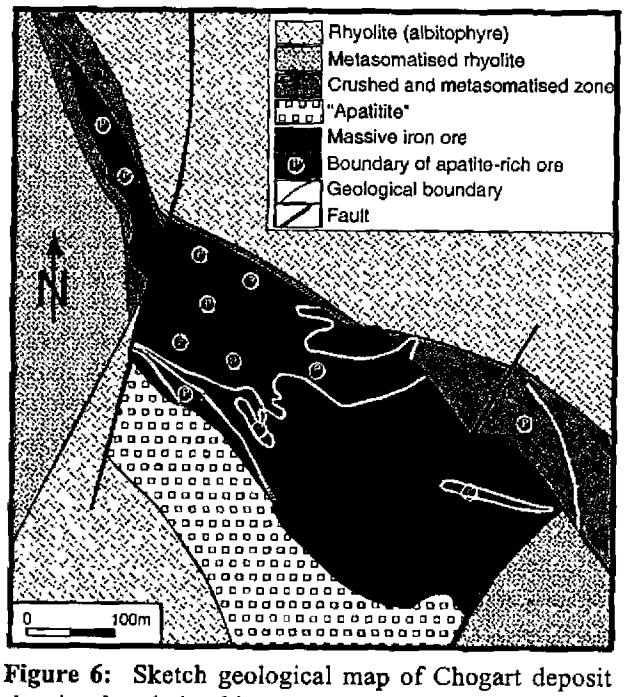


Figure 6: Sketch geological map of Chogart deposit showing the relationship between the magnetite-apatite ore body and the "apatitites" (modified after NISCO, 1980).

enriched in carbonates and the incompatible REE elements and were crystallised into a "non-fragmented" matrix consisting of a second generation of apatite (ap_2), REE minerals (allanite, monazite), hornblende, calcite, quartz, talc, (phlogopite?) and later veins (third stage) of calcite, scapolite and talc. Ap_2 with allanite and monazite form submicroscopic stubby crystals that are intimately associated with late calcite, quartz and other matrix minerals (Fig. 8C, D). In "carbonate-apatitites" (eg., Esfordy, Chogart and Zarigan) calcite is the main matrix component and forms large laths (Fig. 8A, B). Apatite is commonly rich in fluid and solid inclusions.

The samples investigated from the Chogart mine comprise crystal fragments of (ap_1) in a calcite matrix "carbonate-apatitite" (Fig. 8B). The (ap_2) and minor monazite are intimately associated with the carbonate matrix. Quartz and scapolite cross cut the early-formed minerals.

In the samples investigated from the Esfordy deposit, large apatite crystals and crystal fragments (ap_1) occur together with pyroxene crystals and garnet grains in a highly altered matrix of amphiboles, late calcite, quartz and the second apatite generation (ap_2), with allanite and monazite. Amphiboles were in part formed by the alteration of early pyroxenes. The new-formed hornblende is commonly smaller and idiomorphic. Pyroxene crystals are strongly "cataclased" and are infiltrated by an assemblage of calcite and scapolite. Magnetite is an accessory component, while quartz is later than the calcite, and is filled with carbonate inclusions (Fig. 8 C, D).

Geochemistry

For the geochemical studies, apatite samples from two apatite-magnetite deposits (Mishdovan and Chahgaz) and from four "apatitite" occurrences (Chogart, Esfordy, Zarigan and Chahgaz) were considered. In addition, analytical data of apatites from six occurrences (Mishdovan, Chogart, Chadormalu, Anomaly 14A, Chahgaz, Anomaly 13A) were used for comparison (NISCO, 1980).

Analytical Methods

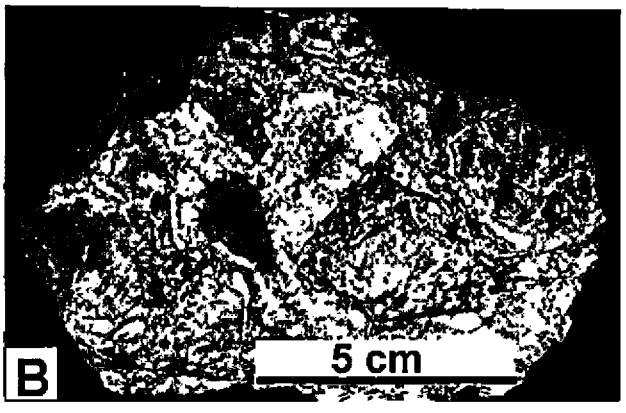
Microprobe analyses of the apatites were performed at the Max-Plank Institute in Heidelberg using an ARL-SEMQ wavelength-dispersive microprobe at a 20 KV accelerating voltage and 20 nA beam current for 30 seconds per element. Semi-quantitative analyses of other minerals were done with a Cameca SX50 at the University of Karlsruhe. Proton-induced X-ray emission data (PIXE) were obtained with the proton microprobe at the Max-Plank Institute in Heidelberg at a proton energy of 2.2-MeV. The analyses were carried out with a beam current of 70 -110 pA for 4000-6000 seconds (Traxel et al., 1995). Apatite samples were analysed in addition for REE with inductively coupled plasma-mass spectrometry (ICP-MS) using a Fions VG-Plasma Quad PQ2 in the University of Karlsruhe. For determination of the cell parameters of the apatites X-ray powder diffraction analysis was applied with a Huber Guinier Diffractometer with Cu Kα1 at the University of Karlsruhe.

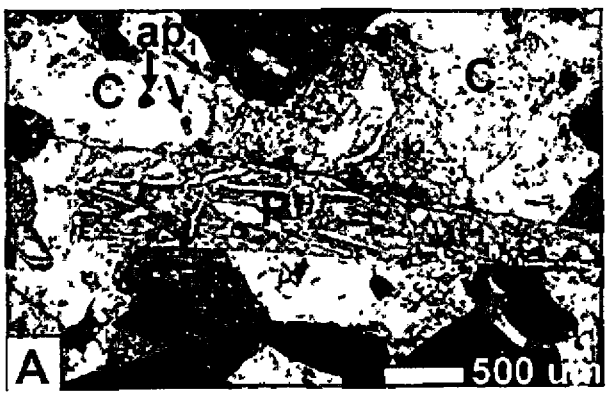


Figure 7:

(A) A dyke-like body of "apatitites" penetrating the Sagand Formation at Zarigan.

(B) Hand specimen from (A) showing splinter of "distorted" megacrytals of apatite (some with a dark core), magnetite (black grains) and pyroxene (not visible here) with interstitial amphibole, carbonate, quartz and REE minerals.







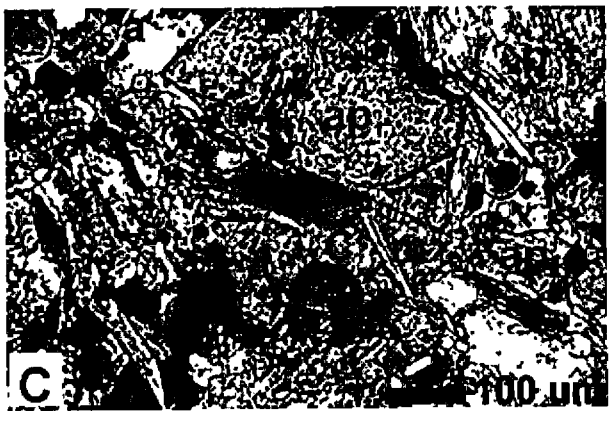




Figure 8: Microphotographs from "apatitites".

(A) Zarigan deposit. Fragments of early pyroxene (p) and apatite crystals (ap_1) in a matrix of large calcite laths (c).

(B) Chogart deposit. Crystal fragments of early apatite (ap_1) in a matrix of calcite associated with monazite (m).

(C-D) Esfordy deposit. Fragments of early apatite (ap_1) and partly altered pyroxene crystals (p) in a matrix composed largely of calcite with minor quartz, hornblende (h) associated with stubby crystals of REE minerals, the second apatite generation (ap_2), monazite (m), and allanite (a).

Results and Discussion

Apatite Chemistry

Apatites of the first generation (ap_1) were analysed for almost all elements, but not for carbon dioxide or water. The results are listed in Tables 1 to 3.

To provide a basis of comparison with other Kiruna-type ores, apatites from Kirunavaara (Sweden) and Durango (Mexico) were also analysed (Tables 2, 3). The ICP-MS results of this study, closely match the data published by Frietsch & Predhal (1995) and Dill & Kantor (1997) for the Kiruna apatite and the data from the Durango apatites (Roeder et al., 1987).

One apatite crystal from the iron ore deposit on Hormoz Island in the Persian Gulf, which seems to belong to the same mineralising event as of the Bafq iron ores (Daliran, 1990), was also analysed for REE (Table 2).

REE Chemistry and Distribution

Apatites from both the apatite-magnetite ores and in the "apatitites" in the Bafq district have similar compositions. Both are enriched in REE, in equal amounts, while the content of the other trace elements is not significant.

Apatites from the Mishdovan iron ores have the highest REE concentrations (1.75 wt% REE), while those from the Chahgaz ore contain the lowest (0.76 wt% REE). A line-scan of an optically zoned apatite crystal from Mishdovan also showed REE chemical zoning.

Bafq apatites have approximately equal concentrations of La and Nd, the former being slightly enriched, while La concentrations are 3 times those of Y. The degree of LREE enrichment relative to HREE, represented by the Ce/Y ratio, varies between 5.5 to 8.5 and indicates the relative compositional homogeneity of the Bafq apatites. There is a positive correlation between the total content of REE and the Ce/Y ratio. La/Nd is even more uniform and fluctuates around 1.

The chondrite-normalised REE patterns of the Bafq apatites (ICPM data) are represented in Figure 9. The patterns evidently all follow the same path, which is marked by a steep slope with LREE enrichment and a pronounced negative Eu anomaly. A slight positive Ce anomaly can also be seen in all of the analysed Bafq apatites. Figure 10 shows an identical pattern obtained for the Bafq apatites using the analytic data of NISCO (1980).

Other Elements

The content of other trace elements is typically low. The apatites contain consistently low amounts of Sr, averaging 300-400 ppm, and only a few ppm Rb. Th concentrations are around 100 ppm, and U is close to the limit of detection. Pb could not be detected. Significant amounts of As (110-345 ppm) were measured in all samples, and may be indicative of their source.

The fluorine content of most analysed apatites is around 1.8 wt %, while chlorine is around 0.6 wt %. Carbon dioxide and water were not determined by EMPA, although the infra-red spectrographic examination of the apatite from the hematite ore of Mishdovan, showed OH-F absorption bands. The lattice constants for the Bafq apatites and the fluor-apatite samples from Durango (Mexico) were calculated and are listed together with ICDD data for F-, Cl- and (OH)-apatites in Table 4 for comparison. It is emphasised that it has not been possible to distinguish between a F- or a Cl- variety of the REE-bearing apatites, because of the composite substitutions, which cause incalculable changes in the X-ray data of the end-member apatites.

Chemistry of Associated Minerals

The EMPA survey of associated minerals showed that apart from the typical REE minerals, monazite and allanite, no REE could be detected. Other relevant trace elements, such as Th, U, Sr or F and Cl, could not be detected either.

Monazite and allanite exhibit a strong LREE enrichment, similar to the apatites, with Ce, La, Nd selectivity, and Y deficiency. A zoned allanite crystal displayed REE zoning with Ce-La enrichment from the core to the rim, controlled by Ca depletion.

The pyroxene is a Ca-rich diopside. Diopside grains contain almost 1 to 2 wt% Na, whereas the amphiboles, particularly the obviously newly formed hornblendes, contain no Na. Actinolite formed from the alteration of pyroxene is impoverished in Ca and enriched in Mg, whereas its Fe remains almost constant. Garnet is a Ca- and Fe-rich andradite variety, and is Al poor. The carbonate matrix was identified as calcite with minor amounts of Fe, Mg and Mn, but without the conspicuous chemistry that characterises carbonatite calcites.

Genetic Discussion

The long-standing debate on the genesis of the Kiruna-type apatite-magnetite ores was based primarily on the ore liquid magma model introduced by Geijer, who published several manuscripts on the Swedish Kiruna ores. This genetic concept, which was applied to the majority of the Kiruna-type ores (Geijer & Ödeman, 1974, Frietsch, 1984; Wright, 1986; Lyons, 1988; Nyström & Henriquez, 1994) was challenged by Parak (eg., 1973, 1975) who contended they were not magmatic, but rather exhalative-sedimentary.

In the Bafq district, the field relationships between the iron ores and the "apatitite" rocks, combined with their petrographic and mineralogical characteristics, provide strong evidence for a common source for both types of occurrence. The mode of emplacement of the iron ore deposits, however, is varied. Fundamental aspects such as syn-sedimentary structures within the ore which are in continuity with the host rock in one group of deposits (eg., Mishdovan), provide sufficient evidence to suggest that iron ore was deposited in a sedimentary environment. Growth of the megacrysts of apatite in this same group of deposits by sedimentary processes however is still ambiguous. Conversely however, there is a lack of sedimentary features in the other group of deposits, which have been assigned a metasomatic origin. A model must therefore be defined that

Table 1: Average composition (wt%) of Bafq apatites (EMPA)

Deposit	Esfordy		Chahgas	Chogart	Mishdovan	
Sample	Apatite-Pyroxenite		Apatite-Pyroxenite	Apatite-Carbonate	Apatite-Magnetite	
Na_2O	0.31	0.34	0.38	0.37	0.60	0.61
MgO	0.05	0.05	0.05	0.07	0.06	0.06
SiO_2	0.25	0.26	0.21	0.29	0.27	0.25
P_2O_5	41.51	41.65	41.76	41.63	41.25	41.11
CaO	53.07	53.10	52.98	52.75	52.10	51.80
MnO	0.03	0.05	0.04	0.04	0.03	0.04
Fe_2O_3	0.08	0.09	0.05	0.07	0.05	0.07
La_2O_3	0.50	0.52	0.32	0.62	0.55	0.56
Ce_2O_3	0.95	1.16	0.84	1.26	1.21	1.32
Pr_2O_3	0.25	0.22	0.19	0.20	0.22	0.23
Nd_2O_3	0.46	0.47	0.41	0.51	0.50	0.62
Sm_2O_3	0.08	0.12	0.07	0.07	0.11	0.16
Eu_2O_3	0.00	0.08	0.03	0.00	0.07	0.07
F	1.84	1.87	1.85	1.85	1.80	1.82
Cl	0.67	0.63	0.76	0.54	0.68	0.67
Total	100.05	100.61	99.94	100.27	99.50	99.39

H_2O and CO_2 were not analysed

Table 2: REE analyses (ppm) of apatites (ICP-MS)

Deposit	Mishdovan	Chahgaz		Hormoz	Durango		Kiruna
Sample	Apatite-Magnetite	Apatite-Magnetite	Apatite-Pyroxenite	Apatite-Hematite	1	2	R17493
La	3175	1310	2400	2050	2995	3460	681
Ce	8570	3590	6770	3825	3825	4180	1740
Pr	934	417	769	415	304	334	220
Nd	3285	1470	2840	1520	945	1010	873
Sm	459	241	406	277	117	122	161
Eu	32	16	27	24	14	14	24
Gd	492	253	432	311	143	160	178
Tb	52	29	49	42	13	16	22
Dy	266	136	245	235	65	70	121
Ho	48	25	44	48	12	14	24
Er	138	66	127	138	34	37	67
Tm	17	7	16	18	4	5	8
Yb	100	39	93	97	24	26	49
Lu	13	5	12	12	3	4	7
Σ REE	*17581*	*7604*	*14230*	*9012*	*8498*	*9452*	*4175*

Table 3: Trace element analyses (ppm) of apatites (PIXE)

Deposit	Mishdovan			Esfordy		Chahgaz	Chogart	Zarigan	Durango
Sample	Apatite-Magnetite			Apatite-Pyroxenite		Apatite-Pyroxenite	Apatite-Carbonate	Apatite-Carbonate-Pyroxenite	Apatite-Magnetite
Mn	79	86	122	112	94	239	115	135	85
Fe	690	757	730	758	742	755	684	586	298
Ni	nd	nd	nd	nd	nd	nd	nd	nd	nd
Cu	nd	nd	nd	nd	nd	nd	nd	nd	nd
Zn	7	10	9	11	6	16	8	15	4
As	345	310	325	340	112	244	213	126	517
Rb	3	1	3	5	nd	3	3	3	6
Sr	363	385	275	360	420	315	349	283	332
Y	1590	1589	1113	1224	1570	1164	1315	1210	292
La	4380	4130	3934	3930	4170	2420	4150	2080	2969
Ce	11390	10575	9740	9030	9470	6680	9630	5800	3580
Pr	1080	958	802	767	933	645	859	638	230
Nd	4290	4020	3560	3240	3585	2850	3670	2640	889
Sm	735	706	463	577	684	558	584	385	100
Eu*									
Gd	512	472	279	424	522	420	368	273	nd
Tb*									
Dy	263	262	230	256	255	231	245	203	nd
Ho	nd	nd	nd	nd	nd	nd	nd	nd	14
Er	149	149	108	141	155	119	138	119	30
Tm	nd	nd	nd	nd	nd	nd	nd	nd	nd
Yb	103	109	65	91	100	70	79	80	15
Lu	nd	nd	nd	nd	7	nd	nd	nd	10
Pb	nd	nd	nd	nd	nd	nd	nd	nd	nd
Th	88	83	63	111	130	51	83	44	115
U	nd	nd	11	11	8	nd	nd	nd	nd
Σ La-Lu	22902	21381	19181	18456	19881	13993	19723	12218	7837

nd = not detected, * = values not reliable due to interferences

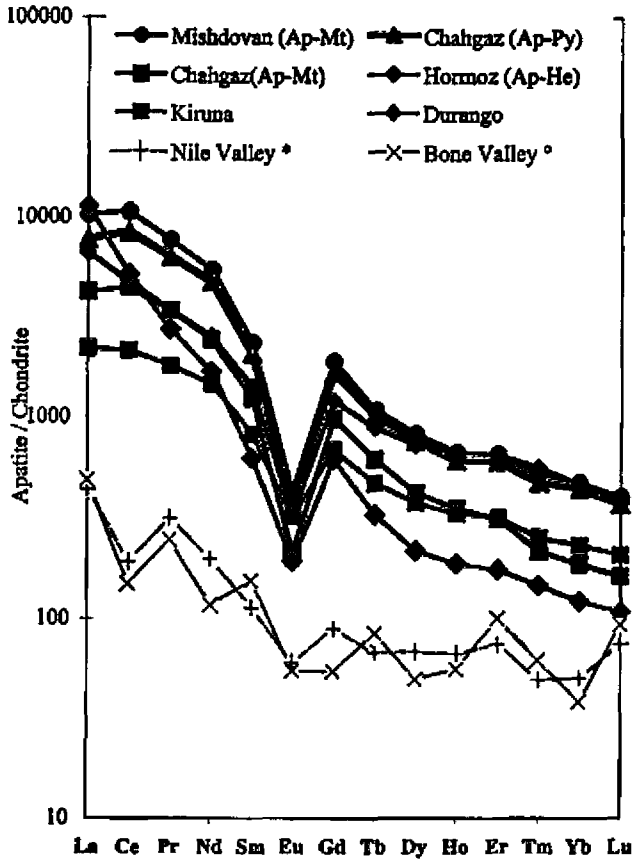


Figure 9: Chondrite-normalised REE patterns of Bafq apatites compared to apatites from Kiruna and Durango (Table 2) and sedimentary phosphorites (* El Kammer et al., 1979; ° Altschuler et al., 1976).

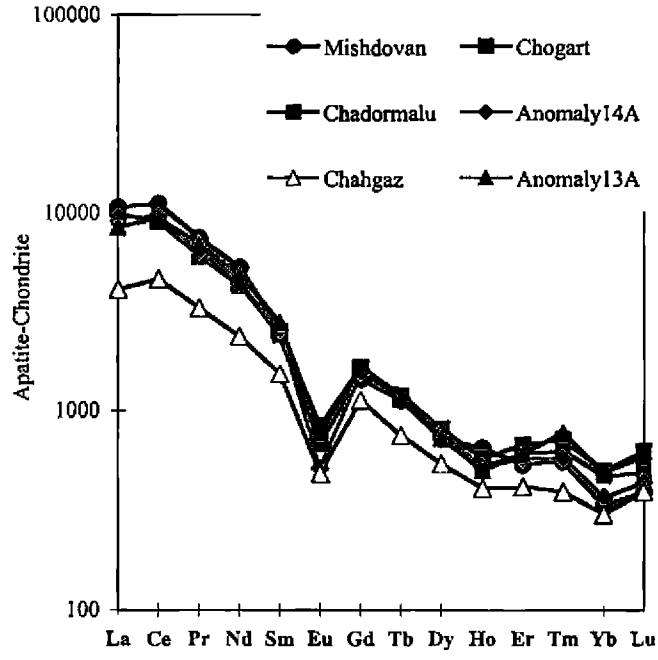


Figure 10: Chondrite-normalised REE patterns of Bafq apatites after analytic data of NISCO (1980).

is able to explain the mode of emplacement of these two different style of mineralisation in the Bafq district.

Comparative Occurrences

REE concentrations and their pattern of distribution can be used as petrological tracers for the classification of the apatites. Roeder et al. (1987) showed that apatites of carbonatitic affinity, commonly exhibit high total REE contents, strong LREE enrichment, and low Y/REE ratios. A similar behaviour was revealed by the study of several other occurrences as compiled in Fleischer & Altschuler (1986), who stated that apatites associated with iron ores resemble those of carbonatites, alkalic ultramafic, and ultramafic rocks. Differing REE patterns are rarely noted. For example Campbell and Henderson (1997), reported a flat, MREE (Mid Rare Earth Element)-enriched chondrite-normalised pattern in apatites with a probable, carbonatitic origin.

For a genetic classification of the Bafq apatites three classes of apatite occurrences can be considered:

1 Iron Ores

Apatite-iron ores comprising both the low-Ti Kiruna-type and the high-Ti iron ores (nelsonites) commonly have REE contents ranging from some tenths of a percent, up to 10 wt%. The chondrite-normalised distribution patterns for the apatites associated with these two groups of iron ores are similar and show enrichment in LREE and a negative Eu anomaly (Kolker, 1982; Landa et al., 1983; Van Marcke de Lummen, 1985; Roeder et al., 1987; Barker, 1995; Frietsch & Perdhal, 1995), as in the Bafq apatites. Frietsch & Perdhal (1995) reported an exception within the Kiruna-type iron ores from the Avnik apatite-magnetite deposit in Turkey, which differs in that it lacks LREE fractionation.

Rare earth concentrations within apatites from Kiruna and Durango (see Tables 2 & 3) are one half to a quarter of that of most of the Bafq apatites. Their chondrite-normalised pattern, however, is similar to the Bafq apatites. The slightly positive, higher Ce anomaly of the Bafq apatites exists also in Kiruna apatite, but is absent in those from Durango(see Fig. 9).

There are many factors which influence the distribution of REE in a mineral. These include ionic radius, ionic charge, temperature, pressure and composition of a system and the fO_2 (Henderson, 1996; Roeder, et. al., 1987). The oxidation states of the Eu and Ce also effect their geochemical behaviour. A common explanation for the negative Eu anomaly in many igneous rocks is its removal by the partitioning of Eu^{2+} in early fractionated plagioclase, as has been assumed for the negative Eu-anomaly associated with Kiruna-type apatites eg., Oyarzun (1985) and Frietsch & Perdhal (1995). Since the genetic relationship between the apatite-bearing rocks and the host rhyolites in the Bafq district is not documented, the explanation for the negative Eu-anomaly within the Bafq apatites remains unclear.

The Bafq apatites crystallised in two stages (ap_1 and ap_2), both of which are enriched in LREE. In addition, the presence of the Ce-rich minerals monazite and allanite, rather than any other HREE mineral, obviously indicates

Table 4: Cell parameters of Bafq apatites, compared to the apatites of different compositions

Cell Parameter	Mishdovan	Esfordy	Chahgaz	Durango	F-Apatite (ICDD)	Cl-Apatite (ICDD)	OH-Apatite (ICDD)
a	9.413	9.410	9.412	9.437	9.358	9.641	9.418
c	6.876	6.880	6.875	6.879	6.884	6.771	6.884

the availability of a Ce-rich source reservoir, rather than any fractionation process occurring during crystallisation. Gerasimovskiy & Mineyev (1981) noticed that, in the presence of other REE minerals, apatite had lower REE concentrations. There is some doubt over this statement however, since the bulk of the apatite (ap_1) crystallised prior to the other REE minerals allanite and monazite. Consequently, it's chemistry could not be influenced by the incorporation of one or another element into these minerals. Furthermore, even in the presence of abundant monazite and allanite the apatites of these samples were among the most REE-rich encountered. Differences in the REE content of the apatites from various localities seems to be unrelated to the type of provenance (apatite-iron oxide ore or "apatitites"), and reflect the REE concentration of the local reservoirs.

2 *Carbonatites*

The apatite-bearing rocks of Bafq show some striking geological, mineralogical, petrographic and geochemical similarities with carbonatite occurrences worldwide (Anderson, 1986; 1987; Woolley & Kempe, 1989; Bailey, 1993; Morteani & Preinfalk, 1996; Wall & Mariano, 1996; Nothholt, 1997). The apatite-carbonatites containing monazite at Kangankunde, Malawi, described by Wall & Mariano (1996), show some striking similarities in their petrographic features to the Chogart "apatitites". Pecora (1956) recognised the apatite-magnetite ores as one of the carbonatite varieties. These apatite-magnetite occurrences have been variously termed phoscorite (foskorite) or camphorite, particularly by geologists of the Soviet school (Russel et al., 1954; Borodin et al., 1973; Zhuravleva et al., 1976; Landa et al., 1983; Sokolov, 1983).
In carbonatite systems, apatites are generally enriched in REE and may contain up to several per cent. As apatite can crystallise at different stages in the development of a carbonatite system, its REE content may be variable within the same occurrence (Anderson, 1986, 1987; Roeder et al., 1987; Hogarth, 1989; Morteani & Preinfalk, 1996; Wall & Mariano, 1996). Apatite that occurs in carbonatite rocks is commonly enriched in LREE. However, where the complete REE spectrum was available (Anderson, 1986, 1987; Roeder et al., 1987; Hogarth, 1989; Mariano, 1989; Morteani & Preinfalk, 1996; Wall & Mariano, 1996; Wu et al., 1996), they do not reveal the same negative Eu anomaly observed in Bafq apatites.

Carbonates of carbonatitic affinity also generally contain variable concentrations of REE (Anderson, 1986, Morteani & Preinfalk, 1996). The calcite from the "apatitite" rocks of Bafq region however, did not reveal any REE concentrations. This might be due to their incorporation in the earlier formed REE-bearing minerals apatite, monazite and allanite.

The tendency for the REE minerals of the Bafq district to form in the final stages of the paragenetic sequence has also been noted in these carbonatite occurrences. Hydrothermal or volatile fluid systems which generate carbonatites have been documented from different examples around the world and confirm that such processes are predominantly responsible for the formation of REE minerals (Anderson, 1986, 1987; Bailey, 1993; Gieré, 1996; Wall & Mariano, 1996). A kind of "filter-press" texture observed in the Bafq "apatitites" may be explained by the observation of Bailey (1993) who described similar features from carbonatite intrusions that he assumes to have been formed by the emplacement of a near-solidus "mush", with interstitial fluid metasomatising the country rocks. Oscillatory growth zoning of apatite samples observed from Mishdovan most probably reflect fluctuations in the composition of the fluids as argued by Gieré (1996) and not by crystallisation from a melt.

The Mishdovan deposit exhibits apparent sedimentary features, but also some mineralogical and geochemical affinities with the carbonatite-related apatite-magnetite and REE mineralisation described at Bayan Obo (Wu et al., 1996; Campbell & Henderson, 1997) and Olympic Dam (Oreskes & Enaudi, 1990; Hitzman et al., 1992).

The evolutionary history of the Bafq district and the timing of the different styles of mineralisation developed in the district (Fe-REE, Th-U, Pb-Zn, Cu-(Au?)) are obviously complex and have not yet been systematically studied. A rift-related mineralising system is nevertheless accepted by some workers (eg., Haghipour, 1974; NISCO, 1980; Daliran, 1990) and by Samani (1993, 1998), who postulated the generation of carbonatite magma in relation to the rifting.

3 *Marine Apatites*

Parak (1973) postulated that the distribution of the REE in the apatites of the Kiruna ores is similar to that found in sedimentary rocks. This statement of Parak's possibly arose from inaccurate analytical results of apatites. Marine apatites or phosphorites have REE contents which are an order of magnitude lower than Bafq apatites and their REE pattern is marked by an enrichment in Y and a Ce deficiency (see Fig. 9), which reflects the composition of the sea water (Altschuler, 1980). These geochemical particulars exclude

a marine source for both the Kiruna ores and the Bafq apatites.

Conclusions

The consistent spatial and temporal association of apatite-magnetite ores and the "apatitite" rocks in the Bafq region provides conclusive evidence that these two assemblages are cogenetic. The result of the present geochemical study, particularly the REE geochemistry of the apatites, leaves no doubt of a common source for the apatites.

At present, the author can find no conclusive evidence that the apatite-magnetite orebodies of the Bafq region were emplaced as a liquid ore magma. The apatite-iron ores of the Bafq district that were studied most likely formed from a source with a fluid-rich component. In some cases, these super-critical fluids carried early crystallised minerals (mega-crystals) to shallow levels of emplacement. The continental rift tectonic setting of the district, with its associated crustal fractures probably provided pathways from deep magmas and for the volatiles and ore fluids to reach higher crustal levels.

The deposition of the mineralising fluids within the Bafq district took place in a variety of different environments, which would explain the diversity of the mode of occurrence of the deposits:

- Fluids released into a lithified environment, mainly rhyolites and subvolcanic granites, pervasively metasomatised the host and resulted in the formation of the replacement type ores with local formation of the "apatitites". Based on the physio-chemical characteristics of a given deposit, two replacement ore types can be distinguished, namely, (1). A *high-temperature metasomatic type,* which appears to be characterised by non-hydrous silicates and enrichment in "apatitites" (eg., Chogart and Esfordy). (2). A relatively *low-temperature hydrothermal type* with extensive albitisation and hydrosilicates (actinolitisation), which is not apparently associated with "apatitites" (eg., North anomaly).

- Fluids discharged onto the basin floor during sedimentation resulted in the development of synsedimentary stratiform ore bodies. This group comprises two subtypes based on mineral assemblages. (1). *Apatite-magnetite-hematite* type (eg., Mishdovan), and (2). The *Mn-Fe-jaspilite* type (eg., Narigan).

The consistent LREE enrichment on a regional scale in the Bafq district implies a primary LREE-rich reservoir. The homogeneous source chemistry has also played a crucial role in the distribution pattern of REE in the apatites. Small differences in the REE contents of the apatites in individual deposits may have been influenced by local conditions.

The enrichment of REE in the Bafq apatites reflects some affinity with alkaline complexes and carbonatites and is similar to the global Kiruna-type ores, which implies a common genesis.

Acknowledgments

My thanks are due to Dr. A. Hushmandzadeh (Pars Kani Co.) and B. Samani (AEOA) for their constructive discussions on the geology of Iran, to the National Iranian Steel Corporation (NISCO) and many of my Iranian colleagues and the mine workers for their warm support during repeated field visits. My special thanks are due to Dr. J. Walther for his endless support with my research works at the Technical University of Karlsruhe and to Prof. D. Stüben for provision of laboratory facilities. The assistance of Dr. M. Metz (EMPA Heidelberg), Dr. Berner, and V. Zibat (Technical University of Karlsruhe) with analyses is appreciated. Dr. L. Campbell (Kingston University) and an anonymous reviewer for Economic Geology are thanked for their critical review of a previous version of the manuscript. Prof. M. Hitzman (Colorado School of Mines) is specially thanked for his advice in reviewing this work and encouraging me to publish it.

References

Altschuler, Z.S., 1980, The geochemistry of trace elements in marine phosphorites, Part 1: Characteristic abundances and enrichment. SEPM Special Publication 29, 19-30.

Altschuler, Z.S., Berman, S., & Cuttitta, F., 1967, Rare earths in phosphorites: Geochemistry and potential recovery. U.S. Geological Survey Professional Papers 575-B, 1-9.

Anderson, T., 1986, Compositional variation of some rare earth minerals from the Fen complex (Telemark, SE Norway): Implications for the mobility of rare earths in a carbonatite system. Mineralogical Magazine 50, 503-509.

Anderson, T., 1987, Mantle and crustal components in a carbonatite complex, and the evolution of carbonatite magma: REE and isotopic evidence from the Fen complex, southeast Norway. Chemical Geology 65, 147-166.

Bailey, D.K., 1993, Carbonate magmas. Journal of the Geological Society, London, 150, 637-651.

Bakhtiar, I., 1973, Petrographische und lagerstättenkundliche Untersuchungen des Narigan-Granits und seines geologischen Rahmens bei Bafg (Zentraliran). Unpublished Ph.D. thesis, University of Aachen, Germany, 118.

Barker, D.S., 1995, Crystallization and alteration of quartz monzonite, Iron Springs mining district, Utah: Relation to associated iron deposits. Economic Geology 90, 2197-2217.

Borodin, L.S., Lapin, A.V., & Kharchenkov, A.G., 1973, Redkometal'nye kamafority. Formatsiya apatit-forsterit-magnetitovykh porod b shchelochno-ultraosnovnykh i karbonatitovykh massivakh. Nauka, Moscow (in Russian).

Bookstrom, A.A., 1995, Magmatic Features of Iron Ores of the Kiruna Type in Chile and Sweden. Economic Geology 90, 469-473.

Borumandi, H., 1973, Petrograpische und lagerstättenkundliche Untersuchungen der Esfordi-Formation zwischen Mishdovan und Kushk bei Yazd/Zentraliran. Unpublished Ph.D. thesis, University of Aachen, Germany, 174.

Boynton, W.V., 1984, Cosmochemistry of the rare earth elements: Meteorite studies, *in* Henderson, P., ed., Rare earth element geochemistry: Developments in Geochemistry 2. Amsterdam, Elsevier, 63-114.

Campbell, L.S., & Henderson, P., 1997, Apatite paragenesis in the Bayan Obo REE-Nb-Fe ore deposit, Inner Mongolia, China. Lithos 42, 89-103.

Daliran, F., 1990, The magnetite-apatite deposit of Mishdovan, East Central Iran. An alkali rhyolite hosted, "Kiruna type" occurrence in the Infracambrian Bafg metallotect. Heidelberger Geowissenschaftliche Abhandlungen 37, 248 (Ph.D. thesis).

Daliran, F., & Amstutz, G.C., 1991, The magnetite-apatite deposit of Mishdovan: An "alkali rhyolite" hosted Kiruna type ore in the Bafg metallotect, East Central Iran. Proceedings of Third Mining Symposium Iran 2, 263-280.

Daliran, F., Tarkian, M., & Tavaf-Djalali, F., 1994, A new occurrence of davidite from the apatite-magnetite ore deposit of Chogart, Bafg district, East Central Iran. Neues Jahrbuch für Mineralogie, Monatshefte 3, 138-144.

Davoudzadeh, M., Soffel, H., & Schmidt, K., 1986, Contribution to the Paleogeography, stratigraphy and tectonics of the Infracambrian and Lower Paleozoic of Iran. Neues Jahrbuch für Geologie und Palaeontologie, Abhandlungen 172, 245.269.

Dill, H.G., & Kantor, W., 1997, Depositional environment, geochemical facies, and attentive classification system of selected types of phosphate occurrences. Geologisches Jahrbuch D-105, 43.

El-Kammer, A.M., Zayed, M.A., & Amer, S.A., 1979, Rare earths of the Nile Valley phosphorites, Upper Egypt. Chemical Geology 24, 69-81.

Fleischer, M., & Altschuler, Z.S., 1986, The lanthanides and yttrium in minerals of the apatite group: An analysis of the available data. Neues Jahrbuch für Mineralogie, Monatshefte 10, 467-480.

Förster, H., & Jafarzadeh, A., 1994, The Bafg mining district in Central Iran: A highly mineralized Infracambrian volcanic field. Economic Geology 89, 1697-1721.

Frietsch, R., 1984, On the Magmatic Origin of Iron Ores of the Kiruna Type- a Reply. Economic Geology 79, 1949-1951.

Frietsch, R., & Predhal, J.-A., 1995, Rare earth elements in apatite and magnetite in Kiruna-type iron ores and some other iron ore types. Ore Geology Reviews 9, 489-510.

Geijer, P., 1910, Igneous rocks and iron ores of Kiirunavaara, Luossavaara and Tuolluvaara. Scientific and practical researches in Lapland arranged by LKAB: Norstedt, Stockholm, 278.

Geijer, F., & Ödeman, O.H., 1974, The emplacement of the Kiruna iron ores and related deposits. Sveriges Geologiska Undersökning C700, 1-48.

Gerasimovskiy, V.V., & Mineyev, D.A., 1981, Rare earths in apatites from apatite-magnetite ores. Geochemistry International 18(1), 67-72.

Gieré, R., 1996, Formation of rare earth minerals in hydrothermal systems, *in* Jones, A.P., Wall, F., & Williams, C.T., eds., Rare earth minerals: Chemistry, origin and ore deposits. London, Chapman & Hall, 105-150.

Haghipour, A., 1974, Etude gélogique de la région de Biabanak-Bafg (Iran Central): Pétrographie et tectonique du socle précambrien et de sa couverture. Unpublished thesis (Doctorat d'Etat), University of Grenoble, France, 403.

Henderson, P., 1996, The rare earth elements: Introduction and review, *in* Jones, A.P., Wall, F., & Williams, C.T., eds., Rare earth minerals: Chemistry, origin and ore deposits. London, Chapman & Hall, 1-19.

Hildebrand, R.S., 1986, Kiruna type deposits: Their origin and relationship to intermediate subvolcanic plutons in the Great Bear magmatic zone, northwest Canada. Economic Geology 81, 640-659.

Hitzman, M.W., Oreskes, N., & Einaudi, M.T., 1992, Geological characteristics and tectonic setting of Proterozoic iron oxide (Cu-U-Au-REE) deposits. Precambrian Research 58, 241-287.

Hogarth, D.D., 1989, Pyrochlore, apatite and amphibole.Distinctive minerals in carbonatite, *in* Bell, K., ed., Carbonatites: Genesis and evolution. London, Unwin Hyman, 105-147.

Hushmandzadeh, A., 1989, An introduction to the geology of the Biabanak-Bafg region. Proceeding of the seminar on reserves and mining potential of the Yazd department 1988. Ministry of Mines and Metals, 341-371 (in Farsi).

Illin, A.V., 1991, The Proterozoic supercontinent: Its Precambrian rifting and breakup into a number of continents. International Geological Review 1, 1-14.

Kolker, A., 1982, Mineralogy and geochemistry of Fe-Ti oxide and apatite (nelsonite) deposits and evolution of the liquid immiscibility hypothesis. Economic Geology 77, 1146-1158.

Landa, E.A., Krasnova, N.I., Tarnovskaya, A.N., & Shergina, Y.P., 1983, The distribution of rare earths and yttrium in apatite from the alkali-ultrabasic and carbonatite intrusions and the origin of apatite mineralization. Geochemistry International 20(1), 77-87.

Lyons, J.I., 1988, Volcanogenic iron oxide deposits, Cerro de Mercado and vicinity, Durango, Mexico. Economic Geology 83, 1886-1906.

Mariano, A.N., 1989, Economic geology of rare earth elements, *in* Lipin, B.R., & McKay, G.A., eds., Geochemistry and mineralogy of rare earth elements. Reviews in Mineralogy 21, 309-337.

Morteani, G., & Preinfalk, C., 1996, REE distribution and REE carriers in laterites formed on the alkaline complexes of Araxa and Catalao (Brazil), *in* Jones, A.P., Wall, F., & Williams, C.T., eds., Rare earth minerals: Chemistry, origin and ore deposits. London, Chapman & Hall, 227-255.

Mücke, A., & Younessi, R., 1994, Magnetite-apatite deposits (Kiruna-type) along the Sanandaj-Sirjan zone and in the Bafg area, associated with ultramafic and calcalkaline rocks and carbonatites. Mineralogy and Petrology 50, 219-244.

NISCO (National Iranian Steel Corporation), 1976, Report on the results of additional exploration of Chogart iron ore deposit as of 1.12.1975. Unpublished Internal Report, 99.

NISCO, 1980, Report on results of search and valuation works at magnetic anomalies of the Bafg iron ore region during 1976-1979. Unpublished Internal Report, 260.

Nothholt, A.J.G., 1997, The economic geology and development of igneous phosphate deposits in Europe and the USSR. Economic Geology 74, 339-350.

Nyström, J.O., 1985, Apatite iron ores of the Kiruna Field,, northern Sweden: Magmatic textures and carabonatitic affinity. Geologiska Föreningens i Stockholm Förhandlingar 107(2), 133-141.

Nyström, J.O., & Henriquez, F., 1994, Magmatic features of iron ores of the Kiruna type in Chile and Sweden. Ore textures and magnetite geochemistry. Economic Geology 89, 820-839.

Oreskes, N., & Einaudi, M.T., 1990, Origin of rare earth element-enriched hematite breccias at the Olympic Dam Cu-U-Au-Ag deposit, Roxby Downs, South Australia. Economic Geology 85, 1-28.

Oreskes, N., Rhodes, A.L., Rainville, K., Sheets, S., Espinoza, S., & Zentelli, M., 1994, Origins and magnetite deposits at El Laco Chile: New evidence from the field studies, fluid inclusions, stable isotopes, and fission track analysis. Geological Society of America, Abstracts with Programs 26(7), A-379.

Oyarzun, J.M., 1985, La métallogenie Andine: Cadre géologique, pétrologique et géochemique et essai d'intérpretation. Unpublished thesis (Doctorat d'Etat), University of Paris-Sud, France, 864.

Parak, T., 1973, Rare earths in the apatite iron res of Lappland together with some data about the Sr, Th and U content of these ores. Economic Geology 68, 210-221

Parak, T., 1975, Kiruna iron ores are not "intrusive-magmatic ores of the Kiruna type". Economic Geology 70, 1242-1258.

Pecora, W.T., 1956, Carbonatites: A review. Bulletin of the Geological Society of America 67, 1537-1556.

Roeder, P.L., MacArthur, D., Ma, X.-P., Palmer, G.R., & Mariano, A.N., 1987, Cathodoluminescence and microprobe study of rare-earth elements in apatite. American Mineralogist 72, 801-811.

Rhodes, A.L., Oreskes, N., & Sheets, S., 1999, Geology and rare earth element geochemistry of magnetite deposits at El Laco, Chile. *in* Skinner, B.J., ed., Geology and ore deposits of the Central Andes. Society of Economic Geologists Special Publication 7, 299-332.

Russel, H.D., Hiemstra, S.A., & Groeneveld, D., 1954, The mineralogy and petrology of the carbonatite at Loolekop, eastern Transvaal. Transaction of the Geological Society of South Africa 57, 197-208.

Samani, B., Zhuyi, G., Xuetao, G., & Chuan, T., 1994, Geology of Precambrian in Central Iran; On the context of stratigraphy, magmatism and metamorphism. Geosciences, Scientific Quarterly Journal of the Geological Survey of Iran 3(10), 40-63 (in Farsi with English abstract).

Samani, B., 1993, Sagand formation, a riftogenic unit of Upper Precambrian in Central Iran. Geosciences, Scientific Quarterly Journal of the Geological Survey of Iran 2(6), 32-45 (in Farsi with English abstract).

Samani, B., 1998, Precambrian metallogenic in Central Iran. AEOI Scientific Bulletin 17, 1-16 (in Farsi with English abstract).

Sokolov, S.V., 1983, The genetic unity of the apatite-magnetite ores and carbonatites in alkali-ultrabasic intrusions. Geochemistry International 20(2), 86-98.

Stoecklin, J., 1968, Structural history and tectonics of Iran: A review. The American Association of Petroleum Geologists Bulletin 52(7), 1229-1258.

Traxel, K., Arndt, P., Braun-Dullaeus, K.-U., Maetz, M., Reimold, D., Schiebler, H., & Wallianos, A., 1995, The new Heidelberg proton microprobe: The success of a minimal concept. Nuclear Instruments and Methods B-104, 19-25.

Treloar, P.J., & Colley, H., 1996, Variation in F and Cl contents in apatites from magnetite-apatite ores in northern Chile, and their ore-genesis implications. Minereralogical Magazine 60, 285-301.

Van Marcke de Lummen, G., 1985, An Fe-Ti oxides-apatite-biotite (nelsonite) deposit related to the Costabonne granite, eastern Pyrennes. Bulletin de Minéralogie 108, 353-365.

Wall, F., & Mariano, A.N., 1996, Rare earth minerals in carbonatites: A discussion centered on the Kangankunde carbonatite, Malawi, *in* Jones, A.P., Wall, F. & Williams, C.T., eds., Rare earth minerals: Chemistry, origin and ore deposits. London, Chapman & Hall, 191-225

Williams, G.H. & Hushmandzadeh, A., 1966, A petrological and genetic study of the Chogart iron ore body and the surrounding rocks. Geological Survey of Iran, Unpublished Report, 18.

Wright, S.F., 1986, On the magmatic origin of iron ores of the Kiruna type: An additional discussion. Economic Geology 81, 192-206

Wu, C., Yuan, Z., & Bai, G., 1996, Rare earth deposits in China, *in* Jones, A.P., Wall, F., & Williams, C.T., eds., Rare earth minerals: Chemistry, origin and ore deposits. London, Chapman & Hall, 281-310.

Wolley, A.R., & Kempe, D.R.C., 1989, Carbonatites: Nomenclature, average chemical compositions, and element distribution, *in* Bell, K., ed., Carbonatites: Genesis and evolution. London, Unwin Hyman, 1-14

Zhuravleva, L.N., Berezina, L.A., & Gulin, Y.-N., 1976, Geochemistry of rare and radioactive elements in apatite-magnetite ores in alkali-ultrabasic complexes. Geochemistry International 13 (5), 147-166.

PGC PUBLISHING

Knight, J., Joy, S., Cameron, J., Merrillees, J., Nag, S., Shah, N., Dua, G. & Jhala, K., 2002 - The Khetri Copper Belt, Rajasthan; Iron Oxide Copper-Gold Terrane in the Proterozoic of NW India; *in Porter, T.M. (Ed.), Hydrothermal Iron Oxide Copper-Gold & Related Deposits: A Global Perspective*, Volume 2; PGC Publishing, Adelaide, pp 321-341.

THE KHETRI COPPER BELT, RAJASTHAN: IRON OXIDE COPPER-GOLD TERRANE IN THE PROTEROZOIC OF NW INDIA

[1]Joe Knight, [2]Sojen Joy, [1]Jon Lowe, [2]John Cameron, [2]James Merrillees, [2]Sudipta Nag, [2]Nalin Shah, [2]Gaurav Dua & [2]Khamalendra Jhala

[1]*BHP Billiton Exploration, Brisbane, Australia*
[2]*BHP Billiton Minerals India, New Delhi, India*

Abstract - The Khetri, Alwar and Lalsot-Khankhera Copper Belts contain widespread Cu±Au±Ag±Co±Fe±REE±U mineralisation over a 150x150 km area of Rajasthan and Haryana, NW India. Mineralisation is hosted by the mid-Proterozoic Delhi Supergroup, which comprises shallow-water, locally evaporitic, sedimentary rocks, with lesser mafic and felsic volcanic rocks. These rocks have been metamorphosed to the low- to mid-amphibolite facies, deformed into NE-SW striking, doubly-plunging folds, and intruded by numerous 1.5-1.7 Ga syntectonic granitoids and 0.75-0.85 Ga post-tectonic granitoids. Post-tectonic granitoids range from tonalite to syenite, contain hornblende and biotite as the dominant mafic minerals and magnetite, titanite, allanite, apatite, fluorite as accessory phases, and are geochemically characterised by A/CNK ratios <1.1, low Al and Ca, high Th and HFSE, and enrichment in LREE, indicating A-type affinities.

The largest deposits in the Khetri Copper Belt are at Khetri (140 mt @ 1.1-1.7% Cu, 0.5 g/t Au), where mineralisation extends over a >10 km strike-length, is hosted by garnet-chlorite schists, andalusite- and graphite-bearing biotite schists, and feldspathic quartzites, and is sited in sub-vertical NE- and NW-striking shear zones. Mineralisation forms sub-vertical lens, comprising stockworks of massive to vein-hosted chalcopyrite-pyrite-pyrrhotite, which are broadly foliation-parallel but also cross-cut bedding and peak-metamorphic fabrics. Gold, Ag, Co, LREE, Mo, S, U and W are variably co-enriched with Cu. Alteration at Khetri comprises amphibole (hornblende, actinolite, cummingtonite, anthophyllite)-albite-quartz-biotite-scapolite-chlorite-carbonate, with magnetite and haematite as dominant oxide phases.

Directly to the east of Khetri, a 50 km wide by > 100 km zone of calc silicate and albite-haematite alteration overprints and cross-cuts metamorphic fabrics. Calc silicate alteration comprises coarse-grained clinopyroxene-hornblende-epidote-apatite-scapolite-titanite-magnetite, whereas albite-haematite alteration comprises assemblages of albite-amphibole-haematite-magnetite-calcite, with variable K-feldspar, biotite, epidote, scapolite, titanite, apatite and fluorite, and locally abundant pyrite and chalcopyrite. Albite-haematite alteration is spatially related to vein systems and breccias, which commonly contain Cu-Au mineralisation, massive magnetite-haematite vein-deposits, fluorite mineralisation and rare uraninite deposits. Calc silicate alteration occurs on the margins of the Khetri Copper Belt, whereas albite-haematite alteration forms a central core to the Belt and locally overprints calc-silicate assemblages. A SHRIMP U-Pb titanite age in the assemblage albite-haematite-amphibole-calcite-titanite constrains the timing of regional alteration to 847±8 Ma. This overlaps the fission-track ages of garnet from ore assemblages at the Madhan-Kudhan Cu mine at Khetri (897±125 Ma).

There is a variation in the sulphide-oxide mineralogy of Cu deposits across the >100 km wide Khetri Copper Belt, with four dominant types recognised: (1) chalcopyrite-pyrite-pyrrhotite ores hosted by graphitic schists at Akwali, in the west, (2) chalcopyrite-pyrite-pyrrhotite-magnetite-haematite ores at Khetri and Kho Dariba, in the east, (3) magnetite-haematite-chalcopyrite-pyrite ores hosted by albite-haematite alteration, in the central part of the Khetri Copper Belt, and (4) haematite-chalcopyrite-baryte ores in the eastern part of the Belt. Types (1) and (2) are hosted by mainly reduced rock types and can be classified as iron sulphide Cu-Au deposits, whereas types (3) and (4) are iron oxide Cu-Au deposits hosted by oxidised rocks. Copper mineralisation in the Khetri Copper Belt is epigenetic, broadly synchronous with late (0.75-0.85 Ga) A-type granitoid emplacement, and has a mineralisation and structural style, and regional- and deposit-scale alteration assemblages comparable to known IOCG and iron-sulphide Cu-Au mineralised districts.

Introduction

Recent research on iron oxide copper-gold (IOCG) deposits has highlighted the diverse styles of mineralisation within this important deposit class (eg., Haynes, 2000; Hitzman, 2000). Hitzman et al. (1992) and Hitzman (2000) document a continuum of IOCG deposit-styles, from magnetite-apatite deposits to iron oxide copper-gold deposits. Haynes (2000) describes a broader transition from iron-oxide Cu-Au deposits, in which Cu sulphides are associated with dominant magnetite or haematite, to iron sulphide Cu±Au deposits, in which chalcopyrite is associated with abundant pyrrhotite and pyrite. The mineralogy and metal-associations of these deposits are controlled by the depth and temperature of mineralisation, the composition of the mineralising fluid (s), and the oxidation states of host-rocks to ore (Haynes, 2000). Iron oxide Cu-Au deposits are hosted by oxidised rocks, whereas iron-sulphide Cu-Au deposits are mainly hosted by reduced carbon-bearing rocks. Unifying features of IOCG and iron sulphide Cu±Au deposits in a given terrane are the association of Cu-mineralisation with regional-scale fault-controlled sodic alteration, comprising albite, magnetite, haematite, actinolite, with variable scapolite, chlorite, epidote, carbonate and titanite, the dominantly brittle nature and late-timing of ore-hosting structures, a likely common hydrothermal-fluid source and composition, and a similar timing of ore deposition (Haynes, 2000).

In this paper, a range of IOCG and iron sulphide Cu-Au deposits are described from the Khetri, Alwar and Lalsot-Khankhera Copper Belts located in Rajasthan and Haryana States, NW India. These Belts form a 150x150 km NE-striking zone of rocks, which hosts numerous Cu±Au±Ag±Ba±Co±Fe±Mo±U±REE deposits (Fig. 1). Host rocks to mineralisation are metamorphosed volcano-

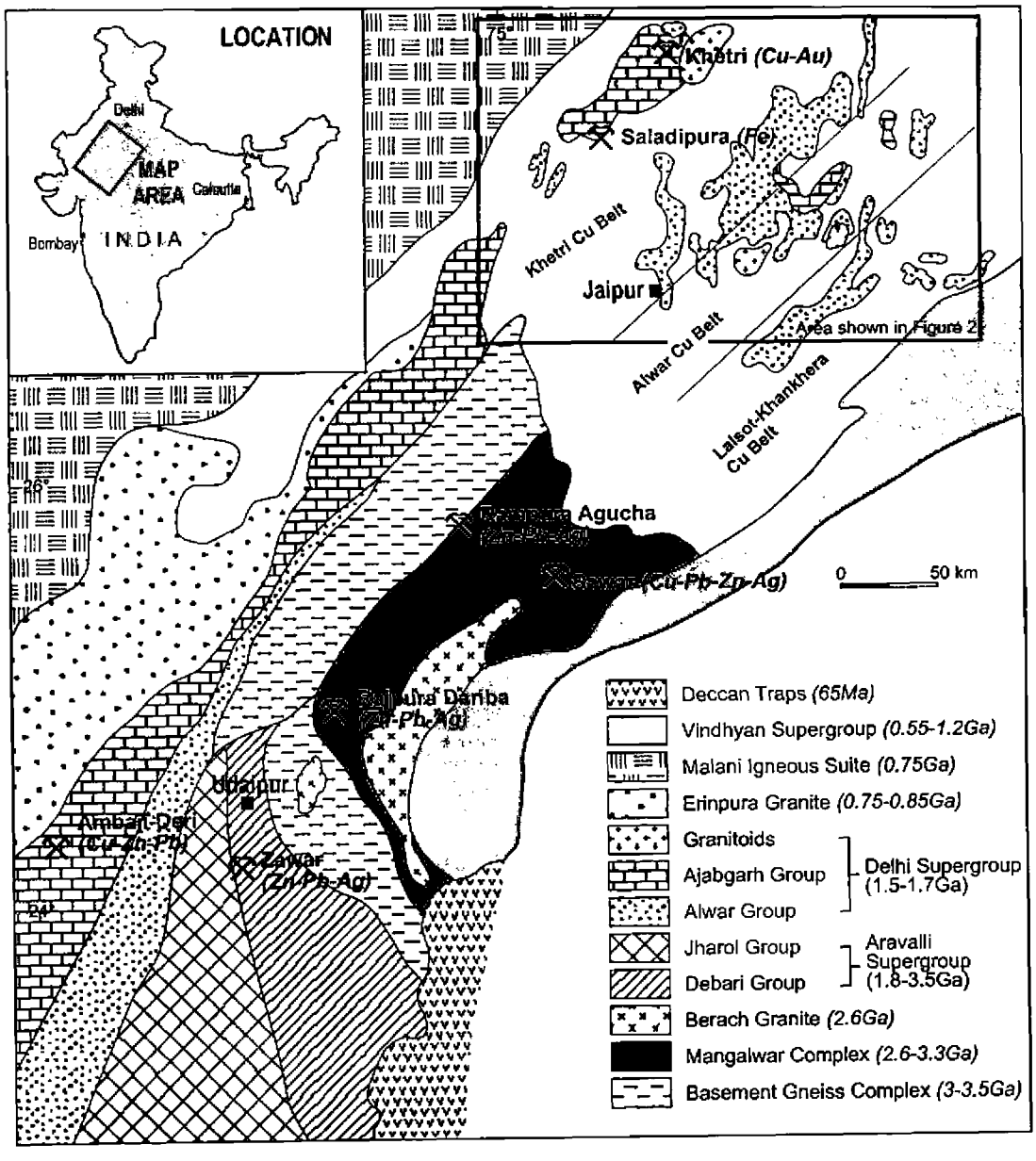


Figure 1. Simplified geology of Southern Rajasthan showing locations of major base metal deposits.

sedimentary rocks of the mid-Proterozoic Delhi Supergroup and, as demonstrated below, Cu deposits within these Belts display common structural controls, ore and alteration mineralogy, and geochemical associations. All belts are therefore described here and the entire copper-mineralised region is referred to as the Khetri Copper Belt (KCB). The KCB is located in the north of Rajasthan which contains major mid-Proterozoic Pb-Zn-Ag deposits at Rampura Agucha (61 Mt @ 13.47% Zn, 1.93% Pb, 45 g/t Ag), Rajpura Dariba (20 Mt @ 2% Pb, 7% Zn, 100 g/t Ag) and Zawar (45 Mt @ 2% Pb, 4% Zn, 50 g/t Ag), and massive pyrite-pyrrhotite±base-metal sulphides deposits at Saladipura (Fig. 1).

Three main models have been proposed for the genesis and timing of mineralisation in the KCB: (1) syngenetic models where the ores formed during sedimentation or diagenesis and were subsequently metamorphosed (eg., Sarkar et al., 1974; Sarkar and Dasgupta, 1980; Basu 1986), (2) hydrothermal models in which mineralisation formed epigenetically, synchronous with, and potentially genetically related to, late granitoid-emplacement (Roy Chowdhury and Das Gupta, 1965; Banerjee 1976) and (3) a combination of models (1) and (2) involving syngenetic mineralisation with subsequent remobilisation and overprinting hydrothermal mineralisation (eg., Das Gupta, 1974). Other research has alluded to the presence of iron oxide copper gold (IOCG)-associated regional alteration in the KCB. Heron (1922), Ray (1987) and Ray and Ghosh (1989) documented the occurrence of 'albitites' in the Khetri region. Ray (1990) defined the "Albitite Line" of northern Rajasthan, a 170 km NNE-trending lineament extending SW from Khetri, characterised by intrusions of albitite, comprising massive pink-red equigranular albite. Das Gupta (1968), Basu and Narsayya (1982, 1983) and Ray (1987, 1990) documented widespread albitisation, fenitisation and Fe-Ti oxide-uraninite-molybdenite-Cu-Fe sulphide-fluorite-calcite mineralisation in the northern part of the KCB and interpreted an igneous origin for the "albitites". Ray (1990) proposed that the "Albitite Line" represents a major intracontinental rift system. In none of these papers however, were the alteration characteristics linked to the Cu deposits at Khetri or the widespread Cu mineralisation in the KCB.

This paper describes the regional geological setting, and nature of wallrock alteration and mineralisation in the KCB, and proposes that Cu±Au±Ag±Co±Fe±REE±U mineralisation was deposited after regional deformation and metamorphism. Furthermore, it is demonstrated that the KCB hosts a range of iron oxide Cu-Au and iron sulphide Cu-Au deposits within a regional-scale calc silicate and sodic alteration system.

Regional Geology

Stratigraphy

The KCB is hosted by the >5 km thick Delhi Supergroup (eg., Singh, 1988), which comprises the basal Raialo Group (metamorphosed carbonate, conglomerate and sandstone, mafic and felsic volcanic rocks), overlain by the Alwar Group (metamorphosed conglomerate and sandstone), which is overlain in turn by the Ajabgarh Group (metamorphosed stromatolitic carbonate, siltstone and shale). Minor felsic and mafic volcanic rocks occur throughout the Ajabgarh and Alwar Groups. Within the KCB, a regionally-continuous, stratigraphically-conformable breccia horizon crops-out. This horizon, named the Hornstone Breccia (Heron, 1917), is broadly at the contact between the Alwar and Ajabgarh Groups (Gangopadhyay, 1974) and comprises angular fragments of quartz and quartzite in a massive Fe-rich chert matrix. It may represent a breccia formed by evaporite dissolution (cf., Corella Formation, Mt Isa: Blake et al., 1990). Outcrop in the KCB is dominated by Alwar Group quartzites, which vary from fine-grained equigranular pure quartzite, to weakly feldspathic quartzite and sericitic quartzite. Towards Jaipur and around Kalyanpura, coarse-grained poly-mictic conglomerates are developed. These rocks comprise matrix-supported conglomerates, with subrounded clasts of quartz, chert, carbonate and meta-siltstone. Banded, locally brecciated, amphibole-bearing dolomitic marble also crops out.

The Delhi Supergroup was likely to have been deposited within a series of intra-cratonic rift basins, developed on Archaean basement rocks, with the depositional environment varying from shelf/shallow marine to fluvial (Singh, 1988; Deb and Sarkar, 1990). Dasgupta (1978) suggested a lagoonal, evaporitic environment for the Ajabgarh Group. The depositional age of the Delhi Supergroup rocks is not known; however, the minimum age is constrained to 1691±4 Ma, the SHRIMP U-Pb in zircon age of the syn-tectonic Gothra Granite, east of Khetri (data from this study, see below). Other estimates of the depositional age of the Delhi Supergroup are based on the 1.5-1.7 Ga Rb-Sr whole-rock ages of syn- and pre-tectonic granitoids (Crawford, 1970; Choudhary et al., 1984).

Metamorphism and Structure

Rocks of the Delhi Supergroup have been metamorphosed to the low- to mid-amphibolite facies. Typical metamorphic mineral assemblages are hornblende-plagioclase-garnet in unaltered mafic rocks, and biotite-muscovite-andalusite-sillimanite, staurolite-garnet-muscovite-biotite-quartz and biotite-chlorite-garnet-amphibole in pelitic rocks (Gangopadhyay and Sen, 1967). Lal and Shukla (1975) estimated peak metamorphic conditions to be 500-600°C at 3-5 kb in the northern part of the KCB using mineral equilibria. Sarkar and Dasgupta (1980) estimated similar metamorphic conditions at Khetri (550-600°C at <5.5 kb).

Two main phases of deformation can be recognised in the KCB: early ductile-deformation and late brittle-deformation. Primary rock types contain a sub-vertical, NE-striking foliation, defined by peak metamorphic minerals, and a steeply plunging mineral lineation. The foliation is axial-planar to NNE-trending regional-scale, locally over-turned, doubly-plunging folds, which have been refolded by a set of NW-trending cross folds. These early structures are cross-cut by NE- and NW-striking brittle and brittle-ductile faults, which play an important role in

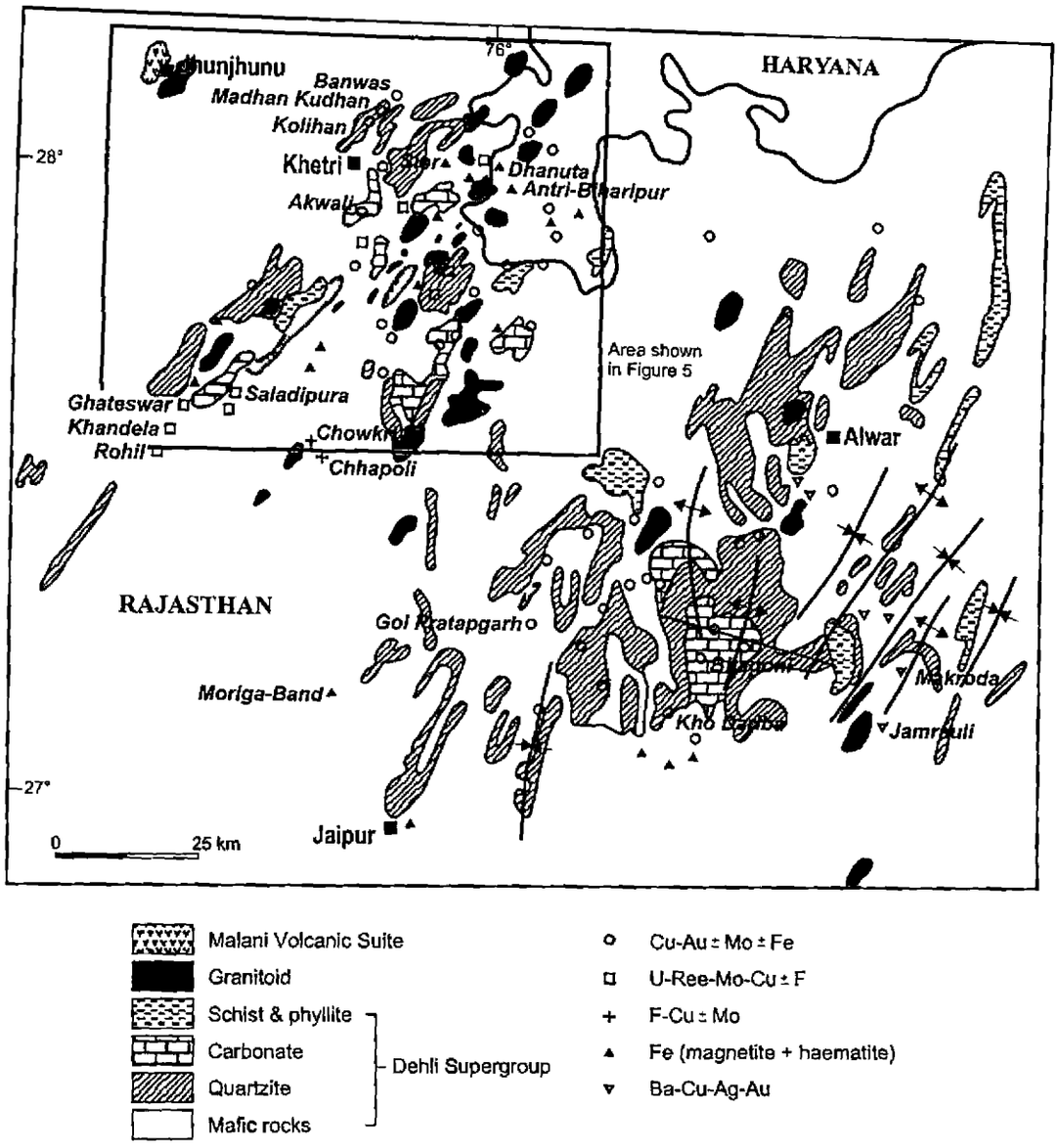


Figure 2. Simplified outcrop geology of the Khetri Copper Belt, Rajasthan showing locations of mineral deposits.

controlling mineralisation and alteration, and are overprinted by late brittle structures (stockworks, breccias, quartz veins), associated with regional alteration (see below).

Granitoids

The KCB is intruded by several poorly exposed granitoids (Fig. 2), which vary from foliated completely-recrystallised bodies, intruded along the axes of regional NNE-trending folds (eg., the Gothra Granite), to small-diameter (<5-10 km) undeformed ovoid stocks that overprint, and therefore probably post-date, peak deformation fabrics. Granitoids range in composition from composite bodies of grey-white tonalite and pink-red syenite, to homogeneous massive pink-red syenite (eg., Bairat), and porphyritic grey tonalite (eg., Sainthal and Pragpura Granites). Foliated granitoid at Ramgarh comprises porphyritic granite-tonalitic granite with minor secondary muscovite.

The pre- or syntectonic, foliated Gothra Granite, located to the east of the Cu-Au deposits at Khetri, is characterised by strong enrichment in the LREE, depletion in the HREE (Fig 3a), no Eu anomaly and a strongly fractionated REE pattern (La_n/Yb_n = 240). The granitoid is enriched in Th and HFSE, and has a very high Na_2O content (8.30%). Primary calcic plagioclase and K-feldspar within the Gothra Granite have been widely replaced by secondary albite, and pods and veins of amphibole-epidote-haematite-feldspar cross-cut the granitoid. In combination, these characteristics suggest that the Gothra Granite has been hydrothermally altered.

Post-tectonic granitoids in the KCB have hornblende and biotite as the dominant mafic minerals and contain magnetite, titanite, allanite, apatite, fluorite and tourmaline as common accessory phases. These granitoids are alkali-rich and meta-aluminous (A/CNK<1.1), with Na/K ratios varying from <1 to >20 (Table 1). Silica contents are

Table 1: **Geochemistry of granitoids from the Alwar and Khetri regions, Rajasthan**

	Gothra	Saladipura	Jat Ki Dhani	Ajit Garh	Ajit Garh	Bairat	Sainthal	Pragpura	Ramgarh
Major elements									
SiO_2 (%)	70.80	69.52	76.58	77.43	76.15	76.58	73.80	73.80	72.51
TiO_2 (%)	0.28	0.58	0.50	0.45	0.45	0.07	0.28	0.27	0.50
Al_2O_3 (%)	13.51	13.09	10.58	11.94	12.07	12.01	14.19	13.15	11.75
Fe_2O_3 (%)	2.67	4.79	3.52	2.16	5.48	1.02	2.99	2.86	4.16
MnO (%)	0.03	0.04	0.02	0.01	0.03	0.01	0.03	0.04	0.03
MgO (%)	0.35	0.76	0.46	0.40	0.32	0.25	0.41	0.48	0.93
CaO (%)	0.71	1.76	0.95	1.44	1.90	0.27	0.84	1.13	0.91
Na_2O (%)	8.30	2.74	4.57	7.43	3.88	7.49	3.22	2.59	2.25
K_2O(%)	0.52	5.64	3.18	0.31	4.78	0.34	7.37	6.10	5.96
P_2O_5 (%)	0.26	0.17	0.08	0.09	0.07	0.01	0.24	0.26	0.41
A/CNK	1.01	0.87	0.83	0.93	0.78	1.05	0.82	0.89	0.86
Na/K	14.33	0.43	1.28	21.19	0.73	19.86	0.39	0.38	0.34
Trace elements									
Ba	117	1080	191	55	1110	213	837	405	763
Hf	6.4	3	5.8	5	5.8	5.2	3.4	2.6	4.4
Li	2.5	25	3	6.5	22.5	15	51	35	81.5
Nb	10.5	21	29.5	27	28	18.5	21.5	18.5	35.5
Rb	20.3	245	98.8	7.2	149	30	496	352	492
Sr	29.6	106	10.7	12.8	38.6	11.1	94.4	61	60.2
Ta	1.1	1.7	3.15	1.9	2.5	2.6	2.25	1.5	3.95
V	40	34	24	20	14	8	16	18	34
Y	32.7	59.8	80.5	82.4	91.6	36.3	30.4	15.9	41
Zr	219	110	199	160	175	116	114	94	155
U	8.8	2.35	6.35	3.85	6.2	17.5	16.3	4.65	10.9
Th	85.3	37.3	41	28.5	28.8	74	34.5	28.3	43.5
Metals and ore elements									
Au (ppb)	bdl	bdl	bdl	bdl	bdl	bdl	1	bdl	bdl
Ag	bdl	bdl	bdl	bdl	bdl	bdl	bdl	bdl	bdl
Bi	bdl	bdl	bdl	0.1	0.8	bdl	0.3	0.1	2.3
Cu	67	10	15	10	15	44	101	119	62
Mo	3	1.2	0.4	2.6	2.2	1.8	2	0.4	2.4
Ni	8	8	4	4	6	6	42	8	10
Pb	10	26	3	8	40	8	53	45	27
Pt (ppb)	bdl	bdl	bdl	bdl	bdl	bdl	bdl	bdl	bdl
Pd (ppb)	bdl	bdl	bdl	bdl	bdl	bdl	bdl	bdl	bdl
S	100	60	40	40	140	60	120	220	120
Sb	bdl	bdl	bdl	bdl	bdl	bdl	bdl	bdl	bdl
W	1	1	bdl	0.5	1	1	1.5	1.5	3.5
Zn	13	47	11	22	23	11	66	55	36
Rare earth elements									
La	870	86.1	79.9	33.5	74.1	38.4	46.3	37.9	66.1
Ce	1680	196	130	104	151	65.4	101	84.9	146
Pr	167	20	18	14.6	17.1	8.02	11.3	10.1	17.1
Nd	523	71.6	71	62.5	66.1	27.6	42	37.3	63.5
Sm	81.6	13	14.6	14	14.5	5.6	8.6	8.05	11.7
Eu	15.5	1.64	1.82	2.16	2.32	0.4	0.88	0.58	0.72
Gd	51.6	11.2	14.6	14.4	14.6	5.2	7.2	6.8	9.2
Tb	4.48	1.72	2.36	2.28	2.36	0.94	1	0.9	1.3
Dy	14.2	10.7	15.5	14.9	15.3	6	6.1	4.2	7.45
Ho	1.54	2.12	3.08	3.06	3.2	1.34	1	0.56	1.38
Er	3.65	6.3	9.3	8.9	9.6	4.45	2.75	1.1	3.75
Tm	0.38	0.92	1.38	1.3	1.4	0.76	0.38	0.12	0.54
Yb	2.4	5.85	9.45	8.25	9.2	5.25	2.25	0.6	3.3
Lu	0.3	0.8	1.4	1.16	1.34	0.78	0.3	0.06	0.42
(La/Lu)n	294.6	10.9	5.8	2.9	5.6	5.0	15.7	64.2	16.0
(La/Yb)n	239.4	9.7	5.6	2.7	5.3	4.8	13.6	41.7	13.2
Eu*	0.7	0.4	0.4	0.5	0.5	0.2	0.3	0.2	0.2
La/Sm	6.5	4.0	3.3	1.5	3.1	4.2	3.3	2.9	3.4
Gd/Yb	17.3	1.5	1.2	1.4	1.3	0.8	2.6	9.1	2.2
Total REE	3415.7	428.0	372.4	285.0	382.1	170.1	231.1	193.2	332.5

Elements were analysed using a combination of ICP-MS and ICP-OES techniques. Bdl = below detection limit.

generally uniform (69.5-77.4%), and the granitoids have low Al and Ca, high Th (28.3-85.3 ppm) and moderate enrichment in the HFSE (Fig 3b). Post-tectonic granitoids in the Khetri region are moderately enriched in LREE, moderately depleted in HREE, have pronounced negative Eu anomalies (Fig. 3a), and weakly fractionated REE patterns (La_n/Yb_n varies from 2.7 to 41.7). These mineralogical and geochemical features indicate that post-tectonic granitoids in the KCB have affinities with A-type granitoids (cf., Whalen et al., 1987).

Available age determinations indicate two main phases of granitoid emplacement within the KCB. Pre- and syn-tectonic granitoids have whole-rock Rb-Sr ages from 1.5-1.7 Ga (Crawford, 1970; Choudhary et al., 1984). Gopalan et al. (1979) calculated a whole-rock Rb-Sr age of 1480±40 Ma for the Udaipur and Saladipura granitoids in the southern KCB. The altered Gothra Granite, to the east of Khetri, has a SHRIMP U-Pb in zircon age of 1691±4 Ma (Fig. 4a and Appendix 1). Zircon U-Pb and Rb-Sr whole rock ages of 0.75 to 0.85 Ga characterise post-tectonic granitoids throughout southern Rajasthan, including the KCB (Crawford, 1970; Deb et al., 2001). This suite probably forms part of the so-called Erinpura Suite of granitoids, which comprises a suite of post-tectonic batholiths, comprising pink-white porphyritic granitoids, located to the SW of the KCB (Heron, 1953, Fig. 1).

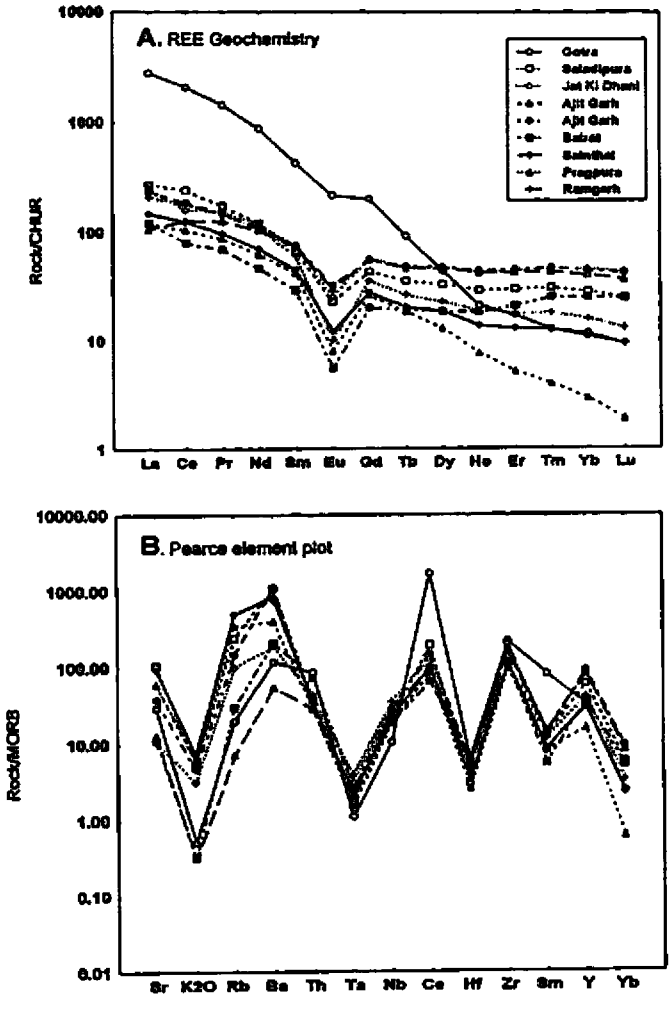


Figure 3: Geochemistry of granitoids in the KCB.

A. Chondrite-normalised REE plot (normalisation factors from Nakamura, 1974).

B. MORB normalised spider plot (element order after Pearce, 1983)

Nature of Mineralisation in the KCB

The largest Cu deposits in the KCB occur at Khetri, which has a total resource of around 140 million t @ 1.1-1.7% Cu and 0.5 g/t Au (production and resources: unpublished Hindustan Copper Ltd data). Smaller Cu deposits occur at Akwali, SW of Khetri, and at Kho Dariba (<1 million t @ 2.5 % Cu) and Bhagoni (5.2 million t @ 1.07% Cu) in the eastern part of the KCB. These deposits are described in further detail below. Numerous other Cu, Cu-Au and Cu±Au±Ag±Co±U±REE prospects have been identified, and partly explored, by the Geological Survey of India throughout northern Rajasthan and the southern part of Haryana (Fig. 2).

Nature of Cu Mineralisation at Khetri

Copper mineralisation at Khetri occurs over a >10 km curvilinear NE-strike length (Fig. 5), which broadly parallels the transition from quartzite-carbonate dominant sequences to the east, to biotite- and andalusite bearing schists to the west. Economic concentrations of Cu and Au at Khetri occur at Madhan Kudhan (66 million t @ 1.12-1.71% Cu, 0.2-0.6 g/t Au, 2-8 g/t Ag), Kolihan-Chandmari (production and resources of around 40 million t @ 1.14-1.62% Cu, 0.2 g/t Au, 2 g/t Ag) and Banwas (resources of around 30 million t @ 1.7% Cu, 0.5-1 g/t Au).

Banwas/Madhan-Kudhan

Mineralisation at Madhan-Kudhan and Banwas is hosted by steeply west-dipping andalusite-bearing phyllites, amphibole-bearing quartzites and garnet-chlorite-amphibole schists, and forms a series of discontinuous layer sub-parallel lodes (Fig. 6a and b). Within lodes, sulphide mineralisation forms: (1) massive zones of pyrite-chalcopyrite-calcite, (2) quartz-chalcopyrite-pyrite-pyrrhotite vein sets (Fig 7a), (3) pyrrhotite-chalcopyrite-amphibole-calcite lenses, and (4) chalcopyrite-pyrrhotite stringers and veinlets. Chalcopyrite-pyrrhotite mineralisation is also hosted by garnet-chlorite-amphibole rock at Madhan Kudhan (Fig. 7b).

Kolihan-Chandmari

In Chandmari, mineralisation is hosted by quartzites, which show a gradation in amphibole and feldspar content across the deposit, with Cu-Au mineralisation broadly sited along the transition between hornblende-bearing and albite-bearing quartzites (Fig. 6d). Mineralisation forms (1) massive amphibole-chalcopyrite-pyrrhotite rock, characterised by a transition in amphibole composition from pale tremolitic amphibole in altered wallrocks to dark green hornblende in ore, (2) massive undeformed quartz-chalcopyrite-pyrrhotite veins, enveloped by albite-hornblende alteration, which cross-cut the regional amphibolite-facies fabric (Fig. 7c), (3) quartz-calcite-chalcopyrite veins, with biotite-chlorite alteration, and (4) stockworks of amphibole-biotite-chalcopyrite-pyrrhotite-

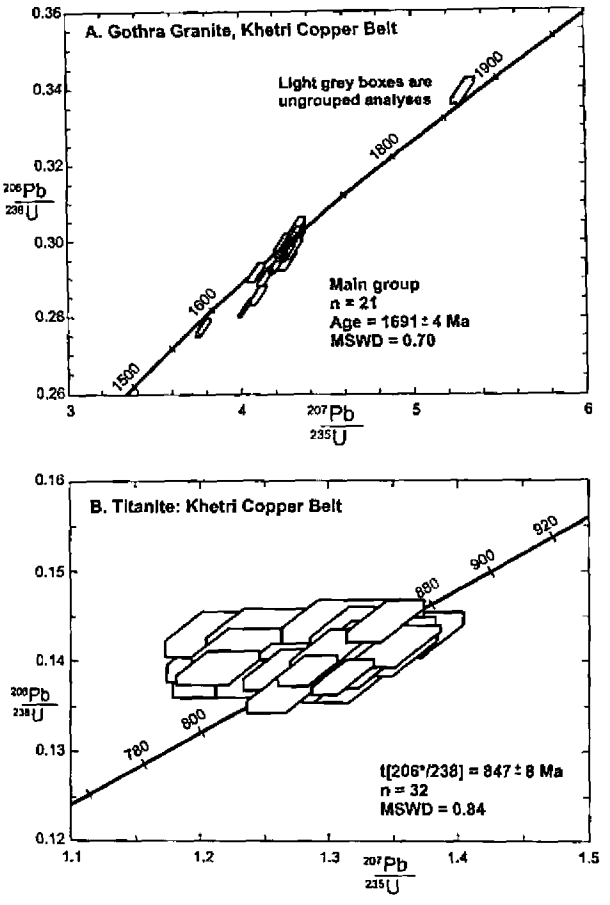


Figure 4: Shrimp II analyses from:

A. Zircons from the Gothra Granite
B. Titanite from regional alteration. Error boxes are 1σ analytical data are tabulated in Appendix 1.

magnetite veins (Fig. 7d). Type 1 mineralisation forms the main ore horizon, with types 2, 3 and 4 hosted in hanging-wall and footwall alteration zones. Disseminated carbonate and magnetite are associated with all styles of mineralisation. Mineralisation at Kolihan is hosted by garnet-chlorite-amphibole schist and comprises massive amphibole-chlorite-chalcopyrite-pyrrhotite-garnet rock with quartz-chalcopyrite-pyrrhotite veins in adjacent wallrocks.

Structural Controls

Mineralisation at Khetri is sited along NE- and NW-striking faults, which cross-cut and therefore post-date regional peak-metamorphic fabrics. At the deposit-scale, orebodies are broadly located along NE-striking faults which are preferentially developed along lithological contacts which dip 40-65° to the W. Sulphide-rich ore-shoots are located at the intersection of steeply-dipping faults. Mineralisation at Madhan Kudhan forms a subvertical cylinder-shaped body at the intersection of NE- and NW-striking faults (Roy Chowdhury and Das Gupta, 1965, Fig. 6a). Other ore bodies at Khetri form series of *en echelon* lenticular lodes, comprising vein sets, breccias and stockworks, which sub-parallel fault zones (Fig. 6). At the vein-scale, mineralised veins and stockworks cross-cut layering and peak metamorphic fabrics. Quartz in mineralised veins at Khetri forms clear, unstrained euhedra and there is little fabric development or evidence of deformation of ore.

Khetri Alteration Assemblages

At the lode-scale, wallrock alteration assemblages contain amphibole, albite, biotite, chlorite and calcite with variable amounts of scapolite, sericite, quartz, magnetite and haematite, and are developed for up to 30-50 m into adjacent wallrocks. Minor magnetite and haematite are disseminated through mineralised veins and altered wallrocks. Distal to mineralisation (>30-50 m), quartzite host rocks contain 10-15% disseminated amphibole, forming radial growths which cross-cut peak metamorphic fabrics. Massive, locally-brecciated Fe carbonate-albite-amphibole-magnetite-epidote±chalcopyrite rocks are developed for several hundreds of metres into the footwall of Cu lodes at Khetri. These rocks grade into quartzites, feldspathic quartzites and carbonate rocks, which contain assemblages of magnetite-feldspar-amphibole-haematite-carbonate, developed for 1-2 km away from known Cu deposits. Magnetite is disseminated throughout footwall quartzites and also forms veinlets cross-cutting and paralleling primary layering. Pink feldspar-amphibole forms small layer-parallel and cross-cutting veinlets, which can also contain epidote and magnetite (Fig. 7e). Regional fabrics and shear zones are commonly overprinted by radial growths of dark green hornblende (Fig. 7f).

Other Significant Cu Deposits in the KCB

Akwali

Akwali, located about 15 km south of Khetri (Fig. 5), is a small Cu deposit (1.23 million t @ 1.7% Cu, 0.5-0.6 ppm Au, 6-8 ppm Ag) hosted by graphitic schist. Mineralisation is located along a sub-vertical NE-striking fault, extends for a strike length of about 5 km and comprises massive zones of chalcopyrite-pyrrhotite-pyrite and carbonate-chalcopyrite-pyrrhotite veins in silicified, carbonate-altered graphite schist. Iron oxides are not present in the ore-zone or associated alteration zones at Akwali. Several other fault-controlled graphitic-schist hosted Cu prospects occur around Akwali.

Kho Dariba

Kho Dariba, located 120 km SE of Khetri (Fig. 2), is hosted by a sequence of massive quartzite, carbonaceous phyllite with cordierite and andalusite, and biotite-muscovite schist. The deposit is sited along the axial-plane of a moderately S-plunging antiform, and consists of a number of small impersistent subvertical shoots (GSI, 1994). These shoots contain veins and stockworks of quartz-pyrrhotite-chalcopyrite and amphibole-biotite-calcite-chalcopyrite-pyrrhotite. Proximal alteration assemblages enveloping vein-sets and stockworks extend for 5-10 m into host rocks and comprise biotite-sericite-carbonate-pyrrhotite-chalcopyrite assemblages. These grade into outer alteration assemblages of amphibole-carbonate-pyrrhotite, with variable biotite and magnetite.

Other Deposits in the KCB

In addition to Cu mineralisation, the KCB hosts deposits of fluorite, Fe-ore, baryte and uranium. The nature of these is summarised below.

Fluorite deposits at Chowkri-Chhapoli are hosted by granitoid, biotite schist and feldspathic quartzite and are associated with calcite-quartz-apatite-hornblende-chalcopyrite veins, with albite-haematite-magnetite wallrock alteration within host rocks (Ranawat, 1979).

Baryte and Cu-baryte deposits occur around Alwar (Fig. 2), in the eastern part of the KCB, where they form subvertical, NE- and NW-striking shear-zone hosted reefs in quartzites and carbonates (Sen Gupta and Bose, 1943; Jain, 1987). Mineralised veins are 1-2 m thick, contain coarse-grained baryte-chalcopyrite-magnetite-haematite, and are enveloped by narrow (<1 m) sericite-haematite-magnetite proximal alteration haloes and wider (5-20 m) distal alteration haloes of albite-haematite-magnetite.

Iron ore deposits, normally comprising sub-equal specular haematite and magnetite, with lesser carbonate, quartz, and apatite, occur throughout the KCB, and generally form massive veins and pods. Iron ore deposits at Morija-Banol, near Jaipur (Fig. 2) are haematite-dominant, with subordinate magnetite and minor apatite, are hosted by coarse-grained quartzites and conglomerates, and form anastomosing veins, reefs and breccia systems with albite-haematite alteration in host rocks (Israili and Absar, 1978). Patwardhan et al. (1987) ascribed a sedimentary origin for magnetite±apatite deposits at Antri-Biharipur, Dhanota and Sior, near Narnaul (Fig. 2), which are hosted by quartzites and carbonates, with abundant pink feldspar-carbonate-epidote-actinolite alteration.

Uranium–Th deposits have been described from several localities in the KCB, but they appear to be concentrated in a NE-SW striking zone lying to the SE of Khetri (Fig. 2). Uraninite-pyrite-pyrrhotite-chalcopyrite-molybdenite-carbonate-fluorite veins at Khandela, SW of Khetri, are hosted by brick-red granitoids, albite-haematite-magnetite breccias and amphibole-albite-haematite-calcite-magnetite rock (Narayan Das et al., 1980; Ray, 1987). Ray (1987) also documented

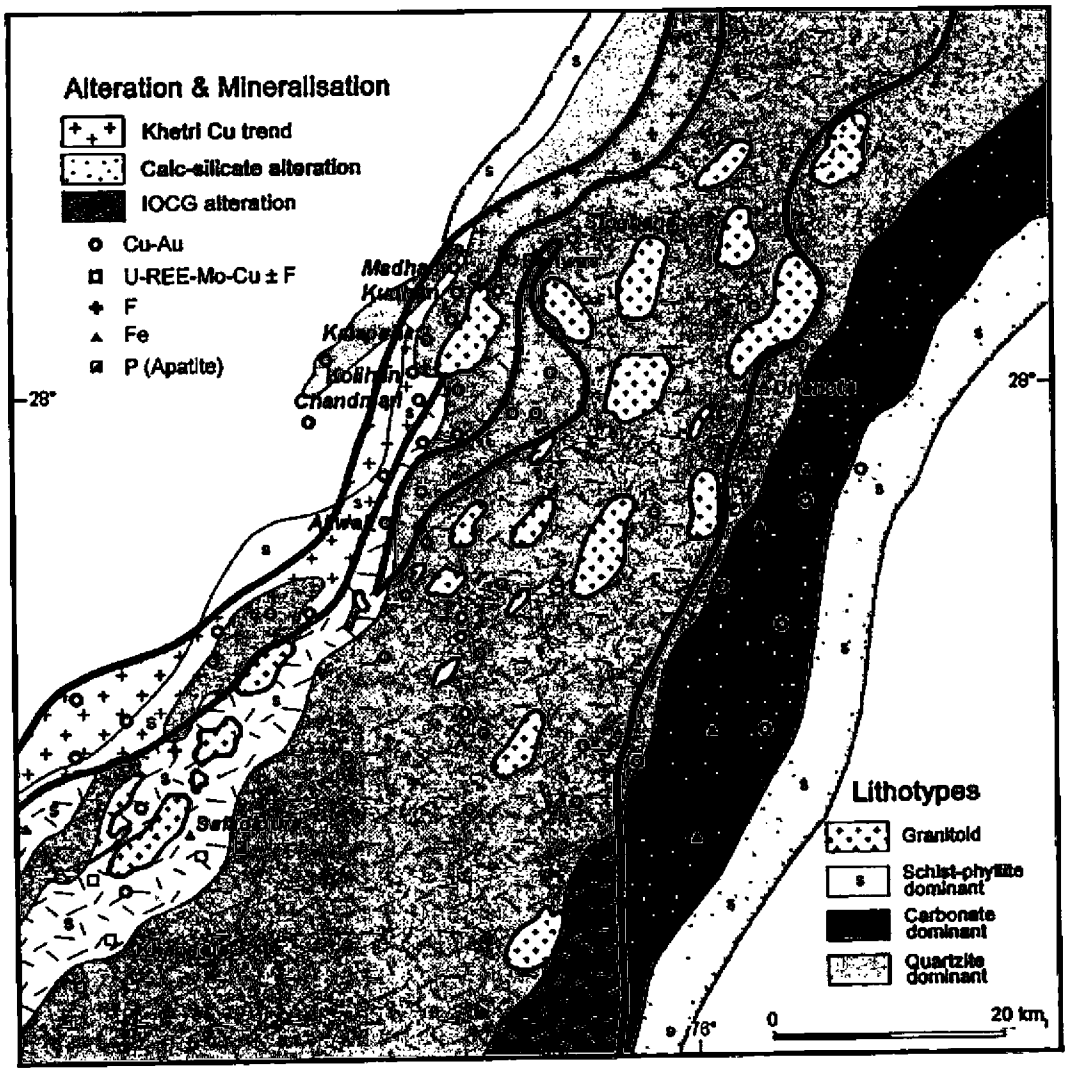


Figure 5: Geology of the Khetri area showing principal rock types, location of mineral deposits, and the distribution of regional alteration types.

chlorite-albite breccias and assemblages of scapolite-tremolite-titanite-apatite-chlorite-calcite associated with U mineralisation at Khandela.

Geochemistry of KCB Cu Ores

Whole rock geochemical analyses of ore samples from Cu deposits at Khetri, Kho Dariba, Gol, Pratapgarh and Nagel, and Cu-baryte deposits at Jamrauli and Makroda (located in Fig. 2) have been determined in order to provide quantitative analytical data on the elemental associations of mineralisation in the KCB. Samples from Khetri include representative composite mill-feed samples from Banwas, Madhan-Kudhan, Chandmari and Kolihan (Table 2). Samples from other deposits are representative grab samples of typical ore types.

Composite feed samples from Khetri show a Cu-Au-Co-S metal association, with elevated Mo and W (Table 2). Lead (<10) and Zn (40-60 ppm) are not enriched, and most metals are at low levels. Of the major elements, only Fe is elevated (14-16%), consistent with the Fe-sulphide rich nature of ore, whereas alkalis are low. Light rare earth elements are moderately elevated and U is low (<2 to 4 ppm). Analysed samples of typical ore from Kho Dariba are enriched in Cu (830-76900 ppm) and Au (6-135 ppb), and variably enriched in Ag (<1 to 12.5 ppm), Ba (14-367 ppm), Bi (0.5-341 ppm), Mo (1.2-204 ppm), Pd (<1 ppb to 35 ppb), U (2.25-63.9 ppm) and LREE (La = 7.5-38.3 ppm). Similar to Khetri, Pb and Zn are present at low levels. Copper deposits at Gol, Nagel and Pratapgarh are also characterised by elevated Cu and Au, with Gol distinguished by elevated As (1620 ppm). Samples of vein material from Cu-baryte deposits at Jamrauli and Makroda are enriched in Ba (3.59-25.3%), Ag (0.5-566 ppm), Au (2-1740 ppb), Cu (65-17700 ppm) and Mo (0.4-39.4 ppm), with variable enrichments in LREE (La = 2.05-23.7 ppm), Bi (1.3-43.5 ppm) and Te (<0.1-18.8 ppm). A Cu-Au signature therefore characterises all copper deposits across the KCB, with associated enrichment in Ag, Ba, Bi, Mo and LREE.

Fluid Properties of Khetri Ores

There are few published data to constrain the P-T conditions and composition of the fluids that deposited, mineralisation at Khetri. Jaireth (1984) analysed fluid inclusions in quartz, pyrite and calcite from three phases of mineralisation identified at Madhan Kudhan and Kolihan. Early barren quartz was deposited from low-salinity, low-density fluids at 540-560°C, whereas ore-related quartz and sulphides were deposited from dense highly-saline (50 wt% NaCl equivalent) fluids in the temperature range 280-480°C. Late unmineralised calcite veins were deposited from low density, moderately saline fluids (23 wt% NaCl equivalent) at 240-260°C. Sahu et al. (1977) estimated that vein quartz from mineralised veins at Kolihan was deposited at >350°C from highly saline fluids (33 wt% NaCl and 17 wt% KCl equivalent).

Sulfur isotope compositions of chalcopyrite and pyrrhotite from Madhan Kudhan ($\delta^{34}S$ = +5.5 to +9.2 per mil) and Kolihan ($\delta^{34}S$ = +5.3 to +8.1 per mil) are broadly similar (Jaireth, 1986), and overlap with the S isotope composition of a number of potential fluid sources, including granitoids, mafic rocks and evaporites (Rollinson, 1993).

Nature of Regional Alteration in the KCB

The KCB contains widespread regional alteration. Two main types can be classified on the basis of mineralogy and texture: (1) calc silicate alteration and (2) albite-haematite alteration. The mineralogy, texture, and temporal and spatial relationships of these alteration types to the widespread Cu-Au-Ag-Ba-Bi-Mo-LREE and Fe ore mineralisation in the KCB are discussed in the following sections.

Calc Silicate Alteration: Mineralogy and Textures

Calc-silicate alteration comprises assemblages of amphibole, clinopyroxene (diopside), scapolite, albite and calcite, with variable epidote, apatite, titanite, specular haematite and magnetite (Fig 7g). Assemblages are generally very coarse grained and are developed in undeformed pods and veins, which both parallel and cross-cut metamorphic and primary layering. Calc silicate minerals also form massive coarse-grained bodies which have entirely replaced primary mineralogy and texture. Typically, alteration consists of simple mono- or bi-minerallic assemblages of clinopyroxene-amphibole, which are cross-cut by veinlets of scapolite, albite or calcite. Titanite, magnetite and apatite are normally present as accessory phases, finely disseminated through altered rocks. Calc silicate alteration is developed in all rock types in the KCB, but is preferentially developed in carbonate rocks where assemblages of coarse bladed pyroxene-amphibole-calcite, with lesser apatite and scapolite are developed. Altered granitoids and quartzites contain veinlets of calcite-pyroxene-apatite-amphibole-magnetite. Elsewhere, assemblages of calc silicate minerals form complex hydrothermal breccias, comprising clasts of amphibole-clinopyroxene altered metamorphosed sedimentary rock, monominerallic amphibole and amphibole ± albite ± haematite, in a matrix of very coarse-grained euhedral calcite (Fig. 7h). These breccias commonly host chalcopyrite-pyrite mineralisation and can contain abundant magnetite.

Albite-haematite Alteration: Mineralogy and Textures

In contrast to calc silicate alteration, albite-haematite alteration is not restricted to particular lithologies, and is developed to varying degrees in all rock types in the KCB. Albite-haematite alteration typically comprises assemblages of pink to red albite-amphibole-magnetite-haematite-calcite, with locally abundant K-feldspar, biotite, scapolite, chlorite, epidote and titanite, and variable but

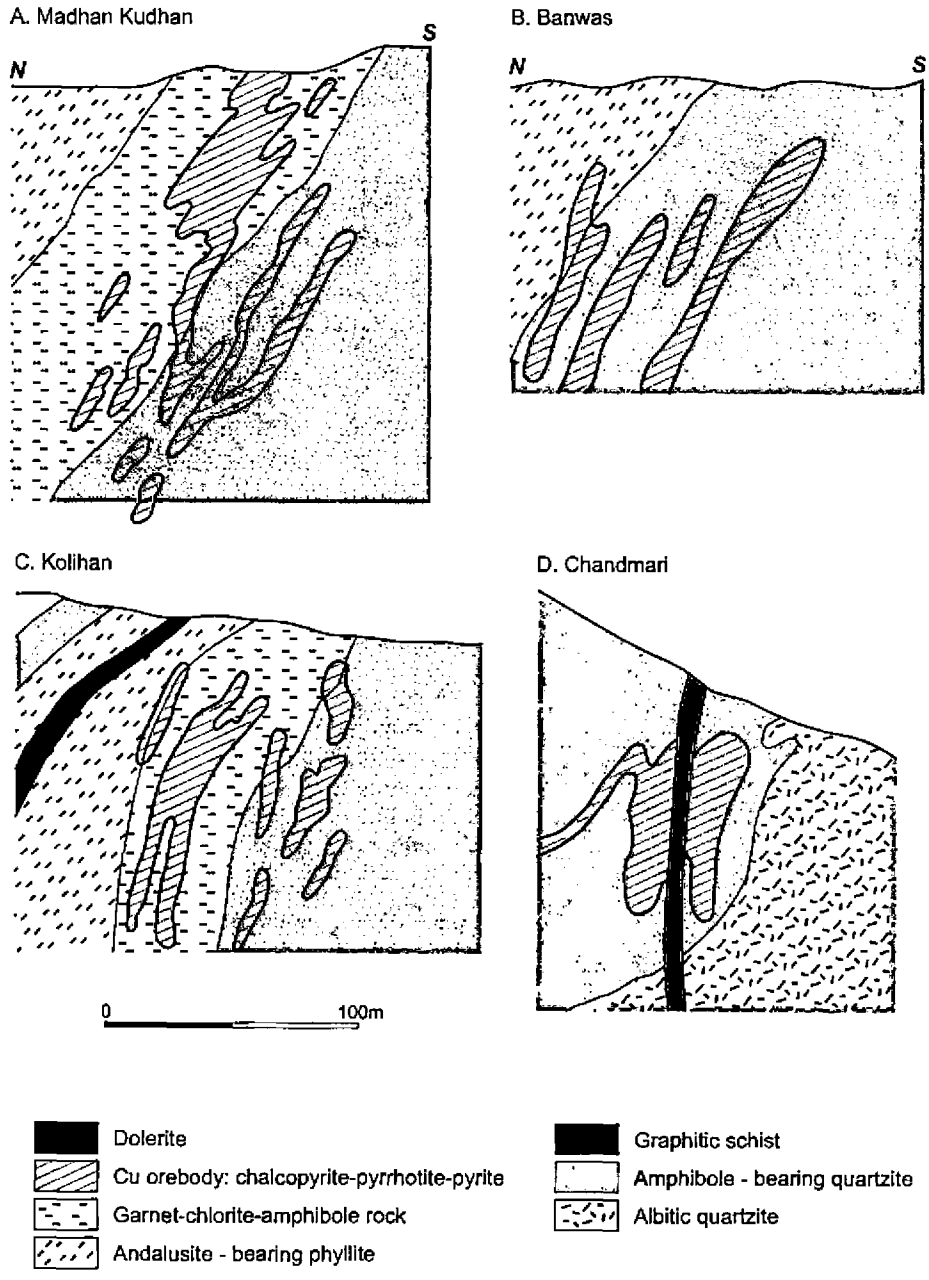
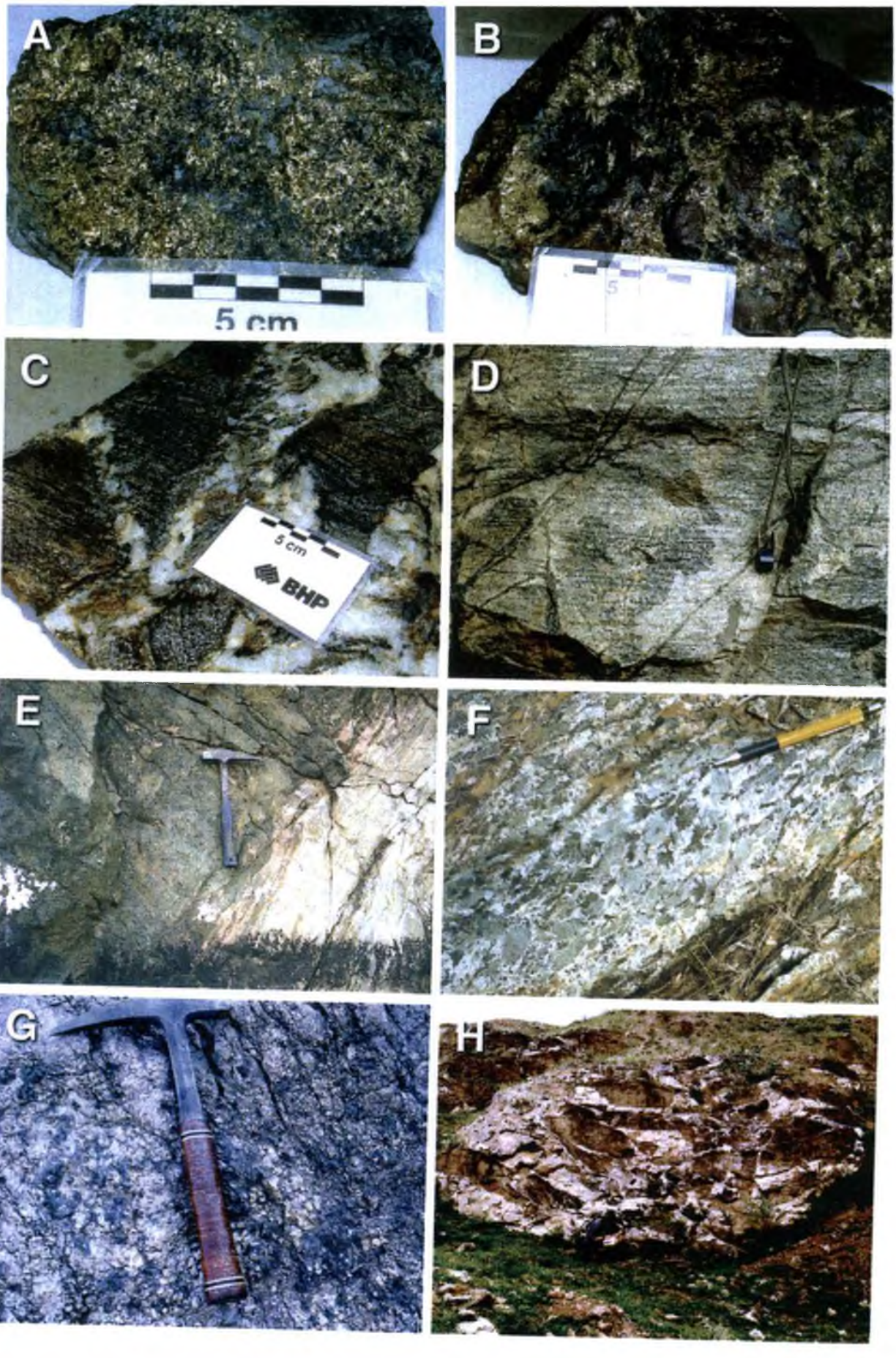


Figure 6: Schematic cross sections through Cu-Au-Ag orebodies at Khetri, Rajasthan (based on unpublished Hindusthan Copper Ltd data).

Figure 7 (facing page): Mineralisation and alteration styles at Khetri and calc-silicate alteration

- **A** Massive chalcopyrite-pyrrhotite ore with amphibole-biotite alteration, Madhan Kudhan.
- **B** Massive to weakly foliated garnet-chlorite-amphibole rock, with coarse chalcopyrite-pyrrhotite, Madhan Kudhan.
- **C** Banded amphibole-plagioclase rock, with weakly disseminated haematite-magnetite, cross cut by quartz-chalcopyrite-pyrrhotite veins, Chandmari.
- **D** Banded-foliated amphibole-albite rock cross-cut by veinlets and stockworks of chalcopyrite-pyrrhotite-magnetite-biotite, Chandmari.
- **E** Steeply dipping feldspathic quartzites overprinted by amphibole-pink albite alteration, Chandmari haul road.
- **F** Strongly foliated coarse-grained conglomeratic rocks overprinted by randomly oriented coarse hornblende, south of Khetri deposits.
- **G** Massive coarse-grained clinopyroxene-amphibole alteration, with lesser feldspar and scapolite and and minor titanite.
- **H** Breccia comprising metre-scale clasts of amphibole-pyroxene altered meta-sedimentary rock in a matrix of very coarse-grained calcite.


A
5 cm
B
C
5 cm
BHP
D
E
F
G
H

Reverse of colour plate, intentionally blank

pink to red and metamorphosed intermediate volcanic rocks contain pink calcic plagioclase partly or completely altered to albite. Primary lithological textures are preserved. With greater degrees of alteration, metamorphic mineralogy and textures are entirely replaced by banded albite-haematite-magnetite-amphibole rock. At the outcrop scale, multiple phases of alteration can be identified: early pink, layer-parallel albite-disseminated haematite is cross-cut by multiple phases of progressively darker red albite-haematite-amphibole alteration (Fig. 8a and 8b).

Copper mineralisation is commonly developed within regional albite-haematite alteration, where it forms pipe-like bodies comprising multiple vein-sets and stockworks, which generally cross-cut banded albite-haematite-magnetite-calcite-amphibole rocks (Fig. 8e). Vein-fill comprises calcite-quartz-amphibole-chalcopyrite-pyrite. Other vein styles commonly developed in albite-haematite alteration include magnetite-haematite-quartz veins, enveloped by albite-haematite-amphibole-magnetite alteration (Fig. 8f), and calcite-apatite-amphibole veins enveloped by pink albite alteration (Fig. 8g). Complex breccia systems are commonly developed and generally comprise angular and rounded fragments of magnetite-amphibole-albite-haematite in a matrix of albite-haematite-calcite-magnetite-amphibole, with minor chalcopyrite-pyrite, and malachite in weathered samples. Establishing paragenetic relationships of discrete phases within regional albite-haematite alteration zones is complicated by multiple overprinting relationships, with several phases of alteration and mineralisation identifiable at outcrop-scale.

Distribution and Zonation of Alteration Types

Regional calc silicate and albite-haematite alteration is developed throughout the KCB, extending over an area of around 100 km wide by 100 km NE strike-length. Alteration probably continues further to the north and south under thick sand dunes and colluvium. In general, the alteration types occur in regional-scale domains. To the east of Khetri, albite-haematite alteration forms a 15-20 km wide central corridor, flanked by >15 km domains where calc silicate alteration is dominant (Fig. 5). These corridors of alteration show a spatial relationship with regional-scale NE-striking faults, which potentially represent re-activated early rift faults (Singh, 1988). The most intense alteration, and associated mineralisation, is developed around intersections of NE- or NNE- and NW-striking faults. At the regional-scale, the most intense albite-haematite alteration appears to be developed where there is a concentration of post-tectonic granitoids to the east of mineralisation at Khetri.

Element-associations of mineralisation are broadly zoned across the KCB, ranging from Cu only at Akwali, to Cu-Au at Khetri and Kho Dariba, to Cu-Au-Fe-Mo-REE-U in albite-haematite regional alteration to the east of Khetri, and Cu-Au-Ba-Ag around Alwar. This chemical variation is reflected in the sulphide-oxide-sulfate mineralogy associated with Cu ores across the KCB, with four dominant types recognised: (1) chalcopyrite-pyrite-pyrrhotite ores hosted by graphitic schists at Akwali in the south west of the KCB, (2) chalcopyrite-pyrite-pyrrhotite-magnetite-haematite ores at Khetri and Kho Dariba, in the east, (3) magnetite-haematite-chalcopyrite-pyrite ores hosted by albite-haematite alteration in the central part of the KCB, and (4) haematite-chalcopyrite-baryte ores in the eastern part of the Belt.

Timing of Mineralisation and Wallrock Alteration

Within the KCB, calc silicate and albite-haematite alteration assemblages, and associated mineralised veins and structures, are generally undeformed and overprint peak-metamorphic assemblages and fabrics. At Khetri, mineralised veins and associated alteration haloes cross-cut regional NE-striking fabrics (eg., Fig. 7c to 7f). Where calc silicate and albite-haematite alteration occur together, assemblages of albite-haematite-amphibole-magnetite appear to overprint calc silicate minerals (Fig. 8h). The silicate mineralogy of wallrock alteration at Khetri (amphibole, biotite-garnet, chlorite) and the mineralogy of both calc silicate and albite-haematite alteration suggest that regional alteration and Cu mineralisation at Khetri formed at relatively high temperatures (low-amphibolite facies).

There are currently no available precise age determinations of Cu mineralisation in the KCB. A mean fission track age of 897±125 Ma has been determined for garnet from ore assemblages at Madhan-Kudhan (Singh et al., 1988). The timing of regional alteration in the KCB is constrained to 847±8 Ma by the SHRIMP U-Pb age of titanite in the assemblage albite-haematite-amphibole-calcite-titanite (Fig. 4b, data are presented in Appendix 1). This suggests that the timing of regional alteration potentially overlaps with both Cu mineralisation and post-tectonic granitoid emplacement.

Relationship Between Cu-Au Mineralisation and Regional Alteration in the KCB

In order to establish whether the KCB is an IOCG terrane, it is necessary to determine the relationship between the widespread Cu mineralisation and regional calc silicate and albite-haematite alteration. The following evidence suggests a genetic and temporal relationship between the two:

1) Both regional alteration and mineralisation are controlled by late brittle and brittle-ductile NE- and NW-striking faults.
2) Textural relationships indicate that Cu mineralisation and regional alteration post-date the main phases of metamorphism and deformation.
3) Similar silicate minerals define ore-related wallrock-alteration assemblages at Khetri (ie., amphibole-albite-biotite-scapolite-magnetite) and regional alteration assemblages, suggesting that they formed from hydrothermal systems with a broadly similar

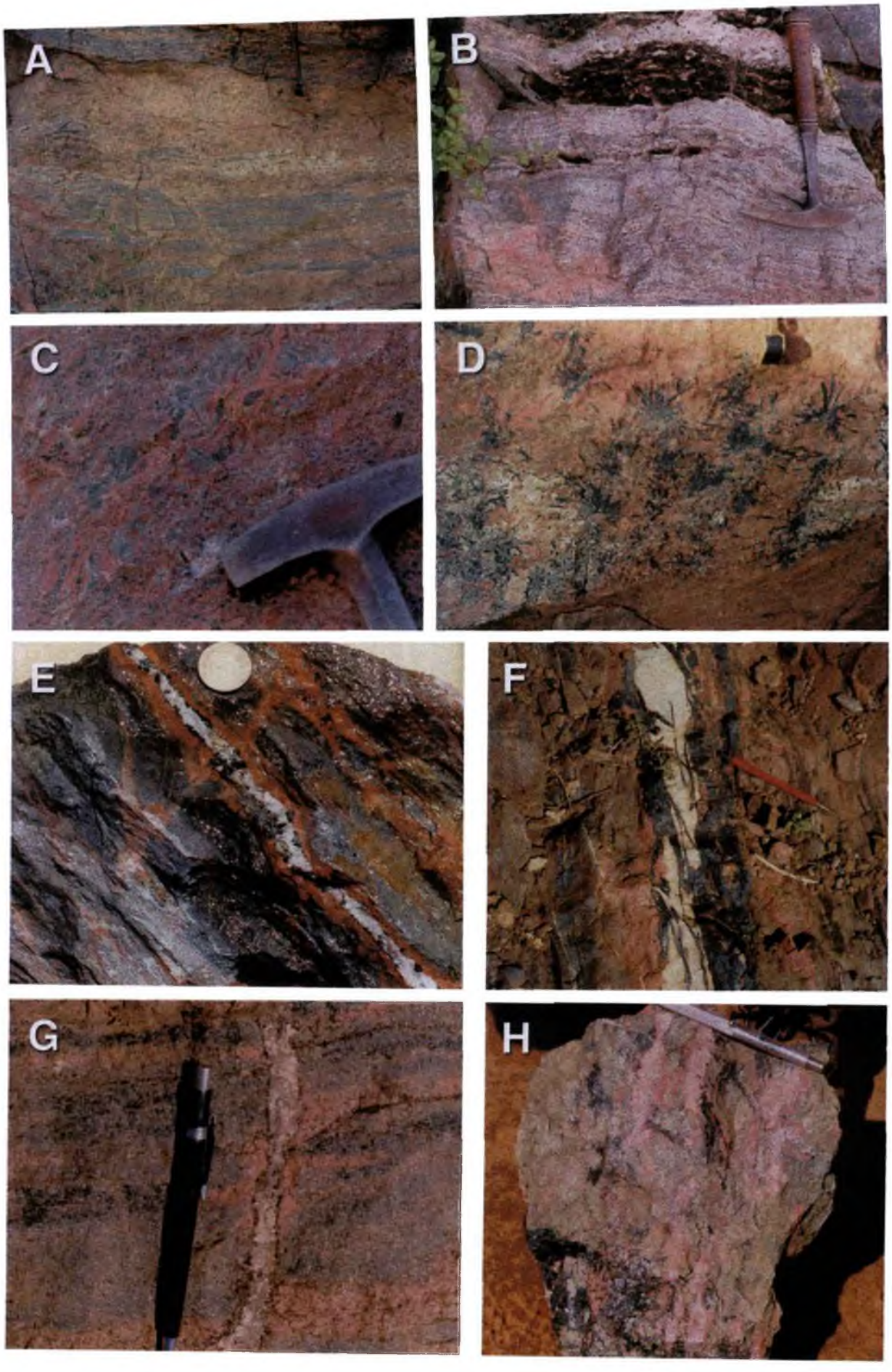
Table 2: Multi-element analyses of composite millhead samples from Khetri and grab samples from other Cu prospects in the KCB

Sample	KCC1	KCC2	KCC3	KCC4	KCC5	KCC6	KCC7	Kho Dariba	Jamrauli	Nagel	Makroda	Pratapgarh	Gol
Major elements (%)													
Si	27.9	19.8	27.1	2.99	2.37	29.2	30.5	na	na	na	na	na	na
Ti	0.28	0.19	0.28	0.03	0.03	0.28	0.28	0.11	0.03	0.03	0.25	0.41	0.59
Al	3.79	2.36	4.26	0.54	0.44	3.75	4.47	3.26	0.84	0.71	4.52	7.12	2.83
Fe	15.9	16.6	14.2	38	42	15	12.4	5.64	0.75	2.13	7.17	2.75	1.19
Mn (pı	1830	595	1700	259	301	1940	1720	932	33	78	464	170	119
Mg	2.31	7.03	2.31	0.39	0.31	2.25	2.45	1.29	0.05	0.06	0.93	0.59	0.1
Ca	0.92	2.94	0.82	0.12	0.11	0.9	0.84	1.69	0.04	0.04	0.13	0.04	0.72
Na	0.61	0.36	0.7	0.1	0.1	0.57	0.71	0.07	0.04	0.03	0.1	0.09	2.25
K	0.74	1.81	0.9	0.16	0.11	0.71	0.94	2.03	0.25	0.12	5.01	3.88	0.09
P (ppr	420	440	440	80	80	440	420	na	na	na	na	na	na
S (ppı	38400	56900	34200	320000	335000	14000	12100	22300	56000	200	3120	200	340
Trace elements (ppm)													
Ba	97	82	115	22	20	128	125	145	253000	54	138000	434	21
Cs	1.7	3.2	1.9	0.3	0.3	1.7	2	na	na	na	na	na	na
Li	11.5	11.5	12.5	1.5	1	13	14	na	na	na	na	na	na
Rb	50.7	154	61.6	8.82	6.76	46.8	61.9	na	na	na	na	na	na
Sr	15.5	14.1	17.3	3.6	3.1	16.2	18.5	na	na	na	na	na	na
Tl	0.3	0.3	0.4	1.4	1.7	0.2	0.3	na	na	na	na	na	na
U	4.15	2.25	4.25	3.25	3.2	4.6	5.1	63.9	2.2	1.65	2.8	5.55	3.3
V	80	40	84	16	16	78	84	na	na	na	na	na	na
Metals and ore elements (ppm)													
Ag	1	1	1	13.5	12	bdl	bdl	5	566	8	2	bdl	bdl
As	9.5	12.5	16.5	60	121	3.5	4.5	1.5	58	30.5	bdl	36.5	1620
Au (pı	273	2250	302	1930	2450	123	143	87	64	1510	215	4	195
Bi	2.2	0.4	4.2	13.6	24	1.4	1.9	14.5	39.5	3.3	1.3	0.2	0.4
Cd	bdl	bdl	bdl	1	1	bdl	bdl	2	bdl	bdl	bdl	bdl	bdl
Cr	85	100	115	20	20	200	110	na	na	na	na	na	na
Cu	13700	25400	11900	180000	141000	2280	1490	18400	17700	53400	6830	203	9890
Co	130	140	118	708	808	108	74	na	na	na	na	na	na
Mo	9	2.4	5.4	35.2	26.4	101	9	204	5.6	2	0.4	23.8	1.6
Ni	82	104	77	350	448	62	56	na	na	na	na	na	na
Pt (pp	bdl	5	5	5	bdl	bdl	bdl	10	bdl	bdl	bdl	bdl	bdl
Pd (pı	5	10	10	25	20	bdl	5	bdl	bdl	5	bdl	bdl	bdl
Pb	6	3	10	24	41	13	8	3	12	bdl	3	10	3
Sb	bdl	0.2	0.2	0.6	1.2	0.2	bdl	2	0.4	0.4	0.2	3.6	0.4
Se	3	6	2	23	24	2	2	bdl	bdl	17	bdl	4	9
Sn	8	9	7	51	43	6	5	bdl	na	na	na	na	na
Te	0.2	0.4	0.2	1.6	1.4	bdl	bdl	bdl	bdl	bdl	bdl	bdl	0.4
W	8.5	4.5	11	3.5	4	10.5	11.5	1.5	1.5	1	3	2.5	3
Zn	61	43	65	396	328	92	54	91	5	17	17	15	12
Rare earth elements (ppm)													
La	37.6	33.6	38.3	13	15.3	39.4	36	10	3.05	13	23.7	5.75	3.65
Ce	71	55.3	73.8	24.9	29.1	75.7	67	20.5	6.85	27.3	51.9	16.1	10.5
Pr	7.76	6.14	8.24	2.8	3.28	8.5	7.4	na	na	na	na	na	na
Nd	32	26.2	33.1	11.5	13.1	33.5	32.3	na	na	na	na	na	na
Sm	7.2	8.6	7.4	2.7	3.2	8.15	7	na	na	na	na	na	na
Eu	2.26	1.68	2.18	0.78	0.92	2.56	2.12	0.36	bdl	1.06	bdl	0.3	0.62
Gd	7.4	11.6	7.4	2.6	3.2	8	7.4	na	na	na	na	na	na
Tb	1	1.82	0.98	0.34	0.38	1.18	0.96	na	na	na	na	na	na
Dy	5	10	5	1	2	6	5	3.85	0.35	2.2	1.35	2	15.1
Ho	1.02	1.78	0.82	0.22	0.26	1.06	0.82	na	na	na	na	na	na
Er	2.4	4	2.15	0.55	0.65	3.15	2.2	na	na	na	na	na	na
Tm	0.32	0.52	0.3	0.08	0.08	0.4	0.3	na	na	na	na	na	na
Yb	2.15	3.15	1.95	0.45	0.45	2.55	2.05	na	na	na	na	na	na
Lu	0.3	0.38	0.28	0.06	0.06	0.36	0.28	0.2	0.06	0.04	0.16	0.26	1.44

SAMPLE DESCRIPTIONS
KCC1. Khetri Mine, Banwas area 180 ML
KCC2. Rougher Feed. Composite sample from Khetri, Kolihan, Chandmari, May 1999
KCC3. Rougher Feed. Composite sample from Khetri, Kolihan, Chandmari, June 1999
KCC4. Final concentrate sample from Khetri, Kolihan, Chandmari, May 1999
KCC5. Final concentrate sample from Khetri, Kolihan, Chandmari, June 1999
KCC6. Final tail sample from Khetri, Kolihan, Chandmari, May 1999
KCC7. Final tail sample from Khetri, Kolihan, Chandmari, May 1999
Elements were analysed using a combination of fire-assay, ICP-MS and ICP-OES techniques. Bdl = below detection limit, na = not analyzed.

Figure 8 (facing page): IOCG alteration and vein styles

- **A** Layered feldspathic-quartzite, with primary layering preserved, overprinted by pink albite-amphibole-calcite-magnetite alteration.
- **B** Layered quartzite with intense layer-parallel amphibole alteration zone, cross-cut by veins and pods of pink (haematite-dusted) albite and amphibole
- **C** Pink-red haematite-dusted feldspar-amphibole-calcite-magnetite-titanite alteration with angular clasts of albitized quartzite.
- **D** Radial clusters of amphibole over-printing massive pink-red haematite-dusted albite-amphibole-magnetite-titanite rock.
- **E** Calcite-chalcopyrite-pyrite-magnetite vein enveloped by red albite alteration in banded biotite-magnetite-pink albite rock.
- **F** Quartz-magnetite-haematite veins enveloped by banded-foliated pink albite-magnetite-amphibole rock.
- **G** Calcite-amphibole-apatite vein, enveloped by pink albite-amphibole alteration, cross-cutting layered feldspathic quartzite with pink albite-amphibole-magnetite alteration.


A
B
C
D
E
F
G
H

Reverse of colour plate, intentionally blank

3) Similar silicate minerals define ore-related wallrock-alteration assemblages at Khetri (ie., amphibole-albite-biotite-scapolite-magnetite) and regional alteration assemblages, suggesting that they formed from hydrothermal systems with a broadly similar composition at similar P-T conditions.
4) Camp-scale alteration assemblages associated with mineralisation at Khetri are characterised by similar mineralogy to regional-scale alteration (ie., amphibole-albite-haematite-magnetite-carbonate, Fig. 7e and f and Fig. 8).
5) Albite-haematite and calc silicate alteration host numerous Cu±Au±Ag±Ba±Co±Fe±U±REE deposits, with no known Cu deposits located outside the area of regional alteration.
6) Diverse styles of Cu mineralisation and associated alteration haloes across the KCB are characterised by similar geochemical enrichments and silicate-sulphide mineralogy.
7) Available age determinations suggest that mineralisation at Khetri and regional IOCG alteration formed broadly synchronously.

Comparison of KCB to Known Iron Oxide Copper-Gold Deposits

Several features of mineralisation and regional alteration in the KCB are similar to those in well-documented IOCG mineralised terranes worldwide (eg., Haynes, 2000; Hitzman, 2000), namely:

1) Mineralisation is sited within a regional-scale alteration system characterised by assemblages of calc silicate minerals (amphibole-clinopyroxene-scapolite-albite-calcite) and assemblages of albite-magnetite-haematite-amphibole-calcite.
2) Copper mineralisation is associated with variable enrichments in Au, Ag, Ba, Co, F, Fe, REE and U.
3) Regional alteration and Cu mineralisation post-date peak metamorphism and deformation.
4) Mineralisation is commonly hosted by, and regional alteration is spatially controlled by, late dominantly brittle faults.
5) Regional alteration and Cu deposits show a broad spatial and temporal relationship with post-tectonic A-type granitoids.
6) Available fluid inclusion data indicate that mineralisation was deposited from highly saline fluids at 280-480°C.

It is proposed therefore that mineralisation in the KCB can be classified as belonging to the Proterozoic iron oxide copper-gold deposit class. Within the KCB, there is a range of iron sulphide Cu-Au and iron oxide Cu-Au deposits and related ore types (cf., Haynes 2000; Hitzman 2000). Mineralisation types include (1) chalcopyrite-pyrrhotite-pyrite ores hosted by reduced graphitic schists (eg., Akwali), (2) chalcopyrite-pyrite-pyrrhotite±magnetite±haematite ores located at the transition between reduced and oxidised rocks (eg., Khetri), (3) magnetite-haematite-chalcopyrite-pyrite deposits hosted by oxidised rocks within regional albite-haematite alteration, (4) magnetite-haematite-apatite deposits (eg., Morija-Banol), and (5) baryte-chalcopyrite-haematite-pyrite ores (eg., Jamrauli, Makroda). Unifying features of mineralisation in the KCB are the structural controls, brittle-nature and late-timing of mineralisation, and the broad geochemical associations and alteration mineralogy of the different ore types.

Summary and Conclusions

The Khetri Copper Belt, and associated sub-parallel copper belts, host widespread Cu±Au±Ag±Co±Fe±Mo±REE±U mineralisation over a 150 km by 150 km area of NW India. These deposits are all:

1) structurally controlled by NE- and NW-striking late faults,
2) texturally late and overprint regional metamorphic and deformation fabrics,
3) enveloped by alteration assemblages containing a combination of the following minerals: albite, amphibole, Fe oxide (haematite or magnetite), carbonate, biotite, epidote, apatite, scapolite and titanite,
4) characterised by simple sulphide assemblages of chalcopyrite±pyrite±pyrrhotite,
5) enriched in Cu and Au, with variable enrichments in Ag, Co, Fe, Mo, REE, U, and
6) sited within regional-scale calc silicate and albite-haematite alteration systems.

These features, in combination with the spatial and temporal association of mineralisation with post-tectonic A-type granitoid emplacement and the gross tectonic setting of the host Delhi Supergroup, suggest that mineralisation in the KCB belongs to the iron oxide copper-gold deposit-class.

Recognition of the likely affinities of Cu mineralisation in the KCB, together with (1) the generally thick deposits of sand, alluvium and colluvium which limit out-crop in northern Rajasthan and Haryana and (2) the lack of IOCG-targeted regional exploration, suggest that the potential for making further discoveries is high.

Acknowledgements

Bob Melsom and Chris Woodman are thanked for drafting the figures, and Sue Buckley is gratefully acknowledged for her assistance in literature searches and data gathering. Tony D'Orazio and Ilam Panneerselvam are thanked for data processing, and Meena Sindhi and Richa Arora for all their assistance during fieldwork in India.

Hindusthan Copper is gratefully acknowledged for allowing access to the copper-gold mines at Khetri.

Marion Marshall and Neal McNaughton are thanked for assistance with the sample preparation and SHRIMP geochronology, respectively. Isotopic data were acquired on a Sensitive High Resolution Ion Microprobe Mass Spectrometer (SHRIMP II), which is operated by a

consortium consisting of Curtin University of Technology, the Geological Survey of Western Australia and the University of Western Australia, with the support of the Australian Research Council.

This paper benefited greatly from reviews by Douglas Haynes and John Ridley who are thanked for their input. This paper is published with the kind permission of BHP Billiton Ltd.

References

Banerjee, A.K., 1976 – Tectonics and ore location in northeastern Rajasthan, India, *Indian Minerals* 29, 1-24.

Basu, S.K., & Narsayya, B.L., 1982 – Carbonatite-alkali metasomatic rock association in the eastern part of Khetri Copper Belt, northeastern Rajasthan, *Indian Minerals* 36, 29-31.

Basu, S.K., & Narsayya, B.L., 1983 – A probable zone of carbonatite and fenitic rock association in the eastern part of the Khetri copper belt, northeastern Rajasthan, *Records of the Geological Survey of India* 113, 7-15.

Basu, S.K., 1986 – Petrology and geochemistry of the Singhana-Muradpur sulphide deposit: A Precambrian syngenetic copper deposit in the Khetri Copper Belt, Rajasthan, India, *Indian Minerals* 40, 1-16.

Blake, D.H., Etheridge, M.A., Page, R.W., Stewart, A.J., Williams, P.R. & Wyborn, L.A.I., 1990 – Mount Isa inlier – regional geology and mineralisation; *in* Hughes, F.E. (ed.), Geology of the Mineral Deposits of Australia and Papua New Guinea, *The Australian Institute of Mining and Metallurgy Monograph* 14, 915-925.

Choudary, A.K., Gopalan, K., & Shastry, C.A., 1984 – Present status of the geochronology of the Precambrian rocks of Rajasthan, *Tectonophysics* 105, 131-140.

Compston, W., Williams, I.S., & Meyer, C., 1984 - U-Pb geochronology of zircons from lunar breccia 73217 using sensitive high mass-resolution ion microprobe, *Journal of Geophysical Research* 89, Suppl. B, 525-534.

Crawford, A.R., 1970 – The Precambrian geochronology of Rajasthan and Bundelkhand, northern Indian, *Canadian Journal of Earth Sciences* 7, 91-110.

Cumming, G.L., & Richards, J.R., 1975. Ore lead isotope ratios in a continuously changing earth, *Earth and Planetary Science Letters* 28, 155-171.

Das Gupta, S.P., 1968 – The structural history of the Khetri copper belt, Jhunjhunu and Sikar districts, Rajasthan, *Geological Survey of India Memoir* 98, 170 pp.

Das Gupta, S.P., 1974 – Geological setting and origin of sulphide deposits in the Khetri copper belt Rajasthan, *Bulletin Geological, Mining and Metallurgical Society of India* 47, 221-238.

Dasgupta, S., 1978 – Sedimentary structures in the Precambrian Delhi Supergroup rocks and their significance, *Indian Journal of Earth Sciences* 5, 177-182.

Deb, M. & Sarkar, S.C., 1990 – Proterozoic tectonic evolution and metallogenesis in the Aravalli-Delhi orogenic complex, northwestern India, *Precambrian Research* 46, 115-137.

Deb, M., Thorpe, R.I., Krstic, D., Corfu, F. & Davis, D.W., 2001 – Zircon U-Pb and galena Pb isotope evidence for an approximate 1.0 Ga terrane constituting the western margin of the Aravalli-Delhi oreogenic belt, northwestern India, *Precambrian Research* 108, 195-213.

Gangopadhyay, P.K., 1974 – Some observations on the nature and origin of 'hornstone breccia' occurring within the Delhi Group in northeastern Rajasthan, *Proceedings 61st Indian Science Congress*, 163

Gangopadhyay, P.K., & Sen, R., 1967 – On the occurrence of andalusite near Bairwas, Alwar District, Rajasthan, *Proceedings 54th Indian Science Congress*, p. 220.

Geological Survey of India, 1994 - Detailed information on copper-lead-zinc ores in Rajasthan-Gujarat, India, *Geological Survey of India Publication.*

Gopalan, K., Trivedi, J.R., Balasubrahmanyan, M.N., Ray, S.K., & Sastry, C.A., 1979 – Rb-Sr geochronology of the Khetri Copper Belt, Rajasthan, *Journal Geological Society of India* 20, 450-456.

Haynes, D.W., 2000 – Iron oxide copper (-gold) deposits: their position in the ore deposit spectrum and modes of origin; *in* Porter, T.M., (ed), Hydrothermal Iron Oxide Copper-Gold & Related Deposits: A Global Perspective, *Australian Mineral Foundation, Adelaide*, pp 71-90

Heron, A.M., 1917 – Geology of Northeastern Rajputana and adjacent district, *Memoir Geological Survey of India* 45, 1-29.

Heron, A.M., 1922 – The geology of Western Jaipur, *Records of the Geological Survey of India* 54, 345-397.

Heron, A.M., 1953 – The geology of central Rajputana, *Memoir Geological Survey of India* 79, 1-339.

Hitzman, M.W., Oreskes, N., & Einaudi, M.T., 1992 – Geological characteristics and tectonic setting of Proterozoic iron oxide (Cu-U-Au-LREE) deposits, *Precambrian Research* 58, 241-287.

Hitzman, M.W., 2000 – Iron oxide-Cu-Au deposits: What, where, when, and why; *in* Porter, T.M., (ed), Hydrothermal Iron Oxide Copper-Gold & Related Deposits: A Global Perspective, *Australian Mineral Foundation, Adelaide*, pp 9-25.

Israili, S.H. & Absar, A., 1978 – Geology and structure of the Morija-Banol iron ore deposits, Jaipur district, Rajasthan, *Geoviews* 4, 17-34.

Jain, V.K., 1987 – Mining and geology of barytes deposit of district Alwar, Rajasthan, *Journal of Mines, Metals and Fuels* 35, 328-330.

Jaireth, S., 1984 – Ore paragenesis and fluid-inclusion thermometry of copper sulphide ores from Madhan-Kudhan and Kolihan deposits, *Special Publication Geological Survey of India* 12, 551-568.

Jaireth, S., 1986 – Igneous source of sulfur of sulphides from Madhan-Kudhan and Kolihan deposits, Khetri Copper Belt, Rajasthan, *Journal of the Geological Society of India* 27, 359-368.

Lal, R.K. & Shukla, R.S., 1975 – Low-pressure regional metamorphism in the northern portion of the Khetri Copper Belt of Rajasthan, India, *Neues Jahrbuch Mineralogy* 124, 294-325.

Nakamura, N., 1974 – Determination of REE, Ba, Mg, Na and K in carbonaceous and ordinary chondrites, *Geochimica et Cosmochimica Acta* 38, 757-775.

Narayan Das, G.R., Sharma, D.K., Singh, G 7 Singh, R., 1980 – Uranium mineralization in Sikar district, Rajasthan, *Journal of the Geological Society of India* 21, 432-439.

Neumayr, P., Ridley, J.R., McNaughton, N.J., Kinny, P.D., Barley, M.E., & Groves, D.I., 1998 - Timing of gold mineralization in the Mt. York district, Pilgangoora greenstone belt, and implications for the tectonic and metamorphic evolution of an area linking the western and eastern Pilbara Craton, *Precambrian Research* 88, 249-265.

Patwardhan, A.M., Patil, D.N. & Sukhtankar, R.K., 1987 – On magnetite quartzites occurring around Narnaul, Haryana, India; *in* Uitterdijk Appel, P.W., & G.L. LaBerge, G.L., (eds), Precambrian Iron Formations *Theophrastus Publications, Athens*, 513-537.

Pearce, J.A., 1983 – Role of the sub-continental lithosphere in magma genesis at active continental margins, *in* Hawkesworth, C.J. & Norry, M.J. (eds), Continental Basalts and Mantle Xenoliths. *Shiva*, 230-249.

Ranawat, P.S., 1979 – Nature of fluorspar mineralization at Chokri-Chhapoli, Sikar-Jhunjhunu districts, Rajasthan, *Journal Geological Society of India* 20, 24-30.

Ray, S.K., 1987 – Albitite occurrences and associated ore minerals in the Khetri Copper Belt, northeastern Rajasthan, *Records of the Geological Survey of India* 113, 41-49.

Ray, S.K., 1990 – The Albitite Line of northern Rajasthan – a fossil intracontinental rift zone, *Journal of the Geological Society of India* 36, 413-423.

Ray, S.K. & Ghosh, S.P., 1989 – The albitite dykes of Dudu sector in Jaipur district, Rajasthan, and their tectonic significance, *Indian Journal of Geology* 61, 129-132.

Rollinson, H.R., 1993 – Using geochemical data: evaluation, presentation, interpretation, *Longman Scientific & Technical, Harlow, Essex*, 352 p.

Roy Chowdhury, M.K. & Das Gupta, S.P., 1965 - Ore localization in the Khetri Copper Belt, Rajasthan, India, *Economic Geology* 60, 69-88.

Sahu, K.C., Panchapakesan, V. & Patil, R.R., 1977 – Fluid inclusion studies on samples from Kolihan Mines of Khetri Copper Belt, *Journal Geological Society of India* 18, 671-674.

Sarkar, S.C., Mukherjee, A.D., Bannerjee, H. & Sarkar, S., 1974 – A note on the pyrite-pyrrhotite mineralization at Saladipura, Sikar district, Rajasthan, *Indian Journal Earth Sciences* 1, 126-128.

Sarkar, S.C., & Dasgupta, S., 1980 – Geologic setting, genesis and transformation of sulphide deposits in the northern part of Khetri Copper Belt, Rajasthan, India – an outline, *Mineralium Deposita* 15, 117-137.

Sen Gupta, K.K. & Bose, A., 1943 – On the copper-barytes ore of Parisal in Alwar State (Rajputana) with a suggestive method of their separation, *Quarterly Journal Geological Mining and Metallurgical Society of India* 15, 151-152.

Singh, S.P., 1988 - Sedimentation patterns of the Proterozoic Delhi Supergroup, northeastern Rajasthan, India, and their tectonic implications, *Sedimentary Geology* 58, 79-94.

Singh, S., Singh, L., Singh, J., & Virk, H.S., 1988 – Fission track dating of some copper ore formations in India; in Khan-Hameed, A., Qureshi-Imtinan, E. & Ahmad-Ishfaq (eds), Solid State Nuclear Track detectors. Nuclear Tracks and Radiation Measurements, *Pergamon, Oxford*, 715-718.

Smith, J.B., Barley, M.E., Groves, D.I., Krapez, B., McNaughton, N.J., Bickle, M.J., &Chapman, H.J., 1998 - The Scholl shear zone, West Pilbara: evidence for a terrane boundary structure from integrated tectonic analyses, SHRIMP U-Pb dating and isotopic and geochemical data of granitoids, *Precambrian Research* 88, 143-171.

Whalen, J.B., Currie, K.L. & Chappell, B.W., 1987 – A-type granites: geochemical characteristics, discrimination and petrogenesis, *Contributions to Mineralogy and Petrology* 95, 407-419.

Appendix 1: SHRIMP Dating

Methods

SHRIMP methods follow Compston et al. (1984) and Smith et al. (1998) for zircons, and Neumayr et al. (1998) for titanite. The procedure involves focussing of an O_2^- ion beam to a 25-30 micron spot on sectioned and polished mineral grains, and measuring secondary ions to obtain isotopic ratios. Analyses were referenced to the CZ3 zircon and Khan titanite standards, analysed concurrently with the samples. The common Pb correction utilized the measured ^{204}Pb (Compston et al., 1984). Data in tables have errors of ±1 sigma, whereas uncertainties in pooled ages are quoted at the 95% confidence level.

Table A1: SHRIMP II isotopic data for zircons from the Gothra Granite.

Grain	U (ppm)	Th (ppm)_	Th/U	f206 (%)	207*/206*	208*/206*	206*/238	207*/235	208*/232	% conc.	207*/206* Age
1-1	285	147	0.52	0	0.1033±6	0.1504±10	0.3036±28	4.323±49	0.0884±10	102	1684±10
2-1	729	307	0.42	0.014	0.0988±4	0.1319±7	0.2774±24	3.781±37	0.0868±9	99	1602±7
3-1	1263	678	0.54	0.155	0.1033±3	0.1654±7	0.2824±24	4.024±37	0.0871±8	95	1685±6
4-1	282	93	0.33	0.017	0.1047±6	0.0965±11	0.298±28	4.302±50	0.0875±13	98	1709±11
5-1	320	102	0.32	0.096	0.1017±6	0.0934±10	0.2916±27	4.09±47	0.0853±13	100	1656±11
6-1	221	42	0.19	0.084	0.1132±7	0.0517±12	0.3391±33	5.292±65	0.0915±24	102	1851±12
7-1	205	69	0.34	0.075	0.1042±8	0.0951±16	0.3004±30	4.315±58	0.0845±17	100	1700±15
8-1	273	114	0.42	0.111	0.1028±6	0.1181±12	0.2993±28	4.244±51	0.085±13	101	1676±12
9-1	542	272	0.5	0.034	0.1035±4	0.1405±8	0.2986±26	4.262±43	0.0836±9	100	1688±7
10-1	343	127	0.37	0.048	0.1035±5	0.1088±9	0.2906±27	4.145±46	0.085±11	97	1687±9
11-1	432	177	0.41	0.079	0.1038±5	0.121±10	0.2941±26	4.21±45	0.087±11	98	1693±9
12-1	370	186	0.5	0.007	0.1041±5	0.1463±10	0.2971±27	4.266±46	0.0867±10	99	1699±9
13-1	253	108	0.43	0	0.1041±6	0.1206±10	0.2988±29	4.288±49	0.0845±11	99	1698±10
14-1	383	227	0.59	0.098	0.104±6	0.1797±13	0.2858±26	4.1±46	0.0866±10	95	1697±10
15-1	523	318	0.61	0.016	0.1035±4	0.1724±9	0.2983±26	4.259±43	0.0845±9	100	1688±8
16-1	245	102	0.42	0.001	0.105±7	0.122±13	0.295±28	4.272±53	0.0861±13	97	1715±12
17-1	241	100	0.42	0.105	0.1037±7	0.121±14	0.2983±29	4.267±54	0.0869±14	99	1692±13
18-1	178	58	0.33	0	0.1034±6	0.0934±10	0.3005±30	4.286±54	0.086±13	100	1687±12
19-1	662	343	0.52	0.032	0.1033±4	0.1485±8	0.2981±26	4.246±42	0.0856±9	100	1684±7
20-1	755	473	0.63	0.033	0.1037±3	0.1791±7	0.3014±26	4.309±41	0.0861±8	100	1691±6
21-1	286	130	0.45	0.036	0.1038±6	0.1291±12	0.2954±28	4.227±49	0.0839±11	99	1693±11
22-1	520	320	0.62	0.049	0.1036±4	0.1777±9	0.2974±26	4.248±43	0.0859±9	99	1690±8
23-1	278	109	0.39	0.003	0.1037±6	0.1111±12	0.3021±29	4.319±51	0.0858±13	101	1691±11
24-1	542	294	0.54	0.055	0.104±4	0.1563±9	0.2947±26	4.228±43	0.0849±9	98	1697±8

CZ3 standard: n = 12, Calibration error = 0.89% (1 standard deviation).
f206 (%) = % ^{206}Pb attributed to common ^{206}Pb.
Common Pb composition = coeval Cumming and Richards (1975) Model III Pb, corrected from ^{204}Pb.
Conc = concordance

Table A2: SHRIMP II isotopic data for titanite from Khetri

Grain	U (ppm)	Th (ppm)	Th/U	f206 %	207*/206*	208*/206*	206*/238	207*/235	208*/232	% Conc	207*/206* Age
10-2	49	147	3	0	0.0676±9	0.9061±92	0.1443±23	1.345±30	0.0436±9	101	856±29
2-2	94	362	3.88	0	0.0689±7	1.1858±85	0.1381±19	1.312±24	0.0423±7	93	896±22
7-5	48	157	3.3	0	0.0668±10	1.0094±101	0.1411±23	1.3±30	0.0432±9	102	832±30
8-2	38	109	2.89	0.152	0.066±20	0.8856±112	0.1442±25	1.312±49	0.0442±10	108	807±65
9-2	50	150	3.03	0.115	0.0665±16	0.919±100	0.1389±22	1.273±39	0.0422±9	102	821±50
1-2	38	108	2.8	0.572	0.0637±28	0.8538±130	0.1428±26	1.255±62	0.0435±11	117	733±93
14-2	92	353	3.82	0.265	0.0633±13	1.175±98	0.1391±19	1.214±32	0.0428±7	117	719±45
15-2	58	204	3.51	0.389	0.0638±21	1.0711±121	0.1412±22	1.242±48	0.0431±9	116	735±71
16-2	52	177	3.39	0	0.0673±11	1.0436±114	0.142±23	1.318±32	0.0438±9	101	848±32
17-1	38	109	2.87	0.153	0.0677±21	0.8554±125	0.1412±26	1.318±50	0.042±11	99	859±63
18-1	54	162	3	0.002	0.0685±16	0.9056±108	0.1392±23	1.316±39	0.0421±9	95	885±48
19-1	39	111	2.83	0.23	0.0685±25	0.8584±128	0.1427±26	1.348±58	0.0434±11	97	885±76
20-1	37	106	2.86	0.195	0.0654±32	0.8852±142	0.1426±27	1.286±70	0.0441±12	109	787±102
21-1	47	138	2.9	0.36	0.0669±25	0.8968±121	0.1386±24	1.278±55	0.0429±10	100	833±78
22-1	39	116	3	0.528	0.0645±34	0.9204±149	0.1401±26	1.247±73	0.043±11	111	759±112
23-1	40	111	2.76	0.728	0.0626±27	0.8316±126	0.1428±26	1.233±60	0.0431±11	124	696±93
24-1	43	122	2.87	0.132	0.0669±24	0.889±126	0.1388±25	1.281±54	0.043±11	100	836±74
25-1	42	119	2.83	0	0.0688±12	0.8577±110	0.1423±25	1.35±35	0.0432±10	96	892±35
26-1	40	113	2.86	0.046	0.0661±29	0.8621±130	0.1427±26	1.301±64	0.043±11	106	810±91
27-1	41	117	2.87	0	0.0679±12	0.9064±116	0.1377±24	1.289±34	0.0435±10	96	866±36
28-1	156	498	3.2	0.085	0.0669±10	0.9728±65	0.1412±17	1.301±26	0.0429±6	102	833±31
29-1	51	161	3.19	0.016	0.0672±18	0.9757±116	0.1435±24	1.33±44	0.0439±10	102	845±56
30-1	42	121	2.85	0.013	0.0683±23	0.8934±124	0.1377±24	1.297±51	0.0431±10	95	878±69
31-1	45	132	2.91	0.044	0.0669±20	0.8825±119	0.1391±24	1.282±47	0.0422±10	101	833±62
32-1	87	329	3.78	0.124	0.0658±17	1.173±105	0.1378±19	1.25±38	0.0427±8	104	801±53
33-1	171	522	3.06	0.006	0.0671±8	0.9191±60	0.1389±16	1.284±23	0.0418±6	100	840±26
34-1	40	111	2.8	0.177	0.0689±20	0.8958±124	0.1408±26	1.337±48	0.045±11	95	896±59
35-1	39	113	2.89	0.429	0.0657±36	0.8689±148	0.1384±26	1.254±75	0.0416±11	105	796±114
36-1	42	119	2.87	0.22	0.066±18	0.8816±122	0.1393±25	1.267±43	0.0428±11	104	807±56
37-1	53	156	2.93	0	0.0673±11	0.9127±111	0.1366±23	1.268±32	0.0426±10	97	847±34
38-1	47	142	3.01	0.404	0.0637±23	0.9032±120	0.1432±24	1.257±52	0.043±10	118	731±76
39-1	56	164	2.94	0	0.0695±11	0.8746±104	0.1414±24	1.354±33	0.042±9	93	912±33

Khan standard: Data collected during two sessions: n = 10 and 10, Calibration error = 1.14% and 1.00% (1 sigma).
f206 (%) = % ^{206}Pb attributed to common ^{206}Pb.
Common Pb composition = coeval Cumming and Richards (1975) Model III Pb, corrected from ^{204}Pb.
Conc = concordance.

PGC
PUBLISHING

Herrington, R., Smith, M., Maslennikov, V., Belogub, E. & Armstrong, R. 2002 - A Short Review of Palaeozoic Hydrothermal Magnetite Iron-oxide Deposits of the South and Central Urals and their Geological Setting; *in Porter, T.M. (Ed.), Hydrothermal Iron Oxide Copper-Gold & Related Deposits: A Global Perspective*, Volume 2; PGC Publishing, Adelaide, pp 343-353.

A SHORT REVIEW OF PALAEOZOIC HYDROTHERMAL MAGNETITE IRON-OXIDE DEPOSITS OF THE SOUTH AND CENTRAL URALS AND THEIR GEOLOGICAL SETTING

[1]Richard Herrington, [2]Martin Smith, [3]Valeriy Maslennikov,
[3]Elena Belogub & [1]Robin Armstrong.

[1]*Department of Mineralogy, The Natural History Museum, London, UK*
[2]*The School of the Environment, University of Brighton, UK*
[3]*Institute of Mineralogy, Russian Academy of Sciences, Miass, Russia*

Abstract - The Urals orogen represents the site of Palaeozoic oceanic crust creation and subsequently a zone of arc development, arc-continent collision, continent-continent collision and post-orogenic collapse. The orogen is host to a number of world-class VMS deposits in the Silurian to Devonian arc sequences but in addition is host to highly significant iron oxide deposits of both hydrothermal and orthomagmatic origin. The hydrothermal ores are developed in Palaeozoic belts associated with rift-related, dominantly mafic, largely subaerial, alkaline volcanism intruded by comagmatic stocks of varying ages, from the Late Silurian to Early Carboniferous. Volcanism, sedimentation and mineralisation all seem to be controlled by major N to NNE trending structures. Much of the mafic volcanic sequence shows hematisation, which is evidence of early oxidation of the lava-tuff packages. Mineralisation comprises massive and disseminated magnetite bodies with elevated REE and ubiquitous accessory apatite. The deposits can be huge, as for example the giant Carboniferous Kachar deposit in Kazakhstan with reserves of over a billion tonnes of >45% Fe are defined. Some of the bodies are true contact skarns developed at the interface between intrusive bodies and volcano-sediments which include limestones. Other bodies, including Kachar, are distal to any possible related intrusions and are developed within regionally extensive scapolite alteration zones. A regionally consistent pattern of early feldspar ± biotite alteration followed by ore-stage pyroxene-garnet-scapolite followed by late hydrous silicate-carbonate alteration is repeated throughout the Urals. Regionally extensive scapolitisation is common in most of the belts. Base metals are generally present in the deposits, often appearing late in the paragenetic sequence, with some bodies having near economic copper grades (0.6% Cu) and significant precious metals.

Introduction

It is widely accepted that the Urals Orogen formed as a result of the closure of a Palaeozoic ocean, involving subduction, continent-island arc collision and finally continent-continent collision, and then later by orogenic collapse. Modern authors generally concur on the development of eastward dipping subduction during the closure of a Palaeozoic ocean attached to the passive margin of the East European craton (Seravkin et al. 1994, Ivanov 1998). The Main Uralian Fault (MUF) is generally agreed to represent the former location of the major subduction zone relating to the later stage of intra-oceanic subduction followed by collision between the East European Craton and the Magnitogorsk island-arc. Units to the West of this suture have been deposited or tectonically emplaced over Pre-Cambrian continental basement (the East European Craton), while those to the East are island arc related volcanic and sedimentary sequences (eg. Puchkov 1997, Brown et al., 1998, Zonenshain et al., 1984).

All the tectonic models concur on the existence of an ocean west of the Main Urals Fault (MUF) which formed in the Ordovician-Silurian and then began closing to produce an arc sequence on oceanic crust east of the MUF. In the north and central Urals, the arc-continent collision probably occurred in Late Silurian to Devonian times (Puchkov 1997). In the south, during the Devonian, the arc sequence developed east of the MUF with the MUF itself the site of obduction and accretion of material from the Urals ocean to the west. This progressive arc sequence is associated with over 60 VMS deposits which form the basis of the extensive copper mining and smelting industry of the south Urals (Herrington et al. 2001). The east European continent collided with the southern arcs in the Late Devonian (Brown et al. 1998) whilst volcanism continued in the east of the Urals through to the lower Carboniferous accompanied by comagmatic intrusive complexes. The major magnetite deposits here are related to this igneous activity. Overlying these are Late Carboniferous platform carbonates. The Lower Carboniferous igneous complexes are compared to those in continental rift settings (Fershtater 2000) and clearly post-date the onset of continent arc collision in the west (Brown et al. 1998). This would imply a change of magma source from subduction of an oceanic slab from

the west and may be the result of deep mantle-sourced magmatism during some form of post-collision extension.

The Urals is also host to a number of iron oxide deposits which occur in a range of settings within the orogen (Smirnov & Dymkin 1989) (Table 1). The three main environments are: a) hosted within units of the continental margin of the East European Craton, b) contemporaneous with rocks of the Palaeozoic ocean-arc assemblage and c) deposits formed in syn to post collisional events within the orogen. These deposits form the basis for iron and steel production in the region which in 1998 amounted to 22 million tonnes of iron ore.

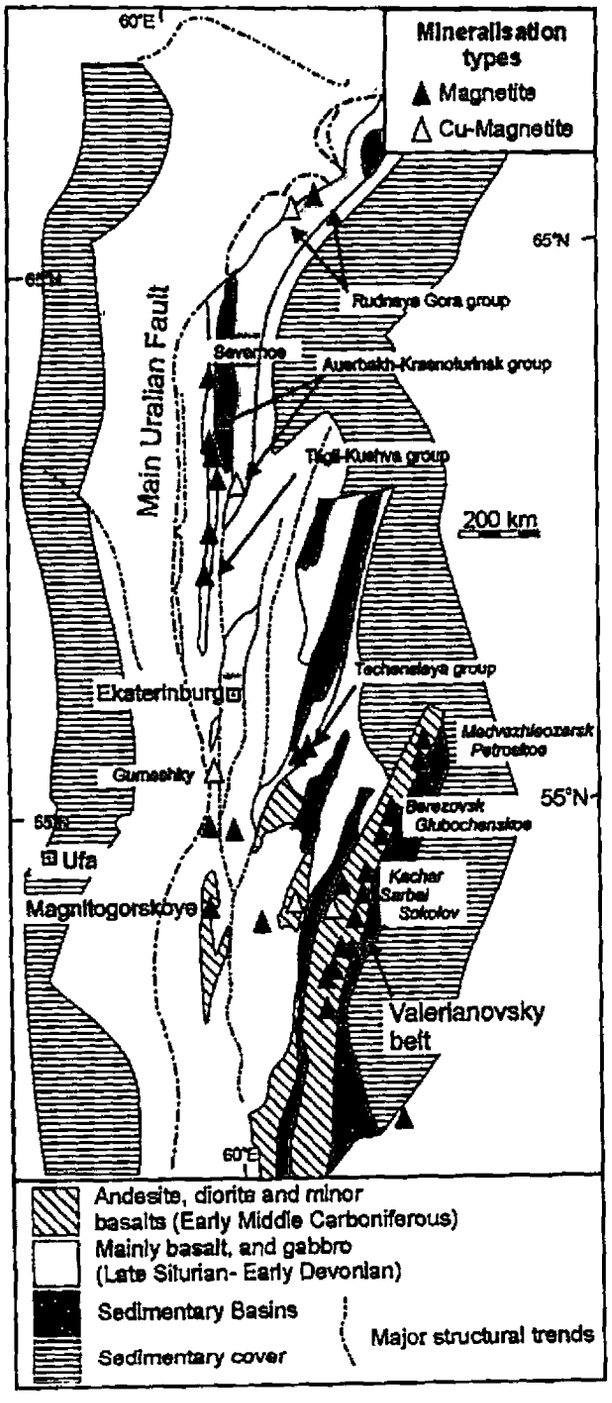


Figure 1: Hydrothermal magnetite deposits of the Urals (modified after Koroteev et al., 1997)

Table 1: Key iron oxide deposits of the Urals and their genetic associations

Genetic association	Petrological association	Deposit name (Age)	Relationship to intrusives
Orthomagmatic	Low-Ti magnetite-bearing intrusives of dunite-pyroxenite association	Kachkanar (Silurian)	Hosted within intrusion
	Titanomagnetite-ilmenite-bearing gabbroic intrusives	Kusinsk, Kopansk (Proterozoic)	Hosted within intrusion
Hydrothermal-(magmatic)	Magnetite calcic-skarn	Magnitogorsk, Vysokogorsk, Goroblagodat (Devonian)	Contact skarn Contact skarn Contact skarn
	Scapolite-albite-*magnetite skarn*	Kachar, Sarbai, Sokolovsk, Glubochensk (Carboniferous)	Stratified replacement Contact skarn + stratified replacement Contact skarn + stratified replacement Contact skarn + stratified replacement

Orthomagmatic Oxide Deposits

The former two groups of deposits, a) and b) above, are related to layered mafic intrusive complexes in Proterozoic rift-related sequences of the East European craton margin and Alpine-type chromite deposits of Palaeozoic oceanic rocks. Examples of the former are the Kusinskaya ilmenite-titanomagnetite occurrences whilst examples of the latter include the world-class Kempirsai chromite deposits in Kazakhstan and the large Kachkanar deposits in the Middle Urals. These deposits are clearly orthomagmatic and are not discussed here (Koroteev et al. 1997).

Hydrothermal Magnetite Deposits

Magnetite dominated iron-oxide deposits that have formerly been grouped together and classified as 'skarns' (Smirnov & Dymkin 1989) include the Palaeozoic deposits of the Auerbakh-Krasnoturinsk, Magnitogorsk and Valerianovsky belts (see Figure 1). These groups of deposits are discussed in the text which follows.

Hydrothermal Magnetite Mineralisation

Auerbakh-Krasnoturinsk

This region hosts a number of 'skarn' magnetite deposits which are notable for their elevated gold and copper values (Sazonov et al. 1998). In this region which is a rather complex tectonic zone between the Tagil volcanic arc and the Precambrian Saldinsk massif in the east (Puchkov 1997), there are numerous porphyry copper prospects and what is described as a Carboniferous-age 'Carlin-type' replacement and vein deposit in limestones and volcanics (Sazonov et al. 1998).

One of the major magnetite bodies in this region is the Peschansk deposit. Peschansk had reserves of 173 million tonnes of magnetite ore in 1977, grading 48.5 to 54% Fe, in four sectors. Significantly, the western sector of the

deposit contained on average, 0.61% Cu (Sokolov & Grigor'ev 1977).

The Peschansk deposit occurs at the margins of a large diorite complex which intrudes Lower Devonian sediments and volcano-sediments. The sediment package includes limestones and andesitic tuffites. The deposits appear to be classic skarns developed directly at the contact between the intrusive and flanking volcanics and sediments. Flanking the zones of massive magnetite are aureoles of metasomatically altered rocks. The skarns are dominated by garnet-pyroxene and garnet assemblages which finger out from the massive magnetite zones. Pervasive epidote alteration of the volcanic rocks occurs outside this.

Massive magnetite, magnetite-sulphide and magnetite skarn ores are recognised with a distinctive sulphide-rich facies in part of the deposit. The deposit carries around 3% S on average throughout.

Tagil-Kushva Group

The Goroblagodat deposit or series of deposits near Kushva is similarly associated with a diorite-syenite porphyry of Upper Silurian to Lower Devonian age which cuts Ludlovian (late Silurian) volcanics and sediments. Reserves were quoted as 140 million tonnes @ 35.5% Fe in 13 stratabound lenses of magnetite. Contact metamorphic zones are characterised by garnet and pyroxene-garnet skarns, magnetite skarns and zones of scapolite alteration. Brecciated magnetite ores are common and pyrite and chalcopyrite are noted disseminated in the magnetite ores (Sokolov & Grigor'ev 1977).

Other deposits in this group are Evstuninskoe, Lebyazhinskoe, Valuevskoe, Osokino and Visokogorskoe. Gold and silver are noted along with enhanced base metals at Visokogorskoe. Rare earth rich apatite is common at Lebyazhinskoe.

Severnaya

This small group of magnetite deposits forms stratabound lenses at the boundaries between Silurian-age limestones and basalts. The main minerals are magnetite with subordinate pyrite, pyrrhotite and often abundant apatite. Skarn assemblages are developed very erratically and comprise magnetite, hematite, mushketovite, pyrite, chalcopyrite, quartz, epidote, chlorite, pyroxene and amphibole. Garnet, titanite and apatite are also found.

Magnitogorsk Region

The magnetite deposits of the Magnitogorsk region was the basis of the large iron and steel complex developed in the city in the 1930s which formed the backbone of Russian production during the second world war. The main deposits of the region are Magnitogorsk (2 main bodies), Maliy Kuibas, Berezky and Dimitrovskoye. In addition the district holds another 30 smaller deposits. The Magnitogorsk resource of some 500 million tonnes of ore is practically exhausted and the only major mine in the region now is the open-pit exploiting the ca. 60 million tonne Kuibas deposit.

The geological structure of the region is dominated by the Devonian to lower Carboniferous volcano-sedimentary rocks, the major part of which comprise subduction related volcanics which are host to major volcanic-hosted massive sulphide deposits (Herrington et al. 2001). The structural grain of the region is dominated by a sequence of parasitic anticlines and synclines aligned sub-parallel to the main N-S trend, with granitic bodies intruded into the cores the fold cores.

These granitoids form two series. The older Devonian suite is comagmatic with the Devonian arc rocks, while the second series is associated with the magnetite skarn-like deposits which are of early Carboniferous age. These younger intrusive massifs are comagmatic with the early Carboniferous volcanics which they intrude. The intrusives show an evolution from gabbro (first stage) to amphibole sub-alkaline granites and syenites (later stage). The ore bodies are located: (a) at the contacts between granites and meta-volcanites (eg. Maliy Kuibas), (b) within granites (eg. Beresky) and (c) along the exocontacts (eg. Magnitogorskoye, Dmitrovskoye etc.). The sequence has been dated at between 333 and 330 Ma (Ronkin 1989). Emplacement of these intrusives is controlled by a major NNE trending structure, indicated on Figure 2. The intrusive igneous suite shows clear evidence of fractionating gabbro to diorite from a common source, with the latest granitic intrusions developed as thin sheets marginal to the gabbros (Fershtater et al. 1997, Fershtater 2000). The main pluton is also zoned from the base, from a lower gabbro to a transitional gabbro-granite breccia to an upper granite. The composition of the plutonic rocks is typical for moderately alkaline continental rift series, comparable to igneous suites from the Afar Rift (Fershtater 2000).

The magnetite bodies at Magnitogorsk itself occur as exoskarns, formed largely at the expense of Tournaisian and Lower Visean (lower Carboniferous) limestones (Figure 3) located on the southern contact of the Magnitogorsk intrusion. The host limestone unit is shown as being underlain by Late Devonian basalts. The footwall is intensely albite-altered close to the limestone unit and the magnetite body, while the overlying Carboniferous volcanics are albitised and overprinted with skarn alteration. The ore-bearing skarn comprises andradite-grossular-garnet, diopside, epidote, calcite and apatite.

The ores are largely magnetite with minor pyrite (carrying up to 5% Co), pyrrhotite and chalcopyrite. Sulphides often form inter-granular aggregates within the magnetite as well as more discrete sulphide-rich lenses.

The Maliy Kuibas orebody is situated 14 km to the NNE of the Magnitogorsk deposit, along the northern flank of the Kuibas granite intrusive. From a structural perspective, as at Magnitogorsk, the deposit lies within the core of a branched anticline of folded volcanic and volcano-sedimentary rocks. The structure is intruded and metamorphosed by the granitoid massif. The deposit itself is clearly related to a tectonic zone within the anticlinal structure (Figure 4). The wall rocks comprise mafic volcanic units, including metamorphosed diabases

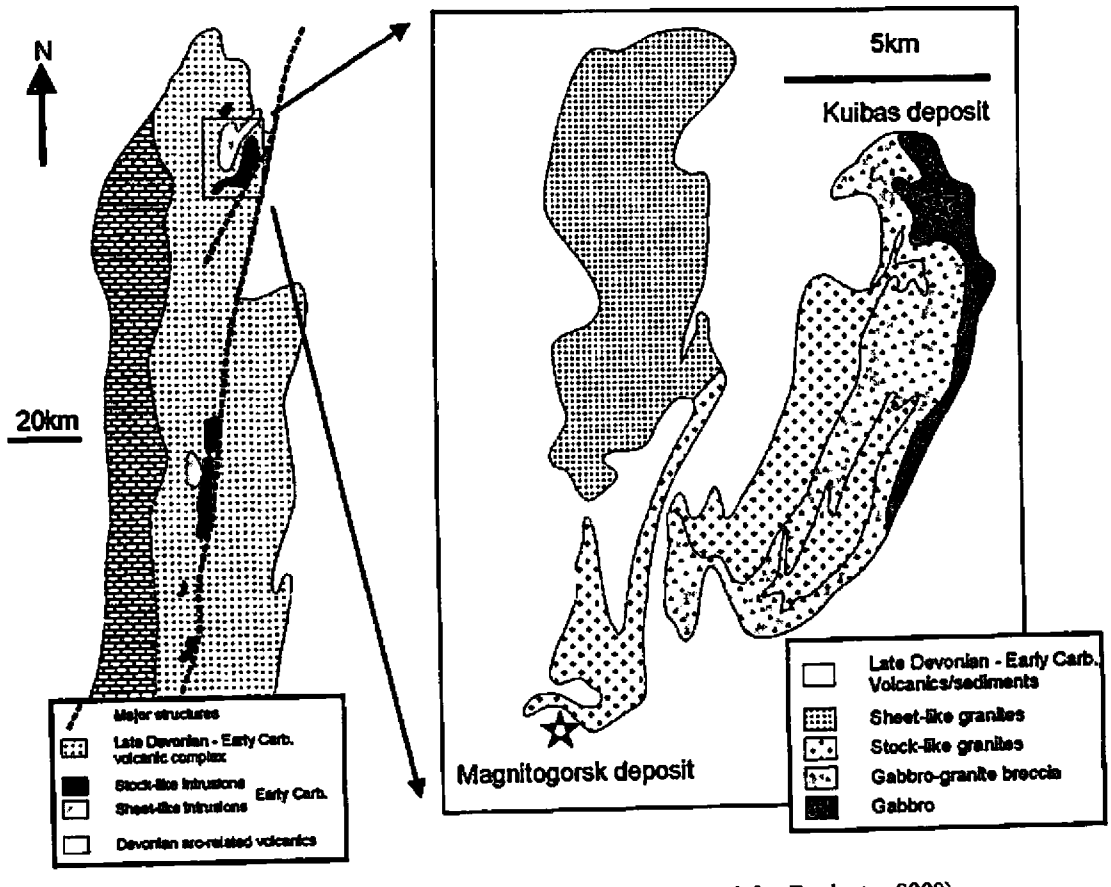


Figure 2: Simplified geology of the Magnitogorsk region (after Fershtater, 2000)

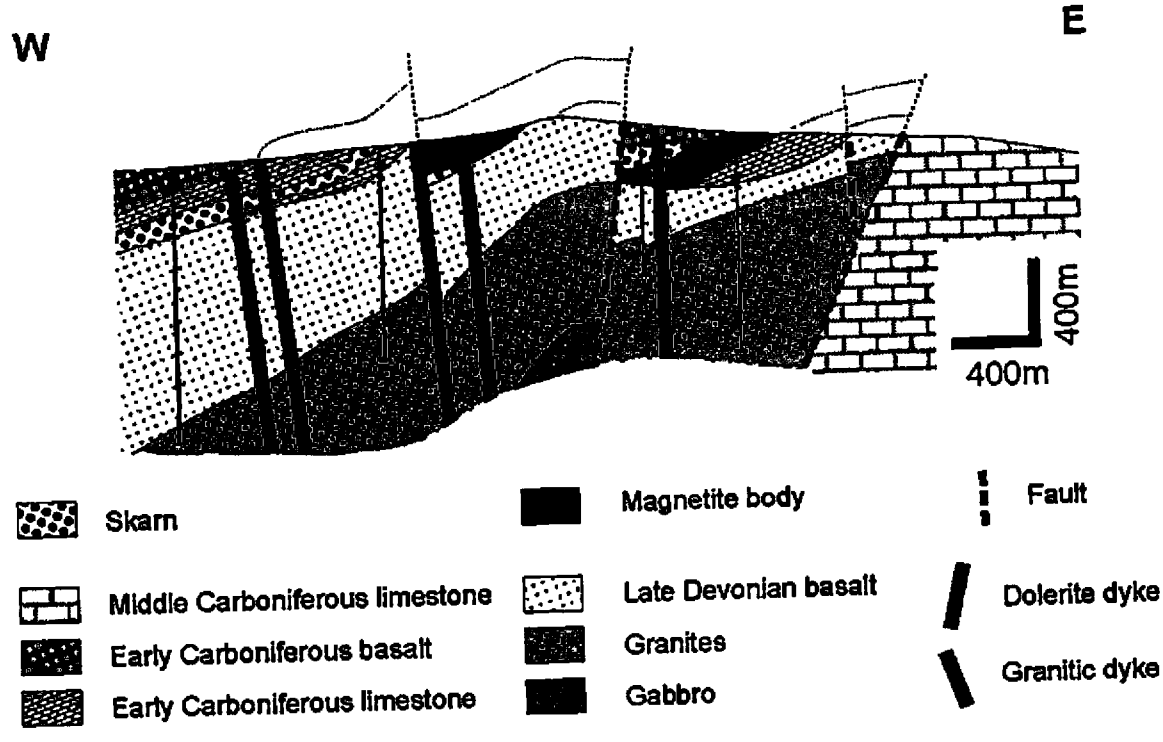


Figure 3: Geological section through the Magnitogorsk deposit (after Ya. Baklaev: unpublished)

(dolerites) and their tuffaceous equivalents, which are plagioclase and pyroxene phyric. In addition, there are granites, gabbros and various hornfels facies which are now represented by a fine-grained rock composed of quartz, plagioclase, hornblende and pyroxene with secondary and accessory leucoxene, epidote, chlorite and titanite.
In the central part of the deposit, pyroxene-feldspar and quartz-feldspar hornfels are developed with skarn and magnetite bodies. These form a zone measuring 200-600x2500 m in extent, elongated parallel to the NNE trend and dipping westwards at 70-85°. Many apophyses and metre wide veins of granite are injected into the ore-zone and separate ore blocks. In detail, there are actually more than 50 individual magnetite lenses in the deposit with sizes varying from 50x50 to 500x300 m, with thicknesses of between 2 and 50 m.

In the limits of the ore zones, granites have progressive transitional contacts with hornfels, tuffs and diabases. Skarns occurs as rims around magnetite ore bodies and veins, and as lens-like inclusions within the ores, granites and hornfels. The mineralogical composition of the skarns comprises: garnet (andradite-grossular, andradite), diopside-hedenbergite, calcite, tremolite, actinolite, bluish hornblende, vesuvianite, scapolite, albite, epidote, chlorites, hematite, pyrrhotite, pyrite, siderite, magnetite and apatite. There are many different mineralogical associations within the skarns, but usually they are dominated by a pyroxene-garnet-association. Skarns are coarse-grain and form zonal veins with cavities and druzy aggregates. The proposed sequence of mineralisation and alteration is summarised in Table 2.

The ore mineralogy is dominated by magnetite with minor pyrrhotite and pyrite, although cobalt is an important trace element. The ores are coarse grained, massive or banded, with breccias being present in places. In the northern part of deposit there is a titano-magnetite-bearing ore body with 16-25% TiO_2,. ulvospinel and herzinite. The deposit is capped by a 5 to 30 m thick supergene blanket.

The composition of typical ores from Maliy Kuibas is (in percent): Fe - 38.5; Co - 0.02; Ni - 0.01; Mn - 0.17; TiO_2 - 0.41; V_2O_3 - 0.05; S - 1.83; P - 0.06; SiO_2 - 16.0; Al_2O_3.- 5.9; CaO - 7.8; MgO - 1.42. For a comparison, the chemical and mineralogical composition of ores from the Magnitogorsk deposit are shown in Table 3.

Valerianov Trend

The 700 km long, NNE striking Valerianov trend (see Figure 1) is host to a major group of magnetite bodies which are described as skarns (Koroteev et al. 1997). This trend contains the major iron-ore producing area of Turgai which includes the Sarbai, Sokolovsk and Kachar deposits. Kachar has a reported resource of some 2 billion tonnes of ore at around 45% contained iron in magnetite. The trend contains two major districts of mineralisation to the south and the north respectively, the Turgai and Glubochensk regions.

Stages of Alteration	Sequence		Mineralogy
	Magmatic stage	Post-magmatic stage	
Telethermal contact hornfels			Labradorite, oligoclase, pyroxene, hornblende, magnetite
Alkaline metasomatism, (oligoclase stage).			Oligoclase, quartz, pyroxene, hornblende, magnetite.
Alkaline metasomatism, albite (albite-orthoclase) stage.			Albite, orthoclase, quartz, actinolite, magnetite, epidote, calcite, sericite.
Skarn-magnetite stage, skarn sub-stage			Pyroxene, garnet, epidote, vesuvianite, wollastonite, hornblende, magnetite, pyrrhotite, apatite.
Skarn-magnetite stage, magnetite sub-stage			Magnetite, garnet, hornblende, pyrite, chlorite, calcite.
Low temperature metasomatism and hydrothermal stage			Quartz, epidote, chlorite, sericite, pyrite, albite, calcite, apatite, siderite.

Table 2: Paragenetic sequence of alteration and mineralisation in the Magnitogorsk area (after Sidorenko, 1973)

Turgai Region

The Turgai region contains the major iron producers of Sarbai, Solovsk and Kachar which have supplied magnetite ore to the Magnitogorsk iron and steel complex since the depletion of virtually all of that complex's associated deposits, with the exception of Kuibas.

The region comprises a NNE trending fault-bounded linear corridor of Tournaisian to Namurian (Carboniferous) volcano-sedimentary rocks developed between large sedimentary basins (Figure 1). The Carboniferous units in the corridor are entirely covered by a 40 to 180 m thick sub-horizontal layer of Mesozoic to Cainozoic sediments. The magnetite bodies were discovered by airborne and ground geophysics in the 1940s, following reports of magnetic compasses being deflected when the area was overflown.

Sarbai

This deposit lies in the south of the belt, at the contact of the Sarbai dioritic intrusion, which comprises a pyroxene-quartz-diorite, accompanied by various dyke phases, culminating in post-ore granite porphyries (Dymkin 1966). The deposits lie above the Valerianov sub-zone of rocks, within andesitic porphyries and diverse volcaniclastic rocks, some of which show extensive early hematite alteration. This host unit defines the Sokolovsk-Sarbai anticline, with the deposits occurring on the western limb. Pre-, syn- and post-ore structure is important in the location of the various intrusive phases and the mineralisation.

Alteration comprises pre-ore hornfelsing and the development of biotite-k spar and albite alteration facies. This phase is followed by pyroxene-scapolite, pyroxene-garnet and epidote-actinolite alteration directly associated with the ore formation. Post ore alteration consists of chlorite-prehnite, calcite-silica and zeolite assemblages. Pervasive scapolite is a noted feature of the Sarbai deposit and of the Turgai province as a whole (Smirnov 1977). Alteration appears to be zoned outward from the Sarbai diorite pluton as follows: a) biotite-albite-scapolite, b) garnet-pyroxene 'skarn', c) 'skarn' ore (dominantly magnetite and scapolite), d) scapolite-pyroxene, and e) pyroxene skarns, passing out into f) hornfels and albitised host rocks.

Orebodies at Sarbai are interpreted as having replaced bituminous limestones, calcareous tuffs and tuffites (Chuguevskaya 1969). The ore layers are conformable and appear bedded, passing laterally into less altered tuffaceous units and calcareous sediments. Post-ore dykes complicate the present geometry. The dimensions of the ore lenses at Sarbai are impressive, with the three main lenses each measuring between 1000 m and 1700 m long, 800 to 1700 m down-dip and are up to 170 to 185 m in thickness. Around half of each of these bodies is present as a higher grade core of approximately 50% Fe, while the remainder is 20-50% Fe. The dominant ore mineral is magnetite, with significant accessory sulphide, mainly pyrite, pyrrhotite and chalcopyrite. Sulphides can form layers in the footwall of the magnetite bodies but are currently not of commercial interest. Other gangue minerals are scapolite, pyroxene, garnet, wollastonite, albite, epidote, actinolite, apatite, calcite and quartz. Quoted reserves in 1970 were 725 million tonnes of ore at a grade of 45.6% Fe, 4.05% S and 0.13% P.

Sokolovsk

This deposit is adjacent to Sarbai and was also discovered in the late 1940s. Like Sarbai, Sokolovsk is similarly located at the margin of a dioritic pluton, and has extensive scapolite alteration accompanying the margins of the mineralisation, forming a hanging-wall blanket to the ore. The deposit has reserves of 967 million tonnes at a grade of 41% Fe, and carries significant sulphide with contents of between 2.5 and 3.3% S in the bulk ore (Sokolov & Grigor'ev 1977).

Element	Content in weight %			Host Minerals
	From	To	Average	
Fe	27	69,8	48,6	Magnetite, pyrite, pyrrhotite, garnet, hornblende
S	0,01	8,6	1,98	Pyrite and others sulphides
P	0,001	0,4	0,04	Apatite
SiO_2	0,3	36,2	8,3	Silicates
CaO	0,02	26,1	1 2,8	Calcite, garnets, epidote, diopside
MgO	-	3,18	1,02	Chlorite, diopside
MnO	0,01	0,26	0,08	Garnets, psilomelane
TiO_2	0,02	0,63	0,21	Titanite, titano-magnetite.
V_2O_5	-	0,12	0,03	Magnetite
Zn	-	0,21	0,03	Sphalerite.
Pb	-	0,1	0,05	Galena
As	-	0,36	0,015	Arsenopyrite.
Cu	-	0,6	0,07	Chalcopyrite
Co	-	-	0,018	Pyrite, magnetite, pyrrhotite.

Table 3: Chemical and mineral composition of ores from the Magnitogorsk deposit (from Sidorenko, 1973)

Kachar

Kachar is the largest of the Turgai region deposits with published ore reserves of 1 billion tonnes of @ 44.9% Fe (Figure 5). More recent press reports indicate that the tonnages may be at least double that figure. As with the other deposits of the district, it was discovered in 1943 by aeromagnetics.

Two supergroups have been recognised in the Carboniferous volcano-sedimentary series in the Kachar region. The older, Lower Carboniferous Valerianovo supergroup comprises approximately 1 km of andesitic volcanics and pyroclastics with interbeds of sediments and carbonates. Anhydrite layers with clay are intercalated with the limestones. The overlying Middle-Late Carboniferous Kachar supergroup contains more than 800m of polymict conglomerates, tuffs and sediments, and andesitic volcanics, basalt and andesite flows and tuff equivalents.
Scapolite-altered granite porphyry bodies cut the host sequence, while the orebody is associated with nearby gabbro-diorite intrusives. Deep geophysics suggests a buried gabbro could also be present, some 2 to 2.5 km below the deposit.

In contrast to the other deposits of the region, Kachar is distinguished by the absence of intrusive bodies immediately proximal to the ore. The high-temperature alteration in and adjacent to the deposit appears to have developed in the absence of a proximal intrusion, with scapolite forming a halo that extends for several hundred metres outward from the ore. In addition, there are broad zones of sulphide alteration accompanied by anhydrite within the deposit, which is enveloped by peripheral alunite (Sledzyuk & Shiryaev 1958).

Extensive scapolite alteration, accompanied by pyroxene, post-dates all the intrusives. Associated phases are actinolite, tourmaline, apatite, chlorite, albite, zeolite and calcite. Pyroxene-albite and pyroxene-garnet suites replace the scapolite alteration in places. Anhydrite occurs as discrete bodies in the limestone and as a replacement phase in the intrusives which are common in the magnetite ores. Belyashov & Plekhova (1965) considered the anhydrite to have originally been syngenetic, and to have been remobilised into the ore, although it only occurs close to ore and appears to be an epigenetic feature.

The ores at Kachar are closely associated in particular with scapolite and albite, in addition to other phases (see Table 4). Sulphides are common accessories although lower than at other deposits. Ores vary from 0.5 up to 3%S, 0.15-0.33% P and 0.02-0.03% Zn with significant vanadium.

Dacite porphyry, interpreted to be extrusive equivalents of the igneous complex in the Kachar ore field, have been dated by Rb/Sr at 315±24 Ma (Sokolov & Grigor'ev 1977).

Glubochensk Region

This region is defined by a group of deposits on the northeastern segment of the Valerianov trend as it enters Russia. The four main deposits of Glubochensk, Berezovsk, Medvezh'yeozersk and Petrovo are currently undeveloped but are similar to those exploited in the Turgai region, although higher grade (>50% Fe) ores are only recorded in the latter two of the group.

Again mineralisation relates to a northeast trending structural zone in the form of a fault-bounded syncline. Volcanic structures of Lower Carboniferous age are an acknowledged feature of the zone and the association of mineralisation with the early Carboniferous volcanism was recognised by Galkin (1963) and Dymkin et al. (1982). The Lower Carboniferous volcano-sedimentary host package has been dated as middle Visean and is subdivided into a lower Valerianovo and upper Kachar supergroup as

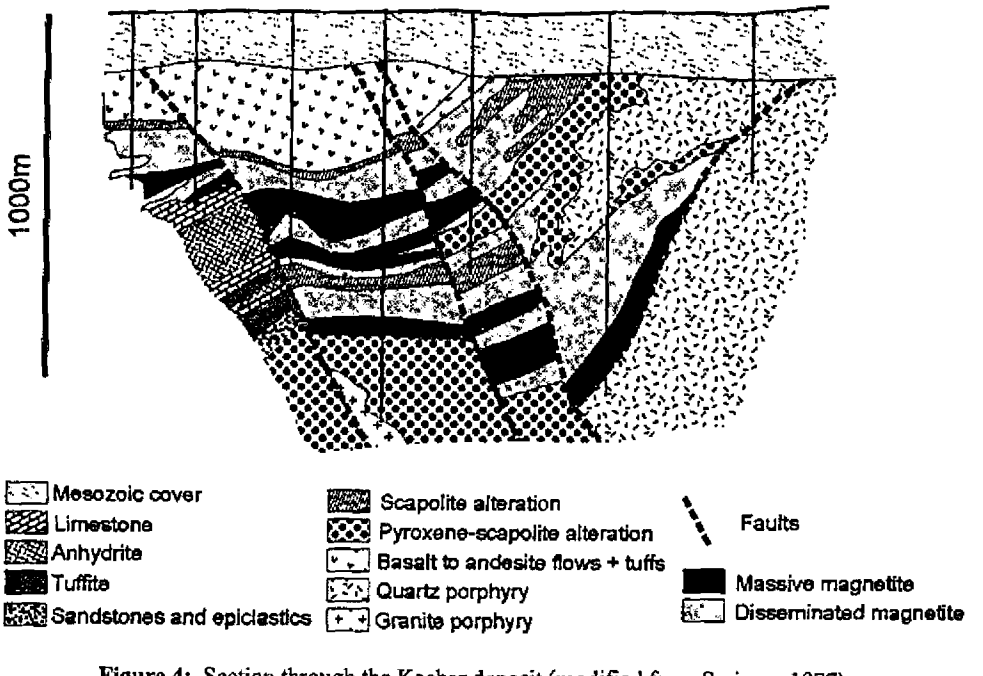


Figure 4: Section through the Kachar deposit (modified from Smirnov 1977)

Deposit	Ore Mineralogy	Alteration Mineralogy
SW Valerianovsk Turgai region		
Sarbai	Mag, pyx, scap, gar, woll, alb, epi, act, apat, py, calc, qtz Sulphide ore: py, po, cpy, sphal	Pre-ore: Biotite, kspar, albite Syn-ore: Pyroxene-scapolite, pyroxene, garnet, pyroxene-scapolite-garnet Post-ore: Chlorite-prehnite, calcite-quartz, zeolite Regional: Scapolite
Sokolovsk	Mag, scap, alb, pyx, gar, act, epi, ido, hem, chl, apat, preh, calc, py, po, ms, cpy, sphal	Pre-ore: Plagioclase-biotite, pyroxene-kspar Syn-ore: Pyroxene-scapolite, pyroxene-garnet Post-ore: Albite-actinolite, epidote, prehnite, calcite, quartz
Kachar	Mag, mat, scap, alb, pyx, gar, epi, act, chl, anhy, apat, titanite, zois, preh, ser, calc, py, po, sphal, cpy, gal, bn, cc	Regional: Scapolite, pyroxene, actinolite, tourmaline, apatite, chlorite, albite, zeolite, calcite Marginal to ore: Pyroxene-albite, pyroxene-garnet, garnet Syngenetic/replacement: Anhydrite
NE Valerianovsk		
Glubochensk	Mag, mart, magh, hem, mush, titano, il (cpy, sphal, gal, py, po, cc, moly, cov, bn, val	Early pervasive: Scapolite, pyroxene-scapolite Skarn: Calcic-garnet, pyroxene-scapolite, epidote-garnet Flanking skarn: Epidote, actinolite, chlorite Late: Calcite, silica, sulphides, anhydrite, gypsum
Sverdlovsk / Ekaterinburg region		
Goroblagodat	Mag, gar, pyx, ortho, scap, py, cpy, calc, epi, chl, alb, preh, zeo (traces: sphal, hem, po, gal, bn, mar, apat, titanite, fluor	Skarn: garnet-magnetite; garnet-epidote-magnetite 'Variolitic': orthoclase-pyroxene-scapolite-magnetite
Peschan'sk	Oxide: Mag, pyx, gar, Sulphide: Mag-cpy, pyx, gar	Distal: Albite, epidote, chlorite, carbonate Proximal: Garnet, garnet-pyroxene
Magnitogorsk region		
Magnitogorsk	Mag, py, po, cpy	Skarn: Garnet(and-gross), diopside, epidote, calcite, apatite
Kuibas	Mag, hem, po, py, apat, cpy	Skarn: Garnet, pyroxene (diopside-hedenbergite), calcite, tremolite, actinolite, vesuvianite, hornblende, scapolite, albite, epidote, chlorite

Table 4 - Summary of key ore and alteration mineralogies for key Urals magnetite deposits

described for Kachar above. In the Glubochensk region, mineralisation is largely confined to the Valerianovo supergroup which comprises mafic to intermediate lavas, tuffs and associated sediments, which include limestones. Limestones are erratically distributed through the supergroup but generally form less than 10% of the sequence.

The Kachar supergroup, which hosts magnetite bodies farther to the southwest, overlies this and comprises dominantly mafic to intermediate volcanics. In the Glubochensk region this supergroup only contains minor magnetite bodies. The volcanics of the Kachar supergroup are alkalic basalts to andesites with trachytes. Flow facies are common and there is a widespread development of mafic tuffs, commonly hematite altered, evidence for an early, probably subaerial, oxidation.

The two supergroups are considered to part of the same mega-volcanic event, although the volcanics of the Kachar supergroup are recognised as having been erupted in a largely subaerial environment (Pumpyanskiy et al. 1985). These volcanics are considered to be co-magmatic with the Sokolovsk-Sarbay intrusive complex, dated as Early to Middle Carboniferous (Ksenofontov & Ivlev 1971).

The chemistry of the igneous suites ranges from basalt to dacite in a continuous series indicating a common igneous source, but also that the Glubochensk rocks are directly comparable to those of the Turgai region. The suites have been compared to continental alkaline basalts formed in a rifted platform environment (Samarkin & Pumpyanskiy 1983).

The orebodies are located where the main NNE trending structures intersect easterly striking faults, with the main mineralised centres seemingly regularly spaced at 30 to 35 km intervals, a similar pattern to that noted in the Turgai district (Teterev 1970). All the orebodies occur as conformable to sub-conformable layers, with the main differences being between those hosted in volcano-sedimentary packages (Glubochensk and Berezovsk) and those in dominantly volcanic host rocks (Medvezh'yeozersk and Petrovo).

At Glubochensk there are three layers of magnetite mineralisation hosted within a volcano-sedimentary

package. The mineralised system extends over a strike length of around 4.5 km, with lenses of magnetite which have dimensions of up to 1300x750 m and may be as thick as 300 m. In its southern sections, sulphides are common, dominated by pyrite, pyrrhotite and chalcopyrite.

The Berezovsk body extends over a strike of 2.8 km and as much as 1.3 km down-dip. The mineralisation takes the form of up to 10 lenses of magnetite, often with abundant disseminated pyrite.

Medvezh'yeozersk is poorly defined, being masked by 400 m of Mesozoic cover, although it is known to comprise a lens of disseminated magnetite some 200 m thick within pyroxene-scapolite and garnet alteration.

Petrovo is almost entirely hosted by volcanics, which are highly altered mafic to intermediate tuffs. These rocks are strongly altered to albite, amphibole, chlorite 'skarns' with common associated garnet-pyroxene skarn and scapolitisation. Magnetite zones are up to 40 m thick with common accessory pyrite, chalcopyrite, pyrrhotite, galena and sphalerite, resulting in a sulphur content within the mineralisation of between 1.5 and 5 weight%.

In summary, the orebodies are characterised by alternating layers of magnetite-bearing and magnetite-poor material. The magnetite-poor zones are generally altered while ore horizons can be massive, disseminated, patchy or veinlet-swarms. The principal ore minerals are magnetite, martite, maghemite, hematite and mushketovite, with minor Ti-bearing spinels. Sulphide mineralisation is widespread, with copper elevated at Glubchensk and Berezovsk whilst zinc and lead are enhanced at Petrovo. Minor molybdenite is recorded.

Alteration is ubiquitous in the host rocks (Pumyanskiy et al. 1985). An early scapolitisation is recorded, accompanied by either pyroxene or epidote-albite, and surrounded by a halo of albitisation. This pattern is observed in both volcanic and intrusive host rocks, indicating the timing to be post volcanism and intrusion. Scapolitisation zones may reach thicknesses of several hundreds of metres, often enclosing small pods of mineralisation. Skarn assemblages in limestone, volcano-sedimentary or volcanic units are common, and are associated directly with magnetite bodies. They comprise calc-silicate assemblages of garnet, pyroxene-garnet and epidote garnet in the case of Glubochensk. These are also developed in intrusive rocks at Berezovsk. The scapolite alteration is over printed by hydrous silicate assemblages of epidote, actinolite and chlorite; often associated with albite and carbonate. The latest stage alteration identified is carbonate, associated with silicification and accompanied by sulphides and gypsum or anhydrite.

Discussion

The hydrothermal magnetite bodies of the Urals span a period from the Late Silurian to Lower Carboniferous, but all appear to show consistent feature of an association with centres of basalt-dominated alkaline volcanism, likely to be related to post-collisional rifting as it migrates from the north southwards along the Urals. The rifts are manifested in the form of sub-parallel, N to NNE striking graben features, now often defined by fold axes. On closer inspection, the classification of the magnetite deposits as simple contact skarns is not so evident and many of these deposits have poorly defined relationships with intrusive rocks. Less than 20% of the magnetite bodies actually form in contact with igneous bodies. The largest body in the Turgai district, Kachar, lies some 18 km laterally and probably more than 2 km vertically (based on geophysical modelling) from the contact zone of any prospective intrusive body of sufficient size to have provided adequate heat-flow. Furthermore, the presence of uniform zones of pyroxene-scapolite alteration many kilometres from the intrusive contact has also been pointed out as incompatible with a simple skarn origin (Belevtsev et al. 1982), although these authors propose a metamorphosed syngenetic origin for the ores. There is also a general lack of spatial association between the extensive zones of scapolitisation and the intrusive bodies, suggesting that the scapolite alteration may not be directly controlled by the presence of igneous bodies. Structure is a key component to deposit formation, both in controlling the large intrusive complexes and for focusing hydrothermal systems.

Table 4 summarises the alteration and mineralisation for key magnetite deposits of the region. Much of the alteration is of a regional nature, developed well beyond the aureole of any of the related intrusive bodies. Evidence for the high chloride activity in the alteration fluids is manifested by the large regional scapolite alteration halos. The fluids were highly oxidised from the bulk mineralogical evidence (magnetite, often anhydrite). Apatite is a ubiquitous associated phase in the deposits.

Undoubtedly contact metasomatic zones (s.s.) are recognised at Magnitogorsk where a classic high-temperature assemblage of plagioclase + pyroxene + hornblende + quartz + magnetite is developed, reflecting an almost isochemical change at the margin of the large Magnitogorsk gabbro-granite pluton. Nevertheless, in the Turgai district and at Goroblagodat, scapolite metasomatism is developed on a regional scale, evidence for major regional fluid flow linked to favourable structural trends rather than simple contact alteration skarn development.

Many of the deposits have base metal sulphides, dominated by copper, as a late phase associated with hydrous silicates and carbonate, similar to many of the Cu-Au bearing iron-oxide camps. In the Auerbakh-Krasnoturinsk camp, the margins of the magnetite bodies are noted to have more sulphide-rich bodies where grades of up to 1.6% Cu are not uncommon. Gold values of up to 6 ppm and silver values of 37 ppm are reported in the sulphides.

Exploration in the Urals for major Cu-Au bodies related to the iron-oxide systems has not been carried out systematically, as these belts have been targeted simply for magnetic iron-ore deposits. There must be potential for large tonnage base metal discoveries, given the scale of

alteration shown by the systems. Existing bodies show significant copper and gold values and currently these are not being recovered.

A further feature to note is the dominance of subaerial mafic volcanic suites in the volcanic sequences of the Urals belts. Previous Russian authors have also noted the presence of early hematisation of these volcanics, another positive indicator for the generation of oxidised, copper and gold bearing fluids in regional hydrothermal systems (Hitzman 2000).

Acknowledgements

Part of the work presented in this publication was funded by the European Communities, Cordis-RTD projects 5th Framework Programme INCO-2, project number ICA2-2000-10011. Chris Stanley and Andy Fleet are thanked for useful comments on a first draft.

References

Belevtsev, Ya. N. et al. 1982, Volcanogenic origin for magnetite ores of the Urals, International Geology Review, 24, pp. 1405-1416.

Belyashov, M.M. & Plekhova, K.R., 1965, The effect of sedimentary anhydrites on the metasomatic processes during the formation of the Kachar magnetite deposit (Turgai downwarp), Geol. Rudn. Mestorozh. 7, pp. 38-49 (in Russian).

Brown, D., Juhlin, C., Alvarez-Marron, A., Perez-Estaun, A. & Olianski, A., 1998, Crustal-scale structure and evolution of an arc-continent collision zone in the southern Urals,Russia, Tectonics, 17, 158-171.

Chuguevskaya, O.M., 1969, The genetic features of the Sarbai and Yrltai magnetite deposits in Turgai, Autoref. Diss. Kand. Geol. Miner. Nauk, Alma Ata (in Russian).

Dymkin, , A.M., 1966, The petrology and origin ot the magnetite deposits of Turgai, Nauka Press, Novisibirsk (in Russian).

Dymkin, A.M., Poltavets, Yu. A. & Nechkin, G.S., 1982, The geological-petrological features of the iron-bearing volcanic-plutonic associations, Sverdlovsk (in Russian).

Fershtater, G., 2000, The Magnitogorsk Gabbro-Granite series and related titanomagnetite and magnetite skarn deposits, in: Seltmann, R. et al. (eds.), The Eroded Uralian Palaeozoic Ocean to Continent Transition Zone: Granitoids and Related Ore Deposits, Excursion Guidebook, Publication 14, IGCP Project 373 pp. 58-68.

Fershtater, G.B., Montero, P., Borodina, N.S., Pushkarev, E.V., Smirnov, V.N. & Bea, F., 1997, Uralian magmatism: an overview, Tectonophysics, 276, pp.87-102.

Galkin, P.S., 1963, Some problems of the geology, volcanism and metallogeny of western Turgai, Trudy I Ural'sk. Petrogr. Soveshch., Vol. 2, pp. 137-141, Sverdlovsk (in Russian).

Herrington, R.J., Armstrong, R.N., Zaykov, V.V., Maslennikov, V.V., Tessalina, S., Orgeval, J-J., Taylor, R.N.A., 2001, Massive sulphide deposits in the south Urals: Geological setting within the framework of the Urals orogen, AGU Urals Monograph (in review)

Hitzman, M.W., 2000, Iron Oxide-Cu-Au Deposits: What, Where, When and Why, in: Porter, M. (ed.), Hydrothermal Iron Oxide Copper-Gold & Related Deposits A Global Perspective, Australian Mineral Foundation Inc.

Ivanov, K.S., 1998, Tectonics and geodynamics of the Urals: a development of mobilistic ideas. Abstracts of papers, Tectonics and geodynamics: general and regional aspects. XXXI Tectonic conference, vol. 1, Moscow: Geos, pp. 207-209. (in Russian).

Koroteev V.A., de Boorder H., Netcheukhin V.M., Sazonov V.N. 1997. Geodynamic setting of the mineral deposits of the Urals. Tectonophysics 276, pp. 291-300.

Ksenofontov, O.K., & Ivlev, A.I., 1971, The magmatism and metamorphism of the Turgai trough, in: The Geology of the USSR, Vol 34 Book 2, Nedra Press Moscow, pp. 9-141 (in Russian).

Puchkov, V.N., 1997, Structure and Geodynamics of the Uralian Orogen, in: Burg, J-P. & Ford, M. (eds.), Orogeny through time, Geol. Soc. Spec. Publ., 121, pp. 201-236.

Pumpyanskiy, A.M., Viryuchev, S.I. & Samarkin, G.N., 1985, The Glubochensk magnetite deposits, Intwernational Geological Review, pp. 93-101.

Ronkin, Yu. L., 1989, Sr isotopes as indicator of the magmatic evolution of the Urals, Yearbook-1988, Inst. Geol. Geochem. Uralian Branch of RAS, Sverdlovsk, pp. 107-109 (in Russian).

Samarkin, G.I., & Pumyanskiy, A.M., 1983, The evolution of the Early Carboniferous magmatism of the Valer'yanovo volcanic belt and its metallogeny, in: The geology and mineral raw-resources of the West Siberian Plate and its folded surroundings, Tyumen, pp. 141-144 (in Russian).

Sazonov, V.N., Murzin, V.V. & Grigoriev, N.A., 1998, Vorontsovsk gold deposit: An example of Carlin-type mineralisation in the Urals, Russia: Geology of Ore Deposits, v.40, pp. 139-151.

Seravkin, I.B., Znamensky, S.E., Kosarev, A.M., Rykus, M.W., Salikhov, D.N., Snaczev, W.I. & Mosejczuk, W.M., 1994, Volcanic metallogenesis of the southern Urals: Moscow, Nauka, 152pp. (in Russian).

Sidorenko, A.V., 1973, Geology of the USSR, V. XII, Moscow.

Sledzyuk, P.E., & Shiryaev, P.A., 1958, The magnetite ores of the Kustanai district and the means of utilising them, Acad. Nauk SSSR Press, Moscow (in Russian).

Smirnov, V.I. & Dymkin, A.M., (eds.), 1989, Magnetite skarn deposits of the Urals: Central and southern Urals), Sverdlovsk: Uralian Branch Acad. Sci. USSR, 212 p. (in Russian).

Sokolov, G.A. & Grigor'ev, V.M., 1977, Deposits of Iron, in: Smirnov, V.I. (ed.), Ore Deposits of the USSR Volume 1, Pitman Publishing, London, ISBN 0 273 01034 4. pp. 7-113.

Teterev, G.M., 1970, The principal patterns of distribution and formation of the skarn-magnetite deposits of Turgai, in: The magmatism and endogenic metallogeny of the Transurals, Kustanay, pp.108-109.

Zonenshain L.P., Korinevski V.G., Kazmin V.G. et al. 1984. Plate tectonic model of the South Urals development. In: Tectonophysics. V. 109. P. 95 – 135

General

PGC PUBLISHING

Smith, R.J. 2002 - Geophysics of Iron Oxide Copper-Gold Deposits; *in Porter, T.M. (Ed.), Hydrothermal Iron Oxide Copper-Gold & Related Deposits: A Global Perspective*, Volume 2; PGC Publishing, Adelaide, pp 357-367.

GEOPHYSICS OF IRON OXIDE COPPER-GOLD DEPOSITS

Robert J Smith

Greenfields Geophysics, Melbourne, Australia
greengeo@bigpond.net.au

Abstract – Geophysics is an essential part of most modern mineral exploration programs for iron oxide copper-gold deposits. This paper reviews the important physical properties, which are the basis for the application of geophysical methods, and attempts to illustrate and summarise the ways they have been applied with data and images from selected deposits. Some comments are provided on their historical effectiveness and the role of these methods in an overall program, which must use all available data from geology, mineralogy, geochemistry and geophysics.

Introduction

The class of iron oxide-Cu-Au deposits has captured the imagination of many explorers in the last decade. There have been notable successes, and extensive exploration programs continue on most continents. There is however, no universally accepted definition of this class of deposits, no comprehensive genetic model and no simple, unambiguous, geometric or mineralogical description.

This paper attempts to take a pragmatic approach and look for common features and physical properties which may affect the application and interpretation of geophysics in further discoveries. These features may be regional or local, they may target either a prospective setting or direct detection and they will be illustrated with real examples, wherever possible.

Deposit Types

Although the author knows no universally accepted and unambiguous definition of iron oxide-Cu-Au deposits, there are certainly common characteristics of many deposits that are commonly included in this class.

Perhaps the primary mineralogical characteristic of all deposits in this class is the abundance of magmatically sourced iron oxide, either magnetite or hematite (including specularite), often, but not always, accompanied by a relative lack of iron sulphides. Hitzman (Hitzman, 2000) considers that magnetite-apatite ("Kiruna-type") deposits are closely related and usually occur as precursors to the introduction of copper and gold. The addition of copper and gold, while economically critical may not always occur, leading to many "barren" magnetite-apatite deposits closely related to this class. Uranium may also be present (eg Olympic Dam) and potassic alteration often accompanies the introduction of copper and gold.

In practise, magnetite is almost always present, although variably abundant, both within the deposit itself and in the surrounding rocks. The presence of magnetite-apatite systems is generally considered to be a favourable indicator of the right tectonic setting. Although some deposits occur close to iron rich BIF's, this is considered an element of structural control and not a primary characteristic of the deposit type (Andrew R.L., pers. comm.).

The presence of copper, as chalcopyrite, sometimes accompanied by variable concentrations of pyrite, is a primary economic characteristic. Gold may also be present, but although it is an important economic feature, it is unlikely to occur in sufficient concentration to affect the physical properties and hence it has little direct relevance to geophysical considerations.

The geometry of these deposits seems to be extremely variable and complex. Apart from size, which is also an economic criterion, there seems little which can be said about the geometry that might affect geophysical targeting. Due largely to the influence of structural control, deposits of this type occur in many shapes, sizes and attitudes, so that any attempt to restrict the geometry may excessively limit the target description. The combination of size and location will ultimately limit the economic potential of most deposits, but that is outside the scope of this paper.
Hitzman (Hitzman, 2000) considers that deposits of this class usually occur in post-Archaean rocks from early Proterozoic to Pliocene. They occur in a range of tectonic environments associated with significant igneous activity, and possibly close to volcanic centres, but generally do not appear to be associated with specific intrusions. They are often localised along fault splays off major, crustal–scale extensional faults, but are located in diverse rock types, resulting in a wide variety of deposit styles and mineralogies. This structural control and diverse nature of the resulting styles of mineralisation results in a high degree of complexity in the final deposits.

Physical Properties

Magnetic Properties *(ref. Clarke, 1997)*

Magnetite is classed as *ferrimagnetic*. On an atomic scale, magnetic moments are antiparallel, but tend to cancel out imperfectly resulting in an appreciable magnetisation. At normal temperatures it exhibits strong magnetic susceptibilities (the susceptibility of 100% massive magnetite ranges from ~ 10 to 150 SI) and often also has significant remanent magnetisation.

Hematite (including specularite) is usually described as *anti-ferromagnetic*. At normal temperatures the antiparallel magnetic moments are deflected from the anti-ferromagnetic plane, resulting in a weak or "parasitic" magnetism. Susceptibilities are typically $6x10^{-4}$ to $2x10^{-3}$ SI. There may also be significant remanent magnetisation, a point that is often forgotten.

Figure 1 illustrates the expected range of magnetic susceptibilities for a number of common rock types and minerals, taken from Clark and Emerson (1991).

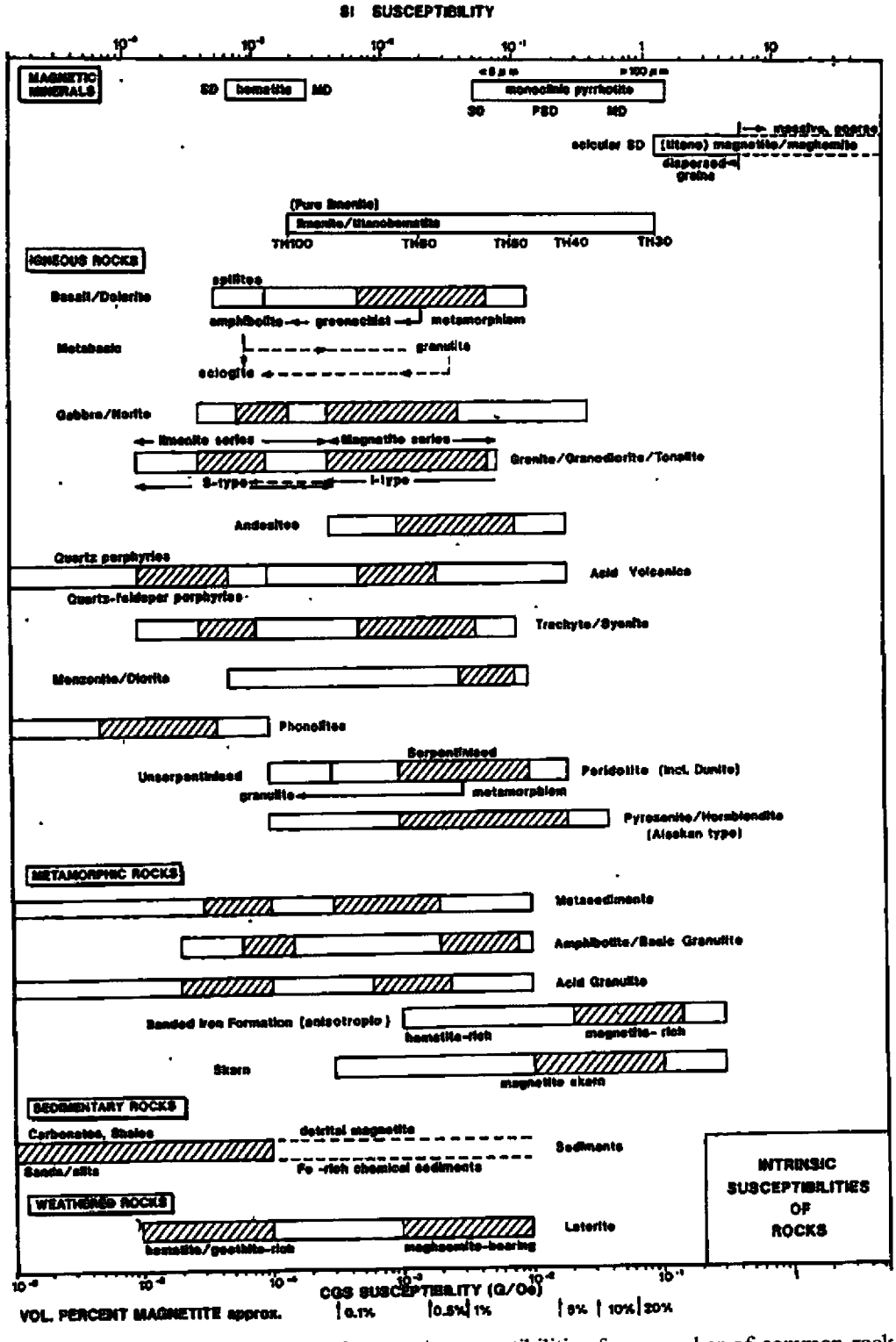


Figure 1: The expected range of magnetic susceptibilities for a number of common rock types and minerals, taken from Clark and Emerson (1991).

In practic, magnetite is usually associated with pronounced magnetic responses or "anomalies" and hematite is not, but this can sometimes be misleading.

Since magnetite is a common rock forming mineral, it occurs in many rocks in varying concentrations and grain sizes. The grain size affects the intrinsic magnetic properties of the mineral. In addition, when disseminated, the effective magnetic properties are diluted and self-demagnetisation effects become important. Dilute dispersions of magnetite grains ($f<0.1$) give susceptibilities of ~3.5f (SI), where f is the volume fraction of magnetite (Clark, pers. comm.). The presence of remanence may either reduce or enhance the effective magnetisation.

The dominant magnetic phase in many rocks is fine grained, magnetically soft multi-domain magnetite, which mainly exhibits viscous remanent magnetisation. This remanence is frequently sub-parallel to the present field and hence it tends to enhance the effective susceptibility without changing the resultant direction of magnetisation. Iron oxide copper-gold deposits are often associated with more coarse-grained magnetite, which tends to retain an ancient remanent direction. It may add to or subtract from the induced magnetisation, or simply skew the resultant magnetisation vector. This would affect quantitative interpretation. Nevertheless, the presence of significant magnetite is usually easily recognised by pronounced magnetic "anomalies".

Hematite, particularly if coarse grained, can sometimes exhibit significant remanent magnetisation resulting in magnetic "anomalies", but this is relatively rare. When it does occur it is generally not aligned with the present field and hence it can distort the resultant direction of magnetisation. This can seriously affect the quantitative interpretation of magnetic sources, where typically only induced magnetisation is considered.

The ratio of remanent to induced magnetisation is termed the Koenigsberger ratio (Q) and some typical values of Q for a number of common rocks are summarised in Figure 2, taken from Clark and Emerson (1991).

In the deposits of interest in this paper, hematite (and maghemite) may result from the partial (or as at Olympic Dam, the almost complete) destruction of magnetite by alteration processes, and hence the two often occur either together or in close proximity. In these cases strong remanent magnetisation is common.

The only common sulphide mineral, which exhibits significant magnetisation at normal temperatures, is pyrrhotite, whose magnetic properties vary from anti-ferromagnetic (hexagonal), with low susceptibility ($\sim 1.5 \times 10^{-3}$ SI) and no remanence, to ferrimagnetic (monoclinic) which has a much higher susceptibility. Monoclinic pyrrhotite has a susceptibility ranging from 0.04 SI for fine grains (<5μm) up to ~10 SI for coarse grained (>100μm) massive monoclinic pyrrhotite. It usually also exhibits strong remanence (Q ranges from 1-10 for coarse (>100μm) grains to >100 for fine grains) which is often quite oblique to the present field (Clark, pers. comm., Clark, 1997). Pyrrhotite is not common in iron oxide copper-gold deposits and hence the magnetic properties of pyrrhotite are not of primary consequence.

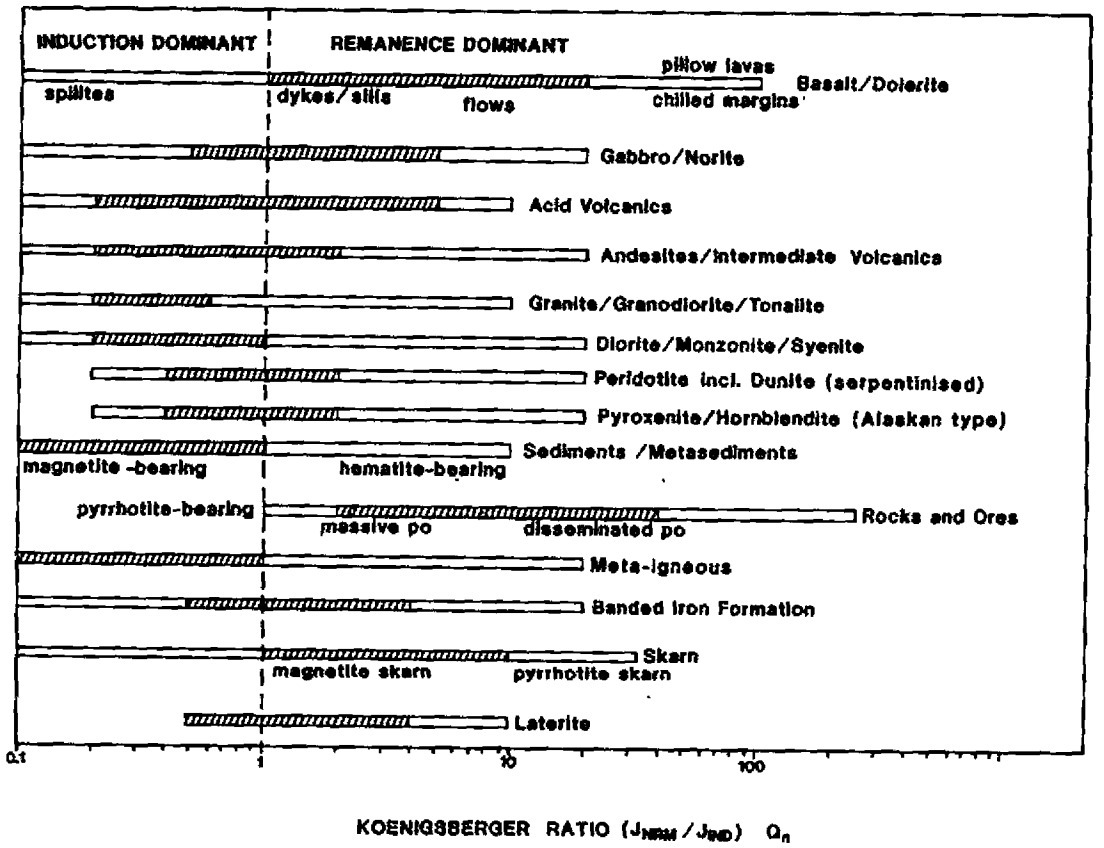


Figure 2: Typical Koenigsberger ratios for common rocks.

Chalcopyrite is paramagnetic and has a typical susceptibility of 30 to $40x10^{-5}$ SI. It does not contribute significantly to any magnetic response.

Gold is weakly diamagnetic and generally occurs in very low concentrations. It does not contribute significantly to any magnetic response.

Most other rock forming minerals are either weakly paramagnetic or diamagnetic and most observed magnetic responses can be attributed to the presence of magnetite, maghemite and, to a lesser extent, hematite.

Specific Gravity

Most rock forming minerals have a well-documented density or specific gravity. The specific gravity of commonly occurring rocks can be estimated from the mineral composition. In real rocks, impurities and other factors result in much more variability. Nevertheless average dry bulk densities for most rock types are generally close to or in the range 2.5 to 3.0 gm/cm^3 as listed below:

Acid igneous (Av.)	2.30 – 3.11 gm/cm^3
Basic igneous (Av.)	2.09 – 3.17 gm/cm^3
Metamorphic (Av.)	2.4 – 3.1 gm/cm^3

(Ref. Tables 2.3 and 2.4 in Telford et. al. 1976)
(Ref. Table 5, Olhoeft G.R. and Johnson G.R. 1989).

By contrast, most ore forming minerals have much higher densities. Olhoeft and Johnson (1989) list the following values for the minerals of interest in this study.

Chalcopyrite	3.6 gm/cm^3
Gold	3.6 gm/cm^3
Maghemite	4.9 gm/cm^3
Magnetite	5.2 gm/cm^3

In all cases they are likely to be much more dense than their host and consequently, if large enough, will result in significant gravity "anomalies". In particular, large hematite associated deposits (eg. Olympic Dam) may be difficult to detect by any other geophysical method.

Electrical Resistivity/Conductivity

The electrical resistivity or conductivity of most minerals is reasonably well documented, however in real rocks there can be significant variations due to impurities, dilution, pore fluids and mode of occurrence. The values quoted generally refer to the properties of a relatively pure mineral specimen. In rocks the inherent variations due to impurities are likely to be minor compared with dilution, due to low concentrations or the presence of saline pore fluids in the overburden or in fractures. In addition there will be major differences between rocks where the conductive mineral particles are either evenly disseminated or interconnected by a network of veinlets.

Nevertheless, the electrical properties of magnetite, hematite (including specularite), chalcopyrite, pyrite and perhaps even gold are of interest.

Most rock forming minerals have very high electrical resistivities and consequently the rocks formed from them are resistive also. Some examples are listed below (taken from Tables 5.4 & 5.5, in Telford et al, 1976). These are typical examples, but there can be wide variations due to weathering, fracturing and other mechanical factors.

Sandstones	$(1\text{-}6.4)x10^8$ (Ωm)
Limestones	$50 - 10^7$ (Ωm)
Dolomite	$3.5x10^2 - 5x10^3$ (Ωm)
Andesite	$4.5x10^4\text{-}1.7x10^2$ (Ωm)
Granite	$3x10^2 - 10^6$ (Ωm)
Basalt	$10 - 1.3x10^7$ (Ωm)

By contrast, magnetite, hematite, chalcopyrite and (gold) are usually several orders of magnitude more conductive, as listed below (from Table 5.2, in Telford et al, 1976):

Magnetite	$5x10^{-5} - 5.7x10^3$(Ωm)
Hematite	$3.5x10^{-3} - 10^7$(Ωm)
Specularite (Av.)	$6x10^{-3}$(Ωm)
Chalcopyrite	$1.2x10^{-5} - 0.3$(Ωm)
Chalcocite	$3x10^{-5} - 0.6$(Ωm)
Pyrite	$2.9x10^{-5} - 1.5$(Ωm)
Pyrrhotite	$6.5x10^{-6} - 5x10^{-2}$(Ωm)
Gold	$2.4x10^{-8}$(Ωm)

In practice, most rocks conduct by movement of ions in the pore fluids. If the rocks are porous (as in the weathered zone) and pore fluids are saline, this can greatly enhance the conductivity. It is common, for example, to measure resistivities in the range 1 to 10 (Ωm) in Australia, due primarily to a deep, porous weathered zone and saline ground water. Nevertheless, in most cases the metallic sulphide minerals will still be much more conductive than barren rocks and even rocks containing magnetite and hematite (specularite) are likely to be relatively conductive.

Several methods are available to measure resistivity (or conductivity) and detect major anomalies in rock resistivity. These include primarily induced polarisation (IP) & resistivity, electromagnetics (EM) and magnetotellurics (MT). Within these broad headings there are numerous subdivisions and variations on the specific method of making the measurement. In principle they could all detect magnetite, hematite and chalcopyrite if they occur in sufficient abundance and in a favourable environment. In practice however there are many complications which may favour one method over another.

IP & Resistivity measurements are usually made together and they are very sensitive to large volumes of even low-grade mineralisation. The addition of an IP measurement contributes to this sensitivity, but it can also respond to many non-economic targets.

EM measurements, whether made from the air or on the ground (or even in drill holes) respond best to a high resistivity contrast, even though the target conductor may occupy a small volume. For example a thin sheet of highly conductive mineralisation may be a good EM target but respond poorly to IP & resistivity.

MT, AMT and CSAMT all respond similarly to resistivity, but they do not include an IP measurement. In some cases they can achieve very great depth penetration to large conductors. MT and AMT are passive measurements, which use natural field variations as an energy source, but these can be unreliable. CSAMT uses an artificial source to ensure sufficient energy for a measurement.

Chargeability *(ref. Parkhomenko E.I., 1967 and 1971)*

Although most host rocks conduct electricity by movement of ions through pore fluids, the "metallic minerals" or those with metallic lustre, usually conduct by movement of electrons through the crystal lattice. This includes most of the metallic sulphides and also includes magnetite and hematite (specularite), graphite and, of course, gold. This mixture of ionic and electronic conduction is the basis of the induced polarisation effect, which can be measured in various ways. The basic parameter, which characterises the magnitude of the response of a mineral to induced polarisation, is "chargeability". Since the measured chargeability is extremely dependent on the concentration and mode of occurrence of the metallic particles (eg. disseminated versus interconnected), as well as the conductivity, it is not usual to list intrinsic chargeabilities for various minerals. It is sufficient to say that chalcopyrite, chalcocite, pyrite, pyrrhotite, gold, magnetite and specularite will all increase the chargeability of a rock when they are present. Dr D.W. Emerson (1994) conducted a petrophysical study of the electrical properties of such ores in a recent AMIRA project (P416).

Although details of the induced polarisation mechanism are still debated, the effect has been shown to be reasonably well described by a mathematical model (the Cole-Cole model, ref. Pelton et al, 1978). In this model, another useful parameter is the "time constant" which appears to be related to the average grain size of the metallic particles. There have been a number of attempts to determine the time constant as well as the chargeability, by measuring at a range of frequencies or over a wide time range, and then using these parameters for mineral discrimination. For example, identifying a specific response for magnetite as distinct from a signature for chalcopyrite would obviously be advantageous. Although there have been specific cases where this appears to have been somewhat effective, in general the time constant appears to be mainly dominated by effective grain size.

In summary, it seems enough to say that magnetite, specularite and chalcopyrite (as well as pyrite and pyrrhotite) can all cause IP anomalies and when they occur in close proximity it is often difficult to distinguish between them.

Radiometrics *(ref. Muller D. and Groves D.I. 1995)*

The radiometric method detects gamma radiation, which is emitted by a number of naturally occurring rocks and minerals, that contain specific elements or, more correctly, specific isotopes of these elements. The only naturally occurring elements of interest as gamma emitters are potassium (K40), uranium and thorium (and their daughter products). Modern gamma ray spectrometers, carried in aircraft, are able to distinguish between emissions from these three sources and, if calibrated, provide a quantitative map of their near surface distribution. These can be used to map near surface lithology and often also to detect overprints from alteration. Perhaps the most important of these is the signature of potassic alteration, which has been associated with many copper-gold deposits.

Although magnetite, hematite and chalcopyrite are unlikely to have a direct radiometric signature, the deposits of interest may have a potassic alteration halo, related directly to the copper-gold mineralisation. If so, this could be detected by airborne or ground based radiometric measurements.

The observed radiometric response is often attenuated, to varying degrees, by soil cover but the nature of the source (eg. K, U or Th) may still be apparent. Potassic alteration is often accompanied by depletion in thorium and hence the K/Th ratio is often used to enhance the alteration signature. Various statistical methods (eg. principal components) can also be used to try to separate alteration overprints from the normal responses relating to cover and lithology. Some examples of this approach can be seen in Wellman (1998, 1999) and Shives et al (1997).

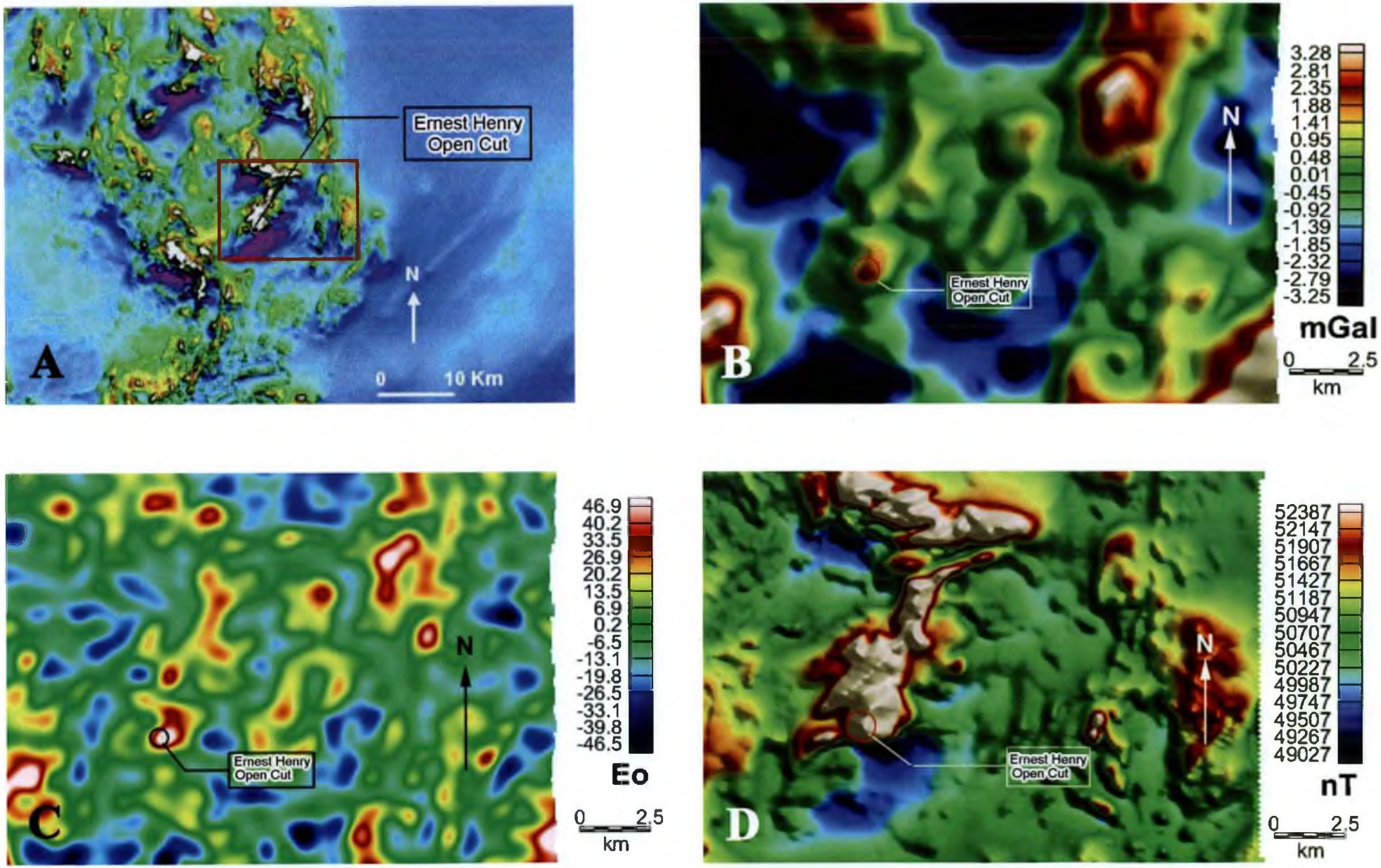
Seismic

Although the acoustic impedance of the ore minerals must increase with increasing specific gravity, the acoustic velocity may compensate due to a decrease caused by faulting and brecciation. In any case, the complex geometry of these deposits is likely to make seismic applications difficult and they are not well documented. Seismic methods do offer high resolution at depth and may find more application in the future.

Regional Responses

Regional geophysical data sets, principally magnetics and gravity, are now becoming readily available in many areas. These data sets are often of high quality and inexpensive, if not free. They are widely used, together with regional geology, as a "first pass" look and as an aid to area selection.

From the discussion of physical properties it should be apparent that iron oxide copper gold deposits are likely to occur in an area of some magnetic activity, although not necessarily coincident with a discrete magnetic anomaly. Haynes (2000) noted this "magnetically active" signature as a characteristic of such mineralised districts at Olympic Dam, Moonta-Wallaroo, Ernest Henry and Candelaria. Plates 1A and 1E show TMI images of the area surrounding Ernest Henry and Olympic Dam. In both cases, there is a notable increase in magnetic activity in the district surrounding the deposits. Numerous possible targets can be easily identified but, in each case, only one has been shown to be associated with economic mineralisation.


Ernest Henry
Open Cut
N
0 10 Km
A
Ernest Henry
Open Cut
B
N
3.28
2.81
2.35
1.88
1.41
0.95
0.48
0.01
-0.45
-0.92
-1.39
-1.85
-2.32
-2.79
-3.25
mGal
0 2.5
km
Ernest Henry
Open Cut
C
N
46.9
40.2
33.5
26.9
20.2
13.5
6.9
0.2
-6.5
-13.1
-19.8
-26.5
-33.1
-39.8
-46.5
Eo
0 2.5
km
Ernest Henry
Open Cut
D
N
52387
52147
51907
51667
51427
51187
50947
50707
50467
50227
49987
49747
49507
49267
49027
nT
0 2.5
km

Regional gravity data tends to show similar character but the available data is usually less detailed. The recent development of an airborne gravity gradiometer by BHP (Falcon), and its deployment on mineral exploration projects will undoubtedly change this in the future. A gravity gradiometer measures the gradient of the gravity field, but it can be converted mathematically to produce maps of the gravity field (Gz), which match conventional ground gravity measurements. These airborne measurements can rapidly produce detailed gravity maps over large areas, similar to the airborne magnetic maps, which have been used extensively for many years.

Plates 1B and 1C show images of gravity (Gz) and vertical gravity gradient (Gzz) derived from an airborne survey by Falcon over Ernest Henry.

Radiometric data is generally collected with a gamma ray spectrometer, together with magnetic data, in modern airborne surveys. In recent years there has been a significant improvement in data quality and it is now common to use the data for lithological mapping, in conjunction with magnetics. In some cases it is also possible to recognise an alteration halo as an overprint on the lithology (Shives et al, 1997; Wellman, 1999). At Candelaria, test surveys after the discovery did confirm the value of radiometrics "in determining areas of potassic alteration when it is outcropping or within 10 to 20 cm of the surface" (Matthews and Jenkins, 1997).

Shives et al (1997) described radiometric data from the Lou Lake area, NWT, Canada. In this area, the Sue-Dianne deposit (Goad, et. al., 2000), which has documented similarities with Olympic Dam, was discovered as a result of a radiometric anomaly detected on survey lines 5 km apart. Subsequently, more detailed surveys were flown by the Geological Survey of Canada and this delineated several new targets as well as the existing ones. Plates 2C and 2D show K and Th/K images respectively from this later survey, taken from Shives et al (1997). In this case they used Th/K to enhance the alteration signature. Plate 2B shows the geology. The large area of enriched K, to the south east of Lou Lake, coincides with numerous showings of vein and disseminated Au-Co-Cu-Bi-W-As. There are also coincident magnetic (>2000 nT) and gravity (3 mgal) anomalies not shown here. Although not yet proven to be economic, subsequent drilling has discovered extensive polymetallic sulphide mineralisation within an extensive zone of potassic alteration and iron enrichment.

Figure 3 shows multi-channel profiles along Line 16, which traverses from east to west across the centre of the area shown in Plates 2B, 2C and 2D. The position of the

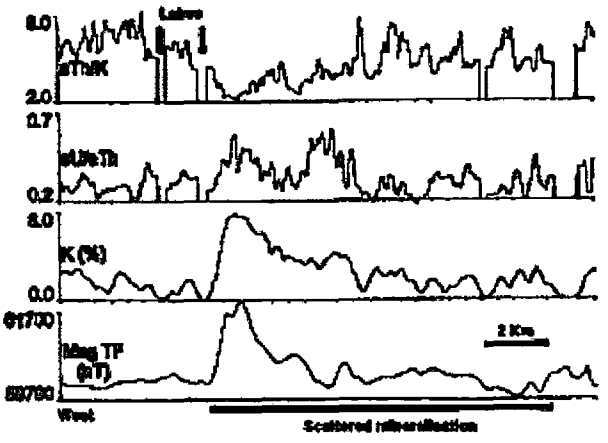


Figure 3 - Multi-channel, partially stacked profiles along Line 16, Lou Lake, NWT, Canada (see Plates 2C & D for location) from a 1993 survey at 500 m line spacing (Shives *et al.*, 1997)

lakes can be clearly seen by a decrease in K response and low values of eTh/K and eU/eTh. Immediately to the east of these lakes there are coincident magnetic and K anomalies which appear to reflect the alteration halo around mineralisation. The alteration zone is also coincident with a zone of increased eU/eTh due to some additional enrichment in U in the mineralised zone. Of course it is well known that there is significant U enrichment in Olympic Dam also, but the depth of cover would mask any similar response to airborne radiometrics.

Deposit Signatures

In detail the geophysical signatures of these deposits are more complex. Although deposits usually occur in an area of significant magnetic relief, they are not always coincident with discrete magnetic anomalies. In the case of the hematite rich Olympic Dam (see Plate 2A) the prominent magnetic anomaly coincident with the deposit appears to come from a deeper source. While it may be genetically related to the mineralisation, it seems unlikely to be directly attributable to it. Plate 1D shows detailed TMI over Ernest Henry. It appears more likely in this case that there is a magnetic response from the mineralisation, but it is only one of many magnetic anomalies in the district and not obviously different from many other possible targets. This is a common feature of these deposits as the related iron oxide is usually much more widespread than the copper sulphide and gold mineralisation.

At Candelaria, in Chile, good quality magnetic data was not obtained until after the initial discovery and earlier

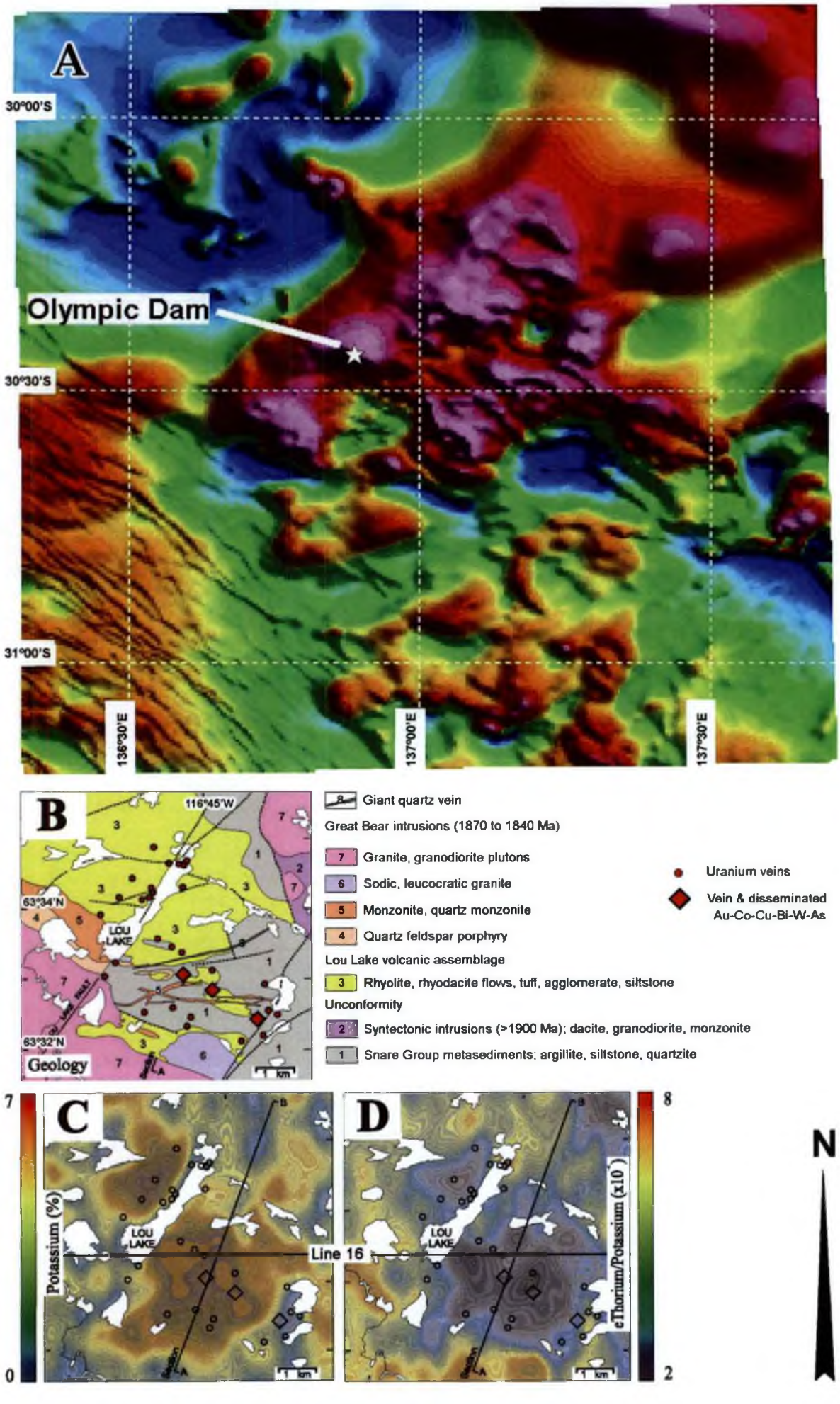
PLATE 1 (see facing page):

A – Shaded TMI Image of Ernest Henry District (courtesy of BHP-Billiton)

B – Shaded Image of Gz over Ernest Henry (courtesy of BHP-Billiton)

C – Image of Gzz over Ernest Henry (courtesy of BHP-Billiton)

D – Detailed TMI over Ernest Henry (courtesy of BHP-Billiton)


A
30°00'S
Olympic Dam
30°30'S
31°00'S
136°30'E
137°00'E
137°30'E
B
116°45'W
63°34'N
63°32'N
LOU LAKE
Geology
1 km
Giant quartz vein
Great Bear intrusions (1870 to 1840 Ma)
7 Granite, granodiorite plutons
6 Sodic, leucocratic granite
5 Monzonite, quartz monzonite
4 Quartz feldspar porphyry
Lou Lake volcanic assemblage
3 Rhyolite, rhyodacite flows, tuff, agglomerate, siltstone
Unconformity
2 Syntectonic intrusions (>1900 Ma); dacite, granodiorite, monzonite
1 Snare Group metasediments; argillite, siltstone, quartzite
Uranium veins
Vein & disseminated Au-Co-Cu-Bi-W-As
C
D
Line 16
Potassium (%)
eThorium/Potassium (x10⁻⁴)
7
0
8
2
N

surveys were of low sensitivity and poorly oriented (Matthews, J.P. and Jenkins, R.A. 1997). Subsequently, high quality data has been obtained. After processing to compensate for the local field inclination (reduction to the pole) an excellent correlation was obtained between the magnetics and mineralisation as shown in Figure 4.

Gravity appears to be more effective in many cases. At Olympic Dam there is also a significant gravity anomaly coincident with the mineralisation which is usually attributed mainly to the ore mineralisation. In fact, early drilling and the discovery hole were sited on the coincident magnetic and gravity anomalies (Rutter, H. and Esdaile, D.J., 1985; Smith, R.J., 1985; Esdaile D.J., et al, 1987).

Similarly, at Ernest Henry, as shown in Plates 1B and 1C, there are both Gz and Gzz anomalies coincident with the deposit. While not unique, they are perhaps more distinctive than the related magnetic features. Detailed ground gravity measurements were used to delineate the deposit and showed good correlation with the mineralisation.

In general one might expect that any significant deposit of the iron oxide copper gold class should have an associated



Figure 4 – Airborne Magnetics (RTP), Candelaria deposit, Chile (Matthews and Jenkins 1997).

PLATE 2 (see facing page):

A – Shaded TMI Image of Olympic Dam District (courtesy of PIRSA)

B – Geology and Legend, Lou Lake, NWT, Canada (Shives et al, 1997)

C – K Image, Lou Lake, NWT, Canada (Shives et al, 1997)

D – Th/K Image, Lou Lake, NWT, Canada (Shives et al, 1997)

gravity response and may or may not have an associated magnetic response.

Although there is often both associated potassic alteration and uranium enrichment in these deposits, radiometric methods are not widely used for direct detection (as distinct from regional reconnaissance). Thickness of cover often obscures any radiometric signature at the surface but down-hole measurements are often useful for ore delineation. The application of down-hole radiometrics would be dependent on the precise mineralogy of the deposit and will not be reviewed here.

Since magnetite, hematite (specularite) and chalcopyrite (and possibly other sulphide minerals) are all conductive, a range of electrical methods can be used for direct detection of these deposits. Historically IP and resistivity have been widely used and with notable success, but modern EM and MT methods have also been shown to be effective in some cases. They all directly detect the target mineralisation, but unfortunately frequently respond also to the associated magnetite and hematite (and pyrite and pyrrhotite, if present). Since these associated conductors are often more laterally extensive than the target mineralisation they will result in many spurious targets. Nevertheless, several notable discoveries have been attributed to these methods.

Olympic Dam is located beneath approximately 300 metres of relatively conductive cover, which would reduce the effectiveness of electrical methods. Early attempts at detecting the deposit with IP were unsuccessful, due primarily to problems attributable to the deep, conductive cover. Subsequent work with more advanced equipment did give a detectable response (Esdaile D.J., et al, 1987).

At Ernest Henry, the strong magnetic anomalies in the area influenced area selection and ground based TEM surveys were used to "filter" the magnetic targets (Ryan A.J., 1998). Copper and gold mineralisation was discovered in 1991 when drilling a moderate amplitude TEM anomaly. Subsequent down-hole TEM suggested that the initial TEM response was primarily due to a supergene zone rich in native copper. The bulk of the primary mineralisation did not produce a TEM anomaly (Webb, W. and Rowston, P., 1995). Typically, these deposits are not massive and their conductivity is generally not ideal for detection by EM methods. If an enriched supergene zone is present it may present a better target. Subsequently, ground magnetic, gravity and induced polarisation methods were used to delineate the deposit at Ernest Henry. Ground magnetic data showed that the main magnetic response was primarily due to magnetite in shears to the north and south of the main deposit, rather than the ore mineralisation itself. IP is much more sensitive than EM to disseminated mineralisation and both surface and down-hole measurements were used at Ernest Henry. It was shown to respond to both the supergene-enriched zone and to the primary ore, and also to "sparsely mineralised magnetite".

At Candelaria, mineralisation was well known and had been mined intermittently from time to time (Matthews and Jenkins, 1997). Initial IP/resistivity surveys over the known mineralisation revealed extensions both laterally and in depth and these guided early drilling. There is abundant non-economic sulphide mineralisation in the area, which also gave pronounced IP responses. IP and resistivity were primary exploration tools but the success obtained relied heavily on starting in the right place, over known deposits.

In summary, IP and resistivity methods have been generally successful in detecting these deposits but they also respond to both iron oxides and barren sulphides, which are often present. EM methods have not been as successful in general, probably due to the disseminated nature of many targets. EM methods are still developing and they may become more effective in the future.

Conclusions

Regional magnetic, gravity and radiometric data sets are now readily available in many parts of the world. They are valuable tools to assist in locating prospective areas, associated with magmatic intrusions and major structural controls. Radiometric data may also indicate potassic alteration haloes in areas where the signature is not obscured by excessive cover.

Specific deposits themselves may or may not have a magnetic signature although they will almost certainly occur in an area of significant magnetic relief. Almost all known deposits in this class do give a significant gravity response but it may be difficult to recognise in areas of complex tectonics or steep terrain.

IP/resistivity has proven to be the most generally useful of the electrical methods, but it also responds to barren sulphides, if present, and to magnetite and specularite. Consequently it will produce many "spurious" targets. EM methods have been less useful in general, due to the often disseminated nature of the targets, but they should not be ignored. Airborne EM may find more application in the future as new systems develop with improved sensitivity. MT methods should also be applicable, particularly where deep penetration is required, but little data is available.

These deposits are difficult to categorise and hence there is no generally applicable recipe for successful exploration. It is important to use a range of tools and integrate all available geological, mineralogical, geochemical and geophysical data to understand them.

Acknowledgments

The author would like to acknowledge contributions from many people, institutions and companies. In particular the illustrations of Ernest Henry geophysics were provided by BHP-Billiton, and regional magnetics over Olympic Dam came from the PIRSA web site. The author was assisted by discussions with Dr. D.A. Clark (CSIRO DEM), Dr. R.L. Andrew and Mr. R.J. Rebek (Rio Tinto Exploration Pty Ltd), and Mr. T.M. Porter (Porter GeoConsultancy Pty Ltd).

References

Clark, D.A. and Emerson, D.W. 1991 – Notes on rock magnetization characteristics in applied geophysical studies; Exploration Geophysics, Volume 22, Number 3, pp 547-555.

Clark, D.A. 1997 – Magnetic petrophysics and magnetic petrology: aids to geological interpretation of magnetic surveys; AGSO Journal of Geology and Geophysics, Volume 17, Number 2, pp 83-103

Emerson D.W. 1994 – Electrical Properties of Magnetite Rich Rocks and Ores, Final Report on AMIRA project P416, August 1994 (originally confidential to sponsors, now available from AMIRA).

Esdaile D.J., Pridmore D.F., Coggon J.H., Muir P.M., Williams P.K., Fritz F.P. 1987 – Olympic Dam Deposit – Geophysical Case History; Exploration Geophysics, Volume 18, Nos 1/2, pp 47-49.

Goad, R.E. et. al., 2000 – Geology of the Proterozoic iron oxide-hosted, NICO cobalt-gold-bismuth, and Sue-Dianne copper-silver deposits, Southern Great Bear Magmatic Zone, Northwest Territories, Canada, *in* Porter, T.M. (Ed), Hydrothermal Iron Oxide Copper-Gold & Related Deposits: A Global Perspective, *Australian Mineral Foundation,* Adelaide, pp 249-267.

Haynes, D.W. 2000 – Iron Oxide Copper (-Gold) Deposits: Their Position in the Ore deposit Spectrum and modes of Origin; *in* Porter, T.M. (Ed), Hydrothermal Iron Oxide Copper-Gold & Related Deposits: A Global Perspective, *Australian Mineral Foundation,* Adelaide, pp 71-90.

Hitzman, M.W. 2000 – Iron Oxide-Cu-Au Deposits: What, Where, When and Why; *in* Porter, T.M. (Ed), Hydrothermal Iron Oxide Copper-Gold & Related Deposits: A Global Perspective, *Australian Mineral Foundation,* Adelaide, pp 9-25.

Matthews, J.P., and Jenkins, R.A., 1997 – Geophysical Exploration and Discovery of the Candelaria Copper-Gold Deposit in Chile; *in* Geophysics and Geochemistry at the Millennium, Proceedings of Exploration 97, Fourth Decennial International Conference on Mineral Exploration, published by the Prospectors and Developers Association of Canada.

Muller D. and Groves D.I., 1995 – Potassic Igneous Rocks and Associated Gold-Copper Mineralisation; Springer

Olhoeft G.R. and Johnson G.R., 1989 – Densities of Rocks and Minerals; *in* Carmichael R.S. (Ed), Practical Handbook of Physical Properties of Rocks and Minerals, CRC Press, Inc., Florida

Parkhomenko E.I., 1967 – Electrical Properties of Rocks; Plenum Press, New York

Parkhomenko E.I., 1971 – Electrification Phenomena in Rocks; Plenum Press, New York

Pelton, W.H., Ward, S.H., Hallof, P.G., Sill, W.R., Nelson, P.H. 1978 – Mineral Discrimination and Removal of Inductive Coupling with Multifrequency IP, Geophysics, Volume 43, pp 588-609.

Porter, T.M. 2000 – Hydrothermal Iron-Oxide Copper-Gold & Related Ore Deposits; *in* Porter, T.M. (Ed), Hydrothermal Iron Oxide Copper-Gold & Related Deposits: A Global Perspective, *Australian Mineral Foundation*, Adelaide, pp 3-5.

Rutter, H. and Esdaile, D.J. 1985 – The Geophysics of the Olympic Dam discovery; Exploration Geophysics, Volume 16, Nos 2/3, pp 273-276.

Ryan, A.J. 1998 – Ernest Henry copper-gold deposit; *in* Geology of Australian and Papua New Guinean Mineral Deposits, Monograph 22, The Australasian Institute of Mining and Metallurgy, pp759-767.

Shives, R.B.K., Charbonneau, B.W., and Ford, K.L. 1997 – The detection of potassic alteration by gamma-ray spectrometry – recognition of alteration related to mineralisation; *in* Geophysics and Geochemistry at the Millennium, Proceedings of Exploration 97, Fourth Decennial International Conference on Mineral Exploration, published by the Prospectors and Developers Association of Canada.

Smith, R.J. 1985 – Geophysics in Australian Mineral Exploration; Geophysics, Volume 50, Number 12, pp 2637-2665.

Telford W.M., Geldart L.P., Sheriff R.E., Keys D.A. 1976 – Applied Geophysics, Cambridge University Press

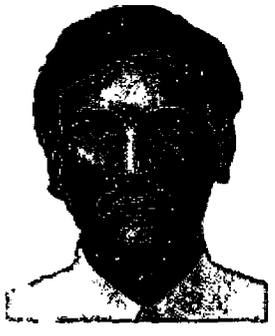
Wellman, P. 1998 - Mapping of a granite batholith using geological and remotely sensed data: the Mount Edgar Batholith, Pilbara Craton; Exploration Geophysics, Volume 29, Numbers 3 & 4, pp 643-648.

Wellman, P. 1999 – Gamma-ray spectrometric data: Modelling to map primary lithology; Exploration Geophysics, Volume 30, Numbers 3 & 4, pp 167-172.

Webb, M. and Rowston, P. 1995 – The geophysics of the Ernest Henry Cu-Au Deposit (N.W.) Qld; Exploration Geophysics, Volume 26, Numbers 2/3, pp 51-59.

Biography

BIOGRAPHIES OF PRINCIPAL AUTHORS



Ricardo Boric received his professional Geólogo degree from the Universidad de Chile, Santiago, in 1980. He then worked until 1988 with SERNAGEOMIN, in northern Chile, compiling metallogenic maps (mainly in the Antofagasta region) and developing ore deposit models for Cu mineralisation, including aspects of hydrothermal alteration, magmatism and tectonics. From 1988 to 1989 he worked as an Exploration Geologist with Compañía Minera El Bronce de Petorca, developing a regional geologic model for the epithermal Au veins of that district. From 1989 to 2001 he held the position of Senior Geologist for Compañía Minera Disputada de Las Condes, El Soldado, developing the geologic model for the mine as well as being responsible for regional exploration. In this capacity he contributed to extending the economic life of the mine by doubling the known ore reserves. Since 1992 he collaborated with the Universidad de Chile faculty in research on isotopes and geochronology of copper mantos (FONDECYT funding), and with faculty and students at Dalhousie University, Halifax, Canada (NSERC funding). Currently he is completing his Masters degree at Dalhousie.

Contact details: c/- Department of Earth Sciences, Dalhousie University, Halifax, Nova Scotia, B3H 3J5, Canada; Currently: Hernando de Aguirre 421, Depto. 42, Providencia, Santiago, Chile; Email: rboric@ctcinternet.cl



Dr. Farahnaz Daliran was awarded a Maitrise (MSc equiv) in Geologie and a "DEA" of Applied Geology from the University of Grenoble, France in 1973 and 1974. In 1975 she started her PhD thesis on the apatite-magnetite deposits of Bafq district and was at the same time Senior Geologist for the National Iranian Steel Corporation. In 1986 she was awarded a Diploma (MSc equiv) in Mineralogie and in 1990 a Dr rer nat (PhD equiv) from the University of Heidelberg, Germany. During 1976-1983 she was assistant lecturer at the University of Esfahan, guest researcher in the University of Cairo, and Chulangkorn. From 1991 to the present she has held post doctoral positions in experimental mineralogy (sulphide systems), and ore deposit research in the Universities of Heidelberg and Karlsruhe, Germany, which was assisted by a consultancy on the mineral deposits of Iran. Her current projects focus on gold and iron oxide-apatite-sulphide systems in Iran.

Contact details: Institut für Petrographie und Geochemie, Kaiserstr. 12, 76128 Karlsruhe, Germany; Phone: +49 721 608 4279; Fax: +49 721 608 7247;
Email: farahnaz.daliran@bio-geo.uni-karlsruhe.de



Dr. Garry Davidson gained his BSc (Hons.) at the Australian National University in 1981, which lead to exploration work with Shell Metals/Billiton Exploration in Australian Proterozoic terrains, seeking sediment-hosted and Broken Hill-type Pb-Zn deposits, and Tennant Creek-style oxide Cu-Au mineralisation. In 1985 he began a PhD on the genesis of the Starra oxide Cu-Au system in the Cloncurry district, extending the scope of the research to include the Osborne deposit (then known as Trough Tank). His post-doctoral studies in the 1990s at the University of Tasmania's Centre for Ore Deposit Research, have specialised in improving the knowledge of the mineralogy and the chemical (including isotopic) and genetic models of oxide Cu-Au systems, including collaborative projects with industry and James Cook University researchers. This work has led to the research discussed in this volume. In addition, his published research includes studies of sediment-hosted Zn-Pb deposits, alkaline alteration in sedimentary basins, sulphur cycling during hydrothermal alteration, and the geochemistry of hydrothermal sediments. Garry is a senior lecturer at the University of Tasmania.

Contact details: Centre for Ore Deposit Research (CODES SRC), University of Tasmania, GPO Box 252-79, Hobart, Tasmania, 7001, Australia;
Phone: +61 3 6226 2815; Fax: +61 3 6226 7662; Email: garry.davidson@utas.edu.au



Russell Dow completed a BSc (Hons) in geology at the University of Western Australia, in 1996. Following graduation he worked for RGC in gold and base metal exploration as well as open pit and underground mining. Currently he is investigation the Arizaro-Lindero Hydrothermal Iron-Oxide Cu-Au systems in northwest Argentina, which is the subject of his descriptive MS Thesis at the Colorado School of Mines. Russell plans to work as an exploration geologist upon completion of his MS at the end of 2002.

Contact details: Department of Geology and Geological Engineering, Colorado School of Mines, Golden, CO, 80401, U.S.A.;
Phone: +1 303 316 2776; Fax: +1 303 273 3859; Email: georuss@hotmail.com

---



Gary Ferris completed a BSc (Hons.) in Geology at University of Adelaide in 1991 and recently submitted a Masters of Exploration Thesis at the Centre for Ore Deposits and Exploration Studies (CODES), University of Tasmania. In 1992 he commenced work with the Department of Mines and Energy, South Australia (now PIRSA) and has worked in the Mineral Assessment Branch working on various commodities and regional bedrock drilling programs. He is currently working in the Gawler Craton Team of the Geological Survey Branch focused on the tectonic evolution of the western Gawler Craton.

Contact details: Geological Survey Branch, Office of Minerals and Energy Resurces, Primary Industries and Resources SA, GPO Box 1671, Adelaide, SA, 5001, Australia;
Phone: +61 8 8463 3123; Fax: +61 8 8226 3200; Email: ferris.gary@saugov.sa.gov.au

---



Dr. Kurt C. Friehauf earned a BSc (Geology) from Colorado State University in 1989 and a PhD. (Geological and Environmental Sciences) from Stanford University in 1998. His research focuses on evolution of porphyry copper deposits and the geology of Fe-oxide (-REE-Cu-Au) type ores. His current projects include work on the magmatic-hydrothermal evolution of porphyry copper-gold and skarn mineralization in the Ertsberg-Grasberg district of Irian Jaya, Indonesia and on Fe-oxide deposits in the northeastern U.S. He is currently an Assistant Professor of Geology in the Department of Physical Sciences at Kutztown University, Pennsylvania.

Contact details: Department of Physical Sciences, Grim-Knedler Building, Room 214, Kutztown University, Kutztown, PA, 19530, USA;
Phone: +1 610 683 4446; Fax: +1 610 683 1352; Email: friehauf@kutztown.edu

---



Christian Grainger graduated from the University of Western Australian with a first class Honours Degree in 1998. Subsequently he worked in gold exploration and mining within the Yilgarn Craton of Western Australia. More recently he was appointed to the position of regional project geologist involved in Fe-oxide Cu-Au exploration within the Carajás Mineral Province of Brazil with Teck Corporation and INCO. Currently he is undertaking a PhD study of the Serra Pelada Au-PGE deposit and its genetic association with Fe-oxide Cu-Au mineralisation within the Carajás Mineral Province. His PhD studies are being conducted through the Centre for Global Metallogeny in the Department of Geology and Geophysics at the University of Western Australian, working with Prof. David Groves and in conjunction with Companhia Vale do Rio Doce and its exploration arm, DOCEGEO.

Contact details: Centre for Global Metallogeny, Dept. of Geology & Geophysics, University of Western Australia, Crawley, WA 6009, Australia;
Phone:+61 8 9380 7150; Fax: +61 8 9380 1178; Email: chriso31@hotmail.com



Nicholas Hawkes was awarded a BSc (Hons) degree in Geology and Mathematics from the Cambridgeshire College of Arts and Technology in the UK in 1986. Since then he has had over 15 years experience in the mineral exploration industry in Australasia, including Australia and PNG, and in central and South America, particularly in Mexico and Perú, working successively for CRA Exploration, Kennecott Exploration and more recently for Rio Tinto Mining and Exploration. In that time he has had extensive experience in exploration for epithermal gold, porphyry copper-gold, iron-oxide-copper-gold and sediment hosted lead-zinc-silver in tropical, arid and semi-arid environments, including the role of project leader and the responsibility for generating and managing projects on a regional scale. He is currently managing major exploration programs for Rio Tinto in Perú.

Contact details: Rio Tinto Mining & Exploration, Manco Copac 551, Miraflores, Lima 18, Perú; Phone: +51 1 241 5187; Fax: +51 1 446 1840;
Email: nick.hawkes@riotinto.com.pe



Dr. Richard Herrington studied at the Royal School of Mines from 1977 and was granted a BSc ARSM in 1980. He then worked as an exploration geologist between 1980 and 1987 within Canada for both Falconbridge and Cominco before undertaking PhD studies on mesothermal gold mineralisation in Zimbabwe between 1987 and 1991 on an RTZ Bursary at the Royal School of Mines. From then until the present he has been a Researcher at the Department of Mineralogy of the National History Museum in London, where he has been involved in laboratory and field based consulting in many parts of the world and for a range of mineral deposit styles. His client portfolio includes Rio Tinto, BHP-Billiton, Cominco, Samax, International Mining Consultants, Redaurum and Avocet Resources. His research and consulting interests include gold deposits, porphyry Cu-Au and epithermal precious metals systems, volcanogenic massive sulphides, and the metallogeny of the Carpatho-Balkan and Urals collision belts. His current positions at the Natural History Museum include: Programme Leader of Mineralogy and Origin of Ore Deposits; Geological Consultant and Marketing Manager for the Department of Mineralogy; and Current Chairman of the Mineral Deposits Studies Group (Geological Society-IMM-Applied Mineralogy Group Min. Soc. Special Interest Group).

Contact details: The Natural History Museum, Cromwell Road, London, SW7 5BD,UK; Phone: +44 207 942 5528; Fax: +44 207 942 5537; e-mail: rmh@nhm.ac.uk.



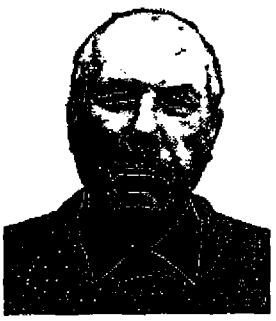
Dr. Jorge Injoque Espinoza studied geology between 1971 and 1975 to obtain his BSc in geology, followed by an engineering degree in 1978. Between 1979 and 1986 he worked for INGEMMET (the Peruvian Geological Survey) researching and exploring, mainly in the Peruvian Coastal belt. Between 1982 and 1985 he undertook post graduate studies to be awarded a PhD from Nottingham University in the U.K. The subject of his thesis was the "Geochemistry of the Cu-Fe-Amphibole Skarn Deposits of the Peruvian Central Coast". Between 1986 and the present he has worked as an exploration geologist in Perú, Chile and Ecuador for a number of mining and exploration companies. This work has exposed him to a range of different geology environments, including deposit types such as Fe Oxide-Cu-Au, precious and base metal epithermals, skarns, porphyries, VMS and mesothermal Au. He is also a part time lecturer at Universidad Nacional de Ingenieria
and Universidad Nacional de San Marcos in Lima, Perú. Currently he is working as an independent consultant in Perú.

Contact details: Casilla 12C, Aptdo 149, Lima 12, Perú;
Email: jinjoque2001@yahoo.com



Dr. Joe Knight received a BSc Honours degree in Geology from Nottingham University, a MSc in Mining Geology from the Camborne School of Mines, and a PhD from the University of Western Australia. He has worked for BHP Minerals for the past five years on base- and precious-metals exploration projects world-wide, concentrating on India. He is currently working for BHP Billiton Exploration as program leader global iron ore and coal.

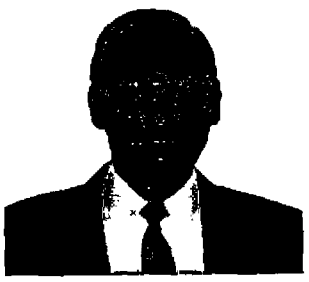
Contact details: BHP Billiton Exploration, QCL House, 40 McDougall Street, Milton, Brisbane, Qld, 4064, Australia;
Phone: +61 7 3307 9600; Email: joe.t.knight@bhpbilliton.com



Dr. Peter Laznicka was granted his first degree from Prague University (then Czechoslovakia) and subsequently an MSc and PhD from the University of Manitoba in Canada where he remained for 27 years to lecture in Economic Geology and a variety of subjects in geoscience. In 1999, he took early retirement from that university and moved to Adelaide, Australia with 15 tonnes of rocks (60 000 samples from 3500 deposits and mineral occurrences) he had systematically collected from around the world, to assume a core position with the Data Metallogenica project for the Australian Mineral Foundation and AMIRA International. Peter is a devotee of 'Metalogenie sans frontiers', trying to relate all metallic ores to all environments and rock associations and to develop a practical systematics of metal accumulations and their settings that field and exploration geologist can use. The set of four "Empirical Metallogeny" books (1985, 1995) and the Total Metallogeny (2001) posters, book and CD-ROM, address this issue. The book "Breccias and Coarse Fragmentites" (Elsevier, 1988) that provides a comprehensive synthesis of these very heterogeneous rocks and their ores, originated with his field research in the Wernecke Mountains, Yukon, in the 1970s and 1980s.

Contact details: AMIRA Data Metallogenica Centre, 63 Conyngham Street, Glenside, SA, 5065, Australia;
Phone: +61 8 8379 5305; Fax: +61 8 8379 6267; Email: peter.laznicka@amira.com.au

---



Dr. Victor Maksaev is Associate Professor of Economic Geology at the Universidad de Chilé, Santiago, Chilé. His qualifications include a BSc from the Universidad de Chilé in 1975 and a PhD conferred by Dalhousie University, Canada in 1990. His main research interests are directed towards the understanding of the metallogeny of the Andes, particularly the processes involved in the formation of copper deposits and their relation to the tectonic and magmatic evolution of the Cordillera. He is currently involved in a detailed geochronological study of the El Teniente porphyry copper ores, attempting to constrain the duration of the hydrothermal processes that originated this enormous copper deposit. He was previously Senior Exploration Geologist for the Barrick and Cambior mining companies from 1994 to 1998, involved in gold exploration in different Latin American countries. Between 1990 and 1994 he was Head of Economic Geology for the Chilean Geological Survey, SERNAGEOMIN, where he spent much of his earlier career involved in geological mapping and metallogenic programs, resulting in the publication of a number of geological and metallogenic maps of northern Chile.

Contact details: Depto. de Geologia, Universidad de Chile, Casilla 13518, Correo 21, Santiago, Chile;
Phone: +56 2 678 4112; Fax: +56 2 696 3050; Email: vmaksaev@cec.uchile.cl



Robert McLean completed a BSc with first class Honours at the University of Western Australia in 1984 and has subsequently worked as an exploration geologist in Australia, Latin America and south-east Asia. He is currently a consultant geologist based in Hanoi, Vietnam.

Contact details: AQ Geological Consultants, Lam Du, Bo De, Gia Lam, Hanoi, Vietnam; Fax: +84 4 514 1694; Email: robertmcl@hn.vnn.vn

---



Dr. H. Richard Naslund is a professor of Geological Sciences at the State University of New York in Binghamton. He received an undergraduate degree in Geology at the University of Illinois in 1972, and Masters and PhD degrees in Igneous Petrology at the University of Oregon in 1977 and 1980 respectively. After teaching at Dartmouth College from 1979 to 1987 he joined the faculty at Binghamton, where he served for six years as the department Chairman. He was a Fulbright Scholar in Chile from 1995 to 1996, and began research on the El Laco deposit at that time. He participated on legs 140 and 176 of the Ocean Drilling Program to investigate the composition, structure, and petrology of the lower ocean crust. His research interests include layered intrusions, differentiated sills, volcanic rocks, experimental petrology, and magmatic ore deposits.

Contact details: Department of Geological Sciences, SUNY, Binghamton, NY, 13902-6000, USA; Email; naslund@binghamton.edu

---



T.M. (Mike) Porter completed a BSc Honours in Economic Geology at the University of Adelaide, South Australia in 1968. He is currently the Principal of Porter GeoConsultancy Pty Ltd, which specialises in arranging and leading professional development courses as the "international study tour series" which take industry geologists to mineral deposits and districts around the world. This has taken him to more than 200 of the worlds more significant ore deposits. He has also been responsible for designing and arranging the technical program of two major conferences and planning, inviting papers and editing the two "Hydrothermal Iron Oxide Copper-Gold and Related Deposits: A Global Perspective" volumes. Prior to establishing his own company in 1996, he worked as an exploration geologist with CRA Exploration Pty Limited for more than 27 years. In this capacity he was involved in exploration for a range of base and precious metals, in a wide variety of geologic and geographic settings, both in Australia and overseas. He worked in the position of Chief Geologist from 1984 to 1996, principally in conceptual work, information synthesis and project generation, particularly from 1990. This included visits to over 150 significant base, ferrous and precious metal ore deposits on all continents, and subsequent research on their regional and local setting.

Contact details: Porter GeoConsultancy Pty Ltd, 6 Beatty Street, Linden Park, SA, 5065, Australia;
Phone & Fax: +61 8 8379 7397; Email: mike.porter@portergeo.com.au



Dr. Gerry Ray served for 3 years with the Northern Rhodesian Police before going to the UK to complete BSc and PhD geology degrees at Bristol and Leeds universities. The latter degree was based on fieldwork with the Malawi Geological Survey. In the early 1970's he worked as an exploration and/or mine geologist with Rio Tinto Zinc in Indonesia and with Falconbridge in Uganda and Zaire. After further work in Saskatchewan and Western Australia, he joined the British Columbia Department of Mines in 1981 where he has focused his attention on skarn deposits. Work as a consultant has also taken him to South America and back to Africa, and his paper on the Productora prospect in Chile in this volume is the result of a project with General Minerals Corporation.

Contact details: British Columbia Geological Survey, PO Box 9320 Stn Prov Gov't, Victoria, BC, V8W 9N3 Canada;
Phone: +1 250 952 0409; Fax: +1 250 952 0381; Email: Gerry.Ray@gems9.gov.bc.ca

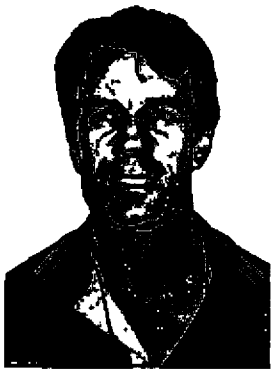
---



Dr. Roger Skirrow is a Senior Research Scientist at Geoscience Australia (formerly AGSO), specialising in Proterozoic metallogeny and Cu-Au systems. He received a BSc in 1980 from the University of Western Australia, a Postgrad. Dip. Sci. in 1983 from the University of Newcastle, NSW, an MSc. in 1987 from Carleton University, Ottawa, Ontario, and a PhD. in 1993 from the Australian National University. He has twenty years experience on gold, copper, lead, zinc and nickel deposits in Australia, Canada and Argentina, working in government surveys, the exploration industry and in universities. Exploration industry experience totalling four years includes project and targeting work with WMC Exploration in South Australia and base metal exploration with BHP in the Yilgarn Block. Roger is currently Project Leader of an Geoscience Australia-PIRSA multi-disciplinary project on the Gawler Craton, focussed on the regional setting and metallogeny of Proterozoic Cu-Au-Fe and Archaean Au systems. Prior to this project, Roger investigated Cu-Au systems and regional alteration in the Curnamona Province, as part of the Broken Hill Exploration Initiative AGSO team. This followed involvement as an economic geologist in AGSO's Geoscientific Mapping of the Sierras Pampeanas (Argentina) project from 1995 to 1997.

Contact details: Minerals Division, Geoscience Australia, Minerals Division, GPO Box 378, Canberra, ACT, 2601, Australia;
Phone: +61 2 6249 9442; Fax: +61 2 6249 9917; Email: roger.skirrow@ga.gov.au

---



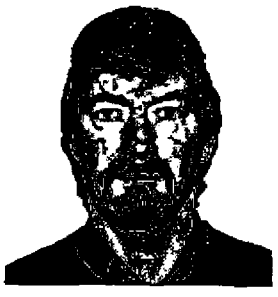
David Sleigh is an MSc graduate from the University of Natal, South Africa. He worked initially in underground mining in the Barberton area of South Africa for Gencor during the mid eighties, and then in gold and base metal exploration for Shell S.A. in the northern and eastern parts of South Africa. During this period he worked on target generation and exploration for a number of Fe-Cu-Au prospects related to the Bushveld acid phases. He then spent 6 years from 1994 developing grass roots Fe-Cu-Au exploration projects in central Zambia, for Gencor and Billiton. Following the changes in the exploration business during the late 1990's he moved to Australia at the start of 2000. Since then he has worked for Selwyn Operations Pty Ltd as Geology Manager, Exploration Manager and now Group Geologist, on their Mt Elliott Cu-Au skarn operation, the Selwyn Line Fe-Cu-Au mines and the regional exploration areas surrounding these mines. He has been involved in exploration and mining for Fe-Cu-Au systems for the last 12 years.

Contact details: Selwyn Mines Australia, PO Box 7966, Garbutt, Qld, 4814, Australia;
Phone: +61 7 4769 6800; Fax: +61 7 4769 6888;
Email: dsleigh@selwynoperations.com.au



Robert J. (Bob) Smith graduated from the University of Melbourne in 1961 and worked for the Bureau of Mineral Resources, Geology and Geophysics as a geophysicist, based in Melbourne and Canberra, between 1961 and 1968. From 1968 until 1973 he was employed by McPhar Geophysics Pty Ltd as Chief Geophysicist, based in Adelaide and Toronto. He established his own consultancy in mining geophysics from 1973 until 1977, when he joined CRA Exploration Pty. Ltd. From 1977 until 2000 he worked initially with CRA Exploration as Chief Geophysicist and subsequently with Rio Tinto Exploration as Chief Consultant - Geophysics. During this period he led the application of geophysics in exploration programs for a variety of commodities throughout the world. Since early 2000 he has again established his own consultancy, Greenfields Geophysics, based in Melbourne. He currently consults in mineral exploration geophysics and geophysical technology.

Contact details: Greenfields Geophysics, PO Box 295, Mont Albert, Vic, 3127, Australia;
Phone/Fax: +61 3 9899 9628; Mobile: +61 4 1734 2422;
Email: greengeo@bigpond.net.au



Colin D. Strickland graduated from Auckland University in New Zealand in 1970 with a BSc (Geology) and commenced his geological career exploring the Tennant Creek Fe-oxide Cu-Au deposits for Geopeko Limited. He has had 30 years experience as a mining and exploration geologist searching for a range of commodities including base metals, uranium, tin-tungsten and gold. Between 1987 and 1998, through his consultancy Triangle Exploration, he actively managed grass-roots projects throughout Queensland, the Northern Territory and West Africa. Since that time he has carried out Cu-Au exploration for General Gold Resources NL throughout Mauritania in both Proterozoic and Archaean terranes.

Contact details: Triangle Exploration Pty Ltd., 29 Aylesford Drive, Marangaroo, WA, 6064, Australia;
Phone: +61 8 9343 8838; Fax: +61 8 9342 2638; Email: strickla@ozemail.com.au

---



Dr. Marcos Zentilli has had a lifelong interest in the geology and metallogeny of the Andes. After receiving his Geólogo degree from Universidad de Chile, Santiago, he studied ore deposit geology at the University of München, Germany. The early part of his career was with the Instituto de Investigaciones Geológicas (now SERNAGEOMIN) as Resident Geologist for Atacama in Copiapó (1964-1968). He continued his study of Chilean geology from Queen's University, Canada, where he completed his Ph.D. in 1974. Since 1972 he has worked in base-metal mineral exploration (Teck - Geophysical Engineering Ltd.) and later joined the Faculty of Dalhousie Univ., where he has been departmental Chair, and more recently Director of the Fission Track Research Laboratory. Apart from teaching economic geology, he has been very active in research undertaking detailed and regional ore deposit studies (base metals, copper, gold) mostly in northern Chile and eastern Canada, and in the last 15 years has concentrated on the time-temperature history of ore-forming processes, such as at Chuquicamata, and studying the involvement of petroleum in ore genesis. He has supervised over 15 PhD and 15 MSc theses. From 1993 he was Co-leader of IGCP Project #342 "Age and Isotopes of South American Ores" from which the El Soldado study arose.

Contact details: Fission Track Research Laboratory, Department of Earth Sciences, Dalhousie University, Halifax, NS, B3H 3J5, Canada;
Phone: +1 902 494 3873; Fax: +1 902 494 6889; Email: zentilli@is.dal.ca

